Wiley Series on Energy
Jay H. Lehr, Series Editor

NUCLEAR ENERGY ENCYCLOPEDIA

Science, Technology, and Applications

Editor-in-Chief: Steven B. Krivit

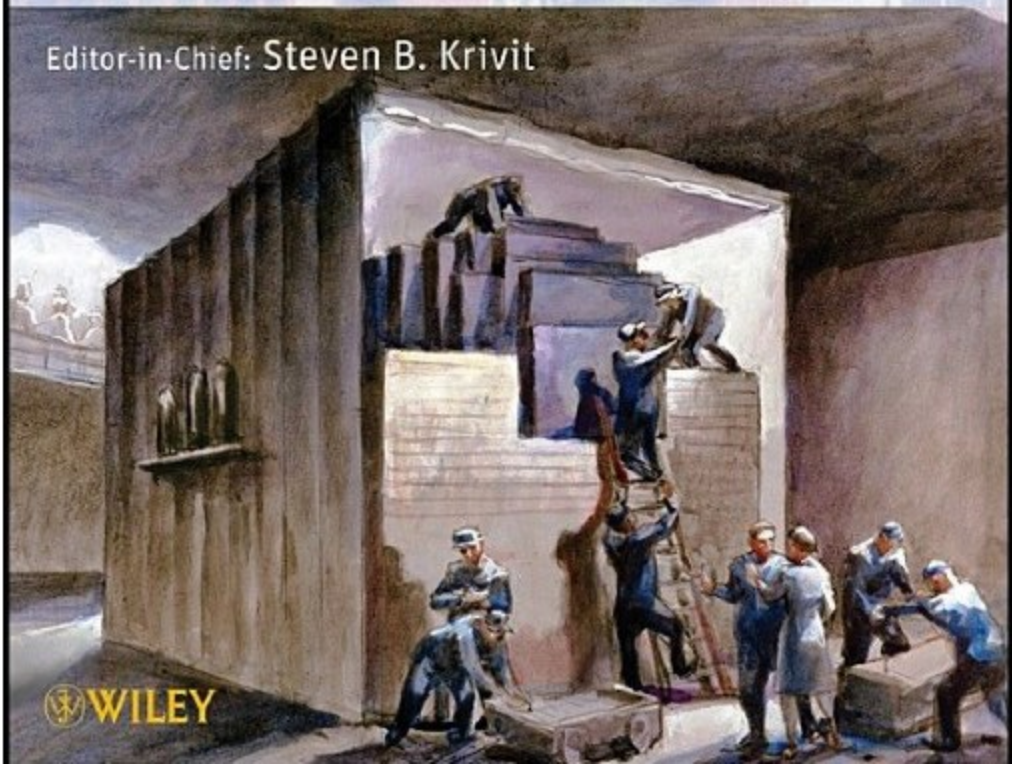

WILEY

NUCLEAR ENERGY ENCYCLOPEDIA

WILEY SERIES ON ENERGY

NUCLEAR ENERGY ENCYCLOPEDIA

Science, Technology, and Applications

Edited by

STEVEN B. KRIVIT, ***Editor-in-Chief***
New Energy Times
San Rafael, CA, USA

JAY H. LEHR, ***Series Editor***
The Heartland Institute
Chicago, IL, USA

THOMAS B. KINGERY, ***Editor***

A JOHN WILEY & SONS, INC., PUBLICATION

Published by John Wiley & Sons, Inc., Hoboken, New Jersey.
Published simultaneously in Canada

Library of Congress Cataloging-in-Publication Data:

Nuclear energy encyclopedia: science, technology, and applications (Wiley series on energy)/Steven B. Krivit, editor-in-chief; Jay H. Lehr, series editor.
p. cm.
Includes index.
ISBN 978-0-470-89439-2 (v. 1 : cloth)
1. Power resources–Encyclopedias. 2. Complete in 5 v. Cf. Wiley encycl. of energy WWW site: xh07 2011-01-21 I. Krivit, Steven II. Lehr, Jay H., 1936– B. III. Title: Encyclopedia of energy.
TJ163.16.W55 2011
621.04203–dc22
2010053086

Printed in Singapore

oBook ISBN: 978-1-118-04349-3
ePDF ISBN: 978-1-118-04347-9
ePub ISBN: 978-1-118-04348-6

10 9 8 7 6 5 4 3 2 1

CONTENTS

PREFACE

STEVEN B. KRIVIT

WE WERE ONCE TERRIFIED OF FIRE, TOO

The discovery of fire 790,000 years ago must have been terrifying to cave men and women [1]. Since that time, many people have died and much property has been destroyed as a result of chemical energy released through fire. Nevertheless, that chemical energy found its place in the world, providing great benefits, and most people take it for granted.

In stark contrast, humankind began to develop and use nuclear energy less than a hundred years ago. According to a 2008 report from the International Energy Agency, nuclear energy provides 13.5% of worldwide electricity [2].

On March 11, 2011, just before we went to press, several of the Fukushima, Japan, nuclear power plants were damaged from a 9.0 magnitude earthquake and a 10-m tsunami. The event dominated headlines and, with some help from the mass media, re-sparked the public's fears of nuclear energy. Some people may look back at Fukushima and consider it a nuclear disaster; others may consider it a nuclear engineering success story, considering the parts of the reactors that did stand up to natural disasters beyond those for which they were designed.

Some members of the public have the misinformed view that radiation has no place in a safe and healthy world. Radiation has always been around us. It comes from a variety of natural sources, and it is widely used in medicine.

The difference between radiation levels that pose a significant health risk and radiation levels that pose negligible or no risks has everything to do with emission rate, concentration, dispersion, distance from, and duration of exposure. Other key factors include the unique properties of each isotope, such as how it affects the body and how long it remains radioactive.

In light of the public's fear, examining how nuclear energy has fared in terms of safety and environment is useful. Remembering that a perfect energy solution for electricity production and transportation does not exist is also useful. Chemical energy and hydroelectric energy have not been without accidents and deaths. Solar and other renewables may have fewer health and environmental risks, but excluding hydroelectric, they provide only 2.8% of electrical power worldwide; they have not demonstrated greater capacity for baseload electrical production.

The public's fear of nuclear energy is an undercurrent that affects all actions related to this industry. This fear must be addressed. Doing that requires exploring the risks and consequences of nuclear energy and other energy technologies. The perceived relationship between nuclear energy and nuclear weapons also contributes to the public's fear.

The 1986 Chernobyl nuclear accident—by far the worst—is most instructive. In 2006, the Chernobyl Forum, an organization comprising the International Atomic Energy Agency, the World Health Organization, the World Bank, and five United Nations organizations working in the areas of food, agriculture, environment, humanitarian affairs, and radiation effects, published an authoritative analysis of the health, environmental, and socioeconomic impacts of Chernobyl [3].

The report concluded that 31 emergency workers died as a direct consequence of their response to the Chernobyl accident. The Forum was unable to reliably assess the precise numbers of fatalities by radiation exposure. The best they were able to do was speculate and make conjecture based on the experience of other populations exposed to radiation. They also wrote that small differences in their assumptions could lead to large differences in their predictions. By 2002, 15 deaths were reported from among 4000 people exposed to radiation and diagnosed with thyroid cancer. These data are in stark contrast to a number of other poorly referenced sources, which have speculated on large numbers of radiation-related deaths.

Concerning environmental impact, the report said that the majority of the contaminated territories are now safe for settlement and economic activity and that the

Chernobyl Exclusion Zone and a few limited areas will have restrictions for many decades.

In August 1975, the Banqiao hydroelectric dam in western Henan province, China, failed as a result of Typhoon Nina, which produced floods greater than the dam was designed to withstand. According to *Encyclopedia Britannica*, 180,000 people died [4].

On April 20, 2010, the Deepwater Horizon offshore oil drilling rig failed and caused 200 million gallons of crude oil to leak into the Gulf of Mexico, according to "PBS News Hour." The leak was out of control for 3 months and 11 men died.

One billion gallons of oil from 21 disasters have been spilled in the oceans since 1967, according to Infoplease [5].

In the United States alone, 260 workers have lost their lives in 21 coal mining accidents since 1970, according to the United States Mine Rescue Association [6].

In Nigeria, on October 18, 1998, a natural gas pipeline explosion took the lives of 1082 people, according to Agence France-Presse [7].

Members of the public would benefit from scrutinizing the comparative safety and track record of clean, emission-free nuclear energy. They would also benefit from learning the basic concepts and principles of nuclear energy production.

The nuclear industry would know that the public is never going to believe—nor should it—that nuclear accidents can't happen. However, it would do well to hear the public's fears and help people understand that nuclear energy has some risks and hazards.

Governments would also do well to show how they are prepared to protect their citizens with effective regulation to minimize radiological emergencies as well as effective response strategies when they occur.

In the absence of the public's understanding of the facts, fear mongers and sensationalist media will surely fill in.

Nuclear energy is certainly not perfect, but the efforts of researchers and industry are significant and crucial. The innovative scientific research and engineering designs shown in this book reflect decades of technological developments in a variety of nuclear applications that are ready to be put to use.

REFERENCES

1. The Hebrew University of Jerusalem, October 27, 2008 press release. http://www.huji.ac.il/cgi-bin/dovrut/dovrut_search_eng.pl?mesge122510374832688760.
2. International Energy Agency's Key World Energy Statistics 2010, Updated February 2011. http://www.iea.org/publications/free_new_desc.asp?pubs_ID=1199.
3. The Chernobyl Forum, *Chernobyl's Legacy: Health, Environmental and Socio-Economic Impacts.* http://www.iaea.org/Publications/Booklets/Chernobyl/chernobyl.pdf.
4. Encyclopedia Britannica, *Typhoon Nina–Banqiao dam failure.* http://www.britannica.com/EBchecked/topic/1503368/Typhoon-Nina-Banqiao-dam-failure.
5. Infoplease, *Oil Spills and Disasters.* http://www.infoplease.com/ipa/A0001451.html.
6. United States Mine Rescue Association, *Historical Data on Mine Disasters in the United States.* http://www.usmra.com/saxsewell/historical.htm.
7. Agence France-Presse, A History of Blasts, in *USA Today*, Nigerian pipeline blast kills up to 200. http://www.usatoday.com/news/world/2006-05-12-nigeria_x.htm.

INTRODUCTION

JAY LEHR

This book marks a significant milestone in the reintroduction of a set of mature nuclear technologies. It also introduces new ideas that expand the frontiers of nuclear science research. It is a timely resource for a world that is awakening to a nuclear renaissance.

Oddly, nuclear energy needs to be reintroduced as if it were a new technology. For a variety of reasons, which vary slightly from nation to nation, the capabilities and capacities of nuclear energy have been under-recognized. In the United States, for example, it supplies 20% of the electric power even though no new nuclear power plant has been designed, approved, and built in the United States in decades.

Nuclear power is a form of terrestrial energy, the same process that heats the center of our earth to 7,000°F. Radioactivity is a natural phenomenon, and indeed, fuel for nuclear power plants comes from natural resources. The concentration of power in the nucleus of the atom is incredible: The disintegration of a single uranium atom produces 2 million times more energy than that produced by breaking a single carbon-hydrogen bond in coal, oil, or natural gas when burned. Nuclear power is an underappreciated marvel of modern technology that harnesses and amplifies a natural process to help satisfy civilization's need for energy.

A 1,000-megawatt coal-fired power plant requires 110 rail cars of coal each day, while an equally powerful nuclear plant requires a single tractor-trailer to deliver new fuel rods once every 18 months. Solar or wind power requires 200 times more land than either coal- or nuclear-powered plants do.

Three decades ago, the average efficiency of nuclear plants was barely 50%, which is to say that they were putting out their rated capacity of energy only half the time. Today, that efficiency has climbed to 94%. Although decades have passed since a nuclear power plant has been constructed in the United States, these reactors produce 25% more power with the same 104 operating plants today than they did 20 years ago.

The real dangers of nuclear power to humans and the environment are vastly different from the propaganda-based exaggerations that have been commonplace in recent decades. Every energy industry has its risks and failures, whether oil spill disasters or coal mine disasters. Prudence and wisdom dictate that decision makers consider the full spectrum of risk and reward in any energy endeavor; this book will help provide sound facts for that purpose.

Future reactors will be even safer than they are today and more cost effective, as well; much has been learned from both successes and failures worldwide.

The United States, at one time a leader in nuclear technology, is lagging in new plant development. The lengthy time required for licensing and construction in the United States remains a significant obstacle to serious investment. According to the Nuclear Energy Institute, applications for 26 new nuclear units are pending with federal regulators, but the most optimistic outlook suggests that only four plants may be built by 2020.

On the other hand, the International Atomic Energy Agency reports that 34 nuclear power plants are under construction in 12 countries besides the United States, including seven in Russia, six in China, and six in India. Many more are on their drawing boards.

Many publications have touted a rebirth of nuclear energy in the United States, but a closer reading often reveals that such support and predictions are tepid at best. Often, the greatest opposition to the clean energy of nuclear power has come from people who maintain a philosophy that more available energy and the progress it will allow will have adverse effects on the environment. In fact, we know that when societies increase their standard of living through economic activity, then and only then can they afford to focus on improving their environment.

During the last few decades, significant misinformation has been propagated worldwide about nuclear energy, often

unknowingly by people with good intentions and care for the environment, although without access to reliable facts. This book helps to bridge that gap.

For decades, nuclear researchers and engineers have been diligently developing and refining new designs and technology. Future-generation nuclear technology will be more passive, no longer requiring coolant to be pumped into vessels in the event of excessive heat. Instead, coolant will be stored at higher elevations, where gravity can do the work.

New plants will have a life of 60 years, spreading their amortized costs. Modular construction will allow quicker and less-expensive assembly. Inherently safe systems, such as the pebble-bed reactor, require fewer safety features because the systems cannot achieve dangerous levels of heat when malfunctions occur. In the case of the pebble beds, the uranium fuel is encased in ceramic spheres the size of tennis balls, and the melting point of the ceramic is well above the level of any heat that can be generated by the uranium.

Waste disposal is not a problem, although it gets the most headlines. Even most critics agree that existing used fuel rods can stay where they are for another 50 or 100 years until permanent storage is determined. In the United States, recycling used fuel has been significantly at odds with the scientific, technical, and even political reality. It is in great need of overhaul.

In 1977, President Jimmy Carter, through a misguided directive, decided that the United States would not reprocess civilian nuclear fuel. According to A. David Rossin, a scholar with the Center for International Security and Arms Control at Stanford University, Carter relied on his advisors and put reprocessing of spent nuclear reactor fuel on hold in the United States. The small amount of mistakenly potentially weapon-grade plutonium produced on reprocessing caused Carter to stop the U.S. program [1]. This decision had several negative consequences.

According to Rossin, Carter hoped that, by setting this example, the United States would encourage other nations to follow its lead. Carter was naive to think that banning reprocessing in the United States, even if based on substantive technical facts, would make the world safer. Why would rogue nations or terrorist groups follow Carter's example? That peaceful nuclear states would voluntarily follow Carter's example to waste nuclear fuel was unrealistic.

As time has shown, other nations have not followed the United States. On October 12, 2010, India announced it had developed its fast breeder reactor technology sufficiently to export it to the world.

Most countries are far more fuel-efficient than the United States and have a fraction of the waste to manage that the United States does. Thus, while U.S citizens diligently strive to recycle their plastic, papers, and many other natural resources, France, for example, gets 80% of its electricity from nuclear power and uses 95% of the available fuel, leaving that country with only 5% waste to manage.

The United States pays a double penalty as a result of Carter's directive, because it uses only 5% of the fuel and wastes 95% of it. Thus, the United States is one of the least responsible nations in nuclear fuel recycling.

There is even greater hope for the future with fast reactors, described in this book, that can use nuclear wastes from a variety of sources as fuel. They are able to unlock energy in waste because they can burn plutonium and neptunium and other materials that are byproducts of current nuclear reactors.

Fast reactors under development in the United States could supply all of the nation's energy needs for 70 years using only nuclear waste in storage today. While costs per kilowatt of capacity will exceed all other nuclear plants, they likely will drop significantly after a few fast reactors come on line.

Nuclear power is progressing technologically and socially, but the battle for the future of mankind's energy is far from won. This book aims to fill a crucial role: to educate industry, policymakers, students, and the public that nuclear energy is the safest and most plentiful form of energy to power the future of civilization. This book offers the most up-to-date collection of all we know about the future of nuclear energy around the world, and it is a bright future indeed.

ACKNOWLEDGMENTS

The editors would like to thank Bob Esposito and Michael Leventhal for their work in producing this book, and John Wiley & Sons, Inc., for publishing it. Steven Krivit would also like to thank the sponsors of New Energy Institute for their support of this project.

We deeply appreciate the contributions of the many experts who, through their work, are helping to advance nuclear science and technology worldwide.

REFERENCE

1. A. David Rossin, *U.S. Policy on Spent Fuel Reprocessing: The Issues*. http://www.pbs.org/wgbh/pages/frontline/shows/reaction/readings/rossin.html.

CONTRIBUTORS

Dr. Alberto Abánades, Institute of Nuclear Fusion-UPM, c/José Gutierrez Abascal, 2, Madrid, Spain

Dr. Rokaya A. Al-Ayat, Lawrence Livermore National Laboratory, 7000 East Avenue, L-580, Livermore, CA, USA

Dr. David E. Ames II, Texas A&M University, Department of Nuclear Engineering, 129 Zachry Engineering Center, 3133 TAMU, College Station, TX, USA

Mr. K. Anantharaman, Reactor Design and Development Group Trombay, Bhabha Atomic Research Centre, Mumbai, Maharashtra, India

Dr. Charles C. Baker, Sandia National Laboratories, Principal Editor-Fusion Engineering and Design, Albuquerque, NM, USA

Mr. Lee Cadwallader, Idaho National Laboratory, Idaho Falls, ID, USA

Carlos H. Castaño, Missouri University of Science and Technology, Nuclear Engineering, 222 Fulton Hall, 1870 Miner Circle, Rolla, MO, USA

Dr. P. Chellapandi, Indira Gandhi Centre for Atomic Research, Kalpakkam, TN, India

Dr. Stephen O. Dean, Fusion Power Associates, 2 Professional Drive Suite 249, Gaithersburg, MD, USA

Dr. Laila A. El-Guebaly, Fusion Technology Institute, 431, Engineering Research Building, 1500 Engineering Drive, Madison, WI, USA

Dr. Hans D. Gougar, Idaho National Laboratory, Idaho Falls, ID, USA

Mr. Christopher Grandy, Argonne National Laboratory, 9700 S. Cass Avenue, Argonne, IL, USA

Ms. Rose A. Hansen, Lawrence Livermore National Laboratory, 7000 East Avenue, L-471 Livermore, CA, USA

Dr. Roger Henning, Nuclear and Hydrogeologic Support Services, 2120 Crooked Pine Drive, Las Vegas, NV, USA

Dr. Robert N. Hill, Argonne National Laboratory, 9700 S. Cass Avenue, Argonne, IL, USA

Dr. Hussein Khalil, Argonne National Laboratory, Nuclear Engineering Division, 9700 S. Cass Avenue; Bldg. 208 Argonne, IL, USA

Mr. Lakshminarayana Venkata Krishnan, Indira Gandhi Centre for Atomic Research, B6, Madhurima Apartments, 32, Conransmith Road, Gopalapuram, Chennai, TN, India

Mr. Steven B. Krivit, New Energy Times, 369-B Third Street; Suite 556, San Rafael, CA, USA

Dr. Antonio Lafuente, Institute of Nuclear Fusion-UPM, c/José Gutierrez Abascal, 2, Madrid, Spain

Dr. Richard T. Lahey Jr., Rensselaer Polytechnic Institute, MANE - NES Bldg., 110 8th Street, Troy, NY, USA

Dr. Jay Lehr, The Heartland Institute, 19 South LaSalle Street #903, Chicago, IL, USA

Dr. J.G. Marques, Instituto Tecnologico, Estrada Nacional 10, Sacavem P-2686-953; Centro de Física Nuclear, Universidade de Lisboa, 1649-003 Lisboa, Portugal

Dr. José M Martinez-Val, Institute of Nuclear Fusion-UPM, c/José Gutierrez Abascal, 2 Madrid, Spain

Dr. Harold McFarlane, Idaho National Laboratory, Idaho Falls, ID, USA

Dr. George Miley, University of Illinois at Urbana-Champaign, Fusion Studies Laboratory, 103 S Goodwin, Urbana, IL, USA

Dr. Alistair I. Miller, Atomic Energy Canada Ltd., 8 Darwin Crescent, Deep River, ON, Canada

Dr. Patrick Moore, Greenspirit Strategies Ltd., 873 Beatty Street #305, Vancouver BC V6B 2M6, Canada

Dr. Edward I. Moses, Lawrence Livermore National Laboratory, 7000 East Avenue, L-466, Livermore, CA, USA

Dr. Robert I. Nigmatulin, Russian Academy of Sciences, Russia

Ms. Saly T. Panicker, Desalination Division, Bhabha Atomic Research Centre, Trombay, Mumbai, Maharashtra, India

Dr. Mireia Piera, Ingenieria Energetica, UNED ETSII-Dp, c/Juan del Rosal, 12, Madrid, Spain

Dr. Igor Pioro, University of Ontario Institute of Technology, Faculty of Energy Systems and Nuclear Science, 2000 Simcoe Street North, Oshawa, Ontario, Canada

Dr. Baldev Raj, Indira Gandhi Centre for Atomic Research, Kalpakkam, TN, India

Dr. P.R. Vasudeva Rao, Indira Gandhi Centre for Atomic Research, Kalpakkam, TN, India

Dr. Francesco Romanelli, JET-EFDA Culham Research Center, Abingdon OX14 3 DB, UK

Dr. William R. Roy, University of Illinois at Urbana-Champaign, Department of Nuclear, Plasma, and Radiological Engineering, 216 Talbot Laboratory, MC-234, 104 South Wright Street, Urbana, IL, USA

Dr. Clifford Singer, Department of Nuclear, Plasma, and Radiological Engineering, University of Illinois at Urbana-Champaign, 216 Talbot Laboratory, MC-234, 104 South Wright Street, Urbana, IL, USA

Dr. Mahadeva Srinivasan, Bhabha Atomic Research Centre (Retired), 25/15, Rukmani Road, Kalakshetra Colony, Besant Nagar, Chennai, TN, India

Dr. Edmund Storms, Kiva Labs, 2140 Paseo Ponderosa, Santa Fe, NM, USA

Prof. Rusi P. Taleyarkhan, Purdue University, College of Engineering, 400 Central Drive, West Lafayette, IN, USA

Dr. J'Tia Taylor, Argonne National Laboratory, 9700 S. Cass Avenue, Argonne, IL, USA

Dr. P.K. Tewari, Bhabha Atomic Research Centre, Desalination Division, Trombay, Mumbai, Maharashtra, India

Mr. Roger Tilbrook, 86 White Oak Circle, St. Charles, IL, USA

Dr. Pavel V. Tsvetkov, Texas A&M University, Department of Nuclear Engineering, 129 Zachry Engineering Center, 3133 TAMU College Station, TX, USA

Dr. Leonid I. Urutskoev, Moscow State University Of Printing Arts, State Atomic Energy Corporation "Rosatom", Expert Dep. ul. Bolshaya Ordynka, 24/26, Moscow, Russia

Dr. Shoaib Usman, Missouri University of Science and Technology, Mining & Nuclear Engineering, 222 Fulton Hall, 1870 Miner Circle, Rolla, MO, USA

Dr. M. Vijayalakshmi, Indira Gandhi Centre for Atomic Research, Kalpakkam, TN, India

Mr. Lester M. Waganer, 10 Worcester Ct., O Fallon, MO, USA

Dr. Winthrop Williams, U.C. Berkeley, 2615 Ridge Rd. #D, Berkeley, CA, USA

Dr. James R. Wolf, Idaho National Laboratory, Idaho Falls, ID, USA

Dr. Joseph. M. Zawodny, NASA Langley Research Center, MS-475, Hampton, VA, USA

NUCLEAR FISSION: GLOSSARY AND ACRONYMS

K. Anantharaman, P.R. Vasudeva Rao, Carlos H. Castaño and Roger Henning

GLOSSARY

Burn-up A measure of energy extracted from nuclear reactor fuel. It is defined as the ratio of the thermal energy released by nuclear fuel to mass of fuel material consumed. It is typically expressed as Gigawatt days per ton of fuel (GWd/t).

Capture cross-section A measure of the probability that an incident particle or photon will be absorbed by a target nuclide.

Chain reaction Neutron-induced fission is a common example. The fission reaction produces neutrons that can sustain the reaction, thus forming a chain of linked reactions. Gasoline combustion is an example from chemistry. A spark initiates the combustion, resulting in a release of energy that is sufficient to propagate the reaction.

Cross-section of a nuclear reaction A measure of the probability that a nuclear reaction will occur. It is the apparent or effective area presented by a target nucleus or particle to an oncoming radiation. The barn is the standard unit for the cross section and is equal to 10^{-24} cm^2.

Enrichment Physical process of increasing the proportion of U235 to U238 material in nuclear fuel element, i.e., increasing the fissile content. It is generally carried out by using high-speed centrifuges or by gaseous diffusion process.

Fast neutron Neutron released during fission, traveling at high velocity and having high energy (>1 MeV).

Fission cross-section The probability a reaction will occur that will cause a nuclide to fission.

Fission product A residual nucleus formed in fission, including fission fragments and their decay products.

Fuel cycle All steps in the use of nuclear material as fuel for a nuclear reactor, including mining, purification, isotopic enrichment, fuel fabrication, irradiation, storage of irradiated fuel, reprocessing, and disposal.

Fuel cycle—Open Spent fuel is removed from the reactor, cooled, and transferred to long-term dry storage. No attempt is made to recover the unused fissile material.

Fuel cycle—Closed Spent fuel is removed from reactor and after a cooling period, it is transferred for reprocessing. The fissile material is recovered for reuse and the fission products are separated for disposal. Reprocessing enables recycling of the fissile isotopes and reduces amount of waste to be disposed.

Half-life The time period required for half of the atoms of a particular radioactive isotope to decay.

Heavy water Water containing an elevated concentration of molecules with deuterium ("heavy hydrogen") atoms. It has chemical properties similar to that of ordinary or light water, but neutronic properties are different. Heavy water absorbs fewer neutrons and is also a better moderator.

Isotope Different isotopes of an element have the same number of protons but different numbers of neutrons. Therefore, the isotopes of an element have different atomic masses. For example, U235 and U238 are isotopes of uranium.

Neutron capture Absorption of a neutron by an atomic nucleus. A measure of the probability that a material will capture a neutron is given by the neutron capture cross-section, which depends on the energy of a neutron and on the composition of the material.

Nuclear fission The process of splitting a heavy nucleus into two lighter nuclei, accompanied by the simultaneous release of a relatively large amount of energy and usually one or more neutrons. Fission is induced through the reaction of an incident radiation with the nucleus. Neutron-induced fission of uranium-235 is a common example. Considerable energy is released during the fission reaction, and this energy can be used to produce

heat and electricity. Spontaneous fission is a type of radioactive decay for some nuclides.

Nuclear fusion The process of forming a heavier nucleus from two lighter ones.

Scrub A substance used to absorb preferentially another in a different phase by providing a preferential chemical reaction or state. Traditionally, the term has been used to designate a liquid to retain gaseous exhausts from a gas stream, but it is applied to other systems as well, including slurries and liquid-to-liquid retention.

Salting Providing extra ions necessary to carry out or improve a particular chemical process. Usually the addition of a salt with the proper ion is meant, but adding the ion in any form can be equally effective (e.g., providing NO_3^- ions by addition of $NaNO_3$ or HNO_3).

Uranium-233 A fissile, manmade isotope of uranium. It is created when thorium-232 captures a neutron through irradiation. It has a half-life of 160,000 years and decays by emitting alpha particles.

Uranium-235 Only fissile isotope of uranium occurring in nature (0.7% abundance). Uranium-235 has a half-life of 700 million years, and it can sustain a chain reaction.

Uranium-238 The most prevalent isotope (>99.3%) of uranium in nature. It has a half-life of about 4,500 million years. Uranium-238 emits alpha particles, which are less penetrating than other forms of radiation. Uranium-238 cannot sustain a chain reaction, but it can be converted by neutron capture to plutonium-239.

Plutonium-239 A heavy, radioactive, manmade fissile isotope of plutonium. It is the most common isotope formed in a typical nuclear reactor formed by neutron capture from U238 and yields much the same energy as the fission of U235. Pu239 has a half-life of 24,400 years and decays by emitting alpha particles. The hazard from Pu-239 is similar to that from any other alpha-emitting radionuclides (Inhalation).

Thorium-232 Th-232 is most stable isotope of thorium, and nearly all natural thorium is Th-232. The isotope thorium-232 is stable, having a half-life of about 14,000 million years, and undergoes alpha decay. Unlike uranium, thorium does not contain any natural fissile isotope. Thorium-232 is not fissile itself, but it can absorb slow neutrons to convert it into U233, which is fissile.

Voloxidation If tritium (^3H) needs to be separated from spent fuel, it is better to do it before the fuel is dissolved, since the tritium would then be isotropically distributed with all the hydrogen in water, solvents, and nitric acid, making its separation much harder. Voloxidation is a process developed by ORNL in which fuel after shearing is then oxidized in a rotating furnace to convert UO_2 to U_3O_8. The latter is less dense, causing the fuel to swell, pulverizing the ceramic fuel and causing the release of occluded gasses. The released gasses (Kr, Xe, etc.) can then be collected, and particularly tritium can then be oxidized and removed as almost pure ultra-heavy water (^3H_2O), all carried out before the fuel is dissolved [M. Benedict, T. Pigford, and H. W. Levi, Chapter 10: Fuel reprocessing, In *Nuclear Chemical Engineering*. McGraw-Hill, New York, 1981, pp. 458–459, 476].

ACRONYMS

Abbreviation	Expansion
AEA	Atomic Energy Act of 1954
AECL	Atomic Energy of Canada Limited, Canada
AHWR	Advanced Heavy Water Reactor
ALARA	as low as is reasonably achievable
BARC	Bhabha Atomic Research Centre, Mumbai, India
BORAX	Boiling Reactor Experiment
BWR	Boiling Water Reactor
CANDU	Canada Deuterium Uranium
CEA	Commissariat à l'Énergie Atomique
CERCLA	Comprehensive Environmental Response, Compensation, and Liability Act of 1980 (Superfund)
CFR	Code of Federal Regulations (U.S.)
CP	Chicago Pile
DOE	(United States) Department of Energy
EBR	Experimental Breeder Reactor
EDF	Électricité de France
EFPD	Effective Full Power Days
EPA	(United States) Environmental Protection Agency
EPRI	Electric Power Research Institute
Euratom	European Atomic Energy Community (legally distinct from the European Union but has the same membership)
FBR	Fast Breeder Reactor
FBTR	Fast Breeder Test Reactor
FEPS	features, events, and processes
FUSRAP	Formerly Utilized Sites Remedial Action Program
HEU	Highly Enriched Uranium
HLLW	High Level Liquid Waste
HLW	high-level radiological waste
HTGR	High Temperature Gas-cooled Reactor
IAEA	International Atomic Energy Agency (independent organization but related to the United Nations)
IGCAR	Indira Gandhi Centre for Advanced Research, Kalpakkam, India

KAMINI	Kalpakkam Mini Reactor
LLW	low-level radiological waste
LWBR	Light Water Breeder Reactor
LWR	Light Water Reactor
MOX Fuel	Mixed Oxide Fuel
MSBR	Molten Salt Breeder Reactor
NEA	Nuclear Energy Agency
NEPA	National Environmental Policy Act of 1969
NRC	(United States) Nuclear Regulatory Agency
NRTS	National Reactor Testing Station
NWPA	Nuclear Waste Policy Act of 1982
ORNL	Oak Ridge National Laboratory, USA
PDRP	Power Demonstration Reactor Program
PHWR	Pressurized Heavy Water Reactor
PIE	Post Irradiation Examination
PRTRF	Power Reactor Thorium Reprocessing Facility
PUREX process	Plutonium-URanium EXtraction process
PURNIMA	Plutonium based Indian research reactor (now dismantled)
PWR	Pressurized Water Reactor
RCRA	Resource Conservation and Recovery Act of 1976
SNF	spent nuclear fuel
SSC	structures, systems, or components
TBP	Tri-n-Butyl Phosphate solvent
THOREX process	THORium-uranium EXtraction process
TRU	transuranic radiological wastes
UMTRCA	Uranium Mill Tailings Radiation Control Act of 1978
USAEC	United States Atomic Energy Commission
WIPP	Waste Isolation Pilot Plant (operated by DOE).

NUCLEAR FUSION: GLOSSARY AND ACRONYMS

LESTER M. WAGANER

GLOSSARY

Availability, Plant availability This metric is a ratio of the hours the plant is available for full power operation divided by the total annual hours. Plant availability is affected by the scheduled maintenance periods and the unscheduled maintenance periods. These maintenance periods are governed by maintainability, reliability, and inspectability.

Advanced (fusion) fuels The D-T fusion reaction is the least demanding reaction, but other fuel combinations are possible that have less energetic neutrons and more charged particles, which enables longer first wall and blanket lifetimes and the possibility of direct conversion into electricity with higher conversion efficiencies.

Blanket The blanket is the power- and fuel-producing component within the power core. The "blanket" name has been adopted to signify that the plasma is almost fully enveloped in a blanketing component. In the early and some present day fusion experiments, the blankets were only shielding blankets in the sense that they captured the plasma thermal and neutron energy, but did not have any tritium breeding function. For the few experiments fueled with D-T, sufficient tritium fuel could be externally supplied for the limited duty cycle operation. As the duty cycle and the power level on future fusion facilities increase, there will be a need to provide a substantial, steady-state supply of tritium. This requires the blanket to be tritium breeding, containing either lithium or a lithium compound. Two design concepts are being pursued, solid and liquid breeder blankets. As the designs move toward power plants, the blanket must operate with higher internal temperatures to enable higher thermal conversion efficiencies. In the present designs, the blanket also supports the first wall.

Burn-up, Burn-up fraction It is the fraction of the fusion fuel elements that are fused to release the nuclear energy. The burn-up fraction is used to determine the throughput of the fuel required to achieve the desired fusion power level.

Capture cross-section A measure of probability that an incident particle/photon will be absorbed by a target nuclide.

Constant dollars An economic analysis with constant dollars assumes that the purchasing power of the dollar remains constant throughout the construction period—the cost for an item measured in money with the general purchasing power as of some reference date. Hence, there is no inflation. However, there are costs associated with the true (or real) interest value. This will not be a realistic situation in the actual world as there are always inflationary (or deflationary) effects, but this "constant dollar" analysis provides a more easily understood, comparative economic metric that avoids making the assumptions about future inflationary/deflationary effects. The rate of interest is usually in the range of 3% to 6% without inflation.

Divertor The divertor is a plasma-facing subsystem, like the first wall. The divertor has a specialized function to intercept the energetic plasma particles of electrons, protons, alpha particles (fusion ash), and other trace impurity elements that are swept out along the magnetic field lines at the plasma magnetic X-point(s). The magnetic geometry of tokamaks can have one or two regions where the confining magnetic fields cross, allowing the energetic particles to escape. Like the first wall, tungsten armor will be required to provide adequate component lifetime. It is highly desired for the divertor lifetime to be (nearly) the same as the first wall and blanket so both subsystems can be removed and replaced at the same time. Thus, the divertor armor must be much more robust than the first wall armor. The divertor modules are located at the bottom (for the single-null divertor) or at the top and bottom (for the double-null divertor) of the power core.

D-T fusion (reaction) The fusing of the two light nuclei of deuterium (D) and tritium (T) is the least demanding fusion reaction resulting in the creation of a 3.52 MeV alpha particle and a 14.07 MeV neutron, resulting in an energy increase of 17.59 MeV. Other fusion fuel combinations are possible, called advanced fuels, because these combinations require more demanding plasma conditions.

Lithium enrichment Physical process of increasing the proportion of lithium-6 to lithium-7 isotopes in blanket breeding materials.

First wall In most current experiments and postulated power plant-relevant facilities, the outer edges of the high temperature fusion plasma ($\sim$100 million $^{\circ}$C) are only a few centimeters away from the first solid surface, the first wall, which protects the power/fuel-producing blanket and is the largest plasma-facing component. The current best candidates for underlying first wall structural materials are ferritic steels or silicon carbide composites. The current thinking is that the candidate first wall materials may not be sufficiently robust to handle the intense heating and occasional bursts of particle flux to last the required operational time. To have additional design margin, a thin layer of tungsten is being considered as an armor material because it is more robust against high heat and particle sputtering with low tritium retention. To accommodate the sizable differential thermal expansion, the tungsten coating will probably be segmented. It will have to be brazed or mechanically attached to the basic first wall to ensure adequate thermal heat conduction.

Fusion cross-section The probability a reaction will occur that will cause two light nuclides to fuse.

Half-life The time in which one half of the atoms of a particular radioactive substance disintegrate into another nuclear form. Measured half-lives vary from a fraction of a second to billions of years.

Heating and current drive The plasma is heated to some degree by the flowing toroidal current, but additional heating is required to reach the necessary fusion temperatures. This is accomplished by radio frequency (RF) heating or maybe neutral beam (NB) subsystems. The interior solenoidal coils will provide the initial toroidal current formation, but RF subsystems will provide the continuing current drive for sustained steady-state operation.

Heavy water Water containing significantly more than the natural proportions (one in 6,500) of heavy hydrogen (deuterium, D) atoms to ordinary hydrogen atoms. It has chemical properties similar to that of ordinary or light water but different neutronic properties. Heavy water is used as a moderator in some reactors because it slows down neutrons effectively and also has a low probability of absorption of neutrons.

Hohlraum target Hohlraum is a hollow cavity with walls in radiative equilibrium with the radiant energy within the cavity. The cavity has one or more holes to admit the radiative beams that strike the inner hohlraum walls, creating a bathing x-ray environment to heat and compress the central fuel target.

Inertially confined fusion energy (IFE) A hot ionized plasma is confined inertially with sufficient pressure, temperature, and time to fuse light elements to other elements with a slightly decreased total mass that yields a net energy release. Confinement can be obtained using laser, light ion, or heavy ion beams directed toward small fuel-containing targets in the center of a spherical or cylindrical chamber. Direct-drive targets require nearly symmetric illumination, whereas indirect drive employs a target with a surrounding hohlraum where laser beams enter the hohlraum from opposite sides.

Isotope Two or more forms (or atomic configurations) of a given element that have identical atomic numbers (the same number of protons in their nuclei) and the same or very similar chemical properties but different atomic masses (different numbers of neutrons in their nuclei) and distinct physical properties. For example, Li-6 and Li-7 are isotopes of lithium, and deutritium (D) and tritium (T) are isotopes of hydrogen.

Liquid breeder blanket Liquid breeding blankets employ either stagnant or moving liquid metal containing a lithium, lithium compound, or lithium eutectic to breed tritium. With the stagnant liquid breeder option, a separate coolant is used to remove the thermal energy. With the moving liquid breeder option, the liquid breeder is the coolant. A separate coolant (such as helium) may also be required to cool the structural material.

Low-activation materials High purity, specialty materials with a composition containing minimal impurities that would transmute into long-lived radioactivity in the presence of fusion neutrons.

Magnetic mirror The magnetic mirror was one of the first magnetic confinement configurations envisioned to confine the energetic fusion plasma ionized particles. It consisted of two high-strength solenoidal coils placed some distance apart. Theoretically, the charged particles would remain in the lower field strength region between the two magnets and be reflected by the higher field regions close to the coils. In experiments, there was an unacceptable amount of plasma "leaking" through the coils. Other coil and field variations were examined to help control the leakage, some by combining a string of solenoidal coils with higher strength yin-yang coils at the ends (tandem mirror). Another arrangement was

arranging the solenoidal coils in a toroid shape call the Elmo Bumpy Torus.

Magnetically confined fusion energy (MFE) A hot ionized plasma is confined magnetically with sufficient pressure, temperature, and time to fuse light elements to other elements with a slightly decreased total mass that yields a net energy release. Small and moderate-sized experiments use normally conducting magnets for the plasma confinement. Larger experiments and eventual power plants have or will incorporate superconducting magnets. Many magnetic configurations exist to confine the plasma, the tokamak being the most studied and demonstrated. Containment can be either pulsed or preferably steady-state.

Neutronics, Nucleonics This branch of physical science estimates the lifetime of first wall and blanket structures due to neutron damage, the effectiveness of the blanket to breed tritium, the radiation damage to the superconducting materials and insulators, the effectiveness of the shields to protect the externals, and the activation of the power core components.

Nominal dollars Nominal dollar cost is the cost of an item measured in as-spent dollars and includes inflation effects. Nominal dollars are sometimes referred to as "current" dollars, "year of expenditure" dollars, or "as spent" dollars. With this analysis metric, a value for inflation must be assumed for the period of construction.

Nuclear fusion The fusing of light atomic nuclei into heavier elements (higher atomic number) with a slightly reduced combined mass that releases a considerable energy (usually in the form of energetic neutrons, alpha particles or radiation) that can heat components surrounding the plasma to produce electricity.

Poloidal field magnets (coils) Poloidal field (PF) magnets are coils that generate magnetic fields in the poloidal direction (around the torus in the short direction) of the device. In the tokamak designs, the coils are a set of 10–20 circular coils that either inductively initiate the plasma current or shape the plasma. Induction coils are located in near the center of the machine inward of the TF coils. In tokamaks, the shaping coils are located above, below, and radially outward of the TF coils.

Radioactive decay The transformation of one radioisotope into one or more different isotopes (known as decay products or daughter products), accompanied by a decrease in radioactivity (compared to the parent material). This transformation takes place over a well-defined period of time (half-life), as a result of electron capture; fission; or the emission of alpha particles, beta particles, or photons (gamma radiation or x-rays) from the nucleus of an unstable atom. Each radioisotope in the sequence (known as a decay chain) decays to the next until it forms a stable, less energetic end product. In addition, radioactive decay may refer to gamma-ray and conversion electron emission, which only reduces the excitation energy of the nucleus.

Scrape-off layer (SOL) The distance between the outer plasma boundary and the first wall is called the scrape-off layer. This is usually on the order of 5–10 centimeters.

Shield The shield is located immediately radially outward from the plasma and behind the blanket and divertor. The shield subsystem function is to capture most of the high-energy neutrons escaping the first wall, blanket, and divertor subsystems and streaming through penetrations and assembly gaps. The requirement for the shield is to provide adequate radiation protection for all the further outboard components (e.g., coils) as well as workers, the public, and the environment. The superconducting coils are quite susceptible to radiation damage, so these are critical components to be shielded. Approximately 10% of the total neutron energy is captured by the shield. This amount of energy is significant, so the current design approach is to employ to layers of shielding if needed. The innermost layer operates at the same temperature of the blanket and contributes to the electrical energy production. A second layer receives much less neutron flux and it cooled with low temperature water.

Solid breeder blanket The solid breeding blankets employ solid pellets or pebbles of lithium ceramic compounds, typically with helium flowing in cooling channels to remove the thermal energy.

Stellarator (configuration) Proposed in 1950 by Spitzer, the stellarator magnetic fusion confinement approach is similar to a tokamak in that it has both toroidal and poloidal magnets to contain and shape the plasma. In stellarators, the stabilizing toroidal plasma current is generated by shaping the toroidal coils to induce the plasma current. Stellarators differ from tokamaks because they are not azimuthally symmetric and less prone than tokamaks to plasma instabilities and disruptions. The first stellarators wound the toroidal coils in a continuous helix to induce the toroidal current. This was appropriate for experiments, but would not be practical for larger experiments or power plants. An improved approach utilized sets of differing individual modular coils that were highly shaped to accomplish the plasma current generation and form a repeating geometrical plasma shape called a period. Stellarators can be designed from two periods up to many periods. Stellarators also need divertors to capture and remove charged particles, ions, and electrons that escape the magnetic field lines. The complex stellarator TF coil geometries complicate the maintenance approach and suggest small replacement assemblies.

Tokamak (configuration) The tokamak is a magnetic fusion confinement approach in the shape of a toroid (donut) configuration that was originally developed by the Russians in the 1950s. This configuration has elliptical D-shaped plasma cross-section formed with equally spaced planar toroidal field (TF) coils to confine the plasma. Additional poloidal field (PF) coils, external to the TF coils, further shape the plasma. Sets of divertor, equilibrium field, and central solenoid coils are necessary to further shape and position the plasma within the toroidal vessel. The solenoidal coils induce a transformer action in the plasma to initiate a toroidal plasma current (10 s of MA). This toroidal current flowing through the plasma is a defining feature for the tokamak that generates a helical component of the magnetic field for plasma stability. Early tokamak experiments created and sustained (for a brief time) the toroidal plasma current with transformer inductance using the solenoidal coils, but pulsed operation is not suitable for power plants. Tokamaks are capable of reaching steady-state operating conditions using current drive systems of radio frequency or neutral beam subsystems. The plasmas of tokamaks (and other magnetic configurations) may suffer instabilities that lead to disruption or edge-localized modes where the plasma bulges out and contacts the walls, thus damaging it. All tokamaks employ divertors in either single or double-null configurations to collect the charged particles, ions, and electrons that escape the magnetic field lines.

Toroidal field (TF) magnets (coils) Toroidal field (TF) magnets are coils that generate magnetic fields in the toroidal direction (around the torus in the long direction) of the device. In the tokamak designs, the coils are a D- or modified D-shape that are planar. There are usually from 12 to 18 identical coils, equally spaced. The tokamak TF coils do not generate a plasma current in the toroidal direction, but rely on the PF coils to initiate the plasma current. The maintenance approach may be a factor that helps define the specific shape. In the stellarator design, the TF coils are highly shaped both non-planar and radially in order to generate a plasma toroidal current as well as the toroidal magnetic field. Early stellarator TF designs were continuously wound coils around the toroid, but later TF coils were desired to be modular for ease of fabrication and maintenance. Other toroid devices use TF coils, combining some of these features.

Vacuum vessel A continued fusion reaction cannot be sustained in the presence of impurities, even if the pressure, temperature, and time conditions are met. Any minor amount of impurities (gases or particulates) would immediately cease the fusion reaction, which is a good safety feature. However, fusion requires an extremely high vacuum with a very clean environment inside the plasma chamber. The typical vacuum chamber design is a D-shaped toroid that completely encloses the plasma, the fusion energy capture and conversion subsystems (first wall, blanket, divertor and shield), internal structure, and heating and current drive launchers/ducts. In tokamaks, the coil subsystems are typically external to the vacuum vessel. Small and large ports are necessary to accomplish maintenance, heating/current drive, instrumentation, and vacuum pumping. A small amount of nuclear energy will escape the internal shielding that will heat the vacuum vessel requiring a low temperature heat removal, typically by water.

ACRONYMS

Abbreviation	Expansion
ITER	ITER is an international collaboration to build a fusion experimental reactor that produces, for a short period, more energy than it consumes. This reactor extends the fusion experimental database to help enable fusion to be a power-producing energy source. The acronym originally meant International Thermonuclear Experimental Reactor, but currently it is using ITER as its name. It is currently being constructed and is expected to produce the first DT plasma in 2026 and operate for a few decades. It is expected to exceed ignition conditions and produce 500 MW of fusion power with an input of 50 MW for 400 seconds.
NIF	National Ignition Facility, a U.S. laser-driven test facility, https://lasers.llnl.gov/
TF	Toroidal Field
PF	Poloidal Field
SOL	ScrapeOff Layer
RAFS	Reduced Activation Ferritic Steel
ODS	Oxide Dispersion Strengthened
SiC/SiC	Silicon-Carbide Composites
LiPb	A lithium lead eutectic is being proposed for use in future fusion power cores as liquid metal tritium breeder and heat transfer media for blankets, shields, and heat transfer loops.The eutectic was originally identified as 17 atom percent lithium and 83 atom percent lead. More recently the lower temperature LiPb eutectic point has been redefined to be 15.7 atom percent lithium and 84.3 atom percent lead. The melting point of the

	LiPb eutectic is 235°C, however the heat transfer loop will typically operate between about 350°C and 700°C, well away from the eutectic temperature.
ELM, ELMs	Edge-Localized Modes are due to instabilities in plasma confinement that release bursts of energy and particles impacting the first wall.
TBR	Tritium Breeding Ratio. The metric for the plant self-sufficiency to breed all tritium required for plant operation considering burn-up, losses, entrapment, and data uncertainties
NbTi	Niobium-Titanium
Nb3Sn	Niobium-Tin
Nb3Al	Niobium-Aluminum
HTS	High Temperature Superconductors
BSCCO	Bismuth Strontium Calcium Copper Oxide
YBCO	Yttrium Barium Copper Oxide
EC	Electron Cyclotron
IC	Ion Cyclotron
H-NB	Heating-Neutral Beam
LH	Lower Hybrid
Q	Ratio of output power to input power
WBS	Work Breakdown Structure
CBS	Cost Breakdown Structure
COE	Cost of Electricity
BOP	Balance of Plant
IDC	Interest During Construction
EDC	Escalation During Construction
AFUDC	Allowance for Funds Used During Construction
EMWG	Economic Modeling Working Group
FCR	Fixed Charge Rate
RF	Radio Frequency
SCR	Scheduled Component Replacement
D&D	Decontamination and Decommissioning

PART I

GENERAL CONCEPTS

1

NUCLEAR ENERGY: PAST, PRESENT, AND FUTURE

JAY LEHR

The Heartland Institute, Chicago, IL, USA

Unlike some aspects of nuclear technology, the process of generating electricity in a nuclear power plant is not very complicated. U235, a naturally occurring element, is one of the few materials on Earth that can be forced to undergo fission—its atoms can be forced to split, releasing prodigious amounts of energy. In a nuclear power plant, uranium pellets arranged in rods are collected into bundles and submerged in water. Induced fission heats the water and turns it into steam, which drives a steam turbine, which spins a generator to produce power.

According to Marshall Brain, whose essay "How Nuclear Power Works" appears on the HowStuffWorks Web site (http://science.howstuffworks.com/nuclear-power.htm), "a pound of highly enriched uranium ... is equal to something on the order of a million gallons of gasoline. When you consider that a pound of uranium is smaller than a baseball, and a million gallons of gasoline would fill a cube 50 feet per side (50 feet is as tall as a five-story building), you can get an idea of the amount of energy available in just a little bit of U235." One metric ton of nuclear fuel produces the energy equivalent of two to three million tons of fossil fuel. Due to the abundance of radioactive minerals in the Earth's crust, nuclear power offers what some believe to be a limitless supply of reasonably priced energy, as long as we safely contain the radioactive material.

Reprinted from ENERGY & ENVIRONMENT, VOLUME 21 No. 2 (2010), MULTI-SCIENCE PUBLISHING CO. LTD., 5 Wates Way, Brentwood, Essex CM15 9TB, United Kingdom

1.1 HISTORY

The first experimental nuclear power apparatus was created in 1942 by Enrico Fermi and his graduate students at the University of Chicago. A product of naval propulsion research, nuclear power emerged in the United States as a commercial power option in the 1950s. A Pennsylvania utility, Duquesne Light, built the first commercial nuclear power reactor at Shippingport, Pennsylvania, in 1954. Nuclear power was commercially attractive because it offered the opportunity to generate power without the air pollution that accompanied the burning of fossil fuels. Waste volumes are comparably scaled: Fossil fuel systems generate hundreds of thousands of metric tons of gaseous, particulate, and solid wastes. By contrast, according to the Nuclear Energy Institute (NEI), boiling water nuclear power reactors produce between 50 and 150 metric tons of low-level waste per year, while pressurized water reactors produce between 20 and 75 metric tons. The volume and mass of the waste can be further reduced by 95% by reprocessing the spent rods.

At present, 33 countries around the world host 444 operating commercial nuclear energy-fueled electric generating facilities. Those facilities have cumulatively recorded over 10,000 years of operation. The United States remains the largest single producer of nuclear energy in the world, with 104 plants that supply over 800 billion kilowatt (kW) hours. In 1998, those plants supplied 674 billion kilowatt (kW) hours.

The gains came as a result of improving equipment, procedures, and general efficiency—not a single new

Nuclear Energy Encyclopedia: Science, Technology, and Applications, First Edition (Wiley Series On Energy).
Edited by Steven B. Krivit, Jay H. Lehr, and Thomas B. Kingery.

nuclear plant was built over that period. The increased efficiency and capacity of the nuclear fleet means the industry added the equivalent of 26 new 1,000 MW reactors to the grid. France has the second largest number of nuclear power plants with 59, and three are under construction. Japan now has 55 nuclear power plants, followed by 35 in the United Kingdom. Russia follows with 29, and then Germany with 20. China currently has seven operational plants and 132 more planned by 2020. Approximately 80% of France's electricity demand is met by nuclear energy, while Britain uses nuclear energy to generate 23% of its electricity. Other countries with significant nuclear power include: Spain, 29%; Germany and Finland, 32%; Sweden, 44%; and Belgium, 58%.

1.1.1 Accidents

The first recorded commercial nuclear power plant accident occurred in the United Kingdom at the Windscale power plant on October 10, 1957 when fire destroyed the core of a plutonium producing reactor sending clouds of radioactivity into the atmosphere, while the chemical accident could have caused fatalities, none were ever reported. The 1979 event at Three Mile Island in the United States occurred because faulty instrumentation gave false readings for the reactor environment. That led to a series of equipment failures and human error. As a result, the reactor core was compromised and underwent a partial melt. Radioactive water was released from the core and safely confined within the containment building structure. Very little radiation was released into the environment, and no health impacts were recorded.

The Three Mile Island incident underscores the relative safety of nuclear power plants. The facility's safety devices worked as designed, preventing injury to humans, animals, or the environment. The accident resulted in improved procedures, instrumentation, and safety systems, meaning nuclear reactor power plants in the United States today are substantially safer than they were in the past. Three Mile Island's Unit One continues to operate with an impeccable record.

The worst nuclear power plant disaster in history occurred when the Chernobyl reactor in the Ukraine experienced a heat (not nuclear) explosion. If such an explosion were to have occurred in a Western nuclear power plant, the explosion would have been safely contained. All Western plants are required to have a containment building: a solid structure of steel-reinforced concrete that encapsulates the nuclear reactor vessel. The Chernobyl plant did not have this fundamental safety structure. The explosion blew the top off of the reactor building, spewing radiation and reactor core pieces into the air. The graphite reactor burned ferociously—which would not have happened if the facility had a containment building from which oxygen could be excluded. The design of the Chernobyl plant was inferior in other ways as well.

Unlike the Chernobyl reactor, Western power plant nuclear reactors are designed to have negative power coefficients of reactivity that make such runaway accidents impossible: When control of the reaction is lost, the reaction slows down rather than speeds up. The flawed Chernobyl nuclear power plant would never have been licensed to operate in the United States or any other Western country. The accident that occurred at Chernobyl could not occur elsewhere. The circumstances surrounding the Chernobyl accident were in many ways the worst possible, with an exposed reactor core and an open building. Thirty-one plant workers and firemen died directly from radiation exposure as a result of the Chernobyl accident.

1.2 RADIATION

In September 2000, the United Nations Scientific Committee on the Effects of Atomic Radiation (UNSCEAR) published its Report to the General Assembly with Scientific Annexes, a document of some 1,220 pages in two volumes. According to the UNSCEAR report and subsequent discussions, roughly 1,800 thyroid cancer cases in children and some adults might reasonably be attributed to radiation exposure after the Chernobyl incident. More than 99% of those cancers were cured. Beyond the thyroid cancers, reported UNSCEAR, there is no evidence of any major public health impact attributable to radiation exposure after the Chernobyl accident.

In countries that do not reprocess their spent nuclear fuel, of which the United States is the primary one, the nuclear waste disposal is a political problem because of widespread fears disproportionate to the risk reality. Waste disposal is not an engineering problem because the United Kingdom and most other countries manage their small volume with relative ease. But in the United States, spent nuclear fuel and high-level radioactive waste have been accumulating for nearly 60 years, when nuclear materials were first used to produce electricity and to develop nuclear weapons.

Nuclear fuel has been used in 104 nuclear power plants in the United States and nearly 200 of that nation's nuclear naval vessels. As in the United Kingdom, the fuel is solid, in the form of ceramic/uranium pellets the size of a pencil eraser. After a few years in a reactor, the uranium pellets in the fuel assembly are no longer efficient for producing electricity. At this point the used, or "spent," fuel assembly is removed from the reactor and placed in a pool of water to cool.

1.3 WASTE AND REPROCESSING

In most other countries where nuclear power is generated, these fuel rods are chemically reprocessed for additional

use. In the United States, however, President Jimmy Carter outlawed this procedure in 1977 as a result of his incorrect assessment that some weapons grade plutonium was created in the process. Although President Ronald Reagan rescinded Carter's executive order, no power plants in the nation have initiated such a recycling program. Thus, without a central disposal site, 60 years of nuclear waste remains in on-site water pools or sealed above-ground in metal canisters within concrete bunkers. U.S. waste that was planned for disposal at the Yucca Mountain storage facility in Nevada resides instead in temporary storage at 121 sites in 39 states. After decades of scientific study, it is clear no legitimate safety issues preclude opening Yucca Mountain for the storage of spent nuclear fuel. Few scientists question the safety of the site, which has been studied for nearly two decades, while few who oppose nuclear power will ever accept any site. For the time being, U.S. President Barack Obama has announced that no work will go forward on the completion of Yucca Mountain as the nation's nuclear waste repository during his term in office.

1.3.1 Recycling Opportunities

If U.S. nuclear power plants were to begin reprocessing spent nuclear fuel, as is done in the United Kingdom, France, and other nations, only 2 to 3% of the material now scheduled to be stored at the Yucca Mountain nuclear repository would have to be stored there, and the whole nuclear waste problem would disappear. After reprocessing, the total unusable portion of three full years of nuclear power production can be stored indefinitely in a dry cask about four times the size of a telephone booth.

The stated rationale, mentioned above, for not reprocessing spent nuclear fuel is the concern that reprocessing nuclear fuel produces weapons-grade plutonium that could, in theory, be smuggled to undesirable entities. What is not commonly recognized, however, is that the plutonium in spent fuel rods is not weapons-grade material. It consists of four different isotopes, which essentially pollute the plutonium necessary to make nuclear weapons.

After the collapse of the Soviet Union, Senators Pete Domenici (R-NM) and Sam Nunn (D-GA) negotiated a remarkable deal with the Russian government under which the U.S. purchases enriched uranium from its stockpile of disassembled weapons and recycles it through U.S. power plants as fuel. As a result, one of every 10 light bulbs in America is now lit by a former Soviet weapon, because 20% of U.S. electricity is produced by nuclear power, and half of the fuel is Russian. The important thing to remember is that the technology currently exists and is being utilized in other countries to virtually eliminate nuclear waste through the reprocessing of spent nuclear fuel. Reprocessing will become more efficient and economical as technology continues to advance. Thus, it is entirely possible, utilizing existing technology, to produce nuclear power without spreading any dangerous chemicals or materials into the environment. But even in the United States, all the high-level by-products from 50 years of nuclear fission could be assembled 10 feet high on a single football field. The French store all their high-grade waste from 30 years of providing nearly 80% of their nation's electricity under a single room in Cap la Hague.

1.4 SAFETY RECORD

It is remarkable that the combination of human fallibility and mechanical failure over the last 40 years has resulted in a nuclear safety record unsurpassed by any other industrial activity. Commercial nuclear electricity has killed zero members of the public over that period. Conventional electric plants powered by coal, oil, and natural gas produce more than 200 accidental deaths per year.

Nuclear power plants also roam the world daily without any significant problems. Every week, one or two nuclear power plants dock at a major port in America or somewhere else in the world. And these power plants have been doing so for half a century now. No accidents of any kind have ever marred these dockings, no leaks have cleared blocks of cities; no emergencies have been declared. It is indeed amazing how thoroughly the United States has lost sight of the fabulous fleet of nuclear submarines that have operated below the radar these past 50 years, since the Nautilus, the first nuclear powered submarine, was launched in 1954. Since then, the U.S. Navy has launched more than 200 nuclear-powered ships, of which 82 are currently in operation. Nuclear ships from all countries are welcomed into 150 ports in 50 countries. They have traveled nearly 150 million miles without a serious incident. Navy reactors have twice the operational hours of our civilian systems. This is a long record of safety, an achievement the public needs to understand.

1.5 THE FUTURE OF NUCLEAR PLANTS

There is no denying that escalating costs of nuclear power plants will impede some growth in their industry. A 2008 study by Synapse Energy Economics, Inc., titled *Nuclear Power Plant Construction Costs* by David Schissel and Bruce Blewald, shows that costs have risen in the past decade from a range of $2 to $4 billion to a range today between $6 and $9 billion, well above coal and natural gas plants. A new generation of nuclear power plants may one day use an innovative technique called the pebble bed modular reactor. This reactor encases the nuclear source material in ceramic spheres about the size of tennis balls and transfers the heat into helium gas, which creates enough

pressure to turn a turbine. The heat generated rises to about 900 degrees centigrade (it would take nearly 3000 degrees to actually melt the ceramic and release any radioactivity). Concurrently, the medium of helium dramatically reduces any potential impact on the environment, were a release to occur. Their costs are expected to be considerably less as a result of the inherent safety features, which also may reduce remaining unwarranted fears held by the public.

On the other hand, if we compare nuclear costs to renewable power such as wind and solar, nuclear is far less expensive, partly because a 1000 megawatt (mW) plant can be built on 200 acres, while an equal amount of wind and solar energy require more than 100 square miles of land area. Barry Brooks, at Web site bravenew climate.com/2009/12/06/tcase7, calculated the quantities of cement, steel, and land required for equivalent solar and nuclear power plants. He found that a solar plant requires 15 times more concrete, 75 times more steel, and 2,530 times more land.

Communications experts say that fear is the best way to get attention when you're trying to win an argument. Groups who oppose nuclear power have certainly mastered that technique by playing to economic, environmental, and safety fears. Perhaps North America should fear that it is falling behind in advancing nuclear power. As a result, North America may be unable to compete with countries that have cheap, clean, reliable nuclear power while they are stuck with a bunch of windmills and solar farms producing expensive, unreliable energy or, more likely, not much energy at all. The prospect of North America ignoring this problem-solving technology that was invented there is unfortunate. In January 2006, U.S. Senator Lamarr Alexander of Tennessee said the Chinese sent a delegation of nuclear scientists and administrators to the UnitedStates on a fact-finding mission. They toured the Idaho National Laboratory, the Argonne National Laboratory, and visited GE and Westinghouse trying to decide which technology to choose for their nuclear program. Perhaps, surprisingly, while the United States hasn't issued a construction permit to build a new reactor in the past 30 years, most countries still look to it for leadership in this technology. The Chinese eventually chose Westinghouse technology for their first reactors. At the time, Westinghouse was an American company. In 2007, Toshiba bought Westinghouse, so it is now a Japanese company. By 2008, the Chinese had shovels in the ground. The first four Westinghouse reactors are scheduled for completion by 2011. They also bought a pair of Russian reactors, which should be finished around the same time. They started talking about building 60 reactors over the next 20 years and just recently raised it to 132. They're in the nuclear business.

What the United States accomplished in the meantime? Senator Alexander says that people have been talking about a "nuclear renaissance." Finally, in 2007, NRG, a New Jersey company, filed the first application to build a new reactor in 30 years. The licensing process at the U.S. Nuclear Regulatory Commission will take five years, after which opponents will file lawsuits and the whole thing will move to the courts. If they're lucky, they might have a reactor up and running by 2020. Other companies have followed suit, and there are now 34 proposals before the NRC, but nobody has yet broken ground. So it isn't likely the Chinese will be coming to us any time soon for more tips on how to build reactors.

Of the 34 proposals before the Nuclear Regulatory Commission, 20 are designed by Westinghouse, now a Japanese company, and nine are from Areva, the French giant.

General Electric, the only American company left on the field, has partnered with Hitachi. They sold five reactors to U.S. utilities but fared poorly in the competition for federal loan guarantees. Two utilities have now cancelled those projects, and there are rumors that GE may quit the field entirely. GE doesn't seem very enthusiastic about nuclear anyway. In the United States, we see GE ads for windmills. They're all over the place. They have an ad for the smart grid, where the little girl says, "The sun is still shining in Arizona." That was pretty good, too. But you won't see any GE ads, in this day of concern about climate change, that 70% of our carbon-free electricity comes from nuclear power. I certainly haven't. It is now completely absurd that so many groups have poisoned the minds of so much of the world against the cheapest, most abundant, and safest form of energy on the planet. Those of us who know better must begin a strong and enduring battle against these forces because our success will improve the plight of the least fortunate, poorest fed, clothed, sheltered, and educated on this planet. As energy goes, so goes the ultimate health of nations. Nuclear energy can solve the world's energy problems, but only if those who know this have the courage to do battle against those who stand in opposition for whatever reason they perceive.

2

BENEFITS AND ROLE OF NUCLEAR POWER

PATRICK MOORE

Greenspirit Strategies Ltd., Vancouver, BC, Canada

Nuclear energy supplies approximately 16% of the world's electricity, a percentage similar to hydroelectric power. Among the 30 countries with nuclear power plants, 21 countries obtain 15% or more of their electricity from nuclear energy, ranging from Canada at 15% to France at nearly 80%. In the United States, about 20% of electricity is produced by 104 nuclear plants, nearly one-quarter of the world's nuclear power.

The 439 nuclear plants operating in 31 countries today are producing clean, reliable, reasonably priced electricity for hundreds of millions of people. And yet nuclear energy remains the most controversial form of power, so much so that some countries and regions have passed laws against it, either pledging to phase it out altogether or placing bans on further development.

Nevertheless, there is a powerful sea change underway, bringing nuclear energy back into favor. This evolution in public opinion and government policy has come about very rapidly, largely due to the convergence of a number of factors, primarily the concerns over global climate change, the urge by many Western governments to reduce their reliance on Middle Eastern and Russian energy sources, and air pollution from fossil fuels. The result has been what is now referred to as a "Nuclear Renaissance."

Nuclear energy came by its controversial reputation honestly. Two atomic bombs killed nearly a quarter of a million people on August 6 and August 9, 1945, in Hiroshima and Nagasaki. This was our first experience with nuclear technology on a grand scale. As a result, a deep fear was indelibly impressed into the human conscience.

In the wake of World War II, the arms race began with the United States, the Soviet Union, and then Britain and France engaging in atmospheric nuclear testing and a build-up of nuclear weapons to be delivered by bombers and missiles. Through the 1960s and 1970s the world lived in constant fear that there would be an all-out nuclear war. In 1953, U.S. President Dwight Eisenhower and Secretary of State John Foster Dulles announced the "Atoms for Peace" program to use nuclear fission to produce energy rather than bombs.[1]

Many people, having been made cynical by the Cold War rhetoric and eventually by the advent of the Vietnam War, saw that as a cover for the continued buildup of weapons. Much public attention was turned toward ever-increasing arms production, more missiles, multiple warheads, and submarines so deadly that one of them could wipe out an entire nation.

Meanwhile, the United States and many other countries embarked on programs to build nuclear reactors for the production of electricity. Most of the 439 reactors operating around the world today were built during the 1960s, 1970s, and into the 1980s. During those early years of the nuclear energy industry, there was an optimistic outlook, and it seemed that nuclear power would sweep the nation and the world.

2.1 THREE MILE ISLAND

That all changed at 4.00 AM on March 28, 1979 when Reactor 2 on Three Mile Island site in Harrisburg, Pennsylvania, had a loss of coolant accident, causing a reactor core meltdown and a wave of fear that spread across the country. It didn't help that the Oscar-winning

Nuclear Energy Encyclopedia: Science, Technology, and Applications, First Edition (Wiley Series On Energy).
Edited by Steven B. Krivit, Jay H. Lehr, and Thomas B. Kingery.

film *The China Syndrome*, starring Jane Fonda and Jack Lemmon, had been released into theaters only two months before the accident. In the film, which was enormously popular, a nuclear plant accident involving a meltdown of the reactor core threatened the world with destruction. The Three Mile Island accident was eerily similar, as if fiction had suddenly turned into reality. For days the news was dominated by the unfolding events in Harrisburg.

But the containment structure around the reactor, five feet of steel and heavily reinforced concrete, did its job and prevented the radioactive material in the core from escaping into the environment.

In the aftermath of the accident there were many follow-up health studies focused on the people living near the reactor. In the end it was determined that there was no negative impact to the public or the workers in the plant.[2]

In many ways, the accident at Three Mile Island turned out to be a success story. It was a major mechanical failure but no one was injured, never mind killed. And it was a wake-up call for the nuclear industry, not just in the United States, but in all Western countries that had reactors. All the safety systems and operating procedures were reviewed and strengthened to make sure such an accident would not be repeated in America. At the time of this writing, Japan is going through a similar process with its Fukushima plant following a devastating earthquake and tsunami.

2.2 CHERNOBYL

Unfortunately, the Soviet Union was still behind the Iron Curtain in 1979, and the lessons learned from Three Mile Island accident had no effect on its nuclear program. Years earlier, the Soviet Union began building reactors around the country for power production. The government took a short cut and simply copied the design of its nuclear weapons production reactors, failing to include a containment structure and not providing adequate safety systems. It was like putting a nuclear reactor in a warehouse. The RMBK class of Soviet reactors were an accident waiting to happen. And it did.

There were four identical reactors at the Chernobyl nuclear complex. In 1986 a group of engineers were assigned to do a test on Unit 4, which had the best operating record in the group. Ironically, the test was designed to improve the safety of the reactors.

When the test went horribly wrong and the operators contravened basic safety procedures, the reactor blew up, breaking through the roof and spewing the contents of the core downwind over the Ukraine, Belarus, and on to Sweden. There, at a Swedish nuclear reactor, alarms went off indicating elevated radiation levels. At first, the operators thought there was a radiation leak at their reactor. It was not until three days later that the Soviets finally admitted there had been an accident at Chernobyl.

In many ways, Chernobyl was symptomatic of everything that was wrong with the Communist system: secrecy, central control, shoddy engineering, lack of concern for human life, and blind obedience to authority in the face of extermination.

It took a week to put out the fire, which was made very difficult due to the huge graphite moderator in the reactor core. Graphite is pure carbon, and when it catches fire, it is extremely difficult to extinguish. Thirty-four people died of radiation and burns in the effort to stop the flames that continued to spread radiation into the atmosphere. When the fire was finally put out, the world was faced with the fact that a large area downwind from the reactor had been contaminated with strontium 90, cesium 137, iodine 131, and other fission products.

After the accident, the Iron Curtain was opened briefly as the Soviets sought help from nuclear scientists in the West. They helped to modify the other RMBK reactors' safety systems and operating procedures so such a situation could not be repeated. It has not, even though the other three reactors at the Chernobyl site continued to operate for 14 years after the accident. Even today there are 11 RMBK class reactors operating, 10 in Russia and one in Lithuania. They will eventually be shut down and replaced with reactors that have proper safety systems.

The Chernobyl accident was quickly adopted by the anti-nuclear movement in the West as proof that nuclear energy should be rejected and that all existing reactors should be closed. Just as the Cold War was coming to an end, this became a new cause to replace the campaign against the buildup of nuclear weapons. In a way, nuclear energy simply replaced nuclear weapons as the cause of the day. Far-fetched proclamations by the Greens in Europe claimed that 300,000 people had died in the aftermath of Chernobyl. To this day Greenpeace claims over 90,000 deaths.[3]

In the wake of the accident, the United Nations established the Chernobyl Forum, an investigative body that involved seven UN agencies, including the World Health Organization, the UN Environment Program, and the International Atomic Energy Agency. In 2006, 20 years later, the Forum published its findings on the impact of the accident. Two facts stand out. First, they concluded that only 56 deaths, including the 34 who died fighting the fire, could be directly attributed to the accident. Second, they acknowledged that the worst effect of the accident was the forced evacuation of 330,000 people from the contaminated zone into tenement blocks on the outskirts of Kiev. The incidence of suicide, drug and alcohol addiction, marriage breakdown, and mental illness far outweighed the possible effects of the slightly increased radiation exposure they would have experienced if they had been left in their country homes. The evacuation was ordered with the best

of intentions, but it would have been better if most of the people had been allowed to stay in their own communities.[4]

Despite the unfortunate fact that injury and death were caused at Chernobyl, nuclear energy is still one of the safest technologies we have invented. Every industry, whether it is construction, farming, steel production, forestry, financial services, transportation, energy production, or mining, has risks associated with it. For the amount of power it produces and the number of people involved in its operations, the nuclear industry is a very safe place to work.

In 2008, workers in the U.S. nuclear industry experienced an accident rate of 0.13 accidents per 200,000 worker-hours. The accident rate for all manufacturing industries combined in the United States was 3.5 per 200,000 worker-hours, 27 times higher than for the nuclear industry.[5]

U.S. Bureau of Labor Statistics confirms that it is safer to work in a nuclear plant than it is to work in either real estate or financial services.[6] A study of 54,000 nuclear workers conducted by Columbia University in New York and published in 2004 found that they had significantly fewer cancers, less disease, and lived longer than their counterparts in the general population.[7]

2.3 PROLIFERATION

Then there is the charge that nuclear power plants increase the risk of nuclear weapons proliferation. This is a more serious issue than safety or terrorism and deserves careful analysis.

For many people who were active in the early years of the environmental movement, this was the real deal-breaker, the association of nuclear energy with nuclear weapons. And here is where many activists made a big mistake.

It is important to note that no nuclear weapon has been manufactured using the plutonium produced in a civilian power reactor. The nuclear weapons states all have dedicated military or research reactors for producing plutonium, which is extracted from used nuclear fuel. It is certainly possible to extract plutonium from the used fuel from civilian power reactors.

This is the first question to consider for people who are concerned that civilian reactors increase the threat of proliferation: If all 439 power reactors are shut down, would that convince the generals and the military to shut down their weapons-producing reactors? It is those reactors that merit concerns and should be considered for decommissioning.

The argument about shutting down civilian power plants becomes weaker still in consideration of the fact that one does not need a nuclear power plant to build a nuclear weapon. In fact, it is much easier to enrich uranium to weapons-grade material with centrifuge technology than it is to extract plutonium from used nuclear fuel. The concern over Iran's nuclear program is primarily due to the fact that it has the centrifuges that are capable of enriching uranium to weapons-grade material. These same centrifuges can be used to produce the far less enriched uranium for fueling a nuclear reactor. This is why the strong international inspection program provided by the International Atomic Energy Agency is crucial.

The simple answer to the question about the rogue states is that shutting down all the nuclear plants in the world would not reduce the threat of leaders, deranged or otherwise, who want to obtain nuclear weaponry. These situations can only be dealt with by political and possibly military means. Turning off a major portion of the world's cleanest electricity would unlikely sway a rogue leader from his determination to build nuclear weapons and developing the means to deliver them.

Since the discovery of fire, it has always been the case that many of our most important tools and technologies can be used for destructive purposes. And many of our most useful and beneficial technologies were originally invented as weapons of war and only later adopted for non-military means. It does not follow that we should outlaw the beneficial uses of a technology simply because it can also be used for destructive or evil purposes. For example, nuclear medicine is used to diagnose and treat millions of people every year, using radioactive materials that are produced in nuclear reactors.

2.4 USED FUEL VS. "NUCLEAR WASTE"

The fuel that originally goes into a typical nuclear reactor is pure uranium. During the nuclear reaction process, part of the uranium is burned, splitting it in two and releasing vast amounts of energy that is used to make steam to run turbines to produce electricity. The results of splitting uranium are called *fission products*.

Uranium splits in many ways, so the fission products are a mixture of many different isotopes, some which decay in less than a second and others that remain radioactive for a few centuries. Most of the used fuel is unburned uranium, and another portion of it is uranium that has been converted, as a result of the nuclear reaction, into plutonium and other heavy elements such as americium and californium.

The fission products such as isotopes of cesium 137, and strontium 90, and iodine 131, are the main components of used fuel that have no useful purpose at the present time and are typically categorized as "waste." These fission products are biologically active and must not be ingested. They must be isolated from the environment until they decay into non-radioactive elements in order to avoid serious health and environmental consequences.

Fortunately, the longest lived fission products of concern decay into non-radioactive elements in about 300 years.

This may seem like a long time, but in reality it is not difficult to design containers, and facilities in which to store those containers, that will be secure for much longer than 300 years.

The good news is that the majority of the used fuel, the uranium and plutonium in particular, can be recycled and made into new nuclear fuel. Used nuclear fuel contains at least 95% of the energy capacity that was in the original fuel. In other words, only about 5% of the energy is extracted from the nuclear fuel in its first cycle through the reactor. It makes no sense to call used fuel "waste" when 95% of it can be reused. Used nuclear fuel is actually one of our most important future energy resources. And even if the original uranium was imported from another country, used fuel can now become a domestic energy resource, thus reducing concerns about energy security.

2.5 RECYCLING USED NUCLEAR FUEL

In the same way that nuclear fission, originally harnessed for weapons, is now used to make energy, we can use recycling technology for the peaceful purpose of producing even more energy rather than making bombs. When critics state that nuclear waste will remain radioactive for millions of years, they are referring to the uranium and the plutonium reaction products, both of which can be used again as fuel and subsequently converted into fission products that have much shorter lives.

This is only one of the benefits of recycling used fuel. Another, of course, is the fact that the uranium that was mined in the first place is now able to produce about 20 times as much energy than merely from a single burn cycle. And not only are the fission products from recycled nuclear fuel much shorter-lived than the uranium and plutonium that was first produced, but there is now much less waste to dispose of because most of the used fuel is recycled.

One of the central principles of the environmental movement is the concept of "reduce, reuse, and recycle" the materials we employ to make goods and energy. The recycling of used nuclear fuel fits squarely into this concept and is therefore a logical, environmentally correct approach to managing nuclear material.

A number of countries are already recycling some of their used nuclear fuel. Of the 290,000 tonnes of used fuel that has been produced over 50 years, about 90,000 tonnes have already been recycled.

Recycling used fuel requires a specialized facility. Given the substantial costs of these facilities and the advanced technology required to run them, it is likely that only a few countries will maintain the capability to build and operate large, centralized recycling centers for used fuel. Countries or jurisdictions without this recycling capability transport their used fuel to these centralized facilities for recycling.

France is in the forefront of this technology with a large recycling facility at Cap la Hague in Normandy that is capable of recycling 1,700 tonnes per year. Once recycled, the fuel can once again be used in reactors that have been appropriately modified. Of France's 59 nuclear power stations, 22 have been modified to burn recycled fuel. Russia, the United Kingdom, and India also have recycling facilities. Japan has recently completed a US$30 billion nuclear fuel fabrication and recycling facility at Rokkasho north of Tokyo. It is modeled on the French technology but with improvements that make it much less susceptible to the risk of proliferation because pure plutonium is never removed from the facility—deep inside the recycling plant, plutonium is mixed with uranium to create mixed oxide fuel (MOX), which cannot be used to make a nuclear weapon. Under the U.S.-Japan Agreement for Cooperation Concerning Peaceful Uses of Nuclear Energy, the United States had to approve of the construction of the recycling plant in Japan. Recycling used nuclear fuel is a very complex subject that cannot be treated in depth here. For those who wish to dig deeper, I suggest beginning with the World Nuclear Association's detailed explanation of the topic.[8]

It is ironic that while the United States is the largest producer of nuclear energy, with 104 of the world's 339 nuclear plants, it does not recycle any of its used nuclear fuel at this time. During the 1960s and 1970s, three recycling plants were built to produce recycled fuel. One, at West Valley, New York, operated successfully from 1966 until 1972. It was shut down when regulations were brought in that made it uneconomical. Another, at Morris, Illinois, incorporated a new technology and did not perform satisfactorily. A third large plant was built at Barnwell, South Carolina, but never operated because the U.S. government changed its policy in 1977 to rule out all civilian recycling technology.

Again, ironically, the policy did not ban the military use of the technology to make weapons-grade plutonium, even though the ban on civilian recycling was rationalized in terms of preventing nuclear weapons proliferation. This ended U.S. attempts to enter the used fuel recycling business. The apparent reason for this will be explained later in this chapter. There is a common misconception that "nuclear waste" is prone to leak out and contaminate the environment. As in the Simpsons cartoon, it is depicted as a yellowish-green corrosive liquid that is roiling around in its container trying to eat its way out. In fact, used nuclear fuel is stored in solid pellets that are not at all corrosive and are securely contained in steel and concrete casks that are built to last for hundreds of years.

The used nuclear fuel that is being stored safely and securely at nuclear reactors around the world will certainly be recycled eventually. One of the reasons it is not all being recycled now is that new uranium is cheaper than recycled

fuel. There is no economic motivation to recycle the used fuel. It can be stored for decades or even centuries without difficulty before it is recycled.

In a typical reactor, one-third of the fuel is removed and fresh fuel added every two years. At this stage, the used fuel is very radioactive and hot and must be cooled to prevent it from melting. This is managed by placing the fuel in a large pool of water outside and adjacent to the reactor. Water is also a very good radiation shield. A person can stand safely for hours above the pool looking directly at the used fuel under six feet of water and not be exposed to harmful levels of radiation. After five to ten years, the fuel has cooled sufficiently that it can be removed from the pool. At this time it can be placed in "dry casks" (they are called "dry casks" because the fuel has been taken out of the water; really, they are just casks made from concrete and steel). These casks have been designed to withstand the most severe imaginable impact by trains, planes, and large trucks.

Because the United States has not established either a recycling program or a long-term waste repository, the used fuel is still stored at the nuclear reactor sites. At some reactors that have been operating for 30 to 40 years, the pools have become full, and the older used fuel is being transferred to dry casks where it is stored on site on concrete pads with secure perimeters. The Nuclear Regulatory Commission has stated the dry casks are capable of containing the used fuel for 120 years, stored outdoors in the weather.[9] This is certainly a very conservative estimate. And if the dry casks were in a building in a controlled climate, they would be secure for 1000 years or longer because they would not be subject to weathering.

All the used fuel produced in U.S. reactors over the past 50 years would fit on a football field stacked 22 feet high. If the used fuel were recycled (we are still in the first cycle from past 50 years), the fission products, the actual "waste," would cover a football field about nine inches in depth. Available technology is more than capable of securely storing this relatively small amount of material until it decays into non-radioactive elements. The United States would demonstrate responsible environmental leadership by joining the other countries that are continuing to improve recycling technology and making use of this most valuable source of energy.

The fact that new uranium is less expensive than recycled used fuel has stopped neither France, Japan, the United Kingdom. nor Russia from moving forward with the technology. One reason for this is that the nuclear industry in these countries is, or has traditionally been, state owned. State-owned corporations do not operate in the free market as is largely the case in the United States. If the French government wants to develop recycling technology, it simply makes the decision to do it and provides the necessary funding. In the United States, the fact that it is less expensive to buy new uranium will cause the private companies that own nuclear plants to choose new uranium. Therefore, the only way that the U.S. nuclear industry will consider investing in recycling is if the government provides sufficient incentives or funding to make it financially attractive.

There are two reasons for the U.S. government to create an environment in which recycling is encouraged. First, unless you are engaged in developing the technology, you can't be a part of the international dialogue about it, you can't work to improve the technology to make it more efficient, and you can't be effective in improving security at an international level to prevent used fuel and its by-products from falling into the wrong hands.

Second, recycling used nuclear fuel is obviously the right thing to do in order to make use of the energy in it, to reduce the volume of waste and the time it takes to decay, and to live up to the principle of reuse, recycle, and reduce. In many cases, it costs more to make new glass and paper than it does to recycle these materials. But we recycle them anyway because it is believed that this is a superior approach from the perspective of sustainability. Recycling used nuclear fuel is simply another way to be better stewards of our planet.

2.6 THE NEXT GENERATION OF REACTORS

Research and development programs are now under way in many countries to design and eventually build the next generation of nuclear reactors. Perhaps the two most important of these new designs are high-temperature gas-cooled reactors and fast neutron reactors, including those called breeder reactors.

Nearly all the "conventional" reactors operating around the world are based on water-cooled low-temperature technology. They are relatively inefficient at converting heat to electricity, and they can't produce steam that is hot enough for most industrial processes. Very high-temperature gas-cooled reactors are much more efficient, produce high-temperature steam that can be used in place of steam produced by fossil fuels, and can produce hydrogen directly by splitting water through a thermo-chemical process. They will be capable of replacing fossil fuel energy in oil refineries, paper mills, chemical plants, and many other industries. They can also be used to desalinate water for domestic, irrigation, and industrial use. China, South Africa, and the United States are leading in this technology.

Fast neutron reactors will be necessary to carry out the complete recycling of used nuclear fuel. Conventional reactors can be used for the first stages of recycling but cannot finish the job. Most importantly, fast reactors can burn a number of by-products from conventional reactors

that they cannot burn, thus making nuclear waste shorter-lived and easier to handle. Fast reactors can also be used to desalinate water. A number of fast breeder reactors have been built and operated. The Russian BN-350 fast reactor ran from 1964 to 1999, producing 135 megawatts of electricity and 16 million gallons of water per day to the town of Altau on the Caspian Sea. Fast reactors are now operating in France, Japan, Russia, and India. Fast reactors are currently under construction in Russia, China, Japan, and India. The United States operated a fast reactor at Hanford, Washington, from 1982 until 1992. It was shut down when the Department of Energy decided there was no further use for it, a decision that many people in the nuclear industry felt was unwise. As a result, the United States is trailing a number of other countries in this fast breeder reactor technology.

Breeder reactors are fast neutron reactors that produce more fuel than they consume. With this technology it is also possible to burn all the uranium 238, thus extracting the maximum amount of energy from nuclear fuel. This will ensure a supply of nuclear fuel that will last for thousands of years.

Another interesting development is the renewed emphasis on small reactors, ranging in size from under 50 megawatts up to 300 megawatts, for electricity, hydrogen, industrial heat, and desalination. Small reactors are not new, but in the past most of them were in either research or military applications. The reactors that power nuclear submarines, aircraft carriers, and icebreakers are in this category. Small reactors are especially applicable in remote areas that are off the electric grid and on islands where the alternative is often diesel generators. Four small reactors are already operating in a remote corner of Siberia that produce steam for district heating and 11 megawatts of electricity each. They have performed well since 1976, much more cheaply than fossil fuel alternatives in the Arctic region.

Russia is developing both 35 megawatt and 200 megawatt floating reactors on self-propelled barges to service remote industries such as oil and gas and mining in Siberia. In addition, Argentina, Japan, Korea, South Africa, and the United States are all in advanced development of various types and configurations of small reactors.[10]

2.7 SWORDS TO PLOWSHARES

There are many positive activities and trends toward turning nuclear weapons programs and materials toward peaceful purposes. One of the first of these involved South Africa.

During the 1970s and 1980s, while the apartheid regime was still in power, South Africa mined uranium, enriched it, and produced six nuclear warheads as a deterrent against invasion. As preparations were made in the early 1990s for the post-apartheid democratically elected government, these weapons were dismantled. South Africa had become the first nuclear weapons state to voluntarily give up nuclear arms.

South Africa had already built two nuclear reactors near Capetown by 1985, both of which are operating today. They had nothing to do with the nuclear weapons program. When the nuclear bombs were dismantled, the highly enriched uranium was stockpiled for the purpose of making medical isotopes for nuclear medicine.

One of the most important medical isotopes, technetium 99m, is produced by bombarding enriched uranium with neutrons from a nuclear reactor, thus producing molybdenum 99, which has a half-life of only 66 hours. The molybdenum is then delivered to hospitals around the world where it then decays into technetium 99m. Technetium is used for over 20 million diagnoses every year, providing the best possible images of the brain, kidneys, liver, lungs, skeleton, blood, and tumors. Eighty-five percent of all nuclear diagnostic imaging is done with this isotope. South Africa is now one of the top three producers of medical isotopes in the world.

Beginning with the first Strategic Arms Limitation Treaty between the United States and the Soviet Union in 1972, the number of nuclear weapons actively deployed in the world has been reduced from 65,000 to just over 20,000, only about 8,000 of which remain in active operation.[11] While this is still more than enough to destroy our civilization, it is certainly a move in the direction of the peaceful application of atomic energy. And while these weapons are a great threat to our future, the uranium and plutonium from the thousands of dismantled warheads offers great potential for application toward the future of clean energy.

The major nuclear powers, the United States, Russia, the United Kingdom, and France, now have great stockpiles of plutonium and highly enriched uranium that is surplus to their nuclear weapons programs. All of this can eventually be used as fuel to produce nuclear energy. The supply is immense, especially considering the much larger stockpiles of depleted uranium that resulted from the enrichment of uranium for bombs. The most common application of depleted uranium is for armored vehicles and tanks and for bullets and shells. It is harder than steel and heavier than lead, so it performs both those military uses well. Alternatively, this depleted uranium could be burned as fuel in fast reactors to power our world.

The most significant example of nuclear swords to plowshares today is the fact that 50% of U.S. nuclear energy is now fueled with uranium from dismantled Russian warheads. Yes, fully 10% of all U.S. electricity is derived from bombs that have been taken apart under disarmament agreements. In 1993 the United States and Russia signed a 20-year agreement for 500 tons of Russian highly enriched uranium (90+% U235) to be downblended to reactor-grade

uranium (4-5% U235) and shipped to the United States for nuclear fuel. As of June 2009, 367 tons of weapons-grade uranium had been converted into 10,621 tons of reactor fuel. This is by far the largest effort to convert nuclear weapons to peaceful purposes.[12] Russia has announced it will not renew the contract when it expires in 2013, presumably because it wants to use it in the 50 new reactors that have been announced as their objective.

2.8 A NUCLEAR RENAISSANCE

In addition to the 439 operating nuclear reactors in 31 countries that provide 15% of the world's electricity, 40 new reactors are under construction. These are mainly in Asia, where China has 18 and India has five reactors under construction. Russia is now building 11 reactors, and others are under way in Finland, Slovakia, Korea, Romania, Japan, Argentina, France, Bulgaria, and Iran. Canada has announced it will build four to eight new reactors in the province of Ontario, which already produces 50% of its electricity from nuclear energy.

There are proposals for new plants in the Canadian provinces of Alberta, Saskatchewan, and New Brunswick as well. In all, there are about 100 committed plans for new reactors beyond those already under construction and proposals for about 250 additional plants. As of late 2009, there were 30 plants in the planning stages in the United States, with 20 of those already in the process of obtaining licenses to build and operate through the Nuclear Regulatory Commission. Most of these are planned for existing nuclear sites where public opinion is strongly in favor of the new plants.

The number of operating reactors may well double in the next 30 to 40 years. This truly is a nuclear renaissance of global proportions.

Endnotes

1. The entire speech can be found at: http://www.iaea.org/About/history_speech.html.
2. http://www.nrc.gov/reading-rm/doc-collections/fact-sheets/3mile-isle.html.
3. http://www.greenpeace.org/international/news/chernobyl-deaths-180406.
4. http://www.who.int/ionizing_radiation/chernobyl/en/.
5. http://www.nei.org/resourcesandstats/documentlibrary/safetyandsecurity/reports/wanoperformanceindicators_08.
6. http://www.nei.org/newsandevents/newsreleases/safetyindicators/.
7. "Analysis of the Mortality Experience Amongst U.S. Nuclear Power Industry Workers After Chronic Low-Dose Exposure to Ionizing Radiation," Radiation Research, November, 2004 (Rad Res 162, 517–526, 2004).
8. http://www.world-nuclear.org/info/inf69.html.
9. www.nei.org/filefolder/Safely_Managing_Used_Nuclear_Fuel_0109.pdf.
10. http://www.world-nuclear.org/info/inf33.html.
11. http://www.ploughshares.org/news-analysis/world-nuclear-stockpile-report.
12. http://nuclearthreatinitiative.org/e_research/cnwm/reducing/heudeal.asp.

3

EARLY HISTORY OF NUCLEAR ENERGY

ROGER TILBROOK

Argonne National Laboratory (Retired), Argonne, IL, USA

Although the peaceful uses of nuclear energy include electricity generation and contributions to the medical, manufacturing, and industrial sectors of the economy, the accelerated development of nuclear energy was clearly rooted in World War II. Although the nuclear age was conceived by 19th-century physicists, it was delivered by the 20th-century physicists who had the objective to save allied lives during wartime.

The history of understanding atomic structure, radioactivity, and finally fission is a commentary on the way science was performed before WW II and the Cold War, when individuals or teams of scientists across Europe and America published their discoveries in specialist journals as soon as they were certain of their results and the need for review panels did not delay publication for months.

In 1896 Antoine Becquerel, studying the natural fluorescence of uranium salts, discovered that the salts fogged photographic plates. Further investigation by other researchers lead to the identification of alpha-, beta- and gamma rays, although their atomic identities were still unknown. During the first two decades of the 20th century, Ernest Rutherford inferred that the energy associated with radioactive decay was about a million times that associated with chemical reactions, developed the nucleus model of the atom based on alpha-ray scattering, and finally showed that one element could be transmuted into another by alpha-ray bombardment. During these years Albert Einstein proposed his theory of the equivalence of mass and energy, $E = mc^2$, and Niels Bohr, based on Rutherford's model of the atom, developed a quantized model of the hydrogen atom.

In 1932 James Chadwick, in England, discovered the neutron. This is an electrically neutral particle that makes up the nucleus of atoms with protons. Being neutral, it is not repulsed by either the electron cloud surrounding an atom or the positive charge of the nucleus. Thus, it can be used to investigate atomic structure and the effect of neutron speed on nuclear behavior and to transmute nuclei from one element or isotope into another. The following year Frédéric and Irène Joliot-Curie, in Paris, demonstrated nuclear transmutation and the creation of artificial radioactivity by bombardment of one element by alpha-rays to create another element, which undergoes radioactive decay.

Meanwhile, other physicists were using the neutron to bombard elements across the periodic table. One such physicist was Enrico Fermi, in Rome, who showed that almost all elements could be transmuted by neutrons. However, when he used uranium, the results could not be explained based on previous experience. He proposed that he was creating "transuranic" elements, elements beyond the top of the then-known periodic table. Teams of scientists across Europe worked on this puzzle for several years. In 1938, the year Fermi received his Nobel Prize and emigrated to the United States, Otto Hahn and Fritz Strassmann, in Berlin, identified one of the "transuranic" elements as an isotope of barium. Having sent their results to the journal *Die Naturwissenschaften*, Hahn wrote to former colleague Lise Meitner. As a refugee from the Nazis, Meitner was in Sweden and very interested in the research. She tried to analyze the results on the assumption that the barium had come from "broken" uranium atoms. The rest of the atom must be other elements, and she determined that their total mass was less than that of the original uranium atom. Over the Christmas holiday 1938, Meitner and her

Nuclear Energy Encyclopedia: Science, Technology, and Applications, First Edition (Wiley Series On Energy).
Edited by Steven B. Krivit, Jay H. Lehr, and Thomas B. Kingery.

nephew, Otto Frisch, another refugee, working with Bohr in Copenhagen, worked on the problem and developed the theory of fission and showed, based on Einstein's $E = mc^2$ relation, that about 200 MeV of energy was released for each atom fissioned.

In the following weeks both Bohr and the Joliot-Curies expressed surprise that they themselves had not seen this process. Indeed, the model of the fission of the nucleus fit with Bohr's liquid-drop model of the nucleus, which he had developed from an idea by George Gamow, a Russian, and with which Frisch was familiar. Meitner and Frisch submitted the fission concept to the journal *Nature* in January 1939, and it was published in February.

In the meantime, Bohr went to the United States to attend the Washington Conference on Theoretical Physics. In transit, he met with Einstein, Eugene Wigner, and John Wheeler at Princeton. The news of fission had arrived in America. The news reached Fermi at Columbia University, New York, and work began immediately on experiments to find the energy pulse from fission. At the conference Bohr met Fermi, who suggested that neutrons could be released during fission, which could enhance the rate of reaction and lead to a chain reaction. Within weeks of the conference, four teams in the United States and two in Europe had confirmed Meitner's and Frisch's hypothesis, and two teams at Columbia had started work to determine the number of neutrons emitted during fission. Their results were published, side by side, in *Physics Review*, April 1939, showing that excess neutrons were created and that a chain reaction was possible.

At the same time Bohr, who was still in the United States, explained why sometimes uranium fissioned, but often did not, behaving like thorium by absorbing the neutron and ejecting an electron from the nucleus, transmuting into another element. For uranium, this new element was an as yet unnamed transuranic; it was later named neptunium. Bohr had picked up on the discovery, just a few years earlier, that natural uranium had a small percentage of a lighter isotope with an odd-numbered atomic weight, 235, compared with the even-numbered atomic weights of thorium, 232, and the main uranium isotope, 238. He ascribed the main fission activity to the lighter uranium isotope, U235. The relative ease with which a captured neutron is absorbed or causes fission changes with the speed of the neutron and is included in the effective area of a nucleus as it appears to the approaching neutron. This is called the cross-section and is measured in "barns" (10^{-24} cm^2). For the next months, physicists were measuring the nuclear characteristics of uranium and trying to find methods to separate U235 from natural uranium in which it represents only 0.7% mass.

Many of the scientists in the United States and England studying the effect of neutrons on uranium were immigrants fleeing from Nazi and Nazi-like influences in Germany or their home countries—for example Fermi and Emilio Segré from Italy, Leo Szilard, Edward Teller, and Eugene Wigner from Hungary, and Otto Frisch from Austria, and many others working in related fields, such as Albert Einstein and Hans Bethe, and later Bohr from occupied Denmark. After the discovery of fission, the press openly published articles discussing the potential of atomic energy. Physicists, seeing the problems revealed by their data, doubted that atomic energy had a future and that bombs would ever be practical. There was no official U.S. government program to aid nuclear research in the universities. Many people in the immigrant scientific community were very concerned by the lack of official action, knowing what Hahn, Strassmann, and Heisenberg in Germany knew and hearing that the Germans had refused to export any uranium ore from the mines in Czechoslovakia. Expecting a Nazi war of aggression in Europe and fearing the development of a German atomic bomb, Szilard and Wigner approached Einstein and explained the current state of nuclear physics. Einstein, who had not been following the subject, immediately understood the importance of the research, resulting in the famous letter to President Franklin Roosevelt in August 1939, less than a month before the German invasion of Poland. Roosevelt did not receive and read the letter until several weeks later, but immediately established the Uranium Committee. There was considerable skepticism, and the Committee did not provide much support to the physicists until, coincidentally, the day before Pearl Harbor. In mid-1942, after other agencies succeeded it, the Committee finally evolved into the Manhattan Project.

Meanwhile, in February 1940, in England, Otto Frisch looked at the four possible combinations of fast- or slow-fission for U238 or U235. Considering the available data, he reasoned that fast neutron fission of U235 was the only practical option for an atomic weapon. He worked with Rudolph Peierls, another immigrant, to estimate the critical mass for a U235 bomb as a few pounds rather than tons for natural uranium. Frisch had been working on Clusius tube separation of uranium isotopes using gaseous thermal diffusion. The suggestion for a U235 bomb, supported by Mark Oliphant, went to the British government's Tizard committee, the committee that overlooked the application of science to the war effort.

During this period, interest in uranium fission devices was ongoing in Germany, the Soviet Union, and Japan. France was peripherally involved inasmuch as Joliot informed the French Ministry of Armaments about German interest in the major stock of heavy water in Norway. The stockpile was shipped out under the nose of the Germans. When France was invaded, the heavy water found its way to England. Later, the Norwegian heavy water plant was sabotaged by commandos, and a major shipment sunk in a fjord on its way to Germany.

Also in this time period, a young radio-chemist named Glenn Seaborg was bombarding uranium at the University

of California's Berkeley campus using Ernest Lawrence's 60 inch cyclotron, trying to transmute uranium into transuranic elements to study, but especially looking for element 94. During 1939, he had separated microgram samples of neptunium, element 93, and samples that might contain element 94. In early 1940 Seaborg and his team focused on "mass production" of neptunium to let it radioactively decay to element 94. In March 1940, the team of Seaborg, Kennedy and Segré, another immigrant, tested element 94 for fissionability and found it behaved much like U235. Element 94 was not named plutonium until 1942.

During 1941 the determination of the best element to act as a "moderator" (to slow the fast neutrons born in fission to improve their chance of interacting with a nucleus) so that a chain reaction experiment could be performed was undertaken. The best moderators needed to be light atomic weight, but also have low cross-sections for absorbing neutrons. Ordinary water is light but absorbs neutrons. Heavy water is a good moderator with a very low cross-section, but is such a small fraction of ordinary water that it is every energy intensive to separate and therefore very expensive. Graphite is good for slowing down neutrons, does not absorb them, is relatively cheap, but tends to have impurities such as boron, which do absorb neutrons. In mid-1941, at Columbia, Fermi and his team, including Walter Zinn and Herb Anderson, started building graphite piles of increasing size to measure the slowing down of neutrons and the "multiplication" of uranium-graphite systems (the number of neutrons in successive generations). There were problems with graphite purity and uranium metal purity. In fact, most of the uranium used in the early experiments was in the form of oxide, which had better purity control than available metal.

Measurements led to improved spacing between the uranium samples in the larger piles and materials purity improved, increasing the number of neutrons in succeeding generations. However a chain reaction still eluded the researchers. In December 1941 the governmental agency, Office of Scientific Research and Development, reorganized the uranium work under Arthur Holly Compton of the University of Chicago. The work on both coasts was to be consolidated in Chicago, not just for collocation but for fear of spies snatching personnel and secrets from sites near the coasts. The groups from Columbia, Princeton, and Berkeley were transferred to the newly created "Metallurgical Laboratory" (the Met Lab) on the campus of the University of Chicago in early 1942. Larger piles were built; as size increases, fewer neutrons leak out of the sides, and putting additional graphite around the sides reflects some of the escaping neutrons back into the uranium core of the pile (see Figs. 3.1 and 3.2). By mid-1942 the nuclear measurements had provided enough data to design a pile with good confidence that a self-sustaining chain reaction could be produced. Material purity had improved to support the design and even some high-purity uranium metal was becoming available in small quantities.

During 1941 and early 1942, it became clear that there were two approaches to an atomic bomb. One was to use U235, and the other was to use element 94. Separating U235 from natural uranium promised to be a major project, but a weapon appeared to be fairly easy to design. On the other hand, producing element 94 needed the chain reaction in uranium to become reality, and then the chemical separation from the irradiated uranium had to be achieved. The problems of designing a plutonium bomb had yet to be discovered.

About this time, the Manhattan Engineering District was established, and in September 1942 the Manhattan Project under General Leslie Groves was formed. Almost immediately land was bought at Oak Ridge, Tennessee, and design started on facilities for the separation of U235 using electromagnetic devices, calutrons, which Lawrence had adapted from his research cyclotrons. This was originally called the Clinton Engineering Works. Even in September 1942, three months before the first chain reaction, plans were developed for the pilot plutonium plant, called the X-10 Graphite Reactor at Oak Ridge, although it was called the Clinton Laboratory at that time. In September it was not clear where the Chicago pile was to be built. Land had been loaned to the Met Lab southwest of the city in the Palos Woods Forest Preserve, and a facility for the pile was being built. However, labor strife slowed construction, and it was decided to build the pile in a squash court under the stands at the unused football stadium of the University of Chicago, Stagg Field.

Starting in mid-October, the team at the Met Lab were fully engaged in building the pile and designing instrumentation. Not knowing the physics constants and pile theory as well as desired, a large balloon cloth bag was purchased from Goodyear Tire and Rubber Company, and the pile, with support timbers, was constructed inside. This provided the option that if the multiplication was near to chain reaction but not quite, then the bag could be sealed and evacuated, removing the nitrogen and its neutron absorption, thus perhaps helping to achieve criticality. As the event transpired, this action was not necessary. Four hundred tons of graphite were brought to the site and machined in the West Stands. Everybody worked at all trades, carrying the graphite bars, machining, drilling, transporting the product to the squash court and assembling the pile (see Figs. 3.1 and 3.2). Professors, students, physicists, tradesmen, and army rejects all worked, getting black as coal miners, working two 12-hour shifts a day up to ninety hours a week. The graphite bars, about 4 $\times$ 4 inches square and 16 inches long, were laid at right angles in alternate layers for stability. Alternate layers had the drilled bars with two 3 1/4 inch holes in each to hold the 22,000 pseudo-spheres of pressed uranium oxide or the

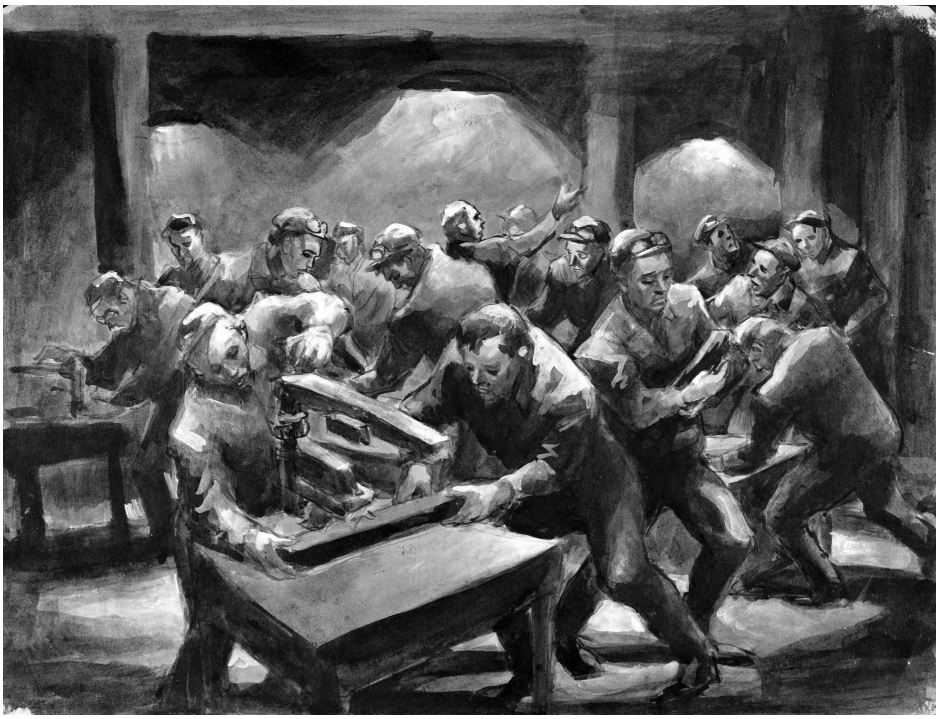

Figure 3.1 Machining the graphite bars. Courtesy of Argonne National Laboratory, managed and operated by UChicago Argonne, LLC, for the US Department of Energy under Contract No. DE-AC02-06CH11357. Artist John Cadel.

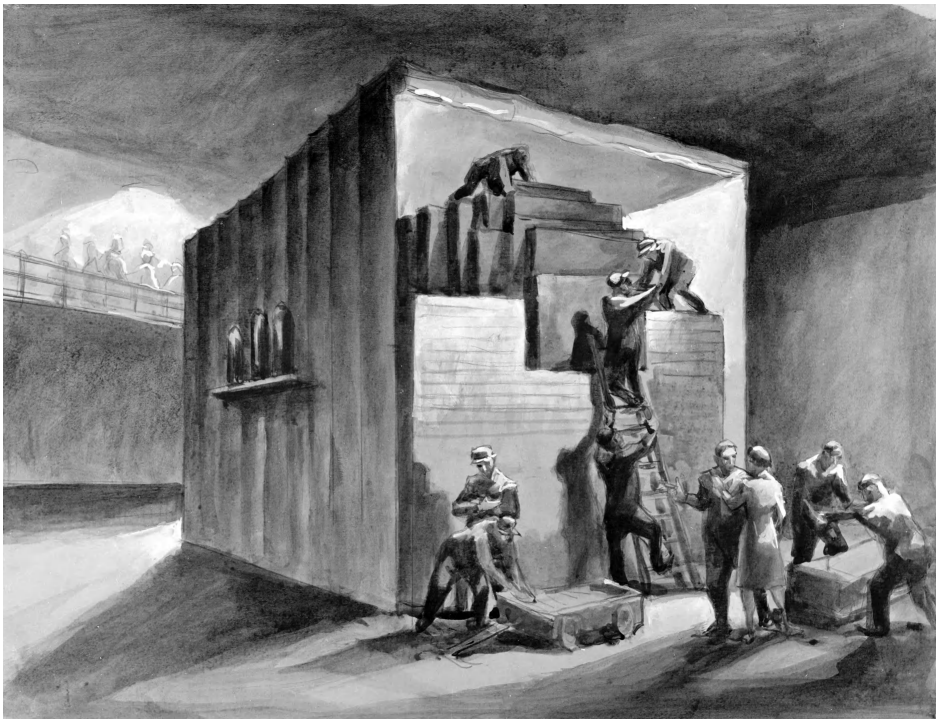

Figure 3.2 Building the reactor pile. Courtesy of Argonne National Laboratory, managed and operated by UChicago Argonne, LLC, for the US Department of Energy under Contract No. DE-AC02-06CH11357. Artist John Cadel.

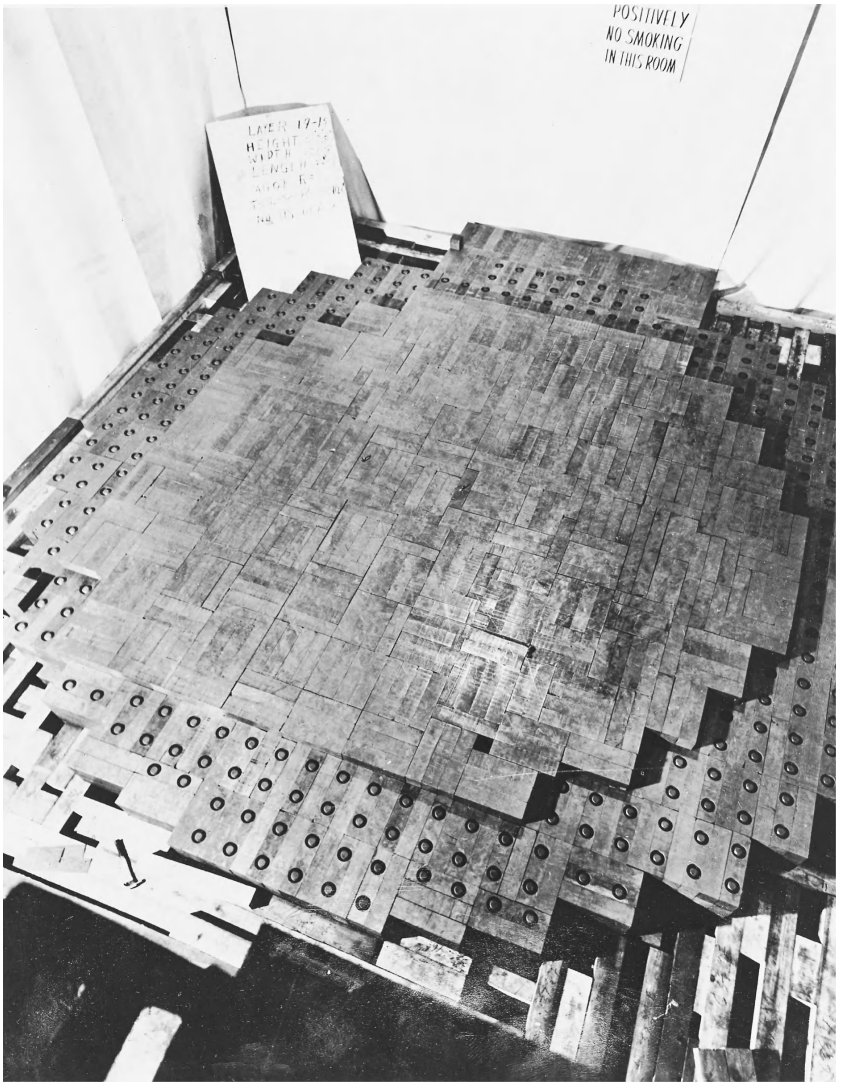

Figure 3.3 CP-1 during construction showing graphite layers with and without uranium oxide pseudospheres. Courtesy of Argonne National Laboratory, managed and operated by UChicago Argonne, LLC, for the US Department of Energy under Contract No. DE-AC02-06CH11357.

much fewer metal slugs (see Fig. 3.3). There were different grades of material, reflecting the various nuclear properties of each batch (primarily the degree of impurities), and the least impure were put nearest to the center of the pile.

Before construction began, Fermi had given a series of lectures explaining the theory of the pile and what to expect as the final test to criticality was performed. There were a series of cadmium (a strong neutron absorber) strips locked in place during each day's construction. These were removed once each day so that radiation measurements could be taken and the approach to the final layers monitored quantitatively. At layer 52, Fermi predicted that layer 56 would permit criticality, but he added a 57th layer for good measure on December 1st without any further measurements.

Before a chain reaction had been achieved, General Groves had bought land at Hanford, near Pasco, Washington, next to the Columbia River, for the plutonium production facility and signed a contract for its design and construction. A lot was riding on this experiment.

On the morning of December 2, 1942, the strips were removed and the cadmium safety and control rods withdrawn. A final safety rod that they called ZIP, a quick-acting device, was made ready for rapid emergency release by using an ax to cut the rope that held the gravity-assisted rod out of the reactor in the event of an electronic signal malfunction to the solenoid release. As a final safety back-up, carboys of cadmium sulphate solution were sitting on top of the pile to be poured into it if all else failed. There was one control rod left in the pile, which Fermi directed

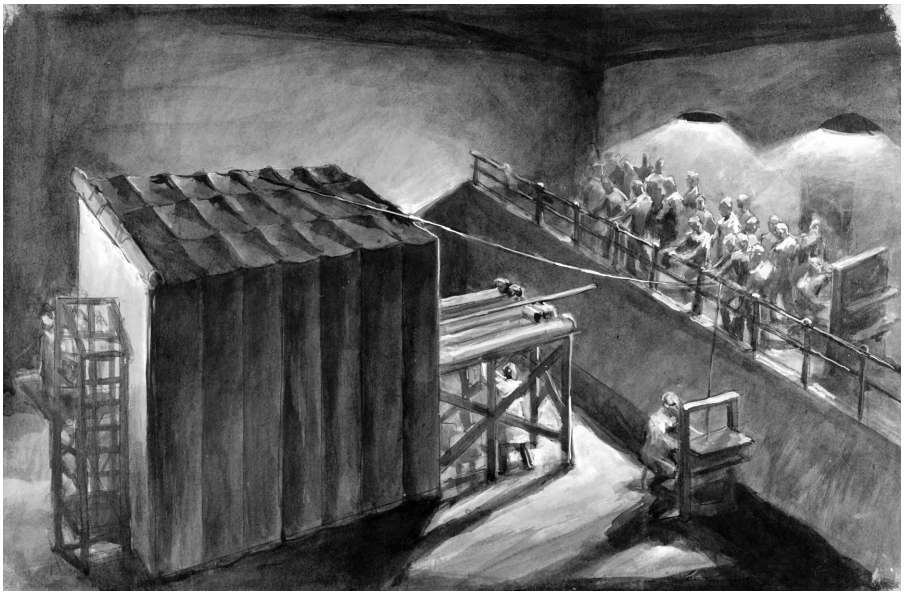

Figure 3.4 The pile showing the control and safety rods with the instrument panel and visitors on the balcony. Courtesy of Argonne National Laboratory, managed and operated by UChicago Argonne, LLC, for the US Department of Energy under Contract No. DE-AC02-06CH11357. Artist John Cadel.

to be removed in increments as he did calculations on his slide-rule based on each set of new instrument readings (see Fig. 3.4).

First, as he had the rod moved about halfway out, the counters increased their rate of clicking and the galvanometer chart trace raised and leveled out at a new value. Fermi ordered another foot removed from the pile. Again, the clicks accelerated to a new intensity, and the trace crept to a new plateau. Now the rod was withdrawn another six inches with the same audible and trace results. This was repeated several times, each time Fermi predicted the level that the trace would reach. At one point, the scalar of the chart had to be reset to keep the pen on the paper. Then there was a crash as the ZIP safety rod inserted. It had reached some set point that had been arbitrarily set at too low a value, there being no data to determine an appropriate value. Rather than continue, Fermi decided to go to lunch and start again in the afternoon. The cadmium rods were reinserted and locked.

After lunch, the rods were withdrawn, the ZIP rod reset, and Fermi had the control rod pulled to a preset value. It was pulled out another foot, and the counters and pen nearly jammed at new high values. The counting ratios and graph scalars were reset. Another six-inch move, then a one-foot move and Fermi announced that this was going to be a self-sustaining chain reaction and the trace would not plateau (see Fig. 3.5). As the clicks mounted and the galvanometer trace changed from convex to concave upwards, Fermi spent some minutes calculating the rate of exponential increase and announced that a chain reaction had been achieved. The ZIP rod was ordered inserted and the counter clicks died away. At this point Wigner produced a bottle of Chianti and all present drank from little paper cups before signing the raffia wrapping of the bottle. Chicago Pile number 1, CP-1, was now history.

Arthur Compton telephoned James Conant, one of the government program overseers, at Harvard.

> Compton, "The Italian navigator has landed in the New World."
>
> Conant, "How were the natives?"
>
> Compton, "Very friendly."

Other piles had been built during the summer and fall before the push for CP-1. These were to test the physics of different pile designs for the next stages of plutonium production, the X-10 Graphite Reactor at the Clinton Laboratory in Tennessee, and then the water-cooled production reactors at Hanford, Washington.

In April 1942, Glenn Seaborg moved to Chicago to establish the chemical processes for separating element 94, now named plutonium, from irradiated uranium. At Berkeley he was working with microgram quantities of neptunium and element 94 from cyclotron bombardment. Here he had to develop a process that could be scaled up to separate gram to kilogram quantities that could be used for testing and property evaluation and finally enough for a weapon.

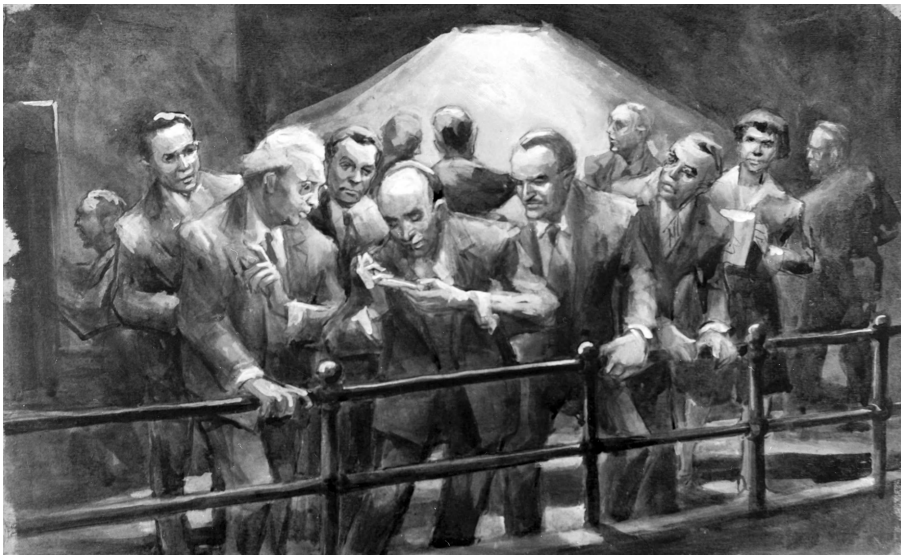

Figure 3.5 Fermi calculates the approach to criticality with Szilard and Compton adjacent. Courtesy of Argonne National Laboratory, managed and operated by UChicago Argonne, LLC, for the US Department of Energy under Contract No. DE-AC02-06CH11357. Artist John Cadel.

CP-1 only operated at Stagg Field for two and a half months, then it was shut down, dismantled and rebuilt, larger and shielded at the Palos Woods facility, known as Site A. This was accomplished in 23 days and renamed CP-2. Under these conditions, it could be operated at higher power and neutron flux levels, and facilities were incorporated for irradiation experiments in the pile. Fuel samples began to come to Seaborg's chemistry department where various techniques were tried to separate the plutonium from the mix of uranium and fission products. Construction started on the Clinton Laboratory Graphite Reactor, X-10, in January 1943. Many of the Chicago team commuted, by train, regularly to the Clinton Laboratory during construction. X-10 went critical on November 3, 1943, the world's first operational reactor, as compared to a pile. In parallel, a chemical separation plant was in preparation to house the processes being developed from Seaborg's microscopic and bench scale experiments. The experiences at the Clinton Laboratory were incorporated into the design of the Hanford production plant, construction of which began in mid-1943. The plutonium from X-10 was used for determining the properties of the element and for experiments to design the plutonium weapon. Furthermore, the Clinton Laboratories trained key staffers for the Hanford reactors and chemical separation plant. Hanford finally became operational in December 1944. The X-10 pile continued to produce plutonium until early 1945. In this period it started to make radioactive lanthanum for taking measurements of the plutonium bomb implosion experiments. The plutonium for the Trinity test and Nagasaki bombs came from the Hanford plant.

FURTHER READING

1. *Controlled Nuclear Chain Reaction—The First 50 Years*. American Nuclear Society, 1992.
2. *The First Reactor*—40th *Anniversary*, U.S. Department of Energy, 1982 (DOE/NE—0046).
3. Clarence Larson, Richard Duffy, David Rudolph, eds., *Historical Perspectives—Dawn of the Nuclear Age*. American Nuclear Society, 1989.
4. Alwyn McKay, The golden age of nuclear fission, ATOM395, September 1989, UK Atomic Energy Authority, pp. 2–5.
5. Richard Rhodes, *The Making of the Atomic Bomb*. Simon and Schuster, 1986.
6. Robert G. Sachs, ed., *Nuclear Chain Reaction—Forty Years Later: Proceedings of a University of Chicago Commemorative Symposium*." The University of Chicago, 1984; especially Appendix C, Albert Wattenberg.
7. Murray A. Rosenthal, *An Account of Oak Ridge National Laboratory's Thirteen Nuclear Reactors,* ORNL/TM-2009/181, August 2009. Availability U.S. Department of Energy (DOE) Information Bridge. http://www.osti.gov/bridge.

4

EARLY COMMERCIAL DEVELOPMENT OF NUCLEAR ENERGY

ROGER TILBROOK

Argonne National Laboratory (Retired), Argonne, IL, USA

The early commercial development of nuclear generated electricity was a multi-pathed progress based within national boundaries and guided by nationalistic ambitions. Each program had a different technical starting point and different degrees of resources that were available or could be brought to bear on problems that arose. Likewise, the changing economic environments as programs progressed made some political decisions inevitable, to the detriment of nuclear progress; for example, the discovery of gas in the North Sea reduced the need to push ahead with nuclear energy in Britain; the subsequent discovery of oil reduced the need still further.

At the end of World War II there were suspicions between the allies (even close allies), which prevented a free flow of nuclear-related information and materials, not only in relation to weapons but even the already contemplated industrial applications.

When World War II ended, the United States had all the resources necessary to further develop nuclear weapons and start to exploit the heat generated in nuclear piles (soon to be called nuclear reactors as their size, uses, and complexity increased). The Metallurgical Laboratory in Chicago had the original Chicago Pile, CP-1, rebuilt as CP-2, and had built a heavy water research pile, CP-3, which went critical in May 1944, ostensibly to provide support for the Hanford plutonium production reactor but also as a basis for maintaining staff that had not been ordered to Hanford and Los Alamos (primarily chemists and physicists respectively). Furthermore, Metallurgical Laboratory staff looking ahead to the post-war period and trying to define their purpose were focused on pile (reactor) development. As part of the allied wartime collaboration, it had been agreed that Anglo-Canadian research efforts would interface, although not closely, with the Met Lab and build a heavy water research pile in Canada using American heavy water. ZEEP (Zero Energy Experimental Pile) was built at Chalk River and went critical in September 1945. It was the first pile (reactor) outside the United States. The project had an international team of scientists, primarily Canadian, British, and French. The international mix of personnel disturbed General Groves, head of the Manhattan Project to which the Met Lab reported, and he insisted that the team be headed by John Cockcroft, a British national.

When the war ended, the United States was the only country that possessed all the necessary elements for a successful nuclear development program: experienced personnel, nuclear piles of different concepts and characteristics, plutonium production and separation plants, and enrichment capabilities all functioning. Out of all the debate within the nuclear, military, and political communities came the Atomic Energy Act of 1946 (the McMahon Act), which established the U.S. Atomic Energy Commission (US AEC) to develop the peaceful uses of nuclear energy, own all the fissile fuel (primarily U235 and Pu239) on behalf of the federal government, and undertake weapons development instead of leaving it the responsibility of the military. The AEC, realizing that the development of nuclear power would be a complex program, postponed all power reactor development and focused research on the effects of radiation on materials and biological life forms and on fissile materials production.

Nuclear Energy Encyclopedia: Science, Technology, and Applications, First Edition (Wiley Series On Energy).
Edited by Steven B. Krivit, Jay H. Lehr, and Thomas B. Kingery.

The development of reactors for research or power demonstration can be classified depending on fuel, moderator, and coolant, and, for power plants, by the turbine, or heat transfer, cycle. The United States, having the only U235 enrichment capability (and plutonium production), had an initial advantage over all other countries in that it could use enriched uranium as fuel (i.e., uranium with added proportions of U235) and thereby consider reactor concepts with different fuel cladding and moderators and coolants to enhance efficiency and/or economics (i.e., reduce capital and/or operating costs) or even concepts that would not be possible without all these options.

After the cessation of hostilities, the foreign scientists who had been loaned to the Manhattan Project by their governments returned home; those who had emigrated to escape Nazism and its fellow travelers in general stayed in the United States, many attaining positions of great influence in the American post-war programs, both in the peaceful aspects and the weapons activities. Therefore, many countries had experienced people available, primarily Britain, France, and Canada, which also had a reactor. Once the German invasion of the Soviet Union had been repulsed, the Soviets accelerated their nuclear research. (Although the country is now known as the Russian Federation, the achievements discussed here occurred before its establishment and will be acknowledged to the Soviet Union.)

The development of commercial nuclear power can be likened to growing a crop with each period lasting about five years. Each country progressed with remarkably similar projects in each period depending on national capacities, facilities, and motivations. Some programs lead to successful *lignes* (reactor types) that succeeded, some *lignes* matured for a while before being culled, and some never made it beyond demonstration units.

4.1 TILLING THE GROUND: 1945–1950

During this time, the United States had several operating reactors to support the collection of nuclear physics data and study radiation and radiation effects. The piles CP-2 and CP-3 and the reactor X-10 were used for materials radiation and isotope preparation. In 1946 the Clementine reactor was built at Los Alamos to study the physics of fast (unmoderated) neutrons. Studies were begun for the world's first materials test reactor (MTR), which started operating in 1952. This high-flux reactor was designed to irradiate, in particular, the structural and cladding materials for power reactors in an accelerated manner so they could be studied for property degradation. This was crucial for safe deployment of power reactors. The MTR was a collaborative effort by three national laboratories, Oak Ridge and Argonne for design and the National Reactor Testing Station (NRTS) in Idaho, which built and operated it. Simultaneously, concept design work began for a submarine motive unit using enriched fuel and light water. The physics test for this concept was called Zero Power Reactor 1 (ZPR-1), which went critical at ANL in 1950. The resulting reactor design (Submarine Thermal Reactor—STR) was provided to Westinghouse to build and operate in Idaho at NRTS. This became the start of Westinghouse's involvement with pressurized water reactors (PWR). When the STR was built, it was done in a submarine shell in a water tank; Captain Rickover, as he was then, did not want any surprises when the reactor was duplicated in a real submarine vessel and put to sea surrounded by water. Simultaneously, design work was ongoing for a sodium-cooled intermediate (speed) neutron reactor for submarine propulsion. The General Electric Company was responsible for this effort.

Meanwhile, north of the border, Canada had used data from ZEEP to design and build the NRX (National Research Experimental) reactor at Chalk River, starting operations in 1947. Its design power was 20 MWt (megawatts thermal). It was used for neutron physics and cross-section data research.[1]

In Britain, a significant group of scientists had returned from North America, including John Cockcroft from Canada and William Penney from Los Alamos. The first pile in Western Europe was the Graphite Low-Energy Experimental Pile (GLEEP) in 1947. It was designed for 100 kWt, although it did operate at significantly higher levels from time to time. The decision was made to pursue atomic weapons, and two plutonium production piles were constructed at Windscale in what is now Cumbria. Operations commenced in 1950 and 1951. It was an air-cooled, open-cycle design.

France resumed its pre-war nuclear research, both with scientists who had been in North America and those who had suffered through the German occupation. France was determined to build on its pre-war role in the discovery of fission and become a nuclear power, both in peaceful applications and militarily. It established the Commissariat à l'Énergie Atomique (CEA) with Frédéric Joliot-Curie as the high commissioner in 1945, doing basic research. Its first reactor was ZOE in 1948.

The Soviets were aware of the potential of uranium as early as 1940; however, it wasn't until two Soviet physicists published a paper in *Physics Review* in June 1940 about their related discoveries—and the response from Americans was dead silence—that the Soviets realized that the work in the United States had gone secret.

Reports requested studies especially of the military implications; however, little could be done until after the Battle of Stalingrad and even until the war was over. Some work was done on the manufacture of pure uranium and graphite. The American bombs that ended the war with Japan spurred further efforts. Consequently, the first reactor outside North America was the F-1 in December 1946 at

the Kurchatov Institute of Atomic Energy, four years after CP-1. Industrial plutonium production, including reactors and separation plant, must have been developed apace because the first Soviet atomic bomb test was September 1949, again only four years after the first American test. And plans were being prepared before the end of the decade for research reactors and their first atomic power station.

4.2 SOWING THE SEEDS: 1950–1955

In 1951 the first nuclear generated electricity was produced in Idaho: by the Argonne National Laboratory designed and built Experimental Breeder Reactor 1 (EBR-1), although it was only enough to power the reactor building. The promise of fast neutron reactors is the potential for breeding more fissile fuel than is consumed, thus allowing for more complete use of mined uranium. EBR-1 demonstrated the practicality of liquid metal coolant (here a sodium potassium eutectic, NaK), nuclear production of electricity (1951), the feasibility of breeding (1953), and, many years later, electricity production from a core with a major inclusion of plutonium (1963). The Submarine Thermal Reactor was extensively tested in Idaho (it was renamed the S1W), and the first nuclear-powered submarine, USS Nautilus, went operational in 1954. Experiments with aqueous homogeneous reactors and molten salt reactor designs were undertaken at Oak Ridge National Laboratory, but the concepts were put aside.

After the successful deployment of the USS Nautilus, the pressurized water reactor (PWR) was now to be developed for civilian power generation, and in 1954 the AEC selected a group of companies to start this project. Meanwhile, at Argonne, thought was being given to the effects of steam bubbles in the core on reactor stability. The ANL test reactor series was built and operated at NRTS. The first boiling water reactor experiment, BORAX-I, began testing in 1953 at 1.4 MWt with gradually increasing in-core boiling. The system remained stable, and finally a series of increasingly sharp reactivity insertions were introduced to test safety margins. Eventually, the reactor was destroyed by a high-temperature thermal-hydraulic expansion, not a nuclear excursion. Boiling Water Reactor (BWR) safety having been demonstrated, the concept's development for a cheaper capital cost generating plant (no steam generators) was assured. BORAX-II (1954) was a larger-size reactor operating at a higher pressure and included a range of U235 enrichments in the fuel plates. This plant was soon converted to BORAX-III by the addition of a turbine generator, and on July 17, 1955, it lit the town of Arco, Idaho, with all-nuclear-generated electricity. BORAX-III was designed for 15 MWt with a 2 MWe capability.

In 1954 the AEC felt that its emphasis on R&D had paid off, and it was time to initiate a civilian reactor building program. This lead to the Atomic Energy Act of 1954, which permitted the private ownership of reactors, although the fuel had to be leased from the government, and permitted the release of information necessary for the design of reactors by commercial vendors. The Act also encouraged international development of nuclear power. The Power Demonstration Reactor Program (PDRP) was announced, inviting industry to make proposals to build power reactors in a range of sizes and apply for financial assistance to make the projects viable to demonstrate the commercial economics of the various designs and concepts. The plant sizes all seem small by today's standards, but there was an emphasis on smaller sizes, and large fossil plants of that era were much smaller than those of today. Also this was the time when vendors and utilities were striving to push steam superheat higher to improve plant efficiency of fossil units. (Superheat is the increase in steam temperature above the saturation temperature corresponding to the system pressure.)

Meanwhile, in Canada work began on the National Research Universal (NRU) reactor in 1951. It was being designed to support NRX by performing more experiments and producing more radioisotopes. There were close technical relations with Britain, and significant work was done for the USAEC and the U.S. Navy. This was primarily irradiation of submarine-related materials. When NRX had its accident in December 1952, Rickover loaned hundreds of Navy personnel to the cleanup to learn how to manage such events. Data from the reactor was also useful in the design of the Savannah River production reactors. Atomic Energy of Canada Limited (AECL) was established in1954 to undertake R&D in peaceful nuclear applications. Two years later, AECL initiated plans with Ontario Hydro and Canadian General Electric for the design of a power plant.

In Britain, the choices for reactor design were constrained by the availability of only natural uranium for fuel and no supply of heavy water–dictated graphite as the moderator. The experience operating the Windscale piles and the successful development of a magnesium-based cladding material called Magnox (magnesium, no oxygen) for the natural uranium fuel rods made practical higher operating temperatures. Christopher Hinton, in charge of fissile material production, proposed a series of PIPPA reactors (Pile for producing Plutonium and Power). Four were planned for Calder Hall, next to the Windscale piles and four more at Chapel Cross in Dumfriesshire, Scotland. Meanwhile, at Harwell a fast neutron critical assembly, Zephyr (1954), had started experiments toward a liquid metal fast reactor.

Across the Channel in France, a second heavy water research reactor (2 MWt) came into operation at Saclay in 1952. Its metallic uranium fuel rods were cooled by carbon dioxide (CO_2), a first. Plans were afoot for plutonium production plants based on graphite as the moderator at

Marcoule. The first plant was to be an air-cooled, open-cycle reactor and later plants were to be power producing. Furthermore, the CEA began studying sodium cooled concepts in 1953.

In the Soviet Union, the early 1950s saw the design of several research reactors and the first atomic power plant. In 1954 at Obninsk, the world's first electric plant (5 MWe) went into operation (APS-1) using enriched uranium. It was of a graphite moderated, boiling water–cooled design, which was later developed to become the RBMK series. And in 1955 the Soviet's first fast reactor program put into operation BR-1, a 100 Watt, thermal, plutonium-fueled reactor for physics experiments.

The end of this period is marked by the 1955 Geneva Atoms for Peace Conference. The shock of the Soviet H-bomb test in 1953 spurred American and other West European leaders to contemplate different approaches to what was becoming a nuclear arms race. In December 1953, President Eisenhower spoke to the United Nations proposing a series of steps to control uranium and fissile materials. This led to many negotiations and exchanges, resulting in the 1955 Geneva Conference. There were representatives from 69 countries and 1,132 papers, many disclosing information previously regarded as secret. It was because of this conference that the Soviets wanted APS-1 to succeed so they could attend as a champion of peaceful nuclear applications. The AEC, also wanting to show a good face, wished to have a reactor to show at Geneva. A modified version of the Oak Ridge swimming-pool Bulk Shielding Reactor (BSR) was selected and operated at Geneva, showing its blue Cherenkov radiation, one of the hits of the conference. After the conference, it was sold to the Swiss government, who moved it to Würenlingen as SAPHIR. Although this conference was all about international cooperation, two other reactors had been built in the 1950s, as cooperative projects—the low-power heavy water/natural uranium Norwegian/Dutch reactor at the Kjeller Center, Norway, in 1951, and a similar reactor near Stockholm as a joint Franco-Swedish venture in 1954.The world's first international nuclear conference had been held in Oslo in1953, starting European nuclear cooperation just as the McMahon Act was being amended.

4.3 TENDING AND THINNING: 1955–1960

The second half of the 1950s decade in the United States was a period of progress for several reactor types, *lignes*. Borax-IV (1956) was operating as a test bed for different fuel types (e.g., changing from plate fuels to fuel rod bundles), and the Experimental Boiling Water Reactor (EBWR) started operation at Argonne, Illinois, also in 1956. It had a capacity of 5 MWe; the thermal power was originally 20 MWt, being raised later to 100 MWt. BORAX V was completed in 1959 to demonstrate that nuclear superheat could be achieved in a BWR just as in conventional fossil-fueled generating plants. The civilian version of USS Nautilus at Shippingport, Pennsylvania, on the Duquesne Light electric grid, went critical on December 2, 1957, 15 years to the day after CP-1 and produced its full power of 60 MWe about a year later.

Meanwhile, in 1954, General Electric was considering what reactor type to pursue. It had experience with a sodium-cooled plant, which had been tried for submarine propulsion in the USS Seawolf (but was replaced by a PWR), and graphite-moderated boiling water–cooled reactors from overseeing the Hanford production reactors for the AEC. The success of the BORAX tests convinced GE that a BWR was technically viable and cheaper than the Hanford-style plants. To test its concepts, GE built the experimental Vallecitos BWR (5 MWe), which began operating in 1957; this received the AEC Power Reactor License No. 1. The Commonwealth Edison Company (now incorporated into Exelon) had had engineers working on assignment on the construction of EBWR. Consequently, GE and ComEd signed a contract for a BWR, the first Dresden plant, which went critical and entered commercial operation in 1960 in a commercial utility environment with no government funding for its 200 MWe capacity. Also in 1960, Yankee Rowe (175 MWe) entered service operating a Westinghouse PWR as part of the PDRP project. Late in this period export orders were also being negotiated.

In Canada, with only the CANDU type reactors under consideration, in the late 1950s, commissioning activity was relatively quiet. Only the NRU went on line (1957), but design work for the prototype power reactor Nuclear Power Demonstration (NPD) to be built at Rolphton, Ontario, was ongoing. In 1959 it was also decided to look at organic liquid-cooled reactors (still heavy water moderated) for smaller-size units and an experimental reactor was planned for Whiteshell, Manitoba.

The British program was moving fast. In October 1956 Her Majesty Queen Elizabeth II opened Calder Hall (Unit A-1). This was a 50 MWe graphite-moderated, CO_2 cooled reactor and the first of four at this site, to be followed by another four units commissioned at Chapel Cross before the end of the decade. But it must be remembered that the units were operated to optimize weapons-grade plutonium production. Also during these years, ZEUS (a fast reactor critical assembly) went into operation in 1959, but primarily the experimental Dounreay Fast Reactor (DFR) went critical with an electrical output of 14 MWe from 60 MWt.

In October 1957, the British nuclear program was given a wake-up call to caution and safety. When graphite is irradiated, the crystal lattice is distorted. Periodically, the graphite must be heated in a controlled manner to release this Wigner stored energy. At the Windscale piles, this was a procedure undertaken every six months. However, in October 1957, the reaction got out of control and caused a fire in the air-cooled pile. It took five days to extinguish

the fire and 22 days before the local milk was no longer impounded. Sir William Penney ran the inquiry into the causes of the incident. It was determined that it would cost too much to retrofit Pile 2, and it was shut down. This did not impact plutonium production excessively because the Calder Hall reactors were now coming on line. The salutary lessons of Windscale benefited the whole nuclear program, which was just taking off.

In France the period 1955 to 1960 saw the startup of the G-1 reactor at Marcoule. It was an air-cooled, open-cycle graphite reactor for plutonium production, similar to the Windscale piles. The follow-on reactors, G2 and G3, were designed to also produce 38 MWe each and were commissioned in 1959 and 1960 respectively. These had horizontal fuel channels and introduced the concept of on-load refueling. The vessels were prestressed concrete. The basic design for the next reactor, EDF-1 (70 MWe), at Chinon was like the G2 plant, but preferred the vertical channel option and chose a steel vessel. However, a crack developed during fabrication in 1959, delaying EDF-1 and EDF-2 (210 MWe) by two or three years. In 1960 the French reverted to prestressed concrete vessels for EDF-3 (400 MWe), and soon thereafter the British ordered their first concrete pressure vessel. In 1957, France started work on Rapsodie, a 20 MWt fast reactor with sodium cooling. This was based on the research reactors Harmonie, Mazurca, and Cabri.

In the Soviet Union, fast reactor projects progressed. BR2 (100 kWt) began operation in 1956. Two years later, it was replaced by BR5 (5 MWt). Later in the 1970s it was upgraded to 10 MWt as BR10. In 1958 the first of the six Troitsk reactors was commissioned. Each unit was a 100 MWe, using enriched fuel and a graphite moderated, pressurized water-cooled concept. Work was also undertaken in the 1950s on PWR technology for use in the navy's submarines (1959) and in the icebreaker fleet, the first of which, Lenin, started up also in 1959.

Also in this period the Second Geneva Atoms for Peace Conference was held in 1958. Argonne had developed the ARGONAUT (Argonne Nuclear Assembly for University Training) reactor (10 kWt) for instruction and research in reactor technology. It was intensively used for the International School of Nuclear Science and Engineering at ANL. A second unit was built, then broken down and shipped to Geneva, where it was reassembled and operated during the Conference. Afterwards, it was returned to Argonne where it was upgraded to JUGGERNAUT to help the "Atoms for Peace" work-horse research reactor CP-5.

4.4 LET ALL THE FLOWERS BLOOM, THEN CULL: 1960–1970

The decade of the 1960s in the United States saw few national laboratory reactors built in support of power generation (for example, the Experimental Breeder Reactor II [EBR II] in 1964 and the Transient Reactor Test Facility [TREAT] in 1959 for examining fast reactor fuel under transient conditions). GE also designed SEFOR (Southwest Experimental Fast Oxide Reactor), a 20 MWt experimental facility to determine the physics of fast reactors with mixed oxide fuel and measure the Doppler coefficient, which was crucial to the safety design. Operating 1968 to 1972, this was a joint program with U.S. utilities, the AEC, and support from Gesellschaft für Kernforschung of Kahlsruhe, West Germany. The results were very important for FBR design.

But this was the age of the PDRP reactors. In 1957 Atomics International operated the AEC's Sodium Reactor Experiment (SRE) at Santa Susana, California, leading in 1962 to the Hallam, Nebraska, (75 MWe) unit with canned graphite and sodium coolant. Failures of some components, including the graphite cans, resulted in its shutdown in 1964, and the concept was put aside, although AI continued interest in sodium technology in support of the fast breeder program. General Electric plants, all BWRs, went into operation in 1963, Big Rock Point, Michigan, (70 MWe) and Humboldt Bay, California, (65 MWe) and in 1968 Nine Mile Point, New York, (500 MWe). And there were exports: Garigliano (Italy), operating in 1963 (150 MWe). All these plants operated successfully for many years. Wesinghouse built the Carolina Virginia Tube Reactor, South Carolina, (CVTR, 17 MWe), a version of the heavy water tube concept, which operated 1964–1967 and then shut down and was not pursued. A small 3 MWe PWR was operated at Saxton, Pennsylvania, from 1962 to 1972. For a time, Westinghouse worked on a basis that the number of coolant loops matched the unit power: Zorita (Spain) had one loop for 153 MWe (1968), Obrigheim (West Germany) had two loops for 340 MWe (1967), San Onofre (California) had three loops for 375 MWe (1967), and Haddam Neck (renamed Connecticut Yankee) had four loops for 575 MWe (1967). There were earlier exports. Trino (Italy) started operations in 1964 (200 MWe) and Chooz A, France, in 1967 (260 MWe). Some of these export plants were built in collaboration with licensees (Obrigheim and Chooz), which led eventually to the major Framatome *ligne* of PWRs and the European collaborations for a European PWR.

Other companies were designing PDRP reactors, many of which tried innovations on the basic BWR designs, which did not prove viable. General Nuclear Engineering Corporation, the company founded by Walter Zinn, former director of ANL, built BONUS (Boiling Nuclear Superheat) in combination with Combustion Engineering in Puerto Rico. Operating from 1964 to 1968 (17 MWe), it was finally shut down due to operating problems. GNEC was absorbed into Combustion Engineering as its nuclear division. Its next plant was a 700 MWe PWR at Palisades, Michigan, in 1971. Babcock and Wilcox, B&W, built Indian Point-1 in New York. It operated from 1963 to 1974 at 270 MWe with oil-fired superheat. Its next plant

was ordered in 1966 for Oconee-1, South Carolina. One of the plants ordered after Oconee was Three Mile Island in Pennsylvania, one of whose units, TMI-2, suffered a classic meltdown accident in 1979. There was no damage outside the containment, and TMI-1 went back on power. Atomics International (AI) built an organic liquid moderated and cooled reactor at Piqua, Ohio, based on the Organic Moderated Reactor Experiment (OMRE) at NRTS. It was designed for 11.4 MWe and operated during 1963–1965 when radiation damage to the organic fluid led to shutdown. Allis-Chalmers (AC) tried two superheat BWRs: Elk River, Minnesota, (22 MWe) featured natural circulation and had coal superheat and Pathfinder, North Dakota, (58 MWe) had nuclear superheat. These plants operated 1963–1967 and 1964–1968 respectively. AC also built a less exotic BWR at La Crosse, Wisconsin, which operated from 1969 to 1987 at 50 MWe. The United States also experimented with the High Temperature Gas-cooled Reactor, HTGR, with the Peach Bottom, Pennsylvania, unit 1 by General Atomics. This operated from 1966 to 1974 and the experience led to the order in 1968 for the 330 MWe Fort St. Vrain plant, Colorado. A group of U.S. utilities and Japanese companies proposed the most ambitious reactor of the first round of the PDRP. The Enrico Fermi Fast Breeder Reactor, EFFBR, was designed by the Atomic Power Development Associates (APDA) for 61 MWe. This sodium-cooled plant was jointly owned by Detroit Edison and the Power Reactor Development Corporation (PRDC). It was connected to the Edison grid and went critical in 1963. It was built before any experience from EBR II, which did not start until the following year. A blockage from a failed safety feature affecting two fuel assemblies occurred in 1966. The plant went back into operation in 1970, but was shut down when a replacement core load could not be obtained.

In Canada, the NPD reactor at Rolphton, Ontario, went into operation in 1962 (23 MWe). Before completion of the NPD, Ontario Hydro and AECL started design work on the 208 MWe Douglas Point plant (Ontario), which was the step-up prototype for commercialization. This unit went into operation in 1968, at which time the first four Pickering units (Ontario), 515 MWe each, were under construction, leading to the CANDU *ligne*. As a variation on the basic CANDU, the CANDU-BLW (Boiling Light Water in the tubes) was tried as Gentilly-1, Quebec. It operated at 250 MWe from 1971 to 1988 and then was closed. The experiment was not repeated in Canada.

In the meantime, in Britain, Magnox power stations were being commissioned regularly at ever increasing outputs. In 1962 the first units at both Berkeley and Bradwell were commissioned by The Nuclear Power Group (TNPG) for the Central Electricity Generating Board (CEGB), although their design was optimized for plutonium production. The stations when completed were 2×137 MWe and 2×150 MWe respectively. Many other design/manufacturing/construction consortia were in the market with plants. In 1964 Hunterston A (2×150 MWe) went on line for the South of Scotland Electricity Board (SSEB), followed by several CEGB plants at Hinkley Point A (2×250 MWe) in 1965, Trawsfynydd (2×275 MWe) also in 1965, Dungeness A (2×275 MWe) in 1966, Sizewell A (2×290 MWe) in1966, Oldbury (2×280 MWe) in 1967, the first British plant with a prestressed concrete vessel, and finally Wyfla in 1971 at 2×590 MWe. Two plants were exported to Italy and Japan, starting up in 1964 (Latina) and 1966 (Tokai Mura). In general, the plant thermal efficiencies improved at each step as gas coolant pressures and temperatures increased. From Calder Hall's 18.8% efficiency, plant thermal efficiencies increased to Oldbury's 33.6%. However, after many years of operation, it was found that at these higher conditions there was increased corrosion, and the utilities had to derate capacity to keep corrosion within acceptable limits. During all the Magnox construction, the Windscale Advanced Gas-cooled Reactor (WAGR) was commissioned in 1963 at 30 MWe. This used enriched oxide fuel in stainless cladding, and after the 5000 MWe Magnox program, the next generation of gas-cooled reactors (GCR) were AGRs, the first orders coming in the late 1960s. However, in spite of steady performance, generally, lack of exports among other economics led to closing the GCR *ligne* in favor of internationally accepted LWR plants.

A prototype heavy water reactor similar to the CANDU-BLW, named the Steam Generating Heavy Water Reactor, SGHWR, was commissioned in 1968 at 100 MWe. It operated until 1990. In the mid-1970s the SGHWR concept was given great credence and was considered to be the preferred successor for a domestic design to the GCRs, but favorable LWR experience in the United States and other countries, and a domestic familiarity with PWR technology from the nuclear submarine program, led to PWR selection for the next plants. Work on fast reactors continued, leading to the 250 MWe Prototype Fast Reactor, PFR, which was commissioned in 1974 after construction delays.

Similarly, in France, domestic *lignes* were pushed ahead only to be passed by for international PWR technology, which was then domesticated. At Chinon, the three EDF 1–3 units went online in 1963 (70 MWe), 1965 (210 MWe) and 1966 (480 MWe). St. Laurent-1 was a copy of EDF-3 and went on line in 1969. Upgraded designs for St. Laurent-2 (515 MWe) and Bugey-1 (540 MWe) went online in the early 1970s. Even though an advanced annular fuel element, with internal and external cooling surfaces was developed for Bugey-1 in an attempt to improve plant economics and the Vandellos plant was exported to Spain (a 480 MWe unit) operating in 1972, a debate raged between the CEA and utility EDF about the next flight of reactor orders. EDF had been exposed to Westinghouse technology with the Chooz A, 310 MWe plant (a Franco-Belgian project), which came online in

1966. In this time period, French PWR R&D was driven by the military with the PAT reactor in 1967, a prototype for its first submarine, which was completed in 1971, thus increasing France's familiarity with the *ligne*. In 1970, EDF ordered its first PWR station, 900 MWe, from the Westinghouse licensee; other orders up to 8,000 MWe soon followed. Various company rearrangements have left Framatome, now Areva, as a major independent PWR designer with plants around the world. And the GCR *ligne* is closed.

Further French design efforts included the EL-4 (Eau Lourde, heavy water), commissioned in 1967 and operating at 70 MWe until 1985. It was heavy water moderated and cooled by CO_2. However, problems with the original beryllium-based cladding required an alternate clad, necessitating enriched fuel, making the plant uneconomic. The experimental fast reactor, Rapsodie, reached its designed 20 MWt in 1967 and was upgraded to Fortissimo (40 MWt) in 1970. Design work for Phénix, 250 MWe, began in 1965–1966, and construction began at Marcoule in 1968. Criticality came in 1973, and grid connection before the end of that year and full power in early 1974. Superphénix, 1200 MWe, came later as an international program.

Meanwhile, in the Soviet Union, the Troitsk series was completed in 1962, but the concept was discontinued. A small organic moderated and cooled reactor (0.75 MWe) was operated and tested in 1963, and later the concept was put aside. BWRs were built, the first being the VK50 (50 MWe). This came into service in 1966 and this concept, too, was abandoned. The three Soviet *lignes* that continued development were the RBMK, VVER (PWR), and fast reactors.

After the small Obninsk reactor, larger units were built at Beloyarsk. Unit 1 was 100 MWe (1964) and unit 2 was 185 MWe in 1967. A series of 950 MWe and 1450 MWe designs were built around the Soviet Union in the 1970s and subsequent years, including the Chernobyl plant, which had the infamous accident at unit 4 in 1986. The VVER (PWR) program was expanded beyond the use in ships and submarines; the first two plants were built at Novo Voronezh, starting operations in 1964 (265 MWe) and 1969 (338 MWe). Novo Voronezh-3 and -4 were both 410 MWe units (1971,1972) as a standard design basis approached 440 MWe. Many VVER plants in the 400 MWe range were exported in the 1970s, mainly to Eastern Europe. The next size increase was to a 900+ MWe range, again with East European exports.

The Soviets' third avenue of nuclear development was the fast reactor. The BOR60 (11 MWe) went operational in 1969, and construction was ongoing for the BN350 at Shevchenko on the Caspian Sea. This went into operation in 1973, producing 135 MWe and steam to the adjacent desalination plant for 120,000 cubic meters per day. This is the only nuclear-powered desalination plant ever built. A 600 MWe FBR was later commissioned with larger plants being considered.

Many other countries initiated nuclear programs based on their own technical creativity, as developments from licensee agreements, or based on technical information transfer included in reactor purchase contracts (abbreviated to "tech transfer"). And there are international design/construction collaborative groups with individual companies providing their own particular expertise to the team. In general, the long-term surviving *lignes* are the PWR, BWR, and a smaller fraction of CANDU designs. All the other concepts have faded away, even though they may still be represented in the world list of operating reactors. Some of the concepts are periodically resurrected for reconsideration due to improvements in materials that may make them viable, but they don't have the experience base of the above *lignes* and would be difficult to sell. The only exception is the liquid metal fast breeder reactor, which several countries regard as necessary to maximize the use of our uranium reserves and reduce proliferation. They are continuing R&D either as national programs or as part of international collaborative efforts with different degrees of financial commitment.

Endnotes

1. Dates quoted for reactors vary by source due to the lack of differentiation between criticality, full power, and connection to the grid. Similarly, the reactor power quoted by different sources does not differentiate between "name plate" rating, power generated, and power at the bus-bar, which subtracts the in-house power needed to operate the plant.

FURTHER READING

1. *Controlled Nuclear Chain Reaction—The First 50 Years.* American Nuclear Society, 1992.
2. Robert Bothwell, *Nucleus—The History of Atomic Energy of Canada Limited,"* University. of Toronto Press, 1988.
3. Bertrand Goldschmidt, *The Atomic Complex—A Worldwide Political History of Nuclear Energy*. American Nuclear Society, 1982.
4. Jack M. Holl, *Argonne National Laboratory: 1946—1996*. University of Illinois Press, 1997.
5. Jacques Leclercq, *The Nuclear Age*. Hachette, 1986.
6. Ray L. Lyerly and Walter Mitchell, III, *Nuclear Power Plants*, Understanding the Atom Series. U.S. Atomic Energy Commission/Div. of Technical Information, 1968.
7. R.F. Pocock, *Nuclear Power—Its Development in the United Kingdom*. Urwin Bros. Ltd., and the Institution of Nuclear Engineers, 1977.
8. Theodore Rockwell, *The Rickover Effect: How One Man Made a Difference*, An Authors' Guild Backprint.com Edition, 2002; originally published Naval Institute Press, 1992.
9. Murray A. Rosenthal, *An Account of Oak Ridge National Laboratory's Thirteen Nuclear Reactors*, ORNL/TM—2009/181, August 2009. Availability U.S. Department (DOE) Information Bridge. http://www.osti.gov/bridge.

5

BASIC CONCEPTS OF THERMONUCLEAR FUSION

Laila A. El-Guebaly

Fusion Technology Institute, University of Wisconsin–Madison, Madison, WI, USA

5.1 BASIC PRINCIPLES OF FUSION

Fusion is the nuclear process that fuses light elements under high temperature and pressure into other light elements with a combined mass less than the initial mass. This decreased mass is converted into energy as defined by Einstein's relationship of matter and energy ($E = mc^2$). This is the process used by the sun and stars that provides light and heat to the Earth. The other nuclear process is fission, which splits apart heavy elements to produce a combination of other heavy elements that also have less combined mass. The same mass-to-energy conversion applies to both fission and fusion.

The first large-scale demonstrations of these two nuclear processes were weapons of mass destruction. Since that time, scientists and engineers have been seeking means to effectively control these processes for peaceful energy production. The peaceful production of fission energy in a power reactor was achieved in the 1950s with many fission power plants now operating throughout the world. Fusion is viewed by many as safe and attractive, but a difficult alternative or supplemental energy source.

Fusion is energy-rich, emits no CO_2 during operation, has much lower levels of radioactive waste, and releases orders of magnitude more energy per unit mass than uranium or fossil fuels. All fusion concepts share a common set of fuel elements: a mixture of hydrogen and/or helium isotopes (such as deuterium (D), tritium (T), and/or helium-3 (^{3}He)). These gases are heated to very high temperatures (exceeding that of the sun) with a corresponding pressure to create an ionized plasma (a collection of charged particles). This plasma is contained long enough for the highly energetic ionized isotopes (D^+, T^+, and/or $^3He^+$) to fuse into heavier nuclei, releasing helium ions (alpha particles), neutrons, and various forms of radiation. The components surround the plasma capture and convert the released energy into thermal energy that can be used to generate electricity or other forms of energy. Direct energy conversion to electricity is possible if the fusion energy release is predominately charged particles.

Most of the fusion efforts to date are devoted to the D-T fuel cycle, since it has the least demanding plasma conditions to reach ignition. To achieve even more environmentally friendly fusion processes, there is ongoing worldwide research on fuel cycles other than D-T that produce many fewer neutrons. The most popular "advanced" fuel cycles are D-D, D- ^{3}He, ^{3}He- ^{3}He, and proton-boron-11 (p-^{11}B). The main drawback of these cycles is the much higher and more difficult temperature and pressure conditions for ignition.

Fusion has an abundant supply of fuel with plentiful resources. Deuterium, an essential isotope for most fusion fuel cycles, is stable, plentiful, and can be extracted at low cost from seawater. Tritium is radioactive with a 12.3-year half-life, does not exist abundantly in nature, but can be created for D-T fuel cycles using lithium (Li) or Li compounds (as neutrons react with Li to produce T). Tritium is then recovered on site from Li-based blankets (wrapped around the plasma) and fed back into the plasma as gas or fuel pellets—a closed cycle that creates fuel as needed (rather than holding large quantities on site) and requires no transportation of T. The worldwide Li supply is more limited compared to D, but its inventory is sufficiently large to supply fusion for thousands of years. The advanced

Nuclear Energy Encyclopedia: Science, Technology, and Applications, First Edition (Wiley Series On Energy).
Edited by Steven B. Krivit, Jay H. Lehr, and Thomas B. Kingery.

fuel element, ^{3}He, is extremely scarce in nature, but can either be created or perhaps mined from the moon.

Fusion offers an intrinsically safe energy source with no risk of runaway power situation, primarily because of the sustainment of the plasma. Since proper plasma condition is difficult to achieve for fusion, any control anomalies or in-leakage of air or other contaminants will cause the plasma to shut down immediately and cease functioning with no chance for a critical runaway condition. The plasma chamber normally contains very low fuel inventory (<1 gram of D+T) and maintains a high vacuum condition ($\sim 10^{-6}$ Pa). Any atmospheric or coolant leak would be inward toward the plasma, which would also cause the plasma to immediately cease power production. Current fusion power plant designs have incorporated safety requirements and inherent safeguards so that public evacuation plans are no longer required. And many extensive, in-depth safety studies performed on fusion designs have confirmed that credible accident scenarios couldn't cause any safety risk to workers or the public.

Almost all fuel cycles, except ^{3}He-^{3}He, produce neutrons at various intensities and energies. The D-D, D-T, and D-^{3}He reactions produce neutrons essentially at the 2.45 and 14.1 MeV energy levels. Most of the D-T fusion energy ($\sim$80%) is carried by 14.1 MeV neutrons. These neutrons deposit their energies in the blanket and breed tritium. However, these neutrons will also transmute the materials surrounding the plasma into radioactive elements and radioisotopes. There is an impetus to exclusively use low-activation materials within the power core region. Low-activation materials are defined as materials with elements that will not be transformed into highly radioactive radioisotopes with long half-lives. This will limit or eliminate the production of long-lived radioactivity, generating only low-level waste (similar to hospital and industrial wastes) for near-surface geological disposal or, preferably, recycling and clearance. Further, an advanced fuel cycle could reduce the radioactivity level by orders of magnitude to minimize the environmental consequences of fusion.

Although fusion science has progressed significantly since its inception in the early 1950s, it has been demonstrated only on a relatively small scale. The International Thermonuclear Experimental Reactor (ITER) in Cadarache, France [1], and the National Ignition Facility (NIF) at Lawrence Livermore National Laboratory (LLNL) in the United States [2] are the largest experiments that respectively use magnetic and inertial confinement methods to achieve and control the plasma. Neither experiment will convert fusion energy into electricity, but both intend to reach energy breakeven conditions and solve many scientific and technical issues and further advance the fusion knowledge database. After almost 50 years of research, achieving fusion energy still remains challenging. Much more R&D effort is required before fusion becomes commercially available as a viable power source. Before fusion joins the commercial market, all the fusion power core components and subsystems need to be developed, prototyped, and validated for inclusion in a demonstration (demo) power plant. This development effort will require additional facilities, such as an advanced physics experiment, a materials test facility, and a component test facility. With sufficient funding and governmental support, it is conceivable the commercial phase of fusion could begin as early as 2035.

To expedite fusion development, many researchers suggested a departure from the primarily stated goal of making electricity and proposed a number of non-electric applications, such as hydrogen production, breeding fissile fuels, transmutation of fission waste, production of medical radioisotopes, desalination of water, space propulsion, explosives detection, and altering materials properties etc [3]. These applications take advantage of the neutron-rich fusion system and offer near-term opportunities to advance fusion development with modest physics and technology requirements. If successful, the world will retain interest in fusion and recognize its potential contributions to the society before fusion penetrates the commercial market as a base-load electrical power station.

5.2 FUSION CONCEPTS

The main concepts that confine the hot plasma for a sufficiently long time to produce energy are magnetic and inertial. In magnetic fusion, magnets generate intense magnetic fields to squeeze the hot plasma (at 100 million $^\circ$C or more) and keep it away from the surrounding walls. The very low-density plasma ($\sim 10^{20}$ particles/m^3) could be sustained by external energy sources (such as radio frequency or neutral beam heating and current drive subsystems in existing fusion experiments) or by self-heating of the alpha particles produced by fusion reactions. In inertial fusion, beams of laser, light ions, heavy ions, or X-rays focus down on tiny targets containing D-T fuel, thus creating very high-density plasma ($\sim 10^{32}$ particles/m^3) under high pressure (to overcome the inertia of the particles) and confine the plasma long enough to ignite and fuse the fuel elements and produce energy.

For decades, continued investigation and development of magnetic and inertial confinement concepts have been conducted for a wide range of design approaches in the United States, Europe, Japan, Russia, and China. Magnetic fusion now encompasses seven concepts: the tokamak, stellarator, spherical torus (ST), reversed-field pinch (RFP), spheromak, field-reversed configuration (FRC), and tandem mirror (TM). The inertial fusion includes the laser and ion (light and heavy) with both direct and indirect drive target

and the Z-pinch driven systems. The physics and design of the magnetic and inertial fusion power cores are quite different at a large scale, but there are many similarities in the technical details. There are distinct differences between the drivers, heating, and current drive systems. On the other hand, there are many near-identical systems in the turbine and electric plants, remote handling equipment, hot cells, fuel cleanup systems, plant control systems, and others. The differences and similarities exist also among magnetic fusion energy (MFE) concepts and among inertial fusion energy (IFE) concepts, but to a lesser extent.

5.3 MAGNETIC FUSION

A wide range of magnetic research programs is ongoing around the world [4]. In the early 1950s, there were four magnetic confinement fusion concepts pursued internationally: tokamak, stellarator, mirror, and pinch. During the 1970–2010 period, more than 50 conceptual power plant studies have addressed the physics, engineering, and technical challenges of all seven magnetic fusion concepts: four original concepts plus ST, FRC, and spheromak concepts. Ultimately, the success of any concept as an energy source will depend on the economical competitiveness of its cost of electricity in the 21st-century energy market.

Figure 5.1 displays the timeline of the 58 large-scale magnetic fusion power plants designed since the early 1970s by research teams in the United States and abroad. Numerous conceptual commercial plant designs were developed for tokamaks—the leading magnetic concept. The decade of the 1980s witnessed a transition period aimed at temporarily suspending the U.S. tokamak studies in order to investigate alternate concepts: stellarator, ST, RFP, spheromaks, FRC, and TM. In the late 1980s, the United States decided to pursue all concepts, except tandem mirrors.

5.3.1 Tokamaks

The tokamak is a toroid (donut) configuration with elliptical D-shaped plasma. Typically, 16 equally spaced toroidal field (TF) coils confine the plasma, as shown in Figure 5.2, along with approximately 10 poloidal field (PF) coils external to the TF coils. A set of divertor, equilibrium field, and central solenoid coils is necessary to further shape and position the plasma within the toroidal vessel. A defining tokamak feature is a current flowing through the plasma that generates a helical component of the magnetic field for plasma stability. Tokamaks are capable of reaching steady-state operating conditions using current drive systems with radio frequency or neutral beam subsystems. The plasmas of tokamaks (and other magnetic configurations) may suffer instabilities that lead to disruption or edge-localized modes where the plasma bulges out, contacts the wall, and damage it. All tokamaks employ divertors in either single or double null configurations to collect the particles, ions, and electrons that escape the magnetic field lines.

The first tokamak experiment began in 1956 in Kurchatov Institute, Moscow, and yielded impressive results and thrust the tokamak confinement scheme to the forefront. Since then, the confinement concept has been successfully demonstrated with approximately 35 experiments operating around the world [5]. The international collaborative effort materialized in the design and construction of ITER in France [1] by a consortium that has grown to include seven parties: the European Union, Japan, United States, Russia, China, South Korea, and India. ITER will further advance the fusion physics and technology knowledge and help the transition from the present fusion experimental basis toward the goal of disruption-free, electricity-producing power plants.

At present, the tokamak concept is more advanced than any of the other six magnetic fusion concepts. High-power-density tokamaks, desired for economic reasons, are compact with significantly higher performance requirements than existing experiments [6]. Some of these requirements are advanced plasma physics, high-performance first walls (>5 MW/m^2 neutron wall loading), advanced divertor systems (>10 MW/m^2 heat flux), high magnetic fields ($\geq$ 16T), and long-lived, radiation-resistant (>200 displacements per atom), low-activation, recyclable materials.

5.3.2 Stellarators

Stellarators cover a variety of configurations and more diverse parameter space than tokamaks. The prime interest in this concept stems from the potential physics advantages over tokamaks in that the complex stellarator TF coils create a helical field that does not require a large toroidal current in the plasma. Stellarators are inherently steady-state devices with no need for large plasma current, no external current drive, no risk of plasma disruptions, and low recirculating power. The downside issues are a very complex TF magnet coil system that complicates access to the internal power core.

Several operational and under construction experiments (such as HSX in United States, LHD in Japan, and W7-X in Germany) intend to approach fusion-relevant conditions. Although the stellarator concept has been around for several decades, only six large-scale conceptual design studies have been performed internationally (refer to Figure 5.1). Figure 5.3 displays an isometric of the most recent ARIES-CS compact stellarator design [7]. The in-vessel components tightly conform to the plasma that changes around the torus. In the case of ARIES-CS, the plasma has three field periods. The shapes of all

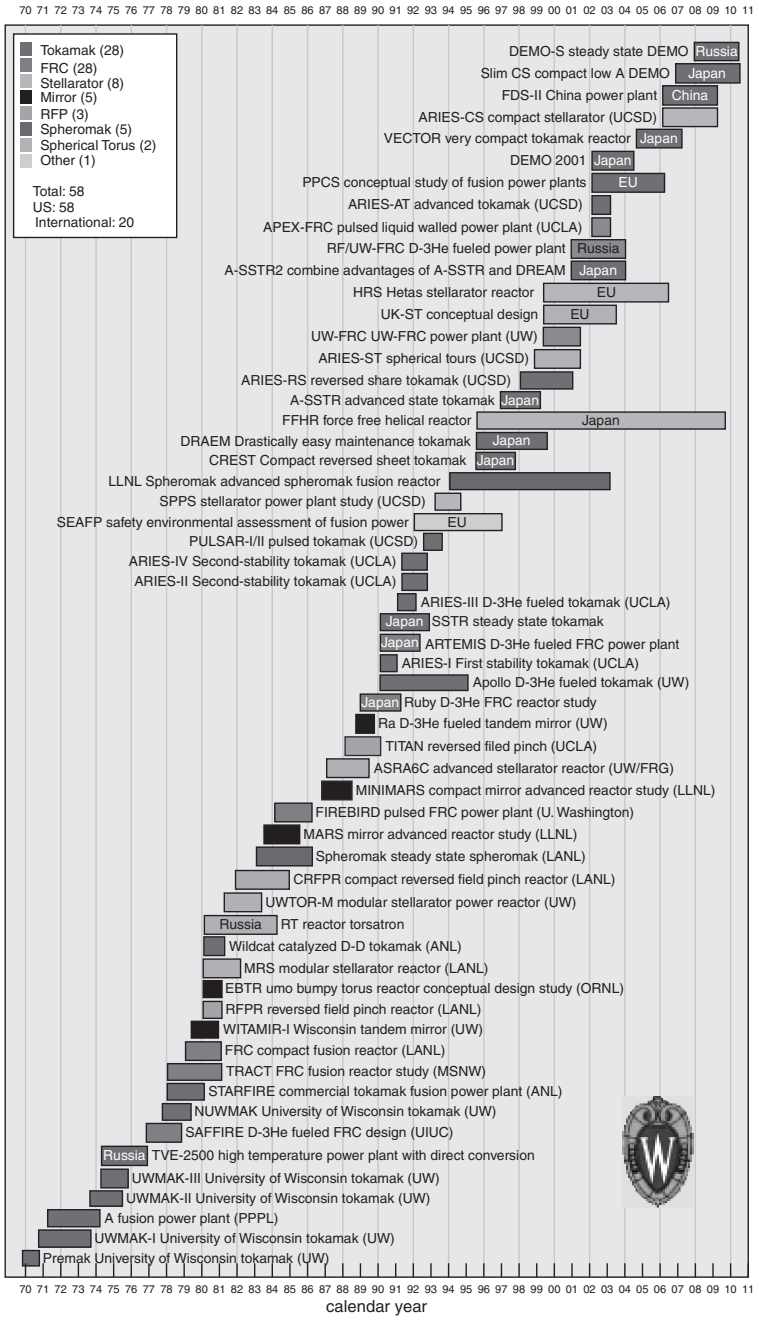

Figure 5.1 MFE timeline of large-scale conceptual power plant designs developed in the United States (38 - unmarked) and abroad (20 - marked).

power core components vary both toroidally and poloidally, representing a challenging 3-D physics and engineering problem and making the design of in-vessel components, overall integration process, and maintenance scheme much more complex than tokamaks with much fewer common parts. Nevertheless, interest in the stellarator concept increased over the years because of physics advantages and advances in construction techniques.

5.3.3 Spherical Tori

Interest in the ST concept began in the 1980s when Peng et al. [8] identified unique physics features for ST as a device with low aspect ratio (<2—ratio of plasma major to minor radii). Geometrically, the ST device is skinny radially and tall (see Fig. 5.4) with a central hole to accommodate the inner legs of the TF coils and their shielding [9]. This highly elongated shape is quite different from

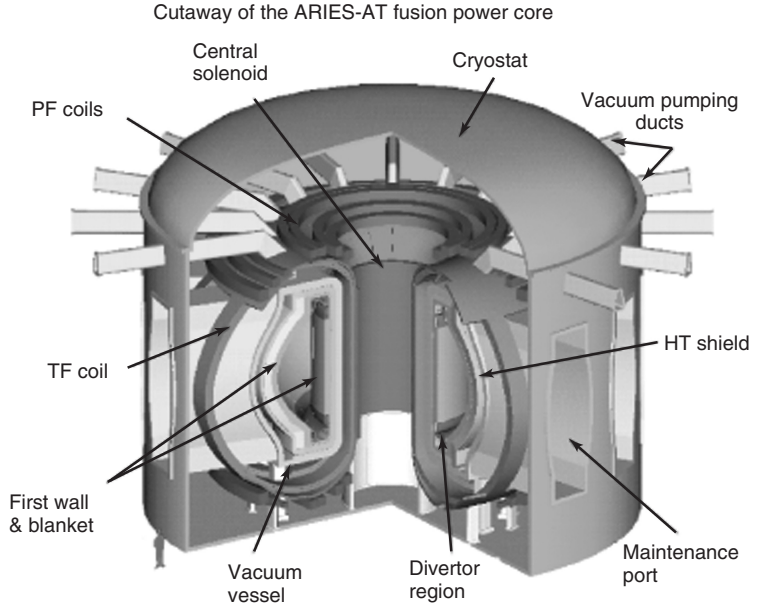

Figure 5.2 Isometric view of ARIES-AT advanced tokamak [6].

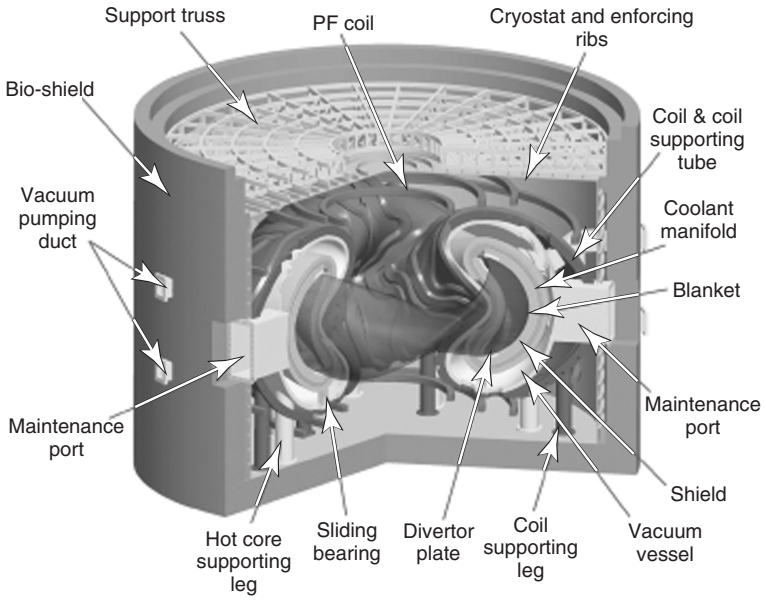

Figure 5.3 Isometric of ARIES-CS compact stellarator [7].

the donut D-shape plasma of tokamaks. Also, the toroidal magnetic field is two- to threefold less in STs compared to tokamaks, allowing normal, non-superconducting magnets with present-day technology and much less shielding requirements. However, the resistive losses in these normal magnets could be significant, requiring large recirculating power.

Among approximately 20 ST operational experiments around the world, NSTX in the United States and MAST in United Kingdom are the largest two facilities. Only two power plant studies have been made of the ST concept in the 1990s (see Fig. 5.1). Both the U.S. and U.K. studies identified the strengths and weaknesses of the ST concept as a power plant, in addition to a set of critical issues to be addressed by dedicated R&D programs.

5.3.4 Reversed-Field Pinches

The RFP configuration is much like a tokamak except for the more than ten-fold weaker toroidal magnetic field. The

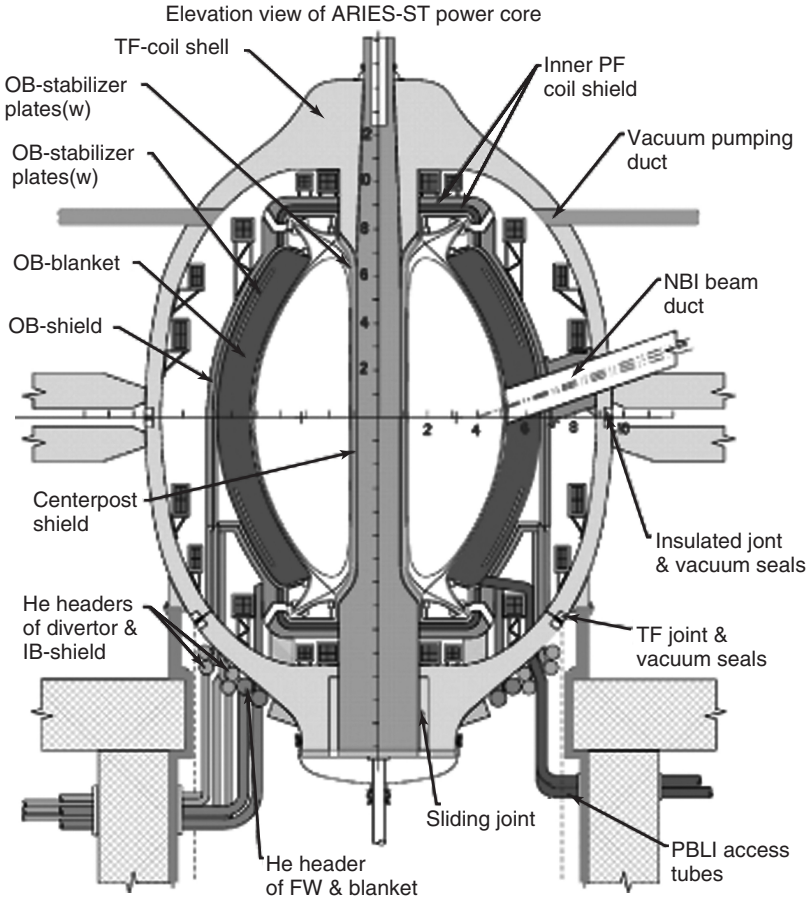

Figure 5.4 Elevation view of ARIES-ST spherical torus [9].

dominant magnetic field at the plasma edge is poloidal. Moving radially away from the plasma axis, the toroidal field reverses its direction, hence the name reversed-field. Figure 5.5 displays the general arrangement of the sole 1990 TITAN power plant design [10]. The weakly applied toroidal magnetic field leads to positive attributes, including high mass power density, compact design with favorable economics, normal (non-superconducting) coils with less shielding, and a single-piece maintenance system with high system availability. A challenging engineering issue is how to handle the intense neutron flux at the wall and surface heat flux at the divertor. The present RFP experiments (such as MST in the United States) aim to validate the TITAN strong, unproven physics assumptions.

5.3.5 Spheromaks

Spheromaks confine the roughly spherical plasma in a cylindrical structure using only a small set of external stabilizing coils as shown in Figure 5.6 [11]. The toroidally symmetric configuration is distinguished from STs and tokamaks by the simple, compact geometry without TF coils and with no inboard center post or materials, offering a truly compact fusion device with very low aspect ratio. A distinct feature of spheromaks is that the confining magnetic fields are self-generated by the plasma. Although the overall design is simple, the plasma dynamo behavior is very complex and difficult to predict or control as it often involves magnetic fluctuations and turbulence.

5.3.6 Field-Reversed Configurations

Geometrically, FRC is a linear, open-ended cylindrical system, quite different from the tokamak and the other toroidal devices. It represents one of the simplest configurations that can be envisioned for a fusion device. The cylindrical chamber permits easy construction, access, and maintenance of all components. The plasma configuration consists of closed and open field lines. The latter guide the charged particles to the chamber ends, offering the possibility of direct energy conversion with efficiencies approaching 60%. Over the past two decades, the FRC has been an important platform for investigating the potential advantages of the advanced D-^{3}He fuel cycle. Figure 5.7 shows a schematic

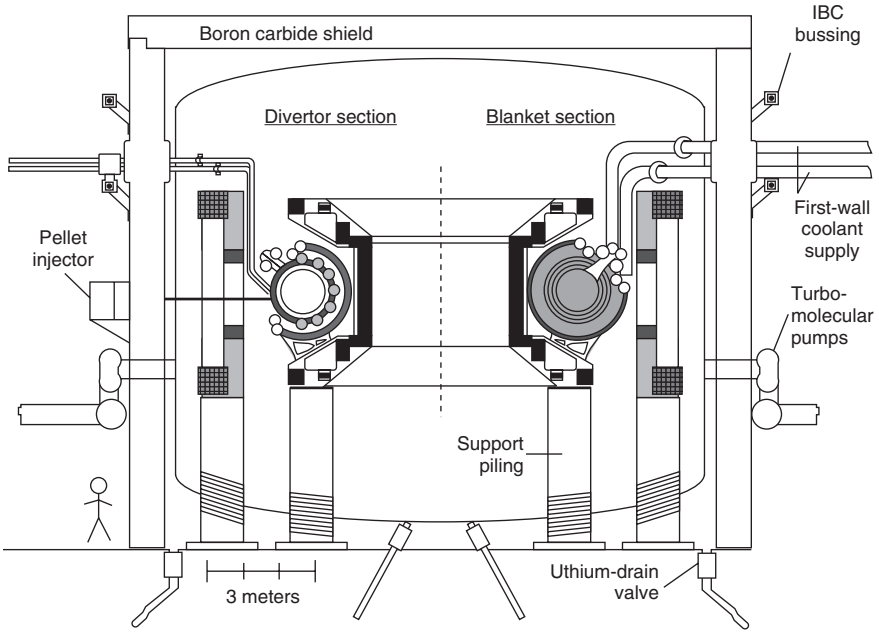

Figure 5.5 Vertical cross section of TITAN-I reversed-field pinch design [10].

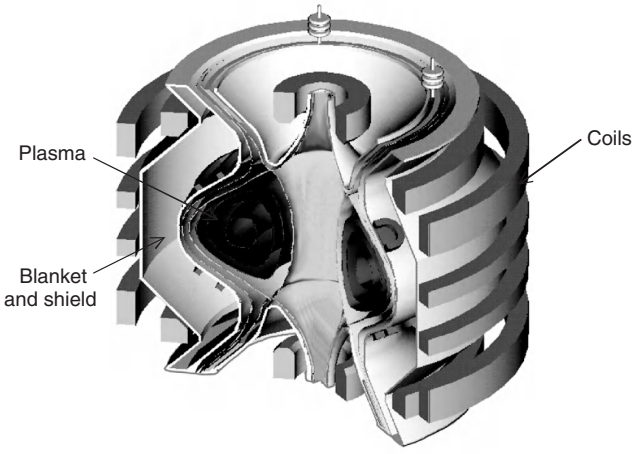

Figure 5.6 Schematic of spheromak power core [11].

of the ARTEMIS power plant [12] with a 25 m long chamber and a 4 m diameter. The remaining challenging issues are plasma stability, energy confinement, and an efficient method for current drive.

5.3.7 Tandem Mirrors

In contrast to tokamaks, tandem mirrors (TMs) are linear in nature, like FRCs. The basic configuration is a long central cell (90–170 m) terminated by end mirror cells. TMs are more amenable to maintenance of the central solenoid as compared to toroidal systems. Other positive attributes include the modest solenoidal magnet technology with ~5T, absence of driven plasma current eliminating disruptions, and the potential for the direct conversion of charged particle power into electricity at high efficiency. In the 1980s, four conceptual power plants were designed (refer to Fig. 5.1), fuelled with both D-T and D-^{3}He. Figure 5.8 demonstrates the D-T fuelled MINIMARS [13]. The United States terminated the TM program in 1986 in favor of the more promising tokamak and five other alternate concepts. Worldwide, the only TM experiment is GAMMA 10 in Japan, which is an educational device, rather than a facility for energy research.

5.4 INERTIAL FUSION

Shortly after the invention of laser in the early 1960s, scientists at the U.S. Lawrence Livermore National Laboratory suggested the implosion of D-T filled targets by laser beams for net energy production. The following decades witnessed serious research when more powerful and efficient lasers made inertial fusion appear more practical for generating net energy. However, some of the target physics basis remained largely classified until the mid 1990s. Besides the electron beam pumped krypton fluoride (KrF) laser and diode pumped solid state laser (DPSSL), other drivers have been identified: light ions, heavy ions (with induction or radiofrequency linac accelerators), and Z-pinches. All drivers share a strong commonality: they deliver very short time pulsed energy to compress a small target (containing

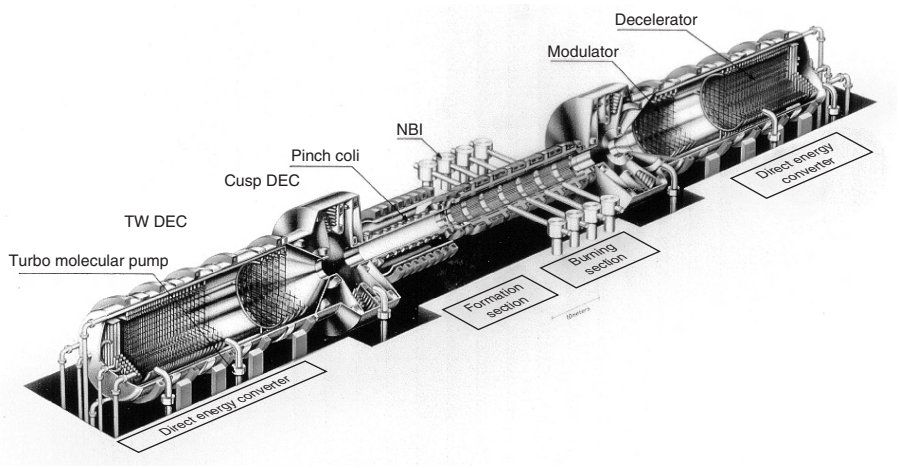

Figure 5.7 Layout of ARTEMIS D-^{3}He fuelled field-reversed configuration power plant [12].

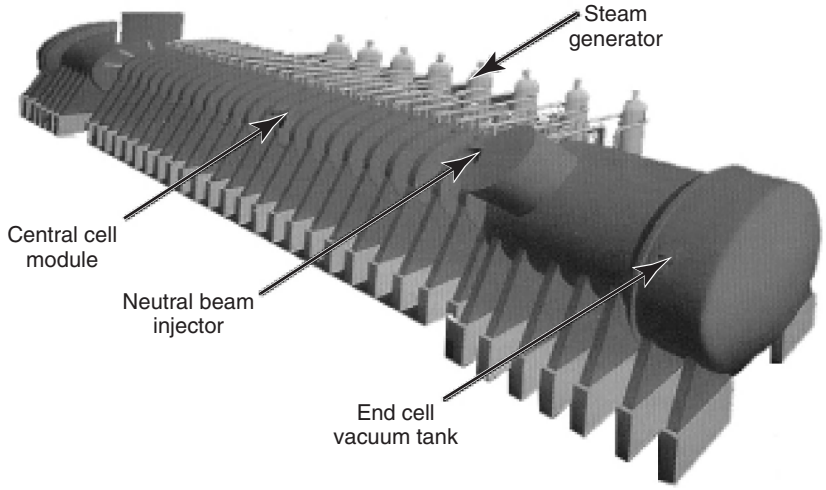

Figure 5.8 MINIMARS layout [13].

the fusion fuel) to reach a plasma state, overcome the inertia and repulsive forces between the fast moving ions, fuse and burn the D-T fuel.

The targets are defined as either direct drive or indirect drive targets (see Figure 5.9). The former is typically cryogenic with many different layers to aid in the compression and heating of the D-T fuel. The most desirable condition is to symmetrically compress a spherical target uniformly from all angles. The complexity of equally dividing the beam power over many beam lines is challenging. In practical terms, the number of beam lines is limited, which introduces non-symmetrical illumination resulting in instabilities and disturbances that grow as the target is compressed. The indirect drive nominally uses two sets of beam lines to direct the compression energy to the target. The target has a much more complex geometry with the D-T fuel contained in a capsule within a metal hohlraum (a German name for hollow area). The beams enter the hohlraum from opposite sides, interact with the hohlraum materials to create X-rays that symmetrically compress and heat the interior fuel capsule and fuse the D-T fuel to ignition. More recently, the fast ignition approach was introduced to separate the compression and heating phases where laser beams compress the D-T fuel to high density, then a short-pulse laser beam ignites the target. The main advantages of the fast ignition approach are the relaxation of the symmetry requirement for imploding the capsule and the reduced laser-driver energy.

The principle of laser and ion inertial fusion is to direct beams at targets that are injected to the center of spherical or cylindrical chamber multiple times a second to create a near-continuous flow of power to the solid or liquid

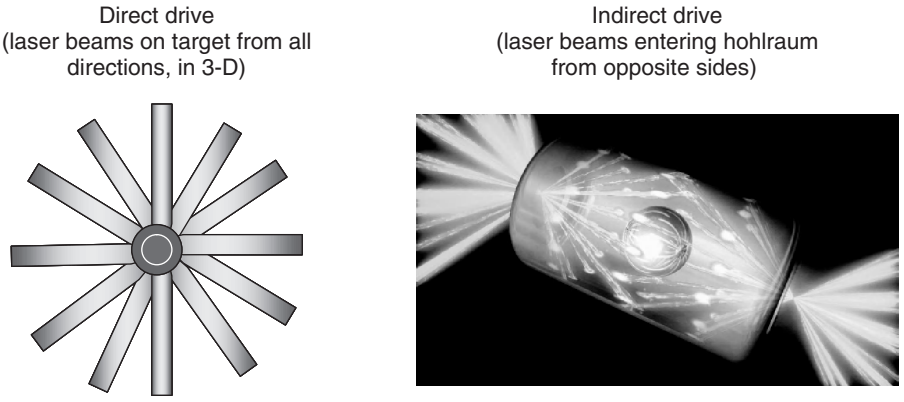

Figure 5.9 Schematic of direct drive target and NIF indirect drive target.

chamber walls. The cryogenic targets must be injected at very high speed to arrive at the center of the chamber intact, at cryogenic temperature, and at the right orientation (in the case of indirect drive targets). This is difficult because the wall of the chamber is quite hot from the previous shot, and the internal atmosphere is turbulent from pumping out the remains of the prior shot. This should happen multiple times a second. There will likely be an active tracking system to initiate the firing sequence of the beam lines. After each shot, all (or most of) the remains of the target must be removed from the chamber. Then the entire sequence is repeated many times a second.

Besides the driver and target, every IFE system requires a spherical or cylindrical chamber where the energy from the fusion reaction is deposited in a blanket and/or shield surrounding the target. The IFE core does not need magnets as in magnetic fusion. Rather, the chamber contains only the blanket and/or shield with the essential penetrations for the laser or ion beams and vacuum ducts. The chamber is quite large to reduce the very brief pulse of energy on the chamber wall surface. Existing experiments are single-shot facilities where the target ignites once every few hours, day, or week. Recently, NIF at LLNL [2] has only fired one shot per day. For power plants, ignition must be done on a repetitive basis, i.e., many times per second. Development is underway to increase the repetition rate required for IFE power plants.

When the target ignites, it emits an intense burst of radiation (X and gamma rays), alpha particles, neutrons, and target debris (from materials surrounding the D-T capsule). Besides breeding tritium, the prime role of the blanket is to convert the kinetic energy of the radiation and particles into thermal energy to be converted into electricity. The heat flux, pressure pulses, thermal stresses, and neutron flux create intense challenges to the integrity of a bare first wall. Most chamber designs increase the distance from the target to the solid wall and/or employ a sacrificial layer to protect the solid wall against the X-rays and target debris [14]. Mitigating options include filling the chamber with gas, attaching tiles to the wall, using thin liquid fluid as a protective layer, and having free-flowing thick liquid metal walls. The time-dependent pressure from evaporation and recondensation of materials within the chamber is very complex. Before each shot, the chamber atmosphere must be reconditioned by removing all target debris and ablated materials in a fraction of a second—a challenging task.

Beginning in the early 1970s and continuing to the present, numerous conceptual power plants based on inertial fusion have been designed in the United States, Japan, and Russia. Figure 5.10 displays the timeline of 50 large-scale conceptual designs developed to date. The following three subsections present a few examples of the most recent conceptual designs: a laser-driven system with solid wall chamber, a light/heavy ion beam driven system with thin/thick liquid wall chamber, and Z-pinch driven system with thick liquid wall chamber. These designs deliver 1 GW_e of net electric power. Like MFE concepts, all IFE concepts are at an early stage of development. More simulations, experiments, and testing have yet to be done to solve and validate the key engineering issues and remaining challenges [15].

5.4.1 Laser-Driven System

In all 28 conceptual laser power plants developed to date, the design consists of a chamber, a laser driver, an array of identical laser beam lines, a target factory, a target injector, a set of optics, and an electrical generator. These are shown schematically in Figure 5.11a, with the exception of the driver and thousands of special lenses and mirrors (placed outside the chamber) that focus the powerful laser beams on the target. Two major laser-driven systems have recently been proposed: the High Average Power Laser (HAPL) [16] and the Laser Inertial Fusion Engine (LIFE) [17]. The latter is based on NIF physics and technology and presently under development at LLNL.

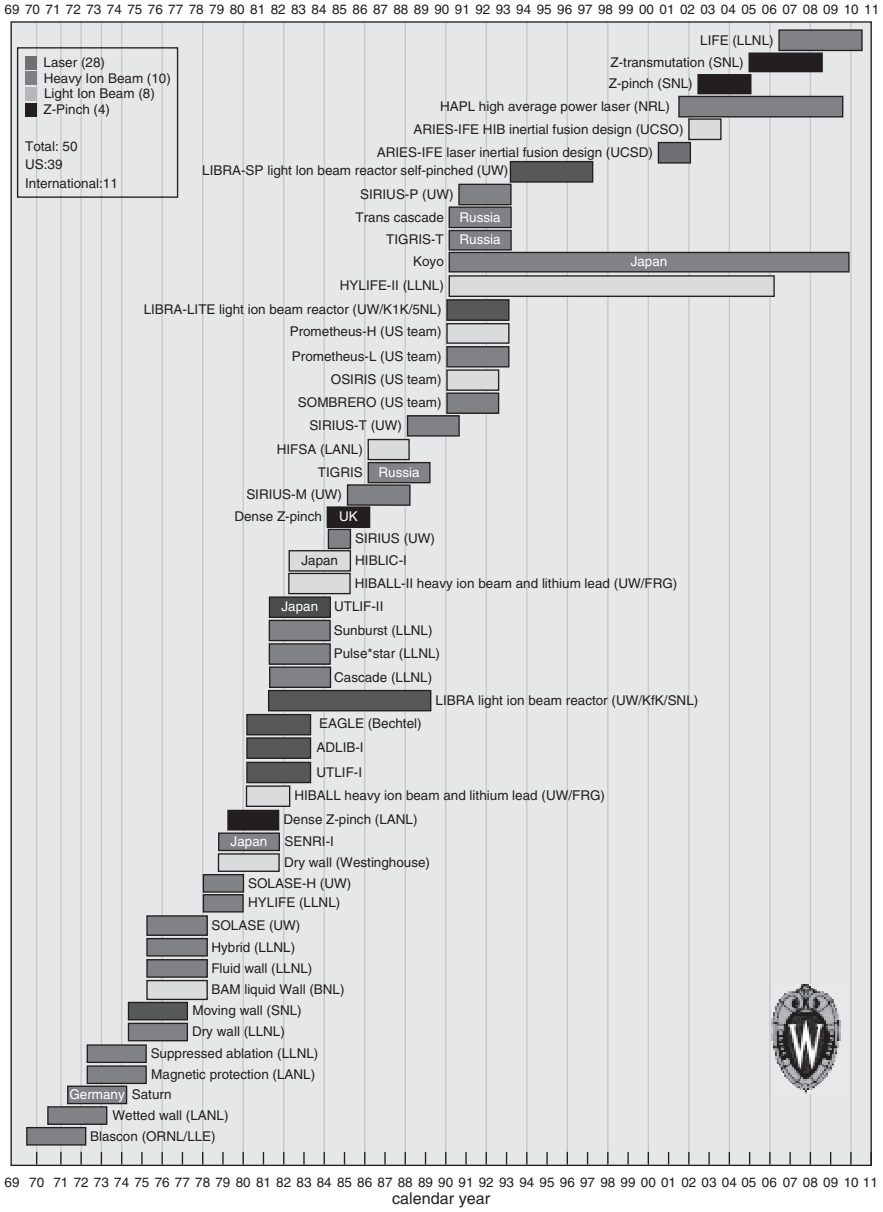

Figure 5.10 Timeline of large-scale IFE conceptual power plant designs developed in the United States (39 - unmarked) and abroad (11 - marked).

The U.S. Naval Research Laboratory (NRL) developed the HAPL conceptual design with direct-drive target and dry wall chamber [16]. In this concept, 40 high intensity laser beams symmetrically compress and heat the D-T target every 0.2 second to obtain a near-continuous power production. Two types of lasers were developed: DPPSL at LLNL and the KrF at NRL. Simulations predict higher target gain (performance) with KrF lasers owing to the shorter wavelength and smoother beam quality. But both types of lasers are viable for fusion energy. During the 2000s, the program addressed the critical components needed for laser IFE, including target fabrication, target engagement, target injection, final optics, and fusion chamber and materials research. One key chamber issue is the survivability of the solid wall under ion bombardment from the target. Two chamber concepts were pursued. In one approach, the chamber is made large enough (21 m in diameter) to withstand the emissions from the target. In another, shown in Figure 5.11b, a relatively modest magnetic field is used to divert the ions (the most damaging component of the target emissions) into external dumps. The HAPL program stressed experimental

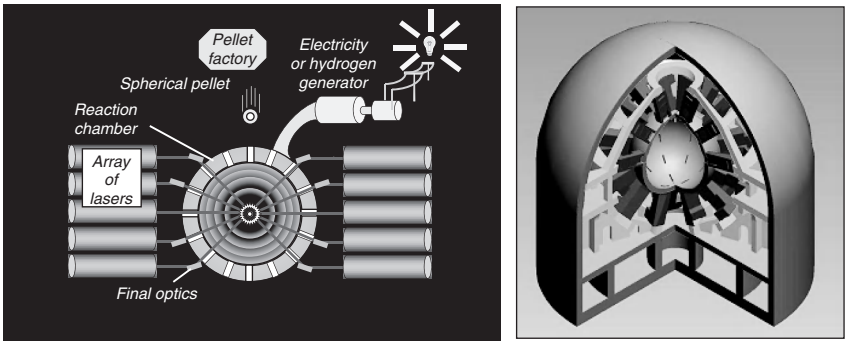

Figure 5.11 (a) Schematic of the essential components for laser driven systems. (b) Cutaway view of HAPL power plant [16].

validation, predictive capability, and the development of fusion energy with a multidisciplinary integrated systems approach. Credible solutions were proposed for much of the needed key technologies.

5.4.2 Ion-Beam Driven System

Pulses of ions (light or heavy) could be delivered to the D-T target using accelerators and/or diodes with several techniques for beam propagation. The intense X-rays and target debris from the target require either wetted wall or thick liquid wall to protect the structure of the chamber. Common design issues are the generation of mist from the chamber liquid walls (vaporized by X-rays) and the mechanism of chamber clearing. Several ion beam driven systems have been proposed (e.g., HIBALL-II [18], Prometheus-H [19], LIBRA-SP [20], and HYLIFE-II [21]).

The **Light Ion Beam ReActor-Self-Pinched** (LIBRA-SP) explored the implications of transporting 24 self-pinched light ion (Li) beams from diodes to a direct drive target located at the center of a chamber. It is an upright cylinder, as shown in Figure 5.12, with many

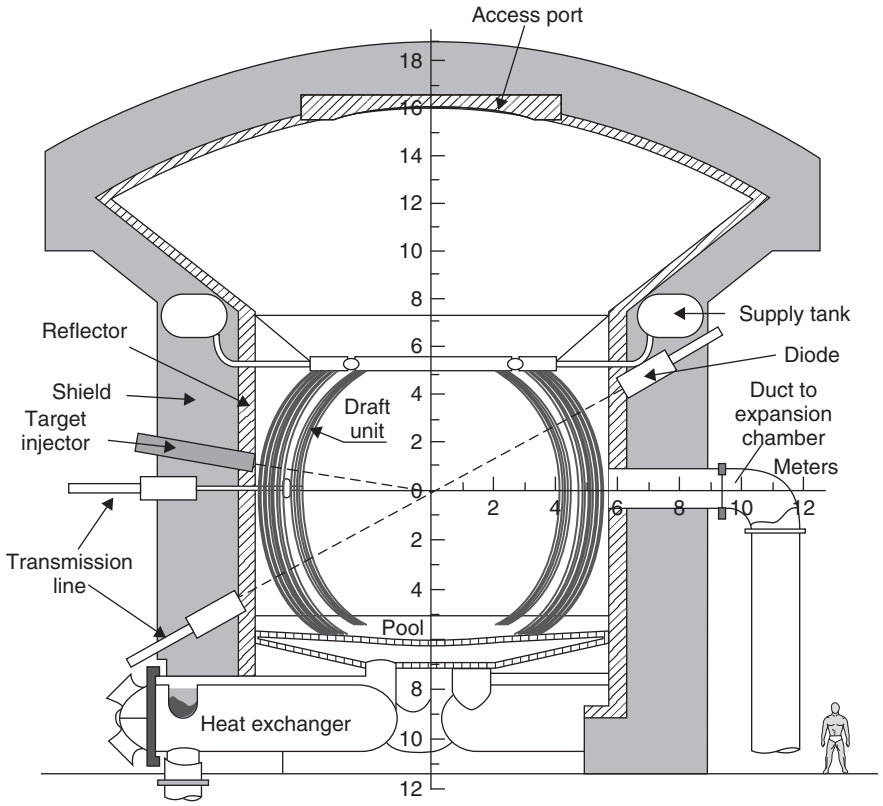

Figure 5.12 LIBRA-SP power plant conceptual design [20].

rigid (to withstand shocks), perforated (to maintain LiPb wetted surface) ferritic steel tubes through which the LiPb breeder/coolant flows. After the shot, a portion of the wetted surface is rapidly vaporized by the X-rays while the target debris is deposited in the just-created LiPb vapor. Six large expansion tubes behind the blanket midplane connect the chamber to an expansion tank that provides volume for the vapor to expand and condense. The LiPb eventually collects in a pool at the base of the chamber, then drains and flows to the heat exchanger before circulating back into the chamber [20].

The **High Yield Lithium-Injection Fusion Energy, version 2** (HYLIFE-II) uses heavy ion beams to heat the target. The driver requires tens of beams from each side of the indirect-drive target (a hohlraum containing a D-T capsule) with final focusing magnets just outside the chamber [21, 22]. Oscillating jets of a molten salt coolant/breeder LiF-BeF2 (called Flibe) are injected around the target in a bell-shape chamber to form a protective blanket and shield (see Figure 5.13). The thick Flibe absorbs the X-ray and debris energies from the target. The Flibe jets expand and disassemble after each shot, increasing the surface area of the liquid and shortening the condensation time of vaporized materials. The chamber is then cleared and the Flibe jets are reestablished in ~0.2 second before the next shot.

5.4.3 Z-Pinch Driven System

The Z-pinch IFE represents a unique class of inertial confinement where a confining magnetic field is produced by a flowing current in a wire array, a puff of gas, or a single fiber. All Z concepts have very high plasma density—a characteristic of an IFE plasma. Achieving a simple linear pinch has been a difficult task. Over the years, scientists identified numerous engineering and physics issues that are not easily solvable for the linear Z-Pinch in particular [23, 24].

In 2005, the Sandia National Laboratories in Albuquerque, New Mexico, developed a spherical Z where the pinch produces X-rays that are used to implode the pellet [25]. Basically, a powerful electric current flows in an array of thin tungsten (or steel) wires surrounding a target containing a D-T capsule. The Recyclable Transmission Line (RTL) connects the pulsed power driver to the target. The high current (~90 MA) vaporizes the wires forming plasma curtain and a strong magnetic field that compresses the plasma, producing high temperature and X-rays that create a shock wave in the target structure, causing the D-T fuel to burn. The RTL is destroyed after each shot, recovered, then a new one is inserted at the top of the 5 m radius chamber, and the process repeats every 10 seconds. Because of the large amount of RTL steel, it must be recycled with advanced remote handling equipment. The fusion yield is quite high (~3 GJ for 1 GW_e plant) relative to other IFE systems (typically <0.5 GJ). Therefore, shock mitigation is a serious issue for Z-pinch and mandates protection of the chamber wall with approximately 65 cm liquid Flibe. Multiple chambers (each cycled every 10 seconds) of the type shown in Figure 5.14 are necessary to deliver the 1 GW_e net output power.

5.5 FINAL REMARKS

Inherent safety, minimal environmental impact, and plentiful, widespread fuel sources are the most notable features for fusion when compared to other energy sources. The fuel, in particular, is abundant and politically more secure and environmentally friendly than uranium or fossil fuels. The plasma contains less than 1 gram of D-T fuel, and there is no possibility of uncontrolled fusion reactions. Even in the case of a severe accident, the low decay heat within the power core precludes melting the structure. The ability to generate only short-lived byproducts and recycle all activated fusion materials significantly minimizes the radwaste burden for future generations. All these salient features would help gain positive public perception and acceptance for fusion, providing proper dissemination of information to the public. Nevertheless, fusion is not commercially available yet. It still has a long lead-time from

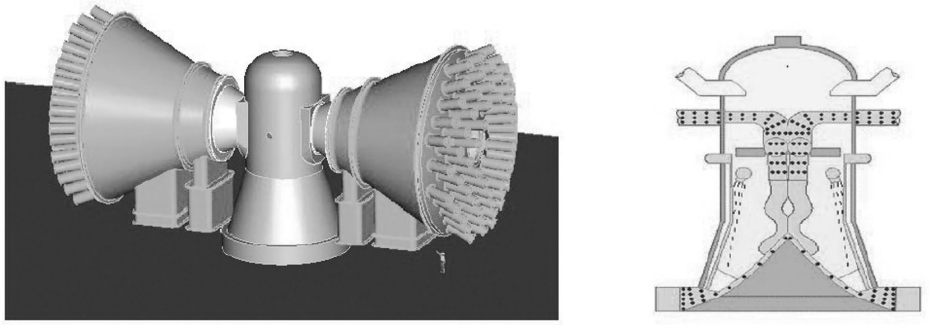

Figure 5.13 Isometric of HYLIFE-II (left) showing heavy ion beams to ignite two sides of target, and vertical view of chamber (right) [22]. Not to scale.

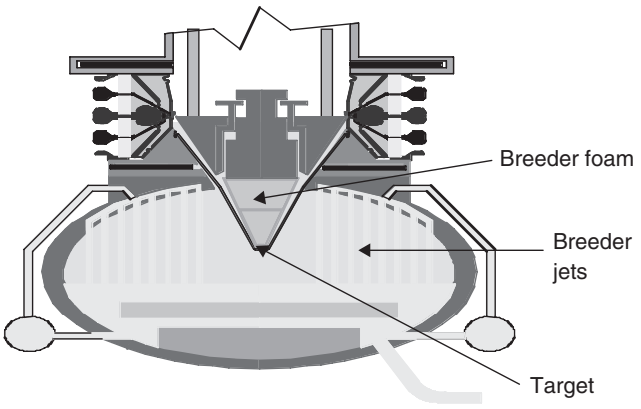

Figure 5.14 Z-pinch chamber [25].

existing experimental devices (ITER and NIF) to putting power on the grid. An electricity-generating fusion plant requires advances in target design and injection, materials development, blanket, divertor, magnet, safety assurance, component reliability, maintenance verification, and power handling. At present, the worldwide MFE and IFE fusion efforts focus on developing more advanced physics and technology, reducing the complexity of all fusion concepts, and improving their economics.

Acknowledgments

The author is extremely thankful to Prof. G. Kulcinski (UW), L. Waganer (Boeing consultant), L. Cadwallader (INL), and J. Sethian (NRL) for their inputs and/or reviews. Special thanks are extended to D. Bruggink (UW) for providing the timelines of MFE and IFE power plants.

REFERENCES

1. The ITER Project. http://www.iter.org, accessed March 2010.
2. The NIF Project. https://lasers.llnl.gov, accessed March 2010.
3. L. Waganer, Assessing a new direction for fusion. *Fus. Eng. Des.,* 2000, **48**, 467–72.
4. L.A. El-Guebaly, History and evolution of fusion power plant studies: past, present, and future prospects, in *Nuclear Reactors, Nuclear Fusion and Fusion Engineering*, A. Aasen and P. Olsson (ed.), NOVA Science Publishers, Inc., Hauppauge, NY, 2009, pp. 217–71.
5. Worldwide Tokamak Experiments. http://www.toodlepip.com/tokamak/conventional-large-tokamaks.htm, accessed March 2010.
6. F. Najmabadi, A. Abdou, L. Bromberg, T. Brown, V.C. Chan, M.C. Chu et al., The ARIES-AT Advanced Tokamak, advanced technology fusion power plant. *Fus. Eng. Des.,* 2006, **80**, 3–23.
7. F. Najmabadi, A.R. Raffray, and the ARIES-CS Team, The ARIES-CS compact stellarator fusion power plant. *Fus. Sci. Tech.,* 2008, **54**(3), 655–72.
8. Y.K.M. Peng, and D.J. Strickler, Features of spherical torus plasma. *Nuclear Fusion*, 1986, **26**, 576.
9. F. Najmabadi and the ARIES Team, Spherical torus concept as power plants–the ARIES-ST study. *Fus. Eng. Des.,* 2003, **65**(2), 143–64.
10. F. Najmabadi, R.W. Conn, N. Ghoniem, J. Blanchard, Y. Chu, P. Cooke, et al., The TITAN Reversed-Field-Pinch Fusion Reactor Study, final report. University of California, Los Angeles UCLA-PPG-1200, 1990.
11. E.B. Hooper, and T.K. Fowler, Spheromak reactor: physics opportunities and issues. *Fusion Technology*, 1996, **30**, 1390–94.
12. H. Momota, A. Ishida, Y. Kohzaki, G.H. Miley, S. Ohi, et al., Conceptual design of the D-^{3}He reactor ARTEMIS. *Fusion Technology*, 1992, **21**, 2307.
13. J.D. Lee (ed.), *MINIMARS Conceptual Design: Final Report*. Lawrence Livermore National Laboratory Report, UCID-20773, 1986.
14. W.J. Hogan, (sci. ed.), *Energy from Inertial Fusion*, STI/PUB/944, International Atomic Energy Agency, Vienna, Austria, 1995.
15. W.R. Meier, A.R. Raffray, S.I. Abdel-Khalik, G.L. Kulcinski, et al., IFE chamber technology—status and future challenges. *Fus. Sci. Tech.,* 2003, **44**, 27–33.
16. J.D. Sethian, D.G. Colombant, J.L. Giuliani, R.H. Lehmberg, et al., The science and technologies for fusion energy with lasers and direct-drive targets. *IEEE Trans. on Plasma Sci.,* 2010, 690–703.
17. LIFE. https://lasers.llnl.gov/about/missions/energy_for_the_future/life, accessed March 2010.
18. B. Badger, K. Beckert, R. Bock, D. Boehne, I. Bozsik, J. Brezina, et al., *HIBALL-II—aAn Improved Conceptual Heavy Ion Beam Driven Fusion Reactor Study*. University of Wisconsin Fusion Technology Institute Report, UWFDM-625, 1984. http://fti.neep.wisc.edu/pdf/fdm625.pdf
19. L.M. Waganer, D.E. Driemeyer, V.D. Lee, R.L. Calkins, et al., *Inertial Fusion Energy Reactor Design Studies, Prometheus-L & Prometheus-H*, Final Report, McDonnell Douglas Aerospace Team, DOE/ER54101, MDC92E0008, 1992.
20. B. Badger, D. Bruggink, P. Cousseau, R. Engelstad, et al., *LIBRA-SP: A Self-Consistent Design of a Commercial Fusion Power Plant Based on Self-Pinched Propagation of Ions*. Fusion Power Associates Report, FPA-94-6, 1994. http://fti.neep.wisc.edu/pdf/fpa94-6.pdf
21. R.W. Moir, R.L. Bieri, X.M. Chen, T.J. Dolan, et al., HYLIFE-II: a molten salt inertial fusion energy power plant design—final report. *Fusion Technology*, 1994, **25**, 5–25.
22. S.S. Yu, W.R. Meier, R.P. Abbott, J.J. Barnard, et al., "An updated design point for heavy ion fusion. *Fus. Sci. Tech.,* 2003, **44**, 266–73.

23. A.E. Robson, Prospects for fusion with dense Z-pinches," Dense Z-pinches, Third International Conference, London, UK, 1993. Published by American Institute of Physics. Proceedings 299 (1994): 707–715.

24. J.D. Sethian, "The Quest for a Z-Pinch Based Fusion Energy Source—A Historical Perspective, Dense Z-Pinches, Fourth International Conference, 1997, Vancouver, Canada. Published by American Institute of Physics. *Proceedings*, 1997, **409**, 3–10.

25. C. Olson, G. Rochau, S. Slutz, C. Morrow, et al., Development path for Z-pinch IFE. *Fus. Sci. Tech.,* 2005, **47**(3), 633.

6

BASIC CONCEPTS OF NUCLEAR FISSION

PAVEL V. TSVETKOV

Department of Nuclear Engineering, Texas A&M University, College Station, TX, USA

6.1 NEUTRON ECONOMY

In the nuclear fission process, energy is released as a result of division of an original heavy nucleus into two or more fission fragments. Examples of such heavy nuclides include U235, Pu239, Am242m, and others. Although ternary fissions are possible, binary events dominate in the secondary particle distributions where two fission fragments are formed. Nuclear fission events can be induced by collisions of heavy nuclei with elementary particles, e.g. neutron-induced fissions. In neutron-induced fission events, neutron collisions with heavy nuclei lead to compound nucleus formation. Unstable compound nuclei release their excitation energy through various channels including fission events.

As atomic weight increases, chances for spontaneous fission events increase, although $\alpha-$particle emissions typically dominate for the majority of radioactive nuclides. A selected group of heavy nuclides, including Pu241, Cm250, and Bk249, decays via $\beta-$particle emissions. The reaction energetics is governed by binding energy per nucleon. For fissile nuclides, such as U233, U235, Pu239, Pu241, fissions can be induced by neutrons of very low energies, while for fissionable nuclides, such as U238, neutron energies must exceed reaction threshold energies. Neutron capture events by such threshold-fissionable nuclides initiate transmutation chains, leading toward fissile nuclides, for example, U-Pu conversion chains.

Particle yields of neutron-induced fission reactions consist of light fission fragments, neutrons and other types of particles, and radiations. These secondary neutrons create a chain of fission events—fission chain reaction. The fission chain reaction can be controlled by managing neutron absorption and scattering as depicted in Figure 6.1. The neutron economy in a reactor system can be managed by maximizing probabilities of neutron moderation and fission events and minimizing parasitic neutron absorption. The factors limiting neutron economy optimization are the requirements of controllability and safety, economics and performance.

Today, on a large scale, fission energy is successfully recovered in nuclear fission reactors and converted into heat energy that is later transformed into electricity or utilized directly in heat processes. Man-made devices take advantage of both neutron-induced fission reactions and spontaneous fissions.

6.2 NUCLEAR FUEL APPROACHES

The probability of neutron capture leading to fission is larger for slow neutrons than for fast neutrons. Therefore, most common reactors are "thermal" reactors, that is, they utilize the higher thermal cross sections. The naturally occurring fuel is the fissile isotope of uranium—U235. As a result, the majority of nuclear reactors utilize this nuclide as a fuel. Alternative fuels include U233 (fissile nuclide produced from Th232) and Pu239 (fissile nuclide produced from U238). The best moderator has high moderation efficiency, low neutron absorption, high resistance to radiation and corrosion, and low cost. The moderators in commercial power reactors are graphite, ordinary water, and heavy water.

Naturally occurring uranium is composed of 0.7% U235 and 99.3% U238. This fraction of fissile U235 is too low

Nuclear Energy Encyclopedia: Science, Technology, and Applications, First Edition (Wiley Series On Energy).
Edited by Steven B. Krivit, Jay H. Lehr, and Thomas B. Kingery.

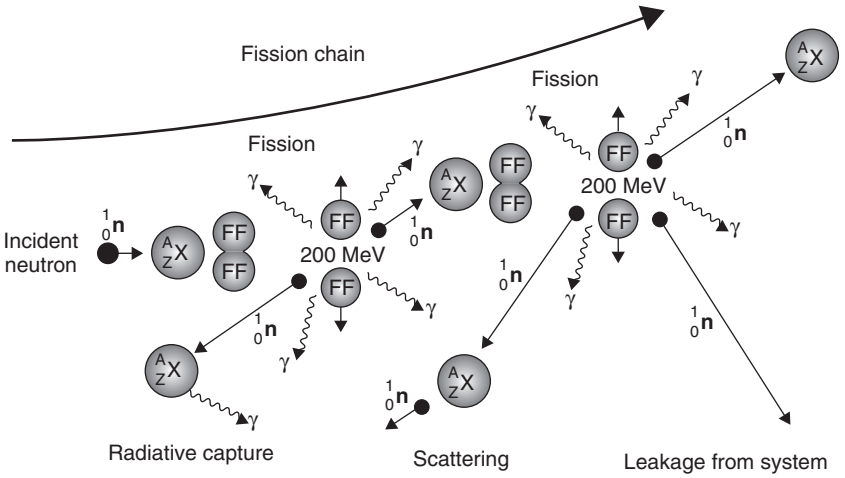

Figure 6.1 Fission chain reaction.

to sustain a fission chain reaction in combination with most neutron moderator materials. To achieve criticality, either the probability of fission must be enhanced by increasing fissile fraction (enrichment) or the moderator effectiveness must be enhanced by facilitating neutron, slowing down and reducing chances of parasitic neutron absorption. Some reactor designs, PWR, BWR, HTR, use enriched fuel in combination with inexpensive moderators like ordinary water and graphite. Other designs, such as CANDU, take advantage of natural uranium in combination with more expensive, but better as moderator, heavy water. Fast fissions in U238 contribute about 3–4% to the fission process in a typical thermal reactor. As mentioned above, some of the fertile U238 is converted to fissile Pu239. The most commonly used nuclear fuel material is uranium dioxide with various enrichments in U235. Some modern designs use mixed oxide fuels containing plutonium in their fresh fuel loadings.

6.3 REACTOR POWER, FUEL BURNUP, AND FUEL CONSUMPTION

When fuel is irradiated, a net decrease in heavy atoms occurs due to fission and the fuel is said to be burned or depleted. The term *burnup* is used as the measure of either the energy obtained from the burned fuel or the fraction of fuel that has fissioned (i.e., burned). The two units most widely used for reporting burnup of fuel are

$$\frac{MWd}{kg\ H.M.} \text{ and } atom\ \%;$$

$\frac{MWd}{kg\ H.M.}$ measures the energy obtained from irradiating fuel: The useful lifetime of fuel in a reactor is indicated by the burnup, this is a measure of the total amount of thermal energy generated per unit quantity of heavy atoms charged to the core,

$$\bar{B}_R\left(\frac{MWd}{kg\ H.M.}\right) = \frac{P_R(MW)\cdot T_f(\mathrm{d})}{m(kg\ H.M.)}.$$

This is the fission energy release per unit mass of fuel. When burnup is reported in MWd/kg H.M., the fuel mass in the denominator includes the initially loaded heavy atoms only (heavy metal (H.M.)). It does not include the oxygen in oxide fuel. The oxide fuel mass *m(kg Oxide)* (if used) must be multiplied by the ratio of the total fuel heavy atoms atomic weight $M(H.M.)$ to the oxide fuel molecular weight *M(Oxide Fuel)*, in order to obtain the heavy atoms mass *m(kg H.M.)* for use in calculating burnup:

$$m(kg\ H.M.) = m(kg\ Oxide)\cdot\frac{M(H.M.)}{M(Oxide\ Fuel)}.$$

In calculating burnup, one must be careful to distinguish between chronological time T_R and time at rated power, T_f. Time at rated power, T_f, is the product of a load factor (or capacity factor) f and a chronological time T_R. The load factor f is the fraction of chronological unit of time during which the reactor is operated at the thermal power level P_R:

$$\text{Time at rated power} = T_f = f\cdot T_R.$$

The reactor operation time between two core reloadings is called the refueling interval T_R. The fuel irradiation process begins at the time of reactor startup after refueling and ends when the reactor is shut down for subsequent refueling. The refueling interval T_R is given in chronological time. Thus, the average fuel burnup, $\bar{B}_R$ (MWd/kg H.M.), during the refueling interval T_R is

$$\bar{B}_R\left(\frac{MWd}{kg\ H.M.}\right) = \frac{P_R(MW)\cdot f\cdot T_R(d)}{m(kg\ Oxide)\cdot\frac{M(H.M.)}{M(Oxide\ Fuel)}};$$

atom % measures the fraction of heavy atoms in the fuel that undergo fission. The two burnup units are related to one another; the ratio of the specific energy value, $\bar{B}_R$ (MWd/kg H.M.), to the percent fission value, $\bar{B}_R$ (atom %), is:

$$\frac{\bar{B}_R\left(\frac{MWd}{kg\ H.M.}\right)}{\bar{B}_R(atom\ \%)} = \frac{\bar{B}_R\left(\frac{MWd}{kg\ H.M.}\right)}{\bar{B}_R\left(\frac{\%\ fissions}{atoms\ H.M.}\right)}$$

$$= \frac{6.023 \times 10^{26} \cdot \left(\frac{atoms\ H.M.}{kg - mol.\ H.M.}\right)}{\left[100 \cdot \left(\frac{\%}{absolute}\right) \cdot 2.9 \times 10^{16} \cdot \left(\frac{fissions}{MW \cdot s}\right) \cdot 0.864 \times 10^{5} \cdot \left(\frac{s}{\mathrm{d}}\right) \cdot 238 \cdot \left(\frac{kg\ H.M.}{kg - mol.\ H.M.}\right)\right]}$$

$$= 10.$$

6.4 FISSION REACTOR CONSIDERATIONS

The primary objective in the design and operation of a nuclear reactor is the utilization of the energy released by a controlled chain reaction of nuclear fission events maintained within the reactor core. Since 2 to 3 neutrons are released in every neutron-induced fission reaction, the probability of a sustained neutron chain reaction is obvious. In the proper environment of fissionable material, these fission neutrons are capable of inducing further fissions with the release of more neutrons, and so on. This sequence of events is known as a chain reaction and is the process by which nuclear energy is utilized in practical applications. A nuclear reactor is a device in which things are so arranged that a self-sustained fission chain reaction can occur in a controlled manner.

The required condition for a stable, self-sustained chain reaction in a nuclear reactor is that exactly one neutron must be produced per fission, which eventually succeeds in inducing another fission. In other words, one fission must lead to another, and if this is the case, the number of fissions occurring per unit time within the system will be constant. If, on the other hand, each fission eventually leads to more than one fission, the fission rate will increase in time, and conversely, it will decrease with time if less than one additional fission occurs per fission. There is competition for the fission neutrons:

- Radiative neutron capture events (n, γ): Some will be absorbed in fuel nuclides as radiative capture events (n, γ) rather than fission events (n, F).
- Neuron disappearance due to non-fuel absorption: Some will be absorbed by non-fuel nuclides and disappear.
- Neutron leakage: Some will leak out of the system.

Elastic and inelastic scattering events, (n, n) and $(n, n^{/})$, do not change a neutron population because in both cases the scattered neutron remains in the system and may still cause a fission event (n,F). However, inelastic scattering events $(n, n^{/})$ may change neutron energies and thus, they affect the relative probabilities of the next fission events.

The nuclear reactor configuration is called critical if it maintains the steady-state fission chain process, which is the stable balance between fission reactions (neutron production) and neutron capture and leakage (neutron disappearance).

The multiplication factor is defined as the ratio of the number of fissions in any one generation to the number of fissions in the immediately preceding generation. When this factor is exactly equal to unity the number of fissions in each succeeding generation, it is a constant, and a chain reaction initiated in the system will continue at a constant rate. Such a system is said to be critical. If the multiplication factor is greater than unity, the number of fissions increases with each succeeding generation. In this case, the chain reaction diverges and the reactor is said to be supercritical. Finally, if the multiplication factor is less than unity, the chain reaction eventually dies out, and the system is called subcritical.

$$k \equiv \frac{P(t)}{L(t)} \Rightarrow \begin{cases} Subcritical\ Configuration:\ k < 1 \\ Critical\ Configuration:\ k = 1 \\ Supercritical\ Configuration:\ k > 1 \end{cases}$$

where it is explicitly noted that the production $P(t)$ and loss $L(t)$ rates may change with time.

In order to maintain a self-sustained chain reaction in a reactor, a careful balance must be established between the rate at which neutrons are produced in the system and the rate at which they disappear. Neutrons disappear in two ways: They either leak from the surface of the reactor or are absorbed within its interior. The rates at which neutron leakage and absorption occur are governed by the size and composition of the system. A reactor will become supercritical or subcritical if its properties are changed in such a way that its multiplication factor becomes different from unity. These changes may occur in a number of ways:

a. Fuel burnup: Initially loaded fissionable material is consumed in an operating reactor at a rate proportional to the power of the system. If fertile materials, such as Th232 or U238, are present, fissile nuclei will be produced (and also consumed) in time. Thus, the fuel composition changes in time, and this effect naturally has an impact on the multiplication factor.
b. Fission product buildup and decay: Some of the fission products are strong neutron absorbers and

may substantially increase the absorption cross section of a composition.

c. Temperature variations: Many reactor parameters depend upon temperature, and the multiplication factor of a reactor is therefore also temperature dependent. Reactor temperature, however, is usually a function of the operating power of the reactor, and changes in power level may lead to changes in the criticality of the system.

d. Reactivity changes due to movement of control rods or other geometrical and material changes within the reactor. Most reactors are controlled by moving rods of neutron-absorbing material that are inserted in their interiors. The movement of these control rods changes the absorption characteristics of the reactor, and this changes the multiplication factor.

e. Environmental changes: Some reactors are coupled to and are therefore affected by changes in their environment.

f. Accidents: Unforeseen events may suddenly change the properties and criticality of a reactor.

Each of these phenomena is characterized by a different time constant. The results of reactivity changes are usually transients with time constant that are determined by the lifetime of the prompt and delayed neutrons in the reactor.

The reactivity effects of fuel depletion must be compensated to maintain criticality over the fuel burnup cycle:

- The major compensating elements are the control rods, which can be inserted to compensate positive depletion reactivity effects and withdrawn to compensate negative depletion reactivity effects.
- Adjustment of the concentration of a neutron absorber (boron) in the water coolant is another method used to compensate for fuel depletion reactivity effects.
- Burnable poisons (B, Cd, Er, Gd) located in the fuel lattice, which themselves deplete over time, can be used to compensate the negative reactivity effects of fuel depletion.

Fuel depletion and the compensating control actions affect the reactor power distribution over the lifetime of the fuel in the core. Depletion of fuel will be greatest where the power is greatest. The initial positive reactivity effect of depletion will enhance power peaking. At later times, the negative reactivity effects will cause the power to shift away to regions with higher neutron multiplication. In general, the fuel depletion effect is to flatten the power distribution because the regions of high power are more rapidly depleted.

Core management deals with the schemes for loading (and unloading) of fuel and, to some extent, with reactivity control. Core management has two main objectives:

- To increase the burnup of the fuel, thereby improving its utilization.
- To achieve a more uniform thermal power distribution in the core, thereby facilitating heat removal.

Efficient core management basically involves the use of fuel with different degrees of enrichment (fissile content) distributed in the core so that the enrichment is high where the neutron flux is low, and vice versa. The thermal power distribution, which is related to the product of the enrichment and the neutron flux, is thus "flattened." Another requirement in core management is to minimize downtime while the reactor is being refueled and is not generating power.

Fuel can be loaded into nuclear reactors either continuously or batch-wise. In batch loading, some fraction of the irradiated fuel is replaced by a fresh batch of fuel at periodic shutdowns for refueling. If one-third of the fuel is replaced, there would be three batches of fuel in the reactor, each with its separate irradiation history. Generally, the refueling interval is one year, primarily because that is convenient for utilities.

The time-dependent phenomena include changes in the neutron population (neutron flux) as well as causally related changes in the reactor system, i.e., composition, temperature. The relationship between the neutron population (neutron flux) and the physical reactor system (composition, temperature, etc.) may occur in either direction; that is, changes in the composition or temperature of the system may cause a change in the flux, or changes in the flux may alter the composition or temperature and thus the density and absorption characteristics of the system. If the flux changes cause changes in the reactor and these changes subsequently "act back" on the flux, the phenomenon is called "feedback." The energy and nuclear reactions that occur during the operation of a nuclear reactor change the material properties of the core and thus the multiplication factor. This change in the reactivity of the reactor is called feedback reactivity.

Reactivity feedback is called "inherent" if its occurrence is based on an unavoidable and thus totally reliable physical phenomenon. An example is the Doppler broadening of resonances that is directly associated with the fuel temperature. Doppler broadening of resonances automatically leads—through reduction in resonance self-shielding—to an increase in neutron absorption and thus to a negative and inherent reactivity feedback (note that resonance capture dominates resonance fission in all thermal power reactors). The reactor reactivity variation with temperature is the principal feedback mechanism determining the inherent stability of a nuclear reactor with respect to short-term fluctuations in power level. Such feedback is called "prompt" if it directly follows the changing fuel temperature. If additional physical phenomena such as material motion or heat transfer are

required to produce a certain feedback effect, a delay exists between the energy production in the fuel and the feedback. The delay of axial fuel expansion is small enough that this expansion can also be considered a prompt feedback effect.

The large negative Doppler coefficient accounts for the stability of thermal power reactors to temperature transients. The Doppler coefficient in a fast reactor depends, in the first place, on the nature and amounts of the fissile and fertile nuclides in the fuel. It is numerically larger in a softer than in a harder spectrum because of the increased flux of neutrons in the 1-keV energy region. The negative Doppler coefficient of U238 is therefore more significant in a fast reactor with oxide fuel than in one with metal fuel. Neutron absorption in Pu239 can result either in parasitic capture (to form Pu240) or in fission, and there are resonances for both types of absorption. If the Doppler broadening is accompanied by an increase in parasitic capture relative to fission, an increase in temperature will produce a decrease in reactivity. On the other hand, if the reverse is true, the reactivity will increase with temperature. Although the effect of temperature on the capture-to-fission ratio in Pu239 depends on the neutron spectrum, it appears that the Doppler coefficient for this nuclide is generally positive but small. In large fast reactors, the fuel consists of about 80% U238 (as oxide); the negative temperature coefficient of the fertile material is thus dominant, and the fuel temperature coefficient is negative. The Pu240 formed during operation of the reactor also has a negative temperature coefficient. Power transients under the influence of temperature-stimulated counteraction (feedback) have been investigated since the realization of the first chain reaction. Feedback, especially prompt and inherent reactivity feedback, is vitally important for the safety of nuclear reactors.

6.5 CONCLUSIONS

The prediction of the physical properties of a reactor throughout its life is one of the most important problems in reactor design. The objective is the utilization of the energy released by a controlled chain reaction of nuclear fission events maintained within the reactor core. At startup, the reactor must be fueled with more fissile material than required for criticality in order to provide for the burnup of the fuel and for other reactivity changes. To compensate for this excess fuel, control rods are inserted into the reactor and then slowly withdrawn to keep the system critical as the fuel is consumed and poisons accumulate.

Today, on a large scale, fission energy is successfully recovered in nuclear fission reactors and converted into heat energy that is later transformed into electricity or utilized directly in heat processes.

7

OKLO NATURAL FISSION REACTOR

L.V. Krishnan

Indira Gandhi Centre for Atomic Research (Retired), Chennai, TN, India

The element uranium as it occurs today has three kinds of atoms, which have different masses. Atoms of the same element with different masses are known as the isotopes of the element. The three isotopes of uranium now found in nature are present in the proportion given in Table 7.1. Analyses of uranium samples obtained from different parts of the world, from the meteorites, and from the moon, show that the isotopic composition of uranium falls within a very narrow range, whatever may be the source. Of the three uranium isotopes, it is U235 that supports the chain reaction in nuclear fission reactors.

In 1972, a French team working a uranium mine in Franceville basin in Gabon in West Africa found that the proportion of the isotope U235, in one of the samples from the mine was slightly less than what is present elsewhere in nature—0.7107% instead of the well established figure of about 0.72%. Repeated measurements confirmed the discrepancy. This led to more extensive collection of samples from the mine. At certain places the isotope U235 was found to be significantly depleted, going down to a level as low as 0.29% instead of 0.72%. Lower levels of the isotope U235 were found at locations of ore body that were also rich in uranium.

The above findings could be explained only by postulating loss of some of that isotope due to fission chain reaction. The occurrence of fission in nature had been considered earlier by a few scientists. The relative proportion of the different isotopes of uranium in nature has varied over time because of the different rates at which each undergoes radioactive transformation (Table 7.1). In geologically ancient times, the content of the isotope U235 was far higher than at present. In 1956, Kuroda published the conditions needed for a fission chain reaction in nature—like an ore body old enough to have a high level of U235, of sufficient size and rich in uranium, absence in it of neutron-absorbing elements, and presence of water in the region [2]. Although the chances of all the conditions being met at one location were considered rare, he suggested a closer search for locations that met these requirements. The abundance of the isotope U235, some 2,000 million years before the present, works out to about 3% as against the current 0.7%. This is a level that could support a fission chain reaction in the presence of sufficient amount of water. Currently operating Light Water Reactors use uranium enriched in the isotope U235 to the extent of 3% and above. Measurements indicated the age of the uranium ore in Gabon to be about 1,800 million years before the present.

After confirming the initial discovery of the discrepancy in the natural abundance of the isotope U235, French scientists undertook a detailed analysis of all the constituents of the ore samples collected from the mine site and produced a report describing how and when a natural fission reactor could have functioned at the site. More recent studies of samples have examined the extent of dispersion of the fission products from the site of the reactor to draw lessons for designing safe disposal schemes for high level waste from currently operating nuclear power reactors in the world.

One of the first questions to be answered related to the manner in which veins rich in uranium came to be formed in the Franceville basin of Gabon. Geological investigations showed that about 2,100 million years ago a sedimentary layer of sandstone had formed in the region (marked FA in

Nuclear Energy Encyclopedia: Science, Technology, and Applications, First Edition (Wiley Series On Energy).
Edited by Steven B. Krivit, Jay H. Lehr, and Thomas B. Kingery.

TABLE 7.1 Uranium Isotopes Found in Nature, Their Abundance and Half-Life

Isotope	Natural Abundance (atom%) [1]	Radioactive Half-life (Million years)
U234	0.0050–0.0059	0.2452
U235	0.7198–0.7202	703.8
U238	99.2739–99.2752	4,468

Fig. 7.1). Placer deposits with about 0.5% uranium formed in the layer. The absence of oxygen in the atmosphere at the time inhibited dissolution and migration of uranium. Over the next about 100 million years, oxygen began appearing in the atmosphere and promoted these processes.

The presence of oxygen in the air also promoted growth of organic life, and the uranium deposit was gradually overlain by black shale rich in carbonaceous material. Over time, the uranium-bearing layer was buried about 3,000 m deep. Fissures in the overburden carried oxygen-laden water to the uranium deposit, leading to dissolution of uranium and its redistribution into several uranium-rich pockets close to the black shale layer. These pockets contained uraninite crystals embedded in a clay matrix.

Water was present in adequate quantity in the ore matrix, and materials that act as parasitic neutron absorbers were absent. As a result, a fission chain reaction was initiated as soon as the uranium content in a pocket reached a certain threshold, depending on its size. This is estimated to have happened around 1,950 million years ago.

Seventeen pockets have been identified as Reactor Zones. They are in three different ore deposits in the Franceville basin of Gabon. Sixteen of them are found at Oklo and nearby Okelobondo with the third one at Bangombe about 30 km away. In each pocket, the chain reaction is believed to have been initiated independently at a somewhat different point in time and proceeded to a different extent depending on the amount of uranium present.

By the time of the discovery of the natural fission chain reaction in Oklo, about half of the contained uranium had been mined. Mining activities at the Basin, however, continued and came to an end in 1997 after excavation of the 310 m deep Okelobondo reactor zone. Three other pockets—i.e. Reactor Zones 10, 13, and 16—also lay at depths of 250 m and more below the surface (Fig. 7.2).

Details of the chain reaction that happened so long ago have been pieced together from an analysis of the amounts of the various residual products of nuclear fission found in the ore. The investigators came from Europe, United States, Australia, and Japan and belonged to several related disciplines like geology, geochronology, geochemistry, radiation chemistry, reactor physics, and nuclear engineering. A wide range of techniques, like solid-state mass spectrometry, inductively coupled mass spectrometry, such as thermal ionization mass spectrometry and secondary ion mass spectrometry as well as the technique of ion imaging *in situ* using an ion microprobe, were deployed for the purpose. Because all of the original radioactive products from the fission reactions had decayed, analyses depended on measurement of isotopic shifts.

Most results have come from studies of samples from Reactor Zone 2 than from any other. For instance, the isotope neodymium-142 is present to the extent of 27.2% in nature, and very little of it is produced in fission of U235 (Fig. 7.3). The ore at Oklo, however, contained a depleted level of 6.6% in that isotope. Correspondingly, there was almost a hundred percent increase in the level of neodymium-143 (produced by neutron capture by neodymium-142 as well as in fission) over the natural level.

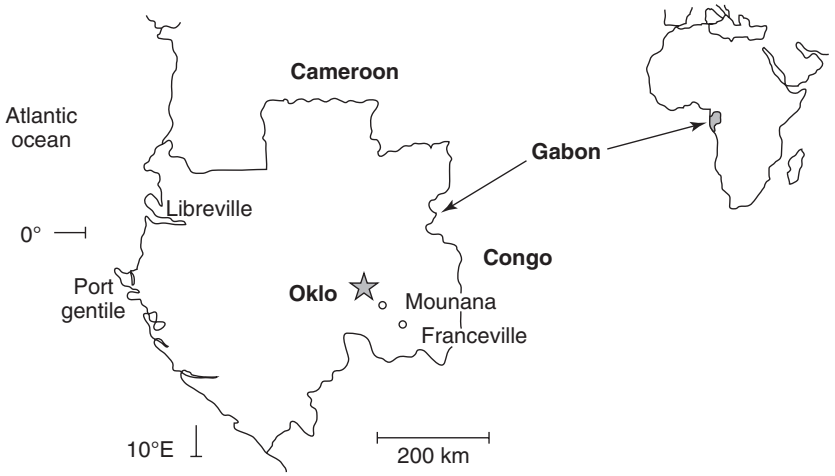

Figure 7.1 Location of the Oklo Uranium Mine in the Franceville Basin in Gabon. (Courtesy http://oklo.curtin.edu.au/where.cfm.)

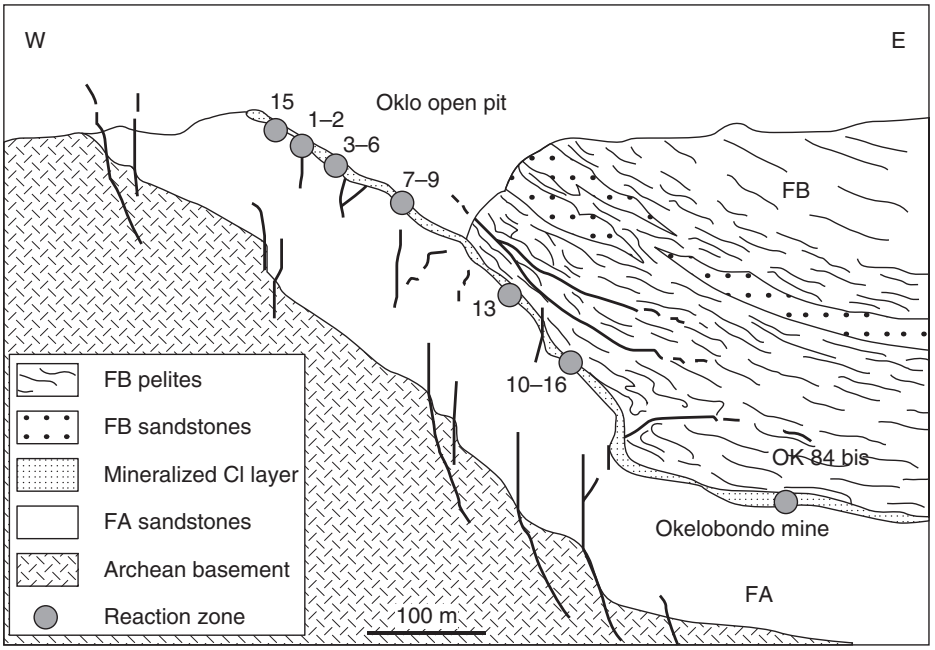

Figure 7.2 Location of the Reactor Zones [3]. (Courtesy of Kyser and Cuney from Sandstone-hosted uranium deposits, in M. Cuney and K. Kyser, *Recent and not-so-recent developments in uranium deposits and implications for exploration*. Mineraological Association of Canada, Short Course Series 39, 2008.)

Similarly, the level of the isotope ruthenium-99 was found to have doubled in the ore, the increase coming from the radioactive transformation of the parent isotope technetium-99, which is a product of uranium fission. Since technetium-99 has a half-life of 211,000 years, almost all of it has been transformed to ruthenium-99 in the ore, after the fission reactions ceased at Oklo.

Ore samples drawn from Reactor Zone 9 were analyzed by solid-state mass spectrometry technique for the isotopic composition of eight selected fission products. This Zone lay at about 100 m depth in the Oklo open pit, but has been nearly mined out. From cumulative yields of fission product palladium, it was possible to infer that the contribution to the total number of fissions that took place amounted to about 88% from U235, with 8% from U238 and 4% from plutonium-239 [4]. These proportions varied somewhat from Zone to Zone. The fission contribution from U238 in Reactor Zone 13 was estimated to be exceptionally high at 18% due apparently to a much shorter total duration of operation [5]. Nearly half of the U235 atoms that underwent fission are believed to have resulted from the decay of plutonium-239. According to one estimate, over two tonnes of plutonium was produced in these reactor zones[6].

It was also possible to estimate the total duration of operation of the chain reaction in this Reactor Zone to be about 220,000 years, taking place intermittently. But the duration was not the same in the different reactor zones, varying from 150,000 to 850,000 years. The average density of fissions in this period was estimated at 0.92×10^{20} per cubic centimeter. The total heat energy generated by the fissions in all the reactor zones put together is estimated as 15,000 Megawatt-years accounting for about 5.5 tonnes of U235 [6]. Because it all happened over a very long period of time, the average heat generation rate was less than about 100 kW. For a 3% presence of this isotope, about 180 Te of natural uranium was involved in the fissions out of the total uranium content in these Zones.

An examination of the ratio of the two isotopes of lutetium, namely Lu-175 and Lu-176, in seven samples from three Reactor Zones provided an indication of the likely temperatures at the time the fission reactions occurred. This was possible because the neutron capture cross section of one of the two (Lu-176) has a significant temperature dependence. The results point to an average temperature of $280 \pm 50^{\circ}$C [7].

Aluminum phosphate grains found in the samples from the Reactor Zones were found to contain very large concentrations of fission product atoms of xenon and krypton. The isotopic composition of the xenon atoms in these grains, however, was quite different from those produced in fission. This difference is explained by postulating that those isotopes that appeared soon after fission migrated out quickly when the temperatures were high. Others that were produced later by radioactive decay of precursors were trapped in the aluminum phosphate

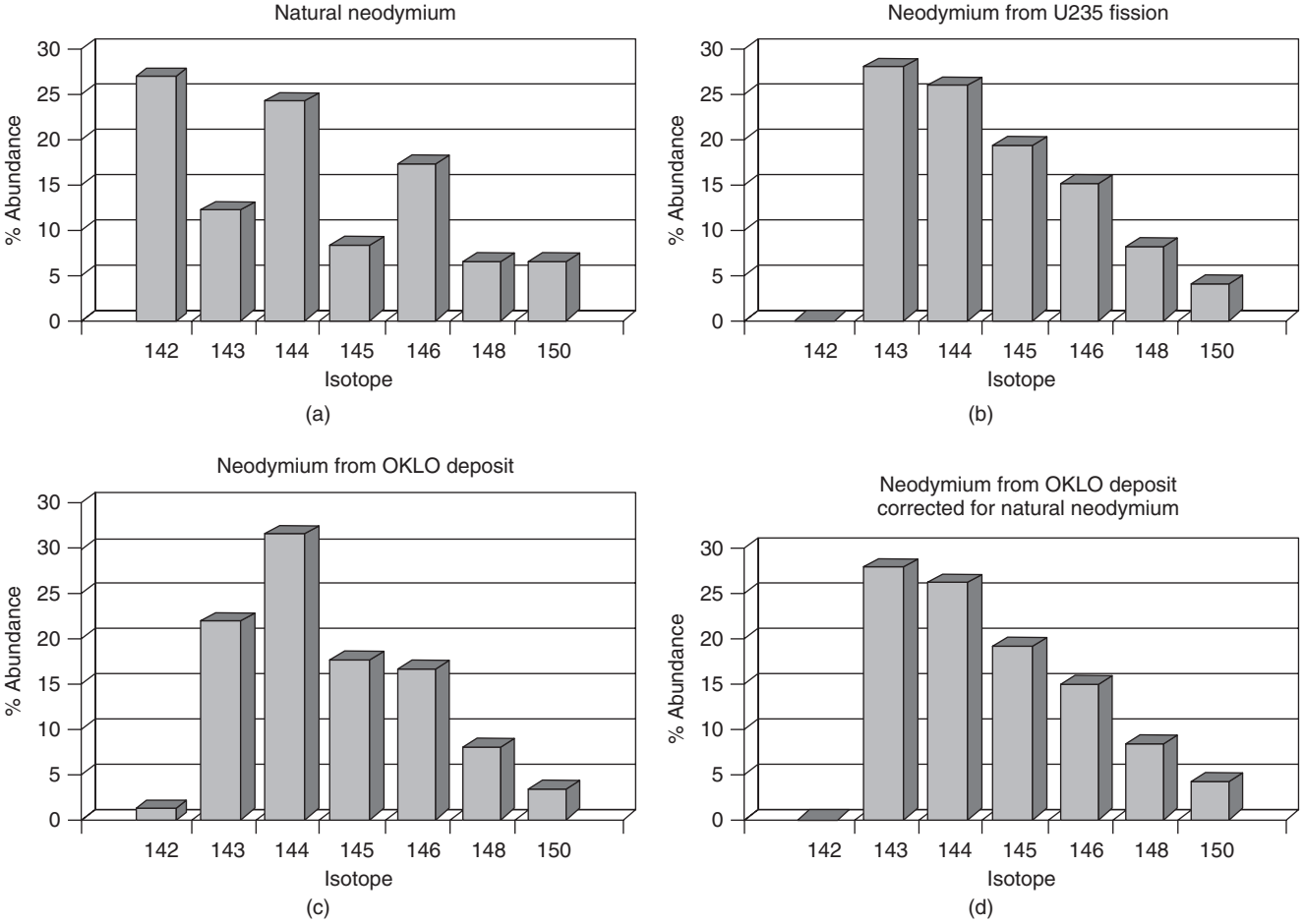

Figure 7.3 Isotopic signature for (a) naturally occurring neodymium, (b) uranium fission, (c) Oklo natural reactor, and (d) Oklo natural reactor corrected for presence of natural neodymium. (Courtesy http://www.grisda.org/origins/17086.htm.)

grains that formed in cooler conditions [8]. Reconstruction calculations indicate that the fission chain reactions must have occurred in short pulses of 30-minute duration separated by a quiescent period of about 2.5 hours. This mode of operation was caused by cessation of the fissions due to loss of the moderating effect of water as a result of heat generated by the fission and subsequent resumption as temperatures dropped in a cyclic process. It is remarkable that these xenon atoms have remained trapped in the aluminum phosphate grains for nearly two billion years.

Various aspects of the fission chain reaction in the reactor zones were studied by developing models [9]. The results for a typical reactor zone indicate that once initiated, the reaction could have reached equilibrium in less than 10 years. The thermal impact of the reaction was probably limited to a distance of less than 40 m from the reaction zone.

Other studies have examined the extent to which the radioactive products arising from the fission reaction have spread out in the environment. Some of the Reactor Zones lay at a depth of over a thousand meters when the reaction occurred, while a few were about 500 meters below the surface [10]. The prevailing temperature and pressure approximated to levels as high as in currently operating human-designed reactors. Subsequently, over the next several hundred million years, tectonic activity and river-caused erosion brought the reactor zones much closer to the surface. About 800 to 900 million years ago, volcanic activity caused the intrusion of a dolerite dyke into the Franceville basin. However, migration of the radioactive products from the Reactor Zones is found to be limited to close in distances. It is believed that these findings would help in conceiving better methods for long term storage of radioactive wastes from the nuclear power programs in the various countries.

Samples from Reactor Zone 2 analyzed *in situ* by the Sensitive High Resolution Ion Microprobe (SHRIMP) technique showed that uranium, rare earth elements, Zr, and Mo have migrated out of the core region to a distance of several meters because of uraninite dissolution and

advective transport during and after the fission reactions [11]. Selenium is believed to have moved further away.

Measurement of isotopic ratios was carried out, with the SIMS technique of high spatial resolution, on a large number of samples from the core and periphery (about 3 m by 1.5 m) in Okelobondo Reactor Zone [12]. The ratio of U235 to U238 was found to vary by 2.5% over a few microns to millimeters and by as much as 17% over a meter (0.00643–0.00776). In five of 18 samples, U235 presence was higher probably due to migration of the plutonium-239 that had formed and its subsequent decay. The transport of plutonium is attributed to water present in the core. The samples most enriched in U235 are found in organic-rich clays adjacent to the core.

Reactor Zones 7-9 were found to be rich in organic substances. The presence of the organic matter is believed to have facilitated the concentration of uranium in sufficient quantities to enable a chain reaction. When the reaction occurred, the heat generated produced liquid bitumen out of the organic matter. As the reaction subsided, the bitumen solidified into a mixture of PAH and cryptocrystalline graphite. Residual uranium and the fission products were trapped in the mixture and have remained immobilized for nearly two billion years [13]. In those reactor zones that contained only traces of carbonaceous matter, fission products including caesium, strontium, and rubidium as also boron have migrated out [14].

Using the solid-state mass spectrometry and the isotope dilution technique, Loss et al analyzed samples from Reactor Zones 2-7 along with other samples from the host rock for comparison [15]. Similar studies were carried out by others on samples from Reactor Zone 9 [16]. Both teams found that fission product elements Pd and Te were retained almost fully within the samples while all of Cd and Ag appear to have migrated out of the Reactor Zone. Cadmium was found to remain in the host rock but there was little presence of Ag.

The UO2 matrix in the ore appears to be efficient at retaining elements such as Mo, Tc, Ru, Rh, Pd, and Te, but not Cd, Cs, Xe, Kr, Rb, Sr, and Ba. Clays and phosphate minerals appear to have played a role in the retention of fissiogenic elements [17].

Water samples were collected from within the Bangombe Reactor Zone located about 10 m below the surface and also from outside the Zone about 3 m away. These were found to contain traces of fission product neodymium at a concentration of about 17 parts per trillion, but not the samples drawn from points much further away at 25 m [18].

Geological studies indicate that a dolerite dyke intrusion occurred close to the Reactor Zones in the Oklo and Bangombe region about 900 million years ago. Analysis shows that the age of the lead content in uraninite grains is only about 500 million years, leading to the inference that thermal impact from the intrusion of the dyke must have caused a certain degree of loss of the Pb component from the uraninite grains [19]. But the intrusion has not affected uranium itself or the fission products.

REFERENCES

1. K.J.R. Rosman and P.D.P. Taylor, Isotopic composition of the elements., *Pure & Applied. Chemistry*, 1998, **70**, (1), 229.
2. P.K. Kuroda, On the infinite multiplication constant and the age of the uranium minerals. *J. Chem. Phys*., 1956, **25**, 1295–1296.
3. Also indicated in the figure are cell parameter "a" of uraninite crystals in the ore in Angstrom units; typical value is 5.4682 (ref: http://www.mindat.org/min-4102.html); oxidation causes reduction in unit cell parameter.
4. R.D. Loss, et al., The Oklo natural reactors: cumulative fission yields and nuclear characteristics of Reactor Zone 9, *Earth and Planetary Science Letters*, July 1988, **89**, 2, 193–206.
5. H. Hidaka and P. Holliger, Geochemical and neutronic characteristics of the natural fossil fission reactors at Oklo and Bangombé, Gabon. *Geochimica et Cosmochimica Acta*, January 1998, **62**, 89–108.
6. A.P. Meshik, *The Workings of an Ancient Nuclear Reactor*, http://www.scientificamerican.com/article.cfm?id=ancient-nuclear-reactor.
7. P. Holliger and C. Devillers, Contribution à l′étude de la température dans les réacteurs fossiles d'Oklo par la mesure du rapport isotopique du lutétium, *Earth and Planetary Science Letters*, 1981, **52**, 1, 76–84.
8. A.P. Meshik et al., Record of cycling operation of the natural nuclear reactor in the Oklo/Okelobondo Area in Gabon. *Phys. Rev. Lett*., 2004, **93**, 182302.
9. F. Gauthier-Lafaye et al., Natural fission reactors of Oklo, *Economic Geology*, December 1989, **84** 8, 2286–2295.
10. B. Barré, *The nuclear reactors of Oklo: 2 billion years before Fermi!*, http://www.euronuclear.org/e-news/e-news-9/issue-9
11. R. Bros et al., Mobilization and mechanisms of retardation in the Oklo natural reactor zone 2 (Gabon)—inferences from U, REE, Zr, Mo and Se isotopes. *Applied Geochemistry*, December 2003, **18**, 12, 1807–1824.
12. C.S. Palenik et al., *Analysis of fission products and Pu migration in the Okélobondo Reactor Zone using SIMS*, http://microtracescientific.com/people/cpalenik/abstracts/GSA_Palenik_FINAL.pdf.
13. B. Nagy et al., *Role of organic matter in the Proterozoic Oklo natural fission reactors, Gabon, Africa*, http://geology.gsapubs.org/content/21/7/655.abstract.
14. D.J. Mossman et al., *Carbonaceous substances in Oklo reactors—Analogue for permanent deep geologic disposal of anthropogenic nuclear waste*, http://reg.gsapubs.org/content/19/1.abstract.
15. R.D. Loss et al., Transport of symmetric mass region fission products at the Oklo natural reactors. *Earth Planet. Sci. Lett*., May 1984, **68**, 2, 240–248.

16. J.R. de Laeter et al., The Oklo natural reactor: Cumulative fission yields and retentivity of the symmetric mass region fission products, *Earth Planet. Sci. Lett*., October 1980, **50**, 1, 238–246.
17. F. Gauthier-Lafaye et al., Natural fission reactors in the Franceville basin, Gabon: a review of the conditions and results of a "critical event" in a geologic system, *Geochimica et Cosmochimica Acta*, December 1996, **60**, 23, 4831–4852.
18. P. Stille et al., REE mobility in groundwater proximate to the natural fission reactor at Bangombé (Gabon), *Chemical Geology*, August 15, 2003, **198**, 3-4, 289–304.
19. L.Z. Evins et al., Uraninite recrystallization and Pb loss in the Oklo and Bangombé natural fission reactors, Gabon, *Geochimica et Cosmochimica Acta*, March 15, 2005, **69**, 6, 1589–1606.

8

ELECTRICAL GENERATION FROM NUCLEAR POWER PLANTS

PAVEL V. TSVETKOV AND DAVID E. AMES II

Department of Nuclear Engineering, Texas A&M University, College Station, TX, USA

8.1 WORLD ENERGY NEEDS AND THE ROLE OF ELECTRICITY

This chapter discusses overall role of the nuclear power and perspectives of its future development focusing on electricity, co-generation and operational aspects. As an illustrative example, Figure 8.1 depicts the turbine hall view of a nuclear power plant.

Our today world is highly dependent on energy. Industrialized nations are totally dependent on an abundant, reliable supply of energy for living and working, and it is a key ingredient in all sectors of modern economies. Even so, it is often taken for granted because it plays such a large role in everyday existence. Meanwhile, in developing countries, there is almost an unquenchable thirst for substantial increases in energy generation and usage. In any case, energy is one of the single most important factors in regards to living standards of individuals across the world. Studies have continually shown an indisputable link between energy consumption and individuals overall well being [1, 3].

Large amounts of data have been collected for comparing average energy consumption per capita to measurements that represent the standard of living or quality of life achieved in any community. One such measure is the Human Development Index (HDI), which incorporates factors such as life expectancy, education, income inequality, poverty rates, Gross Domestic Product (GDP) per capita, and the environment [2]. The HDI is widely considered to be the best and most comprehensive measure for quality of life. The index is normalized to give a value between zero and one, with one representing the highest possible standard of living or most developed country and zero being the least. Countries that score an HDI greater than 0.90 are considered to have a "very high quality of life," while those with values between 0.60 and 0.90 are rated as having an "average quality of life," and those below 0.60 are classified as having a "very low quality of life." Figure 8.2 demonstrates this compelling relationship between the HDI values and energy usage. The data were released by the United Nations Development Program (UNDP) on December 20, 2008. The compilation includes the HDI values and electricity generation per capita (as determined in 2006) for 180 different countries, with some of countries labeled for general reference. As indicated, the results overwhelmingly show that the greater the energy consumption per capita for a community, the greater the standard of living (HDI) for those individuals. Consequently, energy consumption can be used as an overall indicator for the overall well-being of humankind and as a metric to compare conditions around the globe.

Iceland and Norway have the highest HDI at 0.968, while Sierra Leone ranks lowest at 0.329. The United States has an HDI of 0.950 and is ranked number 15 overall. As expected, all nations strive to increase HDI, and the most effective and straightforward way to accomplish this is by adding energy generation capacity. Of particular notice is China and India, the two most populated countries in world, which have HDI values that place them in the lower portion of the "average quality of life" group of nations. As both

Nuclear Energy Encyclopedia: Science, Technology, and Applications, First Edition (Wiley Series On Energy).
Edited by Steven B. Krivit, Jay H. Lehr, and Thomas B. Kingery.

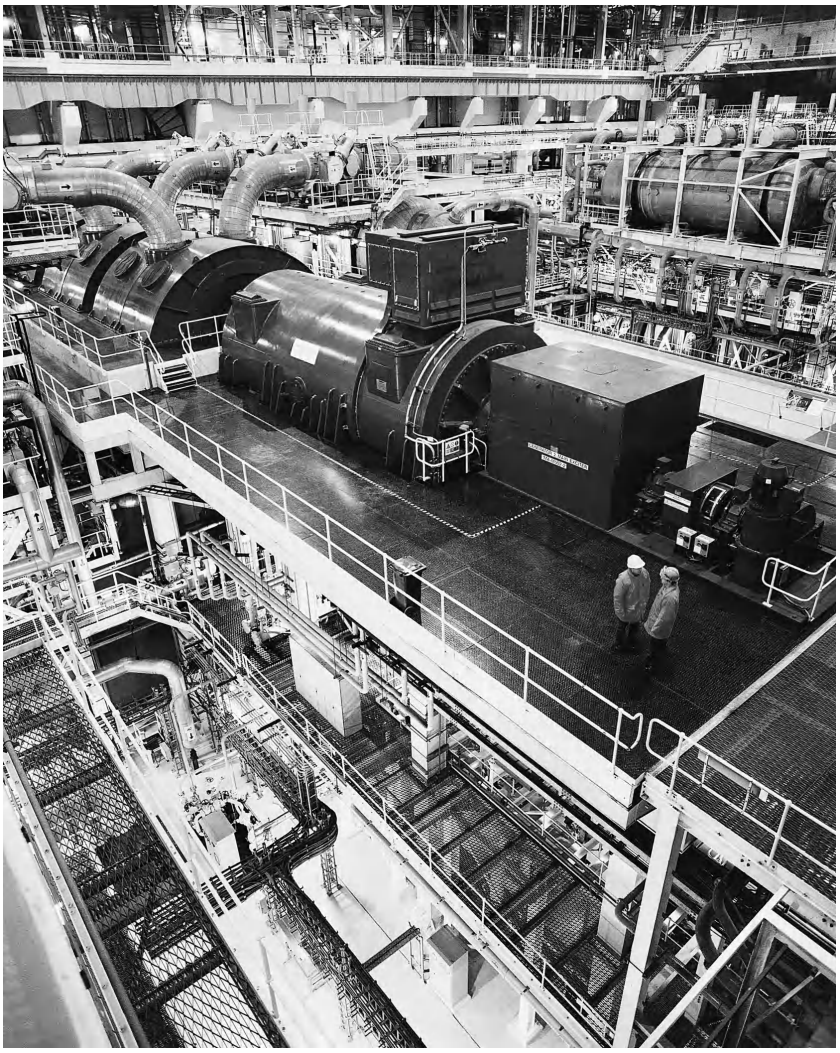

Figure 8.1 Steam generated from nuclear power plant drives electrical turbine-generators. Image Courtesy of World Nuclear Association.

India and China strive to rapidly increase their HDI, it will greatly affect the rest of the world. With over 35% of world's population between them, just a slight increase in either's electricity consumption per capita will have a huge impact on overall energy needs worldwide.

The role of electricity in the overall energy mix is increasing and propagating in all spheres of our society. Our economy and everyday lives depend on electricity. Electricity is vital for state governments, defense systems, transportation, telecommunications, water systems, and industries. Even traditional industries are computerized and automated. Everything halts without electricity. Blackouts due to local hardware failures, grid overloads, and climate disturbances signify the magnitude and the multifaceted nature of humankind dependencies on electricity by freezing our everyday functions and threatening our existence in extremes of natural disasters. The moment when electricity is interrupted in local communities is the moment when everything freezes until the problem is fixed.

Since 1973, the use of non-electric forms of energy, in the United States, for example, has remained relatively flat at 21%. But the use of electricity has increased by 66%—somewhat less than the gross domestic product at 80%. Clearly, electricity has become America's chosen energy source. The Department of Energy says the United States will need 44% more electricity by 2020 to meet growing energy demands.

8.2 ENERGY CONSUMPTION, NUCLEAR POWER, AND ENVIRONMENT

The coupled effect of energy use and living standards leads to an interesting dilemma. Just like energy's link

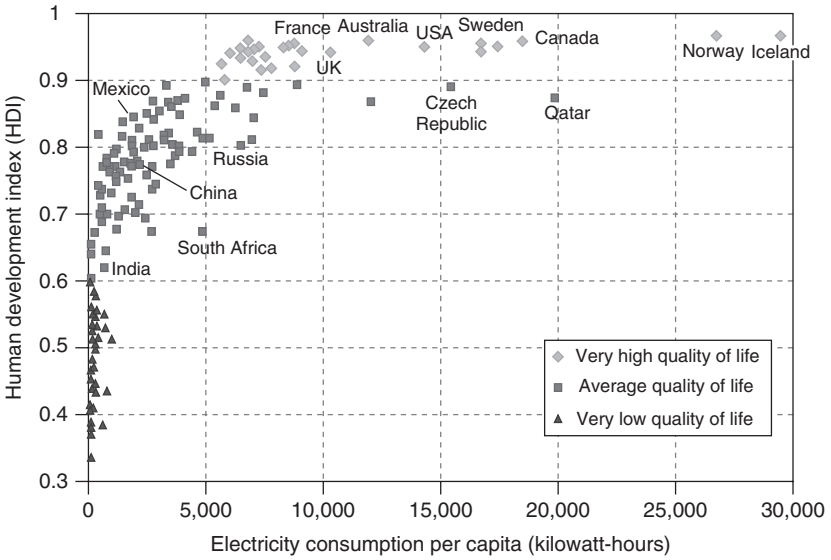

Figure 8.2 Relationship of HDI and electricity consumption per capital.

to quality of life, energy is also intricately entwined with the environment. Much of the global-scale environmental degradation seen today is attributed to the adverse effects of energy production and use. Thus, nations are faced with the struggle to increase energy generation in order to provide a higher standard of living for their citizens, but they must also do so in an environmentally responsible way.

Figure 8.3 displays carbon dioxide (CO_2) emissions and HDI data for 180 countries around the world. The six countries (Bahrain, Kuwait, Oman, Qatar, Saudi Arabia, and the United Arab Emirates) that make up the Gulf Cooperation Council (GCC) are at the top or near the top of the list for CO_2 emitters, mainly due to their high emitting gas production sector, small populations, and exportation of energy. Qatar is the number one emitter, generating 79.3 tons/capita—such a high value that it does not even fit on the scale of the provided plot. Many of the GCC countries have taken aggressive measures to reduce CO_2 emissions, including tightening controls on gas flaring, researching carbon capture and sequestration, and investigating the use of non-CO_2 emitting energy forms such as nuclear energy and wind power.

Counties such as France and Iceland have extremely high HDI values while at the same time generating very low levels of CO_2 emission per capita. Further investigation reveals that France gets about 80% of its electricity

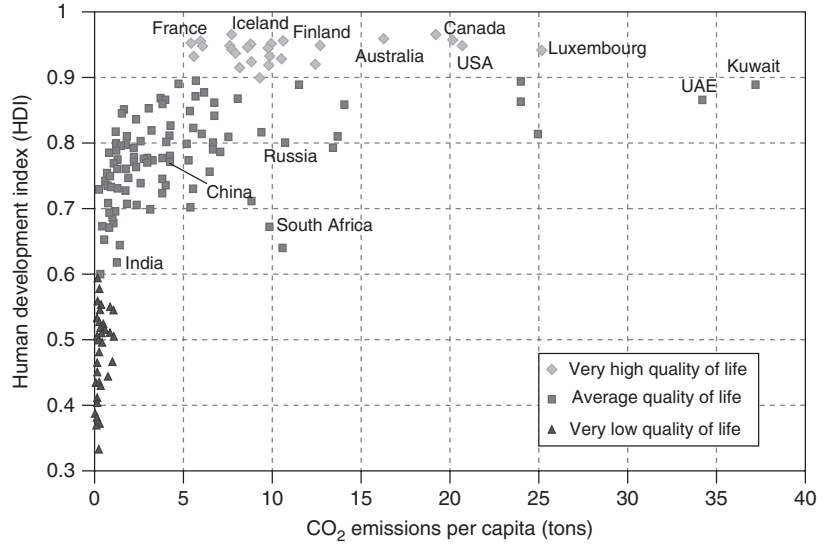

Figure 8.3 HDI vs. CO_2 emissions per capita for 180 countries.

generation from nuclear power, and much of Iceland's energy needs are met by renewable sources (particularly geothermal power), so both countries are fulfilling a large portion of their energy needs by non-CO_2 emitting sources. Iceland and France have something else in common—they both have very few fossil fuel energy resources within their borders. Even so, they have adopted energy plans that have made them much more energy-independent as compared to other industrialized nations. The United States is 9th on the list for CO_2 emissions per capita and 2nd, just behind China, for overall CO_2 emissions. China and India are of major concern due to their large populations and the impact they will have in the future because of their rapidly growing economies.

The world has become much more sensitive to the relationship between energy and the environment, to the point that it has become impossible to discuss one without the other. In response, nations and groups of nations have proposed and/or implemented policies to mitigate the harmful environmental effects associated with energy generation [4, 5]. These energy policies are developed to aid the environment through tactics such as carbon emission caps, emissions trade plans, carbon taxes, efficiency and conservation incentives, clean renewable energy incentives, and others. In addition to the very important environmental issues that have come to the forefront, there are some other important requirements for future energy systems. Important goals and basic principles of future energy sources include the following:

1. Reducing greenhouse gas emissions
2. Minimizing the overall environmental footprint
3. Safety and reliability
4. Sustainability
5. Economics
6. Efficiency
7. Energy independence

Climate change and air quality are putting pressure on fossil fuel-based energy generation. Growing concerns for the environment will favor energy sources that can satisfy the need for electricity and other energy-intensive products on a sustainable basis, with minimal environmental impact and competitive economics. From the onset, nuclear power has shown great promise in meeting all of the above principles. As the technology has matured so has its effectiveness in accomplishing these goals.

Unlike fossil fuel plants, nuclear plants do not release carbon dioxide, sulfur, or nitrogen oxide into the environment. Nuclear energy is America's cleanest large-scale source of electricity, representing two-thirds of the nation's emission-free electricity generation. By using nuclear energy instead of other fuels, electric utilities reduce U.S. emissions of carbon dioxide, the principal "greenhouse" gas. Each year, U.S. nuclear plants prevent the discharge of 174 million metric tons of carbon.

Today nuclear energy is arguably one of the best sources for electricity generation that can meet future needs and requirements. Even so, advances and improvements must be made for nuclear energy to be competitive in the future. The next generation of nuclear systems can provide a vital part of a long-term, diversified energy supply.

8.3 NUCLEAR POWER TODAY AND DEVELOPMENT TRENDS

Consideration of the use of nuclear energy for production of useful power began shortly after the discovery of nuclear fission. At that time, scientists realized that future energy needs could not be met by fossil fuels alone. The development of nuclear reactors as useful sources of power began shortly after the end of World War II. Most of this development has been concentrated on light water reactor (LWR) concepts (pressurized water reactors and boiling water reactors) and their fuel cycle. The success of the LWR is based on the early recognition that natural fissile material was considered scarce and that nuclear energy could develop only if systems with low fissile inventories per unit power would be built in the start phase. LWRs, as initially developed for naval applications, fulfilled this criterion and used simple and relatively cheap technology that enabled a first generation of power stations to be constructed rapidly. The necessary uranium enrichment technology was available from the military development. The significant plutonium generation in LWR fuels was considered to be an asset because plutonium is an excellent fuel for fast reactors, and the anticipated deployment of fast reactors around the turn of the century would have required large fissile inventories.

Today's nuclear energy system is the result of a 50-year development during which this technology has reached industrial maturity and became a reliable resource for our electricity needs. The expansion of nuclear power was initially rapid. In the first half of the 1970s, growth averaged 30% per year, and average growth for the full decade was 21% per year. Nuclear power's share of global electricity increased dramatically.

Near the end of the 1980s, growth slowed substantially. Licensing interventions from growing environmental movements on both sides of the Atlantic often stretched out licensing times and increased costs. The combination of inflation and rising energy costs resulting from the oil shocks of 1973 and 1979 depressed growth in electricity demand and disproportionately raised the cost of capital intensive power plants, like nuclear power plants. Some utilities found the regulatory and transaction costs

of nuclear power simply too high to manage cost effectively. The 1979 Three Mile Island accident severely damaged the reputation of the nuclear power industry in the United States, although it had no off-site impacts, and the Chernobyl accident in 1986, which had substantial off-site impacts, largely stalled the expansion of nuclear power in both Europe and the former Soviet Union. Finally, the price deregulation of electricity markets, particularly in OECD countries, exposed excess capacity, pushed electricity prices lower and made power plant investments more risky. Other things being equal, nuclear power's front-loaded cost structure is a disadvantage in markets that emphasize short-term profits and hence value rapid returns.

In the 1990s, growth in nuclear electricity generation exceeded the growth in nuclear capacity as consolidation in the nuclear industry, management efficiencies, and technological advances progressively raised the average energy availability of the world's nuclear plants. The energy availability factor measures the percentage of time that a power reactor is available to generate electricity, rather than being shut down for refueling, maintenance, or other reasons. The global availability average for nuclear power reactors has risen from 73% in 1990 to 83% in 2004. This increase is equivalent to the addition of 33 new 1000 MW reactors.

Well-run nuclear power plants are generally a competitive and profitable source of electricity. One reason is that while these plants are relatively expensive to build, they are relatively inexpensive to operate. Once a nuclear power plant's construction costs have been fully amortized, it is generally at its most profitable stage. Other things being equal, there is an economic incentive to operate the plant for as long as it is safe to do so, as seen from the continuing pace of license renewals. More than 400 nuclear power plants are currently operating throughout the world, supplying about 16% of the world's electricity:

83.4% are light water reactors (LWR), of which:

- 57.7% are pressurized water reactors (PWR)
- 23.2% are boiling water reactors (BWR)
- 0.6% are advanced boiling water reactors (ABWR)
- 13.8% are water-water energetic reactors (Russian version of PWR) (WWER)
- 4.7% are light water-cooled graphite reactors (LWGR)

7.8% are heavy water-cooled reactors (HWR) (pressure vessel heavy water reactors)

0.2% are heavy water-moderated light water-cooled reactors

8.1% are gas reactors (GR)

0.5% are fast reactors (FBR)

These plants perform safely and reliably, and they help meet the objectives of diversity, independence, and security of their energy supply. In addition to the central station power reactors, there are several hundreds of pressurized water naval propulsion reactors and hundreds of research and special purpose reactors of various types worldwide. Today 31 central station nuclear power reactors are under construction worldwide and are going to be operational in next few years so that the power reactor fleet will consist of 465 reactors worldwide.

Two projections to 2030 published by the IAEA. The low projection assumes that no new nuclear power reactors will be built beyond those already under construction or currently planned. Nuclear power capacity grows only slightly in this projection, to 416 GW(e) in 2020, before leveling off. The high projection incorporates nuclear projects proposed beyond those already firmly committed. Global nuclear power capacity in this projection grows steadily to 640 GW(e) in 2030, an average growth rate of slightly over 2% per year. While both projections show significant differences in different parts of the world, both project greatest growth in the Far East. There is also significant expansion in Eastern Europe in both projections and for North America in the high projection. In Western Europe, there is a contraction in the low projection as retirements outpace new construction, but substantial growth in the high projection. Growth rates are high in the Middle East and South Asia in both projections, although these regions start from a small 2005 base.

Nuclear power is mainly used in industrialized countries. Of the world's operating reactors, 91% is either in OECD countries or countries with economies in transition. In terms of electrical generating capacity, 95% of nuclear generating capacity is installed in these countries. In terms of new construction, however, the pattern is reversed. Sixteen of the new reactors under construction are in developing countries. Current expansion, as well as near term and long term growth prospects, are centered in Asia.

8.4 INNOVATIVE NUCLEAR REACTOR TECHNOLOGY DEVELOPMENT

Nuclear power has had a substantial role in the supply of electricity in the United States for over three decades. Nuclear power reactors in the United States currently produce about 20% of the nation's electricity. Over the past 20 years, the average capacity factor for U.S. nuclear plants has increased from about 60% to over 90%. Over this same period, nuclear safety has been excellent, and there have been substantial reductions in operating and maintenance costs, worker exposures to radiation, and quantities of radioactive waste. There has been steady progress in issues such as long-term disposal of used nuclear fuel. Nuclear

plants emit no greenhouse gases, an attribute of increasing importance in the United States and around the world. Many U.S. nuclear power plant owners have applied to NRC to extend their plant licenses. Nuclear power technology has matured to the point that it is now a vital and extraordinarily valuable part of the nation's electricity supply. The nuclear-generated electricity is safe, clean, and economical and does not emit greenhouse gases. Continued and expanded reliance on nuclear energy is one key to meeting future demand for electricity in the United States and is called for in the National Energy Policy. Nevertheless, no new nuclear plants have been built in the United States in many years.

A lot of work has been done around the world to improve the existing reactor designs. The large base of experience with the current nuclear plants has been used to guide development of the new designs. Common goals are simplification, larger margins to limit system challenges, longer grace periods for response to emergency situations, high availability, competitive economics, and compliance with internationally recognized safety objectives. In the United States and worldwide, the design research activities have been driven by two major objectives: to incorporate passive (inherent) safety features, which ensure safety without reliance on active control systems, and to incorporate modular construction techniques. The trend of development based on the above two objectives remains steady. The U.S. Department of Energy (DOE) has been working with the nuclear industry to establish a technical and regulatory foundation for the next generation of nuclear plants. The DOE Generation IV Initiative will develop technologies that achieve safety performance, waste reduction, and proliferation resistance while providing a nuclear energy option that is economically competitive and ready for deployment before 2030. The Generation IV nuclear energy systems are an ensemble of nuclear reactor technologies that could be deployed by 2030 and present significant improvements in economics, safety and reliability, and sustainability over currently operating reactor technologies.

Generation IV nuclear energy systems would follow three other distinct periods of reactor development:

- Generation I (1950–1970)—experimental and prototype reactors: The first power reactors generation was introduced during the this period and included early prototype reactors such as Shippingport, Dresden, Fermi I in the U.S. and the Magnox reactors in the UK.
- Generation II (1970–1990)—large, central-station nuclear power reactors: The second generation included commercial power reactors built during this period, such as the Light Water-cooled Reactors (LWRs) with enriched uranium, including the Pressurized Water Reactor (PWR) and the Boiling Water Reactor (BWR). In the United States, it includes 104 plants currently in operation. In Canada, it includes the Canadian Deuterium Uranium heavy water moderated and natural uranium fueled (CANDU) reactors. In Russia, this was the era of pressurized water reactor (VVER-1000) and the RBMK-1000 of Chernobyl accident.
- Generation III (1990–2030)—evolutionary designs: The third generation started being deployed in the 1990s and is composed of the Advanced Light Water Reactors (ALWRs) including the Advanced Boiling Water Reactor (ABWR), and the System 80+. These were primarily built in East Asia to meet that region's expanding electricity needs. New designs that are expected to be deployed by 2010–2030 include the Westinghouse Advanced Passive AP600 and AP1000 and European EPR. These are considered as evolutionary designs offering improved safety and economics.
- Generation IV (2030 and beyond)—next generation designs: While the current second- and third-generation nuclear power plant designs provide an economically, technically, and publicly acceptable electricity supply in many markets, further advances in nuclear energy system design can broaden the opportunities for the use of nuclear energy. The fourth generation of nuclear reactors is expected to start being deployed by 2030. The Generation IV reactors are designed with the following objectives in mind: economic competitiveness, enhanced safety and reliability, minimal radioactive waste generation, proliferation resistance.

Although existing designs, which are denoted as Generation II and III, provide a reliable, economical, and publicly acceptable supply of electricity in many markets, further advances in nuclear energy system design can broaden the opportunities for the use of nuclear energy. Described in the roadmap are six system concepts chosen by the United States Department of Energy's Nuclear Energy Research Advisory Committee and the Generation IV International Forum to be researched: Gas-Cooled Fast Reactor (GFR); Very-High-Temperature Reactor (VHTR); Supercritical-Water-Cooled Reactor (SCWR); Sodium-Cooled Fast Reactor (SFR); Lead-Cooled Fast Reactor (LFR); Molten Salt Reactor (MSR). The Generation IV International Forum nations believe that development of these six concepts will result in long-term benefits worldwide.

For new plants, the basis for achieving high performance is also being laid down during the design phase. These include design for online maintenance and short outages. Many other aspects such as better man-machine interface using computers and improved information displays, and better operator qualification and simulator training, which

have been applied at current plants, will contribute to high performance of future plants. The advanced designs also desire plant lifetimes of 60 years and longer.

8.5 NUCLEAR FUEL RESOURCES

From the early days of nuclear energy, the back-end of the fuel cycle was not given the same attention as the reactors, and the concept of geologic disposal of radioactive waste was not yet questioned by the public. Because the known uranium resources increased with prospecting and the growth of nuclear energy did not meet the early expectations, uranium became cheap and the envisaged rapid introduction of fast reactors did not come to pass. In many countries, a once-through open fuel cycle developed where spent fuel is accumulating in spent fuel storage pools and intermediate storage facilities. Other countries embarked on a reprocessing fuel cycle, taking advantage of the PUREX technology, which was also available from the military application, to separate plutonium and uranium. Whereas some of the recovered plutonium is recycled in the form of uranium-plutonium mixed-oxide (MOX) fuel in LWRs, the remaining mix of minor actinides (MA: neptunium (Np), americium (Am), curium (Cm) and higher-Z actinides) and fission products is conditioned for final waste disposal.

Today, after some 40 years of nuclear energy deployment, most countries with nuclear energy programs have a growing stock of spent fuel, or separated plutonium and vitrified high-level waste (HLW), where the further management of this material is uncertain. This situation is particularly uncomfortable since, in the meantime, the back end of the fuel cycle has become the main focus of much of the criticism against nuclear energy, mostly oriented toward the final storage of spent fuel or high level waste (HLW). The solution envisioned is in partitioning and transmutation (P&T) technologies that aim at making nuclear energy more sustainable from the viewpoint of the back-end of the fuel cycle by minimizing the high-level waste with respect to its mass, radiotoxicity, and (possibly) repository risk. P&T mainly deals with the management—i.e., transmutation and/or special conditioning and confinement—of minor actinides and fission products, but involves the closure of the fuel cycle for plutonium as a necessary step.

The extent of energy resources is limited partly by nature and partly by human ingenuity and economics. "Reserves" are the accessible portion of resources at existing prices using existing technology. Reserves therefore depend mainly on how much people are willing to pay for energy services and on the technology available to extract resources and turn them into services. Resources not demanded by the market are just "neutral stuff." Thus, reserves are continually replenished not through the creation of new material, but through growing demand and declining production costs that turn "neutral stuff" into reserves. This is true for both finite and renewable resources, but for finite resources, unlike renewables, there will eventually be a limit.

Nuclear resources include uranium and thorium. Thorium is three times as abundant as uranium, but, as noted above, the reserves, or recoverable quantities, depend on market conditions and technology as well as the geology of different deposits. Currently, uranium is in much greater demand.

All of the world's operating nuclear power reactors use uranium fuel, as will all that are under construction. Identified conventional uranium resources are currently estimated at 4.7 million tons of uranium (MT U) for costs below \$130/ kg. For reference, the spot market price of uranium at the end of January 2006 was about \$94/ kg. Additional conventional resources beyond those already identified are estimated to add another 10.1 MT U. Table 8.1 summarizes how long conventional uranium resources would last at current burnup rates. The top row of numbers assumes that future nuclear power reactors use the same technology as today's reactors, which can only use less than 2% of the energy in natural uranium. The bottom row assumes that, as uranium becomes more expensive, used fuel is eventually recycled, using technologies available today, to extract much more of the available energy. Since all the numbers in the tables are based on current uranium consumption rates, they will all decrease in proportion to any expansion of nuclear power.

Taking unconventional uranium resources into account greatly increases all the numbers in Table 8.1. Unconventional uranium resources include about 22 MT U that occur in phosphate deposits and up to 4000 MT U contained in sea water. The technology to recover uranium from phosphates is mature, although costs are relatively high at \$60–100/ kg U. The technology to extract the large dilute uranium resources in sea water has only been demonstrated at the laboratory scale, and extraction costs are currently estimated at about \$300/ kg U. The impact on nuclear generating costs of any eventual shift to higher cost uranium resources would be limited, given that fuel costs

TABLE 8.1 Years of Uranium Availability for Nuclear Power (IAEA 2006)

Fuel Cycle Scenario	Conventional Resources (years)	Total Resources (years)
Once-through fuel cycle with LWRs	80	270
Closed fuel cycle based on pure recycling in FRs	4,800–5,600	16,000–19,000

are a smaller part of nuclear electricity generating costs (2%) than they are of fossil-fired electricity generating costs (40–70%).

Table 8.1 refers only to uranium. Thorium-fueled reactors were developed in the 1960s and 1970s but never captured a significant share of the market. India, which has far greater thorium than uranium resources, is one country continuing to develop the thorium fuel cycle. Thorium is three times as abundant in the Earth's crust as uranium. Although existing estimates of thorium reserves plus additional resources total more than 4.5 MT, such estimates are considered conservative. They do not cover all regions of the world, and the historically weak market demand has limited thorium exploration.

8.6 LONG-TERM WASTE DISPOSAL

Final repositories for low-level radioactive waste from nuclear power plants and from medical, research, and other applications have been licensed and are in operation in many countries. There is no operating repository for the final disposal of high level waste (HLW) from civilian nuclear power plants, although the scientific and technical communities generally agree that such waste can be disposed of safely in stable geological formations. There is one operating geological repository for the disposal of long-lived transuranic waste generated by research and the production of nuclear weapons, the Waste Isolation Pilot Plant in New Mexico, USA.

Currently, spent fuel generated by operating nuclear power plants is either reprocessed or stored. Reprocessing extracts usable uranium and plutonium from the spent fuel for use in new fuel. What remains is HLW that is currently stored pending final disposal. China, France, India, Japan, and the Russian Federation reprocess most of their spent fuel. Canada, Finland, Sweden, and the United States have opted for the alternative of direct disposal of spent fuel as HLW, although the United States has recently proposed a third approach in which spent fuel would be recycled not to extract usable uranium and plutonium, but to immediately "burn" the plutonium and reduce the volume and toxicity of the waste requiring permanent disposal. Countries that have not yet chosen a strategy are currently storing spent fuel and keeping abreast of developments associated with all alternatives.

There is now over half a century of experience with spent fuel storage technology. The amount of spent fuel is relatively small: The spent fuel produced in one year by all the world's operating reactors would cover a soccer field to a depth of about 1.5 meters. And it is relatively easy to add incremental storage capacity. Where politically acceptable, multinational disposal can be considered as a potentially more cost-effective option, especially for small countries with small nuclear programs and limited repository sites.

REFERENCES

1. Francis M. Vanek and Louis D. Albright, "*Energy Systems Engineering: Evaluation and Implementation*." McGraw-Hill Professional, United States of America, 17 May 2008.
2. *Human Development Report 2007/2009*. Palgrave Macmillan, United Nations Development Program, New York, 2007.
3. A.D. Pasternak, Global *Energy Futures and Human Development: A Framework for Analysis*. Lawrence Livermore National Laboratory, 2000.
4. United Nations, Convention on Climate Change, *KYOTO PROTOCOL to the United Nations Framework Convention on Climate Change*. 11 Dec. 1997. http://unfccc.int/resource/docs/convkp/kpeng.html. Accessed 22 October 2006.
5. Paul P. Portney and Robert N. Stavins, *Public Policy for Environmental Protection*, 2^{nd} *ed*.. RFF Press, Washington DC, 4 August. 2000.

FURTHER READING

1. R. Brogli and R. A. Krakowski, *Degree of Sustainability of Various Nuclear Fuel Cycles*. LA-UR-01-6939, LANL, 2002.
2. M. ElBaradei, ed., *Nuclear Power and Sustainable Development*, April 2006, IAEA, http://www.iaea.org/books.
3. *Generation IV Roadmap: Fuel Cycle Assessment Report*. GIF-014-00, 2002.
4. *Trends in the Nuclear Fuel Cycle: Economic, Environmental and Social Aspects*. OECD-NEA, 2001.
5. P. Wydler and L. H. Baetsle, Closing the nuclear fuel cycle: Issues and perspectives. 6^{th} *Inf. Exch. Meeting on Actinide and Fission Product Partitioning and Transmutation*, Spain, Madrid, December 11-13, 2000, EUR 19783 EN.

9

NUCLEAR ENERGY FOR WATER DESALINATION

SALY T. PANICKER AND P.K. TEWARI

Desalination Division, Bhabha Atomic Research Centre, Mumbai, Maharashtra, India

9.1 INTRODUCTION

Water scarcity is one of the most pressing crises affecting our planet. It is a global issue. Water is indispensable for industrial development, economic growth, social well-being, and for the preservation of natural resources. It is estimated that one-fifth of the world's population does not have access to safe drinking water. Drinking water with physical, chemical, or biological contamination has harmful effects on human beings. Seawater, brackish water, and fresh water have different levels of salinity, which is normally expressed by the total dissolved solids (TDS) concentration. Water is considered potable when its TDS is below 500 parts per million (ppm) as per the World Health Organization (WHO). A virtually inexhaustible reserve of water exists in the sea, which is not fit for drinking.

Desalination is the process of producing pure water from saline water using electricity or heat. The major types of commercial desalination processes are (a) thermal processes, such as multi-stage flash (MSF), multiple-effect distillation (MED), vapor compression (VC), and low temperature evaporation (LTE), where heat energy is used to vaporize fresh water from saline water; and (b) membrane processes such as reverse osmosis (RO) and electro-dialysis (ED), where pure water is separated through suitable membranes using mechanical or electrical energy. Globally, about 60 million cubic meter/day (M^3/d) of fresh water is produced by desalination. The energy for these plants is generally supplied from the conventional fossil fuel power plants. However, the depleting sources and future price uncertainty of the fossil fuels promote production of energy from nuclear or renewable sources.

9.2 NUCLEAR DESALINATION

Desalination is an energy-intensive process. A desalination system, especially the thermal unit, can be integrated with a power plant for directly receiving steam, electricity, and coolant (seawater) return stream as feed. Co-location of desalination and power plants has the benefits of sharing infrastructural facilities, which would lead to the reduction of overall costs. Such dual purpose plants generating power and water have inherent design strategies for better thermodynamic efficiency besides economic optimization.

Production of potable water in a facility in which a nuclear reactor is used as the source of energy for the process is termed *nuclear desalination.* This energy could be low-grade steam (for MSF/MED), waste heat (for LTE), or electricity (for RO/ED). Years of successful operation have proved the technical feasibility and reliability of nuclear desalination.

A power plant coupled with a desalination system utilizing only a part of the total energy for producing water is known as a dual-purpose plant or a cogeneration plant. A power plant exclusively dedicated for water desalination is known as single-purpose plant. For a given power rating, a nuclear power plant, in general, has a larger amount of waste heat than a fossil fuel power plant. The enthalpy of steam available at the inlet to the high pressure (HP) turbine of a nuclear power plant is lower due to the lower pressure and temperature of the saturated steam. Thus, the specific steam consumption in a nuclear power plant is higher as compared to conventional power plant. This leads to availability of a higher amount of steam that could be utilized for desalination (Table 9.1). In addition, a nuclear

Nuclear Energy Encyclopedia: Science, Technology, and Applications, First Edition (Wiley Series On Energy).
Edited by Steven B. Krivit, Jay H. Lehr, and Thomas B. Kingery.

TABLE 9.1 Steam Characteristics of Nuclear and Fossil Power Plants

No.	Parameters	Nuclear power plant	Conventional power plant
1	Type	PHWR	Coal based
2	Steam pressure (MPa)	4	13
3	Steam temperature (°C)	250	535
4	Steam enthalpy at HP turbine inlet (kJ/kg)	2800	3470
5	Specific steam consumption (kg/kwh)	6	3.4
6	Steam pressure at LP turbine outlet (MPa)	0.01	0.01
7	Steam temperature at LP turbine outlet (°C)	45	45

TABLE 9.2 Typical Steam Parameters of Different Types of Nuclear Power Plants

Nuclear Power Plant	Steam Parameters	
	Pressure (MPa)	Temperature (°C)
PHWR	4.0	250
PWR (U-tube SG)	6.5	280
PWR (Once-through SG)	6.9	312
BWR	5.5	270
LMFBR	16.3	510
Fort St. Vrain HTGR	17.3	541
THTR-300	18.1	530

power plant is normally situated in coastal areas, where the feed seawater is available nearby and also there is scarcity of good quality water.

Table 9.2 shows the parameters of steam, produced in various reactor types. A nuclear plant, depending on its type, can provide steam or process heat from about 50 to 150°C for desalination. Liquid Metal Fast Breeder Reactor (LMFBR) and High Temperature Gas Cooled Reactor (HTGR) generate steam at higher temperature and pressure. LMFBRs produce steam at approximately 500°C and HTGRs at still higher temperatures.

9.3 WORLD SCENARIO OF NUCLEAR DESALINATION

The possibility of using nuclear energy for desalination of seawater was realized as early as the 1960s. Experience with nuclear desalination now exceeds 150 reactor-years. Table 9.3 gives a list of the nuclear plants used for desalination of water.

Nuclear desalination has been drawing broad interest among the member states of International Atomic Energy Agency (IAEA) due to acute water issues in many arid and semi-arid areas worldwide. The IAEA is playing an important role as a facilitating agency for creating the awareness, coordinating research projects, identifying important topics of common interest, organizing technical meetings, and providing forums for exchange of information on nuclear desalination. Argentina is exploring the possibilities of using its small reactor, CAREM, for providing energy input to desalination system. China has completed the feasibility study of nuclear desalination project using the NHR-200 type of nuclear reactor. Egypt has completed a feasibility study for a nuclear co-generation plant at El-Dabaa. Construction of a pre-heat reverse osmosis (RO) test facility at El-Dabaa has been completed. France has collaborations with (1) Libya to undertake techno-economic feasibility study for a specific site and the adaptation of the experimental reactor at Tajoura for nuclear desalination and (2) Morocco (The AMANE project) for techno-economic feasibility study of Agadir and Laayoun sites. In Japan, several nuclear reactors are integrated with desalination facilities. The Korean program includes development of an integrated desalination plant with SMART for electricity generation and seawater desalination. Pakistan is establishing an MED based nuclear desalination demonstration plant integrated with the Karachi Nuclear Power Plant (KANUPP). The Russian Federal Agency for Atomic Energy (ROSATOM) is constructing a floating barge mounted co-generation nuclear plant based on ship propulsion reactor KLT-40s of PWR type. Tunisia has completed techno-economic feasibility study for the la Skhira site in the southeast part of the country. Nuclear desalination is one of the missions of U.S. Department of Energy's launched Global Nuclear Energy Partnership (GNEP)'s Grid Appropriate Reactor (GAR) campaign. Indonesia, Saudi Arabia, Algeria, Brazil, Islamic Republic of Iran, Iraq, Italy, Jordan, Lebanon, Philippines, Syrian Arab Republic, and the UAE

TABLE 9.3 Nuclear Desalination Plants

Name and Type Reactors	Gross Power (MWe)	Desalination Process	Water Capacity (M^3/d)
Ikata-1,2 (Japan) PWR	2x566	MSF	200
Ikata-3 (Japan) PWR	890	RO	2000
Ohi-1,2 (Japan) PWR	2x1175	MSF	3900
Ohi-3,4 (Japan) PWR	2x1180	RO	2600
Genkai-4 (Japan) PWR	1180	RO	1000
Genkai-3,4 (Japan) PWR	2x1180	MED	1000
Takahama-3,4 (Japan) PWR	2x870	MED	1000
Kashiwazaki (Japan) BWR	1100	MSF	1000
BN-350 (Kazakhstan)	150	MED	80,000
MAPS (India) PHWR	2x220	MSF & RO (Hybrid)	6300
CIRUS (India) PHWR	40 (MWth)	LTE	30

Figure 9.1 Nuclear Desalination Demonstration Plant (NDDP) at Kalpakkam (India).

are exploring the potential of nuclear desalination in their countries or regions.

9.4 CASE STUDY: NUCLEAR DESALINATION IN INDIA

9.4.1 Utilization of Nuclear Steam

Nuclear Desalination Demonstration Plant (NDDP) set up by Bhabha Atomic Research Centre (BARC) at Kalpakkam (Fig. 9.1) consists of hybrid MSF-RO system of 6300 M^3/d capacity and is coupled to the Madras Atomic Power Station (MAPS). NDDP is the first and the largest nuclear desalination plant based on hybrid technology in the world. The requirements of seawater, steam, and electrical power for the desalination plant are met from MAPS.

The MSF plant (4500 M^3/d) produces water of distilled quality (2–10 ppm TDS), which is good for high end industrial use. The basic principle involved in the MSF process is to heat the sea water to about 90–120°C using the heat of condensation of the vapor produced in the system and external steam (Fig. 9.2). The heated seawater is subsequently flashed in successive stages maintained at decreasing levels of pressure. The vapor produced is condensed and recovered as pure water. MSF can tolerate higher contaminant loading (such as suspended solids, heavy metals, oil, grease, Chemical Oxygen Demand (COD), Biological Oxygen Demand (BOD)) in feed seawater. It requires low-pressure steam as energy input. Long tube design is adopted to reduce energy consumption. Salient features of the MSF section of NDDP are given in Table 9.4.

The basic features of MAPS are shown in Table 9.5. The MSF plant needs about 21 tonnes/hour (T/h) dry saturated steam at 1.8 kg/cm^2 for the brine heater and 0.5 T/h dry saturated steam at 7 kg/cm^2 for the steam jet ejectors. The low-pressure (LP) steam is drawn after the high-pressure (HP) turbine from the cold reheat line before moisture separator (MS) of the nuclear power plant. A moisture separator is provided to entrap moisture of cold reheat steam in order to prevent erosion. It is designed in such a way that the steam becomes almost dry, and the pressure drop is limited to 0.05 kg/cm^2.

In order to avoid any possible ingress of activity from the steam to the brine heater and to the ejector systems, two separate isolation heat exchangers (as barriers) are provided. The HP isolation heat exchanger generates steam for steam jet ejector, and the LP isolation heat exchanger generates steam for the brine heater using low-pressure steam from the exhaust of the high-pressure turbine. These physical barriers isolate the nuclear power plant from the desalination plant and minimize the probability of product water contamination.

9.4.2 Utilization of Nuclear Waste Heat

Because the energy cost component is the major fraction of the desalinated water cost, utilization of waste heat is an attractive option. This is also an eco-friendly way to produce desalinated water, because it does not require chemical pretreatment of the feed. LTE technology

Figure 9.2 MSF Section of NDDP.

TABLE 9.4 Technical Specifications of the MSF Section of NDDP

No.	Parameters	Technical Specifications
1	Capacity (M^3/hr)	187.5
2	Design concept	Recycle type
3	Tube configuration	Long tube
4	No. of flash stages	39 (heat recovery : 36 heat rejection : 3)
5	Top brine temperature (°C)	121
6	Performance ratio	9
7	Feed quality (ppm)	25,000–40,000
8	Product quality (ppm)	2–10

TABLE 9.5 Basic Features of MAPS

No.	Parameters	Technical Specifications
1	Net Electrical Output (MW(e))	220
2	Moderator	Heavy Water (D_2O)
3	Primary Heat Transport System	Heavy Water (D_2O)
4	Secondary Heat Transport System	Water/Steam
7	Condenser Coolant	Seawater

developed by BARC essentially consists of three portions: heater, separator, and condenser. In the heater shell, vertical tubes are used. Feed seawater enters the unit at the bottom of the tubes and partly evaporates by the time it comes out from the top. After the water and vapor mixture comes out of the tubes, the vapor rises through the vertical shell, enters the horizontal tube bundle kept at the top of the vertical shell, and condenses around the tubes (which are cooled by seawater flowing inside), producing desalinated water.

LTE plants are ideally suited for coupling with power/process plants/diesel generator (DG) sets, where waste heat is available. Nuclear research reactors produce significant quantities of waste heat. An LTE plant of 30 M^3/d capacity is coupled to the nuclear research reactor at Trombay, India (Fig. 9.3) for producing distilled water (2–3 ppm TDS) from seawater. The product is used as makeup water in the reactor. An intermediate heat exchanger (IHE) is incorporated between the nuclear reactor and the desalination plant as isolation loop to minimise any possibility of product water contamination.

9.4.3 Utilization of Electricity

In addition to integration with an existing nuclear power plant, NDDP has the specialty of hybridization. Combination of more than one desalination process is termed *hybridization*. NDDP consists of an RO section producing 1800 M^3/d potable water from seawater. The hybrid technology has several advantages. It has the provision for flexibility, redundancy, and usability of warm seawater from the thermal desalination plant as feed to RO, which would enhance the productivity and production of two qualities of desalinated water for the best utilization. The other facilities, such as combined post treatment, common seawater intake and brine discharge systems, and sharing of manpower and facilities helps in reducing the product water cost. Figure 9.4 shows the logistics of NDDP hybridization. The product water (250–500 ppm TDS) from RO is of potable quality. The products from MSF and RO can be blended for providing better quality drinking water.

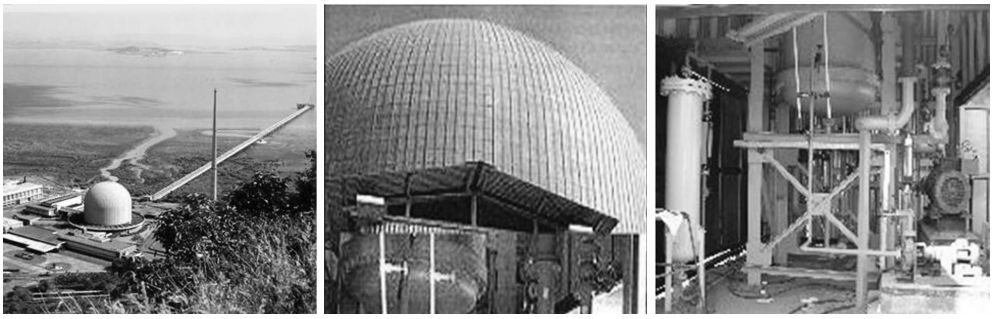

Figure 9.3 LTE Plant Using Nuclear Waste Heat at Trombay.

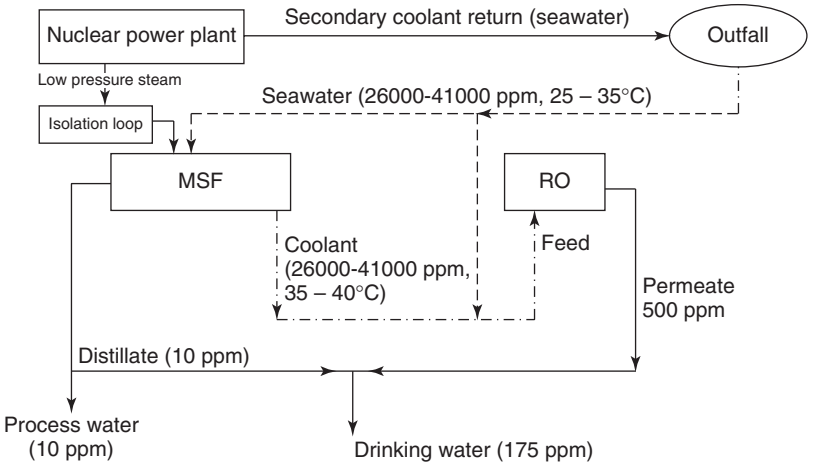

Figure 9.4 Schematics of MSF—RO Hybridization.

Figure 9.5 RO Section of NDDP.

RO is a pressure-driven, membrane-based desalination technology. The physico-chemical properties of the semi-permeable membrane used in the system govern the process of desalination. A typical RO plant consists of three sections: pretreatment, RO membrane, and post treatment. The pretreatment section involves either the conventional system of particulate and fine filtrations or membrane-based ultrafiltration (UF) followed by chemical addition. The second section consists of RO membrane elements through which pretreated saline water is passed under pressure in excess of its osmotic pressure with the help of a high-pressure pump. Pure water permeates through the membrane, effecting desalination. The concentrated stream (reject) contains the total pressure energy supplied, which can be recovered. Various energy recovery devices are available, such as hydraulic turbochargers and pressure exchangers that can recover this energy up to 50%, thus reducing the energy cost. The post treatment section may include (1) lime treatment for pH correction, so as to prevent corrosion of the water distribution systems and (2) chlorination for disinfection. Figure 9.5 shows the RO section of NDDP. The salient features of the plant are given in Table 9.6.

TABLE 9.6 Salient Features of the RO Section

No.	Parameters	Technical Specifications
1	Capacity (M^3/hr)	75
2	Sea water TDS (ppm)	25000–40000
3	Operating pressure (MPa)	45–55
4	Recovery (%)	35
5	Solute Rejection (%)	>98.5
6	Product quality (ppm)	250–500

9.5 CONCLUSION

To meet the challenges of growing demands of power and water, nuclear plants with desalination system coupled to them are going to play a major role. Adopting cogeneration concept along with hybridization would help in cost-effective production of desalinated water. There would be requirements for small, medium, and large size desalination plants coupled to nuclear power stations in coastal areas governed by the demand with respect to quantity and quality of the desalinated water.

10

NUCLEAR ENERGY FOR HYDROGEN GENERATION

ALISTAIR I. MILLER

Atomic Energy Canada Ltd., Deep River, ON, Canada

10.1 INTRODUCTION

Hydrogen is a paradoxical substance in at least three ways. First, in both simple molecular and ionic forms, it abounds in the universe, yet terrestrially, it overwhelmingly exists in chemically combined form as compounds of oxygen, carbon, and other atomic species. Second, molecular hydrogen holds promise of an exceptionally clean and energy-rich fuel—in weight terms—but it is awkward to contain since it occupies relatively large volumes and can escape easily. Third, through unfamiliarity, it suffers from a reputation of being a dangerously flammable substance although its attributes of easy dispersion and a flame that emits little radiant heat make it relatively safewhen compared to gasoline.

Hydrogen could be a large-scale energy vector with relatively small environmental detractions[1] although it has competitors in biofuels and electricity. Biofuels—especially bio-ethanol—are early leaders to displace oil-based fuels, but their detractions of collateral emissions of both carbon dioxide (CO_2) and nitrous oxide (N_2O) and disruption of other agriculture seem likely to limit their usefulness in reducing greenhouse gas (GHG) emissions. Electricity is a much stronger challenger wherever it can be generated with minimal GHG emissions, and battery advances are trending toward affordable pluggable hybrids with enough capacity to be predominantly electric-fueled for light duties. Heavier-duty vehicles offer the most probable application for hydrogen fueling.

Today, hydrogen appears unlikely to be *the* single, silver bullet for CO_2-free transportation, but it could have an important role. However, this will only be possible if there is a satisfactory means for its production without collateral pollution.

To date, nuclear fission has been confined almost entirely to generation of electricity. While electricity is an important component of total energy consumption—typically 25 to 30%—new ways to extend nuclear fission's application to non-electrical applications could allow a larger role for this primary energy source. Producing hydrogen using relatively high-temperature nuclear heat is one possible approach, involving either no electrical input or significantly reduced electrical input compared to that for conventional water electrolysis. This appears to be technically possible for nuclear reactor designs producing fluid outputs of about 800–900°C and possibly as low as 550°C.

Nuclear reactors are usually operated continuously to provide base-load electricity, although in grids where nuclear power is a substantial component of the total supply, the reactor fleet's power output may have to be reduced at times of low electrical demand. This is economically undesirable and creates some technical difficulty. One can envisage diversion of the reactors' output (either as heat or as electricity) for generation of hydrogen during periods of lower electricity demand as a means to avoid reduced-power operation. Thus, while electricity cannot easily be stored for later use, storage is quite practical if the energy has been converted to hydrogen.

10.2 PRODUCING HYDROGEN

Hydrogen does not occur naturally on earth. It must be manufactured and, if it is to contribute to large-scale

Nuclear Energy Encyclopedia: Science, Technology, and Applications, First Edition (Wiley Series On Energy).
Edited by Steven B. Krivit, Jay H. Lehr, and Thomas B. Kingery.

greenhouse gas reduction, manufactured in ways that do not release significant amounts of GHGs. Traditionally, steam-methane reforming (SMR) has been the predominant process for hydrogen manufacture. But the SMR co-produces almost 8 kg of CO_2 per kilogram of hydrogen. Electrolysis of water is also used to manufacture hydrogen but only for small-scale production and for ultra-pure hydrogen, since it is generally more expensive than SMR production. Nonetheless, if the electricity comes from a source with little or no CO_2 emission, this is a route to hydrogen production with low GHG emissions.

Hydrogen is, of course, easily produced by many chemical reactions such as adding an acid or even steam to a metal. One of the simplest ways of producing hydrogen is to react steam with iron:

$$Fe + xH_2O \rightarrow FeO_x + xH_2 \qquad (10.1)$$

This is an old way of producing very pure hydrogen but of little value without an acceptable way of reversing the process. Reversal of this reaction is essentially smelting iron, a complex route that involves conversion of carbon to CO and CO_2, defeating the underlying objective of avoiding GHG production.

Starting in the 1960s, widespread studies began in an attempt to identify suitable chemical cycles that could decompose water into hydrogen and oxygen reversibly using heat either alone or predominantly to effect the decomposition.

In theory, steam can be directly dissociated with heat alone, but the water molecule has strong bonds, thus dissociation is negligible below 2000°C, an unworkably high temperature. Even at 2900°C, equilibrium attains only 10% dissociation. Even worse, recombination occurs rapidly as the mixture cools and there is no evident way of separating the dissociated gases. In thermodynamic terms, the energy needed for a chemical reaction to occur has two components: free energy, usually designated ΔG, and an entropy component, usually designated $T\Delta S$, where T is temperature and ΔS is the entropy change. $T\Delta S$ can be supplied by heat while ΔG cannot. If ΔG is substantially positive, the reaction will only occur with input of work in some form, either electricity or another reaction with a negative ΔG. Because the total energy for a reaction varies only slightly with temperature (unless a phase change occurs), a sufficiently large $T\Delta S$ term will drive ΔG negative. Unfortunately, with water vapor, the $T\Delta S$ term climbs very slowly with temperature, and ΔG is still slightly positive at 4000 K (Fig. 10.1).

However, many reactions have larger entropy changes and thus a $T\Delta S$ term that is much more temperature-sensitive. Consequently, there are many sets of coupled chemical reactions that could, in theory, be used to split the water molecule indirectly with only heat at fairly accessible temperatures. Innumerable alternative processes to split water into hydrogen and oxygen indirectly have been examined. The simplest would be a two-step process illustrated in Figure 10.2.

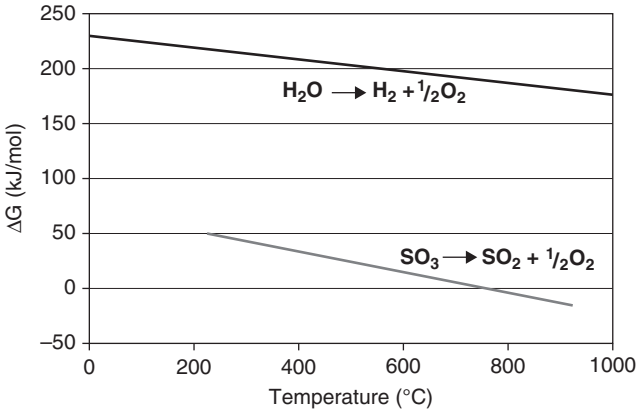

Figure 10.1 Free energies for SO_3 dissociation to SO_2 and O_2 and of water dissociation as a function of temperature.

No practical process using this approach has been identified. So the studies have investigated three- to five-step processes. A few of these are objects of extensive development today. They employ temperatures in the range of 500–1000°C, and some also use some electrolysis. Temperatures of up to about 900–950°C could be supplied either by focused solar heat or very high temperature nuclear reactors (VHTRs) cooled with helium gas.

Two groups of processes currently feature in major government-funded investigations. The first group depends on high-temperature (about 800°C ± 50°C) decomposition of sulfur trioxide (SO_3). The second group depends on changing valence states of metal chlorides.

10.2.1 The Sulfur–Iodine Process

The most prominent of the first group is known as the sulfur–iodine (S/I) process[2]. Over the last decade, this process has been extensively investigated up to pilot-scale by nationally funded programs in Japan, France, the United States, and the Republic of Korea, the work latterly coordinated as part of the Generation IV International Forum (GIF)[3].

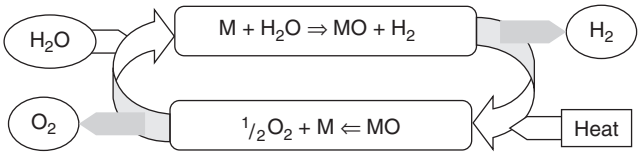

Figure 10.2 Idealized two-step thermochemical process.

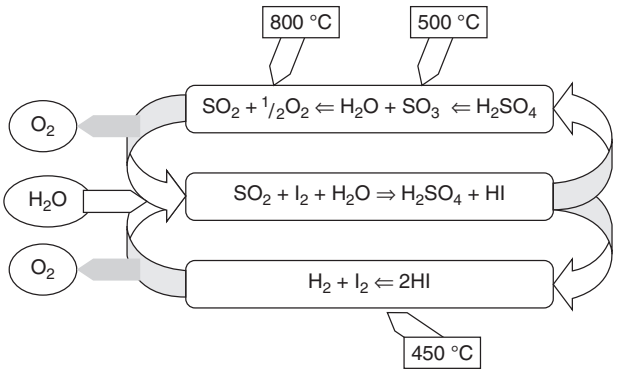

Figure 10.3 The S/I process.

The S/I process is illustrated in Figure 10.3. At its heart is the Bunsen reaction:

$$SO_2 + 2H_2O + I_2 \rightarrow H_2SO_4 + 2HI, \qquad (10.2)$$

which is a low-temperature, exothermic reaction that occurs easily in liquid phase. It is followed by thermal decomposition of the sulfuric acid, first to sulfur trioxide, SO_3, and steam (by 500°C) and subsequently, at yet higher temperature, by decomposition of SO_3 to sulfur dioxide, SO_2, and oxygen:

$$H_2SO_4 \rightarrow SO_3 + H_2O \rightarrow SO_2 + \frac{1}{2}\,O_2 + H_2O \qquad (10.3)$$

At intermediate temperature (450°C), the HI decomposes into hydrogen and iodine, I_2:

$$2HI \rightarrow H_2 + I_2 \qquad (10.4)$$

The SO_2 and I_2 are recycled, and water has been split into hydrogen and oxygen.

Reality is much more difficult than the equations suggest. While the Bunsen reaction is easily produced by bubbling SO_2 through iodine in water, considerable excesses of both water and iodine have been shown to be necessary. Excess water is needed for the reaction to proceed, and excess iodine is required to cause the two acids to separate into two phases, a lighter one containing almost all of the H_2SO_4 and a heavier of almost pure HI_x. Without this phase separation, raising the concentration of HI to 50% causes irreversible side reactions forming hydrogen sulfide, H_2S, and sulfur. Lee et al. [1] report that the optimal form of the Bunsen reaction is actually:

$$5I_2 + SO_2 + 13H_2O \rightarrow [H_2SO_4 + mH_2O] + [2HI + 4I_2 + (11 - m)H_2O] \qquad (10.5)$$

Subsequent removal of this excess water and iodine takes energy and generally increases costs. Most of the excess water stays with the HI phase and has to be evaporated when the temperature is raised to around 220°C to gasify the HI and separate it from the excess I_2. By using a reactive distillation column with vaporization of the HI, this dissociation can occur at about 320°C. The HI dissociation reaction has a negative ΔG.

In comparison with the difficulty of the HI decomposition, decomposition of the sulfuric acid is relatively straightforward, although requiring heat at a higher temperature. While this reaction requires a temperature of about 850°C for ΔG to become negative (Figure 10.1), this temperature is far more accessible than the temperature for direct water decomposition.

Goldstein et al. [2] have estimated the thermal efficiency of the S/I cycle. The theoretical maximum is around 52%; however, their calculations suggest an actual efficiency of only 33 to 36%, although they note that there may be scope for improvement if advanced technologies such as membrane or electrodialysis separations can be developed. Another area for potential improvement would be development of cheaper materials able to resist attack by these two corrosive acids at the required temperatures. However, the large difference between the molecular weights of iodine and hydrogen (127:1) coupled to the need for a large excess of iodine weighs on the economics. The value of the iodine circulating in the S/I process is thousands of times that of the circulating hydrogen, suggesting that iodine holdup is an important variable for process economics and that even slight losses would be economically intolerable.

With 2009 technology, Leybros et al. [3] have estimated a production cost for hydrogen by the S/I process of 12 €/kg ($18/kg). While this cost estimate is almost certainly open to reduction with experience and advances in materials, the estimated cost is so high as to cast severe doubts on the economic viability of the S/I process.

10.2.2 The Hybrid Sulfur Process

Some of the technical and economic difficulties of the S/I process can be avoided by eliminating the iodine component and reconstituting the sulfuric acid by electrolysis:

$$SO_2(aq) + 2H_2O \rightarrow H_2SO_4(aq) + 2H^+ + 2e \qquad (10.6)$$

and, by using a cell with a proton-conducting membrane,

$$2H^+ + 2e \rightarrow H_2(g) \qquad (10.7)$$

The decomposition of H_2SO_4 is identical to the S/I process.

The economics of this process have also been examined by Leybros [4] and his collaborators. While this process uses electrolysis and so is not a pure thermochemical route to hydrogen production, the theoretical voltage is small (~0.25 V in 50% H_2SO_4). Allowing for a typical overvoltage with practical current densities, Leybros

et al. suggest an actual voltage of 0.6 V is possible. (This compares very favorably with the 1.7 or more needed for water electrolysis.) As they note, the main technical challenge is devising an electrolysis cell able to withstand 50% H_2SO_4 at 120°C and a pressure of up to 10 atmospheres. (Hydrogen must be compressed for storage or transmission; compression is most energy intensive at low pressure, and this energy is much more easily and efficiently supplied electrochemically rather than mechanically.) Based on 2009 materials and technology, Leybros et al. estimate a cost for hybrid sulfur of 6.6 €/kg ($10/kg) but caution that their assumptions of cell lifetime and voltage may be optimistic.

10.2.3 Cycles Based on Metal Halides

One of the earliest concepts for indirect thermochemical production of hydrogen was to utilize metal halides and oxides. Numerous cycles based on this approach have been investigated. Although written in 1979—toward the end of the initial period of intensive exploration of thermochemical possibilities—Ihara's [5] review remains definitive.

One of the earliest of the halide-oxide cycles is the UT-3 cycle, which uses calcium and iron oxides and bromides. It has been extensively studied:

$$CaO + Br_2 \rightarrow CaBr_2 + 1/2\ O_2 \text{ at } 550^\circ C \quad (10.8)$$

$$CaBr_2 + H_2O \rightarrow CaO + 2HBr \text{ at } 730^\circ C \quad (10.9)$$

$$Fe_3O_4 + 8HBr \rightarrow 3FeBr_2 + 4H_2O + Br_2 \text{ at } 220^\circ C \quad (10.10)$$

$$3FeBr_2 + 4H_2O \rightarrow Fe_3O_4 + 6HBr + H_2 \text{ at } 650^\circ C \quad (10.11)$$

Here bromine is used to reduce calcium oxide and ferric oxide to regenerate bromine while producing ferrous bromide, which can in turn be oxidized with water to release H_2.

While the temperature requirement is somewhat lower than needed for SO_3 decomposion, the presence of so many solid species is a weakness, and it is difficult to avoid sintering when CaO is converted to $CaBr_2$. Investigators from the French CEA have concluded that it is unlikely to be competitive as a hydrogen production process [6].

10.2.4 Copper Chloride Cycles

The main attraction of processes based on copper chlorides is that the highest temperature required is only 500°C. This temperature is within the reach of various liquid-metal-cooled reactors (using liquid lead or liquid sodium) and supercritical water reactors (SCWRs) as well as gas-cooled reactors operating at lower temperatures than the VHTR. Electrolysis is required for one step.

The following reactions have been proposed:

$$2Cu + 2HCl \rightarrow 2CuCl + H_2 \text{ at } 450^\circ C \quad (10.12)$$

$$2CuCl \rightarrow CuCl_2 + Cu \text{ at } 30^\circ C \text{ with electrolysis} \quad (10.13)$$

$$CuCl_2(aq) \rightarrow CuCl_2(s) \text{ at } 100^\circ C \quad (10.14)$$

$$2CuCl_2 + H_2O \rightarrow Cu_2OCl_2 + 2HCl \text{ at } 400^\circ C \quad (10.15)$$

$$Cu_2OCl_2 \rightarrow 2CuCl + 1/2\ O_2 \text{ at } 500^\circ C \quad (10.16)$$

The first reaction is exothermic. The others are endothermic with reaction 10.13 requiring electrolysis because it has a positive ΔG. Reaction 10.14 is really a purification step in which solid $CuCl_2$ is separated from the mixture in which it was formed.

Atomic Energy of Canada Limited (AECL) has recently developed a variant on this cycle that avoids production of copper metal. Reaction 10.12 is eliminated; reaction 10.13 is replaced by a new electrochemical step:

$$2CuCl + 2HCl \rightarrow H_2 + CuCl_2 \text{ at } 100^\circ C \text{ with electrolysis} \quad (10.17)$$

Avoidance of production of solid copper is a definite advance, and recent experiments by AECL have shown that this process achieves good stoichiometry and a voltage of about 0.7 V is needed at reasonable current densities [7]. This voltage requirement is comparable to the hybrid sulfur process.

All of the reactants in the copper chloride cycles are reasonably inexpensive: HCl costs around $600/tonne and copper around $3,500/tonne. Based on two atoms of copper reacting to produce one hydrogen molecule, a 0.1% loss of copper would add about $220/tonne to the cost of hydrogen. Similarly, based on two molecules of HCl producing one hydrogen molecule (the proper ratio to use is debatable), a 0.1% loss would add about $45/tonne to the cost of hydrogen.

So makeup costs for the copper-chloride process would likely exceed those for the hybrid sulfur process, but they would be far less of an issue than for the S/I process.

10.3 COMPETING NON-THERMOCHEMICAL HYDROGEN-PRODUCING PROCESSES

10.3.1 Steam-Methane Reforming (SMR)

Hydrogen already has a large and growing share in transportation as an additive to transform crude oil into usable products. Crude oil grades processed in refineries have become increasingly sour—rich in sulfur—and hydrogen poor. This requires that they be treated with a range of

hydrogen-consuming processes such as hydrofining and hydro cracking. Almost invariably, the hydrogen has been produced by the SMR process where:

$$CH_4 + 2H_2O \rightarrow CO_2 + 4H_2 \qquad (10.18)$$

Based on a price for crude oil of \$80/bbl, the energy-equivalent price of natural gas is \$13/GJ. Statistically, the North American equivalent price has averaged slightly less than the energy-equivalent price. So crude oil at \$80/bbl should be converted to just over \$11/GJ. Including the use of gas for process heat, 2.86 kg of methane produces one kilogram of hydrogen for a fuel cost of \$1.83/kg plus a processing cost of about \$0.60/kg.

10.3.2 Low-Temperature Electrolysis

Low-temperature ($\sim$70°C) electrolysis (LTE) currently occupies two niches: small-scale production and ultra-pure product. Conversion of water to hydrogen by LTE is accomplished with 70 to 80% efficiency—depending on the current density—making it a reasonably efficient process. Typically, 50 to 55 kWh of electrical energy produces one kilogram of hydrogen. To compete with SMR, hydrogen at \$3.00/kg, electricity must cost less than 6 ¢/kWh. While this would seem to present a substantial obstacle to electrolytic hydrogen, three circumstances can favor it: (1) in locations with large hydroelectric capacity such as Manitoba, where the wholesale price of electricity is about 3 ¢/kWh; (2) using low time-of-day value (and in some jurisdictions, price) of electricity, which can vary greatly and can be very low; and (3) where local production of electrolytic hydrogen produced at the point of fueling avoids the cost of distribution. The cost of electrolytic equipment must also be included. This capital equipment cost for hydrogen production is difficult to estimate on production scales large enough to influence GHG abatement since costs would be immensely greater than the existing production of electrolytic hydrogen. Hydrogenics—a leading developer and supplier of electrolysis equipment—estimates that its cells could be mass-produced for \$500/kA. Cells are robust equipment; amortized over 20 years at 10%/a interest plus the cost of operation, cells are estimated to add about \$0.33/kg to the cost of hydrogen. So, in a few locations favored with low electricity costs, electrolytic hydrogen could be competitive.

However, to be produced widely, intermittent production using off-peak pricing of electricity would be the only competitive approach. Detailed studies using the price paid for electricity in the Canadian provinces of Ontario and Alberta [8] have shown that intermittent production combined with cavern storage (similar to that used for natural gas) can produce hydrogen at about \$3.30/kg.

10.3.3 High-Temperature Electrolysis

As Figure 10.1 implies, the voltage required for water electrolysis falls with rising temperature, and high-temperature electrolysis (HTE) offers the prospect of a far simpler process than a thermochemical cycle, although it appears to need temperatures almost as high as those for SO_3 decomposition plus electrical as well as thermal energy. The technology is almost identical to that already being developed for solid-oxide fuel cells (SOFC) with the important distinction that electrolysis produces oxygen in its nascent and highly reactive state. The most widely used material for both SOFC and HTE is yttrium-stabilized zirconia.

With HTE, the proportion of the energy to dissociate water that needs to be provided electrically falls with rising temperature. At 800°C, the theoretical voltage has dropped to just under 1.0 V. In practice with reasonable current densities, work at Idaho Falls Laboratory of the United States Department of Energy (USDOE), which is developing HTE technology [9], indicates voltages around 1.2 to 1.3 V. This is close to the thermoneutral voltage for water decomposition and about two-thirds of what is typically achieved in a low-temperature electrolysis cell.

This technology is early in its development, but the relatively small reduction in electricity consumption compared to LTE may be insufficient to offset relatively complex equipment and the need for very high temperature heat. More recently, gadolinium-stabilized ceria has been proposed as an alternative separator. It operates at slightly lower temperature.

10.4 CONCLUSION

James Funk, one of the originators of the concept of thermochemical hydrogen production in the early 1960s, wrote in a review article in 2001 [10]:

> ... where cost estimates which yield both capital and operating costs ... the cost numbers do not look good when compared ... with natural gas reforming.

Funk went on to suggest that constraint on CO_2 emission could overcome this. However, for low-emission hydrogen, the competition for thermochemical production processes should be seen as conventional low-temperature electrolysis rather than SMRs. If one starts with 850°C heat, electricity can be generated with about 48% efficiency, giving an overall efficiency of energy conversion to hydrogen by LTE of around 42%. Taking the S/I process as the most studied and developed of the thermochemical processes, its complexity and a *theoretical maximum* conversion efficiency of 52% suggest that the prospect of thermochemical-produced hydrogen remains elusive. Hybrid-sulfur appears substantially better than S/I while other, newer cycles have some promise. Nonetheless,

almost 50 years of study and development have yet to produce an economically viable thermochemical or thermo-electrochemical route to hydrogen production.

Autobiographical Note

Alistair Miller has been a Canadian representative from virtually the inception of the Hydrogen Production Project Management Board of the Generation IV International Forum, which is an international collaboration for development of advanced nuclear reactors. He has written extensively on the economics of energy and hydrogen production in the context of greenhouse-gas abatement. He is a researcher emeritus with Atomic Energy of Canada Limited. He has a PhD in Chemical Engineering from the University of London, Imperial College.

Endnotes

1. Because of its high flame temperature, burning hydrogen can lead to the formation of nitrogen oxides, NO_x. These contribute to formation of photochemical smog and nitrous oxide, N_2O, is a powerful and long-lived greenhouse gas. Care must be taken with design of combustion processes to reduce NO_x to insignificant levels. Water vapor is also a powerful greenhouse gas and energy from burning hydrogen produces 1.5 to two times more water vapor than burning natural gas or oil. This is unimportant in the troposphere where water vapor has a turnover time of only days. However, in the Stratosphere, water vapor is much more persistent, and the potential for a greenhouse gas effect from the use of hydrogen as an aircraft fuel would need careful review.
2. Sometimes reversed to I/S.
3. The GIF is a multinational program of collaboration on the development of advanced nuclear reactors.

REFERENCES

1. B.J. Lee et al., An optimal operating window for the Bunsen process in the I-S thermochemical cycle. *Int. J. Hydrogen Energy*, **33**, 2200–2210, 2008.
2. S. Goldstein, J.-M. Bogard, and X. Vitart, *Int. J. Hydrogen Energy*, **30**, 619–626, 2005.
3. J. Leybros et al., Plant sizing and evaluation of hydrogen production costs from advanced processes coupled to a nuclear heat source; Part I: Sulphur-iodine cycle. *Int. J. Hydrogen Energy*, to be published.
4. J. Leybros et al., Plant sizing and evaluation of hydrogen production costs from advanced processes coupled to a nuclear heat source; Part II: Hybrid-sulphur cycle. *Int. J. Hydrogen Energy*, to be published.
5. S. Ihara, Chapter 5: Thermochemical hydrogen production, from *Solar Hydrogen Energy Systems*, T. Ohta, ed. Pergamon Press, 1979.
6. F. Lemort, C. Lafon, R. Dedryvère, and D. Gonbeau, Physicochemical and thermodynamic investigation of the UT-3 hydrogen production cycle: A new technological assessment. *Int. J. Hydrogen Energy*, **31**, 7, 906–918, June 2006.
7. S. Suppiah, private communication, Atomic Energy of Canada Limited, November 2008.
8. A.I. Miller and R.B. Duffey, Integrating large-scale co-generation of hydrogen and electricity from wind and nuclear sources (NuWind™), 2008 International Congress on Advances in Nuclear Power Plants, Anaheim, CA, 2008 June 8-12.
9. S. Herring et al., *High temperature solid oxide electrolyser system*, USDOE Project PD24, 2005, www.hydrogen.energy.gov/pdfs/review05/pd24_herring.pdf.
10. J.E. Funk, Thermochemical hydrogen production: past and present. *Int. J. Hydrogen Energy*, **26**, 185–190, 2001.

PART II

NUCLEAR FISSION

11

URANIUM-PLUTONIUM NUCLEAR FUEL CYCLE

SHOAIB USMAN

Missouri University of Science and Technology, Mining & Nuclear Engineering, Rolla, MO, USA

Nuclear energy has been a significant part of the energy mix for most of the developed world for the last four decades. At present, an estimated 16% of the world energy is provided by nuclear power [1] and the recent trends are strongly continuing in this direction. Many countries are constructing new nuclear power plans to fulfill their current and future energies needs. Nuclear energy is perhaps the most regulated power industry with monitoring and regulation ranging from local and national levels all the way up to international monitoring organizations. Many aspects of nuclear energy are highly political. The International Atomic Energy Agency (IAEA) headquartered in Vienna, Austria, was established in 1957 with its main goal to promote the peaceful use of nuclear energy and prevent its military use by monitoring and regulating various stages of the nuclear fuel cycle. Through the work of IAEA, international agreements have been put in place between the member countries. This extraordinary political flavor of the industry is primarily due to close similarities between nuclear power production and nuclear weapon development [2]. Concerns for potential environmental impact are significant, as a result of the 1986 Chernobyl accident, but the risk of nuclear weapon proliferation has played the most important role in the international arena.

The term Nuclear Fuel Cycle refers to the extraction of uranium- (or in some special cases thorium-) based minerals from nature, processing the material, and then using the material in the nuclear reactor for power generation. Finally, reprocessing the spent fuel once it is discharged from the reactor to separate the waste from the spent fuel and reusing the useful materials. In the "once through" fuel cycle, the spent fuel is not reprocessed to extract remaining useful materials. Figure 11.1 shows various stages of the nuclear fuel cycle. For each process in the cycle, multiple methods and techniques are applied.

Nearly all nuclear power reactors require the raw uranium to undergo an enrichment process. Natural uranium exists primarily in two isotopic forms, U238 (99.274%) and U235 (0.720%) [3]. Only the U235 portion of natural uranium can undergo fission induced by slow neutrons and will work as fuel for thermal reactors. The process of increasing the weight percent (content) of U235 in the natural uranium such that a chain reaction can be maintained is called enrichment.

It is important to point out that not all reactor types, and therefore fuel cycles, require an enrichment process. For example, the Canadian reactor design CANDU (CANada Deuterium Uranium) uses natural uranium. The goal of the nuclear fuel cycle is to process the material to initiate and maintain safe and efficient fission process:

$$\begin{aligned} &neutron + Nuclear\ Fuel \rightarrow Fission\ Process \\ &\quad \rightarrow Fission\ Products + additional\ Neutrons \\ &n + U235 \rightarrow ff1 + ff2 + x.n \end{aligned}$$

Fission, being an exothermic reaction, is used to produce power. On the average approximately 200 MeV ($\sim 3.204 \times 10^{-11}$ J) of energy is released per fission. The term *chain reaction* refers to the process of utilizing the fission neutrons released (where x varies from 2 to 3) to cause subsequent fission(s). Fission chain reaction will be maintained if one and only one of the fission neutrons (on the average) will cause a subsequent fission. If more

Nuclear Energy Encyclopedia: Science, Technology, and Applications, First Edition (Wiley Series On Energy).
Edited by Steven B. Krivit, Jay H. Lehr, and Thomas B. Kingery.

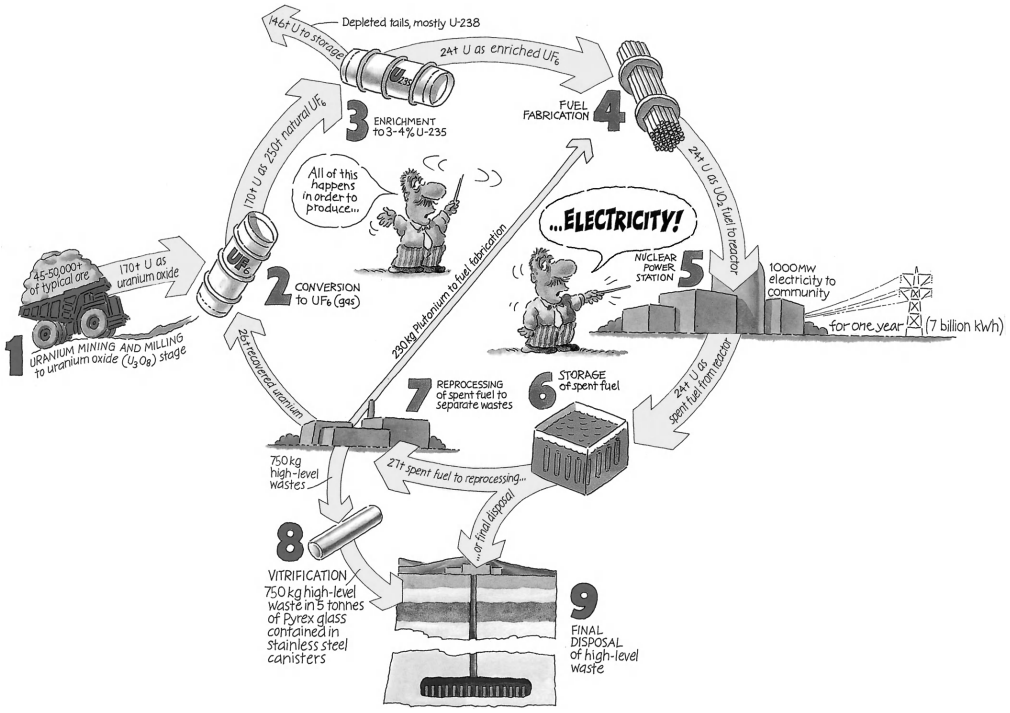

Figure 11.1 Uranium fuel cycle. *Source*: http://www.world-nuclear.org/education/graphics/nfc1-3.gif.

than one fission reactions are caused by the neutrons in the subsequent cycle, the process will be supercritical.

Only a few isotopes can interact with a thermal neutron (that is, in thermal equilibrium, moving at a slow speed of 2200 m/s) to cause fission. For example, uranium exists in nature in three isotopic forms: U234 (0.0055%), U235 (0.720%), and U238 (99.2745%) [3]. Of these, only U235 is fissile (i.e., it will undergo fission induced by thermal neutrons). The secondary challenge arises due to the production of fission products. Due to the statistical nature of the fission process, wide arrays of fission products are accumulated in the reactor. Some of these fission products have a large neutron cross section (that is, they can and do absorb neutrons), and consequently impact the neutron balance in the reactor. On the other hand, some isotopes like U238 are fertile, that is they are not fissile but after absorption of a neutron, they can be converted to fissile material [4]. This means that while the reactor is in operation, some fuel is also produced in the reactor, which is subsequently burned in the reactor. All of these processes make the nuclear fuel cycle a challenging yet very interesting subject. While thorium has the potential of becoming a significant nuclear fuel, at this time uranium is the primary fuel for the nuclear industry.

The nuclear fuel cycle starts from the mining of uranium-bearing minerals. Uraninite (UO_2) and Pitchblende (UO_3, U_2O_5) are the two most common uranium ores while others include torbernite, uranophane, monazite, davidite, and trinitite (Fig. 11.2). There are three methods available to mine uranium from the earth deposits:

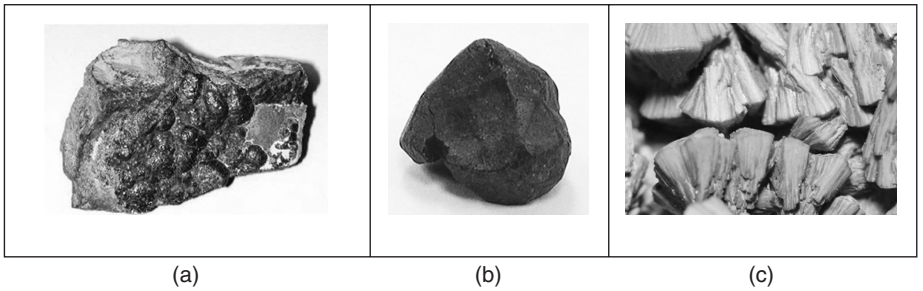

Figure 11.2 Uranium-bearing minerals: (a) uraninite, (b) davidite, (c) tobernite. *Source*: http://www.toroenergy.com.au/ur_whatis.html.

Figure 11.3 Open uranium mine. *Source*: http://pubs.usgs.gov/gip/deserts/minerals/open_pit.gif.

open pit mining (Fig. 11.3), underground mining, and, more recently, leach mining [2]. Each has its own advantages and disadvantages. For example, with underground mining there is a potential risk of accidents. Also, a significant amount of ore embedded with uranium has to be left in the mine to ensure structure integrity of the mine. Presence of high concentration of radon (a radioactive decay product of radium that is invariably present with most uranium ores) is also a significant health issue for the miners. The advantage of underground mining is that the land above the mine is only disturbed at the shaft opening. Open-pit mining results in a large hole in the ground that is environmentally undesirable. Recently, a significant amount of uranium is being mined using in-situ methods (Fig. 11.4), where a solution, mostly carbonate (in earlier implementations, nitric and/or sulfuric acid was also used), is injected in the ore-bearing soil where it then reacts with the ore. The dissolved ore is pumped out from another bore. At present, in-situ is becoming an increasingly popular method for uranium mining because it eliminates ore crushing and milling. Even a low-grade ore can be mined using this technique. Additionally, minimum ground disturbance and radioactivity release to the environment makes the in-situ method an attractive mining option for uranium mining. The disadvantages include low recovery yield and potential release of toxic chemicals to the environment.

Australia, Kazakhstan, South Africa, and United States have the major reserves of uranium in the world. These reserves are categorized in terms of availability and cost of recovery. Known conventional resources of uranium are classified based on the cost of recovery. It is traditional to report them in the following categories: recoverable at less than \$40/ kg of uranium, less than \$80/ kg, and less than \$130/kg [5]. At this time, only the first category (\$40/kg of uranium) is economically feasible. According to a conservative estimate of the known conventional resources (which includes the reasonably assured resources; RAR and estimated additional resources; EAR) a total of

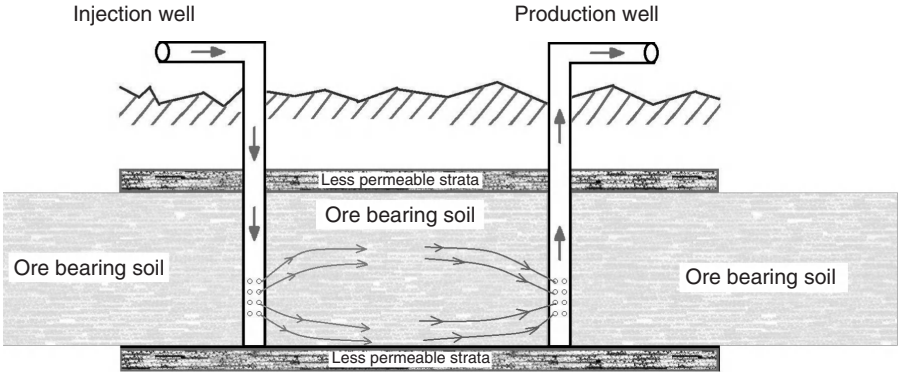

Figure 11.4 In-situ uranium mining. (Drawing by S. Usman).

4 Mt of uranium is available, while significant amounts of additional undiscovered and secondary resources are thought to be present. World uranium resources and fuel processing capacities are summarized by Knief [6]. In addition to these resources, an almost infinite amount of uranium is available in seawater.

For traditionally mined ore, milling is the next step in uranium processing. The ore is crushed and heated to remove organic material from the ore. Solvent extraction is then used to precipitate uranium. Dried product is formed into blocks, or bricks, and is commonly known as yellow cake (U_3O_8) (Fig. 11.5), which is shipped in drums for enrichment.

Waste from the milling process is usually released to a pond. These ponds are controlled due to environmental concerns about leaching of radioactive materials, particularly radium, acid, and slime. Regulations are in place to control mill tailing ponds to protect people and the environment.

The next step in nuclear fuel processing after mining and milling is the step of enrichment. In this step, the isotopic concentration of U235 is increased to approximately 3-5%. Purification of U_3O_8 is the first step in the enrichment process. Small quantities of impurities like boron and cadmium can adversely impact reactor performance. Sodium and other such impurities are likely to get mixed with yellow cake in the mills and during the separation process and must be removed from the feed to the enrichment unit. Plutonium-uranium extraction (or PUREX) is one such method based on aqueous (liquid-liquid) ion exchange process to extract uranyl nitrate using certain organic solvent (Fig. 11.6).

Purified U_3O_8 in fine powdered form is reduced by hydrogen at high temperature in a fluidized bed. High temperature, above 1000°F, is required for this process.

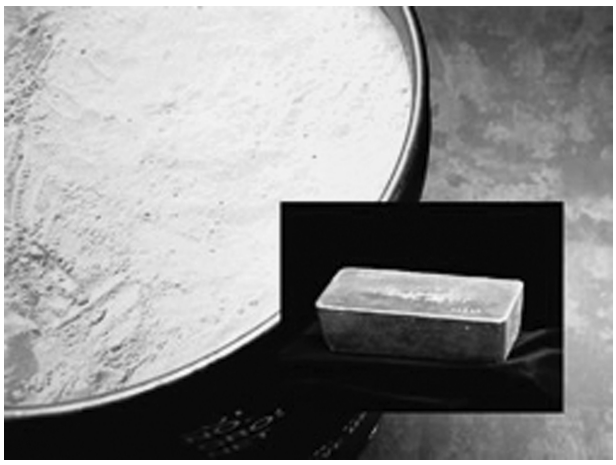

Figure 11.5 Yellow cake (U_3O_8), product of uranium milling. *Source*: http://www.fas.org/programs/ssp/nukes/fuelcycle/centrifuges/_images/Yellowcake_250.jpg.

The product (UO_2) then goes through two hydrofluorination processes:

$$UO_2 + 4HF \rightarrow 2H_2O + UF_4,$$
$$UF_4 + F_2 \rightarrow UF_6.$$

High temperature is required throughout the process. Uranium hexafluoride (UF_6) can exist in solid, liquid, or gas forms with the triple point approximately at 64.05°C and 1.5 bar. Uranium hexafluoride in the gas form is used as feed material for the enrichment process. UF_6 is the only compound of uranium that exists in gas form at comparatively low temperatures, making it a suitable candidate for the enrichment process. Fortunately, the weight fraction of fluoride is not too high in the molecule, allowing economically feasible enrichment.

Gaseous diffusion (Fig. 11.7) has been the primary process in the United States for uranium enrichment. There is a fine difference in the rate of diffusion of $U235F_6$ versus $U238F_6$. Using this difference, UF_6 is diffused through a thin barrier containing microscopic pores to enrich $U235F_6$. The kinetic energy of a gas molecule is

$$kT = \frac{1}{2}mv^2$$

where k is the Boltzmann Constant, T is the absolute temperature, m is the mass of the molecule, and v is the velocity of the molecule. Since there is a fine difference between the mass of $U235F_6$ and $U238F_6$, at a constant temperature there will be a slight difference between the velocities of the two isotopes:

$$\frac{V_{U235}}{V_{U233}} = \left(\frac{M_{U233}}{M_{U235}}\right)^{1/2}$$

The above ratio is called the *separation factor*. For the case of U238/U235, the ratio is only 1.0042. Higher values of the ratio mean that the process is efficient in separating the material. Due to this small ratio, thousands of stages are required to achieve the required enrichment. Figure 11.8 shows a cascade of these stages when the product of one stage is fed as input for the upstream stage and the waste of one stage is mixed with the input of the downstream stage.

Leakage of air into the system will plug the porous barrier and must be prevented at all cost. The cost of enrichment is measured in Separation Work Units (SWUs):

$$SWU = [P.V(x_p) + W.V(x_w) - F.V(x_f)]$$

where $V(x_i)$ is the "separation potential" of the material (product, waste, or feed);

$$V(x_i) = (2x_i - 1)\ln\frac{x_i}{(1 - x_i)}$$

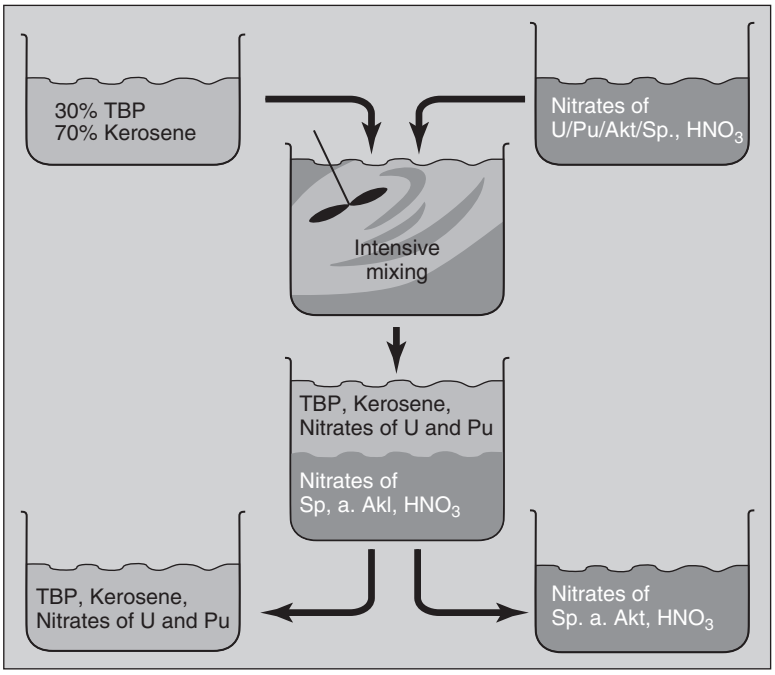

Figure 11.6 PUREX separation for uranium and plutonium. *Source*: http://www.euronuclear.org/info/encyclopedia/p/purex-process.htm.

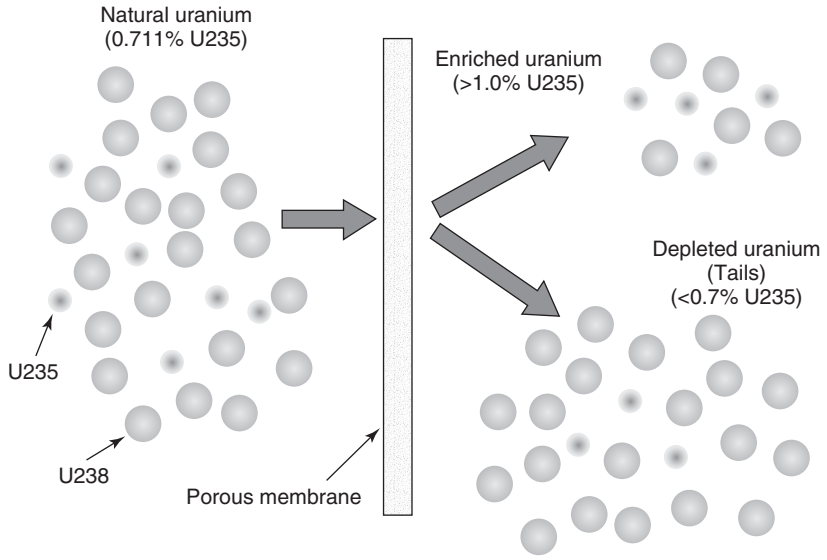

Figure 11.7 Gaseous diffusion uranium enrichment process. *Source*: http://www.nrc.gov/images/materials/fuel-cycle-fac/enrichment-process.gif.

where x_f, x_p, and x_w are the weight fraction of the U235 in the feed, product, and the waste respectively. And F, P, and W are the mass flow rate of feed, product, and the waste respectively.

Other methods of U235 enrichment are also reported in the literature include centrifuge method, nozzle separation method, and atomic vapor laser isotope separation (AVLIS) method.

Because of the energy economics of the centrifuge system, recently this method of uranium enrichment is preferred over gaseous diffusion. The power consumption is about 10% of the gaseous diffusion method per unit product SWU, which is mostly used in overcoming the friction of the rotor drum. Feed is introduced in the center of a high-speed rotating drum. Due to the difference in the molecular masses, the lighter molecules ($U235F_6$) tend to

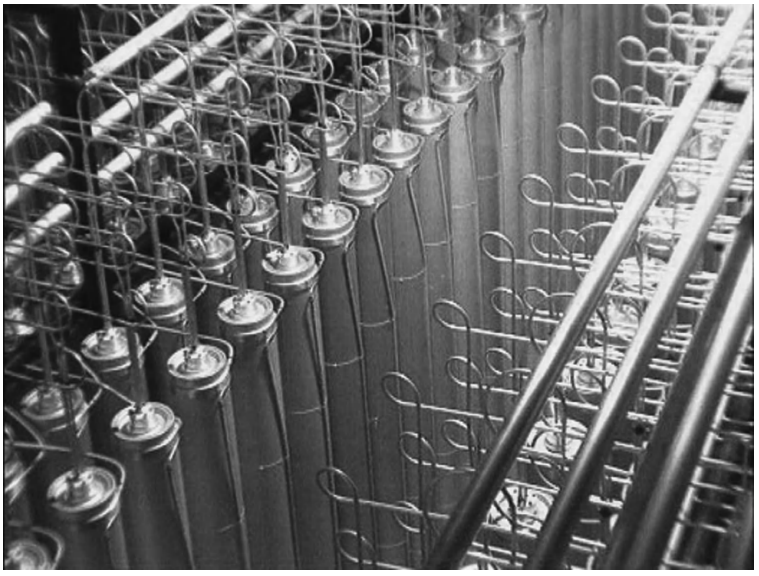

Figure 11.8 Cascade of gaseous diffusion process for uranium enrichment. *Source*: http://www.world-nuclear.org/education/nfc.htm.

concentrate close to the center of the drum while the heavier molecule ($U238F_6$) concentrates toward the outer volume of the drum. Enriched and depleted UF_6 gas is collected from the centrifuge machine and is fed to the next stage of the enrichment. Thousands of these machines must work in series to achieve the desired enrichment.

The nozzle separation method also works on the principle of centrifugal separation. A lean mixture of UF_6 and H_2 is forced to pass through the nozzle. Due to the difference in the centrifugal force, the isotopes are separated and collected at their respective paths. Hydrogen is added to achieve higher gas velocities, which enhance the separation efficiency. Several hundred stages of nozzles are required to enrich the uranium to the desired level.

The atomic vapor laser isotope separation (AVLIS) method is based on the selective ionization of U235. There is a very fine difference between the wavelength of laser light, which would excite and ionize U235 versus U238. This fine difference is used to fine-tune the wavelength of the laser source that selectively ionizes U235, which is separated using a magnetic field. This process is extremely efficient and does not require multiple stages and, hence, high energy-efficiency and enrichment levels are possible. The AVLIS method requires vaporized pure uranium and must be operated at extremely high temperatures. This high-temperature operation puts extraordinary demand on the material's performance. To avoid a high-temperature operation, UF_6-based molecular laser isotope separation (MLIS) techniques are being developed.

After the enrichment process, the U235-rich UF_6 is used as feed material to fabricate uranium fuel. Figure 11.9 shows the process of fuel fabrication. UF_6 is supplied to the fuel fabrication facility under high pressure in solid form. An oven is used for UF_6 production, and the gas is passed through water to produce UO_2F_2. Chemical reaction with ammonia is used to produce ammonium diuranate $(NH_4)_2U_2O_2$. Finally, UO_2 is produced from the precipitate of the chemical process. Powder of UO_2 is

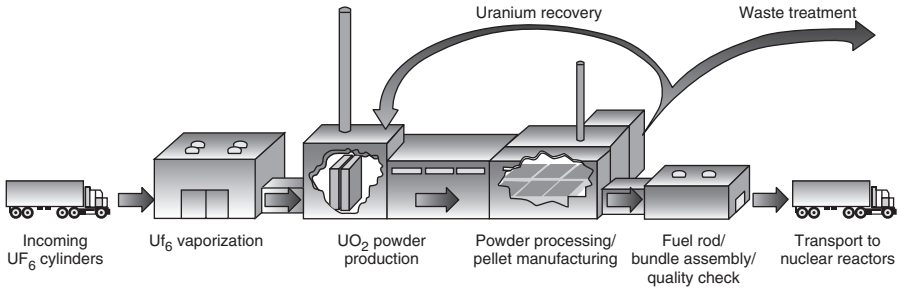

Figure 11.9 The nuclear fuel fabrication process. *Image is public domain from the U.S. Nuclear Regulatory Commission*.

sintered at very high temperature to produce the pellets. These pellets are about 95% of the theoretical density and are machined to accurate diameter and cupped at the ends. High-temperature vacuuming is used to outgas any moisture to avoid corrosion. These pellets are loaded in zircaloy tubes. Zircaloy is an alloy of zirconium containing approximately 1.5% tin and trace amounts of nickel, iron, and chromium. Zircaloy is used as cladding material because of its unique durable properties. A suitable cladding material must prevent fuel corrosion and retain the fission products. In addition, cladding must also have good heat transfer characteristics and mechanical properties to accommodate dimensional changes in the fuel pellets. Moreover, to maintain neutron economy, the cladding must not absorb any significant neutrons produced in the fission process. Only a few materials are available with all of these properties. These materials include aluminum, magnesium, and zirconium. While stainless steel is another good candidate for cladding material Zircaloy is perferred due to its superior neutron economics. In addition to the fuel and the cladding material, some burnable poison is also added to the fuel assembly. The purpose of the burnable poison is to compensate for the excess reactivity of the fresh fuel, which is necessary for long operation without the need for refueling and hence fuel economy. In PWR it is possible to use chemical shim, which is a dissolved poison in the reactor coolant. Most of the burnable poison material will either include boron or gadolinium.

Pellets are loaded in tubes and an array of pins is created to form a fuel assembly. For PWR, the matrix usually ranges from 15×15 to 18×18 rows and columns. Several structural supports, for example, spacing grids, are used to hold the pins together and prevent any bulging. For BWR, a small matrix of 7×7 to 10×10 is used. The objective of the smaller array size is to ensure proper heat transfer. These assemblies are loaded in the reactor and irradiated for power production.

Figure 11.10 shows a typical PWR assembly. The bottom nozzle is used as the intake for the coolant and diffuses the water. Water is passed through the debris catcher, which is installed to prevent any debris from traveling up the flow channel and potentially causing damage to the fuel rods. Various subcomponents are included in the assembly design for structure and heat transfer considerations. Approximately one-third of the fuel assemblies are replaced with fresh ones during a refueling operation, which takes place every 12 to 18 months. The remaining two-thirds of the assemblies are reshuffled in the core to maximize fuel utilization. The topic of in-core fuel management is a sub-topic of nuclear engineering that specializes in optimum utilization of fuel in the core.

Figure 11.11 shows a typical BWR assembly. Most of the design is similar to that of a PWR fuel assembly with the exception of the array size. BWR assemblies are smaller

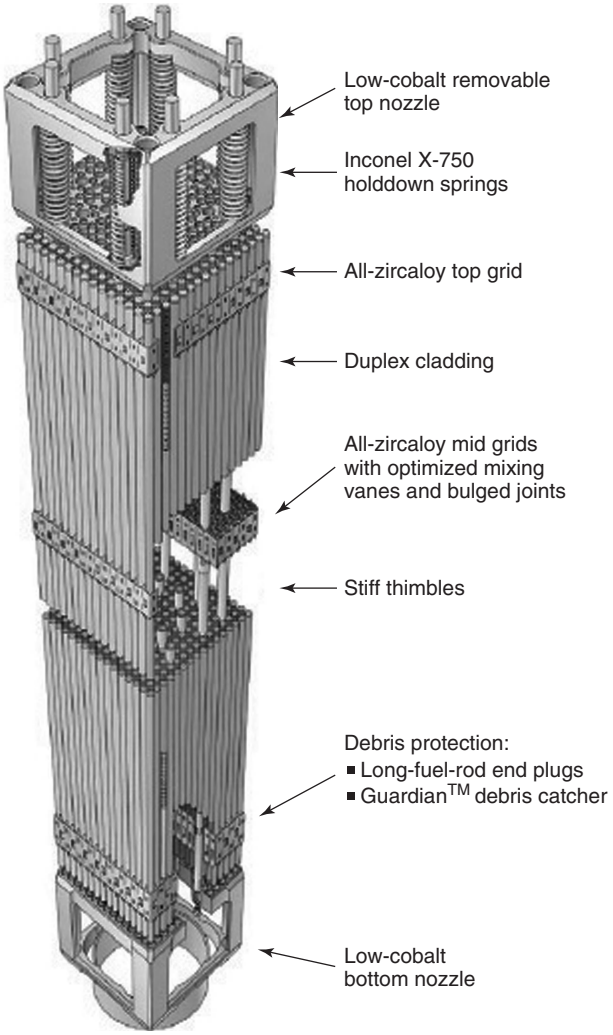

Figure 11.10 Westinghouse 15×15 PWR fuel assembly. *Source*: http://me1065.wikidot.com/fuel-assemblies-in-nuclear-reactors.

(e.g., 7×7) with larger spacing between the fuel pins to allow better heat transfer.

Various reactor designs are available to utilize nuclear fuel for production of power. In general, from the nuclear fuel cycle point of view, reactors can be divided into three groups: the burners, the converters, and the breeders. Most reactors in the current fleet of power reactors are classified as converters; that is, while the fuel is consumed to produce power, additional fuel is converted to fuel by the process called transmutation. Burners are designed to burn the fuel and/or the fission product. Breeder reactors are special converters with a conversion ratio greater than unity. Consequently, the reactor produces more fuel than it consumes. The breeder reactor [7] is a very interesting design concept and therefore is a subject of significant research.

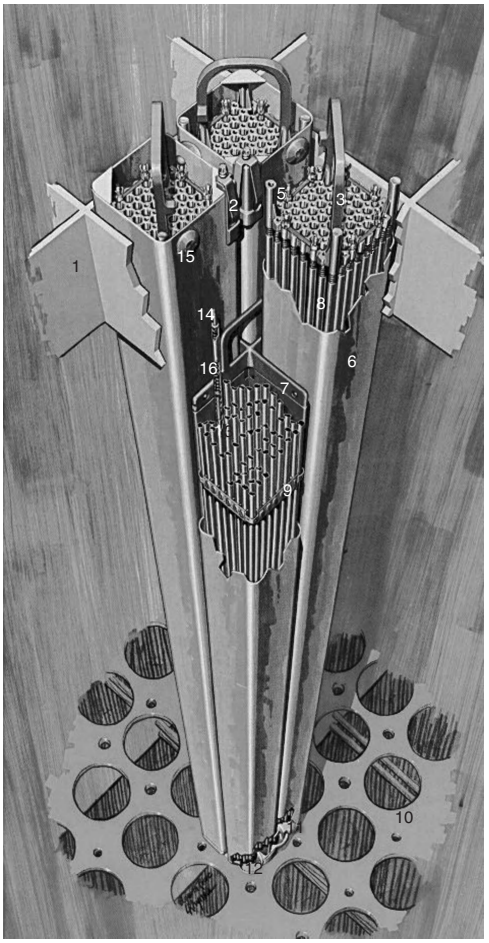

Figure 11.11 General Electric GBWR fuel assembly. *Source*: http://www.architectureweek.com/2011/0316/news_2-2.html.

After producing power in the reactor, the fuel is discharged from the reactors. At this time, the fuel is highly radioactive. Significant cooling time is required to reduce the radioactivity level of the spent fuel. Most, if not all, of the spent fuel maneuvering at the power plant takes place under water, and a small system of spent fuel transportation canals is designed at the reactor facility. Spent fuel is stored at the reactor site for a considerable amount of time. Figure 11.12 shows a spent fuel storage facility. The fuel is kept under water to reduce the radiation exposure. A significant amount of heat is also generated because of the radioactivity. This heat is removed from the fuel by natural circulation and evaporation of the pool water.

The spent fuel contains about 30% of the original U235 plus a certain amount of plutonium produced by the reactor. In addition to these valuable materials, there are also fission products and other activated materials useful for many applications, including medicine and industrial applications. While the spent fuel is commonly referred to as "nuclear waste," the term is somewhat misleading. There are many valuable isotopes present in the spent fuel. However, separation and purification of these materials remains a challenge.

Figure 11.13 depicts the risk factor associated with the spent nuclear fuel as a function of post-discharge time. The source of this radioactivity is a mix of fission products, their decay products, and the actinides produced due to transmutation of the fuel. The high level of radioactivity in the spent fuel is a source of significant health and environmental concerns. As is well-known, the risk persists for millennia. Therefore, proper storage and disposal of the spent fuel generated in the nuclear power cycle is a critical part of the nuclear fuel cycle. As shown in Figure 11.1, there is the option to reprocess the spent fuel, separate the useful material from the waste, and recycle it back to the reactor. This also provides the opportunity to separate useful radioisotopes and use them for other applications and dispose the waste. If recycling is to be employed effectively, a significant (40–50%) saving in the uranium is potentially possible.

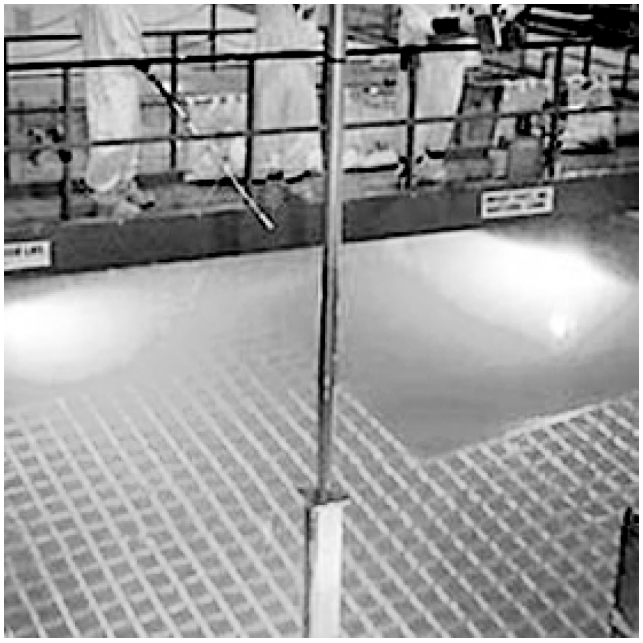

Figure 11.12 Spent fuel storage facility. *Source*: https://www.scientificamerican.com/article.cfm?id=japan-nuclear-renaissance.

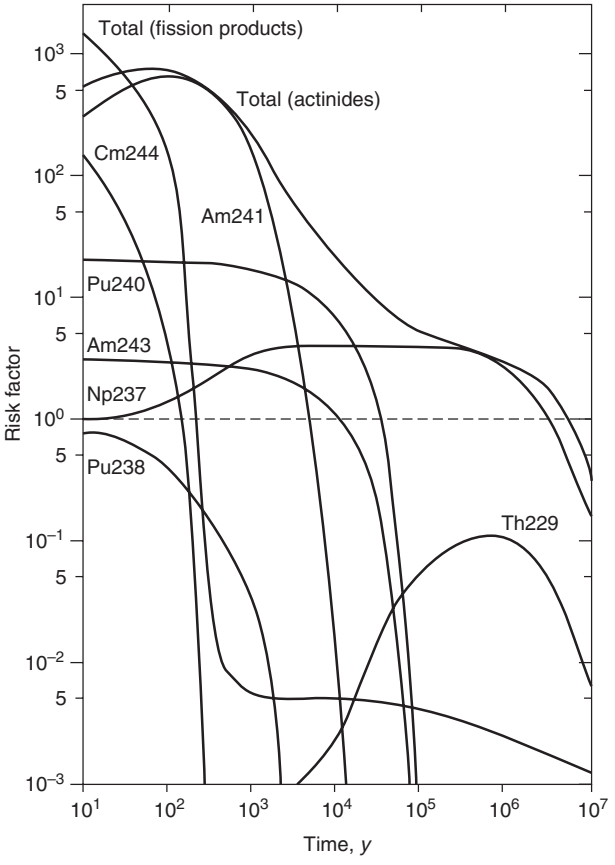

Figure 11.13 Radiation risk factor of spent fuel. *Source*: http://www.fas.org/programs/ssp/nukes/fuelcycle/centrifuges/U_production.html.

In the recycling phase of the nuclear fuel cycle, the spent fuel is cut into small pieces and dissolved in nitric acid. Using solvent extraction and separation methods, the useful materials are separated and collected for recycling to the reactor. The resultant fuel is MOX (Mixed oxide fuel $(U + Pu)O_2$). MOX can be used in the reactors as a fuel; however, due to proliferation concerns, the option of reprocessing was banned in the United States. Recently there has been a significant shift in this approach to the nuclear fuel cycle and the United States is constructing a new MOX fuel fabrication facility in South Carolina to convert the existing stockpiles of plutonium from the weapons program to nuclear fuel for energy production. This bilateral program between the United States and Russia is a positive sign in the development of a healthy approach toward closing the nuclear fuel cycle by virtue of fuel recycling.

In summary, there are several major steps involved in the nuclear fuel cycle as shown in Figure 11.1. And for each of these steps, multiple methods and techniques are available. Feasibility of these options depends on the specific needs and available resources.

DEDICATION

Dedicated to my father, Usman Abdul Ghafoor, for his everlasting inspiration.

REFERENCES

1. Key World Energy Statistics 2007, International Energy Agency, Stedi Media, Paris Cedex, France, 2007. (also available at http://www.iea.org/textbase/nppdf/free/2007/key_stats_2007.pdf).
2. R.G. Cochran and N. Tsoulfanidis, *The Nuclear Fuel Cycle: Analysis and Management*, 2nd Edition, American Nuclear Society, La Grange Park, IL, 1999.
3. C. Normand. (2008, March 30). Karlsruhe Nuclide Chart Database. Nucleonica [Online]. Available: http://www.nucleonica.net/.
4. J.R. Lamarsh and A.J. Baratta, *Introduction to Nuclear Engineering*, 3rd Edition, Prentice Hall, Upper Saddle River, NJ, 2001.
5. R. Price and J.R. Blaise, Nuclear fuel resources: Enough to last?, *NEA News*, **20** 2002.
6. R.A. Knief, *Nuclear Engineering—Theory and Technology of Commercial Nuclear Power*, 2nd ed. Taylor & Francis, Washington, DC, 1992.
7. A.E. Waltar and A.B. Reynolds, *Fast Breeder Reactors*, Pergamon Press, Elmsford, NY, 1981.

12

GLOBAL PERSPECTIVE ON THORIUM FUEL

K. Anantharaman[1] and P.R. Vasudeva Rao[2]

[1]*Reactor Design and Development Group, Bhabha Atomic Research Centre, Mumbai, Maharashtra, India*
[2]*Chemistry Group, Indira Gandhi Centre for Atomic Research, Kalpakkam, TN, India*

12.1 INTRODUCTION

Thorium is a radioactive chemical element that belongs to the actinide series. It is represented by the chemical symbol "Th". Thorium metal was discovered in 1828 by the Swedish chemist Jons Jakob Berzelius, who named it after Thor, the Norse god of thunder. Thorium occurs naturally in low concentrations (about 6–7 ppm) in the Earth's crust. In nature, almost all thorium is as thorium-232 (Th232), although several additional isotopes can be present in a small amount. Th232 decays very slowly (its half-life is 1.41×10^{10} years, about three times the age of the Earth), but other thorium isotopes occur in its decay chain as well as that of uranium isotopes. The final decay product of the Th232 series is the stable lead isotope Pb208.

Thorium is a soft, silvery-white, ductile, heavy metal (about as dense as lead) that is pyrophoric in powdered form. Thorium metal has a very high melting point (1750°C) [1], while the oxide thoria (ThO_2) has the highest melting point (3378°C) of all the binary oxides [2]. When heated in air, thorium turnings ignite and burn brilliantly with a white light. Thorium metal in its pure form retains its lustre for several months. However, when it is exposed to air, thorium slowly tarnishes, becoming grey and eventually black. Thorium is an important alloying element in magnesium and is used to coat tungsten wire for components of electronic equipment. It can also be added to ceramic items such as crucibles to make them more heat resistant, as well as to refractive glass to allow for smaller and more accurate camera lenses and scientific instruments. In addition, thorium is added to tungsten in welding rods and electric bulb filaments to improve product performance.

During the pioneering years of nuclear energy, from the mid 1950s to mid 1970s, there was considerable interest worldwide to develop thorium fuels and fuel cycles in order to supplement uranium reserves. However, the utilization of thorium on a commercial scale has not been pursued intensely, partly due to the easy availability and usage of uranium and mainly due to the technological challenges associated with the thorium-based fuels. Basic research and development has been conducted in Germany, United States, Russia, Japan, United Kingdom, and India. India has large thorium deposits, and thorium would be the main stay of its nuclear power program.

12.2 THORIUM RESOURCES

12.2.1 Sources of Thorium

Thorium is widely distributed in small amounts in the Earth's crust and is about three times as abundant as uranium. The most common source of thorium is the rare earth phosphate mineral monazite, which contains up to about 12% thorium phosphate. Monazite is found in intrusive rocks and pegmatite, as well as in some metamorphic rocks, such as gneiss. However, the richest sources of monazite are placer deposits (these being accumulations of sand in rivers and beaches). Thorium, as well as rare earth metals, are a major component in placer deposits, which are currently mined for titanium.

Thorium is also found in the minerals thorite (thorium silicate) and thorianite (mixed thorium and uranium oxides). While monazite is the primary ore of thorium, thorite is the

Nuclear Energy Encyclopedia: Science, Technology, and Applications, First Edition (Wiley Series On Energy).
Edited by Steven B. Krivit, Jay H. Lehr, and Thomas B. Kingery.

most common thorium mineral. Thorite is also recognized as an important ore of uranium in the form of uranothorite. The isotope Th230, a decay product of U238, is found in uranium deposits as well as in uranium mill tailings (however, natural occurrence is less than 1 ppm).

12.2.2 Recovery from Natural Resources

The two main sources of thorium that could be considered are firstly monazite itself and secondly old residues remaining after removal of the rare earths. Thorium concentrate and nuclear-grade thorium oxide are produced from monazite by following process steps:

- Extraction and pre-concentration of beach sands
- Conversion of ore (beach sand concentrates) to monazite
- Conversion of monazite into thorium concentrate, uranium concentrate, and rare earth
- Storage of thorium concentrates in suitable form or conversion of thorium concentrate to nuclear-grade thorium dioxide powder

The mining and extraction of thorium from monazite is relatively easy and significantly different from that of uranium from its ores. Most of the commercially exploited sources of monazite are from the beach or river sands along with heavy minerals. The individual heavy minerals, namely ilmenite, rutile, monazite, zircon, sillimanite, and garnet, are separated from each other by methods depending up on physical properties, i.e., specific gravity, magnetic susceptibility, electrical conductivity, and surface properties.

The overburden during mining is much smaller than in the case of uranium, and the total radioactive waste production in mining operation is about two orders of magnitude lower than that of uranium. Like uranium, thorium is naturally radioactive, but the "radon impact" from processing thorium ores is easier to handle because its radioactive daughter thoron (Rn220) is shorter lived than its radon counterpart from uranium milling operations. Thus, management of tailings is simpler than in the case of uranium. Significant recoverable amounts of thorium are present in mine tailings. These include the tailings of ancient tin mines, rare earth mine tailings, phosphate mine tailings, and uranium mine tailings. In addition to the thorium present in mine tailings and in surface monazite sands, thorium is also present in the waste ash pile produced by burning coal at the thermal power plants.

12.2.3 Availability of Thorium in the World

International Atomic Energy Agency (IAEA) estimates thorium resources to be about three times that of uranium.

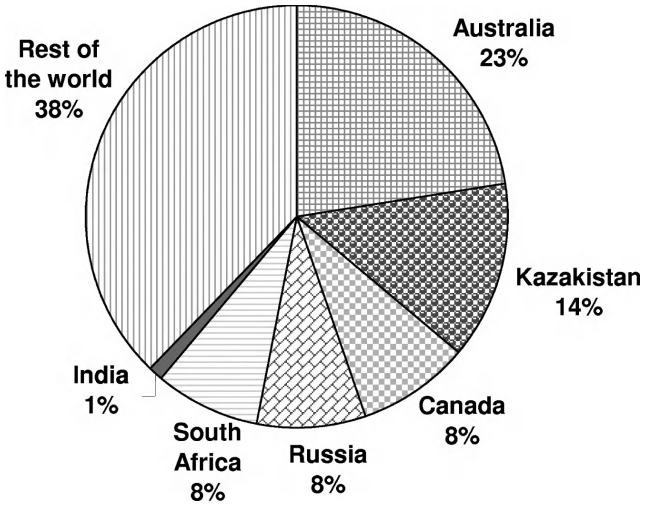

Figure 12.1 Global distribution of uranium [3].

It is a widely distributed natural resource, which is readily accessible in many countries. The present knowledge of thorium resources in the world is limited and incomplete because of the relatively low-key exploration efforts arising out of insignificant demand. Figures 12.1 and 12.2 show the global distribution of uranium and thorium resources respectively [3, 4].

The worldwide thorium resources are estimated to be about 6.08 million tons [5]. The highest resources are reported from Australia, United States, Brazil, Turkey, and India. Thorium resources also occur in Norway and South Africa, where it is associated with carbonatite, pegmatite, and placer deposits.

In Australia, most of the known thorium resources [6] are held in the monazite component of heavy mineral sand deposits, which are mined for their ilmenite, rutile, leucoxene, and zircon content. An average thorium content in monazite is up to 7% in heavy mineral sand deposits. In the United States, thorium production was primarily from the rare-earth-thorium-phosphate mineral monazite, which is recovered as a byproduct of processing heavy-mineral sands for titanium and zirconium minerals or tin minerals. Thorium compounds were produced from monazite during processing for the rare earths. Vein deposits host the largest volume known high-grade thorium resources in the United States [7]. There are two thorium vein districts, the Lemhi Pass district of Montana-Idaho and the Wet Mountains area of Colorado, that dominate the known high-grade thorium reserves of the United States. Norway has major thorium resources [8] in the world as per the U.S. Geological Survey. The knowledge of Norwegian thorium-rich minerals and their grades is mainly based on results from uranium exploration carried out during two periods, from after World War II to 1965 and from 1975 to 1985.

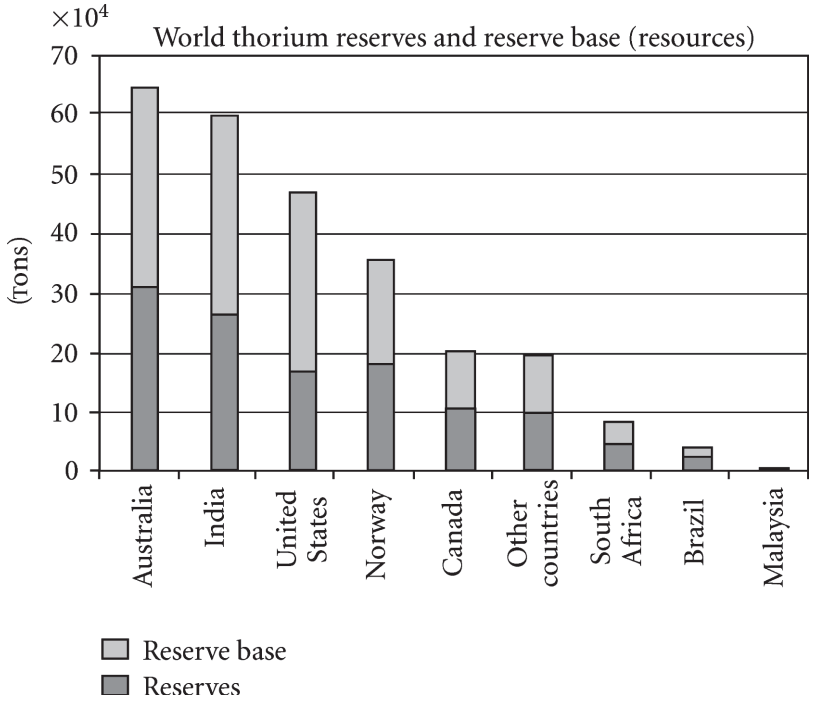

Figure 12.2 Global distribution of thorium [4].

Norway has potential thorium resources, but exploration specifically for thorium has never been undertaken.

12.2.4 Availability of Thorium in India

Thorium is abundantly available in India and constitutes almost one-third of the world resource. Exploration for atomic minerals in India is being carried out solely by the Atomic Minerals Directorate for Exploration and Research (AMD) since 1949. Most of India's thorium reserves are in the beach sands of Southern India (mainly Kerala) and Orissa. The beach sands of the coastal regions of Kerala and Tamil Nadu are very rich in monazite. The total mineral established so far includes about 10.2 million tons of monazite resource under all categories (indicated, inferred, and speculative). The ore is of very high grade with a thorium content of about 10% with 800,000 tons of recoverable thorium metal.

12.3 PHYSICS OF THE THORIUM FUEL CYCLE [9]

12.3.1 Isotopic Composition

Unlike uranium, thorium does not contain any natural fissile isotope. Nearly all natural thorium is Th232, which is relatively stable. Th232 is not fissile, but it can absorb neutrons to convert it into U233, which is fissile. Thus, thorium can also be used as a fuel material in a nuclear reactor, but the reactor operation with thorium fuel cycle depends on the initial feed of the fissile material like U235 or PU239.

12.3.2 Neutronic Properties

The reactor physics aspects associated with thorium are slightly different from that of uranium. Thorium offers better fuel utilization because of its potential neutronic advantages. The absorption of neutron in Th232 produces U233, which has a higher tendency to generate neutrons by fission (in thermal/epithermal neutron flux) than that with U235 or PU239. This will provide better compensation to balance the wastage or loss of neutrons in materials like structures, coolant, and others. Figure 12.3 shows the variation of number of neutrons generated by fissile isotopes (U233, U235, and PU239) with incident neutron energy. The neutron production for U233 is relatively insensitive to temperature changes, thus it is uniform for the energy spectrum.

As a fissile isotope, U233 compares favorably with PU239. At the lower energies of neutrons in the reactor core, the probability of fission reaction (cross section) for U233 is significantly higher than that of either PU239 or U235. At very high energies of neutrons, above 1 MeV, the possibility of fission reaction for PU239 and U233 are about the same and higher than that of U235. Also, the possibility of absorption of slow neutrons (thermal absorption cross

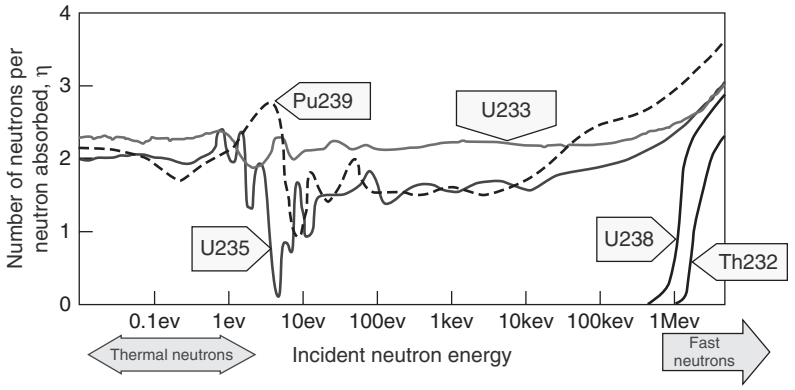

Figure 12.3 Neutron yield per neutron absorbed.

section) by Th232 is higher than that of U238. Therefore, the in-reactor fissile material generation capability of Th232 during long-term irradiation can be higher than that of U238. This will reduce the need for fuel ore and/or fuel enrichment per unit of energy produced.

The major advantages of the thorium-based nuclear fuels that have captured the international attention are (a) the insignificant production of long-lived minor actinides on neutron irradiation as compared to uranium systems and (b) the proliferation resistance introduced by the presence of hard gamma emitters in the U233 produced by neutron irradiation of thorium.

12.3.3 Thermo-Physical Properties

A comparison of the properties of thorium dioxide and uranium dioxide shows thorium dioxide to be superior from the point of view of fuel performance in the reactor. First, thorium dioxide is a highly stable stoichiometric oxide. So, it retains dimensional stability at high burn-up (more residence time in reactor). Due to its relatively inert nature, there is also less concern for the fuel reacting chemically with the cladding around it or with the cooling water, if there be a breach in the cladding. Second, ThO_2 has higher thermal conductivity and lower coefficient of thermal expansion than UO_2. This will result in lower fuel temperatures, also induce lower strains on the cladding, and therefore allow operating for longer in-reactor residence time. The melting point of thorium dioxide (3378°C) is about 500°C higher than that of uranium dioxide (2865°C). This difference provides an added margin of safety in the event of a temporary power surge or loss of coolant. It also has high radiation resistance, better thermophysical properties, and lower fission gas release rates, which result in slower fuel deterioration. The assessments carried for thoria-based fuels show that their thermo-mechanical performance will satisfy the safety limits used for uranium-based fuels. In summary, thorium-based fuels, due to their better thermophysical and thermochemical properties, provide a better scope for operating successfully to higher burn-up.

12.3.4 Reduced Toxicity of Waste from the Thorium Fuel Cycle

Since U233 has a lower mass number compared to the isotopes in natural uranium, the amount of higher actinides (such as neptunium, plutonium, americium, and curium) produced in Th-U fuels per unit of energy generated is insignificant as compared to uranium-based fuels. Consequently, the amount of waste containing minor actinides (americium, curium, etc.) to be disposed of is also very less. Plutonium is completely absent from thorium reactor's waste. The lower production of higher actinides has an important advantage, because the minor actinides contribute significantly to the long-term hazard potential of the waste generated by nuclear fuel reprocessing.

12.4 THORIUM-FUELED REACTORS

12.4.1 Experience [3, 10, 11, 18]

Thorium-based fuels have been loaded in the past, either partially or fully, in the reactor core, worldwide in test reactors and power reactors of different types, including High Temperature Gas-cooled Reactors (HTGR), Light Water Reactors (LWR), Pressurized Heavy Water Reactors (PHWRs), Liquid Metal cooled Fast Breeder Reactors (LMFBR), and Molten Salt Breeder Reactors (MSBR). A brief summary of these reactors is given in Table 12.1.

12.4.1.1 Germany **AVR (Arbeitsgemeinschaft Versuchs Reaktor)** was an experimental HTGR operated at Julich Research Centre, Germany, generating 15 MWe of power, most of the time (about 95%) with thorium fuel. The reactor operated successfully from 1967 to 1988. It used helium coolant at 10 bar pressure and was used

TABLE 12.1 Use of Thorium Based Fuels in Different Reactors Worldwide [18]

Name and Country	Type	Power	Fuel	Operation
AVR, Germany	HTGR Experimental (Pebble bed reactor)	15 MWe	Th + U235 driver fuel, Coated fuel particles, Oxide & dicarbides	1967–1988
THTR-300, Germany	HTGR, Power (Pebble bed reactor)	300 MWe	Th + U235, driver fuel, Coated fuel particles, Oxide & dicarbides	1985–1989
Germany, Lingen	BWR Irradiation-testing	60 MWe	Test Fuel $(Th,Pu)O_2$ pellets	Until 1973
Dragon, UK OECD EURATOM also Sweden, Norway, & Switzerland	HTGR, Experimental (Prismatic Block)	20 MWt	Th + U235 driver fuel, Coated fuel particles, Oxide & dicarbides	1964–1976
Peach Bottom, Pennsylvania, USA	HTGR, Experimental (Prismatic Block)	40 MWe	Th + U235 driver fuel, Coated fuel particles, Oxide & dicarbides	1967–1974
Fort St Vrain, Colorado, USA	HTGR, Power (Prismatic Block)	330 MWe	Th + U235 driver fuel, Coated fuel particles, Dicarbide	1976–1989
MSRE ORNL, Tennessee, USA	MSBR	8 MWt	U233 molten fluorides	1964–1969
Shippingport, Pennsylvania, USA & Indian Point 1, New York, USA	LWBR PWR, (Pin assemblies)	60 MWe, 265 MWe	Th + U233 driver fuel, Oxide pellets	1977–1982, 1962–1974
SUSPOP/KSTR KEMA, Netherlands	Aqueous Homogenous Suspension (Pin assemblies)	1 MWt	Th+HEU, oxide pellets	1974 - 1977
NRU & NRX, Canada	MTR (Pin assemblies)		Th + U235 test fuel	Irradiation of few fuel elements
KAMINI; CIRUS & Dhruva, India	MTR Thermal	30 kWt; 40 MWt; 100 MWt	AL + U233 driver fuel, "J" rod of Th & ThO_2	All in operation
KAPS 1&2; KGS 1&2; RAPS 2,3&4, TAPS 3&4, India	PHWR (Pin assemblies)	220 MWe 540 MWe	ThO_2 pellets (for initial neutron flux flattening)	Continuing in all new PHWRs
FBTR, India	LMFBR (Pin assemblies)	40 MWt	ThO_2 blanket	In operation

for testing the performance of different types of coated particles like $(Th\text{-}U)C_2$, ThC_2, $(Th\text{-}U)O_2$, ThO_2, UO_2, etc. The fuel was in the form of a ceramic carbide or oxide contained within spherical pebbles coated with silicon oxide and pyrolytic graphite. The U235 enrichment varied between 93% and 10%. Most of the fuel could reach high burn-up of about 170 GWd/t for fuel pebbles and about 700 GWd/t for feed particles. The fuel temperatures reached about 1350°C with excellent fission product retention.

Thorium High Temperature Reactor (THTR) was a 300 MWe thorium-fueled, helium-cooled, graphite-moderated, high-temperature reactor at Hamm-Uentrop, Germany [12]. It first went critical in 1983 and operated for six years. The THTR-300 was also a high-temperature reactor with a pebble bed core (similar to AVR), consisting of the spherical fuel elements with U235 and Th232 fuel. During its operation, the reactor itself produced part of its fuel and the burn-up achieved was about 110 GWd/t.

12.4.1.2 United Kingdom The Dragon Reactor Experiment (20 MWth) was the first HTGR with coated particle fuel in prismatic core configuration. Its purpose was to test fuel and materials for the High Temperature Reactor programs pursued in Europe 40 years ago. Dragon Reactor Experiment was run as an OECD/Euratom cooperation project, involving Austria, Denmark, Sweden, Norway, and Switzerland in addition to the United Kingdom. Thorium fuel elements with a 10:1 Th/U (Highly Enriched Uranium) ratio were irradiated in the reactor.

12.4.1.3 United States Irradiation experiments with thoria-based fuels started in early 1950s in the United States. The earliest irradiations of $(Th\text{-}U)O_2$ fuel were done in Chicago Pile 5 at Argonne and in MTR at Idaho Falls. This was followed by irradiation of aluminium-clad $(Th\text{-}U)O_2$ fuel pins in the BORAX-IV reactor and SS304 clad fuel pins in the Elk River reactor. Thoria–urania fuels

containing 93% enriched U235 were used in Indian Point-I, a 265 MWe PWR designed by Babcock and Wilcox.

Peach Bottom Unit-1 was an experimental helium-cooled, graphite-moderated, high-temperature reactor located at Peach Bottom Township, York County, Pennsylvania, USA. It operated from 1967 to 1974 at a power level of 110 MWth (40 MWe). The reactor used prismatic block-type fuel elements containing fertile thorium carbide–coated particles and smaller highly enriched fissile uranium (U235) carbide–coated particles. The reactor was an excellent test bed for HTGR fuel development.

Fort St. Vrain reactor was the only commercial thorium-fueled nuclear plant in the United States and operated during 1976–1989. It was a high-temperature (700°C), graphite-moderated, helium-cooled reactor with a thorium/HEU fuel designed to operate at 842 MWth (330 MWe). The fuel was in microspheres of fertile thorium carbide and fissile thorium/U235 carbide coated with silicon oxide and pyrolytic carbon to retain fission products. It was arranged in hexagonal prisms/columns ("prismatic block type fuel") rather than as pebbles. Almost 25 tons of thorium was irradiated to temperatures greater than 1300°C, and this achieved 170 GWd/t burn-up.

Molten Salt Reactor Experiment (MSRE) of 8 MWth operated during the period 1964–1969 at Oak Ridge National Laboratories in the United States. MSRE was a truly homogeneous reactor using molten fluorides (ThF_4 and UF_4), presenting many advantages such as excellent neutronics, inherent safety, breeding capabilities, in-line venting of fission gases, in-line purification by fluoride volatilization processes, high thermal yields, and a relatively simple design. Corrosion and erosion problems were encountered at the time, which could now possibly be mitigated with more modern materials. It did operate with U233 fuel, but there was no electricity production.

Shippingport, a 60 MWe PWR, commenced commercial operation in December 1957 as the first large-scale nuclear power reactor to be operated solely for electricity production [13, 14]. The USAEC had used it as test bench for a thermal breeder with thermal or epithermal neutrons using special U233 hexagonal fuel elements. The Shippingport plant operated as a Light Water Breeder Reactor (LWBR) between August 1977 and October 1982. Following the operation, inspection of the core indicated that 1.39% more fissile fuel was present at the end of core life than at the beginning of life, proving that breeding had occurred. Shippingport was the only U.S. demonstration program using U233 as the fissile seed material. Although this demonstration was successful from the standpoint that slightly more U233 was bred than consumed, this success was only achieved at the high cost of a sophisticated core design and by sacrificing reactor performance.

12.4.1.4 Canada In Canada, AECL has more than 50 years' experience with thorium-based fuels, including burn-up to 47 GWd/t. About 25 tests were performed until 1987 in research reactors, with fuels ranging from ThO_2 to that with 30% UO_2, although most were with 1–3% UO_2, the uranium being highly enriched. The zircaloy-clad (Th-1.4%Pu)O_2 fuel bundles (six Bruce type) fabricated in the Recycle Fuel Fabrication Facility (RFFL) of AECL were test irradiated under experiment BDL-422 in NRU in order to investigate the suitability of thoria as matrix material for burning of plutonium (weapons grade) in heavy water reactors.

12.4.1.5 Other Countries Other reactors that operated with thorium fuel include the 60 MWe Lingen Boiling Water Reactor (BWR) in Germany and the aqueous suspension reactor project in Netherlands. In Japan, thorium/HEU fuel was used for the criticality experiments at KURRI.

12.4.2 Emerging Concepts

Thorium fuel cycles are feasible in all thermal reactors and fast reactors. In the short term, it should be possible to incorporate thorium fuel cycle in the existing reactors without major modifications in the engineered systems, reactor control, and the reactivity devices. Concepts for advanced nuclear power reactors based on thorium-fuel cycles include Light Water Reactors, with fuel based on plutonium dioxide (PuO_2), thorium dioxide (ThO_2) and/or uranium dioxide (UO_2) particles arranged in fuel rods; Gas Turbine-Modular Helium Reactors (GT-MHRs), which can use a wide range of fuel options, including thorium/HEU, thorium/U233, and thorium/plutonium, Pebble-Bed Modular Reactors (PBMRs); Accelerator Driven Systems (ADS) and fusion breeders. Some of the promising concepts are discussed below in some detail.

12.4.2.1 Pressurized Heavy Water Reactors (PHWR) Today, (U-Pu) MOX (mixed oxide) fuels are used in some conventional nuclear reactors, with PU239 providing the main fissile ingredient. An alternative is to use thorium/plutonium fuel, with plutonium being consumed and fissile U233 bred. The remaining U233 after separation could be used in a thorium/uranium fuel cycle. PHWR type reactors offer great potential in burning plutonium to the extent of 96% using (Th-Pu)O_2 fuel [15]. In the closed fuel cycle, the driver fuel is required to start off and is progressively replaced with recycled U233, so that on reaching equilibrium, 80% of the energy comes from thorium. AECL in fact, envisages a fleet of PHWR type reactors with near Self-Sufficient Equilibrium Thorium (SSET) fuel cycle.

12.4.2.2 Molten Salt Breeder Reactor (MSBR) A reactor system having great potential for the application of thorium fuel cycle is the Molten Salt (thermal) Breeder Reactor (MSBR), capable of achieving a breeding ratio of 1.07 and an overall thermodynamic efficiency of 40% [16]. The fissile inventory needed is very small (about 1.5 kg of U233 per MWe), and the system is expected to have a doubling time comparable to that expected from oxide-fueled, sodium-cooled fast breeder reactors.

The MSBR is a two-region, two-fluid system, with fuel salt separated from the blanket salt by graphite tubes. The fuel salt consists of uranium fluoride dissolved in a mixture of lithium and beryllium fluorides, and the blanket salt is a thorium-lithium fluoride of eutectic composition (27 mole% thorium fluoride). The uranium fluoride provides the fissile material necessary for achieving criticality. The heat transport medium in the MSBR is the fuel salt itself. The energy generated in the reactor fluid is transferred to a secondary coolant salt circuit ($NaF + NaBF_4$) that couples the reactor to a supercritical steam cycle.

The fuel salt in MSBR is processed continuously in an on-line reprocessing plant. The fluoride volatility and vacuum distillation process is employed for core fuel reprocessing. On-site fluoride volatility processing leads to low unit processing costs and economic operation as a thermal breeder reactor. The on-line reprocessing also helps to remove protactinium (Pa233) and parasitic fission products, which affect neutron economy.

12.4.2.3 VVER-T The VVER is the Russian version of the Pressurized Water Reactor (PWR). The Russian Research Centre Kurchatov Institute (KI) evolved the concept of VVER-T reactor utilizing thorium. VVER-T reactor is a water-moderated, water-cooled power reactor using uranium–thorium fuel [17]. The fuel assembly of the VVER-T reactor has two zones, i.e., the seed zone at the center and the blanket zone at the periphery. The basic feature of the reactor is the use of heterogeneous fuel assemblies with mixed uranium-thorium fuel in the blanket region and uranium-zirconium fuel in the seed region instead of traditional uranium fuel assemblies. This type of loading ensures effective transmutation of Th232 to U233 and its burn-up in-situ without refabrication. This scheme enables effective utilization of thorium in open fuel cycle without refabrication of spent fuel. The U233 accumulated in the spent fuel could be utilized once the refabrication technology is industrially established. The seed fuel is discharged after a burn-up of 150 GWd/t, whereas the blanket fuel is kept for a longer time (about 10 years) before discharge for ultimate storage without reprocessing. This fuel cycle results in savings of natural uranium by 20%, as well as reduction in the production of trans-plutonics by about 20 times, as compared to the operating VVERs. The unique combination of non-proliferation qualities, improved efficiency, decreased radwaste accumulation, improved safety, and amenability to use of weapon grade uranium and plutonium makes VVER-T attractive for development and operation in the near future.

12.4.3 Thorium in Fast Reactors

As in the case of uranium, the best utilization of thorium resources for power generation is possible only in fast breeder reactors (breeding fissile material), relative to thermal reactors, which cannot sustain the fissile material production. IAEA has prepared some documents describing the global status of thorium utilization [3, 18]. The various experimental irradiations and studies performed using thorium in Fast Breeder Reactors (FBR) are listed below.

Thorium samples were irradiated in the blanket region of Russian BN-350 reactor up to 1.3 gm/kg of U233 in blanket. The U232 content was 2–11 ppm [19]. This experiment was mainly for confirming reaction rate estimates. Detailed studies have been conducted of ThO_2 irradiation in the core and blankets of BN-800. These studies show that during every cycle, in the radial blanket, a maximum of 5 gm/kg of U233 production is possible. After long irradiations, U232 concentrations reach only a maximum of about 100 ppm. However, if thorium/U233 oxide fuel is considered within the core, U232 concentrations reach a few thousand ppm for high burn-up.

These studies indicate that the best way of utilizing thorium is in the blankets of FBR as breeding ratios close to 1.10 is achievable in the U-Pu MOX fuelled FBR with ThO_2 blankets. It is possible to keep the U232 content in uranium relatively small, below 100 ppm. The U233 so produced may be used to fuel thermal breeder (molten salt) or fast breeder reactors.

In the uranium-plutonium mixed carbide–fueled Indian Fast Breeder Test Reactor (FBTR), about 60 sub-assemblies containing ThO_2 are being irradiated as a blanket.

U233 has been considered as fuel [20] for thermionic emission–based space reactors of the fast type with metal or air coolant.

12.5 THORIUM FUEL CYCLE ASPECTS

12.5.1 Challenges in Thorium Fuel Cycle [9, 18]

Despite the thorium fuel cycle's having a number of attractive features, there are several challenges associated with it. Th232 (the only isotope of the element in nature) is a fertile material, which means that a fissile material (U235 or Pu329) is needed to supply neutrons to convert the Th232 into U233.

Unlike uranium oxide and plutonium oxide, thorium forms only the dioxide, which is very stable. Uranium

dioxide dissolves in nitric acid. ThO_2 and (Th-U)O_2 or (Th-Pu)O_2, containing higher percentages of thorium (>80%), cannot be dissolved with pure nitric acid. This problem is mitigated by the addition of small amounts of hydrofluoric acid (HF). The use of fluoride ions, however, enhances the corrosion of stainless steel equipment and piping. Therefore, selection of material of construction for dissolution equipment poses a challenge. Laboratory-scale parametric studies have been carried out for improving the dissolution of thorium dioxide fuel by using different additives (HF & NaF) in the dissolvent and by adding dopants (magnesium oxide) in the thoria during fabrication. Aluminium nitrate can be added to the dissolvent solution to reduce the fluoride activity, in order to reduce the corrosion.

Another operational difficulty with thorium-based fuel is the formation of protactinium isotope (Pa233, with a half-life of 27 days) in the intermediate stage of conversion of Th232 to U233. This causes buildup of the isotope U233 by decay of Pa233 during a long shutdown. This addition of reactivity has to be accounted for in the reactor design and operation after a long shutdown.

The major concern with respect to thorium fuel cycle is related to the radiological aspects associated with the production of isotope U232 along with U233. U232 is formed via (n, 2n) reactions, from Pa233 and U233. The level of contamination with U232/Th228 depends on the isotopic composition of uranium in the initial thorium fuel, the burn-up and the neutron spectrum encountered in the reactor. The contamination increases with subsequent recycling of uranium with thorium fuel. The half-life of U232 is about 69 years. The isotopes produced in the decay chain of U232 (Bi212 and Tl208) are emitters of hard (high-energy) gamma rays. Therefore, the reprocessed material emits hard gamma rays, and their dose increases with time after separation. As a result, the radioactivity in the uranium separated from irradiated thorium would present several technological challenges in the refabrication and recycling of uranium. Consequently, the processes and equipment must be developed, so that the various steps can be carried out in a shielded facility and within a very small time period after separation.

The thorium recovered from the irradiated spent fuel will also contain traces of Th228 (half-life of 1.91 years). Handling of recovered thorium (by routes employed for freshly mined thorium) will thus be difficult, if the processing is carried out after a short cooling period, because of the presence of the hard gamma emitters. Approximately 20 years (~10 half-lives of Th228) of cooling period is required to bring down the gamma dose in thorium.

The higher energy (n, 2n) reactions encountered by Th232 during the irradiation in nuclear reactors also lead to the formation of long-lived Pa231 (half-life 3.27×10^4 yr), which is almost 100 times more as compared to that in U235 fuel. Since protactinium migrates in soil or water much faster (being present in pentavalent form) as compared to the other radionuclides present in multivalent form, protactinium would be an issue to be addressed in thorium fuel cycle.

The alpha activity of U233 is three orders of magnitude higher than that of HEU and about one order magnitude less than that of weapons grade plutonium.

12.5.2 Fabrication [21, 22]

The use of thorium requires addition of fissile material, and this can be in the form of enriched uranium (U235), plutonium (PU239), or uranium (U233) obtained from reprocessing of thorium fuel. ThO_2, UO_2, and PuO_2 are isostructural (FCC, CaF_2 type). Thoria forms solid solutions with urania and plutonia. The manufacturing processes of thorium-based fuels are, therefore, similar to that of the well-established processes for fabrication of UO_2 and mixed-oxide fuels. The (Th-U) MOX fuel can be fabricated like the conventional uranium fuel, and the (Th-Pu) MOX fuel can be fabricated inside a glove box like that of well established (U-Pu) MOX fuels.

As mentioned earlier, a special feature of thorium/U233 fuel cycle is the high gamma dose associated with the daughter products of U232. The fabrication process of (thorium/U233) fuel requires shielding provisions, and this necessitates considerable technological development. The following techniques, amenable for remotization, have been developed so far for manufacturing ThO_2 and thoria-based mixed-oxide fuels: (1) the "powder-pellet" route, (2) the "Vibro-sol" route, (3) "Sol-gel microsphere pelletization," and (4) the "impregnation technique."

ThO_2, ThO_2-UO_2, and ThO_2-PuO_2 fuels have been manufactured in both "particle" form (microspheres) and "pellet" form for use in water-cooled reactors in the form of "vi–pac" and "pellet-pin" elements respectively. For fabrication of "vi–pac pins", high-density fuel microspheres of one, two, or three size fractions (typically 1000μ, 100μ, and 10μ) are vibratory compacted into fuel cladding tubes to obtain fuel elements of controlled "smear" density. Alternatively, the sintered high-density pellets are loaded in fuel cladding tube and encapsulated to obtain pellet-pin fuel elements for water-cooled reactors. High-density fuel "microspheres" of ThO_2, (Th-U)O_2, or (Th-U)C_2 have been manufactured for HTGRs. The microspheres are subjected to multilayer coatings of pyrolytic carbon and silicon carbide, known as BISO- or TRISO-coated particles, and compacted in graphite matrix. The HTGR fuel is either in the form of spherical balls (known as fuel pebbles used in pebble bed core configuration) or in the form of cylindrical shapes (known as fuel compact used in prismatic core configuration).

12.5.3 Reprocessing [18, 21, 22]

The process for extracting U233 from thorium-based fuel during reprocessing has not matured to the same extent as the process of extraction of plutonium from uranium-based fuel. This is largely due to lack of its immediate application in the technologically developed countries. One of the main hurdles in reprocessing of thorium-based fuel is the highly stable nature of thorium dioxide, which makes dissolution of thoria-based fuels more difficult as compared to urania-based fuels.

For reprocessing of spent thorium-based fuels, the wet chemical route developed in ORNL in the mid 1950s, namely the THORium-uranium EXtraction (THOREX) process, has so far been the most viable route [18, 23–25]. It is based on solvent extraction separation of uranium and thorium from fission products by means of Tri-n-Butyl Phosphate (TBP). Figure 12.4 shows typical schematic diagram of the THOREX process.

In this process, thorium is co-extracted with uranium, using TBP (30 to 42.5% in a paraffin diluent), leaving the fission products in the aqueous phase. A higher acid strip (>0.3 M) is used to remove the bulk of thorium, while very low acid is used to subsequently strip the uranium. One of the challenges encountered in this route is the third phase formation due to poor solubility of thorium–TBP complexes in the paraffin diluent. In order to avoid third phase formation, the solvent loading of TBP phase with thorium is restricted to values much lower than what is normally employed in the case of uranium. Alternatively, aromatic diluents like decalin (decahydronapthalene) in place of dodecane, Shell sol–T, or n-paraffin, can be used to increase the loading of thorium in TBP without third-phase formation.

So far, reprocessing of spent thorium-based fuel has been carried out only in a few countries based on THOREX process, mostly on laboratory or pilot plant scale.

A Power Reactor Thorium Reprocessing Facility (PRTRF) is being established in BARC, and this plant will be used for reprocessing of thorium fuel bundles irradiated in PHWRs.

12.5.4 INTERIM 23 Process for Separation of Uranium

In most countries, the INTERIM 23 process has been used in the past, where partitioning of thorium is omitted, and the uranium is selectively extracted with 1.5 to 5% TBP in a paraffin diluent, with relatively good decontamination factors. The objective of the INTERIM 23 process is to extract only the uranium in the organic phase, and the thorium is passed into the raffinate together with the fission products [18, 23]. However, the uranium thus separated contains a significant amount of thorium as impurity. The U233 product is further purified by anion exchange process in hydrochloric acid medium. The uranium product is precipitated as di-uranate and calcined to uranium oxide.

In recent years, long-chain aliphatic amides are also being considered as potential candidates for the selective extraction of uranium, based on their superior uranium-thorium separation factors [26]. It has been shown that trialkyl phosphates with branching in the carbon chain also have superior selectivity for uranium over thorium. However, these processes are yet to be demonstrated with irradiated fuels.

Much more developmental effort is required even today before the thorium fuel cycle can be commercialized. Nevertheless, the thorium fuel cycle, with its potential for

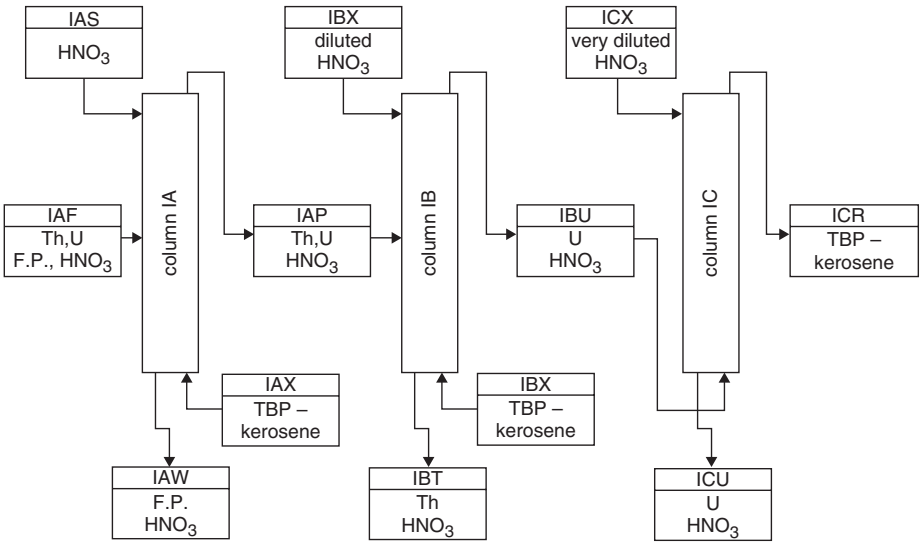

Figure 12.4 Simplified flow diagram for THOREX process.

breeding fuel without the need for fast-neutron reactors, holds considerable potential in the long run. It could be a significant strategy in the long-term sustainability of nuclear energy.

12.6 UTILIZATION OF THORIUM IN INDIA

Worldwide, the highest activity on thorium as a nuclear energy source is in India. It is thus appropriate to describe in some detail the programme for thorium utilization in India.

India has about 1% of the world's uranium resources, while its thorium resources are one of the largest in the world, totaling about 2,25,000 tons [27]. With vast thorium and limited uranium, India has made utilisztion of thorium for large-scale energy production a major goal in its three-stage nuclear power program. Various experimental campaigns have been carried out in India to generate the required reactor physics and performance database for large-scale utilization of thorium fuel.

12.6.1 Thoria Fuel in Research Reactors

Irradiation experiments have been carried out with thoria (thorium oxide) fuel in research reactor Dhruva [28]. Four thoria fuel assemblies were loaded in research reactor Dhruva during its initial days of operation to take care of the excess reactivity of the initial core. These assemblies were successfully irradiated up to 100 Effective Full Power Days. The fissile material U233 has been utilized as a liquid fuel for PURNIMA research reactor. The research reactor KAMINI at Kalpakkam, India, built jointly by BARC and IGCAR, is the only research reactor in the world fuelled with U233. This reactor operates as a neutron source and has facilities for carrying out radiation physics experiments, neutron radiography, neutron activation analysis etc.

12.6.2 Thoria-Based MOX Fuel

Thoria-based MOX fuels and thoria fuel have been successfully irradiated in the Pressurized Water Loop (PWL) of the CIRUS reactor without any failure [28, 29]. These tests were carried out with short-length fuel pins (about 0.5 m long) under simulated power reactor operating conditions. Six (Th4%Pu) MOX pins of BWR type with free-standing clad have been irradiated to a burn-up of 18.5 GWd/t. Two (Th-6.75%Pu) MOX pins of PHWR type with collapsible clad have been irradiated to a burn-up of 10.2 GWd/t.

12.6.3 Thoria Fuel Bundles in Indian PHWRs

Four test fuel bundles containing high-density thorium dioxide pellets were successfully irradiated in PHWR at Madras Atomic Power Station. India has replaced depleted urania bundles with thoria bundles for neutron flux flattening of the initial core after startup in PHWRs at Kakrapar and other reactors subsequently commissioned at Kaiga (I & II), Tarapur (III & IV) and Rajasthan (III, IV, II, and V). Presently, thorium dioxide bundles are used in Indian PHWRs for achieving the flux flattening of the initial core after startup [28, 29]. This represents a unique way of utililizing thorium without any loss of burn-up in UO_2 fuel. To the present time, 256 thoria fuel bundles have been loaded into PHWRs.

12.6.4 Thorium-Fueled Indian Advanced Heavy Water Reactor (AHWR)

The main objective of AHWR is to demonstrate advanced technologies required for large-scale utilization of thorium in reactors and its fuel cycle. Because thorium utilization forms the basis of the third stage of the Indian nuclear power program, AHWR is designed to use (thorium/U233) MOX and (thorium/plutonium) MOX fuel [30].

The AHWR is a 920 MWth (300 MWe) vertical-pressure, tube-type boiling light water reactor. The fuel is moderated by heavy water and cooled by natural circulation of light water. The fuel consists of (thorium/plutonium)O_2 and (thorium/U233)O_2 pins. The fuel cluster is designed to generate major energy out of U233, which is bred in-situ from thorium. The AHWR has been designed to extract major fraction of its power from thorium-based fuel, keeping plutonium consumption as low as possible. The equilibrium fuel cycle for the AHWR is based on the conversion of naturally available thorium into fissile U233 driven by plutonium as the external fissile feed. The AHWR has been designed to be self-sustaining in U233. The fuel cycle is a closed fuel cycle, envisaging recycling of both fissile U233 and fertile thoria back to the reactor. The U233 requirements for the reactor will be met by recycling after reprocessing the spent fuel. The adoption of closed fuel cycle helps in generating a large fraction of energy from thorium. The fuel cycle time of AHWR is 8 years—four years of in-reactor residence, two years of cooling, one year of reprocessing, and one year for refabrication. A part of the recovered thorium from the reprocessing plant will be recycled into the reactor immediately by using it in the fabrication of (thorium/U233) MOX fuel pins.

AHWR is the first of its kind in the world and has been designed for 100 years of plant life. The reactor is one of the innovative next-generation nuclear reactors that incorporate safety and operating conditions at par with emerging international standards. The reactor has a slightly negative void coefficient of reactivity. The AHWR relies heavily on passive processes and components for its operation and accident mitigation. There are several passive safety

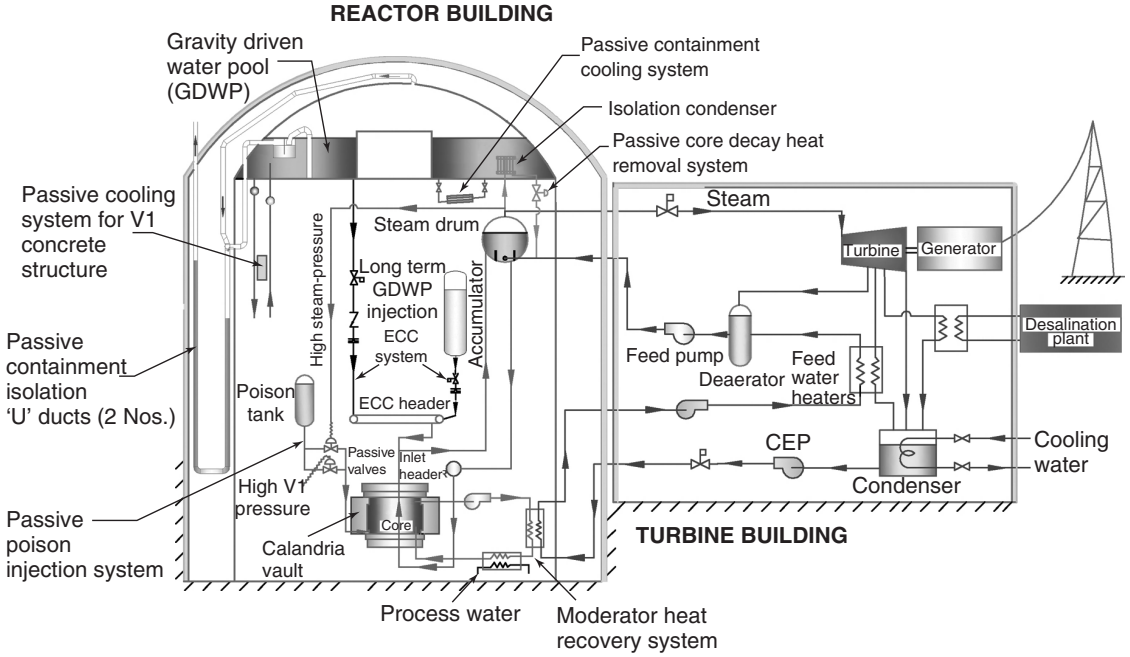

Figure 12.5 Schematic arrangement of various systems in AHWR.

systems for reactor normal operation, decay heat removal, emergency core cooling, confinement of radioactivity, and other processes. These passive safety features are based on natural phenomena for their operation, such as gravity and natural convection, requiring no operator intervention. A schematic arrangement of various systems of AHWR is shown in Figure 12.5.

A number of facilities have been developed and planned to validate the evolutionary concepts. The target core damage frequency is 10^{-7}/ year or less. For achieving this, a series of potential high-consequence events have been visualized even when these events are Beyond Design Basis Accidents (BDBA), according to current standards. The safety features are so engineered that the consequences are mitigated.

Unlike uranium-based fuels, only a small database exists for the thorium-based fuels. A critical facility has been constructed at BARC for carrying out reactor physics experiments as part of the AHWR design and development program. This facility is a low-power research reactor, where lattice physics experiments are being carried out for validation of reactor physics design parameters. The experimental irradiations planned along with the Post-Irradiation Examination (PIE) will provide an insight into the performance behavior aspects of the thorium-based fuels.

Even though production of minor actinide in thorium/U233 fuel is less as compared to those in uranium fuel, the production of minor actinides in AHWR is expected to be higher than that in PHWR, due to the use of PU239 in AHWR fuel, which leads to higher generation of americium and curium isotopes.

A fuel cycle facility is also planned, which will be co-located with AHWR. This facility will fabricate and reprocess the AHWR fuel to recycle the fissile and fertile materials. There will also be provisions for waste management, poolside inspection, and nuclear material storage, so as to meet the fuel fabrication and reprocessing requirements. Thus, thorium-based AHWR will provide a platform for developing thorium fuel cycle technologies.

12.7 CONCLUSION

The increasing energy demands in the future and the depleting of fossil fuel resources would strongly dictate the use of nuclear energy. Thorium, being more abundant than uranium in nature, can be a sustainable nuclear energy resource. Reactor designs for optimum utilization of thorium resources can satisfy the energy needs of the world for a few centuries. Thus, the advantages of thorium fuel cycle could be exploited to enhance the role of nuclear technology in meeting the energy requirements of the future generations. However, considerable investments in R&D would be required to resolve the technology issues and reach the level of maturity that has been attained in uranium-based fuel cycles. In the Indian context, the use of thorium for large-scale commercial electricity generation is of great importance. The time scale for implementing utilization of thorium in different countries will, however, depend on the availability/access to uranium resources.

REFERENCES

1. S. Glasstone and A. Sesonske, *Nuclear Reactor Engineering: Reactor Design Basics*, Volume 1, 4th ed. CBS Publishers and Distributors, 2004.
2. C. Ronchi and J.P. Hiernaut, Experimental measurement of pre-melting and melting of thorium dioxide. *Journal of Alloys and Compounds*, 1996, **240**, 179–185.
3. International Atomic Energy Agency, Thorium fuel utilization: options and trends, *IAEA TECDOC-1319,* November 2002.
4. G. Mazzini, E. Bomboni, et al. (based on U.S. Geological Survey, Mineral Commodity Summaries, January 2007) The use of Th in HTR: state of the art and implementation in Th/Pu fuel cycles. *Science and Technology of Nuclear Installations*, Hindawi Publishing Corporation, Article ID-749736, 2009.
5. OECD, International Atomic Energy Agency (IAEA), Uranium 2007: Resources, production and demand. *Redbook* 2007.
6. T.P. Mernagh and Y. Miezitis, A review of the geochemical processes controlling the distribution of thorium in Earth's crust and Australia's Thorium Resources. *Geoscience Australia Record*, 2008/05, 23–28 ISBN 978-1-921236-78-5 (printed).
7. B.S. Van Gosen, V.S. Gillerman, and T.J. Armbrustmacher, Thorium deposits of the United States—energy resources for the future? US Geological Survey Circular 1336, 2009.
8. Thorium Report Committee, *Thorium as an Energy Source—Opportunities for Norway*, Published by Research Council of Norway (RCN) and the Ministry of Petroleum and Energy (OED), January 2008. ISBN 978-82-7017-692-2 (printed).
9. Michel Lung, A present review of the thorium nuclear fuel cycle. *European Commission Report EUR-17771 EN,* 1997.
10. International Atomic Energy Agency, Thorium based fuel options for the generation of electricity: Developments in 1990s. *IAEA TECDOC-1155,* May 2000.
11. D. Greneche, W.J. Szymczak, J.M. Buchheit, M. Delpech A. Vasile, and H. Golfier, Rethinking the thorium fuel cycle: an industrial point of view, Paper 7367, *Proceedings of ICAPP (International Congress on Advances in Nuclear Power Plants) 2007, The Nuclear Renaissance at Work,* May 13–18, 2007, Nice Acropolis, France.
12. R. Baumer, I. Kalinowski, E. Röhler, J. Schöning, and W. Wachholz, Construction and operating experience with the 300-MW THTR nuclear power plant. *Nuclear Engineering and Design*, 1990, **121**, 2, 155–166.
13. R. Atherton *Water cooled breeder program summary report (LWBR Development Program)*, Bettis Atomic Power Laboratory, Report WAPD-TM-1600, October 1987.
14. G.L. Olson, R.K. McCardel, D.B. Illum, *Fuel summary report: Shippingport Light Water Breeder Reactor*., INEEL/EXT-98-00799 Rev. 2, September 2002.
15. P.G. Boczar, M.J.N. Gagnon, P.S.W. Chan, R.J. Ellis, R.A. Verrall, and A.R. Dastur, Advanced CANDU systems for plutonium destruction. *Canadian Nuclear Society Bulletin*, **18**, 1, Winter 1997.
16. P.R. Kasten et al., Molten salt breeder reactor design studies. *Proceedings of Second International Thorium Fuel Cycle Symposium,* Gatlinburg, Tennessee, USA, May1966, 41–63.
17. N.N. Ponomarev-Stepnoi, G.L. Lunin, E.P. Ryazantsev, A.G. Morozov, V.V. Kuznetsov, V.V. Kevrolev, and V.F. Kuznetsov, Light Water Thorium Reactor VVER-T. *Atomic Energy*, 1998, **84**, 4, 685–699.
18. International Atomic Energy Agency, Thorium fuel cycle—Potential benefits and challenges. *IAEA TECDOC-1450,* May 2005.
19. M.F. Troyanov, V.G. Ilyunin, A.G. Kalashnikov, B.D. Kuz'minov, M.N. Nikolaev, F.P. Raskach, E. Ya. Smetanin, and A.M. Tsibulyaet, Some investigations and developments of the thorium fuel cycle. *Atomic Energy*, 1998, **84**, 4, 225–229.
20. A.K. Hyder, R.L. Wiley, G. Halpert, D.J. Flood, and S. Sabripour, *Spacecraft Power Technologies*. Imperial College Press, January 2000.
21. K. Anantharaman, V. Venkatraj, and A.K. Anand, Performance of thorium-dioxide fuels. *Russian-Indian Workshop on Thorium Fuel Cycle,* Obinsk, Russia, November 1998.
22. K. Anantharaman, A. Ramanujam, H.S. Kamath, S. Majumdar, V.N. Vaidya, and M. Venkataraman, Thorium based fuel reprocessing and refabrication technologies and strategies, Paper-C1352, *Proceedings of INSAC-2000 (11^{th} annual conference of Indian Nuclear Society): Power from Thorium: Status, Strategies and Directions,* June 2000, **2**, 82–107.
23. F.L. Culler, *Proceedings of First International Conference on Peaceful Uses of Atomic Energy*, Geneva, Switzerland, 1955, **9**, 464–483.
24. *Gmelin Handbook of Inorganic Chemistry*, 8^{th} ed., Springer-Verlag Publishers, New York, 1982, 285–288.
25. R.H. Rainey and J.G. Moore, Laboratory development of the acid THOREX process for recovery of consolidated Edison Thorium reactor fuel, *Oak Ridge National Laboratory Report ORNL-3155,* May 1962, 2–28.
26. P.N. Pathak, R. Veeraraghavan, D.R. Prabhu, G.R. Mahajan and V.K. Manchanda, Separation studies of uranium and thorium using di-2-ethylhexyl isobutyramide (D2EHIBA)., *Separation Science and Technology*, 1999, **34**, 13, 2601–2614.
27. DAE Document No.-10, *A Strategy for Growth of Electrical Energy in India,* http://www.dae.gov.in/publ/doc10/index.htm (accessed January 2010).
28. K. Anantharaman, V. Shivakumar, and D. Saha, Utilisation of thorium in reactors. *Journal of Nuclear Materials*, 2008, **383**, 119–121.
29. K. Anantharaman, "Loop experiments with thoria based fuel. *Indo-Japan Seminar on Thorium Utilisation,* Mumbai, India, December 10–13, 1990, 132–135
30. R.K. Sinha and A. Kakodkar, Design and development of the AHWR—the Indian thorium fuelled innovative nuclear reactor. *Nuclear Engineering and Design*, April 2006, **236**, 7–8, 683–700.

13

DESIGN PRINCIPLES OF NUCLEAR MATERIALS

BALDEV RAJ AND M. VIJAYALAKSHMI

Indira Gandhi Centre for Atomic Research, Kalpakkam, TN, India

"Sustainable and green energy" is an imminent global necessity of the 21st century. In this context, nuclear energy plays [1] a pivotal role, with a sustainable fuel cycle and very low CO_2 footprint. Both the types of nuclear power, namely fission and fusion, meet the above two demands. *Fission* refers to release of energy (~200 MeV per fission event) during the disintegration of heavy fissile nuclei of uranium, U235, U233, and Pu239 into lighter fragments, when it is bombarded by an energetic neutron. In *fusion*, energy is released when nuclei of smaller elements are fused together to form a larger nucleus (example, $H_1^2 + H_1^3 \rightarrow He_2^4 + n_0^1 + 17.6$ MeV).

Of the two nuclear sources, fission and fusion, fission technology is well established, while the latter is in its infancy. The 438 fission-based power reactors worldwide [2], accounting for ~15% of global electric power generation, have demonstrated a safe, energy production record in the last three decades. France has established a proven record, meeting 75% of power demand from nuclear resources, while Japan provides 29%. The economics of nuclear power is the major deciding factor for the choice of nuclear power by any country. The widespread public acceptance of nuclear power can be achieved only if key issues such as improved safety, non-proliferation, and waste management are addressed. The advanced, innovative design concepts of emerging nuclear technologies of the 21st century are targeted toward achieving economic, safe, proliferation-resistant nuclear reactors with much lower radioactive waste than the present generation reactors. There is intense international cooperation toward the above goal, although the individual option of nuclear policy varies widely across the globe. Figure 13.1. shows the possible scenario for nuclear expansion in the 21st century. The anticipated technology leap between the advanced design concepts and the present generation reactors is enormous.

Another important aspect of the nuclear industry is the fuel cycle option. The nuclear industry begins with extraction of the nuclear fuel from the ore, burning it in the reactor, followed by the suitable disposal of the burnt or spent fuel. The first stage is called the front end, while the third stage is referred to as the back end of the fuel cycle. The third stage has two options: (1) the open, once-through fuel cycle, in which the entire spent nuclear fuel is treated as nuclear waste and disposed in deep geological repositories, and (2) the closed fuel cycle, in which the spent fuel is reprocessed to yield unburnt fuel for recycling and nuclear waste for burying in deep repositories. Table 13.1 compares the two fuel cycle options and lists the options exercised by various countries.

Any meaningful program on materials development for nuclear industry has to take into account the improved targets of performance of the nuclear industry, consequent developments in the reactor design, and, finally, the changes in the service conditions to which the materials will be exposed in the emerging scenario. Hence, we present a brief introduction to different types of nuclear reactors and the future trends in the nuclear industry before proceeding to a detailed discussion on nuclear materials.

Nuclear Energy Encyclopedia: Science, Technology, and Applications, First Edition (Wiley Series On Energy).
Edited by Steven B. Krivit, Jay H. Lehr, and Thomas B. Kingery.

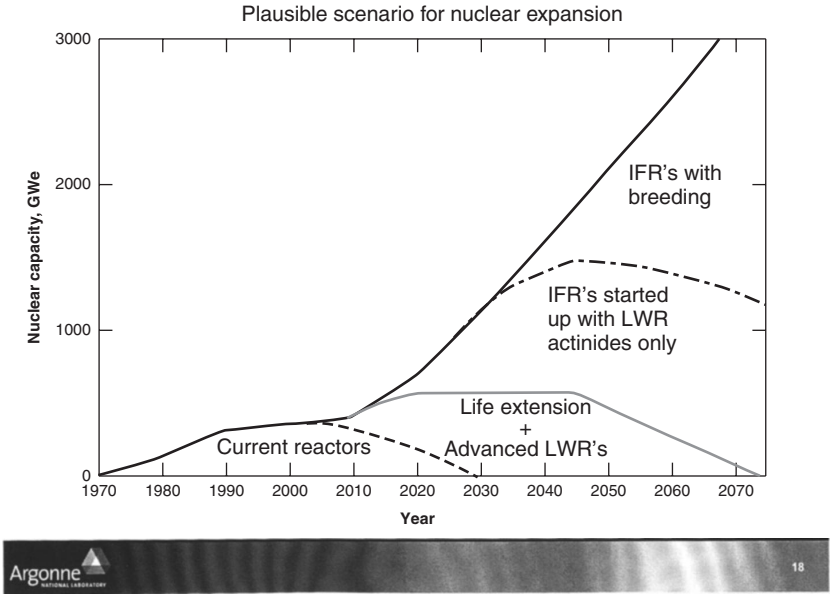

Figure 13.1 Possible scenario for nuclear expansion [3].

TABLE 13.1 Comparison between Two Fuel Cycle Options and the Choice of Various Countries

Name of the Fuel Cycle	Principle/Concept	Advantages	Disadvantages	Countries Following Fuel Cycle
Open	Spent nuclear fuel (SNF) is cooled, vitrified, packed in suitable canisters, and buried deep in geological repositories	No need for establishing reprocessing technologies Cost of reprocessing technologies is reduced from fuel cycle cost Proliferation probabilities is reduced	Possible only if uranium availability is sufficient, since reusable fuel is buried Time for the activity of the SNF to reduce to natural level is of the order of geological time scales Less economic incentive, in terms of loss of usable fuel	United States, UK
Closed	Spent nuclear fuel is cooled, reprocessed to separate the reusable fuel from fission products and minor actinides, before vitrification, packing, and burial in geological repositories	Ensures sustainable nuclear energy Better waste management; time taken by the nuclear waste to reduce to the natural level of activity is reduced by two orders of magnitude. Unused fuel reprocessed from SNF can be reused in more reactors; useful for countries with less uranium resources	Essential to establish cost effective reprocessing facilities Infrastructural facilities Proliferation issues	France, Russia, Japan, and India

13.1 INTRODUCTION TO NUCLEAR TECHNOLOGY

A schematic of the two types of nuclear reactors *i.e*., fission- and fusion-based, is shown in Figure 13.2. In the case of fission-based nuclear reactors, the nuclear fuel consists of fuels like U235, U233, and Pu239, called the fissile nuclei, which undergo nuclear fission. The abundance of U235 in natural uranium, U238, is only 0.07%. Other two fissile nuclei, U233 and Pu239, have to be produced by another nuclear reaction in a reactor, using fertile nuclei like Th232 or U238. The nuclear reactors are broadly classified into either *thermal* or *fast* reactors, depending on the energy of the neutrons used for causing fission. The average energy of neutrons causing fission in thermal reactors is ~0.025 eV, while it is 0.2 to 0.5 MeV in fast reactors. The characteristics of thermal and fast nuclear reactors are compared in Table 13.2.

Fusion power is a promising long-term solution for global energy issues. Only the reactor in which heat is generated using thermonuclear reaction is different, while the remaining components of the power plant are similar to any other power station. The earlier attempts on sustaining the fusion plasma have resulted in launching the ongoing International Thermonuclear Experimental Reactor (ITER). ITER is a joint project in which the European community, Japan, Russia, the United States, Korea, China, and India are participating with the target of testing the commercial feasibility of fusion power and examining the concepts of tritium breeding using test blanket modules. Long-term fusion programs like DEMO, a demonstration fusion power reactor, is being planned for validation of in-service performance of candidate materials in fusion environments.

13.1.1 Present Generation Reactors

Presently, the fission-based light water reactor is the workhorse of the nuclear industry. The fuel used is a mixture of oxides of uranium and plutonium, with the moderator (medium used for slowing down the fission neutrons) and coolant being light water. The satisfactory performance of many thermal reactors has enabled their licensing for a longer service life of 60 years. A few countries, namely Japan, Russia, France, and India have chosen the route of augmenting the thermal reactor capacity with fast reactors. The fast reactor technology in the last three decades has matured, with 390 successful years [5] of operating experience.

It is possible to operate the fast reactors as either *burners* or *breeders*. That is, burners are fast reactors that produce energy by burning the fuel and/or transmuting minor actinides into short-lived nuclear waste. Breeders refer to those reactors that produce more fissile material than they consume. The international initiatives, like INPRO [6] and GEN-IV [7], consider fast breeder reactors as an important option to meet the twin objectives of sustainability of nuclear power and minimizing nuclear waste in the future.

Presently, the back end of the fuel cycle is carried out by industrially proven technologies for the reprocessing and waste management. Reprocessing is carried out using the aqueous PUREX (Plutonium Uranium Recovery by EXtraction) process, while waste management is carried out by vitrification of high-level waste in a matrix of borosilicate before deposition into deep geological repositories.

13.1.2 Future Generation Technologies

The litmus test of the success of future generation nuclear industry is the synergy between the strength of past experience and addressing the present societal concerns: economy of the technology, safety, non-proliferation and waste management.

Internationally, the following steps have been taken up to improve economy. These are basically short-term strategies: increasing the life of the presently installed reactors with assured safety, reducing the shutdown time of the reactors, increasing the thermal efficiency of the reactors and replacing the components with long-lived, cost-effective materials. There are a few innovative concepts with long-term targets: (1) high temperature, multiple-use reactors; (2) improved fuels and better coolants; (3) proliferation resistant reactors; and (4) superior waste management.

The high-temperature, multiple-use reactors are designed to operate at temperatures as high as 1273°K, in addition to using the fission-generated heat for commercial purposes such as the production of hydrogen as fuel, desalination, and heating of buildings. Although this technology was known as early as 1970, the economic competitiveness of light water reactors has gained popularity. The revival of this technology with improved design features is expected to be commercialized in another one or two decades.

In the context of improved fuels and coolants, both the thermal and fast reactors are undergoing evolutionary changes. Intense R&D has been carried out to develop different types of fuels such as the metallic and ceramic (oxide or carbide or nitride of uranium and plutonium) fuels. When the challenge of sustainability has to be met, the metallic fuel, with high breeding capability, appears to provide the best option for those countries with inadequate uranium reserves. The metallic fuels were also used in the early days of nuclear industry, due to its better compatibility with sodium. Its limitations, at that point of time, arose due to low residence time and unacceptable behavior of fuel at high temperatures and irradiation in the reactor. However, certain discoveries in the 1970s with respect to in-service behavior of metallic fuel have provided the required confidence to reconsider the metallic fuel as an

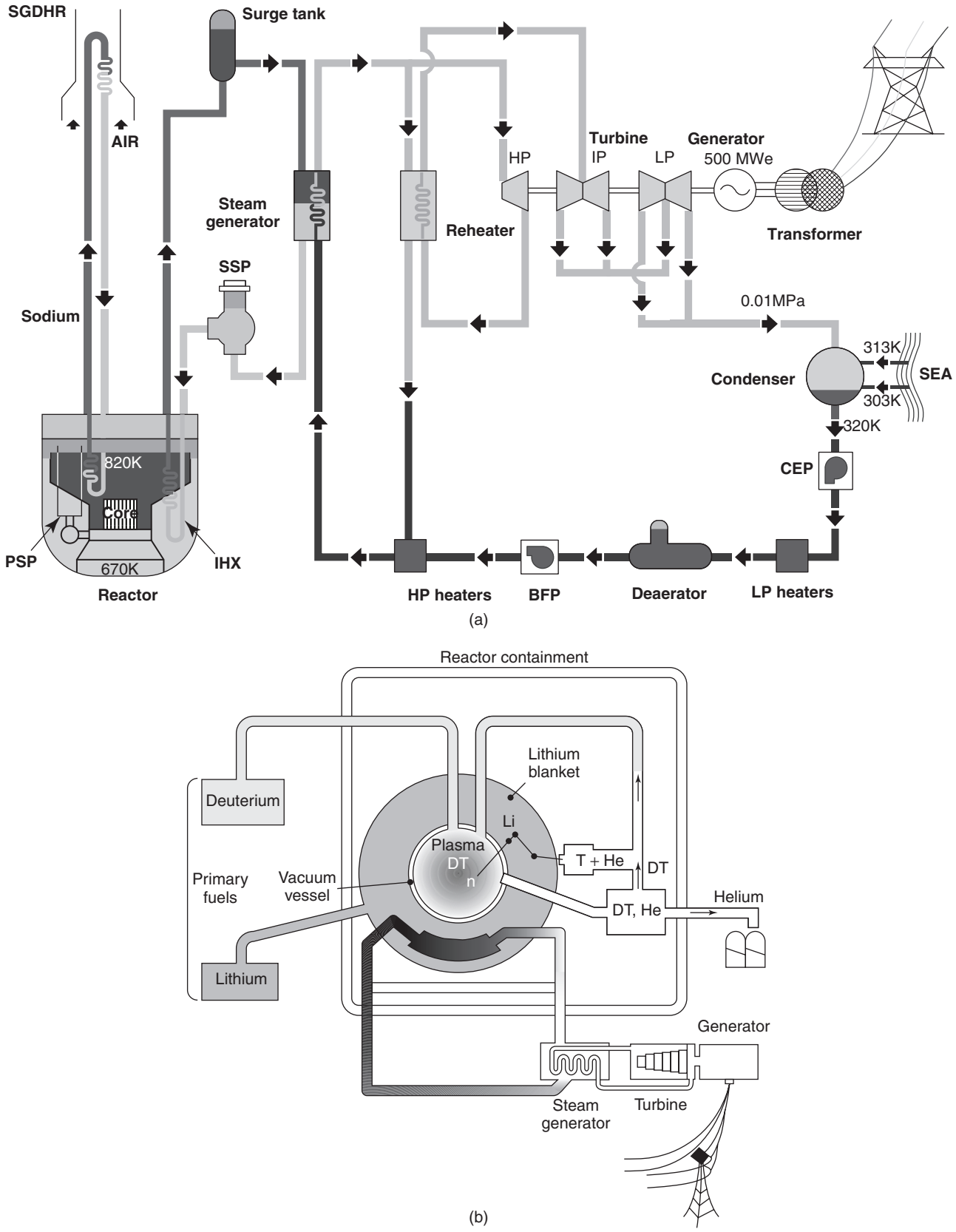

Figure 13.2 Schematic of the two types of nuclear reactors: (a) fission and (b) fusion [4].

TABLE 13.2 Characteristics of Thermal and Fast Reactors in Various Countries

Type of Reactor	Characteristics			Few Countries with the Installations
	Energy of Neutrons	Major Components	Exposure Conditions	
Thermal reactors	<0.1 eV	Fuel: Mixed oxide Moderator: light/heavy water Coolant: same	Neutron flux: 10^{15}n/cm^2/s Fluence or Burn-up: 80 GWd/tonne Temperature: 573K	Argentina, Australia, Austria, Belgium, Brazil, Canada, China, Cuba, Denmark, France, Finland, Germany, Greece, India, Hungary, Iran, Mexico, Netherlands, Norway, Korea, Pakistan, South Africa, Switzerland, UK, USA
Fast reactors	~1 MeV	Fuel: mixed oxide; Coolant: Liquid sodium	Neutron flux: 8×10^{15} n/cm^2/s Burn-up: 100 GWd/t Temp.: 823°K	France, Japan, Russia, USA, and India

acceptable option. The specific discoveries refer to ability of the metallic fuel to withstand high residence time in the reactor, due to release of accumulated fission gas through connected pores in the fuel lattice.

Another option to enhance the fuel availability is to use thorium, Th232, through its conversion to U233. India, with its abundant thorium reserves, has already launched the thorium-based fuel-cycle technologies as an alternate energy option. The major challenge is in the front-end of the fuel cycle. The fabrication procedures for fuels containing U233 have to take into account the presence of isotope U232, which decays ultimately to thallium, Tl208, which is a hard gamma emitter. This necessitated development of remote fuel fabrication technology. The commercial viability is expected in the middle of the present century.

In the context of coolants, gases like helium and carbondioxide are being evaluated for the high-temperature reactors, be it thermal or fast reactors. In the case of fast reactors, alternate liquid coolants like Pb and Pb-Bi are also being evaluated.

Innovative technological solutions are being developed to address the concern regarding non-proliferation and nuclear waste. The long-term goal is to develop advanced back-end technologies to avoid accumulation of spent fuel and make a judicious choice of appropriate fuel cycle options to ensure sustainability. The PUREX process is being replaced by another process called the COEX, developed by France. The spent nuclear fuel from any reactor consists of unburnt U and Pu, fission products, and long-lived radioactive actinides. The first step in the new technology of reprocessing is to partition the reusable U+Pu from the nuclear waste containing fission products and minor actinides. Following the partitioning, U and Pu is co-converted into their oxides, which can be integrated as fuel precursor into the fuel refabrication. Since Pu is not extracted separately, the non-proliferation issue is taken care of using the above emerging reprocessing technology routes. It is hoped that the present R&D efforts will lead to commercialization of the above technologies by the middle of this century.

The technology for waste management has to address the issue of minimizing the time for the nuclear waste to reduce to the level of natural uranium ore. Generally, typical spent nuclear fuel from light water thermal reactors contains 95% uranium, 1% Pu, (unburnt), 4% fission products, and 0.1% minor actinides. Figure 13.3 shows roughly the time taken by each of the above constituents of spent nuclear fuel to reduce its toxicity to that of natural uranium level. The open fuel cycle, which buries the entire spent nuclear fuel, takes geological time scales for the toxicity to reduce to that of natural uranium ore. If the technology can be developed that would finally leave only fission products as nuclear waste, the time taken to reduce the toxicity will be reduced to acceptable level of around hundreds of years. Extensive research has been carried out to develop the new technology of *partitioning and transmutation* to ensure minimization of nuclear waste. In this technology, the mixture of minor actinides and fission products, extracted in the partitioning stage of COEX reprocessing technology, is used as the initial waste matrix. The next step is to examine whether transmutation of these constituents into non-radioactive substance can be achieved. It is known that transmutation of fission products like I, Cs, and Tc is neither feasible nor realistic. The feasibility of transmutation of minor actinides like americium and neptunium in thermal reactors is demonstrated to be impossible. However, the sodium-cooled fast reactors could be successfully employed for the transmutation of the minor actinides. This process reduces the time for radio toxicity of the waste to reach the level of natural uranium ore, from 10,000 years for MA + FP to only 500 years for fission products. These technologies, which are in the R&D stage, would require another two to three decades to become commercial.

In the longer time horizon are the ambitious goals such as accelerator driven systems (ADS) and the fusion technology. The fusion technology has been discussed

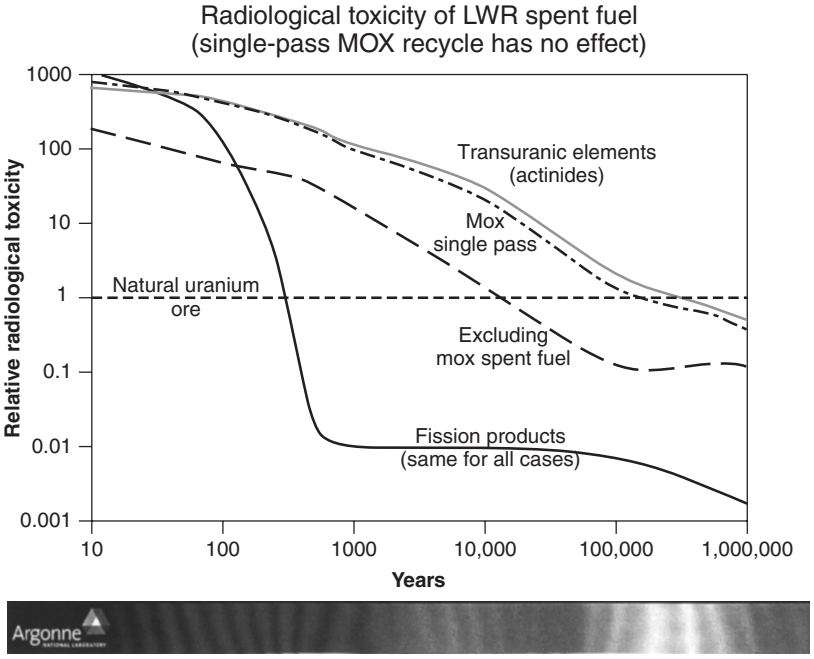

Figure 13.3 Time taken [3] by constituents of spent nuclear fuel to reach the natural radioactivity level.

briefly. ADS is a technology in which the high energy (1 GeV) proton beam from an accelerator strikes heavy elements like liquid lead, resulting in copious yield of *spallation neutrons*, which drive the fission reactions in a subcritical nuclear reactor, be it thermal or fast. This is used for in-situ incineration of nuclear waste, containing the fission products and minor actinides into non-radioactive elements.

Successful commercialization of the above technologies needs a strong R&D backup in all related fields, including materials technology. The safe and reliable performance of fission and fusion systems depends on the choice of appropriate materials and an evaluation of the degradation mechanisms during service. In the past, there have been extensive cross-cutting programs in materials technology that have enabled pooling up of developments in related fields. Examples are the ferritic/martensitic steels for the fast reactors from the fossil-based power program and the composite materials in high-temperature reactors from atmospheric re-entry of nuclear warheads. The development of nuclear materials is evolutionary in character so far. However, future reactors need innovative materials and technologies, which are discussed below.

13.2 DEVELOPMENT OF REACTOR MATERIALS

The nuclear-grade materials can be divided into two categories: the inert cladding and structural materials and the fissile/fertile fuel materials. The present article will provide an overview of the inert nuclear structural materials, confining the discussion to the first category. In any of the technologies discussed so far, the nuclear structural materials play an important role, since they constitute roughly 15% of the cost of the technology.

The challenge toward development of nuclear structural materials arises from the following factors in a nuclear industry: the demanding, hostile environments with respect to the radiation, temperature, and stress, high performance levels, and total guarantee or reliability over the long term. The materials properties that govern the selection criteria depend on the service conditions to which the material would be exposed. The operating conditions depend on the type of reactor and the component. Table 13.3 illustrates the differences in the exposure conditions of a material and consequent crucial material properties that govern the selection criteria.

In view of the diverse environments to which the nuclear materials are exposed, the development of nuclear materials is discussed in the same sequence as the previous session: design principles of present generation materials, challenges in the future generation materials, and development of materials for the back-end technologies.

13.2.1 Design Principles of Present Generation Reactor Materials

13.2.1.1 Thermal Reactors Neutron economy is the most important selection criteria in the case of materials for thermal reactor. Accordingly, zirconium, with an extremely

TABLE 13.3 Selection Criteria of Materials for Components in Thermal and Fast Reactors

Type of Reactor	Component	Selection Criteria
Thermal	Clad	• Low neutron absorption coefficient • Minimum interaction with the fuel pellet • Compatible with the moderator/coolant: stress corrosion cracking • Ability to withstand cladding stress due to fission gas release and thermal expansion • Resistance to irradiation creep
	Structural	• Low neutron absorption coefficient • Minimum irradiation induced damage • Minimum environment-induced changes such as chemical interaction with coolant and fission products, hydrogen damage, enhanced corrosion under stress, irradiation, and environment
	Pressure tubes	• Minimum hydrogen damage like hydrogen embrittlement, blistering, and hydride cracking
Fast	Clad	• Minimum dimensional changes due to void swelling and irradiation creep • Reduced irradiation growth, hardening, and embrittlement • Good compatibility with liquid sodium and fuel • Stability of structure and mechanical properties
	Wrapper	• Acceptable radiation damage and high temperature properties • Good compatibility with sodium • Good weldability and fabricability
	Structural	• Good compatibility with liquid sodium • Excellent structural stability and high temperature mechanical properties • Availability of design data • Good weldability and fabricability • Affordable cost

low absorption cross section, has been selected as the workhorse of thermal reactors. A large number of zirconium alloys have been continuously developed as the core structural material. Persevering efforts to increase the residence time of zirconium-based components inside the reactor have resulted in the development of a series of zirconium alloys: Zircaloy-2 (Zr-Sn-Fe-Cr-Ni), Zircaloy-4, Zr-Nb alloys, and their variants. The detailed performance characteristics of the various materials developed for the thermal reactors are reviewed in many books [8, 9]. Advanced alloys of Zr-Nb, such as Zirlo, M5, E110, and DX-D4 have been developed, which have enabled achieving a burnup (energy production per unit quantity of fuel) of ~60 GWd/tU. Attempts are in progress to enhance the burnup to about ~80 GWd/tU in the next decade, with improved fuel and structural materials.

The properties of concern for zirconium alloys have been hydrogen adsorption from the moderator in thermal reactors and consequent deterioration, oxidation, irradiation growth, and embrittlement. A complex interplay of chemistry, microstructure, out-of-core behavior, and in-reactor performance necessitates detailed evaluation and validation of many zirconium-based alloys before commercial acceptance in the nuclear industry.

One of the attempts to reduce cost has been to enhance the lifetime of the present generation reactors. Materials technologists have developed reliable methodologies for estimating the health of materials and ensuring safe extension of their remaining life. Of late, new deterioration mechanisms under prolonged exposure of materials in thermal reactors have been recognized, like void swelling [10] at doses <1 dpa and at temperatures $\sim 300^{\circ}$C. For structural materials made of austenitic stainless steel, low temperature sensitization (catastrophic, intergranular failure in a corrosive medium at $\sim 700^{\circ}$C) is another problem encountered [11]. Presently, R&D efforts are in progress to find a commercial solution that would facilitate safe, life extension of the reactors, up to even about 100 years.

13.2.1.2 Fast Reactors In the case of fast reactors, the materials are exposed (Table 13.3) to more severe environments than thermal reactors. The major selection criterion for the fast reactor core component materials is the dimensional instability due to two mechanisms called the *void swelling* and *irradiation creep*. Void swelling refers to dimensional increase (Figure 13.4a) of the components due to condensation of vacancies into voids (Figure 13.4b). Vacancies are produced when irradiation in a reactor knocks off atoms from their equilibrium positions, ultimately leading to unacceptable dimensional changes of the components. The extent of void swelling is measured in terms of change in volume. ∇ V/V varies with dose as shown in Figure 13.4c. for 316 austenitic stainless steel, D9 (Ti modified austenitic stainless steel with 15% Cr-15% Ni), and ferritic steels. The major challenge for the materials scientists is to develop materials with as high a threshold 'hreshold dose (*i.e.*, the dose at which ∇ V/V increases rapidly with dose) as possible. Irradiation creep refers to the permanent deformation of the material, leading eventually

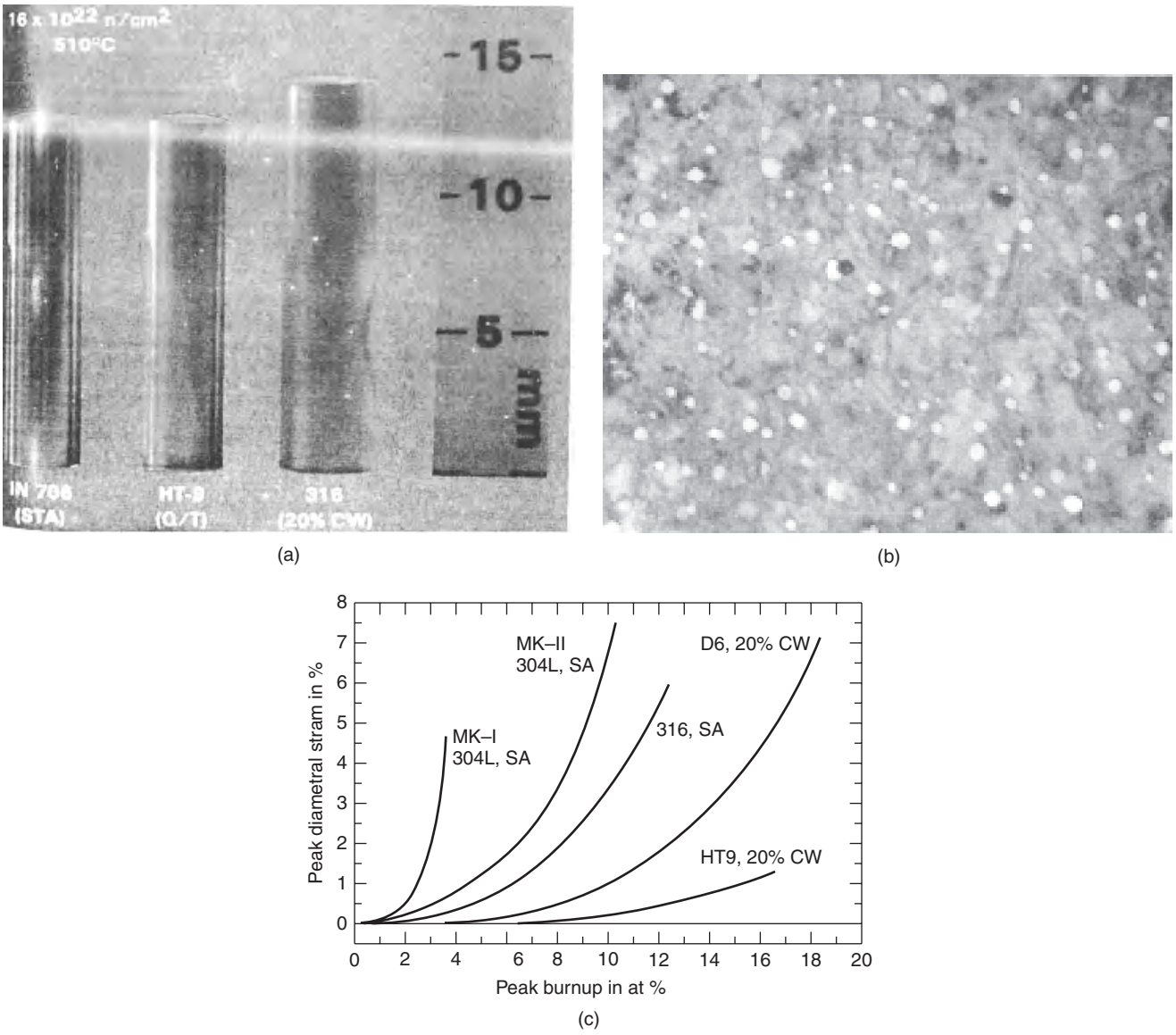

Figure 13.4 Evidence and cause for void swelling in core component materials of fast reactors: (a) Increase in dimensions in three different materials, a nickel based alloy, 12% chromium ferritic steel, and 316 austenitic stainless steel irradiated to a dose of 16×10^{22} n/cm^2 at 510°C; (b) transmission electron micrograph of voids in stainless steel, the first discovered [12] in 1967; and (c) comparison of variation of void swelling of 316 SS with D9 and nearly nil swelling of ferritic steels [13].

to fracture, under combined effects of high temperature, stress, and irradiation.

Since high temperature is one of the concerns, nickel-based super alloys and austenitic stainless steels were the candidate materials in the 1960s. Soon, the realization of embrittlement due to helium produced during irradiation of nickel was realized. Prior to 1974, cold worked austenitic stainless steels received the major thrust. Austenitic stainless steels anchor around various combinations of iron, nickel, chromium, molybdenum, and carbon, with the fcc austenite phase being stable at room temperature. This is known to possess excellent high-temperature mechanical properties, in the absence of irradiation. The acceptable resistance to void swelling by this family of steels is understood in terms of high binding energy (0.26 eV) of nickel with vacancies. The deleterious influence of chromium in void swelling can also be understood in terms of low binding energy between chromium atoms and vacancies, 0.06 eV. Chromium in amounts more than 12% is added to ensure corrosion resistance to the steels and referred to as stainless steel. The dislocations introduced in these steels during 20% cold work enabled annihilation of defects that were produced during irradiation, thereby improving the radiation resistance of the 316 stainless steel.

Until about 1986, variants of austenitic stainless steel were attempted, one of which is D9, whose performance in Superphenix was satisfactory. The high-temperature creep properties [14] of the modified D9 austenitic steels were found to be superior (Figure 13.4c) to the conventional 316 austenitic stainless steel. The threshold dose, at which dimensional instability occurred, was nearly double that of 316 stainless steel. Further improvements were achieved by modifying minor alloying elements. These alloying elements altered two factors: behavior of the fcc matrix in which they had dissolved and the interface of the newly formed precipitates that annihilated the radiation induced defects. Oversized elements with high binding energy with vacancies impart beneficial effects in reducing swelling. Ti, P, Si, and B are beneficial. The binding energy of titanium, phosphorus, silicon, and boron with vacancies is very high, $\sim$0.3 eV. The diffusion or the mobility of P-Vacancy complexes is also very high, thus reducing swelling. At high temperatures, precipitation of phosphides occurs. The interface between the phosphides and the matrix enhances the annihilation rate of point defects and reduces swelling. Boron reduces the mobility of carbon and nitrogen by combining with them and reduces rate of formation of carbides and carbo-nitrides. This enables the fcc matrix to retain beneficial elements like Ni, Mo, Si, and Nb and suppress the deleterious mechanism called the solid solution decay.

Another factor is the preferential bias of undersized and oversized precipitates offer to defects in the austenite matrix. The design principle in the development of austenitic steels is to identify the benefit of trapping vacancies with oversized precipitates like TiC and interstitials with undersized precipitates like Fe_3P by adjusting the concentration of minor elements. Figure 13.5 summarizes the void swelling suppression mechanisms in austenitic stainless steels, using either dislocations or precipitates.

The major design principles learned during the studies in austenitic stainless steels are the following:

- Introduce optimum density of dislocations in the fcc matrix (Figure 13.5a).
- Add oversized elements with high binding energy with vacancies.
- Maximize the mobility of the complexes between the element and the defects.
- Introduce fine coherent second-phase particles, with an optimum combination of oversized and undersized particles (Figure 13.5b and c).
- The interface of oversized particles with fcc lattice attracts vacancies, while the undersized particles attract interstitials, maximizing the benefit.

In a parallel manner, the fossil industry was developing high-temperature materials for increased thermal efficiency at high temperature and high pressure. HT 9, a ferritic steel, based on 12% chromium and marketed by Sandvik, was found [15] to have nearly zero void swelling, even up to double the burnup corresponding to austenitic stainless steel. Following this clue, a large number of ferritic alloys have been evaluated [16] for the nuclear core.

Extensive basic studies on ferritic steels identified the following reasons as the origin of superior swelling resistance in ferritic steels:

1. The relaxation volume for interstitials, *i.e.*, the volume of the matrix in which distortion is introduced by creating an interstitial, in bcc ferrite is larger than fcc austenite. For every interstitial introduced, the lattice distortion is high, hence the strain energy of the lattice. Hence, the bias toward attracting or accommodating interstitials in the bcc lattice is less. This leaves higher density of "free" interstitials in the bcc lattice than fcc lattice. As a result, recombination probability with vacancies increases significantly, and super saturation of vacancy reduces. Consequently, the void nucleation and swelling is less.
2. The migration energy of vacancies in bcc iron is only 0.55 eV, against a high value in fcc austenite, 1.4 eV. Vacancies are more mobile in bcc than fcc, increasing the recombination probabilities in bcc ferrite. Another factor is the high binding energy between carbon and vacancy in bcc iron (0.85 eV), while it is only 0.36 to 0.41 eV in austenite. This leads to enhanced point

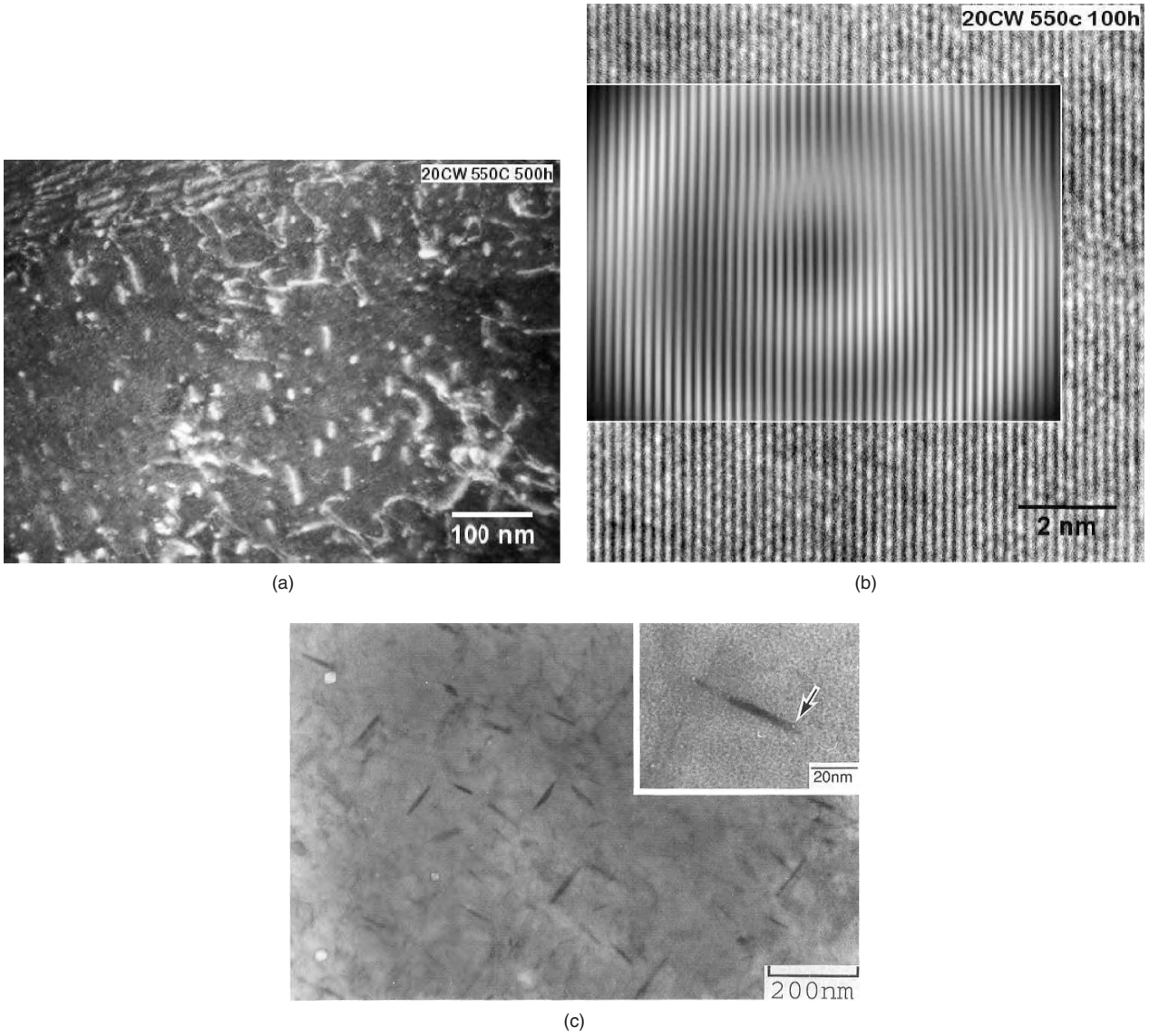

Figure 13.5 Electron micrographs illustrating the void swelling suppression mechanisms: (a) Deformation by increasing the density of dislocations, (b) fine, coherent TiC precipitates, and (c) needle-shaped semi-coherent Fe_3P particles by increasing the recombination probability of vacancies with interstitials produced during irradiation.

defect recombination in bcc than fcc, due to more trapping of vacancies by carbon or nitrogen.

3. In bcc iron, it is known that there is a strong interaction between dislocations and interstitials solutes, forming atmospheres of solutes around dislocations. This reduces the dislocation bias for interstitial capture and also inhibits dislocation climb. Hence, dislocations remain as unsaturable sinks for excess interstitials.

These fundamental differences in the behavior of solutes and point defects in bcc lattice make ferritic steel far superior to austenitic steels with respect to radiation damage.

While attempts were diverted to develop ferritic steels as core component materials, additional limitations (Figure 13.6) of the ferritic steels were recognized [16]: irradiation embrittlement more severe in ferritics than austenitics, the inherently inferior high temperature mechanical properties, and the joining technology of these steels, more difficult due to Type IV cracking in their welds subjected to creep loading, in the context of developing steam generator materials. The minimization of embrittlement and the overcoming of Type IV problems could be

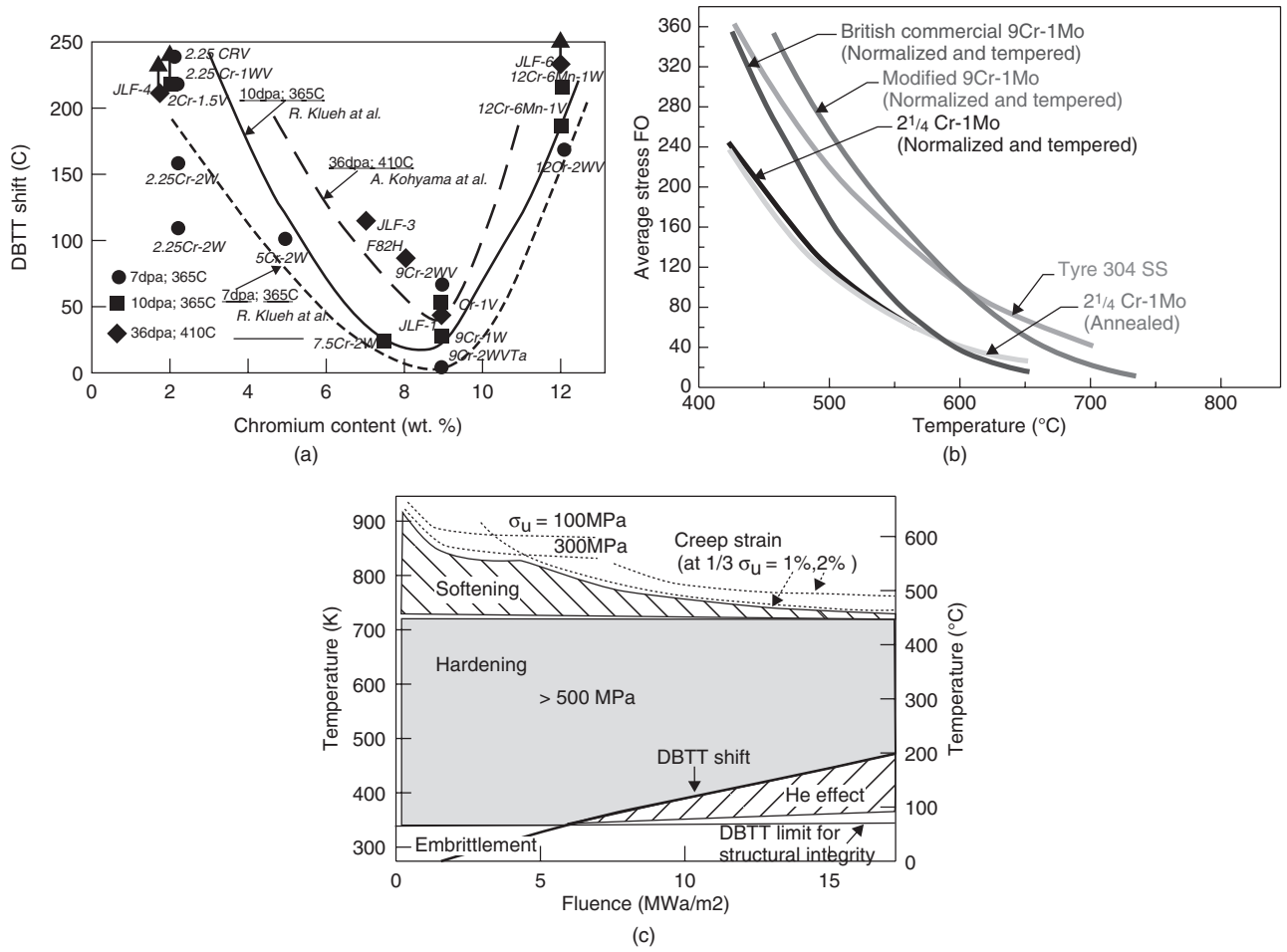

Figure 13.6 Challenges in ferritic steels: (a) embrittlement, being least in steels with 9%Cr [17]; (b) degradation of creep properties at high temperature [18] and (c) degradation mechanisms [19] in the reactor.

carried out by optimizing the chemistry of the steel, especially the chromium content, leading to many commercial steels, mainly revolving around 9% to 12% chromium, where the embrittlement is the least. The major problem was that the inferior high temperature mechanical properties of the ferritic steels limit the operating temperature to around 775°K.

The immediate target of fast reactor technology is to increase the burnup further, with 100 years as lifetime and an operating temperature of about 973°K. These improved targets of the nuclear industry impose the necessity to overcome the limitations of ferritic steels.

13.2.2 Challenges in Future Generation Materials

In recent years, a concerted effort [20] to develop advanced materials for the future reactors is being attempted. Intense R&D to increase the high-temperature creep behavior of ferritics has led to strengthening the steel using 5 nm particles of yttria, leading to the oxide dispersion strengthened (ODS) ferritic steels. Figure 13.7a. shows the electron micrograph of such nano-sized particles in a ferritic steel. These steels have been proven (Figure 13.7b) to be strong at temperatures as high as 873°K. This would enable us to achieve both void swelling resistance up to a burn up of ~200 dpa and reach temperature of around 600°C. The ceramic reinforcements in ODS steels make them perform at temperatures even up to 800°C. The production technology, which is based on powder metallurgy routes, has been demonstrated at the industrial scale. The in-service performance and the suitability in the back-end technologies have yet to be demonstrated before commercial exploitation.

The above concept of oxide dispersion has been extended to austenitic steels and nickel-based alloys to improve radiation resistance and high temperature capability.

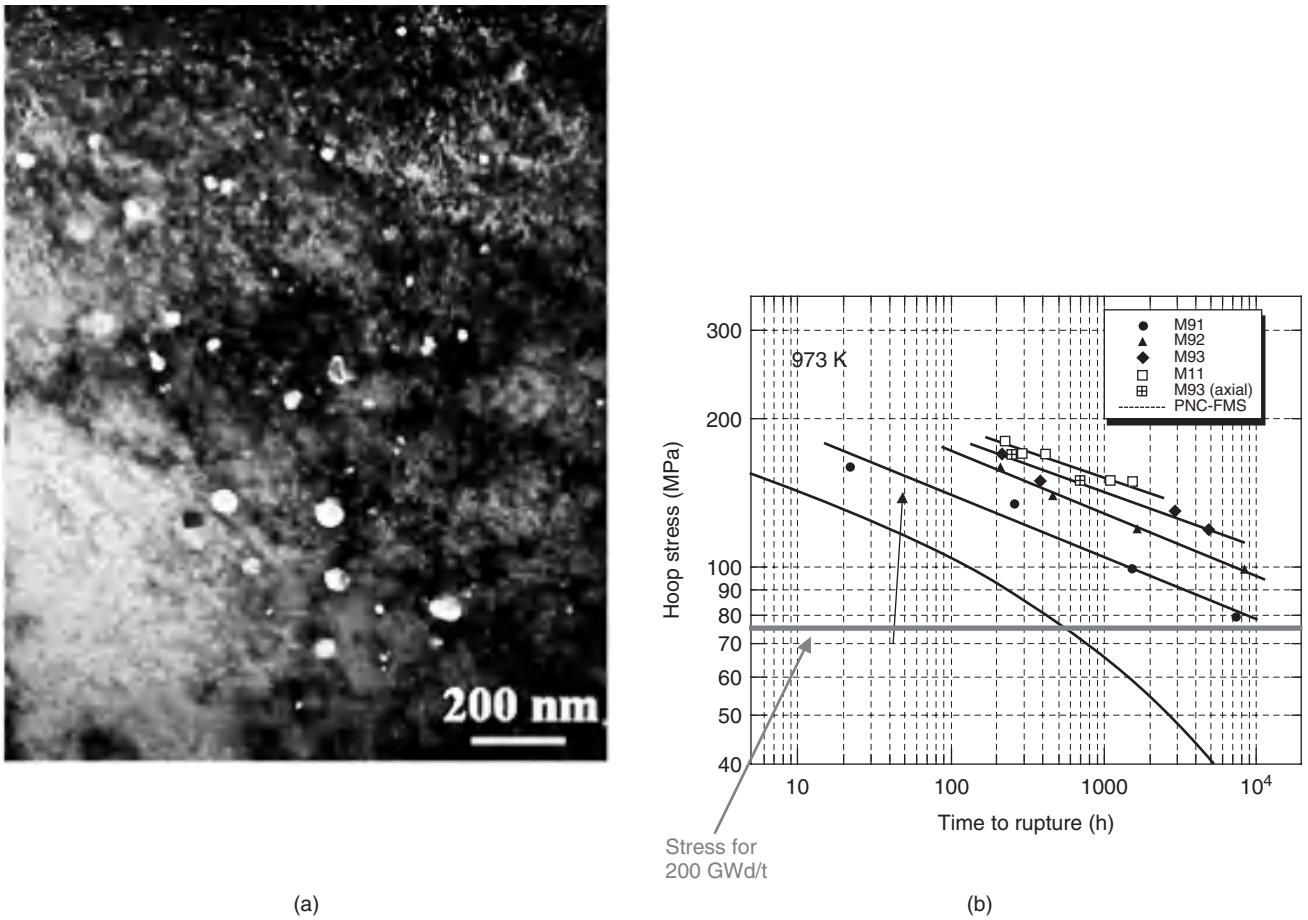

Figure 13.7 (a) Dark field electron micrograph [21] showing Z-contrast of nm-sized oxide dispersions in newly emerging oxide dispersion strengthened ferritic steels, capable of withstanding 700°C up to a burnup of 200 dpa and (b) improved creep properties [22] of ODS in comparison with ferritic steel.

The advanced, high-temperature, multiuse reactors envisage temperatures higher than 1173°K. None of the conventional nuclear materials developed so far can withstand such high temperatures. Hence, a range of new high temperature materials are being explored: refractory alloys based on Nb, Ta, Mo, and W, ceramics, composites, and coatings. The heat-resistant fuel cladding materials that are being developed belong to the family of composites based on either fibers of carbon or ceramics like SiC. These materials are based on completely novel composite honeycomb structure. Experience in the development of similar materials already is available in the space technology as these are used in jet nozzles in fighter aircrafts. Their suitability to the advanced nuclear technologies has to be evaluated.

Once the high-temperature reactors are conceived, it is necessary to augment the conditions of pressure and temperature of steam generators in the conventional side of the reactor. Here again, the experience [23] in the development of materials to withstand the ultra supercritical (USC) steam in thermal power industry is useful. In addition to increasing the thermal efficiency, the release of deleterious gases also is reduced in these domains of pressure and temperatures. The required properties are the resistance to stress corrosion cracking and erosion-corrosion. However, the experience gained in the development of ferritic steels is very useful, since most of these USC materials belong to high-chromium steels. Alternately, nickel-based alloys are also being considered for these applications.

The attempt to improve fuels and coolants requires re-examination of the proven nuclear structural materials. With respect to metallic fuels, the ferritic steels meet the requirement of clad and structural materials. In the context of thorium fuel cycle also, no major problem is anticipated from the materials point of view. However, in both cases, there are concerns in the back-end technologies, which will be discussed in the next section. However, alternate

coolants, which increase the thermal efficiency, can be incorporated only after confirming the compatibility of the candidate materials with the newly selected coolants. Extensive R&D is in progress toward achieving this goal.

13.3 MATERIALS FOR THE BACK-END TECHNOLOGIES

The major selection criteria for the materials for the back-end technologies (Table 13.4), like reprocessing and waste management, are entirely different from that of the reactors, which we discussed in section 13.2.

The structural materials for the dissolver and evaporator of reprocessing of fast reactor fuels have so far been NAG austenitic stainless steel, which has been replaced by Grade 2 Ti, which is superior to stainless steels for applications in highly corrosive boiling nitric acid. An alternative material Ti-5Ta-1.8Nb [24], whose corrosion resistance is five times higher than Ti or Ti-5Ta, has been developed. These alloys have recently been replaced by zirconium alloys for the dissolver tank. Thus, the materials for reprocessing plants also evolve continuously to increase the lifetime of the plants, reducing the fuel cycle cost.

Even for the matured technologies in practice now, the requirements will vary once the fuel, the clad, or the wrapper in the reactor are changed. The proposed change of fast reactor fuel to metallic fuel introduces complications in the reprocessing routes and the compatible materials. Similar situations arise if the thorium fuel cycle is adopted.

Metallic fuels are best reprocessed using pyro-chemical processes with the high-temperature electrochemical route. These processes use highly corrosive molten halide salts. Hence, there is a need for the development of a new range of corrosion-resistant coatings, graphite crucibles coated with ceramic oxides like zirconia or alumina, and refractory container materials. These technologies have reached maturity at the industrial level and require steps for harnessing their potential at the commercial scale. Reprocessing of thorium-based fuels involves the use of fluoride at relatively high concentrations. Extensive R&D efforts are essential to develop advanced materials resistant to corrosion in fluoride media.

Metallic fuels also envisage intense R&D in the newer materials required for disposal of waste generated by pyro-chemical reprocessing. A possible solution with respect to the hull waste (pieces of clad material left behind after fuel is processed) is alloying stainless steels with 15% zirconium and converting to suitable metal waste form. Similarly, suitable matrixes need to be developed for immobilization of other wastes such as salts used in pyro-chemical processes.

The long-term strategies, which are being developed to ensure proliferation-free technologies with minimum waste, are at a stage of benchmarking the process of separation, partitioning, and transmutation. These technologies do not envisage operating conditions that are vastly different from the present generation technologies. Hence, materials *per se* may not impose great restrictions in the commercialization of the newer back-end technologies. The hybrid accelerator-driven system toward the goal of no accumulation of nuclear waste also is presently in the R&D domain. The long-term materials problems are confined to selection of window material, i.e., the material that separates the accelerator from the sub-critical reactor. The selection criterion of the window is to have resistance toward irradiation, corrosion, and embrittlement and possess good thermo-physical properties. Presently, different variants of

TABLE 13.4 Selection Criteria of Materials for the Back-End Technologies

Back-End Technology	Conventionally Used Materials	Selection Criteria
Fuel reprocessing	Nitric acid grade 304L stainless steels, Ti and its alloys, zirconium alloys, boron-coated stainless steels	• Stability against radiation damage • Best corrosion resistance in boiling nitric acid • Necessity to remain sub-critical throughout the reprocessing
Waste management	Immobilization of the waste in borosilicate glass	• High ability to lock up the nuclear waste in a suitable matrix • Ability to accommodate variation in chemistry and physical forms of the waste • High waste loading efficiency
	Vitrification in melter pots: Ni-base alloys	• Ability to withstand high temperatures ~1000 s of °C • Radiation resistant for long durations
	High-level waste canisters and over packs: copper, iron, stainless steel, titanium alloys, and nickel-based alloys	• Excellent resistance to radiation, high temperature, and gradients and chemical compatibility • Long failure-free lifetime during casting, interim storage, and permanent disposal

modified ferritic/martensitic steel or austenitic stainless steel are being explored. There is also an attempt to modify the technology to be without the window. Presently, the ADS technology is in its infancy. It is hoped that the problem of the nuclear waste management would be completely solved, if we can successfully incinerate the nuclear waste, with the success of the ADS technology.

13.4 MATERIALS FOR FUSION TECHNOLOGY

Fusion technology poses great challenges for the materials technologists. This is one system where the temperatures of the components range from millions of degrees Kelvin to liquid nitrogen temperature, with a similar situation for pressure, very low vacuum, to extremely high-pressure plasma. Steep gradients in pressure and temperature and high heat flux exist. The components are subjected to high neutron irradiation, helium and hydrogen flux, and strong mechanical, thermal, and electromagnetic loadings, both static and transient.

The research efforts toward fusion materials can be categorized as *plasma-facing materials* and *structural materials*. The materials for the first wall divertor or the breeding blankets constitute the former. The exposure conditions and the selection criteria are given in Table 13.5. The structural materials should have the least activation from waste management point of view. These demands have led to the development of ceramics, fiber-reinforced composites, refractory alloys, and reduced activation steels.

High thermal conductivity and excellent creep at elevated temperatures, required for components like divertors, have led to the development of tungsten-based refractory alloys, CuCrZr alloys, fiber-reinforced metal matrix composites, carbon-reinforced carbon, Be- and W-based materials. Coating technologies, basically hydrogen permeation barrier coatings, to overcome hydrogen embrittlement also have been developed for the plasma-facing and the heat sink materials.

The development of ferritic steels for the fast reactor core has helped transfer the technology to develop the reduced activation steels by replacing molybdenum and niobium with tungsten. Commercial availability of these steels has already been achieved.

Despite all the above developments in materials technology proceeding in tune with the fusion technology, there is a challenge in the case of proven performance of fusion materials. It is well established that the materials' behavior is sensitive to the environmental conditions. For example, in the case of fission reactors, extrapolation of performance of materials from one reactor to another itself is shown to be inaccurate. In such a situation, prediction of materials' behavior in a fusion reactor environment, based on accumulated experience of materials behavior in accelerators, fast reactors, and modeling could at best be only a short-term solution. It is likely that materials may display entirely new behavior in the real-life fusion reactor, which can be dealt with only after such experiments are carried out. Hence, international efforts to simulate fusion environments are also being planned to launch meaningful materials programs for the fusion technology.

TABLE 13.5 The Exposure Conditions and the Selection Criteria for the Plasma-Facing Materials and Structural Materials in a Fusion Reactor[1]

Components	Exposure Conditions	Materials Issues	Candidate Materials
Plasma-facing components: a. First wall b. Divertor c. Breeding blanket	14 MeV neutrons, with high damage rate (20–30 dpa/year for 3–4 GW reactor); Ten times higher helium production (10–15 appm/dpa) than fission Four times more hydrogen (40–50appm/dpa) than fission High heat flux (0.1–20 MW/m2); High temperatures (775–3475 K)	Radiation damage High-temperature performance sputtering erosion, blistering, exfoliation, hydrogen trapping, and deterioration in properties Thermal shock resistance Thermal conductivity	First wall: Refractory alloys based on tungsten, or tungsten-coated ODS steel or flowing liquid metal like lithium, gallium, or tin Divertor: Tungsten-based alloys; tungsten coated SiC/SiC_f, or flowing liquid metals of lithium, gallium, or tin Breeding blanket: Tritium breeder: solid: Li_4SiO_4, Li_2TiO_3 liquid: Pb-Li Neutron multiplier: Be, $Be_{12}Ti$
Structural materials	High temperatures Radiation damage; mechanical and thermo-mechanical stress	Radiation embrittlement, deterioration in mechanical properties under stress and radiation (similar to fission reactors)	*By 2010:* Low activation ferritic- martensitic steels *By 2015:* ODS ferritic steels, vanadium alloys, SiC/SiC_f

13.5 ROLE OF MODELING IN DEVELOPMENT OF NUCLEAR MATERIALS

Most of the developments of the new engineering materials have so far been only empirical. The nuclear materials are no exception. They are exposed to extreme environments, wherein a large number of damage mechanisms operating simultaneously dictate the useful, safe, reliable life of the components. Presently, lifetimes are computed based on lab-based experimental data, constitutive laws, design rules, and finally the standards or codes. There are two extremes of time and length domains for the radiation damage. The time domains extend from 10^{-18} seconds to 100 years, while the length scales range from interatomic distance to meters. The empirical approaches and extrapolations are reaching their limits, and it becomes necessary to develop predictive tools to estimate materials' behavior for new materials and environments. A few examples, wherein modeling has enabled prediction of materials behavior, are presented in the following sections.

13.5.1 Radiation Damage

The damage to a material exposed to radiation in a nuclear reactor begins at the 10^{-18} th second, when energy is transferred from the energetic incident particle to the atom in the host lattice. A host of events take place following this, leading eventually to unacceptable changes in the material such that it can no longer be retained in the reactor. Extensive work has been carried out in developing basic understanding of the phenomena of radiation damage. Modeling has helped predict the rate of nucleation and growth of voids for different types of lattices. The predictions have also been validated by extensive controlled, in-reactor experiments.

The present challenges to materials scientists are as follows: Can the understanding of these events be built into the currently used codes to provide more accurate prediction of the life of the materials? How can scientists develop methodologies to extend this basic knowledge into domains hitherto unexplored, such as the case of fusion? Of late, a new methodology called *multi-scale modeling* is being developed [25] to examine if "seamless" joining of the concepts at various length and time scales can finally achieve an accurate prediction of lifetime of materials. The strategy that is being adopted is to combine the following powerful theoretical tools, which have been proven successful in their own length and time domains: the *ab initio* calculations, molecular dynamics, Monte Carlo method, the rate theory, dislocation dynamics, finite element methods, and the continuum models. Combining the computation procedures with appropriate experimental validation would produce robust materials research. However, at the moment, it can only be hoped that this combination would provide the much anticipated, acceptable alternative to the existing, empirical procedures for the development of advanced materials.

13.5.2 Embrittlement in Ferritics

One of the inherent problems in ferritic steels is the embrittlement, *i.e*., the loss of impact toughness when in service for a prolonged time or during irradiation. In view of the importance of this class of steels in industry, this problem has been thoroughly studied in the 20th century and the general understanding [26] is that the certain elements called *metalloids*, like phosphorus, antimony, tin, etc., which are present in the steel in ppm level, migrate to grain boundaries during prolonged exposure to medium temperatures and cause the embrittlement.

In a parallel manner, basic studies in the structure of grain boundaries revealed [27] that there are certain types of boundaries called the coincidence site lattice boundaries, which could resist or delay grain boundary phenomena, such as precipitation, segregation, crack nucleation, and growth. This concept was applied to a number of engineering materials to extend their service life. One of the successful applications [28] of this method is the time delay introduced in the intergranular cracking of stainless steels from 200 hrs to 2000 hrs after grain boundary engineering.

The application of such a grain boundary engineering method on ferritic steels, on the other hand, is tougher due to certain basic limitations of the steel. A number of modeling methods, like the Monte Carlo method, percolation model, and fractal analysis, have been carried out [29], in combination with a relatively new technique called *electron back-scattered diffraction*. Figure 13.8 a shows the EBSD micrograph of processed steel. The size of the grains had reduced by 50%. Correspondingly, the ductile to brittle transformation temperature (DBTT), an index of embrittlement, could be reduced only by about 20°C. The fractal analysis of the fractured surface confirmed that the advantage was gained due to larger number of crack deflections or a tortuous path for the crack along its propagation route, as reflected by the high fractal dimension and the fracture energy.

13.5.3 Mass Transfer across Dissimilar Ferritics

In many industrial components, it is impossible to fabricate the component with a single material. Very often, two materials of different chemistry are joined or welded together during fabrication of the component. When such joints are exposed at high temperatures of operation, atoms move, or diffuse, from one material to another, sometimes deteriorating the mechanical properties of the materials.

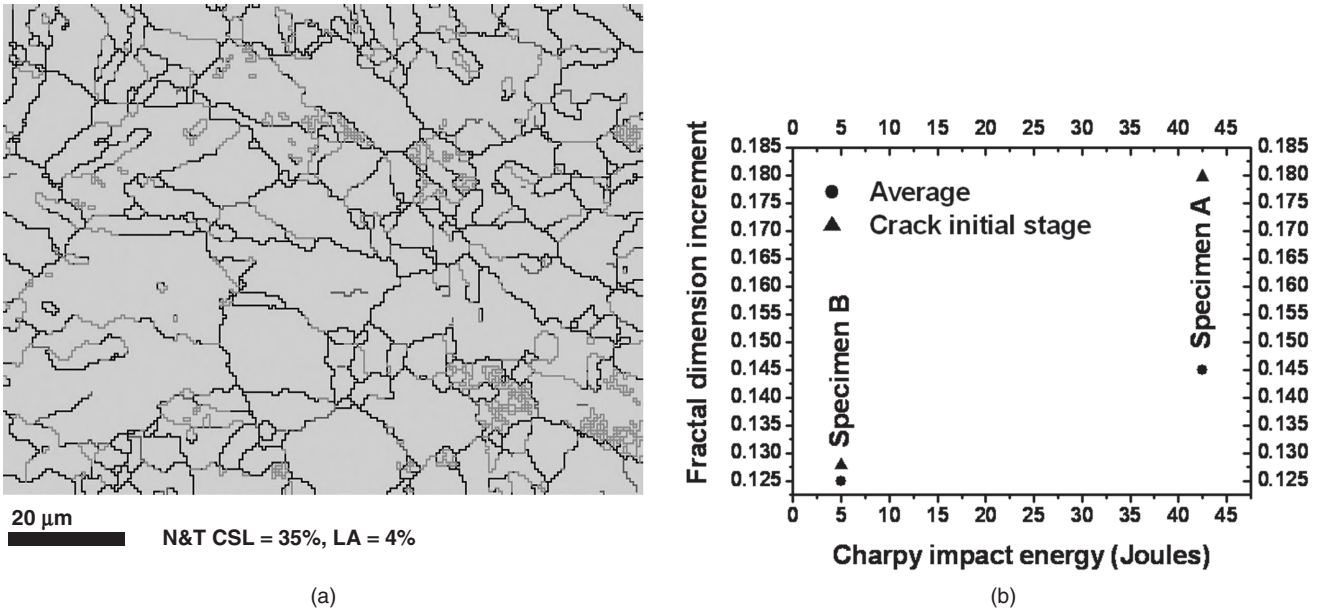

Figure 13.8 (a) EBSD micrograph enabling identification of amount of strong boundaries in steels and (b) fractal analysis [30] of crack propagation in steels.

Modeling methods have proven to be effective in the study of such processes. More importantly, these modeling methods could also be used to predict materials' behavior and prevent completely occurrence of deleterious processes, an example of which is given below.

A joining between two different types of steels with different concentrations of chromium, as shown in Figure 13.9a, is very often used. When such a joint is used at high temperatures, carbon diffuses and a hard, brittle zone forms at the interface, as shown. Material fails at these joints. The finite difference method, Thermo-Calc, and DICTRA and Molecular Dynamics have been used [31, 32] to study this engineering problem. Figure 13.9b. shows the variation of thickness of the deleterious hard zone if different types of barriers are introduced between the two steels. These predictions were validated experimentally using nickel barrier, as shown in Figure 13.9c. The basic understanding of the process was based on molecular dynamics calculations, which showed that the sluggish diffusion of carbon in nickel compared to iron is responsible for preventing the formation of the hard zone. Figure 13.9d shows the hopping sites of carbon in iron lattice obtained using molecular dynamics. Thus, computational simulations followed by experimental validation for few typical cases could reduce the time for probing solutions for an engineering problem.

13.5.4 Prediction of Microstructural Features

Very often, the joints in austenitic stainless steel welds used in fast reactors consist of a duplex structure, containing both fcc austenite and bcc delta-ferrite. The materials scientists have identified that 3 to 8% delta-ferrite is acceptable in the joints, balancing the advantage of hot cracking susceptibility and the disadvantage of conversion of delta-ferrite into brittle sigma phase during service. Under such circumstances, it becomes appropriate to develop models to predict the end-phases based on the composition of the weld and also the morphology of these phases. Figure 13.10 shows the successful application of artificial neural network method to provide [34] the much-needed information to materials scientists to enable them to choose the composition of the filler metal with which they join the two materials.

The successful story of the modeling in developing better materials consists of many more such examples, of which only few have been listed. It is prudent to envisage that modeling would emerge as a complementary tool to lab-scale experiments. The major difficulty in any of the existing modeling methods is the availability of the relevant database, be it interatomic potentials or the properly well-assessed thermodynamic database. These difficulties are compounded when one deals with multi-component systems with more than one phase, with many mechanisms operating simultaneously. In reality, almost all engineering materials fall in this category of multi-component, multi-phase systems, with more than one damage mechanism operating simultaneously, leading to reduction in service life of components. Hence, the replacement of today's empirical practices by knowledge-based design of nuclear or other engineering materials is the most difficult challenge to the materials scientists.

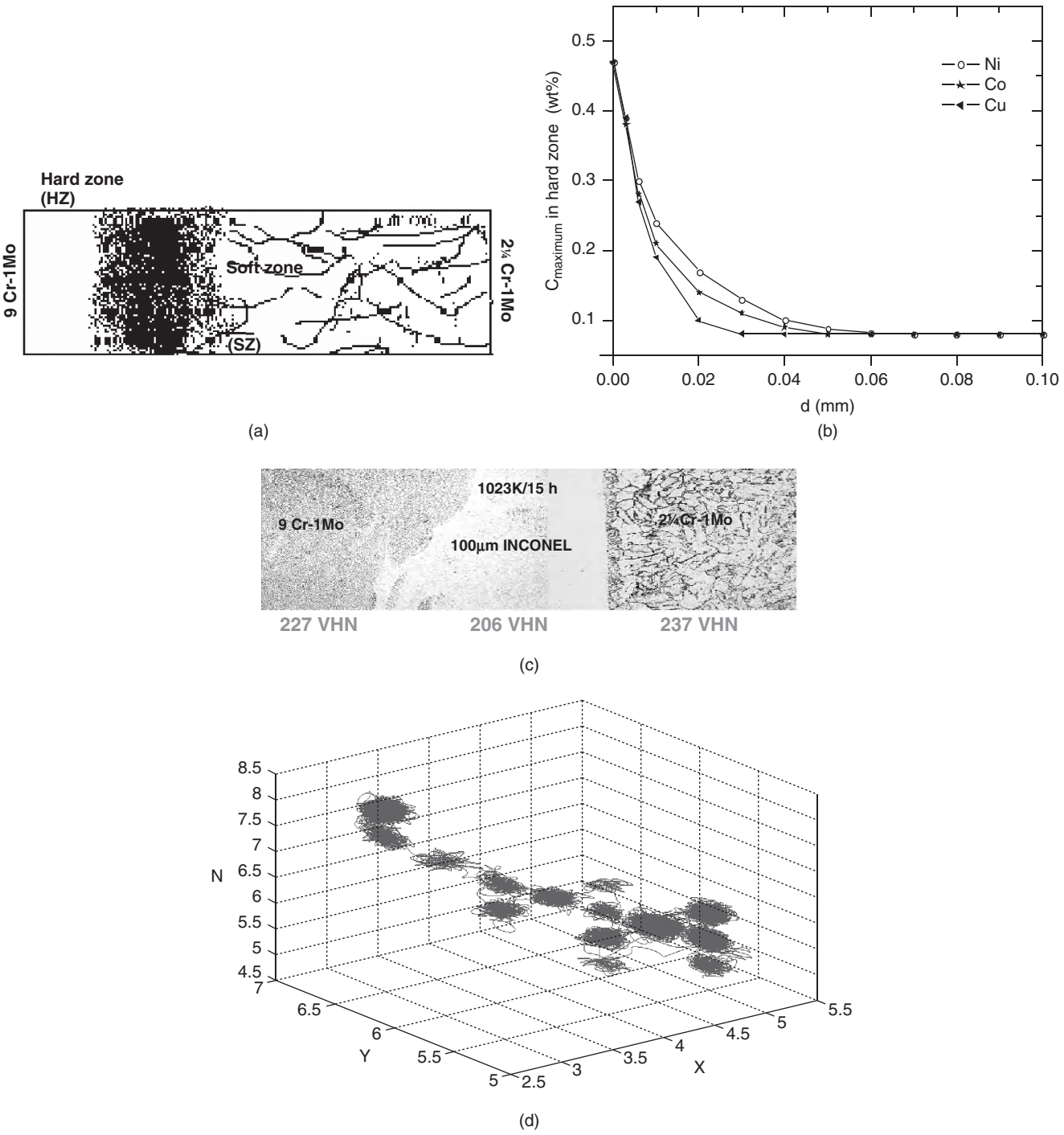

Figure 13.9 Modeling [31, 32] in the prediction and prevention of formation of a hard brittle zone between dissimilar materials during service exposure. (a) Schematic of the two dissimilar systems and the hard zone at the interface; (b) finite difference methods to calculate the thickness of the hard zone for different metals between the two dissimilar materials, for different thicknesses; (c) experimental validation of absence of hard zone for a thickness of few microns of nickel, and (d) molecular dynamics calculation [33] of diffusion of carbon in iron lattice, providing insight into the mechanism.

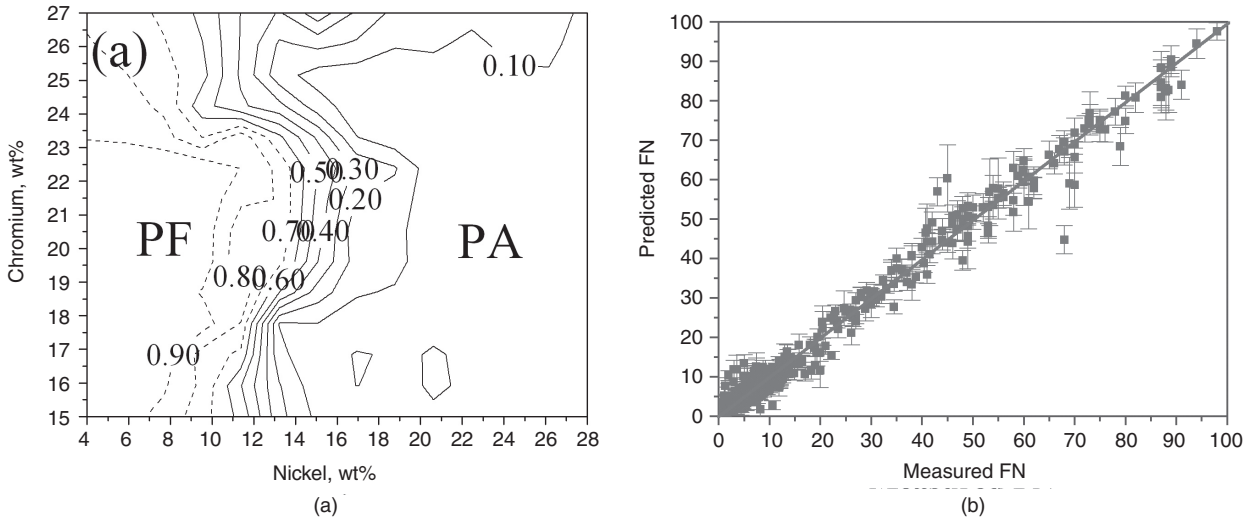

Figure 13.10 Artificial neural network to predict the morphology and microstructure of welds: (a) for different chemistry [35] and (b) good agreement [36] between the calculated and experimentally evaluated ferrite number, which measures the amount of the ferrite phase.

13.6 CONCLUSIONS

The 21st century is experiencing a renaissance in the nuclear industry's meeting the societal concerns of sustainability. The short-term measures to enhance the life of present generation reactors and improve the economy have been successfully implemented. The industry is forging ahead with evolutionary technologies to ensure sustainable, safe, proliferation-resistant nuclear power with minimum nuclear waste. The growth of the nuclear industry has always been supported by challenging modifications in materials technologies, right from the genesis. The spectrum of materials and their performances demanded by the nuclear environments have been continually on the increase, from zircaloy to Zr-Nb alloys, from aluminum alloys to austenitic stainless steels, to ferritic steels to ODS steels for reactors. The back-end technologies have also evolved to use specific nitric acid grade austenitic stainless steels, which have been subsequently replaced with successively superior corrosion-resistant materials such as titanium- and zirconium-based alloys. The underlying foundation for the above successes has been the understanding of scientific principles, including thermodynamics, phase transformations, structure-property correlations, and appreciation of the vital role of modeling and simulation.

However, today, the materials technologists are in a position to explore materials unstudied so far and in exposure conditions not experienced so far. The possible operative mechanisms need to be visualized, experimented, and confirmed. Extrapolation methodologies need to be established. Amid these challenges are demands to develop materials in shorter time domains for situations that cannot be simulated, such as fusion. The key direction is to replace past empiricism, appropriately, with accurate knowledge-based design. The challenges ahead of materials designers are many. Their successful response to these challenges would pave way for our society to enjoy sustainable, pollution-free energy in future.

REFERENCES

1. Baldev Raj, M. Vijayalakshmi, P.R. Vasudeva Rao, and K.B.S. Rao, Challenges in materials research for sustainable nuclear energy. *MRS Bulletin*, 2008, **33**, 327–337.
2. http://www.iaea.org/programmes/a2/index.html.
3. Y.I. Chang, *Integral Fast Reactor and Associated Fuel Cycle System, Part 4*, Lecture notes delivered during Joint ICTP/IAEA School on Physics and Technology of Fast Reactors Systems, The Abdus Salam International Centre for Theoretical Physics, November 9–20, 2009.
4. http://ec.europa.eu/research/energy/fu/fu_rt/fu_rt_pp/images/plasmadt_1541.jpg.
5. http://www.world-nuclear.org/info/inf98.html.
6. http://www.iaea.org/INPRO/.
7. http://www.gen4.org/.
8. Derek O. Northwood, The development and applications of zirconium alloys, *Materials and Design*, 1985, **6**, 2, 58–70.
9. George P. Sabol and Gerry D. Moan, *Zirconium in the Nuclear Industry*, ASTM, STP 1354, 2002. Twelfth ASTM International Symposium held in Toronto, June 15–18, 1998.
10. F.A. Garner F.A. and M.B. Toloczko, Irradiation creep and void swelling in austenitic stainless steel at low displacement rate in light water energy systems. *Journal of Nuclear Materials*, 1997, **251**, 252–261.

11. K. Kiuchi, M. Kikuchi, and T. Kondo, A new type of low temperature sensitization of austenitic stainless steels enhanced with defect-solute interactions. *Journal of Nuclear Materials*, 1991, 179–181, 481–484.
12. C. Cawthorn and E.J. Fulton, Voids in irradiated stainless steel. *Nature*, 1967, **216**, 575–576.
13. J.L. Seral, V. Levy, D. Gilbon, A. Maillard, A. Fissolo, H. Touron, R. Cauvin, A. Chalony, and E. Le Boulbin, Behaviour under neutron irradiation of the 15-15Ti and EM10 steels used as standard materials of the Phenix fuel subassembly, in *Effects of Radiation Materials: 15th International Symposium* ASTM STP 1125, R.E. Stroller, A.S. Kumar, and D.S. Gelles, eds. American Society for Testing and Materials, Philadelphia, PA, 1992, 1209–1233.
14. S. Latha, M.D. Mathew, P. Parameswaran, K.B.S. Rao, and S.L. Mannan, Thermal creep properties of alloy D9 stainless steel and 316 stainless steel fuel clad tubes, *International Journal of Pressure Vessels and Piping*, **85**, 12, 2008, 866–870.
15. E.A. Little and D.A. Stow, Void swelling in irons and ferritic steels: II. An experimental survey of materials irradiated in a fast reactor. *Journal of Nuclear Materials*, 1979, **87**, 1, 25–39.
16. R.L. Klueh and D.R. Harries, *High Chromium Ferritic and Martensitic Steels for Nuclear Applications*. ASTM publication, 2001.
17. A. Kohyama, A. Hishinuma, D.S. Gelles, R.L. Klueh, W. Dietz, and K. Ehrlich, Low activation ferritic and martensitic steels for fusion application. *Journal of Nuclear Materials*, 1996, **233–237**, 138–147.
18. V.K. Sikka, Development of modified 9Cr-1Mo steel for elevated temperature service, in *Proceedings of the ASTM Tropical Conference on Ferritic Alloys for Use in Nuclear energy Technologies*, J.W. Davis and S. Michel, TMS-AIME, 1984, 317–327.
19. A. Hishinuma, A. Kohyam, R.L. Klueh, D.S. Gelles, W. Dietz, and K. Ehrlich, Current status and future R&D for reduced activation ferritic/martensitic steels. *Journal of Nuclear Materials*, 1998, 258–263, 193–204.
20. K.L. Murty and I. Charit, Structural materials for GenIV nuclear reactors: challenges and opportunities. *Journal of Nuclear Materials*, 2008, **383**, 1–2, 189–195.
21. S.Saroja, A.Dasgupta, R.Divakar, S.Raju, E.Mohandas, M.Vijayalakshmi, K.Bhanusankara Rao and Baldev Raj, *J. Nucl. Mat.*, 2011, **409**, 131–139.
22. S. Ukai, S. Mizuta, M. Fujiwara, T. Okuda, and T. Kobayashi, Development of 9Cr- ODS martensitic steel claddings for fuel pins by means of ferrite to austenite phase transformation. *Journal of Nuclear Science and Technology*, 2002, **39**, 7, 778–788.
23. M. Fukuda, The next generation of USC technology in Japan, in *Challenges of Power Engineering and Environment*, Kefa Chen, Yong Chi and Fei Wang, ed., Springer Berlin Heidelberg, 2007, 20–25.
24. S. Saroja, M. Vijayalakshmi, and Baldev Raj, Physical metallurgy of Ti-Ta-Nb alloy, *Transactions of Indian Institute of Metals*, 2008, **61**, 389–398.
25. M. Samaras, M. Victoria, and W. Hoffelner, Nuclear energy prediction: application of the multi-scale modeling paradigm. *Nuclear Engineering and Technology*, 2009, **41**, 1, 1–10.
26. B. Raj, S. Saroja, K. Laha, T. Karthikeyan, M. Vijayalakshmi, and K.B.S. Rao, Methods to overcome embrittlement in ferritic steels. *Journal of Materials Science*, 2009, **44**, 9, 2239–2246.
27. T. Watanabe, S. Tsurekaw, Z. Xiang, and Z. Liang, The coming of grain boundary engineering in the 21st century (p. 43–79), in *Proceedings of the International Conference on Microstructure and Texture in Steels and Other Materials*, A. Haldar, S, Satyam, and D. Bhattacharjee, eds. Jamshedpur, India during February. 5–7, 2008, Springer Dordrecht Heidelberg, 2009.
28. N. Parvathavarthini, S. Mulki, R.K. Dayal, I. Samajdar, K. Mani, and Baldev Raj, Sensitisation control in AISI 316 L(N) austenitic stainless steel: defining the role of the nature of grain boundaries. *Corrosion Science*, 2009, **51**, 9, 2144–2150.
29. T. Karthikeyan, V. Thomas Paul, S.K. Mishra, S. Saroja, M. Vijayalakshmi, and I. Samajdar, Effect of thermo-mechanical treatment on the grain boundary character distribution in a 9Cr-1Mo ferritic steel, *Metallurgical and Materials Transactions A*, 2009, **40**, 9, 2030–2032.
30. T. Karthikeyan, S. Saroja, S. Rachael Reena, and M. Vijayalakshmi, Fractal analysis of Charpy fractured specimens of coarse and fine grained 9Cr-1Mo steel tested at brittle temperature regime. presented in Annual Technical Meeting of The Indian Institute of Metals, Kolkata, November 16, 2009.
31. R. Anand, T. Karthikeyan, A.L.E. Terrance, S. Saroja, and M. Vijayalakshmi, Effectiveness of nickel based diffusion barriers in preventing hard zone formation in ferritic steel joints. *Journal of Materials Science*, 2009, **44**, 1, 257–265.
32. R. Anand, C. Sudha, T. Karthikeyan, A.L.E. Terrance, S. Saroja, and M. Vijayalakshmi, Metal interlayers to prevent 'hard zone' formation in dissimilar weldments of Cr-Mo steels—A comparison between Cu, Co and Ni. *Transactions of Indian Institute of Metals*, 2008. **61**, 6, 1–4.
33. R. Anand, and S.Karthikeyan, Molecular dynamics simulation of carbon diffusion in Fe and Ni lattice—A comparative study, *International Seminar for Research Scholars 2010*, by Indian Institute of Metals, Madras, at IIT, Madras during 20–24 December, 2010.
34. M. Vasudevan, A.K. Bhaduri, Baldev Raj, and K. Prasad Rao, Delta ferrite prediction in stainless steel welds using neural network analysis and comparison with other prediction methods. *Journal of Materials Processes and Techniques*, 2009, **142**, 1, 20–28.
35. M. Vasudevan, A.K. Bhaduri, Baldev Raj, and K. Prasad Rao, Artificial neural network modeling of solidification mode in austenitic stainless steel. *Materials Science and Technology*, 2007, **23**, 451–459.
36. M. Vasudevan, M. Muruganath, A.K. Bhaduri, Baldev Raj, and K. Prasad Rao, Bayesian neural network analysis of ferrite number in stainless steel welds. *Science and Technology of Welding and Joining*, 2004, **9**, 109–120.

14

NUCLEAR FUEL REPROCESSING

Carlos H. Castaño

Missouri University of Science and Technology, Nuclear Engineering, Rolla, MO, USA

Reprocessing is the chemical process of recovering uranium and plutonium from spent fuel and separating it from cladding, fission products, transuranics, and other chemicals used in the separations. The uranium, plutonium, and some transuranics can then be used again as fuel (re-enriching uranium in some cases), some of the remaining radioisotopes can be used in multiple nuclear applications (sources, tracers, materials processing, medical isotopes, gauges, etc), and the rest can be disposed of as high-level waste (HLW) or in some advanced concepts burned in special nuclear reactors (transmutation of nuclear waste).

Immediately after a nuclear reactor shutdown, there are hundreds of neutron-rich radioisotopes, but most of these are very short-lived, lasting from fractions of a second to a few days. When nuclear fuel is removed from the core, it is typically stored on-site under water in a spent fuel pool for a number of years so the most active radionuclides can decay. Waiting 7 to 20 half-lives decreases the concentration of a radioisotope to inconsequential values. For example, a radioisotope with a half-life of one month has almost disappeared before two years elapsed. Only a few fission products, uranium, plutonium, and some transuranics, remain after this cooling period. At this stage, one can either dispose of the spent nuclear fuel as high-level waste or reprocess it to recover the useful isotopes. Also, the final volume of HLW to dispose of after reprocessing is much lower than the original volume of HLW.

Historically, nuclear fuel reprocessing was implemented (as part of the Manhattan Project) before nuclear power was attempted. The original objective was to obtain plutonium for the atomic bomb. Glenn Seaborg and his group at the Metallurgical Laboratory in Chicago (which became Argonne National Laboratory) developed a method of oxidation-reduction using lanthanum-fluoride as a carrier for the plutonium. This early method proved difficult to scale up, so Seaborg's group tried phosphate as a carrier of plutonium, and the first industrial reprocessing plants were built to use this process.

Before summarizing the historic and modern techniques for fuel reprocessing, it is important to understand that reprocessing is a necessary component of any closed nuclear fuel cycle, a highly desirable cycle from economic and resource conservation points of view. Unfortunately, some countries that have both nuclear energy and nuclear weapons programs have developed concerns about reprocessing because of the possible cross-over (or proliferation) of materials from nuclear energy applications to nuclear weapons applications by other countries. Thus, the subject is mired with deep geopolitical undercurrents. As an example, in 1976 in the middle of the presidential campaign in the United States, proliferation concerns started to dominate the discussion about fuel reprocessing. President Gerald Ford decided that reprocessing should not continue until the United States' perceived risk of proliferation could be decreased. His successor, Jimmy Carter, decided to defer fuel reprocessing in the United States indefinitely, and finally the Nuclear Waste Policy Act (NWPA) of 1982 signed by Ronald Reagan declared that the United States will dispose of spent nuclear fuel in a national geological repository (the Yucca Mountain Geologic Repository) in lieu of reprocessing for at least 50 to 100 years. This status of reprocessing applies only to civilian nuclear fuel in the United States. The United States still quietly reprocesses military nuclear fuel, and most countries with significant nuclear industries reprocess their fuel, including Russia,

Nuclear Energy Encyclopedia: Science, Technology, and Applications, First Edition (Wiley Series On Energy).
Edited by Steven B. Krivit, Jay H. Lehr, and Thomas B. Kingery.

Japan, India, United Kingdom, and France. China and South Korea have recently started programs for fuel reprocessing as well.

Let's briefly review the historical techniques used for fuel reprocessing.

14.1 BISMUTH PHOSPHATE PROCESS

The method used by radiochemists to separate the very first microgram quantities of plutonium involved a "carrier precipitation" where a selective insoluble salt of the substance of interest was formed. This insoluble compound was then separated and refined to extract the desired substance. Glen Seaborg found that, by using bismuth phosphate ($BiPO_4$), plutonium in the tetravalent state (Pu(IV)) could be precipitated from aqueous solution while plutonium in the hexavalent state (Pu(VI)) remained soluble.

The first step of the process was to dissolve the spent fuel or irradiated uranium with nitric acid. The plutonium ion in solution was then reduced to the tetravalent state with sodium nitrite ($NaNO_2$). Plutonium phosphate (IV), ($Pu_3(PO_4)_4$) was then formed and precipitated when both bismuth nitrate and sodium phosphate were added to the solution.

The complete purification process included removing most fission products by re-dissolving the plutonium phosphate with sodium bismuthate ($NaBiO_3$) while $BiPO_4$ was precipitated, again leaving the Pu in solution. This was done twice. This method of plutonium separation has a high efficiency (>95%), but it does not recover uranium, and large quantities of radioactive chemicals remain at the end of each batch, creating a large amount of radioactive waste [1].

14.2 REDOX AND TRIGLY PROCESSES

The Redox process, developed at Argonne National Laboratory, improved on the bismuth-phosphate process by recovering uranium. The name originates from the multiple reduction and oxidation stages alternately applied to separate the plutonium and uranium. Basically, uranium (VI) and plutonium (IV and VI) ions are soluble in the organic solvent hexone (methyl isobutyl ketone, $(CH_3)_2CHCH_2C(O)CH_3$), while fission products and plutonium (III) are insoluble [2]. At the same time, hexone is insoluble in water (a similar process has been used to extract uranium from leaching solutions used in uranium mining).

The redox process as implemented consisted of dissolving the spent fuel with nitric acid and forcing all plutonium into hexavalent plutonyl nitrate $PuO_2(NO_3)_2$ by oxidation with dichromate ions (e.g., $Na_2Cr_2O_7$). At this stage, the solution was forced to counter-flow with the hexone solvent, which extracted the plutonium nitrates and hexavalent uranium nitrates into the hexone. Fission product nitrates were removed from the aqueous phase using a "scrub" solution of the "salting" agents aluminum nitrate, sodium nitrate, and sodium dichromate. Salting agents were used to provide nitrate ions in lieu of using more nitric acid to prevent the nitric acid from becoming concentrated enough to dehydrate the hexone.

After this first partition, the hexone (organic phase) was separated and again forced to counter-flow with an aqueous solution of the reducing agent, ferrous sulfamate ($FeH_4N_2O_6S_2$). This converted plutonium to the water-soluble trivalent state $Pu(NO_3)_3$ and a residue of aluminum nitrate ($Al(NO_3)_3$), which maintains uranium in the hexone phase (as uranil nitrate). The uranium and plutonium were then separated for further treatment. The main disadvantages of the redox process are the volatility and flammability of hexone and the addition of significant amounts of $Al(NO_3)_3$ to the volume of radioactive wastes generated by the process.

The Trigly process was developed in Canada at about the same time [1], and it works on a similar principle as the redox process but uses triglycol dichloride ($ClCH_2CH_2OCH_2CH_2OCH_2CH_2Cl$) as the solvent and nitric acid and ammonium nitrate (NH_4NO_3) as salting agents. Hexavalent plutonium has a high degree of separation from uranium ions in this solvent. This process also adds significant amount of NH_4NO_3 to the radioactive waste to be disposed of.

14.3 BUTEX PROCESS

Developed in Chalk River Laboratory, Canada, Butex was the first reprocessing method to avoid adding nitrate salts to the radioactive wastes. It used the solvent dibutyl carbitol (diethylene glycol dibutyl ether, $C_4H_9OCH_2CH_2OCH_2CH_2OH$), which has the advantage of being more stable to nitric acid exposure than hexone. Therefore, no other nitrate salts were required. Also, after the extraction processes, the nitric acid could be evaporated from the aqueous radioactive wastes and reused. Butex uses dibutyl carbitol for the primary separation and purification of uranium and 20% TPB (tributyl phosphate, $(CH_3CH_2CH_2CH_2O)_3PO$) in kerosene for plutonium purification [3]. Dibutyl carbinol has also the advantage of being less flammable than hexone, but it had both higher viscosity and density and forms uranium complexes that are then hard to extract or treat. Butex remained in use in Windscale, UK, until an explosion attributed to the reaction of nitric acid with solvent ended its use.

14.4 PUREX PROCESS

Purex is currently the worldwide de facto standard (with minor modifications) for fuel reprocessing [4].

PUREX is an acronym standing for **P**lutonium **UR**anium **Ex**traction. Purex is similar to the redox process, but it uses a better organic solvent, tributyl phosphate (TPB, $(CH_3CH_2CH_2CH_2O)_3PO$). The purex process was invented in 1947 in the United States [5] and was first implemented by Knolls Atomic Power Laboratory in a pilot plant at Oak Ridge National Laboratory from 1950 to 1952 [1].

The main advantages of purex over redox are that waste volumes are lower since nitric acid used as a salting agent can be recovered by evaporation, TBP is less volatile, less flammable, and more stable against attack by nitric acid than either hexone or dibutyl carbitol, and operating costs are lower.

A typical purex process proceeds as follows:

1. Fuel is decladded using either mechanical (shearing, chopping, sawing) or chemical means (mostly for aluminum-uranium fuel elements) to expose the fuel to the dissolving agent.
2. The broken fuel and cladding are mixed with hot nitric acid to dissolve the fuel while leaving the cladding (steel or Zircaloy) mostly untouched.
3. Depending on local government regulations of the plant, radiokrypton, xenon, ^{14}C, tritium, and other volatile products (iodine, etc.) are either released or collected for disposal. Collection processes might include oxidization, adsorption, absorption, voloxidation, or scrubbing with water.
4. The aqueous solution at this point usually requires some pretreatment, which might include pH adjustment (pH $\sim$2.5), cooling, clarification, or valence adjustment of Pu ions in solution to (IV) by nitrogen peroxide N_2O_4. The cladding husks are washed with water and removed for waste storage.
5. Uranium and plutonium are separated from the fission products by solvent extraction with a solution of 30% (by volume) TBP in a hydrocarbon diluent (e.g., n-dodecane [6]). This step removes about 99% of the fission products from the U and Pu in the solution.
6. Pu is extracted (from the TBP phase) by reducing the Pu to the trivalent state without reducing the uranium. The reducing agent could be ferrous sulfamate ($FeH_4N_2O_6S_2$), tetravalent uranium ions (U^{4+}), hydroxylamine (NH_2OH), or cathodic reduction.
7. Once the plutonium and uranium are separated (different streams), they are treated to precipitate the uranium and the plutonium from their respective phases.
8. Both plutonium and uranium are (usually) further purified by additional cycles of solvent extraction.
9. Plutonium nitrate is converted to PuO_2 by evaporation, calcination, or precipitation with oxalate ($C_2O_4^{2-}$) or a peroxide (R-O-O-R′) followed by calcination.
10. The uranyl nitrate solution is evaporated and then calcinated obtaining UO_3.
11. Nitric acid vapors are condensed and reused.
12. High level wastes are solidified and disposed of (e.g., in a geological repository).

14.5 OTHER PROCESSES

The prevalence and efficiency of the Purex process has led to the development of variants to achieve different objectives. It is interesting to mention some of them briefly:

14.5.1 Urex

The is a purex process modified to prevent the plutonium from being extracted independently. The objective is making purex more proliferation resistant while reducing the amount of waste that needs to be disposed of in a geologic repository. The objective of UREX is to recover 99.9%+ of U and 95%+ of Tc while rejecting 99.9%+ of transuranics. When this is done, the uranium obtained is a class C waste (Low Level Waste, LLW$<$100 nCi/g [7]).This process uses acetohydroxamic acid (AHA, $C_2H_5NO_2$) which interferes with the extraction of Pu and Np (by forming Pu and Np complexes).

14.5.2 Truex

This is a modification of purex aimed at extracting transuranics (TRU) from nuclear waste. It was developed in the United States during the Cold War to deal with TRU waste generated at material production sites. It utilizes CMPO (octyl(phenyl)-N, N-dibutyl carbamoylmethyl phosphine oxide) combined with TPB to form the so-called TRUEX solvent. This solvent is particularly effective at extracting all actinides (with +3, +4, and +6 valences) from acid solutions.

14.5.3 Sanex

Selective **A**cti**N**ide **Ex**traction allows the separation of actinides from lanthanides so that actinides can be used for nuclear fuel (e.g., Am) without lantanides interfering, given their high neutron cross sections. SANEX is still under development, and there are different solvents being studied (i.e., SANEX-N: Bis-triazinyl-pyridines (BTPs), SANEX-S: mix of Cyanex-3017 and 2,2-bipyridyl [8]).

14.5.4 Diamex

DIAMide **Ex**traction uses malondiamide ($CH_2(CONH_2)_2$) to reduce organic waste generated to only C, H, N, O. This

TABLE 14.1 Review of Some Advanced Aqueous Partitioning Methods (adapted from [8])

Process	Purpose	Country	Special Aspects
DIAMEX	Extracts minor actinides and lanthanides (HLLW)	France	**DIA**mide **EX**traction process solvent based on amides as alternate to phosphorous reagent. Generates minimum organic waste as the solvent is totally combustible
TODGA	Extracts minor actinides and lanthanides (HLLW)	Japan	Uses **T**etra-**O**ctyl-**D**i**G**lycol-**A**mide, similar to DIAMEX
TRUEX	Transuranic elements (**TRU**) **EX**traction from HLLW	France Germany	Extraction by using carbamoyl methyl phosphine oxide (CMPO) together with TBP
SANEX-N	**S**elective **A**cti**N**ide **EX**traction process for group separation of actinides from lanthanides	France Germany	Process for separating actinides from lanthanides from HLLW by using neutral N-bearing extractants, viz. Bis-triazinyl-pyridines (BTPs)
SANEX-S	Ditto	China Germany India	Use of acidic S-bearing extractants, for example synergistic mixture of Cyanex-3017 with 2,2-bipyridyl
TALSPEAK	Ditto	USA Sweden	**T**rivalent **A**ctinide **L**anthanide **S**eparation by **P**hosphorus **E**xtractants and **A**queous **K**omplexes. Use of HDEHP as extractant and DRPA as the selective actinide complexing agent
ARTIST	Ditto	Japan	**A**mide-based **R**adio-resources **T**reatment with **I**nterim **S**torage of **T**ransuranics. This process is made-up of (1) phosphorus-free branched alkyl monoamides (BAMA) for separation of U, Pu; (2) TOGDA for actinide and lanthanide recovery; and (3) N-donor ligand for actinide/lanthanide separation
SESAME	**S**elective **E**xtraction and **S**eparation of **A**mericium by **M**eans of **E**lectrolysis	France Japan	Process for separating Am from Cm by oxidation of Am to Am(VI), subsequent extraction with TBP for separation from Cm
CSEX	**Cs EX**traction	USA France	Using Calix-crown extractants
CCD-PEG	Extraction of Cs and Sr from the raffinate	Czech Russia USA, EU	**C**hlorinated **C**obalt **D**icarbollide and **P**oly-**E**thylene **G**lycol (CCD-PEG) in sulfone-based solvent is planned for extraction of Cs and Sr from UREX raffinate
SREX	**Sr EX**traction	USA	Using dicyclohexano 18-crown-6 ether
GANEX	Uranium extraction followed by group extraction of all actinides	France	Group recovery of all actinides based on branched amide compound N, N-di-(2-ethyl-hexyl)-iso-butanamide (DOiBA) and subsequent DIAMEX/SANEX
UREX +	**UR**anium **EX**traction + other processes for further separation	USA	Series of five steps: (1) recovery of Tc and U (UREX), (2) recovery of Cs and Sr (CCD-PEG), (3) recovery of Pu and Np (NPEX), (4) recovery of Am, Cm, and rare-earths TRUEX, and (5) separation of Am and Cm from the rare earth fission products (Cyanex 301).

prevents the creation of acidic gases during evaporations and calcitation steps and, therefore, reduces emissions that can cause acid rain (it will be likely first implemented in Europe).

There are many other processes developed over the years and many more under active current development. Table 14.1 summarizes some of these. It is important to note that these processes are *not* exclusive from each other—for example UREX-1a combines UREX, CCD-PEG, TRUEX, and TALSPEAK (see Figure 14.1). UREX-1a prevents Pu from being recovered in a pure state (proliferation resistance). Pu and minor actinides Np, Am, and Cm, which contribute the majority of the radioactive and heat load (in a geologic repository) will instead be available to be burned in a reactor. Separation of the minor actinides and separation of Ba and Sr allow more compacting of the waste at the disposal site due to decreased heat load demands.

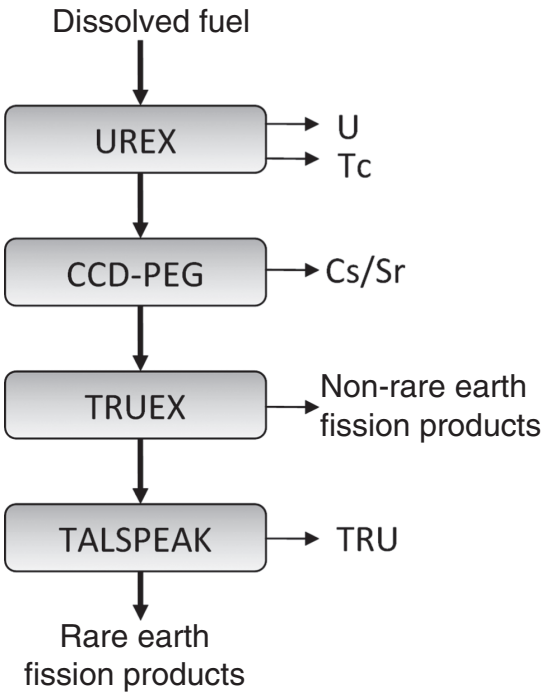

Figure 14.1 Graphic representation of the steps conducted in UREX-1a. (adapted from [10].)

14.6 PYRO-CHEMICAL PROCESSES

An alternative to aqueous methods is to process metals and salts at high temperatures. High-temperature processes are based on a variety of methods including melt-refining, volatilization, gas-solid reactions, fractional precipitation, vacuum distillation, electro-deposition, electro-refining, and electro-winning [8].

The typical pyro-processing process involves dissolution of spent fuel elements in a molten-salt bath (500–800°C) followed by recovery of the constituent elements by some selective technique. In the United States, spent metallic fuel (U-Zr or U-Pu-Zr) is cut into small pieces and mounted on an anode dissolution basket that is then immersed in an eutectic mixture of LiCl/KCl at 773 K. A rod of steel is used as a cathode and $CdCl_2$ is added to transfer most of the actinides and fission products to the electrolyte as chlorides. As a current is forced between the anode and cathode, the uranium in the anode oxidizes and subsequently reduces again at the cathode as uranium metal. After most of the uranium has been extracted, the solid cathode is replaced by a liquid cadmium cathode. In this new cathode U, Pu, and some lanthanides deposit in the cadmium while more reactive fission products remain dissolved in the fused-salt electrolyte. Fission products less reactive than actinides, including noble metals and zirconium, do not dissolve and remain mostly in the anode basket [8, 9].

The advantages of pyro-chemical processing are shorter cooling periods (important in future fuel cycles), short turnaround time for fuel (reduces fissile material inventories), the ability to recover actinides with one process, compact processing plants that can accept a variety of fuels, minimization of TRU waste generated, high proliferation resistance (fuel is highly radioactive, and the plant can be located next to or inside the nuclear reactor facility), it doesn't use any solvent that could potentially create a criticality accident (i.e., no H or C present). The disadvantage is that pyro-processing has a lower separation factor than aqueous methods, and it is expected that it will be implemented in future fast reactors that will tolerate more fuel impurities than current thermal reactors can. On the other hand, the expected lower costs of pyro-processing might trump aqueous processing for reactors in the future.

REFERENCES

1. M. Benedict, T. Pigford, and H.W. Levi, Chapter 10: Fuel reprocessing, in *Nuclear Chemical Engineering*. McGraw-Hill. New York, 1981, 458–459.
2. F.J. Rahn, A.G. Adamantiades, J.E. Kenton, and C.A. Braun, Chapter 14. Reprocessing of nuclear fuel. *In Guide to Nuclear Power Technology: A Resource for Decision Making*. John Wiley & Sons, New York, 1984, 608.
3. P. Paviel-Hartman, B. Benedict, and M.J. Lineberry, Chapter 11: Nuclear fuel reprocessing, in *Nuclear Engineering Handbook*, D.K. Kok, ed. CRC Press, Boca Raton, 2009, 324–325.
4. P. Paviel-Hartman, B. Benedict, and M.J. Lineberry M.J., Chapter 11: Nuclear fuel reprocessing, in *Nuclear Engineering Handbook,* D.K. Kok, ed. CRC Press, Boca Raton, 2009, 331–332.
5. U.S. patent 2924506. H.H. Anderson and L.B. Asprey, 1947.

6. G.F. Vandegrift et al., *Lab-Scale Demonstration of the Urex+ Process*. WM'04 Conference, February 29,–March 4, 2004, Tucson, AZ.
7. J.K. Shultis and R.E. Faw, *Fundamentals of Nuclear Science and Engineering*, 2nd ed. CRC Press, Boca Raton FL, 2008, 376.
8. Development of Advanced Reprocessing Technologies. NTR 2008 Supplement. 52nd IAEA General Conference, 2008.
9. S.X. Li, T.A. Johnson, B.R. Westphal, K.M. Goff, and R.W. Benedict, *Electrorefining Experience for Pyrochemical Processing of Spent EBR-II Driver Fuel Proceedings of GLOBAL 2005*. Tsukuba, Japan, October 9-13, 2005. Paper #487. INL/CON-05-00305. PREPRINT.
10. D. Olander, Nuclear fuels—present and future. *Journal of Nuclear Materials*, 2009, **389**, 1–22.

15

SAFETY OF NUCLEAR FISSION REACTORS: LEARNING FROM ACCIDENTS

J.G. Marques

Instituto Tecnológico e Nuclear & Centro de Fisica Nuclear da Universidade de Lisboa, Portugal

15.1 INTRODUCTION

The safety of nuclear fission reactors is a major public concern with many people believing that nuclear power is particularly risky [1]. These concerns have been increased by the accidents of Three Mile Island (TMI), in the United States in 1979, and Chernobyl, in the USSR in 1986. Mostly as a result of the Chernobyl accident, the public shows an extreme sensitivity to nuclear incidents, regardless of their real impact.

The potential hazards of nuclear fission reactors were recognized very early and features to prevent, contain, and otherwise protect the public from accidents were applied from the outset [2]. Fission reactors generate large amounts of radioactive isotopes, i.e., unstable nuclei that will decay emitting alpha, beta, or gamma radiation. The exposure to this man-made radiation has to be minimized in all situations.

The isotopes produced in fission reactors can be divided in two broad categories: first and foremost the fission products and, second, the activation products. The fission products are nuclei that result directly from the fission of the uranium in the "fuel" of the reactor. The most commonly used nuclear fuel is UO_2, in the form of pellets, encased in tubes of a corrosion-resistant metal alloy, normally zircaloy. The UO_2 provides a stable matrix that retains many of the fission products; the remaining products are confined by the zircaloy cladding. Examples of fission products are I131 (half-life of 8 days) and Cs137 (half-life of 30 years). The activation products have a different origin: they result from the capture of neutrons by impurities in the moderator-coolant when they pass through the reactor core. Tritium (half-life of 12 years), resulting from the activation of deuterium present in trace amounts in light water moderated reactors, is a typical activation product.

In normal operation, some of the activation products are released to the environment in a controlled way, with negligible impact [3]. Trace amounts of fission products can leak or diffuse through the fuel cladding also without impact. However, in accidents that result in damage to the cladding, larger amounts of fission products will enter the reactor coolant and may be released. The release can be airborne, waterborne, or a surface spill; any of these is generically called a "radioactive release," signaling that it contains radioactive isotopes in a liquid, gaseous, or particulate form. The radioactive isotopes of iodine (namely I131) are responsible for most of the short-term dose to individuals exposed in reactor accidents. When considering a longer time period, then Cs137 is the dominant isotope. Actinides (e.g., U, Pu) and other elements of low volatility are retained in the fuel and small fractions may be released as fuel fragments in extreme conditions. Pu was present in the Chernobyl fallout but contributed with less than 1% of the dose beyond 30 km of the reactor [4].

The safety strategies in fission reactors evolved with successive generations of larger capacity plants, and many additional features were introduced. Remote siting was the first implemented measure, its goal being to ensure that the radiation dose is small enough at the border of an exclusion area created around the reactor, in case of any

Nuclear Energy Encyclopedia: Science, Technology, and Applications, First Edition (Wiley Series On Energy).
Edited by Steven B. Krivit, Jay H. Lehr, and Thomas B. Kingery.

accident. The U.S. Navy had a strong influence on the adoption of accident prevention strategies, since remote siting could not be relied upon to acceptably limit the consequences of an accident, nor could containment be reasonably engineered for a nuclear submarine. Defense-in-depth is a safety strategy in use since the 1950s. It relies on having multiple, redundant, and independent layers of safety systems for the critical point in fission reactors: the reactor core. Its application helps to ensure that the three basic safety functions—controlling the power and reactivity, cooling the fuel, and confining the radioactive fission products—are preserved.

Several countries started building nuclear fission reactors at the end of the 1940s. This first generation of reactors included prototypes of technological solutions (different combinations of moderator, coolant, and fuel), research reactors, test reactors, as well as plutonium production reactors. At the first Geneva conference in 1955, about 100 different reactor types were considered, while three years later, at the second Geneva conference, only about 12 types were seriously considered [5]. The first nuclear power station to generate electrical power on an industrial scale was Calder Hall, in the United Kingdom, a Magnox reactor connected to the grid in August 1956. Calder Hall had more than a year's lead on the Shippingport reactor, connected to the grid in the United States in December 1957 [6].

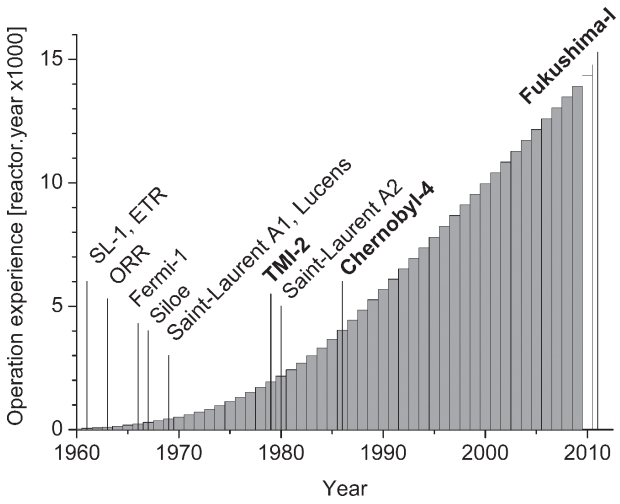

Figure 15.1 Evolution of the cumulative operating experience with nuclear fission reactors (in reactor-years) and timeline of accidents involving fusion of at least part of the core.

Table 15.1 summarizes nuclear accidents in fission reactors involving damage to the fuel in the core, which are documented in open literature [7–11]. Figure 15.1 shows the evolution of the cumulative operating experience with nuclear fission reactors (in reactor years) in the last five decades, as well as the timeline of accidents in the same period. The data for the operating experience until 2009

TABLE 15.1 Reactor Accidents with Core Damage

Year	Location	Reactor	Thermal Power (MW)	Type	Extent of contamination
1952	Chalk River, Canada	NRX	30	Experimental	None
1955	Idaho Falls (ID), United States	EBR-1	1.4	Fast reactor prototype	Trace
1957	Windscale (now Sellafield), United Kingdom	Windscale-1	180	Gas-cooled reactor	$2-5 \times 10^4$Ci I131
1958	Chalk River, Canada	NRU	200	Research	None
1958	Idaho Falls (ID), United States	HTRE-3	0.2	Experimental	Slight
1959	Santa Susanna (CA), United States	SRE	20	Experimental	Slight
1960	Waltz Mills (PA), United States	WTR	60	Experimental	None measured
1961	Idaho Falls (ID), United States	SL-1	3	BWR prototype	10 Ci I131
1961	Idaho Falls (ID), United States	ETR	90	Research	Slight
1963	Oak Ridge (TN), United States	ORR	30	Research	Trace
1966	Newport (MI), United States	Fermi-1	300	Fast reactor prototype	None outside plant
1967	Grenoble, France	Siloe	30	Research	Trace
1969	Lucens, Switzerland	Lucens	30	Gas-cooled reactor	None
1969	St-Laurent-des-Eaux, France	Saint Laurent A1	1650	Gas-cooled reactor	Little, if any
1979	Three Mile Island (PA), United States	TMI-2	2770	PWR	Slight
1980	St-Laurent-des-Eaux, France	Saint Laurent A2	1650	Gas-cooled reactor	Little, if any
1986	Chernobyl, Ukraine	Chernobyl-4	3200	RBMK	Extensive
2011	Fukushima, Japan	Fukushima-I, Units 1–3	1380, 2381, 2381	BWR	Moderate

was obtained from the PRIS database of the International Atomic Energy Agency (IAEA) [12]. The values for 2010 and 2011 were estimated. The accumulated operating experience up to date with fission reactors is approximately 14,000 reactor-years. The operating experience more than tripled between the accident of Chernobyl in 1986 and the one of Fukushima-I in 2011.

The only accidents from Table 15.1 that resulted in a direct loss of life were the ones in the experimental reactor SL-1 in 1961, where three workers died from the effects of the explosion and radiation, and in Chernobyl, where 30 members of the operating and firefighting personnel died, primarily from high radiation doses. In addition, a small number of delayed cancer fatalities is expected from the Windscale accident in the United Kingdom in 1957 [13] and a larger number of delayed fatalities from the Chernobyl accident [14]. At the time of going to press, the consequences of the Fukushima-I are still largely unknown. A brief overview will be done in the following section of all known accidents that occurred before TMI, with the exception of the accident in Saint-Laurent A2, which was grouped together with the one in its sibling Saint-Laurent A1. The accidents of TMI, Chernobyl and Fukushima-I will be discussed in separate sections.

15.2 CORE DAMAGE ACCIDENTS IN THE EARLY DAYS

The National Reactor eXperimental (NRX) was a 30 MW (thermal) heavy water moderated, light water cooled reactor that started working in the Chalk River Nuclear Laboratories (Canada) in 1947 for research and plutonium production [15]. In December 1952, experiments were in progress to measure the effect of fuel irradiation on its reactivity. The reactor was being operated according to procedures that differed from those for normal operation, although similar procedures had been followed before. An operator error, followed by a failure of the control rod system, resulted in a partial meltdown of the core [16] and the release of an unspecified amount of radioactivity [7]. The cleaning operations were extensive and had the assistance of Canadian army and U.S. Navy personnel, including the future U.S. President Carter, at the time a U.S. navy officer [17]. The reactor was brought back into operation in 1954. It was shut down in 1993, after 45 years of operation.

The 1.4 MW (thermal) Experimental Breeder Reactor (EBR-1) in the National Reactor Testing Laboratory (NRTL, now the site of the Idaho National Laboratory), in Idaho (United States), was the first reactor from which electricity was produced, although at a small scale of 0.2 MW_e. This experimental reactor was designed to study the breeding capabilities and the time-response characteristics of reactors of this type. Successful experiments had been performed in the four years of operation before the accident. The EBR-1 suffered a 40 to 50% core meltdown during a test in 1955 in which the power level of the reactor was intentionally raised but, due to operator error, was not reduced promptly. There was a limited contamination of the building, no injuries occurred, and the release of radioactive material was "trivial" [7]. The EBR-1 was deactivated in 1964 and replaced with a new reactor, the EBR-2. The EBR-1 was declared a U.S. National Historic Landmark in 1965 [18].

The United Kingdom built two nuclear reactors at the Sellafield site (then designated Windscale) between 1947 and 1951 for the production of plutonium and other materials for the UK weapons program, the Windscale-1 and 2 "piles," with a power of 180 MW (thermal) each. These were graphite-moderated, air-cooled reactors. "Wigner energy" accumulated in the graphite moderator, as carbon atoms were displaced from their locations in the graphite lattice by neutron impact. To avoid an uncontrolled release of this energy as heat, the graphite was annealed periodically by nuclear heating at low power and reduced airflow to raise the temperature of the graphite until the stored energy was released. An accident occurred in October 1957 in the Windscale-1 pile in the course of one of these annealing operations [19]. This procedure had been done several times before, but it was ill understood, and the thermocouples monitoring the temperature in the core were not well placed [9]. During the annealing, part of the core overheated so that fuel and graphite in that part burned in the air coolant. In the ensuing fire, some of the fission products and activation products contained in a few percent of the core were released into the atmosphere. The fire could only be put out by flooding the reactor with large volumes of water. The most serious consequence was the release of I131, initially estimated to have been 20,000 Ci [7], with more recent estimates going as high as 50,000 Ci [20]. Windscale-2 was also stopped after the fire and none of the reactors was taken back into operation. Decommissioning of the two reactors is underway [21].

The National Reactor Universal (NRU) was a 200 MW (thermal) heavy water moderated and cooled reactor, which started working in the Chalk River Nuclear Laboratories (Canada) in 1957 [15]. It remains one of the main reactors for the production of medical isotopes, namely Mo99 [22]. In 1958 some faulty fuel elements were discovered and promptly removed from the core. However, the tank was contaminated, and the residual activity prevented the operators from identifying other faulty fuel elements. In May 1958, an instrumentation problem allowed the reactor to start up at a rate higher than expected, causing a failure of an undetected faulty fuel element. The pressure shock from this transient caused a spurious signal to be generated, which triggered the withdrawal of the control rods, leading

to another transient that ended up shutting down the reactor. Two fuel elements were damaged, one of which melted after its removal from the core due to deficient cooling. There was some release of radioactivity, confined to the area of the building [7].

The Heat Transfer Reactor Experiment (HTRE-3) was designed to test high-temperature cores in the NRTL, Idaho (United States). In November 1958 a third core was undergoing tests. Changes had been made to the instrumentation to reduce noise in the single power channel used to drive a servomechanism moving the control rods. These changes caused a wrong reading at high power, and the servomechanism proceeded to withdraw the control rods, leading to a power excursion that extensively damaged the core. Small amounts of radioactivity were released within the facility and to the environment [7, 23]. The unintentional removal of control rods is one of the "postulated starting events" considered in modern safety analysis of fission reactors.

The Sodium Reactor Experiment (SRE) was a graphite-moderated and sodium-cooled reactor, with a power of 20 MW (thermal), operated by the Atomic Energy Commission in Santa Susanna (CA). An organic material (tetralin) was used as an auxiliary coolant in the primary coolant pumps [24]. In July 1959 the reactor experienced several failures, spurious shutdowns, and unexplained transients. Once radioactivity was detected in the primary coolant, the reactor was stopped for inspection. More than 20% of the fuel was found severely damaged, possibly due to a power excursion. The primary cause was attributed to the leakage and decomposition of the organic compound. The decomposition products prevented the fuel assemblies from being properly cooled and also blocked some coolant passages. The increase in temperature on the fuel elements went undetected during the operation of the reactor, because only the temperature of the sodium coolant was monitored—although the measured values were higher than usual, they were considered acceptable [7, 25]. The SRE was repaired and restarted the following year. It operated until 1964 [26].

The Westinghouse Testing Reactor (WTR) was a 60 MW (thermal) water-moderated and cooled reactor. In April 1960, tests were being done on the onset of boiling at different coolant flowing rates and powers to validate calculated values. During one such test, at 34 MW, there was a sudden drop of power, compensated with a withdrawal of control rods by an operator, which in turn led to a radiation alarm and shutdown of the reactor. The primary cause was the failure of a fuel element, namely a separation in the bonding between the cladding and the fuel. The de-bonding acted as a barrier for heat removal and led to subsequent melt. There was some release of radioactivity within the plant and into the environment. The reactor was dismantled in 1962 [7, 27].

The Stationary, Low-power SL-1 reactor was a 3 MW (thermal) prototype natural circulation Boiling-Water Reactor (BWR) located at the NRTL. The SL-1 used highly enriched uranium and was intended for heating and electricity production at remote military installations, without need to be refueled for three years. From September 1960 onwards, deterioration of control rod performance was experienced. An accident occurred in January 1961 in which three army technicians were killed when one of them apparently rapidly removed manually the central control rod from the core during maintenance [28]. As a result, there was a rapid increase in reactor output, followed by a steam explosion, leading to lethal levels of radiation within the reactor building. About 20% of the core was destroyed [9]. Most, but not all, of the activity was contained within the building [7]. The remains of the SL-1 reactor are buried near the original site. This reactor design was abandoned after the accident. As a result of this accident, reactors with compact cores are built so that the withdrawal of a single control rod cannot produce the excess reactivity that was possible with the SL-1 design. This is known as the "one stuck rod" criterion and requires complete shutdown capability even with the most reactive control rod stuck in the fully withdrawn position.

The Engineering Test Reactor (ETR) was a 90 MW (thermal) test reactor operated at the NRTL from 1957 to 1982. In December 1961 a Plexiglas sight glass inadvertently left in the reactor vessel during the previous shutdown blocked the coolant flow in part of the core, resulting in a partial melting of six fuel elements. There was a small release of radioactivity [29]. An accident of the same type occurred in the Oak Ridge Research Reactor (ORR), a 30 MW (thermal) research reactor operated in the Oak Ridge National Laboratory from 1958 to 1987 [30, 31]. In July 1963 a neoprene gasket slipped off a fixture on the inside of the reactor tank and blocked the top of one fuel element. This resulted in the melting of one fuel plate when the reactor was taken to 24 MW. There was a minor release of radioactivity to the atmosphere [7]. The faulty fuel element was removed and replaced. Operation of the ORR was resumed the following day. The French research reactor Siloe (30 MW, thermal) experienced a similar accident in 1967, when an unidentified object blocked several flow channels, resulting in the melting of six fuel plates, with a small release of radioactivity [29].

The Fermi-1 reactor in Detroit (United States) was a fast breeder reactor prototype with 300 MW (thermal) power. It featured cooling by liquid sodium. The Fermi-1 reactor suffered a partial meltdown in 1966. The cause of the accident was a blockage in the flow path of the sodium coolant. There were no injuries or significant release of radioactivity, and the reactor was out of service for three years [32]. The Fermi-1 reactor was permanently shut down in 1972 [33].

The Lucens reactor was a 30 MW (thermal) experimental power reactor, moderated with heavy water and cooled with CO_2. It was located inside a natural cave in the canton of Vaud, Switzerland. The Lucens reactor was designed to combine features of the French reactors and the UK Magnox units with heavy water moderation. In 1969 there was a partial fuel melting due to a loss of CO_2 cooling. There was severe damage to the reactor but no radiation release beyond permitted levels [7]. The reactor was not put back into operation, and the site is now open to the public [34].

There were two accidents involving partial core melt in French graphite-moderated, gas-cooled reactors [8, 11]. A human and technical error caused the melt of two fuel elements in the Saint Laurent A1 reactor, 1650 MW (thermal), in the day after its initial inauguration in 1969. Another accident occurred in the Saint Laurent A2 reactor in 1980 when a plate protecting instrumentation became stuck in a channel, causing the melting of three fuel elements. In both cases there were no effects to the environment, but the reactors were out of service for one to two years for cleaning and modifications. In the 1970s France had already started building water-moderated and cooled Pressurized Water Reactors (PWR) and ended up abandoning the line of graphite-moderated reactors [11].

15.3 THE ACCIDENT AT THREE MILE ISLAND

15.3.1 Pressurized Water Reactor

The TMI Power Station is located on an island in the Susquehanna River, close to the town of Harrisburg in Pennsylvania. The power station has two PWRs, which started commercial operation in September 1974 (TMI-1) and December 1978 (TMI-2). The reactor that became TMI-2, with 2770 MW (thermal), was initially planned for the Oyster Creek site in New Jersey, and its design was slightly different from the one of TMI-1, although Babcock & Wilcox manufactured the main components for both. On March 28, 1979, TMI-2 experienced a series of events that resulted in a partial core melt with a small radioactive release to the atmosphere.

PWRs have their origins in the technology developed for the nuclear submarine program of the U.S. Navy [30]. Figure 15.2 shows a simplified schematic layout of the TMI-2 plant [35], highlighting some components that were central to the accident.

In a PWR, the coolant enters the reactor pressure vessel near the top, flows downward between the vessel's inner wall and the core, is distributed at the lower core plate, flows upward through the core, and exits at the top of the vessel. The coolant, which is pressurized to about 15 MPa, typically enters the vessel with a temperature of about 290°C and exits at about 320°C. Primary coolant is pumped to a steam generator where the heat is transferred to a secondary loop through several U-shaped tubes. The dry steam produced in the steam generator flows to a turbine-generator where it is expanded to convert thermal energy into mechanical energy and hence electrical energy. The expanded steam exhausts to a condenser where the latent heat of vaporization is transferred to the tertiary system and the steam is condensed. The condensate is pumped back to the steam generator to continue the cycle. The tertiary loop is the heat rejection loop. Depending on the specific site, this heat is released to a river, lake, ocean, or cooling tower system [36].

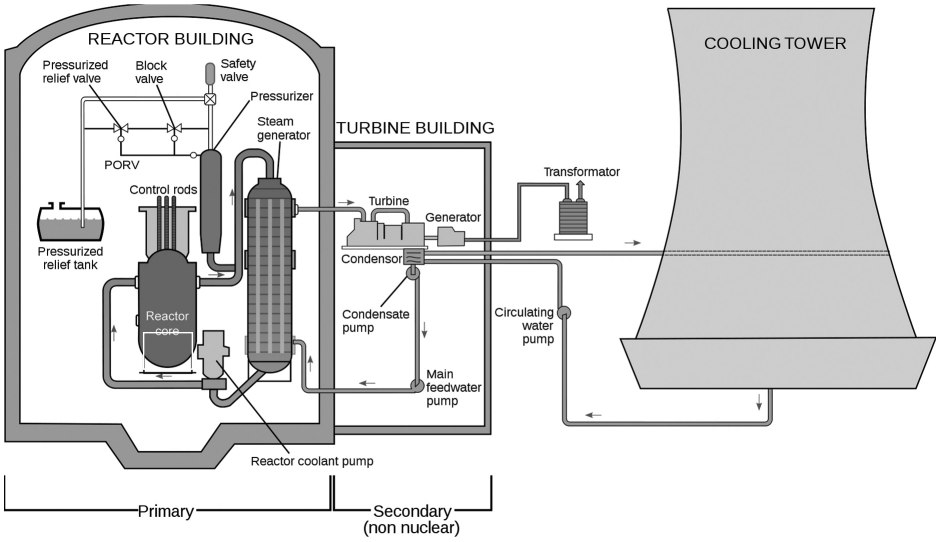

Figure 15.2 Schematic layout of TMI's Unit 2. Courtesy of the World Nuclear Association.

The pressurizer regulates the pressure in the primary loop using electrical heaters and water sprays. Under normal conditions, the pressurizer contains water in the bottom and steam in the top. The trapped steam at the top is under pressure, and this pressure is transmitted through the water at the bottom of the pressurizer and through the connecting pipe to the primary system. The top of the pressurizer is connected to a relief tank. There are two valves in this line: a block valve, which is normally open, and a pressure relief valve, which is normally closed. The block valve serves as a backup in case the pressure-relief valve fails. If the pressure in the pressurizer gets too high, the relief valve opens and relieves the pressure. The steam or water-steam mixture that comes out of the pressurizer passes through the open block valve and through the opened relief valve and into the relief tank. It normally takes only a few seconds to relieve the pressure. If the relief valve fails to close, the block valve can be used to close the line. Safety valves, installed in a parallel pipe, can also be used.

15.3.2 Accident Sequence

Several detailed descriptions of the TMI-2 accident were published *inter alia* in accident reviews [7, 9, 37], special reports [38, 39], dedicated books [40, 41], and in nuclear engineering books [42–44]. We will follow here a simplified outline, with the main events only.

The accident began about 4:00 am on March 28, 1979, when the plant experienced a failure in its non-nuclear section. The reactor was operating at about 97% of power, but with three problems [43]:

- There was a loss of small amounts of coolant, through one or more of the pressurizer valves, which the operators believed to be within limits. This minor loss partially filled the relief tank.
- Two valves on the emergency secondary coolant feedwater lines were unduly closed, following maintenance completed two days before, although the records available to the operators showed them to be open.
- The operating staff of TMI-2 had been trying for several hours to unclog the piping of one of the eight polishers, which remove impurities from the water once the steam that drives the turbines is condensed. During this process there was a condensate pump shutdown at about 4:00 am.

As a result of the cutoff of water from the condensate polishers, the main feedwater pumps that send water to the steam generators stopped. Then the turbine tripped, and the emergency feedwater pumps started automatically. The loss of secondary coolant in the steam generators reduced the rate of heat removal from the primary coolant loop and the reactor core, resulting in what is called a "loss of heat sink" scenario.

As the primary coolant became hotter and pressure increased, the overpressure relief valve in the pressurizer, the so-called "pilot-operated relief valve" (PORV), connected to the top of the pressurizer opened automatically. After a further increase of pressure, and 8 s into the accident, the core protection system caused the control rods to be inserted into the core. Up to this point, all systems operated as could be expected.

The primary system cooled following the decrease in power, and the pressure dropped below the set point for closure of the PORV at about 13 s into the accident, but the valve failed to close. As a consequence, reactor coolant was allowed to escape through the open valve into the relief tank at the bottom of the containment building, which reduced the pressure in the primary coolant system as well as the coolant level.

At 14 s into the accident, the emergency secondary coolant feedwater pumps reached full design pressure, but the two closed valves in the emergency secondary system prevented the coolant from reaching the steam generators. It was another 8 min before an operator from TMI-1 (then shut down for refueling) arrived in the control room of TMI-2 and noticed that these valves were closed—their indicator lights were partially blocked by tags [9]—and immediately opened them to restore secondary coolant to the steam generators.

Meanwhile, the instruments in the control room provided unclear information. As there was no direct measurement of the level of coolant in the core, the operators inferred this from the level in the pressurizer; since this was high, it was assumed that the core was properly covered with coolant. Unfortunately, due to a j-shaped "trap" connection, there was no direct relationship between the coolant levels in the reactor vessel and in the pressurizer. The operators judged PORV to be closed, as per the indication they had in the control room. Within this scenario, nobody realized at the time that the plant was experiencing a "loss-of-coolant accident," although there were no pipe breaks involved.

At about 2 min into the accident, the primary system pressure dropped below the set point of the high-pressure injection system, which then started pumping borated water from a storage tank into the core. Approximately 2 min later, the operators turned off one of the pumps and reduced the other pump, resulting in emergency coolant being added at a slower rate than primary coolant was being lost through the still-open PORV. This was done according to the operators' training. Even with continuing loss of primary coolant, the pressurizer signal indicated a filled system, and the operators had been trained to avoid a "solid" pressurizer (entirely filled with liquid water) because it would prevent the pressurizer from fulfilling its function.

About 73 min into the accident, both primary coolant pumps in the loop to one of the two steam generators were shut down in response to indications of vibrations, low pressure, and low coolant flow. This was done to prevent destruction of seals, which the operators feared would cause a loss of coolant accident. At this point, the operators were still unaware that a loss of coolant accident was already underway. At about 100 min into the accident, the primary coolant pumps in the other loop were also shut down for the same reason. At this point in time the operators expected natural circulation to establish and cool the core, but this did not happen. As long as the pumps were working, the coolant consisted of a saturated mixture of steam and liquid, which still provided some cooling. However, once forced flow was stopped, steam separated from water. The remaining liquid did not cover the core, and decay heat caused continuing vaporization of the non-circulating coolant. At about 111 min into the accident, reactor outlet coolant temperatures rose rapidly and went off-scale ($>330^{\circ}$C). As the core became uncovered, the clad temperatures increased to the point that exothermal Zr-steam reactions occurred, adding energy to the system and producing hydrogen. Once the temperature reached approximately 1800°C, the zircaloy cladding started to melt and began to dissolve the UO_2 fuel, well below the melting point of UO_2 [45].

Pressure in the relief tank increased to a level high enough to lift the safety valve at about 3 min into the accident and break the rupture seal at about 15 min. Thus, primary coolant flowed first into the relief tank and then into the containment building sump. There was a pressure sensor on the relief tank that might have alerted the operators on the loss of coolant. However, its meter was located on a back-facing panel behind the reactor console, out of easy access. In the initial stages of the flooding, the radiation levels were low, as the coolant contained essentially the activation products typical of normal operation [46]. However, once the cladding was damaged, the radiation levels increased as large amounts of fission products were carried by the coolant. The makeup and letdown systems, with tanks located in the auxiliary building, are used to balance the inventory of coolant in the primary circuit. Small leakages were regarded as of no importance during normal operation, as the primary coolant has very little radioactivity. However, in this case these small leakages allowed part of the high-activity primary coolant to escape into the auxiliary building during the accident. Fission gases from the several sources in the auxiliary building were picked up by the ventilation system and were discharged after filtration. The filters removed much of the radioactive iodine but had no effect in the inert noble gases.

About 142 min into the accident, the operators finally closed the block valve in series with PORV, thus blocking the escape route. It was later found that about half of the core had melted during the early stages of the accident. Figure 15.3 shows a representation of the molten core, made with data obtained several years after the accident.

The next 13 hours were spent trying various means to reestablish core cooling, which was ultimately successful. The reactivation of the high-pressure injection at 200 min into the accident recovered the core and filled the reactor vessel. At 224 min into the accident, molten fuel from the core relocated to the lower head of the pressure vessel, as shown in Figure 15.3.

An additional problem, which ended up having a large public impact, was the creation of a sizable hydrogen bubble from the Zr-steam interactions involving about one-third of the zircaloy in the core. The hydrogen was removed during the first week, taking advantage of its variable solubility with water temperature and pressure. A cyclic process was followed, involving dissolution by pressurization in the core, followed by depressurization and release through the pressurizer.

15.3.3 Consequences

Although the TMI-2 plant suffered a core meltdown, it did not produce the consequences that some had long feared. In a worst-case accident, it was feared that the melting of nuclear fuel would lead to a breach of the walls of the containment building and release massive quantities of radiation to the environment.

Nevertheless, the accident caught federal and state authorities ill-prepared. First, they were concerned about the small releases of radioactive gases that were measured off-site by the late morning of March 28 and even more concerned about the potential threat that the reactor posed to the surrounding population. The Nuclear Regulatory Commission (NRC) dispatched the first team of inspectors to the site and other agencies, such as the Department of Energy and the Environmental Protection Agency, also mobilized response teams. By the evening of the first day, the core appeared to be adequately cooled and the reactor appeared to be stable.

However, new concerns arose in the morning of Friday, March 30. A controlled release of radiation from the plant's auxiliary building, performed to relieve pressure on the primary system and avoid curtailing the flow of coolant to the core, caused a great deal of confusion and consternation. Communication between the personnel on site and the involved agencies at local and federal level was difficult. On one hand, there were few telephone lines and the circuits were often busy; on the other hand, important technical details were not always well transmitted and perceived. Several misunderstandings occurred as a result of these difficulties. One such misunderstanding, on the nature of the release on March 30 and on its magnitude, led to a major

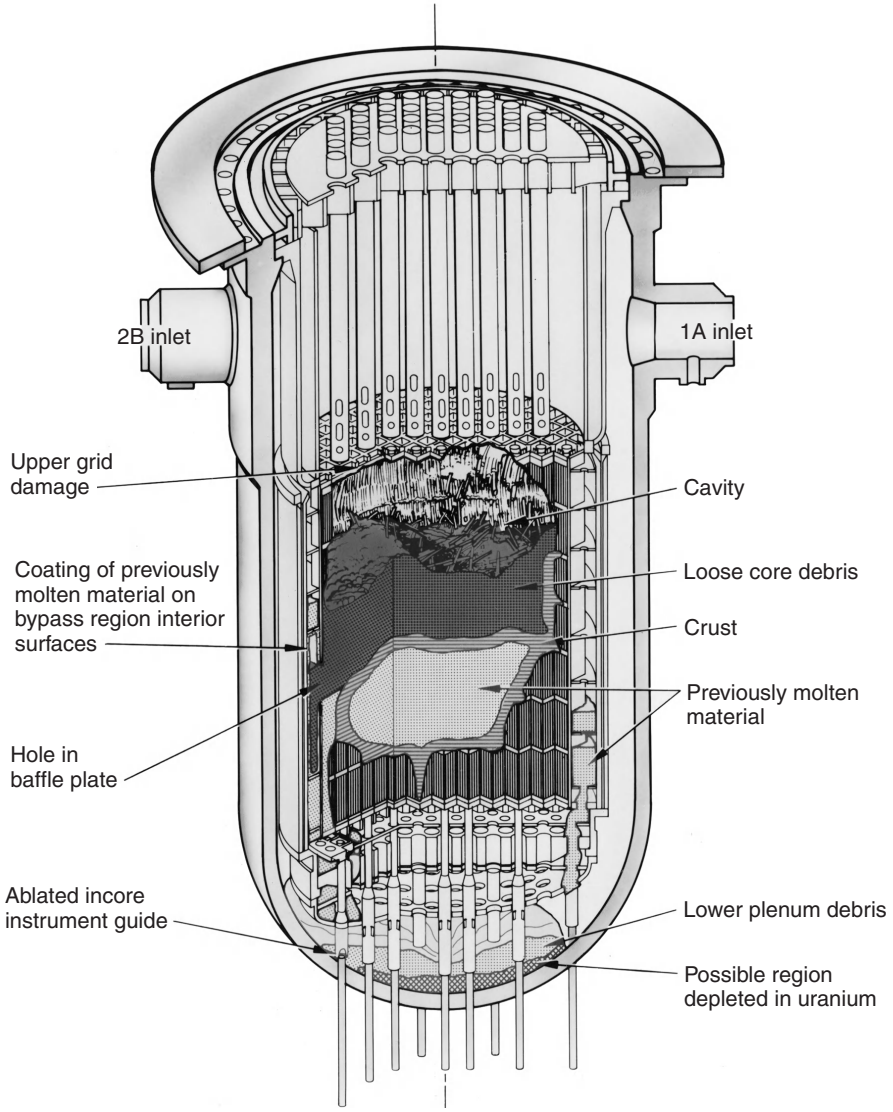

Figure 15.3 Configuration of the damaged core inside the TMI-2 pressure vessel after the accident. Courtesy of the U.S. Nuclear Regulatory Commission.

evacuation in the area. At a press conference at 12:30 pm, the governor of Pennsylvania, Richard L. Thornburgh, advised pregnant women and small children living within a five-mile radius of the plant to leave the area. About 3,500 pregnant women and small children within the five-mile radius were evacuated, corresponding to an estimated 83% of that group. They were joined by approximately 140,000 people living within a 15-mile radius of TMI [41].

Within a short time, the presence of a large hydrogen bubble in the dome of the pressure vessel stirred new worries. The concern was that the bubble might burn or explode and rupture the vessel. In that event, the core would fall into the containment building and eventually breach the containment. Twelve days before the accident, the film *The China Syndrome* had been released in U.S. theaters, with the fictional concept that molten material from an American reactor would melt through the crust of the Earth and reach China. The hydrogen bubble was a source of intense scrutiny and great anxiety throughout Saturday, March 31. The crisis ended on Sunday, April 1, when it was determined that the bubble could not burn or explode because of the absence of oxygen in the pressure vessel. Meanwhile, the TMI-2 operators had well underway the reduction of the amount of hydrogen in the reactor's vessel.

The radioactive releases from the accident were minimal. The noble gas release was estimated at about 10 MCi, mostly of Xe133, while the iodine release was estimated at only 18 Ci, mostly of I131. Soon after the accident, a number of anecdotes about TMI-related symptoms, disease,

and death surfaced [47]. However, the radiation doses to members of the public were quite small. It was determined that the average likely and maximum whole-body gamma-doses for individuals in a five-mile area around TMI-2, during the 10 days after the accident, were 0.09 mSv and 0.25 mSv, respectively [48]. These values are significantly smaller than the annual effective dose from natural background received by an individual in the United States, estimated at 3 mSv [49], or worldwide, estimated at 2.4 mSv [50]. Figure 15.4 shows the mean likely whole-body gamma dose within a five-mile radius of TMI-2, by civil division, from Talbott and co-authors [48]. The doses are indicated in mrem (100 mrem = 1 mSv). The highest exposures occurred in Lower Swatara, Royalton, and Goldsboro. As a reference, the annual dose limit currently adopted for members of the public is 1 mSv; this value does not include exposure due to natural background, nor due to medical applications.

Several public health studies were made since the accident [48, 51–54]. The most recent study, on 32,000 people, confirms previous conclusions that there is no consistent evidence that the radioactivity released during the TMI-2 accident had a significant impact on the mortality experience through 1998 [54]. In particular, the slight trend for female breast cancer and likely gamma exposure seen in an earlier study of the same authors [48] is no longer evident.

15.3.4 Lessons Learned

The TMI-2 accident, in spite of its limited damage, was a wake-up call for the authorities and the nuclear industry. President Carter appointed a special commission to enquire into the causes and the circumstances of the accident. The report of the Kemeni commission identified 18 faults and errors: 5 in design, 2 in regulation, and 11 in operation [38].

An error identified for the NRC was its failure to inform TMI-2 of an earlier problem in the United States with the pressurizer relief valve of the Davis-Bessie plant, which also got stuck in 1977. The same problem had occurred in the Beznau-1 power plant (Switzerland) [7] in 1970. In both cases there were no consequences because the operators acted on time and managed to keep the core always covered.

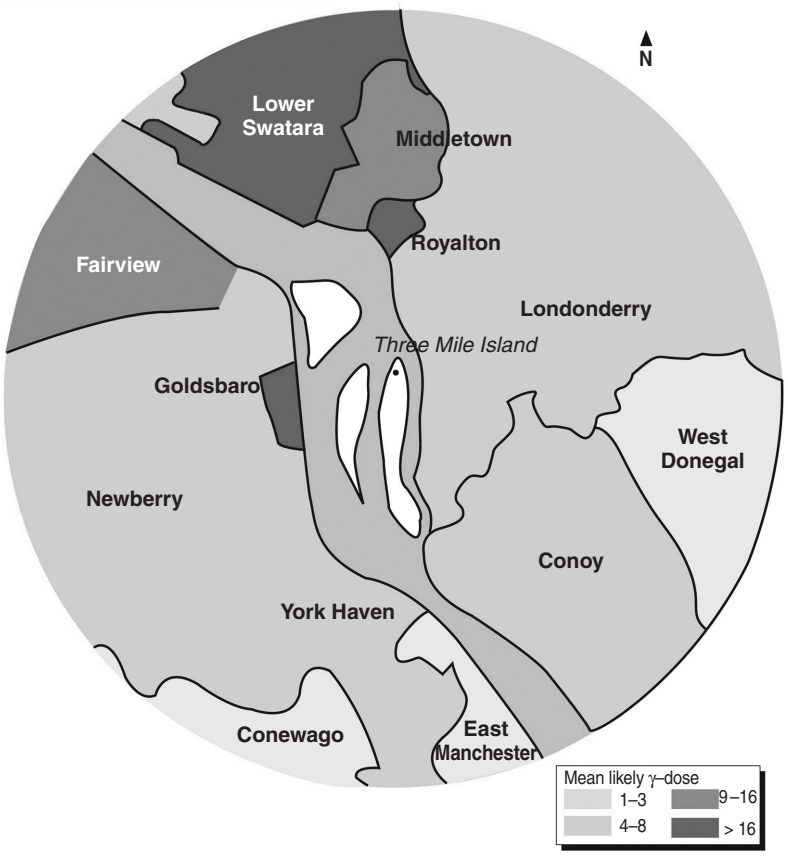

Figure 15.4 Mean likely whole-body gamma dose within a five-mile radius of Three Mile Island, by civil division. The doses are indicated in mrem (100 mrem = 1 mSv). Reproduced from Talbott and co-authors [48] with permission from Environmental Health Perspectives.

This does not mean that the TMI-2 operators have the full responsibility for the accident. In fact, the indicator light of the PORV valve in the control room was misleading. It did not show the actual status of the valve, but the power status of the solenoid that was expected to actuate the valve. The operators, relying on the indicator light, did not pay attention to other indications and were unaware of the PORV failure.

Moreover, the control room had several deficiencies that may have confused the operators during the initial minutes of the accident [38, 55]:

- Over 100 alarms went off in the early stages of the accident with no way to identify and separate the important ones.
- The arrangement of controls and indicators was not satisfactory because some key indicators relevant to the accident were on the back, therefore not easily accessible.
- Several instruments were not designed to follow the course of an accident and went off-scale, depriving the operators of vital information.
- The computer printer registering alarms could not cope with the event rate and at one point jammed, thereby losing valuable information.

Figure 15.5 shows part of the console of TMI-2 with maintenance tags that the operators testified were covering the indications of the closed valves in the emergency secondary coolant circuit [38]. Even if the impact on the accident progression of the 8 min absence of feedwater is not clear [43], this was certainly one of the large pieces of the puzzle.

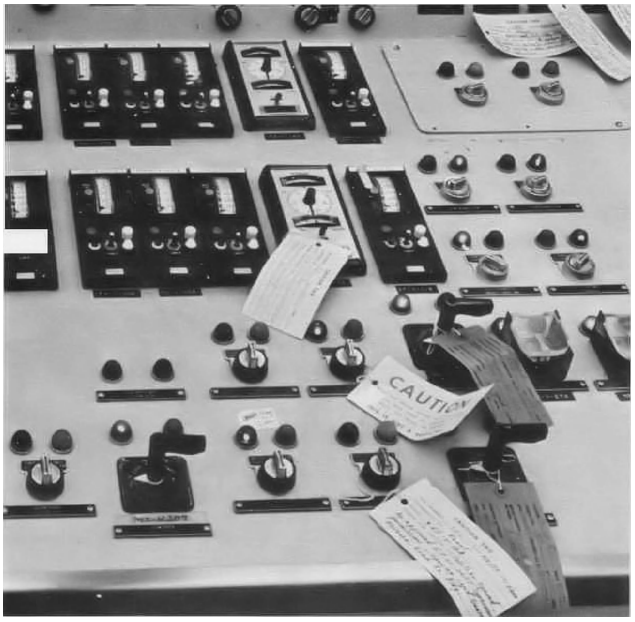

Figure 15.5 Part of the console of TMI-2 showing maintenance tags that covered some essential indicator lights during the early stages of the accident. Courtesy of the President's Commission on the Accident at Three Mile Island.

Modern control rooms are drastically different [56]. In particular, an enormous progress has been done in the human-machine interface, following stringent safety criteria [57]. Figure 15.6 shows a simulated view of the control room of Olkiluoto-3 [58], the first unit of the Evolutionary Pressurized Reactor from Areva, a Generation III+ design. The control room has four separate working areas for reactor and turbine operators, shift supervisor, and, most important, systems and screens to show a plant overview that was so necessary, but lacking, in TMI-2.

The TMI-2 accident has shown that improvements were essential in control room instrumentation, operating procedures, lines of authority, lines of communication, technical support to the operator, emergency planning, and public evacuation. It has also shown that non-technical aspects, e.g., operator training, emergency procedures, organization, and management, are as important as the technical aspects.

After the TMI-2 accident, the nuclear industry formed a new body, the Institute of Nuclear Power Operation (INPO) [59] and its National Academy for Nuclear Training. These two industry organizations have been effective in promoting excellence in the operation of nuclear plants and accrediting their training programs.

Training is now extensively done using computer-driven simulators that faithfully duplicate the control rooms right down to the location of individual gauges and switches on the panels. The actions taken by operators under several scenarios can be tested and evaluated, both for effectiveness and feasibility of implementation. The operating shifts can be evaluated as teams, on crucial tasks such as information flow, and command and control.

Soon after the accident, the NRC created the Office of Analysis and Evaluations of Operating Data (AEOD) to provide better information about plant safety, performance trends, and identify accident precursors. Management changes were implemented in the NRC in 1980, to define more clearly the role of the chairman, particularly during emergencies. The NRC also consolidated its more than 11 sites in the Washington area to a single location in 1988.

Finally, the cleanup of the damaged TMI-2 was finished in 1991, after 12 years of work, at a cost of US$ 973 million [35]. Defueling the reactor vessel was the heart of the cleanup. A total of 342 fuel canisters were shipped for long-term storage at the Idaho National Laboratory. Approximately 1% of the fuel and debris remains in the vessel. TMI-2 is now under Post Defueling Monitored Storage. TMI-1 was only restarted in October 1985. During the shutdown, the plant was modified, and training and

Figure 15.6 Control room of the Evolutionary Pressure Reactor (EPR) from Areva, a Generation III+ PWR reactor. The control room has separate working areas for reactor and turbine operators, shift supervisor, as well as systems and screens to show a global plant overview. Courtesy of Teollisuuden Voima Oyj (TVO), Finland.

operating procedures were revamped in light of the lessons of TMI-2.

15.4 THE ACCIDENT AT CHERNOBYL

15.4.1 The RBMK

The Chernobyl site is located in the eastern part of a large region known as the Byelorussian-Ukrainian woodlands, on the banks of the Pripyat River, about 100 km away from Kiev, the capital of the Ukraine. The site had four Soviet-designed Reaktor Bolshoy Moshchnosty Kanalny'(RBMK, literally translated as "high-power channel reactor") BWRs with 3200 MW (thermal), 925 MW_e (net) power. Unlike Western-designed BWRs, the RBMK reactors do not have a pressure vessel; instead, the fuel assemblies are located inside individual pressure tubes, the so-called "technological channels," with some similarities to the ones of CANDU reactors [60]. However, the RBMK uses graphite as a moderator, instead of water, which makes it much larger than a BWR. The coolant water works as moderator and neutron absorber at the same time [44]. It was originally designed for plutonium and electricity production. The fuel channels are independent and can be isolated from the system, allowing the replacement of fuel assemblies without stopping the reactor [43].

The concept of the RBMK was developed over three generations: the first generation with the units of Chernobyl-1 and 2, Kursk-1 and 2, Leningrad-1 and 2; the second generation with Chernobyl-3 and 4, Kursk-3 and 4, Leningrad-3 and 4, Smolensk-1 and 2, Ignalina-1 and 2; and the third generation with the Smolensk-3 unit [56]. At the time of the accident there were 15 RBMK reactors in operation in the territory of the former Soviet Union.

Figure 15.7 shows a simplified layout of a RBMK reactor [61]. The core consists of an array of square cross-section graphite blocks, with 0.25 m side. The blocks are set together to form a cylinder with approximately 12 m diameter and 7 m height. There are 2,488 columns overall, 1,661 penetrated with fuel channels and 222 with control rod channels. Water is pumped from the bottom of the pressure tubes over the fuel. It removes the heat from the fuel, turns to steam in the process, and leaves the reactor core at the top, to the turbines, in an adjacent building. RBMK reactors use standard 500 MW_e turbines, in groups of two or three.

As in all pressure tube reactors, some (about 5%) of the heat released from fission leaks out to the moderator. In CANDU reactors, where the moderator water is separated from the cooling water, the moderator heat is removed by an independent cooling circuit, which keeps the moderator at about 70°C [60]. A similar arrangement cannot be done with graphite and, as a result, the graphite in the RBMK design operates at around 700°C. At this temperature, graphite cannot be exposed to air, because it would burn. The whole core is put inside a sealed steel case (shown in Fig. 15.7) designed to keep air away from the graphite. A mixture of inert gases (80% helium and 20% nitrogen)

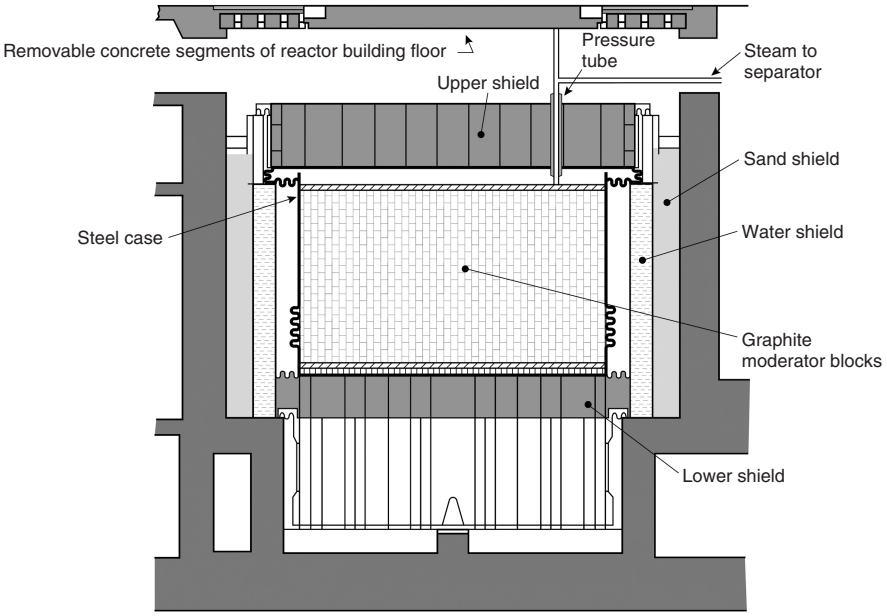

Figure 15.7 Simplified layout of the RBMK reactor of Chernobyl. Courtesy of Canteach.org.

circulates inside the container for additional cooling. The container was built so it could withstand the failure of a pressure tube without bursting and letting in air. The shielding of the RBMK reactor is made up of several blocks. The lateral shields are made of water, sand, and concrete, while the ones on the bottom and top are made of concrete. All the pressure tubes and control rods are attached to the top shield, which is a design feature that played a key role in the accident.

RBMK control rods have a unique combination of materials, with a graphite "follower" below the neutron absorber (boron carbide). The graphite displacer prevented coolant water from entering the space vacated as the rod was withdrawn, thus augmenting the rod's effect on reactivity. The rods were raised and lowered from above the core by a belt cable and motorized drum, at a speed of 40 cm per second for insertion [62]. With this system, full insertion of the control rods, including for emergency shutdown, took nearly 20 s [43], far longer than in Western-designed reactors.

The Chernobyl-4 reactor had only a partial containment. The pipes below the reactor core were inside "leak-tight boxes" connected to a huge pool of water under the whole building, the "bubbler pond." If one of the pipes in the boxes broke, the steam would be forced into the pond, where it would be trapped. In contrast, all steam pipes above the core were inside ordinary industrial buildings. Thus, if one of these pipes broke, particularly if the break were large, a release of radioactive steam would occur. The amount of radioactivity released would depend on how effective the shutdown and emergency cooling were in preventing damage to the fuel.

The USSR had several reasons for pursuing the RBMK design [43, 63]:

- An extensive engineering experience base with graphite-moderated, boiling-water-cooled reactors. The world's first commercial electricity, although at small scale, was generated in 1954 by a 5 MW_e RBMK in Obninsk.
- Existing manufacturing plants could fabricate major components.
- The reactor size was not limited by considerations related to fabrication, transportation, or installation of components.
- A large loss-of-coolant accident was thought to be virtually impossible because of the use of numerous pressure tubes rather than a single pressure vessel.
- Very efficient use fuel enriched to only 2%.
- Use of online refueling could achieve a very high plant capacity factor.

The USSR considered the RBMK to be its "national" reactor and showed considerable pride in the development of the design [63].

15.4.2 Accident sequence

As in the case of TMI-2, several descriptions of the accident at Chernobyl-4 were published, e.g., in accident reviews [9,

37], special reports [61, 63–65], dedicated books [62, 66], and in nuclear engineering books [42–44]. We will follow here a simplified outline, with the main events only.

The Chernobyl-4 reactor was scheduled to be shut down for routine maintenance on 25 April 1986. It was decided to take advantage of this shutdown to test the use of a turbine during its post-trip coastdown as a source of emergency electrical power for cooling the reactor core following an emergency shutdown, for a short period until the diesel emergency power supply would be online. The safe control of a loss-of-coolant accident with a simultaneous loss of off-site power was required by USSR regulations. This was expected to have been demonstrated during trial operation, with a fresh core. However, unit 4 had started operation in December 1983 without having performed this test [67]. Later, in 1985, the test had failed because the power delivered from the running down turbine fell off too rapidly.

The plan called for the power of the RBMK reactor to be reduced from the 3200 MW (thermal) full-power level to about 700–1000 MW (thermal) and for bypassing some safety systems that would have prevented the test conditions from being realized. In this power range one turbo generator would be in operation, and the second one would be switched off. The goal was to disconnect the remaining turbine and use its spinning energy to run a subset of the main pumps for a short while. Four main coolant pumps (including the two standby pumps) should continue to run during and after the test to ensure core cooling. These pumps therefore were connected to the normal electric network. The four remaining main coolant pumps were intended as the load for the turbo generator during the test. Accordingly, these pumps were supplied by the turbo generator prior to the test. It was expected that these pumps would phase out, following the decrease in power of the generator.

As scheduled, the control rods were inserted at 1:00 am on April 25 to reduce slowly the power to about 1600 MW (thermal), reached at 3:47 am. At 2:00 pm, the subsequent power reduction had to be postponed to meet power demand. The emergency core cooling systems were independently switched off at that time to prevent them from drawing power during the test—although this was a clear violation of operating procedures, as the test had just been postponed and the reactor continued to operate at half-power for several hours [64].

The reactor crew only received permission to continue reducing the power at 11:20 pm, with a different crew in control. Shortly after midnight, due to operator error or equipment failure, it was not possible to stabilize the reactor in the intended power range of 1000 to 700 MW (thermal), and the power fell to 30 MW (thermal). The test should have been cancelled at this point, due to the effects associated with the buildup of xenon, a strong neutron absorber.

The radioactive noble gas Xe135 is a known neutron absorber, produced directly as a fission product and indirectly from the decay of I135. The I135 is not a fission product, but appears as the result of the decay of another fission product, Te135. In normal operation at a given constant power, equilibrium is reached between the production of Xe135 and its removal by neutron capture reactions and by decay; the Xe135 "poisoning" thus represents a fixed absorption of neutrons, easily compensated with the control rods. However, when the reactor power goes down suddenly, the removal of Xe135 decreases less than its production, as removal by capture is done at the new, lower, neutron flux, and part of the production comes from the decay of the fission products previously generated at higher power. This creates a negative reactivity peak that has to be compensated with a significant removal of control rods or by waiting for the Xe135 isotope to decay.

The operators chose to withdraw the majority of the control rods to compensate the increase of Xe135, causing the power to climb and stabilize briefly at about 200 MW (thermal). A suitable number of control or safety rods should have been kept in a partially inserted position, for fast reactivity decrease if necessary, but the operators violated this rule [68].

At 1:03 am all eight pumps were activated to ensure adequate post-test cooling. This violated the maximum flow rate limit, so the corresponding automatic shutdown trip was deactivated. The resulting high coolant flow rate reduced coolant temperature and increased its density, thus introducing negative reactivity due to increased neutron absorption in the coolant, which required further control rod withdrawal. The increased coolant density also maximized the positive reactivity worth of coolant voiding. The combination of low power and high flow produced instabilities, which required numerous manual adjustments, causing the operators to deactivate other emergency shutdown signals.

At 1:22 am, the control system computer indicated excess reactivity in the core. In order to be able to complete the test, the operators blocked the last remaining trip signal just before it would have automatically shut down the reactor.

The turbine test was finally started at 1:23 am. As planned, four main pumps ran down. However, the reduction of coolant flow rate in the then-unstable core at low power led to a power excursion. During the power increase, the operators still began to insert the control rods from the fully withdrawn position. However, as the graphite followers of the rods entered the active core before the absorbing material, the replacement of neutron-absorbing water in the lower part of the core with graphite added positive reactivity, further accelerating the power increase.

The power surged to 100 times design full power in the next 4 s and then decreased momentarily. Then there were followed repeated power pulses, one of which may have reached 500 times the design full power. The fuel disintegrated, breached the cladding, and entered the water coolant, causing a steam explosion that lifted the top shield of the reactor core, shearing all the coolant pipes and removing all the control rods—because all these components were attached to the top shield. The explosion was well beyond the containment design basis and penetrated the concrete walls of the reactor building, dispersing burning fuel and graphite, and releasing a plume of radioactive gases and particles.

15.4.3 Consequences

With the containment totally breached, releases from Chernobyl attained a level never previously seen. The releases included fission product gases, other volatiles, particulates and aerosols, plus graphite debris from the reactor core [43]. The heat generated by the burning graphite dispersed the radionuclides high into the atmosphere. The weather conditions changed frequently during the first 10 days (until the fire was controlled) while the main releases occurred, causing radionuclides to be dispersed in several directions. The radionuclides were first transported at great height in a northwestern direction, via Bielorussia, toward Finland and Sweden. On the following day, the wind turned west, spreading the contaminated air masses over central Europe and later the United Kingdom. The release was discovered in Sweden on April 28. The USSR initially considered this matter an "internal affair" and did not acknowledge immediately that an accident had happened. Details were released slowly over the first week [43].

Figure 15.8 shows a simulation by the U.S. Atmospheric Release Advisory Center (ARAC) of the spread of the radioactive cloud on May 5, when it reached the United States. The levels of the various fission products detected in the United States were far below the maximum permissible concentration levels [69].

The total release from the accident is estimated at approximately 320 MCi, including 48 MCi of I131 and 2 MCi of Cs137 [70]. These are the most important radionuclides to consider, because they are responsible for most of the radiation exposure received by the general population.

The accident resulted in 30 early fatalities, mostly due to a combination of thermal burns and acute radiation exposure [14]. Over 1,000 people received large doses of radiation. Many of the nearby population received doses greater than 0.25 Sv, with the most serious in the range 0.4 to 0.5 Sv. All these values are well above the annual dose limit currently adopted for members of the public of 1 mSv.

In addition to those involved in early emergency operations, about 240,000 "liquidators" participated in major mitigation operations in the reactor and within 30 km around it, in the period 1986–1987. Mitigation activities continued at a relatively large scale until 1990. A total of 600,000 persons, civilian and military, have been recognized as liquidators [70]. Over one million people were possibly affected by radiation, according to the national registers in the Ukraine, Russia, and Belarus.

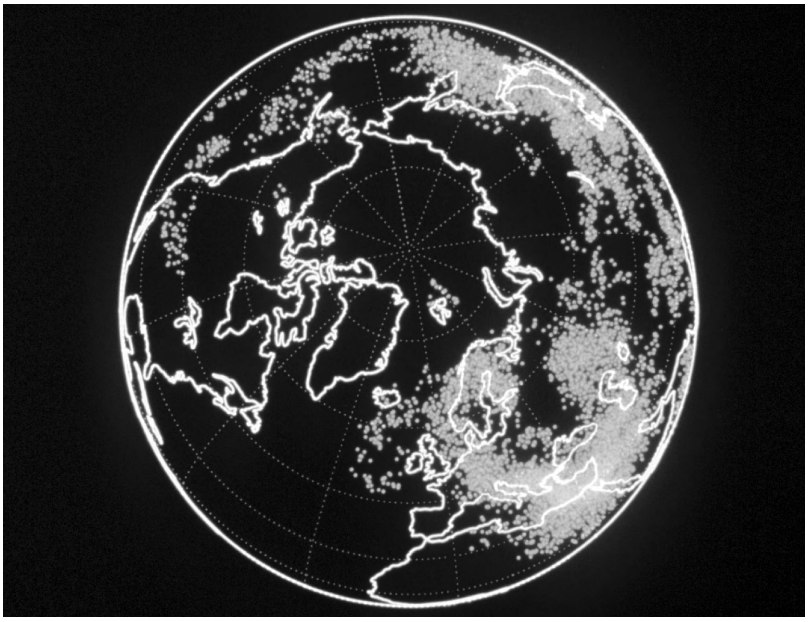

Figure 15.8 Simulation of the spread of radioactive cloud from Chernobyl, day 10. Courtesy of the U.S. Department of Energy.

Several studies on the health effects were made following the accident, see, e.g., references [14, 70–74]. About 4,000 cases of thyroid cancer in exposed children and adolescents have been diagnosed in the 1990–2002 period. However, the rapid increase in detected thyroid cancers suggests that some of it at least is an artifact of the screening process [14]. Thyroid cancer is usually not fatal if diagnosed and treated early. So far no increased risk of leukemia has been observed in children, liquidators, and in the general population. Increases in a number of nonspecific detrimental health effects other than cancer have been observed in liquidators and residents, but these are difficult to interpret, due to a lack of baseline for comparison [14].

The destroyed reactor is now inside a large concrete shelter that was erected quickly in 1987 to allow continuing operation of the other reactors at the Chernobyl site [75]. However, the structure is neither strong nor durable. Some major work on the shelter was carried out in 1998 and 1999. The total inventory of long-lived radionuclides in the shelter is estimated to be about 19 MCi. A new structure will be erected this decade, at an estimated cost of over US$ 1 billion. The direct economic cost of the Chernobyl-4 to the USSR was initially reported at 8 billion rubles (then US$ 13 billion) applied in recovery and purchase of replacement power. Outside the USSR the direct costs were estimated at US$ 1 billion [43].

15.4.4 Lessons Learned

Post-accident assessments identified design-related defects in RBMK reactors [63, 64]:

- Positive coolant void reactivity coefficient.
- Slow shutdown system.
- Easy-to-block safety systems.
- Absence of containment and emergency fission product control systems.

The term *positive void coefficient* is often associated with the RBMK reactors. Reactors cooled by boiling water always contain a certain amount of steam in the core. Water is both a more efficient coolant and a more effective neutron absorber than steam. A change in the proportion of steam bubbles, or "voids," in the coolant will result in a change in reactivity. In reactors where water is both a moderator and coolant, an increase in steam reduces the moderation of neutrons and leads to a reduction in power—this corresponds to a negative void coefficient, typical of Western-designed reactors. In the RBMK design, the neutron-absorbing properties of the cooling water are a significant factor in the operating characteristics. The reduction in neutron absorption as a result of steam production, and the consequent presence of extra free neutrons, increases power—corresponding to a positive void coefficient. The void coefficient is only one components of the global coefficient of reactivity, but in RBMK reactors, it is the dominant one. With a power increase, more steam is produced, which in turn leads to a further power increase. The immediate response to decrease the positive void effect in RBMK reactors was to insert 81 control rods in the core and block their movement. After that, as fuel assemblies were changed, the enrichment was increased to 2.4%.

Another problem was the slow movement of the control rods and their configuration. The graphite displacer increased the reactivity worth during removal. However, when the rod was inserted from the fully withdrawn position, the graphite created a positive effect, or a "positive scram," whose magnitude depended on the spatial distribution of the power density and on the operating regime of the reactor. This unwanted phenomenon had been identified in 1983 at the Ignalina-1 plant in Lithuania, but no corrective actions were taken [73]. After the accident, a minimum rod insertion of 1.3 m was enforced. Additionally, a fast shutdown system, 10 times faster, was tested at the Ignalina plant.

At Chernobyl-4, there was a ready capability for the operators to manually disable certain safety systems, bypass automatic scram trips, and suppress alarm signals. This could be done ordinarily by connecting jumper wires to accessible terminals. The operating procedures permitted such disabling under some circumstances [64]. Automatic engineered safety features were introduced after the accident to prevent disabling of reactor protections [76].

The investigation following the Chernobyl-4 accident also uncovered that two previous accidents had occurred in RBMK reactors, one at Leningrad-1 in 1975, another at Chernobyl-1 in 1982. The accident at Leningrad-1 is even considered to have been a precursor to the Chernobyl-4 accident [64]. The experimental determination of the void coefficients of the reactivity at Leningrad-1 after the accident led to the decision to increase the degree of enrichment from the original 1.8% up to 2%. This, however, did not solve completely the problem. One decisive reason for the disregard for these problems was the absence in the USSR, for a long time, of an independent nuclear regulatory authority, such as the NRC in the United States. The Ministry for Mechanical Engineering was responsible for both construction and monitoring until 1984 [77]. Additionally, the lack of communication and lack of exchange of information between the different organizations in the USSR prevented that lessons could be learned from these accidents.

The responsibility for the sequence of events that led to the accident is obviously largely due to operator error and bad management. Six members of plant management

were subsequently tried and convicted for violation of safety rules, criminal negligence, and abuse of power. The station director, chief engineer, and deputy chief engineer were sentenced to 10 years in a labor camp. However, the positive coolant temperature coefficient and the absence of a containment building designed to withstand overpressure events were also major contributors to the accident and the magnitude of its external effects.

In the period 1986–1989 all operating RBMK units went through several upgrades to correct the identified problems. The German Nuclear Safety Authority (GRS) declared in 1996 that "a repetition of the former explosion-like accident seems to be hardly possible today" [78]. Nevertheless, the RBMK design was effectively abandoned. Figure 15.9 shows the total net power installed with RBMK units since the 1970s. Data on the power and starting year of operation were taken from the PRIS database of the IAEA [12], while data on the expected closure year was taken from the World Nuclear Association [79]. Only two units were completed after the Chernobyl-4 accident, Ignalina-2 and Smolensk-3. On the other hand, Western nations pushed the Ukraine to close all units in the Chernobyl site after the fire in the turbine hall of Chernobyl-2 in 1991; the last unit to close was Chernobyl-3 in 2000. Later, the closure of the two units in Lithuania was negotiated during the accession of this country to the European Union [80]; the last unit to close was Ignalina-2, at the end of 2009. It is foreseen that the last RBMK unit will be closed in 2024 [79].

Meanwhile, Russia is effectively promoting its PWR designs. The AES-92 is a Generation III PWR with 1000 MW_e net electric output [81, 82]. It is based on the well-known VVER-1000 (from Vodo-Vodyanoi Energetichesky Reactor, literally translated as Water-Water Energetic Reactor), of which there are 28 units operating in Russia [83], the Ukraine [84], the Czech Republic [85], Bulgaria [86], and China [87]. The AES-92 is the first Russian design certified to comply with the requirements of European utilities [88]. Two AES-92 units are currently being built in India [89] and two more will be built in Bulgaria [86].

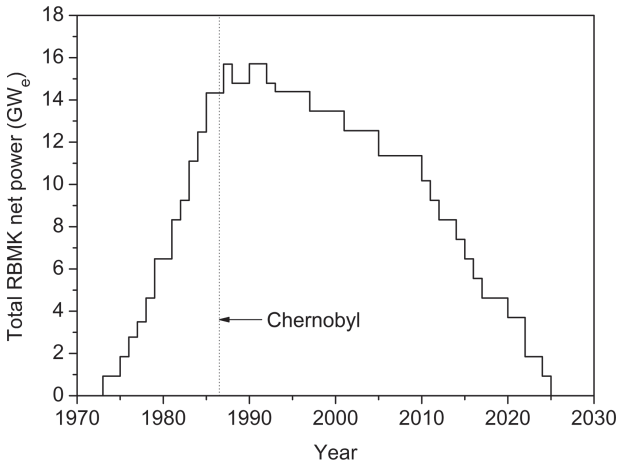

Figure 15.9 Net power installed with RBMK units.

The IAEA introduced the "International Nuclear Event Scale" after the Chernobyl accident, in order to communicate in a consistent way the safety significance of nuclear and radiological events. Events are classified on this scale at seven levels: Levels 1–3 are called "incidents" and Levels 4–7 "accidents" [90]. The scale is designed so that the severity of an event is about ten times greater for each increase in level on the scale. Levels 4–7 are named, respectively, "Accident with Local Consequences", "Accident with Wider Consequences", "Serious Accident" and "Major Accident". Events without safety significance are called "deviations" and are classified "Below Scale" or Level 0. The Chernobyl accident was classified as a Level 7 accident, while the one of TMI-2 was classified as a Level 5 accident, the same level that was attributed to the Windscale accident. The accident at Saint Laurent A2 was classified as a Level 4 event (local consequences only).

15.5 THE ACCIDENT AT FUKUSHIMA-I

15.5.1 Boiling Water Reactor

The Fukushima-I site is located in the eastern coast of the Honshū island, Japan, about 250 km north of Tokyo. The site contains 6 units of the BWR type, designed by General Electric (GE) and supplied by GE (Units 1, 2 and 6), Toshiba (Units 3 and 5) and Hitachi (Unit 4), connected to the grid between 1971 and 1979. The Tokyo Electric Power Company (TEPCO) operates the 6 units in Fukushima-I plus 11 units in other sites.

A BWR is so named because the water in the core is boiled. Steam is formed already in the pressure vessel and goes directly to the turbines, with no need for external steam generators as in a PWR. Both BWR and PWR technologies were developed in the 1950s. The pressure in a BWR is approximately 7 MPa, or about half the one in a PWR. The coolant flows downward between the inner wall of the pressure vessel and the core shroud, is distributed by the core plate, flows upward through the core and upper structure, and exits as steam at about 290 °C. About 30% of the coolant flow is recirculated, which has the net effect of increasing the coolant flow rate in the core [42]. The control of a BWR is different from the one of a PWR, as the direct cycle links thermal power, pressure, and water level. Thermal power in a BWR is changed either by the position of the control rods or through the re-circulation flow rate.

The Fukushima-I units 1 to 5 have containments with GE's Mark I design and Unit 6 has a Mark II type.

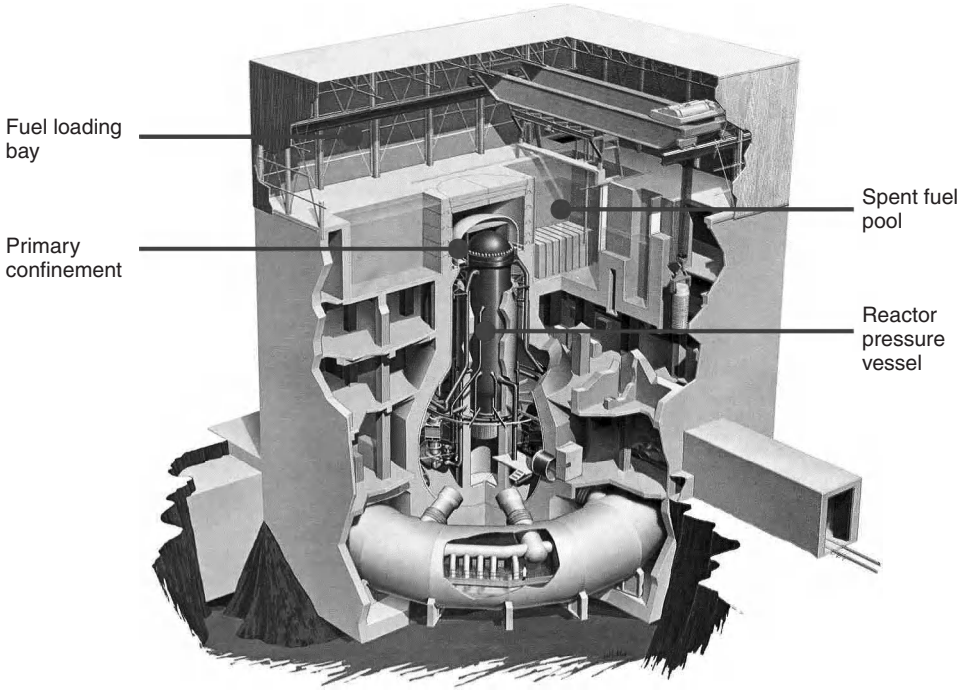

Figure 15.10 Cutaway view of a typical Mark I containment. Adapted from reference [91]. Courtesy of the Nuclear Regulatory Commission.

Figure 15.10 shows a cutaway of a typical Mark I building, adapted from reference [91]. The reactor pressure vessel and the recirculation pumps are inside a light-bulb shaped steel-lined pressure vessel, designated drywell, which is backed in most of its surface with reinforced concrete. The large doughnut-shaped vessel connected to the drywell is called the wetwell or suppression chamber. The wetwell contains a large amount of water and is designed to suppress the pressure surges that might result if all the water in the reactor were suddenly turned into steam. The drywell and the wetwell serve the same purpose for this type of BWR as the containment building does for PWRs. The building is a secondary containment, surrounding the primary containment and houses the core cooling systems and the spent fuel pool [7, 92].

15.5.2 Accident sequence

The accident sequence is not entirely clear at the time of writing. Several agencies, such as the IAEA, the Japanese Nuclear and Industrial Safety Agency (NISA), the NRC, and the French Radioprotection and Nuclear Safety Institute issued periodic reports with information obtained in Japan. The description and analysis given here are preliminary, based on the data available two weeks after the start of the accident [93–95].

The accident began at 2:46 pm (local time) on March 11, 2011, with a magnitude 9 earthquake (Richter scale) with epicenter approximately 72 kilometers east of the Oshika Peninsula of Tōhoku, or 373 km from Tokyo. The earthquake was followed by a tsunami. The Onagawa, Tokai, Fukushima-I and Fukushima-II sites, with a total of 14 power reactors, were the closest ones to the epicenter. Units 4, 5 and 6 at the Fukushima-I site were stopped at the time of the earthquake for routine maintenance and there was no fuel loaded on Unit 4. All operating reactors were automatically shut down by the earthquake. No major safety problems occurred in the Onagawa, Tokai and Fukushima-II sites. However, the earthquake damaged the transmission lines for off-site power to the Fukushima-I site and the tsunami affected the local diesel generators, resulting in a total loss of A/C power at 3:42 pm. Mobile diesel generators were brought on site still on March 11 allowing the limited use of water make-up and cooling systems, but some fuel damage had probably already occurred. Japanese authorities ordered the evacuation of residents within a 3 km radius of the Fukushima-I site and told people within a 10 km radius to remain indoors.

Upon automatic shutdown, the main heat source becomes the decay of the fission products in the core. When a reactor is operating at a certain power, fission products are produced continuously and also decay continuously. Immediately after shutdown these fission products, through their decay, produce about 6% of the power at which the reactor was operating [96]. Since no new fission products are being produced, this power will decrease over time,

although slowly. This decay heat (also named "residual heat") needs to be removed and several provisions exist to this end. However, the loss of power on the site limited the use of the cooling systems designed to keep the core properly cooled and covered. A worst case scenario at this point is that temperature in the fuel temperature rises to the point where exothermal Zr-steam reactions occur, releasing hydrogen and further increasing the temperature until the zircalloy cladding starts to melt, irreversibly damaging part of the fuel, as occurred in TMI-2.

As pressure increased in Unit 1, safety relief valves were used to reduce the pressure inside the reactor pressure vessel. The combination of steam and hydrogen flowing into the wetwell increased the temperature and pressure inside the wetwell. Since there was no means available to cool the water in the wetwell, venting became necessary to avoid a containment breach [92]. Evacuation within a 10 km radius was meanwhile started.

The venting was started at 2:30 pm on March 12 and resulted in a hydrogen explosion at 3:36 pm which damaged the top part of the secondary containment building. The primary containment of Unit 1 remained intact. Media in several countries wrongly reported the hydrogen explosion as an "explosion of the reactor".

NISA confirmed the presence of Cs137 and I131 in the vicinity of the reactor, but with levels decreasing fast. The evacuation zone was then extended to 20 km and iodine tablets started being distributed, although not administered. As a countermeasure to limit damage to the reactor core, TEPCO started injecting seawater mixed with boron into the primary containment of Unit 1 at 8:20 pm. The use of seawater is far from optimal, due to corrosion phenomena in the fuel and risk of blockage of valves and cooling orifices, but the top priority was the immediate cooling of the core.

Meanwhile the conditions in Unit 3 degraded. Venting operations were performed on March 12 and 13, followed by injection of seawater. Another venting operation on March 14 resulted in a hydrogen explosion at 11:01 am. A similar explosion occurred in Unit 2 the following day, March 15 at 06:10 am. High radiation levels were observed at the site at 09:00 am, with a dose rate of 11.9 mSv/h, but decreased fast. At this time, TEPCO informed that the primary containments of Units 1 and 3 were intact, while the wetwell of Unit 2 was possibly damaged.

New concerns arose the same day, this time with the spent fuel pools inside the secondary containment of the reactors. Once fuel is unloaded from a reactor core, it is stored in a pool for cooling before final storage or reprocessing. Water in a spent fuel pool is continuously cooled to remove the heat released by the decay of the fission products in the fuel. Water is used to remove the released heat and also as a radiation shielding. If the fuel is no longer covered by water, this will create a local radiation hazard (high radiation levels) at first and may escalate to a radioactive release if the fuel cladding is damaged. The power supplies to cool the pools at the Fukushima-I were also partially affected during the accident. With higher-than-usual water evaporation rates (and possibly some losses due to damage to the pools during the accident) it became necessary to replenish several times the pools in Units 1 to 4 using fire trucks in the days following the accident. The pools of Units 5 and 6 were not affected.

On March 17 operators were able to start one of the diesel generators in Unit 6 and a second generator 2 days later. The two generators were used to power cooling systems in Units 5 and 6. Unit 5 achieved a safe, cold shutdown on March 20, at 2:30 pm, while the same status was achieved in Unit 6 at 7:27 pm. Off-site power was gradually restored to the affected units during the following days. Fresh water started being injected into Units 1 and 3 on March 25 and in Unit 2 during the following day.

15.5.3 Consequences

At the time of writing it is too early to fully evaluate the consequences of the Fukushima-I accident. It was the first nuclear accident in more than one reactor at the same time. All reactors were automatically shut down with the onset of the earthquake, as expected. There was no apparent damage to the reactors due to the earthquake, even if the intensity was higher than considered in the safety studies. Unit 1 was designed for a peak ground acceleration of 0.18 g and a response spectrum based on the Taft record from the Southern California earthquake of 1952 [97]. No damage to the Fukushima-I units occurred after the 7.4 magnitude earthquake of June 12, 1978, with an epicenter approximately 140 km from the site [97].

The High Scientific Council of the European Nuclear Society declared on this respect that "It will be the task of seismologists and earth scientists to determine if the probability of occurrence of such extreme events have really been underestimated during the reactors design, or if these events are so exceptional that the residual risk could a priori be considered acceptable" [98].

The real extension of the damage to the cores of Units 1, 2 and 3 is unknown. In spite of that, the TMI-2 accident has shown that a core melt can be stopped even in an advanced state by renewed supply of coolant, without any deterioration of the reactor pressure vessel [99].

Radioactive releases from the accident reached the west coast of the U.S. on March 16–17 amidst a lot of attention from the media. A joint statement from the Environment Protection Agency (EPA) and the Department of Energy (DOE) on March 18 revealed traces of fission products in Sacramento (CA), with I131 at a concentration of 0.165 mBq/m^3 and Cs137 at a concentration of 0.002 mBq/m^3 [100]. These values are, respectively, 500 times and 20,000 times lower than the peak concentration

detected after the Chernobyl accident in the Livermore (CA) area [69]. A new statement from EPA on March 22 announced that the detailed measurements of air filters from monitors in California and Washington showed radiation levels hundreds of thousands to millions of times below levels of concern [101]. To put it further into perspective, EPA declared that "In a typical day, Americans receive doses of radiation from natural sources like rocks, bricks and the sun that are about 100,000 times higher than what we have detected coming from Japan. For example, the levels we're seeing coming from Japan are 100,000 times lower than what you get from taking a roundtrip international flight." [101].

The Japanese authorities have rated on March 18 the accidents in each of the Units 1, 2 and 3 as Level 5 in the INES scale, the same level as the TMI-2 accident. On April 12, the Japanese authorities estimated that the radioactive release into the atmosphere from the three units was approximately 10% of the amount released from the Chernobyl accident. The assessment of the Fukushima-I accident in the three units was then upgraded to Level 7, the same as Chernobyl, because the releases into the atmosphere were about 10 times higher than the minimum for a Level 7 event. Two weeks after the start of the accident there were no direct casualties due to radiation, although 17 workers have received doses in excess of 100 mSv, but below the 250 mSv limit defined by the Japanese authorities for this emergency work. The prompt evacuation of the population living in the vicinity of the Fukushima-I site has minimized their radiation exposure, so long-term public health consequences can be expected to be small.

15.6 CONCLUSIONS

The accident at the Chernobyl-4 fission reactor in 1986 was the most severe in the history of the nuclear power, having caused a significant release of radionuclides that spread over part of the northern hemisphere. Learning from accidents is essential to prevent the repetition of serious events and to improve long-term safety.

Edwin E. Kintner, the executive vice president of GPU Nuclear (owners of TMI), who oversaw the decontamination of the damaged TMI-2 reactor, characterized the accident as "a huge and costly safety experiment" that was "not well instrumented and terminated too soon" [43]. The TMI-2 accident did, however, provide a convincing demonstration of the safety of a properly engineered nuclear reactor. Two of the major credible accidents, loss of heat sink and loss of coolant, took place. Meanwhile, the operators were unaware of the real state of the reactor and took about the worst possible actions. Although the core was destroyed, no one got hurt, and radioactive releases were minimal. By the same token, TMI-2 exposed major deficiencies in reactor operating procedures, operator training, and exchange of safety-related operating information, which stimulated extensive subsequent improvements.

The Chernobyl-4 accident is generally judged to identify "no significant new lessons" for the nuclear industry outside the USSR [43]. Design-related lessons were not applicable elsewhere due to the unique characteristics of the RBMK. However, the Chernobyl accident helped to conclude the implementation of post-TMI changes. It was also a catalyst for the completion of several international agreements. The Early Notification of Nuclear Accidents [102] and the Emergency Assistance in the Event of a Nuclear Accident or Radiological Emergency [103] conventions were adopted by the General Conference of the IAEA still in 1986. Later, in 1994, the Convention on Nuclear Safety reaffirmed "the necessity of continuing to promote a high level of nuclear safety worldwide" [104]. The obligations of the parties to this convention cover the siting, design, construction, and operation of nuclear installations, the availability of adequate financial and human resources, and the assessment and verification of safety, quality assurance, and emergency preparedness.

The experience of TMI-2 and Chernobyl-4 has led to an emphasis on passive safety in the design of advanced reactors. The recent accident at Fukushima-I reinforced this approach, given the consequences of the failure of the power supplies necessary for active systems. The objectives of passive safety design are, to the extent possible, for the reactor to be able to maintain a balance between power production and heat removal, to shut itself down when an abnormal event occurs, and to remove decay heat, without requiring operator action or the functioning of engineered safety systems.

Generation III/III+ reactors, whose construction started in the 1990s, have an increased reliance on passive safety [105]. These new designs feature a reduced probability of occurrence of accidents involving core melting, quantified by a Core Damage Frequency (CDF) that is well below the 1×10^{-5} events per reactor-year value recommended by the IAEA in 1999 [106]. The NRC requires plants to have a CDF below 1×10^{-4} events per reactor-year. The CDF of the Economic Simplified Boiling Water Reactor (ESBWR) from General Electric is currently the lowest of all Generation III/III+ designs, at 2.8×10^{-8} events per reactor-year for initiating events occurring during power operation, and at 3.36×10^{-8} events per reactor-year when the plant is shut down [107].

The nuclear fission industry has learned much with nuclear accidents and has taken clear steps to reduce or eliminate the consequences of such accidents through better training, the development of more realistic accident management strategies, and, ultimately, the development of advanced reactor designs.

Acknowledgments

The author gratefully acknowledges Teollisuuden Voima Oyj (Finland) and the World Nuclear Association (UK) for their permission to reproduce images for this work. Mr. Jiri Mandula (International Atomic Energy Agency, Austria) is kindly acknowledged for his assistance in obtaining data from the PRIS database.

REFERENCES

1. J.H. Gittus, *Nuclear Power—A Perspective*, Proceedings of International Approach to Nuclear Safety After Three Mile Island and Chernobyl, June 1988, G.M. Ballard (Ed.), Elsevier Applied Science Publishers, Barking, 1988.
2. F.E. Haskin, A.L. Camp, and S.A. Hodge, *Perspectives on Reactor Safety*, NUREG/CR-6042, Rev. 1. NRC, Washington, 1997.
3. United Nations Scientific Committee on the Effects of Atomic Radiation, *Sources and Effects of Ionizing Radiation*, UNSCEAR 2000, vol. 1, Bernan, Blue Ridge Summit, 2001, 182–188.
4. M. Eisenbud and T. Gesell, *Environmental Radioactivity from Natural, Industrialm and Military Sources*, 4th ed. Academic Press, San Diego, 1997, 418–419.
5. R. Cowan, Nuclear Power Reactors: A Study in Technological Lock-in, *The Journal of Economic History*, 1990, **50**, 541–567.
6. B. Goldshmidt, *The Atomic Complex: A Worldwide Political History of Nuclear Energy*. American Nuclear Society, La Grange Park, 1982, 257–276.
7. H.W. Bertini, *Descriptions of Selected Accidents that Have Occurred at Nuclear Reactor Facilities*, ORNL/NSIC-176, Oak Ridge, TN, 1980.
8. D. Bastien, *Twenty-Nine Years of French Experience in Operating Gas-Cooled Reactors*, International Working Group on Gas-Cooled Reactors (IWGGCR-19), International Atomic Energy Agency, Vienna, 1988, 113–119.
9. D. Mosey, *Reactor Accidents*, 2nd ed. Nuclear Engineering International, Sidcup, 2006.
10. M. Eisenbud and T. Gesell, *Environmental Radioactivity from Natural, Industrial, and Military Sources*, 4th ed. Academic Press, San Diego, 1997, 254.
11. B. Goldshmidt, *The Atomic Complex: A Worldwide Political History of Nuclear Energy*. American Nuclear Society, La Grange Park, 1982, 347–359.
12. International Atomic Energy Agency, Power Reactor Information System (PRIS), http://www.iaea.org/programmes/a2/.
13. R. Wakeford, The Windscale reactor accident—50 years on, *Journal of Radiological Protection*, 2007, **27**, 211–215.
14. World Health Organization, *Health Effects of the Chernobyl Accident and Special Health Care Programmes*. WHO, Geneva, 2006.
15. Atomic Energy of Canada Limited, *Canada Enters the Nuclear Age: A History of Atomic Energy of Canada Limited*. McGill-Queen's University Press, Montreal & Kingston, 1997.
16. T.J. Thomson and J.G. Beckerley, *The Technology of Nuclear Reactor Safety*, vol. 1. The MIT Press, Cambridge, 1964, 619–622.
17. N. Wade, Carter as Scientist or Engineer: What Are His Credentials?, *Science*, 1976, **193**, 462–463.
18. National Park Service, *Listing of National Historic Landmarks by State*, NPS, Washington, June 2010. http://www.nps.gov/.
19. L. Arnold, *Windscale 1957: Anatomy of a Nuclear Accident*, 3rd ed. Palgrave MacMillan, Basingstoke, 2007.
20. J.A. Garland and R. Wakeford, Atmospheric emissions from the Windscale accident of October 1957, *Atmospheric Environment*, 2007, **41**, 3904–3920.
21. Atomic Energy Authority, *Pile Reactors—Phase One Decommissioning*, UKAEA, 2008. http://www.ukaea.co.uk/.
22. Institute of Medicine, *Isotopes for Medicine and the Life Sciences*. National Academy Press, Washington, 1995.
23. T.J. Thomson and J.G. Beckerley, *The Technology of Nuclear Reactor Safety*, vol. 1. The MIT Press, Cambridge, 1964, 636–638.
24. R.L. Ashley, R.J. Beeley, F.L. Fillmore, W.J. Hallett, B.R. Hayward, T.L. Gershun, and J.G. Lundholm, *SRE Fuel Element Damage*. Atomics International, NAA-SE-4488, 1959.
25. T.J. Thomson and J.G. Beckerley, *The Technology of Nuclear Reactor Safety*, vol. 1. The MIT Press, Cambridge, 1964, 638–645.
26. J.W. Carroll, *Sodium Reactor Experiment Decommissioning: Final Report*. Rockwell International, ESG-DOE-13403, 1983.
27. T.J. Thomson and J.G. Beckerley, *The Technology of Nuclear Reactor Safety*, vol. 1. The MIT Press, Cambridge, 1964, 645–653.
28. Atomic Energy Commission, *IDO Report on the Nuclear Incident at the SL-1 Reactor*, IDO-19302. AEC Idaho Operations Office, Idaho, 1962.
29. International Atomic Energy Agency, *Derivation of the Source Term and Analysis of the Radiological Consequences of Research Reactor Accidents*, Safety Reports Series No. 53. IAEA, Vienna, 2008.
30. A.M. Weinberg, *The First Nuclear Era: The Life and Times of a Technological Fixer*. American Institute of Physics, New York, 1994.
31. M.W. Rosenthal, *An Account of Oak Ridge National Laboratory's Thirteen Nuclear Reactors*, ORNL/TM-2009/181. ORNL, Oak Ridge, 2009.
32. R.L. Scott, Fuel melting incident at the Fermi reactor on Oct. 5 1966, *Nuclear Safety*, 1971, **12**, 123–134.
33. R.H. Krieg, E.E. Hickey, J.R. Weber, and M.T. Masnik, Decommissioning of nuclear power plants, *Encyclopedia of Energy*, Volume 4. Elsevier, 2004, 409–420.

34. International Atomic Energy Agency, *Decommissioning of Underground Structures, Systems and Components*, Technical Reports Series No. 439. IAEA, Vienna, 2006, 123–136.
35. World Nuclear Association, Three Mile Island Accident, Information paper No. 36, WNA, 2010. http://www.world-nuclear.org/info/inf36.html.
36. R. Schreiber, Pressurized Water Reactors, in *Nuclear Engineering Handbook*, K.D. Kok, ed. CRC Press, Boca Raton, 2009, 9–82.
37. T. Kletz, *Learning from Accidents*, 3rd ed. Gulf Professional Publishing, Oxford, 2001.
38. J.G. Kemeny, B. Babbitt, P.E. Haggerty, C. Lewis, P.A. Marks, C.B. Marrett, L. McBride, H.C. McPherson, R.W. Peterson, T.H. Pigford, T.B. Taylor, and A.D. Trunk, *Report of the President's Commission on the Accident at Three Mile Island*. Washington, 1979.
39. M. Rogovin, G.T. Frampton Jr, *Three Mile Island—A Report to the Commissioners and to the Public*, NUREG/CR-1250, vol. 1. Nuclear Regulatory Commission, Washington, 1980.
40. B.A. Osif, A.J. Baratta, T.W. Conkling, *TMI 25 Years Later: The Three Mile Island Nuclear Power Plant Accident and its Impact*. The Pennsylvania State Universiy Press, University Park, 2004.
41. J.S. Walker, *Three Mile Island: A Nuclear Crisis in Perspective*. University of California Press, Berkeley, 2004. ISBN 0-520-23490-7.
42. W.M. Stacey, *Nuclear Reactor Physics*, 2nd ed. Wiley-VCH, Weinheim, 2007, 249–255.
43. R.A. Knief, *Nuclear Engineering: Theory and Technology of Commercial Nuclear Power*, 2nd ed. Taylor and Francis, Washington, 1992, 423–450.
44. J.R. Lamarsh and A.J. Baratta, *Introduction to Nuclear Engineering*, 3rd ed. Prentice-Hall, Upper Saddle River, 2001, 686–693.
45. M.S. Veshchunova and P. Hofmann, Dissolution of solid UO_2 by molten zircaloy, *Journal of Nuclear Materials*, 1994, **209**, 27–40.
46. M. Eisenbud and T. Gesel, *Environmental Radioactivity from Natural, Industrial, and Military Sources*, 4th ed. Academic Press, San Diego, 1997, 232–240.
47. J. Mangano, Three Mile Island: health study meltdown. *Bulletin of the Atomic Scientists*, 2004, **60**, 5, 30–35.
48. E.O. Talbott, A.O. Youk, K.P. McHugh, J.D. Shire, A. Zhang, B.P. Murphy, and R.A. Engberg, Mortality among the residents of the Three Mile Island accident area: 1979-1992, *Environmental Health Perspectives*, 2000, **108**, 545–552.
49. National Council on Radiation Protection and Measurements, *Exposure of the Population in the United States and Canada from Natural Background Radiation*, NCRP Report No. 92. NCRP, Bethesda, 1998.
50. United Nations Scientific Committee on the Effects of Atomic Radiation, *Sources and Effects of Ionizing Radiation*, UNSCEAR 2000, vol. 1. Bernan, Blue Ridge Summit, 2001, 84–156.
51. M.C. Hatch, J. Beyea, J.W. Nieves, and M. Susser, Cancer near the Three Mile Island nuclear plant: radiation emissions, *American Journal of Epidemiology*, 1990, **132**, 397–412.
52. M.C. Hatch, S. Wallenstein, J. Beyea, J.W. Nieves, and M. Susser, Cancer rates after the Three Mile Island nuclear accident and proximity of residence to the plant. *American Journal of Public Health*, 1991, **81**, 719–724.
53. S. Wing, D. Richardson, D. Armstrong, and D. Crawford-Brown, A reevaluation of cancer incidence near the Three Mile Island nuclear plant: the collision of evidence and assumptions, *Environmental Health Perspectives*, 1997, **105**, 52–57.
54. E.O. Talbott, A.O. Youk, K.P. McHugh-Pemu, and J.V. Zborowski, Long-term follow-up of the residents of the Three Mile Island accident area: 1979-1998. *Environmental Health Perspectives*, 2003, **111**, 341–348.
55. G.E. Cummings, Operator/Instrumentation interactions during the Three Mile Island incident. *IEEE Transactions on Nuclear Science*, 1980, **NS-27**, 931–934.
56. International Atomic Energy Agency, *Modern Instrumentation and Control for Nuclear Power Plants: a Guidebook*, Technical Reports Series No. 387. IAEA, Vienna, 1999.
57. International Atomic Energy Agency, *Instrumentation and Control Systems Important to Safety in Nuclear Power Plants*, Safety Guide No. NS-G-1.3. IAEA, Vienna, 2002.
58. Teollisuuden Voima Oyj, Nuclear Power Plant Unit Olkiluoto 3, TVO, Helsinki, 09/2008. http://www.tvo.fi.
59. N.J. McCormick, Changes in the nuclear power industry after TMI. *Progress in Nuclear Energy*, 1982, **10**, 245–248.
60. A.I. Miller, J. Luxat, E.G. Price, R.B. Duffey, and P.J. Fehrenbach, Heavy water reactors, in *Nuclear Engineering Handbook*, K.D. Kok, ed. CRC Press, Boca Raton, 2009, 141–196.
61. V.G. Snell and J.Q. Howieson, *Chernobyl—A Canadian Perspective*. Atomic Energy of Canada Limited, 1991. http://canteach.candu.org/.
62. Z. Medvedev, *The Legacy of Chernobyl*. W.W. Norton and Company, New York, 1990.
63. Nuclear Regulatory Commission, *Report on the Accident at the Chernobyl Nuclear Power Station*, NUREG-1250. NRC, Washington, 1987.
64. International Atomic Energy Agency, *The Chernobyl Accident: Updating of INSAG-1*, Safety Series No. 75-INSAG-7. IAEA, Vienna, 1992.
65. Gesellschaft für Anlagen- und Reaktorsicherheit (GRS), *The Accident and the Safety of RBMK Reactors*, GRS-121. GRS, Cologne, 1996.
66. G. Medvedev, *The Truth About Chernobyl*. Basic Books, New York, 1991.
67. Gesellschaft für Anlagen- und Reaktorsicherheit (GRS), *The Accident and the Safety of RBMK Reactors*, GRS-121. GRS, Cologne, 1996, 39.
68. Gesellschaft für Anlagen- und Reaktorsicherheit (GRS), *The Accident and the Safety of RBMK Reactors*, GRS-121, GRS, Cologne, 1996, 48.

69. J.M. Beiriger, R.A. Failor, K.V. Marsh, and G.E. Shaw, Radioactive fallout from the Chernobyl nuclear reactor accident. *Journal of Radioanalytical and Nuclear Chemistry*, 1988, **123**, 21–37.
70. United Nations Scientific Committee on the Effects of Atomic Radiation, *Exposures and Effects of the Chernobyl Accident*, UNSCEAR 2000, vol. 2. Bernan, Blue Ridge Summit, 2001, 451-566.
71. Nuclear Energy Agency, *Chernobyl: Assessment of Radiological and Health Impacts*. NEA, Paris, 2002.
72. M. Rahu, Health effects of the Chernobyl accident: fears, rumours and the truth. *European Journal of Cancer*, 2003, **39**, 295–299.
73. International Atomic Energy Agency, *Environmental Consequences of the Chernobyl Accident and Their Remediation: Twenty Years of Experience*. IAEA, Vienna, 2006.
74. V.G. Bebeshko, D.A. Bazyka, and V. Buzunov, Chernobyl: current situation of non-cancer diseases, *International Congress Series*, 2007, **1299**, 54–59.
75. World Nuclear Association, *Chernobyl Accident, Information Paper No. 7, WNA, 2009*. http://www.world-nuclear.org/info/inf07.html.
76. N.M. Sorokin, B.A. Gabaraev, and Y.M. Cherkashov, Safe operation and life extension of RBMK plants. *Nuclear Engineering and Design*, 2006, **236**, 1648–1656.
77. Gesellschaft für Anlagen- und Reaktorsicherheit (GRS), *The Accident and the Safety of RBMK Reactors*, GRS-121, GRS, Cologne, 1996, 45.
78. Gesellschaft für Anlagen- und Reaktorsicherheit (GRS), *The Accident and the Safety of RBMK Reactors*, GRS-121. GRS, Cologne, 1996, 133.
79. World Nuclear Association, *RBMK Reactors*, Information Paper No. 31, WNA, 2010. http://www.world-nuclear.org/info/inf31.html.
80. Protocol Nr. 4 on the Ignalina Nuclear Power Plant in Lithuania, *Official Journal of the European Union* L 236, 23 September 2003, 944–945.
81. Y. Ermakov and O. Rousselot, EUR Volume 3 AES 92 Subset, European Utility Requirements Seminar 2007, Nice, 2007. http://www.europeanutilityrequirements.org/.
82. International Atomic Energy Agency, *Status of Advanced Light Water Reactor Designs 2004*, TECDOC-1391, IAEA. Vienna, 2004, 337–358.
83. World Nuclear Association, *Nuclear Power in Russia*, Information Paper 45, March 2010. http://www.world-nuclear.org/.
84. World Nuclear Association, *Nuclear Power in Ukraine*, Information Paper 46, March 2010. http://www.world-nuclear.org/.
85. World Nuclear Association, *Nuclear Power in the Czech Republic*, Information Paper 90, April 2010. http://www.world-nuclear.org/.
86. World Nuclear Association, *Nuclear Power in Bulgaria*, Information Paper 87, February 2010. http://www.world-nuclear.org/.
87. World Nuclear Association, *Nuclear Power in China*, Information Paper 63, February 2010. http://www.world-nuclear.org/.
88. P. Berbey, *Status and Near-Term Works on the EUR document—Possible Use by Third Parties*, International Conference on Opportunities and Challenges for Water Cooled Reactors in the 21st Century, IAEA-CN-164-3S01. IAEA, Vienna, 27–30 October 2009. http://www.europeanutilityrequirements.org/.
89. World Nuclear Association, *Nuclear Power in India*, Information Paper 53, March 2010. http://www.world-nuclear.org/.
90. International Atomic Energy Agency, *INES The International Nuclear and Radiological Event Scale User's Manual*, IAEA, Vienna, 2008.
91. Nuclear Regulatory Commission, *Boiling Water Reactor (BWR) Systems*, USNRC Technical Training Center, NRC, Washington, rev 0200 (undated).
92. Nuclear Energy Institute, *Mark I Containment Report*, NEI, Washington, March 19, 2011, http://www.nei.org, accessed March 21, 2011.
93. Nuclear and Industrial Safety Agency, *Seismic Damage Information (56th Release)*, March 27, 2011, NISA, Tokyo, http://www.nisa.meti.go.jp/english/, accessed March 27, 2011.
94. Institut de Radioprotection et de Sûreté Nucléaire, *Situation des installations nucléaires au Japon suite au séisme majeur survenu le 11 Mars 2011: Point de situation du 26 Mars 2011 à 10 heures*, IRSN, Fontenay-aux-Roses, http://www.irsn.fr/, accessed March 27, 2011.
95. International Atomic Energy Agency, *Fukushima Nuclear Accident Update: Update of 27 March 2011*, IAEA, Vienna, <www.iaea.org>, accessed March 27, 2011.
96. American Nuclear Society, *Decay heat power in light water reactors*, ANSI/ANS-5.1-2005, ANS, La Grange Park, 2005.
97. National Bureau of Standards, *An Investigation of the Miyagi-ken-oki, Japan, Earthquake of June 12, 1978*, NBS Special Publication 592, Washington, 1980.
98. European Nuclear Society, *Statement on the Japanese Nuclear Accident*, ENS, Brussels, http://www.euronuclear.org/1-expert/japan2011.htm, accessed March 18, 2011.
99. K.H. Neeb, *The Radiochemistry of Nuclear Power Plants with Light Water Reactors*, Walter de Gruyter & Co, Berlin, 1997, 690.
100. Environmental Protection Agency, *Joint EPA/DOE statement: Radiation monitors confirm that no radiation levels of concern have reached the United States*, EPA, Washington, Released March 18, 2011.
101. Environmental Protection Agency, *Radiation monitors continue to confirm that no radiation levels of concern have reached the United States*, EPA, Washington, Released March 22, 2011.
102. International Atomic Energy Agency, *Convention on Early Notification of a Nuclear Accident*, INFCIRC/335, IAEA, Vienna, 1986.

103. International Atomic Energy Agency, *Convention on Early Notification of a Nuclear Accident*, INFCIRC/336, IAEA, Vienna, 1986.

104. International Atomic Energy Agency, *Convention on Nuclear Safety*, INFCIRC/449, IAEA, Vienna, 1994.

105. J.G. Marques, A Review of Generation-III/III+ Fission Reactors, this volume.

106. International Nuclear Safety Advisory Group, *Basic Safety Principles for Nuclear Power Plants*, 75-INSAG-3 Rev. 1, STI/PUB/1082, IAEA, Vienna, 1999, 11–12. ISBN 92-0-102699-4.

107. Health and Safety Executive, *New Reactor Build: GEH ESBWR Step 2 PSA Assessment*, 2008. http://www.hse.gov.uk/.

16

SPENT FUEL AND WASTE DISPOSAL

Clifford Singer[1] and William R. Roy[2]
[1]*Department of Nuclear Plasma, and Radiological Engineering, University of Illinois at Urbana-Champaign, Urbana, IL, USA*
[2]*Div. State Geological Survey, University of Illinois at Urbana-Champaign, Urbana, IL, USA*

A nuclear fuel cycle follows reactor fuel from the cradle to the grave. The simplest nuclear fuel cycle is the once-through approach. This cycle entails uranium mining, fuel fabrication, burning, followed by cooled storage of reactor fuel discharge under convectively cooling conditions, then permanent underground storage while being conductively cooled. In a more complex approach, spent reactor fuel is set aside for re-use in power production before the completion of the fuel cycle. Four types of nuclear reactors have both been used on a commercial scale for electricity production and are being considered for further use. The coolants in these reactors are (1) ordinary ("light") water, (2) heavy water (deuterium oxide, D_2O), (3) helium, and (4) liquid sodium. Commercial light water reactors have been fueled with uranium oxide and occasionally with a mixture of uranium and plutonium oxides (MOX). Commercial heavy water reactors are fueled with a uranium oxide. Helium-cooled reactors have been fueled with uranium in graphite. With the exception of a few trial projects, commercial nuclear power production uses light and heavy water reactors.

The only liquid sodium-cooled reactor that operated with an average of over half of design capacity was fueled primarily with enriched uranium excess to Soviet military needs. Russia plans to bring online in 2014 a new 800 megawatt-electric (MWe) liquid sodium-cooled reactor that would burn excess weapons plutonium (Podveg, 2010). India has constructed a 500 MWe liquid sodium-cooled reactor to be fueled with plutonium recovered from some of its heavy water reactor discharges.

Fuel discharged from water-cooled reactors is initially stored under water for convective removal of the intense decay heat from short-lived radioisotopes (Fig. 16.1). Upon removal from this pool, there are five possible pathways for spent fuel in the fuel cycle. In ascending order of the amount of energy that can be extracted from the original mined uranium, these are the following: (a) storage in air-cooled ("dry") casks (Fig. 16.2) pending burial, (b) storage in dry casks pending heating to remove volatile materials and reuse as a powder, (c) near-term aqueous/organic extraction to extract plutonium for reuse as MOX fuel, (d) storage in dry casks pending aqueous/organic extraction to extract uranium and plutonium for reuse, and (e) aqueous/organic extraction of plutonium for use in liquid sodium-cooled reactors.

For aqueous/organic extraction, the most common process is called PUREX, which is an acronym for Plutonium-URanium EXtraction. In countries that reuse spent fuel on a large scale, so far primarily France, prompt reprocessing after removal of spent fuel from pool storage has been favored. Reactor discharges contain the isotope plutonium-241, which decays with a half-life of 14.4 years to americium-241 (Table 16.1). Am241 in turn decays with a half-life of 432 years and emits penetrating gamma radiation, which provides an incentive to minimize Am241 content. Commercial reactor fuel fabrication facilities have been built to handle plutonium with increasingly large concentrations of Am241.

Once spent nuclear fuel has aged enough for most of the Pu241 to have decayed, radiolytic destruction of organic compounds used during aqueous/organic extraction is reduced if the fuel has been aged long enough for most of the strontium-90 and cesium-137 to decay as well. Then, the longer the wait until spent fuel is reprocessed, the easier

Nuclear Energy Encyclopedia: Science, Technology, and Applications, First Edition (Wiley Series On Energy).
Edited by Steven B. Krivit, Jay H. Lehr, and Thomas B. Kingery.

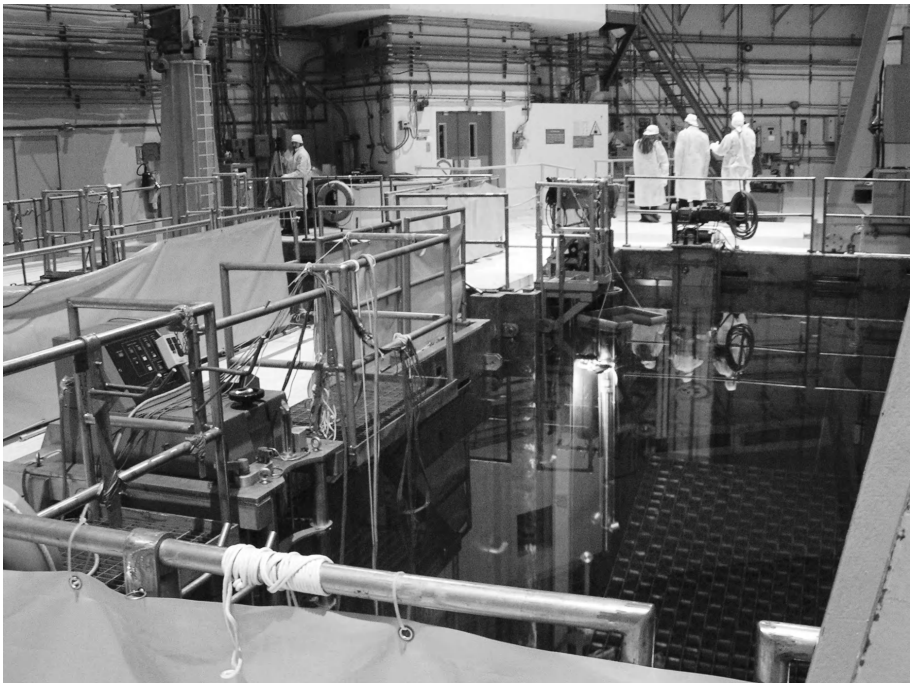

Figure 16.1 Storage of spent nuclear fuel in a pool at a power plant.

Figure 16.2 Dry storage casks for spent nuclear fuel. *Source*: Holtec International, http://www.holtecinternational.com/.

the reprocessing should be. With their high production rates from fission and their respective half-lives of 29 and 30 years respectively, Sr90 and Cs137 dominate the radioactive heat release in spent fuel from less than 10 years to about 100 years after reactor discharge (Table 16.1).

Elements with atomic numbers larger than uranium's 92 protons are called *transuranics* and are all radioactive. In spent nuclear fuel, these can include americium, plutonium, and smaller amounts of neptunium and curium derived from uranium and other transuranics by neutron capture and subsequent radioactive decays. Three major approaches to convectively cooled, underground storage of spent nuclear fuel components that include transuranics have been taken to or beyond the point of submission of site license applications. These are (1) salt deposits such as New Mexico's Waste Isolation Pilot Plant (WIPP),

TABLE 16.1 Some Spent Fuel Isotopes with 10 to 1,000,000 Year Half-lives

Transuranic Actinides		t-1/2 yr	% of Pu	Impact
Plutonium	PU242	380,000	5	Minor
"	Pu241	14	14	Am241 source
"	Pu240	6,537	23	Hard to burn out
"	Pu239	24,110	57	Weapons usable
"	Pu238	88	1	Minor
Americium	Am241	432		Burial density
Fission Products		**t-1/2 yr**	**#/fission**	**Impact**
Strontium	Sr90	29	0.06	Convective cooling
Cesium	Cs137	30	0.06	Convective cooling
Technetium	Tc99	213,000	0.06	Groundwater contaminant

Plutonium fractions are for a typical pressurized water reactor with a comparatively low burnup of 33 GW-days-theraml per metric ton.

Yields per fission are for U235 in a water moderated reactor, after decay of short-lived percursors.

Sources: Lawrence Berkeley Laboratory. 1998. Fission Product Yields http://isotopes.lbl.gov/fission.html, accessed April 15, 2009; Albright, David, Frans Berkhout, and William Walker.

Plutonium and Highly Enriched Uranium 1996: World Inventories, Capabilities, and Policies. Oxford University Press.

(2) crystalline rock in a non-oxidizing environments as used by Finland and Sweden, and (3) volcanic tuff in an oxidizing environment for Nevada's Yucca Mountain site. See Table 16.2 for a comparison of these repository designs.

Salt deposits are thought to be suitable for radioactive material emplacements when there is no intention of recovering the material such as for future reprocessing. WIPP is used for emplacement of those military program transuranics without associated fission products. Materials placed in WIPP are thought not to be suitable for reuse.

Finland and Sweden are enclosing spent fuel in copper casings designed to remain intact for millions of years in a non-oxidizing environment (Figure 16.3), as does native copper in nature. Such a repository is not designed to maintain convective cooling until most of the Am241 decays. Crystalline rocks like granite have higher heat conductivity than volcanic tuff and, thus, allow a greater packing density of the waste packages. However, the amounts of material that Finland and Sweden plan to emplace are respectively only 9,300 and 6,500 metric tons of heavy metal (MTHM, almost all of which is uranium). These amounts are small enough that high packing density was probably not a determining factor in the choice of site type.

The U.S. Nuclear Waste Policy Act of 1982 as Amended (NWPA) restricted the capacity of the Yucca Mountain site to the equivalent of commercial spent fuel containing 70,000 MTHM, with a tenth of the capacity planned to be used for military program materials. With more than the 63,000 MTHM allocated to commercial spent fuel to have been exceeded by U.S. commercial reactor discharges by 2011, U.S. law required the Department of Energy to assess the need for licensing a second repository site starting in 2009. The U.S. administration in place at the time decided instead to reassess the country's entire spent fuel management approach, and appointed a Blue Ribbon

TABLE 16.2 Finnish, Swedish, and U.S. Repositories

Country	Sites	Capacity MTHM	Above Water Table?	Oxygen?	Waste Envelope	Rock Type	Near Reactors?	Earliest Start
Finland	1	6,500	No	Reducing	Copper	Crystalline	Yes	2020
Sweden	2	9,300	No	Reducing	Copper Nickel	Crystalline	Yes	2017
USA	1	70,000	Yes	Oxidizing	Alloy	Volcanic	No	2020

Also, the Waste Isolation Pilot Plant (WIPP) in New Mexico, a salt formation licensed to start taking transuranic defence wastes and isolate them for 10,000 years. Current U.S. requirements for unreprocessed spent nuclear fuel limit exposures to a single individual limit due to releases to groundwater to 100 millirem/year (i.e. less than minimum background exposure) for a million years in addition to a limit of 15 millirem/year for the first 10,000 years. WIPP is not licensed to accept unreprocessed spent nuclear fuel.

Sources: IAEA. 2009. Geological disposal of radioactive waste: Technological implications for retrievability, Technical Report NW-T-1.19; Rampe, Norbert. 2007. Permanent underground repositories for radioactive waste, *Progress in Nuclear Energy* **49**, 365; Vandenbosch, Robert and Sussane Vandenbosch. 2009. The revised radiation protection standards for the Yucca Mountain nuclear waste repository, APS Physics & Society, http://www.aps.org/units/fps/newsletters/200901/vandenbosch.cfm, accessed April 15, 2005.

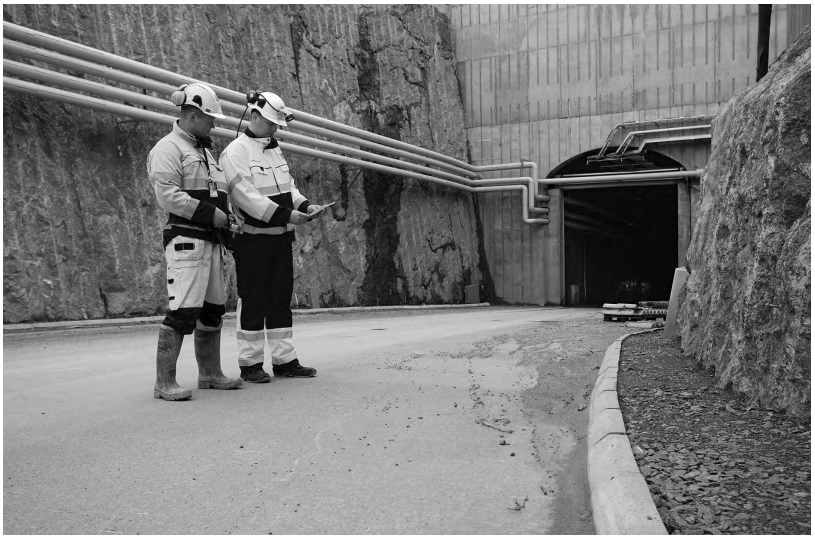

Figure 16.3 Construction of an underground repository for spent nuclear fuel in Finland. *Source*: Posiva Oy, http://www.posiva.fi/.

Commission on America's Nuclear Future to perform such an assessment. This left Finland and Sweden as the only countries having licensed deep underground repositories for commercial spent nuclear fuel.

The design for the Yucca Mountain site license application allowed for closure after 300 years. After that, the temperature in the surrounding rock would be limited by conductive cooling to less than boiling water temperature to avoid mobilization of moisture. Consideration was given to extending the convective cooling period, which would allow for more decay of Am241 and thus denser packing. However, with allowed emplacements already limited by statute to substantially less than the physical capacity of the site, there was little incentive to face the challenge designing to maintain convective cooling well beyond 300 years.

The approaches in Scandinavia demonstrate the existence of a technically viable solution to long-term isolation of spent nuclear fuel in a deep underground repository. However, the possibility of storage in less expensively constructed facilities for a century or more in dry casks like those shown in Figure 16.2 raises the question of whether that would be a preferable option if at some later time the reuse of spent nuclear fuel becomes economically favorable. Assessing how long such retrievable storage might need to be before reprocessing is economical requires study of how the price of extraction of uranium from mines might evolve over time. For example, making and using nuclear fuel that includes reprocessed material was much more expensive in 2010 than using native uranium only.

The inflation-adjusted price of many other minerals has increased historically at most as the 2/9 power of the cumulative amount mined (Scheider and Sailor, 2008). That is, if $p = p_0(u/u_0)^s$, then $s \leq 2/9$, where u_0 is the amount mined up to the point where the price averaged over periodic price fluctuations is p_0. This observation applies both to metals comparably rare to uranium and to other heavy metals. Adjusted to the year 2007, U.S. dollar purchasing power, the average contractual price paid for mined uranium from 1971–2007 in the United States was about \$80/ kg, accounting for about one-thirtieth the median cost of electricity delivered to the transmission grid by U.S. nuclear power plants in 2006 (Koomey and Hultman, 2007). Up to this point, the cumulative global amount of uranium used was about 2.3 million metric tons. If uranium prices on the average increased even as fast as the 2/9 power (i.e. price proportional to $u^{2/9}$ where u is global cumulative uranium mined) of the amount mined, then 512 times more uranium than used through 2006 would have to be mined before uranium costs increase by a factor of four, thereby increasing the cost of nuclear electric energy delivered to the transmission grid by only 10%.

Only if reuse of spent nuclear fuel can be made competitive with mined uranium at about \$150–160/kgU might such reuse be economical as soon as the end of the 21st century, even with some the strongest global nuclear energy use growth scenarios produced for the Intergovernmental Panel on Climate Change (IPPC). Reuse is most likely to become economically competitive for well-aged spent fuel that has been devolatilized and reused as a powder, because this approach can avoid the more complex processes and waste streams associated with aqueous/organic extraction. Aqueous/organic extraction with the ambitious goal of being competitive with mined uranium at over \$240/kgU would not become economically advantageous until after the end of the following century,

if during that century average global rate of use of nuclear energy were twice the value of four trillion watts of nuclear electric energy production rate 2100 in the same IPCC strong nuclear growth rate scenario. If so, then spent fuel aged over 200 years could become economically useful and thus recovered from a deep underground repository before it is sealed off from convective cooling.

Given the inherent uncertainties in long-term extrapolations of uranium prices and reprocessing and fuel fabrication costs, it is likely to remain uncertain for many decades whether or when reprocessing of spent fuel might become economically competitive. The default option of moving to dry cask storage pending a decision on this, which is being adopted in practice albeit sometimes not in principle by most countries other than France and Japan, may thus well persist for many decades to come.

France and Japan have large sunk capital costs committed to PUREX facilities and are thus likely to continue operating them for some time to come, barring serious operational problems arising like those that shut down Britain's Thermal Oxide Reprocessing Plant (THORP) for nearly four years. Most other countries have either been cancelling PUREX reprocessing contracts with France and Britain for production of MOX fuel for light water reactors on economic grounds, or at least have not yet fully committed to building or operating reprocessing facilities for all of the spent nuclear fuel that they will be producing over the next several decades. Whether France or Japan will suspend reprocessing for economic reasons before or at the end of the operational lifetime of their current PUREX plants remains to be revealed.

The fact that nuclear reactors produce plutonium as a by-product has affected attitudes toward spent nuclear fuel because of concerns about the possible near-term use of nuclear reactor products to make more nuclear explosives. For a country that already has a sizable nuclear arsenal, there is no incentive for a government to do this, but spent nuclear fuel still needs to be protected against unauthorized acquisition by private parties. For the first several decades after discharge from a reactor, spent fuel is so radioactive that contact handling needed to fabricate its plutonium into a critical chain-reaction mass would rapidly produce a lethal dose. As the Sr90 and Cs137 decay, this would eventually be no longer the case. However, countries that maintain stocks of active and retired nuclear explosives need in any case to secure that material at one or more storage locations. There would be no sense in a private party absconding with well-aged spent nuclear fuel casks from stored as such a facility or from a different location with comparable security, because it would be far preferential to acquire the comparably well-guarded, weapons-grade nuclear material.

Thus, the main concern about the nuclear explosives potential of reactor discharges lies with countries that do not yet have nuclear weapons. Adoption of any spent fuel reprocessing technology by such a country overcomes most of the hurdles in the way of possible future production of nuclear weapons. This is also true of powdering devolatized well-aged spent fuel if the resulting nuclear fuel is burned in CANDU-type heavy water reactors, which can be a preferred option for material still containing some undesirable elements other than uranium and plutonium. This is because CANDU reactors have online refueling that can produce weapons-grade plutonium in spent fuel in the first discharges during startup, and because enough tritium to substantially boost the yield of nuclear weapons is produced as a byproduct of CANDU reactor operation. Thus there is also nuclear proliferation potential in the approach called DUPIC (direct utilization of spent pressurized water reactor fuel in CANDU reactors).

There have been proposals to ship spent fuel from non-nuclear-weapons states to nuclear weapons states for reprocessing, and then ship the spent fuel fission products back to the countries of origin for disposal. Such proposals have little appeal to most countries, because they can eliminate a perceived national security benefit of retaining control over the nuclear fuel cycle but still saddle the country in question with high-level radioactive waste disposal problem. Only if a nuclear weapons state can solve the domestic political problem of giving one or more of its own regions an adequate incentive to host all needed spent fuel management facilities can it hope to reduce global nuclear proliferation concerns by taking spent nuclear fuel from non-weapons states without returning back fission products. If this can be done, then the current nuclear weapons states could readily absorb the spent fuel produced by states that do not have nuclear weapons for many decades. For example, a recent study suggests than the ratio of spent fuel ready to ship from pool storage in all of the Association of Southeast Asian Nations to that from the United States might increase from 1% to 7% in the 2030s and remain less than 9% for several decades thereafter. Cooperation between the United States and two other nuclear weapons countries could readily accommodate all of the countries without nuclear weapons that were willing to participate in such an arrangement with adding appreciably to the nuclear waste management burden in the recipient countries (Singer and Taylor, 2007).

Global installed nuclear capacities in April 2010 are listed by region in Table 16.3. The EU contains two nuclear weapons states and coordinates civilian nuclear activities through EURATOM in close cooperation with Switzerland. Canada is a member of NATO and appears fully committed to its non-nuclear-weapon position. Japan is likely to manage its own spent nuclear fuel for the foreseeable future, and the Republic of Korea appeared in 2010 to be interested in moving in a similar direction. Taiwan has a unique national security environment that makes the pursuit of nuclear weapons currently impractical.

TABLE 16.3 April 2010 Nuclear Capacities

Who	GWe	% of Global GWe
China Mainland	8.6	2%
EU	115.2	31%
India	4.2	1%
Russia	22.8	6%
USA	101.1	27%
Switzerland	3.3	1%
Canada	12.7	3%
Japan	47.1	13%
Korea	17.7	5%
Taiwan	4.9	1%
Other	36.6	10%
Total	374.1	100%

Source: WNA, 2010.

China and India have nuclear weapons, as does Pakistan with 0.4 GWe installed nuclear electric capacity. The rest of the world had only 10% of installed nuclear capacity, a fraction not likely to increase rapidly given the rapid growth in China and possibly India. The legacy and likely accumulation over three decades of spent nuclear fuel among this set of countries with 10% of installed nuclear capacity without nuclear weapons is small compared to that of the nuclear weapons states.

The problems that the United States has in developing a well-ordered system for managing its spent nuclear fuel derive from its structure as a federal republic and its balanced division of federal governance between legislative, administrative, and judicial branches. The states of Nevada and Utah have fiercely and as of 2010 successfully resisted pressures respectively to accept underground and surface storage facilities for spent fuel. On the other hand, ten U.S. states have legally enforceable impediments to new nuclear reactor construction pending an acceptable national solution of the spent nuclear fuel management problem. The distribution of spent nuclear fuel among the U.S. states as of 2007 is given in Table 16.4. The states with names in italics, Maine and Washington, hosted no still operating nuclear reactors. So far, it is only these states that cannot simply move spent fuel to another operating nuclear reactor in the same state.

Japan faced similar spent fuel management problems to those in the United States. Japanese prefectures pressed to have spent nuclear fuel removed from their jurisdictions, but resisted taking back MOX fuel for burning in their reactors. At considerable expense, the solution was to send all spent fuel for reprocessing at Rokkasho Mura at the northern tip of Japan's main island. Given the preliminary nature of Japan's underground repository program, it is likely that its reprocessing facility will become a de facto storage facility for radioactive material from nuclear reactors for a long time to come.

TABLE 16.4 Spent Nuclear Fuel Discharge

State	Total (MTHM)	Dry Storage (MTHM)	At Morris, IL
Alabama	2600	130	
Arizona	1600	550	
Arkansas	1100	610	
California	2500	400	100
Connecticut	1800	510	30
Florida	2600	75	
Georgia	2200	410	
Illinois	7070	460	140
Iowa	420	110	
Kansas	540	0	
Louisiana	1000	70	
Maine	540	540	
Maryland	1100	560	
Massachusetts	620	130	
Michigan	2300	420	
Minnesota	1000	360	200
Mississippi	700	50	
Missouri	590	0	
NorthCarolina	3100	392	
Nebraska	720	50	200
NewHampshire	400	0	
NewJersey	2200	220	
NewYork	3000	150	
Ohio	1000	30	
Oregon	360	360	
Pennsylvania	5200	910	
SouthCarolina	3500	1200	
Tennessee	1300	200	
Texas	1700	0	
Vermont	550	0	
Virignia	2200	120	
Washington	540	180	
Wisconsin	1200	270	
Total (with Morris)	57780	9467	670

Source: (Ewing et al., 2009).

In many other countries, policymaking on spent nuclear fuel management is more nationally centralized, but in democracies other than Finland and Sweden, there remains substantial resistance to siting long-term management facilities. Thus, spent nuclear fuel and its components are likely to remain at existing facilities in dry storage casks for the foreseeable future, pending decisions on the future of deep underground repositories and reprocessing.

REFERENCES

R.C. Ewing, C. Singer, and P. Wilson, *'Plan D' for Spent Nuclear Fuel*, 2009. University of Illinois at Urbana-Champaign Program in Arms Control, Disarmament, and International Security Report at http://www.acdis.uiuc.edu/Research/ResReports.shtml, accessed April 9, 2010.

J. Koomey and N. Hultman, A reactor-level analysis of busbar costs for U.S. nuclear plants, *Energy Policy*, 2007, **35**, 5630.

P. Podveg, *BN-800 Expected to Be in Operations in 2014*, January 21, 2010, International Panel of Fissile Materials, http://www.fissilematerials.org/blog/2010/01/, accessed March 9, 2010.

E. Schneider and W. Sailor, Long-term uranium supply estimates, *Nuclear Technology*, 2008, **162**, 379.

C. Singer and J. Taylor, *Nuclear's Role in 21st Century Pacific Rim Energy Use*. Global 2007 Advanced Nuclear Fuel Cycles and Systems American Nuclear Society Topical Meeting, Boise, Idado, September 9–13, 2007; available in extended form as *Nuclear's Role in 21st Century Pacific Rim Energy Use: Results and Methods*, University of Illinois at Urbana-Champaign Program in Arms Control, Disarmament, and International Security Report ACDIS SIN:1.2007 at http://www.acdis.uiuc.edu/Research/ResReports.shtml.

WNA (World Nuclear Association), *Fact Sheet on Decommissioning Nuclear Power Plants*, January 22, 2008, http://www.nrc.gov/reading-rm/doc-collections/fact-sheets/decommissioning.html, accessed April 22, 2009.

17

FISSION ENERGY USAGE: STATUS, TRENDS AND APPLICATIONS

PAVEL V. TSVETKOV

Department of Nuclear Engineering, Texas A&M University, TX, USA

17.1 WORLDWIDE POWER REACTOR FLEET

Climate change and air quality are putting pressure on fossil fuel-based energy generation. Growing concerns for the environment will favor energy sources that can satisfy the need for electricity and other energy-intensive products on a sustainable basis, with minimal environmental impact and competitive economics. Consideration of the use of nuclear energy for production of useful power began shortly after the discovery of nuclear fission. At that time, scientists realized that future energy needs could not be met by fossil fuels alone. The development of nuclear reactors as useful sources of power began shortly after the end of World War II. More than 400 nuclear power plants are currently operating throughout the world, supplying over 18% of the world's electricity:

83.4% are light water reactors (LWR), of which:
- 57.7% are pressurized water reactors (PWR)
- 23.2% are boiling water reactors (BWR)
- 0.6% are advanced boiling water reactors (ABWR)
- 13.8% are water-water energetic reactors (Russian version of PWR) (WWER)
- 4.7% are light water-cooled graphite reactors (LWGR)

7.8% are heavy water-cooled reactors (HWR) (pressure vessel heavy water reactors)

0.2% are heavy water-moderated light water-cooled reactor

8.1% are gas reactors (GR)

0.5% are fast reactors (FR)

These plants perform safely and reliably, and they help meet the objectives of diversity, independence, and security of their energy supply. Unlike fossil fuel plants, nuclear plants do not release carbon dioxide, sulfur, or nitrogen oxide into the environment. Nuclear energy, for example in the United States, is the cleanest large-scale source of electricity, representing two-thirds of the nation's emission-free electricity generation. By using nuclear energy instead of other fuels, electric utilities reduce U.S. emissions of carbon dioxide, the principal "greenhouse" gas. The Department of Energy projects the United States will need 44% more electricity by 2020 to meet growing energy demands. If advances are made that fully apply the potential benefits of nuclear energy systems, the next generation of nuclear systems can provide a vital part of a long-term, diversified energy supply.

In addition to the central station power reactors, there are several hundred pressurized water naval propulsion reactors and hundreds of research and special purpose reactors of various types worldwide.

The success of the LWR is based on the early recognition that natural fissile material was considered scarce and that nuclear energy could develop only if systems with low fissile inventories per unit power would be built in the start phase. LWRs, as initially developed for naval applications, fulfilled this criterion and used simple and relatively cheap technology that enabled a first generation

Nuclear Energy Encyclopedia: Science, Technology, and Applications, First Edition (Wiley Series On Energy).
Edited by Steven B. Krivit, Jay H. Lehr, and Thomas B. Kingery.

of power stations to be constructed rapidly. The necessary uranium enrichment technology was available from the military development. The significant plutonium generation in LWR fuels was considered to be an asset because plutonium is an excellent fuel for fast reactors and the anticipated deployment of fast reactors around the turn of the century would have required large fissile inventories.

17.2 NUCLEAR ENERGY AND NUCLEAR POWER APPLICATIONS

All presently developed nuclear power reactors act as sources of thermal energy, producing electricity through the conventional "heat engine" process. In all current central generating station applications, steam is the final working fluid, with conventional steam turbines being used to drive the electrical generators. The thermal energy is generated within the nuclear fuel confined in the nuclear reactor. The process uses no air. Fuel can be added continuously or in batches, daily or annually. The mass of fuel is small relative to the mass of fuel for coal power plants because of large specific potential of energy in nuclear materials.

The thermal energy from nuclear fission is transferred from the fuel by coolant. Water, boiling water, gasses, metals, and other materials may be serving as reactor coolants and secondary working fluids. Gasses and steam may be used directly in the turbine (direct cycle). Alternatively, various types of heat exchangers can be used to transfer heat to secondary working fluids (indirect cycle).

To take full advantage of fission energy, the need for greater energy efficiency is becoming an increasingly important component in development efforts toward sustainable energy resources. Cogeneration systems, producing heat and electricity, offer a solution for optimization of nuclear energy usage and increased energy security. Nuclear power plants represent a viable energy source for cogeneration options. Currently operating nuclear power plants discard thermal energy into a heat sink at temperatures of about 280°C. Heat at these temperatures is suitable for desalination plants and various other process heat applications. Future Very High Temperature Reactors (VHTR) offer much higher temperatures and energy conversion efficiencies that would allow electricity generation, potable water production, and hydrogen production in a single multipurpose cogeneration system. Worldwide, accompanying economic development and rapid population growth, the demand for electricity and fresh water is increasing in some regions at overwhelming rates. Local fresh water needs are approaching or have already exceeded the capability limits of existing supply infrastructures. Half of the world's 6 billion people lack proper sanitation, and a billion cannot get safe drinking water. In many parts of the world 90% of all diseases are related to water. Maximizing electricity generation and fresh water supplies would greatly facilitate regional economic development and raise the standard of living. Numerous concepts and deployable designs are under consideration to address these issues. The desalination of seawater using nuclear energy is a demonstrated option having over 150 reactor-years of operating experience worldwide of which Japan now has over 125 reactor-years. Kazakhstan (Aktau fast reactor BN-350) had accumulated 26 reactor-years of producing 80,000 m^3/day of potable water before shutting down in 1999.

The coupling of a nuclear energy system with a cogeneration facility creates unique challenges. The nuclear energy source determines the maximum energy production rate for all of the coupled energy systems driven by the reactor. The interface between the various product streams will need to be managed such that reactor operation is not challenged. If electricity generation is primary and chemical processing is secondary, then the "product shifting" protocol must be responsive to the needs of the electrical grid. High-demand periods could force the chemical plants into standby mode, whereas low demand periods could see increased chemical production. If chemical processing is primary and electricity generation is secondary, electricity would only be sold as a commodity when demand and availability coincide.

Different countries take different approach to nuclear energy, using it or considering using it for different applications, such as central power, potable water production, district heating, industrial applications including petrochemical applications, high-temperature processes, carbon sequestration, transportable nuclear power stations, and others. In this context, small nuclear power reactors are gaining interest worldwide because of expectations of smaller deployment expenses and versatility of potential applications.

17.3 WORLDWIDE STATISTICS OF NUCLEAR ENERGY USE

Today nuclear power has a prominent role in the worldwide energy portfolio. Table 17.1 summarizes current nuclear power status worldwide. With 14% electricity fraction, 438 units in operation and 54 units under construction, nuclear power provides an expanding contribution into the carbon-free electricity generation.

Furthermore, increasing efficiency of energy conversion yield options for other nuclear energy uses. Projects are underway to develop and deploy nuclear-driven cogeneration solutions allowing for electricity and desalination in the same systems. Future considerations include additions of high temperature industrial applications. There is a coordinated IAEA program focused on potable water and desalination.

TABLE 17.1 Nuclear energy usage in 2009–2010

	Nuclear Electricity		Reactors in Operation		Reactors under Construction		
Country	bil. kWh	%	No.	MWe	No.	MWe	Desalination
Argentina	7.6	7.0	2.0	935.0	1.0	692.0	
Armenia	2.3	45.0	1.0	376.0	0.0	0.0	
Bangladesh	0.0	0.0	0.0	0.0	0.0	0.0	
Belarus	0.0	0.0	0.0	0.0	0.0	0.0	
Belgium	45.0	51.7	7.0	5943.0	0.0	0.0	
Brazil	12.2	3.0	2.0	1901.0	0.0	0.0	
Bulgaria	14.2	35.9	2.0	1906.0	0.0	0.0	
Canada	85.3	14.8	18.0	12,679.0	2.0	1500.0	
China	65.7	1.9	11.0	8587.0	23.0	25,310.0	
Czech Republic	25.7	33.8	6.0	3686.0	0.0	0.0	
Egypt	0.0	0.0	0.0	0.0	0.0	0.0	
Finland	22.6	32.9	4.0	2696.0	1.0	1600.0	
France	391.7	75.2	58.0	63,236.0	1.0	1630.0	
Germany	127.7	26.1	17.0	20,339.0	0.0	0.0	
Hungary	14.3	43.0	4.0	1880.0	0.0	0.0	
India	14.8	2.2	19.0	4183.0	4.0	2572.0	2 PWRs 10,200 m^3/d
Indonesia	0.0	0.0	0.0	0.0	0.0	0.0	
Iran	0.0	0.0	0.0	0.0	1.0	915.0	
Israel	0.0	0.0	0.0	0.0	0.0	0.0	
Italy	0.0	0.0	0.0	0.0	0.0	0.0	
Japan	263.1	28.9	54.0	47,102.0	2.0	2756.0	10 facilities, PWR 10,000–30,000 m^3/d
Jordan	0.0	0.0	0.0	0.0	0.0	0.0	
Kazakhstan	0.0	0.0	0.0	0.0	0.0	0.0	BN-350 80,000 m^3/d, 60%
North Korea	0.0	0.0	0.0	0.0	0.0	0.0	
South Korea	141.1	34.8	20.0	17,716.0	6.0	6700.0	
Lithuania	10.0	76.2	0.0	0.0	0.0	0.0	
Mexico	10.1	4.8	2.0	1310.0	0.0	0.0	
Netherlands	4.0	3.7	1.0	485.0	0.0	0.0	
Pakistan	2.6	2.7	2.0	400.0	1.0	300.0	
Poland	0.0	0.0	0.0	0.0	0.0	0.0	
Romania	10.8	20.6	2.0	1310.0	0.0	0.0	
Russia	152.8	17.8	32	22,811	9	7550	
Slovakia	13.1	53.5	4	1760	2	840	
Slovenia	5.5	37.9	1	696	0	0	
South Africa	11.6	4.8	2	1842	0	0	
Spain	50.6	17.5	8	7448	0	0	
Sweden	50	34.7	10	9399	0	0	
Switzerland	26.3	39.5	5	3252	0	0	
Thailand	0	0	0	0	0	0	
Turkey	0	0	0	0	0	0	
Ukraine	77.9	48.6	15	13,168	0	0	
UAE	0	0	0	0	0	0	
United Kingdom	62.9	17.9	19	11,035	0	0	
United States	796.9	20.2	104	101,119	1	1180	
Vietnam	0	0	0	0	0	0	
WORLD	2558	14	438	374,127	54	56,145	

Source: http://www.world-nuclear.org/info/reactors.html.

South Korea has developed a small nuclear reactor design for cogeneration of 90 MWe of electricity and potable water at 40,000 m^3/day. The 330 MWt SMART (System integrated Modular Advanced Reactor) reactor (an integral PWR) has a long design life and needs refueling only every three years. The feasibility of building a cogeneration unit employing multi-stage flash desalination technology for Madura Island in Indonesia is being studied. Another concept has the SMART reactor coupled to four multi-effect desalination units (MED), each with thermal-vapor compressor (MED-TVC) and producing total 40,000 m^3/day.

China is looking at the feasibility of a nuclear seawater desalination plant in the Yantai area of Shandong Peninsula, producing 160,000 m^3/day by MED process, using a 200 MWt NHR-200 reactor.

Russia has embarked on a nuclear desalination project using dual barge-mounted KLT-40 marine reactors (each 150 MWt) and Canadian reverse osmosis desalination technology to produce potable water.

Pakistan is developing a demonstration multi-effect desalination plant coupled to its KANUPP reactor (125 MWe PHWR) near Karachi to produce 1600 m^3/day (it was earlier projected to produce three times this). It has been operating a 454 m^3/day reverse osmosis desalination plant for its own use.

Morocco has completed a pre-project study with China, at Tan-Tan on the Atlantic coast, using a 10 MWt heating reactor that produces 8000 m^3/day of potable water by distillation (MED). The government has plans for building an initial nuclear power plant in 2016–2017 at Sidi Boulbra, and Atomstroyexport is assisting with feasibility studies for this.

Egypt has undertaken a feasibility study for a cogeneration plant for electricity and potable water at El-Dabaa, on the Mediterranean coast. Late in 2008, plans were being formed for two 1000 MWe reactors to be built there by 2017–2018.

Libya: In mid 2007 a memorandum of understanding was signed with France related to building a mid-sized nuclear plant for seawater desalination.

Iran: A 200,000 m^3/day multi-stage flash desalination plant was designed for operation with the Bushehr nuclear power plant in Iran in 1977, but appears to have lapsed due to prolonged construction delays.

Qatar has been considering nuclear power and desalination for its needs, which are expected to reach 1.3 million m^3 per day in 2010.

Jordan has a "water deficit" of about 1.4 million m^3 per day and is actively looking at nuclear power to address this, as well as supplying electricity.

Argentina has also developed a small nuclear reactor design for cogeneration or desalination alone—the 100 MWt CAREM (an integral PWR).

Most or all these have requested technical assistance from IAEA under its technical cooperation project on nuclear power and desalination. A coordinated IAEA research project initiated in 1998 reviewed reactor designs intended for coupling with desalination systems as well as advanced desalination technologies. This program, involving more than 20 countries, is expected to enable further cost reductions of nuclear desalination.

FURTHER READING

1. S.M. Balashov, E.N. Videneev, A.V. Veresov, V.V. Zorichev, B.K. Mal'tsev, and V.N. Smolin, Electrical heaters for experimental installations and nuclear power stations. *Thermal Engineering*, 2002, **49**, 5, 377–381.
2. L. Birnhack, R. Penn, and O. Lahav, Quality criteria for desalinated water and introduction of a novel, cost effective and advantageous post treatment process. *Desalination*, 2008, **221**, 70–83.
3. M. D. Carelli, IRIS: A global approach to nuclear power renaissance, *Nuclear News*, **46**, 10 (Sept. 2003), pp. 32–42.
4. *Combined Heat and Power*, White Paper, Western Governors' Association's Clean and Diversified Energy Advisory Committee (CDEAC), 2006, http://files.harc.edu/Sites/GulfCoastCHP/Publications/CHPWhitePaper.pdf, accessed 2006.
5. Desalination units powered by renewable energy systems, *Proceedings of the International Seminar* held in Hammamet, Tunisia, September 26, 2005, WIP, INRGREFF, 2005.
6. W. ElMoudir, M. ElBousiffi, and S. Al-Hengari, Process modeling in desalination plant operations. *Desalination*, 2008, **222**, 431–440.
7. El Paso Water Utilities, *Water: Setting the stage for the future*, 2007.
8. J. R. Humphries and K. Davies, *A Floating Desalination/Co-Generation System Using the KLT-40 Reactor and Canadian RO Desalination Technology*, XA0056267, 2001, in IAEA-TECDOC-1172 (Small Power and Heat Generation Systems), IAEA, Austria, 1998.
9. IAEA, *Desalination Economic Evaluation Program*, September 2003.
10. *Innovative Small and Medium Sized Reactors: Design Features, Safety Approaches, and R&D Trends*. May 2005, International Atomic Energy Agency, Vienna, Austria, IAEA-TECDOC-1451.
11. *Introduction of Nuclear Desalination*, Technical Reports Series No. 400, STI/DOC/010/400, International Atomic Energy Agency, Vienna, Austria, 2000.
12. Japan Atomic Industrial Forum, Inc., *MHI Submits Application to NRC for US-APWR Design Certificate*, January 16, 2008.
13. I. C. Karagiannis and P. Soldatos, Water desalination cost literature: review and assessment. *Desalination*, 2008, **223**, 448–456.

14. S. Lattemann and T. Hopner, Environmental impact and impact assessment of seawater desalination. *Desalination*, 2008, **220**, 1–15.
15. P. Nelson and C. Sprecher, *What Determines the Extent of National Reliance on Civil Nuclear Power?*, submitted to 2008 annual meeting of the Institute for Nuclear Materials Management.
16. *Optimization of the Coupling of Nuclear Reactors and Desalination Systems*, June 2005, International Atomic Energy Agency, Vienna, Austria, IAEA-TECDOC-1444.
17. T.M. Pankratz, Nuclear desalination: challenges and options, in IAEA-TECDOC-1524, Status of Nuclear Desalination, IAEA, Austria (2007), *Nuclear Desalination Journal*, 2001.
18. *Small Modular Nuclear Reactors*, May 2001, Report to Congress, U.S. Department of Energy, Office of Nuclear Energy, Science and Technology.
19. *Status of Design Concepts of Nuclear Desalination Plants*, November 2002, International Atomic Energy Agency, Vienna, Austria, IAEA-TECDOC-1326.
20. *Status of Nuclear Desalination in IAEA Member States*, January 2007, International Atomic Energy Agency, Vienna, Austria, IAEA-TECDOC-1524.
21. *Status of Small Reactor Designs without On-Site Refueling*, January 2007, International Atomic Energy Agency, Vienna, Austria, IAEA-TECDOC-1536.
22. Study outlines reactor dD that may be ready for deployment by decade's end. *Nuclear News*, August 2001, DOE Report.
23. N. X. Tsiourtis, Criteria and procedure for selecting a site for a desalination plant. *Desalination*, 2008, **221**, 114–125.
24. *World Nuclear Power Reactors & Uranium Requirements*, http://www.world-nuclear.org/info/reactors.html, accessed 2006.
25. http://www.world-nuclear.org/info/inf71.html, accessed 2006.

PART III

FISSION: BROAD APPLICATION REACTOR TECHNOLOGY

18

LIGHT-WATER-MODERATED FISSION REACTOR TECHNOLOGY

J'TIA P. TAYLOR[1] AND ROGER TILBROOK[2]
[1]*Argonne National Laboratory, Argonne, IL, USA*
[2]*Argonne National Laboratory (Retired), Argonne, IL, USA*

18.1 INTRODUCTION

There are now 440 operating power reactors in 30 countries around the world.[1] There are six different basic plant designs, each with a range of details depending on the vendor, unit size, and age. Vendors modify their designs for different outputs and to reflect greater understanding of plant safety and operations. The six plant designs in operation are pressurized water reactors (PWRs), boiling water reactors (BWRs), heavy water reactors (HWRs), gas-cooled reactors (GCRs), light-water-cooled graphite-moderated reactors (LGRs), and a single liquid-metal-cooled fast breeder reactor operating in Russia.

Light-water reactors (LWRs), which includes PWRs and BWRs, dominate the tables of reactor types and power generation. There are 268 PWRs and 88 BWRs representing 61% and 20% of the total number of reactors, respectively. However, as these designs have been competitively developed over the years by a number of vendors, the sizes have increased in order to reduce the cost per electric unit. Consequently, the fraction of electric power generated by LWRs is increased to 66% and 22% for PWRs and BWRs respectively of the world's total electricity of 375, 594 MWe. The next largest reactor type is the HWRs with 11% of operating plants but accounting for only 7% of the power generation. GCRs and LGRs are specific to their countries of origin, the United Kingdom and Russia, respectively.

Detailed numbers for prospective new plants are not included here owing to the anticipated reassessments of planned reactors and units under construction, including location, size, or vulnerability, owing to the impact of the Fukushima tsunami. Over 100 units were under construction or planned, with about 90% being LWRs (83% PWR, 6% BWR) and the remaining majority being HWRs. Historical commercial development of reactors is covered in Chapter 4. Information about the other reactor types not specifically covered in this chapter is contained in Part III Fission: Broad Application Reactor Technology. The remainder of this chapter discusses PWRs and BWRs, which comprise the majority of operating reactors.

18.2 PRESSURIZED WATER REACTORS (PWRs)

The PWR is a thermal nuclear power plant design that uses light-water as a coolant and moderator for energy generation. The PWR concept was conceived in the late 1940s after a joint government/industry project at the Clinton Laboratories. The Atomic Energy Commission gave design responsibility to Argonne National Laboratory. A zero power physics test, ZPR-1, went critical in 1950 and the subsequent design (submarine thermal reactor, STR) was passed to Westinghouse to build and operate at the National Reactor Testing Station (NRTS) in Idaho. At this reactor, power focused on submarine propulsion rather than electric power generation, but in subsequent submarine configurations other functions within the boat were appended to the reactor power output. The long test of reactor operation concluded in June 1953. In July, work

Nuclear Energy Encyclopedia: Science, Technology, and Applications, First Edition (Wiley Series On Energy).
Edited by Steven B. Krivit, Jay H. Lehr, and Thomas B. Kingery.

began on the development of a PWR-based central power station. This resulted in the design and construction of the Shippingport Atomic Power Station, operated by the Duquesne Light Company near Pittsburgh, Pennsylvania. The design power was 60 MWe and full power was first delivered in December 1958.

Uranium in the nuclear fuel is responsible for the exothermic fission reaction that provides heat energy. Fuel pellets are made of uranium dioxide (UO_2) with enrichment of the U235 isotope. A fuel rod is created from a lengthwise group of pellets surrounded by a metal fuel cladding. Zirconium is typically chosen as the fuel cladding material because of its desirable mechanical properties and low neutron capture cross section. A PWR fuel bundle is typically a 15 × 15 or 17 × 17 square array of fuel and control rods approximately 3.6 m (12 ft) in length. Top and bottom nozzles as well as spring clip grid assemblies connect the rods within the bundle. Figure 18.1 illustrates a fuel assembly, a core cell, and their constituent elements.

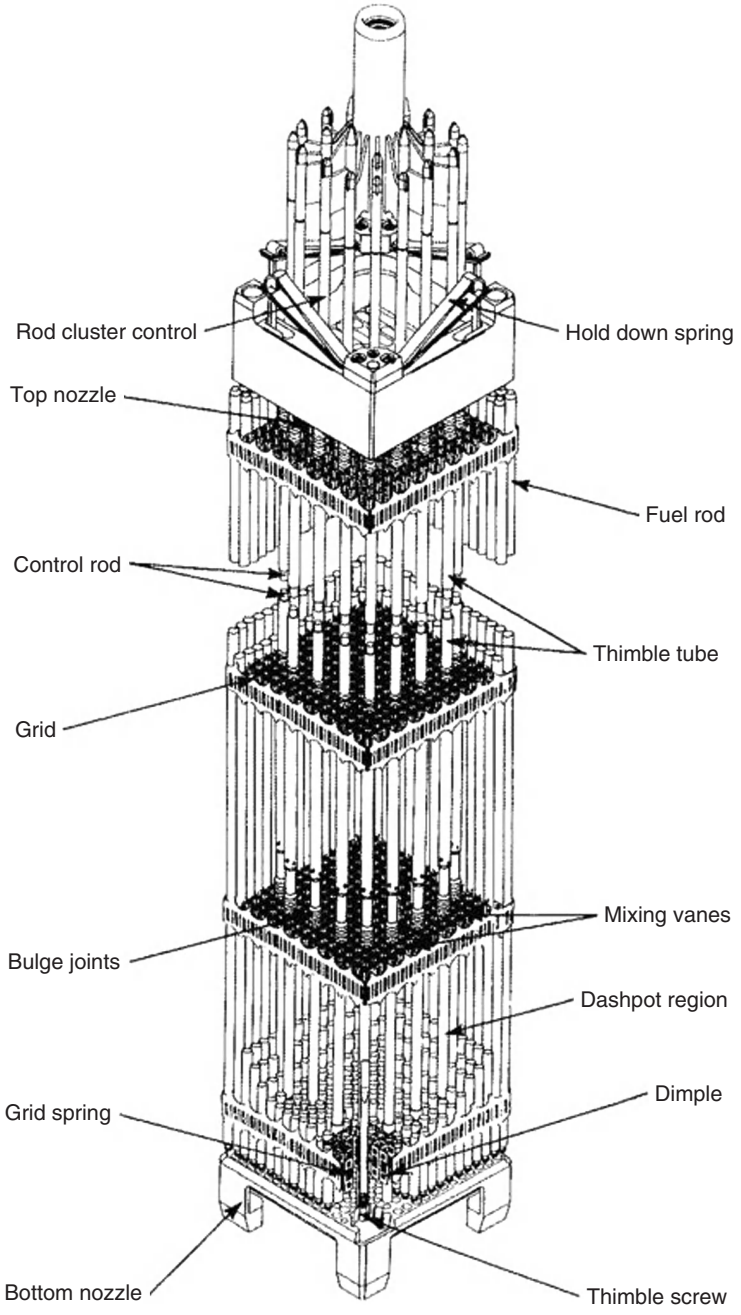

Figure 18.1 Diagram of a pressurized water reactor fuel assembly. *Source*: From Ref. [1]

Reactivity is a measure of the fission reaction and its balance in the reactor. Positive reactivity results in an increase in power and negative reactivity results in a decrease in power. Reactivity is controlled within a PWR using control rods and boric acid concentration. The control rods contain silver–indium–cadmium and boric acid contains boron, which absorbs the neutrons needed to cause fission reactions that produce heat energy and thus power.

The fluid in the PWR core is pressurized typically to 2000–2400 psi. This suppresses boiling in the core, resulting in greater water density and requiring lower uranium enrichments than a BWR. Water flows from the core to a steam generator, where the high pressure hot water passes through a bundle of tubes immersed in warmed water, called the feedwater and is pressurized to about 1000 psi. As heat passes to the feedwater, steam is created and passed to the turbine, which turns the electric generator. The steam above the bundle is very wet. The top of the steam generator contains moisture separators that dry the steam for the turbine and returns the hot water to mix with the entering feedwater.

There is also a pressurizer attached to one of the hot primary pipes between the reactor vessel and one of the steam generators. The pressurizer is a high-pressure vessel, partially filled with water under a cover of steam, with a complex of cooling sprays and heaters to keep the steam pressure within a required range. The water that circulates between the reactor core, pressurizer, and the steam generator is called the primary coolant. The water that flows between the steam generator, the turbine, and the condenser is the secondary coolant. Heat is transferred between the primary and secondary coolants, which are isolated from each other (Figure 18.2).

The historical development of increasing sizes of PWRs is outlined in Chapter 4. Companies pursuing development have PWR designs that are certified or undergoing Nuclear Regulatory Commission (NRC) certification. The Advanced Passive 600 (AP600), Advanced Passive 1000 (AP1000), and System 80+ are advanced PWR designs developed by Westinghouse and certified by the NRC. The US Evolutionary Power Reactor (US EPR) and the US Advanced Pressurized Water Reactor (US APWR) are advanced designs by AREVA and Mitsubishi, currently under review. Other vendors have designs in a range of sizes, which are being prepared for NRC consideration.

The AP1000 design, an increased capacity design based on the AP600, decreases the number of components including pipes, wires, and valves, decreasing equipment failure. The AP1000 also features Westinghouse Passive Core Cooling System (PCCS), which removes core heat independent of electrical systems. Construction of units began in Zhejiang, China, at the Sanmen Nuclear Power Plant in 2008 with six units expected on completion. Additional construction is underway in Shandong, China, at the Haiyang Nuclear Power Plant in 2008 with six units expected on completion. A single unit AP1000 is rated at thermal and electric power capacities of 3400 and 1540 MW, respectively, with a design discharge burnup of 50 GWd/t.

18.3 BOILING WATER REACTORS (BWRs)

The Boiling Water Reactor (BWR) is a thermal nuclear power plant design that uses light-water as a coolant and moderator for energy generation. A distinct feature of the BWR, in comparison to other light-water reactors,

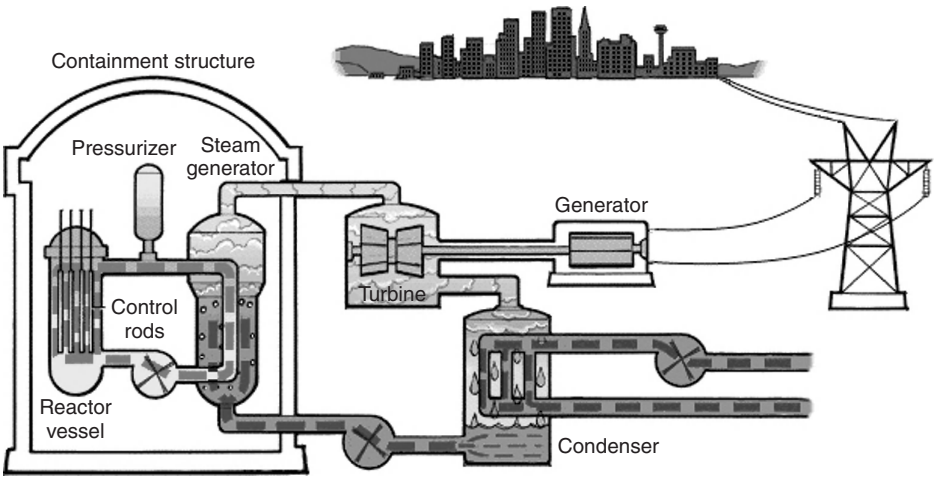

Figure 18.2 Diagram of a pressurized water reactor power plant. Image taken from the Nuclear Regulatory Commission website (http://www.nrc.gov/reading-rm/basic-ref/students/animated-pwr.html)

is the generation of steam in the reactor core. Before the development of BWR technology, it was thought that in-core boiling would result in unstable conditions. The BORAX experiments of the 1950s disproved this assertion and illustrated the viability of in-core boiling. Research, development, and commercial construction of BWRs are a result of partnership between US government-sponsored national laboratories and private companies such as General Electric–Hitachi. BWRs are in operation in many nations including the United States, Japan, and Spain and account for approximately 20% of reactors currently in operation. General Electric–Hitachi has continued to develop new designs using in-core boiling technology resulting in the advanced boiling water reactor (ABWR) and economic simplified boiling water reactor (ESBWR) advanced designs.

The BWR designed by General Electric–Hitachi includes six distinct designs including the initial BWR/1, introduced in 1955, and the final BWR/6 design, introduced in 1972. BWR began construction in the mid-1960s and construction of BWR and the advanced designs continue to the present day. A BWR plant produces electricity by converting heat energy into mechanical energy and, by way of turbine generators, into electrical energy. The electricity production process of a BWR power plant is illustrated in Figure 18.3. Nuclear fuel in the core undergoes an exothermic, heat-releasing, fission reaction. Heat, released from fission in the fuel, is transferred to water flowing through the reactor core. As designed, temperature and pressure conditions within the core cause the water to undergo phase change and become steam. The force of the steam entering the turbine causes it to rotate. The turbine is connected to an electric generator containing magnets. Electricity is produced in the generator by electromagnetic induction, caused by the rotation of the magnets. After leaving the turbine/generator, the steam condenses, undergoes a phase change, and becomes water. The water is then heated and returned to the reactor core to repeat the process.

Uranium in the nuclear fuel is responsible for the exothermic fission reaction that provides the heat energy in the BWR. Fuel pellets are made of UO_2 with enrichment of the U235 isotope. Different enrichment levels, ranging from 2% to 4% U235, are used in pellets located within the core.

A fuel rod (also called a fuel pin), with an approximate diameter of 1.3 cm, is created from a lengthwise group of pellets surrounded by a metal fuel cladding. Zircaloy is chosen as the fuel cladding material because of its desirable mechanical properties and low neutron capture cross section. After the fuel rod is loaded with pellets, it is evacuated and filled with an inert, nonreactive gas, such as helium, and sealed with welded Zircaloy plugs at either end. The plenum located within and at each end of the

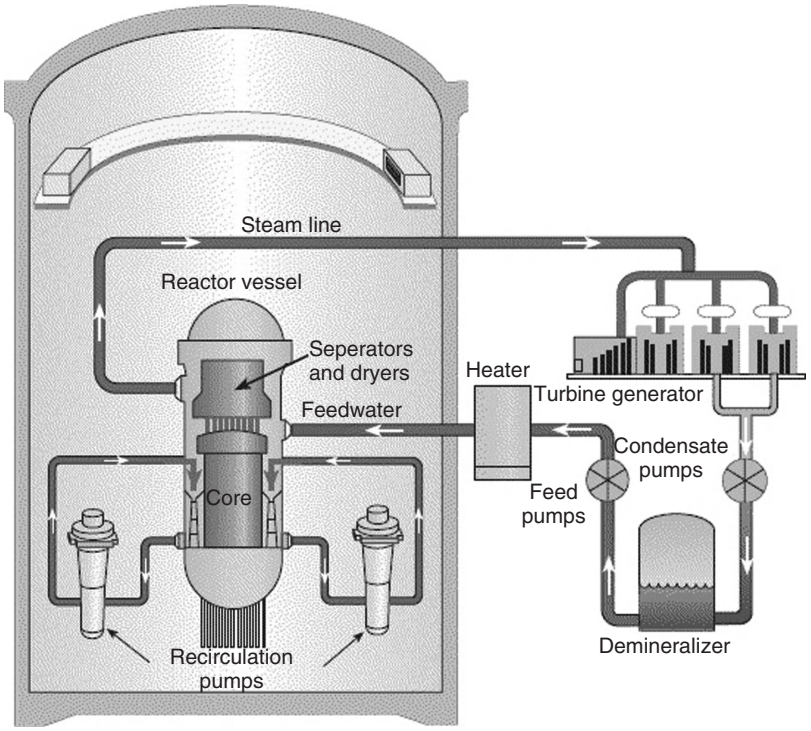

Figure 18.3 Diagram of a boiling water reactor power plant. Image taken from the Energy Information Administration website (http://www.eia.doe.gov/cneaf/nuclear/page/nuc$_r$eactors/bwr.html)

fuel rod contains springs that limit the movement of the fuel pellets during transportation and allow compensation space for fission gases escaping the UO_2 fuel pellets. A fuel bundle is created from a group of 64 rods in a square (8×8) matrix configuration. Upper and lower tie plates connect the rods within the bundle.

These rods also retain their spacing throughout the bundle by means of interim spacers between the tie plates. Each fuel bundle is surrounded by a Zircaloy metal fuel channel, which separates coolant flow between assemblies, giving structure to the assembly, and providing control rod access. A fuel assembly is composed of a fuel bundle and the surrounding channel with a width and length of 14 cm, and a height of 4 m being typical. A core cell is composed of four fuel assemblies with a bladed control rod in their cross section. Figure 18.4 illustrates a fuel assembly, a core cell, and their constituent elements.

Reactivity is a measure of the fission reaction and its balance in the BWR and is typically measured from the critical state of the reactor. Positive reactivity results in an increase in power and negative reactivity results in a decrease in power. Reactivity is controlled within a BWR using control rods, fuel pellet composition, and coolant flow. Short-term reactivity is altered through small movement of control rods during operation and adjustment of the reactor coolant flow rate. An increase in coolant flow rate increases heat removal, thus lowering the temperature. A decrease in temperature leads to a decrease in in-core boiling, which raises neutron moderation, fission reactions, and ultimately, reactivity. As a result of the increased reactivity, the power as well as the temperature rise gives way to a decrease in reactivity. This cycle, beginning with an increase in coolant flow rate, results in a critical-state reactor at a higher power than its initial level.

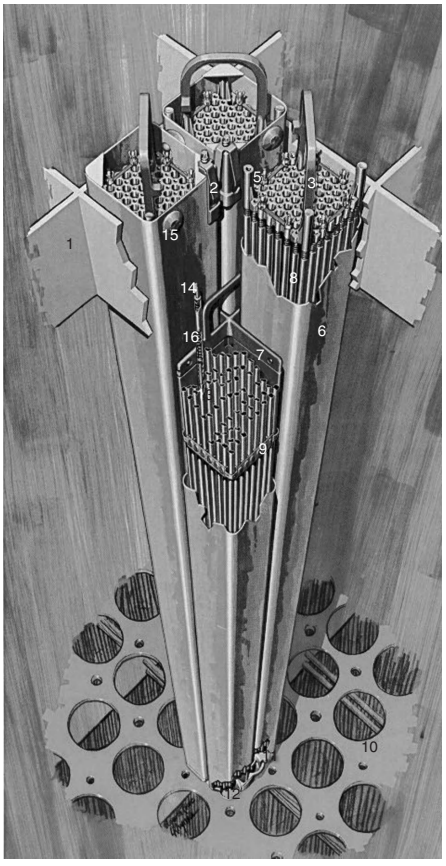

Figure 18.4 Diagram of a boiling water reactor fuel assembly. *Source*: From Ref. [1]

Long-term reactivity changes such as reactor start-up, shutdown, and other large power level variations are controlled using control rods in the BWR. Control rods are inserted into the core from the reactor bottom because of steam voids in the upper plenum. Each control rod contains 84 neutron absorber rods, divided into four sheaths. Each sheath has access holes to allow for coolant flow with the control rod. The neutron absorber rods are steel tubes with compressed boron carbide (B_4C) powder and steel balls that act as spacers. Long-term reactivity changes due to fuel depletion are controlled through the insertion of neutron-absorbing compounds, such as gadolinium oxide Gd_2O_3, into the uranium dioxide of specific fuel pins. Roughly four fuel rods in an assembly contain reactivity control compounds.

The BWR is moderated and cooled by ordinary light-water, which is also used as the heat transport fluid. The water enters the lower plenum of the reactor located below the core area. The water migrates into the core containing the fuel assemblies where energy, released by fission reactions in the fuel, is absorbed by the water. The energy absorbed by the water includes the latent heat, which vaporizes water and creates steam. The multiphase mixture rises into the upper plenum and then onto the steam separators. The steam separator divides most of the mixture into steam and water; with the water flowing into the downcomer and the steam rising above the water level into the dryer. The steam exits the reactor containment vessel via the steam line that leads to the turbine/generator and condenser systems. An illustration of the reactor vessel is given in Figure 18.5.

The in-core creation of steam, with a temperature of approximately 290°C, renders the heat transfer fluid radioactive after passing through the core. This leads to radiation shielding of the systems that use fluid in the steam line. In the PWR, a steam generator is used to create steam and a pressurizer is used to avoid in-core boiling. The pressure in a BWR, approximately 1000 psi, is roughly half the pressure of a PWR. The heat exchanger and pressurizer systems are two major systems that are not needed in the BWR design.

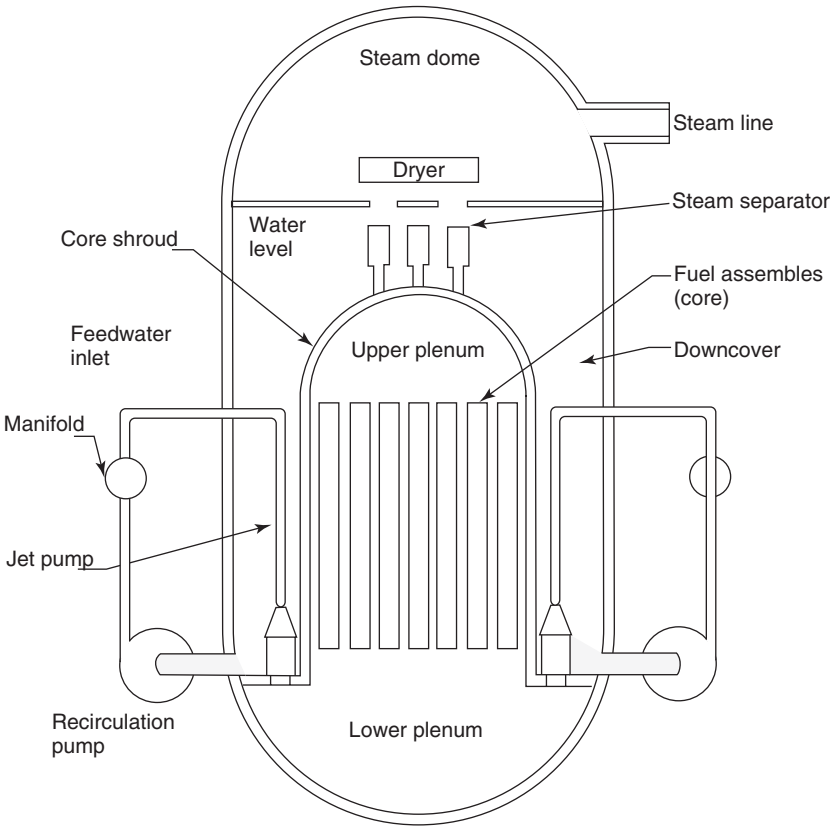

Figure 18.5 Diagram of boiling water reactor. Courtesy J. Taylor

BWR technology is continually under research and development. General Electric–Hitachi advanced designs of the technology include the ABWR and the ESBWR. The ABWR design is based on simplification of BWR technology. Major changes include the exclusion of recirculation pumps in favor of the reactor internal pumps (RIPs) located at the bottom of the reactor pressure vessel, and refined movement capabilities of control rod via the fine motion control rod drives (FMCRDs).

The US NRC certified the standardized design of the ABWR in 1997. This design certification removed major regulatory obstacles to construction and operation in the United States. Subsequently, NRG Energy, a nuclear company, indicated its intention to construct two ABWRs in Texas and has filed for construction and operation licenses. Four ABWRs are operating in Japan, two units at the Kashiwazaki–Kariwa Nuclear Power Plant, and single units at the Hamaoka and Shika Nuclear Power Plants. A single unit ABWR is rated at thermal and electric power capacities of 3926 and 1350 MW, respectively. ABWR units are also under construction in Japan and Taiwan.

The ESBWR uses the basic BWR technology and advances of the ABWR while emphasizing passive safety features and delivering a larger power capacity. The ESBWR uses natural circulation and contains no recirculation pumps in contrast to the ABWR. The design also uses a gravity-driven cooling system, which operates without pumps and generators. The ESBWR also features isolation condenser and containment cooling systems outside of the radiation containment boundaries, allowing for easier access and less worker radiation exposure. There are no operating ESBWR units; however, two US consortia of companies have stated interest in construction and operation. A single unit ESBWR is rated at thermal and electric power capacities of 4500 and 1590 MW, respectively, with a design discharge burnup of 50 GWd/t.

18.4 CONCLUSIONS

The PWR and BWR designs described in this chapter differ in one fundamental way. A BWR generates steam inside the core, whereas the PWR produces steam via a secondary coolant system. This difference leads to a larger core for the BWR to accommodate equipment such as steam separators and dryers at the top and control rods at the bottom. Fuel with slightly higher uranium enrichment is required for the BWR due to steam/water effects. The steam generated in the BWR core that flows to the turbine contains trace

radionuclides that require radiation shielding throughout the core and turbine systems. The core containment vessel is smaller for a PWR; however, the higher operating pressure requires more resistant materials in the primary coolant system. The PWR also requires additional systems for steam generation and pressurization. Secondary coolant system use by the PWR slightly reduces plant thermal efficiency but this is compensated by the higher pressures compared to the BWR. Other nuances exist between PWR and BWR design beyond the discussion above.

This chapter is being written even as the scenarios for the Fukushima Dai-ichi units are evolving. It is noted that all operating units shut down automatically and promptly in response to a seismic event considerably beyond their design basis. However, the 7- to 10-m tsunami resulting from the 9.0 Richter scale earthquake destroyed the plant's power grid connections and overwhelmed the constructed sea-wall defense of the plant resulting in loss of the emergency diesel generators. This loss of power and consequent loss of cooling event affected not only the reactors but also the spent-fuel storage pools.

All reactors are designed, licensed, and built to withstand a range of accidents initiated internally and externally. These include different worst-case scenarios based on reactor design and location. The location defines a number of potential natural hazards as being Beyond the Design Basis Accident (BDBA) for the plant, meaning the probability of occurrence is so small that the risk is acceptable. The applied design basis may change in light of experience. The Fukushima event will cause close reconsideration of such criteria around the world, just as after the Three Mile Island and Chernobyl accidents.

Endnotes

1. The numbers here are based on the Reference Issue of *Nuclear News*, the magazine of the American Nuclear Society, March 2011; they have been adjusted to delete Fukushima Dai-ichi units 1–4, which were rendered inoperable by the March 11, 2011 tsunami.

REFERENCES

1. W. Stacy, *Nuclear Reactor Physics*, Wiley-VCH GmbH & Co. KGaA, Weinham, 2007.

FURTHER READINGS

J. Lamarsh and A. Baratta, *Introduction to Nuclear Engineering*, Prentice Hall, Upper Saddle River, 2001.

A. Nero, *A Guidebook to Nuclear Reactors*, University of California Press, Berkeley, 1979.

19

CANDU PRESSURIZED HEAVY WATER NUCLEAR REACTORS

RUSI P. TALEYARKHAN

College of Engineering, Purdue University, West Lafayette, IN, USA

19.1 INTRODUCTION

CANDU (CANadian Deuterium Uranium) reactors are a form of nuclear reactors that traditionally use heavy water for both cooling and moderation (i.e., to bring down or moderate the energy of neutrons to states where they may be able to produce a sustainable nuclear fission chain reaction). Due to historical, mainly security reasons (post World War II), enriched uranium technology and the related infrastructure was not available to nor feasible for the Canadians, so the CANDU concept was forced to use natural uranium, a resource that is plentiful in Canada. This decision on part of the United States (to not share uranium enrichment technology) made it imperative for Canada to use heavy water (which is identical to ordinary water, except that the hydrogen atom is replaced with the isotope deuterium, a form of hydrogen that is twice as heavy since it has an extra neutron in its nucleus), but this was feasible for Canadians to undertake since they also possessed experience working with heavy water.

Together with use of heavy water as moderator and natural uranium as fuel, CANDU reactors become large in size relative to reactors, which use enriched uranium and light water for moderation and cooling. The Canadians developed a novel design to overcome key limitations related to the need for large pressure vessels of significant thickness to house the fuel, the moderator, and coolant. Instead, they placed the uranium fuel within hundreds of small diameter fuel channels, which are pressurized. The bulk of the heavy water moderator is placed within a common, large unpressurized tank called a *calandria*. The individual fuel rods within pressurized tubes run horizontally, and liquid heavy water performing as a coolant runs through them for carrying away most of the heat energy from nuclear fission of uranium. However, such a design mandates a second water circuit to cool the moderator tank, since the moderator outside of the pressure tubes will also receive some of the energy of fission. The energy of fission lost to the moderator tank becomes unavailable for electricity production but may be useful as process heat. On the plus side, a design such as this permits the reactor to remain at full power while nuclear fuel from within individual pressure tubes is changed out; hence, a CANDU reactor may theoretically never have to shut down. This feature has provided the CANDU concept the advantage of a high capacity factor—that is, CANDU reactors are available round the clock without interruption of power for refueling outages as is mandatory for reactors that use light water and enriched uranium. On the downside, CANDUs must use heavy water, which is expensive, must operate at lower coolant temperatures, and must release the natural uranium-based nuclear fuel after significantly lower consumption (burnup) compared with pressurized light water reactors. Lower coolant temperatures also result in lower thermodynamic efficiencies.

The particular design of the CANDU reactor causes the system to possess a positive (albeit, small) void reactivity coefficient. This feature is undesirable from a safety perspective during accident conditions. A positive void coefficient causes the reactor power to rise just as

Nuclear Energy Encyclopedia: Science, Technology, and Applications, First Edition (Wiley Series On Energy).
Edited by Steven B. Krivit, Jay H. Lehr, and Thomas B. Kingery.

cooling capacity is reducing and the liquid coolant has started to boil. Fortunately, the use of heavy water as moderator makes such a runaway scenario controllable in time, since the rate of such runaway is much slower than for light water reactors. The CANDU system uses two independent sets of control systems for shutdown to prevent runaway power excursions. The balance of the CANDU system utilizes an approach similar to light water reactor systems such as the pressurized water reactor (PWR); that is, hot coolant from the reactor is made to flow through tubes within a heat exchanger. Low-pressure light water flows outside of the heat exchange tubes get heated to boil and produce steam, which drives a turbine generator set to produce electricity.

Various design schemes have evolved for CANDU system steam generator that are uniquely suited for heavy water moderator-coolant based systems. Present-day systems have migrated to using PWR-type, light-bulb-shaped, vertically oriented steam generator designs. With the availability of enriched uranium, future CANDU systems are being designed so they can be made more compact, even allowing boiling within the pressure tubes, and with promising advantages relative to other reactor technologies for impacting not just the uranium fuel-based cycle that the world has used for the past 50 years, but also for the exciting thorium fuel cycle, which is presently gaining increased attention as a viable alternative to the uranium-based fuel cycle for power production. Presently, CANDU reactors are being used for power production in Canada, India, South Korea, Argentina, Romania, and China. Of the world's approximately 444 reactors generating about 372 GWe, about 46 of these reactors are of the CANDU design (22 in Canada, 24 elsewhere), and they contribute about 24 GWe in total electricity worldwide.

19.2 HISTORICAL EVENTS LEADING TO THE CANDU CONCEPT [1–3]

Allied countries during World War II co-operated as part of the well-known *Manhattan Project*. However, in July 1946, the United States passed the McMahon Act. As a consequence, nuclear-related research and development (R&D) became cloaked in secrecy. This included reluctance on part of the United States to share uranium enrichment technology [1]. Western European leaders and Canada had no choice but to consider natural uranium (of which only about 0.7% is the type of uranium called U235, which produces most all of the nuclear energy during uranium fission in power reactors). The world's first test reactor, Chicago Pile-1 (CP-1), in which the Canadians had taken part during 1942, also had used natural uranium. Earlier, since 1930s, Canadians already had experience (together with cooperation with the British) with use of heavy water. It was known that using heavy water with natural uranium could possibly lead to a power-producing nuclear reactor. If ordinary water were to be used in the reactor, the uranium ore would need to be enriched so that about 3% of the total uranium was made of U235, something the Canadians were not given access to at the time, and which was impractical to develop on their own. As a consequence, after the 1946 McMahon Act was passed, the Canadians decidedly seized upon the potential of the natural uranium-fueled, heavy water moderated-cooled reactor for its long-term nuclear power program. Figure 19.1 provides a timeline

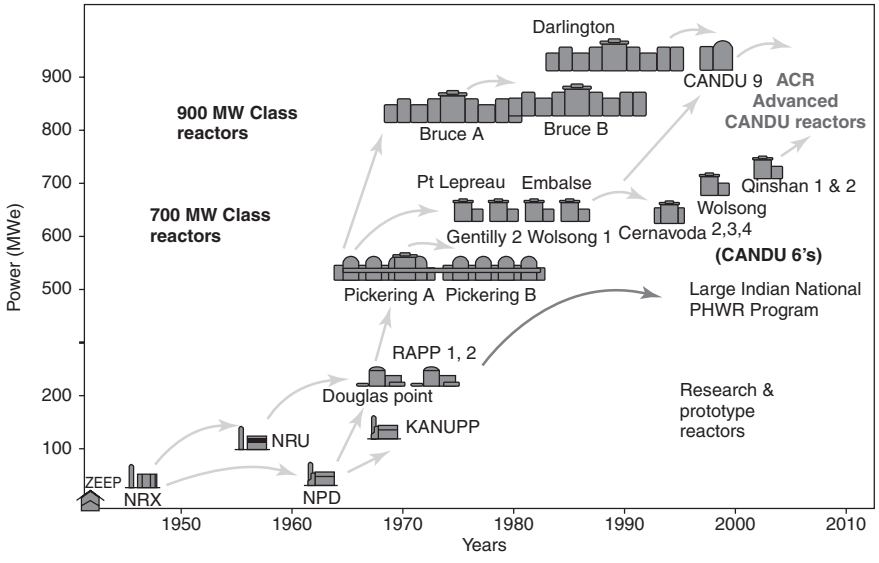

Figure 19.1 Timeline of developments related to the CANDU Pressurized Heavy Water Reactors [2].

of the development for the pressurized heavy water–based CANDU-type reactors [2].

The initiation of a Canadian power reactor program mandated front-end research to assess for the various nuclear and thermal-hydraulic aspects of a heavy water, natural-uranium-fueled nuclear reactor. The Chalk River Laboratory [2] on the Ottawa River was established, and soon thereafter, on September 5, 1945, the Zero Energy Experimental Pile (ZEEP), the first nuclear reactor outside of the United States, was started up. At the time, Canada was the only nation besides the United States to start nuclear development during WWII. Key nuclear data on a heavy water-natural uranium reactor were obtained from ZEEP. This then led to the design and successful operation of Canada's National Reactor Experimental (NRX) 22 MW-t reactor on July 22, 1947. The success of NRX led to the development, starting in 1951, of the 200 MW National Reactor Universal (NRU), a reactor system that had the added mission to serve as a workhorse for producing medical and other industrial isotopes; a mission that has been successfully carried out until the present. To date, since its successful start on November 3, 1957, NRU has supplied over 60% of the world's supply of key medical and industrial isotopes, such as cobalt-60 and molybdenum-99.

In 1952, Canadian Prime Minister Louis St. Laurent established a Crown Corporation, Atomic Energy of Canada Limited (AECL), at heart of which were the personnel of Chalk River Laboratories. Within two years of establishment, AECL initiated development of a 25 MWe electricity-producing power reactor, aptly named the Nuclear Power Demonstration (NPD) plant at Rolphton, Ontario. Even before completion of NPD, AECL and Ontario Hydro initiated plans to build a 200 MWe, commercial prototype at Douglas Point (with the nuclear plant dubbed "Douglas Point") on Lake Huron, Canada. In 1962, a CANDU forerunner, the 20 MWe NPD, was completed and began feeding electricity into the Canadian grid. The 200 MWe Douglas Point was commissioned in 1966. Some studies were conducted that suggested that use of organic liquid coolants could provide superior thermal-to-electrical efficiencies, but those pathways were abandoned. Hydro Quebec together with AECL completed a 685 MWe CANDU 6 (Gentilly 2) plant at Trois Rivières in Quebec, together with multi-unit stations at the Bruce Peninsula, Ontario, the Pickering Station, and the Darlington Stations, respectively, for a total of 22 currently operating CANDU reactors in Canada. Canada also exported its technology to India, Romania, Argentina, South Korea, and Pakistan. Currently [3], a world total of about 46 CANDU-type reactors produce about 34 GWe, enough to supply the western world needs of about 40 million people.

19.3 NUCLEAR PHYSICS CONSIDERATIONS FOR HEAVY WATER REACTORS RELATIVE TO LIGHT WATER REACTORS

Nuclear fission [1, 4] of heavy nuclei such as U235 occurs when a neutron is absorbed within the nucleus of U235 and destabilizes it in such a way that the nucleus breaks apart. During this breaking apart, smaller elements are formed, along with release of a large amount of energy, about 200 MeV (compare this with only about 2–4 eV for fossil fuel combustion). In a nuclear reactor that is based on fission of uranium, the incoming neutron must be of a suitable energy, which is down in the 0.01 eV range; if not, the U235 nucleus will not let it readily enter and cause fission. However, when U235 does fission, it releases multi-MeV energy neutrons. How does one now bring down the energy from MeV to sub-eV levels? Enter the "moderator," so-called because it acts to moderate the neutrons from fission to an orderly level down in the sub-eV range. Water (H_2O) is one such moderator. Heavy water (D_2O) is another such moderator. Neutrons impinge upon the atoms of H_2O or D_2O and successively lose their energy, much like billiard balls striking each other. H_2O is a much better moderator since the "H" atom is about the same mass as a neutron. A neutron striking the nucleus of a "H" atom can lose all its energy in a single head-on collision (although collisions at various other angles can also take place). It takes fewer collisions on average to bring down the energy from MeV to the eV range for H atoms than for D atoms [4]. For example, with H atoms, it would take about 18 collisions for a neutron to come down from 2 MeV to 0.025 eV in energy, versus about 25 such collisions with a "D" atom. However, this is not all one needs to consider. One must also take into account the likelihood or probability of such collisions taking place and the probability that during each such collision the neutron may actually become absorbed by the moderating medium. The distance a neutron would have to travel in D_2O before colliding is about six times greater than in H_2O. This feature means that a D_2O-moderated reactor would have to be several times larger than a H_2O-moderated reactor. For example, the diameter of the c*alandria* (the moderator tank) of a CANDU system is about 8 m ($\sim$26 ft)^3, whereas the diameter of a 1000 MWe PWR is much smaller, about 4.5 m (15 ft) [5]. However, unlike the CANDU, the PWR vessel must be thick walled ($\sim$0.33 m) and hence, expensive to manufacture. Such a heavy forging must be without flaws; a major undertaking. For CANDUs, the calandria tank is only about 0.001m thick (since the moderator fluid is maintained at about 1 bar, and $<80^\circ$C). The large-size feature is detrimental from an economics viewpoint, since D_2O can cost [3] between $300 and $500 per kg.

However, D_2O possesses a key positive attribute relative to H_2O: dealing with parasitic absorption during collision

with neutrons. The currency of a successful power-producing nuclear fission reactor is the "neutron." The more the neutrons at a given time, the greater will be the number of fissions and more energy is produced. If neutrons produced from fission get absorbed, they would then not be available to keep the chain reaction sustained, and the reactor power will die down. Fortunately, D_2O absorbs neutrons to a much smaller (almost negligibly) compared with H_2O—in fact about 600 times less. The combination of scattering and absorption characteristics are characterized by the key metric [4] called *moderating power*, which is ~21,000 for D_2O and only ~58 for H_2O. This attribute of D_2O itself becomes a key factor, which permits the neutrons from fission to remain available for sustaining a chain reaction without needing uranium enrichment. H_2O-moderated reactors, because of their tendency to lose neutrons to water via absorption, require more U235 to keep the chain reaction going (and hence, must used enriched uranium).

From a safety perspective, a nuclear fission reactor must be controllable and self-stabilizing. That is, if a state of non-equilibrium is reached in which the power rises and the fuel starts to heat up or the coolant starts to boil and escape, the nuclear feedback must remain negative such that the neutron population (and hence fission reactivity events and the nuclear energy released) comes down automatically. Any nuclear fission reactor licensed in the United States must have this feature; otherwise, the U.S. Nuclear Regulatory Commission (USNRC) will not authorize licensing the facility. However, as a consequence of the nuclear performance of a CANDU reactor, the loss of D_2O from within the pressure tubes results in a "positive" fission reactivity behavior [3, 4, 6]—this is why no CANDU reactor has ever been licensed for sale in the United States. Fortunately, for CANDU systems, the rate of change of neutron population is much slower. This is because of the longer distances a neutron must travel before coming down in energy from MeV to eV levels and diffusing before a fission reaction can take place. The lifetime of a prompt neutron (i.e., the neutrons emitted immediately within picoseconds after a fission event occurs) in a D_2O moderator system is ten times longer [4] in a D_2O-moderated system versus in a H_2O-moderated system: i.e., ~1 ms in D_2O, versus about 0.1 ms in H_2O. When in a prompt critical mode, this leads to a so-called reactor period (the time needed to exponentially grow the reactor power) of about 1 s for a D_2O-moderated system, versus about 0.2 s for a H_2O-moderated system. That is, in 1 second, a 1 MW power level could rise to 2.7 MW (i.e., about three times) with D_2O, but to 148 MW (or about 150 times) with H_2O. This inherent, built-in sluggishness of a CANDU reactor to transient change is taken advantage of by CANDU designers to enable installation of fast-enough operating digital control systems that can react with sufficient rapidity to prevent fuel overheating despite the positive void-reactivity coefficient of a CANDU system. H_2O-moderated water reactors do not possess positive reactivity coefficients. This aspect is covered later on when we discuss safety aspects and control systems.

In summary, while a CANDU system using D_2O as moderator permits use of natural uranium (since D_2O does not like to absorb neutrons like H_2O does), the size of the reactor must be much larger than a H_2O-moderated reactor. The vastly longer neutron lifetimes in D_2O versus H_2O save the day and enable the CANDU reactor, by virtue of its sluggishness to sudden changes in power, to remain adequately controllable from a safety and operational viewpoint.

19.4 THE CANDU REACTOR SYSTEM [1, 3, 4, 7–11]

As mentioned earlier, due to the moderating properties of D_2O, a tube-shell type design was developed by AECL designers. Such a system is depicted schematically in Figure 19.2. The large outer tank is called the calandria, which is filled with D_2O and is not pressurized. In the horizontal direction are several hundred fuel channels (e.g., 380 in the ~700 MWe CANDU 6 design, to 480 in the ~900 MWe CANDU 9 design). Each of the fuel channels will have multiple (e.g., 37 for the Bruce B reactor) fuel bundles placed one behind the other (Fig. 19.2a). The fuel channels are grouped together and directed into steam generators from headers, after which the coolant flows back into the reactor. Either one or two such loops have been used. There is also a second separate moderator flow circuit, which is put in place to avoid having the unpressurized D_2O in the calandria become overheated past 80°C. The steam generators produce dry steam, which is fed into turbine-generator sets to produce electricity thereafter. Table 19.1 presents information on operational characteristics of the various CANDU plants. Generally, the moderator tank is at low (close to atmospheric pressure, and the D_2O moderator therein is maintained at ~70°C. The pressurized fuel channels have high-pressure (10 MPa) coolant entering at ~250°C and leaving to the steam generators at ~310°C (which is low compared with LWRs and leads to reduced plant efficiency). Fuel burnup (i.e., consumption) is generally in the 8,000 MWd/MTU range, which is significantly lower than the values of about 60,000 MWd/MTU for LWRs. As a consequence of the low fuel burnup due to use of natural uranium in CANDUs, and for enhancing availability, online refueling is used in which about 8 to 12 fuel bundles are removed and refueled each day. Such online refueling at full power is one of the reasons why CANDU plants have traditionally enjoyed the highest capacity factors of all nuclear reactors worldwide

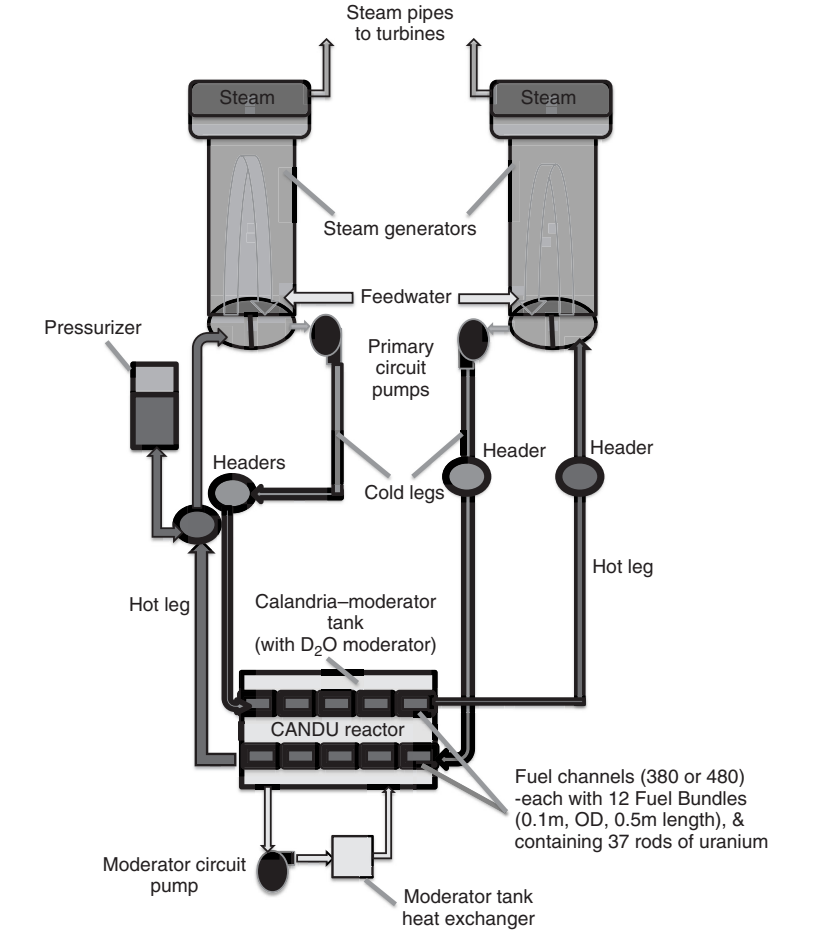

Figure 19.2 (a) CANDU Reactor and two heat transfer circuits. (b) CANDU 37 element fuel bundle [11].

TABLE 19.1 Comparison of Operating and Design Parameters for Various CANDU Systems

Plant	Power (MWe) -Net	# Fuel Channels	# Loops	Header Pressure (MPa)	Max. Channel Flow (kg/s)	Steam Generator Area (m^2/SG)	Steam Pressure (MPa)
Gentily-2	638	380	2	10	24	3200	4.7
Embalse	600	380	2	10	24	2800	4.7
Pickering (4 Units)	515	390	2	8.7	23	1850	4.1
Bruce B (4 Units)	860	480	1	8.7	24	2400	4.7
Darlington (4 Units)	881	480	2	10	27.4	4900	5.1
ACR-1000*	1087	520	2	11.1	28	NA	5.9

—ACR-1000 uses H_2O as coolant; outlet temperature = 319°C; Efficiency increased to 34%; compared with ~28% to 30% for present-day CANDU systems; Fuel bundle comprises 43 elements (versus 37 in existing CANDUs); Fuel is enriched (2–3 w/o U235); Burnup is increased to ~20,000 MWd/MTU vs <8,000 MWd/MTU (for existing CANDUs).

Other Pertinent Design Data: Calandria diameter: ~7.6 m for CANDU 6; ~8.5 m for CANDU 9; ~7.5 m for ACR-100. Pressure tube thickness: ~4 mm for CANDU 6/Darlington; ~6.5 mm for ACR-100. Lattice Pitch: ~286 mm for CANDU 6/Darlington; ~240 mm for ACR-100. Outlet Header temperature: ~310°C for CANDU 6/CANDU 9; ~319°C for ACR-100. Steam Generator tube diameter: 15.9 mm (CANDU 6/9); 17.5 mm (ACR-1000). Steam temperature: ~260°C (CANDU 6); ~265°C (CANDU 9/-Darlington); ~275.5°C (ACR-1000). Steam pressure: ~4.6 MPa (CANDU 6); ~5 MPa (CANDU 9/Darlington), 5.9 MPa (ACR-1000). Steam quality: ~0.9975 (CANDU 6/9); ~0.999 (ACR-1000). Online refueling: ~8 to 12 fuel bundles are replaced each day for all CANDU designs.

(approaching ~90%). The continuous refueling aspect is in contrast to LWRs where fuel assemblies remain in the reactor core for over two years before replacement, causing downtimes of over one to two months for refueling.

The CANDU reactor is connected to steam generators that produce steam, which is sent to turbine generator sets. The reactor system, along with steam generators and emergency cooling and shutdown systems, are housed within an envelope that forms the containment building of a type and construction similar to those used for conventional LWR systems (Fig. 19.3). Containments have the primary purpose of trapping radionuclides, if released from nuclear fuel during normal operation (e.g., from fuel failures), or more importantly, during accidents, and also to protect the nuclear reactor from external threats such as missiles, wind, fires, or others. Steam pipes from the steam generators lead to the outside of the containment where buildings house the turbine-generator sets, which are connected to the switchyard and transmission lines.

19.5 STEAM GENERATORS FOR CANDU REACTORS [12–15]

A critical mission-relevant component of any steam-driven, electricity-producing nuclear plant is the steam generator. While the boiling water reactor [4] (a type of LWR) design produces steam directly from within the nuclear reactor vessel itself, the rest of the water-cooled/moderated nuclear reactor systems worldwide utilize steam generators.

Steam generators are a form of heat exchangers thath exchange heat from the hot primary side pressurized coolant running through the nuclear reactor with a low-pressure liquid flowing on the secondary side that enters the steam generator, heats up, and boils to produce steam. This steam is dried (i.e., water droplets are removed) and then passed on to conventional turbine-generator sets to produce electricity. Steam generators in nuclear plants, as such are critical components in relation to the primary mission of the plant. The CANDU system concept utilizes steam

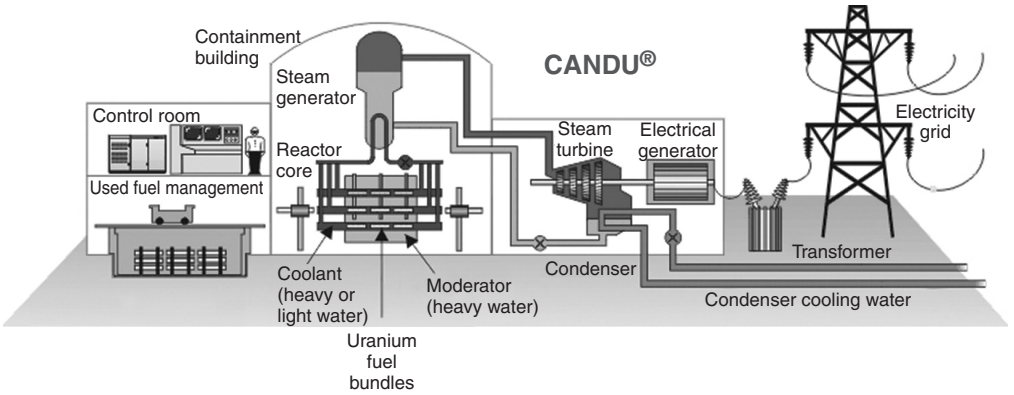

Figure 19.3 CANDU power plant [7].

generators, which have evolved somewhat uniquely since the first designs used for NPD and Douglas Point and owe their roots to the WWII–era submarine designs. Much of the evolution has been driven with the requirements for higher power, high steam quality, the use of D_2O as primary side coolant (which can become radioactive with tritium), cost, robust reliable operation, and compactness.

As part of appreciation for Canadian contributions to the WWII war effort, a request was made by Canada [12] early on for enabling a jump start in the nuclear technology arena, a key component being to receive design details of U.S. nuclear submarine steam generators via the Babcock Wilcox Canada company (BWC) Ltd. This design was adapted for Canada's first 20 MW steam generator for its NPD plant. This submarine-based design for the boiler included a horizontal steam drum positioned above the horizontally positioned U-tube heat exchanger. The steam drum was connected via riser and downcomer tubes to the shell side of the heat exchanger. Use was made of cyclone-generating steam separators to produce dry steam to send to the turbine-generator set. Several useful lessons were learned in relation to complexities related to fretting induced wear around steam generator tubes held in place at grid support plates.

The success at NPD led to work on SGs for the Douglas Point plant where the horizontal heat exchanger was changed to a U-tube hairpin type vertically positioned heat exchanger. Thereafter, for Pickering Station's 500 MWe boilers, BWC designed a variant of the PWR steam generator, but took heed for minimizing the volume of the primary side (to account for the cost of heavy water). Significant knowledge was gained therein on fretting and vibration issues, which then helped later on in the design of steam generators for the modern CANDU fleet of nuclear plants. At first, for the Bruce A station, a common steam drum was utilized for multiple steam generators, resulting in boiler level control issues. This led to dismissing of cross-drum boiler designs and the advent of the current day light-bulb type designs as shown in Figure 19.4.

The CANDU steam generator systems [12, 13], as with other light water reactor plants, face several operational issues such as fretting, leakages, and fouling. Fretting and leaks are normally addressed by plugging the individual tubes. Fouling, on the other hand, can lead to significant degradation of performance due to buildup of magnetite (a corrosion product on the inside of steam generator tubes), which must be periodically cleaned. This issue gains added importance for CANDU plants where the primary side D_2O coolant can become contaminated with tritium (a radioactive gas). In the past, cleaning of tubes would normally be performed using chemical and mechanical brushing techniques. Recently, two shot-blast techniques have been developed [14, 15] that use robotic manipulators to shoot tiny pellets of metal using high-pressure air through one side of the heat exchange tubes and then collect the shot together in a single vessel within the bowl of the CANDU heat exchanger.

19.6 SAFETY AND CONTROL OF CANDU REACTORS [3, 6, 8, 10, 16]

CANDU nuclear reactors use two independent digital computer-controlled systems to monitor plant status continually, with one performing the task at any given point in time and the other acting as a backup. Reactivity control, as

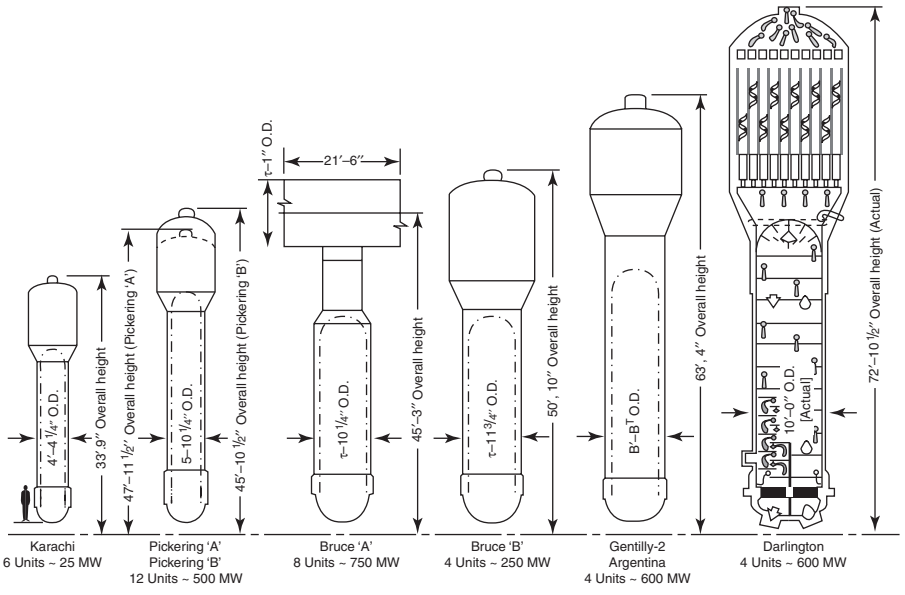

Figure 19.4 CANDU steam generator types [13].

well as power shaping within the reactor, is accomplished using fuel management (since CANDUs can be refueled online while at full power), as well as with a set of adjuster rods made of steel or cobalt. Both steel and cobalt can absorb neutrons and thus reduce the power level where they are placed. In fact, the use of natural cobalt has a secondary benefit in that with neutron absorption a valuable industrial isotope (cobalt-60) can be produced and used for applications ranging from cancer therapy to gamma scans of containers to use for sterilization or food preservation [8]. If boiling occurs in a coolant channel, steam gradually displaces coolant. The name of this effect is *voiding*. A partial or total void in a channel affects resonance capture, parasitic absorption, fast fission, and leakage. The void reactivity is commonly related to the change in reactivity for 100% voiding of all coolant channels. It is positive in CANDU reactors. The actual value varies from reactor to reactor but is about +10 mk (milli-k) for the Bruce reactors and can be up to 15 mk for CANDU 6 type reactors. The letter "k" in nuclear reactor theory [3] is used to provide an indication of how reactive the fuel-water system is. Positive "k" values are an indication of increased uranium fission (i.e., reactivity), hence a condition in which fission power will rise. Conversely, negative "k" values are indicative of decreased reactivity. When voiding of coolant occurs, there is no moderation of the high-energy fission neutrons, which can then reach neighboring fuel channels. This has two major effects, both a result of use of natural uranium (where the principal uranium isotope is U238): (a) An increase of fast neutron induced fission in U238 takes place, which generates energy; and (b) an increasing number of neutrons escape, being absorbed and removed as they would otherwise do before they leave the fuel. More neutron availability means that these escaping neutrons into the moderator tank will next be available to produce more fission events when they come back into the fuel at lower energies. Now, a +10 mk is a very large positive reactivity and able to cause an unacceptably fast power rise if it were to be inserted all at once. However, it is not ordinarily possible for all the coolant to flash instantly to steam, even on a large pipe break. In fact, the first second after a large loss-of-coolant accident can result in a positive reactivity insertion of only about 4 to 5 mk. The CANDU safety systems are designed to detect and stop the power rise long before the +10 mk of reactivity is ever inserted. There are two independent, fast, automatic, safety shutdown systems to make sure a shutdown occurs.

Reactor shutdown is accomplished via two independent, fast-acting systems [3, 8, 10, 16]: (1) Shutdown System 1(SDS 1), which consists of cadmium (a neutron poison) rods that are gravity driven, and, (2) Shutdown System 2 (SDS 2), a high-pressure injection of a liquid neutron poison (gadolinium nitrate) into the low-pressure moderator tank (calandria). Both SDS 1 and SDS 2 are independently capable of shutting down the reactor, if and when they receive the appropriate signals from independent triple-logic-based, online nuclear radiation sensor systems. Each shutdown system can be actuated within 1 s and can cause a large negative reactivity (e.g.,−50 mk) in the first second after actuation. Therefore, despite the fact that it is often cited as a concern that conventional CANDU systems possess a positive void reactivity coefficient, the relatively sluggish response of a D_2O-moderated system such as CANDU, the fact that all coolant voiding instantaneously is impossible, and in fact readily controllable by the shutdown systems, makes this somewhat of a red herring (albeit, a worrisome psychological) issue.

In addition to the two independent shutdown systems, CANDU plants include two other safety systems: the emergency core cooling systems (ECCS) and the containment system. Figures 19.5 and 19.6 display the safety and control systems. The ECCS is designed to re-establish fuel cooling in the unlikely event of a loss-of-coolant accident (LOCA) and incorporates three stages: injection stage, intermediate stage, and recovery stage. The injection stage uses pressurized air to inject water from tanks located outside the reactor building into the heat transport system. The intermediate stage supplies water from the dousing tank. When this water supply is over, the recovery stage system pumps water that has spilled over and collected in the reactor building sump and pumps it back into the heat transport system to keep the fuel rods from overheating. The containment system (Figs. 19.3 and 19.7) is a full containment system in the sense the entire reactor system, including the heat exchangers, is covered within a large reinforced concrete building under negative pressure with a water spray (dousing system) to condense any steam within the building and to prevent overpressure-based breaches. The ECCS and containment systems are similar to those utilized for western PWR and BWR systems.

A convenient quantitative metric for judging the relative safety of nuclear plants is based on the use of Probablistic Safety Assessments (PSAs). PSAs are currently used by the regulatory bodies (e.g., USNRC), for risk-informed decision making. For CANDU systems, such an analysis has been conducted for a variety of CANDU plants [17]. The results of PSAs are provided in terms of the frequency (or likelihood) of the occurrence of fuel failure and severe core damage leading to release of fission products from breached fuel rods, when taking hundreds to thousands of possible pathways for failures to occur. The PSAs conducted for the Wolsong Power Station in South Korea (a 700 MWe CANDU 6 design) and the Darlington Power Station in Canada (a 900 MWe CANDU 9 design) reveal a total (summed) severe core damage frequency of $\sim 6.1 \times 10^{-6}$/y and 3.8×10^{-6}/y, respectively—that is, one chance in about half a million that in a given year a severe core damage event will occur. These core damage frequencies

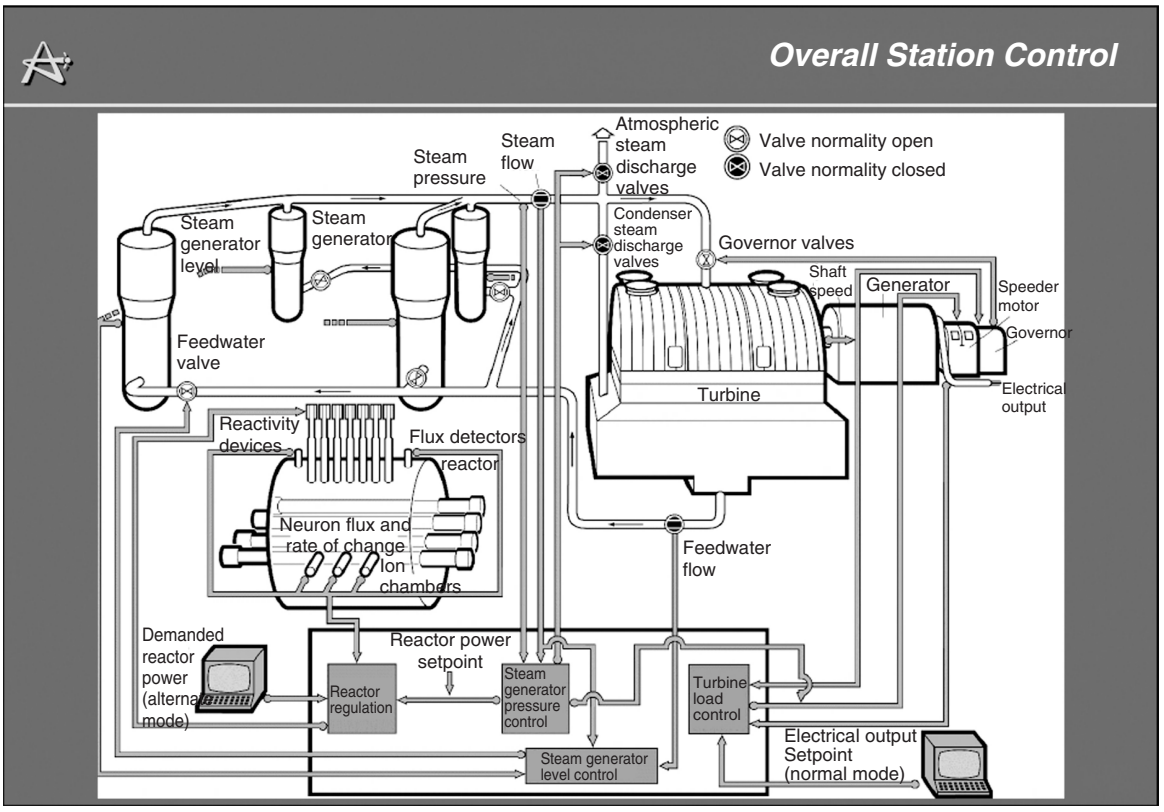

Figure 19.5 CANDU reactor and plant control systems [16].

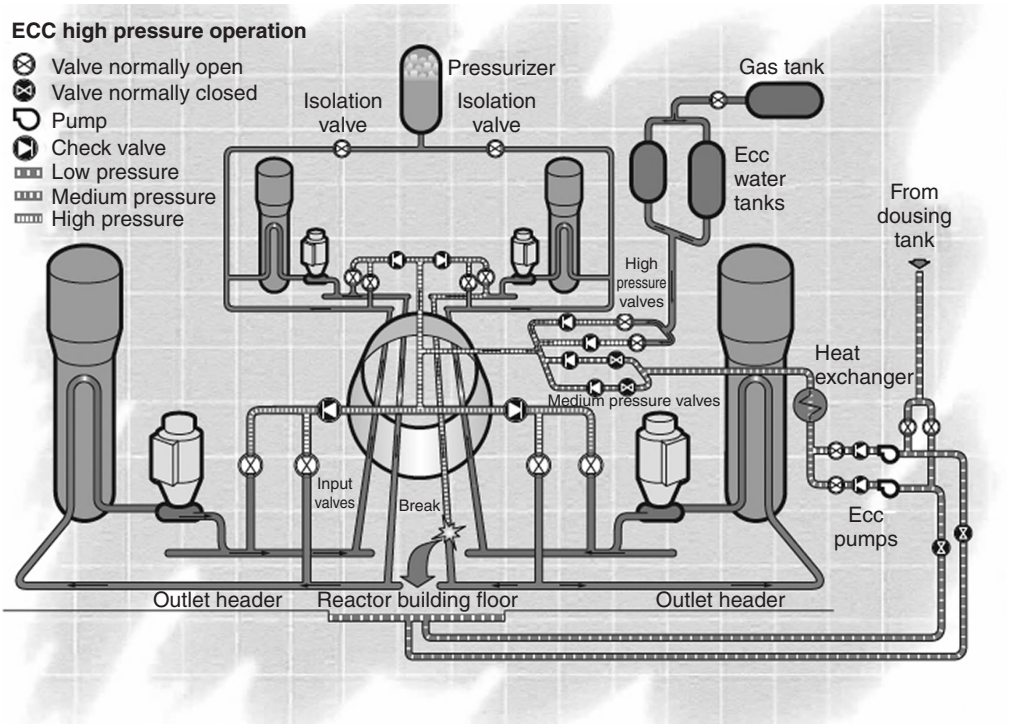

Figure 19.6 CANDU safety systems—emergency core cooling circuits [14].

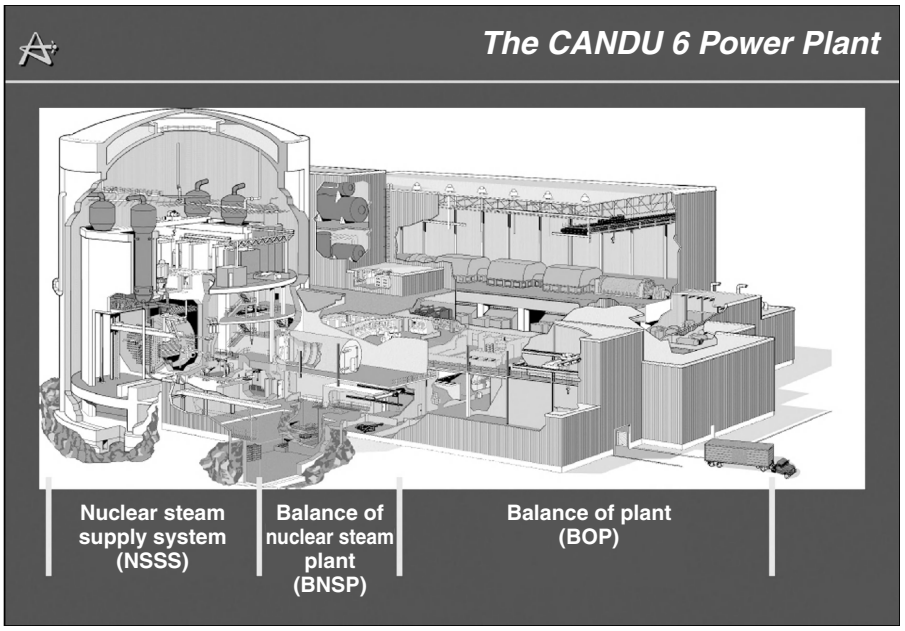

Figure 19.7 CANDU 6 plant layout [16].

are comparable with existing LWRs. The USNRC [18] mandates [19] that the risk of cancer from nuclear plants to the population near it should not exceed 0.1% of the sum of cancer risk from all other causes. The U.S. Environmental Protection Agency (EPA) estimates [20] that cancer risk from natural sources of ionizing radiation is 1 in 100 or about 0.01. Including other causes such as smoking and other life factors would increase this value. 0.1% of 0.01 amounts to $10^{-2} \times 10^{-3}$ or $\sim 10^{-5}$. The frequency for core damage (i.e., onset of a severe accident) for CANDU systems was found to be below these values.

The core damage frequency in CANDU plants due to failure of the two independent shutdown systems is evaluated [18] to be even smaller at 3×10^{-8}/y or about 1 chance in about 33 million years, a value that is commensurate with a large meteorite striking the earth capable of causing massive damage to life and earth (e.g., similar to that which is considered to have wiped off the dinosaurs).

19.7 NEXT GENERATION ADVANCED CANDU DESIGNS [3, 9, 20, 21]

CANDU reactor designs have evolved over three generations (GEN): GEN-0 (ZEEP, NRX, NRU), GEN-1 (22 MWe Nuclear Power Demonstration plant), GEN-2 (the 200 MWe Douglas Point plant), and, GEN-3 (the ~700 MWe CANDU 6 designs of Gentilly, Wolsong, and others; the ~900 MWe CANDU 9 plants at Bruce and Darlington stations). In recognition of negative perception issues related to a positive void reactivity coefficient, as well as the low (compared with other LWRs) thermal-to-electric conversion efficiency, to improve the safety and economics of the CANDU plant, AECL has come up with improvements to the baseline CANDU systems of the past with the development of their so-called ACR (Advanced CANDU Reactor) as the GEN III+ offering of the CANDU line of nuclear plants.

The ACR [21] is an evolutionary design offered at two power levels: the 700 MWe (ACR-700) and the 1,200 MWe (ACR-1000) class heavy water reactor-based plants. The ACR reactor core consists of fuel and light water coolant in pressure tubes with the heavy water moderator outside in the calandria. The fuel is enriched (i.e., 2% to 3% of U235 by weight) to allow higher burnups, and the use of light water together with enriched fuel makes the void reactivity coefficient a negative value of about −3 mk (compared with over 10 mk for baseline CANDU plants [21]). Together with modular construction and the claimed ability to not only burn uranium fuel, but also thorium and mixed oxide fuels, and for possible applications in hydrogen production and development of Canadian oil-sands reserves, the ACR is being marketed by the developers at AECL as the next generation CANDU system [20]. Table 19.1 compares some of the salient design features of the ACR versus other CANDU systems.

REFERENCES

1. *"Controlled Nuclear Chain Reaction—The First 50 Years."* American Nuclear Society, 1992.

2. K. Hedges, ACR Workshop, *Introduction*, 2002. Canteach document: http://canteach.candu.org/aecl.html#ACR, accessed June 2010.
3. B.P. Bromley, *Heavy Water Reactors: Physics, Concepts and History*., Joint ICTP-IAEA Workshop on Nuclear Reaction Data for Advanced Reactor Technologies, May 26/27, 2008.
4. S. Glasstone and A. Sesonske, *Nuclear Reactor Engineering*. Van Nostrand Reinhold Company, 1967.
5. *Pressurized Water Reactor (PWR) Systems, Reactor Concepts Manual*. USNRC Technical Training Center, www.**nrc**.gov/reading-rm/basic-ref/. . . /animated-**pwr**.html, accessed June 2010.
6. *Main Steam and T/G Systems, Safety*. Canteach document, www.canteach.candu.org/library/191980104.pdf, accessed June 2010.
7. Canadian Nuclear FAQ, http://www.nuclearfaq.ca/cnf_sectionA.htm#c, accessed June 2010.
8. *CANDU Fundamentals*. Canteach document, canteach.**candu**.org/library/20040721.pdf, accessed June 2010.
9. B. Garland, *The Canteach Project*. www.canteach.candu.org.
10. CANDU 6 Program Team, *CANDU 6 Technical Summary*. Atomic Energy Canada Limited, June 2005.
11. R.B. Lyon, *Heavy Water Reactors: Status and Projected Development*, Technical Reports Series No. 407. International Atomic Energy Agency, Vienna, Austria, 2002.
12. J.M. Dyke and W. J. Garland, *Evolution of CANDU Steam Generators—a Historical View*. May 19, 2006. Canteach document: www.canteach.**candu**.org/library/20060101.pdf, accessed June 2010.
13. W.J. Garland, *Reactor Thermalhydraulic Design Reference Text*. Thai-Canadian Nuclear Human Resources Development Linkage Project, Canteach document: www.canteach.candu.org/library/20043701.pdf, accessed June 2010.
14. G. Kramer and F. Amman, *Method for the Cleaning of Heat Exchange Tubes and Collecting Device for the Collection of Deposits from Heat Exchange Tubes*, Canadian Patent No. 2,280,348, October 12, 2004.
15. E. Wilson, Mechanical cleaning for steam generator. *Nuclear Engineering International*, January 2008, www.aecl.ca/Assets/Publications/NEI-Steam_Generators.pdf, accessed June 2010.
16. V.G. Snell, *CANDU Safety—Emergency Core Cooling*. Canteach document www.canteach.candu.org/library/19990107.pdf, May 24, 2001.
17. V.G. Snell and R. Jaitly, *CANDU Safety—Probabilistic Safety Analysis*. Canteach document, www.canteach.candu.org/library/19990121, May 24, 2001.
18. www.nrc.gov/reading-rm/doc-collections/fact-sheets/reactor-risk.html, accessed June 2010.
19. *Radiation Risks and Realities*. United States Environmental Protection Agency, EPA-402-K-07-006, May 2007.
20. F. Nuzzo, Advanced CANDU reactor, evolution and innovation. *Proceedings of the 18th International Conference. on Structural Mechanics in Reactor Technology (SMIRT 18)*, Beijing, China, August 7–12, 2005.
21. P. Chan, *ACR Workshop Core Design and Reactor Physics*. Canteach document, www.canteach.candu.org/library/20031205.pdf, accessed June 2010.

20

GRAPHITE-MODERATED FISSION REACTOR TECHNOLOGY

PAVEL V. TSVETKOV

Department of Nuclear Engineering, Texas A&M University, College Station, TX, USA

20.1 GRAPHITE AS MODERATOR

Graphite is one of the best moderators among typical materials used in nuclear reactors. It has been used as a reactor moderator since the beginning of nuclear era because of its high scattering and low absorption rates. Low neutron absorption in graphite allows using natural or low enriched uranium as reactor fuel. Only heavy water has better moderator properties than graphite. Because carbon nuclei are sufficiently large to lead to relatively long neutron mean free paths, graphite-moderated reactors are typically large. Notably, graphite interactions with air result in graphite oxidation, leading potentially to graphite fires. To avoid this, inert coolants are used, typically helium and nitrogen.

Although CO_2 has been used as the coolant in the MAGNOX class of natural uranium-fueled, graphite-moderated reactors for many years in the United Kingdom, most of the current interest is directed at HTGRs using helium under high pressure to cool a reactor fueled with enriched uranium and moderated by graphite. The helium coolant is then passed through steam generators to transfer the thermal energy on to a secondary loop containing water as a working fluid.

If graphite is used as the moderator, it is possible to configure graphite components and fuel elements into composite assemblies. In these configurations, coolant channels are typically arranged through the graphite medium or through the annular fuel elements.

As reactor material, graphite can be found in inherently safe Generation IV helium-cooled very high temperature reactors (VHTRs) evolving from historical high-temperature, gas-cooled reactors (HTGRs) and in boiling water-cooled graphite moderated reactors (RBMK—high-power channel reactor—reactor bolshoy moshchnosty kanalny), one of which was destroyed in the Chernobyl accident in Ukraine.

20.2 HISTORY OF GRAPHITE-MODERATED FISSION REACTORS

Graphite-moderated reactors have a long history of operation worldwide. In the United Kingdom, experience at the Windscale nuclear reactor with air-cooled, graphite-moderated reactors for plutonium production was considered safer than experience at Hanford with water-cooled reactors. By 1956, this experience resulted in the Calder Hall dual-purpose design for power and plutonium. The design used natural uranium metal as the fuel, graphite as the moderator, and carbon dioxide gas under pressure as the coolant. Several advanced (Hinkley Point B type) nuclear plants, intended primarily for power generation and using slightly enriched uranium dioxide as the fuel, have followed the same basic design principles as the Calder Hall reactors.

In 1967, in the United States, a high-temperature, gas-cooled reactor, with helium gas as the coolant and graphite as the moderator, started commercial operation at Peach Bottom, Pennsylvania. In 1976, a similar reactor of higher power (330 MW electric) was completed at Fort St. Vrain, Colorado.

Today, high-temperature, gas-cooled reactors are in operation in Japan, HTTR with prismatic block core, and

Nuclear Energy Encyclopedia: Science, Technology, and Applications, First Edition (Wiley Series On Energy).
Edited by Steven B. Krivit, Jay H. Lehr, and Thomas B. Kingery.

in China, HTR10 with pebble bed core. Taking advantage of its experience with HTR-10, China is building a commercial pebble bed reactor prototype. In United States, the Generation IV Next Generation Nuclear Power Plant is being considered as a VHTR with either pebble bed core or prismatic block core.

20.3 "MAGNOX" AND AGR POWER PLANTS

The "Magnox" reactors are graphite-moderated, CO_2-cooled reactors fueled with natural uranium, with metal cladding with a magnesium alloy. They have derived their generic name from this latter feature, metal clad with a magnesium alloy. The Magnox reactors were pioneered in United Kingdom and in France and were a natural outgrowth of earlier air-cooled, graphite-moderated research and plutonium production reactors. Many Magnox reactors were built in Britain and France with a few exported to other countries. Early versions used steel reactor pressure vessels with external heat exchangers (boilers) and gas circulating blowers. Later versions employed prestressed concrete pressure vessels incorporating the reactor core, heat exchangers, and coolant circulation blowers. This was primarily a cost reduction measure, although supported by safety advantages with respect to risk of coolant system rupture. Primarily because of coolant temperature limitations imposed by the uranium metal fuel and the Magnox cladding, only relatively modest turbine steam conditions are achievable, limiting the station overall efficiency to $\sim$30% .

As is typical of all natural uranium power reactors, the Magnox reactors are fueled on-load. This is because large quantities of excess reactivity, in the form of additional U235, is not "built into" the new fuel. The in-service availability of the Magnox reactors has proven to be relatively good. On-load refueling helps in this regard. Nevertheless, their relatively high capital cost and relatively modest achievable fuel utilization has led to the discontinuation of construction of further reactors of this type.

The AGR (Advanced Gas-cooled Reactor) has been developed in the United Kingdom as a successor to the Magnox line of reactors. Several are now under construction. They differ from the latest Magnox reactors primarily by the fuel used. The fuel is UO_2, and they have stainless steel cladding. This permits rather higher fuel temperatures and, hence, coolant temperatures to be achieved, leading to conventional fossil fuel steam conditions (2400 psi, 1025°F). The fuel is in the form of a cluster of small diameter rods, permitting relatively high power levels to be achieved. This reduces the size of the reactor core relative to the Magnox reactors, where the fuel is in the form of large single elements. However, because of these fuel changes, the AGR requires some fuel enrichment.

20.4 HTGR POWER PLANT CONCEPT

The High-Temperature Gas-cooled Reactors (HTGR) can be considered as the next evolutionary step in the Magnox-AGR line of gas-cooled, graphite-moderated reactors. The HTGR concept can be considered as an alternative to conventional LWRs. It uses graphite as a moderator and helium as a coolant. In many countries, HTGRs are being developed and have already been built and operated as experimental reactors aimed at electric power generation.

The HTGR differs from the AGR in two major respects. The first is the use of helium as the coolant in place of CO_2. This permits even higher coolant temperatures without inducing a chemical reaction with the graphite moderator. The second relates to the fuel. It is manufactured in very small spheres that are coated with pyrolytic graphite, the latter providing the cladding. These spheres are compacted into large graphite elements.

Helium is an inert gas, and graphite has good mechanical properties at high temperatures. Moreover, since there is no possibility of a phase change of the coolant within the reactor, the system can operate at a high temperature without pressurization. As a consequence of these factors, the primary coolant can attain much higher temperatures than in water-cooled reactors with the gas pressurized only to the extent required to facilitate removal of heat from the core. The very high achievable coolant temperatures lead to high steam cycle efficiencies, or alternatively, make possible the ultimate use of gas turbines directly driven by the coolant.

The fuel probably represents the major development problem yet to be completely solved in terms of achieving attractive long-term fueling costs. This reactor type, because of its high thermal efficiency, should see some preference. The development of the direct cycle gas turbine version would be particularly attractive. Thus, in the HTGR, the moderator is graphite and the coolant is helium gas. After heating in the reactor core: (1) direct cycle—the hot gas passes to a direct gas turbine and then back to the reactor; (2) indirect cycle—the hot gas passes to a heat exchanger and then back to the reactor; this constitutes the primary loop. In the heat exchanger, steam is generated in a secondary loop. The steam is expanded in the turbines, condensed, and returned as liquid water to the heat exchanger, just as in a PWR.

The graphite is used for fuel particle coating, fuel structural material, moderator, and coolant channel walls. Helium is used as a coolant. The use of all-ceramic fuel elements results in low parasitic neutron capture in the core and good fuel cycle economics. The coated fuel particle design results in high specific powers and high fuel burnups. Furthermore, because of the use of graphite, high coolant exit temperatures are possible, resulting in high plant thermal efficiencies.

Coated fuel particles consist of a kernel of oxide or carbide (of U, Th, or Pu with about 95% theoretical density) coated with various layers of pyrolytic carbon (PyC). The fuel kernel has to be porous in order to accommodate fission gasses. In addition to fuel kernel porosity, a gap between kernel and coating and an inner low-density buffer layer are present for further fission fragment accommodation. It has been experimentally confirmed that it is necessary to have the inner low-density PyC layer to prevent fission fragment damage to other coating layers. A layer of silicon carbide (SiC) is sometimes used in the coating in order to improve the retention of metallic fission products. The coating thickness is of the order of 0.2 mm. If no SiC is present, the coating consists of an inner low-density buffer layer and an outer high-density layer (BISO or duplex particles). If SiC is used, the coating consists of an inner low-density buffer layer, an inner high-density pyrolytic carbon layer, a silicon carbide layer, and an outer high-density pyrolytic carbon layer (TRISO or triplex particles).

The HTGR concept can be considered as an alternative to conventional light water-cooled and moderated reactors. It uses graphite as a moderator and helium as a coolant. In many countries HTGRs have already been built and operated as experimental reactors aimed at electric power generation. Within the frame of worldwide investigations in the HTGR concept field, experience of operation of several HTRs and facilities assures further development and deployment:

Fort Saint Vrain nuclear power station—330 MW(e) US HTGR operated for 14 years (837 MW(t), USA).

THTR-300—300 MW(e) German demonstration pebble bed reactor with steam turbine operated for 5 years (750 MW(t), Germany).

HTTR—30 MW(t) Japanese HTGR reached criticality in 1998 (Japan).

HTR-10—10 MW(t) Chinese HTGR reached criticality in 1999 (China).

AVR-15—15 MW(e) Experimental pebble bed reactor operated for 21 years in Germany (46 MW(t), Germany).

PROTEUS—Critical test facility in Switzerland (LEU-HTR PROTEUS, Switzerland).

The following proposed detailed reactor designs have to be noted:

Separate Pebble Bed Type Gas Cooled Reactor (SPGR, Japan).

HTR-MODUL (MHTGR)—80 MW(e) German modular pebble bed reactor design by Siemens/Interatom, licensed in 1987 (Germany).

HTR-100—100 MW(e) German modular pebble bed reactor design by HRB/BBC (Germany).

GT-MHR—300 MW(e) US HTGR, helium turbine design (United States).

INCOGEN HTR—Inherently safe Nuclear Cogeneration with HTR using a direct cycle gas turbine (20 MW(t), the Netherlands).

PBMR-400—400 MW(th) High-temperature helium-cooled reactor using a direct cycle gas turbine (South Africa).

20.5 VHTR POWER PLANT CONCEPT

The Very High Temperature Reactor (VHTR) is a commercial followup for the VHTR prototype technology being developed as the Next Generation Nuclear Plant (NGNP) to be constructed at the Idaho National Laboratory (INL). The main design targets are high temperature and passive safety.

The VHTR will produce both electricity and high temperature heat for applications such as hydrogen production, district heating, desalination, and petrochemical applications. The process heat for industrial applications, and possibly the electricity production, will be transferred through an intermediate heat exchanger (IHX). The reactor thermal power and core configuration will be designed to assure passive decay heat removal without fuel damage during any hypothetical accident. The fuel cycle will be a once-through, very high burnup, low-enriched uranium fuel cycle. An outlet temperature near 1000°C will allow the reactor to be used for a large number of other process heat applications.

The VHTR may have either a pebble-bed core or a prismatic block core. The current designs for the prismatic block-type and pebble-bed-type VHTRs have common features such as (1) low enriched uranium (LEU) fuel, (2) annular core, (3) control rods located in the core and/or in the side reflector, (4) and a high effective height-to-diameter (H/D) ratio. The physics characteristics of the VHTR system differ substantially from operating light water–cooled reactors (LWRs): an annular core design, solid graphite moderator, higher enrichment of the uranium fuel, and TRISO fuel particles. Because of the VHTR design features, a suite of core physics models and analysis tools different from those utilized for analyzing the LWRs is required for accurately representing the physics of the VHTR system. These models are based on Monte Carlo codes and associated libraries and the deterministic code systems (lattice physics and whole-core analysis codes) that can accurately represent the core physics impacts of the coated fuel particles, neutron streaming along channels (prismatic block-type) or through porous bed and at core top (pebble-type), inner reflector-core interface in the annular VHTR core design. Figures 20.1–20.3 show pebble design, pebble bed, and prismatic reactor design elements.

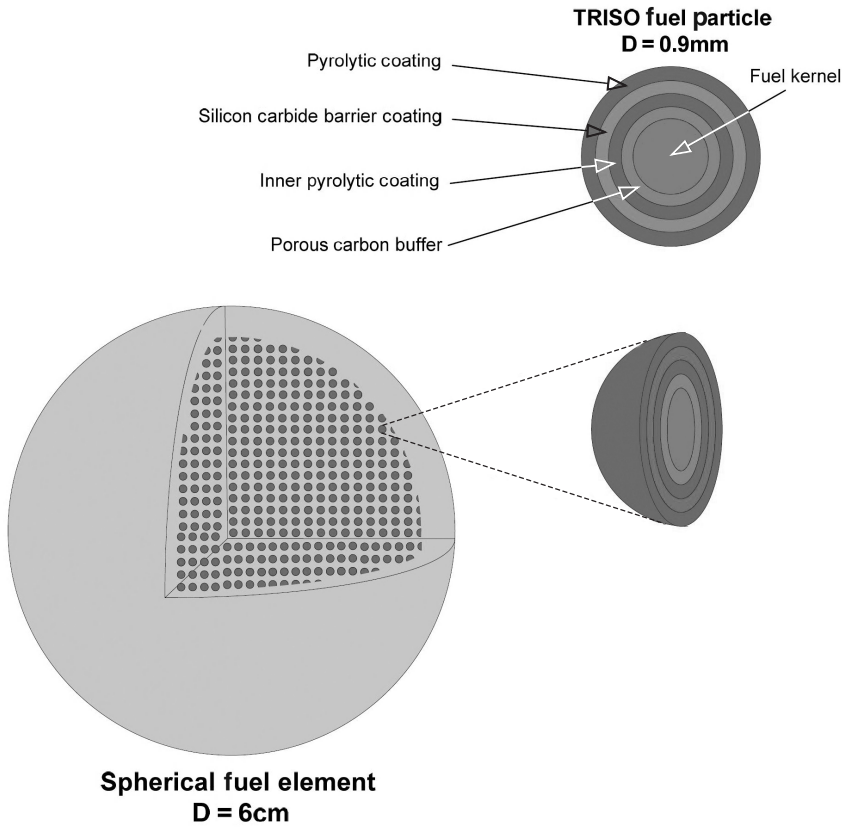

Figure 20.1 TRISO fuel and pebble bed design.

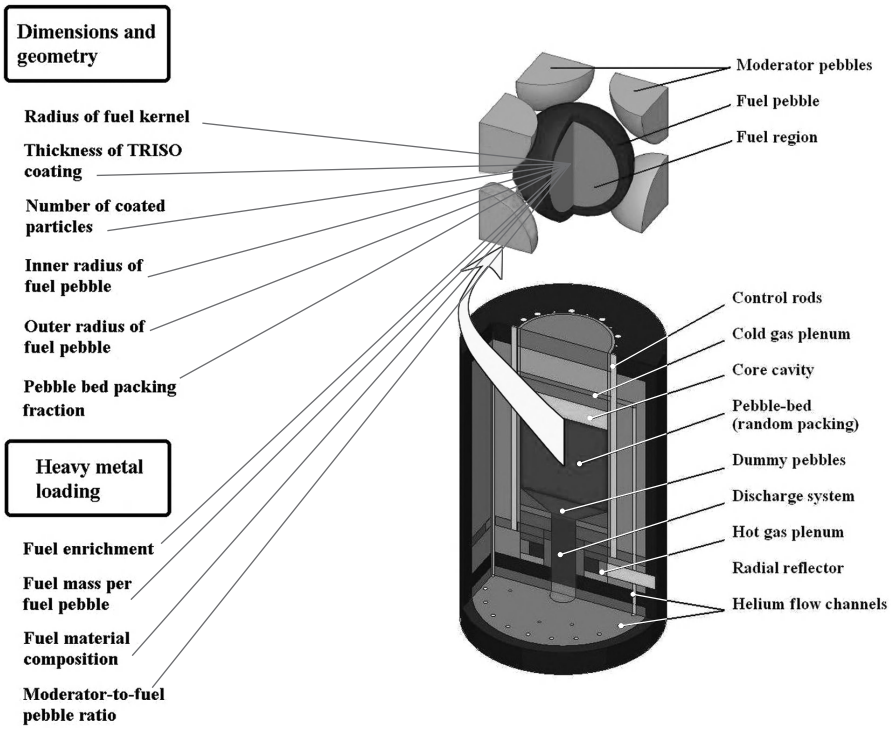

Figure 20.2 Pebble bed reactor design considerations.

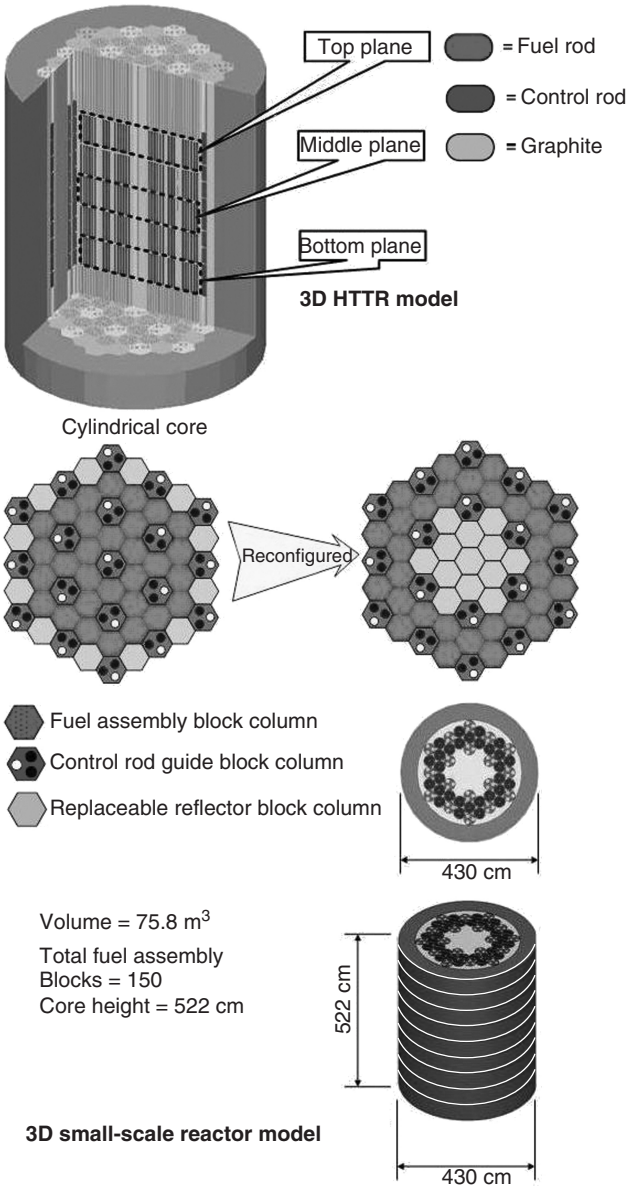

Figure 20.3 Japanese HTTR model.

20.6 BOILING WATER–COOLED GRAPHITE-MODERATED REACTORS (RBMK)

Designed in the USSR, RBMK (high-power channel reactor—reactor bolshoy moshchnosty kanalny) is a pressurized water reactor with individual fuel channels using ordinary water as its coolant and graphite as its moderator. It is very different from most other power reactor designs because it derived from a design principally for plutonium production and was intended and used for both plutonium and power production.

Pellets of slightly enriched uranium oxide are enclosed in a zircaloy tube 3.65 m long, forming a fuel rod. A set of 18 fuel rods is arranged cylindrically in a carriage to form a fuel assembly. Two of these, end on end, occupy each pressure tube. Within the reactor, each fuel assembly is positioned in its own vertical pressure tube or channel about 7 m long. Each channel is individually cooled by pressurized water, which is allowed to boil in the tube and emerges at about 290°C. When fuel channels are isolated, these fuel assemblies can be lifted into and out of the reactor, allowing fuel replenishment while the reactor is in operation. A series of graphite blocks surround, and hence separate, the pressure tubes. They act as a moderator to slow down the neutrons released during fission so that a continuous fission chain reaction can be maintained. Conductance of heat between the blocks is enhanced by a mixture of helium and nitrogen gas. Boron carbide control rods absorb neutrons to control the rate of fission. A few short rods, inserted upwards from the bottom of the core, even the distribution of power across the reactor. The main control rods are inserted from the top down and provide automatic, manual, or emergency control. The automatic rods are regulated by feedback from in-core detectors. If there is a deviation from normal operating parameters (e.g., increased reactor power level), the rods can be dropped into the core to reduce or stop reactor activity. A number of rods normally remain in the core during operation. Two separate water coolant systems, each with four pumps, circulate water through the pressure tubes to remove most of the heat from fission. There is also an emergency core cooling system that will come into operation if either coolant circuit is interrupted. Steam from the heated coolant is fed to turbines to produce electricity in the generator. The steam is then condensed and fed back into the circulating coolant. There is no secure containment in the sense accepted in the West. The reactor core is located in a concrete-lined cavity that acts as a radiation shield. The upper shield or pile cap above the core is made of steel and supports the fuel assemblies. The steam separators of the coolant systems are housed in their own concrete shields.

The combination of graphite moderator and water coolant is found in no other power reactors. The design characteristics of the reactor mean that it is unstable at low power levels, and this was shown in the Chernobyl accident. The instability was due primarily to control rod design and a positive void coefficient. A number of significant design changes have now been made to address these problems. After the accident at Chernobyl unit 4, the primary concern was to reduce the positive void coefficient. All operating RBMK reactors in the former USSR had the following changes implemented to improve operating safety: To improve the operational reactivity margin, the effective number of manual control rods was increased from 30 to 45; the installation of 80 additional absorbers in the core to inhibit operation at low power; an increase in fuel enrichment from 2% to 2.4% to maintain fuel burnup with

an increase in neutron absorption (ie less reliance on cooling water for this). These factors have reduced the positive void coefficient from +4.5 beta to +0.7 beta, eliminating the possibility of power excursion. Beta is the delayed neutron fraction, which is neutrons emitted from each fission with a measurable time delay. The next consideration was to reduce the time taken to shut the reactor down and eliminate the positive void reactivity. Improvements include: scram (rapid shut down) rod insertion time cut from 18 to 12 seconds; the redesign of control rods; the installation of a fast scram system; precautions against unauthorized access to emergency safety systems. There are 179 of 211 control rods, inserted into the core from the top. To improve their effectiveness, they are equipped with "riders" fixed to their bottom end but with a gap between the rider and the bottom tip of the control rod. Approximately 1.0 m water columns remain under and above it. When the control rod is in its uppermost position, the rider is in the control rod cooling tube within the fueled region of the core. Because the rider is made substantially of graphite, it is almost transparent to neutrons, while water, which would occupy the tube otherwise, plays as an absorber. When the reactor is "poisoned" with xenon and with partially inserted control rods, the major part of the power is produced within the lower region of the core. This means that when the rod started to move down from its uppermost position, the rider removed water from the lower part, causing an increase in reactivity and hence in power.

FURTHER READING

GT-MHR: http://www.ga.com/gtmhr/R_GTMHR_Project.html.

HTGR-Related Links: http://www.iaea.org/programmes/ne/nenp/nptds/htgr/links/links.htm.

The IAEA Knowledge Base: http://www.iaea.org/inis/aws/htgr.

PBMR: http://www.eskom.co.za/nuclear_energy/pebble_bed/pebble_bed.html.

21

STATUS OF FAST REACTORS

BALDEV RAJ AND P. CHELLAPANDI

Indira Gandhi Centre for Atomic Research, Kalpakkam, TN, India

21.1 BASIC PRINCIPLES OF FAST NEUTRON SPECTRUM REACTORS

In any nuclear reactor, fissile materials, such as U233 or U235 or Pu239 are destroyed, and U233 and Pu239 are produced by conversion of the fertile materials Th232 and U238 respectively. The ratio of fissile material produced and fissile material destroyed is termed the *conversion ratio*. The conversion ratio, if greater than 1, is called breeding ratio. If η is the number of neutrons produced per neutron absorbed, the necessary condition for breeding is: $\eta = 2 + \mathrm{x}$, to account for one neutron for a new fission, one for a new conversion, and x for leakages or parasitic captures. Figure 21.1 shows that the condition for breeding is well fulfilled in fast spectrum reactor (FR), in particular for Pu239, for which the value of η averaged over the high energy spectrum is about 2.3. Hence, in a fast neutron reactor, there is a net production of fissile material that can be used to fuel another reactor. This is the fundamental characteristic of fast neutron reactors. The rate of generation of fissile materials in the fast reactor (FR) core itself is higher than that of a pressurized water reactor (PWR) of equivalent power, but it remains less than 1. The conversion ratio in a typical 1000 MWe FR oxide core is $\sim$0.72 and 0.6 for PWR. However, significant benefit is derived from the conversion in the blankets of the FR core. The conversion ratio rises to 1.12 with the additional conversion in the blanket with uranium oxide. This is not the case with PWR; surrounding the core with a blanket does not significantly change its conversion ratio of 0.6 due to the low number of neutrons leaking out of the core. Hence, it is relatively easy to modulate the breeding ratio in the FR by enhancing the number of neutrons that are captured by changing the thickness of the blankets appropriately.

21.2 POTENTIAL OF FAST SPECTRUM REACTORS

As per the Nuclear Energy Agency, the proven resources of uranium in the world are 11.5 metric tonnes. In addition, about 3.3 metric tonnes could be extracted, which has some uncertainty. These quantities are equivalent to 150 Giga tonnes of oil equivalent (Gtoe). At the current rate of global consumption (0.6 Gtoe/year), this can support open-cycle water reactors for about 250 years. The primary energy needs are expected to grow strongly from the current consumption of about 9.8 Gtoe to about 40 Gtoe by 2050. To meet these needs, nuclear power should increase its share from 0.6 to 4 Gtoe/year by 2050. This is possible only through fast neutron reactors, which use the U238 reserves currently stored as tails from enrichment plants effectively by multiple recycling and thus allow for increased energy reserves up to a factor of about 60 in comparison to the current light water reactor (LWR) technology. For example, FR with the breeding ratio of 1.2 would yield a power greater than 6 Gtoe/year in 2050. The plutonium requirement would be met through 60 years of LWR operation. Hence, the fast reactors are the key to an efficient use of uranium resources.

Owing to their high level of neutron flux (10 times higher than that of an LWR) and to the ratios of capture cross sections to fission cross sections of major actinides being more favorable in the fast spectrum by a factor of 10

Nuclear Energy Encyclopedia: Science, Technology, and Applications, First Edition (Wiley Series On Energy).
Edited by Steven B. Krivit, Jay H. Lehr, and Thomas B. Kingery.

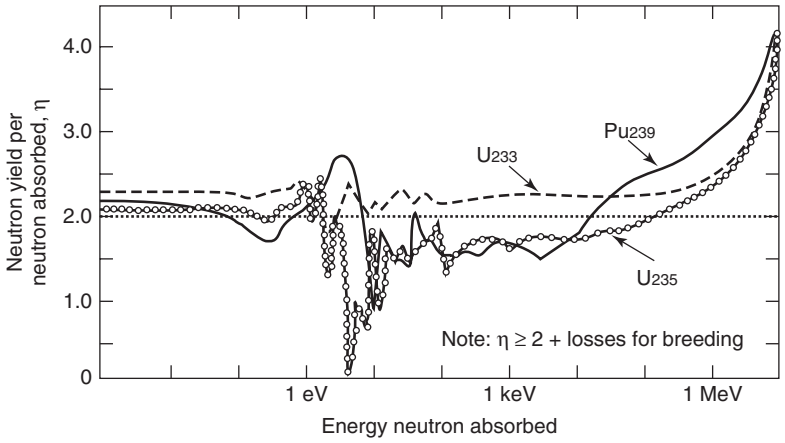

Figure 21.1 Neutron yield in a fission versus energy of neutron absorbed.

(Fig. 21.2), it is easier in FR to transmute the transuranium or minor actinides, such as plutonium, americium, cesium, strontium, and curium. These elements are also primarily responsible for the decay heat that can cause repository temperature limits to be reached. The cesium and strontium can be stored separately for 200 to 300 years, and plutonium, americium, and curium can be recycled for transmutation and/or fission. Hence, there is less impact on the fuel cycle (e.g., in fuel fabrication), and also, large gains in repository space are possible. Further, the FR technology offers means to reduce waste generation by features such as improved thermal efficiency, effective use of fuel resources, and the development of superior waste forms from the FR with closed fuel cycle. It is estimated that the ultimate accumulated long-lived radioactive isotopes, which need to be disposed in repositories, shall contribute less than 0.1% of all the fission products after multiple recycling in FR. FR with closed fuel cycle minimizes the waste management burdens by about 200 times in terms of storage space (Fig. 21.3) and less than 700 year time span for the activity to become close to the background value (Fig. 21.4). It also is obvious that FR contributes to the reduction of the greenhouse effect (CO_2 emissions) compared to electricity generation using fossil fuels.

The FR has the flexibility to operate as a breeder to achieve net creation of transuranics, as a convertor to balance the transuranic production and consumption, and as a transmuter to convert the long-lived minor actinides and other radioisotopes to short-lived ones. An appropriately designed FR has the flexibility to perform in any of the operating modes. The desired actinide management strategy depends on the priority between waste management and resource extension considerations. Further, by developing and introducing adequate advanced separation technologies for an optimal management of nuclear fission products and minor actinides, the FR system has the possibility for a breakthrough in meeting the sustainability and energy security considerations. These facts, in the long-term view,

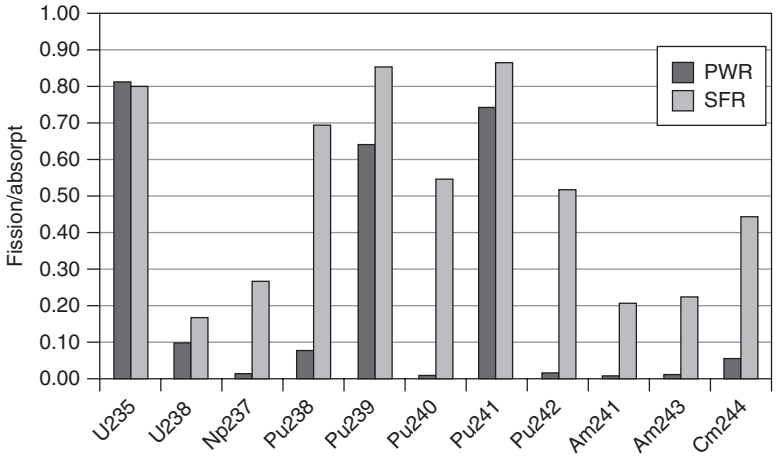

Figure 21.2 Fission to absorption cross sections.

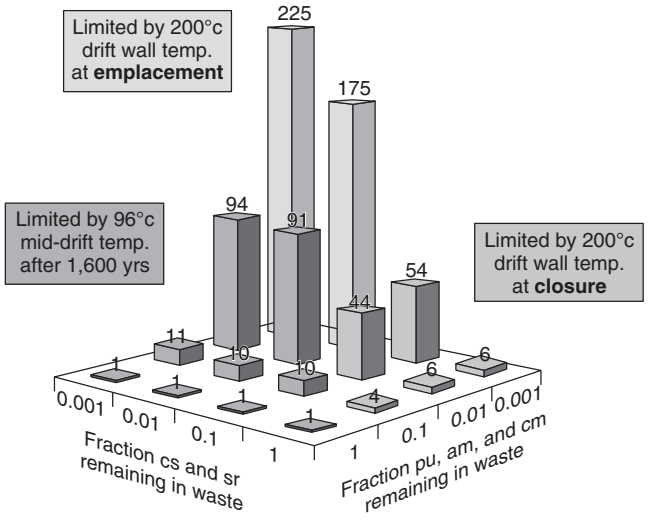

Figure 21.3 Storage space requirements.

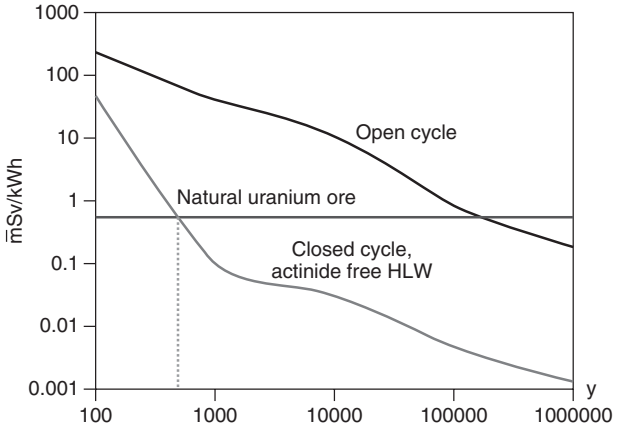

Figure 21.4 Radioactive waste decay time.

favor the acceptability and usefulness of nuclear energy in terms of providing sustainable energy security and clean environment worldwide.

The IAEA is pursuing an international project on Innovative Nuclear Reactors and Fuel Cycles (INPRO). A specific joint study has been carried out with the objectives to assess the innovative fast reactor with closed fuel cycle (CNFC-FR) to determine paths for its deployment and to establish frameworks and areas for collaborative R&D work. The study indicates that both water reactors and fast spectrum reactors will stay side by side, and both open and closed cycle strategies will also be used in the 21st century. A faster growth rate is possible with CNFC-FR systems. However, the time scale for introduction depends on the national and global strategies. Further, the study concluded that the sodium-cooled fast reactors have high potential for near-term deployment by 2015 to 2020. The CNFC-FR, in the global context, would start making contributions in a commercial scale from 2020 onwards. Countries such as China, India, and Russia are planning to increase their nuclear power capacity significantly; hence, FR systems with higher breeding are envisaged. The joint assessment study on CNFC-FR has concluded that this innovative energy system satisfies the sustainability criteria.

21.3 GENERIC SAFETY FEATURES OF FAST REACTORS

The three generic characteristics of FR core, which are claimed to be disadvantages for the FR system compared to PWR, are the following: (1) high power density (specific power is 300–600 MW/m^3 in FR, about five times higher than that of PWR), (2) short lifetime of prompt neutrons (about 4.5×10^{-7} s in FR and 2.5×10^{-5} s in PWR), and (3) a small number of delayed neutrons (overall fraction is 0.35% in FR and 0.6-0.5% for PWR, depending upon the burnup). These issues are addressed in the following paragraphs.

The high power density signifies low thermal capacity of the core; hence, the consequences of the disturbances cause very fast temperature changes, which in turn actuate the fast and continuous feedback by the Doppler and fuel expansion effects. The temperature changes represent the status of the core, which would be known at the core outlet with very small time delay, so that at right time, it is possible to carry out counter measures. This temperature monitoring is carried out, in addition to the neutron flux monitoring. High power density also means small core dimensions and hence, the reactor can be shutdown within short time (<1 s) with short travel of the control and safety rods. Thus, the high power density of the FR core is demonstrated as a safety-oriented advantage. The negative consequence of the high power density is that during the primary pump pipe rupture event without shutdown or with the total loss of coolant flow, high thermal gradients would result. However, any sudden stoppage of the coolant flow is physically impossible due to the high mass moment of inertia of coolant and pumps, and further mismatch between power and coolant flow would soon initiate a fast-scram. Further, the simultaneous failure of pumps and failure to scram is an extremely improbable accident.

Even with small number of delayed neuron fractions, FRs are more stable, due to the benefits derived from fast neutrons. Variations in the operating parameters, for example, inlet temperature, coolant flow, and power have a considerably less influence on the reactivity (about \$0.0015/K compared to \$0.01 – 0.1/K for PWR). Hence, the contribution expected from the delayed neutron fraction

is relatively small. This apart, the short shutdown time of FR adds a large safety margin.

Critical examination of the underlying facts, briefed above, thus reveals that the issues assumed against FR do not pose any significant disadvantages to FR. The dedicated experiments, conducted in the 20 MWt reactor, called SEFOR (Southwest Experimental Fast Oxide Reactor in United States) confirmed the role of Doppler feedback to arrest super-prompt critical transients.

The reactivity loss due to fuel burnup is small in FR due to breeding of fuel and low absorption cross section of fission products to fast neutrons. In thermal reactors, due to the absorbing fission products, much negative reactivity is added, especially by Xenon 135 (half-life of 9.2 h). Within a short period after the shutdown, the reactivity increases considerably due to the decay of Xenon 135. Since its effective cross section, in contrast to the fission cross section, is very much smaller in the fast spectrum than in the thermal spectrum, this effect does not practically play any role in the FR.

In view of special geometrical features, viz. large-dimensioned, thin-walled shell structures with large liquid coolant mass associated with the liquid free levels, the seismic design issues have to be critically investigated from the structural integrity, reactivity variations, pump seizure, and reactor scramability points of view. There are a few critical issues with reference to coolant that are addressed in the section 21.7.1.2. It is worth mentioning that there are only a few postulated initiating events in FR. There exists high potential for decay heat removal capability in case liquid-metal-cooled fast reactors by utilizing the natural circulation. The freedom to choose high-ductile structural materials, such as austenitic stainless steel, offers high energy-absorbing potential in FR systems.

21.4 MAJOR FAST REACTOR OPTIONS

The generation IV international forum (GENIV) has identified six advanced nuclear energy systems that have the potential to meet the sustainability requirements including economics, safety, and reliability, apart from proliferation resistance and physical protection requirements. Out of these, three are fast reactor systems, Sodium-Cooled Fast Reactors (SFRs), Lead Cooled Fast Reactors (LFRs), and Gas-Cooled Fast Reactors (GFRs). These systems can operate on a range of fuel types including oxide, nitride, and dispersion fuels (all); metal fuel (liquid metal coolant); and oxycarbide fuel (gas cooled). There is considerable operating experience for oxide and metal fuels but limited experience with the other types. All three systems can use fuels that are compatible with aqueous processing and pyroprocessing for recycling.

21.4.1 Sodium-Cooled Fast Reactors (SFRs)

The SFR system features a fast-spectrum, sodium-cooled reactor (Fig. 21.5) and a more fully closed fuel cycle for efficient management of actinides and conversion of fertile uranium. The fuel cycle employs full actinide recycle. Plant size options under consideration range from smaller-sized (150 to 500 MWe) modular reactors to larger plants (up to 1,500 MWe). Fuel cycle options are either a metal alloy fuel

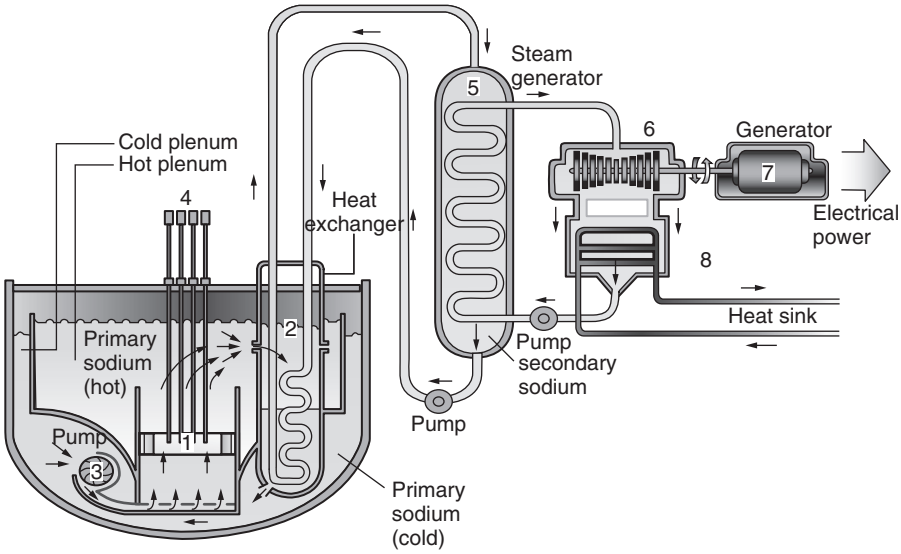

1-core, 2-heat exchanger, 3-pump, 4-control rods, 5-steam generator, 6-turbine, 7-generator, 8-condenser

Figure 21.5 SFR schematic.

that contains uranium and transuranic elements, supported by pyrometallurgical processing of spent fuel in facilities integrated with several collocated reactors, or a mixed uranium-transuranic oxide fuel supported by advanced aqueous processing of spent fuel at a central location serving a number of reactors. The outlet temperature is approximately 550°C for all options. SFR is designed for management of high-level wastes and, in particular, management of plutonium and other actinides. Important safety features of the system include a long thermal response time (the reactor heats up slowly), a large margin between operating temperatures and the boiling temperatures of coolant (less chance for accidental boiling), a noncorrosive coolant (protects pipes and vessels), a primary system that operates near atmospheric pressure (piping is not pressurized), and an intermediate sodium system between the radioactive sodium in the primary system and the water and steam in the power plant. SFR's fast spectrum makes it possible to utilize available fissile and fertile materials (including depleted uranium) considerably more efficiently than thermal reactors such as LWRs.

21.4.2 Lead and Lead-Bismuth-Cooled Fast Reactor System (LFR)

The LFR system features a fast-spectrum reactor using pure lead or lead/bismuth eutectic liquid as coolant and a more fully closed fuel cycle for efficient conversion of fertile uranium and management of actinides. The system supports the actinide management mission with central or regional fuel cycle facilities. Options have a range of plant ratings including a battery of 50–150 MWe reactors (Fig. 21.6) that features a very long interval between refueling to reduce the number of shipments of nuclear fuel, a modular system rated at 300–400 MWe, and a large plant option at 1200 MWe. The fuel is metal or nitride, containing fertile uranium and transuranics. The LFR battery concept is cooled by natural circulation with current development on a reactor outlet coolant temperature of 550°C, possibly ranging up to 800°C with advanced structural materials. The higher temperature enables process heat applications including the production of hydrogen by high-temperature electrolysis processes. A lower temperature variant (~480°C) could be demonstrated with less technical risk but with a somewhat lower thermal efficiency. The LFR battery is a small factory-built turnkey plant operating on a closed fuel cycle with a very long refueling interval (15 to 20 years) with a cassette core or replaceable reactor module. Its features are designed to meet market opportunities for electricity production in isolated locations or on small grids and for countries that may not wish to deploy an indigenous fuel cycle infrastructure to support their nuclear energy systems. The battery system is designed for distributed generation of electricity and other energy products including hydrogen and potable water.

21.4.3 Gas-Cooled Fast Reactor System (GFR)

The GFR system features a fast-spectrum, helium-cooled reactor (Fig. 21.7) and a fully closed fuel cycle. Like thermal-spectrum, helium-cooled reactors, the high outlet temperature of the helium coolant makes it possible to deliver electricity, hydrogen, or process heat with high efficiency. The reference reactor is a helium-cooled system, ranging from 288 MWe to 1,200 MWe, operating with an outlet temperature of 850°C. Several innovative fuel forms are candidates that hold the potential to operate at very high temperatures and to ensure an excellent retention

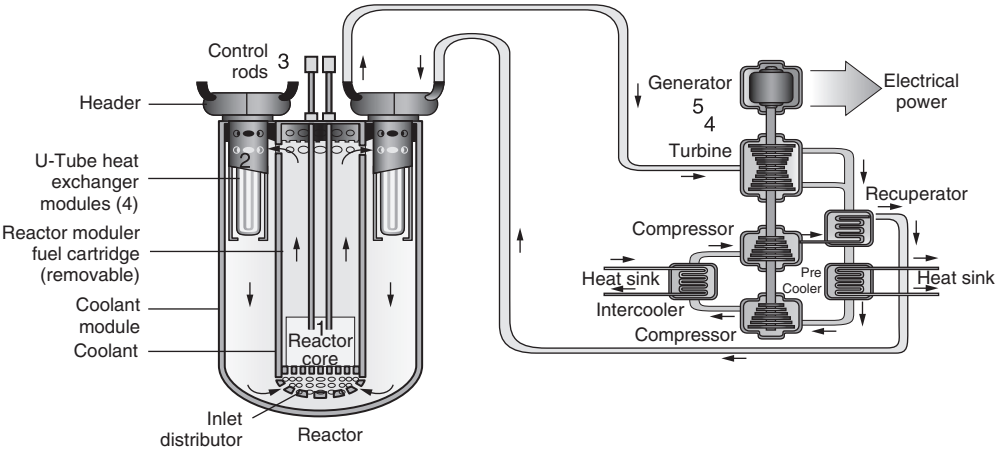

1-core, 2-heat exchanger, 3-control rods, 4-turbine, 5-generator

Figure 21.6 LFR schematic.

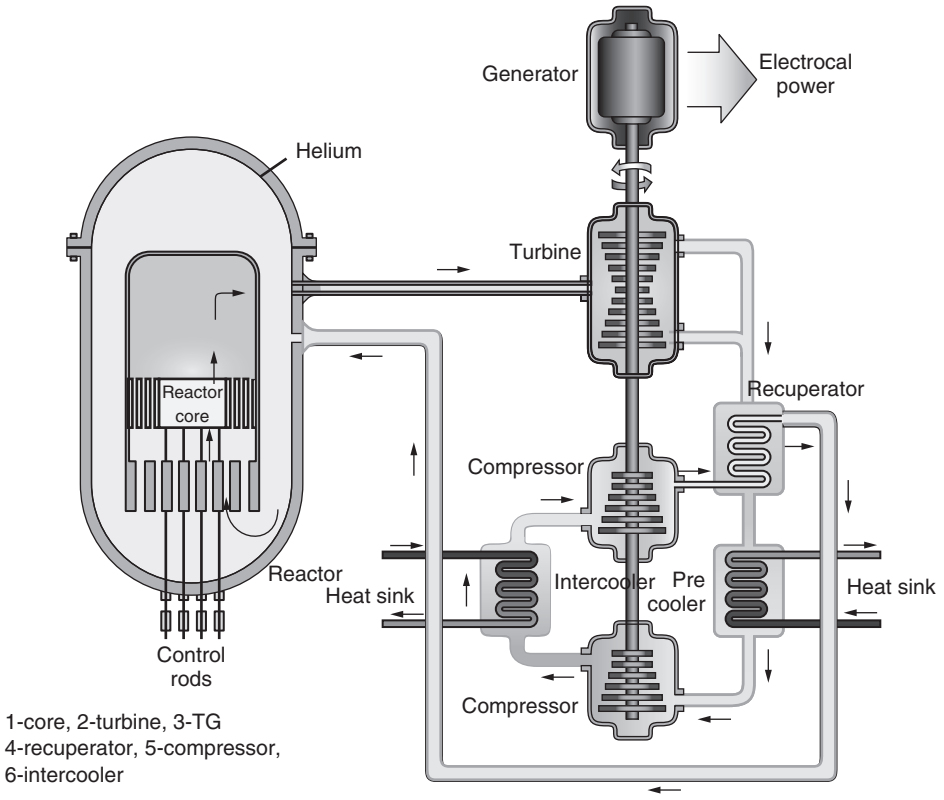

Figure 21.7 GFR schematic.

of fission products: composite ceramic fuel, advanced fuel particles, or ceramic clad elements of actinide compounds. Core configurations may be based on prismatic blocks or pin- or plate-based fuel assemblies. The GFR reference has an integrated, on-site used fuel treatment and refabrication plant. The reference GFR uses a direct Brayton cycle helium turbine for high thermal efficiency in electricity generation or can optionally use its process heat for production of hydrogen. Steam-cycle GFRs have been designed in the past, operating at lower temperatures.

21.4.4 Molten Salt Reactor (MSR)

The MSR system produces fission power in a circulating molten salt fuel mixture with an epithermal-spectrum reactor and a full actinide recycle fuel cycle (Fig. 21.8). The fuel is a circulating liquid mixture of sodium, zirconium, and uranium fluorides. The molten salt fuel flows through graphite core channels, producing an epithermal spectrum. The heat generated in the molten salt is transferred to a secondary coolant system through an intermediate heat exchanger, and then through a tertiary heat exchanger to the power conversion system.

Main MSRs are characterized by the following unique features:

- Neutron balance in the core is adequate for burning and transmutation of actinides or extensive fuel breeding.
- Temperature is sufficiently high for thermochemical production of hydrogen.
- Molten salts are characterized by very low pressure of saturated vapors; as a result, the probability of vessels and pipelines rupturing is reduced.
- The reactor is inherently safe, because it could be provided with a catcher for fuel retaining in case of emergency and a passive cooling system; it also has low percentage of fissile materials in fuel.
- Refueling and removal of fission products can be performed without shutdown of the reactor; therefore, high availability factors can be potentially achieved.
- Easy adding of various materials to molten fuel makes it possible to use the reactor for burning of long-lived actinides and transmutation, thereby reducing significantly the amount of long-lived radionuclides in nuclear waste.

MSRs can be used within a uranium-thorium fuel cycle with maximum (up to 1.07) fuel breeding ratio; as a converter reactor of Th–U233 characterized by minimum inventory of weapons-grade material and, consequently,

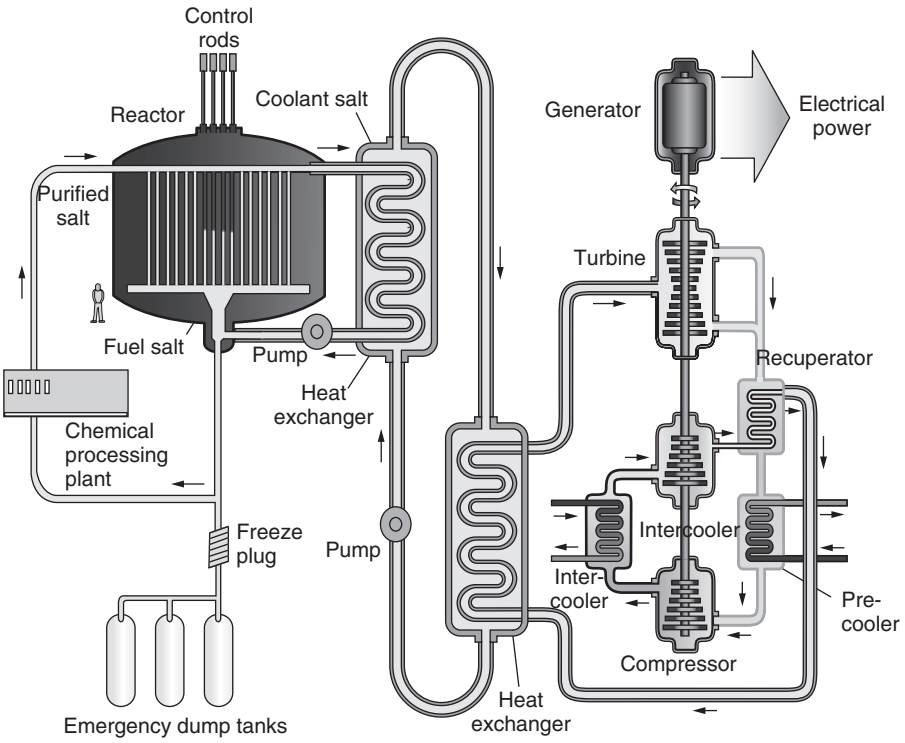

Figure 21.8 MSR schematic.

fully resistant to proliferation; as an incinerator of actinides (plutonium and minor actinides: Np, Am, Cm); and as a burner of actinides in case of continuous recycling of fissile materials.

In the nearest future, the major application of MSR remains as the source of electricity. In this case, sodium and zirconium fluorides will be used as dissolving agents. Radiochemical processing of fuel will be necessary if the reactor would be used only for production of electricity, hydrogen, or for burning of actinides. If the values of the breeding ratio are similar to those at the existing LWR, molten fuel shall be replaced once in several years. Molten U238 and Th232 fluorides can be used as breeding material. In the initial period, MSR may operate with low-enriched uranium or any other fissile material.

In recent years, several multinational collaborative programs on thorium utilization in MSR have been initiated. In France, the AMSTER concept is being pursued. AMSTER is a thermalized molten salt reactor working on Oh232–U233 fuel cycle with an online reprocessing unit for removal of fission products and for feeding of heavy nuclei (U, Th, etc.) to the MSR. Russian and OECD studies have identified MSR as a potential component of thorium-based *closed* fuel cycle to efficiently burn actinides and reduce the long term radiotoxicity of nuclear wastes. In the United States, MSBR with a Multiheat Helium Brayton cycle is being examined with different thorium fuel cycle options, primarily for actinide waste burning with the secondary interests of production of electricity and hydrogen and breeding and burning of *fissile* fuels without separating them.

21.5 FAST BREEDER REACTORS IN THE WORLD AND OPERATING EXPERIENCES

Operating experience provides important input into the design process and has the potential to influence the maturity of the various fast reactor concepts. The greater the number of operating experience years, the greater the opportunity to modify the design based on operating lessons learned. The SFR relies on technologies already developed and demonstrated for sodium-cooled reactors and associated fuel cycles that have successfully been built and operated in worldwide fast reactor programs. The first electricity generation was demonstrated by EBR-I, a fast neutron reactor in 1951. Subsequently, many test/experimental/prototype FRs have been built and operated in France, India, Japan, the United Kingdom, Russia, Ukraine, and the United States, accumulating about 400 reactor years of operating experience. An experimental FR in Germany was built but never operated. Experience gained so far is not significant compared to LWR, which has accumulated about 13,000 reactor years. This is due, of course, to the fact that the long-term benefit of FRs is counterbalanced by the short-term additional costs involved in the use of a sodium coolant that

requires a more robust technology. The countries mastering the FR technology follow the strategy of attaining purely technical targets, i.e. mastery of plutonium and sodium through test/experimental reactors and subsequently validation of design options that will lead to industrial and economic solutions through prototype reactors. Table 21.1 lists the existing test/experimental reactors in the world. These reactors had essentially twofold aims: to provide experience in the operation of sodium-cooled reactors on a sufficient scale and to allow the development of a fuel element capable of withstanding high burnup. The next phase is that of demonstration reactors. These reactors are electricity generators with a power ranging between 100 and 600 MWe, and their purpose is to prepare for the introduction of high-power reactors by validating their concepts. Table 21.2 lists the demonstration fast reactors in the world.

The last phase involves the construction of high-power prototype reactors, between 750 and 1500 MWe, in order to achieve economic competitiveness. The first such project was the Super Phénix (SPX) reactor designed and built by a European consortium composed of France, Germany, and Italy. The reactor was connected to the grid in 1985 and shut down in 1998. BN-800, which is under construction in Russia, could also come under this category.

Some important details of a few fast reactors that have given valuable experience are presented in the following paragraphs.

21.5.1 Enrico Fermi

The world's first commercial FR, and the only one ever built in the United States, was the 94 MWe Unit at the Enrico Fermi Nuclear Generating Station. It was designed by Dow Chemical and Detroit Edison in a joint effort as part of the Atomic Power Development Association Consortium. First pour of concrete began in Lagoona Beach, Michigan (near Monroe, Michigan) in 1956. The plant went into operation in 1963. However, it was shut down on October 5, 1966, due to high temperatures caused by a loose piece of zirconium that was blocking the molten sodium coolant nozzles. Partial melting damage to six subassemblies within the core was eventually found. The zirconium blockage was removed in April 1968, and the plant was ready to resume operation by May 1970, but a sodium coolant fire delayed its restart until July. It subsequently ran until August 1972, when its operating license renewal was denied. Figure 21.9 shows the schematic sketch of the reactor.

21.5.2 Fast Flux Test Facility

The construction activities of 400 MWt, mixed-oxide-fueled, loop-type experimental reactor (FFTF) in United States began in 1970, with initial criticality was achieved in February 1980. The reactor provided an excellent experimental base for extensive testing of various fuels and structural materials under intense fast flux. From April 1982 to April 1992, it operated as a national research facility to test various aspects of commercial reactor design and operation, especially relating to breeder reactors. The FFTF is not a breeder reactor itself, but rather a sodium-cooled fast neutron reactor, as the name suggests. Figure 21.10 depicts the schematic sketch of FFTF. It is to be noted that by late 1983, three full cycles of operation had been completed with 99.5% capacity factor and an availability factor of 100% with maximum fuel burnup of 1,05,000 MWd/t. The reactor continued to provide good

TABLE 21.1 Test/Experimental Reactors in the World

Name	Thermal Power	Criticality	Country	Status
Clementine	0.02 MW	1946	USA	Stop 1952
EBR-I	1.4 MW	1951	USA	Stop 1963
BR-1		1955	Russia	
BR-2	0.2 MW	1956	Russia	Stop 1957
BR-5/BR-10	5/10 MW	1958/1973	Russia	Stop 2002
LAMPRE	1MW	1961	USA	Stop 1965
DFR	75 MW	1959	UK	Stop 1977
EBR-II	60 MW	1963	USA	Stop 1993
EFFBR	200 MW	1963	USA	Stop 1972
RAPSODIE	24/40 MW	1967/1970	France	Stop 1983
BOR 60	60 MW	1968	Russia	Running
SEFOR	20 MW	1969	USA	Stop 1972
KNK1-KNK2	60 MW	1972/1977	Germany	Stop 1991
JOYO	50 MW	1977	Japan	Running
FFTF	400 MW	1980	USA	Stop 1992
FBTR	40 MW	1985	India	Running

TABLE 21.2 Demonstration Reactors in the World

Name	Power	Start	Country	Status
EFFBR	100 MWe	1963	USA	Stop 1972
BN 350	150 MWe	1972	Kazakhstan	Stop 1993
Phénix	250 MWe	1973	France	Stop 2009
PFR	250 MWe	1974	UK	Stop 1994
BN 600	600 MWe	1980	Russia	Running
SNR 300	300 MWe		Germany	Given up
Monju	280 MWe	1992	Japan	Shut down
CFBR	280 MWe	2010	China	Construction
PFBR	500 MWe	2011	India	Construction

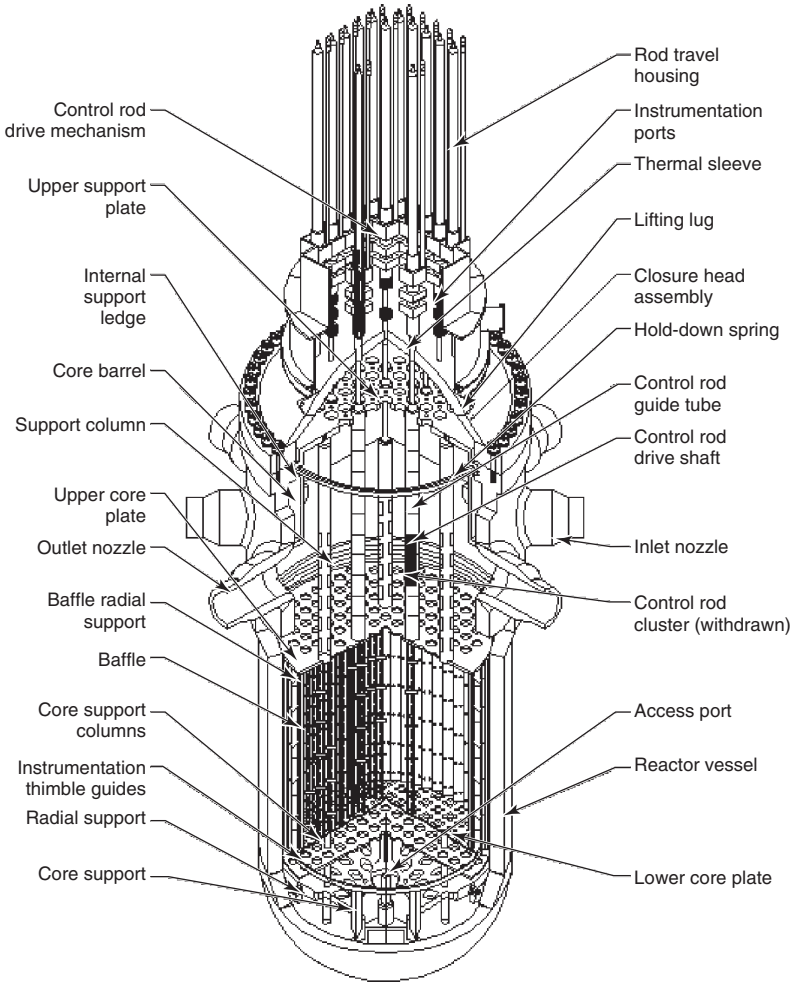

Figure 21.9 Enrico Fermi schematics.

results and demonstrated the safe operation of a fast reactor with excellent capacity and availability factors until its shutdown in April 1992. Lack of mission and funding has forced the reactor to remain shut down since that date. However, in view of the Clinton administration's non-proliferation policy, issued on September 27, 1993, seeking to discourage the civil use of Pu worldwide, it has since been decided to permanently shut down the reactor.

In May 2005 the core support basket was drilled to drain the remaining sodium coolant. This effectively made the reactor unusable; however, a technical study is being pursued with regard to repairing the reactor. As the coolant was drained, the system was back filled with high purity

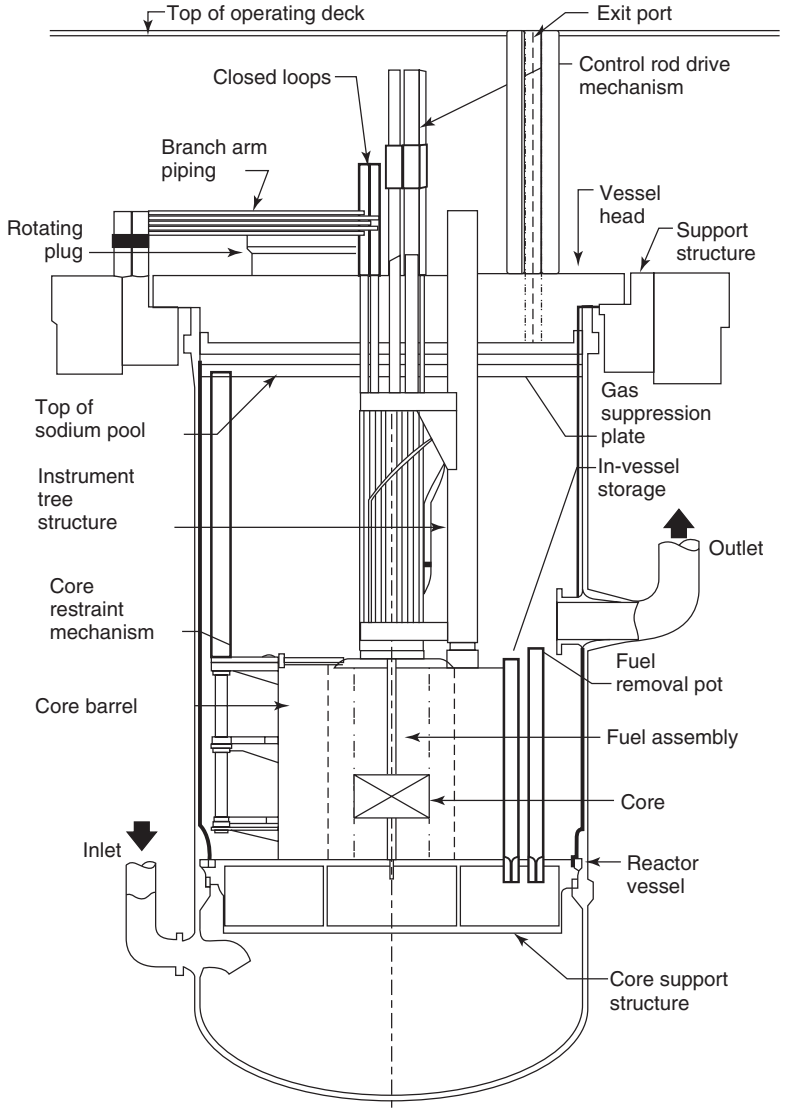

Figure 21.10 FFTF schematics.

argon gas to prevent corrosion. The support basket is an unpressurized area; the reactor core has not yet been breached (as of June 2006).

There seems to be a renewed interest in the FFTF since the global atmosphere with regard to nuclear energy has changed due to current oil prices, and the United States is pursuing nuclear power once again. To build a similar facility would cost an estimated $2 to $5 billion. In April 2006, the FFTF was honored by the American Nuclear Society as a "National Nuclear Historic Landmark." Achievements cited include radiation exposure to operators was 1/100th of commercial power reactors, it established a world record for fuel performance; produced extremely high-quality rare radioisotopes for medicine and industry; conducted the first passive safety testing; demonstrated commercial viability of breeder reactor components, materials, and fuels; provided fundamental experimental data for fusion programs, advanced fuels, and materials development for space nuclear power; demonstrated miniaturized reactor test techniques; and demonstrated the feasibility of transmuting radioactive Technetium 99 into a non-radioactive element using a reactor. Technetium 99 is one of the most troublesome long-lived components of the nuclear waste stream. Processing of this isotope and destroying it in a reactor represents a permanent solution to reducing the nuclear risk in waste.

21.5.3 EBR-II

The experimental breeder reactor II (Figure 21.11), 62.5 MW(th)/20 MW(e) was designed as power plant and to include an integrated fuel reprocessing and refabrication

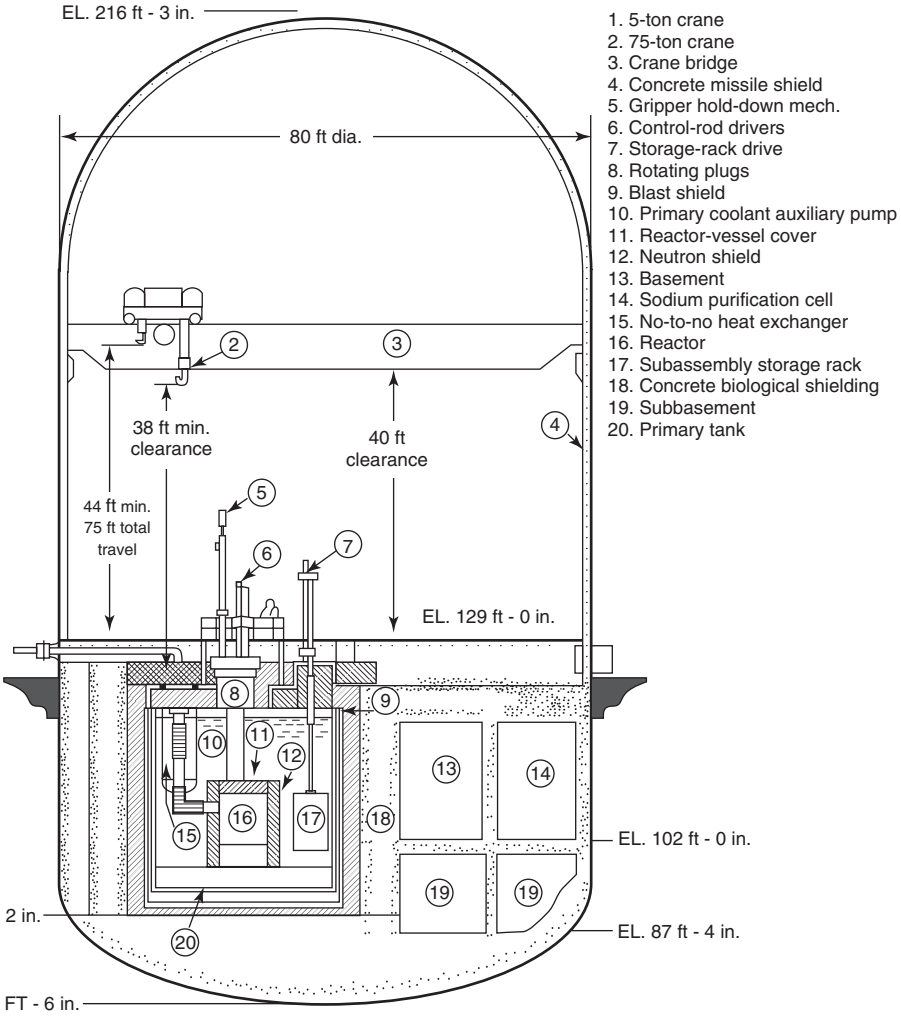

Figure 21.11 EBR II Schematic.

facility in order to demonstrate the complete closed fuel cycle of FRs. Difficulties with some components delayed wet criticality until November 1963 (plant was constructed in 1961). In April 1963, pump 1 became difficult to rotate and had to be removed. Inspection showed that the pump labyrinth was cocked with respect to the shaft center line owing to the tilt of the bottom flange of the shield. The pump bowed owing to the high temperature caused by its rubbing on the aluminum-bronze labyrinth bushing. The shield plug bottom flange was re-machined and a new shaft and labyrinth bushing were installed. The ascent to power began in July 1964, and an extensive irradiation test program for fuels and structural materials was started in 1965. The experiments consisted of various fuel types (oxides, metal, carbides, and nitrides). Peak burnups of 19 at.% for MOX fuel and 18.5 at.% for metal fuels have been reached. An integrated fuel cycle was demonstrated. The EBR-II before closure was operated as the integral fast reactor (IFR) prototype, demonstrating important innovations in safety, plant design, fuel design, and actinide recycle. The ability to passively accommodate anticipated transients without scram has resulted in significant benefits related to simplification of the reactor plant, primarily through less reliance on emergency power and by virtue of not requiring the secondary sodium or steam systems to be safety-grade. The uranium-plutonium-zirconium alloy fuel is fundamental to the superior safety and operating characteristics of the reactor. In January 1994, the Department of Energy mandated the termination of the Integral Fast Reactor (IFR) Programme, effective as of October 1, 1994. To comply with this decision, Argonne National Laboratory-West (ANL-W) prepared a plan providing detailed requirements to place the EBR-II in a radiologically and industrially safe condition, including removal of all irradiated fuel assemblies from the reactor plant, and removal and stabilization of the primary and secondary sodium used to transfer heat within the reactor plant.

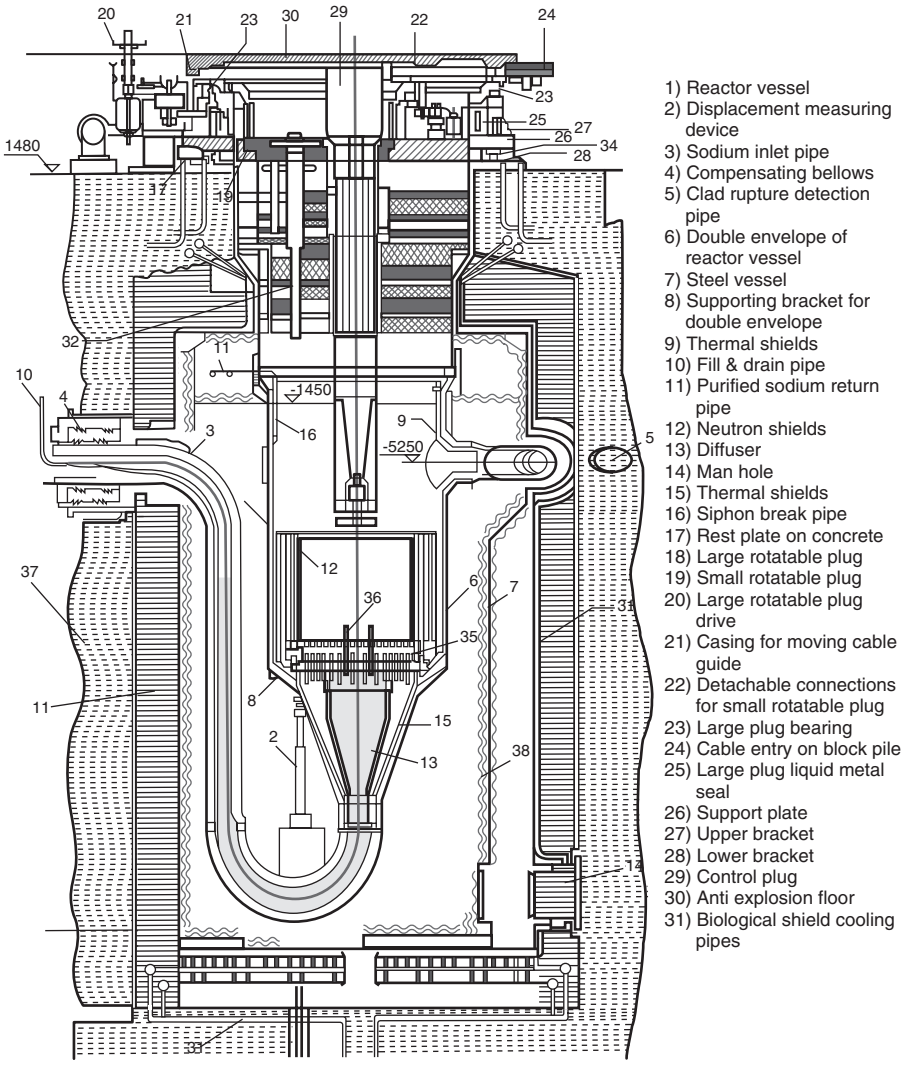

Figure 21.12 Rapsodie schematic.

21.5.4 Rapsodie

In France, the first chapter in the history of fast reactors was the construction of the Rapsodie reactor (1962–1966) that used sodium as a coolant and mixed oxide fuel (Fig. 21.12). The construction was started in 1962 within an association of CEA and EURATOM. The reactor went critical on January 28, 1967, reaching 20 MWt power on March 17, 1967. The core and equipment were modified in 1970 to increase the thermal power level to 40 MWt. The operating parameters were similar to those in large commercial-size reactors. During 16 years of operation, ~30,000 fuel pins of the driver core were irradiated, of which ~10,000 reached a burnup beyond 10%; 300 irradiation experiments and more than 1,000 tests have been performed. The maximum burnup of the test fuel pins was 27% (173 displacement per atom). In 1971, the irradiations performed in the core revealed a phenomenon of irradiation swelling in the stainless steel of the wrapper and the fuel cladding in the high neutron flux. The Rapsodie results have been extrapolated in the Phénix reactor. The decision to stop running the reactor was taken after two successive defects were detected in the primary system containment (double envelope of reactor vessel). The first defect, which appeared in 1978, consisted of a sodium micro leak: Radioactive sodium aerosols were found in the double-wall reactor vessel. Investigations did not find any liquid sodium in the gap nor locate the defect. The reactor was subsequently operated at a reduced power level (~0.6 P_N), which was high enough for irradiation needs but did not cause the leak to reappear. The second defect appeared in 1982 and consisted of a small leak from the nitrogen blanket surrounding the primary system.

Before the final shutdown of the reactor, a series of end-of-life tests were conducted in April 1983. Two series

of tests were performed on the Rapsodie reactor, the purpose of which was to investigate the serviceability of this reactor's core and of the reactor as a whole under extreme conditions that were characterized by an exceedingly high temperature. The first series of tests to be performed called for an experimental inquiry into the behavior of fuel elements during fuel melting. Over the course of these tests, the fuel pin linear power observed on two test subassemblies reached 1000–1060 W/cm; i.e., two times greater than that normally used in commercial reactors. The second series of experiments simulated the most serious accident, which consisted of the shutdown of the primary-circuit and secondary-circuit pumps, as well as the ternary-circuit fans, and the non-operation of the safety rods. Here, reactor output reached 21.2 MW (more than 50% of the rated value), while the mean coolant temperatures at the reactor inlet and outlet came to 402°C and 507°C, respectively. A comparison of calculation results and experimental data demonstrated that the fuel residing in the core shared a state of coalescence with the fuel cladding and expanded with the cladding upon heating up. It is in such instances precisely that good agreement is reached between the calculation results and the experimental data concerning the coolant temperature at the subassembly outlet.

21.5.5 FBTR

The Fast Breeder Test Reactor (FBTR) is a sodium-cooled, loop-type 40 MWt/13.2 MWe experimental reactor operating at Kalpakkam, India, since 1985 (Fig. 21.13). Its design is same as that of Rapsodie-Fortissimo, obtained under agreement signed with CEA, France, in 1969, except for incorporation of steam generators (SGs) and a turbo-generator (TG). The FBTR has two primary and two secondary sodium loops, and each secondary loop has two once-through, serpentine-type SGs. All the four SG modules are connected to a common steam-water circuit having a TG and a 100% steam Dump Condenser. The first criticality was achieved in October 1985 with a small core of 22 fuel subassemblies of MK-I composition (70% PuC + 30% UC), with a design power of 10.6 MWt and peak linear heat rating (LHR) of 250 W/cm. Progressively, the core was expanded by adding subassemblies at peripheral locations. With a goal of increasing the core size and hence the reactor power, carbide fuel of MK-II composition (55% PuC + 45% UC) was inducted in the peripheral locations in 1996. MK-I carbide fuel has so far seen a burnup of 165 GWd/t without any pin failure. TG was synchronized to the grid for the first time in July 1997. The reactor has so far been operated up to a power level of 17.4 MWt by raising the LHR of MK-I fuel to 400 W/cm in 2002. Fuel discharged from FBTR up to a burnup of 100 GWd/t has been successfully reprocessed by the PUREX process, and the reprocessing of fuel with a burnup of 150 GWd/t is in-progress. With the successful operation of about 25 years, the FBTR has given credible confidence in fuel cycle technology and formed a backbone of regulatory perception and a cradle for human resources for India. Further, the reactor life is planned to be extended by 20 years to serve as an irradiation facility for the development of future metallic fuels and core.

It is worth highlighting three notable incidents during the long operation of FBTR. The first incident is fuel handling problem, which occurred during an in-pile fuel transfer for performing a low-power physics experiment in

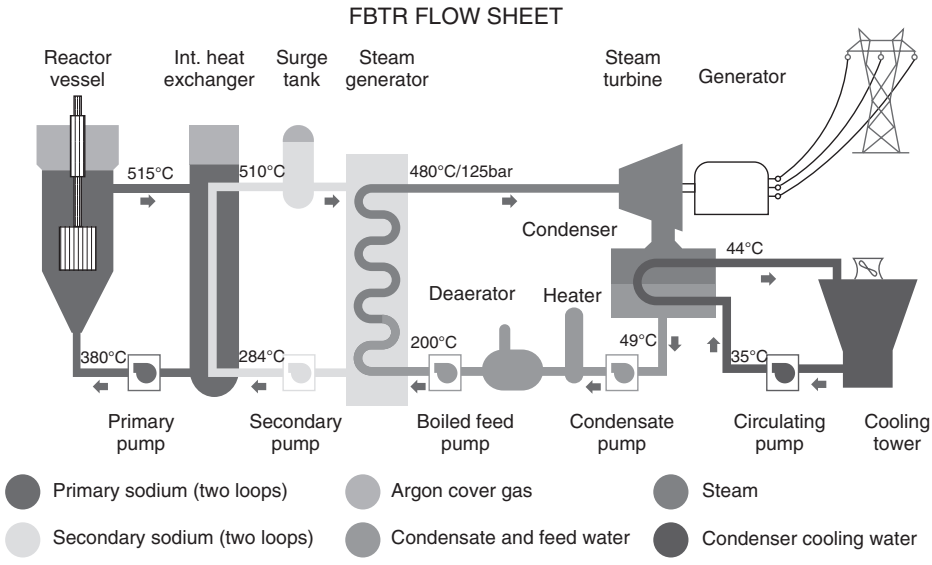

Figure 21.13 FBTR Schematic.

May 1987. The incident was due to the plug rotation logic during fuel handling remaining in bypassed state, resulting in the rotatable plugs being rotated with the foot of a fuel subassembly protruding into the core during the in-reactor transfer. The foot of the subassembly, as well as the heads of 28 reflector subassemblies on the path of its rotation, were bent. In a complex mechanical interaction that took place during subsequent plug rotation, the guide tube was bent by about 320 mm. By developing innovative tools and techniques, the reactor operation could be resumed in May 1989. There were three reactivity incidents in 1994, 1995, and again in 1998–1999. With ther exception that all these were positive reactivity incidents, the characteristics of all the three incidents were totally different in terms of magnitude, permanent gain, and reproducibility. Although the exact causes could not be established even after extensive testing, they are suspected to be caused by core deformations arising out of steep thermal gradients inherent in the small core. With the progressive expansion of the core, they are no longer seen. The core cover plate housing the thermocouples for monitoring the subassembly outlet temperatures got stuck in fuel handling position in 1996, resulting in core temperature anomalies, especially of the MK-II fuel subassemblies in the core periphery. An eddy current flow meter has been developed for periodic monitoring of flows through the subassemblies during fuel handling to supplement the core temperature supervision. There was a leak of about 75 kg of primary sodium in 2002 due to a defect in the body of a sodium valve. The leak was contained within the inerted primary purification cabin, and the system was normalized without any exposure or contamination.

21.5.6 Joyo

Japan's first experimental FR, Joyo is located at Japan Atomic Energy Agency's O-arai Research and Development Centre. It became critical in 1977 with the MK-I breeder core. The schematic sketch of JOYO is shown in Figure 21.14. The objective of the reactor is to conduct irradiation tests on fuel and materials, carry out experiments for gaining operating experience, and validate innovative technology for development of future FRs. The Joyo has been supporting the development of sodium-cooled fast reactors by providing valuable irradiation testing of advanced fuels and materials, as well as improvements in fast reactor safety and operation. The first major upgrade of Joyo to the 100 MWt MK-II irradiation test bed was successfully operated from 1982 to 2000. Work began in 2000 on the 140 MWt MK-III program, which was the second major upgrade to improve the irradiation capability of Joyo. Start-up testing of the MK-III core was conducted from June to October 2003. The rated power operational cycle of MK-III core was started in May 2004. A few of the important tests that have been carried out are an irradiation test of Self-Actuated Shutdown System (SASS), fuel failure simulation test, and irradiation tests on oxide-dispersion-strengthened ferritic steel (ODS) and MOX fuel with 5% americium and neptunium. Beyond 2010, fuel slow transient safety testing, anticipated-transients without scram (ATWS) testing, and in-service inspection and repair demonstrations are being considered. Currently, the reactor is under shutdown due to some fuel handling problems. The Joyo is going to serve as a powerful irradiation test facility for the fast reactor development needs of Japan and the world.

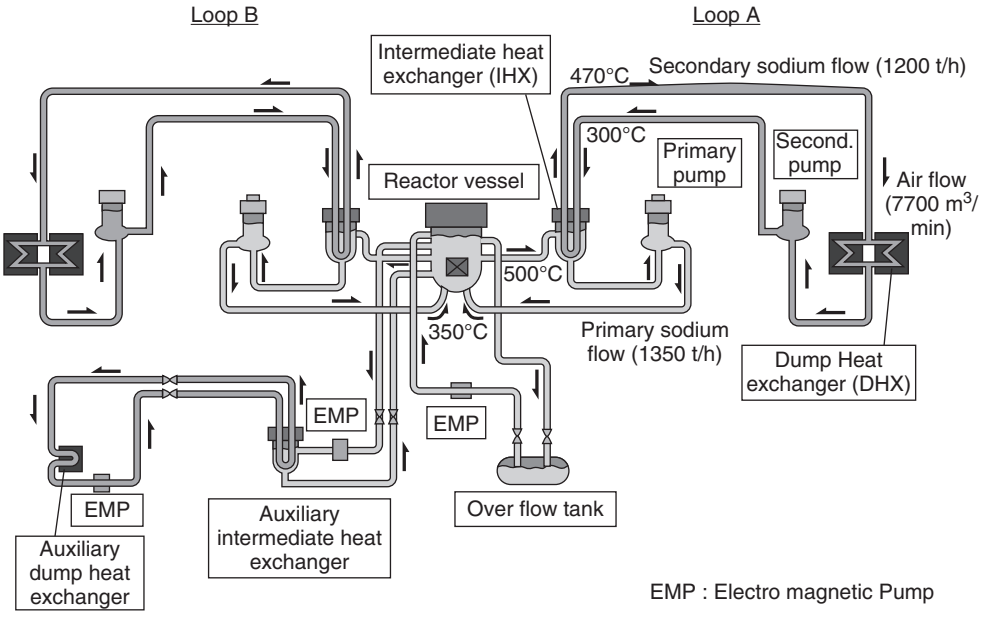

Figure 21.14 Joyo schematics.

21.5.7 Monju

Monju is a loop-type sodium-cooled reactor designed to generate 280 MWe (714 MWt), fueled with Pu-U mixed oxide with a rated capacity of 714 MWt/280 MWe (Fig. 21.15). It is located in Tsuruga, Fukui Prefecture, Japan. The objectives of the development of Monju are to demonstrate the performance, reliability, and safety of an FR power plant; to establish the sodium-handling technology during the design, fabrication, construction, operation, and maintenance of the plant; and to contribute to technology development for commercialized FR cycle systems in Japan and worldwide. In the reactor core, there are two kinds of fuel assemblies with different plutonium enrichments; the higher enriched fuel assemblies are loaded in the outside region to level the radial power distribution. The initial burnup will be 80,000 MWd/t (average of unloaded fuel assemblies). Refueling is planned every six months approximately, and about one-fifth of the core and blanket fuel assemblies will be exchanged at each operating cycle. The stainless steel reactor vessel contains the core and core internals. The shield plug has a single rotating plug in which the upper core structure is installed. The upper core structure contains control rod drive mechanisms that position control rods consisting of three fine regulating rods, 10 coarse regulating rods, and six backup safety rods. The sodium inventory (total quantity of the primary, secondary, and ex-vessel storage tank systems) is about 1,700 t. Most of the piping that connects the primary system components is installed at high level, and guard vessels are provided for the reactor vessel, the primary main circulation pumps, the intermediate heat exchangers, and the connecting piping. With this design, sufficient coolant for core cooling is guaranteed even if coolant leakage occurs. Moreover, compartments of systems with radioactive sodium are kept in a nitrogen atmosphere, and their floors and walls are lined with steel plate so that leaked sodium cannot ignite. In addition to the main cooling system, there is an auxiliary cooling system to remove decay heat from the core when the reactor is shut down for refueling or in an emergency. The auxiliary cooling system, which is separated from the secondary sodium system, has an air cooler in parallel with the steam generator. During shutdown, the primary and secondary sodium are circulated by the primary and secondary main circulation pumps driven by pony motors. Spent fuel is taken from the core and transferred to a tank in the lower part of an in-vessel transfer machine. This is done by a fuel-handling machine of the pantograph fixed-arm type. After the fuel has been removed from the reactor

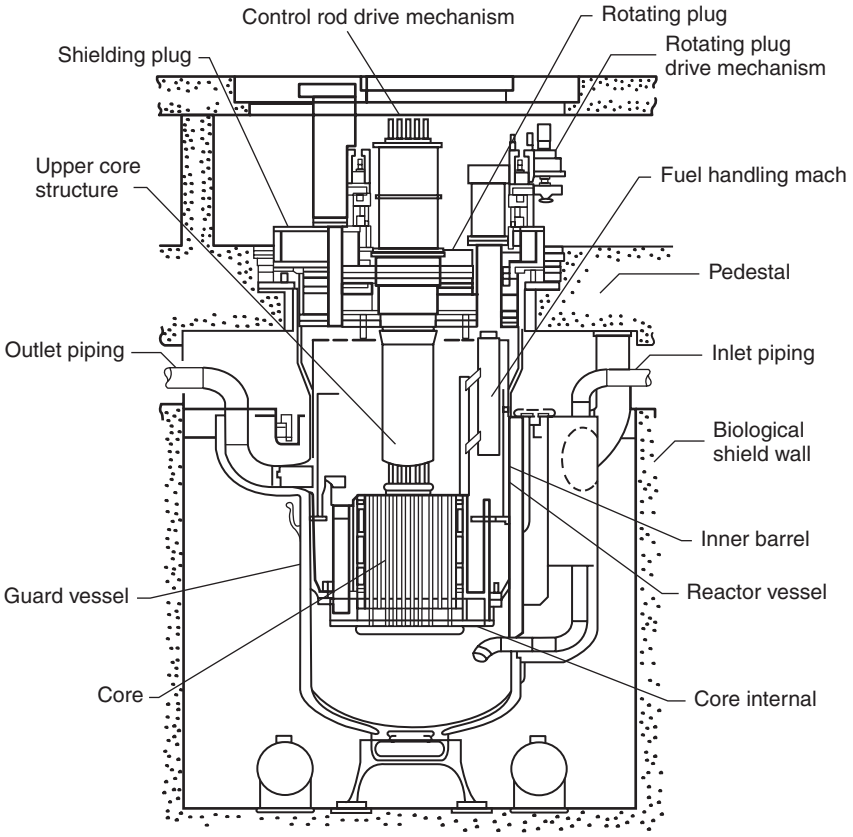

Figure 21.15 Monju schematics.

vessel with an ex-vessel transfer machine, it is transferred through a containment equipment hatch. Later, it is stored in a fuel cooling pond after sodium cleaning.

Monju successfully achieved its first criticality in April 1994 and supplied electricity to the grid initially in August 1995. However, the preoperational test of the plant was abruptly interrupted by a sodium leak accident in the secondary heat transport system in December 1995 during a 40% power operation test. The leak of about 750 kg of sodium was due to failure of a thermowell caused by high-cycle fatigue due to flow-induced vibration. After carrying out the investigation and the comprehensive safety review for two years and the necessary licensing procedure, the permit for plant modification (countermeasures against potential sodium leak, etc.) was issued in December 2002 by the Ministry of Economy, Trade and Industry. JAEA has started preparatory work for modification, after given prior approval by the local governor of Fukui in February 2005, and the main modification work has been in progress since September 2005. The function test for modified systems has been in progress since December 2006. The main modification work was completed by May 2007, and the modified system function test was done in August 2007. The entire system function test is in progress since August 2007, and 43 tests out of 114 tests were achieved by the end of January 2008. Sequentially, the comprehensive system function test, considering the long period of plant shutdown, is scheduled in the near future. The reactor was restarted in May 20, 2010.

21.5.8 BN350

BN-350 (1973) was the first full-scale Soviet FR. Constructed in Chevchenko on the Mangyshlak Peninsula in Kazakhstan and on the shores of the Caspian Sea, it supplied 130 MW of electricity plus 80,000 tons per day of desalinated fresh water to the city of Aktau. Its total output was regarded as the equivalent of 350 MWe. The reactor, which uses UO_2 fuel, has a loop arrangement of the primary circuit components, i.e., the primary sodium pumps, intermediate heat exchangers, and valves are disposed in separate compartments (cells) and are connected with the reactor and interconnected by pipelines. The reactor includes the reactor vessel, which contains the core diagrid with neutron reflector and a set of core and blanket fuel assemblies; the reactor refueling system; and the above core structure and in-core instrumentation guides. The diameter of the cylindrical part of the reactor vessel is 6000 mm, and the wall thickness is 30 mm. In the middle section of the vessel there is a support belt by which the reactor is located on 16 roller bearings arranged on a support shell of 5850 mm diameter transmitting the reactor weight load onto the foundations (Fig. 21.16).

The reactor vessel is enclosed in a guard vessel. The reactor unit is set in a concrete well covered by the upper stationary shield, which is composed of steel shot and serpentinite concrete layers. Between the reactor and the wall of the well is a radiation shield consisting of an iron ore concentrate-filled cage. Six cells enclosing the primary circuit thermo-mechanical equipment are adjoined to the reactor well. Figure 21.16 shows the schematic sketch. The reactor plant includes the reactor assembly, six primary loops, six intermediate (secondary) loops, steam generators, the refueling complex (integrated mechanical system), the primary and secondary sodium purification system, and the automated process control system, including the reactor control and protection system (CPS) and diagnostic systems for monitoring the operating state of the safety-related components and systems. During power operation, core heat removal and transport to the working medium (steam-water) are provided by a three-circuit flow scheme. The primary circuit is composed of six intermediate heat exchangers (IHX), six primary coolant pumps (PSP), and sodium pipelines with gate and non-return valves. The pressure chamber with the core diagrid and the upper mixing plenum above the core are the common sections of primary sodium flow path. Sodium flow is distributed from the diagrid into the core and the radial blanket fuel assemblies. A portion of the primary sodium (250 t/h) is removed from the pressure chamber through throttles and utilized for cooling the reactor vessel and its outlet nozzles. There is a capability to isolate each primary loop from the reactor using two gate valves on the suction and pressure pipelines of the circuit. On the pressure pipeline of each loop downstream of the PSP, a flap-type check valve is provided, eliminating coolant backflow in the event of a PSP trip in one loop when the other PSP are operative. The secondary sodium circuits comprise IHX heat transfer tubes, pipelines, secondary sodium pumps, and steam generators. Due to utilization of the reactor energy for fresh water production, the steam-water system has some specific features. Steam from the SG is supplied to turbines of two types: a condensing turbine and a back-pressure turbine.

21.5.9 Phénix

The prototype fast reactor, Phénix, a pool-type reactor, 250 MWe, went into commercial operation in 1974. Fifty-one cycles were run, and more than 20 billion KWhs were produced. Since the initial design life of the reactor was 20 years, the reactor should have been shut down in 1994, but in the mid-1990s, the role of the reactor changed: It was to be used as an irradiation tool, acting as a support to the R&D transmutation program of the CEA within the framework of the 1991 French law relating to long-lived radioactive waste management. This new objective required an extension of the planned reactor lifetime. A large

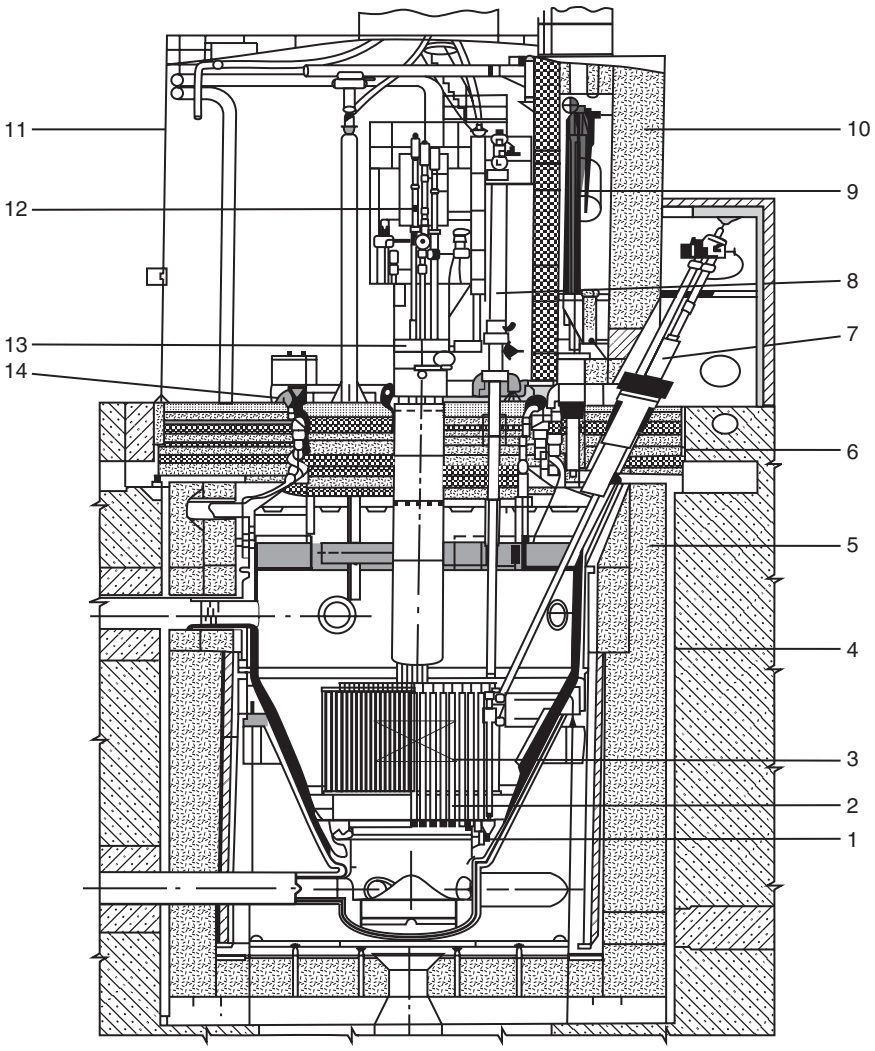

Figure 21.16 BN 350 schematics.

refurbishment program was defined and carried out in two phases within six years, the first phase lasting from 1994 to 1997 and the second from 1999 to 2003. These two phases were separated by one operating cycle, and the plant resumed power at the end of 2003. It operated at its nominal power throughout 2004 and 2005. Five operating cycles (representing 600 EFPD) have been scheduled to carry out the experimental irradiation program until final shutdown of the plant in 1999. Preliminary studies on one end-of-life test and expertise programs were performed and proposed to the international scientific community in the prospect of SFR development.

For the reactor assembly, the pool-type concept is adopted (Fig. 21.17). The fuel is uranium dioxide mixed with plutonium dioxide (UO_2-PuO_2). The three primary sodium pumps are variable speed units (150 to 970 rpm) delivering about 950 kg/s at 825 rpm, which is their normal service speed. Each secondary loop is connected to a steam generator consisting of an evaporator, superheater, and reheater, in 12 modules for each stage. The behavior of the subassemblies was strongly improved by the choice of specific steels, for wrapper and cladding, with low swelling properties. The maximum burnup achieved was 136,000 MWd/t of oxide. Eight cladding failures, with

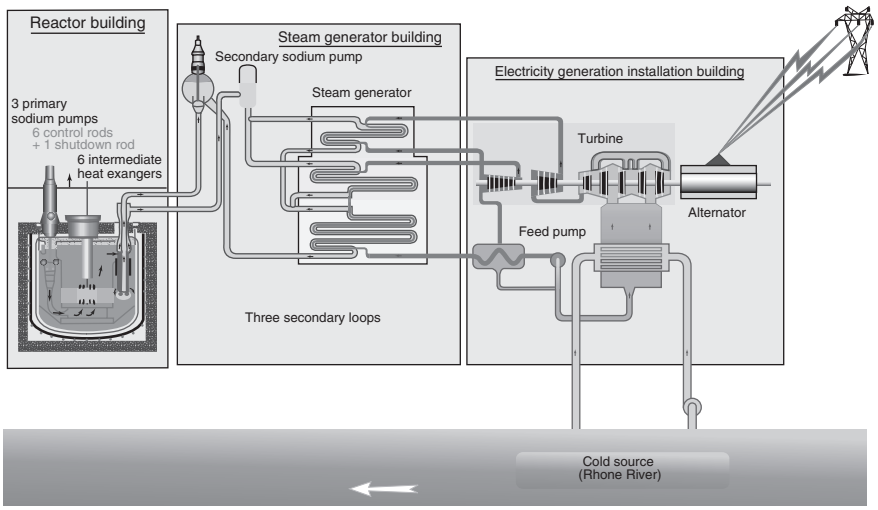

Figure 21.17 Phénix schematics.

delayed neutron emission, occurred during these 10 years. Consequences on reactor operation were small, failed subassembly identification being fast and replacement often shorter than three days. This short time of radioactive element emission allowed both primary sodium and argon cover gas to be kept at very low levels of activity. An unusual event appeared in 1989, shown as a quick decrease and rise of core reactivity, involving automatic reactor scram by reaching the "negative reactivity" threshold. In spring 1990, the power of the reactor was limited to 500 MWth, because of a safety request: to check the decay heat removal ability, in case of failure of the normal decay heat removal circuits. Over the operating period, the irradiation program was continued: for example, wrapper and cladding materials. Spreading over the span of 10 years, leaks in IHX have resulted in limited periods of operation at two-thirds of full power, operating on two secondary circuits. On three occasions in summer 1989, the reactor was stopped by automatic emergency shutdown, the negative reactivity threshold (10 pcm) being exceeded. This reactivity variation was very fast: first a minimum after 50 ms followed by an increasing oscillation, and then a decrease, caused by the control rod drop, 200 ms after the start of the transient. The first two events were thought to be spurious (a neutronic chamber fault), and the reactor was restarted. The normal plant instrumentation did not allow proper recording of the transient, so following the second trip, special instrumentation was installed. After the third trip, the reactor was shut down in order to identify the cause of the events. An expert committee was then set up and an extensive study of all the possible phenomena was started. It was also decided to fit the plant with special monitoring equipment, including fast recording systems, and to perform tests. Around 200 data were concerned. Tests on vessel and component mock-up were also planned. The tests were performed with the reactor shut down, critical at zero power (since October 1991) and at 350 MW_{th} power (for around 12 days—February 1993). In the same time, checks were performed on the plant, especially on the reactor, its components, and auxiliaries. Reactor tests were very satisfactory: They proved the good behavior of the instrumentation, and data are now stored as reference of steady state power and emergency shutdown conditions. By the end of 1993, studies had not led to a clear explanation of the phenomenon: "False" reactivity variations (a "neutronic mask" between core and neutronic chambers, or a spurious signal) are thought to be impossible. Among "real" reactivity variations, a sodium void effect or variation of the relative displacement of fuel and control rods are also thought to be impossible. There remains only a radial core volume variation, the origin of which (a "pressure wave") has not been found. These studies confirm that the reactor safety was not affected. Operation with special instrumentation seems to be the only way to understand the origin of these negative reactivity trips. In March 2010 the reactor was shut down after completing all the planned end-of life tests.

21.5.10 PFR

The UK fast reactor program was conducted at Dounreay, Scotland, from 1957 until the program was cancelled in 1994. Two fast reactors were built, along with fabrication and reprocessing facilities for fuel that were co-located. The Dounreay Fast Reactor (DFR) achieved its first criticality in 1959 with uranium metal fuel. It used NaK coolant and produced 14 MWt of electricity. This was followed by the sodium-cooled 250 MWe Prototype Fast Reactor (PFR) in the 1970s. Figure 21.18 depicts the whole plant view.

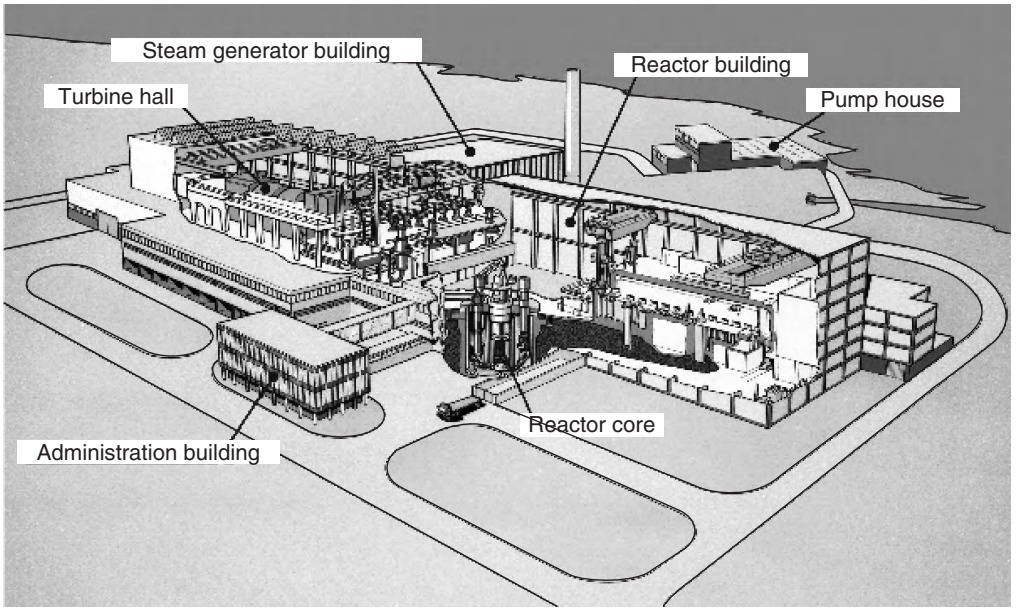

Figure 21.18 PFR Fermi schematics.

The PFR, which was the first reactor with a UO_2-PuO_2 core, attained criticality in March 1974. Physics parameters for the core and for the reactivity effectiveness of, and interaction between, the control and shut-off rods agreed with prediction within the expected uncertainties. The hot dynamic test was completed in June 1974. The operating history of the PFR power plant can be divided into two phases. For the first 10 years, electrical output was limited, mainly because of a series of leaks in the steam generator units, and the highest load factor in any year was 12%. After 1984, with the steam generator weld problems dealt with, plant performance improved, and in the final year of operation the load factor was about 57%. In 1985, PFR was able to operate, for the first time since the commissioning period, with a full set of steam generator units. In the second decade of operation, there was one major outage in 1991/1992. In this period, until 1991, the reactor and primary circuit equipment were responsible for only a very small fraction of unplanned outage time. On June 25, 1991, a leakage of oil from a bearing of one of the primary pumps into the primary sodium led to interruption of reactor operation for 18 months. PFR was started up for the last time on January 14, 1994. A total of 37 leaks were experienced in PFR SG units in the period 1974 to 1984, with 33 of these occurring in evaporators, three in superheaters, and one in a reheater. All the leaks originated at the welds between the tubes and the tube plates associated with cracking of the tube-to-tube plate welds. These were hard and had high residual stresses because there was no post-weld heat treatment. The type of direct tube-to-tube plate weld (the "butt/fillet" weld adopted initially at PFR), which could not be heat treated after manufacture, is being avoided in future fast reactor SGs. In the decay heat removal system of PFR, leaks were detected in the air heat exchanger (heat exchanger between the NaK circuit and the atmosphere). These were associated with anomalous temperature differences between tubes in the heat exchanger, due to aspects of the design together with difficulties in achieving filling with NaK. The PSP bearing oil spilled into the reactor sodium experienced during PFR operation resulted in an 18-month stoppage, which was spent in cleaning the primary sodium and in making preparations for examination of the three primary pump filters and the inlet filters on some of the fuel assemblies that had shown temperature increases at the time of the spillage. The EFR design was changed following the PFR oil ingress incident by the introduction of the innovative magnetic bearing and "ferro-fluid" seals to eliminate oil completely and remove the potential hazard of its ingress in to the sodium. PFR was shut down in 1994 as the British government withdrew major financial support for nuclear energy development.

21.5.11 BN 600

The longitudinal section of the BN-600 reactor is presented in Figure 21.19. The heat transfer from the primary circuit to the secondary one is provided by two intermediate heat exchangers with "sodium-sodium" in each loop. Heat from the secondary circuit to the steam-water medium of the tertiary circuit is transferred in sectional/modular steam generators (SG) having eight sections in each loop. Each

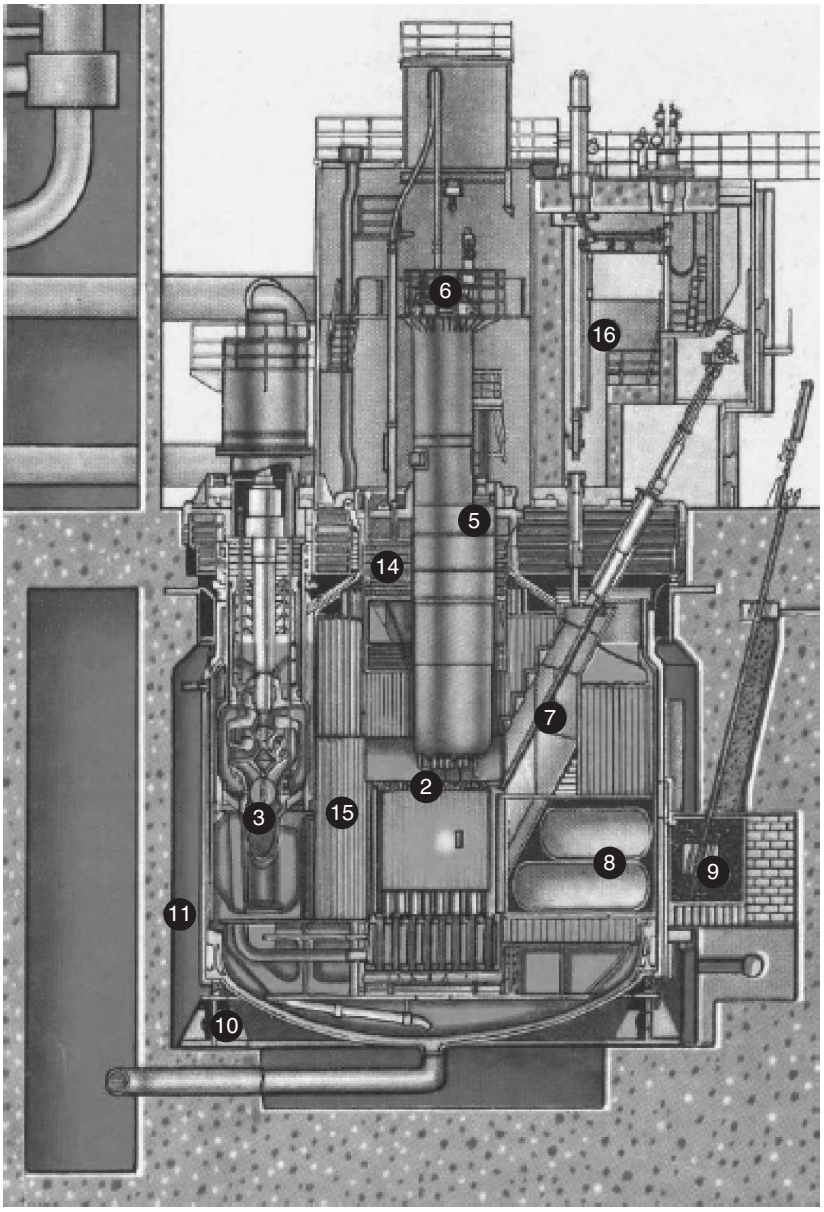

1,2-Core, Fuel assembly, 3-Primary pump, 4-Intermediate heat exchanger (IHX), 5-Central column, 6-Control rod drive mechanism, 7-Loading-unloading elevators, 8-Neutron channel, 9-Neutronic measurement chambers, 10-Reactor supports, 11-Reactor vault, 14-Rotating plug, 15-Neutronic protection, 16-Refuelling cell

Figure 21.19 BN600 schematics.

SG section can be isolated from the secondary and tertiary circuit by cut-off valves. The reactor facility can operate with two loops (when the third loop is shut down) at the power level up to 70% of rated value.

Successful operation of the BN-600 reactor with core designing for fuel burnup of 10% heavy atoms along with substantial R&D input allowed to enhance the burnup up to 11.1% heavy atoms. From spring 2004 till autumn 2005, a transition to a new core modification 01M2 with four-fold reactor refueling was implemented. The new BN-600 reactor core has the same characteristics as the previous core configuration and an increased design value of a fuel burnup and more prolonged refueling interval accordingly. The structural materials of fuel pin cladding and fuel subassembly duct remained the same. The average load factor for the period of commercial operation of the BN-600 power unit from 1982 tot 2006, excluding the initial stage of power mastering, is equal to

73.5%. As regards reliability indices, the BN-600 power unit is one of the best Russian NPP for a period of several years. The BN-600 reactor's more than 25 years in operation have demonstrated high parameters of safety and operating reliability. During this period, the long-duration tests of large-size sodium components, mastering sodium technology, development and optimization of operating modes, and mastering the technology of replacement and repair of sodium components, including pumps and steam generators, have been demonstrated. The *s*ectional/modular steam generators (SG) used in the BN-600 reactor have demonstrated high performance for the whole period of power unit operation. During the whole period of reactor operation, about 27 sodium leaks were experienced, of which 12 leaks are from steam and water into sodium. All the leaks were suppressed by regular means, and thus they have not resulted in emergencies. There was only in one case of leak and fire of radioactive sodium from the primary circuit; the design algorithm of confinement of sodium fire consequences was implemented successfully. In this case, radioactivity release (10.7 Ci) was well below the permissible limit. There was no need to use drainage-based firefighting systems. Unique experience has been gained in the operation of sodium leak-confinement systems, showing their effectiveness.

The systematic life extension program demonstrated that it is possible to justify the extension of the lifetime of evaporators from 50,000 hours design value up to 105,000 hours and, hence, assure single replacement of the evaporators instead of three replacements planned for the whole lifetime of the power unit. The scheduled replacement of SG evaporator modules has been carried out in the mid-1990s. Since 1995, seizure of the small rotating plug was observed during reactor refueling, and this seizure became stronger with time. Investigation confirmed that bearing unit was plugged with sodium and, in addition, the small deformation of a lateral surface of the small rotating plug was revealed. The operations on replacement of the bearing unit and increase of a gap between the large and small rotating plugs by means of sweep and treatment of the lateral surface of the small plug were performed to solve the problem.

The successful operation of the power unit with BN-600 reactor during almost 27 years testifies to successful industrial development of technology of fast reactors with sodium coolant. The technology of replacement and repair of sodium equipment, including the main equipment (pumps, steam generators), also has been mastered. The operational experience accumulated at the BN-600 reactor demonstrates that after mastering sodium technology by the personnel, the specific features of sodium coolant have no significant influence on safety and operational parameters of the power unit.

21.5.12 Super Phénix

Construction of the Super Phénix (SPX) plant, in cooperation with Germany and Italy, lasted from 1977 to 1985. Full power was reached in 1986, and until the end of 1996, the plant operated for 4.5 years at different levels of power, with scheduled periods of maintenance and tests. It remained shut down for 4.5 years, although still in an operational state, due to administrative procedures underway and a little more than two years went by following technical incidents and repairs. The last operating year was remarkable; the complete program of overall qualification by successive stages of 30, 60, and 90% nominal power progressed without difficulty. Super-Phénix 1 (SPX), worldwide the first large LMFR, was connected to the grid on January 14, 1986. Full power was reached on December 9, 1986. As a whole, the operating experience of SPX was incomplete: Over 11 years of existence, it has been operating during four and a half years, producing 7.9 billion kWh (half of it in 1996). However, experience feedback on large components remains significant in spite of the short operating period. Primary and secondary pumps put in a total of more than 60,000 hours on the main motor, and the continuous improvement of maintenance operations has allowed an increase in reliability and availability. As far as the steam generators are concerned, the sodium/water reaction detection systems have been improved on the basis of validated analytical methods through experience. The only experience in the world with Alloy 800 helically wound, 750 MWt SG units were obtained in SPX, where such SG units were installed and very successfully operated. Numerous draining and filling operations (more than 30 for the secondary loops and more than 20 for the decay heat removal emergency circuits) have allowed validation of the corresponding procedures. Knowledge of primary circuit behavior has in fact been improved, thanks to natural convection tests that showed that natural convection was established in the core in about five minutes. After an interruption of activity for more than five years, all the parameters were found to be normal. Following the declaration made to the French National Assembly on June 19, 1997, the French government decided on February 2, 1998, to shut down the plant permanently. The decree of December 31, 1998, finalized the immediate and permanent shutdown of the plant. Figure 21.20 depicts the schematic sketch of reactor block of SPX.

21.6 FRS UNDER CONSTRUCTION

21.6.1 China Experimental Fast Reactor (CEFR)

In the framework of the National High-Tech Program, the CEFR project has been under way since 1990. The CEFR is a sodium-cooled 65MWt experimental fast reactor

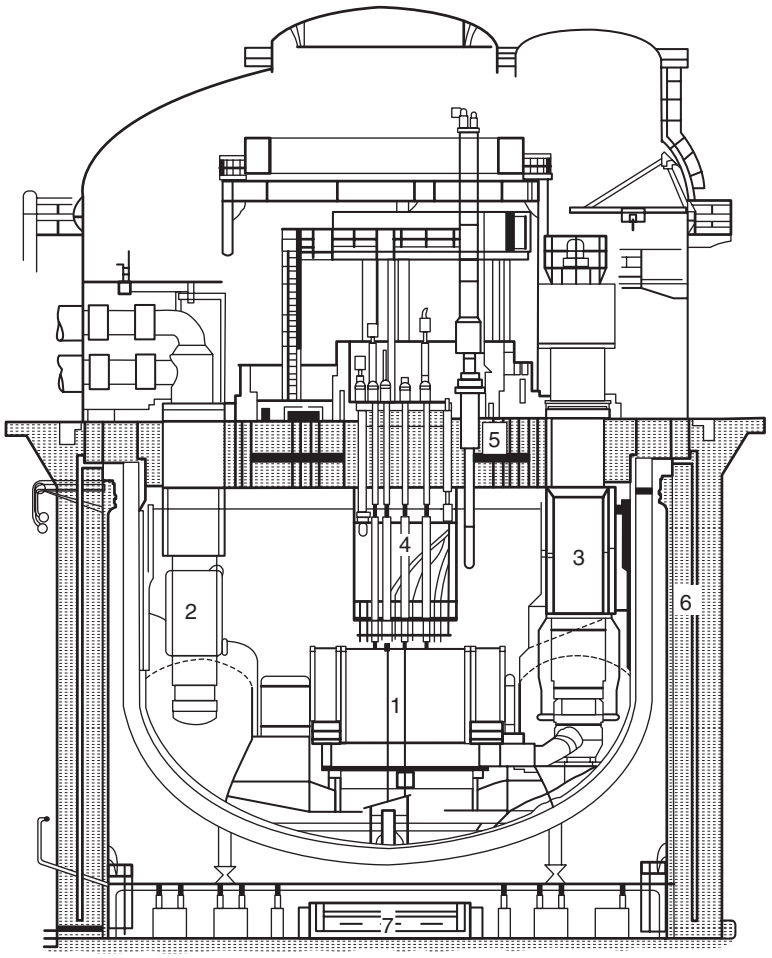

1-Core, 2-IHX, 3-Pump, 4-Control plug, 5-Rotatable plug,
6-Reactor vault, 7-Neutron channels

Figure 21.20 SPX schematics.

with $(Pu,U)O_2$ as fuel, but UO_2 as the first loading, Cr-Ni austenitic stainless steel as fuel cladding and reactor block structural material, bottom-supported pool type, two main pumps, and two loops for primary and secondary circuits respectively. The water-steam tertiary circuit has also two loops, but the superheat steam is incorporated into one pipe, which is connected with a turbine. Design work was started in 1990 and preliminary safety analysis report review was carried out during 1998–2000. Figure 21.21 depicts the details of the component layout. The CEFR reactor assembly is composed of a main vessel and a guard vessel, supported from the bottom on the floor of reactor pit with the diameter of 10 m and height of 12 m. The reactor core is composed of 81 fuel subassemblies and is supported on lower internal structures. Three safety subassemblies, three compensation subassemblies, and two regulation subassemblies, followed by 336 stainless steel reflector subassemblies and 230 shielding subassemblies and, in addition, 56 positions for primary storage of spent fuel subassemblies, are included. Two main pumps and four intermediate heat exchangers are supported on upper internal structures. These two structures are mounted on the main vessel. Two DHR heat exchangers are hung from the shoulder of main vessel. The double rotating plugs, on which control rod driving mechanisms, fuel handling machine, and some instrumentation structures are mounted, are supported on the main vessel top. The erection of a few reactor assembly components is shown in Figure 21.22. The reactor was commissioned in June 2010.

21.6.2 Prototype Fast Breeder Reactor (PFBR-India)

The overall flow diagram, comprising a primary circuit housed in reactor assembly, a secondary sodium circuit and the balance of plant (BoP), is shown in Figure 21.23. The nuclear heat generated in the core is removed by circulating sodium from a cold pool at 670°K to the hot pool at

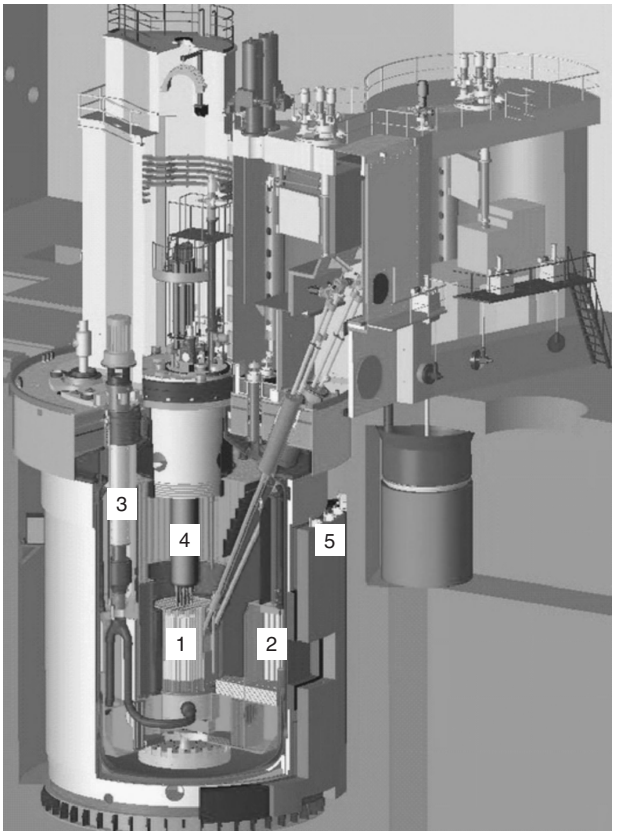

1-Core, 2-IHX, 3-Pump, 4-Control plug, 5-Reactor vault

Figure 21.21 CEFR details.

820°K. The sodium from hot pool, after transporting its heat to four intermediate heat exchangers (IHX), mixes with the cold pool. The circulation of sodium from the cold pool to the hot pool is maintained by two primary sodium pumps, and the flow of sodium through the IHX is driven by a level difference (1.5 m of sodium) between the hot and cold pools. The heat from IHX is in turn transported to eight steam generators (SG) by sodium flowing in the secondary circuit. Steam produced in SG is supplied to turbo-generator. In the reactor assembly (Figure 21.24), the main vessel houses the entire primary sodium circuit, including the core. The sodium is filled in the main vessel, leaving the argon cover gas space at the top. The hot and cold sodium pools are separated by the inner vessel, which is supported on the grid plate. The reactor core consists of 1,757 subassemblies, including 181 fuel subassemblies. The control plug, positioned just above the core, houses mainly 12 absorber rod drive mechanisms. The top shield supports the primary sodium pumps, IHX, control plug, and fuel handling systems.

21.6.2.1 Construction Status of PFBR The nuclear island, housing a total of 17 buildings, including safety-related structures, is under construction. Out of 17 buildings, eight buildings—namely, the reactor containment building, two SGBs, two electrical buildings, the control building, the radwaste building, and fuel building—are connected together as a single structure, which is called Nuclear Island Connected Buildings (NICB). The NICB is supported on a common raft foundation that covers an area of approximately 102 × 93 m. The reactor vault construction has been successfully completed, meeting the stringent dimensional tolerances required for the specified erection tolerances. The excavation work for the balance of plant (BOP) has been completed. Figure 21.25 shows the status of civil construction of NICB.

The nuclear steam supply system components have been manufactured successfully by the Indian industries, based on the experience gained through technology development and including the feedback from the in-sodium testing. Manufacture of large-size components, such as the safety vessel, main vessel, inner vessel, and thermal baffles, have been completed, meeting the stringent tolerance requirement. The safety vessel, incorporated with delicate thermal insulation panels, is the first major nuclear equipment and was erected successfully in June 2008; subsequently, the main vessel was lowered in December 2009 (Fig. 21.26).

Transportation of reactor vessels Erection of reactor vessels

Figure 21.22 Erection of reactor components of CEFR.

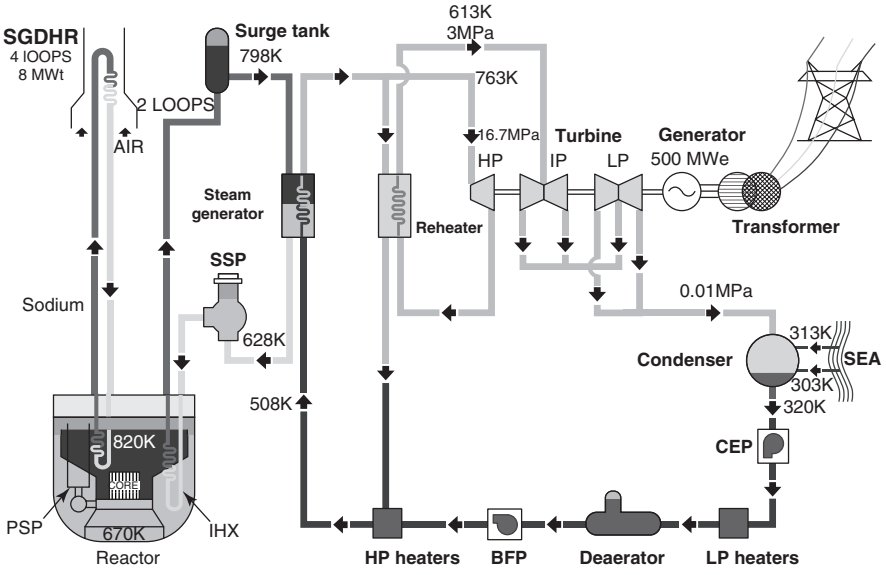

Figure 21.23 PFBR flow sheet.

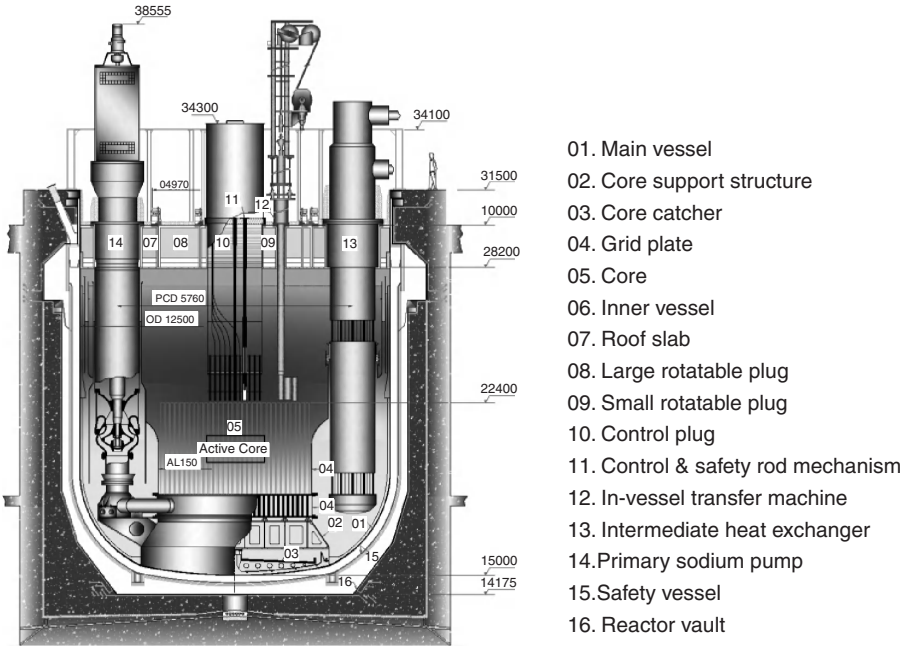

Figure 21.24 Schematic of PFBR assembly.

Because the manufacturing tolerances are very crucial for meeting the functional and structural integrity considerations, tighter values have been specified for the same. Better tolerances (form tolerances less than the half of the wall thickness) have been achieved consistently for all the large-size components. This achievement is possible due to the extensive manufacturing development work completed as a pre-project activity as well as well coordinated efforts of task forces involving IGCAR and Bharatiya Nabhikiya Vidyut Nigam (BHAVINI) constituted for these purposes. Elegant methodology has been finalized for the subsequent erection of main vessel along with the internals and the top shield, respecting various erection tolerances given due considerations of time and economy. Figure 21.27 shows the manufacturing status of a few important components. Sodium has been transferred safely to storage tanks.

The erection of permanent components of reactor assembly would be completed within June 2011, and the reactor will attain the first criticality in 2013.

Figure 21.25 Construction of NICB.

Figure 21.26 Erection of safety vessel and main vessel.

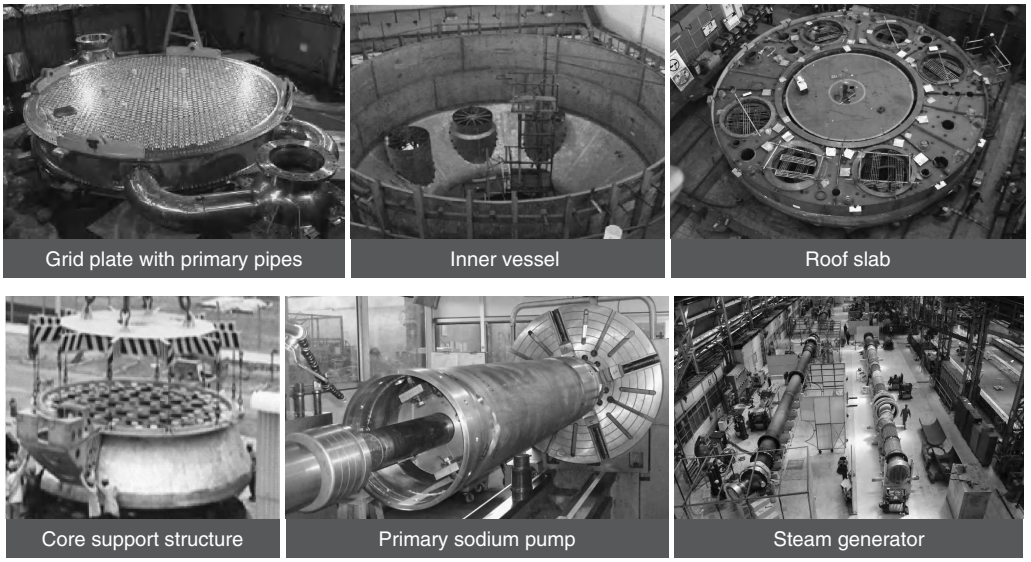

Figure 21.27 Manufacturing status of a few important components.

21.6.3 BN-800 (Russia)

Construction of the fourth power unit with the BN-800 reactor on Beloyarsk NPP site is carried out in accordance with the Program of Development of Nuclear Power in the Russian Federation for 2000–2005 period and the reactor is expected to be completed in 2014. The executed improvement of the BN-800 design has allowed increasing its electric power from 800 MW up to 880 MW (with the same thermal power of the reactor equal to 2100 MW), extending its lifetime from 30 years to 40 years, thus improving the technical and economical characteristics of the power unit. On the whole, the BN-800 reactor design has not undergone cardinal changes, and all basic parameters of the reactor plant and key design approaches have been kept practically unchanged. One of the main issues that should be resolved on the BN-800 reactor is a demonstration of the closed nuclear fuel cycle. An opportunity for use of the BN-800 reactor for recycling stocks of weapon-grade plutonium is also under discussion now. The longitudinal section of the BN-800 reactor is presented in Figure 21.28.

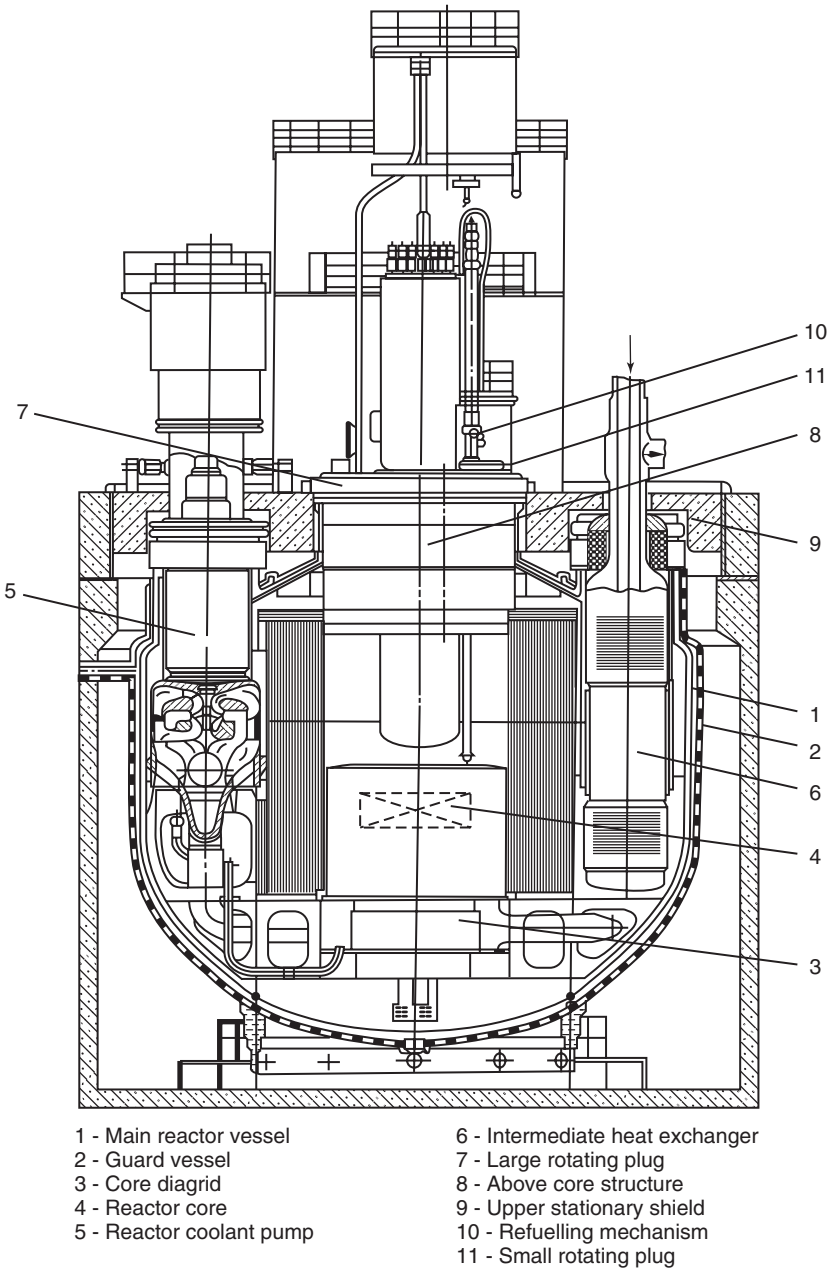

Figure 21.28 BN-800 schematic.

The BN-800 reactor design is a logical development of the BN-600 reactor design. Experience gained during BN-600 reactor operation has allowed considerable improvement in the technical decisions adopted for the BN-800 reactor design and has enhanced its safety. The most important changes and modifications inserted into the BN-800 design compared to the BN-600 design are one turbine for the power unit, steam reheating instead of sodium, a special decay heat removal system that dissipates heat outside through heat exchangers, "sodium-air" connected to the secondary circuit, a core catcher for collecting core debris in the case of its melting, a special sodium cavity over the core to reduce sodium void reactivity effect, and an additional passive shutdown system with hydraulically suspended rods.

The reactor vessel erection status is shown in Figure 21.29. Construction completion and power unit commissioning are scheduled for 2012.

21.7 EMERGING DESIGNS

Cumulative experience of approximately 400 reactor years, gained in design, construction, and operation of test, prototype, and power reactors in different countries demonstrates that the infrastructure and human resources to design, construct, commission, and operate the SFRs can be organized in most of the advanced countries. Comprehensive assessment of various issues involved in the commercialization of the FR system indicates that the most important one relates to its capital cost. The current designs are costlier, mainly due to high capital cost varying from 20% to 60% as compared to well-established water reactors. Recent studies have identified various high-impact factors governing capital cost. R&D efforts should be enhanced significantly to minimize the capital cost, through which it is possible to demonstrate that the SFR systems would be economically competitive as compared to thermal reactor systems or even fossil power systems. A Russian study demonstrates that the specific capital costs of current and evolving designs such as Japanese SFR (JSFR), the Russian BN is consistent with the status of the reactors, and the Indian CFBR are comparable to reference PWR. Further, the steel consumption and in turn capital cost can be brought down significantly in future designs with enhanced R&D inputs.

In this section, a few emerging designs, which are in the advanced conceptual design stage, are presented after highlighting a few major design options still under consideration.

21.7.1 Main Design Concepts under Consideration

The choice of design concepts is crucial at the start of conceptual design stage in order to meet the requirements for achieving safety and economy concurrently. The operating experiences with fast reactors have provided issues to investigate critically, including the choice of fuel, coolant, and pool versus loop concepts. These are discussed below:

21.7.1.1 Fuel Mixed-oxide fuels (UO_2-PuO_2) have provided the reference program fuel material for all nations pursuing the breeder option for at least the last decade. Interest in this fuel system logically followed from the wealth of experience gained from oxide fuels in the water-cooled power reactors. Principal factors that motivated interest in mixed oxides for the FR were the recognition of the high burnup potential and the existence of an established industry for manufacturing oxide fuels. For LWR applications, oxide fuels have demonstrated very satisfactory dimensional and radiation stability, as well as chemical compatibility with cladding and coolant materials. However, the environment in an FR is considerably more hostile (higher temperatures and much larger exposure), and some alterations, beyond enrichment, must be made to the fuel to maintain satisfactory performance. The principal disadvantages of mixed-oxide fuel for FR use are its low thermal conductivity and low density. The former property leads to high temperature gradients in the fuel and low values for linear power, and the latter property is undesirable from a breeding-ratio point of view.

Among the several compounds of uranium and carbon, UC has been given the most attention because of its high

Figure 21.29 Erection of the BN-800 reactor vessel.

uranium density. UC is a densely packed, face-centered cubic structure that contains 4.8 weight percent carbon for a stoichiometric composition. Like UO_2, UC can be fabricated by compacting and sintering powders to achieve the degree of porosity desired. The primary factor of interest in UC as a fast reactor fuel, beyond its relatively high density, is its good thermal conductivity.

Uranium nitride (UN) has also received appreciable attention. It has physical properties quite similar to UC. Uranium nitride is more compatible with cladding than UC (no carburization), but much less in-pile experience exists upon which to judge its overall merits. Fabrication problems are somewhat complicated, particularly if an arc-casting process is used, because of the need for a nitrogen atmosphere to prevent nitrogen loss. Thermal decomposition of UN occurs above 2000°C, which may raise certain safety questions but should not affect steady-state performance.

All the early low-power fast reactors employed metallic uranium fuel. It is relatively easy to fabricate, has excellent thermal conductivity, and has a high density (19.0 g/cm^3 at room temperature). The principal problem with metal fuel is its highly anisotropic growth patterns upon irradiation and the large associated dimensional change. If fully dense metallic fuel is used, along with a small initial fuel-cladding gap in order to achieve a high smear density, burnup is limited to the order of 10 MWd/kg, far too low to be economical. However, at least two techniques have been proposed to improve metal fuel burnup capability. The challenge is to fabricate an axial hole in the fuel to accommodate fuel swelling internally. The second technique, developed in association with the EBR-II project, involves increasing the initial fuel-cladding gap filling with sodium to accommodate such swelling. Success in this approach with metal alloy fuels was demonstrated in EBR-II. The thorium based fuels, such as the Th232–U233 fuel system, could be employed in a breeder reactor, although with an inherently lower performance with regard to breeding ratio and doubling time. Because the potential to breed does exist for such a system, it is appropriate to provide some background on the potential of thorium-based fuel systems for fast reactor application. Relative to uranium, thorium metal has both a higher thermal conductivity and a lower coefficient of thermal expansion. Both these properties tend to reduce the thermal stress in the fuel elements, but the latter property would tend to reduce the negative reactivity feedback during a power excursion.

Thorium has a considerably lower density than uranium. Perhaps the most significant difference with regard to in-pile performance is that thorium has an isotopic cubic crystalline structure (face-centered cubic) and, therefore, undergoes appreciably less dimensional change upon thermal cycling and irradiation than does the anisotropic uranium. Thorium also has higher irradiation creep resistance, higher ductility, and a higher melting point (1700°C). The latter property somewhat complicates the fabrication process since melting and casting are more difficult. Thorium, however, is fertile material from which fissile material U233 can be generated. In the early years of nuclear energy, there was enthusiasm for thorium worldwide, and several thorium-based reactor systems were examined. However, due to easy availability of uranium and saturation in energy demand in the developed world, interest in thorium could not be sustained. Considering the modest uranium reserves available in the world, large growth in nuclear power can be realized only through efficient conversion of fertile materials into fissile materials and utilizing the latter to produce energy. In view of its high-energy neutron spectrum, the FR system has the ability to trigger a larger transmutation and hence is essential for achieving fast growth rate in the energy production. Once the FR system is fully matured, the option of utilizing thorium through the FR route would be fully studied.

21.7.1.2 Coolant In any reactor system, the coolant significantly influences the reactor design. This is an important issue for the fast reactor system, since power density is very high in the fast reactor core, thus demanding a very efficient coolant. Hence, generally liquid metal is preferred. For the fast reactors designed and developed so far, sodium has been the universal choice, thanks to the very attractive nuclear, physical, and even some of its chemical properties. Further, sodium is the most common of the alkali metals. It is widespread in nature but only in the form of compounds. Since its density is low (900kg/m^3), the mechanical loadings, viz. dead load and seismic forces are low. Further, the sodium remains in the liquid state even under extreme high temperature conditions without calling for any pressurization. In view of these features, the structural wall thickness for the vessels can be as small as possible, which are generally decided by stability requirements from manufacturing and handling conditions. The sodium corrosion to structural materials such as austenitic stainless steel is insignificant, provided its purity is maintained. However, the sodium has a major limitation—its chemical toxicity. It can have a violent reaction with the air, causing a great concern for safety. However, it is worth mentioning that, due to the low volatility, the sodium flames are very short, and the heat produced by the fire is rather low; thus, it is possible to extinguish the fire by spreading a powder, a mixture of Na carbonate, Li carbonate, and graphite.

Sodium reacts exothermically with water, and potentially with violence, as a function of local conditions. The reaction with water produces sodium hydroxide and hydrogen gas, inducing hazards to be analyzed when the sodium is used as a coolant. This reaction is strongly exothermic (162 kJ/mole of Na) and extremely fast. For these reasons, sodium-water

interaction, which can occur in the steam generator units, is considered as an important issue, and safety means are developed and implemented to mitigate this event.

In normal operation, evaporation rapidly attains an equilibrium level (condensation = vaporization). Consequently, in the various gas plenums, and more particularly in the primary vessel, the mass transfer toward the colder roof of the slab is rather limited, particularly in the presence of argon, due to its low thermal conductivity. Nevertheless, the SFR operational feedback shows that there is the possibility of observing some sodium aerosols deposited in upper structures or narrow gaps. It is necessary to foresee vapor and aerosol traps in cover gas to prevent any related issues. Sodium has only one stable isotope namely: $^{23}_{11}$Na. The neutron flux leads to the formation of radioactive isotopes: Two other isotopes are created: Na24 (half life 14.98 h), creating the necessity to wait for decay before some interventions on primary circuits, and Na22 (half life: 2.6 years), to be taken into account during decommissioning and sodium treatment. This low activation is also a very attractive property of sodium for nuclear use in SFR. The sodium has extensive operating experience, more than 350 reactor years.

The periodic in-service inspection and repair of components is difficult in sodium due to its opaqueness. Further, safe disposition of huge amounts of radioactive sodium during the decommissioning stage requires high investment, operational cost, and complex technologies. Sodium poses a few specific structural mechanics problems, viz. thermal striping and thermal fluctuations, which severely affect the structural integrity of structures. These are the critical issues, responsible for inspiring the researchers to study alternate coolants, such as gases (helium and CO_2), steam, and alternative liquid metals (lead and lead-bismuth). The problems related to sodium are being addressed in the current designs through detailed analyses employing sophisticated numerical modeling and simulation techniques, testing and evaluations, and lessons learned from the operating experiences worldwide. The risk of sodium leaks can be minimized with the advanced leak detection systems, reduction of welds in piping, adopting improved materials, advanced manufacturing technologies, compact layout with fewer sodium loops, and state-of-art inspection and repair techniques. Future designs are conceived with the objective to practically eliminate the problems with double-wall sodium piping, double-wall tubes in steam generators, and the introduction of innovations such as sodium discharge into a pan with hydrolock and sodium discharge into a tank blanketed by inert gas for self-extinguishing the sodium fires when sodium is leaking from the circuits. With these features, it can be stated that issues related to sodium leakage and fires can be managed in a comprehensive manner, to the satisfaction of designers, utilities, and regulators.

The technological maturity of the potential alternate coolants is yet to be attained for the actual reactor application. In case of lead and lead-bismuth coolant, the major areas calling for significant R&D support are the chemistry and activation control of the coolant and the corrosion products, especially the oxygen control and Po210 activation product control in the Pb–Bi option. The heat transport system design requires innovative solutions such as natural circulation, lift pumps, and in-vessel steam generators. Further, high temperature structural materials also would have to be developed especially for the reactor system design in the temperature range of 750–800°C apart from environmental issues with lead. Since the density is much higher (11 g/cc) compared to sodium (9 g/cc), the seismic forces generated due to inertial effects and pumping power are significantly higher. The envisaged cost would override the economical benefits derived by elimination of sodium. In the case of gases, apart from high temperature materials, performance-related R&D is required in areas that include development of high-performance helium turbine and efficient coupling technologies for process heat applications and the high-temperature nuclear heat in the core. It is worth mentioning that, in gas-cooled fast reactors, the associated fuel cycle would be significantly different, requiring extensive R&D; much larger as compared to future fuels for SFRs.

21.7.1.3 Pool- versus Loop-Type Concepts Two types of primary systems are generally used, the pool system and the loop system. In the pool system, the entire primary system (i.e., primary circuit, primary pumps, and IHXs) is located in a large sodium pool in the reactor vessel. In the loop system, the primary pumps and IHXs are located in cells outside the reactor vessel with interconnecting piping. The heat transport systems for both the loop and pool designs are shown schematically in Figure 21.30. The term *loop* applies to a sequential series of components in the heat transport system between the reactor and the turbine, each operating independently of the other loops in the system. In an FR loop system, each loop consists of a single primary and secondary pump and one or more IHXs and steam generators. For the pool system, the term *loop* refers to the IHXs and secondary sodium system; there is no requirement that the number of primary pumps and loops be the same, though they frequently are. Most commercial-size demonstration plants have four loops; most of the smaller prototype plants have three loops.

A thorough analysis of pool/loop concepts shows that the option of reactor unit power level can influence the choice of design variants, as concerns the SFR system. The factors favoring the pool concept are that there is no relevant accident scenario of loss of primary coolant. The primary sodium inventory is managed by safety provisions

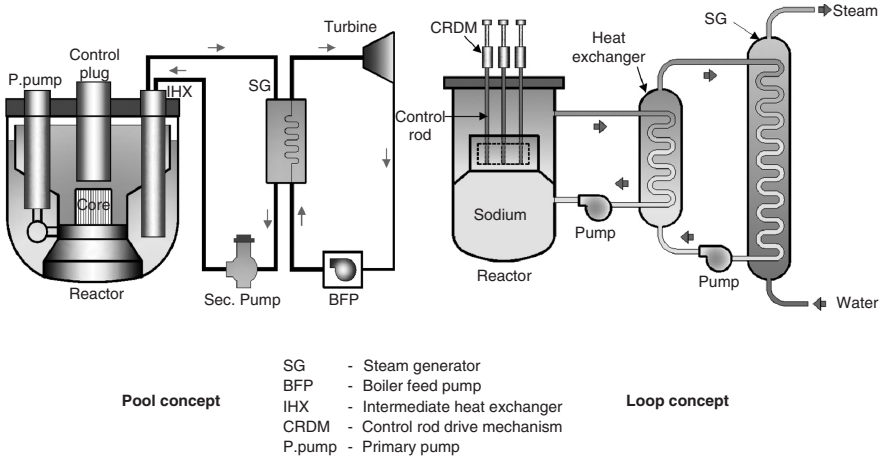

Figure 21.30 Heat transport circuits of SFR power plant.

(e.g., safety vessel); the large thermal inertia of the reactor-block contributes to slow down any transient of loss of heat sink; there is no risk of breaking the hydraulic loop from the core outlet toward the core inlet; a very efficient natural circulation of the primary circuit is expected, as a flow backup at reactor shutdown state; in case of loss of the forced flow mode (e.g., pumps trip), there exists a cold sodium plenum at the pumps' suction upstream that acts as buffer against either thermal chocks or gas entrainment toward the core; in practice, there is no risk of a radioactive sodium fire, except for limiting events leading to a core disruptive accident (CDA); good mechanical behavior of the primary containment against energetic CDA; and ease of radiation protection in normal operation. On the other hand, matters related to competitiveness and flexible operational conditions remain as challenges. There exists limited access for inspection and repair of the under-sodium internal equipments, seismic behavior of sodium free-level and large structures is complicated, and reactor-block compactness poses imitation due to integrated large components. Nevertheless, slight differences are expected between pool and loop concepts, based on existing technology, regarding the construction cost.

The factors favoring the loop-type concept are ease of access for maintenance and repair of the primary components located outside the reactor-block (e.g., IHX), compactness of the reactor-block (e.g., vessel diameter) and reduction of the number of primary loops, and the potential for further construction cost reduction and for innovative change of primary and intermediate equipment (e.g., pump design, integrated components, intermediate circuit change, and any rotating pump-shaft is away from the core vicinity). In return, the designer has to solve issues such as the prevention of loss of the primary coolant (e.g., pipe integrity) and provisions to keep a hydraulic loop through the core, whatever the abnormal operating conditions are. Also, the potential consequences of a LOCA, phenomena inside (e.g., gas entrainment) and outside the primary circuit (e.g., active sodium fire) have to be addressed. Provision is needed against asymmetric operating faults (e.g., trip of one of the pumps leading to reverse flow), and suitable implementation of several decay heat removal (DHR) systems is necessary in order to cope with different accidental configurations of the primary circuit.

21.7.2 Advanced Reactor Concepts Considered

21.7.2.1 France Prospective studies carried out by the CEA and industrial partners led to the creation of an R&D strategy for France to support the development of nuclear reactors for the continuous and sufficient supply of energy through the 21st century. The proposal for development of these systems contains two tracks of R&D: the Sodium Fast Reactor and the Gas Fast Reactor. Closely linked to R&D on reactor concepts, a consistent program on fuel cycle technologies is also conducted with the objective of achieving significant progress on the nature of final waste and on optimized management and recycling of minor actinides. The SFR project is in an innovating phase. Advanced Sodium Technological Reactor is developed for Industrial Demonstration (ASTRID) with 600 MWe capacity, mainly to demonstrate the industrial-scale feasibility of such a reactor by qualifying the innovative options under investigation, particularly in safety and operability. A preliminary analysis was performed in 2009 and it is planned to commission this reactor during 2017–2020. Investigations since 2006 focused mainly on three directions: (1) improvement of the pool concept, which allows capitalizing on the experience feedback gained in France on Phenic, Super Phénix, SPX2, and EFR; (2) evaluation of the loop concept with innovative proposals; and (3) investigating new concepts and solutions to assess the potentialities.

At this stage, the complete comparison between all the presented options is difficult, mainly because studies are not at the same levels. However, the gain provided by the higher compactness of loop concept seems limited if the number of primary loops is increased to three from a safety point of view. The loop concept does not provide definitive interest regarding decay heat removal (DHR) diversification and in-service inspection and repair possibilities, except for repair and removability if it is conceived specifically for this objective. DHR diversification is under study, aiming at providing alternative solutions regarding the sodium/air heat exchangers common mode failures. The trend of increasing reactor compactness was confirmed to be beneficial for seismic resistance and costs. However, this trend is detrimental for thermal hydraulics. The GFR system is promising (first results confirm the potential of the concept) and requires significant breakthroughs in the field of fuel, materials, and system arrangement. Some common R&D interests with the SFR are emerging.

The next step is to construct a prototype SFR in the range 250–600 MWe (ASTRID) to demonstrate economics and the safety of new options, to be commissioned in 2020, subsequent to the selection of the main options in 2012. For GFR, an experimental reactor, ETDR, in the range of 50 MWth to demonstrate viability of key GFR technologies, is planned to be operational in 2020.

21.7.2.2 Commercial Fast Breeder Reactor (CFBR-India) India started its fast breeder reactor program by constructing a 40 MWt/13.5 MWe loop-type fast breeder test reactor (FBTR) at Kalpakkam, which has been in operation since 1985. This was followed by the design and development of a 500 MWe capacity Prototype Fast Breeder Reactor (PFBR). The construction of PFBR was started in 2003 and scheduled to be commissioned by 2011. Beyond PFBR, six 500 MWe reactors are planned for construction by adopting the twin unit concept (three 2×500 MWe reactors). One twin unit would be built at Kalpakkam, near PFBR. Commissioning of these reactors is planned by 2023. Since these units are Commercial Fast Breeder Reactors (CFBRs), many innovative features are introduced, particularly in the reactor assembly design to achieve significant cost reduction, retaining the MOX fuel, the two-loop concept, and reactor vault design features. Apart from the twin unit concept, the other features are optimum shielding with advanced shielding materials such as ferro boron, use of SS 304 LN in place of SS 316 LN for cold pool components and piping, 3 SG modules per loop with increased tube length of 30 m (PFBR has four modules per loop with 23 m length), enhancing the design life to 60 years (for PFBR, 40 years), reduced construction time of 5 years (7.5 years for PFBR), and enhanced burnup to 200 GWd/t to be achieved in stages (100 GWd/t for PFBR).

In particular for reactor assembly, improvements/innovations have been introduced based on the feedback from design and construction experiences of PFBR, the international trend of innovative design of FRs worldwide, accumulated experience on focused R&D during last 40 years and above, and technical perception. These efforts have yielded a net material saving of approximately 25% in the reactor assembly components. Further, the challenges involved and the approach in implementing the new concepts and associated R&D works required to be completed in the domain of technology development, in-service inspection, and performance qualifications have been identified. The improvements conceived for the reactor assembly of CFBR are schematically depicted in Figure 21.31.

21.7.2.3 Japan Sodium-Cooled Fast Reactor (JSFR) Based on the Japanese policy, a Fast Reactor Cycle Technology Development (FaCT) project was launched as an advanced stage toward the commercialization of fast reactor cycle technology. The main development issues were identified as 13 issues for fast reactor and 12 issues for fuel cycle, based on the results of FS phase-II study. In the FaCT project, both the conceptual design study for the advanced loop-type fast reactor named Japan Sodium-Cooled Fast Reactor (JSFR) and the developments of the innovative technologies are now being executed by paying attention to the consistency between the design and the relevant technologies, aiming at deciding the adoption of innovative technologies by judging their applicability in 2010, and presenting the conceptual designs of commercial and demonstration facilities in 2015.

JSFR is an advanced loop-type SFR with an MA-bearing MOX fueled core. Figure 21.32 shows the schematic view of JSFR, and the major specifications for the 1,500 MWe plant are included in the figure. In the JSFR design, there are seven innovative technologies to enhance the economy, three technologies to assure the reliability, and three to improve the safety, which shall be developed toward their demonstration and commercialization. In order to reduce the component size, the diameter of the Reactor Vessel (RV) shall be minimized, and the reactor internal structures shall be simplified. In order to select the most advantageous concept of the cooling system, the loop number, primary piping system, and applicability of the integrated components have been comprehensively examined from the viewpoints of the reduction of component size, safety, maintainability, and manufacturability. As a result, shortening of piping, a two-loop cooling system, and an integrated IHX with primary pump are introduced into the design.

21.7.2.4 KALIMER-600 (Korea) The third national mid- and long-term nuclear R&D program was newly

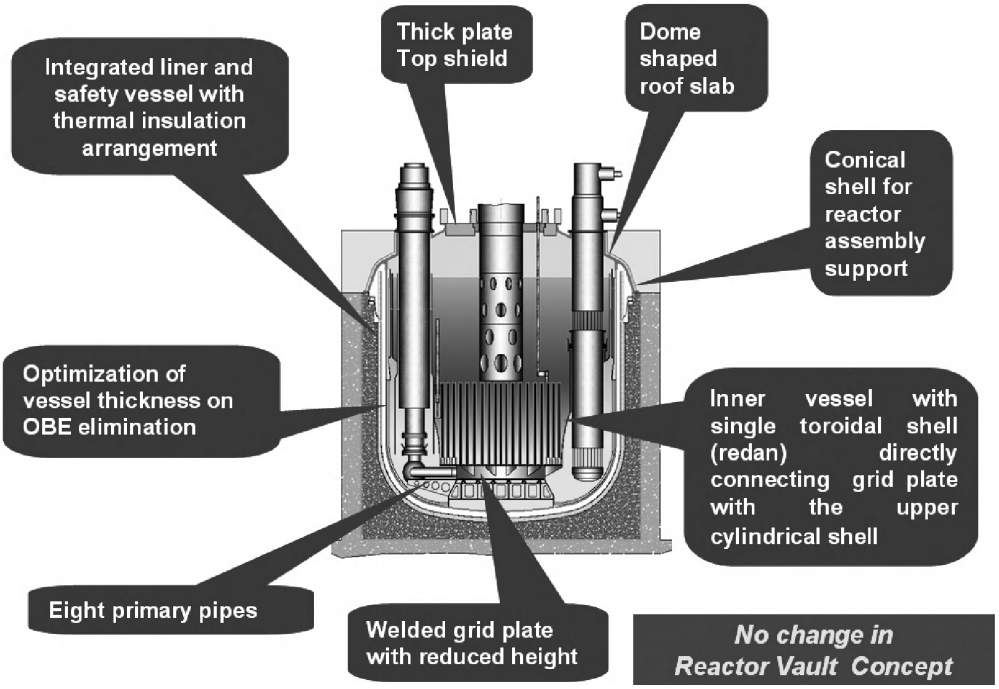

Figure 21.31 Major improvements introduced in the CFBR reactor assembly.

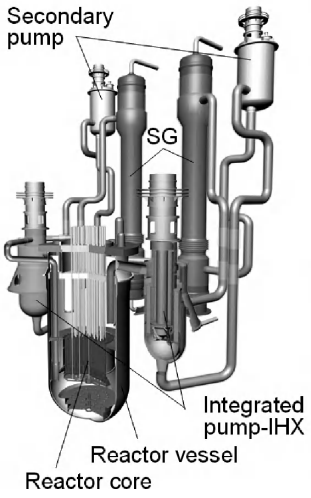

Items	Specifications
Output	3,570MWt / 1,500MWe
Number of loops	2
Primary sodium outlet temperature and flow rate	550 /395 degree C 3.24 x 10^7 kg/h/loop
Secondary sodium temperature and flow rate	520 / 335 degree C 2.70 x 10^7 kg/h/loop
Main steam temperature and pressure	497 degree C 19.2 MPa
Feed water temperature and flow rate	240 degree C 5.77 x 10^6 kg/h
Plant efficiency	Approx. 42%
Fuel type	TRU-MOX
Breeding ratio	Break even (1.03), 1.1, 1.2
Cycle length	26 months or less, 4 batches

Figure 21.32 Major improvements introduced in the CFBR reactor assembly.

launched as a five-year program in 2007. The SFR technology development project is now being carried out by KAERI. The long-term Advanced SFR R&D plan authorized by the KAEC targets the construction of an Advanced SFR demonstration plant by 2028 in association with the pyroprocess technology development. Based upon the experiences gained during the development of conceptual designs for KALIMER, KAERI is developing key technologies for an Advanced SFR. There are three categories of activities under way: (1) advanced concept design studies, (2) development of the Advanced SFR technologies necessary for its commercialization, and (3) development of basic technologies. KALIMER-600, which is a pool-type reactor loaded with metal fuels of U-TRU-Zr, has the capacity of 600 MWe and breakeven characteristics. That is, KALIMER-600 produces the same amount of TRUs that it consumes. With a strong emphasis on proliferation resistance, the core design of KALIMER-600 has been evolved to have a single enrichment zone without any blankets. In addition, passive residual heat removal, shortened IHTS piping, and seismic isolation was realized in the system design. The KALIMER-600 design serves as a starting

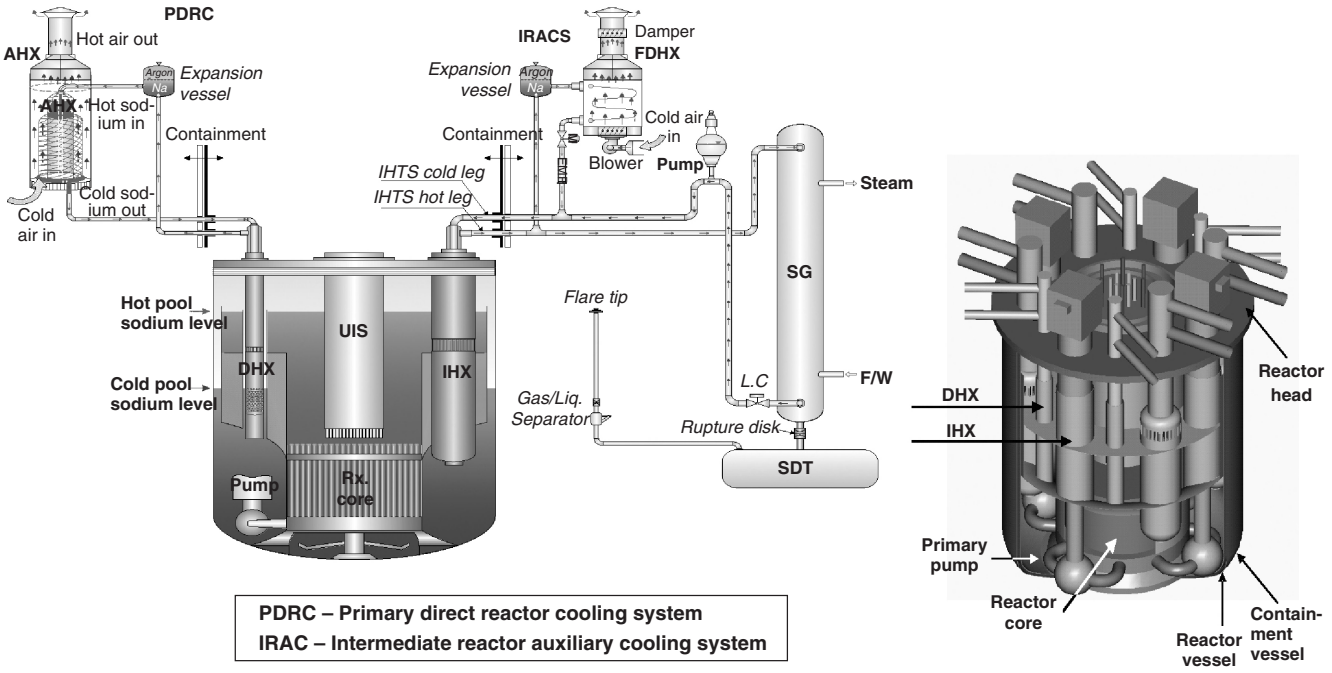

Figure 21.33 Flow sheet and details of reactor assembly component layout of KALIMER.

point for developing a new advanced design. Figure 21.33 shows the flow sheet and details of reactor assembly component layout.

21.7.2.5 BN-1800 (Russia) In Russia, research studies continue that are aimed at the development of the conceptual design of commercial NPP with a large-size, sodium-cooled fast reactor (BN-1800). The conceptual design is in progress. The salient features are as follows:

- a traditional three-circuit design of power unit a pool-type arrangement of the primary circuit with all sodium systems, including cold traps, located in the reactor vessel, making it possible to eliminate, in fact, the danger of radioactive sodium release outside the reactor vessel and its fire
- moderate parameters of sodium and tertiary circuits
- number of loops in the primary circuit–four (each loop contains one IHX and one primary sodium pump)
- number of loops in the secondary circuit–four (each loop contains one IHX, one MCP-2, and one SG
- once-through vessel-type SG of integrated type
- number of turbine units per power unit–two
- steam reheating
- operation of the NPP at the stable (mainly, rated) power level envisaged with a load
- factor equal to at least 0.9
- a closed nuclear fuel cycle
- excluding that a stage of extraction of a pure plutonium
- the exception of intermediate storage drums of fresh and spent fuel subassembly (SFSA) and organization of a capacious in-reactor vessel storage (IVS), providing exposure of SFSA over more than 1.5 years that allows carrying out a direct unloading of FSA from the IVS into washing cells and further into an exposure pool
- the variant of decay heat removal system connected directly to the reactor vessel considered as basic one
- the variant with bottom support of the reactor vessel and
- loop-type variant of the hydraulic scheme of the basic circulation circuit of the primary sodium considered as a basic option.

The flow diagram of the BN-1800 is shown in Figure 21.34, and a longitudinal section of the BN-1800 reactor is presented in Figure 21.35.

21.7.2.6 Integral Fast Reactor (United States) The Integral Fast Reactor (originally Advanced Liquid-Metal Reactor) was a design for a fast reactor distinguished by a nuclear fuel cycle using reprocessing via electro refining at the reactor site itself (Fig. 21.36). This reactor is cooled by liquid sodium and fueled by a metallic alloy of uranium and plutonium. The fuel is contained in steel cladding with liquid sodium filling in the space between the fuel

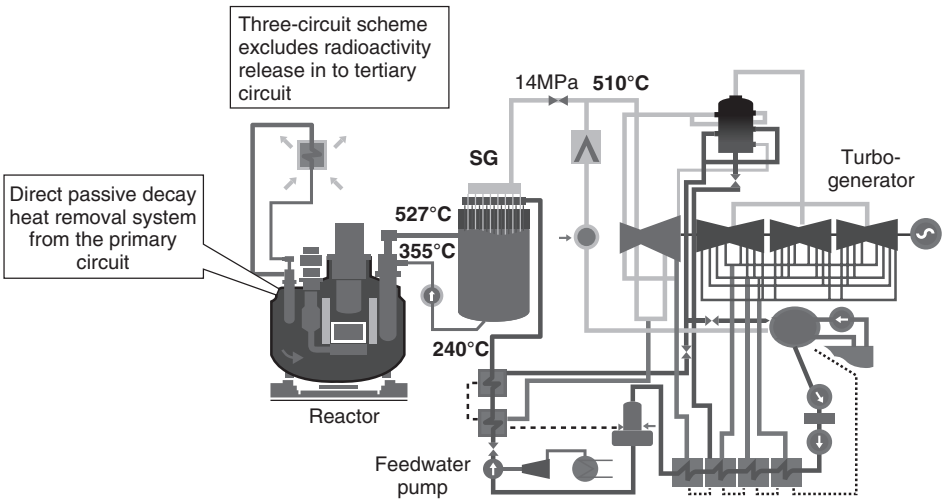

Figure 21.34 Flow sheet of the BN-1800.

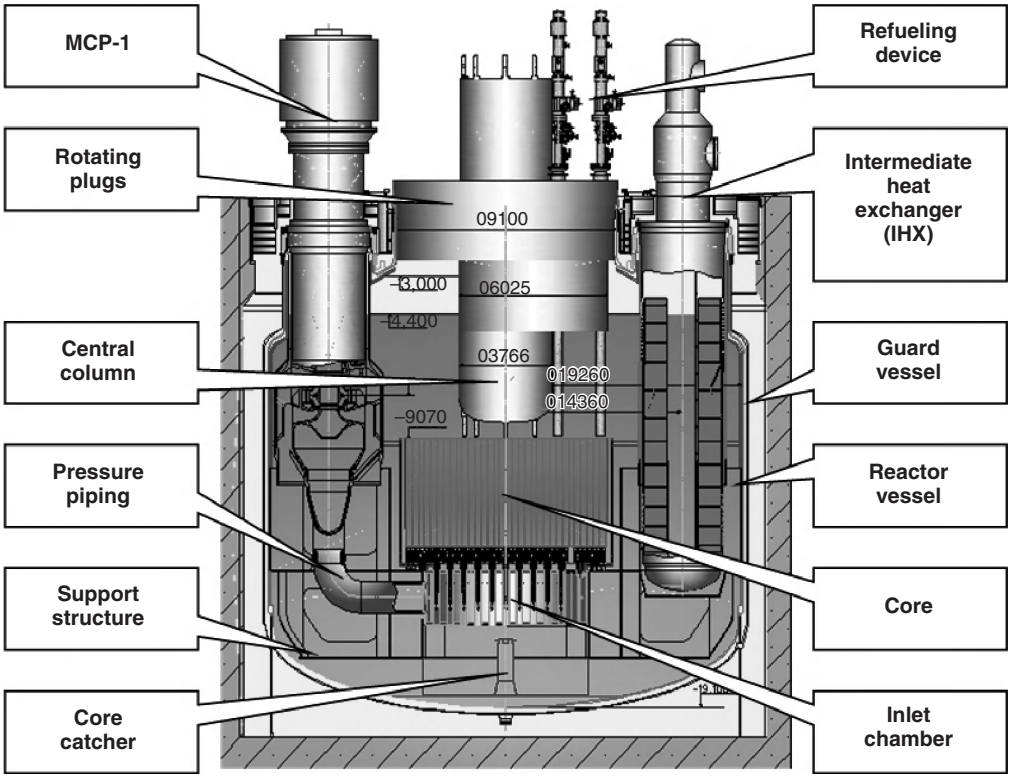

Figure 21.35 Reactor assembly of BN-1800.

and the cladding. The IFR utilizes a passively safe fuel configuration. The fuel and cladding are designed such that when they expand due to increased temperatures, more neutrons would be able to escape the core, thus reducing the rate of the fission chain reaction. At sufficiently high temperatures, this effect would stop the reactor even without external action from operators or safety systems. This was demonstrated in a series of safety tests on the prototype. To reduce the risk of explosions following a leak of water from the steam turbines, the IFR design (as with other sodium-cooled fast reactors) includes an intermediate liquid-metal coolant loop between the reactor and the steam turbines. The purpose of this loop is to ensure that any explosion following accidental mixing of sodium and turbine water would be limited to the secondary heat exchanger and not pose a risk to the reactor itself.

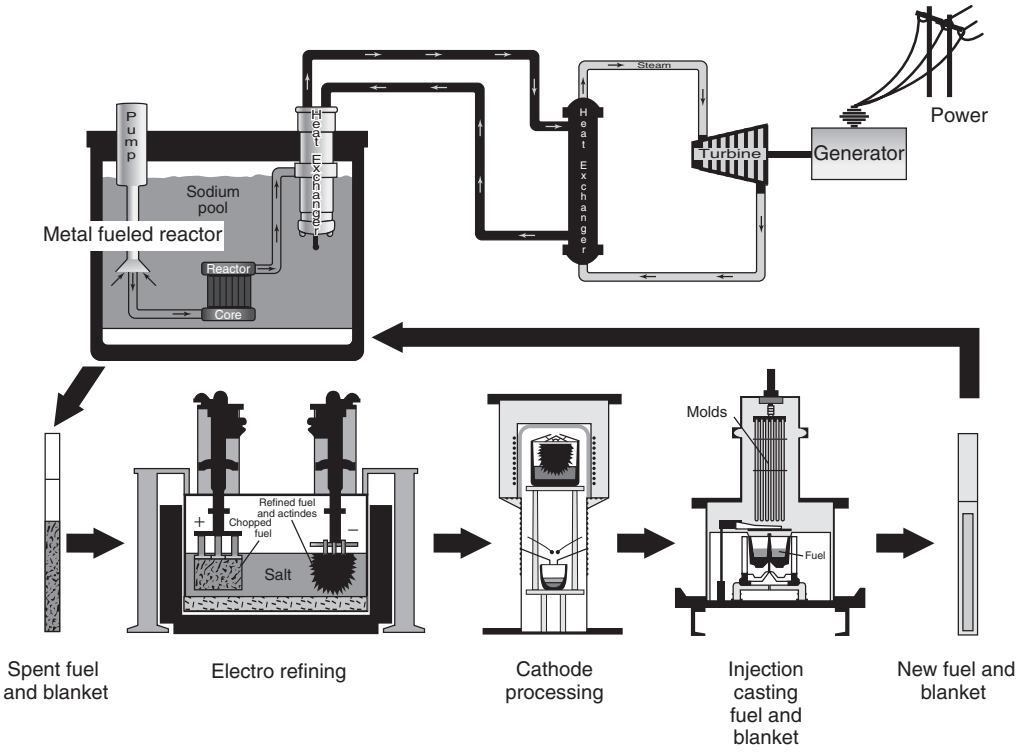

Figure 21.36 IFR schematic.

According to IFR inventor Charles Till, no radioactivity will be released under any plausible circumstance. A wide range of unexpected events that would cause destructive and hazardous failures in other reactor systems would not damage the IFR.

The goals of the IFR project were to increase the efficiency of uranium usage by breeding plutonium and eliminating the need for transuranic isotopes ever to leave the site. The reactor was an unmoderated design running on fast neutrons, designed to allow any transuranic isotope to be consumed (and in some cases used as fuel). Compared to current light water reactors with a once-through fuel cycle that induces fission (and derives energy) from less than 1% of the uranium found in nature, a breeder reactor like the IFR has a very efficient (99.5% of uranium undergoes fission) fuel cycle. The basic scheme used is electrolytic separation to remove transuranics and actinides from the wastes and concentrate them. These concentrated fuels were then reformed, on site, into new fuel elements. The available fuel metals were never separated from the plutonium, and therefore there was no direct way to use the fuel metals in nuclear weapons. Also, plutonium never had to leave the site, and thus was far less open to unauthorized diversion. Another important benefit of removing the long half-life transuranics from the waste cycle is that the remaining waste becomes a much shorter-term hazard. After the actinides (reprocessed uranium, plutonium, and minor actinides) are recycled, the remaining radioactive waste isotopes are fission products, with half-life of 90 years (Sm151) or less or 211,100 years (Tc99) and more, plus any activation products from the non-fuel reactor components. Tc99 and Iodine-129 are also candidates for nuclear transmutation to stable isotopes by neutron capture. The result is that within 200 years, such wastes are no more radioactive than the ores of natural radioactive elements. U.S. national laboratories would design and direct the third component, the Advanced Fuel Cycle Facility, a modern state-of-the-art laboratory designed to serve reactor fuels research needs for the next 50 years.

21.7.2.7 Advanced Burner Reactor (ABR) Under the GNEP program, the United States is also planning to develop and demonstrate Advanced Burner Reactors (ABR), or advanced fast reactors, as a key element of a new, integrated U.S. recycling capability. As they produce power, advanced fast reactors consume transuranic elements (plutonium and other long-lived radioactive material), potentially eliminating the need for their disposal in the geologic repository at Yucca Mountain, Nevada. ABRs would destroy almost all the transuranics in used fuel from nuclear power plants, significantly reducing the limitations on accommodation of this radioactive, radiotoxic, and heat-producing material in a geologic repository. As part of GNEP, the United States is moving from a once-through

fuel cycle to an improved approach based on recycling of spent nuclear fuel. Specifically, recycling would comprise uranium extraction plus (UREX+). Research has shown that UREX+ can separate uranium from spent fuel at a very high level of purification that would allow it to be recycled for re-enrichment, stored in an unshielded facility, or simply buried as a low-level waste. In addition, long-lived fission products, technetium and iodine, could be separated and immobilized for disposal in Yucca Mountain. Short-lived fission products, cesium and strontium, could be extracted and prepared for decay storage until they meet the requirements for disposal as low-level waste. Finally, transuranic elements (plutonium, neptunium, americium, and curium) separated from the remaining fission products could be fabricated into fuel for an advanced fast reactor. To develop and deploy an integrated recycling capability, the Department of Energy is investigating the feasibility, interest, and ability of industry to collaborate with the U.S. national laboratories and international partners on both recycling and fast reactor technologies.

Originally, the ABR program was conceived as a two-phase project, viz. Advanced Burner Test Reactor (ABTR) to qualify fuels, support nuclear regulatory commission design certification, validate codes, and subsequently support technology development for standard ABR design. The current focus is to utilize existing technology to design/construct an ABR prototype. The plant sizes, ranging from 500–2000 MWt, are studied for both reactor and separations facilities.

Figure 21.37 provides the details of ABTR. The objectives of ABTR are to demonstrate actinide transmutation in fast spectrum, demonstrate innovative technologies and design features that could be applied to ABR, and demonstrate SFR safety features. It is of 250 MWt size. The flux level is sufficient for meaningful irradiation testing of fuels and materials; it also has the capability to irradiate lead test assemblies and metal fuel. It has favorable passive behavior for off-normal transients and benign response to severe accidents such as unprotected loss of flow, loss of heat sink, and transient overpower. The fuel-handling system has a single rotating plug and a pantograph fuel-transfer machine. The vessel diameter is reduced by 1 m compared to double rotating plug. Further, it simplifies the fuel handling procedure. For the decay heat removal, Direct Reactor Auxiliary Cooling System (DRACS), which operates by passive natural convection flow, is used instead of Reactor Auxiliary Cooling System (RVACS) to avoid high vessel temperature inherent to RVACS. Seismic isolation based on multiple friction pendulum system is employed for the reactor building base mate. Supercritical CO_2 power conversion system is used for the power generation.

21.8 CONCLUSION

The fast spectrum reactors with closed fuel cycle effectively utilize the limited uranium resources in near future and abundant thorium in far future, cause less environmental burden because of less waste generation and possibility of reduced storage time (∼500 yrs) for the radioactivity to attain the natural background value. Fast reactors have obtained sufficient technological maturity by accumulating approximately 400 reactor years by operating prototype, test, and experimental reactors. Among various reactor types, sodium-cooled fast reactors have high potential for the commercial exploitation from 2020 onwards. Russia and India are embarking upon the construction of commercial reactors by 2020. Although the safety aspects of sodium-cooled fast reactors have been addressed comprehensively through the successful operation of a few prototypes, there is renewed emphasis on improving sodium-related issues, which can be solved with innovative technologies, being pursued intensively by the countries with clear interest in fast reactor technology.

With reference to fuel option, which has a large impact on the fuel cycle technology, oxide-based fuels with rich experience are the first to be exploited because these fuels require minimum R&D. However, for realization of nuclear power in a faster rate, high breeding ratio and transmutation are essential, which are possible by using carbide, nitride, and metallic fuels. Focused R&D activities to achieve enhanced economy and safety need to be pursued in the reactor and fuel cycle systems. Alternate coolants, such as gas, lead, and lead-bismuth alloys, also need significant technological maturity to go to the stage of commercial exploitation.

The above advantages have created a renewed and enhanced interest in the development of fast reactor system globally. The GEN IV international forum and the IAEA Joint assessment Study on closed nuclear fuel cycle with fast reactors (CNFC-FR) have recently brought out the importance of fast reactor systems as the inevitable and sustainable energy option in first half of the 21st century. These initiatives, apart from bringing out the challenges and opportunities in developing FR system, have clearly emphasized the importance of international collaborations and the common perspectives required in sharing the vision, scientific and technical information, and unique facilities to ultimately utilize the unique merits of fast reactor technology toward meeting the sustainability and other inevitable requirements for future.

The fast spectrum reactors offer many research and technology challenges and opportunities to generate immense excitement as well as motivation for the young minds worldwide.

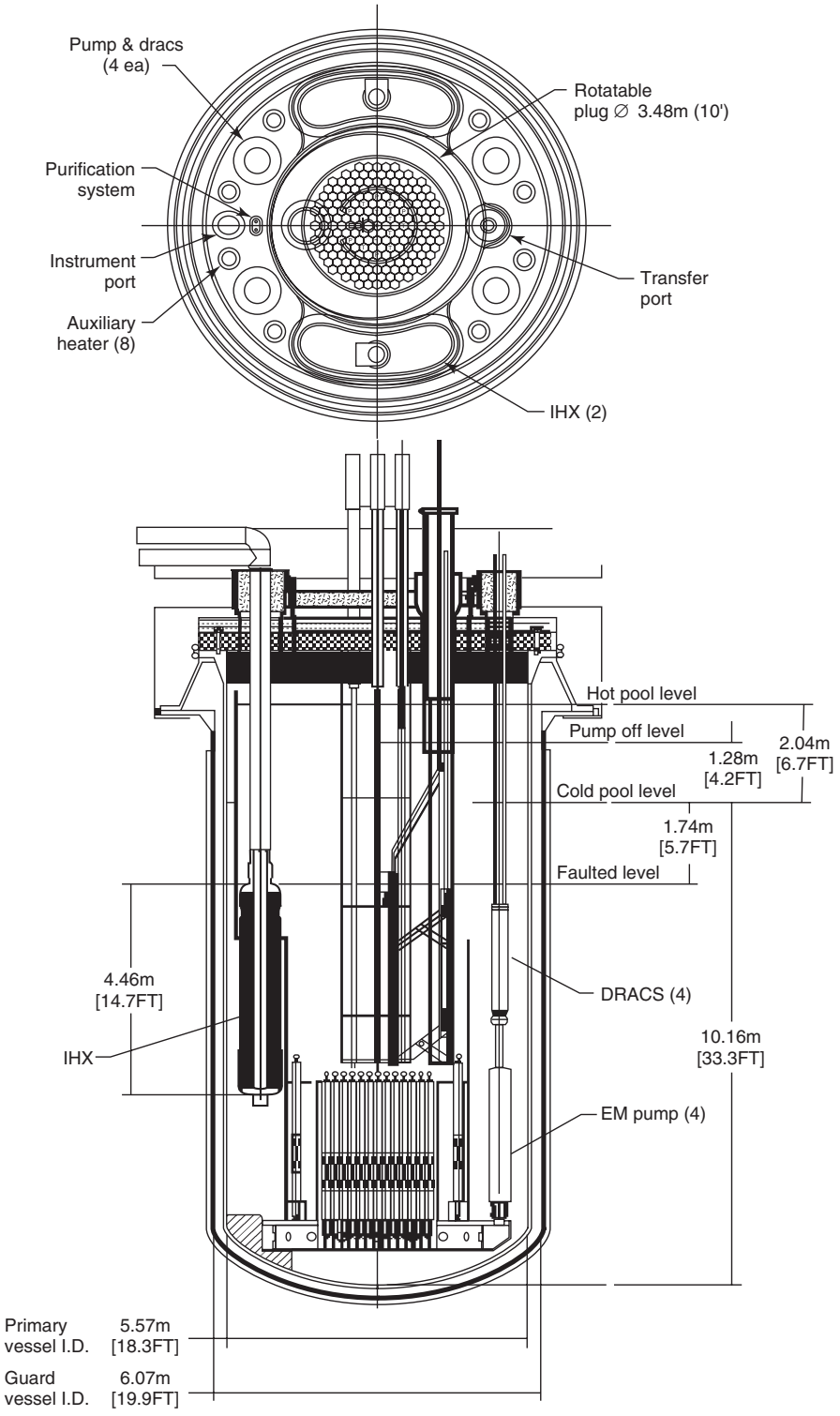

Figure 21.37 ABR schematic.

Acknowledgments

The information provided by colleagues at IGCAR and individuals and organizations from India and abroad are sincerely acknowledged.

FURTHER READING

A Technology Roadmap for Generation IV Nuclear Energy System, G.F-002-00, December 2002, issued by U.S. DOE Nuclear Energy Research Advisory Committee and the Generation IV International Forum.

CEFR: Xu Mi, *Chinese Fast Reactor Technology Development'*, China Institute of Atomic Energy, KAERI-CRIEPI Technical Meeting on LMR on 11-12 November 1999, at Kaeri, Korea.

Fast Reactor Database, IAEA-Tecdoc-866, February 1996.

Gen-IV International Forum Annual Report, 2007, Printed by OECD Nuclear Energy Agency for the Generation IV International Forum.

INPRO Joint Study on Assessment of Innovative Nuclear Systems Based on Closed Fuel Cycle with Fast Reactors, IAEA INPRO-TECDOC-1639, IAEA, Vienna, 2010.

International Working Group on Fast Reactors, Eleventh annual meeting, Summary Report, IAEA, 1978.

International Working Group on Fast Reactors, Meeting on In-service Inspection and Monitoring of LMFBRS, Bensberg, Germany, 20 May 1980.

International Working Group on Fast Reactors, Fourteenth annual meeting, *Summary Report*, IAEA, 1981.

JSFR: Mamoru Konomura and Masakazu Ichimiya, Design challenges for sodium cooled fast reactors., *Journal of Nuclear Materials*, 2007, **371**, 250–269.

KALIMER: Dohee Hahn, Yeong-Il Kim, Seong-O Kim, Jae-Han Lee, and Yong-Bum Lee, Design concept of KALIMER-600, *Proceedings of GLOBAL 2005*, Tsukuba, Japan, 9-13 October 2005, Paper No. 437.

41st Meeting of the Technical Working Group on Fast Reactors (TWG-FR), IAEA Vienna, 26–29 May 2008.

42nd Meeting of the Technical Working Group on Fast Reactors (TWG-FR), IGCAR, Kalpakkam, 26–29 May 2009.

Status of Fast Reactor Technology, 40th Annual Meeting, Kyoto, Japan, IAEA/TWG-FR, 15–18 May 2007.

Status of Liquid Metal Cooled Fast Reactor Technology, IAEA-Tecdoc-1083, April 2009.

Super Phénix: Novotome, 10 rue Juliette Reeca, ier, BP 3087, 69398, Lyon Cedex 03, France.

Tsutomu Yanagisawa, *The Role of Monju for FBR Development*., The Fourth Tsuruga International Energy Forum, 27 April 2004, Japan.

A.E. Waltar and A.B, Reynolds, *Fast Breeder Reactors*, Pergamon press, 1981.

22

REVIEW OF GENERATION-III/III+ FISSION REACTORS

J.G. MARQUES

Instituto Tecnológico e Nuclear & Centro de Fisica Nuclear da Universidade de Lisboa, Portugal

22.1 INTRODUCTION

The nuclear power industry has been developing and improving reactor technology over five decades. Several generations of reactors are commonly distinguished. The reactors in operation today were mostly built in the 1970s and 1980s. They are considered Generation II reactors, because they are based on the experience gained with the Generation I reactors built in the 1950s and early 1960s. The accumulated operating experience to the present time with current reactors exceeds 14,000 reactor-years [1]. Building of Generation III reactors started in the early 1990s, with improved safety and economics, while Generation III+ reactors include further developments. We will refer to Generation III and III+ reactors simply as Gen III/III+ in this review. Generation IV designs are still on the drawing board, and it will take two to three decades for them to be operational.

Gen III/III+ designs present a set of distinctive characteristics [2–4]:

- simpler and more rugged design, making the reactors easier to operate and less vulnerable to operational disturbances.
- Greater use of passive safety features that require no active controls and rely on natural phenomena.
- Reduced probability of occurrence of accidents involving core melting.
- New mitigation measures in case of core melt accidents, in order to reduce significantly the impact of such accidents to the environment and to the public.
- Resistance to the impact of a large aircraft.
- Standardized designs, able to reduce licensing and construction time, as well as capital cost.
- Longer time interval between refueling, resulting in a higher availability.
- Higher burnup to increase fuel use and reduce the amount of waste produced.
- Longer operating lifetime, 60 years, already from design.

Table 22.1 shows the main Generation III/III+ designs constructed, under construction, or undergoing pre-licensing/licensing procedures [3, 5], in alphabetical order by their abbreviation. The characteristics of these reactors will be presented below, divided in the categories of Pressurized Water Reactors (PWR), Boiling Water Reactors (BWR), Pressurized Heavy-Water Reactors (PHWR), and High-Temperature, Gas-cooled Reactors (HTGR), after a general presentation of relevant features of Gen III/III+ designs with their impact on safety and economic aspects.

22.2 SAFETY FEATURES OF GENERATION III/III+ FISSION REACTORS

The safety of nuclear fission reactors has always been an important issue. Redundancy and diversity are commonly applied principles for tolerance against faults that can be traced back to the first reactor built by Fermi in 1942 [2]. Gen III/III+ designs have an increased reliance on passive systems, when compared with designs of previous

Nuclear Energy Encyclopedia: Science, Technology, and Applications, First Edition (Wiley Series On Energy).
Edited by Steven B. Krivit, Jay H. Lehr, and Thomas B. Kingery.

TABLE 22.1 Main Gen III/III+ Reactor Designs

Reactor[a]	Developer(s)	Net Electric Output (MW_e)	Type[b]	Status
ABWR	General Electric, Toshiba, Hitachi	1315	BWR	Start of operation in Japan, 1996
ACR-1000	Atomic Energy of Canada	1085	PHWR	Start of operation in Canada, 2016[c]
AES-92	Gidropress	1000	PWR	Start of operation in India, 2011[c]
AP1000	Westinghouse	1117	PWR	Start of operation in China, 2013[c]
APR-1400	Korea Hydro & Nuclear Power	1350	PWR	Start of operation in South Korea, 2013[c]
APWR	Mitsubishi	1600	PWR	Start of operation in Japan, 2017[c]
EC6	Atomic Energy of Canada	700	PHWR	Design certification ongoing in Canada
EPR	Areva	1600	PWR	Start of operation in Finland, 2012[c]
ESBWR	General Electric Hitachi	1333	BWR	Design certification ongoing in the US
GT-MHR	General Atomics and others	280	HTGR	Start of operation in Russia, 2021[c]
IRIS	Westinghouse and others	335	PWR	Design certification in the US to start in 2012[c]
NuScale	Nexant-Bechtel and others	35	PWR	Design certification in the US to start in 2012[c]
SWR-1000	Areva	1250	BWR	Compliance with European requirements, 2002

[a] ACR-1000 and EC6 are registered trademarks of Atomic Energy of Canada Limited; AP1000 is a trademark of Westinghouse Electric Company, LLC; APR1400 is a trademark of Korea Hydro & Nuclear Power Company; EPR and SWR-1000 are trademarks of the Areva Group.

[b] BWR = Boiling Water Reactor; PHWR = Pressurized Heavy Water Reactor; PWR = Pressurized Water Reactor; HTGR = High Temperature Gas-cooled Reactor.

[c] Expected.

generations. The use of passive systems circumvents the eventual disruption of external sources of electricity, cooling water, and other essential supplies following an extreme event. Several Gen III/III+ designs provide for the physical presence of large thermal capacity heat sinks available to cool the reactor core without depending on the availability of externally powered pumps, relying rather on cooling by natural convection, radiation, and conduction. When valves are required for the activation of passive safety systems, they are generally "fail safe," because they require power to stay in their normal, closed position, and loss of power causes them to open; their movement is made using stored energy from compressed gas, batteries, or springs.

Gen III/III+ designs are characterized by a reduced probability of occurrence of accidents involving core melting, quantified by a Core Damage Frequency (CDF). The International Atomic Energy Agency (IAEA) issued its *Basic Safety Principles for Nuclear Power Plants* in 1988, prepared by an INternational Safety Advisory Group (INSAG) [6], which recommended that the CDF value for advanced designs should not exceed 1×10^{-5} events per reactor-year. This recommendation represented an improvement of a factor of 10 over the U.S. Nuclear Regulatory Commission (NRC) requirement for the CDF of current plants to be below 1×10^{-4} events per reactor-year. The INSAG recommendation has been widely adopted both by utilities and manufacturers for new nuclear power plants.

Figure 22.1 shows a graphical representation of CDF values (in events per reactor-year) for typical Gen III/III+ PWR and BWR designs, compared with the NRC requirement for current plants, a typical value for current plants, and the INSAG limit. The CDF value taken as representative for current plants is 5×10^{-5} events per reactor-year, even if this is subjected to large variations by design and country [7]. The CDF for new designs is typically two to three orders of magnitude below the INSAG limit. Gen III/III+ BWR designs tend to have a smaller CDF than PWR designs, as already happens for current reactors [7]. Specific CDF values for Gen III/III+ designs will be presented later.

A core melt does not necessarily lead to a large radioactive release from the reactor. The INSAG recommended that severe accident management and mitigation measures should reduce by a factor of at least 10 the probability of large off-site releases requiring short-term off-site response [6], and this has been systematically taken into account in new reactor designs [8]. The provision in several reactors to cool and contain the corium, i.e., the molten fuel-structure mixture resulting from a core melt, is a significant contributor for this reduction.

Corium cooling is essential, since the release of fission products and the generation of non-condensable gas stop as the melt/debris temperature drops below approximately 1000°C [9]. The cooling and contention are achieved in Gen III/III+ designs by ex-vessel or in-vessel structures, represented schematically in Figure 22.2.

An ex-vessel structure, or "core catcher," adds an additional barrier that aims at limiting and restricting the consequences of an accident with core melting to the immediate vicinity of the plant. As this requires an intact

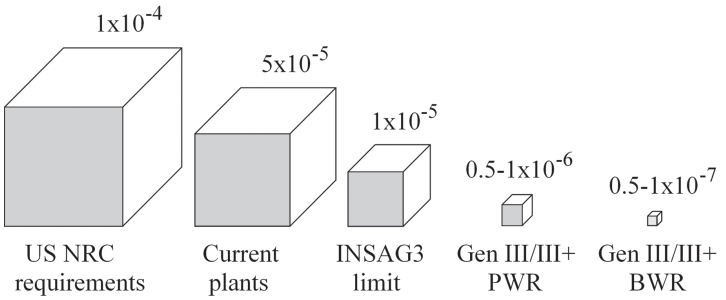

Figure 22.1 Graphical representation of the core damage frequency (in events per reactor-year) for typical PWR and BWR Gen III/III+ reactor designs, compared with the NRC limit for current reactors, the INSAG-3 limit for advanced reactors, and a typical value for current plants. The volume of each cube is proportional to the core damage frequency.

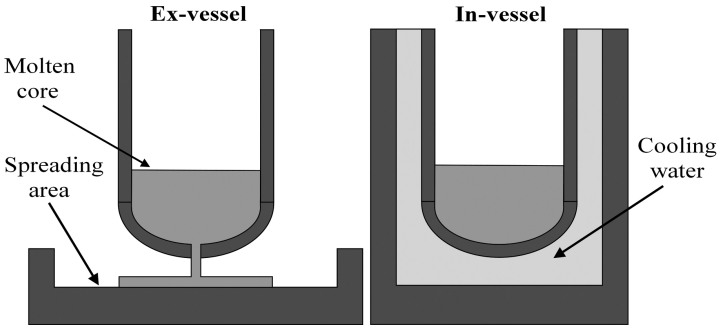

Figure 22.2 Simplified representation of ex-vessel and in-vessel corium cooling and retention systems.

confinement, it is necessary to avoid an attack of the molten core on the containment basemat. An ex-vessel core catcher increases the surface-to-volume ratio of the melt after its release from the reactor pressure vessel (RPV) and allows for the effective quenching and stabilization of the melt before it can attack the structural concrete. The corium in the core catcher can be cooled passively or actively. The deliberate interaction with sacrificial materials (concrete or oxide materials) on a first layer helps to cool the corium and to keep it liquid over a wider temperature range, so that it spreads efficiently. The use of non-limestone aggregate concrete (so called basaltic concrete) minimizes further production of carbon-based non-condensable gases, such as CO and CO_2, which could contribute to eventual containment failure.

The basic idea of in-vessel retention of corium is to prevent RPV melt-through by flooding the reactor cavity and transferring the decay heat from the corium on the lower head of the RPV to the water surrounding the vessel [10]. This heat transfer must be efficient so that the RPV wall maintains its structural properties and is able to support the mechanical load that results from the weight of the corium and the lower head and from possible pressure inside the vessel. The RPV thus maintains its function as a barrier against the release of fission products. An obvious advantage of this type of corium retention scheme is the fact that all ex-vessel phenomena are avoided, such as direct containment heating, corium-concrete interactions, and eventual steam explosions [9]. The first structure of this type was approved by the Finnish Radiation and Nuclear Safety Authority (STUK) for the Loviisa plant, equipped with Russian VVER-440 reactors [11].

22.3 ECONOMIC FEATURES OF GENERATION III/III+ FISSION REACTORS

Fission reactors are excellent base load generators because the cost of the electricity they produce is essentially fixed during the lifetime of the plant. Investment costs represent about 59% of the total cost of electricity, while operation and maintenance represent 26% and fuel costs represent 15% of the total [12]. These three main contributors to the total cost are fairly stable, thus pointing in the direction of essentially fixed production costs. In a very competitive energy market, it is important to improve construction and exploitation issues that have an economic impact, namely standardization, lifetime of the plant and its availability, and increased use of the fuel.

Most nuclear power plants built in the past were one of a kind. The concept of standardized design entered this field only toward the end of Generation II, but it is firmly established in Gen III/III+ designs. Standardization has a direct impact on reducing licensing time, construction time, and capital costs, as well as exploitation costs. Currently, the NRC approves a nuclear power plant design (the so-called Design Certification"), independent of an application to construct or operate it. By issuing a Combined Operating License (COL), the NRC then authorizes a given licensee to construct and operate a nuclear power plant at a specific site, with specified conditions, in accordance with established laws and regulations. In this way, the utilities benefit from the previous certification of a given standard reactor design [13]. Several other regulatory authorities follow similar procedures. As an example of another impact of standardization, a systematic decrease (from 75 to 61 months) was observed of the time from start of civil works to connection to the grid of French REP-900 reactors (PWR, 900 MW_e), as construction of this series progressed [14].

Plant lifetime is ultimately limited by the lifetime of the RPV, which is normally the only component that is not replaceable. As a result of the irradiation with fast neutrons released from the fuel, the RPV steel can become more brittle (reduced ductility and fracture toughness) in certain areas [15]. The important factors governing radiation embrittlement of the RPV are the sensitivity of the steel to embrittlement, the neutron fluence and energy spectrum, and the irradiation temperature [16]. The major contributors to the sensitivity to embrittlement (i.e., copper and phosphorus impurities, as well as high nickel content) were revealed in the early 1970s, and the specifications of the steels were correspondingly updated [17]. The neutron emission may be reduced to some extent all around the core or just at the "hot spots" by tailored core-loading patterns. Other measures to decrease the neutron irradiation of the RPV are the implementation of a larger water gap between the core and the inner wall of the vessel or the use of a neutron reflector [18]. The neutron reflector has the added advantage that it increases the neutron fraction that is available to take part in the chain reaction and can thus improve fuel utilization. Studies carried out in several countries have indicated that the RPV of current reactors can remain in safe operation for a period of at least 50 to 60 years for most designs [19]. Gen III/III+ reactors take full advantage of this accumulated knowledge in order to have a vessel lifetime of 60 years already from design, keeping the fast neutron fluence well below 10^{19} n/cm^2.

The availability of the plants should, naturally, be as high as possible. This is achieved, namely, through a reduction in the number of unplanned outages, an increase in the maintenance that can be done with the reactor running, a reduction in the time needed to refuel the reactor, and an increase in the time between successive refueling operations. Gen III/III+ designs feature refueling intervals up to 24 months, while the typical value for previous generations is 12 months. In 2008, 16 reactors achieved an energy availability factor of 100% (this indicator is defined as the ratio between the net electrical energy supplied by the reactor and the one that would have been supplied for a continuous operation at the reference unit power, during a given period). From these 16 reactors, 12 were in the United States, two in Japan, one in Korea, and one in Taiwan [20]. High availability values are not an exclusive of countries with a large infrastructure: The only plant in Slovenia, Krsko, achieved an energy availability factor of 98.6% in 2008, with an average energy availability factor of 95.2% from 2004 to 2008 [20].

Figure 22.3 shows the worldwide evolution of the median value of the energy availability factor in the last three decades, using values from the PRIS database [21] of the IAEA, compared with the expected value for Gen III/III+ reactors. The median availability factor has increased significantly in this period, from 74% to 86%. The best quartile also increased significantly from 83% to 92%. All Gen III/III+ designs have a planned availability factor above 90%, averaged over the lifetime of the plant.

Fuel burnup should, in principle, be as high as feasible.

Figure 22.4 shows the evolution of average fuel burnup achieved worldwide for both BWR and PWR reactors in the last three decades, using data from Watteau and co-authors [22], compared with the expected values for Gen III/III+ reactors. Although burnup values have increased significantly in this period, recent studies show that there

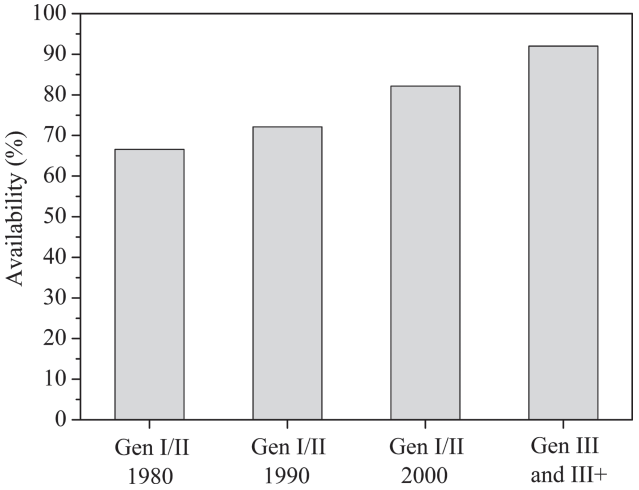

Figure 22.3 Evolution of the energy availability of reactors in the last three decades and expected value for Gen III/III+ reactors. The values for current reactors were obtained from the PRIS database [21], maintained by the International Atomic Energy Agency.

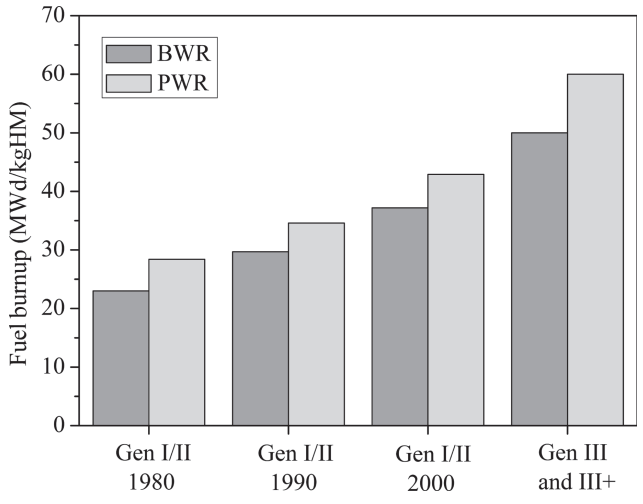

Figure 22.4 Evolution of fuel burnup for BWR and PWR reactors in the last three decades and expected values for Gen III/III+ reactors. The values for current reactors were obtained from Watteau and co-authors [22].

is little economic gain in increasing the burnup above 60 MWd/kgHM with the current fuel cycles [23], even if this would be technically feasible. A significant number of Gen III/III+ designs are expected to approach this burnup value; further improvements are only expected with Generation IV reactors, using different fuels and fuel cycles [24].

Table 22.2 presents a set of general characteristics of Gen III/III+ reactor designs. Details and references on the values for the different designs are given in the text below.

22.4 GENERATION III/III+ PRESSURIZED WATER REACTORS

PWRs have their origins in the technology developed for the nuclear submarine program of the U.S. Navy [25, 26]. The U.S. Atomic Energy Commission sponsored the development of the 90 MW_e Shippingport PWR, completed in 1957, while the first commercial PWR, Yankee Rowe (167 MW_e), was completed in 1960. The first Russian PWR started operating in 1964; it was a VVER-210 prototype (Novovoronezh-1), with 210 MW_e power. It was followed in 1969 by a 365 MW_e unit, a VVER-365 prototype (Novovoronezh-2) [27, 28].

PWR is the most popular design, with 264 units out of a total of 438 units in operation at the end of 2008, having provided nearly two-thirds of the integrated power throughout the world in that year [29]. The reference fuel for PWR is UO_2 in pellet form, enriched in the isotope U235, and protected from the coolant by stainless steel or a modified zirconium-tin alloy that became known as Zircaloy. The enrichment varies from about 2% to 4%, or more, depending on the burnup objective. A typical fuel assembly consists of a 17×17 array of fuel rods of about 1 cm diameter. The coolant flows in an open lattice structure that permits some flow mixing and is under sufficient pressure that no boiling occurs under normal operation [30].

The core of a PWR contains typically 190–240 fuel assemblies with 90,000–125,000 kg of UO_2, has overall approximate dimensions of 3.5 m in diameter by 3.5 to 4.0 m height, and is located inside the RPV. The coolant typically enters the RPV near the top, flows downward between the RPV inner wall and the core, is distributed at the lower core plate, flows upward through the core, and exits at the top of the RPV. The coolant, which is pressurized to about 15 MPa, typically enters the vessel with a temperature of about 290°C and exits at about 325°C. The coolant is pumped to the steam generator, where the heat is transferred to a secondary loop through several U-shaped tubes. The dry steam produced in the steam generator flows to a turbine-generator where it is expanded to convert thermal energy into mechanical energy and hence electrical energy. The expanded steam exhausts to a condenser where the latent heat of vaporization is transferred to the cooling system and the steam is condensed. The condensate is pumped back to the steam generator to continue the cycle [31].

22.4.1 AES-92

The AES-92 is an advanced PWR of Russian design with 1000 MW_e net electric output (1068 MW_e gross electric output), also designated NPP-92 or V-392 [32, 33]. The AES-92 is based on the well-known VVER-1000 (from "Vodo-Vodyanoi Energetichesky Reactor," literally translated as "Water-Water Energetic Reactor"), of which there are 10 operating units in Russia (Balakovo-1 to 4, Kalinin-1 to 3, Novovoronezh-5, Rostov 1 and 2) [34], 13 in the Ukraine (Khmelnitski-1 and 2, Rovno-3 and 4, South Ukraine-1 to 3, Zaporozhe-1 to 6) [35], two in the Czech Republic (Temelin-1 and 2), two in Bulgaria (Kozloduy-5 and 6) and two in China (Tianwan-1 and 2). A review of improvements made to VVER reactors based on the accumulated operating experience was recently made by Dragunov and Denisov [36].

The AES-92 uses a combination of active and passive safety systems. Its reactor coolant system is shown in Figure 22.5.

It consists of four circulating loops and a pressurizing system connected to the reactor with each loop containing a horizontal steam generator, a main circulating pump, and an accumulator as a passive part of the emergency core cooling system [37]. Each accumulator stores 50 m^3 of borated water, which is automatically injected if

TABLE 22.2 General Characteristics of Selected Gen III/III+ Reactor Designs. The values are detailed and referenced in the text

Parameter	Design[a]								
	ABWR	ACR-1000	AES-92 (V-392)	AP1000	APR-1400	APWR (US)	EPR	ESBWR	SWR-1000
Type[b]	BWR	PHWR	PWR	PWR	PWR	PWR	PWR	BWR	BWR
Thermal output (MW)	3926	3180	3000	3415	4000	4451	4300	4500	3370
Gross electric output (MW_e)	1356	1165	1068	1200	1450	1700	1720	1600	1290
Gross efficiency (%)	34.5	36.6	35.6	35.1	36.3	38.2	40.0	35.6	38.3
Net electric output (MW_e)	1315	1085	1000	1117	1390	1600	1600	1535	1250
Net efficiency (%)	33.5	34.1	33.3	32.7	34.8	35.9	37.2	34.1	37.1
Construction time (months)	44	42	59[c]	36–48	48–55	60	42	42	48
Average fuel cycle (months)	24 (max)	36[d]	12	18	18	24 (max)	18	24 (max)	24 (max)
Availability (%)	87	90	85	93	90	95	92	92	94.5
Core damage frequency (per reactor-year)	1.6×10^{-7}	$<8 \times 10^{-7}$	10^{-7}	5.1×10^{-7}	2.7×10^{-6}	1.2×10^{-6}	6.1×10^{-7}	6.2×10^{-8}	8.4×10^{-8}
Average fuel burn-up (MWd/kgHM)	45	20	43	53	60 (max)	49	45	42	65 (max)
Lifetime (years)	60	60	40	60	60	60	60	60	60

[a] ACR-1000 is a registered trademark of Atomic Energy of Canada Limited; AP1000 is a trademark of Westinghouse Electric Company, LLC; APR1400 is a trademark of Korea Hydro & Nuclear Power Company; EPR and SWR-1000 are trademarks of the Areva Group.

[b] BWR = Boiling Water Reactor; PHWR = Pressurized Heavy Water Reactor; PWR = Pressurized Water Reactor.

[c] AES-92/V-466B.

[d] Operational cycle, as refueling is done online.

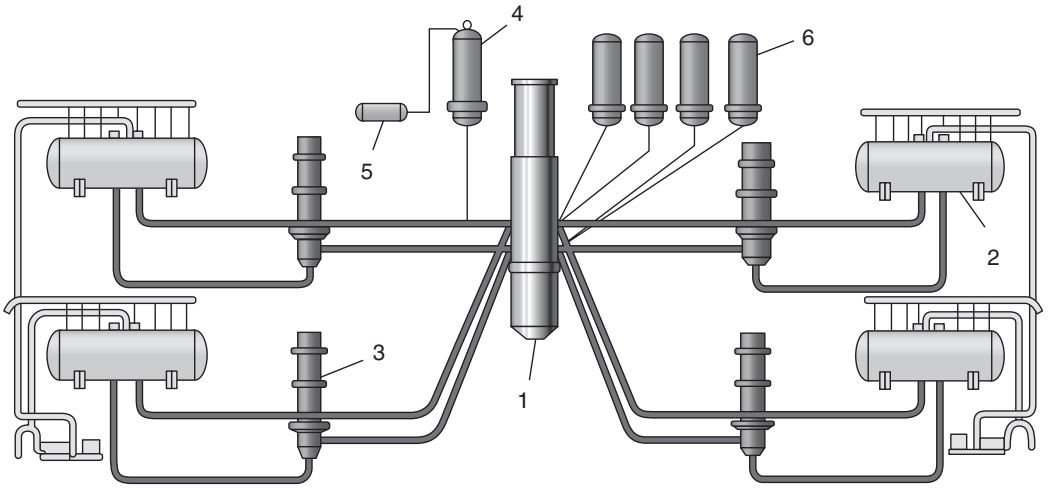

1. Reactor, 2. Steam generator, 3. Main coolant pump,
4. Pressurizer, 5. Pressurizer relief tank, 6. Accumulator

Figure 22.5 Reactor coolant system of the AES-92 design, showing its characteristic horizontal steam generators. Reproduced from Agrawal and co-authors [37] by permission of Elsevier.

the primary circuit pressure falls during a Loss of Coolant Accident (LOCA). An ex-vessel core catcher is provided as mitigation measure, similar to the one of the previous AES-91 design installed in China [38]. The sacrificial material contains gadolinium oxide, a neutron absorber, in its composition so that the molten mass will remain subcritical.

The compliance assessment of the AES-92 with the European Utilities Requirements (EUR) was successfully completed in June 2006 [39]. Two AES-92 units, in the V-412 variant, are currently being built in India (Kudankulam-1 and 2) and are expected to enter commercial exploitation in 2011 [40]. Additionally, two AES-92 units (variant V-466B) will be built in Bulgaria (Belene-1 and 2) [41, 42]. The V-466B design has a planned lifetime of 60 years, while the other AES-92 variants were planned for 40 years. The construction time of the V-466B is given as 59 months [42]. The calculated CDF for the AES-92 in India is 10^{-7} events per reactor-year [37].

Gidropress (Russia) also developed the AES-2006 (sometimes designated VVER-1200), a Gen III+ design with a thermal output of 3200–3300 MW and net electric output of approximately 1200 MW_e. The inner vessel diameter of the AES-2006 will be 10 cm larger than the one of the AES-92 to decrease the neutron fluence in the RPV [43]. Compared with the AES-92 (V-392), the AES-2006 (V-392M) will have a lifetime increased from 40 to 60 years, availability increased from 85% to 90%, and average burnup increased from 43 to at least 50 MWd/kgHM [43, 44]. The first AES-2006 is planned for the Novovoronezh II plant in Russia in 2012 [34]. Russia signed an agreement with India in early 2010 that includes eight new VVER reactors of the AES-92 or AES-2006 designs [40].

22.4.2 AP1000

Westinghouse (US) has a new series of Advanced Passive PWRs, available in two models—the AP600 with 600 MW_e net electric output (619 MW_e gross), and the AP1000 at 1117 MW_e net electric output (1200 MW_e gross) [45, 46]. The AP600 is a Gen III design approved by the NRC in 1998, but no units were built. The AP1000 is a Gen III+ design, based on the AP600, with higher power. For both, the reactor vessel is the same as that for a standard Westinghouse three-loop plant, with nozzles adjusted to accommodate the two loops of the new designs. The internals are also standard, with minor modifications.

The safety systems for both AP600 and AP1000 include passive safety injection, passive residual heat removal, and passive containment cooling. The passive safety systems are significantly simpler than conventional PWR safety systems. They have typically three times fewer remote valves than active systems, and they contain no pumps. This type of design is less expensive to build than a conventional PWR due to a significant reduction in the number of pipes, wires, valves, and associated components.

Figure 22.6 illustrates the action of the Passive Containment Cooling System (PCCS) of the AP1000. The PCCS effectively cools the containment following an accident so that the pressure is rapidly reduced, and the design pressure is not exceeded. The steel containment vessel provides the heat transfer surface that removes heat from inside the containment and rejects it to the atmosphere. Heat is

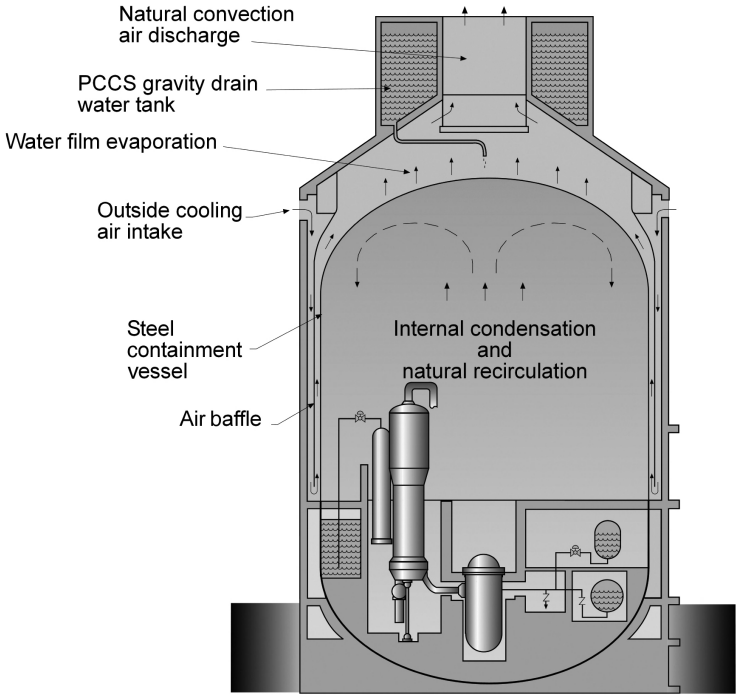

Figure 22.6 Passive containment cooling system of the AP1000. Courtesy of the Westinghouse Electric Company LLC.

removed from the containment vessel by continuous natural circulation of air. During an accident, the air cooling is supplemented by evaporation of water, which drains by gravity from a tank on top of the containment shield building. The positioning of this tank and the central chimney give the reactor building of the AP1000 an outer appearance different from the classical dome shape. In the event of a core melt, the operator can flood the reactor cavity space immediately, surrounding the reactor vessel with water to submerge the reactor vessel; this cooling is sufficient to prevent molten core debris in the lower head from melting the steel vessel wall and spilling into the containment. The CDF of the AP1000 is 3.0×10^{-7} events per reactor-year for initiating events occurring during power operation, and 2.1×10^{-7} events per reactor-year while shutdown; in both cases the CDF values include internal events, plus fire and flood [47].

The core of the AP1000 is surrounded by a radial reflector [48]. The average and maximum burnup values for a UO_2 core are 53.2 MWd/kgHM and 57.2 MWd/kgHM, respectively [49]. The AP1000 can also use a 50% Mixed Oxide (MOX, a blend of oxides of plutonium and uranium) core without changes [49]. The expected availability for the AP1000 is better than 93% for an 18-month cycle or alternating 16-/20-month cycles, with 17 days for refueling [46].

The AP1000 has a design lifetime of 60 years based on the service life of the RPV. All other components of the primary system can be replaced. The target construction time for the AP1000 is 36–48 months, taking advantage of modular construction [50].

The AP1000 was the first Gen III+ design certified by the NRC in December 2005 [51]. It successfully passed all steps of the analysis of compliance with the EUR in June 2006 [39], as well as Step 3 of the Generic Design Assessment in the UK in November 2009 [52], and Phase 1 of the Pre-Project Design Review by the Canadian Nuclear Safety Commission (CNSC) in January 2010 [53]. The construction of the four AP1000 units in China started in 2009 (Sanmen-1 and 2, Haiyang-1 and 2) [54]. As of September 2010, the NRC had received COL requests for the construction of 14 AP1000 units in the United States [55].

The Simplified Pressurized Water Reactor (SPWR) is a Japanese project based on the AP600, with an electric output in the range of 1000–1200 MW_e [56]. The European Passive Plant (EP1000) is a 1000 MW_e extrapolation of the AP600 design with three loops [57], developed by Westinghouse and GENESI (a consortium formed by Ansaldo and Fiat). It successfully passed all steps of the analysis of compliance with the EUR in December 1999 [39].

22.4.3 APR1400

The System 80+ reactor is a Gen III design of Combustion Engineering (US) and its successor owners Asea Brown

Boveri (Switzerland) and Westinghouse. It is an evolution of the three System 80 reactors built in the Palo Verde plant in the United States (1310 MW_e each). The System 80+ was certified by the NRC in May 1997 [58], but no units were built. However, it provided a basis for the South Korean Optimized Power Reactor OPR1000 and the Advanced Power Reactor APR1400 designs.

The APR1400 is a Gen III two-loop PWR with 4000 MW thermal power and 1390 MW_e net electric output (1450 MW_e gross) [59]. The refueling cycle of the core is 18 months with a maximum discharge burnup of 60 MWd/kgHM [60]. The expected availability is above 90% [61].

The APR1400 is equipped with a combination of active and passive safety measures [62] and an in-vessel corium retention system [63]. The CDF for internal initiating events was estimated at 2.3×10^{-6} events per reactor-year, and for external events it is 4.4×10^{-7} events per reactor-year, including fire- and flood-induced events [64].

The APR1400 was certified by the Korean Institute of Nuclear Energy in 2003. The construction permit for Shin-Kori-3 and 4, which are the first APR1400 plants in Korea, was issued in April 2008; commercial exploitation of these units is expected in 2013–2014 [65]. The planned construction time for the first two APR1400 units is 55 months, to be reduced to 48 months as construction of this series progresses [66]. A Korea Electric Power Corporation (KEPCO)-led consortium won a tender in the United Arab Emirates in early 2010 and will supply four APR-1400 units. The first of the four units is scheduled to begin providing electricity to the grid in 2017, with the three later units being completed by 2020 [65].

22.4.4 APWR

The Advanced Pressurized Water Reactor (APWR) was developed by Mitsubishi (Japan). It is a PWR with 4451 MW thermal output and 1538 MW_e gross electric output [67]. The version proposed for the U.S. market has a gross electric output close to 1700 MW_e (approximately 1600 MW_e net output) for the same thermal power [68]. The APWR features several design enhancements including a neutron reflector, improved efficiency, and improved safety systems. It uses a combination of passive and active safety systems [69]. The neutron reflector reduces neutron the RPV fast neutron fluence by a factor of three, as compared with a previous four-loop Japanese PWR design (which typically received a fast fluence of about 2×10^{19} n/cm^2 over 40 years) and improves the reliability of the vessel [67].

The availability factor of the APWR is expected to be 95%, with a refueling cycle of up to 24 months [67]. The average discharge burnup of the fuel is 49 MWd/kgHM [70]. The CDF for the APWR is 1.2×10^{-6} events per reactor-year (internal events, all power states) [71].

The construction of the first APWR in Japan (Tsuruga-3) is expected to start in 2012, with commercial operation scheduled for 2017 [72]. The NRC accepted in 2008 the application for design certification of the APWR and, as of September 2010, it received COL requests for the construction of two APWR units in the United States [55].

Mitsubishi is also working on a Gen III+ design, together with Areva. The ATMEA1 is a three-loop PWR, with thermal power of 3150 MW and net electric output of 1100–1150 MW_e [73]. The ATMEA1 will be equipped with three independent emergency core-cooling trains, each with capacity for complete safe shutdown and residual heat removal. The ATMEA1 will also feature an ex-vessel core catcher, similar to the one of the European Pressurized Reactor, described in the next section.

22.4.5 EPR

The European Pressurized Reactor or Evolutionary Pressurized Reactor (EPR) is a Gen III+ PWR from Areva. It is an evolution of the French N4 and German Konvoi reactors. It is one if the largest reactors available, with a thermal power of 4300 MW and net electric output of 1600 MW_e (gross 1720 MW_e) [74]. The version for the U.S. market has a slightly higher thermal power of 4590 MW [75].

The EPR has four independent cooling systems, an extra cooling and containment area in the bottom to catch the molten core if a core meltdown should occur, and a containment building that can withstand a direct crash by a large airplane [76]. An availability of 92% over its 60-year lifetime is expected [48]. A refueling cycle of 18 months was taken as reference, with the possibility to increase it up to 24 months. The EPR was designed for UO_2 fuel, but having the capacity to use MOX fuel at 50% [77]. The discharge burnup for UO_2 fuel is 45 MWd/kgHM [74].

Redundancy is achieved through four "trains" of protection, with each train able to provide 100% of the safety duty required to enable safe shutdown and post trip cooling. Additional protection comes from the physical segregation of each of the trains, located in separate buildings. This architecture allows maintenance to be done on one of the trains during plant operation, without requiring a shutdown, as there is still three-fold redundancy, thus helping to ensure a high availability [48].

The basic concept of the EPR for corium stabilization is its spreading into a large lateral compartment, followed by flooding, quenching, and cooling with water from the top, drained passively from an internal reservoir, the in-containment refueling water storage tank (IRWST). The corium is initially retained in the reactor pit and is only discharged into the spreading compartment after most of the core inventory is accumulated. This strategy has the

advantage of achieving a spatial separation of the functions to withstand the thermo-mechanical loads during RPV failure and to transfer the melt into a coolable configuration. The spatial separation leads to a simplification of the design of the retention device and preserves the freedom to replace it by an alternative solution if necessary [78].

Figure 22.7 shows a three-dimensional view of the RPV of the EPR, its corium spreading area, and the nearby IRWST.

The CDF for initiating events occurring during all power states is 6.1×10^{-7} events per reactor-year [79]. The EPR successfully passed all steps of the analysis of compliance with the EUR in December 1999 and June 2009 (revision B) [39]. The construction license of the first EPR, in Finland (Olkiluoto-3), was granted in February 2005, while the construction of the second EPR, in France (Flamanville-3), was authorized in 2007 [80]. The EPR passed Step 3 of the Generic Design Assessment in the UK in November 2009 [81]. The application for design certification by the NRC was submitted in late 2007 [82]. Besides the two EPR units under construction in Europe, there are also two more under construction in China (Taishan-1 and 2). As of September 2010, the NRC had received COL requests for the construction of four EPR in the United States [55]. The typical construction time for the EPR in the United States is given as 42 months, from first concrete pouring to fuel loading [75]. The construction of the two EPR units in Europe suffered from initial delays due to problems with concrete placement [83].

22.4.6 IRIS

The International Reactor Innovative and Secure (IRIS) is a medium-sized PWR, developed by an international consortium led by Westinghouse. Its thermal output is 1000 MW, for a net electric output of 335 MW_e [84].

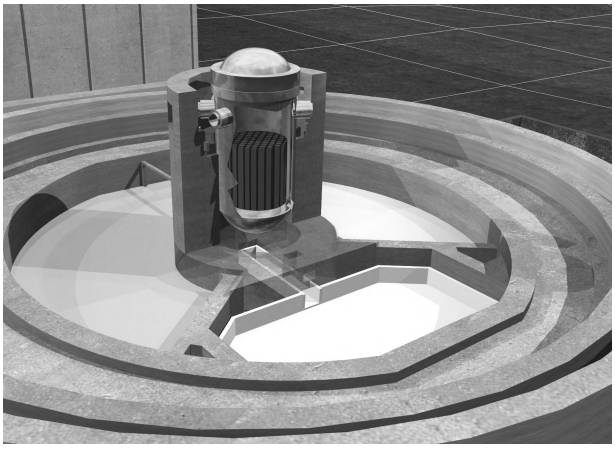

Figure 22.7 Location of the corium spreading area (rectangular zone) and in-containment refueling water storage tank relatively to the pressure vessel of the EPR. Courtesy of Teollisuuden Voima Oyj.

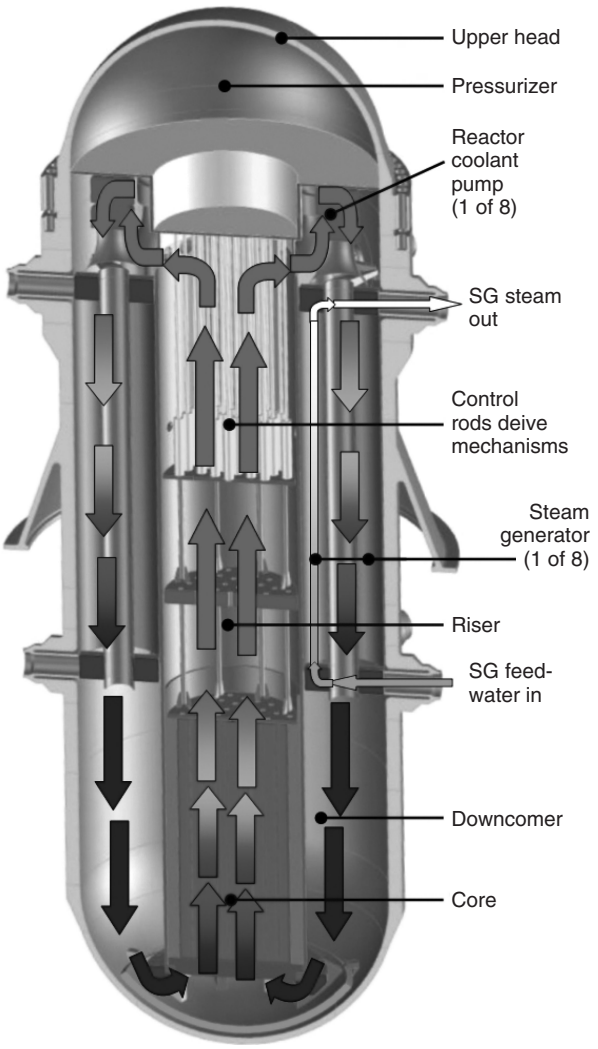

Figure 22.8 The IRIS integral primary system. Reproduced from Carelli and co-authors [86] by permission of Elsevier.

IRIS has an integral reactor coolant system layout, shown in Figure 22.8.

The RPV houses not only the fuel and control rods, but also all the major reactor coolant system components, including eight small coolant pumps, eight small helical-coil steam generators, a pressurizer located in the upper head of the vessel, the control rod drive mechanisms, and a neutron reflector in the downcomer region. Water flows upward through the core and then through the riser region (defined by the extended core barrel). At the top of the riser, the coolant is directed into the upper annular plenum where the suction of the reactor coolant pumps is located. Eight pumps are employed, and the flow of each pump is directed downward through its associated helical coil steam generator module. The flow path continues

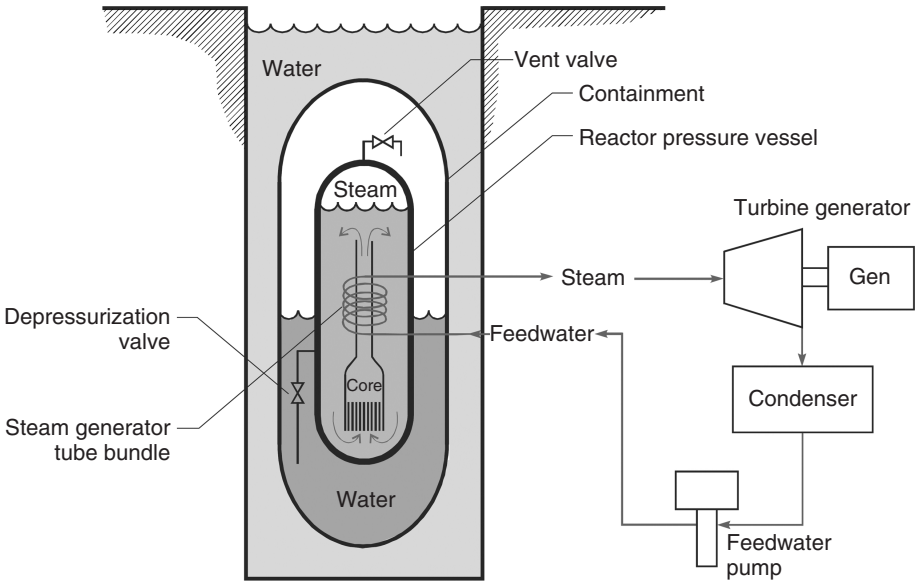

Figure 22.9 Baseline design concept of the MASLWR. Reproduced from Reyes and co-authors [94] by permission of Elsevier.

downward through the annular downcomer region outside the core to the lower plenum and then back into the core, completing the circuit [85].

The IRIS vessel has an internal diameter of 6.2 m and an overall height of 22.2 m, which makes it approximately 50% larger than the RPV of the AP1000. Nevertheless, the size of the IRIS containment is a fraction of the size of corresponding loop reactors, resulting in a significant reduction in the overall size of the plant [86].

The IRIS "safety-by-design" approach is to eliminate by design the possibility for an accident to occur, rather than dealing with its consequences. If it is not possible to eliminate the accident altogether, then the design should inherently reduce its consequences or decrease its probability of occurrence, without resorting to intervention of active or passive means. The integral configuration of this design eliminates large LOCA altogether, since the usual primary penetrations of the reactor vessel or large loop piping do not exist. The IRIS is equipped with an in-vessel core retention system [87].

The initial fuel loading is designed to provide a four-year cycle utilizing nearly standard PWR fuel with up to 5% enrichment, but with improved fuel utilization, with an average fuel burnup in the 48–53 MWd/kgHM range [86]. The core design parameters are selected so that future UO_2 and MOX reload cores with higher fissile content (and longer cycle) are feasible. An eight-year core lifetime is foreseen using UO_2 or MOX fuel with a fissile content in the 7–10% range [88].

The CDF calculated at the conceptual phase of IRIS (internal events only) is 1.2×10^{-8} events per reactor-year [89]. The design certification review of the IRIS by the NRC is expected to start in 2012 [90], and Westinghouse anticipates to be able to deploy the reactor by 2015 [86].

22.4.7 NuScale

The NuScale design of NuScale Power Inc. (US) [91] is an integral PWR, based on the Multi-Application Small Light Water Reactor (MASLWR) project developed in the United States by Nexant-Bechtel, the Oregon State University, and the Idaho National Engineering and Environmental Laboratory [92]. The MASLWR has a thermal output of 150 MW and net electric output of 35 MW_e. It is a natural circulation reactor, with the core and helical coil steam generators located in a common vessel.

There is previous experience in the use of natural circulation PWR in the military sector. The reactors powering the Rubis-class submarines of the French Navy, commissioned in the 1980s and 1990s, are based on an integral vessel arrangement and natural circulation is used up to about 30 MW power (about two-thirds of the maximum thermal power). This arrangement is one of the factors that make the Rubis-class submarines smaller than their British or U.S. counterparts [93].

Figure 22.9 shows the baseline design concept of the MASLWR [94]. The reactor vessel is surrounded by a cylindrical containment partially filled with water. The containment provides pressure suppression and liquid makeup capabilities during a LOCA. The reactor vessel can be depressurized using automatic valves discharging into various locations within containment. The containment

vessel is partially submerged in a water pool that acts as the ultimate heat sink.

The design of the NuScale is modular-based, with the provision of up to 12 modules on the same site. Each containment vessel module containing reactor and steam generator has overall dimensions of 18 m by 4.2 m and will weigh approximately 450 metric tons. The refueling cycle is 24 months long, using fuel enriched at 4.95%. An initial pre-application review meeting was held with the NRC in July 2008, and NuScale anticipates filing the design certification application in 2012 and having the first reactor connected to the grid by 2018 [95].

22.4.8 Other Designs

Babcock & Wilcox (US) is developing the mPower, a modular-based integral PWR, with 125 MW_e electric output and passive safety systems [96]. The mPower is planned for a four-and-a-half-year operating cycle between refueling, using fuel enriched to just below 5%. The reactor will be contained below ground and will have provisions to store the spent fuel underground for the 60 years lifetime of the reactor. Three big U.S. utilities, Tennessee Valley Authority, First Energy Corporation, and Oglethorpe Power Corporation, signed an agreement with Babcock & Wilcox in early 2010, committing to get the new reactor approved for commercial use in the United States.

Other integral PWR in different stages of design are the Central ARgentina de Elementos Modulares (CAREM), with thermal output of 100 MW, under development in Argentina [97], the System-integrated Modular Advanced ReacTor (SMART), with thermal output of 330 MW, under development in Korea [98], and the Integrated Modular water Reactor (IMR), with thermal output of 1000 MW, under development in Japan [99].

22.5 GEN III/III+ BOILING WATER REACTORS

BWR reactors, like PWRS, have their origins in the technology initially developed for the U.S. Navy. BWR is the second most-used design, with 94 units out of a total of 438 units in operation at the end of 2008, providing approximately 23% of the integrated power throughout the world in that year [29]. The reference fuel for BWR is also UO_2 in pellet form, enriched to 2–4%, clad in Zircaloy. A typical fuel assembly consists of an 8×8 array of fuel rods of about 1.3 cm diameter and 4 m height. The 8×8 array is surrounded by a Zircaloy fuel channel to prevent cross-flow between assemblies. A group of four assemblies constitutes a module, together with a cruciform control rod in the center. The core of a BWR contains typically 750 fuel assemblies with 140,000 to 160,000 kg of UO_2. The coolant typically enters at about 7 MPa, flows downward between the RPV inner wall and the core shroud, is distributed by the core plate, flows upward through the core and upper structure, and exits as steam at about 290°C. About 30% of the coolant flow is recirculated, which has the net effect of increasing the coolant flow rate in the core [100]. The control of a BWR is different from the one of a PWR, as the direct cycle links thermal power, pressure, and water level. Thermal power, and hence the steam flow rate, is changed either through the recirculation flow rate or by the position of the control rods. Typically, automatic load following is achieved by changing the recirculation flow above 65% power and by using the control rods below that level.

Dresden-1 was the first large-scale BWR (200 MW_e) developed by General Electric (US), which started operating in 1960. Oyster Creek was the first direct cycle BWR (650 MW_e), that started operating in 1969 and was characterized by the elimination of the steam generators and the use of five external recirculation loops. The Dresden-2 plant first featured in 1970 internal jet pumps, which improved recirculation flow so that only two external recirculation loops were needed [101].

22.5.1 ABWR

The Advanced Boiling Water Reactor (ABWR), developed by General Electric (US), Toshiba and Hitachi (Japan) [102], was the first Gen III reactor to enter commercial operation in 1996. A significant feature of the ABWR is the absence of large nozzles below the elevation of the top of the core. The ABWR has 10 internal recirculation pumps inside the RPV, replacing the external pumps of older BWR designs, together with all their piping, valves, and snubbers. The internal pumps are an improved version of a model previously used in European plants [103]. This configuration of the RPV precludes any large pipe ruptures at or below the elevation of the core and is a key factor in the ability of ABWR safety systems to keep the core completely and continuously flooded for the entire spectrum of design basis LOCA. The CDF (internal events) for the ABWR is 1.6×10^{-7} events per reactor-year [104], nearly an order of magnitude lower than General Electric's BWR/6 older design [105]. The ABWR also features a basaltic floor with passive cooling features that will terminate the flow of corium in the event of a core melt [106]. The thermal power of the Kashiwazaki-Kariwa twin units is 3926 MW, with a net electric output of 1315 MW_e [21, 107]. The ABWR availability factor is 87% or greater, with a refueling interval up to 24 months [108].

The ABWR is certified or licensed in three countries: Japan, Taiwan, and the United States. The NRC issued a final rule certifying the ABWR design in May 1997 [109]. The compliance assessment with the EUR requirements was successfully completed in December 2001 [39].

Four ABWR units are currently in operation in Japan (Kashiwazaki-Kariwa-6 and 7, Hamaoka-5 and Shika-2), two are under construction in Taiwan (Lungmen-1 and 2), and one unit is under construction in Japan (Shimane-3). The average time from start of construction to connection to the grid of the first four ABWR units built in Japan was 44 months, while the average time from start of construction to start of commercial operation was 52 months [21]. The two units in Taiwan, whose construction started in 1999, are expected to start commercial operation in 2011–2012 [110]. The unit in Japan, whose construction started in the end of 2005, is expected to start commercial operation in early 2012 [72]. Two ABWR units are slated to start operation in the United States (South Texas Project) in 2016–2017 [111]. The average energy availability factor of the first two units in Japan, over the first 10 years of operation, was 82%; this value later decreased due to extraordinary inspections after the earthquake in July 2007 [20].

22.5.2 ESBWR

In the late 1980s General Electric began a BWR design project that incorporated advanced, passive safety features. The Simplified Boiling Water Reactor was a natural circulation reactor rated at 600 MW_e [112]. This ultimately evolved into the Gen III+ Economic Simplified Boiling Water Reactor (ESBWR) design, with thermal power of 4500 MW and net electric power of 1535 MW_e (gross 1600 MW_e) [113], which took several technological features from the ABWR already in operation. Significant experience with natural circulation BWR was obtained with the 200 MW Humboldt Bay-3 reactor in the United States [114], operated from 1963 to 1976, and with the 183 MW Dodewaard reactor in the Netherlands [115], operated from 1969 to 1997.

The ESBWR has no recirculation pumps, external or internal, thereby greatly increasing design integrity and reducing overall costs. The passively safe characteristics are mainly based on isolation condensers, which are heat exchangers that take steam from the vessel or the containment, condense it, transfer the heat to a water reservoir, and introduce the water into the vessel again. All safety systems operate without using pumps, thereby further increasing design safety reliability and reducing costs. The core is made shorter than conventional BWR plants to reduce the pressure drop over the fuel and improve natural circulation [116, 117]. The ESBWR is equipped with an ex-vessel core catcher, which uses thick concrete and a passive cooling system to prevent escape of the corium from the containment [118].

The design and operation simplification contribute to a 20% operation and maintenance cost advantage [119]. The expected ESBWR availability factor is 92% or greater, with a refueling interval up to 24-months [117]. General Electric puts the construction time of the ESBWR at 42 months, using proven ABWR construction techniques [120].

The CDF of the ESBWR is currently the lowest of all Gen III/III+ designs, at 2.8×10^{-8} events per reactor-year for initiating events occurring during power operation and at 3.36×10^{-8} events per reactor-year when the plant is shut down (in both cases, the CDF values include internal events, plus fire and flood) [121].

The design certification review of the ESBWR by the NRC was started in 2005. The NRC issued a final safety evaluation report and final design approval in March 2011. Step 2 of the Generic Design Assessment in the UK was completed during 2008 [118]. As of September 2010, the NRC had received COL requests for the construction of five ESBWR units in the United States [55].

22.5.3 SWR-1000

The Siedewasserreaktor (SWR, "Boiling Water Reactor" in German) is a Gen III+ design developed by Siemens/Framatome (Areva) in a joint venture with German, Finnish, and other European utilities, which started in 1992. The SWR-1000 has a thermal output of 3370 MW and a net electric output of 1250 MW_e [122]. The safety concept of the SWR-1000 is based on a combination of passive safety systems and a reduced number of active safety systems. All postulated accidents can be controlled using passive systems alone. Nevertheless, service-proven active safety systems are still intended to operate, if possible, before passive safety equipment takes over. The functional scope and degree of redundancy of these active systems could, however, be reduced [123].

Figure 22.10 shows a comparison of the RPV of the SWR-1000 with the older design for the Kruemmel plant (1350 MW_e, Siemens Product Line 69) built in the late 1970s. The active core height of the SWR-1000 was reduced from 3.7 to 3.0 m, and, as a result, the top of the core is positioned lower inside the RPV. Since the overall height of the RPV remains the same as before and the main steam and feedwater nozzles are positioned at a higher elevation on the RPV shell, this arrangement provides a much larger water inventory above the core for accident control purposes. The volume of water above the core is such that, during post-accident reactor depressurization, no active supply of makeup coolant to the RPV is needed to maintain fuel cooling. To increase the effective water inventory even further, a chimney is provided above the core in which the steam-water mixture is routed through pipes.

The SWR-1000 is equipped with four emergency condensers for passive removal of heat from the RPV to the water of the core flooding pools, plus four core cooling condensers for passive heat removal from the containment to the water pools situated above. An eventual molten core is retained inside the RPV. The bottom of the drywell is

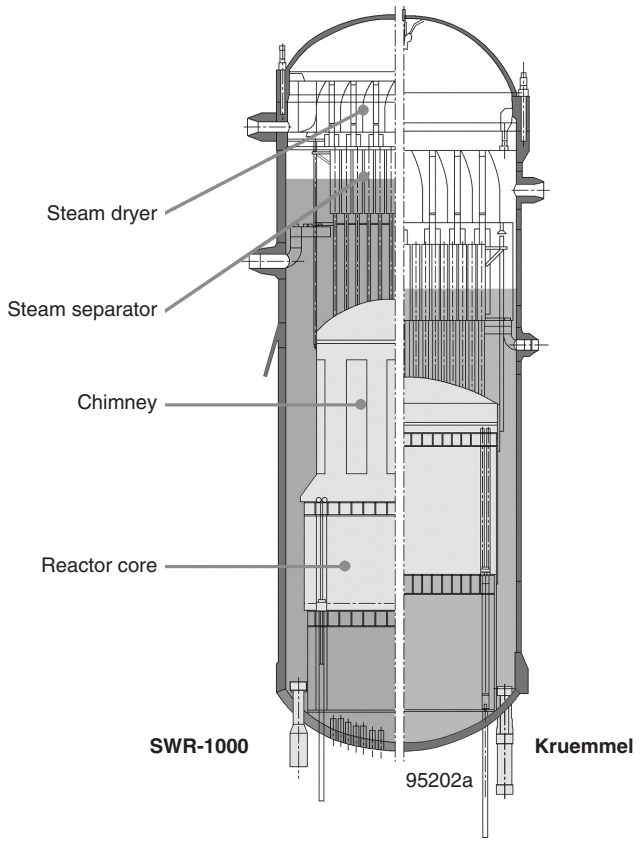

Figure 22.10 Comparison of the pressure vessel of Areva's SWR-1000 reactor with the one of the Kruemmel reactor. Reproduced from Stosic and co-authors [122] by permission of Elsevier.

flooded using water from the core flooding pools to cool the RPV [124].

The average availability for a plant lifetime of 60 years and 12 months long refueling cycle is 94.5%. The SWR-1000 can have fuel cycles up to 24 months [122].

The CDF of the SWR-1000 is one of the lowest for Gen III/III+ designs, at 4.3×10^{-8} events per reactor-year for initiating events during operation at power, and 4.1×10^{-8} events per reactor-year while shutdown [122]. A preliminary safety assessment published by STUK in 2001 confirmed that there were no safety technical obstacles for the SWR-1000 to be approved in Finland [125]. The compliance assessment with the EUR was successfully completed in February 2002 [39]. The process to start the design certification by the NRC was started in 2002 [126].

22.6 GEN III/III+ PRESSURIZED HEAVY WATER REACTORS

In the 1950s and 1960s, heavy water reactor technology was explored in several countries [127]. However, it was in Canada that this line of reactors was selected as the preferred type, which would become known as CANada Deuterium Uranium (CANDU). At the end of 2008 there were 44 PHWR units in operation worldwide, of Canadian and Indian origin, providing approximately 6% of the integrated power throughout the word in that year [29]. The main attraction for the development of PHWR is the comparative simplicity of a system that does not depend on uranium enrichment. Further simplicity was introduced with the choice of pressure tubes, rather than a pressure vessel, to contain the operating pressure. The use of natural uranium and of pressure tubes makes this technology relatively easily accessible. Fuel manufacture has been successfully developed virtually everywhere where these reactors have been built, and the dependence on very specialized large component fabricators to produce pressure vessels has been avoided [128].

The CANDU series of reactors developed by Atomic Energy of Canada Limited (AECL) is designed to use natural uranium, but it can also use low enriched uranium [129] or a variety of fuels, including fuel discharged from light water reactors [130], and thorium, in combination with uranium or plutonium [131–133]. CANDU reactors are refueled on-power, thus avoiding the need for a refueling outage typical of other designs.

The core of a CANDU reactor is contained in a cylindrical stainless steel tank (calandria) that holds the heavy water moderator at low temperatures ($<80^{\circ}$C) and low pressure (about 0.1 MPa). The ends of the cylinder are closed with two parallel end shields that are perforated with holes for the fuel channels, the holes being arranged in a square lattice pattern. Thin-walled Zircaloy tubes are fastened to each inner tube sheet and act as stays for the end shields to form a leak-tight tank. The holes in each end shield are connected with stainless steel tubes (lattice tubes). Each fuel channel (approximately 400 in total) consists of a pressure tube joined to end fittings and occupies the tubular holes or lattice sites formed by each combined lattice tube and calandria tube. The coolant enters the pressure tube at about 265°C and exits at about 310°C. Each fuel channel contains 12 bundles, resulting in a loading of about 100,000 kg of natural UO_2 [134].

The calandria is not a reactor vessel and is not subjected to the high pressures that are required in order to circulate liquid reactor coolants; its function is to hold the heavy water moderator and permit its recirculation. A RPV for a heavy water moderated reactor must be very large. Since deuterium in D_2O is twice as heavy as hydrogen in H_2O, fast neutrons lose (on average) less energy per collision in D_2O and travel greater distances before reaching thermal energies than in H_2O. The core of a D_2O-moderated reactor is thus larger than the one of a H_2O-moderated one [135]. Siemens developed two PWHR with a RPV for Argentina, Atucha-1 (operational in 1974) and Atucha-2

(started in 1981 but still unfinished). The RPV of Atucha-1 (335 MW_e) has a 6.2 m diameter, 12.2 m height, and weighs 470 metric tons, while the one of Atucha-2 (692 MW_e) has an 8.4 m diameter, 14.3 m height, and weighs 971 metric tons [136].

The use of natural uranium and the initial use of heavy water as both moderator and coolant resulted in a lower operating temperature of the coolant fluid, when compared with a light water reactor, and thus in a slightly smaller efficiency [135].

22.6.1 EC6

AECL has developed a Generation III CANDU design, the Enhanced CANDU 6 (EC6), with 750 MW_e gross electric output. The EC6 is a heavy-water moderated and heavy-water cooled pressure tube reactor, based on the latest CANDU-6 (Generation II) plants built by AECL in China (Qinshan III-1 and III-2), which were connected to the grid in 2002–2003. The target operating life for the EC6 is 60 years (while that of CANDU6 is 30–40 years), with some critical components being replaced around mid-life.

The EC6 has a projected availability factor of over 90% [137]. The lifetime energy availability factor for all CANDU-6 reactors (11 units in five countries) was 88.1% until the end of 2008 [20]. The expected overall project duration for the EC6 is 66 months, with the possibility of having a second unit in service six months later. The Qinshan III twin CANDU-6 units took 54 and 57 months from start of construction until connection to the grid [21].

The CNSC completed Phase 1 of the Pre-Project Design Review of the EC6 in March 2010 [138].

22.6.2 ACR-1000

AECL also developed a Gen III+ design, the Advanced CANDU Reactor (ACR), which uses low enriched uranium instead of natural uranium as previous models. The use of enriched uranium is expected to result in operational savings [129]. The ACR will have a small negative coolant void coefficient [139], in contrast with the earlier designs, which feature a small positive void coefficient [140].

The coolant of the ACR will be light water instead of heavy water, which will be retained only as moderator. The new design will simplify the complex system of cooling pipes running through a more compact core [141] and will use new alloys for the piping in order to guarantee a lifetime of 60 years [142]. Two versions were developed, the ACR-700 with thermal output of 1980 MW and gross electric output of 731 MW_e [143], and the ACR-1000 with thermal output of 3180 MW and gross electric output of 1165 MW_e [139].

The ACR-1000 has a planned lifetime capacity factor greater than 90% [144]. It will have a three-year operational cycle, with 21-day maintenance outage, achieved through an increase of online maintenance [144]. The fuel enrichment of the reference core is 2.4%, and the average fuel burnup is 20 MWd/kgHM [145], while for a typical CANDU-6 it is 7.5 MWd/kgHM [139]. Even if a typical PWR fuel burnup is three to six times higher than the value for a CANDU-6, this is the result of fuel enrichment, not of a higher fuel efficiency, as the uranium utilization is lower by about 25% in a CANDU-6, due to its neutron economy [146].

Figure 22.11 shows a three-dimensional view of the calandria, steam generators, and main heat transport system of the ACR-1000. The heat transport system with light water coolant is disposed in a two-loop configuration, with four steam generators, four heat transport pumps, four reactor outlet headers and four reactor inlet headers. Figure 22.11 also shows the arrangement of the pipes that connect the fuel channels (at their lower ends) to the headers (at their upper ends) on the two sides of the calandria. This configuration is similar to the one of CANDU-6 reactors. The lattice pitch of the ACR-1000 is 240 mm, while the one of a CANDU-6 is 286 mm. This makes significant differences in the calandria size. The calandria of the ACR has a diameter of 7.5 m, nearly identical to the one of a CANDU-6, but with higher power; in contrast, the one of the ACR-700, which has approximately the same power of the CANDU-6, has a diameter of only 5.2 m.

The CDF of the ACR-700 for internal initiating events during power operation is 3.4×10^{-7} events per reactor-year [147]. The corresponding values for the ACR-1000 are expected to be lower due to design improvements over the ACR-700, such as a four-quadrant configuration, more reliable emergency feed-water system, passive makeup systems, and passive containment cooling. The target CDF value for the ACR-1000 for internal events at power and shutdown, plus fire and flood, is in the range of $8 \times 10^{-8} - 8 \times 10^{-7}$ events per reactor-year [148].

In October 2004 the NRC concluded a pre-application review of the ACR-700 [80]. The CNSC started a pre-licensing of the ACR-700 in May 2003, which resulted in a report issued in April 2006 [80]. Meanwhile AECL had decided to redirect its efforts to the development of the ACR-1000. The CNSC completed Phase 2 of the Pre-Project Design Review of the ACR-1000 in 2009 and found no barriers to license the reactor [149]. The ACR-1000 design also successfully completed step 2 of the Generic Design Assessment in the UK in 2008 [148]. The first ACR-1000 is expected to be operational in Canada around 2016.

22.7 GEN III/III+ HIGH-TEMPERATURE, GAS-COOLED REACTORS

The concept of HTGR evolved from the family of gas-cooled reactors built since the 1950s. At the end of

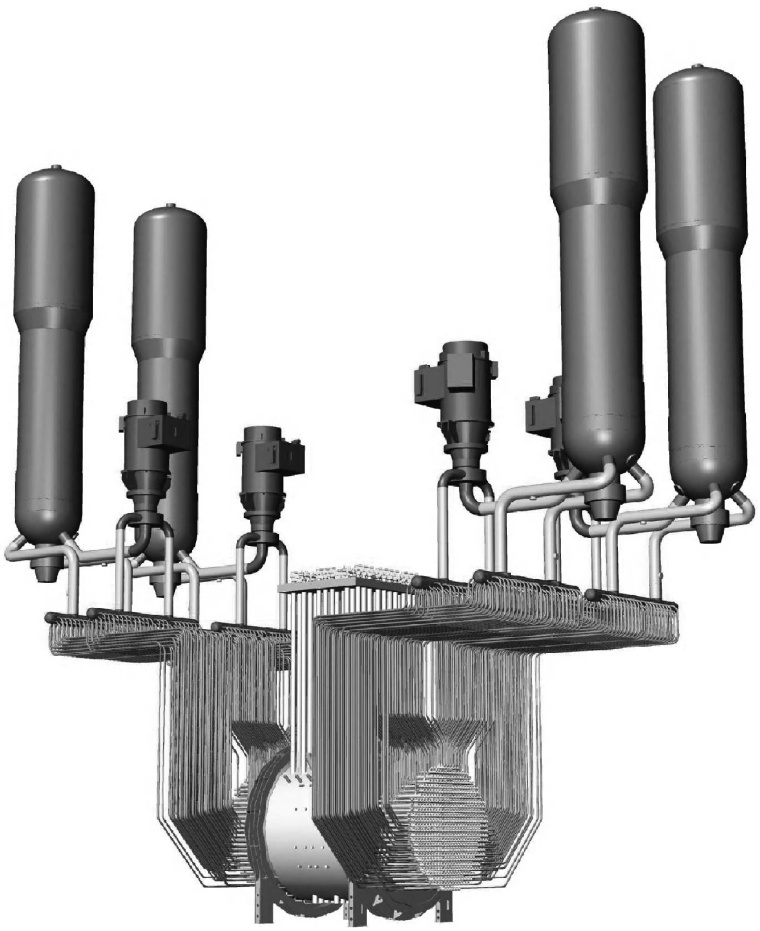

Figure 22.11 Calandria, steam generators, and main heat transport system of the ACR1000. Reproduced from Pedherney and co-authors [141] by permission of the American Society of Mechanical Engineers.

2008 there were 18 gas-cooled reactors in operation worldwide, corresponding to about 2% of the integrated power throughout the world in that year [29]. HTGRs use helium instead of air or CO_2 as the coolant, in combination with a graphite moderator, as this offers enhanced neutronic and thermal efficiencies. It also makes it possible to produce high temperature nuclear heat, and hence the name HTGR [150]. Early HTGR were the Dragon test reactor in the UK (20 MW, 1965), the Peach Bottom-1 in the United States (115 MW, 1967), and the AVR in Germany (49 MW, 1968). These were followed by the Fort St. Vrain plant [151] in the United States (842 MW, 1979) and the THTR plant in Germany (750 MW, 1985). In addition to demonstrating the use of helium coolant (with outlet temperatures as high as 950°C) and graphite moderator, these plants also demonstrated coated particle fuel, a fuel form that employs ceramic coatings for containment of fission products at high temperature.

HTGR use fuel that is significantly different from that used in current reactors: 1 mm-diameter spheres containing a kernel of fuel surrounded by three layers of carbon and one layer of silicon carbide (SiC) formed by Chemical Vapor Deposition (CVD), in a design called tri-isotropic (TRISO)-layered particles, developed in Germany within a program started in the 1960s [152].

Figure 22.12 shows a schematic view of a coated fuel particle as well as spherical and block-type fuel elements for HTGR [153]. The spherical fuel elements have a diameter of approximately 60 mm, similar to a tennis ball, while the block-type fuel hexagonal elements are 600–800 mm long by 360 mm across. In the block-type elements, the TRISO-coated particles are mixed with a carbonaceous matrix and formed into cylindrical fuel compacts, approximately 13 mm in diameter and 50 mm long [154].

Research is ongoing on the use of zirconium carbide (ZrC) in addition to or replacing SiC as coating in TRISO fuel, as some particles coated with ZrC layers have been shown to survive irradiation at higher temperatures than those with SiC [152] and can thus further improve operating margins.

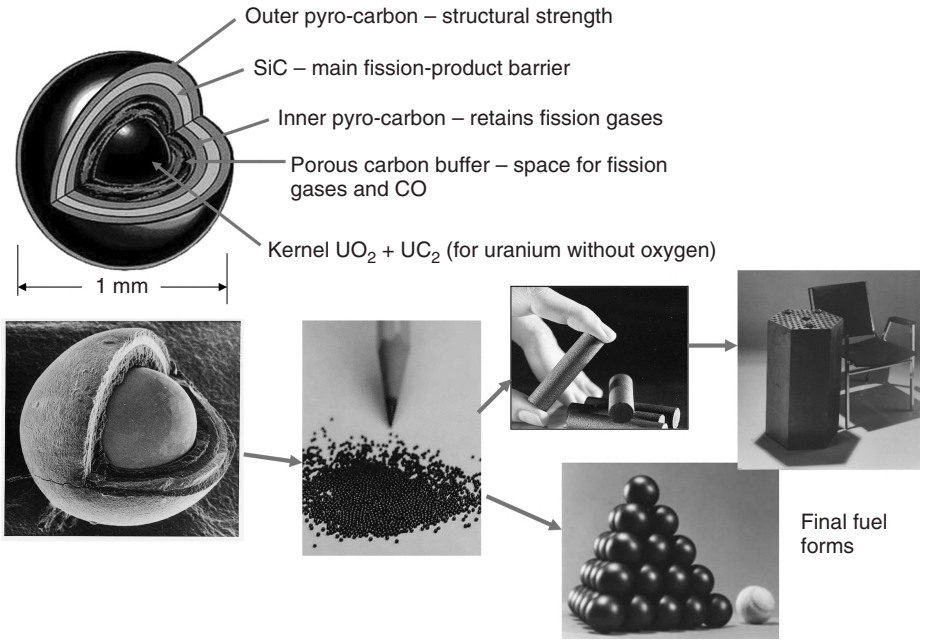

Figure 22.12 Schematic of coated fuel particle and fuel elements for high-temperature, gas-cooled reactors. Reproduced from Olander [153] by permission of Elsevier.

22.7.1 GT-MHR

General Atomics (US) and the Experimental Design Bureau of Machine Building (OKBM, Russian Federation) have jointly developed the Gas Turbine Modular Helium Reactor (GT-MHR). The overall goals are to develop the GT-MHR for the disposition of surplus weapons plutonium in Russia and then to offer GT-MHR plants fueled by uranium to the international market for electricity generation [155]. The GT-MHR will use block-type TRISO fuel elements, with the same design as the ones of the Fort St. Vrain demonstration plant built by General Atomics [151]. The standard fuel block contains about 20 million coated fuel particles; only 0.7 kg of weapons-grade plutonium is loaded per 115 kg mass of graphite fuel block. This design is expected to achieve an average burn-up of 640 MWd/kgHM [155].

The GT-MHR consists of two interconnected units, each inside a pressure vessel: the modular high-temperature reactor and the direct gas turbine cycle power conversion unit. The power conversion unit uses reactor outlet helium in a direct Brayton cycle. It consists of a gas turbine, a recuperator, a pre-cooler, low-pressure and high-pressure compressors, an intercooler, and a generator.

Figure 22.13 shows the layout of the two interconnected pressure vessels in the 1994 design by General Atomics, very close to the current, optimized design [156].

The thermal power of the GT-MHR is expected to be 600 MW, achieving a net efficiency between 46.5% and 47.5% at 850°C [156]. Other options for the power conversion unit were considered, namely Rankine and Brayton indirect cycles, but these were abandoned for the higher efficiency of the direct Brayton cycle. Although the GT-MHR could deliver helium at temperatures up to 1000°C, a temperature of 850°C was chosen for the current design as a compromise between efficiency and material limitations. Deployment of the GT-MHR is expected by 2021 [157].

22.7.2 PBMR

The Pebble Bed Modular Reactor (PBMR) is being developed by PBMR Pty (South Africa) for the utility Eskom. The founder investors of PBMR Pty are Westinghouse, Eskom, and the Industrial Development Corporation of South Africa Ltd. BNFL (UK) and Exelon (US) participated in the initial feasibility study. The PBMR reactor core takes the form of a tall annulus, 11 m high with inner and outer diameters of 2 and 3.7 m. This annular space is filled with some 450,000 fuel spheres 60 mm in diameter, each one having 9 g of enriched uranium. The fission heat is removed from the spheres by high-pressure helium driven downwards through the annular fuel bed. Spent fuel spheres are discharged and replaced with new ones while the reactor remains at power. All 450,000 spheres stay in the reactor for approximately three years, during which time they make six passes down through the core. The PBMR can achieve a fuel burnup of 93 MWd/kgHM at discharge [158].

The reactor vessel of the PBMR is large when compared with a modern PWR: the vessel of the PBMR is 28.5 m high

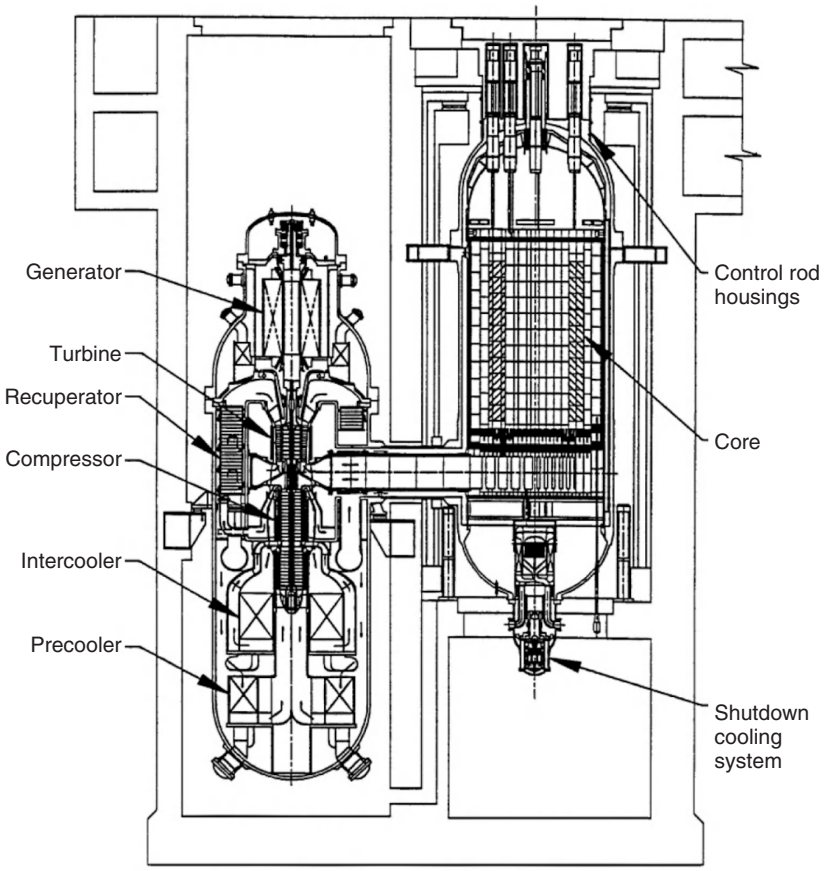

Figure 22.13 Design of the GT-MHR by General Atomics in 1994. Reproduced from Baxi and co-authors [156] by permission of C.B. Baxi (General Atomics).

and has a inner diameter of 6.2 m, or double the height (and 1.5 times the diameter) of the vessel of the AP1000 [158].

The thermal power of the PBMR was initially planned at 400 MW for a net electric output of 165 MW_e, thus achieving a net efficiency of 41% while operating at 900°C using a direct Brayton cycle. However, the thermal output was later reduced to 200 MW, the output temperature was reduced from 900°C to 750°C, and the design was changed into using a Rankine cycle in order to simplify the plant and expedite its licensing [159]. These changes would bring the net electric output of the PBMR close to 80 MW_e. The lack of experience and knowledge from predecessor plants raised several issues at the start of the licensing procedure in South Africa [160]. It was expected that the first PBMR would be operational in the Koeberg site (near Cape Town), around 2020, but the project was cancelled in late 2010.

22.7.3 Other Designs

The Japan Atomic Energy Research Institute is working on the design of a 600 MW (thermal) reactor, the Gas Turbine High Temperature Reactor (GTHTR), aimed at co-production of hydrogen [161]. This program started with the construction of the 30 MW (thermal) High Temperature Test Reactor (HTTR), which achieved first criticality in 1998, full power with a reactor outlet coolant temperature of 850°C in 2001, and full power with outlet coolant temperature of 950°C in 2004 [162].

Work on a pebble bed concept is also going on in China, which started with a test reactor, the HTR-10, with 10 MW thermal output, that went critical in 2000, and has the goal of achieving a demonstration plant, the HTR-PM, with two 250 MW thermal output units around 2013 [163].

22.8 CONCLUSIONS

Building of third-generation fission reactors began in the early 1990s and will dominate the market in the coming decades. The nuclear power industry developed a broad range of advanced designs with improved safety and more stringent safety objectives and requirements, including a significant reduction of the probability for core melt accidents. Economic aspects are only second to safety and were also considered: The new designs offer improvements

in construction and exploitation issues for increased competitiveness. Gen III/III+ designs thus positively address the main concerns of the post-Chernobyl era.

Acknowledgments

The author gratefully acknowledges Prof. Donald Olander (University of California, Berkeley, US), Dr. Karl Verfondern (Research Center Jülich, Germany), Dr. Mario Carelli (Westinghouse Electric Company, US) and Dr. Chandrakant Baxi (General Atomics, US) for making available images from their work for reproduction in this review. Teollisuuden Voima Oyj (Finland), the Westinghouse Electric Company, and General Atomics are acknowledged for their authorization to reproduce images. Mr. Jiri Mandula (International Atomic Energy Agency, Austria) is kindly acknowledged for his assistance in obtaining data from the PRIS database.

REFERENCES

1. World Nuclear Association, *Safety of Nuclear Power Reactors*. Information Paper 6, March 2011. http://www.world-nuclear.org/. Accessed March 27, 2011.
2. W. Frisch, and G. Gros, Improving the safety of future nuclear fission power plants. *Fusion Engineering and Design*, 2001, **56–57**, 83–93.
3. I. Hore-Lacy, *Nuclear Energy in the 21st Century*. World Nuclear University Press, London, 2006, pp. 64–68.
4. J.G. Marques, Evolution of nuclear fission reactors: third generation and beyond, *Energy Conversion and Management*, 2010, 51, 1774–1780.
5. World Nuclear Association, *Advanced Nuclear Power Reactors*. Information Paper 8, March 2011. http://www.world-nuclear.org/. Accessed March 27, 2011.
6. International Nuclear Safety Advisory Group, *Basic Safety Principles for Nuclear Power Plants*, 75-INSAG-3 Rev. 1, STI/PUB/1082. IAEA, Vienna, 1999, 11–12.
7. W.F. Werner, M. Hirano, S. Kondo, G. Johanson, J.M. Lanore, J.A. Murphy, and U. Schmocker, Results and insights from level-1 probabilistic safety assessments for nuclear power plants in France, Germany, Sweden, Switzerland and the United States. *Reliability Engineering and System Safety*, 1995, **48**, 165–179.
8. International Atomic Energy Agency, *Status of Advanced Light Water Reactor Designs 2004*, TECDOC-1391. IAEA, Vienna, 2004.
9. B.R. Sehgal, Stabilization and termination of severe accidents in LWRs. *Nuclear Engineering and Design*, 2006, **236**, 1941–1952.
10. J.M. Seiler, B. Tourniaire, F. Defoort, and K. Froment, Consequences of material effects on in-vessel retention, *Nuclear Engineering and Design*, 2007, **237**, 1752–1758.
11. O. Kymäläinen, H. Tuomisto, and T.G. Theofanous, In-vessel retention of corium at the Loviisa plant. *Nuclear Engineering and Design*, 1997, **169**, 109–130.
12. L. Echávarri, *Energy for the 21st Century: The Potential for Nuclear Power*. IAEA Scientific Forum at the General Conference 2007. Vienna, Austria, September 2007.
13. Nuclear Energy Institute, *Licensing New Nuclear Power Plants Fact Sheet*. NEI, Washington, October 2010. http://www.nei.org/. Accessed March 27, 2011.
14. E. Bertel and G. Naudet, *L'Économie de L'Énergie Nucléaire*, EDP Sciences, Les Ulis, 2004.
15. T.L. Dickson and S.N.M. Malik, An updated probabilistic fracture mechanics methodology for application to pressurized thermal shock. *International Journal of Pressure Vessels and Piping*, 2001, **78**, 155–163.
16. M.T. Simnad, Nuclear reactor materials and fuels, in *Encyclopedia of Physical Science and Technology*, Third Edition, R.A. Meyers (Ed.), Academic Press, 2001, pp. 775–815.
17. C. Leitz and, J. Koban, Development of reactor pressure vessel design, neutron fluence calculation, and material specification to Minimize Irradiation Effects, in *Radiation Embrittlement of Nuclear Reactor Pressure Vessel Steels - An International Review*, ASTM STP 1011, Third Volume, Steele LE (Ed.), American Society for Testing and Materials, Philadelphia, 1989, 130–144.
18. Jendrich U, Tricot N, Neutron Fluence at the Reactor Pressure Vessel Wall—a Comparison of French and German Procedures and Strategies in PWRs, Eurosafe Forum, Berlin, November 2002. http://www.eurosafe-forum.org. Accessed March 27, 2011.
19. Nuclear Energy Agency, *Nuclear Power Plant Life Management and Longer-term Operation*, NEA, Paris, 2006. ISBN 92-64-02924-9.
20. International Atomic Energy Agency, *Operating Experience with Nuclear Power Stations in Member States in 2008*, IAEA, Vienna, 2009, 656–657. ISBN 978-92-0-159909-4.
21. International Atomic Energy Agency, *Power Reactor Information System (PRIS)*, http://www.iaea.org/programmes/a2/. Accessed March 27, 2011.
22. M. Watteau, B. Estève, R. Güldner, R. Hoffman, and A.N.P. Framatome, ANP extended burnup Experience and views on LWR fuels, *Proceedings of the World Nuclear Association Annual Symposium*, London, 2001. http://www.world-nuclear.org/.
23. Nuclear Energy Agency, *Very High Burn-ups in Light Water Reactors*, NEA, Paris, 2006.
24. U.S. Department of Energy Research Advisory Committee and the Generation IV International Forum, *A Technology Roadmap for Generation IV Nuclear Energy Systems*, GIF-002-00, DOE and GIF, 2002. http://www.gen-4.org. Accessed March 27, 2011.
25. A.M. Weinberg, *The First Nuclear Era: The Life and Times of a Technological Fixer*. American Institute of Physics, New York, 1994.
26. R.L. Murray, *Nuclear Energy*: *An Introduction to the Concepts, Systems, and Applications of Nuclear Processes*, Sixth Edition. Butterworth-Heinemann, Burlington, MA, 2009, pp. 323–337.

27. V.P. Denisov, Y.V. Markov, V.A. Sidorenko, S.A. Skvortsov, V.V. Stekol'nikov, and L.M. Voronin, Development of atomic power plants with water-moderated, water-cooled reactors in the Soviet Union. *Atomic Energy*, 1971, **31**, 1076–1085.
28. Nuclear Energy Institute, *Source Book on Soviet-Designed Nuclear Power Plants in Russia, Ukraine, Lithuania, Armenia, the Czech Republic, the Slovak Republic, Hungary and Bulgaria*, Fifth Edition. NEI, Washington, 1997. http://www.nei.org/. Accessed March 27, 2011.
29. International Atomic Energy Agency, *Nuclear Power Reactors in the World*, Reference Data Series No. 2, 2009 Edition, IAEA, Vienna, 2009.
30. R. Schreiber, Pressurized water reactors, in *Nuclear Engineering Handbook*, K.D. Kok (Ed.). CRC Press, Boca Raton, 2009, pp. 9–82.
31. W.M. Stacey, *Nuclear Reactor Physics*, Second Edition. Wiley-VCH, Weinheim, Germany, 2007, pp. 249–250.
32. Y. Ermakov and O. Rousselot, EUR Volume 3 AES 92 Subset, European Utility Requirements Seminar 2007, Nice, 2007. http://www.europeanutilityrequirements.org/. Accessed March 27, 2011.
33. International Atomic Energy Agency, *Status of Advanced Light Water Reactor Designs 2004*, TECDOC-1391. IAEA, Vienna, 2004, 337–358. 104804-1.
34. World Nuclear Association, Nuclear Power in Russia, Information Paper 45, March 2011. http://www.world-nuclear.org/. Accessed March 27, 2011.
35. World Nuclear Association, Nuclear Power in Ukraine, Information Paper 46, February 2011. http://www.world-nuclear.org/. Accessed March 27, 2011.
36. Y.G. Dragunov and V.P. Denisov, Securing Safe Operation of VVER Reactor Systems in Nuclear Power Plants, *Atomic Energy*, 2006, **101**, 539–543.
37. S.K. Agrawal, A. Chauhan and A. Mishra, The VVERs at KudanKulam, *Nuclear Engineering and Design*, 2006, **236**, 812–835.
38. V.B. Khabensky, V.S. Granovsky, S.V. Bechta and V.V. Gusarov, Severe Accident Management Concept of the VVER-1000 and the Justification of Corium Retention in a Crucible-Type Core Catcher, *Nuclear Engineering and Technology*, 2009, **41**, 561–574.
39. P. Berbey, *Status and Near-Term Works on the EUR document—Possible Use by Third Parties*, International Conference on Opportunities and Challenges for Water Cooled Reactors in the 21st Century. IAEA-CN-164-3S01, IAEA, Vienna, 27–30 October 2009. http://www.europeanutilityrequirements.org/. Accessed March 27, 2011.
40. World Nuclear Association, *Nuclear Power in India*, Information Paper 53, March 2011. http://www.world-nuclear.org/. Accessed March 27, 2011.
41. World Nuclear Association, *Nuclear Power in Bulgaria*, Information Paper 87, March 2011. http://www.world-nuclear.org/. Accessed March 27, 2011.
42. *Belene Nuclear Power Plant General Information*, http://www.belene-npp.com. Accessed March 27, 2011.
43. Y.G. Dragunov, S.B. Ryzhov, V.P. Denisov, and V.A. Mokhov, Prospects for development of VVER-type pressurized light-water reactor installations. *Thermal Engineering*, 2007, **54**, 343–347.
44. V. Mokhov and N. Trunov, *VVER Reactors: Clean and Reliable Source of Energy in the Past and in the Future*, International Conference on Opportunities and Challenges for Water Cooled Reactors in the 21st Century, IAEA-CN-164-10KS. IAEA, Vienna, 27–30 October 2009.
45. International Atomic Energy Agency, *Status of Advanced Light Water Reactor Designs 2004*, TECDOC-1391. IAEA, Vienna, 2004, pp. 279–306.
46. T.L. Schulz, Westinghouse AP1000 advanced passive plant, *Nuclear Engineering and Design*, 2006, **236**, 1547–1557.
47. Health and Safety Executive, *Step 3 Probabilistic Safety Analysis of the Westinghouse AP1000*, November 2009. http://www.hse.gov.uk/. Accessed March 27, 2011.
48. J. Wood, *Nuclear Power*, IET, Hertfordshire, UK, 2007, pp. 151–174.
49. R.J. Fetterman, AP1000 core design with 50% MOX loading. *Annals of Nuclear Energy*, 2009, **36**, 324–330.
50. T.L. Schulz, *AP1000 Nuclear Power Plant*, IEEE Power and Energy Society General Meeting 2008, Pittsburgh, July 2008. http://www.ieee.org/. Accessed March 27, 2011.
51. Federal Register, 71 FR 4464, January 27, 2006.
52. Health and Safety Executive, *Report of the System Design and Security Review of the AP1000 Nuclear Reactor (Step 3 of the Generic Design Assessment Process)*, November 2009. http://www.hse.gov.uk/. Accessed March 27, 2011.
53. Westinghouse Electric Company, *Westinghouse AP1000 Completes Phase 1 of Canadian Pre-Project Design Review*, Press Release, February 2010. http://westinghousenuclear.mediaroom.com/. Accessed March 27, 2011.
54. World Nuclear Association, Nuclear Power in China, Information Paper 63, March 2011. http://www.world-nuclear.org/. Accessed March 27, 2011.
55. US Nuclear Regulatory Commission, *Combined License Applications for New Reactors*, NRC, Washington, September 2010. http://www.nrc.gov/reactors/new-reactors/col.html. Accessed March 27, 2011.
56. H. Tabata and M. Yoshimura, SPWR Potential Features to the Environment, *Progress in Nuclear Energy*, 2000, **37**, 59–64.
57. D. Adomaitis, G. Saiu and M. Oyarzabal, European Passive Plant Program: A Design for the 21st Century, *Nuclear Engineering and Design*, 1998, **179**, 17–29.
58. Nuclear Regulatory Commission, *Final Safety Evaluation Report Related to the Certification of the System 80+ Design*, NUREG-1462, NRC, Washington, August 1994, and Supplement No. 1, May 1997.
59. International Atomic Energy Agency, *Status of Advanced Light Water Reactor Designs 2004*, TECDOC-1391 IAEA, Vienna, 2004, pp. 254–278.
60. S.-S. Lee, S.-H. Kim, and K.-Y. Suh, The design features of the Advanced Power Reactor 1400 *Nuclear Engineering and Technology*, 2009, **41**, 995–1004.

61. D.S. Kim, *Nuclear Reactor Development in Korea: Its History and Status*, 13th International Conference on Emerging Nuclear Energy Systems, Istanbul, Turkey, June 2007. http://www.icenes2007.org/. Accessed March 27, 2011.
62. I.C. Chu, C.H. Song, B.H. Cho, and J.K. Park, Development of passive flow controlling safety injection tank for APR1400. *Nuclear Engineering and Design*, 2008, **238**, 200–206.
63. K.H. Kang, R.J. Park, S.K. Kima, K.Y. Suh, F.B. Cheung, and J.L. Remped, Simulant melt experiments on performance of the in-vessel core catcher. *Nuclear Engineering and Design*, 2007, **237**, 1803–1813.
64. S.J. Oh and Y.S. Cho, *APR1400 Design: Its Safety Features and Associated Test Program*, Proceedings Workshop on Advanced Nuclear Reactor Safety Issues and Research Needs. Paris, February 2002, NEA, Paris, 2002, pp. 131–142.
65. World Nuclear Association, *Nuclear Power in Korea*, Information Paper 81, March 2011. http://www.world-nuclear.org/. Accessed March 27, 2011.
66. Y.S. Kim, *Introduction to APR1400 Design Characteristics*, Seminar at the Finnish Nuclear Society, October 2008. http://www.ats-fns.fi/. Accessed March 27, 2011.
67. International Atomic Energy Agency, *Status of Advanced Light Water Reactor Designs 2004*, TECDOC-1391, IAEA, Vienna, 2004, pp. 116–138.
68. Mitsubishi Heavy Industries Ltd, *Design Control Document for the US-APWR*, Chapter 1, MUAP- DC001, Revision 2, October 2009, MHI, Tokyo. http://www.nrc.gov/. Accessed March 27, 2011.
69. Y. Tujikura, T. Oshibe, K. Kijima, and K. Tabuchi, Development of passive safety systems for next generation PWR in Japan, *Nuclear Engineering and Design*, 2000, **201**, 61–70.
70. Y. Nakano, T. Okubo and Y. Koma, Effect of Decontamination Factor on Core Neutronic Design of Light Water Reactors Using Recovered Uranium Reprocessed by Advanced Aqueous Method, *Journal of Nuclear Science and Technology*, 2009, **46**, 436–442.
71. Mitsubishi Heavy Industries Ltd, *Design Control Document for the US-APWR*, Chapter 19, MUAP- DC019, Revision 2, October 2009, MHI, Tokyo. http://www.nrc.gov/.
72. World Nuclear Association, Nuclear Power in Japan, Information Paper 79, February 2011. http://www.world-nuclear.org/. Accessed March 27, 2011.
73. K. Tabuchi, M. Takeda, K. Tanaka, J. Imaizumi, T. Kanagawa, Concepts and Features of ATMEA1™ as the latest 1100 MWe-class 3-Loop PWR Plant, *Mitsubishi Heavy Industries Technical Review*, 2009, **46**, 8–13.
74. Teollisuuden Voima Oyj, *Nuclear Power Plant Unit Olkiluoto 3*, TVO, Helsinki, 09/ 2008. http://www.tvo.fi. Accessed March 27, 2011.
75. Areva, *US EPR*, ANP-U-227-V2-06-ENG, Areva NP Inc, Lynchburg, February 2007. http://www.us.areva-np.com. Accessed March 27, 2011.
76. M. Fisher, The severe accident mitigation concept and the design measures for core melt retention of the European pressurized reactor. *Nuclear Engineering and Design*, 2004, **230**, 169–180.
77. G. Sengler, F. Forêt, G. Schlosser, R. Lisdat, and S. Stelletta, EPR core design. *Nuclear Engineering and Design*, 1999, **187**, 79–119.
78. D. Bittermann, U. Krugmann, and G. Azarian, EPR accident scenarios and provisions. *Nuclear Engineering and Design*, 2001, **207**, 49–57.
79. Health and Safety Executive, *New Reactor Build: EDF/AREVA EPR Step 2 PSA Assessment*, 2008. http://www.hse.gov.uk/. Accessed March 27, 2011.
80. Health and Safety Executive, *New Reactor Build GDA Step 2 Summary of Overseas Regulatory Assessments*, March 2008. http://www.hse.gov.uk/. Accessed March 27, 2011.
81. Health and Safety Executive, *Report of the System Design and Security Review of the UK EPR Nuclear Reactor (Step 3 of the Generic Design Assessment Process)*, November 2009. http://www.hse.gov.uk/. Accessed March 27, 2011.
82. Nuclear Regulatory Commission, http://www.nrc.gov/reactors/new-reactors/design-cert/epr.html. Accessed March 27, 2011.
83. Nuclear Regulatory Commission, *Construction Experience with Concrete Placement*, NRC Information Notice 2008-17, October 2008, NRC, Washington.
84. M.D. Carelli, IRIS: a global approach to nuclear power renaissance. *Nuclear News*, 2003, **46**, 10, 32–42.
85. M.D. Carelli, L.E. Conway, L. Oriani, B. Petrovic, C.V. Lombardi, M.E. Ricotti, A.C.O. Barroso, J.M. Collado, L. Cinotti, N.E. Todreas, D. Grgic, N.M. Moraes, R.D. Boroughs, H. Ninokata, D.T. Ingersoll, and F. Oriolo, The design and safety features of the IRIS reactor. *Nuclear Engineering and Design*, 2004, **230**, 151–167.
86. M.D. Carelli, The exciting journey of designing an advanced reactor. *Nuclear Engineering and Design*, 2009, **239**, 880–887.
87. International Atomic Energy Agency, *Status of Advanced Light Water Reactor Designs 2004*, TECDOC-1391, IAEA, Vienna, 2004, 581–604.
88. B. Petrovic, M.D. Carelli, E. Greenspan, H. Matsumoto, E. Padovani, F. Ganda, Innovative Features and Fuel Design Approach in the IRIS Reactor, Proceedings Second Workshop on Advanced Reactors with Innovative Fuels, Chester, October 2001, Nuclear Energy Agency, Paris, 2002, 185–192.
89. Y. Mizuno, H. Ninokata and D.J. Finnicum, Risk-Informed Design of IRIS Using a Level-1 Probabilistic Risk Assessment from its Conceptual Design Phase, *Reliability Engineering and System Safety*, 2005, **87**, 201–209.
90. Nuclear Regulatory Commission, http://www.nrc.gov/reactors/advanced/iris.html. Accessed March 27, 2011.
91. P. Lorenzini and J. Reyes, Compact and Bijou: a New Approach to Design, *Nuclear Engineering International*, October 2008, 14–18.

92. S.M. Modro, J.E. Fisher, K.D. Weaver, J.N. Reyes, J.T. Groome, P. Babka, T.M. Carlson, *Multi-Application Small Light Water Reactor Final Report*, INEEL/EXT-04-01626, INEEL, Idaho Falls, December 2003.
93. S. Zimmerman, *Submarine Technology for the 21st Century*, Second Edition. Trafford, Victoria, 2000, 26-27. ISBN 1-55-212330-8.
94. J.N. Reyes, J. Groome, B.G. Woods, E. Young, K. Abel, Y. Yao, and Y.J. Yoo, Testing of the multi-application small light water reactor (MASLWR) passive safety systems. *Nuclear Engineering and Design*, 2007, **237**, 1999–2005.
95. Nuscale Power, http://www.nuscalepower.com/. Accessed March 27, 2011.
96. Babcock & Wilcox Modular Nuclear Energy LLC, *mPower: Delivering Clean Energy to the World*, B&W, E201-1002, Lynchburg, 2010. http://www.babcock.com/. Accessed March 27, 2011.
97. M.V.I. Fukami and A. Santecchia, CAREM project: innovative small PWR. *Progress in Nuclear Energy*, 2000, **37**, 265–270.
98. M.H. Chang, S.K. Sim, and D.J. Lee, SMART behavior under over-pressurizing accident conditions. *Nuclear Engineering and Design*, 2000, **199**, 187–196.
99. K. Hibi, H. Ono, and T. Kanagawa, Integrated modular water reactor (IMR) design. *Nuclear Engineering and Design*, 2004, **230**, 253–266.
100. W.M. Stacey, *Nuclear Reactor Physics*, Second Edition. Wiley-VCH, Weinheim, Germany, 2007, pp. 250–255.
101. K. Theriault, Boiling water reactors, in *Nuclear Engineering Handbook*, K.D. Kok (Ed.). CRC Press, Boca Raton, FL, 2009, pp. 83–139.
102. A. Omoto, A. Tanabe, K. Moriya, and C.W. Dillmann, ABWR evolution program. *Nuclear Engineering and Design*, 1993, **144**, 205–211.
103. T. Saito, M. Akasaka, O. Maekawa, Y. Kanazawa, K. Matsumura, Y. Takahashi, and H. Uozumi, Design improvement of weld design of the reactor internal circulation pump motor casing to the reactor pressure vessel nozzle, *Nuclear Engineering and Design*, 1994, **153**, 11–18.
104. Nuclear Regulatory Commission, *Final Safety Evaluation Report Related to the Certification of the Advanced Boiling Water Reactor Design*, NUREG-1503, NRC, Washington, DC, 1993.
105. A.K. Nayak and R.K. Sinha, Role of passive systems in advanced reactors. *Progress in Nuclear Energy*, 2007, **49**, 486–498.
106. General Electric Hitachi, *Advanced Boiling Water Reactor Fact Sheet*, GEA-14576E, GE Hitachi, 2008. http://www.gepower.com/. Accessed March 27, 2011.
107. A. Tsuji, A. Endoh, and Y. Asada, Completion of ABWR plant—Kashiwazaki-Kariwa Nuclear Power Station Unit Nos. 6 and 7, *Hitachi Review*, 1998, 47, 157–163.
108. International Atomic Energy Agency, *Status of Advanced Light Water Reactor Designs 2004*, TECDOC-1391, IAEA, Vienna, 2004, 63–86. ISBN 92-0-104804-1.
109. Federal Register, 62 FR 25800, May 12, 1997.
110. World Nuclear Association, Nuclear Power in Taiwan, Information Paper 115, September 2010. http://http://www.world-nuclear.org/. Accessed March 27, 2011.
111. Nuclear Engineering International, EPC Contract Signed for South Texas ABWRs, February 2009. http://www.neimagazine.com/. Accessed March 27, 2011.
112. B. Wolfe and D.R. Wilkins, Future Directions in Boiling Water Reactor Design, *Nuclear Engineering and Design*, 1989, **115**, 281–288.
113. GE-Hitachi Nuclear Energy, *ESBWR Design Control Document Tier 2*, Chapter 1, 26A6642AD, Revision 4, GEH, September 2007.
114. R.H. Krieg, E.E. Hickey, J.R. Weber, and M.T. Masnik, Decommissioning of nuclear power plants, in *Encyclopedia of Energy*, Volume 4. Elsevier, 2004, pp. 409–420.
115. T.H.J.J. Van Der Hagen, D.D.B. Van Bragt, F.J. Van Der Kaa, J. Karuza, D. Killian, W.H.M. Nissen, A.J.C. Stekelenburg, and J.A.A. Wouters, Exploring the Dodewaard Type-I and Type-II stability: from start-up to shut-down, from stable to unstable. *Annals Nuclear Energy*, 1997, **24**, 659–669.
116. D. Hinds and C. Maslak, Next generation nuclear energy: the ESBWR. *Nuclear News*, 2006, **49**, 35–40.
117. International Atomic Energy Agency, *Status of Advanced Light Water Reactor Designs 2004*, TECDOC-1391. IAEA, Vienna, 2004, pp. 207–231.
118. Health and Safety Executive, *Conclusions of the Fundamental Safety Overview of the ESBWR Nuclear Reactor (Step 2 of the Generic Design Assessment Process)*, HSE-GDA/003 2008/41278, March 2008. http://www.hse.gov.uk/. Accessed March 27, 2011.
119. General Electric Hitachi, *Natural Circulation in ESBWR Fact Sheet*, GEA-14842A, GE Hitachi, 2007. http://www.gepower.com/. Accessed March 27, 2011.
120. General Electric Hitachi, *ESBWR Fact Sheet*, GEA-14429G, GE Hitachi, 2008. http://www.gepower.com/. Accessed March 27, 2011.
121. Health and Safety Executive, *New Reactor Build: GEH ESBWR Step 2 PSA Assessment*, 2008. http://www.hse.gov.uk/. Accessed March 27, 2011.
122. Z.V. Stosic, W. Brettschuh, and U. Stoll, Boiling water reactor with innovative safety concept: the Generation III+ SWR-1000. *Nuclear Engineering and Design*, 2008, **238**, 1863–1901.
123. W. Brettschuh and D. Pasler, *The Safety Concept of the SWR 1000 with Active and Passive Safety Systems, Transactions of the International Topical Meeting on Safety of Nuclear Installations (TOPSAFE 2008)*. European Nuclear Society, Brussels, 2008.
124. Areva NP GmbH, *SWR 1000: The Boiling Water Reactor with a New Safety Concept*, G-1-V4-07-ENG, Areva NP, Offenbach am Main, Germany, 2007. http://www.arena-np.com. Accessed March 27, 2011.
125. Finnish Radiation and Nuclear Safety Authority (STUK), *Preliminary Safety Assessment of the New Nuclear Power*

Plant Project, STUK, Helsinki, 2001. http://www.stuk.fi/. Accessed March 27, 2011.

126. International Atomic Energy Agency, *Status of Advanced Light Water Reactor Designs 2004*, TECDOC-1391, IAEA, Vienna, 2004, 313–335. ISBN 92-0-104804-1.
127. B. Goldschmidt, *The Atomic Complex: A Worldwide Political History of Nuclear Energy*, American Nuclear Society, La Grange Park, 1982. ISBN 0-89448-550-4.
128. A.I. Miller, J. Luxat, E.G. Price, R.B. Duffey, P.J. Fehrenbach, Heavy Water Reactors, in *Nuclear Engineering Handbook*, Kok KD (Ed.), CRC Press, Boca Raton, 2009, 141–196. ISBN 978-1-4200-5390-6.
129. D.F. Torgeson, B.A. Shalaby and S. Pang, CANDU Technology for Generation III+ and IV Reactors, *Nuclear Engineering and Design*, 2006, **236**, 1565–1572.
130. C.J. Park, K.H. Kang, H.J. Ryu, C.Y. Lee, I.H. Jung, J.S. Moon, J.H. Park, S.H. Na, K.C. Song, Irradiation Tests and Post-Irradiation Examinations of DUPIC Fuel, *Annals of Nuclear Energy*, 2008, **35**, 1805–1812.
131. E. Teller, Remarks on the thorium cycle. *Annals of Nuclear Energy*, 1978, **5**, 287–296.
132. P.G. Boczar, P.S.W. Chan, G.R. Dyck, R.J. Ellis, R.T. Jones, J.D. Sullivan, and P. Taylor, Thorium fuel-cycle studies for CANDU reactors, in *Thorium Fuel Utilization: Options and Trends*, TECDOC-1319. IAEA, Vienna, 2002, pp. 25–41.
133. S. Şähin, K. Yıldız, H.M. Şahin, N. Şahin, and A. Acır, Increased fuel burn-up in a CANDU thorium reactor using weapon grade plutonium. *Nuclear Engineering and Design*, 2006, **236**, 1778–1788.
134. W.M. Stacey, *Nuclear Reactor Physics*, Second Edition. Wiley-VCH, Weinheim, Germany, 2007, p. 257.
135. J.R. Lamarsh and A.J. Baratta, *Introduction to Nuclear Engineering*, Third Edition. Prentice Hall, Upper Saddle River, NJ, 2001, pp. 163–168.
136. H. Hantsch, K. Million, H. Zimmermann, H. Cerjak, D. Pellkofer, and J. Schmidt, Sub-arc narrow gap welding of the Atucha 2 reactor pressure vessel closure head. *Atomkernenergie*, 1983, **43**, 25–29.
137. Atomic Energy of Canada Ltd, *Enhanced CANDU 6: Continuing the Tradition of Excellence*. AECL, 2006. http://www.aecl.ca/. Accessed March 27, 2011.
138. Canadian Nuclear Safety Commission, *Status of Pre-Project Design Reviews*, http://www.cnsc-ccsn.gc.ca/. Accessed March 27, 2011.
139. Atomic Energy of Canada Ltd, *ACR-1000 Technical Summary*. AECL, 2007. http://www.aecl.ca/. Accessed March 27, 2011.
140. V.G. Snell and J.Q. Howieson, *Chernobyl—a Canadian Perspective*. AECL, 1999. http://canteach.candu.org/. Accessed March 27, 2011.
141. B. Pedherney, M. Elgohary, and J. Alizadeh, *ACR-1000 Plant Layout*, Proceedings of the 16th International Conference on Nuclear Engineering (ICONE16). ASME, New York, 2008.
142. R.L. Tapping, Materials performance in CANDU reactors: the first 30 years and the prognosis for life eExtension and new designs, *Journal of Nuclear Materials*, 2008, **383**, 1–8.
143. C. Gerardi and J. Buongiorno, Pressure-tube and calandria-tube Deformation Following a Single-Channel Blockage Event in ACR-700, *Nuclear Engineering and Design*, 2007, **237**, 943–954.
144. K. Petrunik, ACR-1000 Ready to Deliver: Evolutionary Technology, Experienced Team and Proven Track Record, *Nuclear Technology International 2008*, Sovereign Publications, London, 2008.
145. N. Popov, R. Ion, S. Yu, R. Duffey, ACR-1000: Advanced CANDU Based on Proven Safety of CANDU Reactors, Transactions of the International Topical Meeting on Safety of Nuclear Installations (TOPSAFE 2008), European Nuclear Society, Brussels, 2008. ISBN 978-92-95064-06-5.
146. B. Rouben, *CANDU Fuel-Management Course*, AECL, 2003. http://canteach.candu.org/. Accessed March 27, 2011.
147. Health and Safety Executive, *New Reactor Build: AECL ACR 1000 Step 2 PSA Assessment*, 2008. http://www.hse.gov.uk/. Accessed March 27, 2011.
148. Health and Safety Executive, *Conclusions of the Fundamental Safety Overview of the ACR-1000 Nuclear Reactor (Step 2 of the Generic Design Assessment Process)*, HSE-GDA/001 2008/41268, March 2008. http://www.hse.gov.uk/. Accessed March 27, 2011.
149. Atomic Energy of Canada Ltd, *Canadian Nuclear Regulator Finds "No Fundamental Barriers" to Licensing AECL's Advanced CANDU Reactor (ACR-1000)*, Press Release, September 2009.
150. A. Shenoy and C. Ellis, High-temperature gas cooled reactors, in *Nuclear Engineering Handbook*, K.D. Kok (Ed.). CRC Press, Boca Raton, FL, 2009, pp. 197–226.
151. A.L. Habush and A.M. Harris, 330-MW(e) Fort St.Vrain high-temperature gas-cooled reactor. *Nuclear Engineering and Design*, 1968, **7**, pp. 312–321.
152. K. Verfondern, H. Nabielek, and J.M. Kendall, Coated particle fuel for high temperature gas cooled reactors. *Nuclear Engineering and Technology*, 2007, **39**, 603–616.
153. D. Olander, Nuclear fuels—present and future. *Journal of Nuclear Materials*, 2009, **389**, 1–22.
154. M.P. LaBar, A.S. Shenoy, W.A. Simon, and E.M. Campbell, Status of the GT-MHR for electricity production, *Proceedings of the World Nuclear Association Annual Symposium*, London, 2003. http://www.world-nuclear.org/. Accessed March 27, 2011.
155. N. Kodochigov, Y. Sukharev, E. Marova, N. Ponomarev-Stepnoy, E. Glushkov, and P. Fomichenko, Neutronic features of the GT-MHR reactor. *Nuclear Engineering and Design*, 2003, **222**, 161–171.
156. C.B. Baxi, A. Shenoy, V.I. Kostin, N.G. Kodochigov, A.V. Vasyaev, S.E. Belov, and V.F. Golovko, Evaluation of alternate power conversion unit designs for the GT-MHR. *Nuclear Engineering and Design*, 2008, **238**, 2995–3001.

157. D.T. Ingersoll, Deliberately small reactors and the second nuclear era. *Progress in Nuclear Energy*, 2009, **51**, 589–603.

158. D. Matzner, The pebble bed modular reactor, in *Future Energy: Improved, Sustainable and Clean Options for our Planet*, T. Letcher (Ed.). Elsevier Science, 2006, 241–257.

159. J. Kriek, Developing a high temperature reactor for local and global Markets, Proceedings of the World Nuclear Association Annual Symposium, London, 2009. http://www.world-nuclear.org/. Accessed March 27, 2011.

160. G.A. Clapisson and A. Mysen, The First Stage of Licensing of PBMR in South Africa and Safety Issues, Proceedings Workshop on Advanced Nuclear Reactor Safety Issues and Research Needs, Paris, February 2002, NEA, Paris, 2002, 209–221.

161. X. Yan, K. Kunitomi, R. Hino, S. Shiozawa, GTHTR Design Variants for Production of Electricity, Hydrogen or Both, Proceedings of Third Information Exchange Meeting on Nuclear Production of Hydrogen, Oarai, Japan, 2005, NEA, Paris, 2006, 121–139.

162. S. Fujikawa, H. Hayashi, T. Nakazawa, K. Kawasaki, T. Iyoku, S. Nakagawa, N. Sakaba, Achievement of Reactor-Outlet Coolant Temperature of 950°C in HTTR, *Journal of Nuclear Science and Technology*, 2004, **41**, 1245–1254.

163. Z. Zhang, Z. Wu, D. Wang, Y. Xu, Y. Sun, F. Li, and J. Dong, Current status and technical description of Chinese 2×250MWth HTR-PM demonstration lant, *Nuclear Engineering and Design*, 2009, **239**, 1212–1219.

23

TOMORROW'S HOPE FOR A PEBBLE-BED NUCLEAR REACTOR

JAY LEHR

The Heartland Institute, Chicago, IL, USA

The first application for a new nuclear reactor in over 30 years was filed with the Nuclear Regulatory Commission (NRC) in 2007. By the middle of 2010, 34 applications had been filed. The NRC, which had laid off hundreds of employees over the years, has now hired 1,000 additional personnel to deal with these applications.

It is clear that a new generation of nuclear power plants is taking shape, and the emphasis is on making them ever more safe in the minds of the public. The most critical difference is that new designs are simpler and rely less on human or mechanical intervention in the case of accidents. New designs rely on gravity to supply emergency cooling water instead of pumps, and many safety features are redundant. Government estimates of new plant safety state that accidents that could damage a reactor core would occur only once in 10 million years, and even then radiation would not likely escape. And since the September 11, 2001, terrorist attack, all containment structures must be able to withstand the direct impact of a jet liner.

The Nuclear Energy Institute, the trade group for the nuclear industry, estimates that to meet U.S. power demands in 2050, 187 new nuclear power plants will be needed, considering that current plants only have a life of 60 years.

The two current technologies in primary use are pressurized water reactors (PWR) and boiling water reactors (BWR). In the pressurized water reactor, superheated water is pumped under pressure to the reactor core, which then transfers its thermal energy to a secondary system that turns a turbine to generate electricity. In a boiling water reactor, the water is injected directly into the core, creating a water-steam mixture that turns a turbine. Most plants today are pressurized systems.

An exciting new design that has yet to be built for commercial operation is the pebble-bed nuclear reactor, considered by many to be a future answer to many nuclear power problems since its conceptualization in the 1970s by Dr. Rudolf Schulten. His idea was to combine fuel, structure, containment, and a moderator into a large number of strong, small spheres. He envisioned the use of silicon-carbide-coated ceramic spheres containing sand-size particles of uranium fuel mixed with pyrolitic carbon spheres into a container where the geometry of the tightly packed tennis-ball-sized spheres would provide the ducts or piping through which the heat transfer fluid could be conducted at extremely high temperature.

As currently envisioned today, a Pebble-Bed Reactor (PBR) producing 120 MW_e might contain as many as 360,000 of these pebbles, creating a reactor core cooled by a semi-inert gas such as helium or perhaps carbon dioxide or nitrogen. Its major attraction would be a dramatically reduced need for safety features that would preclude or combat a possible meltdown. The feature inherent in this design is referred to as Doppler broadening, explained as follows.

When the nuclear fuel increases in temperature, the fuel sees a wider range of neutron speeds and is most likely to absorb fast neurons at high temperatures, which reduces the neutrons available for fission, thereby reducing the power of the reactor in what is called a negative feedback.

Nuclear Energy Encyclopedia: Science, Technology, and Applications, First Edition (Wiley Series On Energy).
Edited by Steven B. Krivit, Jay H. Lehr, and Thomas B. Kingery.

This Doppler broadening occurs around 900°C, while the ceramic-coated pebbles will not melt below 2000°C, thus allowing a higher operating temperature with no fear of a meltdown.

When helium is used as the coolant, it will directly turn low-pressure turbines without intervening losses from heat exchangers. Helium is chemically inert so it cannot be transformed into a radioactive element that would affect the energy-producing turbine.

These so-called inherent safety features preclude the necessity for redundant safety features that are the norm for other designs, thus having the potential to both reduce costs and increase safety. The use of gas as a coolant also significantly reduces the problem of a cooling liquid absorbing radioactive material in some type of accident. There also exists no conventional piping, which can become brittle over time and result in ruptures, to carry the cooling fluid. In the pebble bed, the pore channels between the pebbles act as the piping itself.

Because of its ability to operate at higher temperatures, a pebble-bed reactor can be as much as 50% more efficient than conventional nuclear power plants, which is to say it gets a great deal more energy from each pound of fuel.

Additionally, the hot exhaust from the turbine system can be used to warm buildings on the power plant campus.

The pebble-bed systems can be temperature controlled by altering the flow of gas coolant through the system in a very precise manner, allowing the system to operate in a narrow range of radioactive output. Conventional light water reactor nuclear plants control the system by inserting non-radioactive rods around the nests of radioactive rods that alter the density of radioactivity and thus its output. These systems require the plants to operate on a much wider scale that is more complicated and less efficient.

Another advantage of the pebble-bed design is that it does not have to be shut down periodically to refuel by replacing spent fuel rods with new fuel rods. In the pebble-bed design, there is always an opening at the bottom of the container through which pebbles can be removed while new pebbles are added at the top. The pebbles that are removed are tested for their radioactivity; if they are still active enough, they are transferred to the loader at the top. This virtual continuous throughput system will generally move the same pebble through the container 10 times before it is deemed ready for waste disposal.

One problem that has yet to be completely solved is the ability to maintain a constant porosity within the pebble container. Depending on the packing arrangement of the pebbles, the porosity and, ultimately, natural piping can range from 26 to 40%. This porosity must be kept constant in order to ensure against overheating in different parts of the reactor core.

As with conventional nuclear power plants, the pebble-bed reactor itself is in a container whose walls are two meters thick. The reactor is enclosed in a containment structure built to withstand the crash of any large airplane.

Perhaps the greatest benefit of the pebble-bed reactor is its modular capability. Units can be added as needed from an electrical demand standpoint as well as availability of new investment. Economies of scale can be realized, and several reactors can share control equipment. Small reactors can be mass produced, which will enable rapid safety certification and design acceptance.

While the concepts and experimental designs were first developed in Germany the research there was ended for primarily political reasons and now continues in a variety of countries around the world including South Africa, Holland, China, and the United States.

24

HYDROGEOLOGY AND NUCLEAR ENERGY

ROGER HENNING

Nuclear and Hydrogeologic Support Services, Las Vegas, NV, USA

Hydrogeology is the realm of geology that specifically deals with the occurrence, distribution, quantity, quality, and movement of ground water in the soil and rocks of the earth's crust. It also includes the transport of materials (including contaminants), as dissolved or colloidal, in the ground water. The term *geohydrology* is often used interchangeably. Because hydrogeology deals with water in a complex subsurface environment, it is a complex science.

Most nuclear fission facilities are built on the land surface over ground water. When they were built, there was no intention to discharge to the ground water, but as with any industrial operation, inadvertent or unplanned releases can occur. In addition, waste disposal facilities built at or below grade are sometimes below the water table. As such, given time, releases to the ground water and potential transport to the accessible environment by ground water is expected. International safety guides recognize that understanding and evaluating the ground-water system in relation to nuclear facilities is recommended and often required by regulation.

The general broad concerns that relate to ground water as they apply to nuclear energy include geotechnical and foundation issues for facilities, development of conceptual models to evaluate the consequences of uncertainty, characterization investigations, monitoring of ambient conditions, risk assessment, protection of public health and welfare, detection of inadvertent or unplanned releases, remediation should releases above standards occur, and system performance assessment modeling. Most governments require that operators of nuclear faculties understand the natural environment, including ground water, as well as report plant discharges and results of environmental monitoring around their operations to ensure that potential impacts are detected and reviewed.

Hydrogeology requirements and needs vary internationally based mostly upon the regulatory climate, as well as the political systems of the countries utilizing nuclear power. As an example of some of the differences, some countries separate protection of the human population and protection of non-human environment into different regulations and strategies. Some countries require, in addition to protection of public health and welfare, that facilities also take appropriate technical measures to avoid, in the event of an accidental release, any significant environmental damage, or to mitigate the extent of such consequences [1]. The methods of investigation, as well as the identification of potential source of releases to the ground water, pathways, and potential receptors, tend to be quite similar. Much of this chapter focuses on U.S. regulations because of their complexity and maturity, but many of the concepts translate to other locations with specific differences for the different facility designs, locales, and political drivers. In the United States, regulation and control of all nuclear material is covered by *The Atomic Energy Act of 1954* [2]. According to the

NOTE: This chapter discusses hydrogeology as it relates to nuclear fission and not the front end of the fuel cycle (mining, refining, and fuel fabrication) or recycling. Also not discussed are cleanup activities related to legacy weapons production and testing. In addition, CERCLA, RCRA, UMTRCA, FUSRAP, or other cleanup activities that may occur at nuclear installations are not discussed. Limited instances within European-based references of words such as programme and Organisation were translated to American English. In addition, any use of the word groundwater *was changed to the common United States usage of* ground water *except in the titles of references*.

Nuclear Energy Encyclopedia: Science, Technology, and Applications, First Edition (Wiley Series On Energy).
Edited by Steven B. Krivit, Jay H. Lehr, and Thomas B. Kingery.

Nuclear Regulatory Commission (NRC), this is

> . . . the fundamental United States law on both the civilian and the military uses of nuclear materials. It covers the laws for the development and the regulation of the uses of nuclear materials and facilities in the United States.

In addition, the *National Environmental Policy Act of 1969* (NEPA) ensures that every proposal for a major federal action significantly affecting the quality of the human environment requires a detailed statement on, among other things, the environmental impact of the proposed action and alternatives to the proposed action. Together, for nuclear installations, these laws are the basis for ground water protection [3].

Many other countries are not overly concerned about ground water protection, although most do subscribe to the International Atomic Energy Agency (IAEA) safety standards (see below). Some power plant facilities are in coastal areas with highly saline or brackish waters. For inland locations, the resource may not be potable or has already been contaminated by past activities unrelated to power generation. Future geologic disposal may be located in zones of highly saline water, or the geologic host rock unit may contain little recoverable or usable water (e.g., thick, dense clay units or very deep, poorly fractured igneous rock). In these circumstances, the safety case may be driven more by other aspects and potential pathways than by transport by ground water.

Investigations aimed at hydrogeological solutions at United States and many international sites usually include phased investigations, including development of nuclear safety design bases, identification of conceptual models consistent with available information, and comparison of results of different conceptual models to evaluate the consequences of uncertainty; evaluation of potential features, events, and processes (FEPS); site characterization investigations; refinement of conceptual models (where FEPs can be evaluated for inclusion or exclusion); system performance assessment modeling (or formal risk assessments), followed by detection monitoring, compliance monitoring; or performance confirmation monitoring, as appropriate to the facility [4]. Table 24.1 provides a summary of information needed in a conceptual model.

Figure 24.1 illustrates the progress from the initial reconnaissance study to design phases.

Performance confirmation verifies that the data used by and the predictions generated by the performance assessment are sufficiently accurate and that a facility is behaving within expected limits. This monitoring is aimed at determining whether the actual ground water within the area of the model is behaving consistently with simulations developed to represent the subsurface system. This approach is suggested especially when a site has a very long compliance period (for example, for permanent waste disposal sites), and it is unlikely that any releases would be detected during the compliance period. In these cases, the goal is to confirm that the predictions are likely and that uncertainties contained within the model are either better quantified or shown to not factor significantly. If the subsurface system is shown by monitoring and testing to behave differently than expected, then changes to the facility or modification of the conceptual model may be necessary, both of which may lead to revision of the performance assessment [4].

Detection monitoring is appropriate for facilities where there is no expectation that releases have occurred, but may occur as unplanned of inadvertent releases to the soils and ground water. Compliance monitoring can follow detection monitoring if the potential of a release is indicated or actual indicators of releases are found. Monitoring of this type is often required for regulated facilities where releases have been documented, but no action is necessary yet to protect the public. If a release to ground water is documented, assessment monitoring is often required to determine the nature and extent of the release, as well as the source [4].

Should it be determined that contamination exists and may impact receptors at some time, active or passive remediation and remediation monitoring may be suggested.

Post-closure monitoring may be required to confirm that no unexpected releases are occurring after cessation of operations, to detect any changes that may have occurred on the site after closure, and to determine that the closed facility has been left in an acceptable condition [4].

The use of a graded approach is common in the nuclear industry, and responsible regulatory agencies help to determine the level of investigation, characterization, or monitoring of a site necessary to ensure a degree of confidence needed to minimize risk and verify the performance of the system [4]. Figure 24.2 illustrates an integrated ground water monitoring strategy logic diagram. As such, each facility or installation may have very different ground water investigation, characterization, and monitoring plans, yet still meet the needs of the regulatory agencies and general public. An example of a completed probabistic risk-based assessment for a proposed repository can be found in the "Total System Performance Assessment Model/Analysis for the License Application" for Yucca Mountain [5]. At sites with higher risk of contamination, such as more complex hydrogeology or a greater amount of contamination, an elevated program is recommended [6].

In the end, the acceptance by regulators and the public depends upon the ability of the operator or licensee to demonstrate confidence in the overall safety program. An evaluation of confidence in long-term safety is based upon an evaluation of the robustness of the system concept (i.e., the extent to which the system concept favors safety and minimizes uncertainties and/or the effects of uncertainty

TABLE 24.1 Summary of Information in a Conceptual Model for Contaminant Fate and Transport in Ground Water

Contaminant Inventory	• Contaminant inventory and uncertainty in the amount, location, and concentration, nature, and history of contaminant releases • Source release information, such as container type and expected degradation rates, source control, and other proposed remedial actions
Demographic*	• Location and information on human (and perhaps ecological) receptors under current and anticipated future conditions
Geological	• Regional and site geologic settings, structures, faults, and fractures • Depositional environments and paleogeology • Lithologic facies, distribution, thickness, and transmissive features • Borehole core descriptions, geologic units, and boundaries • Geophysical data such as log and seismic data interpretations • Anthropogenic features including buried corridors and heterogeneous fill materials that control ground water flow and contaminant migration
Hydrologic & Meteorological	• Characteristics of surface water bodies, locations, depths, flow rates, and recharge and discharge analysis • Seasonal or temporal variation of surface water bodies • Precipitation distributions in time and space • Meteorological and climatic records, evapotranspiration potential
Hydrogeologic	• Characteristics of vadose zone and aquifer structures or heterogeneity, identification of preferential flow or barriers • Water content variation in vadose zone • Hydraulic gradients and the variation in temporal and spatial domain • Hydraulic properties, including the conductivity, storage, porosity, transmissivity, homogeneity, and anisotropy of these parameters • Aquifer boundary conditions • Ground-water recharge and discharge • Ground-water interaction with surface water • Quantitative description of ground-water flow field • Ground-water level trend analysis • Aquifer usage information, location and production data for water-supply wells, and estimates of future uses
Geochemical	• General geochemical conditions at the site • Chemical characterization of sources for ground water contamination • Geochemical processes that affect or are indicative of contaminant transport and fate and mineralogy • Temporal trends and variations of contaminant sources and concentrations, mobility of contaminants in each phase • Sorption information, distribution coefficients, and sorption mechanisms • Potential for mobilization of secondary contaminants contaminant attenuation processes
Biological*	• Identification of plants and animals that could facilitate contaminant transport in the near surface • Plants and animal communities that could occupy the site in the future

**Demography and biology are not integral parts of the CSM for the Integrated Ground Water Monitoring Strategy.*

Source: NRC [4].

on safety, the quality of the assessment capability, and the reliability of its application in performance assessment) [7].

With any natural system, it is neither necessary nor possible to demonstrate without any question or uncertainty that the system is fail-safe, only that the uncertainties are understood and incorporated in the process. Decision making requires only that a safety case has been compiled that gives adequate confidence to support the decision at hand, and that an efficient strategy exists to deal at future stages with any uncertainties in the description that have the potential to compromise safety [7].

24.1 IAEA INTERNATIONAL CONSENSUS NUCLEAR SAFETY STANDARDS

Over 130 states have agreed to international consensus standards of the IAEA. The IAEA states that while these standards are not legally binding, they represent an essential basis for safety; the incorporation of more detailed requirements, in accordance with national practice, may also be necessary. Moreover, there will generally be special aspects that need to be assessed on a case-by-case basis. One of the statutory functions of the IAEA is to establish

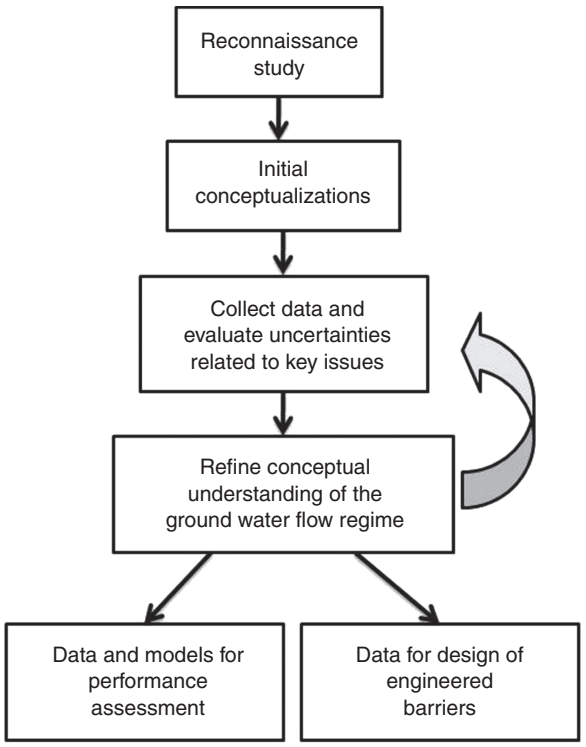

Figure 24.1 Flow diagram of hydrogeological investigations and aims. *Source*: Nuclear Waste Policy Act of 1982 [24].

or adopt standards of safety for the protection of health, life, and property in the development and application of nuclear energy for peaceful purposes. It is also to provide for the application of these standards to its own operations as well as to assisted operations and, at the request of the parties, to operations under any bilateral or multilateral arrangement, or, at the request of a state, to any of that state's activities in the field of nuclear energy.

For nuclear installation siting, the IAEA recommends in its safety guide [8] that the following site information should be evaluated specific for dispersion of radioactive material through ground water:

- A description of the ground-water hydrology of the region shall be developed, including descriptions of the main characteristics of the water-bearing formations, their interaction with surface waters, and data on the uses of ground water in the region.
- A program of hydrogeological investigations shall be carried out to permit the assessment of radionuclide movement in hydrogeological units. This program should include investigations of the migration and retention characteristics of the soils, the dilution and dispersion characteristics of the aquifers, and the physical and physicochemical properties of underground materials, mainly related to transfer mechanisms of radionuclides in ground water and their exposure pathways.
- An assessment of the potential impact of the contamination of ground water on the population shall be performed by using the data and information collected in a suitable model.

In addition, specific to ground water monitoring, the *Dispersion of Radioactive Material in Air and Water and Consideration of Population Distribution in Site Evaluation for Nuclear Power Plants* safety guide [9] states:

- A monitoring program should be established for both surface water and ground water. The purpose of such a program is to provide a baseline for site evaluation and to determine whether the hydrological characteristics of the region have altered since the site evaluation and before the commencement of plant operation.
- The monitoring program for ground water should be initiated about two years before the start of plant construction. The site area should be monitored before the foundation work is begun to verify possible changes in the ground water regime, and monitoring should be continued after construction has finished.
- Ground water is monitored by means of samples taken from boreholes and wells. The samples can

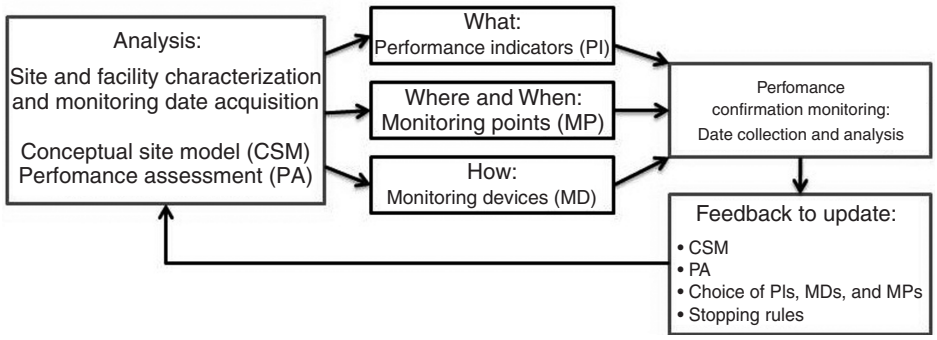

Figure 24.2 Integrated ground water monitoring strategy logic diagram. *Source*: NRC [4].

also be taken from ground water reaching the surface in springs or in natural depressions. The monitoring program should be continued throughout the lifetime of the plant. Boreholes and wells should be kept in an operable state for the same period of time.
- The monitoring program for surface water should also commence well before the start of construction of the plant and should continue for its lifetime.
- All surface water and ground water in the site region should be sampled regularly, at intervals that will depend on the half-lives of the radionuclides that could potentially be discharged.

For predisposal waste storage, the IAEA recommends in its two safety guides (one for low and intermediate and one for high level [10, 11]), the following hydrogeology related site information should be evaluated:

- Meteorology and climatology of the site and region
- Hydrology and hydrogeology of the site and region
- Geology of the site and region
- Geomorphology and topography of the site
- Terrestrial and aquatic flora and fauna of the site (in terms of their effects on the facility)

In addition, for waste sites, or plant sites where discharges have occurred or may occur near ground water resources that may be receptors to human and ecological communities, it may be necessary to investigate the relationships of the following and how they are treated in the conceptual and system performance models:

- Precipitation
- Infiltration
- Flow properties of the unsaturated (vadose) and saturated zones
- Sorption
- Advection
- Matrix diffusion
- Dispersion

24.2 U.S. NUCLEAR POWER PLANTS

When the current fleet of United States nuclear power plants was built, there was no intention to discharge to ground water. Plant design and control systems were expected to isolate the facility from the subsurface environment. As such, hydrogeological studies for those plants were mostly limited to those necessary for foundation and geotechnical needs.

With any industrial operation, inadvertent or unplanned releases can occur. At some facilities, discharges of non-radioactive materials to the subsurface environment have occurred. These may include releases from underground fuel storage systems (e.g., for emergency generators or vehicles) or discharges from construction and maintenance facilities (e.g., solvents and cleaning agents). In addition, storm water discharges from parking lots, streets, roofs, and other facility areas occur. Releases of this type are covered by other state and federal regulations where different standards may apply than for radiological releases.

The basis for environmental monitoring and effluent monitoring at nuclear power plants is 10 CFR 50 [12], General Design Criteria 60, 61, and 64 of Appendix A. The criteria require that a licensee control, monitor, perform radiological evaluations of all releases, and document and report all radiological effluents discharged into the environment. EPA environmental standards that apply to all "Uranium Fuel Cycle" activities that include power plants are covered by 10 CFR 190 [13]. There are separate standards for normal operations (§ 190.10) and variances for unusual operations (§ 190.11).

Regulations to limit offsite releases and their associated radiation doses are much more restrictive than those required for the current fleet of reactors. In 1975, in 10 CFR 50.34 and 50.36 and a new Appendix I, NRC provided numerical guides for design objectives and limiting conditions for operation to meet the radiation dose criterion "as low as is reasonably achievable (ALARA)." These regulations require that plant releases be kept to doses well below the radiation exposure limits for the public in 10 CFR 20 [14].

For liquid effluent releases, the ALARA annual offsite dose objective is 3 mrem to the whole body and 10 mrem to any organ of a maximally exposed individual who lives in close proximity to the plant boundary. This ALARA objective is 3% of the annual public radiation dose limit of 100 mrem [15].

The EPA dose-based drinking water standard is 4 mrem per year for beta emitters. For tritium, this is a maximum contaminant level of 20,000 picocuries per liter (pCi/L). If other similar beta emitters are present, in addition to tritium, the sum of the annual dose from all radionuclides shall not exceed 4 mrem per year [16]. Separate standards apply for other radioactive contaminants. For combined radium 226/228 the standard is 5 pCi/L; the gross alpha standard is15 pCi/L (not including radon and uranium); and for uranium the level is 30 μg/L [17].

The NRC requires nuclear power plants to check for the presence of radioactive materials on site property and in the environment. Licensees must:

- Keep releases of radioactive material to unrestricted areas during normal operation as low as reasonably

achievable (as described in NRC regulations provided in 10 CFR 50.36a), and
- Comply with radiation dose limits for the public (10 CFR 20 [14]).

Power plants routinely check their site and the environment for the presence of radioactive materials in extremely small concentrations. As a result of one or more of the causes listed below, radioactive materials, usually tritium, have been identified in soils or ground water at several commercial nuclear power plants:

1. System leaks (e.g., pipes, valves, tanks)
2. Evaporation of liquids
3. Condensation of vapors
4. As the result of routine, approved releases.

NRC's regulations require proper accounting of all discharges of radioactive materials. Licensees report radioactive discharges and the results of all ground-water monitoring efforts in annual reports to the NRC.

As an initial step toward standardization of approach, NEI developed a Ground Water Protection Initiative [18]. The initiative identified actions to improve utilities' management and response to instances where the inadvertent release of radioactive substances may result in low but detectible levels of plant-related materials in subsurface soils and water. Like many other waste-related investigations, the initiative identified the following for a ground water protection program:

1. Ensure that the site characterization of geology and hydrology provides an understanding of predominant ground water gradients based upon current site conditions.
2. Identify site risks based on plant design and work practices.
3. Establish an on-site ground water monitoring program to ensure timely detection of inadvertent radiological releases to ground water.
4. Establish a remediation protocol to prevent migration of licensed material off-site and to minimize decommissioning impacts.
5. Ensure that records of leaks, spills, remediation efforts are retained and retrievable to meet the requirements of 10 CFR 50.75(g) [12].

The NRC conducts reviews of renewals for existing power plants under 10 CFR 51, *Environmental Protection Regulations for Domestic Licensing and Related Regulatory Functions* [19]. This also provides guidance to prepare plant-specific SEISs to the GEIS. NUREG-1555, *Standard Review Plans for Environmental Reviews of Nuclear Power Plants Supplement 1: Operating License Renewal* is currently in the comment resolution phase [20]. The draft report provides guidance and acceptance criteria that also include hydrogeological issues.

In addition to other environmental monitoring and radiological protection items, there are specific criteria for:

- Soils and geology
- Water use and quality
- Environmental consequences and mitigating actions for hydrogeology, which includes:
  - Potential of atmospheric releases to ground water
  - Water use conflicts
  - Surface/ground water interactions (e.g. for cooling ponds, canals)
  - Ground water quality degradation
  - Ground water and soil contamination
  - Radionuclides released to the ground water

The environmental impacts of postulated accidents including mitigation are also covered.

For plants without active ground-water monitoring and analysis programs, the following general program is recommended:

1. If not yet completed, conduct geologic and hydrologic investigations to understand the hydrogeologic and physico-chemical setting of the site.
2. Evaluate the potential for detectible levels of licensed material from planned releases of liquids and/or airborne materials (e.g., rain-out and condensation).
3. Consider migration pathways should a release occur.
4. Evaluate if it is necessary to place sentinel wells closer to structures, systems, or components (SSCs) where leak detection capability is limited or that have the highest potential for releases that could reach ground water.
5. Install ground-water-monitoring wells down gradient from the plant.
6. Develop sampling and analysis plans and protocols for ground water and soil.
7. Establish a program for long-term ground-water monitoring.
8. Develop a long-term program for preventative maintenance of ground water wells
9. Periodically review of the ground-water monitoring program.
10. Develop a written procedure outlining the decision-making process for the remediation of leaks and spills or other instances of inadvertent releases.

24.3 NUCLEAR WASTE DISPOSAL

All countries in the world using nuclear power have developed interim storage facilities for either spent fuel or reprocessed waste. Almost all countries using nuclear energy have conducted in-depth studies of facilities for final storage of nuclear waste. European research done until now has proven that there are no insurmountable problems related to radioactive waste geological disposal, neither from the points of view of safety nor of feasibility.

The IAEA has stated in its technical report series, *Hydrogeological Investigation of Sites for the Geological Disposal of Radioactive Waste* [21],

> There is a far reaching international consensus that high level radioactive waste can be safely isolated in deep geological repositories using a system of engineered and natural barriers. In a normal situation the pathway having the greatest potential for transferring radionuclides to the human environment is transport by groundwater.
>
> Therefore, a good understanding of the hydrogeological characteristics of the repository site is important. The range of variation in the properties of potential sites for deep geological repositories is considerable. For example, saturation states can vary from fully saturated to unsaturated conditions. The approaches used to characterize the hydrogeological environment in the various geological media are correspondingly different. However, despite these differences there are certain hydrogeological criteria which must be fulfilled by any potential geological repository.

Such a disposal site has already been selected and approved in Finland, where construction has started. Nuclear power companies in Sweden jointly established the Swedish Nuclear Fuel and Waste Management Company (SKB), which recently has completed site selection and submitted applications to build the repository in Forsmark. There are issues that must be solved to reduce uncertainties, to increase confidence (in general, but particularly of the public and politicians) in the practical implementation of safety studies, and to prove and improve concepts and understanding of the risks involved, which are affected by very long time spans, but at extremely low probabilities [22]. In addition, radionuclides in ground water are difficult to extract using existing technologies, so prevention and performance confirmation of systems is preferred to reliance on remediation technologies.

Calculations of the transport processes that could bring radioactive waste finally back into the biosphere show that this will only happen after a time in which the nuclides have sufficiently decayed. Geological uncertainties have been considered, and calculations have been supported by measurements in experimental repositories, and in natural analogues (mines, the Oklo site in Gabon, and others) [22].

24.4 U.S. SPENT NUCLEAR FUEL (SNF), HIGH-LEVEL WASTE (HLW), AND TRANSURANIC WASTES (TRU)

The NRC was created as an independent agency by Congress in 1974 to enable the nation to safely use radioactive materials for beneficial civilian purposes while ensuring that people and the environment are protected. The EPA has the responsibility to establish general environmental standards for SNF, HLW, and TRU and to develop regulations at specific waste disposal sites (e.g., the WIPP repository and the proposed deep geologic repository). The NRC regulates all commercial reactors in the United States, including nuclear power plants that produce electricity and university research reactors. The agency regulates the possession, transportation, storage, and disposal of SNF produced by the nuclear reactors [23].

24.5 U.S. LOW-LEVEL RADIOLOGICAL WASTE

Low-level radiological waste (LLW) is defined as radioactive material that is not HLW, SNF, TRU waste, or byproduct material as defined in section 112(2) of the AEA of 1954 [2]. It is also radioactive material that the NRC, consistent with existing law, classifies as LLW [24]. LLW is comprised of a large volume of radioactive wastes produced by a variety of different processes, including the nuclear fuel cycle, medical or biotechnological research, the production of radioactive chemicals, the manufacture of commercial products, and government military operations. Radioactive waste resulting from the operations, decontamination, and decommissioning of fuel cycle facilities is also classified as LLW, which varies widely in the hazard it poses [23].

In general, all LLW facilities land disposal sites must conform to NRC requirements of 10 CFR 61 [25] (specifically § 61.53, *Environmental Monitoring*) and requirements for environmental protection set by the EPA or its designated state representative.

According to 10 CFR 61.53, *environmental monitoring* requires:

> (a) At the time a license application is submitted, the applicant shall have conducted a *preoperational monitoring program to provide basic environmental data on the disposal* site characteristics. The applicant shall obtain information about the ecology, meteorology, climate, hydrology, geology, geochemistry, and seismology of the disposal site. For those characteristics that are subject to seasonal variation, data must cover at least a twelve month period.
>
> (b) The licensee must have plans for taking corrective measures if migration of radionuclides would indicate that the performance objectives of subpart C may not be met.

(c) During the land disposal facility site construction and operation, the licensee shall maintain a monitoring program. Measurements and observations must be made and recorded to provide data to evaluate the potential health and environmental impacts during both the construction and the operation of the facility and to enable the evaluation of long-term effects and the need for mitigative measures. The monitoring system must be capable of providing early warning of releases of radionuclides from the disposal site before they leave the site boundary.

(d) After the disposal site is closed, the licensee responsible for post-operational surveillance of the disposal site shall maintain a monitoring system based on the operating history and the closure and stabilization of the disposal site. The monitoring system must be capable of providing early warning of releases of radionuclides from the disposal site before they leave the site boundary.

The EPA sets standards for low-level mixed waste under 10 CFR 266 [26]. The Low-Level Radioactive Waste Policy Amendments Act of 1985 [27] made U.S. states responsible for low-level radioactive waste disposal. It encouraged states to enter into compacts that would allow several states to dispose of waste at a joint disposal facility. Most states have entered into compacts. However, no new disposal facilities have been built.

24.6 U.S. DOE TRANSURANIC REDIOACTIVE WASTE AT WIPP

The Waste Isolation Pilot Plant, or WIPP, safely disposes of the nation's defense-related TRU. WIPP began disposal operations in March 1999 and is the DOE geologic repository for TRU wastes. It is located in the Chihuahuan Desert, outside Carlsbad, New Mexico, on 10,240 acres of land in a salt deposit 2,150 feet underground. It was developed specifically to permanently store TRU and mixed wastes that are currently being temporarily stored on federal reservations across the United States [28].

Ground water monitoring at the WIPP began in 1972 when the first site selection investigations were initiated. Several updates were included as the site characterization continued. WIPP was certified by the EPA in 1998 [28]. The portion of the law that is applicable to ground water monitoring can be found in:
Subpart B of 40 CFR § 191.14:

(b) Disposal systems shall be monitored after disposal to detect substantial and detrimental deviations from expected performance. This monitoring shall be done with techniques that do not jeopardize the isolation of the wastes and shall be conducted until there are no significant concerns to be addressed by further monitoring.

As part of certification, EPA issued required criteria as 40 CFR 194 [29]. The portions of 40 CFR 194 applicable to ground water monitoring are paraphrased below and can be found in Subpart B Compliance: Certification and Re-Certification Applications and Subpart C Compliance: Certification and Re-Certification General Requirements.

Subpart B § 194.15, Content of Compliance Re-Certification Application(s)

(a) Requires that any previous compliance application be updated to provide EPA with sufficient information to determine whether or not the WIPP continues to be in compliance with the regulations. Updated documentation shall specifically include: all additional geologic, geophysical, geochemical, hydrologic, and meteorologic information; all additional monitoring data, analyses and results; and any additional information requested by the EPA.

Subpart C § 194.42 monitoring

(a) Requires that DOE conduct an analysis of the effects of disposal system parameters on the containment of waste in the disposal system, include analysis results in any compliance application and use analysis results in developing plans for pre-closure and post-closure monitoring. The analysis shall include ground water flow, effects of human intrusion in the vicinity of the disposal system and brine quantity, flux, composition, and spatial distribution, among other parameters.

(b) Requires that DOE document and substantiate the decision not to monitor a particular disposal system parameter.

(c) Requires, to the extent practicable, that DOE conduct pre-closure monitoring of significant disposal system parameters where significance is defined as the system's ability to contain waste or the ability to verify predictions about the future performance of the disposal system. Such monitoring shall begin before waste emplacement is initiated and shall end at the time at which the shafts of the disposal system are backfilled and sealed.

(d) Requires, to the extent practicable, that DOE conduct post-closure monitoring (commencing when shaft backfilling and sealing has been completed) to detect substantial and detrimental deviations from expected performance. Post-closure monitoring shall be complementary to hazardous waste regulations using techniques that do not jeopardize waste containment and may be terminated when DOE can demonstrate to EPA that there are no significant concerns to be addressed by further monitoring.

(e) Requires that any compliance application submitted by DOE shall include detailed pre-closure and post-closure monitoring plans. Such plans shall identify the parameters that will be monitored and how baseline values will be determined, indicate how each parameter will be used to evaluate any deviations from the expected performance of the disposal system; and discuss the length of time over which each parameter will be monitored to detect deviations from expected performance.

From the *Strategic Plan for Groundwater Monitoring at the Waste Isolation Pilot Plant* [26], as an operating facility, ground-water-monitoring activities at WIPP are an integral part of the requirements to ensure protection of the environment, the health and safety of workers and the public, proper characterization of the disposal system, and compliance of the WIPP with applicable regulations.

The ground water-monitoring program comprises three basic elements:

1. Ground water measurements
   - Ground water quality sampling
   - Ground water level monitoring
   - Pressure-density surveys
   - Injection well surveys
2. Well maintenance and replacement
   - Evaluation of integrity of wells
   - Maintenance as feasible
   - Plugging and abandonment of degraded or unnecessary wells
   - Replacement, as necessary, for determining ground water flow and gradients
3. Investigative studies
   - Culebra geohydrologic unit water level rises
   - Shallow water infiltration into the WIPP exhaust shaft

Long-term programs, such as the ground-water-monitoring program, must be reassessed periodically to determine if the current programs are implemented in the most efficient and effective manner. Future updates to the program include three basic issues of the ground-water strategy:

1. Continued compliance that meets the regulatory drivers and other DOE commitments
2. Effectiveness and efficiencies
   - Improvements in well integrity/longevity
   - Assurances of data relevance and quality
   - Minimization of network requirements (optimize well locations based on data relevance/needs)
   - Advancements in data collection techniques (e.g., automated remote monitoring)
   - Improvements in well design, testing and data analysis
   - Recognition and resolution of long-term issues
3. Operational needs that may include issues that arise from operation of the site and are not generally tied to regulatory drivers (e.g., nature and origin of water leaking into the exhaust shaft).
4. Other regulatory requirements also apply to the WIPP site under the United States Bureau of Land Management, the New Mexico Office of the State Engineer, and the New Mexico Environment Department Hazardous Waste Bureau.

24.7 U.S. HIGH-LEVEL RADIOLOGICAL WASTE

High-level radioactive wastes are the highly radioactive materials produced as a byproduct of the reactions that occur inside nuclear reactors. Commercial HLWs take one of two forms:

- Spent (used) reactor fuel when it is accepted for disposal
- Waste materials remaining after spent fuel is reprocessed

Significant quantities of HLW are also produced by the defense reprocessing programs at Department of Energy (DOE) facilities, such as Hanford, Washington, and Savannah River, South Carolina, and by commercial reprocessing operations at West Valley, New York. These wastes, which are generally managed by DOE, are not regulated by NRC. In addition, the U.S. Navy intends to dispose of naval propulsion nuclear reactor cores in a national repository. These federal government-owned HLWs, along with SNF, must be included in any HLW disposal plan.

SNF, HLW, and TRU management and disposal is covered by 40 CFR 191 [30]. This generally applicable standard provides limits for the release of radionuclides into the accessible environment for management and disposal of SNF, HLW, and TRU. It applies to most such wastes generated by commercial activities regulated by the NRC and defense activities under the jurisdiction of DOE. This EPA regulation covers the operating WIPP and a yet-to-be-developed, deep geological repository. Yucca Mountain had been selected as the site for the deep geologic repository and would have met 10 CFR 63 [31] requirements that were specifically modified by the NRC for the Yucca Mountain environs.

On June 3, 2008, the DOE submitted an application to the NRC for a license to construct a repository at Yucca Mountain. With this application, the DOE moved forward in meeting its congressionally mandated directive to develop, build, and operate a deep-underground facility that will safely isolate SNF and HLW from people and the environment for hundreds of thousands of years. The site has been studied exhaustively for 30 years, and as much as $10 billion has been expended in scientific research. Seldom in history has such a small piece of real estate been

subjected to such a thorough and comprehensive study. And yet the selection of this site has been mired in political controversy from the very beginning.

Yucca Mountain was one of nine sites initially studied for the first repository under the Nuclear Waste Policy Act of 1982 (NWPA) [24]. Its identification as a potential site followed early work by the U.S. Geological Survey showing that disposal in the unsaturated zone would offer advantages in deep geologic disposal of SNF and HLW.

The conclusion was based on the premise that, because water was the medium that would eventually transport radionuclides away from the repository, a repository site in an environment with limited water would be a benefit to repository performance provided by the natural system. Figure 24.3 illustrates FEPs important to saturated zone flow and transport at Yucca Mountain.

The DOE began the formal program of site characterization at Yucca Mountain in 1988, consistent with the provisions of Section 113 of the NWPA, as amended. The site characterization plan [32] described comprehensive studies to gather the information needed for a comparative evaluation of the site with regard to NRC regulations, U.S. Environmental Protection Agency standards, and DOE siting guidelines (10 CFR Part 60 [33], 40 CFR Part 191 [30], and 10 CFR Part 960 [34], respectively) in effect at the time. The site characterization program conducted between 1988 and 2001 included surface-based and underground tests, laboratory studies, and design and modeling activities necessary to provide the technical basis for evaluating repository performance.

The DOE recommended the site to the president in 2002. That same year, Congress approved Yucca Mountain as the site for the nation's first permanent repository for HLW. Congress directed DOE to submit a license application to the NRC.

The submittal of the 8,600-plus page license application was based on more than 2,700 other scientific and technical documents and contained information that has been compiled, updated, integrated, and analyzed over the course of more than 25 years.

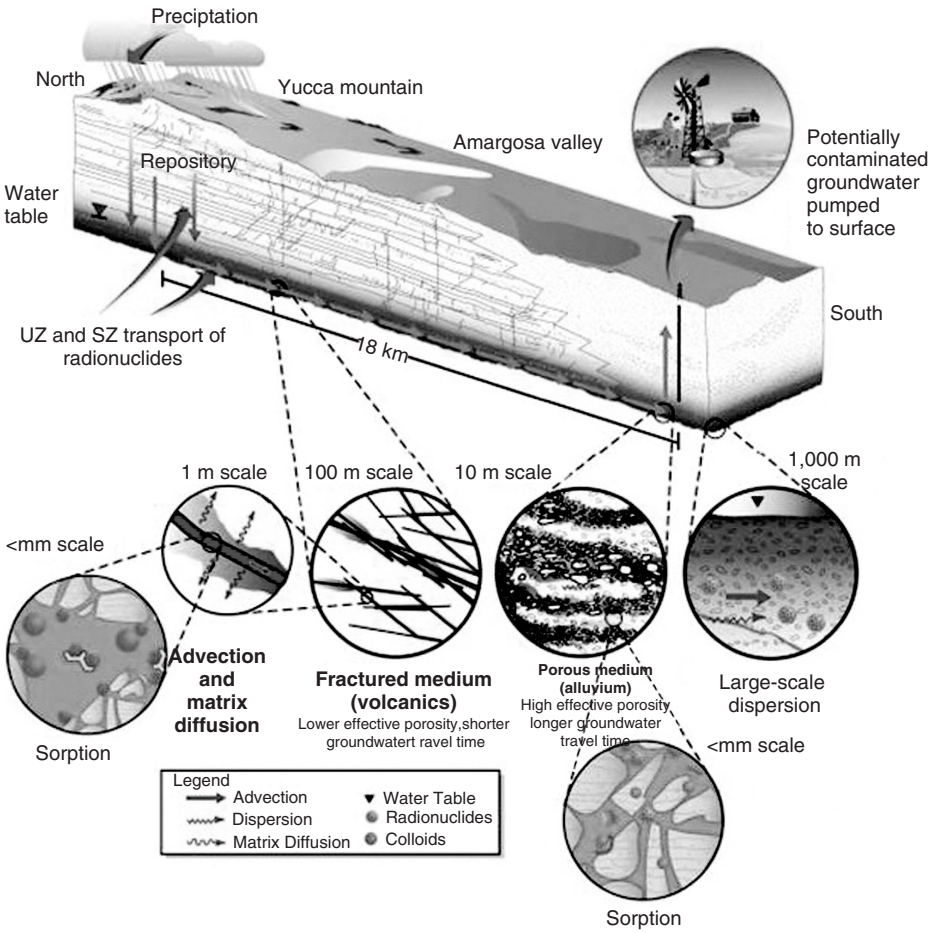

Figure 24.3 Conceptualization of features and processes important to saturated zone transport. *Source*: Sandia National Laboratories (SNL [5].

On March 3, 2010, the Secretary of Energy filed a motion to withdraw the license application for Yucca Mountain. Later filings stated that the Department's judgment was not that Yucca Mountain is unsafe or that there are flaws in the license application, but rather that it is not a workable option and that alternatives will better serve the public interest. The future of Yucca Mountain will likely be mired in political and legal areas for a considerable time. Should another location be selected, then the conditions related to 10 CFR 60.36 may again apply (at the discretion of the NRC), as they did for generic geologic repositories prior to the designation of the Yucca Mountain site.

The Yucca Mountain site was unique as it was located in the unsaturated zone far above the saturated zone. Other sites in the United States that may be considered would likely be below the water table in the saturated zone. As such, additional requirements would apply for siting saturated zone sites, as well as characterization, total system performance assessment, performance confirmation, and postclosure monitoring of hydrogeologic conditions because the repository would be in direct contact with the last natural barrier (the saturated zone), which also would be the last pathway to potential receptors if ground water is used as a resource.

10 CFRs 60.15 through 18 list the high level requirements for a plan for site characterization as well as ongoing review of the activities. 10 CFR 60.122 specifies the siting criteria that would need to be satisfied for a geologic repository other than Yucca Mountain. From the complexities and lengths of these criteria, it should be clear that very few sites within the United States would be able to meet these criteria for waste isolation from the accessible environment (in this case, the ground water as a resource). Those criteria that specifically apply to hydrogeology and ground water are the following:

. . .

b. *Favorable conditions*.

1. The nature and rates of tectonic, hydrogeologic, geochemical, and geomorphic processes (or any of such processes) operating within the geologic setting during the Quaternary Period, when projected, would not affect or would favorably affect the ability of the geologic repository to isolate the waste.

. . .

2. For disposal in the saturated zone, hydrogeologic conditions that provide:
   (i) A host rock with low horizontal and vertical permeability;
   (ii) Downward or dominantly horizontal hydraulic gradient in the host rock and immediately surrounding hydrogeologic units; and
   (iii) Low vertical permeability and low hydraulic gradient between the host rock and the surrounding hydrogeologic units.
3. Geochemical conditions that:
   (i) Promote precipitation or sorption of radionuclides;
   (ii) Inhibit the formation of particulates, colloids, and inorganic and organic complexes that increase the mobility of radionuclides; or
   (iii) Inhibit the transport of radionuclides by particulates, colloids, and complexes.
4. Mineral assemblages that, when subjected to anticipated thermal loading, will remain unaltered or alter to mineral assemblages having equal or increased capacity to inhibit radionuclide migration.
5. Conditions that permit the emplacement of waste at a minimum depth of 300 meters from the ground surface. (The ground surface shall be deemed to be the elevation of the lowest point on the surface above the disturbed zone.)
6. A low population density within the geologic setting and a postclosure controlled area that is remote from population centers.
7. Pre-waste-emplacement ground water travel time along the fastest path of likely radionuclide travel from the disturbed zone to the accessible environment that substantially exceeds 1,000 years.
8. For disposal in the unsaturated zone, hydrogeologic conditions that provide:
   (i) Low moisture flux in the host rock and in the overlying and underlying hydrogeologic units;
   (ii) A water table sufficiently below the underground facility such that fully saturated voids contiguous with the water table do not encounter the underground facility;
   (iii) A laterally extensive low-permeability hydrogeologic unit above the host rock that would inhibit the downward movement of water or divert downward moving water to a location beyond the limits of the underground facility;
   (iv) A host rock that provides for free drainage; or
   (v) A climatic regime in which the average annual historic precipitation is a small percentage of the average annual potential evapotranspiration.

c. *Potentially adverse conditions*. The following conditions are potentially adverse conditions if they are characteristic of the postclosure controlled area or may affect isolation within the controlled area:

1. Potential for flooding of the underground facility, whether resulting from the occupancy and modification of floodplains or from the failure of existing or planned man-made surface water impoundments.
2. Potential for foreseeable human activity to adversely affect the ground water flow system, such as ground water withdrawal, extensive irrigation, subsurface injection of fluids, underground pumped storage, military activity or construction of large-scale surface water impoundments.
3. Potential for natural phenomena such as landslides, subsidence, or volcanic activity of such a magnitude

that large-scale surface water impoundments could be created that could change the regional ground water flow system and thereby adversely affect the performance of the geologic repository.

4. Structural deformation, such as uplift, subsidence, folding, or faulting that may adversely affect the regional ground water flow system.
5. Potential for changes in hydrologic conditions that would affect the migration of radionuclides to the accessible environment, such as changes in hydraulic gradient, average interstitial velocity, storage coefficient, hydraulic conductivity, natural recharge, potentiometric levels, and discharge points.
6. Potential for changes in hydrologic conditions resulting from reasonably foreseeable climatic changes.
7. Ground water conditions in the host rock, including chemical composition, high ionic strength, or ranges of Eh-pH that could increase the solubility or chemical reactivity of the engineered barrier system.
8. Geochemical processes that would reduce sorption of radionuclides, result in degradation of the rock strength, or adversely affect the performance of the engineered barrier system.
9. Ground water conditions in the host rock that are not reducing.
10. Evidence of dissolutioning such as breccia pipes, dissolution cavities, or brine pockets.

. . .

19. Evidence of drilling for any purpose within the site.
20. Rock or ground water conditions that would require complex engineering measures in the design and construction of the underground facility or in the sealing of boreholes and shafts.
21. Geomechanical properties that do not permit design of underground opening that will remain stable through permanent closure.
22. Potential for the water table to rise sufficiently so as to cause saturation of an underground facility located in the unsaturated zone.
23. Potential for existing or future perched water bodies that may saturate portions of the underground facility or provide a faster flow path from an underground facility located in the unsaturated zone to the accessible environment.
24. Potential for the movement of radionuclides in a gaseous state through air-filled pore spaces of an unsaturated geologic medium to the accessible environment.

In addition to siting criteria, should a site be selected, considerable performance assessment modeling (consistent with the requirements of 10 CFR 60.113 36) and development of a performance confirmation plan (consistent with the requirements of 10 CFRs 60.140, 60.141, and 60.142 36) that would be required to meet the criteria for a license application safety analysis report consistent with 10 CFR 60.21 36.

REFERENCES

1. Euratom, *Draft Euratom Basic Safety Standards Directive Version 24 (final)*. The European Atomic Energy Community, February 2010.
2. *Atomic Energy Act*, Public Law 83–703, as amended, 42 USC 2011 et seq., 1954.
3. *National Environmental Policy Act of 1969*, Public Law 91–190, 42 U.S.C. 4321–4347, January 1, 1970, as amended by Pub. L. 94-52, July 3, 1975, Pub. L. 94-83, August 9, 1975, and Pub. L. 97–258, § 4(b), Sept. 13, 1982.
4. NRC, *Integrated Ground-Water Monitoring Strategy for NRC-Licensed Facilities and Sites: Logic, Strategic Approach and Discussion*, (NUREG/CR-6948), by Advanced Environmental Solutions, LLC, for United States Nuclear Regulatory Commission, Washington, DC, 2007.
5. Sandia National Laboratories (SNL), *Total System Performance Assessment Model/Analysis for the License Application*, MDL-WIS-PA-000005 REV00. Las Vegas, NV, Sandia National Laboratories, 2008.
6. Electric Power Research Institute (EPRI), *Groundwater Protection Guidelines for Nuclear Power Plants, Public Edition*. Electric Power Research Institute, Palo Alto, California, 2008.
7. Nuclear Energy Agency (NEA), *Confidence in the Long-term Safety of Deep Geological Repositories, Its Development and Communication*. Organisation for Economic Cooperation and Development, 1999.
8. IAEA, *Site Evaluation for Nuclear Installations—Safety Requirements*, Safety Guide No. NS-R-3. International Atomic Energy Agency, 2003.
9. IAEA. *Dispersion of Radioactive Material in Air and Water and Consideration of Population Distribution in Site Evaluation for Nuclear Power Plants*, Safety Guide No. NS-G-3.2. International Atomic Energy Agency, 2003.
10. IAEA, *Predisposal Management of Low and Intermediate Level Radioactive Waste*, Safety Guide No. WS-G-2.5. International Atomic Energy Agency, 2003.
11. IAEA. *Predisposal Management of High Level Radioactive Waste*, Safety Guide No. WS-G-2.6. International Atomic Energy Agency, 2003.
12. 10 CFR 50, *Energy: Domestic Licensing of Production and Utilization Facilities*.
13. 40 CFR 190, *Protection of the Environment: Environmental Protection Standards for Nuclear Power Operations, Final Rule*.
14. 10 CFR 20, *Energy: Standards for Protection Against Radiation*.
15. Nuclear Regulatory Commission (NRC), *Environmental Monitoring*, Fact Sheet. U.S. Nuclear Regulatory Commission, Washington, DC, 2002.
16. U.S. Environmental Protection Agency (EPA), Drinking water regulations: radionuclides. *Federal Register*, July 9, 1976, **41**, 133, 28402–28409.
17. 40 CFR 141, *Protection of the Environment: National Primary Drinking Water Regulations; Radionuclides;* § 141.15

Maximum contaminant levels for radium-226, radium-228, and gross alpha particle radioactivity in community water systems; § 141.16 Maximum contaminant levels for beta particle and photon radioactivity from man-made radionuclides in community water systems; and § 141.66 Maximum contaminant levels for radionuclides.

18. Nuclear Energy Institute (NEI). *Industry Ground Water Protection Initiative—Final Guidance Document*, NEI 07-07. Nuclear Energy Institute, Washington DC, 2007.
19. 10 CFR 51, *Energy: Environmental Protection Regulations for Domestic Licensing and Related Regulatory Functions*.
20. NRC, *Standard Review Plans for Environmental Reviews of Nuclear Power Plants Supplement 1: Operating License Renewal* (NUREG-1555). Nuclear Regulatory Commission, Washington, DC [in review].
21. International Atomic Energy Agency (IAEA), *Hydrogeological Investigation of Sites for the Geological Disposal of Radioactive Waste*, Technical Reports Series No. 391. International Atomic Energy Agency, 1999, p. 9 (Fig. 1).
22. Euratom, *European perspective on Nuclear Fission, Strategic and Technical Considerations for the Future Development of the Nuclear Energy in the European Union*. Scientific Technical Committee of the European Atomic Energy Community, December 2008.
23. EPA, *Radiation Protection at EPA: The First 30 Years*. U.S. Environmental Protection Agency, Office of Radiation and Indoor Air, Washington, DC, 2000.
24. *Nuclear Waste Policy Act of 1982*, Public Law 97–425, 42 USC 10101, January 7, 1983.
25. 10 CFR 61, *Energy: Licensing Requirements for Land Disposal of Radioactive Waste*.
26. 40 CFR 266, *Protection of the Environment: Conditional Exemption for Low-Level Mixed Waste Storage, Treatment, Transportation and Disposal*, Subpart N.
27. *Low-Level Radioactive Waste Policy Amendments Act of 1985*, Public Law 99–240 99 Stat. 1842, January 15, 1986.
28. DOE, *Strategic Plan for Groundwater Monitoring at the Waste Isolation Pilot Plant*, DOE/WIPP 03–3230. U.S. Department of Energy, 2003.
29. 40 CFR 194, *Protection of the Environment: Criteria for the Certification and Re-Certification of the Waste Isolation Pilot Plant's Compliance with the 40 CFR Part 191 Disposal Regulations*.
30. 40 CFR 191, *Protection of the Environment: Environmental Radiation Protection Standards for Management and Disposal of Spent Nuclear Fuel, High-Level and Transuranic Radioactive Wastes*.
31. 10 CFR 63, *Energy: Disposal of High-Level Radioactive Wastes in a Geologic Repository at Yucca Mountain, Nevada*.
32. DOE, *Site Characterization Plan Yucca Mountain Site, Nevada Research and Development Area, Nevada*. DOE/RW-0199. Nine volumes. United States Department of Energy, Washington, DC, 1988.
33. 10 CFR 60, *Energy: Disposal of High-Level Radioactive Wastes in Geologic Repositories*.
34. 10 CFR 960, *Energy: General Guidelines for the Preliminary Screening of Potential Sites for a Nuclear Waste Repository*.

PART IV

FISSION: GEN IV REACTOR TECHNOLOGY

25

INTRODUCTION TO GENERATION-IV FISSION REACTORS

HAROLD MCFARLANE

Idaho National Laboratory, Idaho Falls, ID, USA

More than a dozen nations with advanced nuclear energy capabilities are developing the technology for a fourth generation of nuclear power systems. Collectively, these advanced fission systems are called Generation-IV nuclear reactors. They are being designed to achieve an ambitious set of goals believed to be necessary for a world with thousands of nuclear power plants operating safely for millennia. When this fourth generation of reactors significantly penetrates the energy market in the second half of the 21st century, it will mark the culmination of Dwight D. Eisenhower's vision for nuclear energy set forth in his 1953 "Atoms for Peace" speech at the United Nations.

25.1 EVOLUTION OF NUCLEAR POWER GENERATION

Categorizing nuclear power plants into discrete generations gained acceptance around the turn of the century when 12 countries plus Euratom banded together to develop a new generation of reactors. The advanced technology employed in these reactors was inspired as much by international policy goals as by user requirements. While the first three generations of nuclear energy progressed through evolution of those technologies that proved to be successful, the fourth generation is taking new development paths that target more ambitious goals.

Starting in the late 1950s, Generation-I power reactors consisted of a collection of individually designed and operated innovative plants of modest generating capacity, ranging from several tens of megawatts to several hundred megawatts. By 1970, larger-scale commercial plants were being introduced. These Generation-II reactors proved to be commercially viable and became the backbone of the global nuclear industry, with some units of this generation still being constructed well into the 21st century. Although Generation-III reactors began to be introduced by the mid-1990s, for the most part, they comprise the large plant designs that are currently competing to enter the global nuclear generation market. However, by 2010, small modular Generation-III reactors were being designed to compete in markets where the physical infrastructure or the financial conditions make large plant construction impractical. The earliest introduction of true fourth-generation reactors will be as prototype or demonstration plants after 2020. Generation-IV designs are intended to be completely new technology development tracks, rather than further refinement of the water-cooled plants that have evolved as the dominant civilian nuclear energy technology.

Figure 25.1 illustrates the concept of four generations of nuclear energy, with specific examples in each generation. This categorization began as an American construct to distinguish state-sponsored advanced reactor research from the commercial, globally competitive nuclear power industry. Even though this framework best reflects U.S. experience, it is readily adaptable to other nuclear-technology-developing nations. In order to accommodate national and technology differences, the timelines in the figure are broad and illustrative rather than precise.

Although some 30 countries have deployed nuclear power plants and perhaps another 60 have indicated a desire to do so in the future, significant nuclear power technology

Nuclear Energy Encyclopedia: Science, Technology, and Applications, First Edition (Wiley Series On Energy).
Edited by Steven B. Krivit, Jay H. Lehr, and Thomas B. Kingery.

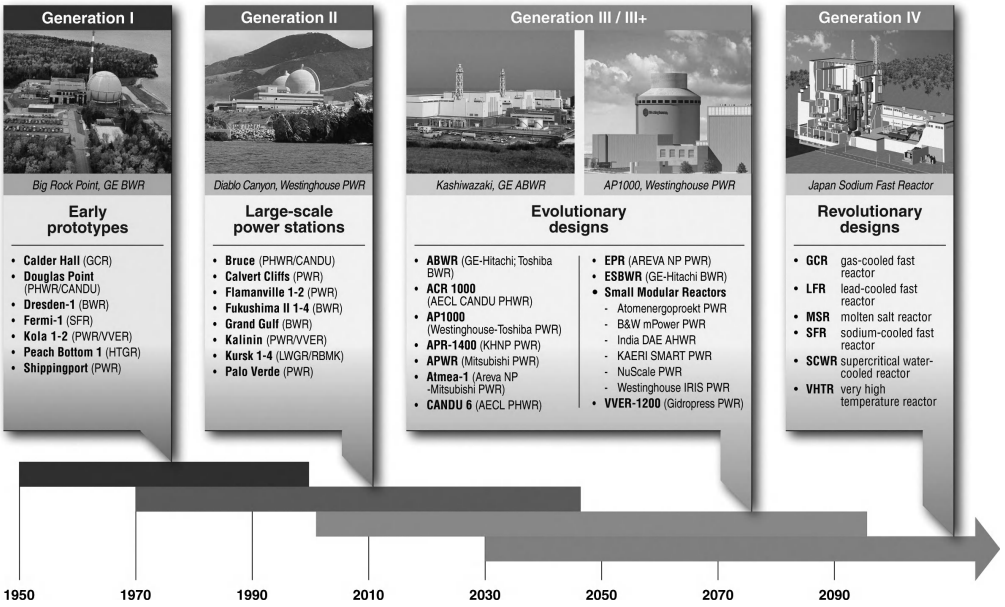

Figure 25.1 The four generations of civilian nuclear energy.

development has been limited to about a dozen nations. Further, only countries that had access to at least some nuclear technology shortly after World War II developed the early prototypes during the 1950s. Following the introduction of the Atoms for Peace Program in 1954 other technologically advanced nations could begin developing indigenous reactor concepts.

25.1.1 Generation-I

During the 1950s and 1960s there was no shortage of reactor design concepts. The overriding constraint was uranium, the only essential reactor material. At the time, uranium was incorrectly believed to be very rare; refined uranium was stored in only a handful of countries. The fissile isotope U235 comprises only 0.7% of natural uranium. The technology needed to enrich the percentage of U235 is complex, expensive, and closely held. Availability of enriched uranium, either through indigenous production or international supply, greatly expanded a country's reactor design options. Using only natural uranium, two development paths were feasible—fuel in a graphite matrix cooled by a gas or fuel moderated and cooled by heavy water (deuterium oxide).

The Generation-I plants were of modest size, designed to produce electricity on a scale of approximately 30 to 600 megawatts. Not expected to be immediately competitive, they were first-of-a-kind demonstration plants, early prototypes, or simply steps in the scale-up to full commercialization. Scientists and engineers developed scores of concepts that combined prospective coolants (water, liquid metals, molten salts, gases, organic liquids) with moderators (graphite, beryllium, light (ordinary) water, heavy water) and fuels (metals, ceramics, composites, solutions; natural, slightly and highly enriched uranium; thorium bearing). Although concepts involving some unusual combinations of fuel, moderator, and coolant reached the demonstration stage, commercial prototypes focused on two types of light-water-cooled reactors, heavy water reactors, two types of graphite reactors, and sodium-cooled reactors. Each of these technology choices found champions in at least one of the five countries that dominated reactor demonstrations in the 1960s.

With ample enriched uranium availability, the United States demonstrated the feasibility of light-water-cooled reactors during the 1950s. Commencing operation in 1960, Dresden was first commercial boiling water reactor (BWR) plant. A commercial pressurized water reactor (PWR) followed immediately in 1961 with the completion of Yankee Rowe. U.S. utilities operated another four BWRs and two additional PWRs during the decade of the 1960s. The U.S. Department of Energy (then Atomic Energy Commission) also constructed and operated the Hallum sodium-cooled graphite reactor, the Piqua organically cooled and moderated reactor, and two small BWR plants. Carolinas CTVR, a pressurized heavy water reactor (PHWR), was operated by a private consortium from 1963 until 1967. Peach Bottom Unit 1 was 40 MW high temperature gas-cooled (helium) reactor (HTGR) that started operation in 1967. In 1966 the Power Reactor Development Corporation began operation of the 61 MW Fermi-I sodium-cooled fast reactor (SFR).

Like the United States, the Russian Federation (then USSR) was unconstrained by uranium access. Russia

focused on developing three classes of prototypes: the light-water-cooled graphite reactor (LWGR), the PWR, and the SFR. The first two LWGRs started operations in 1964 and 1965. The LWGR design that was later commercialized was known as RBMK. Russia also began developing its own pressurized water technology known as VVER in the 1960s, with its first 200 MW demonstration plant being completed in 1969. More than any other nation, Russia has pressed ahead with liquid-metal-cooled fast reactor technology, first building a 350 MW SFR in Kazakhstan in 1973. This unique plant produced both electricity and water for three decades.

The United Kingdom took yet a different direction, developing a CO_2-cooled graphite reactor that was established in Calder Hall units 1 through 4 from 1956 through 1959. An advanced gas-cooled reactor (AGR) with a different fuel type and higher efficiency was first demonstrated in 1963, some 13 years prior to its commercial introduction. Like other advanced nuclear nations, the UK pursued SFR technology, building a small fast reactor at Dounrey in northern Scotland in 1962, followed by a commissioning of the 250 MW Dounrey Prototype Fast Reactor in 1976.

France followed quickly on the heels the UK, building eight CO_2-cooled graphite reactors of its own design between 1959 and 1971. The earliest unit was 38 MW, which was scaled up to 515 MW with the last plant. France also moved aggressively with SFR development, building a 233 MW prototype fast reactor at Marcoule in 1974. France even demonstrated a 70 MW heavy-water gas-cooled reactor (HWGCR) in 1968. After uranium enrichment was deployed, the French utility EdF decided to use standardized PWRs to expand its nuclear fleet. Although a single 310 MW PWR prototype began operation in 1968, EdF was able to leapfrog to larger second-generation plants by initially licensing US PWR technology.

Holding vast uranium reserves, but lacking enrichment capability, Canada embarked on a path of developing the pressurized heavy water reactor (PHWR). Using natural uranium fuel in individually pressurized tubes, these PHWRs featured on-line refueling. Known as CANDU reactors, the first demonstration plant was a 22 MW unit built in 1962. Scale-up was achieved with the operation of a 206 MW prototype reactor in 1968.

German laboratories and industry were heavily engaged in nuclear development in the 1960s and 1970s. They built and operated small BWRs, PWRs, a PHWR, an HTGR, and an HWGCR. Germany also built, but never operated, a 300 MW SFR. Germany's considerable momentum in nuclear technology development was slowed when the national government adopted an anti-nuclear policy. Among Germany's lasting contributions to nuclear energy development, its production method for high quality HTGR fuel is still notable.

Asian nations were not first movers in developing and demonstrating Generation-I nuclear plants. Taking advantage of strong research and development programs, Japan, South Korea, and China were well prepared to deploy second-generation technology and develop internal supply chains.

India established its nuclear technology development program in the mid-1950s, but it also imported Generation-I BWR and CANDU technology during the 1960s. It is unusual that these Generation-I plants are still operating in 2010. After refusing to sign the Nuclear Nonproliferation Treaty in the late 1970s, India did not engage in further international nuclear energy trade for 30 years. During that isolation period, India developed its own indigenous first-generation PHWR and began to build and operate them in the 1980s.

Generation-I was a crucial foundation for establishing a thriving nuclear energy enterprise. The determination of national governments to add a nuclear component to energy portfolios allowed sufficient investment in a variety of nuclear power options to make informed decisions about potential commercialization. The early Generation-I experience is summarized in Table 25.1.

The two light-water technologies, PWR and BWR, went on to dominate the world market, accounting for 88% of the nuclear power capacity in operation in 2010.

TABLE 25.1 Summary of Early Generation-I Reactor Experience

Type	Fuel	Coolant	Moderator	Nation(s)	Outcome
PWR	EU	light water	light water	USA, Russia, France, Germany	Dominant global technology
BWR	EU	light water	light water	USA, Germany	Widespread international deployment
PHWR	U	heavy water	heavy water	Canada	CANDU deployment in Canada, Asia
LWGR	EU	light water	graphite	Russia	RBMK deployed; development then terminated
GCR	U	carbon dioxide	graphite	UK, France	Gen-II deployed, then development terminated
SFR	EU	sodium	none	USA, Russia, UK, France, Germany, Japan	Deployment deferred; broad international development
HTGR	EU	helium	graphite	USA, Germany	Deployment deferred; broad international development

U—natural uranium; EU—enriched uranium

Canada has continued with CANDU pressurized heavy water development. India has focused on deploying its indigenous PHWR for the first phase of its nuclear power expansion. In 2009 PHWRs accounted for about 6% of global nuclear generating capacity.

Gas-cooled reactors were quickly deployed in the UK, accounting for most of nuclear's 22% share of the national electricity market. However, construction of GCRs stopped prior to 1990, with a national decision to switch to PWR technology. France terminated its GCR deployment much sooner than the UK. Nevertheless, GCRs still provide 2.4% of global nuclear generating capacity.

Like the GCRs, light-water-cooled graphite reactors briefly succeeded in a constrained market, still providing 2.7% of global capacity into the 21st century. However, the Russian Federation eventually decided to halt RBMK development; the technology was not commercially developed in other countries.

High-temperature gas reactors and sodium fast reactors have been deferred for Generation-IV development. Nevertheless, a 600 MW SFR has continuously operated for 30 years in the Russian Federation. In 2010 a 250 MW SFR restarted operation in Japan after being shut down for 14 years due to a sodium leak. While these two plants are important for demonstrating aspects of the technology, they are not considered to be true Generation-IV.

Generation-I prototype and early commercial plants compiled a safety record adequate for proceeding with nuclear power implementation. The most notable accident occurred in 1966 when debris blocked the part of sodium flow in the Fermi-1 reactor, resulting in partial melting of some of the fuel assemblies. No injuries resulted, and the reactor was repaired. Lessons learned from the event resulted in important changes in fuel design to prevent such flow blockages in the future.

25.1.2 Generation-II

Beginning in 1970 with the scale-up of plants to medium and large size, Generation-II era has continued for 40 years. Generation-II is primarily the era of the large PWRs and BWRs, although the PHWR took root in Canada and made inroads in parts of Asia. For a while, large RBMK graphite reactors competed with VVER pressurized water reactors in the Russian Federation. Fifty years after the first commercial reactors were introduced, 438 power reactors are operating in some 28 countries. The distribution by type is shown in Table 25.2.

TABLE 25.2 Operating Nuclear Power Plants—May 2010

Type	No.	Capacity (MW)	Percentage
BWR	92	83951	22.6%
FBR	1	560	0.2%
GCR	18	8949	2.4%
LWGR	15	10219	2.7%
PHWR	46	22840	6.1%
PWR	266	245487	66.0%
	438	372006	100.0%

The predominance of PWRs is due in part to international licensing of the technology. France, Japan, South Korea, and China have all licensed foreign technology as a low-risk approach to quickly developing a nuclear industry. In each case the technology has been improved to meet domestic needs and allowed faster construction of nuclear plants at competitive prices. The trend of designing larger plants continued. French PWR plants constructed around 1980 were typically 900 MW; a decade later the typical size was 1330 MW. The very large 1500 MW plants went into operation after 2000. France achieved 80% nuclear electricity rather quickly by building standardized plants, with stages of standardization to accommodate size and other improvements. This was a significant departure from the customized plant construction that took root in the United States during Generation-I.

Two widely reported accidents involving second-generation reactors slowed nuclear growth at least in parts of the world. In 1979 a 900 MW PWR suffered a fuel melting accident at Three Mile Island, Pennsylvania. Although no physical injuries resulted, the financial loss was very high. Coming at a time when electric utilities had excess capacity, the accident effectively ended new nuclear plant orders in the United States for at least 35 years.

A much worse accident involving a 925 MW RBMK reactor took place in Ukraine in 1986. A reactor power excursion caused a steam explosion and subsequent fire in the plant. A substantial release of radioactive fission products into the atmosphere drifted over much of Europe. Thirty-one people were killed by the explosion and acute radiation exposure to emergency personnel. Another 19 died as a result of injuries during the next few years. Design flaws and operational errors were responsible for the accident. Construction was cancelled on three RBMK units in Ukraine and Russia. Safety improvements were made on the remaining 14 operating units, but nevertheless provisions were made to close them between 1996 and 2023. LWGR development was eventually terminated. One impact of the Chernobyl accident was to slow nuclear deployment in Europe.

A positive impact from these two accidents was a global commitment to improved nuclear safety through more effective regulation, improved cooperation among safety authorities in different countries, establishing industry organizations focused on safe operations, and adopting more challenging safety goals for new designs. The global nuclear enterprise recognized that an accident anywhere

could have a devastating effect on the industry. The Institute for Nuclear Power Operations (INPO), established after Three Mile Island event, establishes performance measures for the U.S. nuclear industry, performs detailed evaluations of plants, and aids underperforming plants. Formed in 1989, the World Association of Nuclear Reactors (WANO) shares operating experience, performs peer reviews, and provides technical assistance on a global basis.

Performance of the Generation-II plants went through an extended learning curve. From 1970 to 2000 average plant availability improved from 5060% to 90% in some countries. Overall performance has been strong for a decade, resulting in low production cost for nuclear plants.

Some characteristics of Generation-II plants were not planned during their initial deployment. Because of their profitable performance, plant owners have invested in relatively expensive upgrades that have allowed the power rating for a number of plants to be increased. Since 1977 the U.S. Nuclear Regulatory Commission has approved some 125 power uprates amounting to more than 5600 MW of additional nuclear capacity. In 2010, Rosenergoatom announced that the 4% power uprates completed on all VVER-1000 reactors would contribute 311 MW of additional capacity. Most older VVER-440 reactors are undergoing 5% power uprates. Power uprates have also been embraced in Europe, but are not yet commonplace in Asia.

The United States licensed Generation-II plants for 40 years; most other countries issue licenses for shorter periods. One characteristic of the Generation-II reactors is that many of them are fast approaching the 40-year limit, even as their operational performance is better than ever. Virtually all U.S. reactors are applying for a 20-year life extension, a trend that seems sure to continue if performance remains strong. Research programs are studying the scientific basis for plant aging, with the expectation that the physical limit may be closer to 80 to 100 years. Generation-II nuclear plants will remain an important supply component throughout the first half of the 21st century.

25.1.3 Generation-III

Generation-III is the next generation of nuclear power plants. Some early Generation-III reactors were designed in the 1990s, well before the term was coined. The third or fourth evolution of large water-cooled reactors, the new designs incorporated enough new features to be deserving of their own identity. The large graphite reactors, both the Russian water-cooled RBMK and the British gas-cooled AGR, ended development in Generation-II. Advanced heavy-water reactors have been designed as a Generation-III option for that niche market. The term Generation-III+ has also been coined, but because no broadly accepted definition has emerged to distinguish the III+ from III, only Generation-III is used here.

The Generation-III plants typically have the following features that distinguish them from earlier plants:

- Very large PWRs or BWRs (1100 to 1700 MW).
- Standardized design for each model to expedite licensing through design certification.
- Risk of serious accidents involving fuel damage or offsite radiation releases much lower than required by licensing regulations.
- Designed to protect against airplane impact in a post-9/11 world.
- Digital instrumentation and control.
- Higher thermal efficiency than Generation-II predecessors.
- Designed for 60-year life.

Features that do not apply to all entrants in the Generation-III competition, but that are nevertheless mark significant changes, include the following:

- Compact designs that eliminate a significant fraction of components and commodities (steel, concrete, copper).
- Natural circulation of the coolant, eliminating some mechanical pumps.
- Reliance on passive or inherent features for ultimate safety.
- Ability to use mixed plutonium-uranium oxide (MOX) fuel.
- Modular construction.
- Developed by international alliances rather than a single vendor.

The earliest Generation-III designs were developed in the 1990s through cooperation of the U.S. Department of Energy and the commercial nuclear industry. An advanced boiling water reactor (ABWR) derived from an earlier General Electric Design became the Generation-III BWR. Improvements on the Combustion Engineering System 80 design became the initial basis for the Generation-III PWR. The advanced system was called the System 80+.

The U.S. Nuclear Regulatory Commission certified both the ABWR and the System 80+ designs. Four ABWRs were built in Japan, another is under construction there, and two more are being built in Taiwan. Completed in 1996 and 1997, the two Japanese ABWRs were the only third-generation reactors that started operating in the 20th century. The System 80+ design was never offered for sale, but Westinghouse bought the Combustion Engineering nuclear business in 2000 from ABB. Many features of the

System 80+ are incorporated in South Korea's Generation-III APR-1400. South Korea licensed the earlier System 80 technology and used it as a basis for designing domestically produced nuclear plants, eventually evolving it into true Korean products that could be exported as well as sold domestically. The Korea Electric Power Company is constructing two APR-1400 plants. In 2010 the United Arab Emirates ordered four APR-1400 units.

Other Generation-III designs that were under construction in 2010 include the Areva NP Evolutionary PWR (EPR), Westinghouse AP-1000, Russian VVER-1000 and VVER-1200. The first European EPR is being built in Finland, with a second unit now under construction in France. China is constructing four AP1000 units. Advanced VVER plants are being constructed in India, China and Russia. Designs with specific customers, but without having started construction, include the Mitsubishi APWR and the GE-Hitachi ESBWR.

The emergence of strong EastWest alliances to design and market Generation-III reactors is a major change from the initial Generation-II business model. Toshiba (Japan) now owns a majority stake in industry leader Westinghouse (US); General Electric (US) has teamed with Hitachi (Japan) to market both its advanced boiling water reactor designs; and Areva (France) has teamed with Mitsubishi (Japan) on some projects. Following somewhat the French, Japanese, and Korean model, China has imported and leased new reactor technology with the aim of adapting it and eventually supplying its own huge domestic market.

Table 25.3 lists many of the large LWR designs with near-term market potential. In some cases, slightly smaller units are being designed to fit markets that will not accommodate the largest plants. For example, Russia has a Generation-III 1000 MW VVER that is markedly improved from the earlier VVER designs of that size. Westinghouse initially designed a 600 MW version (AP600) of its larger AP1000. S. Korea has designed a 1000 MW Generation-III PWR for some portion of its domestic market. Canada's AECL has a 700 MW version of the ACR 1000.

Generation-III reactors seem poised to dominate nuclear energy production in the 21st century. Driven primarily by the developing countries, most credible projections of global energy demand anticipate at least a 50% electricity growth by 2030, much of it will be supplied by nuclear plants. Globally, there were 57 nuclear reactors under construction by mid-2010, amounting to more than 54 gigawatts of new capacity. China has the most aggressive energy development policy, with a large nuclear component. Japan, India, and South Korea also had plans for significant nuclear capacity addition. While Asia dominates expected energy growth, Europe, North America, and virtually every other region also anticipate the need for significant energy growth. The market for Generation-III reactors will also be driven by the need to replace the aging Generation-II nuclear plants, and perhaps aging mid-size fossil power plants as well.

Estimates of nuclear generating capacity throughout the 21st century vary widely. Starting from 367 gigawatts in 2010, the range of credible estimates for nuclear capacity in 2030 varies from a low of approximately 600 gigawatts to a high of slightly more than 1300 gigawatts. Most, if not all, of the additional capacity will be due to construction of Generation-III reactors.

Competition for the large Generation-III designs has arisen from small modular reactors of less than 300 MW. Initially, these designs were developed to meet the electrical demand in countries or regions without the infrastructure to support more than 1000 MW in a single unit. The normal guideline is that a single plant should not provide more that 10% of the capacity on the electrical grid.

TABLE 25.3 Some Large Generation-III Plant Designs with Current Market Potential

Reactor Design	Developer	Type	Efficiency (%)	Power MW(e)	Initial Market	Design Certification Application
AP-1000	Westinghouse USA	PWR	35.1	1200	US, China, India	USA-NRC[1]
ABWR	GE-Hitachi USA; Toshiba Japan	BWR	35.0	1400	Japan, Taiwan, USA	USA-NRC, Japan
EPR	Areva NP France-Germany	PWR	37.2	1600	Europe, China, USA	EUR[2], US-NRC
ESBWR	GE-Hitachi USA	BWR	34.7	1560	US, India	US-NRC
APWR	Mitsubishi Japan	PWR	38.2	1700	USA, Japan	US-NRC, Japan
APR-1400	KHNP S. Korea	PWR	36.2	1450	S. Korea, UAE	KINS[3]
VVER-1200	Gidropress Russia	PWR	37.5	1200	Russia, China, India, Europe	EUR; Rostechnadzor
ACR	AECL Canada	PHWR	~37	1180	Canada	CNSC[4]

[1]US Nuclear Regulatory Commission.

[2]European Utility Requirements.

[3]Korean Institute of Nuclear Safety.

[4]Canadian Nuclear Safety Commission.

In market-driven economies, the capital cost of a large nuclear plant is a significant barrier to most utilities. Modular reactors potentially can be built faster and return revenue sooner than a large plant. In principle, additional units can be phased in to meet demand growth. Small plants would use the economies of mass production to compete against the economies of scale of large plants. Figure 25.1 lists some of potential small modular reactor designs that range from 45 to 300 MW. Specific sizes are not listed because most of these designs lack sufficient engineering maturity to be locked into a specific power rating. Transportation limitations, market conditions and proposed legislation have been drivers for changing design target power for SMRs.

25.1.4 Generation-IV

In 2001 a majority of the world's leading nuclear nations came together to create a framework for developing the nuclear power systems that are expected to supplant LWR technology later in the century. Although advanced reactor development was under way in many parts of the world, it wasn't until the formation of the Generation-IV International Forum (GIF) that the collection of future reactor concepts had a name, common goals, and broad international cooperation. Creation of the Forum was also important because it helped focus the advanced concepts from more than 100 to just six promising systems.

The GIF agreement was among ministry-level officials, which ensured that participating nations would share at least some unique facilities, development pathways, and costs. Table 25.4 lists both the founding members of GIF and more recent entrants such as China and Russia.

With construction on Generation-III power plants only now beginning around the world, it seems clear that they represent the next dominant reactor technology. Development of the fourth-generation systems is driven by goals based on the assumption that the Generation-III reactors will be very successful. The expectation is that as the number of reactors doubles, and doubles again to meet the rapidly increasing demand for low-carbon energy, economic and social factors will drive the demand for advanced systems.

With more than 1,000 reactors worldwide, it can be reasonably anticipated that there will be pressure on uranium resources, a more urgent need to deal effectively with used nuclear fuel, an increased potential for an accident somewhere, and more political concern about increased nuclear proliferation risk. The multinational goals of Generation-IV are set out to address these issues. The sustainability of nuclear power depends upon deploying systems that are super-safe, economically practical, capable of significantly extending uranium resources for centuries and minimizing waste while simultaneously easing proliferation concerns. Table 25.5 lists the four overarching goals for Generation-IV as articulated by GIF.

All Generation-IV (Gen-IV) systems will operate at higher temperatures than their predecessors, thus exhibiting superior thermal efficiencies of 40-50% compared to about to about 35% for LWRs. None of them will use conventional water as coolant—rather, liquid metals, helium, liquid salt, and supercritical water are needed for the higher temperature technology. Where practical, Generation-IV reactors are designed assuming a closed fuel cycle, i.e., reprocessing and recycling of plutonium, uranium, and possibly minor actinides such as neptunium and americium. Some of the systems can operate at high enough temperatures to supply high quality heat for several types of industrial operations.

TABLE 25.4 Generation-IV International Forum Membership

Country	Signatory	Implementing Agents
Argentina	CNEA—National Atomic Energy Commission	Inactive
Brazil	CNEN—National Nuclear Energy Commission	Inactive
Canada	NRCan—Department of Natural Resources	NRCan
China	MOST—Ministry of Science and Technology	CAEA[1]/MOST
Euratom	JRC—European Commission's Joint Research Center	JRC
France	CEA—Commissariat á l'énergie atomique	CEA
Japan	MFA—Ministry of Foreign Affairs	MFA
Korea	MOST—Ministry of Science and Technology	MOST/KOSEF[2]
Russia	FAEA—Federal Agency for Atomic Energy (ROSATOM)	ROSATOM
South Africa	DME—Department of Minerals and Energy	DME
Switzerland	SER—State Secretariat for Education and Research	SER
United Kingdom	DTI—Department of Science and Energy	inactive
United States	DOE—Department of Energy	DOE

[1]China Atomic Energy Authority.

[2]Korea Science and Engineering Foundation.

TABLE 25.5 The Four Goals for Generation-IV Nuclear Energy Systems

Sustainability	Economics	Safety & Reliability	Proliferation Resistance & Physical Protection
Provide sustainable energy generation that meets clean air objectives and provides long-term availability of systems and effective fuel utilization for worldwide energy production. Minimize and manage their nuclear waste and notably reduce the long-term stewardship burden, thereby improving protection for the public health and the environment.	Have a clear life-cycle cost advantage over other energy sources. Have a level of financial risk comparable to other energy projects.	Excel in safety and reliability. Have a very low likelihood and degree of reactor core damage. Eliminate the need for offsite emergency response.	Increase the assurance that they are very unattractive and the least desirable route for diversion or theft of weapons-usable materials, and provide increased physical protection against acts of terrorism.

Table 25.6 lists some primary characteristics of the six types of reactor systems that have been selected by GIF for international development. On closer examination, it becomes clear that there are more than six systems because each type allows pursuit of variations in such important options as size, coolant outlet temperature, and average neutron spectrum. Three systems operate at very low pressure compared to LWRs, while the other three are high-pressure systems. With minor design variations, each system is capable of operating with thorium in the fuel cycle.

The Gen-IV systems face some common challenges, most notably advanced materials that can stand up to extreme temperatures, high radiation fields, and repeated thermal shocks over periods of years to decades. The goals of Gen-IV are deliberately ambitious in order to drive an aggressive research and development agenda. Corrosion control is a major issue for the supercritical water, molten salt, and lead systems. Instrumentation is a common challenge in the high-temperature, harsh environments of the Gen-IV systems. For systems with opaque coolants (sodium or lead) or solid moderator (graphite), inspection and maintenance present new development opportunities.

Because nuclear components such as new fuels, pressure boundary vessels, and internal structure can take 10 years or more to qualify for licensing, the ambitious goals for the systems may be approached in an evolutionary strategy. For example, the first high-temperature reactors may operate at 800°C rather than 1000°C in order to allow currently qualified materials to be used. The low end of the operating range for the lead-cooled fast reactor outlet temperature (480°C) may be selected initially in order to control corrosion in the relatively near term.

25.1.4.1 Generation-IV System Descriptions Three of the six Generation-IV systems have been in development with significant testing over several decades: the sodium-cooled fast reactor (SFR), the very high temperature gas-cooled reactor (VHTR), and the lead-cooled fast reactor (LFR). There is little experience with the other three systems, although a small demonstration molten salt reactor (MSR) was operated in the United States during the 1960s.

TABLE 25.6 Characteristics of the Six Generation-IV Nuclear Energy Systems

System	Neutron Spectrum	System Pressure	Coolant	Temperature (°C)	Fuel Cycle	Size (MWe)
VHTR (Very high temperature reactor)	Thermal	High	Helium	900–1000	Open	250–300
SFR (Sodium-cooled fast reactor)	Fast	Low	Sodium	550	Closed	30–150; 300–1500; 1000–2000
SCWR (Super-critical water cooled reactor)	Thermal/fast	High	Water	510–625	Open/closed	300–700; 1000–1500
GFR (Gas-cooled fast reactor)	Fast	High	Helium	850	Closed	1200
LFR (Lead-cooled fast reactor)	Fast	Low	Lead	480–800	Closed	20–180; 300–1200; 600–1000
MSR (molten salt reactor)	Epithermal	low	Fluoride salts	700–800	Closed	1000

The gas-cooled fast reactor (GFR) is a relatively new concept with little nuclear testing experience because it requires a very advanced type of fuel that is only in the early stages of development. Supercritical water has been demonstrated in fossil energy plants, but its unusual physical and chemical characteristics present interesting challenges within the core of a supercritical water-cooled reactor (SCWR).

A frequently asked question is whether the sodium-cooled and gas-cooled reactors built and operated in the past (and currently) are in fact Generation-IV systems. They are not true Gen-IV systems for a variety of reasons, but fundamentally they were not designed to attain the Gen-IV goals. They fall short in some combination of fuel sustainability, operating temperature, reliability, economic competitiveness, resilient safety, and waste minimization. Nevertheless, the earlier test, demonstration, and prototype reactors have contributed immeasurably to the technology development

Sodium Fast Reactor—SFR For many nuclear pioneers and subsequent generations of nuclear engineers, the sodium-cooled fast reactor was the holy grail of reactor technology. Before the abundance of uranium was established, the ability of these fast-spectrum systems to breed more fuel than they consumed was considered essential if nuclear energy was going to expand and flourish. Somewhat ironically, they are also very efficient consumers of excess nuclear material (plutonium or uranium) and minor actinides such as neptunium and americium if the design is optimized for such an application. This trait of consuming minor actinides has been exploited by designers interested in using SFRs as a key part of a comprehensive nuclear waste management system.

Sodium has beneficial properties that were exploited—it has a low absorption cross section for energetic neutrons, it is abundant, and it is chemically benign to the fuels and structural materials used in fast reactors. Further, if the sodium becomes contaminated from a fuel rod failure or other cause, the fission products and other contaminants are readily removed with slipstream filters. Sodium is an effective coolant that has a relatively high boiling temperature of 882°C, allowing a high outlet temperature of about 550°C, with a correspondingly high thermal efficiency above 40%. Sodium-cooled systems can be operated at near atmospheric pressure, a significant safety advantage.

On the negative side, sodium is reactive with air and water, requiring an inert argon gas barrier between the sodium surface and the vessel boundaries. This chemical reactivity has also driven a requirement for a secondary heat transport loop between the reactor and the steam generator, which results in a capital cost penalty. Further, a positive power transient can result if sodium is voided in the central regions of the reactor core. This has been a key design challenge for SFRs. A basic diagram for an SFR system is shown in Figure 25.2.

SFR development has been ongoing for more than 60 years, dating back to the first production of nuclear electricity in Experimental Breeder Reactor-I (EBR-I) in 1951. The amount of worldwide experience with construction and operation of SFR systems is extensive for

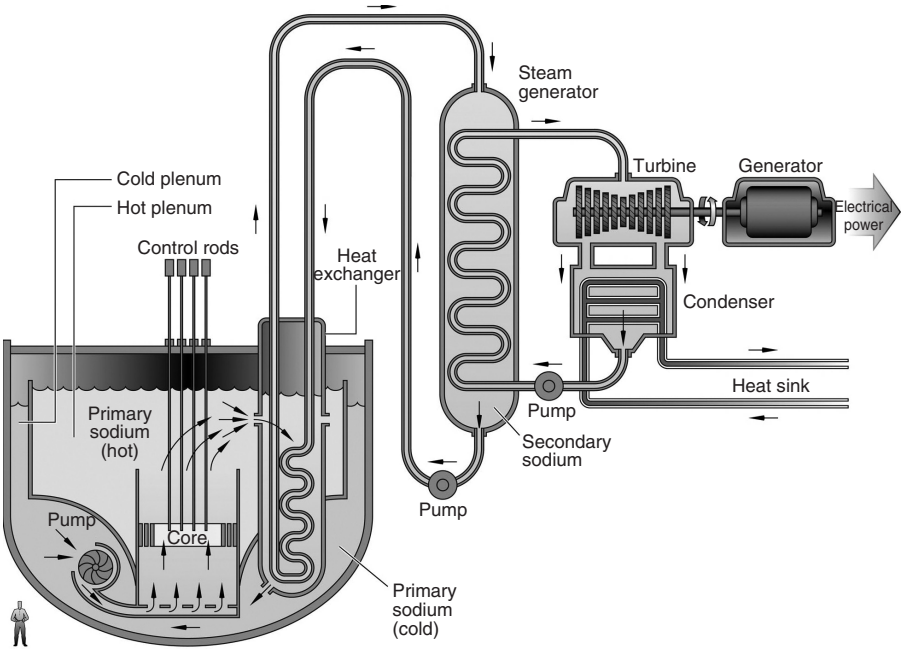

Figure 25.2 Sodium-cooled fast reactor.

TABLE 25.7 International Sodium-Cooled Fast Reactor Experience

Sodium Fast Reactor	Nominal Power (MWe)	Country	Start Date	Status
EBR-1	0.2	United States	1951	Shut down 1963
BR-5	5 (thermal)	Russian Federation	1959	Operating
DFR	14	United Kingdom	1962	Shut down 1977
EBR-II	20	United States	1964	Shut down 1994
Enrico Fermi-1	60	United States	1966	Shut down 1972
Rapsodie	40 (thermal)	France	1966	Shut down 1982
SEFOR	20 (thermal)	United States	1969	Shut down 1972
BOR 60	12	Russian Federation	1969	Operating
BN-350	350	Kazakhstan	1972	Shut down 1999
Phénix	250	France	1974	Shut down 2009
Dounrey PFR	250	United Kingdom	1976	Shut down 1994
KNK-II	17	Germany	1977	Shut down 1991
Joyo	140 (thermal)	Japan	1978	Undergoing repair
FFTF	400 (thermal)	United States	1980	Shut down
BN-600	600	Russian Federation	1981	Operating
SN300	300	Germany	N/A	Never operated
Superphénix	1240	France	1985	Shut down 1998
FBTR	40 (thermal)	India	1985	Operating
Monju	280	Japan	1994	Restarted 2010
PFBR	500	India		Under construction
BN-800	800	Russian Federation		Under construction

a design concept that is not expected to be commercialized until the post-2030 time frame. Table 25.7 summarizes key reactor facilities comprising the global SFR experience.

The worldwide results of testing, demonstration, and industrial experience with SFR systems has been mixed. In Russia, BOR-60, BN-600, and the BN-350 reactor built in Kazakhstan have all achieved notable success over long operating histories. In the United States, FFTF and EBR-II proved to be remarkable experimental facilities, while the premature prototype Enrico Fermi-1 suffered fuel melting from flow blockage due to debris in the coolant. The event caused neither human nor environmental damage. In France Phénix had a long and illustrious career. On the other hand, Superphénix was beset with troublesome balance of plant problems, became embroiled in national politics, and was shut down prematurely. The UK's Dounrey Prototype Fast Reactor was afflicted by steam generator problems—a key concern for SFRs. Japan's prototype Monju reactor was shut down for more than 14 years while working out regulatory approval at the local and national levels following a relatively minor sodium leak. All SFRs have experienced sodium leaks, but because of the low pressure and system design, physical recovery from the events has in most cases taken no more than a few weeks.

Within the GIF framework, the SFR enjoys more participation than any other system. Extending well beyond GIF cooperation, major R&D programs are ongoing in France, Japan, Russia, South Korea, China, India, and Euratom. The U.S. Department of Energy maintains an active advanced fuels and recycling program, but much of the creative SFR design work is now in the private sector. India plans to build six medium-size SFRs before 2020, with the first one scheduled for completion in 2011. GIF is embracing small, medium, and large SFR designs within its cooperative framework.

The major options being studied in SFR research and development programs have to do with economics, fuel type, and safety approach. Economic-based targets include improving the compactness of the plant design, reduction of expensive commodities used in construction, and increased reliability. Although several advanced fuel designs are being investigated, the primary choice is between oxide ceramic and metal alloy options. Component work is going on with compact heat exchangers, power production by a supercritical CO_2 Brayton cycle, and under-sodium viewing technology for inspection and maintenance. In the safety arena, research focuses on design options that include accident prevention, mitigation, active systems, passive systems, and inherent safety. National regulatory frameworks strongly influence choices on safety approaches to SFR design.

Nonproliferation goals are specifically being addressed in some SFR concepts by designing ultra-long-life cores that can be sealed for 20 to 30 years. More broadly, nonproliferation goals are addressed through multiple features in the reactor and fuel design. These features can include underground siting, advanced monitoring technology, and highly radioactive fresh fuel.

Very High Temperature Reactor—VHTR As its name implies, the Very High Temperature Reactor is the most extreme of the Gen-IV systems in terms of temperature goals. These helium-cooled, graphite-moderated systems were originally designed for highly efficient electricity generation. However, the Gen-IV goals for the VHTR envisioned a system that could generate electricity as well as process heat at a temperature sufficient for the thermochemical production of hydrogen from water, i.e., above 900°C.

With time, the nuclear research community realized that the heat energy from nuclear power plants could have a variety of applications over a range of temperatures. While nuclear reactors had been successfully used for water desalinization and district heating, the concept of opening up new industrial markets of the scale of the nuclear electricity market is a 21st century opportunity driven by record oil and natural gas prices. The high core outlet temperatures of Gen-IV systems opened possibilities for economical applications in petroleum refining, oil production from shale and sand fields, steam reformation of natural gas, and hydrogen production. Figure 25.3 shows a conceptual illustration of how an integrated VHTR site might look in the future.

The VHTR stands out from other Gen-IV systems in several respects. Fundamentally, the VHTR comprises a unique fuel type, graphite, which serves both as structural material and neutron moderator and a helium coolant. A noble gas, helium is chemically inert and is a single-phase fluid over the full range of operating and potential transient conditions.

The VHTR is being developed along two distinct conceptual lines—a prismatic graphite core and a pebble-bed graphite core. In the prismatic concept (shown in Figure 25.4) the fuel remains fixed until it is replaced. In the pebble-bed concept, fuel-loaded graphite spheres roughly the size of a tennis ball move through the core, are discharged, and are reintroduced back into the core until the fuel is spent.

The unique TRISO particle fuel is the key to VHTR technology. Uranium, in the form of an oxide or an oxycarbide, is dispersed throughout millions of particles of less than 1 mm diameter in the core of a VHTR. Figure 25.5 shows an example of the fuel particles. The particles are loaded into discrete compacts that fit inside the graphite core structure or in the pebbles. The uranium kernels are coated with two layers of pyrocarbon and an outer silicon carbide. Even in a thermal transient, these fuel particles are designed to retain the fission products, thus providing a very high margin of safety.

Although the global experience base is still somewhat limited, experience with helium-cooled high-temperature reactors dates from the 1960s. The early test reactors were DRAGON (1963–1976) in the UK and AVR (1967–1988) in Germany. Technology demonstrations took place in the United States (Peach Bottom-1 and Fort St. Vrain) and Germany (THTR). Small test reactors are currently operating in Japan (HTTR—30 MW) and China (HT10—10 MW).

The VHTR is strongly supported within the GIF framework. Most member organizations have been involved in VHTR technology development. For the United States, this technology has been the primary focus of Gen-IV national

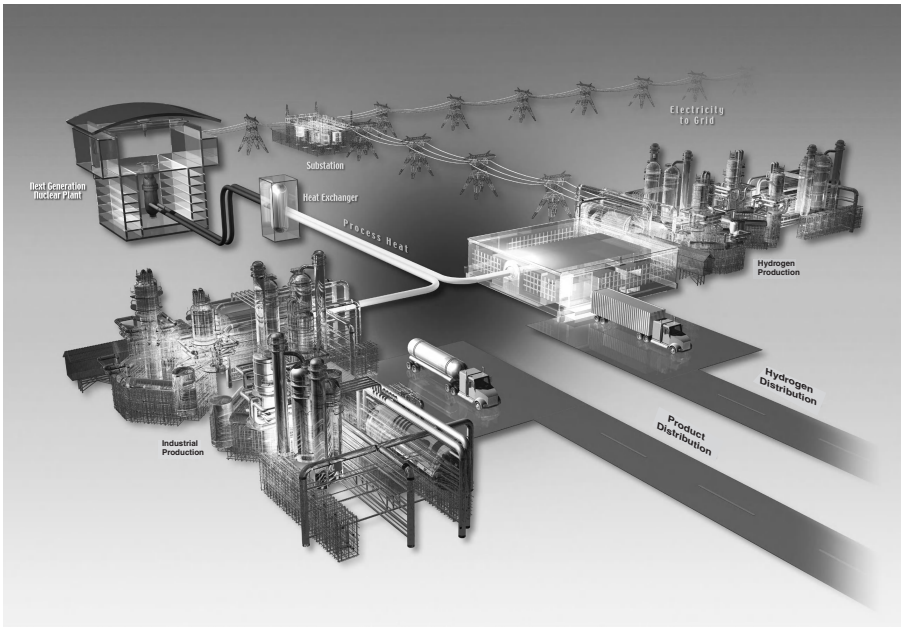

Figure 25.3 Conceptual illustration of an integrated VHTR site.

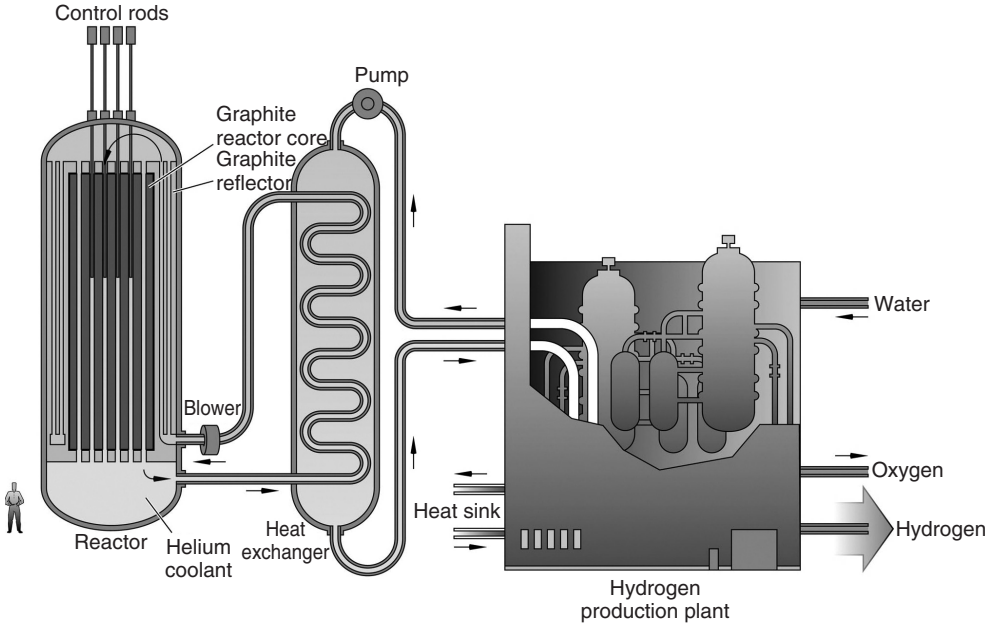

Figure 25.4 The VHTR concept.

Figure 25.5 VHTR fuel particles.

investment in the Next Generation Nuclear Plant (NGNP) program. The main international activities include development of analysis methods, fuel and fuel cycle, materials, components and high-performance turbomachinery, hydrogen generation options, and process heat applications.

Unlike the other GIF concepts, the VHTR size is relatively modest when measured in megawatts. The limit is approximately 600 MW thermal, or less than 300 MWe. Although very large high-temperature reactors were proposed decades ago, the safety limit is governed by the maximum temperature of the fuel particles during accident conditions. The large graphite mass provides thermal inertia for absorbing excess heat if helium flow is lost. Like other concepts, the VHTR designs have a decay heat removal system for off-normal conditions, which is more effective at smaller sizes. Because VHTRs are high-temperature, but low-power density systems, the size of the pressure vessel for a 600 MW VHTR is comparable to that of a large (>1 GW) LWR.

Lead-Cooled Fast Reactor—LFR Lead has long been considered as an alternative to sodium as a fast reactor coolant, because unlike sodium it is not reactive with water or air, while having good thermal and physics properties. Among coolant choices for advanced reactors, lead uniquely provides excellent shielding properties. The boiling temperature for lead is 1745°C, twice that of sodium, therefore potentially offering a wide safety margin. Molten lead's thermal conductivity is less that of sodium, but it has a much higher heat capacity. With a melting point of 327°C and a density higher than most types of nuclear fuel, lead presents its own unique challenges.

Molten lead's chemical corrosion of reactor structural and cladding metals has been a difficult challenge. Controlling the chemistry of molten lead has been the subject of considerable research. Lead's high density presents

challenges for holding the fuel in place and for inserting control rods, both of which would float if not mechanically constrained. Seismic design also becomes more challenging with a high-density coolant.

The Russian Federation has the only significant reactor experience with lead-cooled reactors. Russia has successfully used a lead-bismuth eutectic (LBE) in submarine reactors. LBE has similar properties to lead, but melts at only 125°C, and corrosion control is simplified. One disadvantage is that irradiated bismuth produces polonium, a prolific alpha emitter that exacerbates the challenges of radiologic control. Russia has now extended this LFR design experience to the commercial world, offering SVBR-75/100, a small modular reactor for application in some remote areas. Russia has also carried out design studies for BREST, a large LBE-cooled fast reactor with an advanced fuel cycle.

The basic concept for a generic lead-cooled fast reactor is shown in Figure 25.6. Until 2010 there have been no formal research activities within the GIF framework, although there have been strong programs within the member organizations. The focus of these activities has been on transferring the LBE experience, economics, compact seismic design, in-vessel steam generator, safety, under-lead component handling, support of fuel elements, and design of a reliable decay heat removal system.

Although the United States has carried out some design activities on a 20–180 MWe small modular design of an LFR, most research effort has gone into the design of a 600 MWe European concept. In order to control lead corrosion, the outlet temperature of this design is being limited to 480°C, far below the ultimate goal of 800°C for a Gen-IV LFR system.

Supercritical-Water-Cooled Reactor—SCWR The only water-cooled Gen-IV reactor concept, the supercritical-water-cooled reactor builds on many years of experience in advanced water-cooled reactor and supercritical fossil plant development. It also builds on advanced systems from both industries such as turbine technology. The SCWR operates above the thermodynamic critical point of water (above 374°C, 22.1 MPa). The main advantage of the SCWR is improved economics because of the higher thermodynamic efficiency and plant simplification opportunities that are made possible by the use of a high-temperature, single-phase coolant.

The SCWR offers exceptional design flexibility. It can be designed with a thermal or a hard neutron spectrum; the outlet temperature can reach up to 650°C; the thermodynamic efficiency can approach 50%; it is amenable to both a pressure vessel and a pressure tube design; and it is adaptable to conventional or advanced fuel

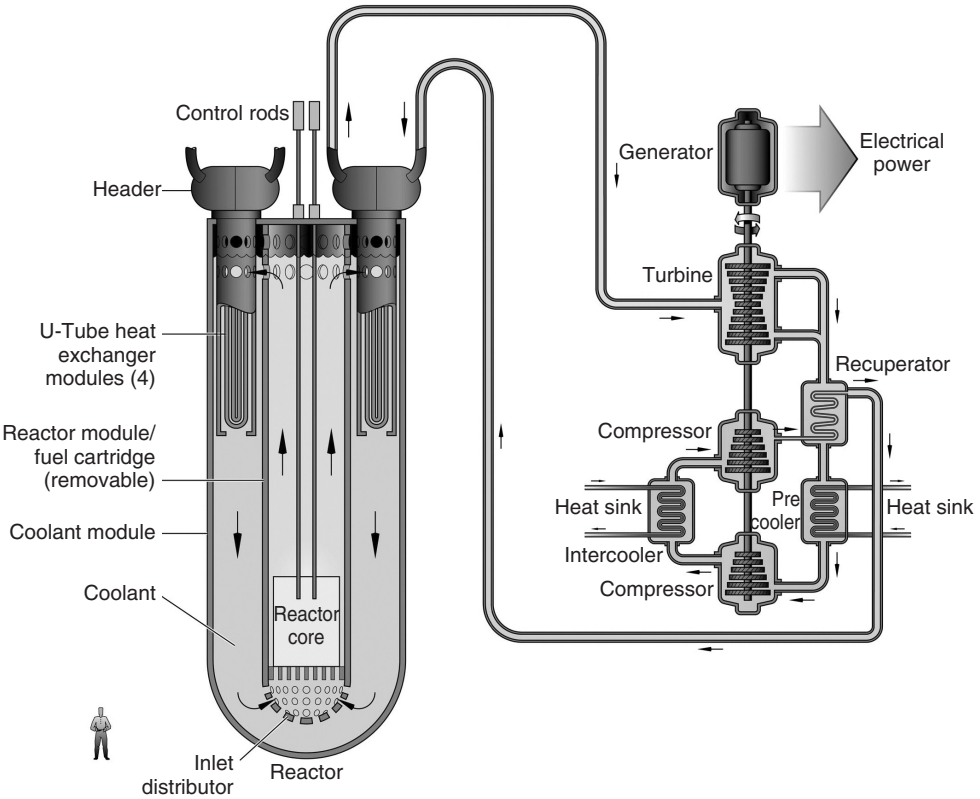

Figure 25.6 Lead-cooled fast reactor.

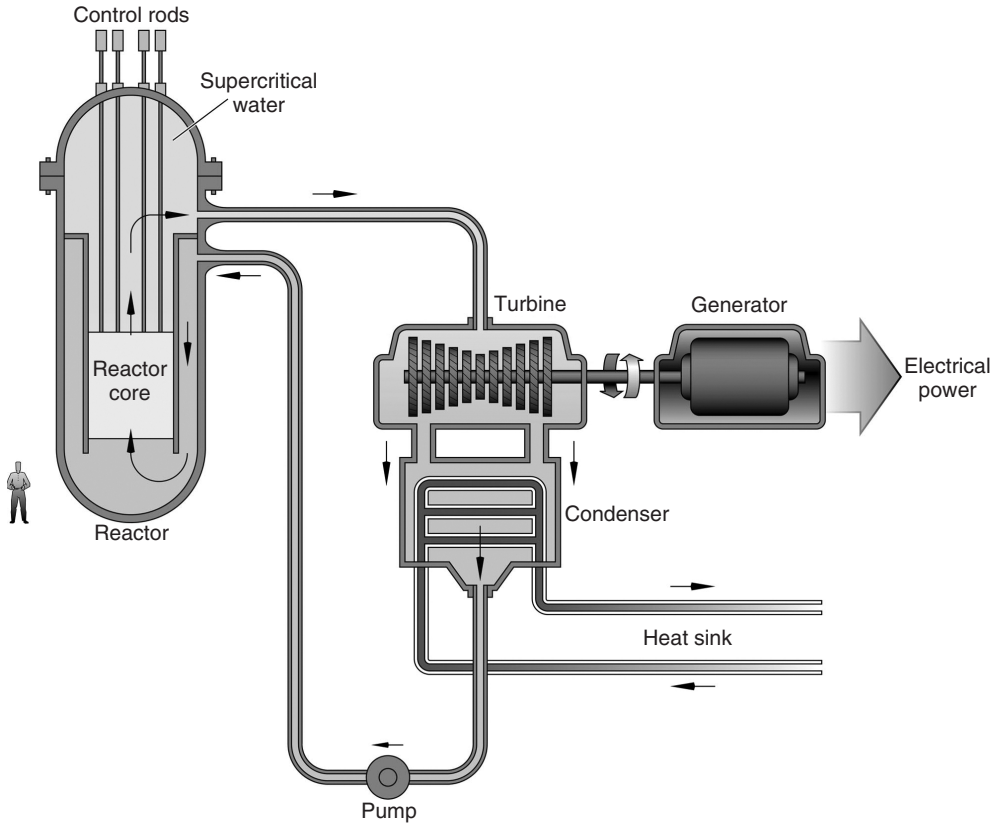

Figure 25.7 Supercritical-water-cooled reactor.

cycles. Using established technology from related industry, commercialization would seem to be straightforward. However, there are materials and safety issues that require resolution prior to nuclear application. One basic concept for the SCWR is shown in Figure 25.7.

Canada, Euratom, Japan, South Korea, and France all have active SCWR development programs. Because the density changes as supercritical water moves through the core, one of the main challenges is to understand basic thermal-hydraulic phenomena, safety, and stability. Supercritical water chemistry under these temperatures and pressures is in question, particularly in the presence of radiolysis. Only very large reactor concepts in the 1500 MWe range are being considered in order to take advantage of the high power density and economies of scale.

Molten Salt Reactor—MSR The molten salt reactor is actually a collection of technology pathways to developing a unique Gen-IV concept. The technology has its roots in the Molten Salt Reactor Experiment (MSRE) that was conducted at Oak Ridge National Laboratory during the late 1960s. The MSR diverges from other Gen-IV concepts in almost every respect. In the base concept, the fuel is dissolved as a fluoride salt in a liquid salt mixture of LiF plus other fluoride salts such as BeF_2, CaF_2, KF, and NaF. The minimum salt melting temperature is above 360°C, and the design operating temperature is more than 700°C.

The basic MSR concept is illustrated in Figure 25.8. The most notable feature in the illustration is a chemical processing plant that is included in the system. While this significantly complicates the design, it eliminates the need for development of high-temperature, high-strength cladding material. Online processing also prevents significant accumulation of fission products and permits continuous adjustment of the fuel mixture. Thus, in principle, the reactor would not require periodic shutdown for refueling.

At this early stage, the MSR has not focused on a preferred line of development. The concept offers exceptional flexibility in designing a system. The various research teams are considering both epithermal and fast spectrum systems. The MSR is readily scalable to any reasonable size. Since the outset of MSR research, thorium has been considered as a potential fuel component. Both thorium and U233 were used in the MRSE. Liquid salt is an excellent heat transport medium that has been considered for solar thermal applications and for coupling nuclear heat production to industrial processes.

A new type of reactor concept has emerged that uses the coolant properties of molten salt with the high-temperature

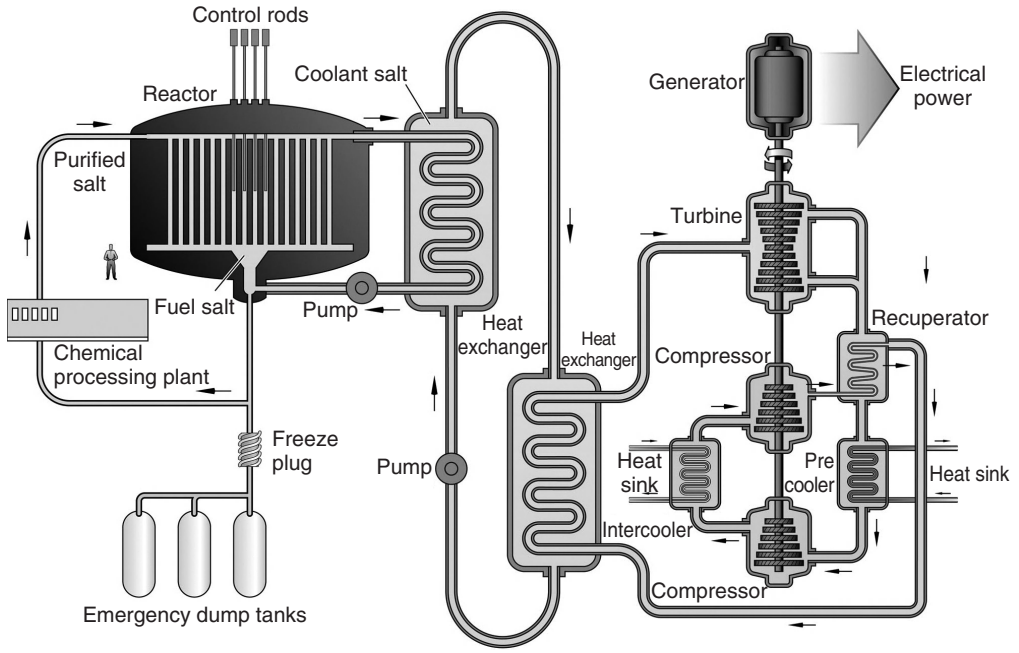

Figure 25.8 Molten salt reactor.

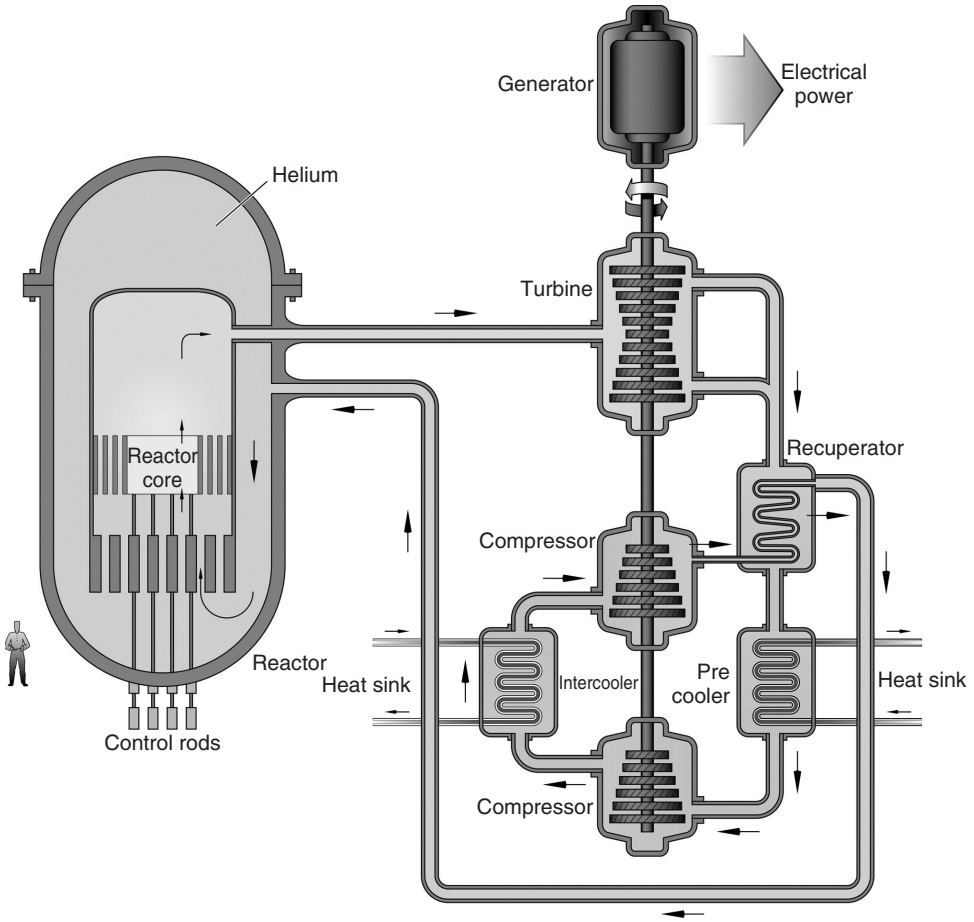

Figure 25.9 Gas-cooled fast reactor.

graphite reactor. In this concept the helium coolant in the VHTR concept is replaced by molten salt. This allows a significant increase in power density for a reactor of the same physical size. The solid fuel is in either a prismatic graphite or a pebble form.

The MSR is being pursed at some level in France, Euratom, Japan, Russia, and the United States. Research activities include flow sheet development, high temperature structural materials, tritium management, analysis methods development, measurements of fuel properties, and measurements of thermodynamic properties.

Gas-Cooled Fast Reactor—GFR The gas-cooled fast reactor is the least developed of the Gen-IV concepts. It has been promoted as an alternative to the SFR, considering Gen-IV goals from the outset. Operating at high temperature, it can be used for efficient electricity production, hydrogen production, or industrial heat applications. With its fast spectrum, the GFR can be used for as a key element in a closed fuel cycle—extending uranium resources, burning minor actinides, or breeding plutonium. The GFR can be designed for small or larger sizes, although early development has focused on the large plants. An illustration of a conceptual GFR is shown in Figure 25.9. This unit is assumed to be a 1200 MWe helium-cooled system operating with an outlet temperature of 850°C using a direct Brayton cycle gas turbine for efficiently generating electricity.

The many potential advantages of the GFR come at the price of an extensive development program requiring new fuel forms, new cladding materials, and qualified structural materials. Fuel work has focused on nitride and carbide ceramics. A silicon carbide matrix is favored for cladding development.

The innovative GFR technologies and design features are intended to overcome the challenges of using a high-pressure gas with poor thermal characteristics to cool a high-power-density core with a low thermal inertia. The principal challenge is decay heat removal following a depressurization event. Research effort is going into methods development and safety analysis. The GFR development activities are centered in Europe, with strong participation from Euratom, France, and Switzerland. Japan also engages in GFR development.

FURTHER READING

The Generation-IV International Forum http://www.gen-4.org/index.html.

International Atomic Energy Agency http://www.iaea.org/.

Proceedings of any International Congress on Advanced Nuclear Power Plants (ICAPP).

World Nuclear Association http://www.world-nuclear.org/info/default.aspx?id=530&terms=Generation%20iV.

26

THE VERY HIGH TEMPERATURE REACTOR

HANS D. GOUGAR

Idaho National Laboratory, Idaho Falls, ID, USA

26.1 INTRODUCTION

26.1.1 Basic Concepts

The Generation-IV (Gen-IV) Nuclear Energy program was launched by the U.S. Department of Energy around the year 2000 to explore innovative nuclear plant concepts that focused on four main objectives: enhanced safety, proliferation resistance, reduced waste, and economic viability.

Many new reactor concepts were considered, and a group of experts narrowed this list down to the six most promising technologies from the broad collection of new concepts. The Very High Temperature Reactor (VHTR) was on this list, which also included a supercritical water reactor, sodium- and lead-cooled fast reactors, a molten salt reactor, and several others. Other countries were invited to conduct research into one or more of these and share knowledge through the Generation IV International Forum. The United States chose to invest most heavily in the VHTR concept because it is most suitable—because of the high outlet temperature—to the production of hydrogen as an alternative combustion fuel. The development and deployment of a VHTR for this purpose was set up as a DOE project called NGNP (the Next Generation Nuclear Plant) and is intended to be a partnership between DOE and private industry. The technology and designs we discuss in this chapter are candidate designs proposed by some reactor vendors involved with the NGNP project. The NGNP mission has changed somewhat over time; however, the fundamental technology has remained unchanged. A high temperature gas-cooled reactor is to be used to drive industrial processes such as hydrogen or fertilizer production.

The *High Temperature Reactor* (HTR) and *Very High Temperature Reactor* (VHTR) are types of nuclear power plants that, as the names imply, operate at temperatures above those of conventional nuclear power plants currently generating electricity in the United States and other countries. Like existing nuclear plants, heat generated from the fission of uranium or plutonium atoms is carried off by a working fluid that can be used to generate electricity. The very hot working fluid also enables the VHTR to drive other industrial processes that require high temperatures not achievable by conventional nuclear plants as shown in Figure 26.1. For this reason, the VHTR is being considered for nonelectrical energy applications. The reactor and power conversion system are constructed using special materials that make a core meltdown virtually impossible.

The key to VHTR technology is the use of refractory materials to contain the fuel and fission products at temperatures that would cause conventional reactor structural materials to degrade. The bulk of the reactor core consists of graphite, a material that does not melt and can absorb excess heat while moderating the neutrons that sustain the fission chain reaction. The ceramic fuel is cast in the form of microspheres encapsulated in robust ceramic coatings and embedded in the graphite. Coolant is pumped through the graphite core to carry away the fission heat and drive the power conversion system. In most designs, this coolant is helium and the reactor is often called a hightemperature *gas-cooled* reactor (HTGR). Helium is chemically inert and possesses good heat transfer properties. In a HTR, the helium exits the core at a temperature between 700

Nuclear Energy Encyclopedia: Science, Technology, and Applications, First Edition (Wiley Series On Energy).
Edited by Steven B. Krivit, Jay H. Lehr, and Thomas B. Kingery.

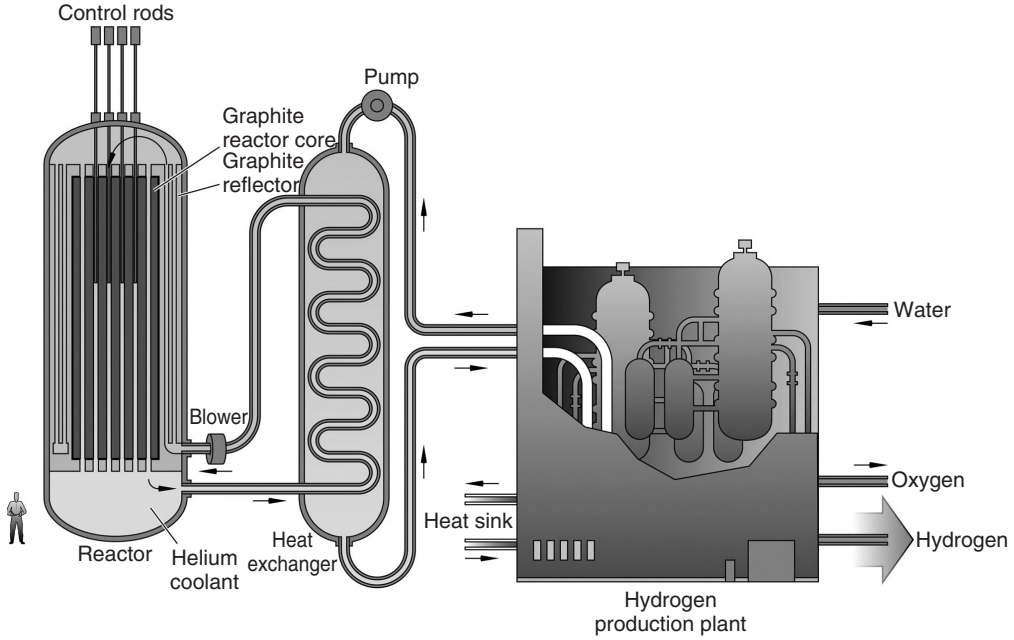

Figure 26.1 Hydrogen plant driven by a VHTR. (U.S. Department of Energy [DOE].)

and 850°C. In a VHTR, the exit temperature can be much higher, approaching 1000°C. VHTR research and development efforts are focused on fabricating and qualifying the fuels and materials that can sustain operation at these temperatures.

What follows is a summary of the history of HTRs, the features that distinguish them from other types of reactors and allow them to operate safely at elevated temperatures, and the technical challenges to widespread deployment. Finally, the potential role of the HTR/VHTR as a carbon-free source of non-electrical energy is discussed.

26.1.2 History

The idea of a nuclear reactor operating at high temperature (>700°C) was first conceived in the early days of nuclear power plant development, and government programs were instituted to develop the fuels, materials, and power conversion systems that could withstand these temperatures [1]. Most HTR concepts employed a gas coolant, hence, the term high-temperature gas-cooled reactors (HTGRs). A small number of experimental HTRs have been built in Europe and Asia to test these concepts (Figure 26.2). Unless otherwise stated, the reactors described hereafter are all cooled by helium gas.

26.1.3 Early Prototypes and Test Reactors

The first HTR was the DRAGON test facility built in Winfrith, England, and operated by the United Kingdom Atomic Energy Authority. Its purpose was to test fuel and materials for the European HTR research and development program and was thus managed as an international project under the auspices of the Nuclear Energy Agency of the Organization for Economic Cooperation and Development. Construction commenced in 1959 and was completed in 1962. Operation at 20 megawatts of thermal power (MWt) began in 1965 and continued until 1976; this thermal energy was never used to generate electricity. The reactor was partially decommissioned in 2005.

The AVR (a German acronym for Arbeitsgemeinschaft Versuchsreaktor) was a prototype HTR built and operated at a research center in Jülich, Germany. Construction began in 1960. Regular operation began in 1967 and continued until 1988 [2]. The AVR had a thermal output of 40 MWt, of which about 17 were converted to electricity for the local grid. The AVR was used to develop and test a wide variety of fuels and machinery in support of the German HTR development program (http://www.nextgenerationnuclearplant.com/). It was the first so-called pebble-bed reactor wherein the fuel was encased in graphite spheres about the size of tennis balls. The AVR provided the foundation for pebble-bed HTR developments later undertaken in South Africa and China.

The HTR-10 is one of two HTRs operating at the beginning of the 21st century. Built in China, the HTR-10 is a small, 10 MWt experimental reactor running on pebbles fabricated to German specifications. The HTR-10 has been used to demonstrate the inherent safety features of the HTR and is a test bed for development of a larger power module under development in China [3].

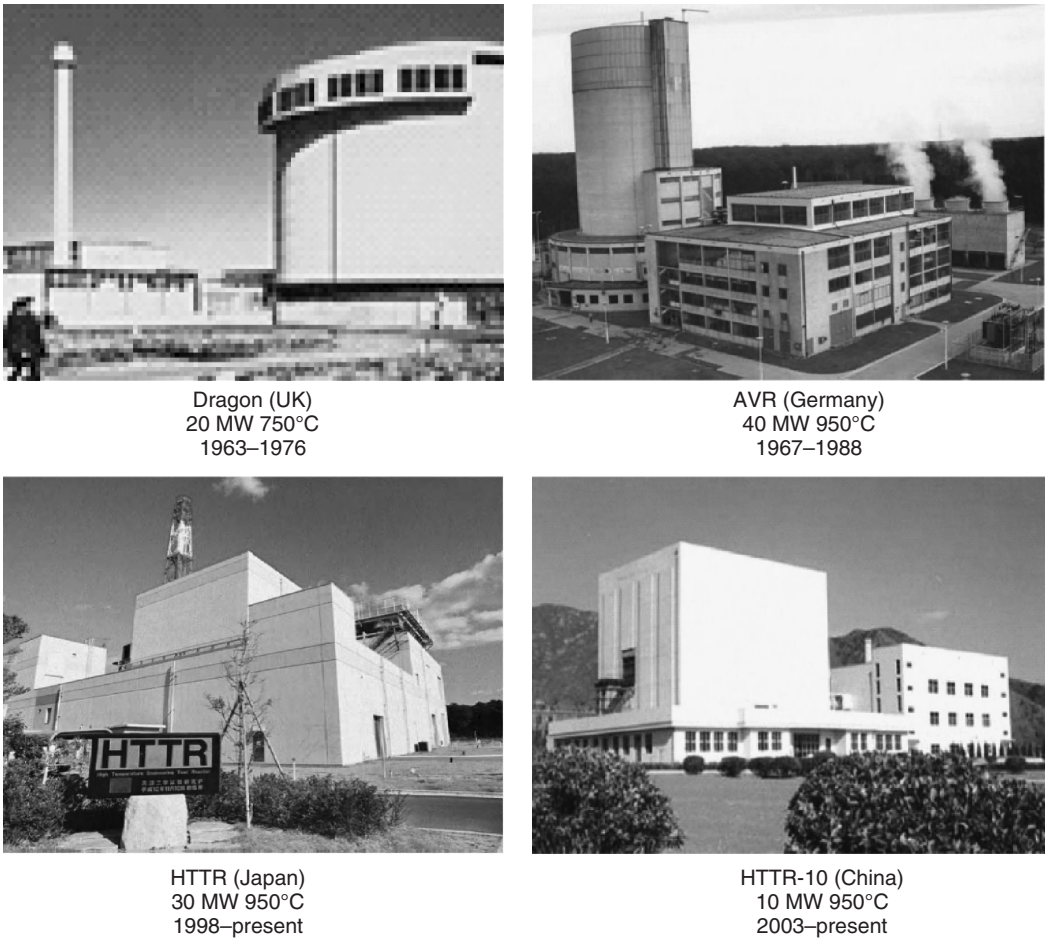

Figure 26.2 Past and existing experimental HTRs. (U.S. Department of Energy.)

The other operating HTR is the High Temperature Engineering Test Reactor (HTTR) located in Oarai, Japan. This 30 MWt reactor employs a prismatic core and also features inherent safety characteristics in addition to operating with an outlet temperature of 950°C. The HTTR is being used by Japan as a test bed to develop a larger power reactor based upon HTR technology [4].

26.1.4 Early Commercial Designs and Plants

Power reactor development of the HTGR was pursued by companies in the United States and Germany with plants licensed by state regulatory agencies and operated for commercial use (Fig. 26.3). While much of the early development of light water reactors was conducted by the U.S Navy in support of its ship propulsion program [5], from the beginning HTGRs were largely a commercial power venture. These early HTGR power plants thus experienced technical challenges typical of first-of-a-kind technology. Although the reliability of these plants did not match the performance of modern LWRs, they did demonstrate that the HTR could evolve into an industrial energy source.

The Peach Bottom Atomic Power Station was built 50 miles (80 km) southeast of Harrisburg, Pennsylvania. The Philadelphia Electric Company was a pioneer in the commercial nuclear industry when it ordered Peach Bottom Unit 1 in 1958. Peach Bottom Unit 1 operated from 1966 to 1974 with a rated power of 115 MWt. Designed and built by General Atomics, this was the first of the so-called *prismatic* or block fuel reactors in which the fuel was embedded in large blocks of graphite and stacked into a large cylinder to form the reactor core. Although it was considered an experimental reactor, Peach Bottom 1 converted 40 of its 115 MW of thermal power into electricity and supplied the grid with an 88% *capacity factor* (the ratio of actual energy produced to what could have been generated if operated continuously at full power).

The THTR-300 (German: Thorium Hoch Temperatur Reacktor) was a pebble bed rated at 300 MWe. Located in Hamm-Uentrop, in the German state of North Rhine Westphalia, Hochtemperatur-Kernkraftwerk GmbH

Peach Bottom 1 (USA)
115 MW 725°C
1967–1974

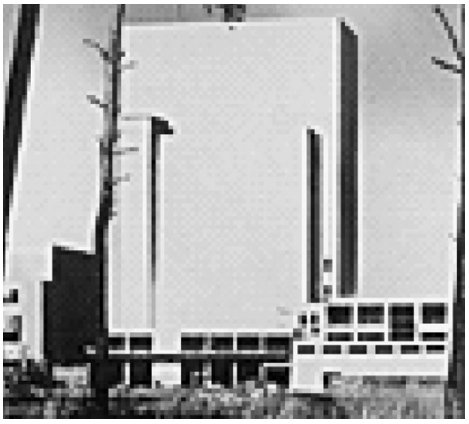

THTR (Germany)
750 MW 750°C
1986–1989

Fort St. Vrain (USA)
842 MW 775°C
1976–1989

Figure 26.3 Commercial-scale HTRs. (U.S. Department of Energy.)

financed construction of the THTR-300. The plant operated from 1983 to September 1, 1989. The THTR was synchronized to the grid for the first time in 1985 and started full power operation in February 1987. The THTR-300 served as a prototype and, unlike other HTRs, used thorium rather than uranium as its primary fuel. In 1988, however, a combination of political and financial factors led to a decision not to restart the plant after a planned maintenance outage.

The Fort St. Vrain Generating Station was built by near Platteville, Colorado, in 1974, the only nuclear plant built in that state. Like its predecessor, Peach Bottom 1, Fort St. Vrain was a prismatic core design built by General Atomics. It ran from 1977 to 1989 with a rated power of 842 MW of thermal energy of which 330 was converted to electricity for the grid. Fort St. Vrain differed from other nuclear plants in that it required no high-strength concrete structure to contain its radiological inventory in case it escaped from the primary cooling system. This function was carried out by the reactor vessel and the special coated particle fuel that is the key technical feature of HTRs. Like the THTR, Fort St. Vrain was shut down before the end of its planned lifetime due to technical difficulties that undermined its commercial viability.

The *modular* HTGR concept was introduced the early 1980s with the design of the HTR Modul 200 by the German industrial firms Kraftwerk Union and Siemens/Interatom. Although one was never built, the design was mature enough to be submitted to the German nuclear licensing authorities. The design stressed simplicity and inherent safety even in the most severe of accidents [6]. The HTR Modul 200 would produce 200 MW of thermal energy that could be used to make electricity or drive a heat-consuming industrial process. It featured a recirculating pebble-bed core, one in which the fuel pebbles were constantly circulated and reloaded into the core during operation. Modular construction techniques would be used to lower capital costs and large electricity demands could be met by building multiple units of the same (relatively small) 200 MWt plant on the same site. The small reactor vessel, combined with the robust coated particle fuel, obviated the need for extensive engineered safety systems that drive up costs. The HTR Modul 200 was designed to be able to

withstand a complete loss of coolant to the core without sustaining fuel damage.

During the 1980s, General Atomics was also developing a prismatic version of the modular HTGR. The 350 MWt Modular High Temperature Gas-Cooled Reactor (MHTGR) also featured a passively safe core that would remain intact even in the event of a complete loss of coolant flow to the reactor [7]. Research and development of the MHTGR was supported by DOE into the 1990s. Design and safety analyses [8] were submitted to the U.S. Nuclear Regulatory Commission (NRC) in support of a license application, but this NRC review was discontinued in 1996.

With renewed interest in nuclear power as a safe, carbon-free, and "home-grown" technology, the HTR has been the focus of new government-sponsored research and development programs around the world. The safety, environmental, and economic features of this heat source have gained the attention of policy makers in Washington and other nations. New designs that build on the fuel and modularity concepts developed in previous decades are now being developed. The following sections explore the technology of the HTR and present some of the new designs that are under development.

Figure 26.4 UO_2 pellet. (U.S. Nuclear Regulatory Commission.)

Figure 26.5 LWR fuel assembly. (U.S. Nuclear Regulatory Commission.)

26.2 TECHNOLOGY

26.2.1 Conventional Nuclear Plants vs. HTRs

Conventional nuclear power plants that currently generate about 20% of the electricity used in the United States are light water reactors (LWRs), so called because water (as opposed to heavy water) cools the fuel and moderates the neutron energy. The fuel is in the form of small pellets of uranium dioxide (Fig. 26.4), a ceramic that has a melting point of 2,840°C. The UO_2 pellets are loaded into 12-foot alloy cladding tubes. These fuel rods are arranged into square arrays called assemblies (Fig. 26.5). Inside the reactor core, water is pumped through the gaps between the rods to carry away the heat generated by the fission reaction. Water also functions as the *moderator*, a substance that slows down the neutrons emitted from the fissioned uranium atoms. Slower neutrons are much more likely to cause fissions and sustain the chain reaction.

The assemblies must remain immersed in water at all times to prevent the rods from melting and releasing their radioactive contents into the reactor cooling system. LWRs are designed with multiple and redundant water injection systems in order to keep the core covered with water under all postulated normal and accident conditions.

The tremendous amount of heat energy absorbed by the cooling water would cause it to boil away quickly if not kept under pressure (about 2,250 psi) inside a very thick steel pressure vessel. The outlet temperature of the coolant is limited to about 330°C to prevent over-pressurization.

In an HTR, the uranium dioxide or uranium carbide is formed into tiny spherical particles and coated with layers of refractory materials that contain the radioactive material even if the coolant (helium) is lost. The bulk of the reactor core consists of graphite, which moderates the neutron energy but also serves to absorb excess thermal energy in the event that coolant flow is stopped. This combination of fuel and core design prevents the core from melting even under the most severe accident conditions. It also allows the coolant to be safely heated to much higher temperatures (>750°C) suitable for high-efficiency electricity generation or process heat applications. These features are discussed in detail in the next section.

26.2.2 Fuel and Core

The keystone of HTR safety and performance is the coated particle fuel. A coated particle with a diameter of just under 1 millimeter is shown in the upper left of Figure 26.6. Such fuels have been extensively studied around the world over the past four decades. Layers of carbon and silicon carbide surround the uranium core or kernel (the active part of the particle) thus forming the so-called *tri-isotropic* coated particle fuel (TRISO). Each HTR core would contain billions of these multilayered coated particles. The particles are mixed with graphite and then pressed into either small cylinders called *compacts* for the prismatic reactor or tennis-ball-sized spheres called *pebbles* for the pebble-bed reactor (see Fig. 26.5).

The TRISO layers make this fuel extremely resistant to physical assault from temperature and radiation, thus providing robust protection for the nuclear material and outstanding retention of the radioactive material produced during fission. The silicon-carbide layer is extremely hard and will not decompose until the temperature exceeds 2,000°C. Extensive testing in Germany in the 1970s and 1980s demonstrated that outstanding performance of high-quality low-defect TRISO-coated particle fuels can be achieved under both normal operation and potential but highly improbable accident conditions. That performance is now being duplicated and extended in tests sponsored by DOE.

Another important aspect of HTR safety is the shape and composition of the reactor core. In both the prismatic and pebble-bed versions of the HTR, the blocks or pebbles comprising the fueled portion of the core are stacked into cylinders or annuli, which are much taller than they are wide. Figure 26.7 shows a cutaway view of a prismatic HTR vessel. The vertical red regions in the middle of the vessel are the graphite blocks containing the TRISO

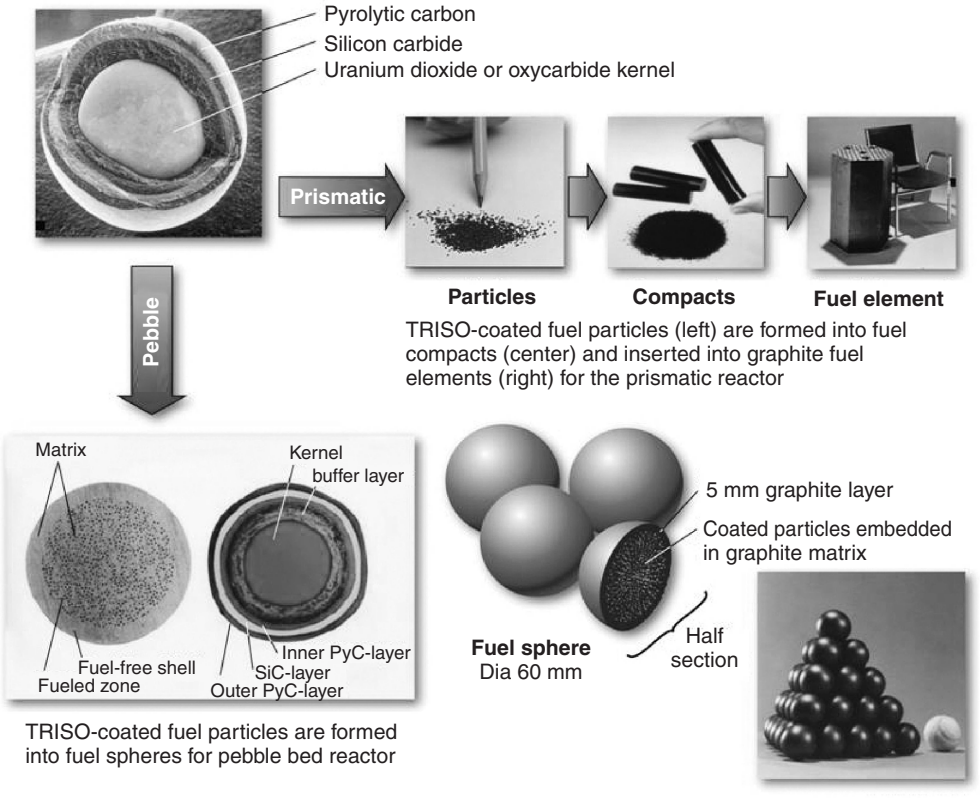

Figure 26.6 TRISO-coated particles are formed into spheres for a pebble bed HTR and compacts for a prismatic HTR. (U.S. Department of Energy.)

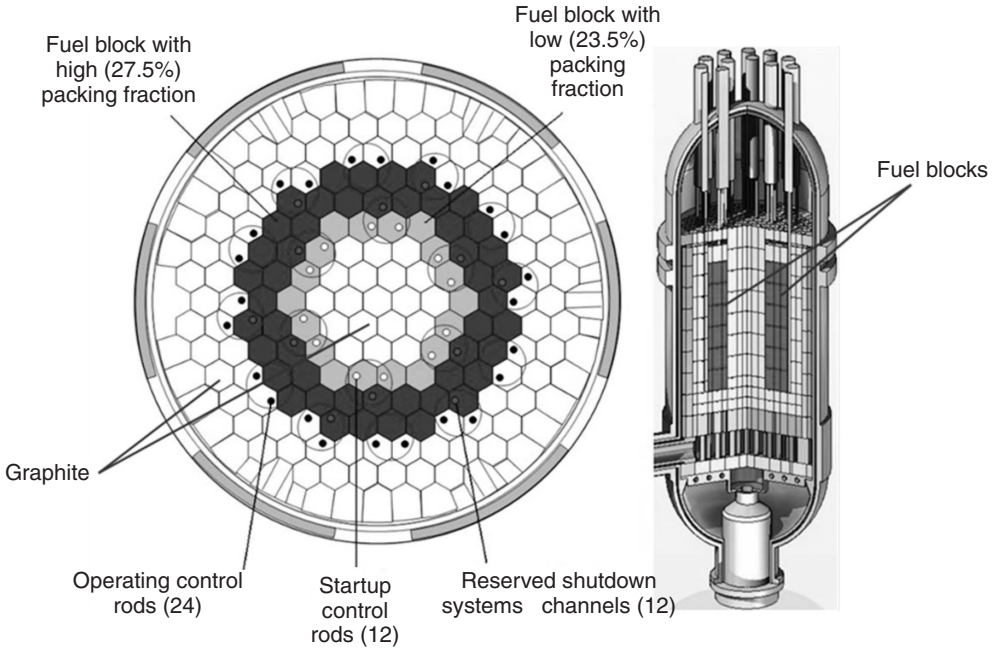

Figure 26.7 Top and side views of a prismatic HTR vessel with core (red) surrounded by a graphite reflector (DOE).

fuel particles. The surrounding material (grey) consists of blocks of pure graphite. Normally, helium coolant flows downward through the fuel region to carry away heat. In the event that the coolant pumps are tripped, the core region immediately starts to heat up. This has a negative feedback effect on the fission reaction, thus the temperature increase causes the reactor to shut itself down. The heat in the core then conducts naturally into the surrounding graphite and eventually out of the vessel. The high aspect ratio of the core (the ratio of the height to the width) means that the thermal energy never has to travel very far to escape the core. Thus, the core temperature increases somewhat (to about 1,600°C), but never exceeds the failure temperature of the coated particle fuel.

This ability to reject heat naturally was demonstrated in the German AVR [2]. In safety tests, the reactor control system was deliberately disabled, and the primary coolant pumps were tripped. As in all nuclear plants licensed in the United States, the rise in temperature caused the fission chain reaction to stop immediately. The loss of coolant flow, however, would lead to the melting of a water-cooled reactor core by the residual (decay) heat from fission products. Yet, in the AVR, the excess heat conducted out of the core over a period of about 120 hours during which the maximum temperature stayed well below the value above which fuel failures would occur. After the test ended, the reactor was restarted for normal operation.

26.2.3 Power Conversion

In order to be commercially viable, the energy produced in the HTR must be in a form that can drive industrial processes. Until recently, electricity production was thought to be the most economical use of high temperature nuclear heat because the power conversion systems were mature and the high capital/low fuel costs of nuclear plants compelled continuous full-power operation. First-generation HTRs in the United States and Germany employed steam generators and turbines commonly used in nuclear and fossil fuel plants for electricity generation.

The Pebble Bed Modular Reactor (PBMR) project, which began in the 1990s in South Africa, featured a novel *gas turbine* system in which the helium gas heated in the reactor vessel would be sent directly to turbo-generators before being cooled, recompressed, and sent back to the reactor. Recent advances in heat exchanger technology enabled the development of high-efficiency gas turbine cycles using helium as the working fluid similar to the technology used in modern natural gas power plants and aircraft engines. Figure 26.8 shows an early version of the PBMR pebble-bed nuclear plant design with a closed cycle gas turbine power conversion system. Helium would exit the reactor (red) at 950°C and 145 psi and be delivered to the gas turbine connected to a generator. The system is designed with a thermodynamic efficiency of 41%, compared with the 33% efficiency typical of an LWR.

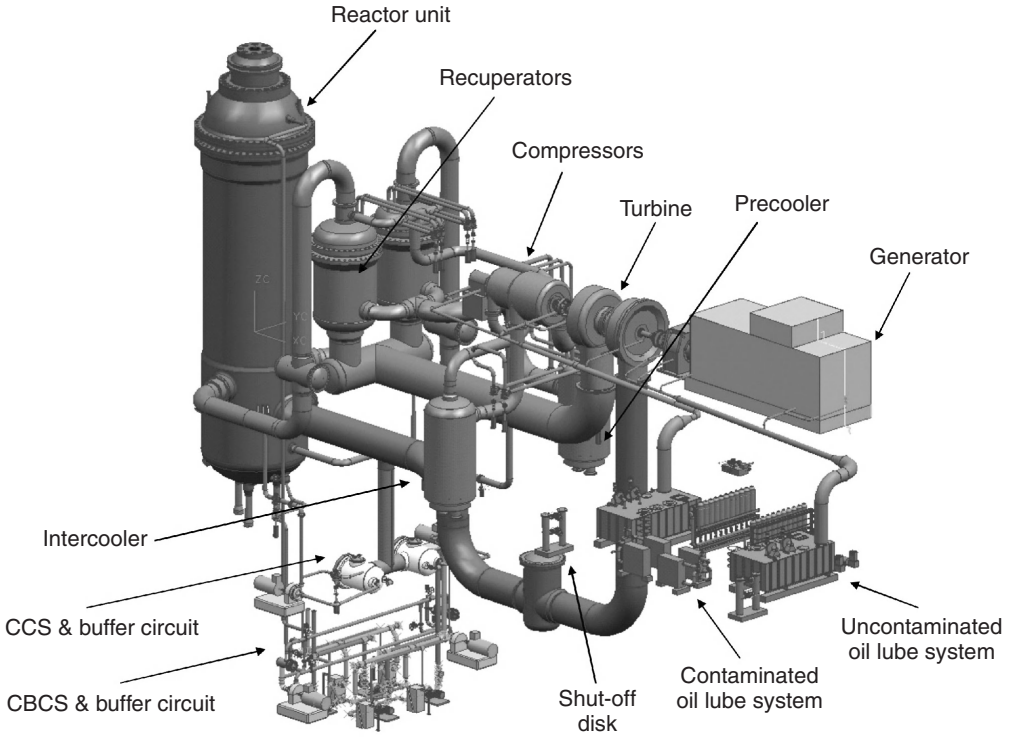

Figure 26.8 Early PBMR design with closed cycle gas turbine for electricity production. (courtesy of PBMR (Pty) Ltd.)

Development efforts have recently shifted toward *cogeneration* applications that would supply both high temperature steam and electricity to a process facility, such as a petrochemical plant or refinery. Extraction and refinement of hydrocarbons from the Alberta (Canada) oil sands or Colorado oil shale deposits are an example of such a multicomponent end use. Integration of the HTGR technology with refining processes, coal to synthetic fuels, and ammonium fertilizer production have been investigated.

Hydrogen production has been the subject of research over the past decade because hydrogen is viewed as a long-term enhancement or replacement to fossil fuels for transportation fuel and petrochemical production. Hydrogen production processes (thermochemical and electrolytic) become more efficient and cost-effective with an increase in temperature of the feedstock (steam or methane). An HTGR generating steam at 850°C can be a significant *domestic* source of carbon-free hydrogen. Figure 26.9 shows one concept of a combined electricity-hydrogen plant driven by an HTR.

Development has therefore shifted toward small (<400 MWt) modular designs that employ flexible heat exchangers and other components that can be tuned to the energy demands and duty cycles of the end user. The plants must also be compatible with the codes, standards, and regulatory requirements associated with both the industrial process and the co-located nuclear plant.

26.3 NEW DESIGNS AND INNOVATIONS

Most of the HTR designs now under development around the world are based on the modular HTGR concepts born in the 1980s, mainly the pebble-bed HTR Modul 200 and the prismatic MHTGR. With variations, all employ the TRISO-coated particle fuel, helium coolant, and a core that can be shut down and cooled without active safety systems or operator action. Developments have focused on raising the outlet temperature of the coolant to accommodate more power conversion systems and higher efficiency. All can be fitted to a steam plant or gas turbine, depending upon the user's needs.

None of the metallic alloys used in conventional nuclear plants are qualified for sustained exposure to the temperatures encountered in VHTRs. Both the AVR and HTTR have operated safely with an outlet temperature of 950°C for months at a time to test components and demonstrate VHTR capability. A full-size power plant, however, is expected to operate at elevated temperatures for 40 years or more, and no pressure vessel alloys have yet been qualified for such sustained operation. Research and

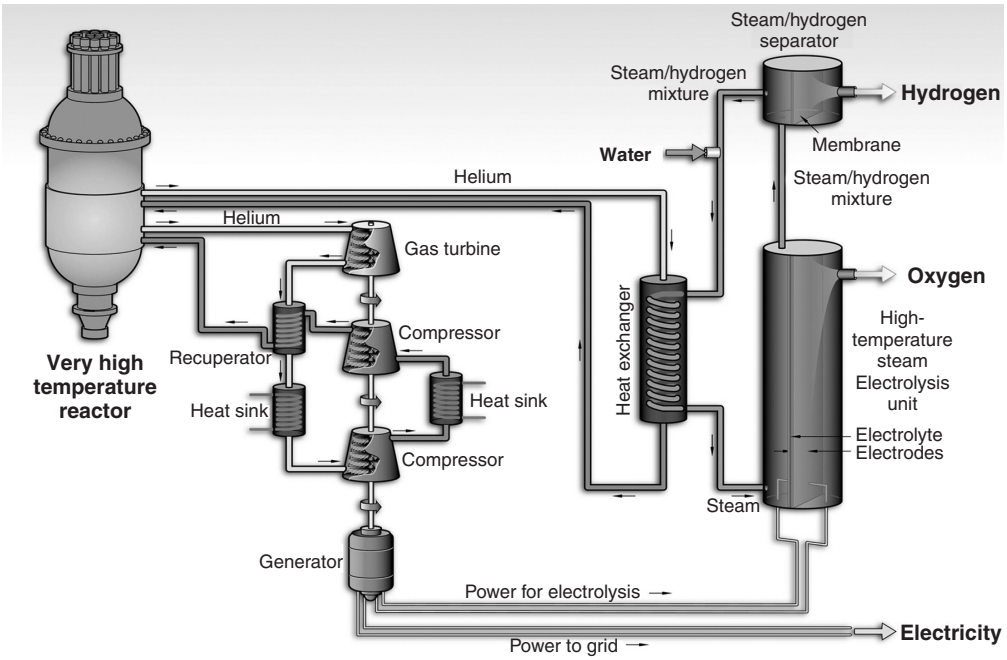

Figure 26.9 Combined electricity/hydrogen plant powered by a high temperature nuclear reactor (DOE).

development into advanced materials is needed to identify the alloys or composites needed for the pressure vessel, heat exchangers, and control rod components. Some of this research is currently underway on behalf of DOE.

26.3.1 Pebble Bed Reactors

The pebble bed fuel concept developed and deployed in Germany has been adopted by both South Africa and China. Both countries are developing modular pebble-bed reactors very similar to the HTR Modul 200, the German design that was developed to the licensing stage but never been built.

In the mid 1990s, South Africa chartered the largely state-owned PBMR company to acquire the German technology and adapt it for its own growing industrial needs. South Africa possesses considerable coal deposits but is otherwise bereft of indigenous fossil reserves. It also has a considerable *coal-to-liquids* (CTL) infrastructure built up over many decades when access to foreign petroleum sources was restricted. The coal-to-liquids technology, also pioneered in Germany in the early 20th century, employs high-temperature steam to turn coal into various transportation and other liquid fuels. It is an energy intensive process that emits considerable amounts of pollutants in addition to the main product. The PBMR is being considered as a clean and reliable alternative to the fossil boilers that drive the CTL process.

PBMR has an industrial partner in Toshiba/Westinghouse and together they are developing a pebble bed HTR for the African market and North America. Depending on the power level and end-user requirements, the PBMR reactor core consists of either an annulus or cylinder of 6 cm fueled pebbles (Fig. 26.10).

The roughly 10 meter high core is surrounded by thick graphite layers that act to support sustained nuclear fission and containment of the neutrons produced from fission. The pebbles make up the core that is located within the annulus formed by the side and center reflectors. The core and reflectors are contained within a core barrel. The reactor vessel is the primary structural and pressure retaining component of the reactor. Lower-temperature helium coolant enters the vessel through the outer part of a large coaxial pipe. From there it travels to the top of the core, flows down through the core, and exits at the bottom through the inner pipe of the coaxial duct. The annulus between the inner and outer vessel walls contains a small flow of lower temperature helium as part of the insulation system for the reactor outlet piping and the vessel. This helium flows up through an annulus between the core barrel and the reactor pressure vessel and rejoins the principal core inlet helium in the upper plenum. The nuclear reaction is controlled with control rods that penetrate the side reflectors from the top.

The pebble-bed reactor is refueled online so that the reactor need never shut down except for maintenance and repairs. The fuel-bearing pebbles enter the core through loading tubes at the top of the vessel. Over a period of many months, each pebble trickles downward through the

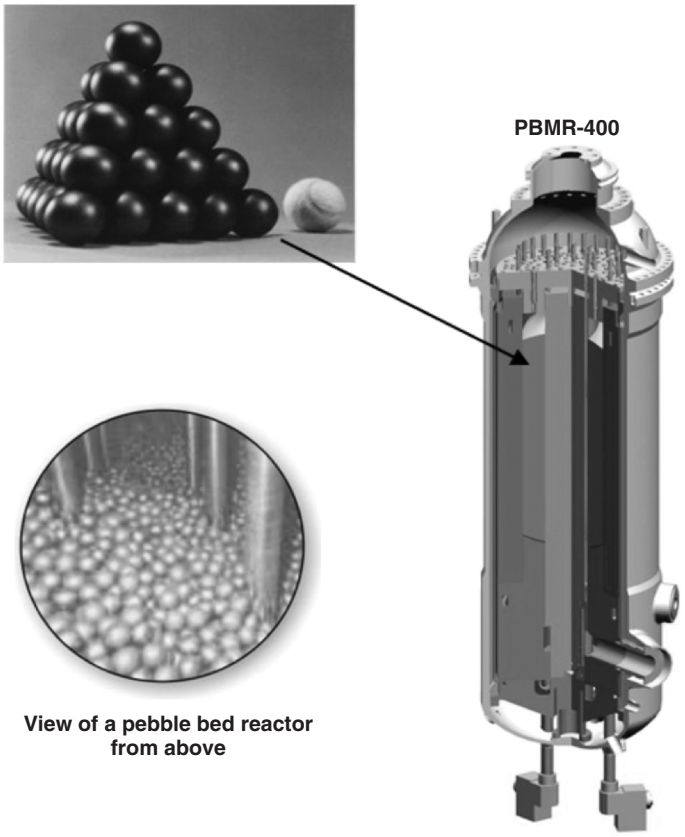

Figure 26.10 Fuel elements and core geometry in a pebble bed HTR. With permission from Tom Ferreira.

core, pushed by gravity and the coolant flow, and exits from the bottom of the vessel. It is then examined in the plant fuel handling system to determine if it has reached its burnup limit or is damaged. In these cases it is removed from the system and a fresh pebble is inserted. Otherwise, the pebble is returned for another pass through the core. Depending on the final power level, core shape, and pebble flow rate, a typical pebble will make between six to 15 passes through the core.

In the 250 MWt PBMR cogeneration plant, the heat transport system and balance of plant employ an indirect cooling system. Coolant from the reactor is passed through an intermediate heat exchanger in which the heat is transferred to a secondary helium loop. The secondary loop includes a steam generator and a secondary intermediate heat exchanger in series with the steam generator (see Fig. 26.11). Steam from the steam generator drives a turbo-generator for the production of electricity; the secondary intermediate heat exchanger supplies hot gas to a process heat plant. Excess electricity can be delivered to the local grid.

China is also developing a pebble-bed reactor based upon German technology. The HTR-PM will produce 250 MW of thermal energy coupled to a steam generator for electricity production. The core consists of an annulus of fueled pebbles surrounding an inner column of pure graphite pebbles. The outlet temperature is 750°C.

26.3.2 Prismatic Reactors

The close cousin to the pebble-bed reactor is the prismatic or block reactor pioneered in the 1960s by General Atomics, a U.S. company. The TRISO particles are embedded in small graphite cylinders called compacts (see Fig. 26.6). The compacts are then loaded into holes drilled into graphite blocks. Holes are also drilled into the hexagonal blocks to allow the helium coolant to pass through and carry away the thermal energy. Unlike the pebble bed reactor, the blocks do not move during operation so that the reactor must be shut down at regular intervals (18–24 months) for refueling. Refueling involves removing spent fuel blocks, shifting partially spent blocks to different locations, and adding fresh fuel blocks.

Although the Peach Bottom I and Fort St. Vrain power plants provided valuable operating experience, modern prismatic HTGRs resemble the MHTGR, the General Atomics modular HTR that was designed but never built.

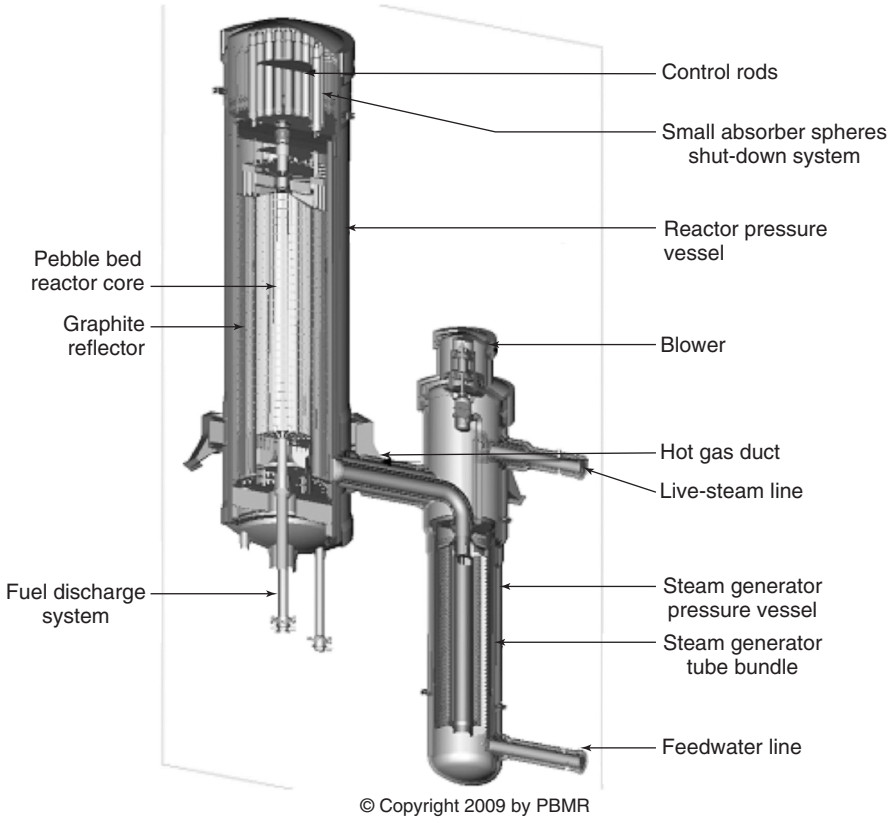

Figure 26.11 PBMR design with heat exchangers for combined electricity/process heat production.

General Atomics and the French firm AREVA have recently proposed similar prismatic block reactor designs. An AREVA reactor design, called ANTARES, is shown in Figure 26.12. The blocks are arranged two to three layers deep, depending on the power level of the reactor, which can be between 300 and 600 MW. The ANTARES plant is designed for electricity production and includes a direct Brayton cycle gas turbine in a horizontal configuration fed from the heat exchanger shown in the figure. A variant of ANTARES similarly employs a secondary coolant loop supplying a combined cycle turbine configuration for electricity production along with a parallel loop supplying high-temperature gas to a prototype hybrid sulfur hydrogen production facility [9].

The General Atomics MHTGR design evolved into the Gas Turbine-Modular Helium Reactor (GT-MHR) shown in Figure 26.13. The primary reactor coolant loop drives a gas turbine in a vertical configuration to produce electricity as shown in Figure 26.14. General Atomics added a second parallel loop, supplying heat to a compact intermediate heat exchanger that in turn supplies heat to a prototype sulfur-iodine hydrogen production facility.

Both AREVA and General Atomics revised their plant designs to drive a steam generator in the primary loop, supplying steam for both process heat and electricity production. Two reactor power levels—350 and 600 MW—are proposed with reactor outlet temperatures between 750 to 800°C.

26.3.3 Alternative Fuels and Coolants

26.3.3.1 Spent Fuel Reduction Spent nuclear fuel from the current fleet of LWRs as well as that from future HTRs contains plutonium and other transuranic elements (TRUs) that pose waste disposal and nuclear proliferations challenges. TRUs can be "burned" further in a nuclear reactor if they can be cast into a form that can stay in a reactor for long periods of time. The robust TRISO coatings offer a potential option. TRU from light water reactor (LWR) or HTR spent fuel can be separated from fission products, cast into TRISO fuel particles, and reinserted into the HTR core for incineration as shown in Figure 26.15. This fuel-burning approach is called "deep burn" and refers to the large fraction of the initially loaded TRU that can be destroyed (up to 60–70% fissions per initial metal atom) during a single pass through a high-temperature reactor. The concept is particularly attractive because it would employ the same reactor designs described above

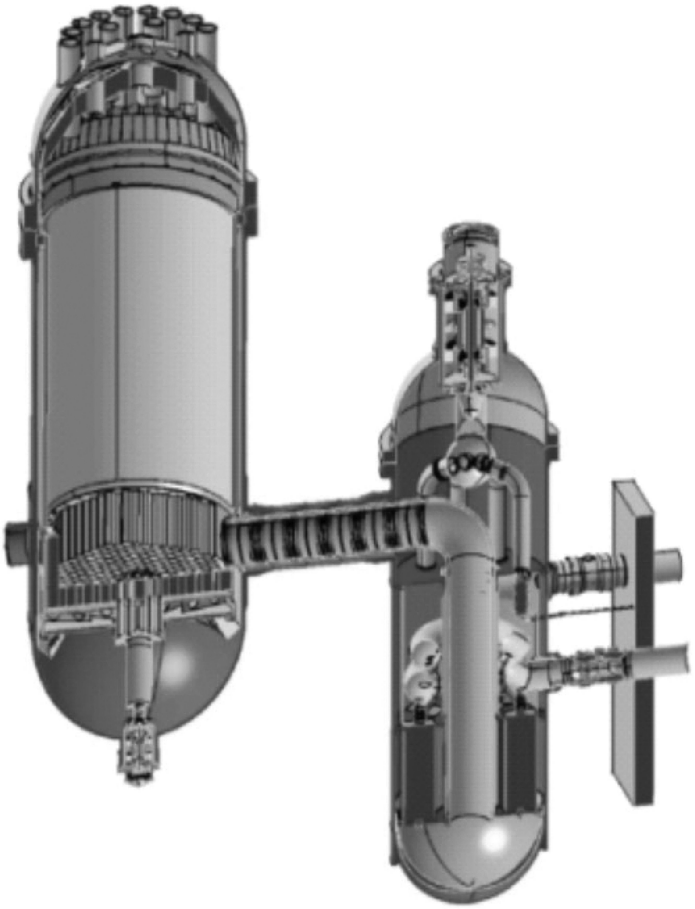

Figure 26.12 ANTARES. (Courtesy AREVA.)

with the same potential for highly efficient electricity, hydrogen production, and other process heat applications. The spent fuel remaining after a deep burn can be placed directly into long-term storage to provide containment of the residual radioactivity or further recycled in fast reactors once that technology is deployed on a large scale. Deep burn could rapidly and effectively reduce the inventory of TRU from spent fuel without the need for repeated recycles, precluding the possible weapons-related use of the residuals. Recent research and computer modeling at laboratories and universities around the world has confirmed the basic physics of the deep burn concept, but fuel testing needs to be performed.

26.3.3.2 Alternative Fuel Uranium is the most common fuel used in nuclear power production, but it is not the only one. Thorium exists in abundance in the earth's crust and can supply fuel for nuclear plants for decades, perhaps centuries. The only naturally occurring isotope of thorium, Th232, is not fissile, however, and thus cannot sustain a fission reaction. (Natural uranium is a mixture of 99.3% non-fissile U238 and 0.7% fissile U235. In a separation process called enrichment, the percentage of U235 can be increased to levels that can sustain a fission reaction, usually 3 to 5%). Instead, thorium must be added to a reactor containing a fissile isotope. In the neutron-rich environment of an operator reactor, thorium is converted into fissile U233, which can then be chemically separated from the unconverted thorium and burned.

Thorium fuel cycles have been used in power plants in the United States (Fort St. Vrain, Shippingport), Germany (THTR), and India. A fissioned U233 atom emits, on average, slightly more neutrons than does U235. This physical feature enabled the Shippingport reactor to breed more U233 fuel from thorium than it consumed during operation. Given the known reserves of uranium and thorium ore, nuclear fuel supplies are thus ensured to last for many centuries.

26.3.3.3 Advanced Coolants All of the HTR concepts so far discussed use helium as a coolant. Helium is chemically inert, neutronically transparent, and has good

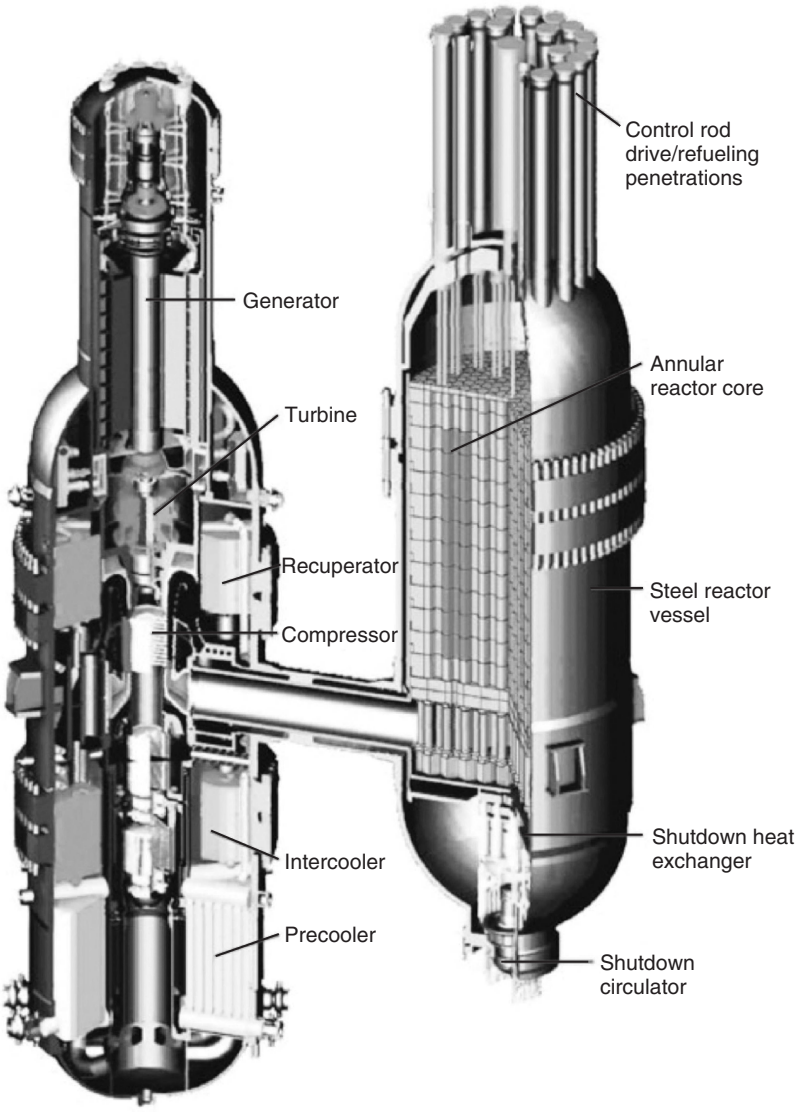

Figure 26.13 GT-MHR. (Courtesy General Atomics.)

heat transfer properties for a gas. Nonetheless, as a gas its ability to absorb and carry away nuclear heat is considerably less than liquids such as water or molten metal. Preliminary investigations have shown that certain liquid salts such as a mixture of lithium fluoride and beryllium fluoride (FLIBE) are compatible with HTR structural materials and are much better carriers of heat, as shown in Figure 26.16. An HTR using FLIBE as a working fluid can operate at a much higher power and lower system pressure because this coolant is far superior at transporting heat from the reactor core. Liquid salt coolants have their own challenges (salt chemistry must be carefully controlled to limit corrosion in the vessel) but have the potential to increase plant efficiency and reduce the probability of certain types of system failures. Although HTR design vendors have no current plans to use liquid salt coolants, they remain fertile territory for further research and development at labs and universities.

26.4 ROLE IN ENERGY PRODUCTION

The real benefit of HTRs lies in expanding nuclear energy beyond its traditional role in electricity production. For the past two decades, nuclear power from LWRs consistently supplied about 20% of U.S. electricity. LWRs are optimized for this market, and it is unlikely that HTRs will displace LWRs in this role. Expanded use of nuclear energy beyond the grid, however, can contribute significantly to the three inter-linked energy challenges that industry and U.S.

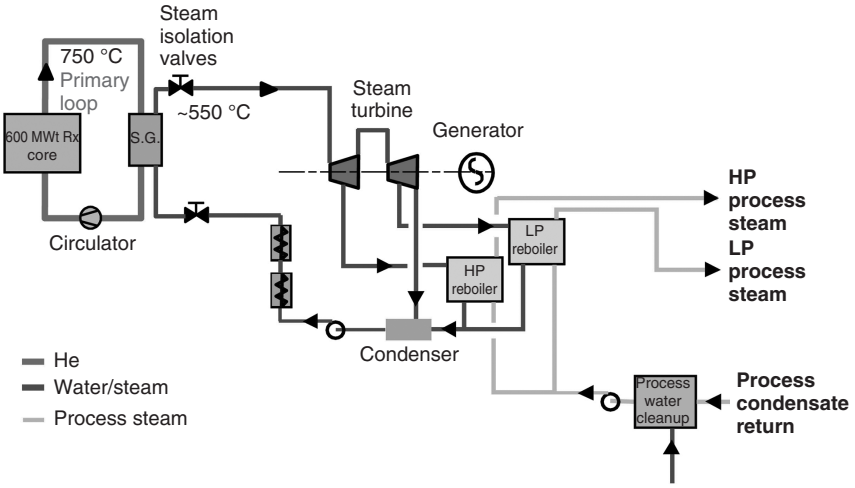

Figure 26.14 Proposed General Atomics HTGR cogeneration plant configuration. (Courtesy General Atomics.)

Figure 26.15 Transuranic components of spent nuclear fuel can be recycled in an HTR.

government face: the rising and volatile prices for premium fossil fuels such as oil and natural gas, dependence on foreign sources for these fuels, and the risks of climate change due to carbon emissions. Expanded use of nuclear energy could:

- Replace conventional fossil fuels by providing electricity for electric-powered vehicles.
- Generate high-temperature process heat, electricity, and valuable chemical feedstocks for the production of premium fuels and fertilizer products.
- Produce hydrogen for vehicles that utilize fuel cells.
- Provide clean water for human consumption by desalination and promote wastewater treatment using low-grade nuclear heat all the while dramatically reducing greenhouse gas emissions.

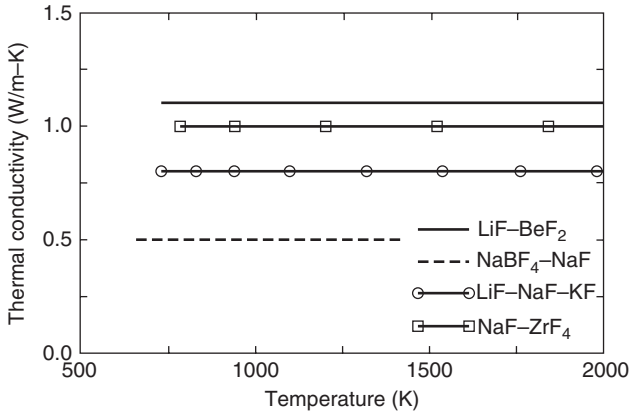

Figure 26.16 Comparison of thermal conductivity of candidate liquid salts (DOE).

Figure 26.17 provides a perspective of the energy picture in the United States in 2007. Nuclear energy provides 20% of electric power generation or about 8% of the total energy usage in the United States. A mature LWR technology operating at a maximum temperature of ~300°C could produce all of the nuclear electric power in the United States. Coal currently supplies 50% of the electricity in the United States and is responsible for 80% of the atmospheric emissions from the electricity sector. If all coal-fired power built before 1980 were replaced with nuclear energy, by 2050, greenhouse gas emissions from the electric power sector would be reduced to 60% of the current level. This task would require 270 new LWRs to replace approximately 850 existing coal facilities.

Table 26.1 lists the contributions of various sectors of the U.S. economy to total fossil fuel emissions and to total U.S. CO_2 emissions.

As seen in Table 26.1, there are many opportunities within the transportation and industrial sectors for nuclear energy to replace the use of fossil fuels, thereby eliminating

TABLE 26.1 CO_2 Emissions Percentages in Various U.S. Sectors

Sector	Total U.S. CO_2 Emissions (%)	CO_2 Emissions Caused by Direct Use of Fossil Fuel (%)
Transportation	33	33
Industrial	28	17
Residential and commercial	39	10

CO_2 emissions. However, the process heat needed for many petrochemical and other industrial processes require temperatures approaching 800°C, the range of HTR outlet temperatures. If all industrial coal and coke heating and 50% of industrial natural gas heating were replaced with heat from HTRs, greenhouse gas emissions from the industrial sector could be reduced to 28% below current levels by 2050.

Substantial reductions in CO_2 emissions (>95% reduction), significantly improved yields (over 250% increase over current process) in the liquids produced by the Fischer-Tropsch process, and reductions in reliance on foreign energy resources can be achieved by integrating HTRs with coal conversion processes such as gasification and coal-to-liquids (e.g., Fischer-Tropsch process) to produce transportation fuels and hydrocarbon feedstocks. Preliminary market analysis indicates that about 15 coal-to-liquids plants (each with an output of about 100,000 barrels per day) integrated with 480 modular HTRs can reduce U.S. oil imports by 25%.

For perspective, recent collaborative work with a major petrochemical company for one of its large facilities has indicated that six to ten modular HTRs would be required to meet the cogenerated steam, electricity, and other process heat needs for that facility. Thus far, evaluation of such potential applications has been shown

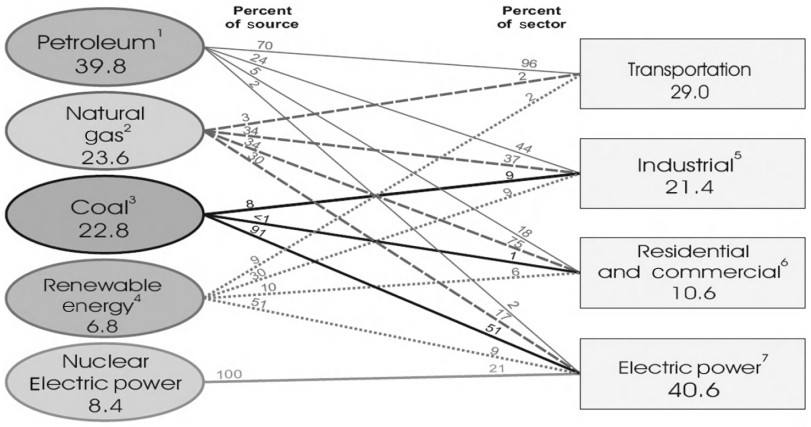

Figure 26.17 Primary U.S. energy consumption by source and sector in 2007 (Quadrillion BTU).

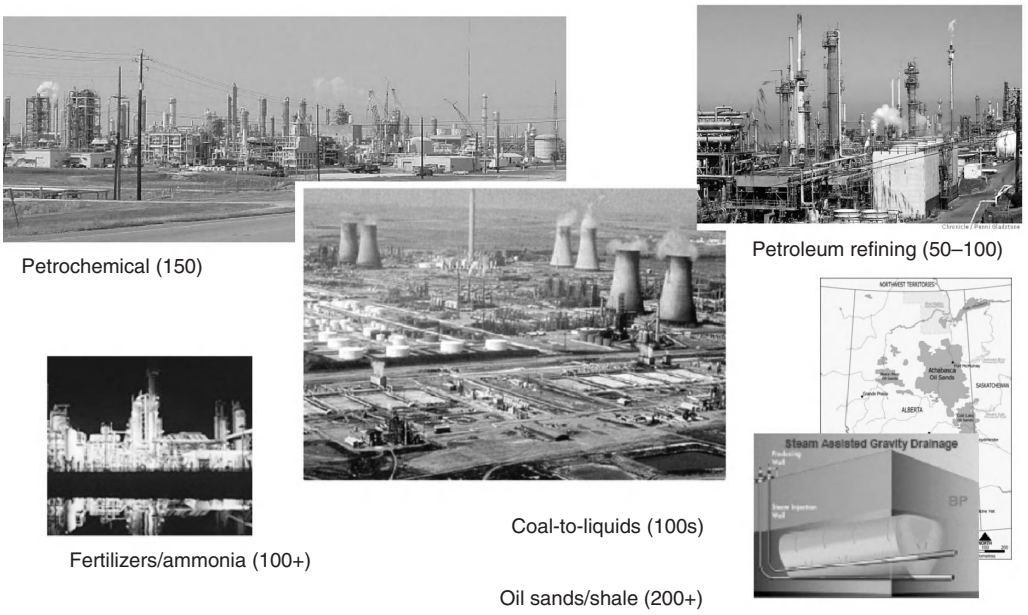

Figure 26.18 Potential industrial applications of HTR process heat and the number of HTRs needed to displace current fossil suppliers.

them to be economically viable. If the conversion of coal to hydrocarbon feedstocks and transportation fuels proves economically viable, as suggested by recent studies, several hundred additional modular HTGR reactors could be required as shown in Figure 26.18.

Coupling nuclear reactors to large chemical customers also poses daunting scientific challenges. Analysis of the interaction between nuclear reactor kinetics and the kinetics of the chemical plant will require more sophisticated computer models and more computing power than that previously used. In addition, developing efficient and robust methods for producing hydrogen will require an understanding of solid-gas interactions, corrosion, high-temperature molecular transport, and the slowly changing morphology of solid electrolytic cells. The examination of these cells already requires scanning and transmission electron microscopy, tunneling-imaging microscopy, x-ray, Auger and Raman spectroscopy to characterize the long-term operation of solid oxide cells and catalysts. The long-term application of massive amounts of heat and steam to fossil deposits will require an understanding of the behavior of geological formations in highly stressed circumstances.

In summary, the expanded use of nuclear energy would provide enhanced energy security by enabling deep reductions in oil and natural gas imports and substantially increasing the amount of liquid fuels produced from domestic fossil resources. Nuclear energy is the only technology that will allow the U.S. heavy manufacturing and transportation industries to reduce their emissions in a cost-effective manner while still using the current hydrocarbon supply infrastructure.

REFERENCES

1. A.J. Goodjohn, Summary of gas-cooled reactor programs. *Energy*, 1991, **16**, 1/2, 79–106.
2. VDI-Verlag GmbH, AVR—experimental high-temperature reactor—twenty one years of successful operation for a future energy technology. *The Society for Energy Technologies*, 1990.
3. Z. Zhong and Z. Qin, Overview of the 10 MW high-temperature gas-cooled reactor test module. *Proceedings of the Seminar on HTGR Application and Development, Beijing, China (PRC)*, March 2001.
4. G. Lohnert (Ed.), Japan's HTTR. *Nuclear Engineering and Design*, October 2004, **233**, 1–3.
5. J.W. Simpson, *Nuclear Power from Underseas to Outer Space*. La Grange Park, IL.: American Nuclear Society, 1995, p. 467.
6. G.H. Lohnert and H. Reutler, The modular HTR—a new design of high-temperature pebble-bed reactor. *Nuclear Energy*, June 1983, **22**, 3, 197–200.
7. M. Simnad, The modular HTGR: its possible role in the use of safe and benign nuclear power. *Proceedings of the International Conference on Global Climate Change: Its Mitigation Through Improved Production and Use of Energy*, American Institute of Physics, Los Alamos, NM, October 1991, 307–321.
8. P.M. Williams, T.L. King, and J.N. W, PROJ0672 NUREG-1338 1989-03-31 2007-03-07 NUREG-1338, *Draft Preapplication Safety Evaluation Report for the Modular High-Temperature Gas-Cooled Reactor*, U.S. Nuclear Regulatory Commission Office of Nuclear Regulatory Research,
9. J. Gauthier, G. Brinkmann, B. Copsey, and M. Lecomte, ANTARES: the HTR/VHTR project at Framatome ANP. *Nuclear Engineering and Design*, March 2006, **236**, 526–533.

27

SUPERCRITICAL WATER REACTOR

JAMES R. WOLF

Idaho National Laboratory, Idaho Falls, ID, USA

27.1 INTRODUCTION

The Gen–IV supercritical water-cooled reactor (SCWR) concept is extremely promising as a nuclear power reactor because of its high thermal efficiency (i.e., about 45% vs. about 33% efficiency for current light-water reactors, LWRs) and considerable plant simplification [1]. SCWRs are basically LWRs operating at higher pressure and temperatures with a direct once-through cycle. The increase in overall thermodynamic efficiency is due to the high-temperature, high-pressure reactor operating conditions that are above thermodynamic critical point of water (374°C, 22.1 MPa or 705°F, 3208 psia).

The main mission of the SCWR is generation of base load electricity. The SCWR concept builds upon two proven technologies: LWRs, which are the most commonly deployed nuclear power generating reactors in the world, and supercritical fossil-fired boilers. It should be noted that almost all new fossil-fired boilers operate in the supercritical thermodynamical range. A typical SCWR, depending on the exact core design, will have a predominantly thermal neutron spectrum with light-water moderation.

The major components that make up a typical SCWR are shown in Figure 27.1 [2].

The key advantages to the SCWR concept include the following:

- Base load electrical operation.
- Significant increases in thermal efficiency can be achieved relative to current generation light-water reactors (LWRs). Estimated efficiencies for SCWRs are in the range of 44–45% compared to 32–34% for state-of-the-art LWRs.
- Direct cycle.
- Thermal spectrum with light-water coolant (and moderator) with low-enriched uranium oxide fuel.
- The higher enthalpy content of supercritical water results in a much lower coolant mass flow rate per unit core thermal power. This leads to a reduction in the reactor coolant pumping power and smaller or fewer steam lines due to lower steam mass flow rates and higher steam density.
- A lower coolant mass inventory results from the reduced size of the system. This results in lower containment loadings during a design basis loss of coolant accident (LOCA) and the ability to utilize smaller containment buildings.
- No boiling or core phase change eliminates concerns about departure from nucleate boiling or dry out during normal operation.
- Because the coolant does not undergo a change of phase, the need for steam dryers, steam separators, recirculation and jet pumps, as well as steam generators, is eliminated.

The elimination of several major components that are found in other reactor designs, such as LWRs and boiling water reactor reactors (BWR), results in a considerable amount of plant simplification and containment volume reduction.

Nuclear Energy Encyclopedia: Science, Technology, and Applications, First Edition (Wiley Series On Energy).
Edited by Steven B. Krivit, Jay H. Lehr, and Thomas B. Kingery.

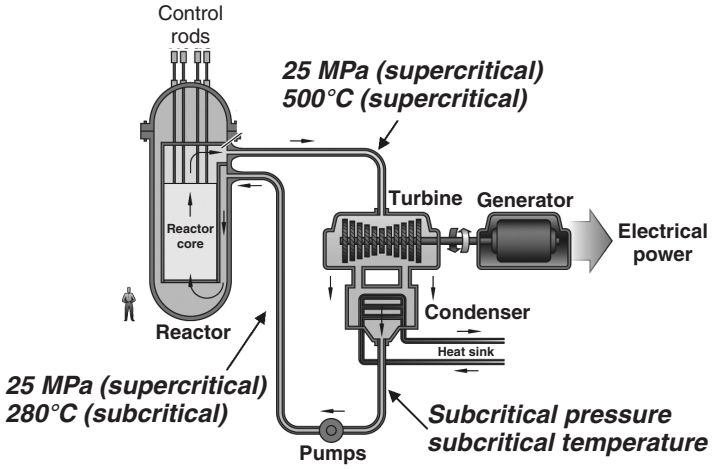

Figure 27.1 Primary components of an SCWR.

27.2 TYPICAL SCWR REFERENCE DESIGN

A typical SCWR reference design is a direct cycle, thermal spectrum, light-water-cooled and moderated reactor with an operating pressure of 25 MPa and inlet/outlet coolant temperature of 280/500°C [3]. The reference power is 3575 MWt, the net electric power is 1600 MWe, and the thermal efficiency is 44.8%. The fuel is low-enriched uranium oxide and the plant is designed primarily for base-load electrical operation. Typical SCWR Reference Design Parameter Values are contained in Table 27.1.

During normal operation, the inlet flow splits, partly to a down-comer and partly to a plenum at the top of the reactor pressure vessel, to flow downward through the core in special water or solid moderator rods to the inlet plenum. This strategy is employed to provide good moderation at the top of the core, where the coolant density is only about 15-20% that of liquid water.

The SCWR uses a power conversion cycle similar to that used in supercritical fossil-fired plants and consists of high-, intermediate-, and low-pressure turbines employed with one moisture-separator reheater and up to eight feedwater heaters.

TABLE 27.1 Typical SCWR Reference Design Parameter Values

Parameter	Value
Thermal power	3575 MWt
Net electric power	1600 MWe
Net thermal efficiency	44.8%
Operating pressure	25 MPa
Reactor inlet temperature	280°C
Reactor outlet temperature	500°C
Reactor flow rate	1843 kg/s
Plant lifetime	60 years

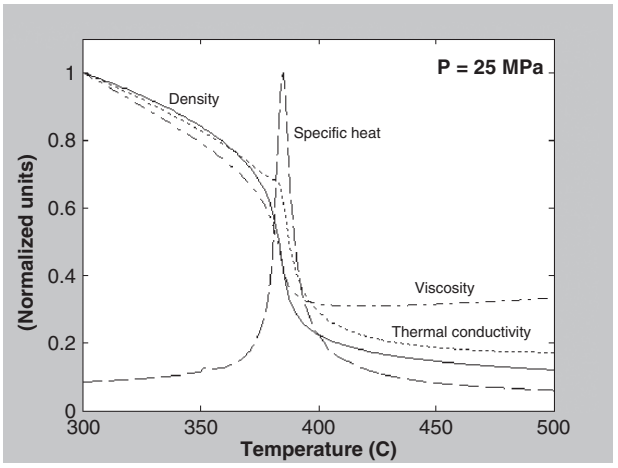

Figure 27.2 Thermo-physical variation of water properties at constant supercritical pressure.

27.3 SUPERCRITICAL OPERATION

Operation above the critical pressure eliminates coolant boiling, so the coolant remains single-phase throughout the system. In a typical SCWR reactor system, pressure is maintained at 25 MPa; the coolant enters the reactor core at subcritical temperature of 280°C and exits at supercritical temperature of 500°C or higher depending on design.

The variation of the thermo-physical properties of water over the typical SCWR operating temperature range and at a pressure of 25 MPa is shown in Figure 27.2. Note that the property variation is rather dramatic, albeit continuous. The "transition" occurs about the so-called pseudo-critical temperature, which is 385°C; the reference SCWR pressure is 25 MPa [4].

It is important to point out that the thermal characteristics of the SCWR are unique. The large temperature gradient

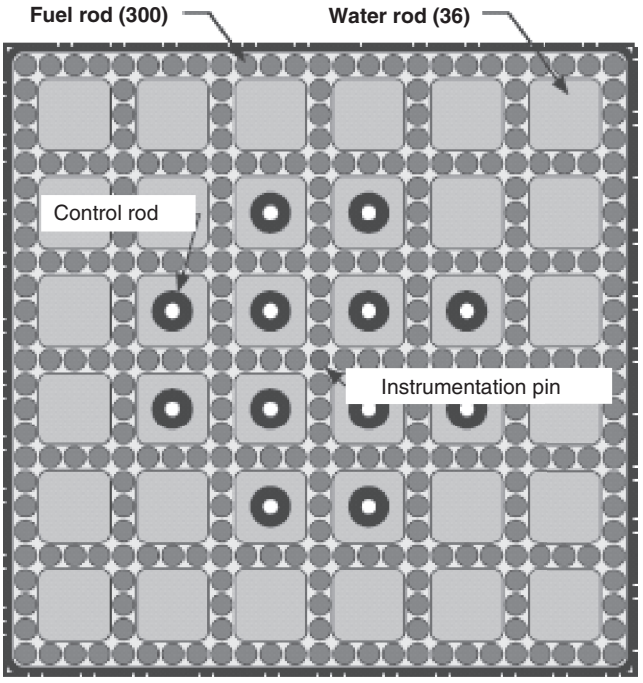

Figure 27.3 Typical reference core design.

in the core is associated with significant density decrease (from about 760 kg/m^3 at the core inlet to about 90 kg/m^3 at the core outlet). The low coolant density in the upper part of the core requires additional engineered features to enhance the moderation. In reactor-vessel-type SCWRs, this is accommodated via water rods in which the cold coolant flows down, or via solid moderator rods as shown by the core illustration in Figure 27.3 [3].

27.4 SCWR RESEARCH AREAS

There are a number of key technical issues that must be addressed through an active research and development program before an actual SCWR can be built. These issues include the following:

- Materials
  - Structural
  - Cladding
- Thermal hydraulics
  - Tube bundle heat transfer
  - Data for critical (or choked) flow at supercritical conditions

In the area of needed materials research and development, the identification of appropriate chemistry and materials for the SCWR structural and cladding systems is the primary key challenge for the establishment of viability for this reactor. Currently, there is little on the general behavior of any candidate materials in supercritical water. Below the pseudo-critical temperature, the density and chemistry of supercritical water is similar to water in conventional light-water nuclear plants. However, at the pseudo-critical point, the water properties change rapidly, and around this point the effects on materials are less known. It is speculated that above the pseudo-critical point corrosion is similar to behavior in gas.

Specifically, materials structural and cladding data is needed in the areas of [5]:

- Oxidation.
- Corrosion and stress corrosion cracking.
- Radiolysis and water chemistry.
- Strength, embitterment, and creep resistance.
- Dimensional and micro structural stability.

In the area of thermal hydraulics, existing thermal-hydraulic correlations and models and codes commonly used for safety analysis of LWR systems are not validated for water at supercritical conditions. Simulation of nuclear reactors cooled by supercritical water is made inherently more complicated by the large variation of the thermodynamic and transport properties over the pressure and temperature range of interest. Supercritical-water thermal-hydraulics is also fundamentally different from two-phase flow thermal-hydraulics due to lack of interfaces with surface tension and because the variation of the properties is continuous, albeit large, for a supercritical fluid, while discontinuous for a two-phase fluid. For these reasons, the heat transfer, critical flow, and other correlations and models used by the LWR codes are not generally applicable to supercritical conditions.

There is also a lack of data for critical (or choked) flow at supercritical conditions. Critical (or choked) flow phenomena are of great importance in designing/operating the reactor safety/relief valves and the automatic depressurization system as well as in the analysis of loss of coolant accident (LOCA) events.

27.5 SUMMARY

Overall, the SCWR concept has great potential for future high-efficiency base-load electrical generation. However, there are several key technical issues that still need to be resolved before a prototype can be developed and deployed.

These issues include:

- Suitable material for structures and cladding has not been identified.
- Heat transfer and critical flow data still needed at supercritical-water conditions.

REFERENCES

1. Generation IV International Forum (GIF), *A Technology Roadmap for the Generation IV Nuclear Energy Systems*, Issued by the U.S. DOE Nuclear Research Advisory Committee and the Gen IV International Forum, December 2002, Report No. GIF-002-00, 2002.
2. J. Buongiorno and P. MacDonald, *Supercritical Water Reactor (SCWR), Progress Report for the FY-03 Generation-IV R&D Activities for the Development of the SCWR in the U.S.*, INEEL/EXT-03-01210. Idaho National Engineering and Environmental Laboratory, September 2003.
3. J. Buongiorno and P. MacDonald, *Feasibility Study of Supercritical Light Water Cooled Reactors for Electric Power Production*, INEEL/EXT- 04–02530. Idaho National Engineering and Environmental Laboratory, January 2005.
4. I. Pioro and R. Duffey, Heat transfer and hydraulic resistance at supercritical pressures in power engineering applications, in *Physical Properties of Fluids in Critical and Pseudocritical Regions*. ASME Press, New York, 2007, pp. 8–16.
5. J. Buongiorno, *Supercritical Water Reactor (SCWR) Survey of Materials Experience and R&D Needs to Assess Viability*, INEEL/EXT-03-00693. Idaho National Engineering and Environmental Laboratory, September 2003.

28

THE POTENTIAL USE OF SUPERCRITICAL WATER-COOLING IN NUCLEAR REACTORS

DR. IGOR PIORO

Faculty of Energy Systems and Nuclear Science, University of Ontario Institute of Technology, Oshawa, Ontario, Canada

Prior to a general discussion on Supercritical Water-cooled nuclear Reactor (SCWR) concepts, it is important to define special terms and expressions used at these conditions. For better understanding these terms and expressions several figures (Figs. 28.1–28.6) and tables (Tables 28.1–28.3) are shown below.

28.1 DEFINITIONS OF SELECTED TERMS AND EXPRESSIONS RELATED TO CRITICAL AND SUPERCRITICAL REGIONS

Compressed fluid is a fluid at a pressure above the critical pressure, but at a temperature below the critical temperature (see Fig. 28.1).

Critical point (also called a *critical state*) is a point in which the distinction between the liquid and gas (or vapor) phases disappears, i.e., both phases have the same temperature, pressure, and volume or density (see Fig. 28.1). The *critical point* is characterized by the phase-state parameters T_{cr}, P_{cr}, and V_{cr} (or ρ_{cr}), which have unique values for each pure substance (see Table 28.1).

Deteriorated Heat Transfer (DHT) is characterized with lower values of the wall heat transfer coefficient compared to those at the normal heat transfer, and hence has higher values of wall temperature within some part of a test section or within the entire test section (see Fig. 28.2).

Improved Heat Transfer (IHT) is characterized with higher values of the wall heat transfer coefficient compared to those at the normal heat transfer, and hence has lower values of wall temperature within some part of a test section or within the entire test section. In our opinion, the improved heat-transfer regime or mode includes peaks or "humps" in the heat transfer coefficient near the critical or pseudo-critical points (see Fig. 28.2).

Near-critical point is actually a narrow region around the critical point, where all thermo-physical properties of a pure fluid exhibit rapid variations (see Fig. 28.4).

Normal Heat Transfer (NHT) can be characterized in general with wall heat transfer coefficients similar to those of subcritical convective heat transfer far from the critical or pseudo-critical regions, when are calculated according to the conventional single-phase Dittus-Boelter-type correlations: $\mathbf{Nu} = 0.023\ \mathbf{Re}^{0.8}\mathbf{Pr}^{0.4}$ (see Fig. 28.2).

Pseudo-boiling is a physical phenomenon similar to subcritical pressure nucleate boiling, which may appear at supercritical pressures. Due to heating of supercritical fluid with a bulk-fluid temperature below the pseudo-critical temperature (high-density fluid, i.e., "liquid"), some layers near a heating surface may attain temperatures above the pseudo-critical temperature (low-density fluid, i.e., "gas") (see Figs. 28.1 and 28.3a). This low-density "gas" leaves the heating surface in the form of variable density (bubble) volumes. During the pseudo-boiling, the wall heat transfer coefficient usually increases (improved heat-transfer regime).

Nuclear Energy Encyclopedia: Science, Technology, and Applications, First Edition (Wiley Series On Energy).
Edited by Steven B. Krivit, Jay H. Lehr, and Thomas B. Kingery.

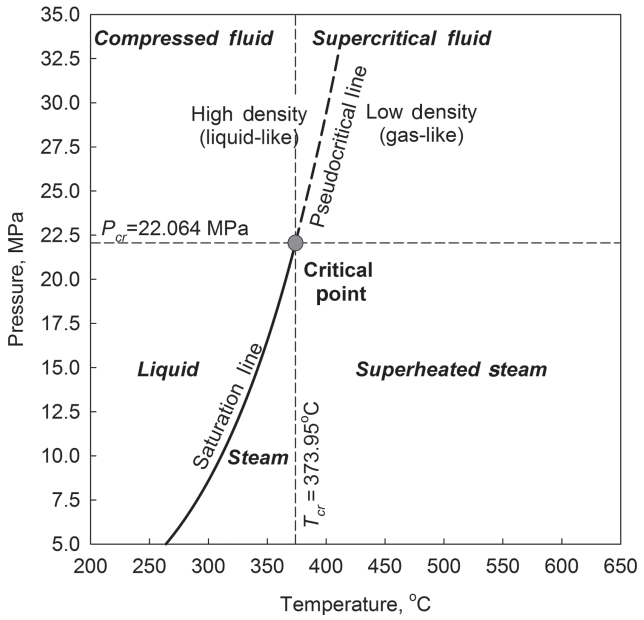

Figure 28.1 Pressure–Temperature diagram for water.

Pseudo-critical line is a line that consists of pseudo-critical points (see Fig. 28.1).

Pseudo-critical point (characterized with P_{pc} and T_{pc}) is a point at a pressure above the critical pressure and at a temperature ($T_{pc} > T_{cr}$) corresponding to the maximum value of the specific heat at this particular pressure (see Figs. 28.1, 28.3e, 28.5, and Tables 28.2 and 28.3).

Pseudo-film boiling is a physical phenomenon similar to subcritical-pressure film boiling, which may appear at supercritical pressures. At pseudo-film boiling, a low-density fluid (a fluid at temperatures above the pseudo-critical temperature, i.e., "gas" (see Figs. 28.1 and 28.3a)) prevents a high-density fluid (a fluid at temperatures below the pseudo-critical temperature, i.e., "liquid") from contacting ("rewetting") a heated surface. Pseudo-film boiling leads to the deteriorated heat-transfer regime.

Supercritical fluid is a fluid at pressures and temperatures that are higher than the critical pressure and critical temperature (see Fig. 28.1). However, in the present chapter, the term *supercritical fluid* includes both terms—a *supercritical fluid* and *compressed fluid*.

Supercritical "steam" is actually supercritical water, because at supercritical pressures fluid is considered as a single-phase substance. However, this term is widely (and incorrectly) used in the literature in relation to supercritical "steam" generators and turbines.

Superheated steam is a steam at pressures below the critical pressure, but at temperatures above the critical temperature (see Fig. 28.1).

28.2 THERMOPHYSICAL PROPERTIES AT CRITICAL AND PSEUDOCRITICAL PRESSURES

General trends of various properties near the critical and pseudo-critical points (Pioro, 2008; Pioro and Duffey, 2007) can be illustrated on a basis of those of water. Figure 28.3 shows variations in basic thermo-physical properties of water at the critical ($P_{cr} = 22.064$ MPa) and three supercritical pressures ($P = 25.0$, 30.0, and 35.0 MPa) (also, in addition see Fig. 28.4). Thermo-physical properties of water and other 83 fluids and gases

TABLE 28.1 Critical Parameters of Selected Fluids (Pioro and Duffey, 2007)

Fluid	P_{cr}, MPa	T_{cr}, °C	ρ_{cr}, kg/m^3
Ammonia (NH_3)	11.333	132.25	225.0
Argon (Ar)	4.863	−122.46	535.6
Carbon dioxide (CO_2)	7.3773	30.978	467.6
Ethanol (C_2H_6O)	6.15	240.8	276.0
Freon-12 (Di-chloro-di-fluoro-methane, CCl_2F_2)	4.1361	111.97	565.0
Freon-13B1 (Bromo-tri-fluoro-methane, $CBrF_3$)	3.95	67.0	770.0
Freon-22 (Chloro-di-fluoro-methane, $CHClF_2$)	4.99	96.145	523.84
Freon-114a (1,1-Dichlorotetrafluoroethane, $C_2Cl_2F_4$)	3.257	145.68	579.97
Freon-134a (1,1,1,2-tetrafluoroethane, CH_2FCF_3)	4.0593	101.06	511.9
Helium (He)	0.22746	−267.95	69.641
Hydrogen (H_2)	1.315	−239.96	30.118
Methanol (CH_4O)	8.1035	239.45	275.56
Nitrogen (N_2)	3.3958	−146.96	313.3
Oxygen (O_2)	5.043	−118.57	436.14
Water (H_2O)	22.064	373.95	322.39

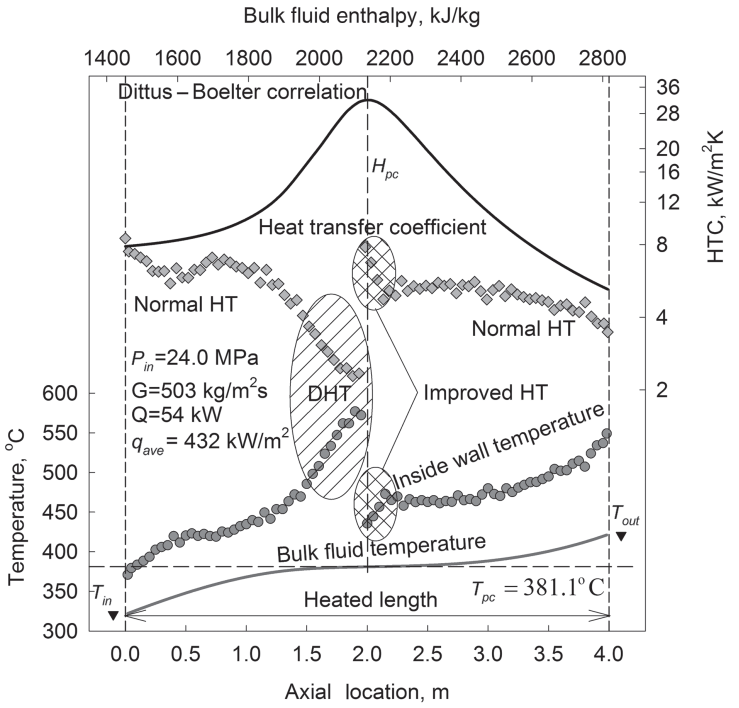

Figure 28.2 Temperature and heat-transfer-coefficient profiles along heated length of vertical circular tube (data by Dr. Kirillov et al., IPPE, Obnisk, Russia): Water, inside diameter 10 mm and heated length 4 m.

at different pressures and temperatures, including critical and supercritical regions, can be calculated using the NIST REFPROP software (2010).

At the critical and supercritical pressures, a fluid is considered as a single-phase substance (Clifford, 1999), in spite of the fact that all thermo-physical properties undergo significant changes within the critical and pseudo-critical regions. Near the critical point, these changes are dramatic (see Fig. 28.3). In the vicinity of pseudo-critical points, with an increase in pressure, these changes become less pronounced (see Figs. 28.3 and 28.6).

Also, it can be seen that properties such as density and dynamic viscosity undergo a significant drop (near the critical point this drop is almost vertical) within a very narrow temperature range (see Figs. 28.3a, b and 28.4), while the kinematic viscosity and specific enthalpy undergo a sharp increase (see Figs. 28.3d, g and 28.4). The volume expansivity, specific heat, thermal conductivity, and Prandtl number have peaks near the critical and pseudo-critical points (see Figs. 28.3c, e, f, h, 28.4 and 28.5). Magnitudes of these peaks decrease very quickly with an increase in pressure (see Fig. 28.6). Also, "peaks" transform into "hump" profiles at pressures beyond the critical pressure. It should be noted that the dynamic viscosity, kinematic viscosity, and thermal conductivity undergo through the minimum right after the critical and pseudo-critical points (see Fig. 28.3b, d, f).

The specific heat of water (as well as of other fluids) has the maximum value at the critical point (see Fig. 28.3e). The exact temperature that corresponds to the specific-heat peak above the critical pressure is known as the pseudo-critical temperature (see Fig. 28.1 and Table 28.2). At pressures approximately above 300 MPa (see Fig. 28.6) a peak (here it is better to say "a hump") in specific heat almost disappears, therefore, such term as a *pseudo-critical point* does not exist anymore. The same applies to the *pseudo-critical line*. It should be noted that peaks in the thermal conductivity and volume expansivity may not correspond to the pseudo-critical temperature (see Table 28.3 and Figure 28.5).

In early studies, i.e., approximately before 1990, a peak in thermal conductivity was not taken into account. Later, this peak was well established (see Fig. 28.3f) and included in thermo-physical data and software. The peak in thermal conductivity diminishes at about 25.5 MPa for water (see Fig. 28.3f and Table 28.3).

In general, crossing the pseudo-critical line from left to right (see Fig. 28.1) is quite similar to crossing the saturation line from liquid into vapor. The major difference in crossing these two lines is that all changes (even drastic variations) in thermo-physical properties at supercritical pressures are gradual and continuous, taking place within a certain temperature range. On the contrary, at subcritical pressures, we have properties discontinuing on the saturation line: one value for liquid and another

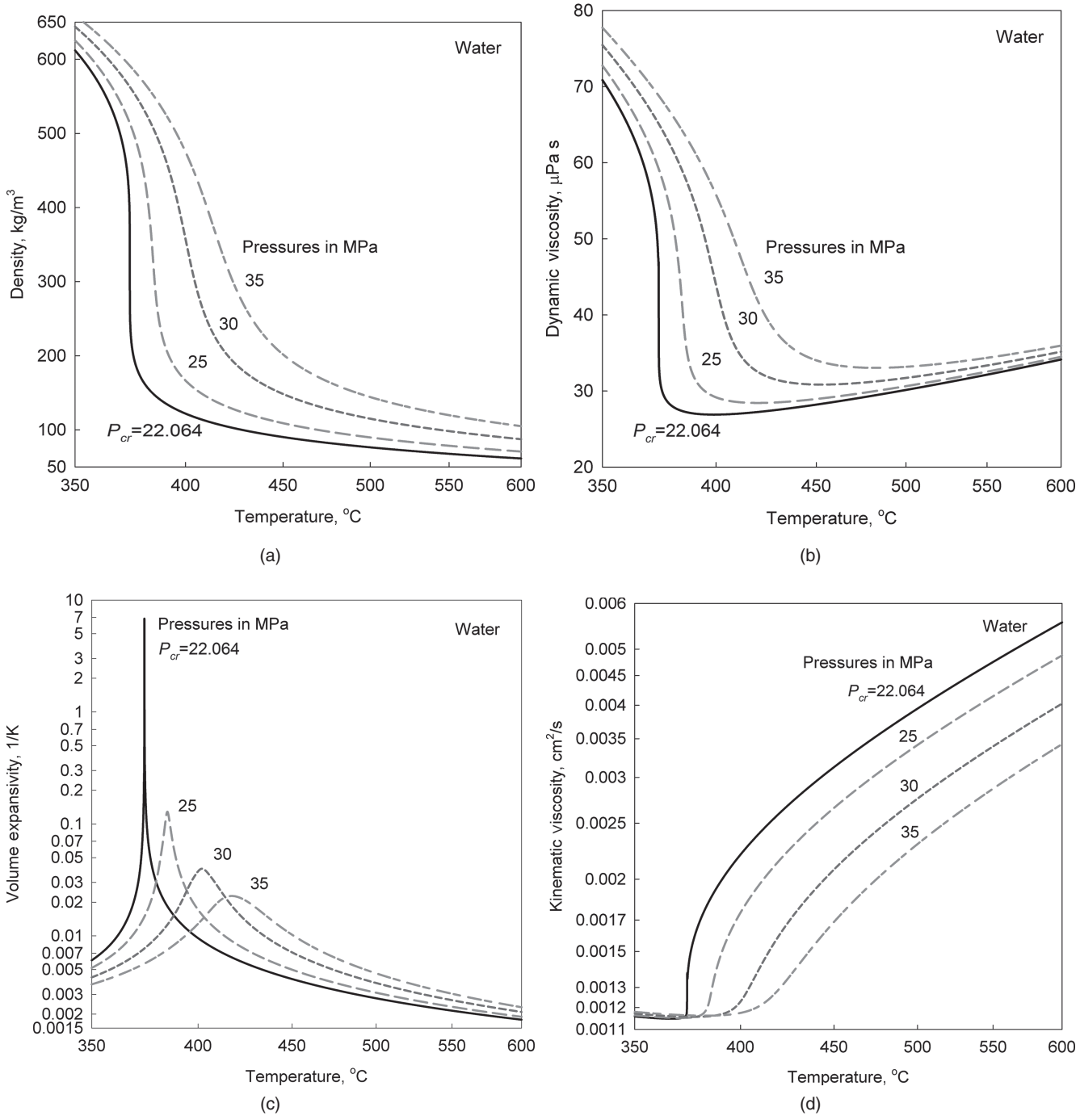

Figure 28.3 (a) Density vs. Temperature: Water. (b) Dynamic viscosity vs. Temperature: Water. (c) Volume expansivity vs. Temperature: Water. (d) Kinematic viscosity vs. Temperature: Water. (e) Specific heat vs. Temperature: Water. (f) Thermal conductivity vs. Temperature: Water. (g) Specific enthalpy vs. Temperature: Water. (h) Prandtl number vs. Temperature: Water.

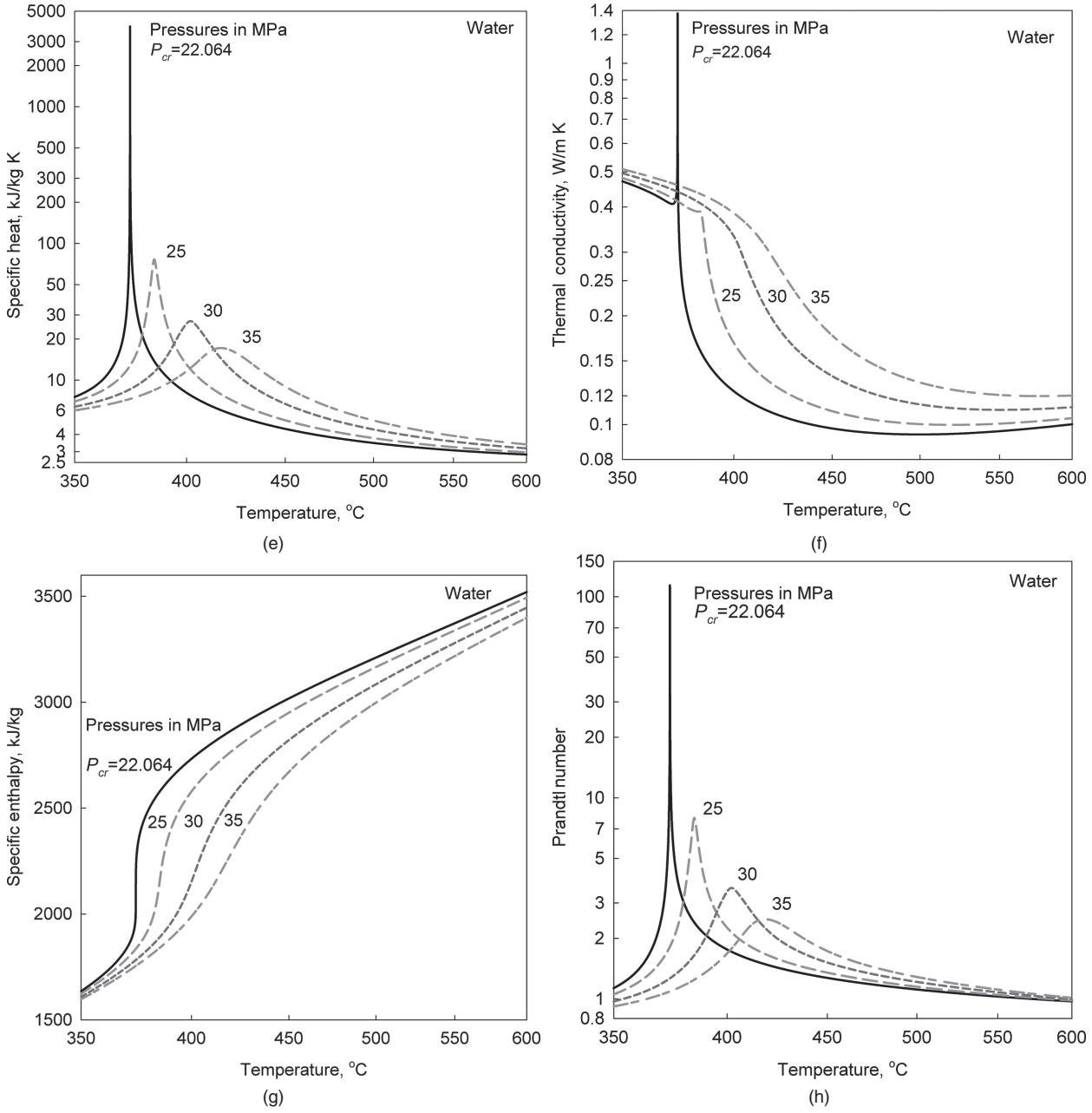

Figure 28.3 (*Continued*)

for vapor. Therefore, supercritical fluids behave as single-phase substances. Also, dealing with supercritical fluids, we apply usually a term "*pseudo*" in front of a *critical point, boiling, film boiling*, etc.

28.3 HISTORICAL NOTE ON USE OF SUPERCRITICAL PRESSURES AND FLUIDS

The use of supercritical fluids in different processes is not new and was not invented by humans. Mother Nature has been processing minerals in aqueous solutions at near or above the critical point of water for billions of years (Levelt Sengers, 2000). Scientists only started using this natural process, called hydrothermal processing, in their labs in the late 1800s for creating various crystals. During the last 50 to 60 years, this process (operating parameters—water pressures from 20 to 200 MPa and temperatures from 300 to 500°C) has been widely used in the industrial production of high-quality single crystals (mainly gemstones) such as quartz, sapphire, titanium oxide, tourmaline, zircon, and others.

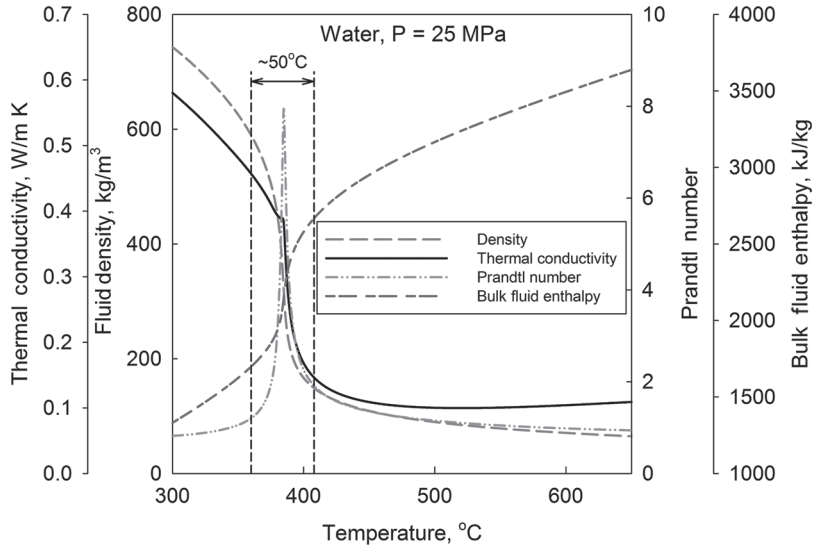

Figure 28.4 Variations of selected thermophysical properties of water near pseudocritical point: Pseudocritical region at 25 MPa is about ~50°C.

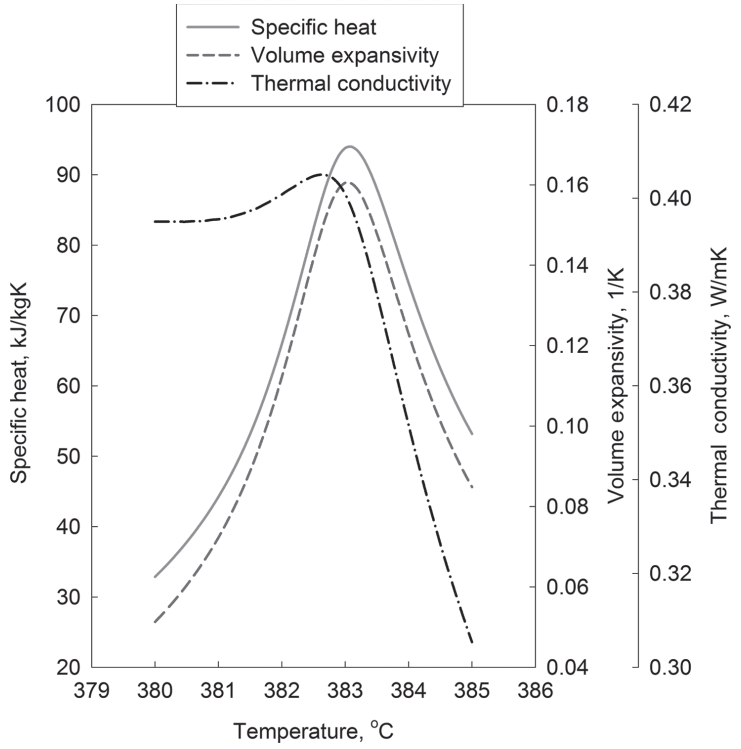

Figure 28.5 Specific heat, volume expansivity and thermal conductivity vs. temperature: Water, $P = 24.5$ MPa.

The first works devoted to the problem of heat transfer at supercritical pressures started as early as the 1930s. Schmidt and his associates investigated free-convection heat transfer of fluids at the near-critical point with the application to a new effective cooling system for turbine blades in jet engines. They found that the free convection heat-transfer coefficient at the near-critical state was quite high and decided to use this advantage in single-phase thermosyphons with an intermediate working fluid at the near-critical point (Pioro and Pioro, 1997).

In the 1950s, the idea of using supercritical water appeared to be rather attractive for thermal power industry.

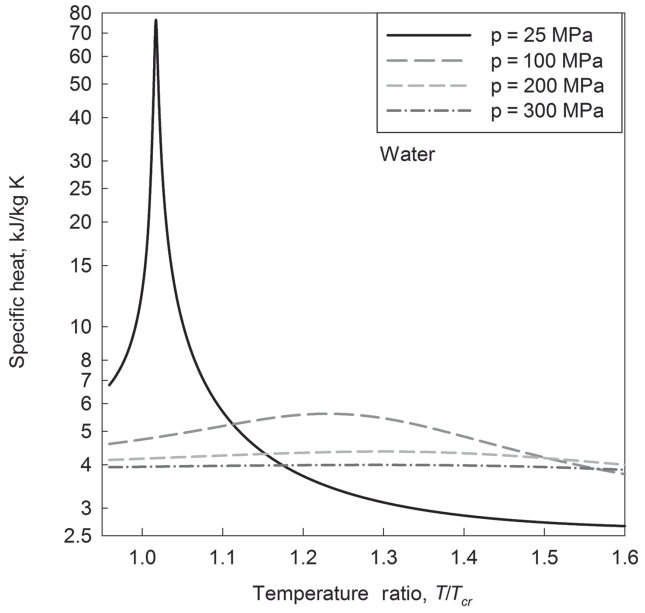

Figure 28.6 Specific heat variations at various supercritical pressures: Water.

TABLE 28.2 Values of Pseudocritical Temperature and Corresponding Peak Values of Specific Heat within Wide Range of Pressures

Pressure, MPa	Pseudo-Critical Temperature, °C	Peak Value of Specific Heat, kJ/kg·K
23	377.5	284.3
24	381.2	121.9
25	384.9	76.4
26	388.5	55.7
27	392.0	43.9
28	395.4	36.3
29	398.7	30.9
30	401.9	27.0
31	405.0	24.1
32	408.1	21.7
33	411.0	19.9
34	413.9	18.4
35	416.7	17.2

The objective was to increase the total thermal efficiency of coal-fired power plants. At supercritical pressures, there is no liquid-vapor phase transition; therefore, there is no such phenomenon as Critical Heat Flux (CHF) or dryout. Only within a certain range of parameters may a deteriorated heat transfer occur. Work in this area was mainly performed in the former USSR and in the United States in the 1950s through 1980s (*International Encyclopedia of Heat & Mass Transfer*, 1998).

In general, the total thermal efficiency of modern thermal power plants with subcritical-parameters steam generators is about 36 to 38%, but reaches 45 to 50% with supercritical parameters, i.e., with a "steam" pressure of 23.5–26 MPa and inlet turbine temperature of 535–585°C, thermal efficiency is about 45% and even higher at ultra-supercritical parameters (25–35 MPa and 600–700°C).

At the end of the 1950s and the beginning of the 1960s, early studies were conducted to investigate the possibility of using supercritical water in nuclear reactors (Pioro and Duffey, 2007). Several designs of nuclear reactors using supercritical water were developed in Great Britain, France, the United States, and the former USSR. However, this idea was abandoned for almost 30 years with the emergence of Light Water Reactors (LWRs) and regained interest in the 1990s following LWRs' maturation.

Use of supercritical water in power-plant steam generators is the largest application of a fluid at supercritical pressures in industry. However, other areas exist in which supercritical fluids are used or will be implemented in the near future (Pioro and Duffey, 2007; Levelt Sengers, 2000; Clifford, 1999):

- Using supercritical carbon-dioxide Brayton cycle for Generation-IV Sodium Fast Reactors (SFRs), Lead-cooled Fast Reactors (LFRs) (see Fig. 28.7) and High Temperature helium-cooled thermal Reactors (HTRs).
- Using supercritical carbon dioxide for cooling printed circuits.
- Using near-critical helium to cool coils of superconducting electromagnets, superconducting electronics, and power-transmission equipment.
- Using supercritical hydrogen as a fuel for chemical and nuclear rockets.
- Using supercritical methane as a coolant and fuel for supersonic transport.
- Using liquid hydrocarbon coolants and fuels at supercritical pressures in cooling jackets of liquid rocket engines and in fuel channels of air-breathing engines.
- Using supercritical carbon dioxide as a refrigerant in air-conditioning and refrigerating systems.
- Using a supercritical cycle in the secondary loop for transformation of geothermal energy into electricity.
- Using SuperCritical Water Oxidation (SCWO) technology for treatment of industrial and military wastes.
- Using carbon dioxide in the Supercritical Fluid Leaching (SFL) method for removal uranium from radioactive solid wastes and in decontamination of surfaces.
- Using supercritical fluids in chemical and pharmaceutical industries in such processes as supercritical fluid

TABLE 28.3 Peak Values of Specific Heat, Volume Expansivity and Thermal Conductivity in Critical and Near Pseudo-Critical Points

Pressure, MPa	Pseudocritical Temperature, °C	Temperature, °C	Specific Heat, kJ/kg·K	Volume Expansivity, 1/K	Thermal Conductivity, W/m·K
$p_{cr} = 22.064$	$t_{cr} = 374.1$	—	∞	∞	∞
22.5	375.6	—	690.6	1.252	0.711
23.0	—	377.4	—	—	0.538
	377.5	—	284.3	0.508	—
23.5	—	379.2	—	—	0.468
	—	379.3	—	0.304	—
	379.4	—	171.9	—	—
24.0	—	381.0	—	—	0.429
	381.2	—	121.9	0.212	—
24.5	—	382.6	—	—	0.405
	—	383.0	—	0.161	—
	383.1	—	93.98	—	—
25.0	—	384.0	—	—	0.389
	384.9	—	76.44	—	—
	—	385.0	—	0.128	—
25.5	386.7	—	64.44	0.107	no peak
26.0	388.5	—	55.73	0.090	0.355
27.0	392.0	—	43.93	0.069	0.340
28.0	395.4	—	36.29	0.056	0.329
29.0	398.7	—	30.95	0.046	0.321
30.0	401.9	—	27.03	0.039	0.316

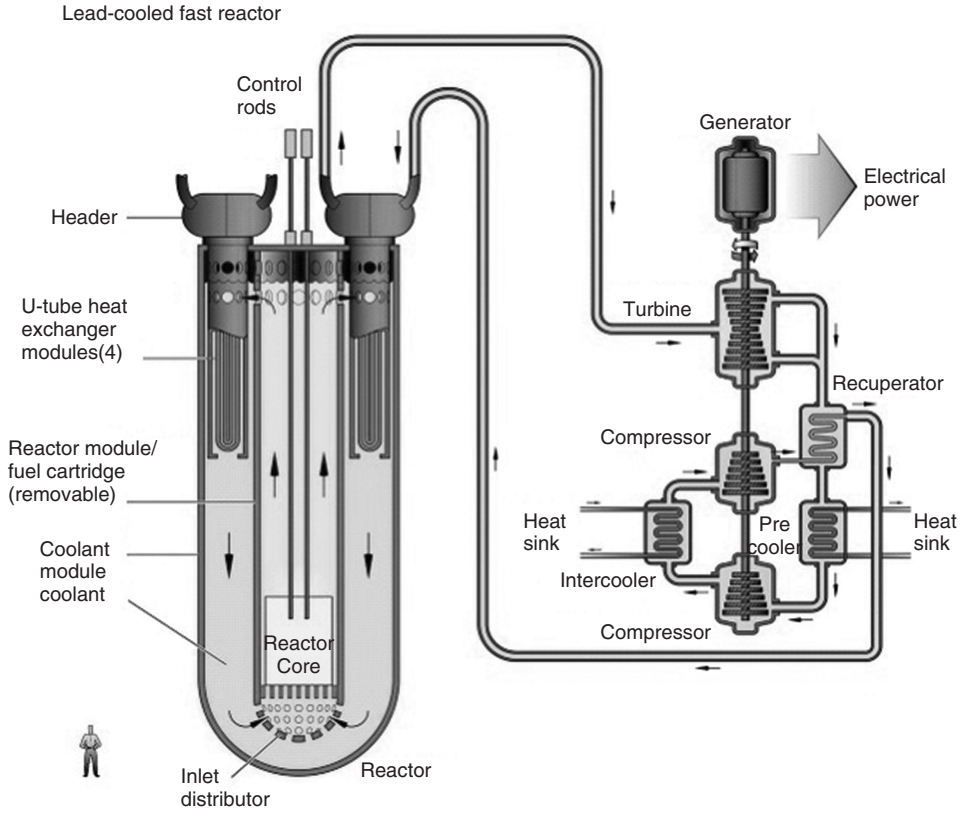

Figure 28.7 Lead-cooled fast reactor with supercritical carbon dioxide Brayton cycle (Courtesy of USDOE).

extraction, supercritical fluid chromatography, polymer processing, and others.

28.4 SUPERCRITICAL WATER-COOLED NUCLEAR REACTORS (SCWRs)

28.4.1 General Considerations

Concepts of nuclear reactors cooled with water at supercritical pressures were mainly studied in the United States and the former USSR as early as the 1950s and 1960s. After a 30-year break, the idea of developing nuclear reactors cooled with supercritical water became attractive again as the ultimate development path for water cooling. Many countries (Canada, China, Germany, Japan, Korea, Russia, United States, and others) have started to work in this direction. However, none of these concepts is expected to be implemented in practice before 2015–2025.

The main objectives of using supercritical water in nuclear reactors are (1) to increase thermal efficiency of modern Nuclear Power Plants (NPPs) from 30–35% to about 45–50%; (2) to decrease capital and operational costs and, hence, decrease electrical energy costs; and (3) explore the possibility for cogeneration of hydrogen.

SCW NPPs will have much higher operating parameters (see Fig. 28.8) compared to modern NPPs (a pressure of about 25 MPa and outlet temperature up to 625°C) and a simplified flow circuit, in which steam generators, steam dryers, steam separators, etc., can be eliminated. Also, higher supercritical water temperatures allow direct thermo-chemical production of hydrogen at low cost due to increased reaction rates (Naterer et al., 2010).

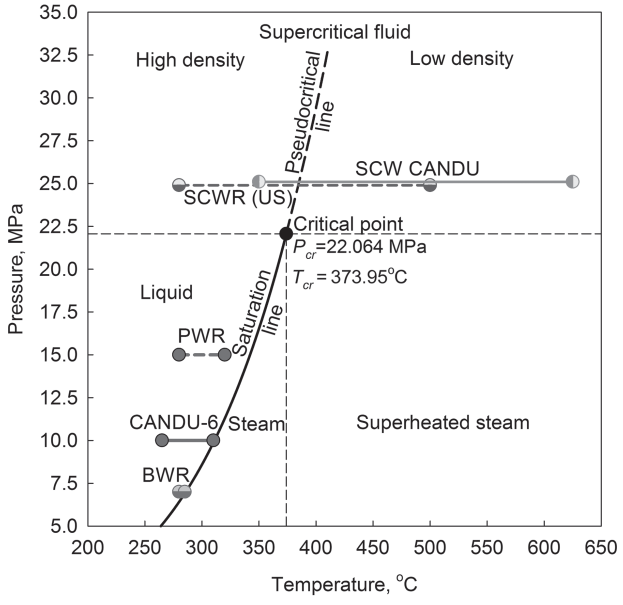

Figure 28.8 Pressure-Temperature diagram of water for typical operating conditions of SCWRs, PWRs, CANDU-6 reactors, and BWRs.

The design of SCW nuclear reactors is seen as the natural and ultimate evolution of today's conventional modern water-cooled reactors[1]. Development of SCWRs is based on the following three proven technologies: (1) modern Pressurized Water Reactors (PWRs), which operate at pressures of 15–16 MPa, i.e., quite high pressures; (2) Boiling Water Reactors (BWRs), which are a once-through or direct-cycle design, i.e., steam from a nuclear reactor is forwarded directly into a turbine; and (3) modern supercritical turbines with pressures about 23.5–35 MPa and inlet temperatures up to 625°C, which operate successfully at coal-fired thermal power plants for more than 50 years (Pioro and Duffey, 2007). In addition, some experimental reactors used nuclear steam reheat with outlet steam temperatures well beyond the critical temperature (up to 550°C), but at pressures below the critical pressure (3–7 MPa), to increase the gross thermal efficiency of NPP (for details, see Figs. 28.9 and 28.10, and Tables 28.4 and 28.5) (Pioro et al., 2010).

However, the major problem for SCWR development is reliability of materials at high pressures and temperatures, high neutron flux, and an aggressive medium, such as supercritical water. Unfortunately, until now nobody has tested candidate materials at such severe conditions.

28.4.2 Supercritical-Pressure Coal-Fired Thermal Power Plants

The cornerstone in SCWR development is using supercritical-water technology and equipment from coal-fired thermal power plants. The basic idea here is "to replace" a supercritical-"steam" generator with an SCWR, and due to that, to achieve significant savings in development of supercritical turbines and related power-plant equipment (of course, some modifications will be required). Therefore, the best approach is to design an SCWR with the same parameters as modern supercritical coal-fired power-plant turbines.

The supercritical "steam" cycle was first introduced in coal-fired power plants in 1957. Due to material issues associated with the supercritical-"steam" pressure and temperature that hindered component reliability, supercritical "steam" was not widely used in its early days. Since the 1970s, the advancements in metallurgical technology have significantly improved the reliability of the supercritical "steam" generators and turbines. As a result, SC "steam" generators and turbines have been widely deployed in newly built coal-fired power plants (with the exception of combined-cycle power plants) to achieve higher thermal efficiency, better economy and cleaner electricity generation. Currently, hundreds of supercritical "steam" coal-fired power plants operate around the world.

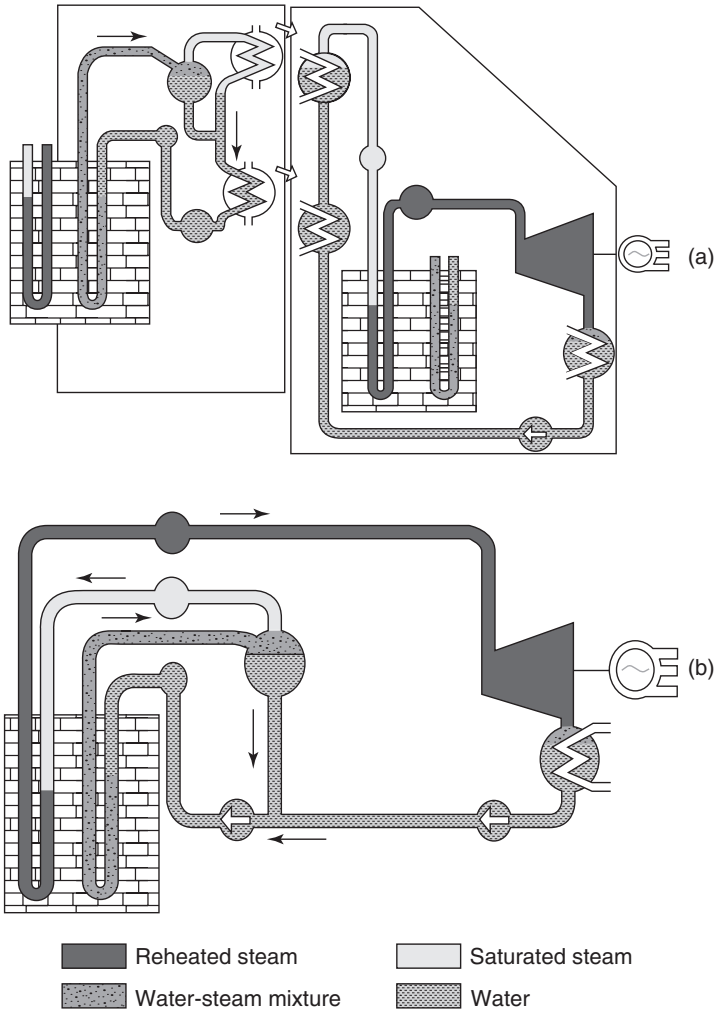

Figure 28.9 Beloyarsk NPP (Russia) reactors schematic: (a) Unit 1 with indirect steam cycle and (b) Unit 2 with direct steam cycle (Courtesy of Dr. Yurmanov, NIKIET, Russia).

The parameters 25 MPa and 600°C are common supercritical "steam" parameters in state-of-the-art coal-fired power plants (see Fig. 28.11), and a few plants even operate at pressures as high as 35 MPa and at temperatures as high as 650°C. The capacity of supercritical turbines ranges from 300 MW_{el} to 1200 MW_{el}. The gross overall steam-cycle efficiency of supercritical fossil-fueled power plants typically ranges between 47% and 54% (i.e., net plant efficiencies between 38% and 43% on a Higher-Heating Value[2] (HHV) basis). Tables 28.6 and 28.7 list parameters of selected supercritical turbines (additional information on supercritical turbines is also listed in Pioro and Duffey, 2007).

The steam-cycle configuration of a supercritical cycle is very similar to a subcritical cycle in a modern fossil-fueled power plant. Steam is usually reheated once in a steam generator after passing through the High-Pressure (HP) turbine, in order to achieve the higher efficiency. The regenerative feedwater-heating system consists of Low-Pressure (LP) and High-Pressure (HP) feedwater heaters (closed type) and a deaerator (mixing type). Usually, supercritical-"steam" cycles involve 8 to 10 stages of feedwater heating, while subcritical-steam cycles typically involve 8 to 9 stages of feedwater heating.

While the modern supercritical turbines share many common merits, they also vary in many aspects, depending on manufacturer preference. These differences can include turbine type (impulse or reaction), shaft combination (tandem or cross compound), cylinder arrangement, parameter choices (feedwater temperature, reheat pressure), and others. Individual manufacturers take different approaches in these areas based on their design experiences. Some features (e.g., unit capacity, feedwater temperature) are flexible within certain ranges if required by customers.

The supercritical "steam"-turbine technology is experiencing continuous improvements. For example, Project

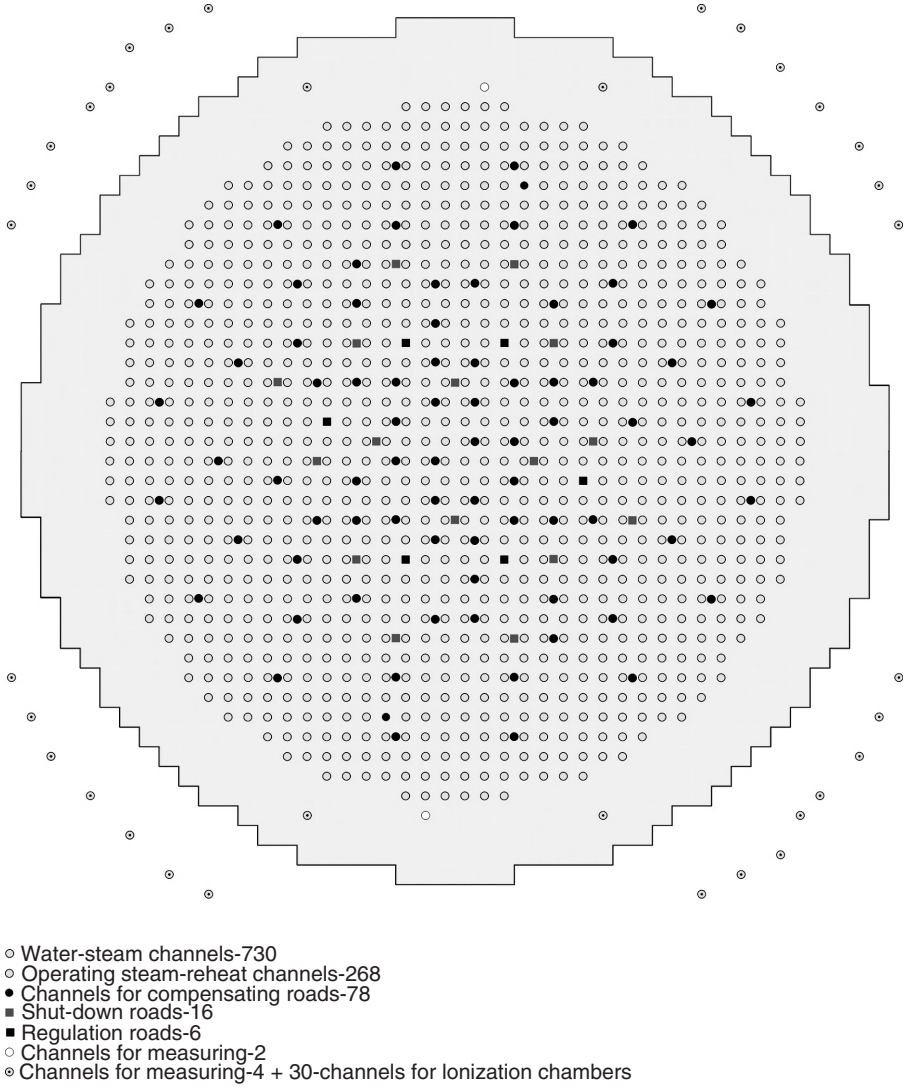

Figure 28.10 Beloyarsk NPP Unit 1 channels layout (drawing prepared by W. Peiman, UOIT).

TABLE 28.4 Main Parameters of Beloyarsk NPP Reactors

Parameters	Unit 1 (730 EChs & 268 SRChs)	Unit 2 (732 EChs & 266 SRChs)
Electrical power, MW_{el}	100	200
Number of K-100-90-type turbines	1	2
Inlet-steam pressure, MPa	8.5	7.3
Inlet-steam temperature, °C	500	501
Gross thermal efficiency, %	36.5	36.6
Uranium load, t	67	50
Uranium enrichment, %	1.8	3.0
Square lattice pitch, mm	200	200
Core dimensions, m: Diameter Height	7.26	7.26

EChs—Evaporating Channels; SRChs—Steam-Reheat Channels

TABLE 28.5 Average Parameters of Beloyarsk NPP Unit 1 before and after Installation of Steam-Reheat Channels (SRChs)

Parameters	Before SRChs Installation	After SRChs Installation
Electrical power, MW_{el}	60–70	100–105
Steam inlet pressure, MPa	5.9–6.3	7.8–8.3
Steam inlet temperature, °C	395–405	490–505
Exhaust steam pressure, kPa	9–11	3.4–4.0
Water mass flowrate (1st loop), kg/h	1400	2300–2400
Pressure in steam separators, MPa	9.3–9.8	11.8–12.7
Gross thermal efficiency, %	29–32	35–36
Electrical power for internal needs, %	10–12	7–9

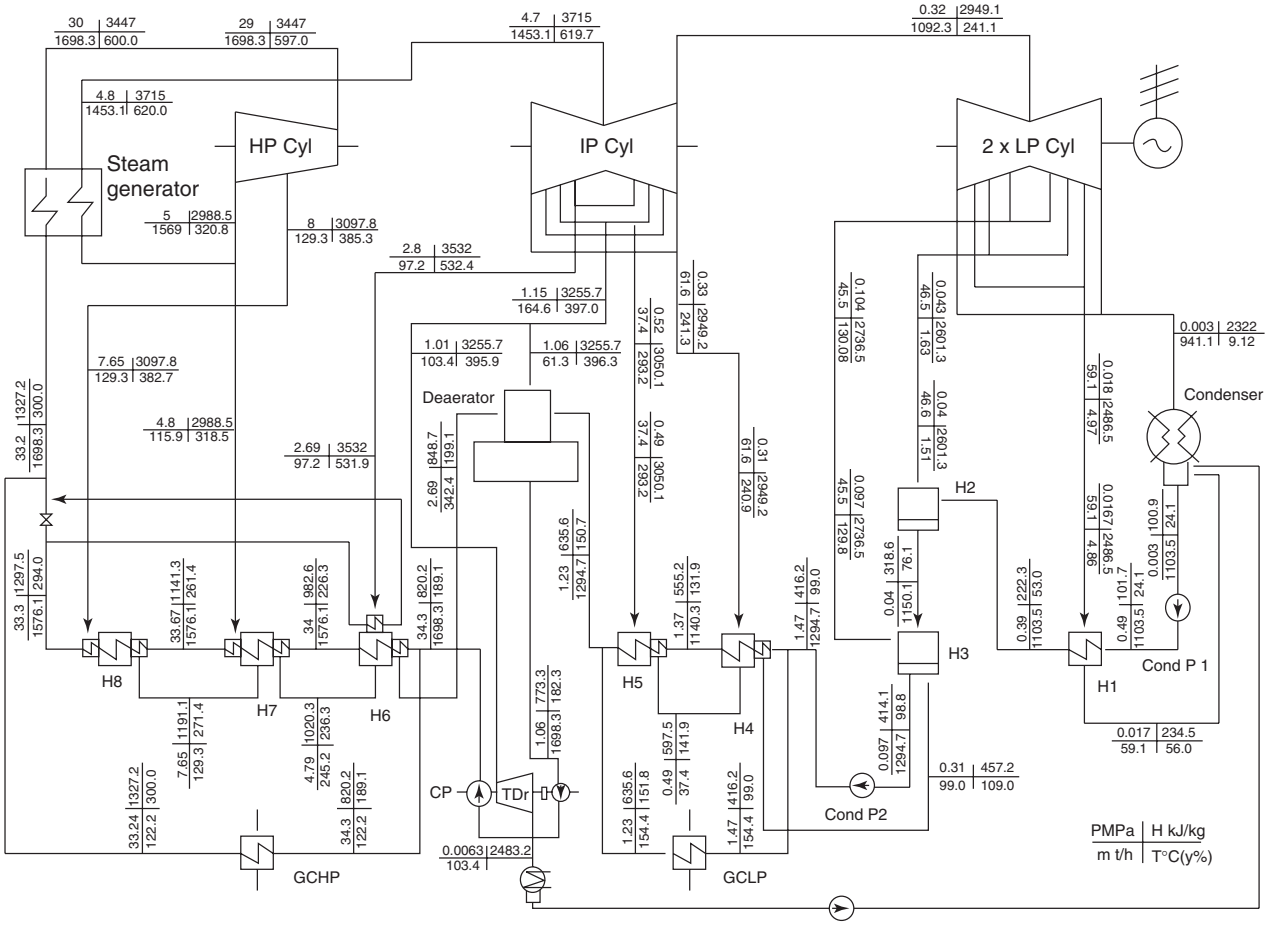

Figure 28.11 Single-reheat-regenerative cycle 600-MW_{el} Tom'-Usinsk thermal power plant (Russia) layout (Kruglikov et al., TsKTI, Russia, 2009). Cyl—Cylinder; H—Heat exchanger (feedwater heater); CP—Circulation Pump; TDr—Turbine Drive; Cond P—Condensate Pump; GCHP—Gas Cooler of High Pressure; and GCLP—Gas Cooler of Low Pressure.

Thermie-700 in Europe is developing a coal-fired "steam" generator-turbine unit for "steam" parameters of 35 MPa and 700°C with a target plant efficiency of 50–55%.

Based on the abovementioned, the following conclusions can be made:

- The vast majority of the modern and upcoming supercritical turbines are single-reheat-cycle turbines.
- Major "steam" inlet parameters of these turbines are: The main or primary supercritical "steam" $-P = 24–25$ MPa and $T = 540–600$°C; and the reheat or secondary subcritical-pressure steam $-P = 3–7$ MPa and $T = 540–620$°C.
- Usually, the main "steam" and reheat-steam temperatures are the same or very close in value

TABLE 28.6 Major Parameters of Selected Hitachi Supercritical Plants (turbines)

First Year of Operation	Power Rating MW_{el}	Pressure MPa(g)	T_{main}/T_{reheat} °C
2011	495	24.1	566/566
2010	809	25.4	579/579
	790	26.8	600/600
2009	1000	25.0	600/620
	1000	25.5	566/566
	600	24.1	600/620
2008	1000	24.9	600/600
	887	24.1	566/593
	677	25.5	566/566
2007	1000	24.9	600/600
	870	25.3	566/593
2006	600	24.1	566/566
2005	495	24.1	566/566
2004	700	24.1	538/566
2003	1000	24.5	600/600
2002	700	25.0	600/600
1998	1000	24.5	600/600
1994	1000	24.1	538/566
1992	700	24.1	538/566
1991	600	24.1	538/566
1989	1000	24.1	538/566
	700	24.1	538/566
1985	600	24.1	538/566
1984	600	24.1	538/538
1983	700	24.1	538/538
	600	24.1	538/566
	350	24.1	538/566
1981	500	24.1	538/538
1979	600	24.1	538/566
1977	1000	24.1	538/566
	600	24.1	538/566
	600	24.1	538/552/566*
1975	450	24.1	538/566
1974	500	24.1	538/566
1973	600	24.1	538/552/566*
	450	24.1	538/566
1972	600	24.1	538/566
1971	600	24.1	538/566

*Double-steam-reheat-cycle turbines.

(for example, 566/566°C; 579/579°C; 600/600°C; 566/593°C; 600/620°C).

- Only very few double-reheat-cycle turbines have been manufactured so far. The market demand for double-reheat turbines disappeared due to economic reasons after the first few units were built.

28.4.3 SCWR Design Considerations

The SCWR concepts therefore follow two main types, the use of either (a) a large reactor pressure vessel (Fig. 28.12) with a wall thickness of about 0.5 m to contain the reactor core (fuelled) heat source, analogous to conventional PWRs and BWRs, or (b) distributed pressure tubes or channels analogous to conventional CANDU®[3] nuclear reactors (Fig. 28.13). In general, mainly thermal-spectrum SCWRs are currently under development worldwide. However, several concepts of fast SCWRs are also considered (see Table 28.8).

28.4.3.1 Pressure-Vessel SCWRs The pressure-vessel SCWR design (see Table 28.8) is being developed largely in China, the European Union (EU), Japan, and some other countries. This type of reactor, which is based on proven technologies in PWRs and BWRs, uses a traditional high-pressure circuit layout. However, due to significantly reduced flow rates (at supercritical conditions flow rates can be up to eight times less than those in current reactors), high outlet temperatures, and some other parameters, significant fuel-sheath temperature non-uniformities may appear, which in turn can lead to sheath damage. Another challenge associated with pressure-vessel SCWRs is manufacturing the pressure vessel due to quite large wall thickness. Also, in pressure-vessel reactors, nuclear steam reheat at subcritical pressures is not possible. More information on thermal and fast pressure-vessel SCWRs can be found in the latest book by Oka et al. (2010).

28.4.3.2 Pressure-Channel SCWRs The pressure-channel SCWR designs (see Table 28.8) are developed mainly in Canada (Fig. 28.13) and in Russia (Pioro and Duffey, 2007). Figure 28.13 shows also the maximum possible outcome from SCWRs. Within those two main classes, pressure-channel reactors are more flexible to flow, flux, and density changes than pressure-vessel reactors. In addition, a nuclear steam reheat can be implemented inside a pressure-channel SCWR based on the experience obtained from the operation of several experimental BWRs in 1960s and 1970s (see Figs. 28.9 and 28.10 and Tables 28.4 and 28.5), which makes it completely suitable to modern supercritical direct single steam-reheat-cycle turbines. All these make it possible to use the experimentally confirmed, better solutions developed for these reactors. One of them is channel-specific flow-rate adjustments or regulations. Also, a pressure tube at such pressures will have a wall thickness of about 7–9 mm compared to about 400–500 mm for a pressure vessel. Therefore, a design whose basic element is a channel that carries a high pressure has an inherent advantage of greater safety than large vessel structures at supercritical pressures.

In general, pressure-channel SCWRs can be with horizontal fuel channels or vertical fuel channels. Horizontal orientation has significant benefits if online refueling is considered. However, at supercritical pressures, online refueling is an extremely challenging task, and thus, it might be abandoned. In this case, the vertical orientation can be

TABLE 28.7 Parameters of Largest Russian Supercritical Turbines

Parameters	K-1200-240	K-800-240	K-800-240*
Power, MW_{el} (max power)	1200 (1380)	800 (850)	800 (835)
	Main Steam		
Pressure, MPa	23.5	23.5	23.5
Temperature, °C	540	540	560
Max Flow Rate Through HP Turbine, t/h	3950	2650	2500
	Reheat Steam		
Pressure, MPa	3.5	3.2	3.4
Temperature, °C	540	540	565
No. of Steam Extractions	9	8	8
Outlet Pressure, kPa	3.6	3.4	2.9
	Cooling Water		
Temperature, °C	12	12	12
Flow Rate, m^3/h	108,000	73,000	85,000
Feedwater Temperature, °C	274	274	270
	Turbine Layout		
No. of Cylinders	5	5	6
No. of High Pressure (HP) Cylinders	1	1	—
No. of Intermediate Pressure (IP) Cylinders	2	2	—
No. of Low Pressure (LP) Cylinders	2	2	—
	Turbine Mass and Dimensions		
Total Mass, t	1900	1300	1600
Total Length, m	48	40	40
Total Length with Electrical Generator, m	72	60	46
Average Diameter of HP Turbine, m	3.0	2.5	2.5

*Double-shaft turbine.

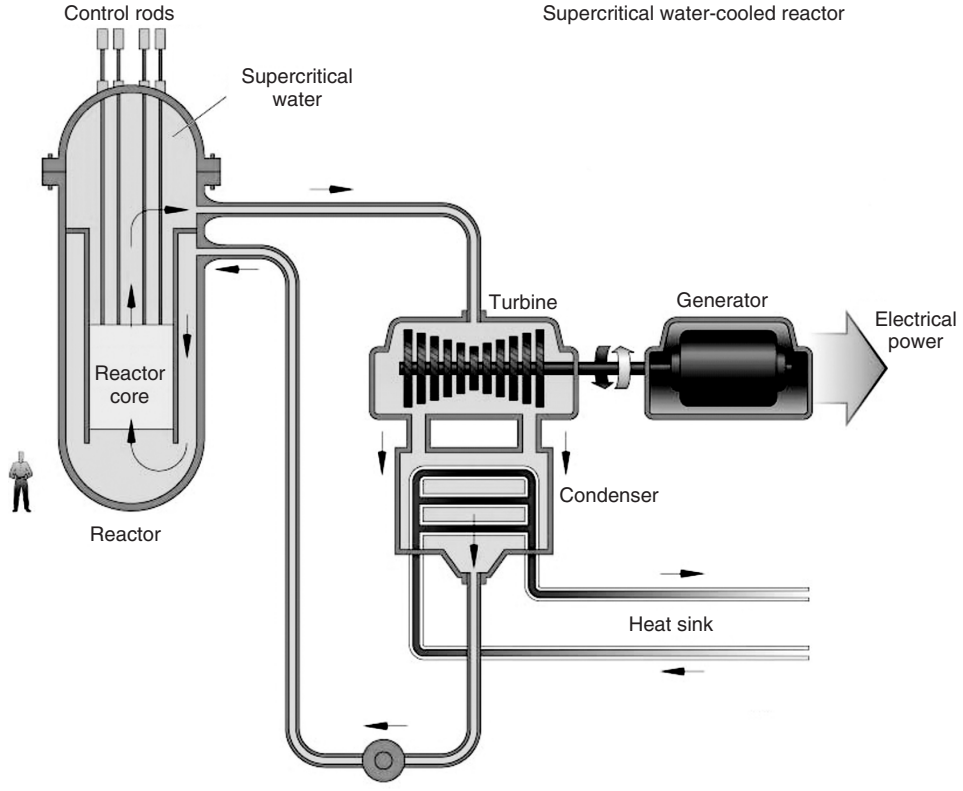

Figure 28.12 Pressure-vessel SCWR schematic (Courtesy of USDOE).

TABLE 28.8 Modern Concepts of SCWRS (Pioro and Duffey, 2007)

Parameters	Unit	SCW CANDU	HPLWR	SCLWR-H	SCFBR-H	SCWR	B-500 SKDI	ChUWR	ChUWFR	KP-SKD	PVWR	WWPR-SCP	SCWR-US
Reference	—	Bushby et al., 2000; Khartabil et al., 2005	Squarer et al., 2003	Yamaji et al., 2004	Oka and Koshizuka, 2000	Bae et al., 2004; Bae, 2004	Silin et al., 1993	Kuznetsov, 2004 (project from 1980s)	Gabaraev et al., 2003a,b, 2004	Gabaraev et al., 2005	Filippov et al. 2003	Baranaev et al. 2004	Buongiorno, MacDonald 2003
Country	—	Canada	EU/Japan	Japan		Korea	Russia	Russia	Russia	Russia	Russia	Russia	USA
Organization	—	AECL	EU/U of Tokyo	University of Tokyo		KAERI/Seoul NU	Kurchatov Institute		RDIPE (IEEEYO)		VNIIAM/ Kurchatov Institute	IPPE (OYE)	INEEL
Reactor type Spectrum	—	PT	RPV	RPV	RPV	RPV	RPV	PT	PT	PT	RPV	RPV	RPV
	—	Thermal	Thermal	Thermal	Fast	Thermal	Thermal	Thermal	Fast	Thermal	Thermal	Fast	Thermal
Power thermal	MW	2540	2188	2740	3893	3846	1350	2730	2800	1960	3500	3830	3575
electrical linear	MW	1140	1000	1217	1728	1700	515	1200	1200	850	1500	1700	1600
max/ave	kW/m		39/24	39/18	39	39/19		38/27		69/34.5		35/15.8	39/19.2
Thermal eff.	%	45	44	44.4	44.4	44	38.1	44	43 (48)	42	43	44	44.8
Pressure	MPa	25	25	25	25	25	23.5	24.5	25	25	25	25	25
T_{in} coolant	°C	350	280	280	280	280	355	270	400	270	280	280	280
T_{out} coolant	°C	625	500	530	526	508	380	545	550	545	550–610	530	500
Flow rate	kg/s	1320	1160	1342	1694	1862	2675	1020		922	1600	1860	1843
Core height	m		4.2	4.2	3.2	3.6	4.2	6	3.5	5	3.5	4.05	4.87
	m	~4		3.68	3.28	3.8	2.61	11.8	11.4	6.45	2.92	3.38	3.91
Diameter													
Fuel	—	UO_2/Th	UO_2 or MOX	UO_2	MOX	UO_2	UO_2	UCG	MOX	UO_2	UO_2	MOX	$UO_2$95%
Enrichment	% wt.	4	<6%	~6.1		5.8	3.5	4.4		6			5
Cladding material	—	Ni alloy	SS	Ni alloy	Ni alloy	SS	Zr alloy/SS	SS	SS	SS		Ni alloy	TBD
# of FA		300	121	121	419	157	121	1693	1585	653	37	241	145
# of FR in FA		43	216/252	300		284	252	10	18	18		252	300
D_{rod}/δ_w	mm/mm	11.5 and	8	10.2/0.63	12.8	9.5/0.635	9.1 (Zr),	12/1	12.8	10/1	Sphere 1.8	10.7/0.55	10.2/0.63
Pitch	mm	13.5	9.5			11.5	8.5 (SS)				mm	12	11.2
T_{max}sheath (cladding)	°C	<850	620	650	620	620	425	630	650	700	630–730	630	
Moderator	—	D_2O	H_2O	H_2O	H_2O	ZrH_2	H_2O	Graphite	—	D_2O	H_2O	$ZrH_{1.7}$	H_2O

Explanations to the table: Concepts appear according to the alphabetical order of the country of origin. ChUWR—Channel-type Uranium-graphite Water Reactor with annular-type elements cooled from inside; ChUWFR—Channel-type Uranium-graphite Water Fast Reactor; FA—fuel assembly; FR—fuel rod; HPLWR—High Performance Light Water Reactor; KP-SKD—Channel Reactor of Supercritical Pressure (in Russian abbreviations); PT—Pressure Tube (reactor); PVWR—Pressure-Vessel Water reactor; RPV—Reactor Pressure Vessel; SCFBR-H—SuperCritical Fast Breeder Reactor with High temperature; SCLWR-H—SuperCritical Light Water Reactor with High temperature; Seoul NU—Seoul National University; SKDI—SuperCritical Pressure Integral (reactor) (in Russian abbreviations); TBD—To Be Determined; U of Tokyo—University of Tokyo; VNIIAM—All-Union Scientific-Research Institute of Atomic Machine Building (in Russian abbreviations); WWPR-SCP—Water-Water Power Reactor ("VVER" in Russian abbreviations) of SuperCritical Pressure.

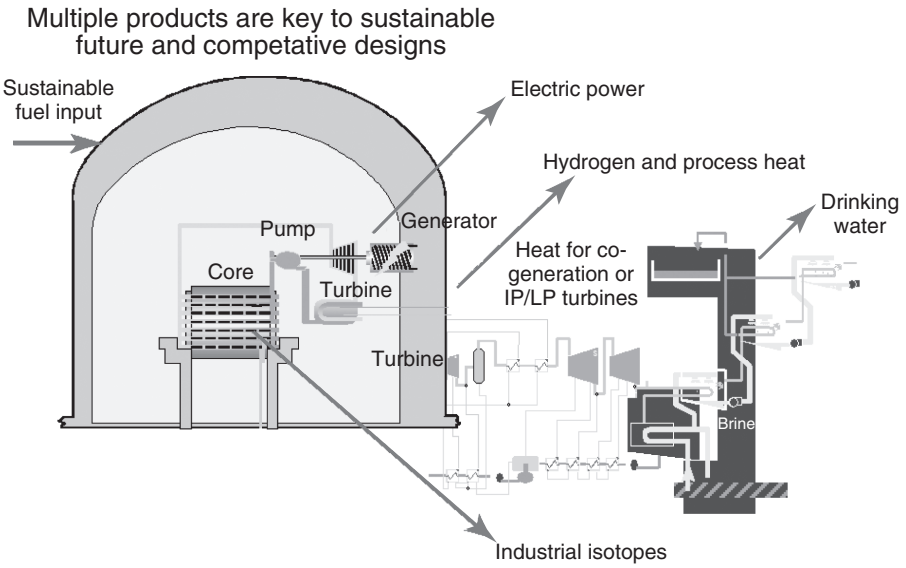

Figure 28.13 General scheme of pressure-channel SCW CANDU reactor: IP—intermediate-pressure turbine and LP—low-pressure turbine (Courtesy of Dr. Duffey, AECL).

a better option. Figure 28.14 shows a possible fuel-channel layout of the generic 1200 MW_{el} pressure-channel SCWR.

From moderator point of view, pressure-channel SCWRs can be with a liquid moderator (heavy water) or with a solid moderator. After the Chernobyl NPP disaster (Ukraine, 1986), it seems that graphite as a moderator will not be used in any water-cooled reactors. However, other solid moderators may be used, for example, beryllium, beryllium oxide, ZH_2.

With a solid moderator, the fuel-channel design can be simplified, because we don't need to worry about heat losses from the hot pressure tube. In this case, for example, Re-Entrant Channels (RECs) without thermal insulation can be used (Fig. 28.15). Due to lower inlet temperatures (about 300°C), a pressure tube can be manufactured from zirconium alloys, but a flow tube should be from stainless steels or Inconels (currently, these materials are considered as candidate materials for application at SCWR conditions).

A liquid moderator has a unique feature that functions as an extra safety system during emergency fuel-channel cooling. The moderator in CANDU reactors acts as a backup heat sink in the unlikely event of loss of coolant combined with loss of emergency core cooling. The moderator cooling system removes heat deposited in the moderator during normal operation. The moderator cooling system can also remove decay heat in certain postulated accident scenarios. In the SCWR design, the moderator operates slightly subcooled, which makes it possible to use a flashing-driven passive loop to remove the moderator heat (see Fig. 28.16).

However, fuel channels in SCWR with the liquid moderator will have more complicated designs (see Figs. 28.17–28.19) to prevent high heat losses from the hot pressure tube to the low-temperature moderator. A challenging task in these designs is a thermal insulation.

28.4.4 Possible Thermodynamic Cycles for SCWRs

In general, the following thermodynamic cycles can be used in SCW NPPs (Naidin et al., 2009; Duffey et al., 2008; Pioro et al., 2008):

1. Direct single-reheat regenerative thermodynamic cycle (Rankine cycle) (see Fig. 28.20 and Tables 28.8 and 28.9), which is the basic cycle for the vast majority of modern supercritical coal-fired thermal power plants.
2. Indirect single-reheat regenerative thermodynamic cycle (see Fig. 28.21).
3. Direct no-reheat regenerative thermodynamic cycle (see Fig. 28.22 and Tables 28.8 and 28.9).
4. Indirect no-reheat regenerative thermodynamic cycle (see Fig. 28.23).
5. Dual regenerative thermodynamic cycles (see Figs. 28.24 and 28.25).

In the direct cycle, supercritical "steam" from an SCWR is fed directly into a supercritical turbine. This concept eliminates the need for complex and expensive equipment such as steam generators (heat exchangers). From a thermodynamic perspective, this allows for high steam pressures and temperatures and results in the highest cycle thermal efficiency for the given parameters. The

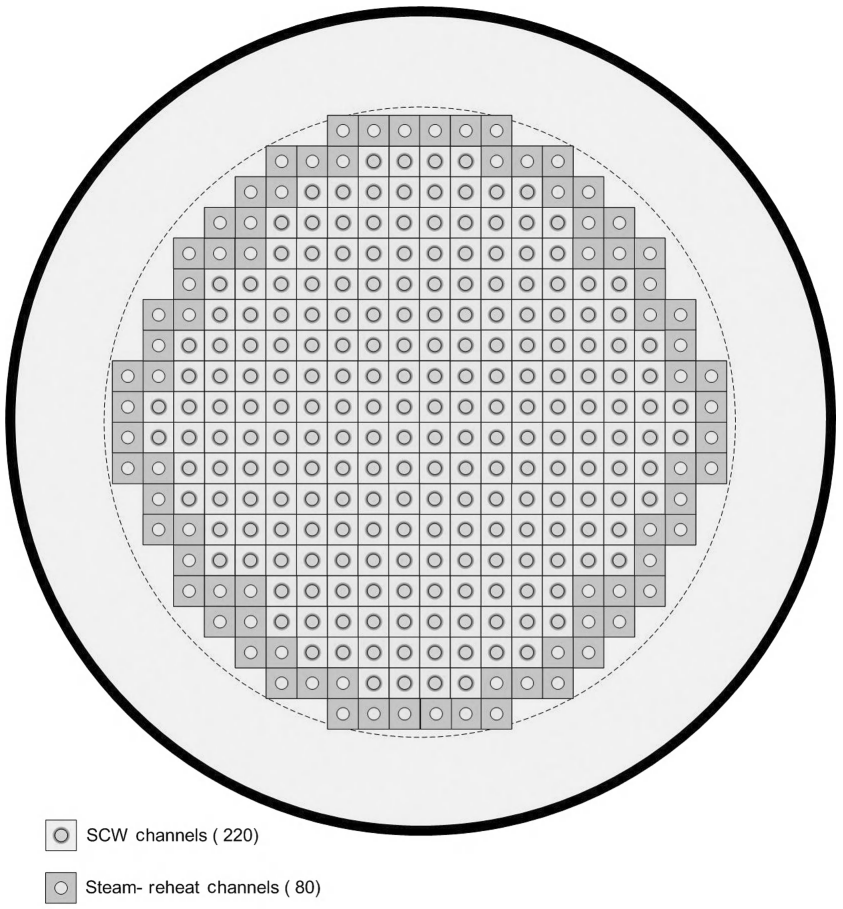

Figure 28.14 Possible fuel-channel layout of generic 1200-MW_{el} pressure-channel SCWR (drawing prepared by W. Peiman, UOIT).

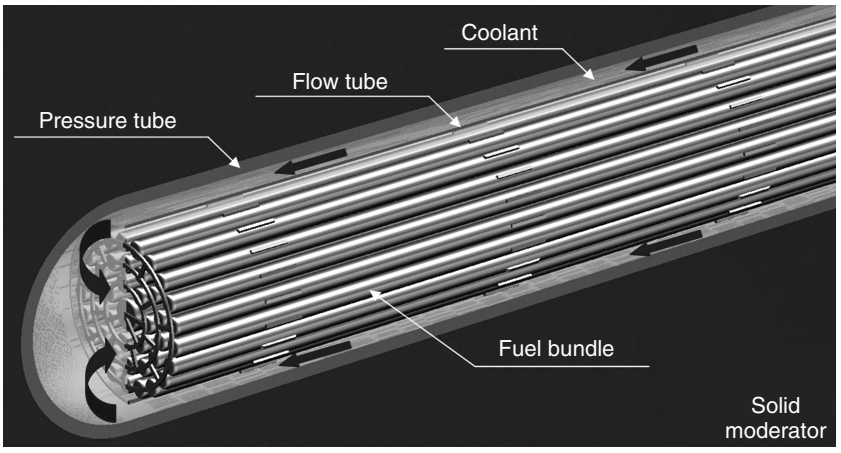

Figure 28.15 Re-Entrant Channel (REC) for SCWR with solid moderator (drawing prepared by W. Peiman, UOIT).

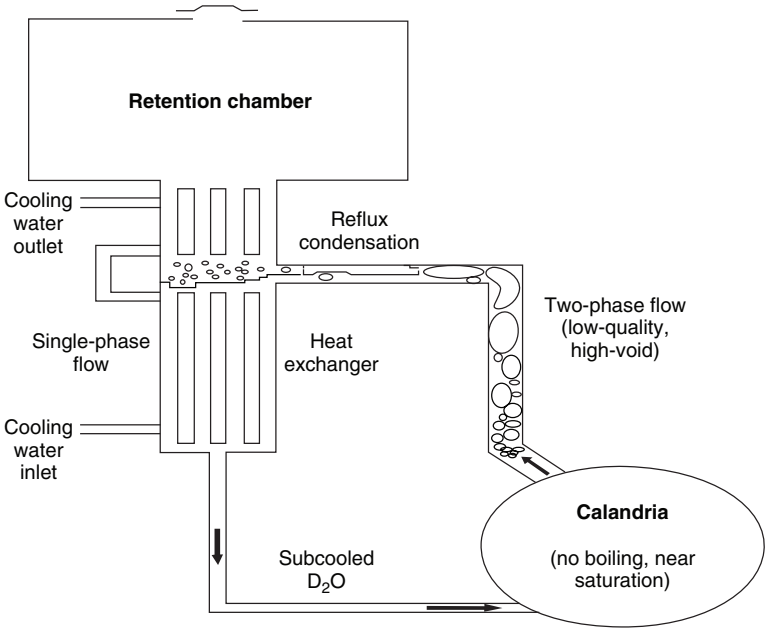

Figure 28.16 Passive moderator-cooling concept—"walk away safety" with no core melting (Courtesy of Dr. H. Khartabil, AECL).

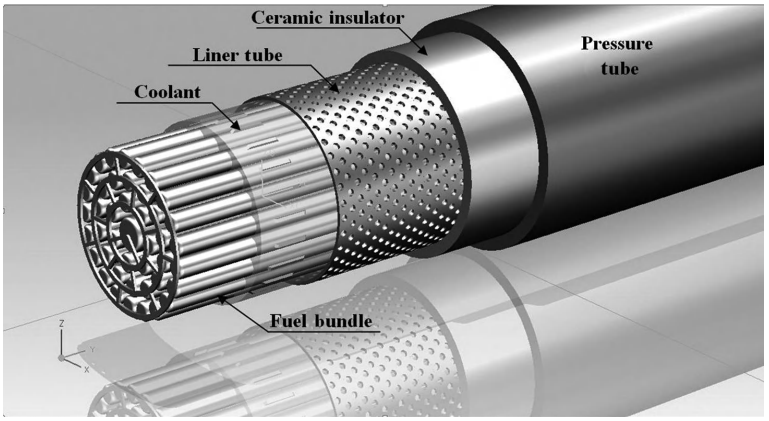

Figure 28.17 High-Efficiency Channel (HEC) with ceramic insert (AECL design) (drawing prepared by W. Peiman, UOIT).

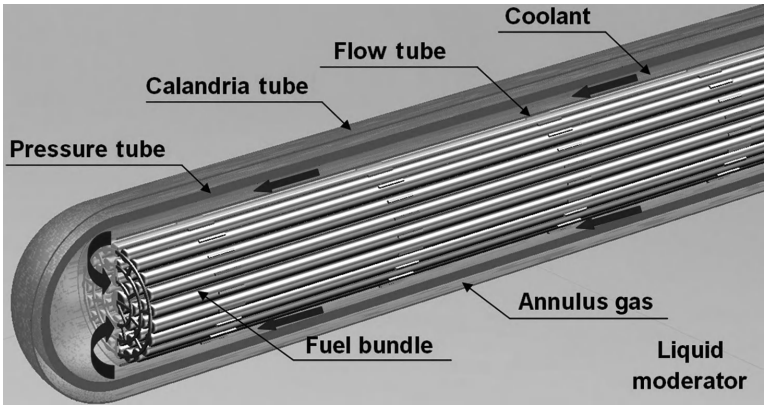

Figure 28.18 Re-Entrant Channel (REC) with annulus gas as thermal insulation for SCWR with liquid moderator (drawing prepared by W. Peiman, UOIT).

direct single-reheat cycle with current supercritical "steam" parameters will have gross thermal efficiency of about 52% and the no-reheat cycle, about 51%. However, the direct single-reheat cycle is easier to implement in pressure-channel SCWRs and might be impossible to implement in pressure-vessel SCWRs. The direct no-reheat cycle can be implemented in both types of SCWRs.

The single-reheat cycle is widely used in thermal power industry, but we have not found any information on thermal power plants operating on the no-reheat cycle. The major technical challenge for the no-reheat cycle is relatively high moisture content at the outlet of the LP turbine (about 19%). However, the moisture can be reduced by implementing contoured channels in the inner casing for draining the water and moisture removal stages.

The indirect and dual cycles utilize heat exchangers (steam generators) to transfer heat from the reactor coolant to a turbine. The indirect cycle has the safety benefit of containing the potential radioactive particles inside the primary coolant. Also, this cycle arrangement prevents deposition of various substances from the reactor coolant on turbine blades. However, the heat-transfer process through

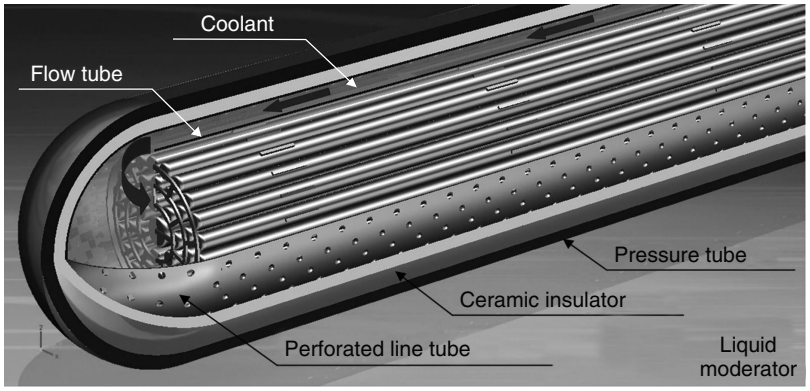

Figure 28.19 Re-Entrant Channel (REC) with ceramic insulator for SCWR with liquid moderator (drawing prepared by W. Peiman, UOIT).

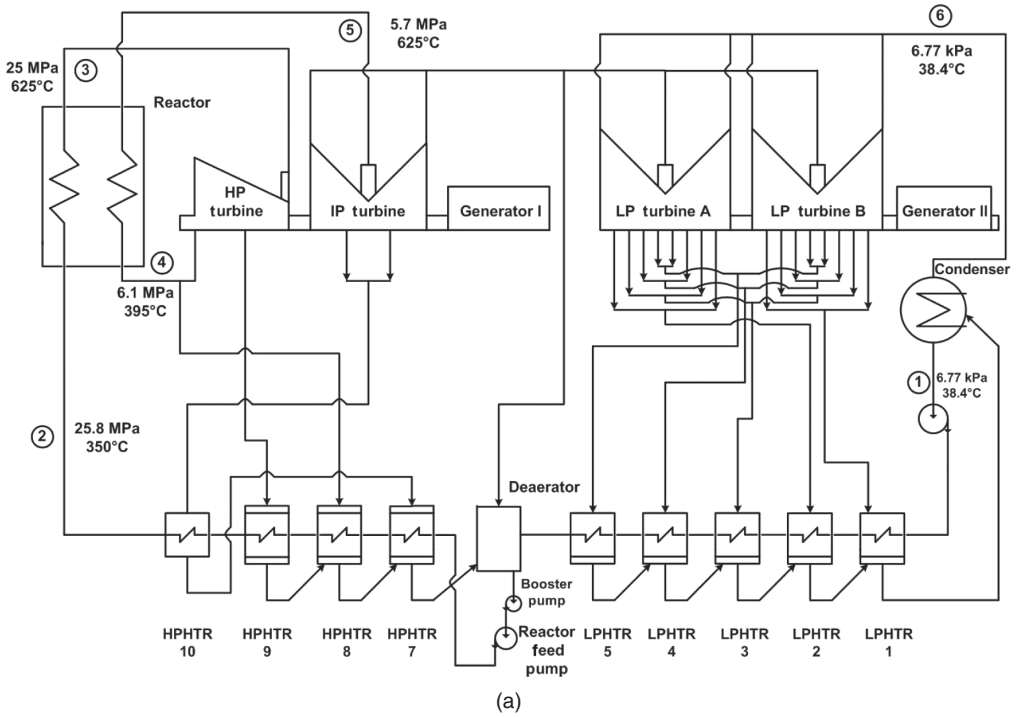

(a)

Figure 28.20 Direct single-reheat regenerative thermodynamic cycle for 1200-MW_{el} pressure-channel SCW NPP (Naidin et al., 2009): (a) Schematic and (b) Temperature-Entropy diagram.

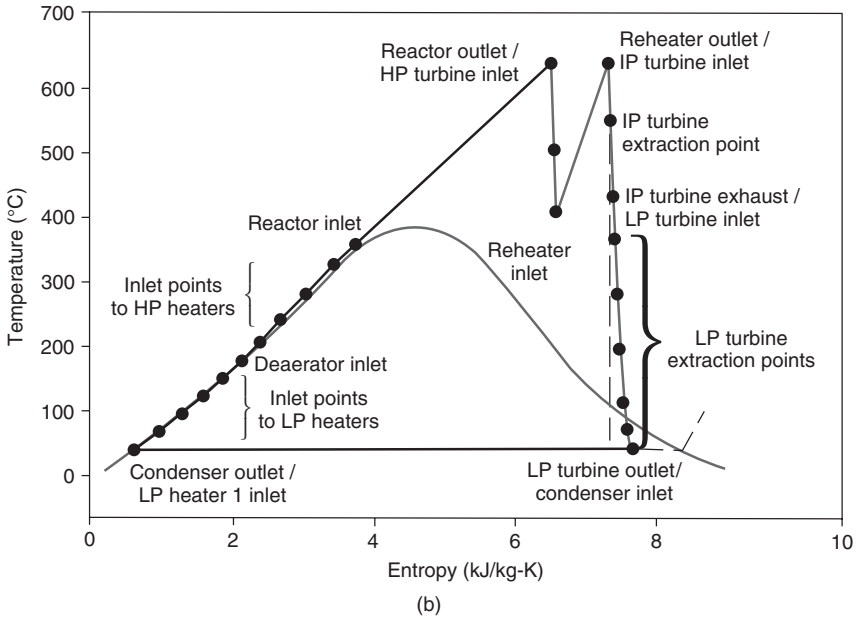

Figure 28.20 (*Continued*)

TABLE 28.9 Selected Parameters of Proposed SCW NPP Direct Cycles

Parameters	Unit	Description/Value	Description/Value
Cycle type	—	Direct Single-Reheat (see Fig. 28.20)	Direct No-Reheat (see Fig. 28.22)
Reactor type	—	Pressure Tube	
Reactor spectrum	—	Thermal	
Fuel	—	$UO_2(ThO_2)$	
Cladding material	—	Inconel or Stainless steel	
Reactor coolant	—	H_2O	
Moderator	—	D_2O	
Power thermal	MW_{th}	2300	2340
Power electrical	MW_{el}	1200	1200
Thermal efficiency	%	52	51
Pressure of SCW at inlet	MPa	25.8	25.8
Pressure of SCW at outlet (estimated)	MPa	25	25
T_{in} coolant (SCW)	°C	350	350
T_{out} coolant (SCW)	°C	625	625
Pressure of SHS at inlet	MPa	6.1	—
Pressure of SHS at outlet (estimated)	MPa	5.7	—
T_{in} coolant (SHS)	°C	400	—
T_{out} coolant (SHS)	°C	625	—
Power thermal SCW channels	MW_{th}	1870	2340
Power thermal SRH channels	MW_{th}	430	—
Power thermal/SCW channel	MW_{th}	8.5	8.5
Power thermal/SRH channel	MW_{th}	5.5	—
fuel channels (total)	—	300	270
# of SCW channels	—	220	270
# of SRH channels	—	80	—
Total flow rate of SCW	kg/s	960	1190
Total flow rate of SHS	kg/s	780	—
Flow rate/SCW channel	kg/s	4.37	4.37
Flow rate/SRH channel	kg/s	10	—

SHS—SuperHeated Steam; SRH—Steam ReHeat (Channel).

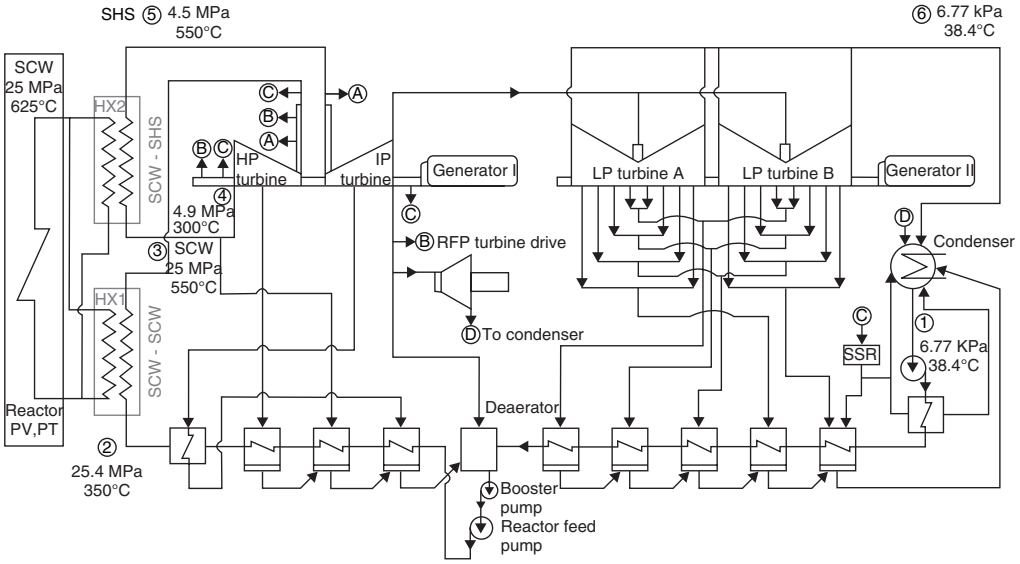

Figure 28.21 Schematic of in-direct single-reheat regenerative thermodynamic cycle for 1200-MW_{el} pressure-vessel or pressure-channel SCW NPP (drawing prepared by H. Thind, UOIT).

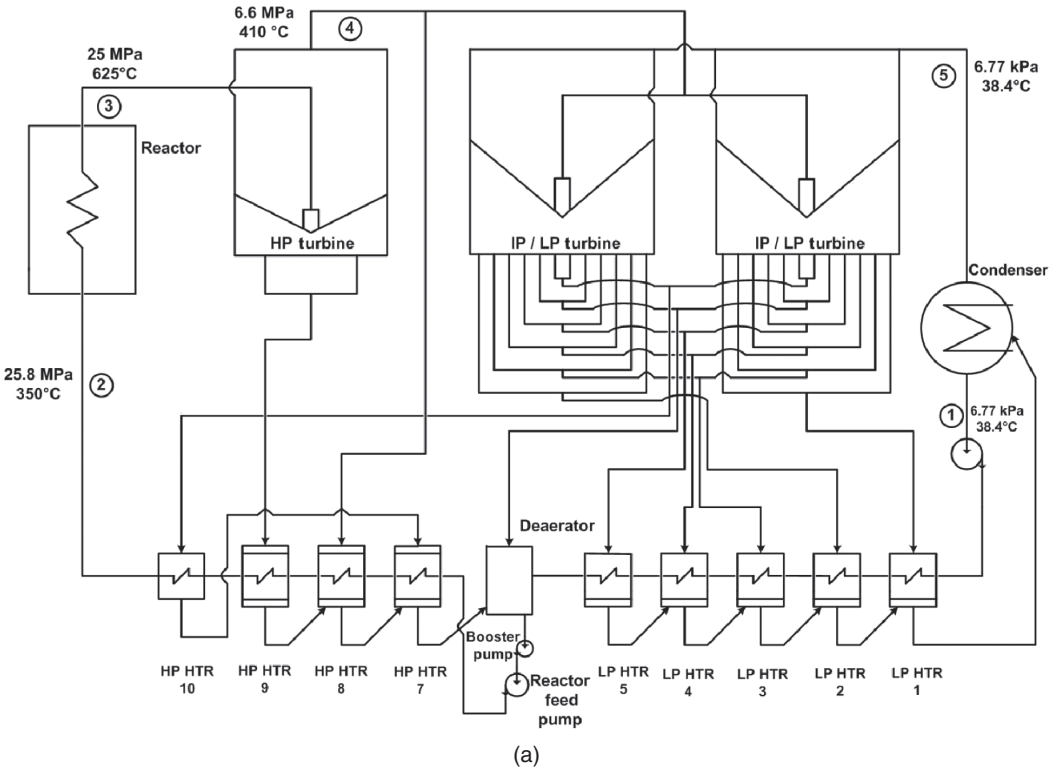

(a)

Figure 28.22 Direct no-reheat regenerative thermodynamic cycle for 1200-MW_{el} pressure-vessel or pressure-channel SCW NPP (Naidin et al., 2009): (a) Schematic and (b) Temperature-Entropy diagram.

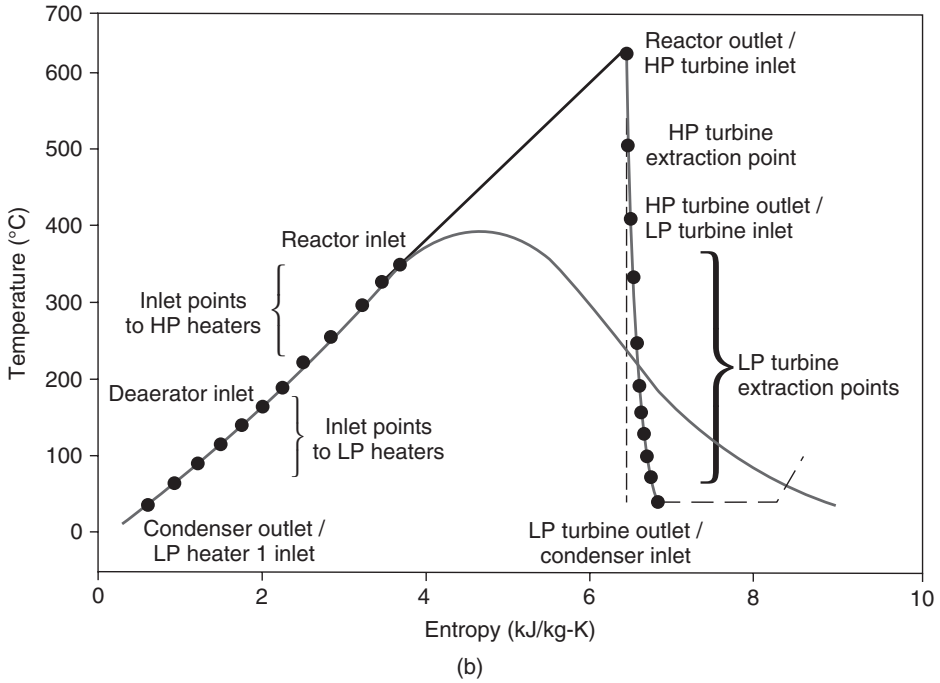

(b)

Figure 28.22 (*Continued*)

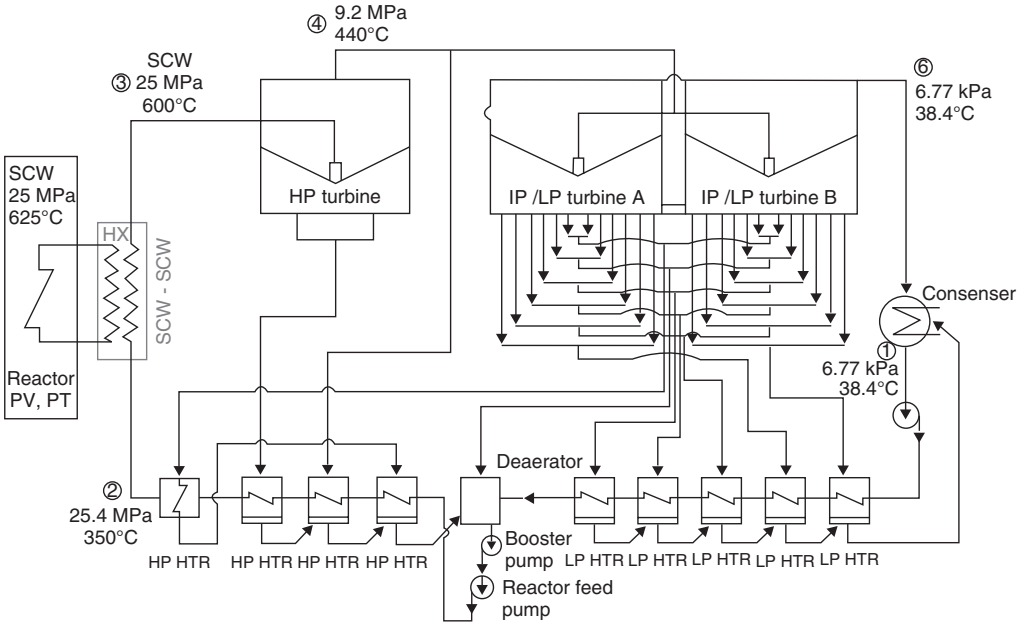

Figure 28.23 Schematic of in-direct no-reheat regenerative thermodynamic cycle for 1200-MW_{el} pressure-vessel or pressure-channel SCW NPP (drawing prepared by H. Thind, UOIT).

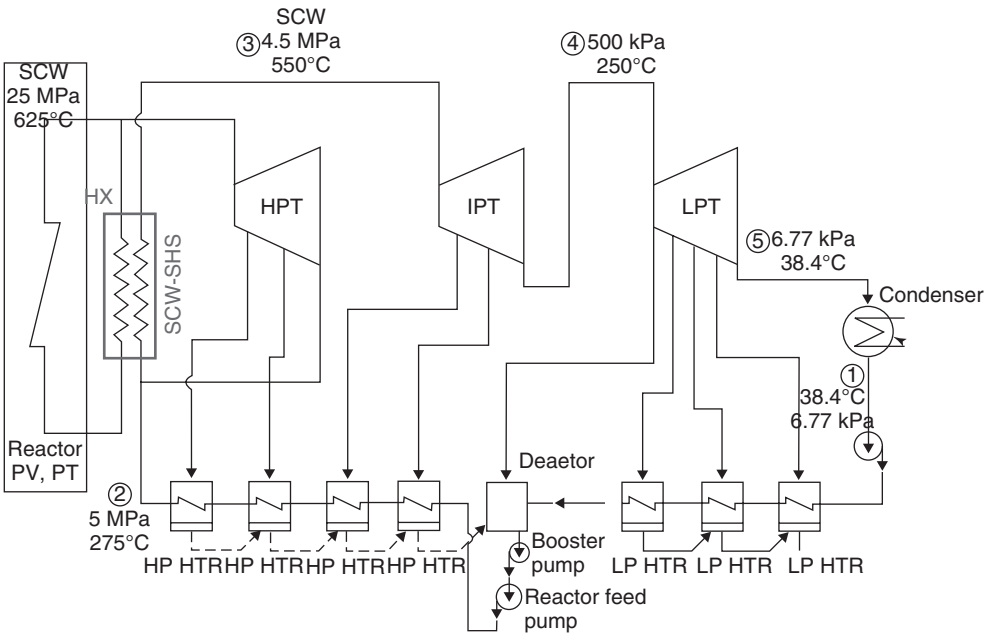

Figure 28.24 Schematic of dual no-reheat primary (SCW) loop and single-reheat secondary (superheated steam) loop regenerative thermodynamic cycle for 1200-MW_{el} pressure-vessel or pressure-channel SCW NPP (drawing prepared by H. Thind, UOIT).

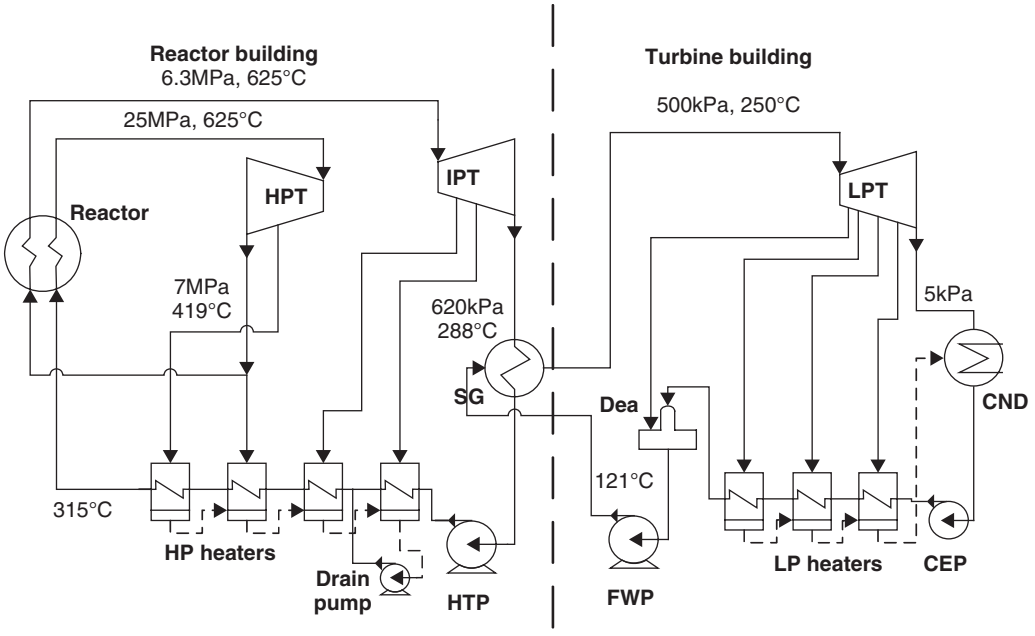

Figure 28.25 Schematic of dual single-reheat regenerative thermodynamic cycle for 1200-MW_{el} pressure-channel SCW NPP: High-pressure units located in Reactor Building for increased safety.

TABLE 28.10 Selected Parameters of Proposed SCWR Fuel Channels

Parameters	Unit	Description/Value		
Maximum cladding temperature (design value)	°C	850		
Maximum fuel centerline temperature (industry accepted limit)	°C	1850		
Heated fuel-channel length	m	5.772		
# of bundles/fuel channel	—	12		
# of fuel rods per bundle	—	43		
Bundle type (AECL designs) (see Fig. 28.26)	—	**CANFLEX**	**Variant-18**	**Variant-20**
# of heated fuel rods	—	43	42	42
# of unheated* fuel rods	—	—	1	1
Diameter of heated fuel rods (& of rods)	mm	11.5 (35) & 13.5 (8)	11.5	11.5
Diameter of unheated fuel rod	mm	—	18	20
Hydraulic-equivalent diameter of fuel channel	mm	7.52	7.98	7.83
Heated-equivalent diameter of fuel channel	mm	9.04	9.98	9.83
Heated area of fuel channel	m^2	9.26	8.76	8.76
Flow area of fuel channel	mm^2	3625	3788	3729
Pressure tube inner diameter	mm	103.45		
Average parameters of fuel channels in single-reheat (see Fig. 28.20) and no-reheat (see Fig. 28.22) options				
Heat flux in SCW channel (both cycles)	kW/m^2	918	970	970
Heat flux in SRH channel (single-reheat cycle)	kW/m^2	594	628	628
Mass flux in SCW channel (both cycles)	kg/m^2s	1206	1154	1172
Mass flux in SRH channel (single-reheat cycle)	kg/m^2s	2759	2640	2682

heat exchangers reduces the maximum temperature in the secondary-loop coolant at least by 25 to 75°C, thus lowering the efficiency of the cycle. Also, heat exchangers (steam generators) can be quite large units with about 200,000 square meters of heat-transfer surfaces.

From the SCWR design point of view, the following can be concluded:

- The single-reheat cycle has an advantage of higher thermal efficiency (compared to that of the no-reheat cycle) and reduced development costs due to a wide variety of single-reheat supercritical turbines manufactured by companies worldwide. The major disadvantage is the increased design complexity associated with the introduction of steam-reheat channels to the reactor core (see Fig. 28.14).
- The no-reheat cycle offers a simplified SCW NPP layout, contributing to lower capital costs. However, the efficiency of this cycle is lower, and no-reheat supercritical turbines have to be developed.

28.4.5 Forced-Convection Heat Transfer at Supercritical Conditions in Bundle and Bare Circular Tube Flow Geometries

In general, SCWRs, the same as many other reactor designs, have several limits, for example: (1) A design limit on the maximum fuel-sheath temperature and (2) an industry-accepted limit on the maximum fuel centerline temperature (1850°C for UO_2 nuclear fuel). The first limit (for an SCW CANDU reactor, it is 850°C) is important in terms of fuel-sheath integrity. It is well known that the strength of any materials decreases very fast with temperature increase. Therefore, at certain pressures and temperatures, the fuel sheath can collapse, and a fuel can be in direct contact with a reactor coolant. The second limit is also important in terms of a possible fuel melting, because the fuel centerline temperature is the highest temperature in a reactor.

Therefore, heat-transfer calculations in fuel-bundle geometry is an important task (some results of these calculations are listed at the end of this chapter). Unfortunately, the vast majority of heat-transfer experiments and the corresponding correlations are related to supercritical water and carbon dioxide flowing in bare-tube flow geometry (Pioro and Duffey, 2007). Currently, there is just one SCW heat-transfer correlation for fuel bundles developed by Dyadyakin and Popov (Russia) in 1977. This correlation was obtained in a 7-element helically-finned bundle (see Fig. 28.27). However, heat-transfer correlations for bundles are usually quite sensitive to a particular bundle design. Therefore, this correlation cannot be applied to other bundle geometries.

To overcome this problem, a wide-range heat-transfer correlation based on bare-tube data can be used as a conservative approach. The conservative approach is based on the fact that heat-transfer coefficients (HTCs) in bare tubes are generally lower than those in bundle geometries, where heat transfer is enhanced with appendages (grids, endplates, bearing pads, spacers, buttons, etc.).

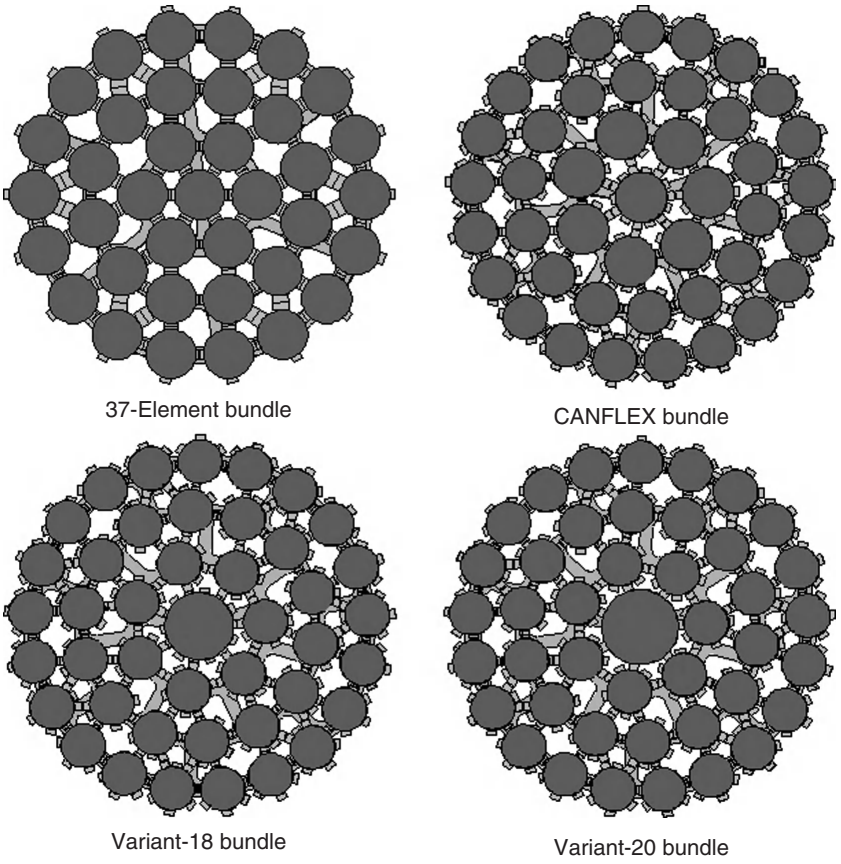

Figure 28.26 CANDU-reactor fuel bundles (Courtesy of Dr. L.K.H. Leung, AECL): 37 elements-current CANDU reactor design and 43-elements (the rest) - new designs.

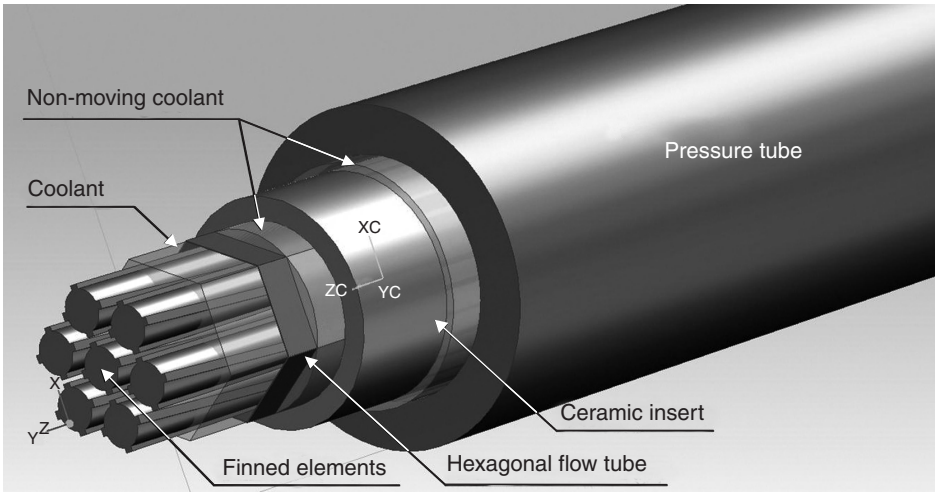

Figure 28.27 Tested 7-element helically finned bundle cooled with supercritical water and heated with electrical current (drawing prepared by W. Peiman, UOIT).

A number of empirical generalized correlations have been proposed to calculate the heat-transfer coefficient in forced convection for various fluids including water at supercritical pressures. However, differences in calculated heat-transfer coefficient values can be up to several hundred percent (Pioro and Duffey, 2007).

The most widely used heat-transfer correlation at subcritical pressures for forced convection is the Dittus-Boelter correlation (Pioro and Duffey, 2007). In 1942, McAdams proposed using the Dittus-Boelter correlation in the following form for forced-convective heat transfer in turbulent flows at subcritical pressures:

$$\mathbf{Nu}_{\mathrm{b}} = 0.0243\ \mathbf{Re}_{\mathrm{b}}^{0.8}\mathbf{Pr}_{\mathrm{b}}^{0.4}. \tag{28.1}$$

However, it was noted that Eq. (28.1) might produce unrealistic results within some flow conditions (see Fig. 28.2), especially, near the critical and pseudo-critical points, because it is very sensitive to variations in properties.

In general, experimental heat-transfer coefficient values show just moderate increase within the pseudo-critical region. This increase depends on flow conditions and heat flux: higher heat flux, less increase. Thus, the bulk-fluid temperature might not be the best characteristic temperature at which all thermo-physical properties should be evaluated. Therefore, use of the cross-sectional averaged Prandtl number (see below), which accounts for thermo-physical property variations within a cross section due to heat flux, was proposed in many supercritical heat-transfer correlations instead of the regular Prandtl number. Nevertheless, this classical correlation (Eq. (28.1)) was used extensively as a basis for various supercritical heat-transfer correlations.

In 1964, Bishop et al. conducted experiments in supercritical water flowing upward inside bare tubes and annuli within the following range of operating parameters: $P = 22.8–27.6$ MPa, $T_b = 282–527^{\circ}$C, $G = 651–3662$ kg/m^{2}s and $q = 0.31–3.46$ MW/m^2. Their data for heat transfer in tubes were generalized using the following correlation with a fit of $\pm 15\%$:

$$\mathbf{Nu}_{\mathrm{b}} = 0.0069\ \mathbf{Re}_{b}^{0.9}\overline{\mathbf{Pr}}_{b}^{0.66}\left(\frac{\rho_w}{\rho_b}\right)^{0.43}\left(1 + 2.4\frac{D}{x}\right) \tag{28.2}$$

Equation (28.2) uses the cross-sectional averaged Prandtl number, and the last term in the correlation, $(1+2.4D/x)$, accounts for the entrance-region effect. However, in the present comparison, the Bishop et al. correlation was used without the entrance-region term as the other correlations (see Eqs. (28.1), (28.3), and (28.4)).

In 1965, Swenson et al. found that conventional correlations, which use a bulk-fluid temperature as a basis for calculating the majority of thermo-physical properties, were not always accurate. They have suggested the following correlation in which a majority of thermophysical properties are based on a wall temperature:

$$\mathbf{Nu}_{\mathrm{w}} = 0.00459\ \mathbf{Re}_{\mathrm{w}}^{0.923}\overline{\mathbf{Pr}}_{\mathrm{w}}^{0.613}\left(\frac{\rho_w}{\rho_b}\right)^{0.231}. \tag{28.3}$$

Equation (28.3) was obtained within the following ranges: pressure 22.8–41.4 MPa, bulk-fluid temperature 75–576°C, wall temperature 93–649°C and mass flux 542–2150 kg/m^{2}s. This predicts the experimental data within $\pm 15\%$.

In 2002, Jackson modified the original correlation of Krasnoshchekov et al. from 1967 for forced-convective heat transfer in water and carbon dioxide at supercritical pressures to employ the Dittus-Boelter-type form for $\mathbf{Nu}_0$ as the following:

$$\mathbf{Nu}_{\mathrm{b}} = 0.0183\ \mathrm{Re}_{\mathrm{b}}^{0.82}\mathrm{Pr}_{\mathrm{b}}^{0.5}\left(\frac{\rho_w}{\rho_b}\right)^{0.3}\left(\frac{\overline{c}_p}{c_{pb}}\right)^{n}, \tag{28.4}$$

where the exponent n is defined as following:

$$n = 0.4 \quad \text{for } T_b < T_w < T_{pc} \text{ and for } 1.2T_{pc} < T_b < T_w;$$

$$n = 0.4 + 0.2\left(\frac{T_w}{T_{pc}} - 1\right) \quad \text{for } T_b < T_{pc} < T_w; \text{ and}$$

$$n = 0.4 + 0.2\left(\frac{T_w}{T_{pc}} - 1\right)\left[1 - 5\left(\frac{T_b}{T_{pc}} - 1\right)\right] \quad \text{for } T_{pc} < T_b < 1.2T_{pc} \text{ and } T_b < T_w.$$

An analysis performed by Pioro and Duffey (2007) showed that the two following correlations—(1) Bishop et al. (1964) and (2) Swenson et al. (1965)—were obtained within the same range of operating conditions as those for SCWRs.

The majority of empirical correlations were proposed in the 1960s–1970s, when experimental techniques were not at the same level (i.e., advanced level) as they are today. Also, thermo-physical properties of water have been updated since that time (for example, a peak in thermal conductivity in critical and pseudo-critical points within a range of pressures from 22.1 to 25 MPa was not officially recognized until the 1990s).

Therefore, recently a new or an updated correlation based on a new set of heat-transfer data and the latest thermo-physical properties of water (NIST, 2010) within the SCWRs operating range was developed and evaluated (Mokry et al., 2009):

$$\mathbf{Nu}_{\mathrm{b}} = 0.0061\ \mathbf{Re}_{\mathrm{b}}^{0.904}\overline{\mathbf{Pr}}_{\mathrm{b}}^{0.684}\left(\frac{\rho_w}{\rho_b}\right)^{0.564}. \tag{28.5}$$

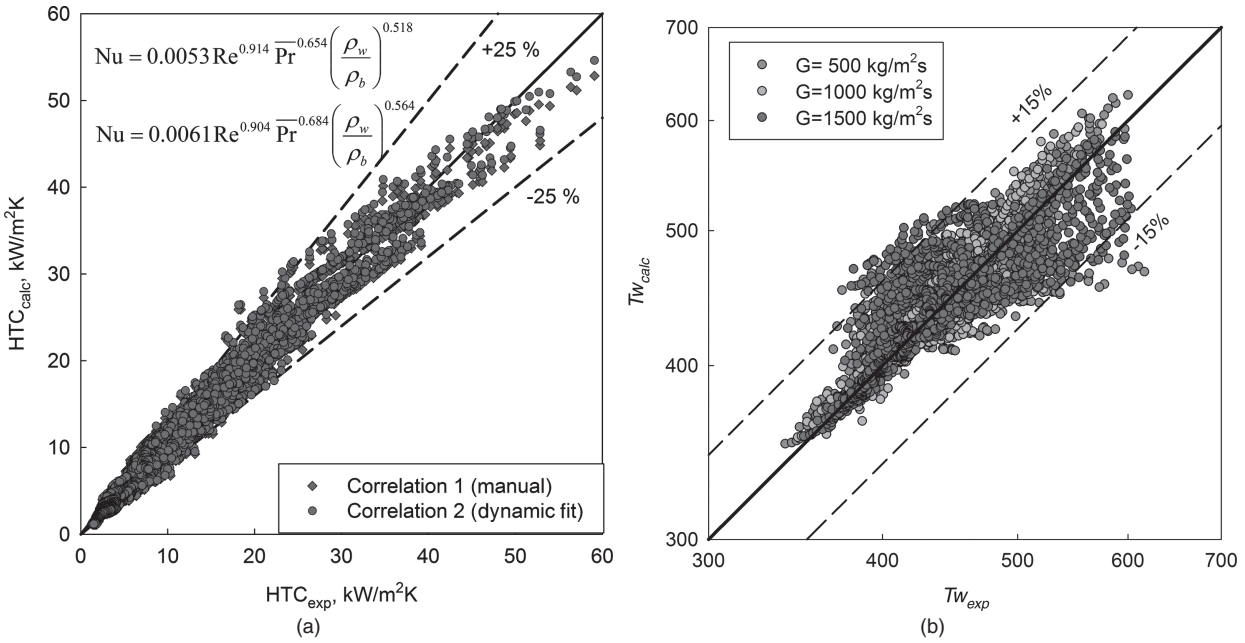

Figure 28.28 Comparison of data fit (Eq. (28.5)) with experimental data: (a) for HTC and (b) for wall temperature.

Figure 28.28 shows scatter plots of experimental HTC values versus calculated HTC values according to Eq. (28.5), and calculated and experimental values for wall temperatures. Both plots lie along a 45-degree straight line with an experimental data spread of ±25% for the HTC values and ±15% for the wall temperatures.

Figure 28.29 shows a comparison between experimentally obtained heat-transfer coefficient values and wall-temperature values and those calculated with the Dittus-Boelter, Bishop et al., Swenson et al., and Jackson correlations. Figures 28.30–28.33 show a comparison of the latest correlation (Eq. (28.5) with experimental data. Figure 28.34 shows a comparison between experimentally obtained HTC and wall-temperature values and those calculated with FLUENT CFD code and Eq. (28.5).

It should be noted that all heat-transfer correlations presented in this chapter are intended only for the normal and improved heat-transfer regimes.

The following empirical correlation was proposed for calculating the minimum heat flux at which the deteriorated heat-transfer regime appears:

$$q_{dht} = -58.97 + 0.745 \cdot G, \ \text{kW/m}^2. \tag{28.6}$$

Figures 28.30–28.34 show that the latest correlation (Eq. (28.5)) closely represents experimental data and follows trends closely even within the pseudo-critical range. Also, the Swenson et al. correlation showed good predictions with experimental data. CFD codes are a nice and modern approach. However, not all turbulent models are applicable to heat transfer at supercritical pressures, plus these codes should be tuned first on the basis of experimental data and after that used in similar calculations.

A recent study was conducted by Zahlan et al. (2010) in order to develop a heat-transfer look-up table for the critical/supercritical pressures. An extensive literature review was conducted, which included 28 datasets and 6,663 trans-critical heat-transfer data. Tables below list results of this study in the form of the overall weighted average and Root-Mean-Square (RMS) errors: (a) within three supercritical sub-regions for many heat-transfer correlations including discussed in this chapter (Table 28.11); and (b) for subcritical liquid and superheated steam (Table 28.12). In their conclusions, Zahlan et al. (2010) determined that within the supercritical region, the latest correlation by Mokry et al. (Eq. (28.5)) showed the best prediction for the data within all three sub-regions investigated. Also, the Mokry et al. correlation showed quite good predictions for subcritical liquid and superheated steam compared to other correlations.

Usually, heat-transfer calculations are backed up with hydraulic-resistance calculations. Pressure drop at supercritical pressures has also some specifics compared to that at subcritical pressures. These specifics are listed in Pioro and Duffey (2007) or Pioro et al. (2004). Another important issue at supercritical and subcritical pressures is uncertainties of measured and calculated parameters. Pioro and Duffey (2007) dedicated a separate Appendix D to this important issue in their book.

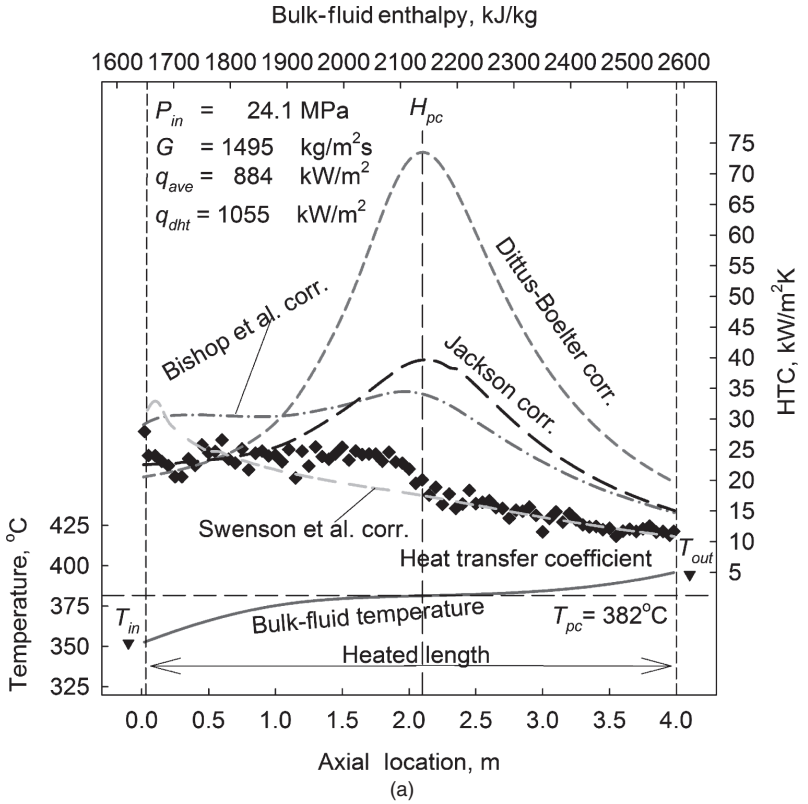

Figure 28.29 Comparison of HTC values calculated with several well-known correlations with experimental data along 4 m circular tube ($D = 10$ mm) (data by Dr. Kirillov et al.): $P_{in} = 24.1$MPa and $G = 1500$ and 200kg/m^{2}s.

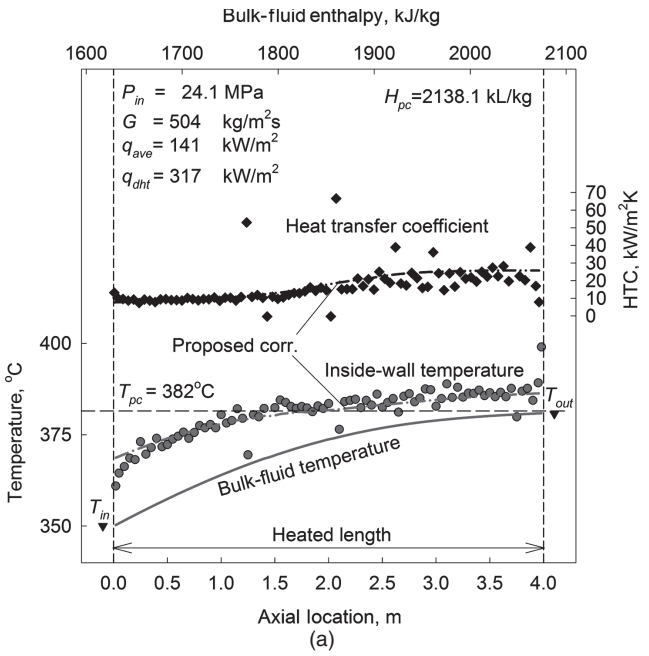

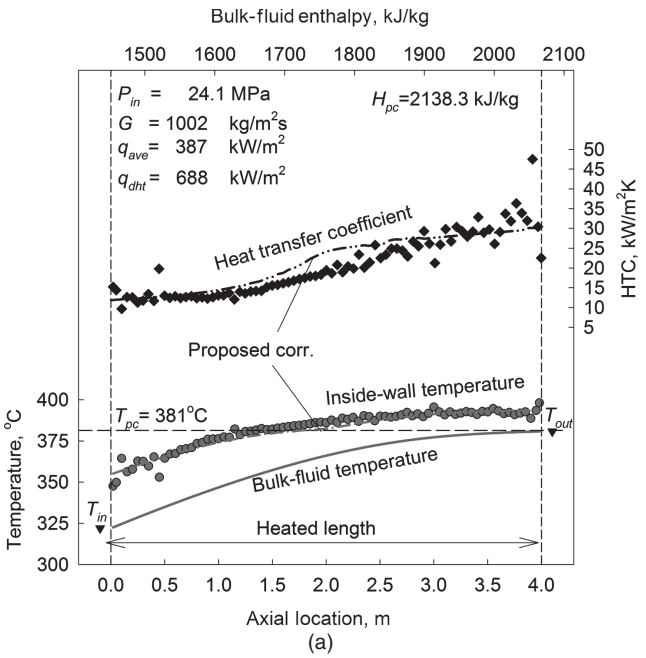

Figure 28.30 Temperature and HTC profiles at various heat fluxes along 4 m circular tube ($D = 10$ mm) (data by Dr. Kirillov et al.): $P_{in} = 24.1$ MPa and $G = 500$ kg/m^{2}s.

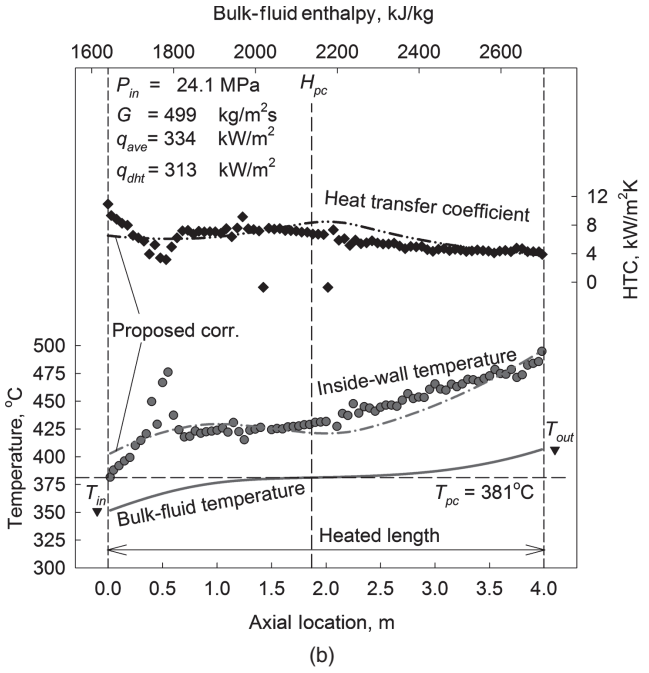

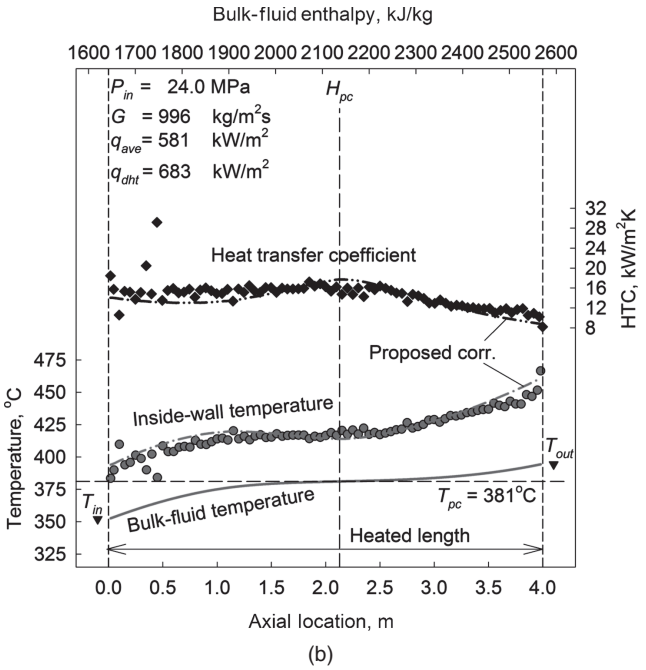

Figure 28.31 Temperature and HTC profiles at various heat fluxes along 4 m circular tube ($D = 10$ mm) (data by Dr. Kirillov et al.): $P_{in} = 24.1$ MPa and $G = 1000$ kg/m^{2}s.

28.5 SCWR FUEL-CHANNEL CALCULATIONS

SCWR technology is currently in its early design phase. A demonstration unit has yet to be designed and constructed. Fuel materials and configurations suited to supercritical conditions are currently being studied. This section describes thermal-design options of fuel bundles with respect to the maximum fuel centerline temperature to be restricted to 1850°C and the maximum sheath temperature to be restricted to 850°C.

A model used in the current thermal-design analysis is a generic PT SCWR with 300 fuel channels and 1200 MW_{el}

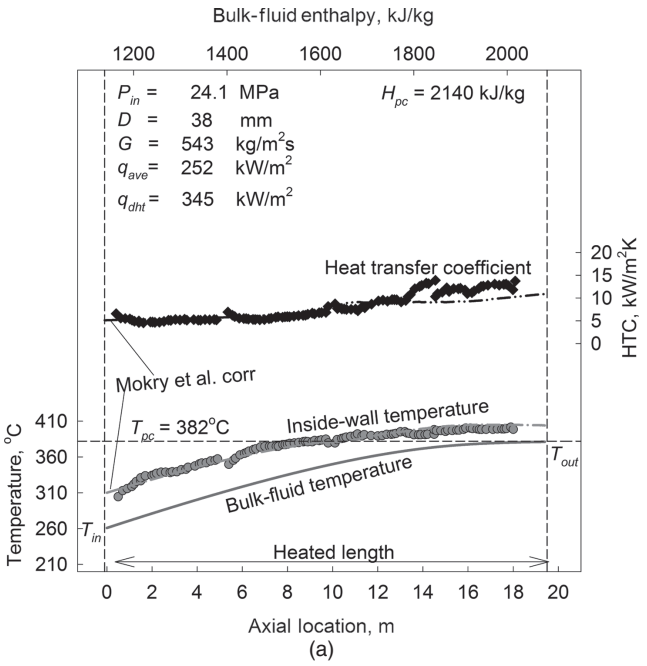

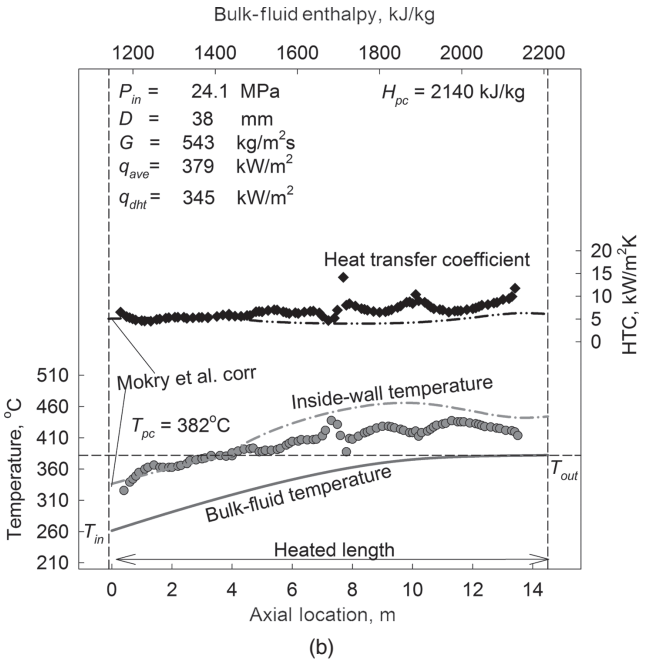

Figure 28.32 Temperature and HTC profiles along circular tube at various heat fluxes: Nominal operating conditions—P_{in} = 24.1MPa and D = 38 mm (Lee and Haller, 1974).

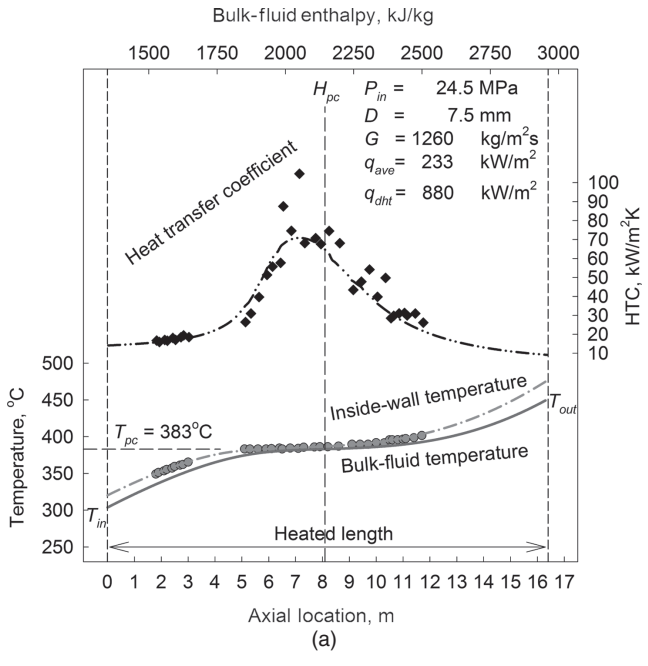

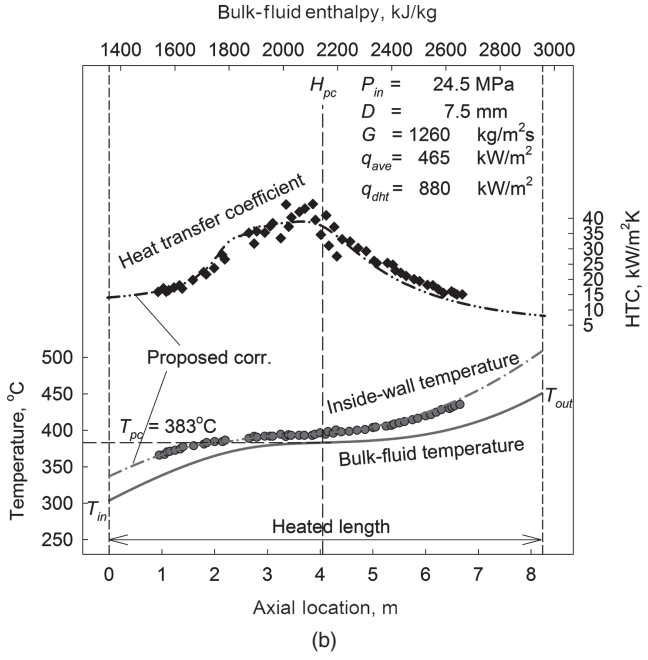

Figure 28.33 Temperature and HTC profiles along circular tube at various heat fluxes: Nominal operating conditions—P_{in} = 24.5 MPa and D = 7.5 mm (Yamagata et al., 1972).

power. A heated-channel length of 5.772 m is assumed. The anticipated fuel string consists of 12 bundles. Calculations consider the fuel-rod length to be equal to the heated-channel length, i.e., end-plates and end-caps of a bundle are not considered. Pressure drop along the channel was not accounted for, and pressure was assumed to be a constant 25 MPa. The contact resistance between a fuel pellet and sheath was considered to be negligible. Steady-state conditions with several uniform and cosine Axial Heat Flux Profiles (AHFPs) were applied. A coolant mass-flow rate per channel was assumed to be a constant 4.4 kg/s; and the produced power per channel to be 8.5 MW_{th}.

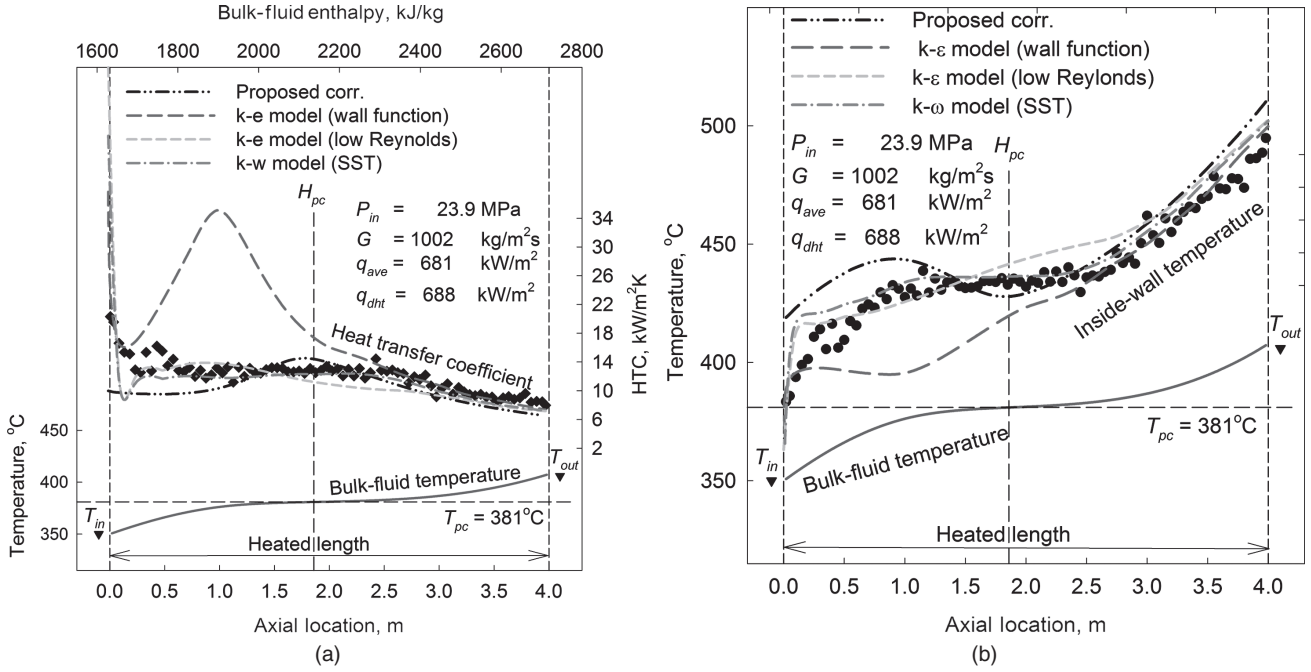

Figure 28.34 Comparison of HTC and wall temperature values calculated with proposed correlation (Eq. (28.5)) and FLUENT CFD-code (Vanyukova et al., NIKIET, 2009) with experimental data along 4 m circular tube ($D = 10$ mm): $P_{in} = 23.9$MPa and $G = 1000$kg/m^{2}s.

TABLE 28.11 Overall Weighted Average and RMS Errors within Three Supercritical Sub-regions (Zahlan et al., 2010)

	Supercritical Region					
	Liquid-Like		Gas-Like		Critical or Pseudo-Critical	
	Errors, %					
Correlation*	Average	RMS	Average	RMS	Average	RMS
Bishop et al. (1965)	6.3	24.2	5.2	18.4	20.9	28.9
Swenson et al. (1965)	1.5	25.2	−15.9	20.4	5.1	23.0
Krasnochekov et al. (1967)	15.2	33.7	−33.6	35.8	25.2	61.6
Watts & Chou (1982)	4.0	25.0	−9.7	20.8	5.5	24.0
Chou (1982)	5.5	23.1	5.7	22.2	16.5	28.4
Griem (1996)	1.7	23.2	4.1	22.8	2.7	31.1
Jackson (2002)	13.5	30.1	11.5	28.7	22.0	40.6
Mokry et al. (2009)	−3.9	**21.3**	−8.5	**16.5**	**−2.3**	**17.0**
Kuang et al. (2008)	−6.6	23.7	**2.9**	19.2	−9.0	24.1
Cheng et al. (2009)	**1.3**	25.6	**2.9**	28.8	14.9	90.6
Hadaller & Benerjee (1969)	7.6	30.5	10.7	20.5	—	—
Sieder & Tate (1936)	20.8	37.3	93.2	133.6	—	—
Dittus-Boelter (1930)	32.5	46.7	87.7	131.0	—	—
Gnielinski (1976)	42.5	57.6	106.3	153.3	—	—

In bold—the minimum values.

*Many of these correlations can be found in Pioro and Duffey (2007).

TABLE 28.12 Overall Average and RMS Errors within Subcritical Region (Zahlan et al., 2010)

	Subcritical Liquid		Superheated Steam	
	Error, %			
Correlation	Average	RMS	Average	RMS
Sieder and Tate (1936)	27.6	37.4	83.8	137.8
Gnielinski (1976)	−4.3	**18.3**	80.3	130.2
Hadaller and Banerjee (1969)	27.3	35.9	19.1	34.4
Dittus-Boelter (1930)	10.4	22.5	75.3	127.3
Mokry et al. (2009)	**−1.1**	19.2	**−4.8**	**19.6**

In bold—the minimum values.

A study was performed to analyze different design features in SCW pressure-channel nuclear reactors. This study was performed using a Variant-20 fuel bundle (see Fig. 28.26) with the uranium dioxide fuel, a uniform AHFP, and a fuel-average thermal conductivity. This study has shown that the fuel centerline temperature might exceed the industry accepted limit of 1850°C for UO_2 fuel (see Figure 28.35).

Therefore, other nuclear fuels with higher thermal conductivity and other AHFPs (cosine, upstream-skewed, and downstream-skewed cosine profiles (see Fig. 28.36)) were considered. The fuels compared below are uranium dioxide (UO_2) (as a reference case), uranium carbide (UC), uranium dicarbide (UC_2), and uranium mononitride (UN). The main objective was to achieve a fuel composition with a lower fuel centerline temperature suited for the SCWR use. Uranium dioxide is commonly used in current reactors. However, it has a very low thermal conductivity that decreases as the temperature increases (see Fig. 28.37).

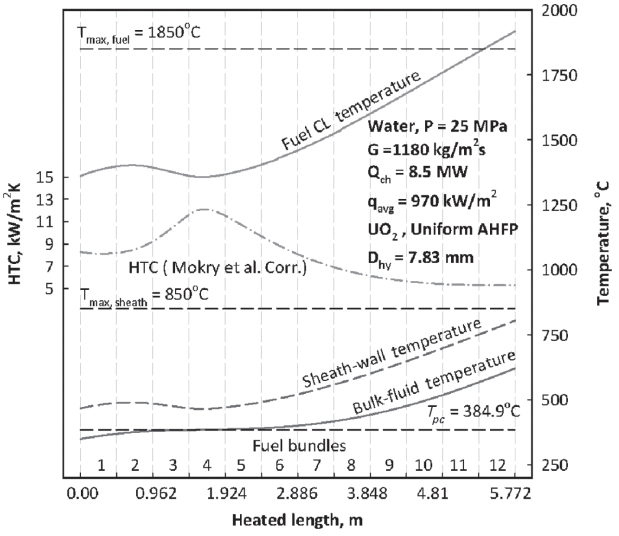

Figure 28.35 Temperature and HTC profiles of UO_2 along heated length of fuel channel (centreline fuel temperature based on average thermal conductivity of UO_2).

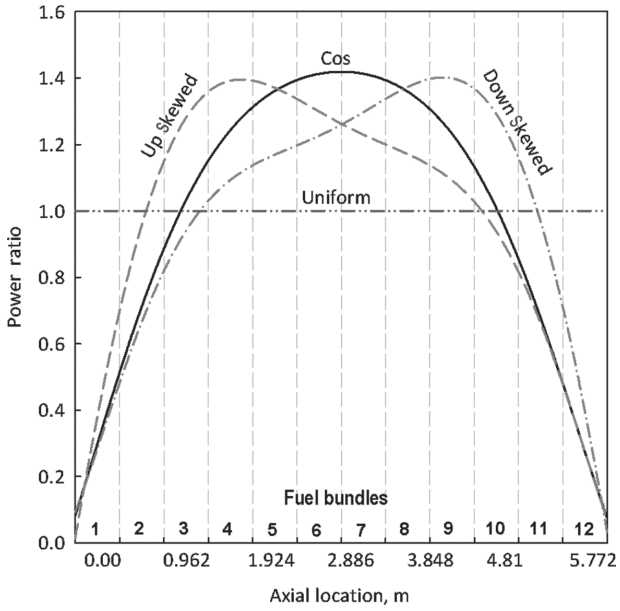

Figure 28.36 Non-uniform AHFPs (based on profiles shown by Dr. L.K.H. Leung, AECL).

As shown in Figure 28.37, thermal conductivities of UN, UC, and UC_2 fuels are many times higher than that of conventional nuclear fuels such as UO_2, MOX, and ThO_2, and their thermal conductivities increase with increasing temperature. A fuel with a rising trend in thermal conductivity would increase heat transfer through a pellet and decrease fuel centerline temperature. This rising trend in thermal conductivity would be a key safety factor for SCWRs.

Table 28.13 lists important thermo-physical properties of nuclear fuels. In general, there are many parameters, such as density, porosity, method of manufacturing, and others, that might affect the thermal conductivity of any potential fuel. Therefore, only generic thermal conductivities of nuclear fuels with densities equal to 95% of theorectical density were used in the following calculations.

Thermo-physical properties of a coolant at the sheath temperature and thermal conductivities of the sheath and fuel were calculated using an iterative method. In general, coolant properties were estimated based on a bulk-fluid

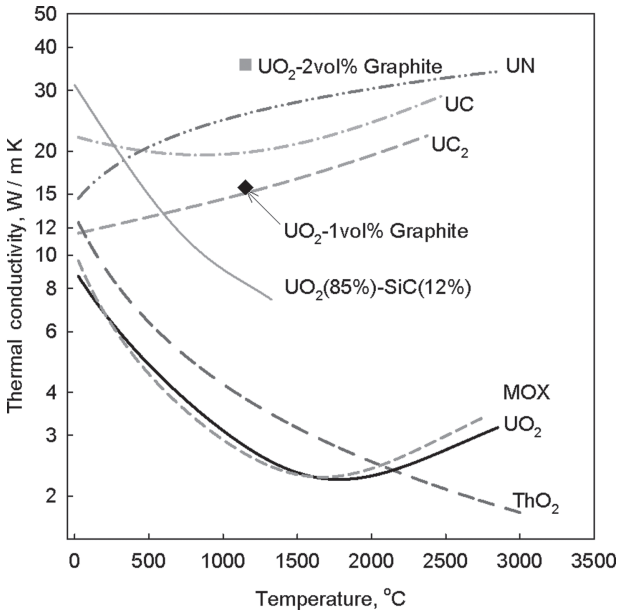

Figure 28.37 Comparison of thermal conductivities of nuclear fuels.

temperature, i.e., an average coolant temperature in a cross section. All calculations were performed along the heated-bundle length with a 1-mm increment.

The bulk-fluid temperature was calculated through the heat-balance method. With the bulk-fluid temperature known and sheath temperature assumed, all properties can be determined at these temperatures, and using the Mokry et al. correlation, the heat transfer coefficient can be calculated through iterations.

Uranium dioxide fuel centerline temperature surpasses the industry accepted limit of 1850°C for all considered AHFPs (see Figs. 28.35 and 28.38).

Figure 28.39 shows variations in temperatures and HTC profiles along the heated-bundle length at non-uniform AHFPs for UC_2, which has the lowest thermal conductivity compared to that of UN and UC fuels. An analysis shows that all calculated cases with UC_2 nuclear fuel have significantly lower fuel centerline temperatures compared to those of UO_2 fuel at all uniform and non-uniform AHFPs due to their high thermal conductivity. The most desirable case in terms of the lowest fuel centerline temperature is UN fuel with the upstream-skewed cosine AHFP. In this case, the fuel centerline temperature does not exceed even the sheath-temperature design limit of 850°C.

However, with UN, UC, and UC_2 fuels, there are factors beyond the scope of this chapter in regards to porosity, density, manufacturing process, high-temperature stability, chemical compatability, thermal-shock resistance, irradiation induced creep, volumetric swelling, etc., which must be accounted for when determining the feasibility of these substances as nuclear fuels for SCWRs.

Acknowledgments

Financial supports from the NSERC Discovery Grant and NSERC/NRCan/AECL Generation IV Energy Technologies Program are gratefully acknowledged.

NOMENCLATURE

A_{fl}	flow area, m^2
c_p	specific heat at constant pressure, J/kg·K
$\overline{c}_p$	average specific heat, J/kg·K, $\left(\frac{H_w - H_b}{T_w - T_b}\right)$
D	diameter (usually inside diameter), m
D_{hy}	hydraulic-equivalent diameter, m, $\left(\frac{4A_{fl}}{P_{wet}}\right)$
G	mass flux, kg/m^2s,
H	enthalpy, J/kg
h	heat transfer coefficient, W/m^2K
k	thermal conductivity, W/m·K
m	mass-flow rate, kg/s
P,p	pressure, Pa
P_{wet}	wetted perimeter, m
Q	heat-transfer rate, W

TABLE 28.13 Thermophysical Properties of Ceramic Nuclear Fuels at 0.1 MPa and 25°C

Property	Units	Fuel					
		UO_2	MOX*	ThO_2	UN	UC	UC_2
Molar mass	kg/kmol	270.3	271.2	264	252	250	262
Theoretical density	kg/m^3	10,960	11,074	10,000	14,300	13,630	11,700
Melting temperature	°C	2850 ± 30	2750	3227 ± 150	2850 ± 30	2365 ± 165	2800 ± 30
Boiling temperature	°C	3542	3538	> 4227	—	4418	—
Heat of fusion	kJ/kg	259 ± 15	285.3	—	—	195.6	—
Specific heat	kJ/kg·K	0.235	0.240	0.235	0.190	0.200	0.162
Thermal conductivity	W/m·K	8.68	7.82**	9.7	14.58	21.24	11.57
Coefficient of linear expansion	1/K	$9.75 \cdot 10^{-6}$	—	$8.9 \cdot 10^{-6}$	$7.52 \cdot 10^{-6}$	$10.1 \cdot 10^{-6}$	—

*MOX—Mixed Oxides $(U_{0.8}Pu_{0.2})\ O_2$, where 0.8 and 0.2 are the molar parts of UO_2 and PuO_2.

**at 95% density.

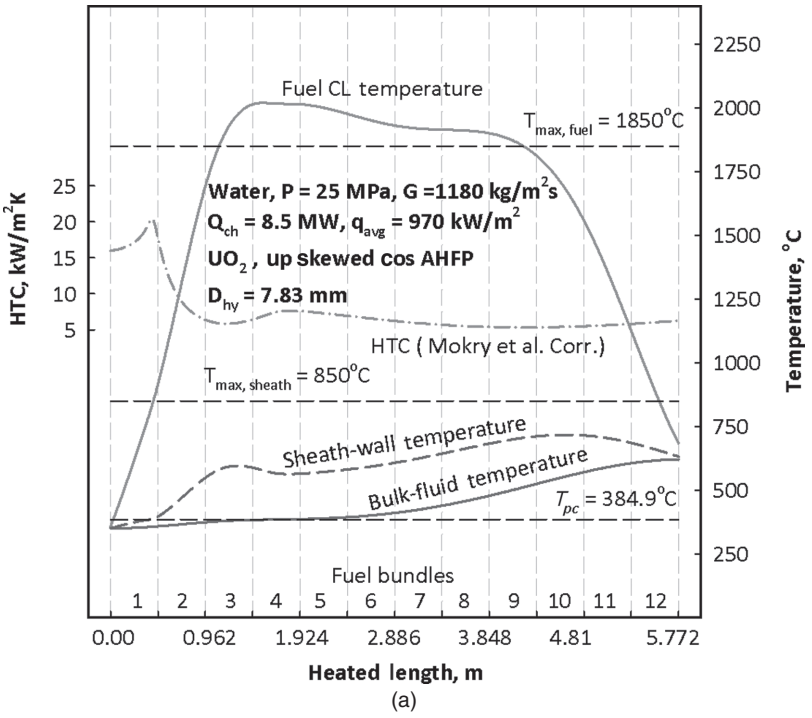

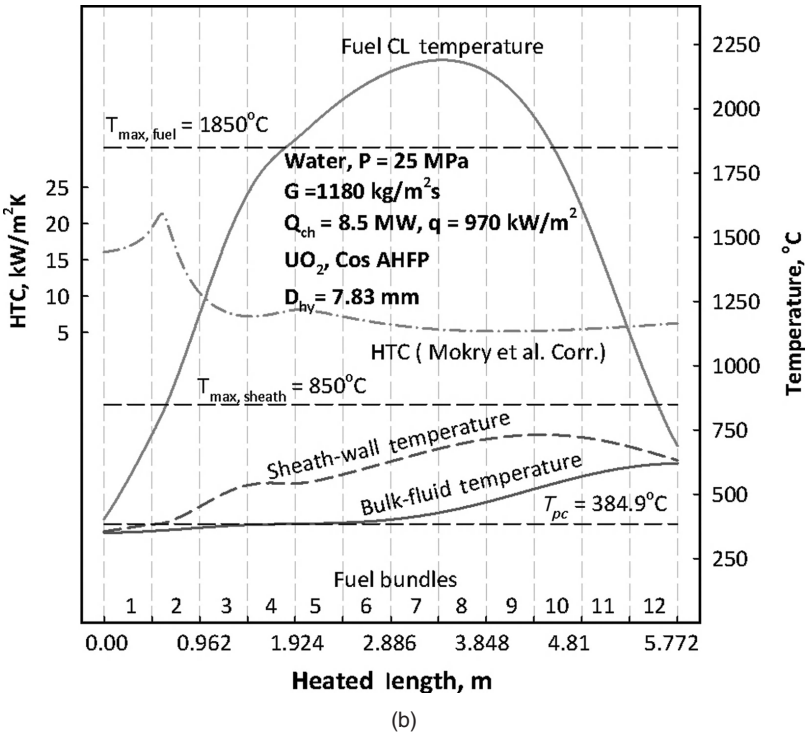

Figure 28.38 Temperature and HTC profiles for UO_2 fuel: (a) at upstream-skewed cosine AHFP and (b) at cosine AHFP.

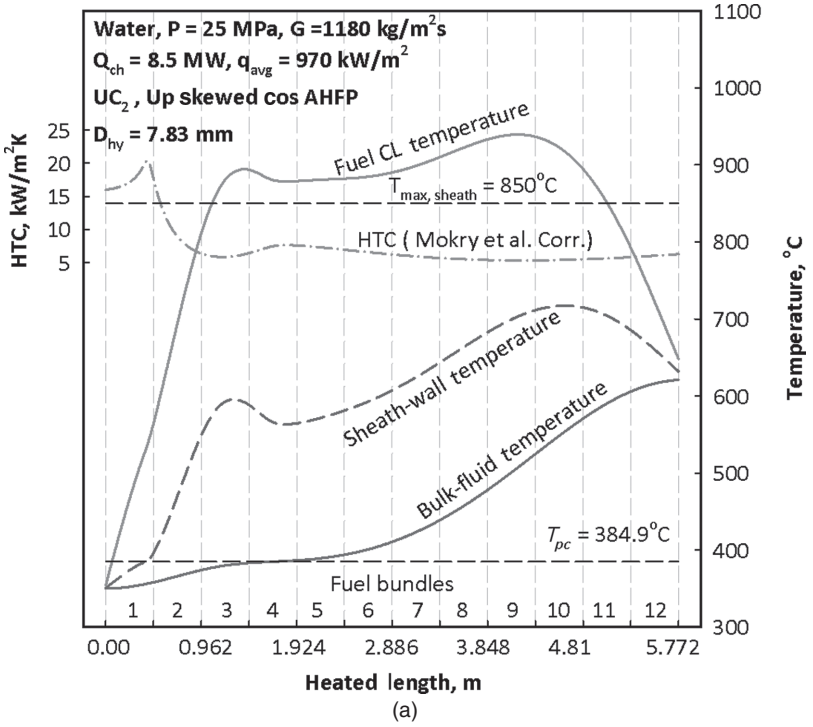

Figure 28.39 Temperature and HTC profiles along heated length of fuel channel for UC_2 fuel: (a) at upstream-skewed cosine AHFP, (b) at cosine AHFP, (c) at downstream-skewed cosine AHFP, and (d) at uniform AHFP.

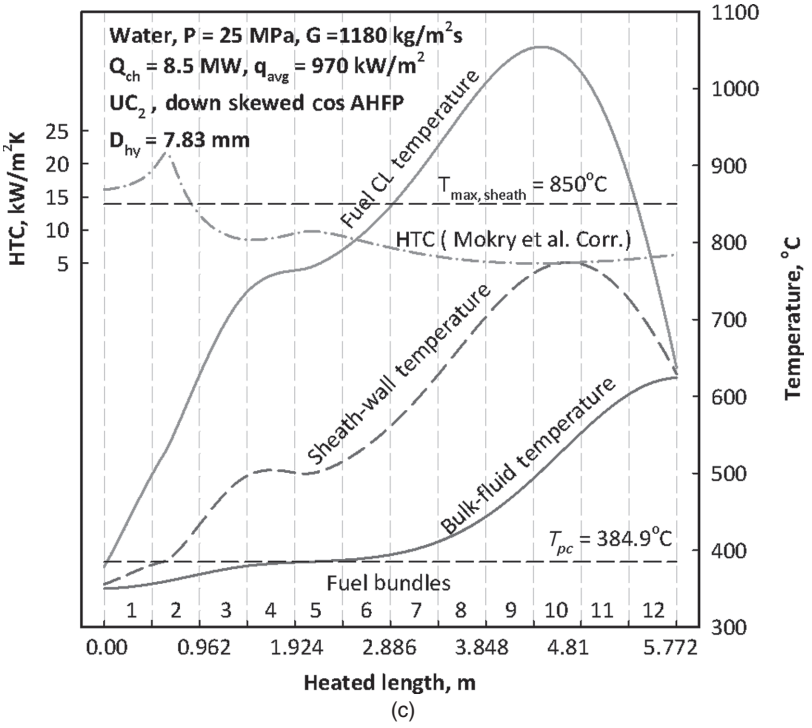

(c)

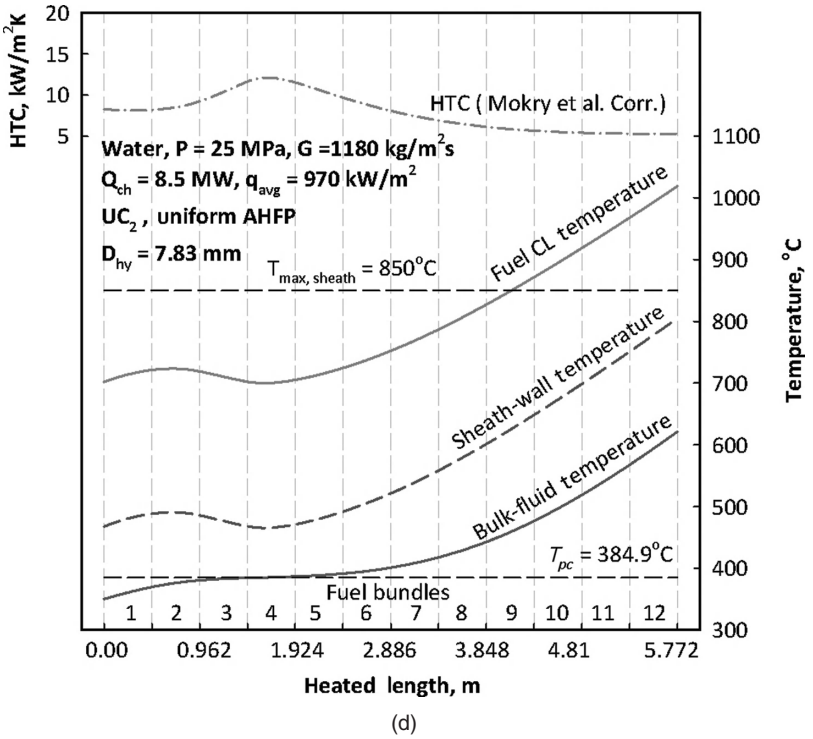

(d)

Figure 28.39 (*Continued*)

q	heat flux, W/m^2
s	entropy, J/kg K
T,t	temperature, $^\circ$C
V	volume, m^3
x	axial location, m

Greek Letters

δ	thickness, m
μ	dynamic viscosity, Pa·s
ρ	density, kg/m^3

Dimensionless Numbers

Nu	Nusselt number $\left(\frac{h \cdot D}{k}\right)$
Pr	Prandtl number $\left(\frac{\mu \cdot c_p}{k}\right)$
$\overline{\mathbf{Pr}}$	average Prandtl number $\left(\frac{\mu \cdot \overline{c}_p}{k}\right)$
Re	Reynolds number $\left(\frac{G \cdot D}{\mu}\right)$

Subscripts

ave	average
b	bulk
calc	calculated
ch	channel
cr	critical
dht	deteriorated heat-transfer
el	elctrical
exp	experimental
hy	hydraulic
in	inlet
max	maximum
out	outlet
pc	pseudocritical
th	thermal
w	wall

Abbreviations

AECL	Atomic Energy of Canada Limited
AGR	Advanced Gas-cooled Reactor
AHFP	Axial Heat Flux Profile
BWR	Boiling Water Reactor
CANDU	CANada Deuterium Uranium
CANFLEX	CANDU FLEXible (fueling)
CEP	Condensate Extraction Pump
CHF	Critical Heat Flux
CND	CoNDenser
Dea	Deaerator
DHT	Deteriorated Heat Transfer
DOE	Department of Energy
ECH	Evaporating CHannel
FWP	Feedwater Pump
GCR	Gas-Cooled Reactor
HEC	High Efficiency Channel
HHV	Higher Heating Value
HP	High Pressure
HPT	High Pressure Turbine
HTC	Heat Transfer Coefficient
HTP	Heat-Transport Pump
HTR	HeaTeR or High Temperature Reactor
IHT	Improved Heat Transfer
IP	Intermediate Pressure
IPPE	Institute for Physics and Power Engineering
IPT	Intermediate Pressure Turbine
LFR	Lead-cooled Fast Reactor
LGR	Light-water Graphite-moderated Reactor
LP	Low Pressure
LPT	Low Pressure Turbine
LWR	Light-Water Reactor
MOX	Mixed OXide
MSR	Moisture Separator Reheater
NHT	Normal Heat Transfer
NIKIET	Research and Development Institute of Power Engineering (Moscow, Russia)
NIST	National Institute of Standards and Technology (United States)
NPP	Nuclear Power Plant
PHWR	Pressurized Heavy-Water Reactor
PT	Pressure Tube
PWR	Pressurized Water Reactor
RBMK	Reactor of Large Capacity Channel type (in Russian abbreviations)
REC	Re-Entrant Channel
RFP	Reactor Feedwater Pump
SC	SuperCritical
SCW	SuperCritical Water
SCWO	SuperCritical Water Oxidation
SCWR	SuperCritical Water Reactor
SFL	Supercritical Fluid Leaching
SFR	Sodium Fast Reactor
SG	Steam Generator
SH	Sheath
SHS	SuperHeated Steam
SRCh	Steam-Reheat Channel
SRH	Steam ReHeat
SS	Stainless Steel

Endnotes

1. In 2009–2010, 439 power reactors operate around the world, including 415 water-cooled reactors: 262 PWRs, 94 BWRs, 44 Pressurized Heavy-Water Reactors (PHWRs), and 15 Light-water Graphite-moderated Reactors (LGRs) or RBMKs; 22 Gas-Cooled Reactors (GCRs) and Advanced GCRs (AGRs) (both types cooled with subcritical carbon dioxide); and 2 SFRs.
2. The heating value depends on the phase of the H_2O products. The heating value is called the HHV when the H_2O in the products is in the liquid form.
3. CANDU® (CANada Deuterium Uranium) is a registered trademark of Atomic Energy of Canada Limited (AECL).

REFERENCES

A.A. Bishop, R.O. Sandberg and L.S. Tong, Forced convection heat transfer to water at near-critical temperatures and supercritical pressures, *Report* WCAP-2056, Westinghouse Electric Corporation, Atomic Power Division, Pittsburgh, PA, USA, December, 1964.

T. Clifford, *Fundamentals of Supercritical Fluids*. Oxford University Press, New York, 1999.

R. B. Duffey, I. Pioro, T. Zhou, et al., Supercritical Water-Cooled Nuclear Reactors (SCWRs): Current and future concepts—steam-cycle options. *Proceedings of the 16th International Conference on Nuclear Engineering (ICONE-16)*, Paper 48869., Orlando, Florida, May 11–15, 2008.

J.D. Jackson, Consideration of the heat transfer properties of supercritical pressure water in connection with the cooling of advanced nuclear reactors, *Proceedings of the 13th Pacific Basin Nuclear Conference*, Shenzhen City, China, October 21–25, 2002.

P.A. Kruglikov, Yu. V. Smolkin, and K.V. Sokolov, Development of engineering solutions for thermal scheme of power unit of thermal power plant with supercritical parameters of steam, (In Russian), *Proc. of Int. Workshop "Supercritical Water and Steam in Nuclear Power Engineering: Problems and Solutions"*, Moscow, Russia, October 22–23, 2009.

R.A. Lee, and K.H. Haller, Supercritical water heat transfer developments and applications, *Proceedings of the 5th International Heat Transfer Conference*, Tokyo, Japan, September 3–7, **IV**, Paper No. B7.7, 1974, 335–339.

J. M. H. L. Levelt Sengers, Supercritical fluids: Their properties and applications, Chapter 1, in E. Kiran et al. (eds.), *Supercritical Fluids*, NATO Advanced Study Institute on Supercritical Fluids—Fundamentals and Applications, NATO Science Series, Series E, Applied Sciences. Kluwer Academic Publishers, Netherlands, 2000, Vol. 366, pp. 1–29.

S. Mokry, A. Farah, K. King, et al., Development of supercritical water heat-transfer correlation for vertical bare tubes. *Proceedings of the International Conference "Nuclear Energy for New Europe,"* Paper 210. Bled, Slovenia, September 14-17, 2009.

M. Naidin, S. Mokry, I. Pioro, R. Duffey, and U. Zirn, SCW NPPs: Layouts and thermodynamic cycles. *Proceedings of the International Conference "Nuclear Energy for New Europe,"* Paper 704. Bled, Slovenia, September 14-17, 2009.

G.F. Naterer, S. Suppiah, L. Stolberg, et al. Canada's program on nuclear hydrogen production and the thermochemical Cu-Cl cycle, *Int. J. of Hydrogen Energy (IJHE)*, 35, 2010, 10905–10926.

National Institute of Standards and Technology, *NIST Reference Fluid Thermodynamic and Transport Properties-REFPROP*. NIST Standard Reference Database 23, Ver. 9.0. U.S. Department of Commerce, Boulder, CO, 2010.

*Y. Oka, S. Koshizuka, Y. Ishiwatari, and A. Yamaji, *Super Light Water Reactors and Super Fast Reactors*. Springer, New York, USA, 2010.

I. L. Pioro, Thermophysical properties at critical and supercritical pressures, Section 5.5.16 in *Heat Exchanger Design Handbook*. Begell House, New York, 2008.

*I. L. Pioro and R. B. Duffey, *Heat Transfer and Hydraulic Resistance at Supercritical Pressures in Power Engineering Applications*. ASME Press, New York, 2007.

I. Pioro, R. Duffey, and T. Dumouchel, Hydraulic resistance of fluids flowing in channels at supercritical pressures (survey). *Nuclear Engineering and Design*, 2004, 231, 2, 187–197.

L. S. Pioro and I. L. Pioro, *Industrial Two-Phase Thermosyphons*. Begell House, Inc., New York, 1997.

I. Pioro, E. Saltanov, M. Naidin, et al., *Steam-reheat option in SCWRs and experimental BWRs*, Report for NSERC/NRCan/AECL Generation IV Energy Technologies Program (NNAPJ) entitled "Alternative Fuel-Channel Design for SCWR" with Atomic Energy of Canada Ltd., Version 1. UOIT, Oshawa, ON, Canada, March 2010.

I. Pioro, U. Zirn, R. Duffey, et al., Supercritical water-cooled nuclear reactors: Thermodynamic-cycles options. *Proceedings of the 6th International Conference on Heat Transfer, Fluid Mechanics and Thermodynamics (HEFAT-2008)*, Paper PI1, June 30?July 2, 2008, Pretoria, South Africa.

Supercritical heat transfer. In G.F. Hewitt, G.L. Shires and Y.V. Polezhaev (eds.), *International Encyclopedia of Heat & Mass Transfer*. CRC Press, Boca Raton, FL, 1998, pp. 1112–1117.

H.S. Swenson, J.R. Carver, and C.R. Kakarala, Heat transfer to supercritical water in smooth-bore tubes, Journal of Heat Transfer, Transactions of the ASME, Series C, 87 (4), 1965, 477–484.

*The most important references to the topic.

V.K. Vikulov, Yu. I. Mityaev, V.M. Shuvalov, Some issues on Beloyarsk NPP reactor physics, (in Russian), *Atomic Energy*, 30(2), 1971, 132–137.

K. Yamagata, K. Nishikawa, S. Hasegawa, et al. Forced convective heat transfer to supercritical water flowing in tubes, *International Journal of Heat & Mass Transfer*, 15(12), 1972, 2575–2593.

H. Zahlan, D. Groeneveld, and S. Tavoularis, Look-up table for trans-critical heat transfer. *Proceedings of the* 2nd *Canada-China Joint Workshop on Supercritical Water-Cooled Reactors (CCSC-2010)*, Toronto, Ontario, Canada, Canadian Nuclear Society (CNS), April 25–29, 2010.

29

GENERATION-IV GAS-COOLED FAST REACTOR

J'TIA P. TAYLOR

Argonne National Laboratory, Argonne, IL, USA

29.1 INTRODUCTION

The Generation-IV International Forum (GIF) is an organization composed of technical experts and governmental representatives with the goal of developing fourth-generation nuclear power reactors through international cooperation. The GIF began meeting in January 2000, and current state members include Argentina, Brazil, Canada, China, Euratom, France, Japan, Republic of Korea, the Russian Federation, Republic of South Africa, Switzerland, the United Kingdom, and the United States. The current technical secretariat for GIF is the Nuclear Energy Agency (NEA) under the Organization of Economic and Council Development (OECD), who, along with the International Atomic Energy Agency (IAEA), are permanent observers.

First-generation reactors include early prototypes such as the U.S. Shippingport and the British Magnox nuclear power plants implemented in the 1950s. Second-generation reactors include most currently operating commercial reactors: the PWR, BWR and CANDU reactors first implemented in the 1960s. Third-generation reactors include the advanced designs of second-generation reactors such as the CANDU6 and the AP600. The generation of reactors currently being implemented in China and elsewhere are deemed Generation III-plus (III+) and include the ABWR, AP1000, EPR, and ESBWR designs.

Revolutionart fourth-generation designs (Gen-IV) encompass increased safety, sustainability, proliferation resistance, and physical security features. The GIF selected six systems for further study: Very-High-Temperature Reactor (VHTR), Supercritical Water-Cooled Reactor (SCWR), Sodium-cooled Fast Reactor (SFR), Lead-cooled Fast Reactor (LFR), Molten Salt Reactor (MSR), and the Gas-cooled Fast Reactor (GFR). Gen-IV designs are proposed for implementation between 2015 and 2030 based on international collaboration. The content presented focuses on the Gas-cooled Fast Reactor concept, including ongoing research and development.

29.2 OVERVIEW OF GFR CONCEPT

The GFR concept cites a thermal power of 2400 MW and electric power of 1100 MW, with an outlet temperature of 850°C for an individual reactor. Like other reactor concepts, the GFR produces heat energy, which is then converted into mechanical energy and ultimately into electrical energy. The GFR uses a fast neutron spectrum, helium gas as the coolant and heat-transfer fluid in contrast to Light Water Reactors (LWR), which constitute nearly all currently operating power reactors. Helium flows through the reactor core where uranium and other actinides in the nuclear fuel are responsible for the exothermic fission reaction that provides the heat energy. The helium, increased in temperature from energy released through fission reactions, flows to the gas turbine used for converting the heat energy into mechanical energy. The gas turbine powers the electric generator, converting the mechanical energy into electricity. Figure 29.1 gives an illustration of a GFR concept. The primary purpose of the GFR is power production; however, three other purposes are cited as advantages for the GFR concept: actinide transmutation, process heat for chemical and/or heating processes, and direct energy conversion with a gas turbine.

Nuclear Energy Encyclopedia: Science, Technology, and Applications, First Edition (Wiley Series On Energy).
Edited by Steven B. Krivit, Jay H. Lehr, and Thomas B. Kingery.

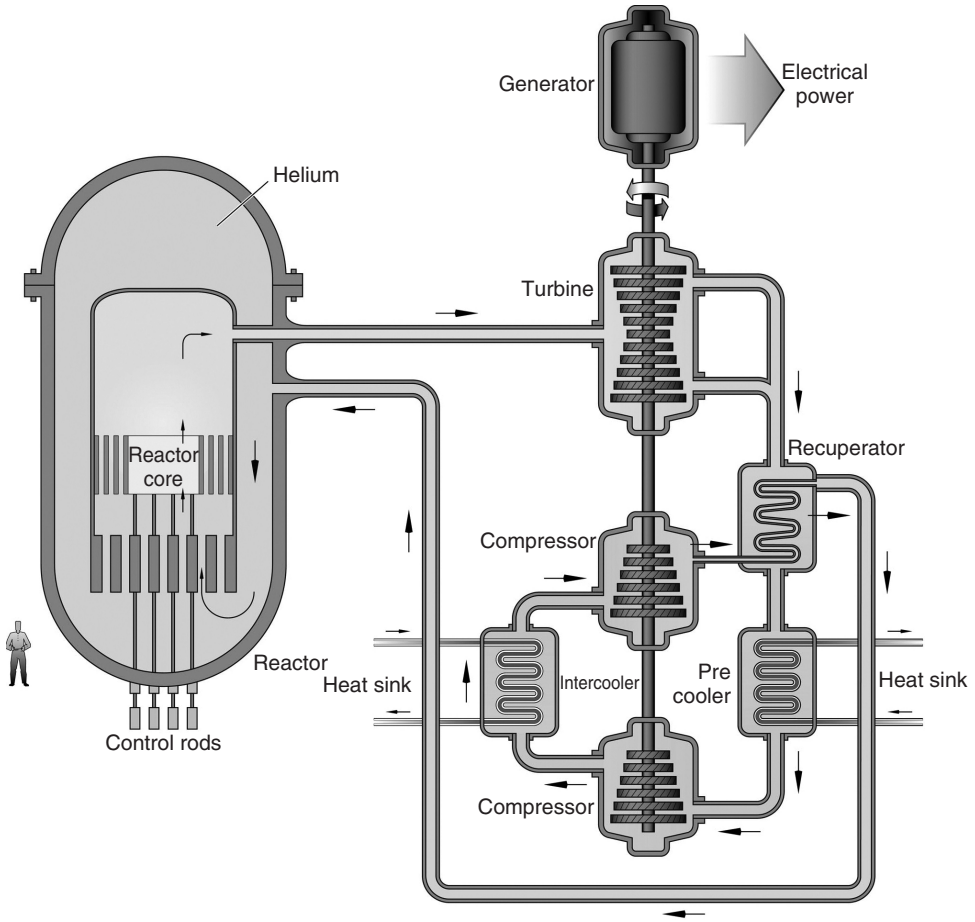

Figure 29.1 Schematic of a Gen-IV gas-cooled fast reactor power plant.

The fast neutron spectrum allows unique interactions between neutrons and fuel material. Fast neutrons interact with actinides, such as the U238 isotope, causing fission and releasing energy. In contrast, reactors using a thermal (or slow) neutron spectrum garner fission reactions and energy primarily from fissile material such as U235. Uranium in its natural state is comprised of approximately 99.2% U238 and 0.7% U235. Fast neutron fission reactions in the more abundant isotope result in a higher uranium utilization, meaning that more power is produced out of a given amount of uranium. Fast neutrons also interact with actinides, causing transmutation (or transformation) into different isotopes. The isotopes that are a product of the transmutation result in less radiotoxicity and heat emission than the starting actinides.

In one of the GFR concepts, helium leaves the core at approximately 850°C, much higher than the typical 290°C seen in LWRs. The use of helium as a heat transfer fluid is conducive to the higher outlet temperature due to its low reactivity and phase stability. The use of high-temperature helium allows the use of a gas turbine to convert heat energy into mechanical energy.

The use of a gas turbine for energy conversion is a significant departure from the operation of typical LWR nuclear power plants (NPP). Typical NPPs use pressure from the generated steam to turn a turbine and produce electricity. A gas turbine generates pressure from an exothermic reaction caused by the burning of the helium gas. A gas turbine is similar to the system used in automobiles, where fuel is ignited to power pistons, which power wheel shafts.

GFR use of a gas turbine leads to a thermal efficiency of approximately 45%, higher than typical nuclear reactors using a steam turbine at an approximate 33% thermal efficiency. Finally, the exhaust gas from the gas turbine can be routed to serve as a heat source for other processes. The processes could be used as heat sources for chemical applications, desalination of water, and district/residential heating. Nuclear power has been used for water desalination in Kazakhstan, India, and Japan. Projects to use nuclear power in water desalination are underway in many nations, including Spain, UK, China, and Jordan. Technical assistance for such projects is provided by the International Atomic Energy Agency (IAEA) and involves

more than 20 nations. District heating using nuclear power has been proven in Sweden, Russia, Switzerland, and Canada. In Switzerland, the Beznau Nuclear Power Plant provides heat to approximately 20,000 people.

29.3 FUTURE DEVELOPMENT

The Gas-cooled Fast Reactor concept is currently under research and development. The concept faces many technological hurdles to successful implementation. These hurdles, as cited in "A Technology Roadmap for Generation IV Nuclear Energy Systems," include development of materials, high-performance gas turbines, and coupling technologies for high-temperature heat and process heat applications. Research and development plans call for establishing the viability of the GFR by 2020, a design by 2019, and a prototype reactor by 2025.

FURTHER READING

Generation IV International Forum, *A Technology Roadmap for Generation IV Nuclear Energy Systems*, 03-GA50034, 2002. Available online at http://www.ne.doe.gov/genIV/documents/gen_iv_roadmap.pdf.

Generation IV International Forum, *GIF R&D Outlook for Generation IV Nuclear Energy Systems*. Available online at http://www.gen-4.org/PDFs/GIF_RD_Outlook_for_Generation_IV_Nuclear_Energy_Systems.pdf, accessed August 21, 2010.

J. Lamarsh and A. Baratta, A., *Introduction to Nuclear Engineering*. Prentice Hall, Upper Saddle River, NJ, 2001.

30

GENERATION-IV SODIUM-COOLED FAST REACTORS (SFR)

Robert N. Hill, Christopher Grandy and Hussein Khalil

Argonne National Laboratory, Argonne, IL, USA

The Generation-IV Technology Roadmap [1] identified three major missions for Generation-IV systems:

1. Electricity production
2. Supply of heat for hydrogen production, seawater desalination, and industrial uses
3. Actinide management

The fast reactors identified in the Roadmap, and particularly the Sodium-cooled Fast Reactor (SFR), were identified as crucial to perform the actinide management mission (as explained below) and able to perform the electricity and heat production missions.

30.1 FAST REACTOR PHYSICS

Fission reactor concepts that rely on high-energy neutrons are termed *fast reactors* because the neutrons remain "fast" (at high energy) between fission events. The energy spectrum of the neutron population of five Generation-IV advanced reactor systems is compared to a conventional Pressurized Water Reactor (PWR) in Figure 30.1. Similar to conventional LWRs, the Very High Temperature Reactor (VHTR) and SuperCritical Water Reactor (SCWR) designs employ *moderators* (carbon and supercritical water respectively) to slow down the fission neutrons. Conversely, in a fast spectrum reactor, moderating materials are avoided. Three different fast reactor options are identified in the Generation-IV Roadmap: the Sodium-cooled Fast Reactor (SFR), Lead-alloy-cooled Fast Reactor (LFR), and the Gas-cooled Fast Reactor (GFR). With regard to the system's physics behavior, the neutron energy spectra of the three reactor types are similar as shown in Figure 30.1.The fast spectrum systems have no low-energy neutrons, and most neutron reactions occur around the flux peak at 100 keV.

The variation of nuclear interactions with energy spectrum is illustrated in Figure 30.2; the fission-to-absorption ratio is compared for dominant actinides in the PWR and SFR spectra. The fission/absorption ratios are consistently higher for the fast spectrum, over 80% of fast neutron absorptions in fissile isotopes (e.g., U235 and Pu239) result in fission. The fast fission ratio can rise to 50% for fertile isotopes (e.g., Pu240), while remaining low (<5%) in a thermal spectrum. Thus, in a fast spectrum, actinides are preferentially fissioned, not transmuted into higher actinides. This implies that fast systems are more "efficient" in destroying actinides because fewer neutrons are lost to capture reactions before eventual fission; this enables enhanced utilization of resources through efficient conversion of U238. Furthermore, the generation rate of higher actinides through neutron capture is inhibited; this mitigates the generation of higher actinides that complicates the recycle and/or disposal of used nuclear fuel.

The Generation-IV SFR system uses liquid sodium as the reactor coolant, allowing high power density with low coolant pressure. Plant-size options under consideration range from small (50 to 300 MWe) modular reactors to

Nuclear Energy Encyclopedia: Science, Technology, and Applications, First Edition (Wiley Series On Energy).
Edited by Steven B. Krivit, Jay H. Lehr, and Thomas B. Kingery.

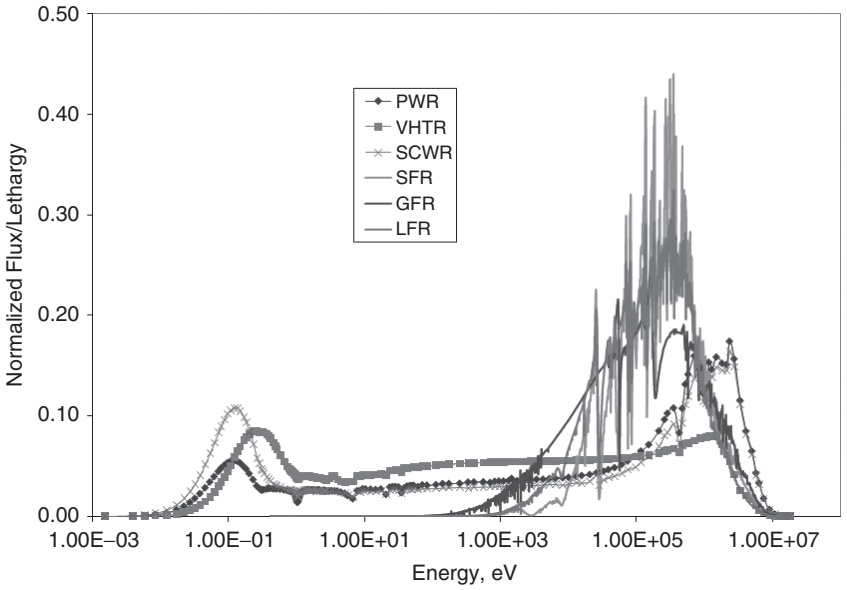

Figure 30.1 Comparison of neutron energy spectra of Gen-IV reactors.

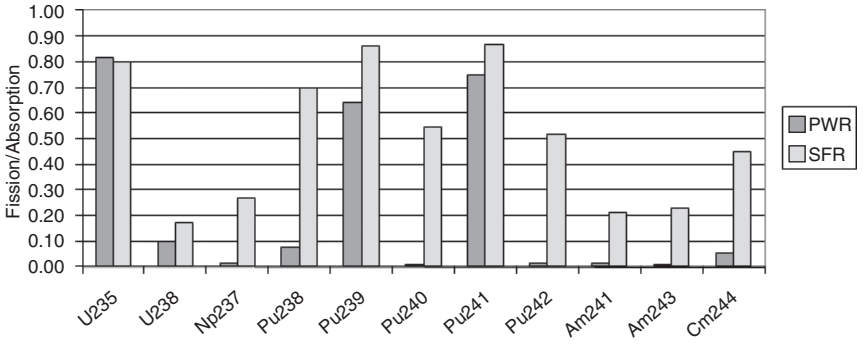

Figure 30.2 Comparison of fission/absorption ratio for PWR and SFR.

larger plants (up to 1500 MWe). The SFR technology was evaluated as most mature of the Generation-IV concepts and is a promising technology to perform the actinide management mission. If enhanced economics for the system can be realized, it can also satisfy the electricity and heat production missions.

30.2 SODIUM-COOLED FAST REACTOR (SFR) BACKGROUND AND EXPERIENCE

The base SFR system relies on technologies already developed and demonstrated in worldwide fast reactor programs. Sodium-cooled fast spectrum reactors have been designed and operated successfully for several decades throughout the world in countries such as France, Germany, India, Japan, Russia, United Kingdom, and the United States. In the United States, SFR technology was employed in the 20 MWe EBR-II that operated from 1963 to 1994. EBR-II research and development included development and testing of metal fuel, demonstration of a closed fuel cycle, and passive safety tests. The 400 MWt Fast Flux Test Facility (FFTF) was completed in 1980. FFTF operated successfully for 10 years with a full core of mixed oxide (MOX) fuel and performed SFR materials, fuels, and component testing.

Significant SFR research and development programs have also been conducted in Russia, Japan, France, India, and United Kingdom. The only current fast *power* reactor is BN-600 (Russia), which has reliably operated since 1980 with a 75% capacity factor. Recent and current operating *test* reactors include PHENIX (France), JOYO (Japan), BOR-60 (Russia), and FBTR (India). The most modern fast reactor construction project was the 280 MWe MONJU (Japan) that was completed in 1990. In addition, SFR technology programs have recently been started in

TABLE 30.1 Experimental Sodium-Cooled Fast Reactors

Plant	Primary Configuration	Status
Rapsodie (France)	Loop	Shut down, deactivated
KNK-II (Germany)	Loop	Decommissioned
FBTR (India)	Loop	Operating
PEC (Italy)	Loop	Decommissioned
JOYO (Japan)	Loop	Operating
DFR (UK)	Loop (NaK)*	Decommissioned
BOR-60 (Russian Federation)	Loop	Operating
EBR-II (USA)	Pool	Shut down, deactivated
Fermi (USA)	Loop	Decommissioned
FFTF (USA)	Loop	Shut down, deactivated
BR-10 (Russian Federation)	Loop	Shut down
CEFR (China)	Pool	Operating

*NaK is sodium-potassium alloy.

both Korea and China, with the Chinese Experimental Fast Reactor scheduled for startup in 2010. Overall, approximately 300 reactor years of operating experience have been logged on SFRs, including 200 years on small test reactors and 100 years on larger demonstration reactors.

Tables 30.1–30.3 show the primary plant configurations for the historical, current, and potential future fast reactor systems from around the world as documented in the IAEA Fast Reactor Database [2]. Table 30.1 provides information on the experimental sodium-cooled fast reactors. Table 30.2 provides information on demonstration-size sodium-cooled fast reactors and design concepts. Table 30.3 provides information on the commercial-scale sodium-cooled fast reactors and proposed reactor designs.

TABLE 30.2 Demonstration or Prototype Sodium-Cooled Fast Reactors

Plant	Primary Configuration	Status
Phenix (France)	Pool	End of Life Testing
SNR-300 (Germany)	Loop	Never built
PFBR (India)	Pool	In construction
MONJU (Japan)	Loop	Shutdown will restart 2010
PFR (UK)	Pool	Shut down, deactivated
CRBRP (USA)	Loop	Designed, not built
BN-350 (Russian Federation)	Loop	In decommissioning
BN-600 (Russian Federation)	Pool	Operating
ALMR (USA)	Pool	Conceptual design, not built
KALIMER-150 (Korea)	Pool	Conceptual design

TABLE 30.3 Commercial Size Sodium-Cooled Fast Reactors

Plant	Primary Configuration	Status
Super-Phenix 1 (France)	Pool	Shut down, deactivated
Super-Phenix 2 (France)	Pool	Conceptual, not built
SNR-2 (Germany)	Pool	Conceptual, not built
DFBR (Japan)	Loop	Conceptual, not built
CDFR (UK)	Pool	Conceptual, not built
BN-1600 (Russia)	Pool	Conceptual, plans to build
BN-800 (Russia)	Pool	In construction
EFR (France)	Pool	Conceptual design
ALMR (USA)	Pool	Conceptual design, not built
BN-1800 (Russia)	Pool	Conceptual
JSFR-1500 (Japan)	Loop	Conceptual

30.3 SODIUM-COOLED FAST REACTOR SYSTEM DESCRIPTION

The coolant for an SFR is liquid sodium. Sodium is used as the reactor core's coolant because of its favorable heat transport properties, low density, and lack of neutron moderation. These features allow operation at ~500°C without pressurization, large margins to boiling, modest pumping power, and a fast neutron energy spectrum. Sodium coolant[1], which is chemically reactive with air, must be maintained under an inert atmosphere to prevent chemical reactions between molten sodium and water vapor or oxygen. Argon, nitrogen, and helium gases are used as the inerting gas atmospheres.

In the basic SFR configuration (see Fig. 30.3), the reactor core will contain either enriched uranium or plutonium/uranium fuel. The fuel will absorb fast neutrons and undergo fission (see Fig. 30.2), which produces heat. Typically, plants built for electricity generation use a steam cycle, and a common characteristic of the different designs is the use of a secondary (also called intermediate) coolant heat transport loop also containing sodium. Heat from the reactor's core is transferred from the primary sodium to the secondary sodium in an intermediate heat exchanger (IHX). The primary sodium will undergo neutron capture reactions in the core region, making it mildly radioactive. Thus, the main purpose of the secondary sodium circuit is to isolate the radioactive primary coolant from the

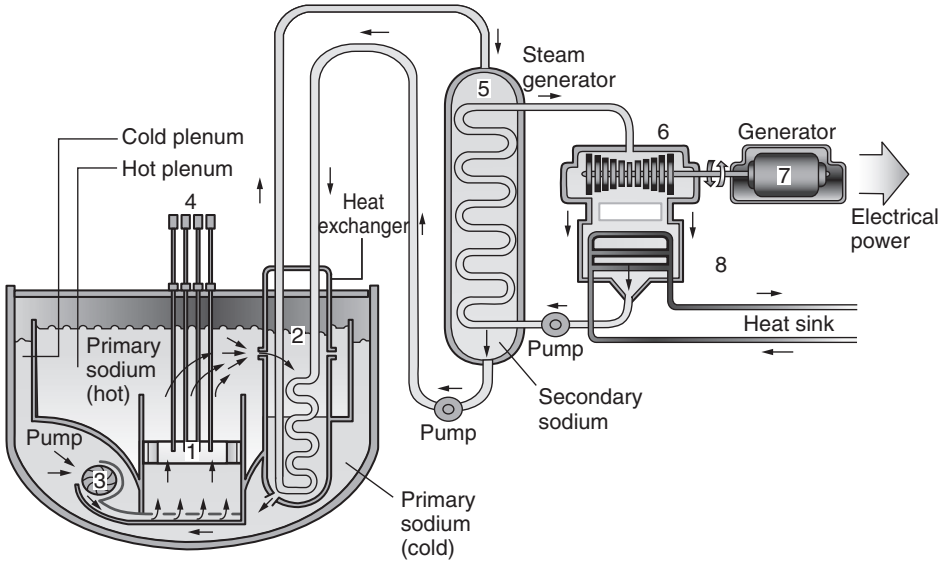

Figure 30.3 Generic sodium-cooled fast reactor.

water/steam circuit, thereby preventing any sodium/water reaction generated in the steam generator (e.g., in the event of a steam generator tube leak) from releasing radioactive reaction products through the sodium water reaction protection relief system to the environment or having sodium/water reaction products enter the reactor core region of the plant. Sodium-cooled reactors built to date have all had a secondary loop filled with flowing sodium. The water-sodium boundary is located only in the secondary sodium circuit. Even in fast reactor plants that do not produce electricity and the heat is rejected directly into the atmosphere (e.g., the former Fast Flux Test Facility in Washington State) or used for process heat (e.g., hydrogen generation), an intermediate sodium loop is still used to isolate the radioactive primary coolant from the ambient air or process heat fluid. Although there are incentives for eliminating the intermediate sodium loop (e.g., potentially reducing capital costs, increasing the plant's thermal efficiency, reducing maintenance costs) the risk of a steam generator tube leak or rupture has forestalled the design of sodium-cooled reactors with primary radioactive sodium coolant flowing directly within the steam generator.

The principal components of the primary heat transport system in a sodium-cooled reactor are the reactor vessel and reactor enclosure (head) that contain the primary radioactive sodium, reactor core region, with an upper and lower plenum, a lower core support structure and associated pressure balanced inlet plenum, a primary sodium-to-intermediate sodium heat exchanger, a primary pump, and the necessary piping, valving[2], and instrumentation. Two basic arrangements have been developed for the configuration of the primary coolant components:

1. **Loop design**. In this arrangement (Fig. 30.4), the reactor and individual primary components are housed in separate vessels with interconnecting piping. The reactor vessel has connected to it two or more loops of piping, each containing, in series, a pump, an IHX, and necessary valves. Each primary loop is dedicated to a particular secondary circuit and steam generator. All of the primary system components contain radioactive sodium, thus suitable radiation shielding and inerted cells must be provided within the containment building.

   A choice exists as to the location of the primary pump; it may be located between the reactor vessel and the IHX (in the hot leg of the loop) or after the IHX (in the cold leg of the loop). In the former case, the pump will operate at the high coolant operating temperature (reactor outlet temperature of approximately 480–550°C). In the latter case, the pump operates at the lower coolant operating temperature (reactor inlet temperatures of approximately 310–380°C). Determination of the primary pump position requires balancing the high-temperature thermal design problems of a hot-leg pump against the necessary available net positive suction head requirements of a cold leg pump, which in turn affects the size of the primary pump and the IHX.

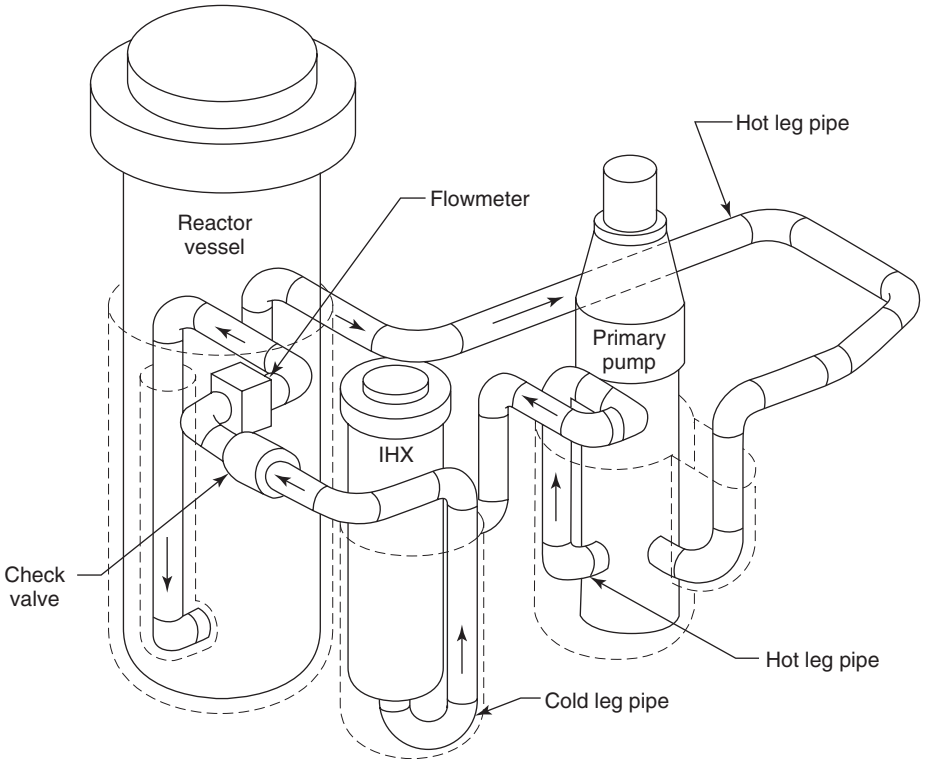

Figure 30.4 Loop plant configuration with hot leg pump.

A system of piping (and possibly valving) connects the IHX and primary pumps with the reactor vessel. The primary piping is designed to accommodate thermal expansion and contraction as a result of sodium coolant temperature changes during normal and transient conditions. Therefore, the piping generally has large bends and expansion loops to reduce the thermal stresses on the piping system. Some designers have proposed the use of large bellows to accommodate the piping system's thermal expansion and contraction, but these have never been deployed commercially in sodium applications.

2. **Pool design**. In a typical pool reactor (see Fig. 30.5), the whole primary heat transport system, comprising the core, intermediate heat exchangers, primary circulating pumps, the associated structures, and primary (radioactive) sodium are contained within the reactor vessel (essentially a tank), typically suspended from the reactor vessel enclosure assembly that forms part of the primary sodium containment boundary. High-temperature sodium leaving the reactor core enters a large inner pool (hot pool) containing the IHXs in which heat is transferred to the secondary sodium. Primary sodium flows downward through the IHX (typically on the shell side) and discharges from the IHXs into a relatively low-temperature outer pool (cold pool), which is separated from the hot inner pool by an insulated inner tank (sometimes referred to as a redan). The primary vessel is maintained at the low temperature (essentially core inlet temperature). The low-temperature sodium is suctioned into the primary pumps, located in the outer cold pool, from which it is discharged via piping and ducts into the inlet plenum, which distributes the sodium into the core assemblies. The core, with its associated shielding and core barrel, is mounted on the lower internal structure, which is integral with the primary vessel. Generally, the primary vessel, the redan, lower internal structure, and core barrel are permanent structures of a pool plant configuration.

In both pool and loop configurations, the major structural components need to be shielded from the radiation field emanating from the reactor core to reduce the radiation damage to the permanent structures and thus extend the life of the reactor plant. The radiation damage to the permanent structures must be sufficiently low so that the structures can last for the life of the plant with sufficient structural margins. Reactors with both pool and loop configurations have been successfully designed and operated. There have been arguments in favor of both types of primary plant configurations, and neither type offers an overwhelming or clear advantage over the other in key areas such as economics, safety,

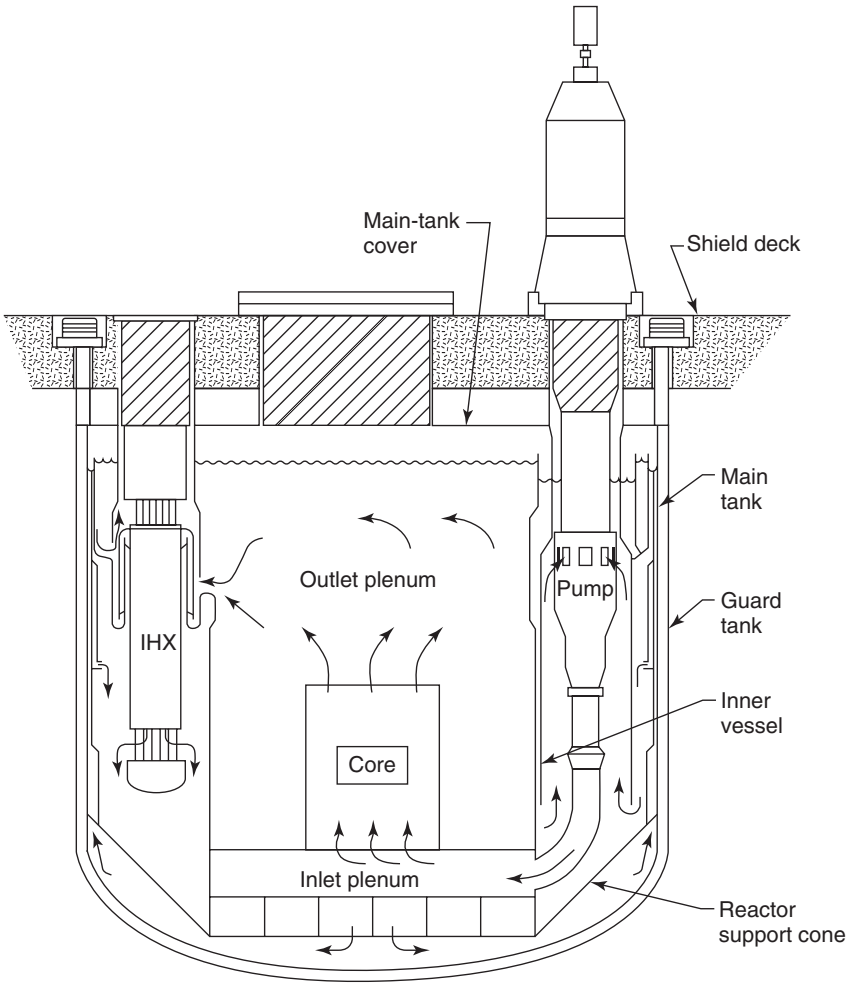

Figure 30.5 Pool plant configuration.

or operations. The one possible exception is the fact that in the loop concept, radioactive sodium is present throughout the reactor containment building, in the shielded and inerted hot cells (one cell for each primary loop), while for the pool concept all of the radioactive sodium is contained within the reactor vessel, which takes up less planar (floor) area within the reactor containment building. Both plant configurations are technically feasible and there are trade-offs with each plant configuration. The size of the reactor has not been a determinant in the choice of the primary plant configuration, as multiple sizes have been designed and built in both plant configurations.

Some countries' reactor development programs evolved from loop to pool designs, and others evolved in the opposite direction. Operating experience has basically confirmed their performance similarities. Currently, advanced SFRs are being designed with both pool and loop primary plant configurations, e.g., General Electric's Power Reactor Inherently Safe Module (PRISM) [3] is a modular pool plant configuration, and the Japan Sodium Fast Reactor (JSFR) [4] is a loop plant configuration.

30.4 GENERATION–IV SFR OBJECTIVES

The Generation-IV International Forum (GIF) is a cooperative international endeavor organized to carry out the research and development (R&D) needed to establish the feasibility and performance capabilities of Generation-IV systems. It has selected six systems for further R&D: the Gas Fast Reactor (GFR), the Lead Fast Reactor (LFR), the Molten Salt Reactor (MSR), the Sodium-cooled Fast Reactor (SFR), the Super-Critical Water Reactor (SCWR), and the Very High Temperature Reactor (VHTR) [1]. Although the SFR technology was evaluated as most mature of the GIF concepts, the scaled capital cost of previous experimental reactors has been high compared to commercial LWRs. Recent cost studies [5] estimate that the capital

cost of current designs may be 25% greater than conventional LWRs. Since it is important to achieve a level of economic competitiveness for SFRs that facilitates deployment, the GIF collaboration on SFR systems is focused on multilateral R&D of innovative SFR design features to improve the system performance and reduce the capital cost including:

- *Configuration simplifications.* These include a reduced number of coolant loops by improving the individual loop power rating, improving the containment design, refining (and potentially integrating) component design, and possibly eliminating the intermediate coolant loop.
- *Improved Operations & Maintenance (O&M) technology.* Innovative ideas are being considered for in-service inspection and repair. Remote handling and sensor technology for use under sodium are being developed, including ultrasonic techniques. In addition, increased reliability for sodium-water steam generators (e.g., by using double-wall tube configuration with leak detection) is being pursued and advanced detection and diagnostic techniques are being developed.
- *Advanced reactor materials.* The development of advanced structural materials may allow further design simplification and/or improved reliability (e.g., low thermal expansion materials and greater resistance to fatigue cracking). These new structural materials need to be qualified, and the potential for higher-temperature operation evaluated.
- *Advanced energy conversion systems.* The use of a supercritical CO_2 Brayton cycle power-generating system offers the potential for surpassing 40% thermal efficiency; a more compact design may also be possible. Cost and safety implications must be compared to conventional Rankine steam cycle balance-of-plant design.
- *Fuel handling.* Techniques and components employed in previous fast reactors were reliable, but very complicated and expensive. Recent design innovations may simplify the fuel-handling system, but require the development and demonstration of specialized in-vessel handling and detection equipment.

The total cost of electricity also includes the plant operation cost. This can be reduced by enhancing the plant load factor by making the reactor cycle length longer and capacity factor higher (e.g., by robust materials and improved system reliability). The fuel cycle cost can also be reduced by increasing the fuel burnup. For this purpose, advanced cladding materials together with high-burnup transuranic fuel will be crucial.

30.5 EXAMPLES OF GENERATION-IV SODIUM FAST REACTOR SYSTEMS

The SFR system uses liquid sodium as the reactor coolant, allowing high power density with low coolant volume fraction. While the oxygen-free environment prevents corrosion, sodium reacts chemically with air and water and requires a sealed coolant system. The primary system operates at near-atmospheric pressure with typical outlet temperatures of 500–550°C; at these conditions, austenitic and ferritic steel structural materials can be utilized, and a large margin to coolant boiling is maintained. The reactor unit can be arranged in a pool layout or a compact loop layout. Typical design parameters of the SFR concept being developed in the framework of the Generation-IV System Arrangement are summarized in Table 30.4. Plant sizes ranging from small modular systems to large monolithic reactors are considered.

Many sodium-cooled fast reactor conceptual designs have been developed worldwide in advanced reactor development programs. In particular, the European Fast Reactor in EU [6], the Advanced Liquid Metal Reactor (PRISM) and Integral Fast Reactor (IFR) Programs in United States [3, 7], and the Demonstration Fast Breeder Reactor in Japan [8] have been the basis for many SFR design studies. Within the following sections, three reactor concepts are briefly described as examples of Generation-IV SFR concepts. These designs cover a wide range of reactor size and configuration options.

30.5.1 Large Loop Configuration SFR

To promote favorable economies of scale, many SFR designs have targeted large monolithic plant designs. For this approach, a prominent recent concept is the Japan Atomic Energy Agency (JAEA) Sodium Fast Reactor (JSFR) [4], which is a sodium-cooled, MOX (or metal) fueled, advanced loop-type evolved from Japanese fast reactor technologies; the conceptual plant design is shown in Figure 30.6.

TABLE 30.4 Typical Design Parameters for Generation-IV SFR

Reactor Parameters	Reference Value
Outlet Temperature	500–550°C
Pressure	~1 Atmosphere
Power Rating	50–2000 MWe
Fuel	Oxide, metal alloy, others
Cladding	Ferritic-Martensitic, Oxide Dispersion-strengthened steel (ODS), others
Average Burnup	150 GWD/MTHM
Breeding Ratio	0.5–1.30

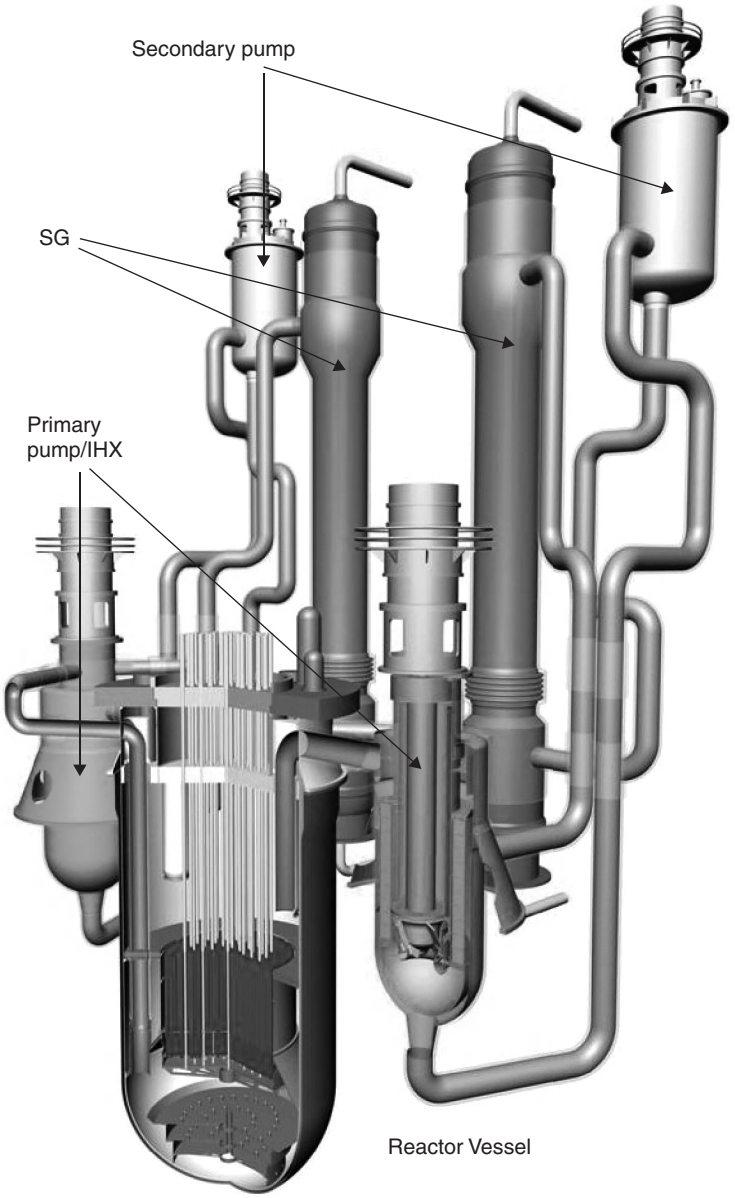

Figure 30.6 JAEA Sodium-cooled Fast Reactor (JSFR).

The JSFR design employs several advanced technologies to reduce the construction cost: compact design of reactor structure, shortened piping layout, reduction of loop number, integration of components, and simplification of decay heat removal system through enhancement of natural circulation capability. These measures include innovative technologies such as 12Cr-steel with high strength and low thermal expansion, an advanced structural design standard at elevated temperature, three-dimensional seismic isolation, and re-criticality free core.

The JSFR design utilizes passive safety measures to increase its reliability. The improvement of the ISI&R technology is concentrated to confirm the integrity of internal structures, including core support structure and coolant boundaries. The means of access is taken into account in design.

The JSFR design studies consider plant sizes ranging from a modular system composed of medium-size reactors to a large monolithic system. The large-scale sodium-cooled reactor utilizes the advantage of economies of scale by setting the electricity output at 1500 MWe. On the other hand, a medium-scale modular reactor would offer advantages of flexibility in power requirements from utility companies and the reduction of development risk compared with large-scale reactors.

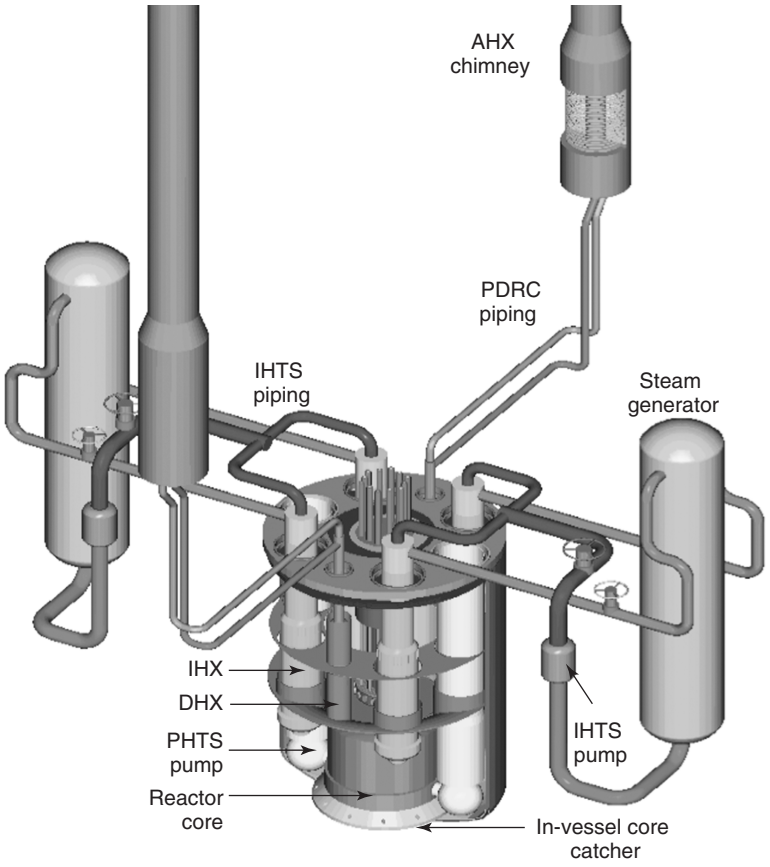

Figure 30.7 KALIMER-600 system configuration.

30.5.2 Medium Pool Configuration SFR

Moderate-size SFR designs have also been proposed; in this case, cost reduction relies on design simplification, factory fabrication techniques, and rapid attainment of Nth of a kind. A recent example is the KALIMER-600 [9] pool-type reactor design, shown in Figure 30.7. A pool-type reactor provides many important design advantages in plant economy and safety. The entire primary heat transport system (PHTS) piping and equipment is located inside the vessel, completely eliminating the possibility of a PHTS piping break outside the reactor vessel. Also, the large thermal inertia characteristics of a pool-type reactor enhance passive safety mechanisms. The safety of KALIMER is enhanced further by loading its core with metal fuel, which has inherent safety characteristics resulting from large negative power reactivity coefficients and a very low probability of a Core Disruptive Accident (CDA).

For the improvement of plant economy over previous designs, KALIMER reduces the number and/or eliminates equipment by design simplification and novelty, compact design, and higher plant efficiency. Its net plant efficiency is designed to reach 39.3% with conventional steam plant. The introduction of the innovative passive decay heat removal circuit (PDRC) system could enable an increase in the size of the system to 1,000 MWe or more. KALIMER requires neither active component operation nor operator action in managing accidents. Also, it does not require a safety-grade emergency electricity generator. These safety design features provide very high reliability in the safety management and can accommodate design basis events (DBE) and beyond design basis anticipated transients without scram (ATWS) events without any operator action or support of active shutdown system operation. The grace period during accidents can be measured in days without violating core protection limits.

30.5.3 Small Modular SFR

The Small Modular Fast Reactor is aimed at exploiting characteristics inherent to fast reactors for application to small grid applications. In a recent U.S. study [10], a reactor size of 50 MWe was selected for a specific niche market where industrial infrastructure is not sufficient for larger systems, and the unit cost of electricity generation is very high with conventional technologies. Examples of this situation are remote areas in Alaska, small grid systems in developing countries, and Pacific-basin islands. The basic

goal is to make the operation, safety, and fuel management as simple as possible; for example, by the application of a long-lived reactor core that eliminates the need for refueling. The SFR characteristics that enable this approach are the following:

- The noncorrosive character of sodium coolant does not degrade the reactor core material and primary system components even over very long residence times.
- The excellent neutron economy of fast spectrum and metal fuel can be exploited to design a small core with a conversion ratio near unity, obviating the need for refueling to account for reactivity losses over an extended cartridge lifetime.

Innovative design features have been incorporated into the SMFR design, including a metallic fueled core with high internal conversion ratio, inherent passive safety characteristics, simplified reactor configuration for modular construction and transportability, and supercritical CO_2 Brayton cycle power conversion system. The primary and intermediate systems and Brayton power conversion are depicted in Figure 30.8; the primary and intermediate systems are embedded below the ground level for physical protection. The primary system is configured as a typical pool arrangement with the core, pumps, intermediate heat exchangers, and auxiliary cooling decay heat exchangers all contained within the reactor vessel. The intermediate sodium exits the vessel and flows to the sodium-to-CO_2 heat exchangers.

A key design feature of the SMFR is the long-lived core–30 years with no refueling. This long lifetime improves proliferation resistance by eliminating all aspects of on-site fuel management: new fuel acceptance, spent fuel handling, and out-of-reactor storage. The SMFR incorporates all the passive safety features developed for SFR applications to avoid plant damage; this includes a passive decay heat removal system directly from the primary coolant pool.

The SMFR utilizes a metal fuel form with similar burnup and fluence limits as employed for the KALIMER design. However, the SMFR operates at a significantly reduced power density to achieve the 30-year lifetime design goal. Thus, the system size is increased compared to a conventional SFR high-power density design, and

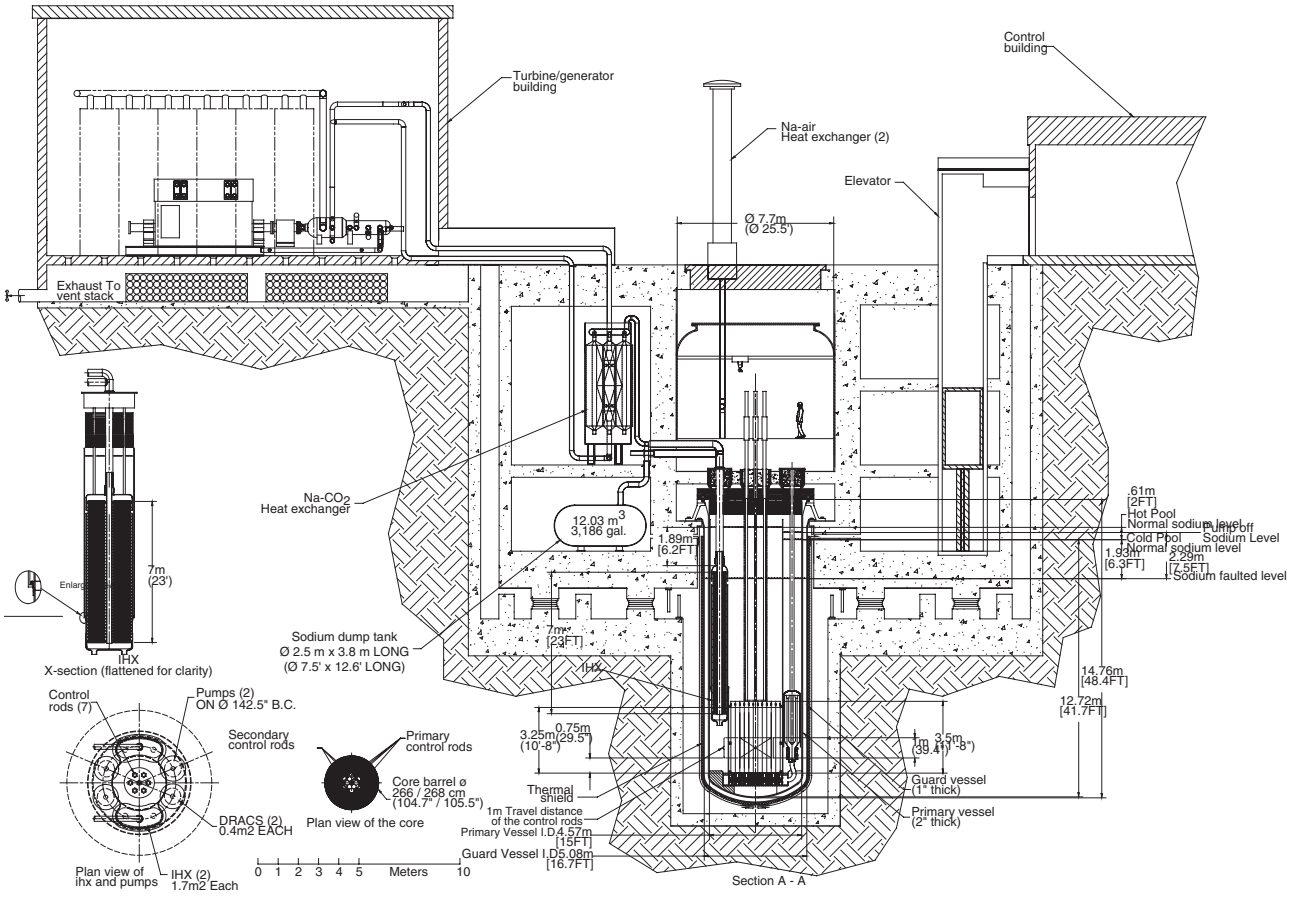

Figure 30.8 Elevation view of SMFR system.

TABLE 30.5 Key Design Parameters of Generation-IV SFR Concepts

Design Parameters	JSFR	KALIMER	SMFR
Power rating, MWe	1,500	600	50
Thermal power, MWt	3,570	1,525	125
Plant efficiency, %	42	42	~38
Core outlet coolant temperature, °C	550	545	~510
Core inlet coolant temperature, °C	395	370	~355
Main steam temperature, °C	503	495	480
Main steam pressure, MPa	16.7	16.5	20
Cycle length, years	1.5–2.2	1.5	30
Fuel reload batch, batches	4	4	1
Core diameter, m	5.1	3.5	1.75
Core deight, m	1.0	0.8	1.0
Fuel type	MOX(TRU bearing)	Metal(U-TRU-10%Zr Alloy),	Metal(U-TRU-10%Zr Alloy),
Cladding material	ODS	HT9M	HT9
Pu enrichment (Pu/HM), %	13.8	24.9	15.0
Burnup, GWd/t	150	79	~87
Breeding ratio	1.0–1.2	1.0	1.0

this results in a higher system cost per unit power generation. However, the SMFR energy-generation cost is acceptable for the intended niche market application where the small size and design simplicity are more important considerations.

30.6 SUMMARY AND CONCLUSIONS

Table 30.5 summarizes the key design parameters of the example Generation-IV SFR design concepts. It is important to note that all of these SFR systems are designed with a large degree of flexibility in size, specific fuel design, and fuel-loading configuration. These particular designs are indicative of current international SFR design studies that cover a wide range of power applications (sized from 50 to 1500 MWe). The question of size involves a cost reduction approach of economies of scale for large systems as compared to modular factory fabrication for small systems. Other factors, such as capital investment limits or electrical grid limitations, may dictate the optimal deployment system power rating.

With regard to the fuel and loading, any of the systems can be designed for different actinide management missions. The converter mode designs given in Table 30.5 could readily be modified to breeder or transmuter configurations by changing the fuel assembly design to impact the uranium loading. Furthermore, the SFR reactor performance can be achieved with different fuel forms.

In conclusion, sodium-cooled fast reactor technology has been around for decades, but the technology has not been deployed commercially like light water reactors. Generation-IV sodium fast reactors are one of six Generation-IV reactor concepts within Generation-IV International Forum. Nuclear energy generation is increasing worldwide, and there are incentives and opportunities to increase the performance of systems to better meet social, environmental, and economic requirements of the 21st century. Sodium fast reactors and other Generation-IV nuclear energy systems are under development to meet these future needs. Sodium fast reactors employ advanced technologies and designs to improve upon the performance of current and advanced light water reactors, particularly through improved waste management, improved utilization of fuel resources, enhanced proliferation resistance and physical protection, increased safety and reliability, and improved economics.

Endnotes

1. Fast reactors have operated with sodium, sodium-potassium alloy, and lead (Russian experience) as coolants. The focus of this chapter in general is on the experience of sodium-cooled fast reactors.
2. Valving is not typically used in the primary sodium system for a pool plant configuration. Most designers try to eliminate valves in the primary heat transport system for either the pool or loop plant configuration.

REFERENCES

1. The U.S. DOE Nuclear Energy Research Advisory Committee and the Generation IV International Forum, *A Technology Roadmap for Generation IV Nuclear Energy Systems*, GIF-002-00. United States Department of Energy, December 2002.
2. *Fast Reactor Database 2006 Update*, IAEA-TECDOC-1531. International Atomic Energy Agency, December 2006.

3. C. Boardman, A. Dubberley, D. Carroll, M. Hui, A. Fanning, and W. Kwant, A description of the S-PRISM plant. *Proceedings of ICONE 8*, Baltimore, MD. American Society of Mechanical Engineers, April 2–6, 2000.
4. S. Kotake, Y. Sakamoto, M. Ando, and T. Tanaka, Feasibility study on commercialized fast reactor cycle systems/current status of the FR system design. *Proceedings of Global 2005*, Tsukuba, Japan. Atomic Energy Society of Japan, October 9–13, 2005.
5. Nuclear Energy Agency, Organization for Economic Cooperation and Development (OECD), *Accelerator-Driven Systems (ADS) and Fast Reactor (FR) in Advanced Nuclear Fuel Cycle—A Comparative Study*, OECD-NEA Report. 2002.
6. J. Lefevre, C. Mitchell, and G. Hubert, European fast reactor design. *Nuclear Engineering Design*. Elsevier, 1996, **162**, 133–144.
7. Y.I. Chang, Status of progress in IFR development. *Proceedings of ASME Joint International Power Generation Conference*, Phoenix, AZ. American Society of Mechanical Engineers, October 2–6, 1994.
8. T. Inagaki, M. Ueta, M. Hamada, and T. Kobayashi, *Current status of development of the demonstration FBR in Japan*. 11th Pacific Basin Nuclear Conference, Banff, Canada. Elsevier, 1998.
9. D. Hahn, Y. Kim, S. Kim, J. Lee, and Y. Lee, Design concept of KALIMER-600. *Proceedings of GLOBAL 2005*, Tsukuba, Japan. Atomic Energy Society of Japan, October 9–13, 2005.
10. Y. Chang, M. Konomura, and P. Lo Pinto, A case for small modular fast reactor. *Proceedings of Global 2005*, Tsukuba, Japan. Atomic Energy Society of Japan, October 9–13, 2005.

PART V

THERMONUCLEAR FUSION

31

HISTORICAL ORIGINS AND DEVELOPMENT OF FUSION RESEARCH

Stephen O. Dean

Fusion Power Associates, Gaithersburg, MD, USA

The origins of fusion can be traced to the origins of nuclear physics and are a natural evolution of it. Sir Ernest Rutherford received the Nobel Prize in 1908 for his seminal work on the theory of atomic structure and for showing how radioactive elements transform themselves into other elements of the periodic table. In 1919, Rutherford also performed experiments showing how heavier elements could be produced by the collision of lighter elements—a process later to be called "fusion." In the same year, British physicist Francis Aston, using a mass spectrometer he had invented (and for which he later also received a Nobel Prize), demonstrated the existence of different "isotopes" of the same element (i.e., atoms of the same elements that have different atomic weights) and discovered the then-astonishing fact that the mass of a helium nucleus was less than the sum of the hydrogen nuclei of which it was composed. In 1920, Sir Arthur Eddington, in a speech to the British Academy for the Advancement of Science, suggested that the "fusion" of light elements, starting with hydrogen to helium, was the source of energy in the Sun and stars. The lightest element in the periodic table, hydrogen, consists of a single proton and has two isotopes, deuterium (with a proton and a neutron in the nucleus) and tritium (with a proton and two neutrons in the nucleus). Deuterium was first identified in 1932; tritium in 1934, although the existence of both had been predicted earlier. During the 1930s, scientists around the world were actively investigating the makeup of the periodic table and the reactions that might explain the energy processes of the Sun and stars. In 1934, Rutherford and his colleagues demonstrated the fusion of deuterium and deuterium to form helium, using a Cockroft-Walton particle accelerator.

A 1936 review article by Hans Bethe in *The Reviews of Modern Physics* led to the first recorded interest in building a fusion experiment in the United States, that of Kantrowitz and Jacobs in 1938, working at the Langley lab of the National Advisory Committee for Aeronautics (NACA, the predecessor agency of NASA). They built a simple torus with coils wrapped around it to produce a magnetic field and fed in about 150 watts of power from a radio transmitter, hoping to heat the hydrogen gas to a million degrees. The experiment failed to produce the desired result and was abandoned. In 1939, Australian physicist Peter Thonneman conceptualized a fusion reactor. He later played a key role in the UK fusion program.

Scientists in the United Kingdom and the United States working on the atomic bomb during WWII were already thinking beyond fission to fusion. In 1946, two British physicists, Sir George Thompson and Moses Blackman, filed a secret patent application for a doughnut-shaped, current-driven "pinch" fusion device they had designed at Imperial College. In 1947, two doctoral students at Imperial College, Stan Cousins and Alan Ware, built and operated a small magnetic "pinch" experiment there. One of those active in the UK fusion program in those early days was Jim Tuck, who had worked at Los Alamos during the war, returned to the United Kingdom, and then returned to Los Alamos to work on the H-bomb. Tuck, known for his sense of humor, built a pinch device in 1952 at Los Alamos he called the "Perhapsatron" because, he said, "perhaps it will work and perhaps it will not." (Fig. 31.1)

Nuclear Energy Encyclopedia: Science, Technology, and Applications, First Edition (Wiley Series On Energy).
Edited by Steven B. Krivit, Jay H. Lehr, and Thomas B. Kingery.

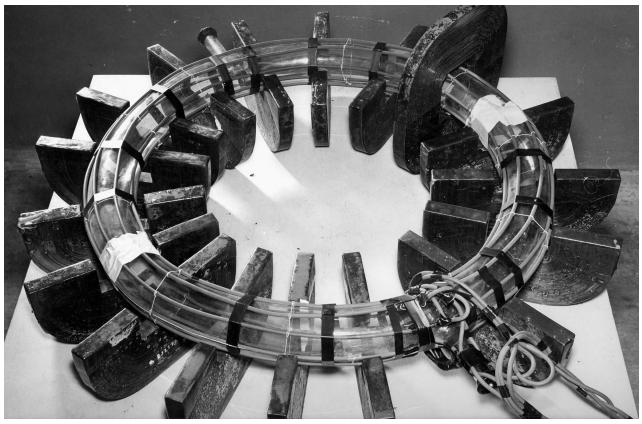

Figure 31.1 Perhapsatron: First U.S. fusion experiment.

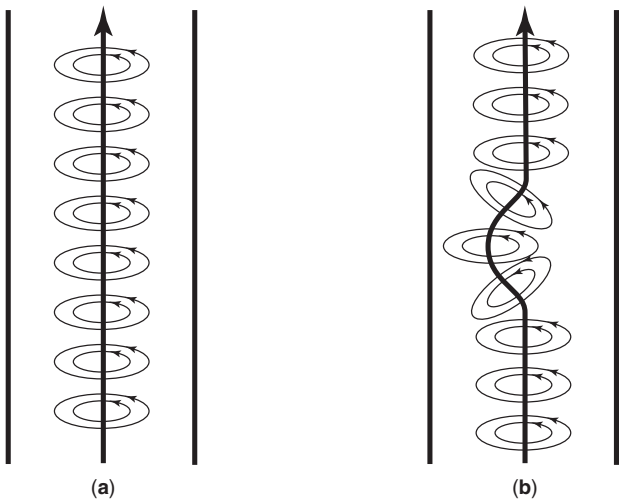

Figure 31.2 The linear pinch configuration (a) before any instabilities develop and (b) with a kink instability that disrupts the discharge.

Although during the 1940s, scientists in the U.S. atomic weapons labs informally discussed fusion from time to time, largely in the context of how to build a hydrogen bomb, the real stimulus for controlled fusion research is usually attributed to a front-page article in the New *York Times* on March 25, 1951, reporting that Argentina claimed to have a working fusion power plant. Although the claim ultimately proved untrue, it gained the attention of scientists and politicians in the United States, United Kingdom, and Soviet Union, and serious efforts to investigate the possibilities were launched. Soon thereafter, in the United States, experiments were underway at Los Alamos under Jim Tuck, at Princeton University under Lyman Spitzer, and at the University of California Radiation Laboratory (now Lawrence Livermore National Laboratory) under Edward Teller, Herb York, and Richard Post. The U.S., UK, and Soviet programs were all highly classified.

In the Soviet Union, it is believed that Oleg Lavrentiev was the first to call attention to fusion in letters he wrote to the government in 1949 and 1950. These letters, in turn, aroused the interest of Soviet scientists Igor Tamm and Andrei Sakharov. In 1951, the government formally launched a fusion program under the direction of Igor Kurchatov, director of the Institute of Atomic Energy in Moscow. He set up an experimental program under the direction of Lev Artsimovich and a theoretical effort under the direction of Mikhail Leontovich. Other institutes were brought into the effort from Kharkov, Leningrad, and Sukhumi.

Early efforts to produce and control fusion reactions were based on then well-known principles of electromagnetic theory. A current passing through a gas was known to strip electrons from the gas atoms (ionization), to raise its temperature, and to produce a magnetic field surrounding the current. Raising the current increased the degree of ionization, the temperature, and the magnetic field strength. The magnetic field exerted a confining force on the column of ionized gas (dubbed "plasma" in a 1928 paper by Irving Langmuir) and, as the current and magnetic field were raised, the column of plasma would be compressed, raising its density and further raising its temperature. This was known as the "pinch effect" and was the basis of most of the early attempts to produce fusion conditions in the laboratory. The "pinch effect" had been predicted in 1934 by W. H. Bennett and, independently, in 1937 by Lewi Tonks, but little subsequent effort was devoted to pinch plasma properties in the 1930s. In the 1950s, some of these "magnetic pinch" devices studied for fusion were linear in geometry (Fig. 31.2) and some were doughnut-shaped (toroidal) (Fig. 31.3). Pinch devices were fashioned into what came to be called "magnetic bottles" for the plasma. They went by a variety of sometimes-colorful names: Perhapsatron and Columbus (at Los Alamos), Zeta (in the UK).

It was recognized early that plasma would rapidly leak out the ends of a linear pinch unless something was done to "plug" the ends. One solution was already being studied in toroidal configurations (which have no "ends"). Another solution to this problem emerged in the form of strengthening the magnetic field at either ends of the pinch by using external magnets. This geometry came to be known as the "magnetic mirror" configuration (Fig. 31.4) and was championed in the United States by Post and colleagues at the University of California's Livermore Laboratory.

Pinches had serious problems, however. It was rapidly observed that, as the plasma column was pinched, the plasma twisted and moved in an unstable fashion and quickly hit the walls of the chamber. A variety of such instabilities were observed in the various pinch configurations, receiving names such as "kink instability"

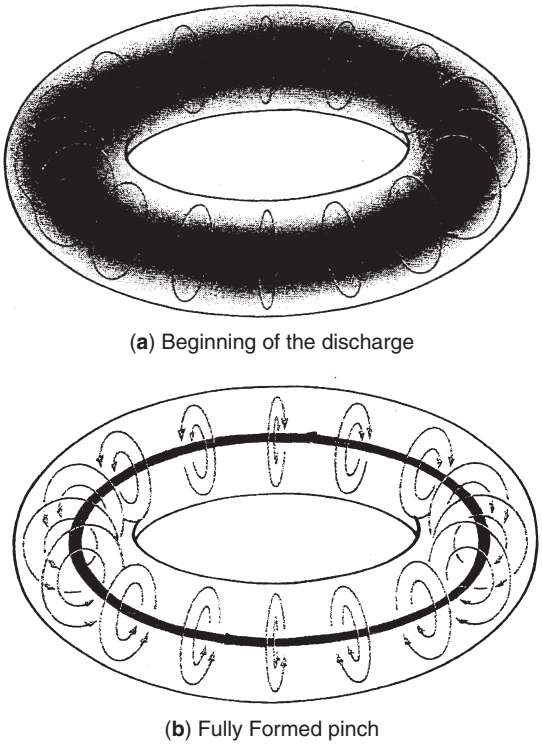

Figure 31.3 Toroidal pinch.

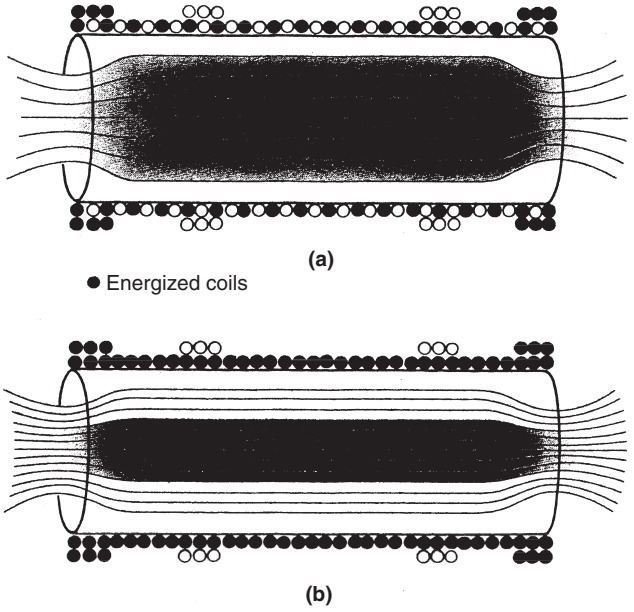

Figure 31.4 Magnetic mirror (a) simple configuration and (b) with magnetic compression.

(Fig. 31.2b) and "sausage instability." Much of the first two decades of fusion research was devoted to developing an understanding of these and related instabilities, all belonging to a class to be known as magnetohydrodynamic (MHD) instabilities or macroscopic instabilities.

Another early approach to creating a magnetic bottle was invented by Princeton University astrophysicist Lyman Spitzer while riding the ski lifts in Aspen. He asked himself how one might contain on earth a plasma similar to that existing in stars. He envisioned a toroidal magnetic configuration he called the "stellarator" since it was a designed to contain a man-made equivalent of a star on earth. In this concept, the confining magnetic field is produced by external magnets. It was similar in some respects to the toroidal pinch configuration (Fig. 31.3) but differed in that the primary confining magnetic field was to be produced by magnets and not by a current in the plasma. Even in this configuration, however, the plasma had many surprises in store for the researchers. These, more subtle, types of plasma loss mechanisms in the stellarator geometry came to be known as "microinstabilities" and are still the subject of active research. The stellarator is still a promising configuration for fusion plasma confinement, although the magnets needed to provide the appropriate magnetic field properties have become increasingly complex to manufacture.

As part of the Atoms for Peace initiatives of the late 1950s, and as scientists realized the extreme complexity of plasma behavior in fusion experiments, the United States, the United Kingdom, and the Soviet Union agreed to remove the veil of secrecy that had surrounded their fusion research efforts and to present their research programs at the Second Geneva Conference on the Peaceful Uses of Atomic Energy, in Geneva, in 1958. Thus began a spirit of friendly competition and cooperation among fusion scientists worldwide that has lasted to the present day.

At the 1958 Geneva conference, the Soviets described experiments in which the toroidal pinch geometry was supplemented by fields provided by external magnets. In some ways, the geometry resembled a marrying of the pinch and stellarator ideas being studied separately elsewhere. One version of this configuration that evolved during the 1960s was called tokamak (from Russian words meaning toroidal magnetic chamber). By the late 1960s, this configuration showed dramatic improvement in confining the plasma compared to other geometries. A worldwide shift to this configuration began after the 1969 fusion conference sponsored by the International Atomic Energy Agency (IAEA) in Novosibirsk. The tokamak configuration now dominates world fusion research.

It was recognized early that simply passing a current, no matter how large, would not suffice to raise plasma temperature to that necessary for sustained fusion. Consequently, the science and technology for "supplemental" heating of the plasma also was pursued. The supplemental methods included compression (see, e.g., Fig. 31.4b),

injection of accelerated particles, and the injection of high-power radio-frequency waves. It was also clear that high field superconducting magnetic fields would be needed; otherwise, if the magnets were not superconducting, too much power would be needed to run the magnets. Consequently, a vigorous program in magnet development was initiated, including the development of new forms of superconducting wire. These developments were vigorously pursued in the 1960s and 1970s.

As research progressed, the properties of materials in the chamber walls became increasingly important. The plasma temperature declined if small amounts of material from the chamber contaminated the plasma. Also, long-range power reactor design studies showed that materials damage from fusion products would limit reactor lifetime if improved materials were not developed. These technology development issues remain critical ones on the path to successful commercial fusion.

The invention of the laser in 1960 gave rise to a whole new approach to fusion called "inertial confinement fusion." The hydrogen bomb showed that fusion could be initiated by a sufficiently strong compressive force exerted on small amounts of fusion fuel. In the case of the bomb, this force was provided by a fission-based atomic bomb surrounding the fusion fuel. Scientists in and outside the weapons laboratories began to speculate on whether a fusion reaction of practical interest could be initiated by focusing a high-power laser on a small capsule containing fusion fuel. The effort, begun in the 1960s in the United States and the Soviet Union, showed that, while theoretically possible, lasers far beyond those available at the time would be required. Larger and larger lasers were built during the 1970s and 1980s, culminating in the National Ignition Facility (NIF), located at the Lawrence Livermore National Laboratory in California. This 192-beam laser, which began operation in mid-2009, is designed to produce a net output of fusion energy compared to the laser energy required to initiate the fusion reaction.

During this same period of the 1970s and 1980s, tokamaks capable of creating "near breakeven" conditions (in which the fusion energy released approximately equaled the energy put in to heat the plasma) were constructed and successfully operated in the United States, Europe, and Japan. The experience gained from these and other tokamaks around the world has led to initiation of the International Thermonuclear Experimental Reactor (ITER) being constructed in France as a joint venture of the European Union and six other country partners.

As fusion research progressed beyond 1958, countries other than the United States, the United Kingdom, and Russia initiated substantial fusion research efforts and are making important contributions to what is still a vigorous international collaborative effort. These countries include Germany, France, Japan, Republic of Korea, China, India, and others. The European Union (EU) is coordinating fusion research among all the EU countries, and the IAEA has continued its world fusion coordination activities, begun in 1958, through its biennial conferences, technical working groups, and the International Fusion Research Council (IFRC).

32

PLASMA PHYSICS AND ENGINEERING

FRANCESCO ROMANELLI

JET-EFDA Culham Research Center, Abingdon, UK

32.1 INTRODUCTION

Fusion is the energy source that powers the sun and the other stars. It has a number of advantages:

- The fuels (deuterium and lithium) are abundant and available worldwide. At the present consumption rate there is enough deuterium and lithium to produce energy for a few tens of million years.
- It does not produce greenhouse gases.
- It is intrinsically safe. In case of accident, it is sufficient to stop fueling the reactor, and the reactions stop. Fusion power plant conceptual studies [1] show that even in the case of the worst accident driven by in-plant energies, no evacuation of the population is needed.
- It is environmentally responsible. The primary reaction does not produce wastes. There is a limited problem with the activation of the structural materials of the reaction chamber but, with a proper choice of materials, radioactivity decays in a few tens of years, and after 100 years all the materials can be recycled in another fusion reactor.

In the core of the sun, hydrogen nuclei (protons) fuse to produce helium nuclei (alpha particles). The proton cycle is an extremely slow process and cannot be used for practical applications on Earth. In order to produce fusion energy, different reactions must be employed, such as the reaction between two hydrogen isotopes, deuterium and tritium. The products of the reactions are an alpha particle and a neutron with 80% of the energy being released as neutron energy.

Deuterium is a stable hydrogen isotope mostly produced during the big bang and very abundant (0.0115% of hydrogen atoms). In each liter of water, there are approximately 25 mg of deuterium. Deuterium can be extracted at a reasonable cost from water through distillation, electrolysis, and various chemical exchange processes. Tritium is a radioactive isotope with a half-life of 12.33 years. Therefore, its natural abundance is almost zero, and it must be produced in a fusion reactor as part of the fuel cycle.

Other reactions can also be used in principle for energy production. The most important are the reaction between two deuterium nuclei, which produces either a He3 nucleus (i.e., a nucleus with two protons and a neutron) and a neutron or a tritium nucleus and a proton (the two channels have the same probability), and the reaction between deuterium and He3, which produces an alpha particle and a proton. The advantage of the two reactions is that they do not need tritium. In addition, the amount of energy released through neutrons (that may be absorbed by the structural materials of the reaction chamber and activate them) is much smaller than for the D-T reaction. However both the D-D and the DHe3 reactions require a much larger value of the temperature of the reactants in order to achieve a significant amount of fusion power. Furthermore, the amount of He3 on Earth is very small, and although proposals have been made to extract it from lunar rocks, the near-term perspective of using such a reaction is very limited. Table 32.1 lists the most important fusion reactions.

The energy released is typically measured in MeV (million of electron volts) with 1 eV $\approx 1.6022 \times 10^{-19}$ J.

Nuclear Energy Encyclopedia: Science, Technology, and Applications, First Edition (Wiley Series On Energy).
Edited by Steven B. Krivit, Jay H. Lehr, and Thomas B. Kingery.

TABLE 32.1 Most Important Fusion Reactions

D + T	→ He4 (3.5 MeV) + n (14.1 MeV)
D + D	→ T(1.01 MeV) + p (3.02 MeV) 50%
	He3 (0.82 MeV) + n (2.45 MeV) 50%
D + He3	→ He4 (3.6 MeV) + p (14.7 MeV)
T + T	→ He4 + 2n + 11.3 MeV
He3 + T	→ He4 + p + n + 12.1 MeV 51%
	→ He4 (4.8 MeV) + D (9.5 MeV) 43%
	→ He5 (2.4 MeV) + p (11.9 MeV) 6%
p + Li6	→ He4 (1.7 MeV) +He3 (2.3 MeV)
p + Li7	→ 2He4 + 17.3 MeV 20%
	→ Be7 + n−1.6 MeV 80%
D + Li6	→ 2He4 + 22.4 MeV
p + B11	→ 3He4 + 8.7 MeV
n + Li6	→ He4 (2.1 MeV) + T (2.7 MeV)
n + Li7	→ He4 + T + n−2.5 MeV

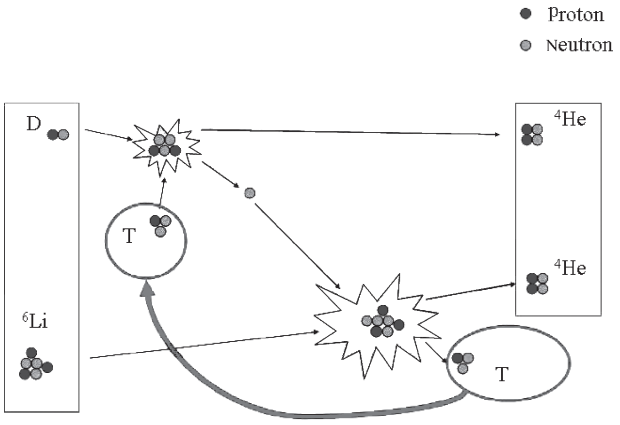

Figure 32.1 The deuterium-tritium cycle. The reaction between deuterium and tritium produces an alpha particle and a neutron. The neutron reacts with lithium in a blanket surrounding the gas of reactants. The reaction between neutron and lithium produces an alpha particle and a tritium nucleus that is recirculated inside the reactor.

If the D-T reaction is considered, tritium must be produced as part of the fuel cycle, and for this purpose lithium is used (Fig. 32.1).

Natural lithium is made by two isotopes Li7 (93%) and Li6 (7%). The reaction between a neutron and Li6 produces a tritium nucleus and an alpha particle. This reaction also releases 4.8 MeV. The reaction between a neutron and Li7 produces a tritium nucleus, and alpha particle plus an additional neutron. This reaction is endothermic with a threshold at 2.5 MeV. The tritium nucleus produced in both reactions can be extracted and reinjected into the fuel cycle. Thus, by surrounding the gas of reactants with a blanket made by lithium, it is possible to breed tritium. At the same time, the blanket absorbs the energy of the fusion neutrons and the energy produced in the reaction between neutrons and lithium. Through a heat exchanger, the energy can be extracted and used to produce electricity (Fig. 32.2).

In ideal conditions, for each neutron, a tritium nucleus is produced. In reality, part of the neutrons are absorbed by the structural materials of the blanket (that become activated), and neutron multipliers made either by beryllium or by lead must be present in the blanket in order to compensate for these losses.

32.2 THE PLASMA STATE

Reacting nuclei are charged particles and repel each other. In order to overcome the electrostatic repulsion and bring nuclei at sufficient small distance to fuse, the reactants must be heated to very high temperatures of the order of 200 million Kelvin (K). These temperatures are about 20 times higher than the temperature in the core of the sun.

At these temperatures, matter is not in an ordinary state (solid, liquid, gas) but is in the so-called *plasma* state. In ordinary states, electrons are bound to the nuclei. As temperature increases above 3000 K, the electron kinetic energy associated with their thermal motion becomes sufficient to overcome the attraction of the nuclei, and the gas of neutral atoms becomes a superposition of two gases: one of positively charged ions and one of negatively charged electrons. This is the plasma state.

Examples of plasmas are common in nature: stars, solar wind, lightning, the *aurora borealis*, flames, and fluorescent lamps are plasmas with different degrees of ionization.

The characteristic values of density and temperature for these plasmas are shown in Figure 32.3.

Plasma temperatures are usually measured in electron-volts rather than in degrees, with 1 eV being approximately 11600 K.

At the temperatures needed for fusion, matter cannot be confined in ordinary containers since any material would be rapidly destroyed by the interaction with the plasma. Two methods are used: magnetic and inertial confinement. In magnetic confinement systems, the charged particles composing the plasma are kept far from the walls of the reaction chamber by intense magnetic fields. The plasma is maintained for very long durations (or even in steady-state conditions) and continuously fueled. In inertial confinement, a fuel capsule is compressed to very high density and temperature for short times by intense beams of radiation or particles. Throughout the rest of this chapter, we will focus on magnetic confinement only. A comprehensive review of the present status of magnetic confinement physics and engineering can be found in references [2–9]. Introductory textbooks to plasma and fusion physics are listed in references [10–14].

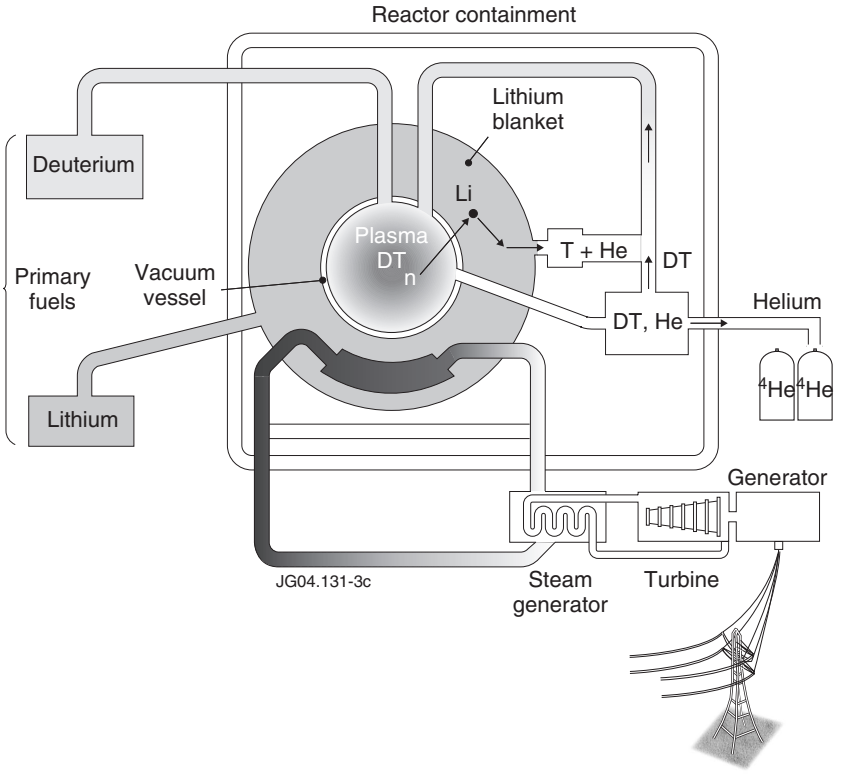

Figure 32.2 Scheme of a fusion reactor. The energy of the fusion neutrons is absorbed in the blanket and extracted through a heat exchanger for the production of electricity.

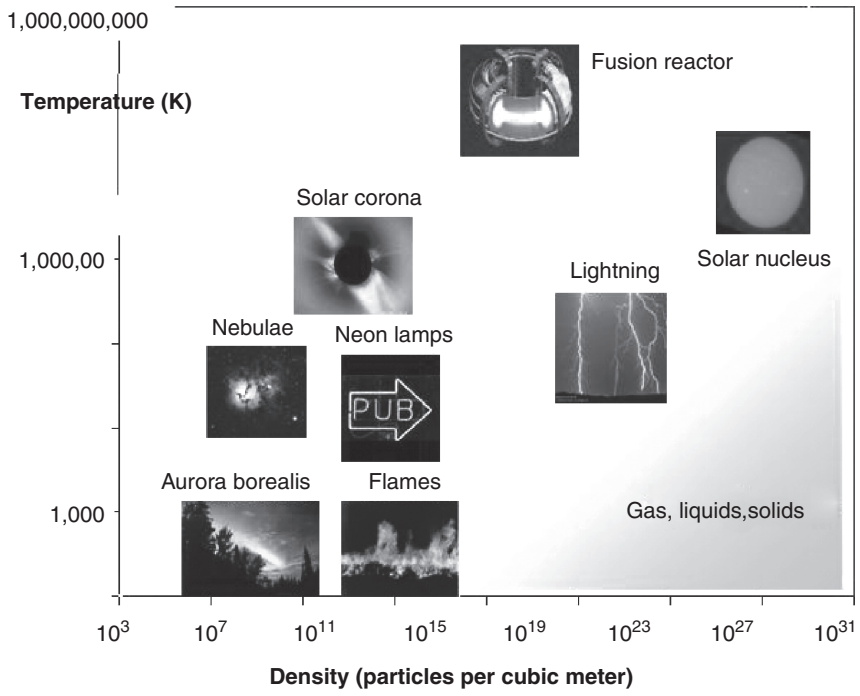

Figure 32.3 Examples of plasmas.

32.3 THE LAWSON CRITERION

In order to have net electricity production, the amount of power generated inside the reaction chamber by fusion reactions must be sufficiently larger than the power used to keep the gas of reactants at high temperature. The power generated by D-T fusion reactions is given by

$$P_{fus} = 17.6 \text{ MeV } n_D n_T <\sigma v> V \qquad (32.1)$$

where n_D is the particle density of deuterium nuclei (number of deuterium nuclei per unit volume), n_T is the particle density of the tritium nuclei, $<\sigma v>$ is the fusion reactivity that takes into account the velocity distribution (assumed to be Maxwellian) of the reacting gases, and V is the plasma volume. The Maxwellian reactivity is only a function of the temperature of the reactants (Fig. 32.4). Detailed numerical fits can be found in [15]. In the temperature range 10–20 keV, the Maxwellian reactivity can be approximated by $<\sigma v\ (m^3/s)> \approx 10^{-24}\ T(keV)^2$.

The power lost by the plasma is associated with thermal conduction/convection and radiation. The power P_{cond} lost through conduction and convection is due to small-scale turbulence and can be quantified in terms of the energy confinement time τ_E

$$P_{cond} = W/\tau_E \qquad (32.2)$$

where $W = (3/2)\ (n_e T_e + \Sigma_j\ n_j\ T_j)$, V is the internal energy of the plasma assumed as the superposition of ideal gases of electrons and ions with the sum extended to all the ion species (deuterium, tritium, helium, and impurities), and $T_e(T_i)$ the electron (ion) temperature. The energy confinement time is a measure of the thermal insulation of the plasma. It corresponds to the time needed to reduce the plasma temperature by a factor 1/e (with e the base of natural logarithms) after all the heating sources are switched off. It must be stressed that the energy confinement time has nothing to do with the time a plasma can be confined. In a machine like ITER, the energy confinement time is of the order of four seconds while the plasma can be confined for a few hundreds seconds [2].

The power lost by radiation is mostly associated with Bremsstrahlung emitted by the electrons accelerated by the electrostatic field of the nuclei. The Bremsstrahlung losses are given by

$$P_{brem}(MW) = 1.69 \times 10^{-4}\ Z_{eff}\ n_e(10^{20} m^{-3})^2\ T_e(eV)^{1/2} V(m^3) \qquad (32.3)$$

with n_e the particle density of electrons and $Z_{eff} \equiv \Sigma_j Z_j^2 (n_j/n_e)$ the average charge of the plasma ions.

Since the plasma must be locally neutral, the electron density n_e must be equal to the sum of the ion densities n_j times their charge Z_j

$$n_e = \Sigma_j\ Z_j\ n_j \qquad (32.4)$$

Thus, at fixed electron density, the amount of deuterium and tritium decreases if other species are simultaneously present. To retain plasma purity is therefore mandatory both to avoid fuel dilution and to reduce Bremsstrahlung losses to a minimum.

In stationary conditions the power released by fusion reactions in the form of alpha particles (1/5 of the fusion power P_{fus}) plus the power P_{aux} injected from external sources must be equal to the power lost by conduction/convection and radiation (power balance condition)

$$P_{fus}/5 + P_{aux} = P_{cond} + P_{brem} \qquad (32.5)$$

Defining the fusion gain $Q = P_{fus}/P_{aux}$ (i.e., the amplification factor of the auxiliary power), we obtain

$$Q = [(P_{cond} + P_{brem})/P_{fus} - 1/5]^{-1} \qquad (32.6)$$

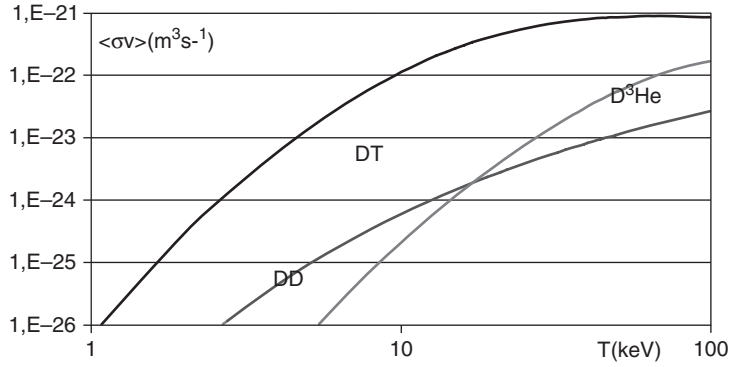

Figure 32.4 Maxwellian reactivity as a function of temperature for the DT, DD and DHe3 reactions.

The fusion gain Q becomes infinite for $P_{aux} = 0$, meaning that the fusion reactions are self-sustained, i.e., for $P_{fus}/5 = P_{cond} + P_{brem}$. This is the so-called ignition condition.

For a pure deuterium and tritium plasma ($n_D = n_T = n_e/2$) with equal electron and ion temperatures, the ignition condition can be written as,

$$n_e(10^{20}m^{-3})\ \tau_E(s) = 3.42 \times 10^{-3}T(keV)/ [<\sigma v>(10^{-20}m^3/s) - K\ T(keV)^{1/2}] \quad (32.7)$$

with $K = 3.82 \times 10^{-4}$ m^3 s^{-1} keV$^{-1/2}$. This is the Lawson criterion. It expresses the requirement in terms of the product of density and confinement time to achieve ignition as a function of the plasma temperature.

The $n_e\tau_E$ value given by the Lawson criterion is plotted as a function of temperature in Figure 32.5.

The quantity in the right-hand side of the Lawson criterion has a minimum corresponding to $n_e\tau_E \approx 1.6 \times 10^{20}$ m^{-3}s at about 25 keV. Since this corresponds to the minimum requirements on confinement, fusion machines are designed to operate close to this temperature. For temperatures approaching 4.3 keV, the $n_e\tau_E$ product tends to infinity. This is the so-called ideal ignition temperature and represents the minimum temperature above which the plasma must be heated in the ideal case of no losses associated with conduction and convection (i.e., $\tau_E = \infty$). Below this temperature, Bremsstrahlung losses are always larger than the fusion power associated with alpha particles, and the power balance condition cannot be satisfied without auxiliary power.

Fusion research has made enormous progress toward the achievement of reactor conditions. In Figure 32.6 the triple product $n_e\tau_E T$ is shown as a function of the ion temperature.

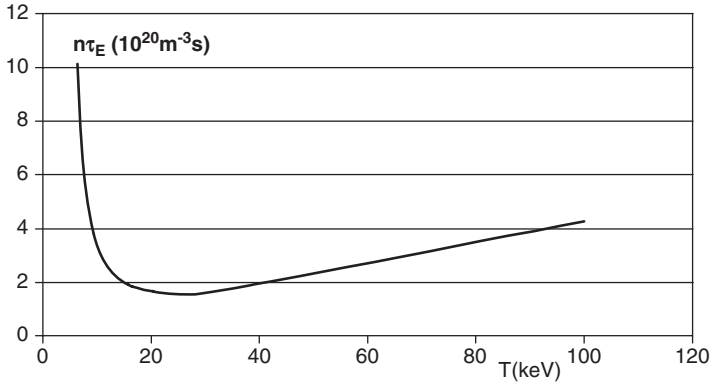

Figure 32.5 Value of the product $n\tau_E$ as a function of temperature to achieve ignition (Lawson criterion).

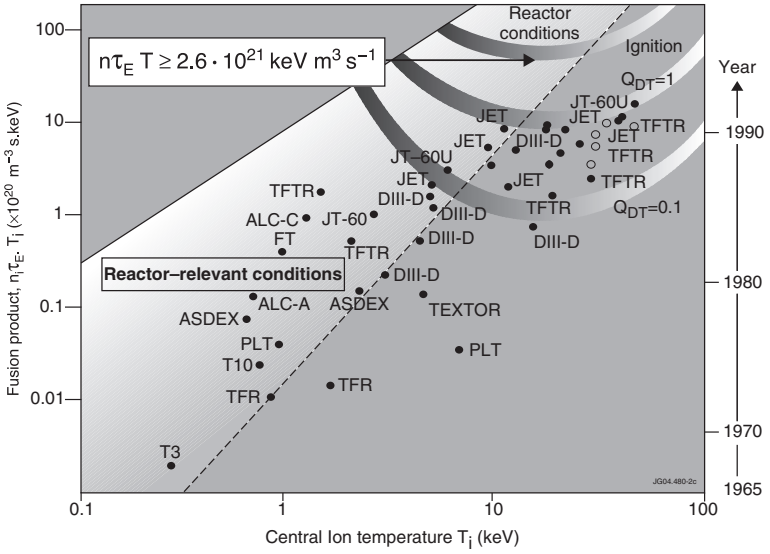

Figure 32.6 Triple product $n\tau_E T$ vs. temperature achieved in present and past fusion devices (*courtesy of EFDA JET*).

With the largest tokamak devices (JET, JT60U, and TFTR) plasma conditions corresponding to a fusion gain up to Q = 1 have been already achieved since the 1990s with values of the triple product within a factor 5 the value expected in ITER. ITER is expected to achieve values of the fusion gain up to Q = 10, whereas values around Q = 30 are envisaged for a commercial reactor.

32.4 MAGNETIC CONFINEMENT OF PARTICLES

No material can withstand the temperatures typical of a fusion reactor core. In order to confine fusion plasmas, it is possible to take advantage of the charged nature of their constituents (electrons and nuclei) and use intense magnetic fields. In a uniform magnetic field **B**, charged particles move along a helix with the axis aligned along the magnetic field lines. The radius of the helix, ρ_{Larmor} (the Larmor radius), is given by

$$\rho_{\text{Larmor}} \equiv \mathrm{v}_{\perp}/\Omega \tag{32.8}$$

with $\mathrm{v}_{\perp}$ the component of the particle velocity perpendicular to **B** and $\Omega = q\mathbf{B}/\mathrm{m}$ the cyclotron frequency with q and m the charge and the mass of the particle. Since Ω is proportional to the magnetic field B, if the magnetic field is sufficiently intense (typical values for a reactor are in the range 5 T to 10 T, i.e. 10^5 times the average Earth's magnetic field at the surface), the particle remains confined in the direction perpendicular to **B**. The particle, however, remains free to move along the magnetic field line, and confinement would be limited by the end losses that occur where the field line intercepts the reaction chamber.

In order to avoid the problem of the end losses, it is necessary to modify the magnetic configuration in such a way that magnetic field lines never intercept the reaction chamber. A simple way to achieve this would be to close the magnetic field line in a circle of radius R as shown in Figure 32.7a. Upon considering a cylindrical coordinate system (R, Z, ϕ), the magnetic field along the ϕ-direction is called *toroidal* magnetic field. Looking at Figure 32.7b, it is clear that end losses would be avoided also by closing the magnetic field lines in smaller circles of radius a in the plane orthogonal to $\boldsymbol{\phi}$. The associated magnetic field $\mathbf{B}_{\mathrm{p}}$ is called *poloidal* magnetic field. In general, the confining magnetic field will be given by a superposition of the toroidal and the poloidal magnetic fields.

These two recipes (intense magnetic fields and toroidal geometry) are at the basis of all the magnetic confinement systems foreseen for energy applications even though the magnetic configuration can be produced in very different ways.

However, in the presence of non-uniform magnetic fields such as the toroidal magnetic field, particles no longer follow simple Larmor orbits but, in addition, undergo secular drifts that can cause loss of confinement. In order to ensure full confinement, the magnetic configuration has to satisfy certain constraints briefly reviewed below.

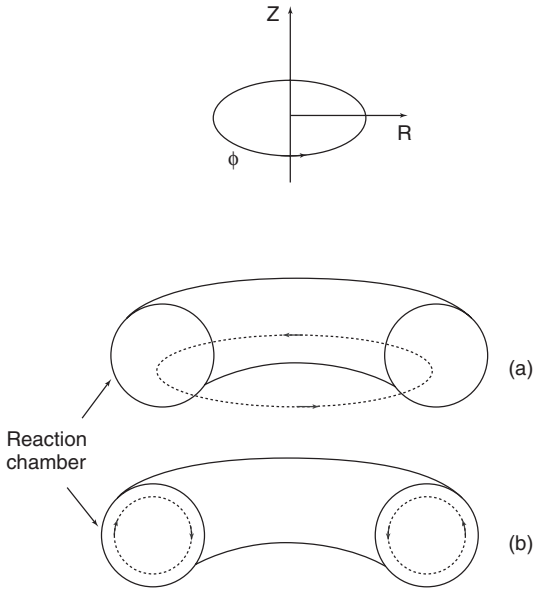

Figure 32.7 (a) Toroidal field and (b) poloidal field.

In order to understand the origin of the drifts in the presence of a non-uniform magnetic field, let us consider first the case of a magnetic field directed along the z axis with the intensity B being a function of the coordinate y (Fig. 32.8).

During a Larmor orbit, an electron (with charge q = −e) experiences a magnetic field lower at point *a* and higher at point *c*. The Larmor orbit will therefore tend to increase its radius at point *a* and reduce it at point *c*. The net effect is a drift in the direction orthogonal to both **B** and ∇B (called

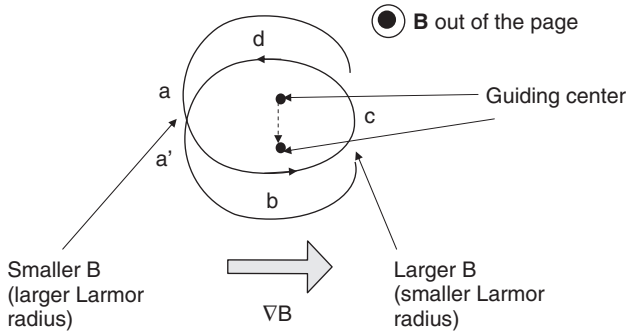

Figure 32.8 Drift of an electron in a magnetic field (coming out of the plane) with intensity varying in the direction perpendicular to the field. A drift is produced as explained in the text. For ions, the mechanism is the same, but the Larmor motion occurs in a clockwise manner instead of counter-clockwise. As a result, the drift is in the opposite direction.

∇B drift) given by

$$\mathbf{v}_{\nabla B} = mv_{\perp}^2 \nabla B \times \mathbf{B}/(2qB^3) \tag{32.9}$$

Similarly, in the presence of a finite radius of curvature R_c of the magnetic field lines, a charged particle moving along the magnetic field with velocity $v_{||}$ experiences a centrifugal force $F_c = mv_{||}^2/R_c$. In the presence of an external force **F**, the particle decreases its energy during the part of its Larmor orbit in which the force has the opposite direction of the velocity (abc in Fig. 32.9 in which the example of an electron is again taken) and increases its energy in the other part (cda′ in Fig. 32.9).

The increase (decrease) in the particle energy leads to an increase (decrease) of its Larmor radius, and the average effect is again a drift in the direction perpendicular to both **F** and **B**. In the case of the centrifigal force, the drift takes the form

$$v_c = mv_{||}^2 \, \boldsymbol{\kappa} \times \mathbf{B}/(qB^2) \tag{32.10}$$

with $\boldsymbol{\kappa} \equiv \mathbf{b}\cdot\nabla\mathbf{b}$ being the magnetic field line curvature ($\kappa \propto 1/R_c$) and $\mathbf{b} \equiv \mathbf{B}/B$. This is the so-called *curvature drift*. Both curvature and ∇B drifts depend on the charge and have therefore opposite directions for electrons and ions.

Non-uniform magnetic fields also affect the motion of particles along the field lines. It is possible to show that if the non-uniformity of the field is sufficiently weak (i.e., if the characteristic variation length of the equilibrium magnetic field is much larger than the particle Larmor radius), the magnetic moment $\mu \equiv mv_{\perp}^2/(2B)$ of a particle is an adiabatic invariant. The parallel velocity of a particle is therefore given by

$$v_{||} = \pm[2(E - \mu B)/m]^{1/2} \tag{32.11}$$

with $E \equiv mv^2/2 = m(v_{||}^2 + v_{\perp}^2)/2$ the particle kinetic energy, which is an exact invariant in the absence of electric fields. Since the magnetic field intensity B varies along the particle orbit, $v_{||}$ is not constant. Two cases can be distinguished:

- *Circulating particles*. If $E > \mu B_{max}$ (with B_{max} the maximum value of the magnetic field along the field line), the parallel velocity never vanishes. In particular if $E \gg \mu B$, the parallel velocity is only weakly modulated by the B variation.
- *Trapped particles*. If $E < \mu B_{max}$, the particle oscillates between the points where $B = B_{mirror} = E/\mu$.

Finally, in the presence of a uniform and static electric field, a charged particle drifts in the direction orthogonal to both the electric under the effect of the external force q**E**. The resulting drift velocity is given by

$$v_E = \mathbf{E} \times \mathbf{B}/B^2 \tag{32.12}$$

and is independent of both charge and mass.

Thus, the particle trajectory is the combination of the Larmor orbits and of the *guiding center* motion, with the latter being given by the perpendicular and parallel drifts discussed above.

The presence of magnetic drifts implies that a plasma cannot be confined purely by a toroidal field. Such a magnetic field is produced by a toroidal solenoid and from Ampere law and Stokes theorem, the magnetic field inside the solenoid is given by

$$B_\phi = \mu_o \, I_M/(2\pi R) \tag{32.13}$$

with I_M being the current in the solenoid and R the radial distance from the axis of the solenoid. Therefore, charged particles in a purely toroidal magnetic field are subject to both the ∇B($\nabla B = -(B_\phi/R)\boldsymbol{R}$, with $\boldsymbol{R}$ the unit vector in the radial direction) and curvature drifts ($\boldsymbol{\kappa} = -\boldsymbol{R}/R$) both directed along the axis of the solenoid (Z axis in Fig. 32.10). Since the drift velocity is opposite for ions and electrons, a charge separation is produced that, in turn, creates an electric field. The electric field produces an outward E × B drift for both ions and electrons, and plasma confinement is lost.

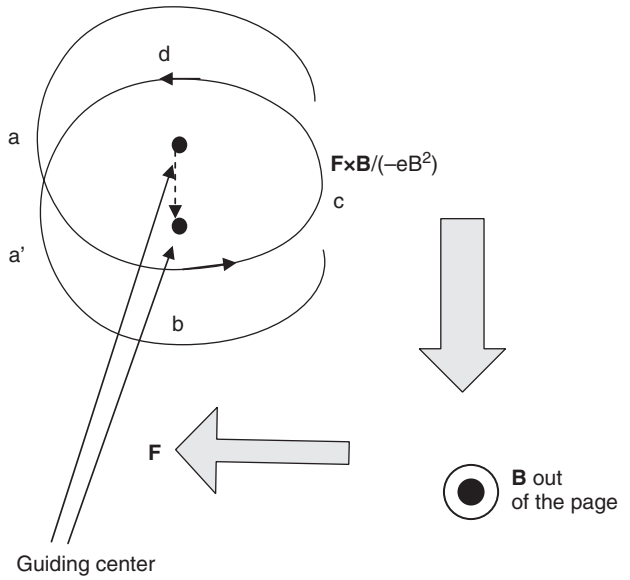

Figure 32.9 Drift of an electron in an external force. Here the drift arises as a result of the change of the particle energy due to the work done by the external force F. As in Figure 32.8, the drift is opposite for ions.

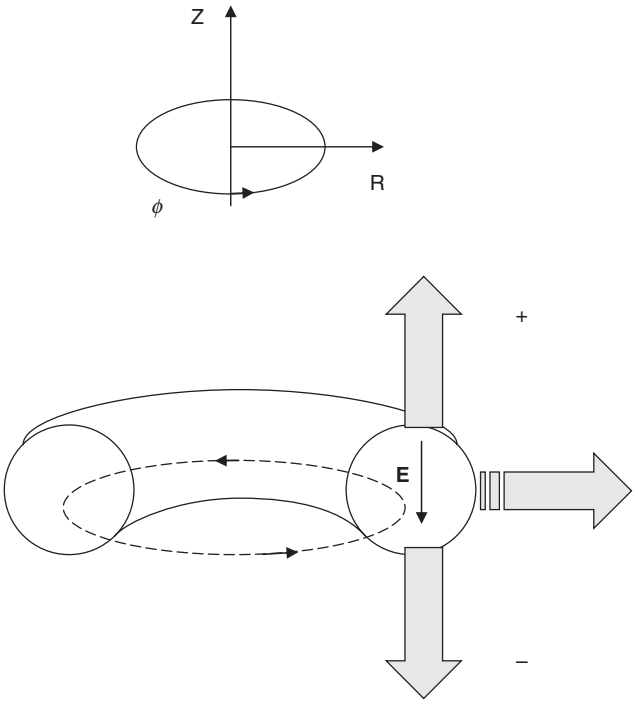

Figure 32.10 Particle drifts in the presence of a purely toroidal magnetic field. The ∇B and curvature drifts produce a charge separation, which, in turn, produces an electric field with an associated outward drift for both ions and electrons and loss of confinement.

In order to confine the plasma, it is necessary to superimpose a poloidal magnetic field in such a way that moving along the magnetic field, the drift experienced by charged particles is periodically directed toward and away from the center of the magnetic configuration, resulting in a zero net effect. In order to achieve this result, the magnetic configuration must have a net *rotational transform*.

The definition of rotational transform is shown below. The magnetic field is the superposition of the toroidal magnetic field and the poloidal magnetic field. Magnetic field lines cover magnetic surfaces topologically equivalent to tori. Magnetic surfaces form a set of simply nested surfaces around a limiting magnetic surface (the magnetic axis). It is convenient to take the magnetic axis as the origin of the system of coordinates in the (R, Z) plane. If we take a section of the magnetic surface with a poloidal plane $\phi = \phi_o$, the section will be a closed curve. The way in which the magnetic field line covers the magnetic surface is described by the rotational transform. Starting at $\phi = \phi_o$, a magnetic field line after one toroidal transit will intersect the poloidal plane at a different angle along the section of the magnetic surface (Fig. 32.11).

Let us call the rotation angle $2\pi\iota_1$. After a second toroidal transit, the rotation angle will be $2\pi\iota_2$. The

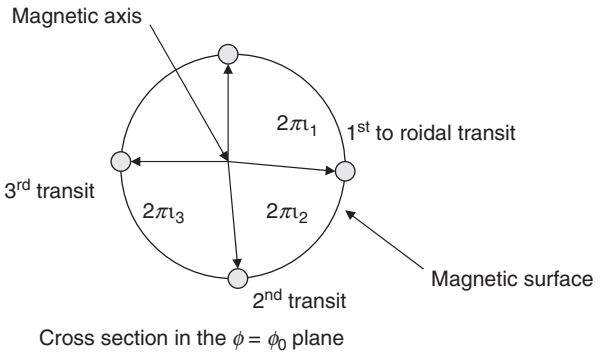

Figure 32.11 Rotational transform. The cross-section of a magnetic surface at a generic angle $\boldsymbol{\phi} = \boldsymbol{\phi}_o$ is shown. A field line starting at the top after the first toroidal transit intersects the magnetic surface at an angle rotated by $2\pi\iota_1$.

rotational transform is defined as the limit

$$\iota = \lim_{N\to\infty} (1/N)\,\Sigma_{k=1,\,N}\,\iota_k \qquad (32.14)$$

and represents the average rotation angle in a toroidal transit. Its inverse is called the *safety factor* $q \equiv 1/\iota$. The rotational transform takes in general different values on different magnetic surfaces. Safety factors and rotational transform play a special role in the stability of toroidal plasmas.

In order to see how the poloidal magnetic field associated with rotational transform is produced, it is necessary to briefly discuss the classification of toroidal magnetic configurations. Magnetic configurations can be broadly divided in two-dimensional (2D) and three-dimensional (3D). In 2D configurations, the magnetic surfaces are symmetric for rotation around the axis of the torus (the Z axis), i.e., the equilibrium quantities are independent of the toroidal angle ϕ. Examples of 2D configurations are the *tokamak* and the *reversed field pinch* (RFP). In 3D configurations, the equilibrium quantities are functions of all the three spatial variables, and the cross-section of a magnetic surface is different at different toroidal angles. The different categories of *stellarators* belong to this class.

2D configurations are intrinsically simpler, and the existence of magnetic surfaces can be proven to be a consequence of the axisymmetry (although in real experiments the presence of magnetic fluctuations can in fact lead to regions of stochastic magnetic field and associated reduction of confinement, a particularly severe problem for RFPs). However, in order to produce the poloidal field associated with the rotational transform, a net toroidal plasma current is needed. On one hand, this requirement leads to the possibility of instabilities driven by the plasma current (see below); on the other hand, it implies

that specific systems to generate the current in steady-state conditions must be in place (see section 32.8).

3D configurations have the advantage that the poloidal field can be produced entirely by external coils, avoiding in this way both current-driven instabilities and current drive systems, but they are intrinsically more complicated, and small errors in the external coils position can lead to stochastic magnetic fields in the plasma. In Figure 32.12 (a and b), the tokamak and the stellarator configurations are shown [14].

In the presence of a rotational transform, the particle guiding centers are confined on surfaces called drift surfaces. A particularly simple case is the motion of the guiding center for axisymmetric configurations where the equilibrium is independent of the variable ϕ. In this case, the canonical momentum $p_\phi \equiv R(mv_\phi + qA_\phi)$ is an exact invariant of the motion, with A_ϕ, the toroidal component of the vector potential, related to the poloidal flux ψ by $RA_\phi = \psi$. The deviation of the drift surface from the magnetic surface is of the order of $\Delta \equiv \rho_L(B/B_p)$. Circulating particles follow a drift surface similar in shape to the magnetic surfaces but displaced by a quantity of the order of Δ, whereas trapped particles follow "banana" orbits in the low toroidal magnetic field region (Fig. 32.13).

Since the poloidal field in the tokamak core is mostly produced by the toroidal plasma current ($B_p \approx \mu_o I_p/(2\pi a)$, with a the minor radius of the torus), the requirement that the size of the alpha particles' drift surfaces must be much smaller than the minor radius implies that a tokamak configuration needs a minimum plasma current in order to confine the alphas, $I_p \geq 3$MA.

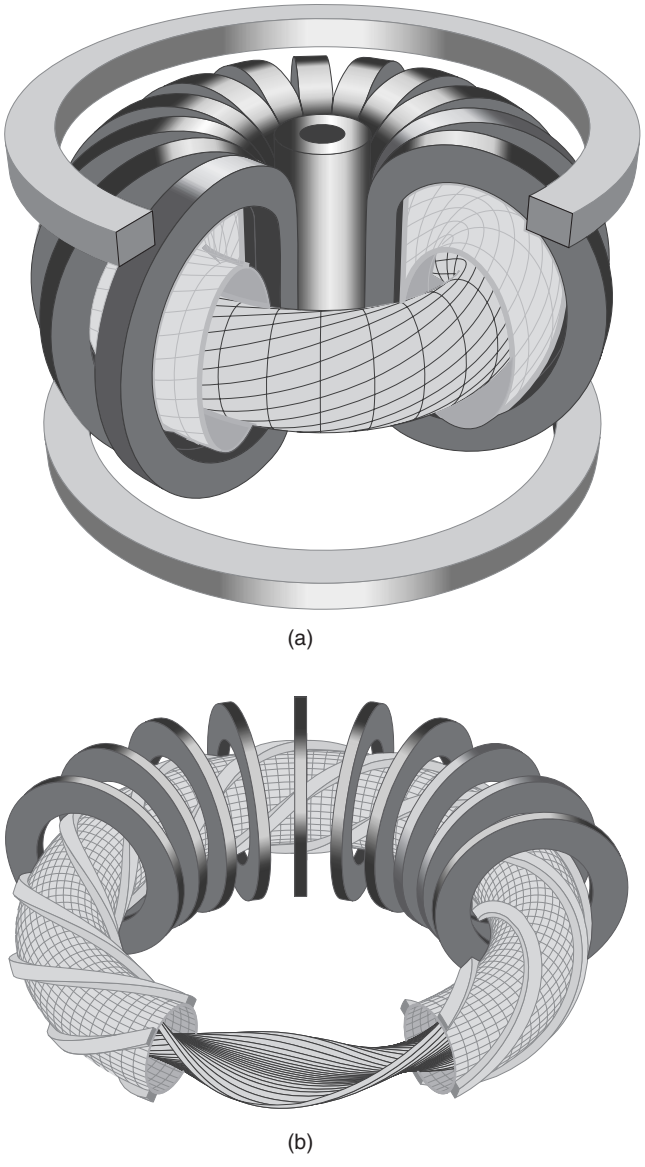

Figure 32.12 Example of two-dimensional (a) and three-dimensional (b) configurations. The poloidal, toroidal, and helical field coils are shown (*courtesy of Max Planck Institute*).

32.5 PLASMA EQUILIBRIUM, CONTROL, AND MACROSCOPIC PLASMA STABILITY

At the simplest level, the macroscopic plasma equilibrium and stability are described by the ideal magnetohydrodynamic (MHD) model. A review of the MHD equilibrium and stability can be found in [16]. The MHD equations can be written as follows

$$\rho d\mathbf{v}/dt = -\nabla p + \mathbf{j}\times\mathbf{B} \tag{32.15}$$

$$d/dt\ (p\ \rho^{-5/3}) = 0 \tag{32.16}$$

$$\mathbf{E} + \mathbf{v}\times\mathbf{B} = 0 \tag{32.17}$$

$$d\rho/dt + \rho\nabla\cdot\mathbf{v} = 0 \tag{32.18}$$

$$\partial\mathbf{E}/\partial t + \nabla\times\mathbf{B} = 0 \tag{32.19}$$

$$\nabla\times\mathbf{B} = \mu_o\mathbf{j} \tag{32.20}$$

$$\nabla\cdot\mathbf{B} = 0 \tag{32.21}$$

with $\mathbf{v}$ the plasma fluid velocity, ρ the plasma mass density, $\mathbf{j}$ the current density, p the plasma pressure and $d/dt \equiv \partial/\partial t + \mathbf{v}\cdot\nabla$. The equilibrium of a magnetically confined system in the absence of macroscopic flow ($\mathbf{v} = 0$) is described by the force balance equation

$$\nabla p = \mathbf{j}\times\mathbf{B} \tag{32.22}$$

The equilibrium equation can be simplified in the case of axisymmetric systems. It is possible to show that the most general expression of an axisymmetric magnetic field is $\mathbf{B} = \nabla\psi \times \nabla\phi + F\nabla\phi$ with $\psi = \psi(R, Z)$ and F a generic function of R and Z. The force balance equation implies $\mathbf{B}\cdot\nabla p = 0$, which, together with the definition of $\mathbf{B}$, implies

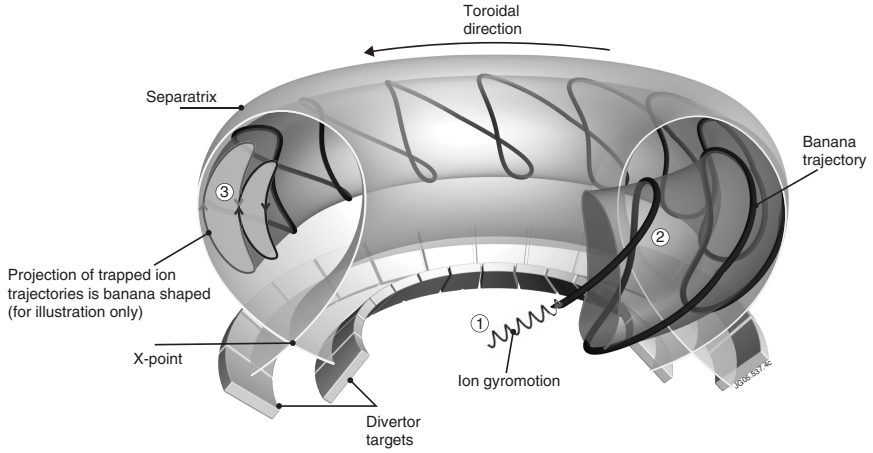

Figure 32.13 Banana orbits. A trapped particle oscillates between the two mirror points at which its parallel velocity vanishes. In combination with the radial drift, this produces a guiding center orbit with a characteristic banana shape. Banana orbits have a precession velocity in the toroidal direction (*courtesy of EFDA JET*).

$p = p(\psi)$. The current density can be evaluated from Ampere's law and can be written as

$$\mathbf{j} = \nabla F \times \nabla\phi - \nabla\phi\nabla^2\psi \qquad (32.23)$$

Since the equilibrium equation also implies $\mathbf{j}\cdot\nabla p = 0$ and $\nabla p = p'(\psi)\nabla\psi$, the expression for $\mathbf{j}$ also implies $F = F(\psi)$. Finally, taking the $\nabla\psi$ component of the equilibrium equation the Grad-Shafranov equation is obtained

$$R(\partial/\partial R)[(1/R)(\partial\psi/\partial R)] + \partial^2\psi/\partial Z^2 + \mu_o R^2 dp/d\psi + F\, dF/d\psi = 0 \qquad (32.24)$$

which is an elliptic partial differential equation for the function ψ once the two arbitrary function $p(\psi)$ and $F(\psi)$ are assigned together with appropriate boundary conditions.

The function ψ is called poloidal flux. It represents the flux of the poloidal magnetic field through a given R = constant surface. Magnetic surfaces are the loci where $\psi(R, Z)$ = constant. The plasma pressure is constant on a magnetic surface and the magnetic field and plasma current lie on it (Fig. 32.14).

It is possible to demonstrate that a plasma cannot be confined in a finite region of space only with currents generated within the plasma itself (virial theorem) [17]. In order to confine a plasma, either passive conductors or active coils must be located around it.

As an illustration, let us consider the equilibrium of a ring with variable major radius R and minor radius a carrying a toroidal current I_p. In the absence of other coils, no equilibrium solution exists. The ring tends to expand in order to minimize the magnetic energy. In order to find an equilibrium solution, a vertical field $\mathbf{B}_v$ must be supplemented. The exact solution for a circular plasma,

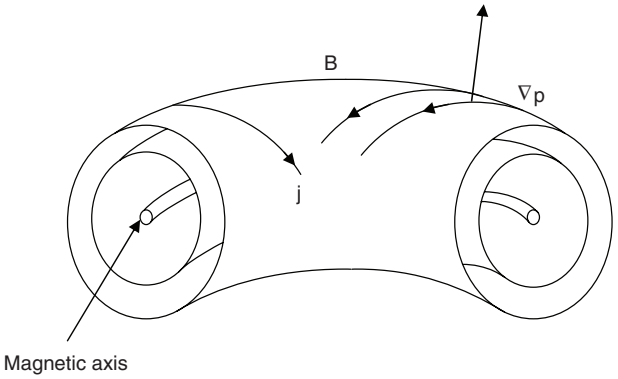

Figure 32.14 Magnetic surfaces for an axisymmetric system. Also shown are the magnetic axis and the equilibrium current density j, magnetic field B and pressure gradient ∇p.

obtained from the Grad-Shafranov equation in the limit of large aspect ratio R/a, yields

$$B_v = (\mu_o I_p/4\pi R)[\ln(8R/a) - 1.5 + l_i/2 + \beta_p] \qquad (32.25)$$

with β_p (poloidal beta) being the ratio between the average plasma pressure and the magnetic pressure associated with the poloidal field. The vertical field is produced by a pair of coils with current in the opposite direction of the plasma current. By varying the current in the coils it is possible to maintain the plasma at a fixed radial position when, e.g., either the internal inductance or the plasma pressure change in time. The control of the horizontal position is the simplest example of plasma control.

Another example of the control of magnetic equilibrium quantities is the control of the shape of magnetic surfaces. Stability arguments show that the optimal shape of the

magnetic surface in a tokamak requires a finite vertical elongation κ (the ratio between the vertical and the horizontal extension of the plasma) and triangularity δ (a measure of the deformation of the magnetic surfaces into a D-shape). Shape is controlled by external coils. Coil currents in the same direction of the plasma current tend to pull the plasma toward the coil, while currents in the opposite direction tend to push the plasma away from the coil. A set of magnetic sensors measures the poloidal flux ψ at different locations, and a control algorithm changes in real time the currents in the external coils to maintain the desired shape. The elongation of a magnetic surface cannot be increased arbitrarily. Above a certain value of κ, the plasma becomes unstable for vertical displacements. In a vertical displacement event, the plasma is accelerated toward the upper or the lower end of the vacuum chamber, and the plasma current tends to flow through the metallic structures, producing large electromagnetic forces on the components inside the vacuum chamber and on the chamber itself [3, 8].

It is important also to note that the currents in the control coils alter the topology of the magnetic surfaces. Considering for simplicity only the plasma and the lower coil (with current in the same direction as the plasma current in order to elongate the plasma), the poloidal magnetic field vanishes at an intermediate location called "X-point." The magnetic surface where the X-point lies is called magnetic separatrix, with the topology of the magnetic surfaces changing across the magnetic separatrix (Fig. 32.15).

The presence of a magnetic separatrix is important since, as it will be shown in section 32.9, it provides a natural solution for the plasma exhaust. Furthermore, the reference regime of operation of ITER (the H-mode, see section 32.6), characterized by enhanced energy confinement, requires the presence of an X-point inside the reaction chamber.

Plasma equilibria can be either stable or unstable [3]. The stability of an MHD equilibrium can be expressed using variational principle in term of the so-called MHD energy δW as a functional of an infinitesimal displacement $\boldsymbol{\xi}(\mathbf{v} \equiv \partial\xi/\partial t)$ to the plasma equilibrium

$$\begin{aligned}\delta W(\boldsymbol{\xi}*, \boldsymbol{\xi}) &= (1/2\mu_o) \int d\mathbf{r}[|(\nabla \times (\boldsymbol{\xi}_\perp \times \mathbf{B}))_\perp|^2 + B^2|\nabla \cdot \boldsymbol{\xi}_\perp \\ &+ 2\boldsymbol{\xi}_\perp \cdot \boldsymbol{\kappa}|^2 + (5/3)\mu_o p|\nabla \cdot \boldsymbol{\xi}|^2 - 2\mu_o(\boldsymbol{\xi}_\perp * \cdot \boldsymbol{\kappa}) \\ &(\boldsymbol{\xi}_\perp \cdot \nabla p) - (j_{||}/B)\boldsymbol{\xi}_\perp * \times \mathbf{B} \cdot (\nabla \times (\boldsymbol{\xi}_\perp \times \mathbf{B}))_\perp]\end{aligned} \tag{32.26}$$

The condition for stability $\delta W > 0$ can be violated only through the last two terms in the expression above, the first three being always positive definite. Thus, the free-energy sources that make a plasma equilibrium unstable are associated either with:

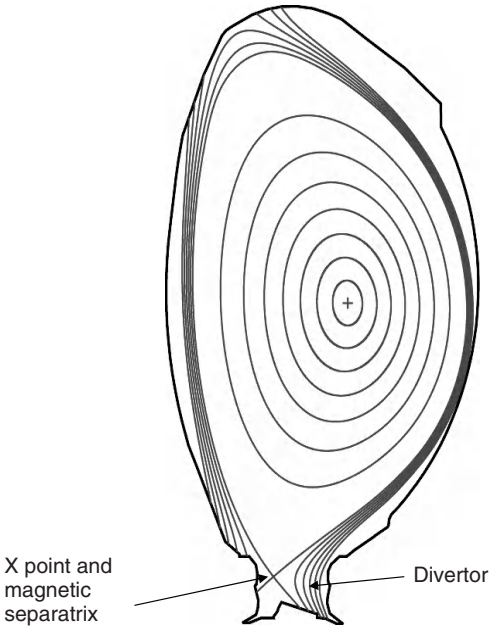

Figure 32.15 Magnetic separatrix and X-point (*courtesy of EFDA JET*).

- The combined effect of a pressure gradient ∇p and of the curvature $\boldsymbol{\kappa}$ of the magnetic field lines; or
- The component $j_{||}(\equiv \mathbf{j} \cdot \mathbf{B}/B)$ of the plasma current in the direction of the equilibrium magnetic field $\mathbf{B}$.

Macroscopic plasma stability is typically described by two parameters:

- $\beta \equiv \mu_o < p > /B^2$, the ratio between the average value $< p >$ of the pressure across the plasma volume and the magnetic pressure; and
- q_{edge}, the edge value of the safety factor (here the edge is conventionally defined at 95% the value of the poloidal flux at the magnetic separatrix since, due to the presence of the X-point, $q \to \infty$ on the magnetic separatrix).

In reality, plasma stability depends also on a number of other features, such as the radial profile of the plasma pressure and of the safety factor, as well as on effects not described by the MHD model such as the presence of a population of energetic particles (such as the α particles in fusion plasmas).

At the simplest level, both theory and experiments indicate that tokamak stability requires operation at $q_{edge} \geq 3$ and $\beta > (5\beta_N/2\pi)(\mu_o I/aB)$, with the parameter β_N depending on the shape of the radial pressure and safety factor profile with typical values between 1.5 and 3 in the absence of a stabilizing conduction wall close to the plasma.

Violating these conditions leads to a macroscopic distortion of the magnetic configuration that grows on a very short time scale (of the order of a few μs) and leads to the interaction between the plasma and the walls of the reaction chamber with a rapid loss of confinement (disruption).

The minimum safety factor at which a tokamak can operate sets a limit on the maximum plasma current. This is important since, as shown before, fast particle confinement requires a minimum plasma current. It will be shown later that also the energy confinement improves with plasma current. A convenient parametrization of the edge safety factor as a function of the equilibrium quantities is

$$q_{edge} = 2\pi a^2 B_\phi/(\mu_o I_p R)[1 + \kappa^2\ (1+2\delta^2 - 1.2\delta^3)]/2 \\ (1.17 - 0.65\varepsilon)/(1 - \varepsilon^2)^2 \qquad (32.27)$$

with $\varepsilon = a/R$ the inverse aspect ratio. From the expression of q_{edge}, it is clear that in order to increase the plasma current at fixed q_{edge}, it is necessary to increase either the toroidal magnetic field (but this possibility is limited by the use of superconducting coils technology) or the dimensions of the machine. However, at fixed toroidal field and dimensions, the plasma current can be maximized by acting on the shape of the magnetic surfaces and, specifically, on the elongation.

While tokamak operations can be effectively performed far from the stability boundaries in q_{edge} and β_N described above, MHD activity can still be present and lead to reduction of confinement. Among the most common instabilities it is important to recall saw teeth, neoclassical tearing modes, edge localized modes, and resistive wall modes. These instabilities have characteristic times longer than those leading to disruptions, and adequate control methods can be put in place to cope with them.

Saw teeth are periodic relaxation of the central part of the plasma, namely the region where the safety factor falls below one. They eject heat and particles from the $q < 1$ region and are overall benign (avoiding impurity accumulation in the plasma center), provided their amplitude is not too high. Large ("monster") saw teeth can be produced by a population of energetic particles (such as the alpha particles produced in fusion reactions) and must be avoided since they can produce a large seed perturbation for other instabilities such as the neoclassical tearing modes. Saw teeth can be controlled by modifying the current density around the $q = 1$ surface.

Neoclassical tearing modes (NTM) are modes that are stable within the classical MHD model but are driven unstable by the (lack of) bootstrap current (see below) at the location of the mode if the plasma pressure becomes sufficiently large (typically for $\beta_N \approx 2$ to 3). NTMs can be controlled and suppressed by the use of electron cyclotron waves (see Section 32.8).

Edge localized modes (ELM) are periodic relaxations of the plasma edge that occur as a consequence of the formation of a steep pressure gradient when a transport barrier is produced at the plasma edge. While ELMs do not generally have a detrimental effect on plasma confinement (avoiding impurity accumulation), if their amplitude is too large, they produce unacceptably large transient heat loads on the plasma-facing components (see section 32.9). Therefore, the energy release per ELM must be reduced to something of the order of 1 MJ for a machine like ITER. Several control methods are under development, such as the use of resonant magnetic perturbations and the injection of frozen deuterium pellets.

Resistive wall modes are produced above the no-wall beta limit. In the presence of a perfectly conducting wall close to the plasma, the stability limit can be somewhat increased above $\beta_N \approx 3$. However, any wall is not a perfect conductor and resistive wall modes (RWM) growing on the time scale of the resistive diffusion time of the wall are produced. RWMs can be controlled by active coils placed around the plasma.

A different class of instabilities is that driven by energetic particles such as the fusion alpha particles. Energetic particles affect plasma stability through resonant and non-resonant interaction with plasma waves due, e.g., to the proximity of their velocity to the Alfvén velocity. The role of energetic particle driven modes is a field of active research and will be fully addressed in ITER [5].

32.6 TURBULENT TRANSPORT

Energy confinement in magnetic fusion devices is affected by small-scale instabilities driven unstable by the plasma free-energy sources associated with the density and temperature gradients. These instabilities do not produce a loss of macroscopic confinement but lead to enhanced heat and particle losses [2]. Vortex structures are produced with a radial correlation length of the order of the ion Larmor radius and an autocorrelation time of the order of the transit time of an ion around the torus.

Under normal conditions, a tokamak plasma is in the so called L(ow)-mode of confinement. Numerical simulations of plasma turbulence show that in L-mode conditions, highly anisotropic vortex structures, elongated in the radial direction, are produced. A reactor using L-mode confinement would be very large and not optimized in terms of plasma parameters.

In the early 1980s, a different regime of operation called H(igh)-mode of confinement was discovered. It was characterized by the suppression of plasma turbulence in the region of the plasma close to the magnetic separatrix. This regime is very reproducible and has become the basis for the design of ITER. The theoretical explanation of the access

to H-mode is still a field of active research. Empirically, H-modes are obtained above a certain threshold in the heating power, with the threshold increasing with plasma density and magnetic field. Numerical simulations of plasma turbulence show that at the transition between L- and H-mode, a sheared flow is produced at the plasma edge that reduces the radial correlation length of the vortex structures, reducing in this way the turbulent transport and leading to the formation of a "transport barrier" characterized by a steep pressure gradient. This process is limited by the onset of edge localized modes above a critical value of the edge pressure gradient.

The energy confinement time in H-mode is estimated through semi-empirical scaling laws. The scaling law that fits at best the experimental data is the ITER98y2 scaling

$$\tau_{\mathrm{ITER98(y,2)}}(\mathrm{s}) = 0.0562 \mathrm{I_p(MA)}^{0.93} \mathrm{B}_{\phi}(\mathrm{T})^{0.15} \mathrm{P(MW)}^{-0.69} \mathrm{n}(10^{19}\mathrm{m}^{-3})^{0.41} \mathrm{M}^{0.19} \mathrm{R(m)}^{1.97} \varepsilon^{0.58} \kappa^{0.78} \quad (32.28)$$

with P the heating power, n the average plasma density, and M the average ion mass [2]. It is important to stress the almost linear dependence of the energy confinement time on the plasma current. As shown in Figure 32.16, the results of the various tokamak experiments span about three orders of magnitude. The extrapolation between the largest experiment (JET) and ITER is about a factor of three with an expected confinement time of about 4.3 s. Stellarators also exhibit similar trends in the energy confinement.

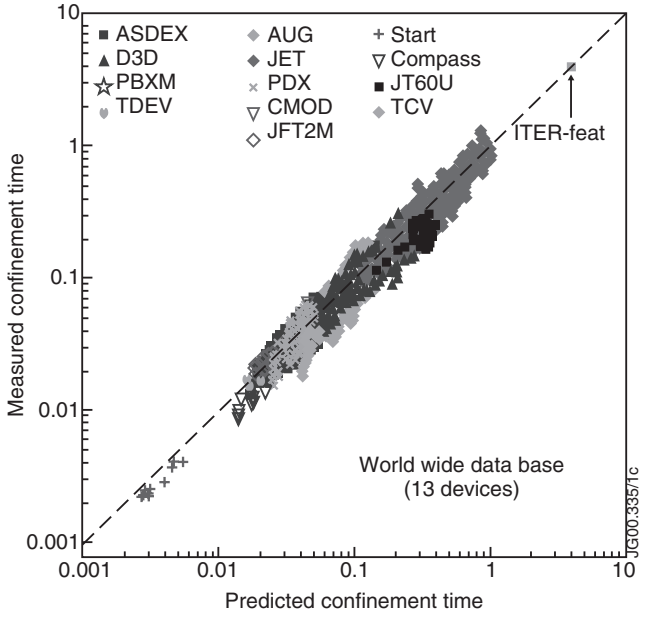

Figure 32.16 Comparison between the experimental values of the energy confinement time and the ITER98(y2) scaling law (*courtesy of EFDA JET*).

It has to be noted that the empirical approach for the determination of the scaling laws for the energy confinement time is supported by the present theoretical understanding of plasma turbulence. It can be shown that by using an appropriate rescaling of the various physical quantities, at fixed geometry (aspect ratio, shape of magnetic surfaces, etc.) and fixed radial profile shapes, the equations describing plasma phenomena in a torus can be cast in a form that depends only on three dimensionless physical parameters: the normalized Larmor radius $\rho^* \equiv \rho_\mathrm{i}/\mathrm{a}$, the normalized pressure β, and the normalized collisionality $\nu^* \equiv \mathrm{R}/\lambda_{\mathrm{mfp}}$, with λ_{mfp} the mean free path between Coulomb collisions (see section 32.7). This situation is similar to that found in the dynamics of neutral fluid where the turbulent flow properties (e.g., for the design of aerodynamic components) can be determined by scaled-down experiments in "wind tunnels." It implies that the energy confinement time can be expressed in dimensionless form as

$$\Omega\tau_\mathrm{E} = \mathrm{f}(\rho_*, \beta, \nu*) \quad (32.29)$$

Dedicated experiments have confirmed that machines working at different dimensional parameters (magnetic field, dimensions, etc.) but same dimensionless parameters, do indeed have the same value of the energy confinement time (in normalized form), demonstrating that energy confinement is the result of plasma physics dynamics (rather than, e.g., atomic physics phenomena), difficult to describe but in principle scalable to different devices. The ITER98y2 expression does indeed satisfy this constraint.

32.7 COULOMB COLLISIONS

The charged nature of the plasma components alters significantly the behavior of a plasma from that of an ordinary gas. Particles interact through the Coulomb force. This is a long-range force, but its effect in a plasma is reduced, due to the screening of the other charged particles, at distances above the Debye length $\lambda_{\mathrm{Dj}} \equiv \mathrm{v_{thj}}/\omega_{\mathrm{pj}}$, with $\mathrm{v_{thj}} \equiv (2\mathrm{T_j}/\mathrm{m_j})^{1/2}$ the thermal velocity and $\omega_{\mathrm{pj}} \equiv (\mathrm{n_j q_j^2}/\varepsilon_\mathrm{o}\mathrm{m_j})^{1/2}$, the plasma frequency of the j-th species. Here $\mathrm{T_j}, \mathrm{n_j}, \mathrm{m_j}$, and $\mathrm{q_j}$ are the temperature (expressed in energy units), density, mass, and charge of the j-th species, respectively.

Coulomb collisions are associated with several effects: energy equipartition between different species, frictional drag in the presence of a difference in the average velocity of the various species, radial transport, and others. In the following discussion, we limit to the first two effects. Radial transport due to Coulomb collision is typically smaller than that associated with plasma turbulence.

Charged particles collisions are described by the Rutherford cross-section. In Figure 32.17, the collision between two particles in the center of mass system is shown.

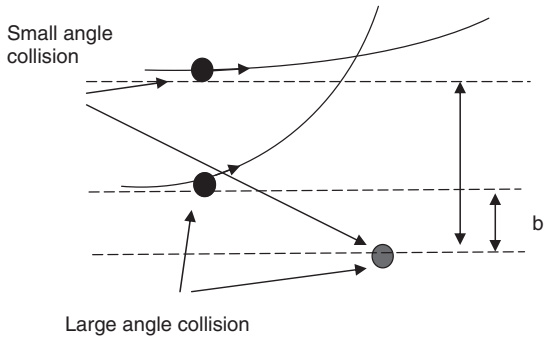

Figure 32.17 Collision between particles. The effects of Coulomb collisions are dominated by small angle events.

The final trajectory after the collision depends on the impact factor b: at a small impact factor, the particle is deflected by a large angle, while at a large impact factor, the particle is deflected by a small angle. In each collision, energy and momentum are exchanged between the colliding particles. The net effect of the collision of a test particle of charge q_b and mass m_b passing through a plasma is the result of the collisions with all the field particles of each species. Since the Coulomb force is a long-range force, the effect of collision is dominated by the large number of high-impact factor collisions, rather than from the small number of low-impact factor events. However, due to the Debye screening, only the particles located at an impact factor $b \leq \lambda_{Dj}$ affect the test particle. In addition, the net momentum and energy transfer from the test particle depends on the average over the velocity distribution function of the field particles (typically a Maxwellian). For the case of a test particle with velocity much larger than the ion thermal velocity and smaller than the electron thermal velocity, it can be shown that the energy transfer is described by

$$dE/dt = -(2E/\tau_{SD})[1 + (E_{cr}/E)]^{3/2} \qquad (32.30)$$

with the slowing down time $\tau_{SD} \equiv 3(2\pi)^{1/2}(2\pi\varepsilon_o^2 m_b^2/n_e Z_b^2 e^4 \ln\Lambda)\, T_e^{3/2} m_e^{-1/2} m_b$ and Λ the number of particles in a Debye sphere. Above a critical energy $E_{cr} = 14.8 T_e A_b (\Sigma_i n_i Z_i^2/(n_e A_i))^{2/3}$ (with A_b and A_i the mass number of the test and field ion particles), the test particle slows down mostly via collisions with the electrons.

The second important effect associated with Coulomb collision is the frictional drag between species with different average velocity. In particular, collisions between thermal electrons that carry the plasma current and ions determine the plasma resistivity $\eta = 1.65\text{l}\ n\Lambda Z_{eff}/T_{keV}^{3/2} 10^{-9} \text{ohm} - \text{m}$. It should be noted that plasma resistivity does not depend on density: As density increases, the collision frequency and the density of current carrying charges increase in the same way. Plasma resistivity is enhanced by the presence of trapped electrons that do not carry a net current.

Finally, it is important to note that Coulomb collisions occur on a time scale much longer than that for a transit around the torus. For example, the mean free path for electron-electron collision (which is of the same order of that for ion-ion collision in plasma with similar electron and ion temperature), $\lambda_{mfp,e} \equiv v_{the}/\nu_{ee}$, with $\nu_{ee} \sim e^4 n_e \ln\Lambda/(\varepsilon_o^2 m_e^2 v_{the}^3)$, is typically $10^2 - 10^3$ times the circumference of the torus, i.e., a collision occurs only after hundreds of transits of the electron around the torus.

32.8 PLASMA HEATING AND CURRENT DRIVE

In axisymmetric configurations such as the tokamak, a net toroidal plasma current is necessary in order to maintain confinement. The plasma current is initially produced through a transformer formed by a cylindrical solenoid (central solenoid) placed along the symmetry axis of the torus (Fig. 32.18).

The change $\Delta\Phi$ in the magnetic flux of the central solenoid induces a toroidal plasma current I_p given by

$$\Delta\Phi = L_p I_p \qquad (32.31)$$

with $L_p = \mu_o R[\ln(8R/a) - 2 + l_i]$ the self-inductance of the plasma and l_i the internal inductance of the plasma that depends on the toroidal current distribution. After the current has achieved the required value, the plasma resistivity would lead to a decay of the current unless a toroidal electric field is induced to accelerate the electrons. If the duration of the plasma pulse is finite, the electric field can be produced by the residual flux available in the central solenoid. Since the plasma resistivity is very low at thermonuclear temperatures, current flat top durations between few seconds and few hundred seconds, depending on the size of the machine, can be obtained. However, this method is intrinsically limited by the amount of residual flux in the central solenoid and prevents the achievement of fully steady-state conditions. To operate a steady-state tokamak [6] requires methods for producing the plasma current in non-inductive ways [9].

A large part of the current can be produced by the plasma itself through the so-called bootstrap mechanism, provided sufficiently high values of the plasma pressure are achieved. The origin of the bootstrap current can be explained by considering neighboring electron banana orbits passing through a point (point 3 in Fig. 32.13). In the presence of an electron density gradient, there is a net parallel velocity that is transferred to the circulating electrons through electron-electron collisions. This acceleration force acting on the circulating electrons is balanced by the friction between circulating electrons and ions. As a result, the current density of the circulating electrons turns out to be

$$j_{bootstrap} \approx -0.33\varepsilon^{1/2}(1/B_p)|\nabla p| \qquad (32.32)$$

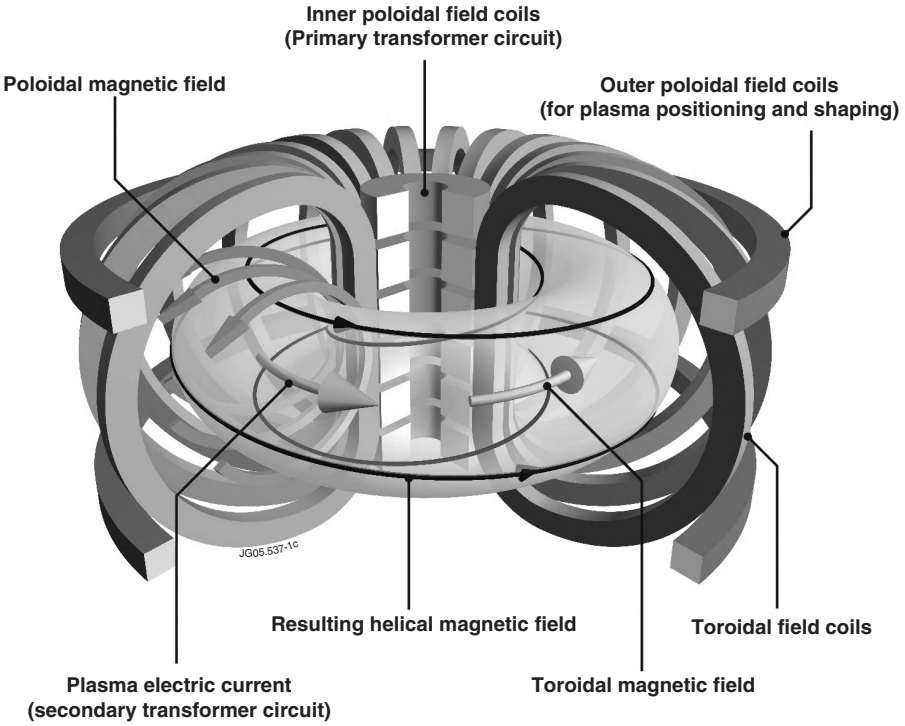

Figure 32.18 The central solenoid (inner poloidal field) coil acts as the primary transformer circuit with the plasma being the secondary circuit. A change in the central solenoid current induces an electric field in the plasma that drives the toroidal current, producing the poloidal field. (*courtesy of EFDA JET*).

The fraction $f_{Bootstrap}$ of the total plasma current associated with the bootstrap current is proportional to $f_{Bootstrap} \propto \varepsilon^{-1/2} q_{edge} \beta_N$. For conventional aspect ratio values and $q_{edge} \approx 5$, to achieve a fraction of the total current between 60% and 80% in the form of bootstrap current requires values of $\beta_N > 3$ [6]. Stability calculations and experimental results show that this is possible through the optimization of the plasma equilibrium profiles.

The bootstrap current is generally not fully aligned with the equilibrium current density profile associated with the magnetic equilibrium configuration, and a residual current has to be produced in the plasma location where the bootstrap current is insufficient or subtracted where the bootstrap mechanism is overdriving the current. In order to generate such a residual plasma current, auxiliary current drive systems are used. The auxiliary systems involve both the use of beams of high-energy ions and high-power electromagnetic waves in different frequency ranges [9].

32.8.1 Neutral Beam Heating and Current Drive

Positive or negative ions are produced by a source and accelerated by electrostatic fields up to energies ranging from 50 keV to 1 MeV. After being accelerated, the ions are neutralized by passing through a region of neutral gas. The resulting high-energy neutral particle beam is then injected inside the vacuum chambers through a port. In the plasma, neutral particles are ionized by the interaction with the plasma particles (mostly via electron impact ionization, charge exchange, and ion impact ionization) and deposit their energy and momentum via Coulomb collisions.

The energy of the beam is determined by the needs of depositing the particle in the plasma core and of driving the plasma current with high efficiency. When applied to thermonuclear-grade plasmas, both conditions require high-energy beams: In ITER the beam energy is 1 MeV, and even larger beam energy values are needed in a fusion reactor. The technology of the injector is determined by the requirement of achieving high efficiency. Above beam energies around 100 keV amu^{-1}, the neutralization efficiency of a positive ions drops to values below 20% while that of a negative ion remains constant at about 60%. As a result, for beam energies above 200 keV, negative-ion-beam technology must be used. However, while negative ions are easy to neutralize, they are more difficult to produce than positive ions. Present negative-ion sources do not exceed values of 25 mA/cm^2, about an order of magnitude lower than positive energy sources. Other issues associated with negative-ion sources are maintainability, extraction efficiency, and uniformity.

The injection of beams always heats the plasma. By injecting the beam tangentially to the equilibrium magnetic field, it is also possible to produce a net plasma current. The mechanism for the generation of plasma current by energetic beams is well understood in terms of classical plasma physics. The current produced by the beam is partially screened by the current produced by electrons, leading to an exact cancellation if the beam and thermal ion charge are the same. Other effects, such as electron trapping, reduce the screening effect and contribute to achieving a net plasma current.

The amount of current that can be driven for unit of neutral beam power injected in the plasma is commonly referred to as current drive efficiency γ

$$I_{CD} = \gamma P_{aux}/(n_e R) \tag{32.33}$$

with n_e the average electron density. In the case of neutral beam current drive typical values of the current drive efficiency for ITER scenarios are in the range $\gamma_{NBCD} \approx 0.3 \times 10^{20}$ m^{-2} A/W. The neutral beam current drive efficiency increases with electron temperature due to the increase of the slowing down time of the beam ions. For beam ion velocities close to the Alfvén velocity, beam ions can destabilize MHD modes.

32.8.2 Electron Cyclotron Heating and Current Drive

The electron cyclotron heating and current drive system uses the resonant absorption of electromagnetic waves by the electrons at the spatial location where the wave frequency equals the electron cyclotron frequency. The development of steady-state powerful generators (gyrotrons) in this frequency range is still an area of active research. With the present technology, it is possible to produce steady-state 1 MW sources up to 170 GHz, corresponding to a resonant magnetic field of 6T.

The main advantages of the use EC waves are the following:

- The very localized absorption, which allows very fine modifications of the temperature and current density profiles, provided the plasma density is below the cut-off density.
- The simplicity of the coupling since, due to the high frequency, the wave can be launched in vacuum and propagate in the plasma core without being affected by the edge plasma conditions.

The typical value of the current drive efficiency is a factor 2–3 lower than for neutral beams $\gamma_{ECCD} \approx 0.1 \times 10^{20}$ m^{-2} A/W. However, for many applications, the low efficiency is not a limitation, since the wave absorption is very localized. This property is used, e.g., for NTM stabilization.

32.8.3 Lower Hybrid Heating and Current Drive

Lower hybrid waves are slow waves with a frequency in the range of the geometric mean of the ion and electron cyclotron frequency corresponding to a few GHz. Klystrons have been developed up to 5 GHz for this purpose.

Wave absorption occurs when the parallel phase velocity of the wave equals the electron velocity. The wave is injected in the plasma through an array of waveguides. By controlling the relative phase of adjacent waveguides, it is possible to produce a spectrum with the phase velocity predominantly in one direction, generating in this way a net plasma current. The coupling of lower hybrid waves is sensitive to the edge plasma conditions, and different antenna concepts have been developed to overcome this problem. The main advantage of lower hybrid is the high current drive efficiency $\gamma_{LHCD} \approx 0.3 \times 10^{20}$ m^{-2} A/W and weak dependence on the plasma temperature, which makes this method the best candidate for driving current in the outer part of the plasma in ITER.

32.8.4 Ion Cyclotron Heating and Current Drive

The ion cyclotron heating and current drive system uses the resonant absorption of electromagnetic waves by the ions at the spatial location where the wave frequency equals the ion cyclotron frequency. Since the ion cyclotron frequency typically falls in the radio frequency range (20 MHz–60 MHz), high-power sources are commercially available as well as transmission lines. The main issues related to the use of ion cyclotron waves is the sensitivity of the antenna-plasma coupling to the edge plasma conditions, especially in the presence of fast edge relaxations associated with ELMs.

Current can be produced in this frequency range via electron absorption when the wave parallel velocity matches the electron velocity. Typical values of the current drive efficiency are about an order of magnitude smaller than for neutral beam current drive $\gamma_{ICCD} \approx 0.03 \times 10^{20}$m^{-2} A/W.

32.9 POWER AND PARTICLE CONTROL

The heat transported from the center of the plasma to the edge by the turbulent process described in section 32.6 needs to be continuously removed from the reaction chamber [4]. Similarly, the He ashes produced after the fusion alphas have transferred all their energy to the plasma need to be continuously removed to avoid poisoning the fuel (dilution). Plasma exhaust takes place at special locations, called *divertors*, in the reaction chamber sufficiently remote from the hot plasma that the heat and particle removal can take place without disturbing the dynamics of the plasma inside the separatrix.

After crossing the magnetic separatrix, heat and particles flow along the magnetic field lines to the divertor (Fig. 32.15). Particles arriving at the divertor are much less energetic than those in the plasma, but even at energies of a few tens of electronvolts, the bombardment of the divertor plates can produce a substantial damage. Thus, the divertor must be operated in conditions where the temperature of the plasma in front of the divertor plates is reduced to a few eV.

Since electrons are faster than ions, they tend to be more easily lost to the divertor plates, which become negatively charged. This negative potential accelerates the plasma ions toward the plate up to velocities of the order of the plasma sound velocity. In ideal conditions, such a flow of ions keeps the impurities released from the plates confined into the divertor region. Furthermore, the He ions coming from the hot plasma are neutralized at the divertor plates, and sufficiently high He pressure can be built up in the divertor to allow effective He pumping, and impurities do not flow back in the plasma.

The heat load on the divertor plates is large, since all the heating power (apart from the fraction radiated on the wall of the reaction chamber) is deposited in a narrow region of the divertor. The R&D for ITER has produced actively cooled components made either of carbon fiber composite (CFC) or tungsten capable of withstanding up to 20 MWm^{-2} in steady-state conditions, with expected heat loads in the range 5–10 MWm^{-2}. A specific issue is the effect of transient heat loads such as those generated by ELMs. Transient loads must be kept below a certain threshold to allow a sufficiently long life of the materials.

The choice of the material for the plasma-facing component in a fusion reactor is constrained by several requirements: resistance to steady-state and transient heat loads, compatibility with plasma operation, and low activation properties under neutron irradiation. Presently, the use of tungsten is envisaged for reactor applications.

32.10 PLASMA DIAGNOSTICS

Diagnostics in fusion devices plays a key role not only for the measurement of various quantities aimed at a better understanding of the physical phenomena, but also for the real-time control of plasma discharges [7]. Diagnostics can be conveniently grouped according to the measurement technique: magnetics, probes, spectroscopy, microwaves, laser-aided, and particle and fusion products.

32.10.1 Magnetics

Magnetic diagnostics are used to measure basic equilibrium parameters such as the plasma current, the position and the shape of the plasma, as well as magnetic fluctuations associated with plasma turbulence. They cover the frequency range between 100 Hz to a few MHz. Magnetic diagnostics are conventional systems in present devices. However, the effect of neutron and gamma radiation on the measurements will already pose challenges to the use of these diagnostics in ITER.

32.10.2 Microwave Diagnostics

Microwave diagnostics cover the frequency range 1 GHz to 3 THz and are used with different techniques:

- Reflectometry measures the phase shift of a wave injected from outside and reflected at the plasma position where the wave frequency is equal to the cut-off frequency.
- Electron cyclotron emission (ECE) measures the electron temperature radial profile: the amplitude of the emitted black body radiation is proportional to the electron temperature, and its frequency is the local value of the electron cyclotron frequency (associated with the local value of the magnetic field whose radial dependence is known).
- Interferometry measures the phase difference between a wave passing through the plasma and a wave traveling in a vacuum, providing a measure of the average plasma density along the path of the wave; in addition, by measuring the change in polarization (polarimetry), it is possible to infer information on the poloidal magnetic field.

32.10.3 Spectroscopy

Spectroscopy covers the frequency range between 10 nm to 10 μm in which it is possible to measure the continuum Bremsstrahlung spectrum and the line radiation from various impurity ions. It provides information not only on the ion composition of the plasma but also on electron temperature (from the relative intensity of lines that have a different dependence of the excitation rate on the electron temperature) and plasma rotation (from the Doppler shift).

32.10.4 Laser-Aided Diagnostics

Thomson scattering is the most widely used diagnostic for measuring the electron density and temperature from the laser radiation scattered by the plasma electrons. The spectral broadening of the laser radiation due to the Doppler effect provides the temperature and the amplitude of the scattered signal the density. The spatial resolution presently achieved is up to about 1/100 of the minor radius and the time separation between consecutive pulses is between 10 μs and 100 ms. The laser source typically employed for

this diagnostic is ruby or Nd:YAG lasers with wavelengths in the visible range, much smaller than the Debye length of the plasma ($\approx 30\,\mu m$). In these conditions, electrons behave as independent particles (incoherent Thomson scattering).

For laser wavelengths comparable to the Debye length, scattered radiation is due to the contribution from different electrons and their surrounding shielding cloud (coherent Thomson scattering). Since shielding is partially due to the ion contribution, information about the ion distribution function can be obtained from this method. For laser wavelengths much larger than the Debye length, the scattered radiation is associated with the collective motion of electrons and collective Thomson scattering can be used to measure density fluctuations.

Laser-induced fluorescence is also used to determine the density of molecules or atoms brought into an excited state by the laser radiation and measuring the spontaneous emission of the photons when they decay back to the ground state (fluorescence).

32.10.5 Probes

Probes are electrodes in direct contact with the plasma and therefore can be used only in low-temperature regions of the plasma where they can give information about the local values of density and temperature.

32.10.6 Particle Diagnostics

Besides conventional neutral particle analyzers, it is important to mention in this context charge exchange recombination spectroscopy for the measurements of ion temperature, density and rotation, and heavy ion beam probes and the electrostatic plasma potential and lithium beam probes to measure the density and magnetic field from the Zeeman splitting.

32.10.7 Fusion Products

The most commonly used diagnostics belonging to this category are those that measure the emission of the neutrons produced in the fusion reactions. In addition, charged particle products can be collected by probes situated at the edge. Techniques based on gamma radiation emitted in the interaction between fast ions and the plasma intrinsic impurities have been recently developed.

REFERENCES

1. D. Maisonnier, D. Campbell, I. Cook, L. Di Pace, et al., Power plant conceptual studies in Europe. *Nucl. Fusion*, 2007, **47**, 1524–1532.
2. E.J. Doyle, W.A. Houlberg, Y. Kamada, V. Mukhovatov, et al., Plasma confinement and transport. *Nucl. Fusion*, 2007, **47**, S18–S127.
3. T.C. Hender, J.C. Wesley, J. Bialek, A. Bondeson, et al., MHD stability, operational limits and disruptions. *Nucl. Fusion*, 2007, **47**, S128–S202.
4. A. Loarte, B. Lipschultz, A.S. Kukushkin, G.F. Matthews, et al., Power and particle control. *Nucl. Fusion*, 2007, **47**, S203–S263.
5. A. Fasoli, C. Gormenzano, H.L. Berk, B. Breizman, et al., Physics of energetic ions. *Nucl. Fusion*, 2007, **47**, S264–S285.
6. C. Gormezano, A.C.C. Sips, T.C. Luce, S. Ide, et al., Steady state operation. *Nucl. Fusion*. 2007, **47**, S285–S336.
7. A.J.H. Donné, A.E. Costley, R. Barnsley, H. Bindslev, R. et al., Diagnostics. *Nucl. Fusion*, 2007, **47**, S337–S384.
8. Y. Gribov, D. Humphreys, K. Kajiwara, E.A. Lazarus, et al., Plasma operation and control. *Nucl. Fusion*, 2007, **47**, S385–S403.
9. J. Jacquinot, S. Putvinski, G. Bosia, A. Fukuyama, et al., Plasma auxiliary heating and current drive. *Nucl. Fusion*, 1998, **38**, 2495–2539.
10. R. J. Goldston and P. H. Rutherford, *Introduction to Plasma Physics*. Institute of Physics Publishing, Bristol, UK, 1995.
11. J. P. Freidberg, *Plasma Physics and Fusion Energy*. Cambridge University Press, Cambridge, UK, 2007.
12. F. Chen, *Introduction to Plasma Physics and Controlled Fusion*. Springer, New York, 2006.
13. J. Wesson, *Tokamaks (third edition)*. Clarendon Press, Oxford, UK, 2004.
14. M. Wakatani, *Stellarator and Heliotron Devices*. Oxford University Press, New York/Oxford, 1998.
15. H. S. Bosch and G. M. Hale, Improved formula for fusion cross-sections and thermal reactivities. *Nucl. Fusion*, 1992, **32**, 611–631; and H. S. Bosch and G. M. Hale, Erratum. *Nucl. Fusion*, 1993, **33**, 1919.
16. J. P. Freidberg, Ideal magnetohydrodynamic theory of magnetic fusion systems. *Rev. Modern Physics*, 1982, **54**, 801–902.
17. V. D. Shafranov, Plasma equilibrium in a magnetic field. *Review of Plasma Physics*, Vol. III, edited by M.A. Leontovich. Consultant Bureau, New York, 1966.

33

FUSION TECHNOLOGY

LESTER M. WAGANER
Fusion Consultant, O'Fallon, MO, USA

33.1 INTRODUCTION

Fusion energy has the inherent advantages of an abundant power supply, minimal resource constraints, no greenhouse gas emissions, low-level waste production, minimal safety concerns for the general public, and no restrictive site limitations. A significant disadvantage is that sustained and controlled nuclear fusion is difficult to achieve and sustain. Research on controlled nuclear fusion commenced in the 1950s with hydrogen ions trapped in magnetic fields within a cylindrical vacuum chamber. The magnetic fields reflected the ions back and forth (i.e., a simple magnetic mirror). Other magnetic configurations were considered and tested with the tokamak configuration exhibiting the most stable plasma conditions. Inertially confined plasmas are an alternative approach to achieving sustained fusion energy production. The origin of inertially confined fusion is the demonstration of the hydrogen bomb in 1952. This burst of nuclear energy began the search for controlled fusion energy.

The hydrogen bomb was initiated by a fission bomb that heated and compressed the core containing fusion fuel materials. Theoretically, the necessary heat and compression for ignition can be achieved on a much smaller scale by using laser, light-ion or heavy-ion beams—all of these methods have been employed in small- and moderate-scale experiments for pulsed containment. The U.S. National Ignition Facility [1] announced completion of its first integrated ignition experiment on October 6, 2010 with the ultimate goal to produce net energy gain.

Many magnetic confinement experiments world-wide have been operated with increasing fidelity with the intent to achieve energy breakeven and an ignited plasma. The ITER [2] experimental facility is currently starting construction; it is the most ambitious tokamak experiment to date. It is expected to exceed ignition conditions and produce 500 MW of fusion power with an input of 50 MW for 400 seconds with first plasma around 2018. The main fusion research emphasis, to date, is to fully understand and control the plasma conditions. Assuming ITER is successful (and it likely will be), the emphasis will shift to advancing, refining, and validating the necessary technology and engineering solutions of producing a viable fusion power plant.

There have been a multitude of fusion power plant designs, both for magnetically and inertially confined plasmas, since the early 1970s. The magnetic confinement fusion approach for energy production has had the most emphasis, fidelity of analyses, and depth of developmental work; thus, this chapter will focus on that plan. The details of the two confinement systems will be significantly different as is the pulsed nature of the energy release for the inertial confinement. There are many areas of similarity in the materials, tritium breeding, heat removal, energy conversion, magnetic coils, shielding, and control systems.

There are significant challenges that need solutions to advance from the experimental phase into the demonstration phase and ultimately into the commercial realm:

- Tokamak experiments have generally operated in the pulsed mode for a few minutes, with a few existing experiments employing current drive systems to induce a short steady-state mode. A power plant must operate at steady-state and stable conditions for months at a time; thus, a reliable non-inductive current drive system must be developed and validated.

Nuclear Energy Encyclopedia: Science, Technology, and Applications, First Edition (Wiley Series On Energy).
Edited by Steven B. Krivit, Jay H. Lehr, and Thomas B. Kingery.

A steady-state tokamak power plant is essentially mandatory, because a pulsed facility would require a costly energy storage system. Also, all power core subsystems will be constantly cycled on and off (hot and cooler), which induces fatigue failures (implying lower reliability). An inertially confined fusion power plant intrinsically must be pulsed at a few cycles per second, so the inner power core sees distinct pulses of heat and neutrons while the heat removal and generating systems can operate at or near steady-state conditions.

- High energy discharges or plasma disruptions in tokamaks remain as an unsolved problem that can be quite damaging to the plasma-facing walls. Either the plasma must be more well-controlled or the plasma-facing components must be developed to be significantly more robust.
- The fusion fuel of choice has been, and will continue to be for the next several decades, deuterium (D) and tritium (T) as this fuel has the most favorable conditions for ignition. However fusing the D-T fuel creates a high energy alpha particle (3.5 MeV) and a highly energetic neutron (14.1 MeV). The alpha particle causes erosion of the divertor plates, and the high-energy neutrons cause transmutation and atom displacements in the power core materials. Thus, the innermost fusion power core components have a finite lifetime and must be replaced many times during the life of the plant. Access to the power core is very restrictive due to the surrounding power core components. The core environment is quite radioactive, which makes the maintenance of a fusion power core very difficult and time-consuming with fully robotic maintenance equipment. Long-duration maintenance times are acceptable for an experiment, but they are not acceptable for an operational power plant.
- The deuterium fuel is quite abundant, but tritium is naturally very scarce and must be bred within the power core to maintain a steady supply of fuel. Adding lithium or lithium compounds to the power core will create tritium when the energetic neutrons interact with the lithium atoms. Breeding-blankets containing lithium or lithium compounds are placed directly behind the first wall to provide a continuous supply of tritium. Tritium is an isotope of hydrogen that tends to diffuse everywhere, thus it is difficult to contain.

These are a few of the challenges that remain to be solved to achieve commercially viable fusion energy. Research and development are proceeding at differing levels in all of these areas, but all proposed solutions need to be analyzed as prototypes in relevant environments, upgraded to demonstration subsystems, and then validated for inclusion in an integrated prototypical demonstration power plant facility. This chapter will discuss the current status of the outstanding technical challenges and highlight a few of the proposed solutions.

33.2 FUSION POWER PLANT GOALS, REQUIREMENTS, AND TECHNICAL ENVIRONMENT

The ultimate goal of fusion research is to provide an abundant energy source with minimal resource limitations, safety issues, and environmental concerns. Fusion has the inherent capabilities to achieve these goals, providing certain technologies are developed and validated. These technologies have been on hold or funded at low levels pending solutions to plasma confinement and performance issues, which are nearing fruition. The intensity for development and validation will soon be shifting to the engineering technology aspects to achieve the required power plant goals (see Table 33.1).

These top-level goals and requirements, in turn, determine lower-level requirements and criteria that influence and establish the requirements for the fusion power core components, subsystems, and systems. The magnetically confined plasma must operate in a very clean and low-vacuum environment to create the necessary fusion conditions. Any minute amount of impurity, even air or water, will cause the plasma to immediately cease operation. This is a good attribute as this prevents any runaway condition and assures leak-tight containment of tritium. However, this means that the vacuum vessel, shown in Figure 33.1, of a

TABLE 33.1 Fusion Power Plant Top Level Requirements and Goals

- Competitive cost of electricity (or hydrogen or process heat)
  - Reasonable capital and operating costs
  - Efficient conversion and capture of alpha and neutron power
  - Competitive plant availability
  - High levels of reliability
  - Efficient remote maintenance
  - Highly efficient thermal conversion
  - Reasonable recirculating power
- No evacuation plan needed
- Generates no radioactive waste greater than Class C
- Workers are not exposed to a higher risk than other power plants
  - Efficient tritium and waste containment
  - Reliable remote maintenance
- Plants use an on-site closed fuel cycle

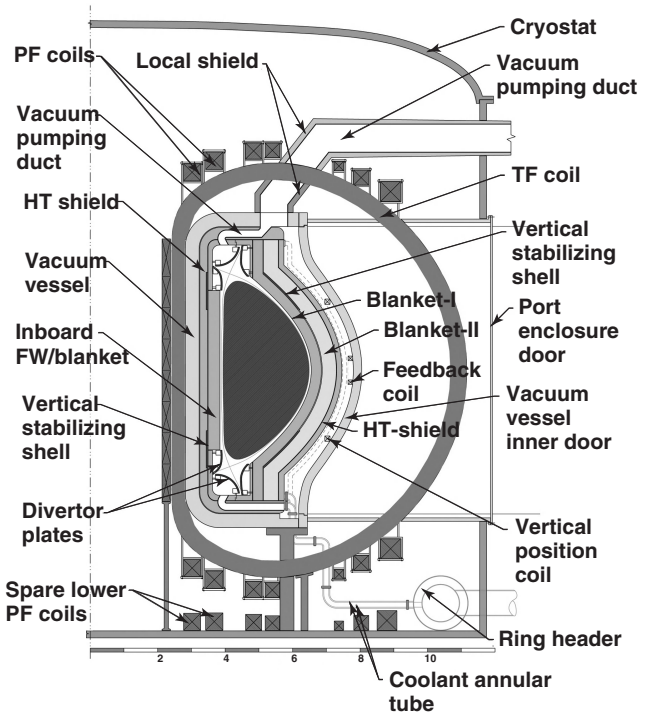

Figure 33.1 Typical cross section of a tokamak power core in a future power plant.

typical tokamak power core and all contained components must have very high vacuum and out-gassing requirements. Also, the alpha particle and neutron by-products of the D-T fusion process are life-limiting to the inner power core components. Yet to achieve the high availability requirement, these components, subsystems, and systems must be highly reliable and must be capable of being replaced very quickly and efficiently. Superconducting magnets must be used to achieve low recirculating power demands. These magnets must be highly reliable, life-of-plant components. Further, to achieve competitive electricity cost, the alpha particle and neutron capture elements of the blanket and divertor must operate at a high temperature that is suitable for very efficient thermal to electric conversion.

33.3 CROSS-CUTTING TECHNOLOGIES

Several technologies encompass all the power core systems and components, such as materials, neutronics, reliability, maintainability, safety, and economics.

Unique, high-purity, specialty, low-activation materials are required for components inside the fusion power core to limit the detrimental out-gassing that would poison the plasma, exhibit low activation to significantly reduce the neutron transmutation into high level radioactive waste, and decrease the susceptibility of materials to neutron damage (such as in displacements of atoms) and helium entrapment.

An early favorite structural material in the 1980s was 316-stainless steel, but it proved to swell rapidly under neutron irradiation and to have many constituents and trace elements that would transmute into high-level waste products. One current favorite structural material is ferritic-martensitic steel for moderate temperature blanket and divertor subsystems (up to 550°C for reduced activation ferritic steel [RAFS] or up to 650°C for oxide dispersion strengthened [ODS] steel containing oxide particles and the newer technology nano-sized particles). Small specimens of RAFS and ODS steels have been tested in fission test reactors to better predict their behavior in fusion plants. To achieve higher levels of energy conversion, the maximum temperature limits of the structures could be increased to ~1000°C by using silicon-carbide composites, SiC/SiC. There have been some encouraging test results for this innovative material, but more testing is required to qualify a SiC/SiC composite structural material for fusion applications.

Plasma facing materials, which may be armor on the first wall, divertor, or radio frequency launchers, must be designed to achieve the same lifetime as the underlying structure, yet they are subject to the most harsh fusion environment, intense radiation, streaming alpha particles, high-energy neutrons, and infrequent minor plasma disruptions or runaway electrons. At present, it is not considered feasible for the armored surfaces to withstand major disruptions without damage or failure. Present low-power experiments have employed beryllium or carbon tiles; however, as the power and the neutron fluence of the fusion devices are increased, both beryllium and carbon will be inadequate. Tungsten is now considered as a likely armor material for the most severe plasma-facing surfaces. It has a reasonably high thermal conductivity, so the challenge is to conduct the heat into the coolant with a sufficiently high thermal conductivity.

The proposed high-temperature heat transfer fluids (coolants), such as the current favorites of lithium lead eutectic ($Li_{15.7}Pb_{84.3}$) or high-pressure (8–10 MPa) helium, must be compatible with the blanket and divertor structural materials. The LiPb coolant has the added advantages of being a tritium breeding material (Li) and a safer material (lower chemical energy release) than pure lithium, but the lead content makes the coolant heavy, difficult to quickly flow in the piping, and an environmentally hazardous material. When the liquid metal coolants are drained from the blankets, the blankets are relatively light weight. Since LiPb is conductive and moving at a high velocity in a high magnetic field, this will increase the magneto-hydrodynamic drag on the coolant in the power core unless insulating sleeves or coatings are used inside the coolant passages. Helium coolant could be the primary blanket coolant as well as in the divertor. Designs for helium-cooled divertors have been proposed to handle the

high levels of heat flux (presently 10 MW/m^2) with some experimental confirmation. The helium pumping power can be prohibitively high if the internal fluid pressure drops are excessive with high flow rates.

Due to the intense neutron environment, the ability to predict the neutron interaction with the power core materials is essential. This branch of physical science is called neutronics, or more correctly, nucleonics. It calculates how the high-energy neutrons degrade the first wall and blanket structures, the effectiveness of tritium breeding materials, changes to the superconducting materials and insulators, the effectiveness of the shields, and the activation of the power core materials.

The degradation of the power-core materials severely limits the lifetime of the inner power-core components, which makes periodic maintenance mandatory. Moreover, the high levels of radiation within the power core require that the maintenance be accomplished with remote equipment. The complex geometry of the magnets and surrounding power core structures makes maintenance of the power core very complex. Existing experiments, including ITER [3, 4], use remote maintenance of moderately sized modules, 1 m by 1 m, with articulated booms through a few maintenance ports plus added support from temporarily deployed rails. This is suitable for experiments with a minimal availability factor, but the future power plant must have an availability in the range of 90%. This level of availability mandates that the only suitable maintenance approach is one of removing very large sections of the power core, preferably a sector associated with each toroidal field coil. The maintenance approach is so design-specific that it impacts all aspects of the power core, power-core building, and hot-cell design. Furthermore, the maintenance must be accomplished very quickly with high accuracy, which will likely mandate that the remote maintenance be accomplished with autonomous computer-guided robotic equipment.

The promise of fusion energy is to be a safe power producer for the workers and the general public. To achieve that goal, all the power-core and facility systems must be designed, evaluated, and validated to ensure that all safety requirements are met, such as containment of tritium, attenuation of the high-energy neutrons, minimization of chemical, thermal, and pressure energy release of blanket and coolant materials, and all other potentially hazardous conditions.

Economics is such a cross-cutting aspect that it touches all the power-core elements. The fusion components and systems are high-technology and high-cost items. The tokamak confinement concept favors large power cores and facilities, making it and most other magnetically confined fusion power plants capital intensive. The operational expenses should be relatively fixed and perhaps at a lower cost than competing technologies. The day-to-day maintenance actions are anticipated to be highly automated and autonomous with only a minimal staff required. The hot-cell refurbishment and disposal processes will require some human intervention, but most operations will be remote and autonomous. Fuel costs will be limited to deuterium and lithium (for tritium fuel generation). The cost of scheduled replaceable items is sizable but predictable.

33.4 FIRST-WALL TECHNOLOGY

In magnetically confined fusion devices, the intense magnetic fields contain the very low pressure, but very high temperature, plasma in a well-defined, three-dimensional geometry. In most current experiments and postulated power plant–relevant facilities, the outer edges of the high-temperature fusion plasma ($\sim$100 million$^\circ$C) are only a few centimeters away from the first solid surface, the first wall, which protects the power/fuel-producing blanket and is the largest plasma-facing component. The distance between the outer plasma boundary and the first wall is called the scrape-off layer. The current best candidates for underlying first-wall structural materials are ferritic steels or silicon carbide composites. The more near-term ferritic steels can either be RAFS or ODS. One, or a combination of these steels, will likely be the first-wall structure of the demonstration power plant. The silicon carbide composite (SiC/SiC) first-wall structure is a more advanced, higher capability option. This ceramic composite material allows higher operating temperatures, greater thermal conversion efficiency, and much less quantity of generated material waste. On the other hand, the SiC/SiC material is not yet well-developed and is presently very expensive.

Although the plasma does not physically touch the first wall during normal operation, the first wall is subject to intense thermal radiation from the high-temperature plasma and to the emitted high-energy neutrons. The very high-heat flux requires a highly capable heat transfer system to remove the surface heat, while the wall must operate at high temperature for efficient thermal conversion. The first choice for a coolant may be the liquid metals typically used for the blanket system, but these designs might not have enough heat transfer capability for this first-wall application. The most favored designs employ high-pressure helium, in the range of 8–10 MPa (80–100 atmospheres) pressure, and high flow rates to maintain a high temperature and high heat-transfer coefficient. The high energy neutrons impart more thermal energy throughout the volume of the first wall by interacting with the wall materials. However, since the first-wall structure is quite thin (3–4 cm), this volumetric heating in the wall is small in comparison to the radiative surface heating. The more difficult issue is that the high-energy neutrons cause atom displacements in the first-wall structural material, which continues to degrade the

material properties. This continued degradation establishes a finite lifetime for the first wall in the power core, after which the wall must be replaced. With the present first-wall material candidates, this lifetime is thought to be on the order of four to five years. Besides activating the main first-wall material components, neutrons can also interact with the atomic structure of the wall materials to create new elements and their isotopes, some of which can be radioactive. For this reason, the ferritic steels and SiC/SiC composites are carefully selected to minimize creation of the highly radioactive isotopes. Moreover, these radioisotopes will limit the material composition by minimizing any alloying elements that will increase the unwanted radioactivity; hence the name "reduced activation." Significant developmental efforts will be necessary to select, test, and verify these first-wall materials in power-plant-relevant environments.

The current thinking is that the candidate first-wall materials may not be sufficiently robust to handle the intense heating and occasional bursts of particle flux to last the required operational time. To have additional design margin, a thin layer of tungsten is being considered as an armor material because it is more robust against high heat and particle sputtering. To accommodate the sizable differential thermal expansion, the tungsten coating will probably be segmented. It will have to be brazed or mechanically attached to the basic first wall to ensure adequate thermal heat conduction.

In addition to the normal operational environmental requirements for the first wall discussed above, there may be off-normal plasma events that impose short-term, intense local discharges of the plasma energy in the form of electrons and protons. One of these discharges is the edge-localized modes (ELMs) due to instabilities in plasma confinement that release bursts of energy and particles impacting the first wall. The plasma can also be displaced, typically vertically, and contact the wall if the magnetic confinement is compromised. These energetic disturbances have frequently occurred in the past on tokamak experiments; however, there are developmental efforts directed toward the control, mitigation, and elimination of these damaging effects on future demonstration and power plants. The intent is to either mitigate the cause or effects of these off-normal events so that the normal operational lifetime is not compromised.

33.5 BLANKET TECHNOLOGY

Behind the first wall is the power- and fuel-producing component called a breeding blanket. The "blanket" name has been adopted to signify that the plasma is almost fully enveloped in a blanketing component. In the early and some present day fusion experiments such as ITER [2], the blankets were only shielding blankets in the sense that they captured the plasma thermal and neutron energy, but did not have any tritium breeding function. In the earlier and present fusion experiments, most experiments were conducted only with hydrogen and deuterium. For the few experiments fueled with D-T, sufficient tritium fuel could be externally supplied for the limited duty cycle operation. As the duty cycle and the power level on future fusion facilities, such as component test facilities and demonstration plants, increases, there will be a need to provide a substantial, steady-state supply of tritium. This requires the blanket to be tritium breeding containing either lithium or a lithium compound.

A breeding blanket has two primary functions—breed tritium and capture the thermal energy of the high-energy neutrons. A secondary function is to support the first wall. As the second radial component from the plasma, it also serves a shielding function by capturing many of the neutrons, thus protecting the outer power core components. The blanket materials must be selected to generate tritium as well as to slow down and thermalize the high-energy neutrons. As discussed in the first wall section, the blanket must be maintained at a high temperature by circulating a high-temperature coolant to remove the thermal energy of the neutrons. The high-temperature and high-energy neutron environment imposes extraordinary requirements on the structural materials. Like the first wall, both ferritic steels and SiC/SiC composites are favored structural materials.

As the ideas and concepts for breeding blankets have been developing and are being tested, two classes of breeding blankets have evolved—solid and liquid breeding blankets.

The solid breeding blankets employ solid pellets or pebbles of lithium ceramic compounds, typically Li_4SiO_4, Li_2TiO_3, or Li_2ZrO_3. Due to the low breeding capacity of solid breeders, this class of breeders usually requires neutron-multiplying materials, such as Be and $Be_{12}Ti$. The thermal energy from neutrons and gamma rays is extracted by forcing high-pressure helium through multiple layers of pebbles and multipliers and through cooling channels in the structure. A technical concern is the ability to effectively conduct the heat away from the pebbles, multipliers, and structure with helium or water while not inducing too much parasitic drag and pumping power losses. Care must be taken in the design of the blankets to make sure there is sufficient tritium being bred because the tritium breeding ratio needs to be sufficiently above unity to serve as a design margin. This is especially important in solid breeders with a beryllium neutron multiplier. The lithium used in the solid breeder blanket probably needs to be enriched (increased content of Li6) from the natural state of 92.5% of Li7 and 7.5% of Li6. Lithium-7 can breed tritium in

an endothermic reaction (consuming 2.467 MeV), which detracts from the useful energy within the blanket. On the other hand, lithium-6 can breed tritium with neutrons of any energy level in an exothermic reaction that yields an increased energy of 4.78 MeV. Enriched lithium will be expensive for higher percentages of Li6. The cost of enriched lithium is speculative as there are presently no commercial processes or sources to supply large amounts of enriched lithium for demonstration or commercial fusion power plants.

The liquid metal breeding blankets can use either natural lithium, lithium alloys (e.g., the molten salt LiF-BeF2 called FLiBe) or eutectic of lithium and lead ($Li_{15.7}Pb_{84.3}$). The beryllium and lead serve as neutron multipliers. If lead is used as a constituent, the lithium probably will be enriched with higher levels of lithium-6. Designs must also be tailored to provide adequate tritium breeding (TBR$>$1 + some design margin [5]). Structural materials can either be ferritic steels or SiC/SiC composites. Presently, there are two approaches to liquid metal blankets—one is a self-cooled blanket only using a liquid metal as the cooling media, and the second is a dual coolant blanket only using a slower-moving liquid metal in the large blanket chambers and a higher velocity and pressure helium to cool the blanket structures. To efficiently remove the thermal energy in self-cooled blankets without overheating the structure, the lithium liquid must have relatively high velocities through the internal passages. Since the lithium fluids are conductive and in the presence of high magnetic fields, large magneto-hydrodynamic Lorentz forces occur within the liquid metal flows that are significantly higher than inertial and viscous forces. This effect can be mitigated with electrical/thermal insulating sleeves that are near, but not necessarily attached to, any conductive coolant channel walls. In the dual-cooled blankets, the liquid metal moves slower and the heat-transfer coefficient is not sufficient to adequately cool the structure, so a separate helium cooling circuit is provided for passages within the structural walls. The slower liquid metal flow rate allows the volumetric heating to increase the central region of the coolant flow above the temperature of the structural walls and adjacent coolant. This arrangement allows a slightly higher coolant exit temperature than the structural material temperature limit.

Recent plasma physics and coil engineering findings indicate the need to have an active or passive conductive vertical stabilizing coil (or shell) within the blanket region to provide enhanced plasma stability. There also might be a conducting shell to provide feedback for a resistive wall mode. The material probably will be tungsten for radiative cooling. The placement of the coil or shell may be at the front of the blanket, in the middle, or behind the blanket, depending on the blanket configuration and the ability to achieve an adequate tritium breeding ratio.

The present thinking is that the first wall and blanket are physically connected together, and this integrated assembly is a replaceable module. To enhance the plant availability, the operational lifetime of these combined assemblies should be a long as possible. The current projected lifetime is in the order of four to five years.

To maximize the plant availability, the reliability of the blanket (and all other subsystems) must be improved with reliability-enhancing design and material improvements supplemented with validating testing programs.

33.6 MAINTENANCE TECHNOLOGY

One of the primary requirements for a successful power plant is to achieve a competitive cost of electricity. There are many factors that influence the cost of electricity, and plant availability is one of the most influential. Extending the operation lifetime and improving the reliability of the replaceable components, discussed in prior sections, will directly enhance the plant availability. Another availability enhancement is the capability to remove and replace the life-limited internal power core components as quickly as possible. One approach is to reduce the number of first-wall/blanket modules in the power core to speed the maintenance actions and increase the plant availability. For power-plant-relevant maintenance, the concept of smaller module replacement with robotic arms and manipulators is being superseded by removing much larger modules or even whole sectors equated with the number of toroidal field coils. Whole sectors can be removed and moved to a hot cell for refurbishment, and previously refurbished sectors can be reinstalled in a shorter time period with higher quality assurance. Since the neutron damage to the blanket is a decreasing function of the radial distance from the first wall, blanket designers have begun to create two distinct blanket zones. The innermost blanket region is life-limited, which will be replaced several times over the life of the power core. The outer blanket region has a lower neutron flux resulting in an extended lifetime, while still efficiently capturing the neutron energy and generating tritium.

The first-wall/blanket modules are designed to preclude any neutron-streaming pathways, such as radial helium passages or assembly gaps between modules. Coolant manifolds for the first-wall/blanket structure and breeding media are usually at the rear of the modules. The first-wall/blanket modules are attached to the next component, the shielding. The gravity loads of the internal components are then supported by the floor of the vacuum vessel. The maintenance concept is to remove and replace all life-limited components on a regular basis inside the vacuum vessel. Furthermore, it is possible that any power-core component might need to be repaired or replaced sometime in the

plant's lifetime. Thus, remote assembly and maintenance of all power-core components is a mandatory requirement.

33.7 DIVERTOR TECHNOLOGY

The divertor is a plasma-facing subsystem, like the first wall. However, the divertor has a specialized function to intercept the energetic plasma particles of electrons, protons, alpha particles (fusion ash), and other trace impurity elements that are swept out along the magnetic field lines at the plasma magnetic X-point(s). The magnetic geometry of tokamaks can have one or two regions where the confining magnetic fields cross, allowing the energetic particles to escape. Like the first wall, tungsten armor will be required to provide adequate component lifetime. It is highly desired for the divertor lifetime to be (nearly) the same as the first wall and blanket so both subsystems can be removed and replaced at the same time. Thus, the divertor armor must be much more robust than the first-wall armor.

The divertor modules are located at the bottom (for the single-null divertor) or at the top and bottom (for the double-null divertor) of the power core. The double-null geometry is more favored for the higher-power and longer-duration fusion plants because of the increased area for interception of the particle and heat flux. From a geometry standpoint, the double-null configuration has vertical mirror-symmetry that offers more duplication of power-core components and modules.

The nominal, steady-state heat flux design requirement for double-null divertors is presently around 10 MW/m^2, which is a very challenging goal. Some proposed divertor designs have been shown to analytically and experimentally meet this goal by using high-pressure helium jet impingement, small passages, and high velocities inside tubes and fingers to achieve necessarily high heat-transfer coefficients. But the fabrication of the high-tolerance parts and small unit sizes are not conducive to high reliability at a reasonable cost with the high number of individual elements necessary for the large divertor surface area in the power core. Studies are being conducted to achieve the same performance using more fabrication-friendly designs and higher-reliability approaches. Some divertor designs with lower heat flux requirements use liquid metals to cool the divertor. The helium-cooled divertors usually incorporate tungsten as the structural material with ferritic steel as the manifolds and shielding. The liquid metal-cooled divertors are postulated to use SiC/SiC with tungsten protective armor. The steady-state peak heating design requirements are still being formulated, but it is likely that regions of the divertor will see peak heating in excess of the steady-state nominal requirements. Short-term transient peak heating must also be addressed.

The divertor region has a reduced neutron wall loading as compared to the first-wall regions. Thus, it is not as imperative to have tritium breeding in the divertor region. The divertor subsystems in current conceptual design studies operate at high temperature and contribute their captured energy to the power cycle.

33.8 SHIELDING TECHNOLOGY

Located immediately radially outward from the plasma and behind the blanket and divertor is the shield subsystem. The first wall, blanket, and divertor intercept and capture much of the high-energy neutrons depositing their energy; however, a significant fraction of that energy ($\sim$10%) will pass through those subsystems and into the shield. The requirement for the shield is to provide adequate radiation protection for all the further outboard components as well as workers, the public, and the environment. The superconducting coils are quite susceptible to radiation damage so these are critical components to be shielded.

In the previous and current fusion experimental facilities, including ITER [2], there was no breeding blanket, but these designs usually had a shielding blanket. In the early fusion conceptual power-plant designs studies, there was a breeding blanket subsystem with a low-temperature shield. All the energy collected in the shield was either discarded or used for feedwater heating. More recent fusion power-plant studies have concluded there was sufficient neutron energy escaping through the blanket and divertor subsystems that a part or all of the shield subsystem could be operated at high temperature and supply the thermal energy conversion system with high-quality heat. The coolant would probably be the same as the blanket coolant [6]. The presently favored material for the shielding function is borated ferritic steel. Alternatively, tungsten carbide (WC) could be substituted, which would reduce the shield thickness. However, the use of WC would significantly increase the decay heat and temperatures during a loss-of-coolant accident. The structural material could be ferritic steel or SiC/SiC. The high temperature shield is a stand-alone component that also serves as the structural backbone of the power core sector that is removed in the sector replacement scheme. This high-temperature structural element supports the first wall, blanket, divertor, and all related plumbing and manifolds as a single replaceable unit. Most of the shield and the structural unit will be designed as life-of-plant components. In the hot cell, new replaceable modules would be installed on the removed shield/structure to form a refurbished sector awaiting installation into the power core.

In some instances, a second shielding component would be located immediately outside the high temperature shield, cooled with low temperature water. This low-temperature

shield would be attached to or integrated with the vacuum vessel.

There are many penetrations in the power core, and most of these penetrations will need to be cooled with helium or water. Typical penetrations are the vacuum vessel maintenance ports, vacuum pumping ports, and plasma fueling and heating ports. These penetrations are surrounded with local shields to protect the magnets and externals.

33.9 VACUUM VESSEL TECHNOLOGY

The vacuum vessel is an important subsystem that provides vacuum integrity for the plasma core and supports and aligns the power-core components. It acts as a heat sink in case of an accident and provides maintenance access to the core components. In all power-core designs, it also provides a shielding function. The base vacuum requirement would be on the order of 1.3×10^{-6} Pa or 10^{-8} torr. The vessel design is quite specific to the plasma and power core arrangement. The vessel is a low-temperature and low-technology subsystem that can be built with conventional fabrication processes. It is probably a double-walled vessel of ferritic steel that is cooled with water. To provide additional shielding protection for the superconducting coils to the level of 10^{19} n/cm^2 ($E_n > 0.1$ MeV) over the lifetime of the plant, spheres of tungsten carbide or borated ferritic steel are added between the walls of the vessel. The tungsten carbide option can provide thinner walls on the inboard regions to help shrink the plasma major radius and reduce the overall power-core cost. The vacuum vessel could either completely enclose the toroidal field and poloidal field coils, which would result in a very large vacuum vessel, or it could closely enclose the shield with the toroidal field and poloidal field coils outside the vessel. The latter approach represents the minimal volume and cost, minimal vacuum pumping requirements, and most direct structural support approach.

The maintenance approach will have a significant effect on the design of the maintenance ports. If the smaller modular approach is adopted, fewer and smaller maintenance ports will be required in the vacuum vessel for articulated maintenance booms. The favored European Union (EU) approach is to remove a larger grouping of blanket modules vertically through two or more large maintenance ports in the upper part of the single-null power core and to use ports at the bottom to remove the lower single-null divertor. The U.S. and Japanese approach is to remove complete blanket, divertor, and shield sectors through large maintenance ports between each toroidal field coil. In each design approach, the vacuum vessel is sealed with an inner vacuum vessel door. Vacuum maintenance port enclosures are provided to remove the modules or sectors without spreading contamination. Outer vacuum doors on the ducts are provided for added vacuum integrity during operation.

33.10 VACUUM PUMPING TECHNOLOGY

It is necessary to create an ultra-high vacuum inside the power core, on the order of 1.3×10^{-6} Pa or 10^{-8} torr, before introducing the fuel components in order to maintain a low level of plasma impurities. As the plasma is operating at steady-state, the typical pumping speed is around 175 m^3/s for a typical 1750 MW fusion power plasma. These vacuum requirements can be satisfied by the use of a combination of existing technology roughing and compound cryopumps, which use cryocondensation for hydrogen isotopes and cryosorption for helium. The nominal arrangement is to have these pumps connected to the main plasma chamber with a vacuum duct for each sector. The likely arrangement would be to have at least two cryogenic pumps at each duct, in order to have one operational while the other is being regenerated or replaced.

33.11 COIL TECHNOLOGY

One key enabling system for the magnetically confined tokamak fusion plasmas is the magnetic coil system. The most prominent is the toroidal field (TF) coils that create the strong toroidal magnetic fields with modified D-shaped coils that envelope the plasma-core elements. In the sector-maintained tokamaks, the D-shaped coils are enlarged sufficiently to allow room for maintenance ports to remove the power core sectors. The poloidal field (PF) coils are located (1) inboard of the toroidal field coils to inductively initiate the plasma and (2) outboard of the toroidal field coils to shape the plasma. Ideally, the inboard and outboard coils would be continuous conducting shells, but fabrication issues and maintenance access suggest the use of discrete coils. The location of the maintenance and other necessary ports dictate areas where the poloidal field coils may need to be relocated. Recent plasma confinement studies have indicated the need for additional plasma control coils directly outside the shield and within the vacuum vessel. Some of these can be passive while others need to be active, feedback-controlled coils. These control coils are normally conductive coils and operate in the 200–300°C temperature range.

In smaller magnetically confined fusion experiments, the toroidal field and poloidal field coils were reasonably low-current, normally conductive coils. As the plasma size, power, and duty factor increased, the coil currents became very large, and the resistive power losses with normally conducting coils were no longer tolerable. The

larger coils for power plants employ low-temperature superconductive conductors to reduce the coil power. For fields up to 8–10 Tesla (T), niobium-titanium (NbTi) superconducting conductors are favored because they are ductile and easily fabricated to shape at a reasonable cost. For magnetic field levels in the range of 11–16 T, niobium-tin (Nb_3Sn) is more suitable superconductor material; however, this conductor is more brittle and must be formed in-situ to its final size before a reactive heat treatment. Niobium-aluminum (Nb_3Al) offers slightly higher fields, but has been proposed only for a few conceptual designs. For higher fields up to 25–30 T, high-temperature superconductors (HTS) are being proposed, but they are not yet commercially available in large quantities at a reasonable cost. The best known high-temperature ($30-70^{\circ}K$) superconductors are bismuth strontium calcium copper oxide (BSCCO) and yttrium barium copper oxide (YBCO).

The typical design for the toroidal field and poloidal field superconducting coils is to have the conductor cooled with integral cooling channels. These conductors are separated with insulating layers and encased in a structural case to withstand the electromagnetic forces. There is a bucking cylinder inboard of the toroidal field coils to counteract the inward coil forces. There are additional toroidal field support structures, usually at the top and bottom of the toroidal field coils, to withstand normal and abnormal overturning moments.

33.12 PLASMA FORMULATION AND SUSTAINMENT TECHNOLOGY

The solenoidal coils inductively help create the initial toroidal current within the plasma, but additional subsystems are needed to ionize and heat the plasma to critical conditions before it can be self-sustaining. The transformer action of the solenoidal coils has a limited capability that must be supplemented by a current drive system to maintain the steady-state operation of the plasma for an extended duration. For power-plant applications, these startup and heating/current drive subsystems are various radio frequency systems, such as ion cyclotron resonance frequency fast wave, lower hybrid wave, and electron cyclotron resonance frequency. These radio frequency subsystems are efficient, well coupled to the plasma, and require only small openings in the first wall and power core. Heating and current drive are essential for ITER to reach its intended goals. ITER [7] will be using a combined power level of 73MW with electron cyclotron (EC), ion cyclotron (IC), heating-neutral beam (H-NB), and possibly lower hybrid (LH) subsystems for heating and current drive. This experiment will be the most relevant demonstration of these technologies to date for future power-plant applications.

Neutral-beam technology has been employed as a current drive system in some experiments, but large openings in the first wall and straight beam-lines through the power core are required. This decreases the first-wall surface area for power and tritium production and creates line-of-sight channels promoting detrimental neutron streaming. Neutral beams are not currently viewed as applicable to power plant facilities.

Stability control subsystems are likely to be needed to provide adequate robust control of the plasma. These subsystems are just being designed and will likely be an application for RF technology.

This category of plasma sustainment will also include the plasma fueling and component control. It will likely be accomplished by particle injection or gas puffing to inject the fuel or impurity mixture into the plasma in the appropriate location. This component may also be used to rapidly terminate the plasma when necessary.

These radio frequency and neutral-beam technologies are reasonably available for future fusion applications as most or all have been utilized on prior or existing experiments. Certainly, there will have to be some scale-up on power level. The launcher components will have to be customized for each application, requiring some design and development effort. The prototypes will have to be validated in relevant environments.

33.13 OTHER FUSION TECHNOLOGIES

Supportive to the above fusion subsystems, there are several other subsystems that are very necessary for the integrated fusion power plant. These include the main heat transfer and transport, radioactive materials treatment and management, fuel handling and storage, autonomous remote maintenance equipment, and instrumentation and control. All of these technologies are reasonably available with substantial experience databases. Certainly, there will be an extension of certain capabilities to satisfy the fusion plant requirements, but these are reasonable extrapolations. Some developmental work will be required, and prototypes will have to be verified in relevant fusion environments.

33.14 SUMMARY

Fusion may soon move from the experimental era of fusion science into that of fusion energy. ITER will be the largest tokamak experiment and will demonstrate a significant gain in energy, $Q \geq 10$, with an ignited D-T plasma, perhaps as soon as 2018. It, and prior fusion experiments, will have demonstrated some of the key principles and technologies necessary to achieve fusion ignition for short periods of time. However, in the beginning era of fusion

energy development, those demonstrated technologies must be enhanced and matured to create a more powerful, robust, reliable, maintainable, and affordable energy source. Technologies in this class are magnetic coils, shielding, heating, and current drive. These enhanced technologies will have to be incorporated into power-plant-ready, validated subsystems.

There is another class of fusion technologies that has not been demonstrated to any great degree in the relevant environment, i.e., the first wall, breeding blankets, divertors, and instrumentation (diagnostics). In the prior existing and planned fusion experiments, there have been some preparatory or lower capability technologies employed, but they have not yet demonstrated the necessary capabilities for fusion energy subsystems in terms of neutron flux and operating time. This will require design, development, and rigorous testing in relevant environments to validate the subsystems for use in demonstration and power-plant applications.

A third class of fusion technologies are those that currently are readily available as commercial technologies, such as vacuum vessels, vacuum pumping, fueling, heat transport, instrumentation and controls, radioactive waste processing, and remote handling. These available technologies will be integrated into the evolving fusion power-plant design and validated for use in the relevant environment.

In the cross-cutting technologies, fusion power-plant-relevant materials are the key to obtaining fully capable first walls, blankets, and divertors. Without a validated materials database, these subsystems cannot be employed. The full understanding of the materials and the power-core components cannot be developed to the level necessary without a higher level of understanding of fusion neutronics. The advent of 3-D neutronics is a significant improvement, but additional research and more complete databases are needed to enable the needed material and design advances. Fusion experiments can achieve their goals with a limited duty cycle (low availability), but the competitive power-plant environment mandates the need to achieve plant availabilities in excess of 90%, even for the first of a kind fusion power plant. This stringent requirement emphasizes the need to have components and subsystems with very high levels of reliability and maintainability. Prior examples of high reliability in other scientific fields have been achieved with rigorous quality assurance, testing, and validation programs, but these approaches have proven to be too expensive. New reliability enhancement programs must be employed to achieve the necessary program goals. Maintainability goals can be achieved when maintainability is integrated into the facility design at the early design stages and high-fidelity modeling and simulation are employed.

REFERENCES

1. The National Ignition Facility Project: https://lasers.llnl.gov/.
2. The ITER Project: *http://www.iter.org/.*
3. T. Ihli, D. Nagy, C. Koehly, and J. Rey, High availability remote maintenance approach for the European DEMO breeder blanket options. *Proceedings of the 21st IAEA Fusion Energy Conference*, Chengdu, China, October 16-22, 2006, International Atomic Energy Agency, http://www-naweb.iaea.org/napc/physics/fec/fec2006/html/node295.htm#58758, 2006, FT/P5-11 [proceedings not published in paper form, only in HTML on web].
4. T. Ihli, L. Boccaccini, G. Janeschitz, C. Koehly, D. Maisonnier, D. Nagy, C. Polixa, J. Rey, and P. Sardain, Recent progress in DEMO, fusion core engineering: improved segmentation, maintenance and blanket concepts. *Fus. Eng. Des.*, 2007, **82**, 2705–2712.
5. L. A. El-Guebaly and S. Malang, Toward the ultimate goal of tritium self-sufficiency: technical issues and requirements imposed on ARIES advanced fusion power plants. *Fus. Eng. Des.*, December 2009, **84**, 2072–2083.
6. L. A. El-Guebaly, Nuclear performance assessment of ARIES-AT. *Fus. Eng. Des.*, January 2009, **80**, 99–110.
7. J. Jacquinot, F. Albajar, B. Beaumont, A. Becoulet, T. Bonicelli, D. Bora, D. Campbell, A. Chakraborty, C. Darbos, H. Decamps, G. Denisov, R. Goulding, J. Graceffa, T. Gassmann, R. Hemsworth, M. Henderson, G. T. Hoang, T. Inoue, N. Kobayashi, P. U. Lamalle, A. Mukherjee, M. Nightingale, D. Rasmussen, S. L. Rao, G. Saibene, K. Sakamoto, R. Sartori, B. Schunke, P. Sonato, D. Swain, K. Takahashi, M. Tanaka, A. Tanga, and K. Watanabe, Progress on the heating and current drive systems for ITER. *Fus. Eng. Des.*, 2009, **84**, 125–130.

34

ITER—AN ESSENTIAL AND CHALLENGING STEP TO FUSION ENERGY

CHARLES C. BAKER

Sandia National Laboratories, Albuquerque, NM, USA

ITER will be the world's first power-plant scale fusion experiment aimed at providing the basis for the demonstration of the scientific and technological feasibility of fusion power for peaceful purposes. As such, it is the critical step from today's magnetic fusion experiments to possible future fusion energy demonstration power plants.

The ITER device is a large toroidal or donut-shaped machine based on the tokamak concept first developed by the Russians in the 1950s and 1960s. This device employs magnetic fields to confine a very high-temperature gas, called a plasma, with temperatures in excess of a hundred million degrees. The magnetic fields are created for the most part by using superconducting magnets. The ITER tokamak is shown in Figure 34.1. The size of the device can be appreciated by noting the small human figure in the lower right of the figure.

34.1 ITER TECHNICAL OBJECTIVES

The fuel in the plasma will be a mixture of deuterium and tritium (D-T), two isotopes of hydrogen, yielding typically fusion power outputs of 500 MW. ITER will achieve this level of plasma performance with most of the energy to sustain the plasma for long periods coming from fusion reactions within the plasma, i.e., a self-heating fusion energy system. The relevant figure of merit is the fusion power amplification factor, Q, which is the ratio of the fusion power created to the power needed to sustain the plasma. Commercial fusion power plants will need Q values of 20 to 30. The technical objectives of ITER are to achieve a Q of at least 10 for 300 to 500 seconds and to demonstrate steady-state operation with a Q of at least 5 for pulse lengths of several thousand seconds. These have been the principal goals of fusion research for over 50 years.

In addition, ITER will incorporate many of the technologies required for fusion demonstration reactors and will also test materials and tritium breeding blankets required for such reactors. To carry out nuclear and high-heat flux component testing relevant to a future fusion reactor, the engineering requirements are an average neutron flux $\geq$ 0.5 MW/m^2 and an average neutron fluence $\geq$0.3 MWa/m^2. These neutron fluxes and fluences are not able to fully test the materials and components needed for a fusion demonstration power plant.

ITER is being designed to achieve a duty factor (duty factor is the ratio of the plasma burn duration to total pulse length) of about 25% for operation in long pulse inductive and non-inductive modes. In the final part of the 20-year operation, ITER will also be required to operate at very high availability for periods lasting one to two weeks. The goals for ITER for the pulse lengths, duty cycles, and availabilities are a very large extrapolation from current experience and place a large demand on design integration, component reliability, and maintenance procedures. However, the data derived from ITER on these issues are essential to realizing practical fusion power plants.

Nuclear Energy Encyclopedia: Science, Technology, and Applications, First Edition (Wiley Series On Energy).
Edited by Steven B. Krivit, Jay H. Lehr, and Thomas B. Kingery.

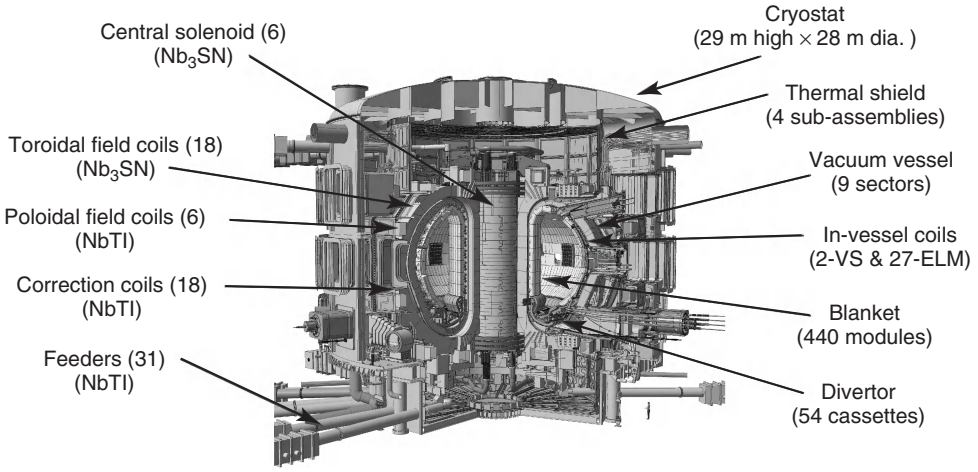

Figure 34.1 The ITER tokamak (Courtesy of the ITER Organization).

34.2 ITER RESEARCH PROGRAM

ITER's research phase is expected to last about 20 years. The ITER operation will be divided into four phases. Before achieving full deuterium-tritium (D-T) operation, which itself is split into two phases, ITER is expected to go through two operation phases, a hydrogen/helium phase, and a deuterium phase for commissioning of the entire plant.

The hydrogen/helium phase is a non-nuclear phase, mainly planned for full commissioning of the tokamak system in a non-nuclear environment where full remote handling is not required. In the deuterium phase, while the fusion power is low, the activation level inside the vacuum vessel will not allow human access after several hundred seconds of deuterium plasma operation. Many plasma operational and control techniques that are necessary to achieve the technical goals of the D-T phase will have been demonstrated in these first two phases.

D-T operation will be divided into two phases, oriented predominantly toward physics and engineering goals, respectively. During the first DT phase, the fusion power and burn-pulse length will be gradually increased until the inductive operational goal of $Q = 10$ at several hundred MW for several hundred seconds is reached. Non-inductive, steady-state operation will also be developed. The power reactor-relevant test blanket modules will be tested whenever significant neutron fluxes are available. The second phase of full DT operation will emphasize improvement of the overall performance and the testing of components and materials to higher neutron fluences. This phase should address the issues of higher availability of operation and further improved modes of plasma operation.

A typical experimental sequence would begin by introducing the fuel into the vacuum vessel chamber by a gas injection system. The gas would be ionized, and then the plasma would progress from a near-circular configuration to an elongated divertor configuration as the plasma current is ramped up. A divertor causes some of the magnetic flux lines on the outside of the plasma to be directed to a chamber where heat and particles escaping from the plasma can be collected and removed.

An elongated shape results in improved plasma performance, especially the ability to achieve higher plasma pressures. As the current develops (nominally up to 15 MA), subsequent plasma fueling (gas or pellets) and additional heating leads to a controlled high-energy gain burn with a fusion power of about 500 MW with the injection of about 50 MW of auxiliary power.

By maintaining the plasma current with energy and momentum input from the plasma heating systems, it is envisaged that the burn duration will ultimately be extended toward 3,000 seconds. This phase is followed by plasma current ramp-down and finally by plasma termination. When the plasma current is driven by magnetic induction, the nominal burn duration is 300 to 500 seconds, with a pulse repetition period as short as 1,800 seconds.

ITER will have extensive plasma and engineering diagnostic systems for its research program. These systems provide information on plasma behavior and performance; plasma burn dynamics, including behavior of alpha particles produced by DT reactions; machine protection and basic machine control; advanced plasma control; plasma-wall interactions; and many others. Examples of plasma diagnostics include magnetic measurements embedded in the in-vessel components, measurements of neutrons and fusion products, optical systems such as Thomson scattering, spectroscopic instruments, neutral particle analyzers, and microwave diagnostics.

Testing tritium-breeding blankets is also a critical element of the ITER mission. Mock-ups of tritium breeding blankets for demonstration fusion power plants, called Test

Blanket Modules, will be inserted and tested in ITER in dedicated equatorial ports directly facing the plasma. ITER will provide the first experimental answers on the performance of the breeding blankets, a vital issue on the path to fusion power.

With these capabilities and a comprehensive research program, ITER will allow for the exploration of the science relevant to magnetic confinement fusion power, as well as testing some of the key technologies for future power plants.

34.3 A FULLY INTERNATONAL PROJECT

ITER is perhaps the most ambitious international science research project ever undertaken. It has been fully international since its inception, beginning with a conceptual design phase in the late 1980s, proceeding to an engineering design and research and development (R&D) phase in the 1990s, to today's construction phase. ITER is projected to make its first plasma in late 2019 and to begin its full DT experiments in 2026/2027.

Today seven governments or members, representing most of the world's population, are participating in ITER—China, European Union, India, Japan, South Korea, Russian Federation, and the United States. A Council made up of representative of the seven ITER members governs ITER. A Director General appointed by the ITER Council leads the ITER Project. The resources for constructing ITER are made up of in-kind contributions (mainly components and subsystems) from each of the members and an International Organization (IO) headed by the Director General that is responsible for design integration and overall management of the construction of ITER. ITER is being built at Cadarache, France, about an hour north of Marseilles. The ITER IO is headquartered at this site. In addition, each member has established a Domestic Agency (DA) to manage its contributions to ITER. Together, the IO and seven DAs make up the day-to-day management team for ITER.

34.4 DESIGN OF THE ITER DEVICE AND SYSTEMS

The ITER design is based on scientific data and experience derived from the operation of the many tokamaks and from fusion technology R&D programs around the world. It is designed as an experimental device with extensive diagnostics and considerable flexibility in shaping, heating, current drive, and fueling methods. It is also possible to change the first-wall and divertor materials. This flexibility is essential for accommodating uncertainty in physics projections, for exploring new operating regimes for an attractive fusion power plant, and for investigating new aspects of plasma physics that may arise from significant alpha particle heating, large size, and extended burn. The design underwent a major international design review from 2006 to 2008.

In order to achieve the desired level of plasma performance, especially the value of Q and total fusion power, the device must have sufficient size, magnetic field strength, and toroidal plasma current. The main machine parameters are summarized in Table 34.1.

The major components of the tokamak shown in Figure 34.1 are the coils that magnetically confine, shape, and control the plasma and a toroidal vacuum vessel and its internal components. The total weight of these systems is about 24,000 metric tons.

Inside the vacuum vessel, the internal, replaceable components include blanket modules, divertor cassettes with high-heat-flux components, radio frequency heating antennas, test blanket modules, and diagnostic modules. These components absorb the radiated heat as well as most of the neutrons from the plasma and protect the vessel and magnet coils from excessive nuclear radiation. The heat deposited in the internal components and in the vessel is removed by the tokamak cooling water system. The entire tokamak is enclosed in a cryostat, with thermal shields between the hot components and the cryogenically cooled magnets.

The magnet system consists of 18 toroidal field (TF) coils, a central solenoid (CS), six poloidal field (PF) coils, and 18 correction coils (CC). The 18 TF coils determine the basic toroidal segmentation of the machine and were chosen to meet the requirements of access ports (both number and size) and the magnetic ripple at the plasma edge. The CS coil is made of six modules and serves as the primary of a transformer with the large toroidal plasma current being the secondary "winding" of the transformer. In this way, the plasma current is formed and sustained for moderate pulse lengths by magnetic induction.

The TF, CS, and PF coils are superconducting coils cooled with supercritical helium at 4.2–4.5°K. The TF and CS coils operate at high peak magnetic fields, 11.8T and 13.0T respectively, and therefore are made of Nb_3Sn

TABLE 34.1 Main Parameters of ITER

Total fusion power	500 MW
Additional heating power	50 MW
Q-fusion power/additional heating power	$\geq$10
Average 14 MeV neutron wall loading	$\geq$0.5 MW/m^2
Plasma inductive burn time	300-500 s
Plasma major radius (R)	6.2 m
Plasma minor radius (a)	2.0 m
Plasma current (I_p)	15 MA
Toroidal field at 6.2 m radius (B_T)	5.3 T

cable-in-conduit superconductors with currents of 68 kA and 40–55 kA, respectively. The PF and CC coils operate at lower magnetic fields and are made of NbTi superconductors. The large TF coil has a stored energy of about 40 GJ. The entire magnet set weighs about 10,000 metric tons.

The vacuum vessel (VV) is a torus-shaped, double-wall structure with in-wall shielding and cooling water between the shells. The vacuum vessel design is an all-welded structure in which the inner shell serves as the first confinement barrier. The VV is divided into nine toroidal sectors joined by field welding. At the upper level, there are 18 ports of a similar design. At the equatorial level, there are 14 regular equatorial ports and three ports for injection of the neutral beams. At the lower level, there are five ports for divertor cassette replacement and/or diagnostics, and four ports for vacuum pumping.

A copper-conductor, water-cooled coil system, which consists of a resonant magnetic perturbation (RMP) coil system and a vertical stabilization (VS) coil system, is proposed for installation inside the vacuum vessel. The two systems have distinctly different functions. The RMP coils generate magnetic perturbations just inside the plasma edge in order to minimize high-power deposition in the divertor induced by energy pulses produced by edge localized modes (ELMs). The coils can also be used to control moderately unstable resistive wall modes. The VS coils provide fast vertical stabilization of the plasma. Two sets of coil systems are installed between the blanket modules and the outboard inner wall of the vacuum vessel.

The cryostat is a fully welded, stainless steel vessel with a large number of horizontal penetrations for access to VV ports at three levels and further horizontal penetrations for coolant pipe work at upper and lower levels and cryo and current feed lines to magnets at the upper and lower levels. Furthermore, penetrations for manned access for repair or inspection are included in the lower cryostat cylinder for horizontal entry and in the top lid of the cryostat for vertical entry. The thermal shield system minimizes heat loads transferred by thermal radiation and conduction from warm components to the components and structures that operate at 4.5°K.

The blanket system provides a physical boundary for the plasma transients, absorbs the power from the plasma, and contributes to the thermal and nuclear shielding of the VV and external machine components. The blanket system consists of 440 modular shielding elements, which are attached to the VV and are made up of plasma-facing first-wall panels mounted on a shield block.

The ITER divertor consists of 54 cassette assemblies, which are inserted radially through three lower level ports and moved toroidally before being locked into position. The high-heat-flux components mounted on the divertor cassettes and the first-wall panels constitute ITER's plasma-facing components (PFCs). The lifetime of the PFCs is a critical issue because of the greatly increased stored energy of the ITER burning plasma. This means that control of transients will be critical to avoid reaching material melting or sublimation points, at which erosion rates will attain levels far beyond even the relatively high values expected in steady-state operation. The present scaling of the amplitudes of certain plasma instabilities at the edge of the plasma, called edge localized modes (ELMs), predicts that the divertor heat loads could be unacceptably high if no mitigation measures are taken. For inductive operation in ITER, two primary approaches are being investigated for mitigation of the ELM heat load: resonant magnetic perturbation and frequent ELMs triggered by pellet injection. Transient heat loads associated with disruptions and vertical displacement events must also be mitigated by techniques such as massive gas injection.

Key plasma-wall interaction issues include the level of tritium retention in the vacuum vessel and the production and transport of dust. To allow flexible operation over a wide range of operating conditions, the divertor target heat flux regions will initially use a carbon fiber composite as a plasma-facing material, due to its favorable thermal characteristics, especially for pulsed heat loads. However, R&D performed to date indicates that the estimated rate of tritium retention has a large uncertainty and would not be acceptable in the worst-case scenario, due to the very limited number of high power D-T pulses that would be possible within the allowed limit. A divertor with all-tungsten plasma-facing materials will therefore be installed in advance of D-T operation, but after the demonstration of successful mitigation of transient heat loads, with the aim of significantly reducing the tritium retention rate.

An extensive and flexible plasma heating and current drive system will be required for ITER to meet its performance goals. The system is a combination of neutral beams and radio frequency units. Neutral beams with a total power input of 33 MW will be provided. Such beams will need energies of 1 MeV to penetrate deeply into the ITER plasma and to drive current efficiently. In order to produce such beams with high efficiency, negative-ion sources will be used. Developing such beams is a major R&D challenge. The radio frequency system will be primarily based on ion cyclotron units that deliver 20 MW of power at about 50 MHz and electron cyclotron units that also deliver 20 MW at 170 GHz. Lower hybrid units at 5 GHz may also be used. Upgrade options are available to increase the total installed power to 130 MW.

34.5 ITER PLANT SYSTEMS

The ITER fuel cycle systems are based, for the most part, on proven technologies that must operate with a very high level

of reliability. In particular, safe handling and confinement of tritium needs to be assured under all operating conditions. Control of the helium and impurity content of the burning plasma requires continuous pumping of the neutral gas flux at the divertor and hence a continuous supply of fresh fuel to the plasma. At the maximum available fueling throughput, ITER will eventually need to recycle about 200–400 kg tritium per year with a maximum on-site inventory level of about 4 kg in the later phases of DT operations. This throughput rate is orders of magnitude higher than any preceding tritium facility. Additional complexity comes from requirements to separate hydrogen isotopes, from the need to recover tritium from tritiated water, and from off-gas detritiation prior to any discharge.

Fueling systems play a key role in achieving the necessary plasma particle densities as well as limiting the heat loads to the divertor by injection of gases. High-speed pellet injection is the main tool for supplying fuel particles deep inside the plasma with high efficiency of delivery. And, as noted above, another important mission of the pellet injection system is to control the frequency of ELMs and to avoid damage to the first wall.

Tritium for ITER operation will come from outside sources; at least 20–25 kg of tritium is expected to be available during the D-T phase through tritium extraction from heavywater-moderated fission power plants, although the maximum on-site inventory at any time will be limited to 4 kg.

Due to the presence of hazardous materials (e.g., beryllium), radiological contamination (tritium and dust), and high radiation during the latter phases of operation, the success of ITER operations will depend on the ability to remotely access and maintain critical components. During assembly and upgrades, the significant weight of components will also require remote handling tools and cranes of large lift capacity. Maintenance of ITER systems located within the ITER tokamak building will depend to a very significant extent on the ITER remote handling capability, for example, for all of the in-vessel components. With the exception of the neutral beam cell, which has a dedicated remote maintenance system, ITER components will be removed from the tokamak building and taken to the ITER hot cell facility for maintenance, repair, or disposal.

The Cadarache site for the ITER plant was selected in 2005. An area of 182 hectares is now designated as

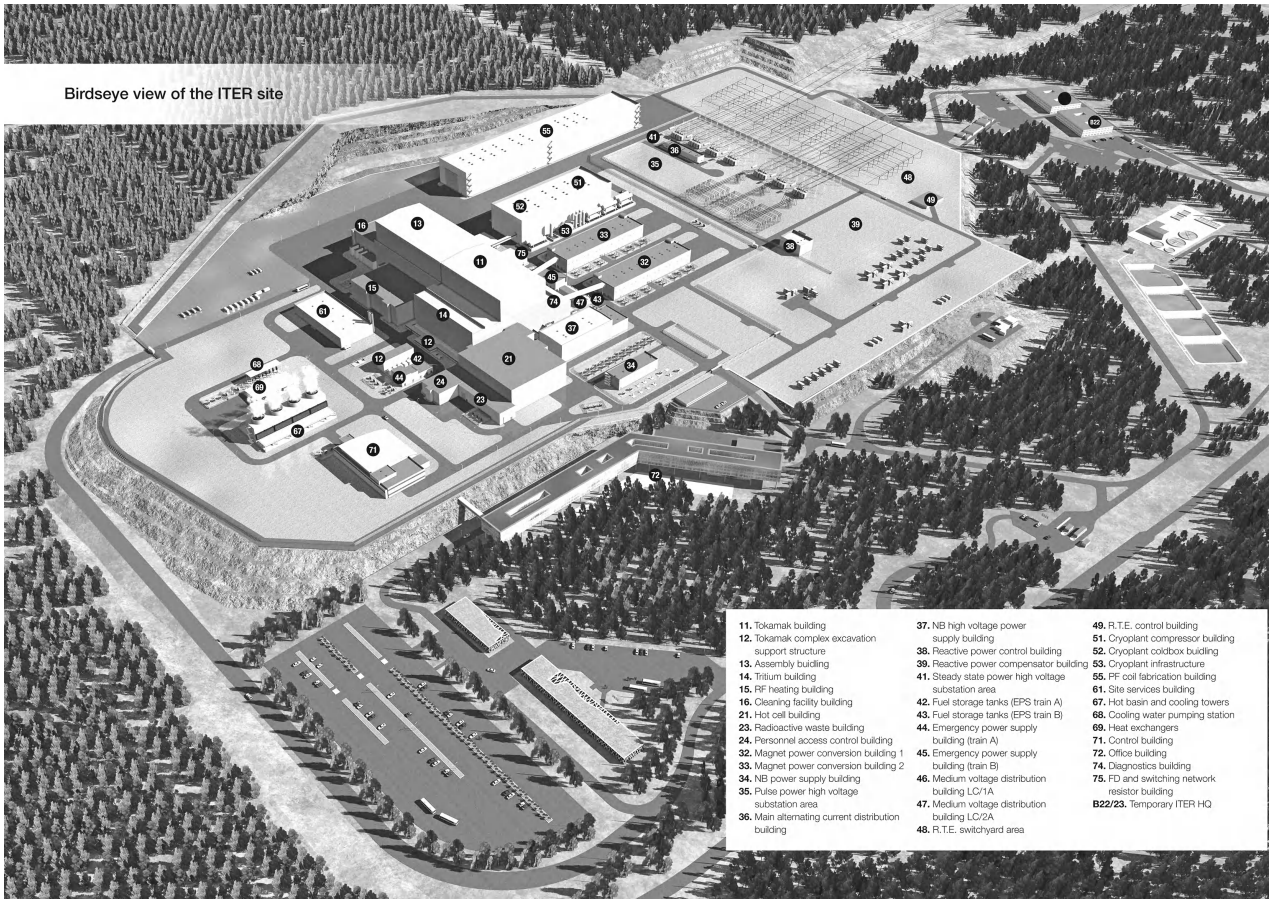

Figure 34.2 The ITER site (Courtesy of the ITER Organization).

international territory, covered by the statutes of the ITER Organization. The heart of the ITER project plant, shown in Figure 34.2, is the tokamak complex, including the tokamak building. This complex is a nuclear-rated structure of reinforced concrete and is mounted on seismic isolators. The building roof level is approximately 57 meters high above ground level, and the basement floor is approximately 11 meters below ground. The assembly hall is connected directly to the tokamak complex and is served by a 1500 metric ton capacity bridge crane.

The ITER electrical power distribution system provides up to 500 MW, 200 MVA, of pulsed power for the preprogrammed plasma scenarios, including the plasma current, position, and shape control, including vertical stabilization; the heating and current drive power supplies; the superconducting magnet coils; and the in-vessel coils. The power demand for all other loads is approximately 155 MW. About 13 MW of the total demand must be provided even in case of a loss of off-site power. Autonomous diesel power generators will be used as backup during such events.

The heat deposited in the internal vessel components and the vacuum vessel is rejected to the environment via the tokamak cooling water system. This system has the capacity to remove 1 GW of heat, including about 700 MW from the first-wall and blanket system. Heat is exchanged between this system and the component cooling water system to preclude the release of tritium and activated corrosion products to the environment. Ultimately, heat is rejected to the environment through cooling towers and basins.

A cryoplant produces liquid helium, which is distributed by the cryodistribution system to auxiliary cold boxes feeding the magnet and other loads such as the cryopumps for the pumping of the vacuum vessel.

34.6 ITER SAFETY AND ENVIRONMENTAL FEATURES

ITER will be the world's first large-scale fusion nuclear facility, and one of its objectives is to demonstrate the safety and environmental potential of fusion and thereby provide a good precedent for the safety of future fusion power plants. As such, it will be licensed and monitored under the appropriate French nuclear authorities.

The project's safety approach will be driven by taking advantage of fusion's favorable safety characteristics: e.g., the fuel inventory in the plasma is always below 1 gram, so that the fusion energy content is small; the plasma burn is terminated inherently when fueling is stopped due to the limited confinement by the plasma of energy and particles; and the plasma burn is passively terminated by the ingress of impurities under abnormal conditions.

Acknowledgments

The technical information in this paper has been taken from project documents developed by the ITER International Organization. The author appreciates the very helpful comments received from David Campbell, Ned Sauthoff, and Harold Forsen.

35

POWER PLANT PROJECTS

Laila A. El-Guebaly

Fusion Technology Institute, University of Wisconsin-Madison, Madison, WI, USA

The progress of fusion over the past five decades has been connected to the construction of numerous experimental facilities aiming to achieve power-plant-relevant parameters and operating conditions. In the meantime, the power-plant projects presented an essential element of the developmental process in order to understand the future trends. They provide a guide to physics and engineering criteria for advanced designs, highlight emerging technical issues and challenges, and present a perspective on potential fusion concepts. The mission of such projects include the following:

- Performing self-consistent integrated designs, stressing constructability, fabricability, operability, and maintainability of fusion power plants.
- Focusing on practicality, safety, and economic competitiveness of fusion power.
- Engaging multi-institutional, multifunctional design teams with expertise in plasma physics, neutronics, magnets, materials, heat transfer, power conversion, maintenance, safety, and economics.
- Uncovering physics and technology challenges.
- Helping the fusion community and funding agencies understand major design issues.
- Suggesting research and development (R&D) programs to deliver attractive and viable end products.

In the early days of fusion, nearly five decades ago, there were a multitude of fusion concepts searching for a viable confinement approach. The advent of the tokamak confinement concept, notably the Russian T3 experiment in 1968, was heralded as a significant confinement improvement. Larger tokamak experiments followed in the 1980s and still continue with excellent experimental results. However, the advocates for alternate magnetic and inertial fusion concepts continue to offer attractive potential solutions. Some of these concepts failed critical confinement and engineering requirements, while others continue to be developed with larger successful experiments. Some of the enduring magnetic confinement concepts are stellarator, spherical torus, field-reversed configuration, reversed-field pinch, and spheromak, while inertial configurations include direct/indirect laser, light/heavy-ion, and Z-pinch.

Despite continued investigation and preliminary development of the alternate confinement concepts, the magnetically confined tokamak is currently regarded as the most viable candidate to demonstrate commercial fusion energy generation. The tokamak program accounts for over 90% of the worldwide magnetic fusion effort. For these reasons, this section focuses on tokamak power-plant projects developed in the United States and abroad. Recent power plant projects for D-T (deuterium-tritium) fueled tokamaks have stressed the following key points:

- Fusion has favorable safety and environmental features:
  - Low-activation materials that minimize long-lived radioactivity.
  - Design features that support public and worker safety.
  - Passive containment systems to eliminate the need for an evacuation plan in the event of accidents.
  - Design and material usage to enable a high level of material recycling and clearance.

Nuclear Energy Encyclopedia: Science, Technology, and Applications, First Edition (Wiley Series On Energy).
Edited by Steven B. Krivit, Jay H. Lehr, and Thomas B. Kingery.

  - Radwaste reduction scheme through compactness, blanket segmentation, permanent components, and recycling/clearance.
  - No CO_2, NO_2, or hazardous material emissions.
- Compact high-power density machines provide economical benefits while integrating advanced physics and technologies to improve performance:
  - Innovative first-wall design operating at >5 MW/m^2 neutron wall loading (compactness).
  - Advanced divertor system withstanding >10 MW/m^2 heat flux (compactness).
  - Radiation-resistant structural materials handling >200 dpa (longer component life and waste reduction).
  - High field magnets providing >16 Tesla (compactness):
    - Superconductors as opposed to resistive Cu magnets (electrical efficiency).
    - Development of high-temperature superconductors offers higher fields (compactness) and lower cryogenic demands (recirculating power efficiency).
- Advanced power plants with the following attributes could compete economically with other energy sources:
  - Steady-state operation.
  - On-site tritium fuel production.
  - Breeding blanket converting nuclear energy at high temperature $>700^\circ$C for highly efficient thermal conversion to electricity or hydrogen production.
  - External heat transfer system that safely handles high temperatures ($700-1100^\circ$C), yielding high energy conversion efficiency (40–60%).
  - Successful operation for >50 years with expedient blanket and divertor replacements (every 3–5 years).
  - Outer power core components (shield, vacuum vessel, and magnets) operating reliably for entire plant lifetime.
  - Advanced low-cost fabrication techniques for all components to enhance economic viability.
  - High availability ($>90\%$) for competitive power production:
    - Highly reliable components to minimize unscheduled outages.
    - Expedient power core maintenance to minimize downtime.
  - 24/7 operation to provide continuous base-load power to grid or other power need.
  - At least 1 GW_e of net output power (larger plant power levels offer lower unit power costs, but may be limiting to the connected grid).

Numerous tokamak studies [1], extensive R&D programs, more than 35 worldwide operational experiments [2], impressive international collaboration in all areas of research, and a large body of accumulated knowledge have led to the current wealth of tokamak information and understanding. Recent international collaborative effort materialized in designing and starting ITER [3]—an International Thermonuclear Experimental Reactor—that will be a significant advance in the understanding and demonstration of ignited tokamak plasmas and related technologies. Most of the studies and experiments are currently devoted to the D-T fuel cycle, as it has the least demanding plasma temperature and pressure conditions to achieve ignition. The emphasis on fusion safety has stimulated worldwide research on other more demanding fuel cycles with less neutron generation, such as deuterium-deuterium (D-D), deuterium-helium-3 (D-He3), proton-boron-11 (P-B11), and He3-He3.

35.1 KEY TOKAMAK FEATURES

The plasma is confined by a large set of equally spaced toroidal field (TF) and poloidal field (PF) coils. Sets of divertor, equilibrium field, central solenoid, and vertical position coils are necessary to create, shape, position, and stabilize the plasma within a toroidal vessel of a D-shaped elliptical cross section. An isometric of the ARIES-AT power core [4] is shown in Figure 35.1, which is typical of a tokamak configuration.

The dominant physics feature of a tokamak is a flowing current in the plasma that generates a helical component of the magnetic field for plasma stability. Experimental tokamak devices use solenoidal coils to inductively create and sustain the plasma current for short periods of time for pulsed operation. It is highly likely that commercial tokamaks will operate in a steady-state mode to eliminate the cyclic fatigue induced in all systems and to avoid the need for an energy storage system [5, 6]. A steady-state operating condition is achievable with neutral beam or radio-frequency current drive systems. Once the plasma ignites, the alpha particles from the fusion reaction provide nearly all the plasma heating. Most tokamaks employ divertors in either single (usually at the bottom) or double (at top and bottom) configurations to collect the created alpha particles, ions, and electrons that escape the magnetic field.

The components surrounding the plasma must capture the energy of radiated heat and energetic particles, convert the high-energy neutrons into thermal energy,

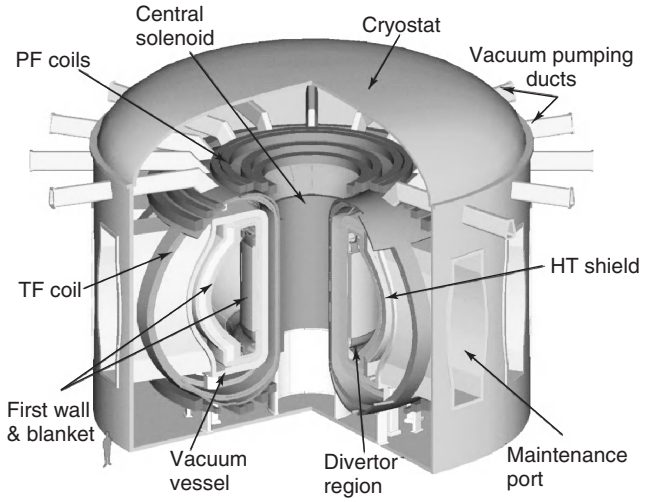

Figure 35.1 Cutaway isometric view of the ARIES-AT power core [4].

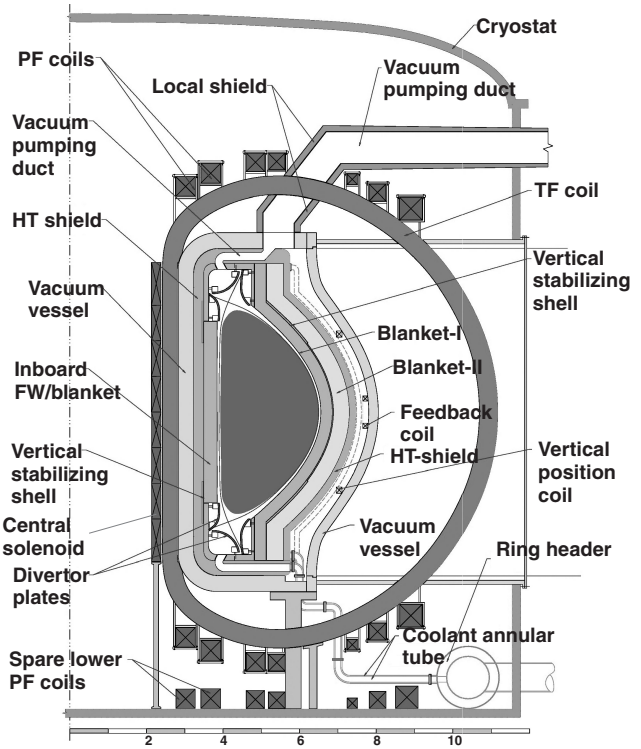

Figure 35.2 Vertical cross section of ARIES-AT power core configuration [4].

breed tritium fuel in the case of D-T fueled fusion systems, and protect the vacuum vessel, magnets, and other external components against radiation. There are a variety of specialized components and subsystems that work together to achieve the overall energy capture, breeding, and shielding requirements. Different advocates offer various design solutions for each of these components with the final choices to be determined and refined before integration and implementation on demonstration (Demo) power plant.

The first wall covers the inboard and outboard blankets and is designed to handle both the high surface heat flux and neutron flux. It is a thin component (a few centimeters thick) with very high cooling capability and no breeding function in most cases. The inboard and outboard blankets (see Fig. 35.2) are of varying thicknesses, contain various lithium compounds to breed tritium for fuel self-sufficiency, and convert the kinetic energy of the neutrons into thermal energy. Usually, the first wall and blanket are combined into a single assembly. The high thermal stresses suggest small blanket modules on the order of a few meters on a side. Due to the high neutron fluence (15–20 MWy/m^2), the life of the first wall/blanket is limited to three to five years. The divertor subsystem is a specialized component that intercepts the high-energy (3.5 MeV) alphas and other charged particles. It has a surface heat flux on the order of 10 MW/m^2 with a lower neutron wall loading than the first wall. The design requirement is to have a similar lifetime to that of the first wall and blanket.

In the depth of the power core behind the blanket and divertor where the neutron flux is too low for efficient production of tritium, there is still significant flux for damage to other components. For this reason, a specialized shield is employed at inboard, outboard, top, and bottom of the plasma core to protect the magnets [7]. If the volumetric neutron flux is sufficiently high, this shield is cooled with high-temperature coolants for power production. As a part of an integrated power-core design, this hot shield also functions as a structure that integrates all the inner core components, including high-temperature coolant manifolds. For horizontal segment maintenance scenarios, this complete assembly can be removed and replaced as a single segment module. In recent ARIES tokamak designs [8], the recommended maintenance approach is to remove each of the 16 core sectors between the outer TF coil legs through large maintenance enclosures. The recent EU Demo designs feature vertical maintenance of 52 large Multi-Module Segment assemblies and divertor cassettes through two vertical ports in the top of the power core [9].

The TF and PF coils are typically located just outside the vacuum vessel. The design requirement is for the coils to be sufficiently protected from the energetic neutrons for the life of the plant by the inner in-vessel components. With horizontal segment removal, the outer PF coils (normally located near the horizontal centerline) should be permanently relocated above and below the maintenance port enclosures.

The challenging fusion environment (14.1 MeV neutrons, high heat flux, high magnetic fields, thermo-mechanical stresses, and chemical compatibility issues)

mandates employing advanced low-activation structural materials (ferritic steels, vanadium alloys, and SiC/SiC composites) to assure the successful development of economical fusion energy [10, 11]. Fusion materials should contain benign alloying elements and extremely low levels of impurities to achieve very low induced radioactivity to allow the recycling and/or clearance of all fusion components [12].

Besides breeding sufficient tritium for plasma operation, the ultimate purpose of the fusion power core is to produce high-quality useful thermal energy. The higher the output coolant temperature, the higher the efficiency of the thermal conversion system. This high-temperature coolant is produced in the first wall, blanket, divertor, hot shield, and, perhaps, some other specialized components. When using liquid metals or metal alloys, insulating liners or coatings will be necessary. Multiple loops with isolating heat exchangers may be necessary for coolant compatibility issues or tritium migration to the turbine system and ultimately to the environment. The heat-transfer and transport system must be able to efficiently handle high-temperature heat-transfer media (700–1100°C) consistent with advanced energy conversion systems [13, 14].

Reliability and maintainability are immensely important to achieve high availability and low operational cost. Plant availability must exceed 85% in order for fusion to compete economically with other energy sources in the time frame for fusion introduction. Advanced low-cost fabrication techniques can be developed for all components to lower the initial capital and recurring costs [7].

Numerous studies have predicted that fusion potentially has favorable safety and environmental features. Top-level safety objectives have been defined and implemented into the conceptual designs to assure public and worker safety, no need for an evacuation plan during accidents, and an attractive low-level waste reduction scheme through innovative designs, recycling/clearance, and smart choice of low-activation materials [15]. In addition to safety and environmental attractiveness, economics remains an important consideration [16, 17]. According to researchers in various countries, fusion could be cost effective compared to other energy sources, particularly when external costs are added to the cost of electricity [18, 19]. There is a need to develop low-cost techniques [7] to fabricate power-core components because existing techniques are too expensive and may not be able to handle the complex shapes that are necessary. Recent studies continue to indicate an economical power plant should deliver at least $1GW_e$ of net output power. Larger sizes (>1 GW_e) are more economical due to economy of scale, but would present higher financial risk for utilities and more complexities for integrating and handling multi-GW sources [20].

35.2 U.S. TOKAMAKS

In the United States, the tokamak conceptual studies progressed steadily from the early 1970s pulsed UWMAK series [21, 22], to STARFIRE [23] (1980) that first promoted steady-state current drive, to the more advanced 1990s steady-state ARIES series [8]. The earlier designs of the 1970s demonstrated how fusion plants could be designed and operated, but also uncovered undesirable aspects of pulsed operation with an energy storage system and low power density machines, plasma impurity control problems, and maintainability issues. These pioneer studies contributed significantly to the basic understanding of the field of fusion power plant design and technology. In fact, many of the proposed 1970s technologies are still considered in recent fusion designs: 316-SS structures, lithium (Li) and lithium-lead (LiPb) liquid breeders, $LiAlO_2$ solid breeders, beryllium multipliers, helium and water coolants, NbTi and Nb_3Sn superconductors, low-Z liner for first wall and solid divertor, liquid Li divertor, and remote maintenance.

More in-depth power plant studies were initiated in the 1980s to identify, understand, and resolve the physics and technology challenges of tokamaks. While these studies proposed solutions for known problems, they uncovered other areas that needed further assessment and development, such as disruption control, current drive technology, high heat flux divertor design, and high-temperature blankets. STARFIRE, shown in Figure 35.3, represented the first tokamak power plant that operated in a steady-state, current drive mode without an energy storage system. Other STARFIRE design features include advanced physics, lower-hybrid current drive, beryllium-coated first wall (FW), modular water-cooled solid breeder blanket, attractive safety characteristics, and a sector maintenance scheme. In the 1990s, the ARIES team [8] produced a series of advanced tokamak power plant design studies, emphasizing the safety and economic competitiveness of fusion power and taking into consideration the fabricability, constructability, operability, and maintainability of the machine. The ARIES physics, engineering, and economics proceeded interactively to produce an integrated design approach, while the systems code determined the reference parameters by varying the physics and engineering parameters, subject to pre-assigned physics and technology limits, to produce an economically optimized plant design.

Each ARIES design was conceived to investigate various options that may provide an improvement; basically, a technical sounding board that helps evaluate the viability of different physics and engineering concepts. The first design of the ARIES series (ARIES-I [24]) operated in the first-stability plasma regime—the closest to the present database—with a ceramic breeder blanket and SiC/SiC

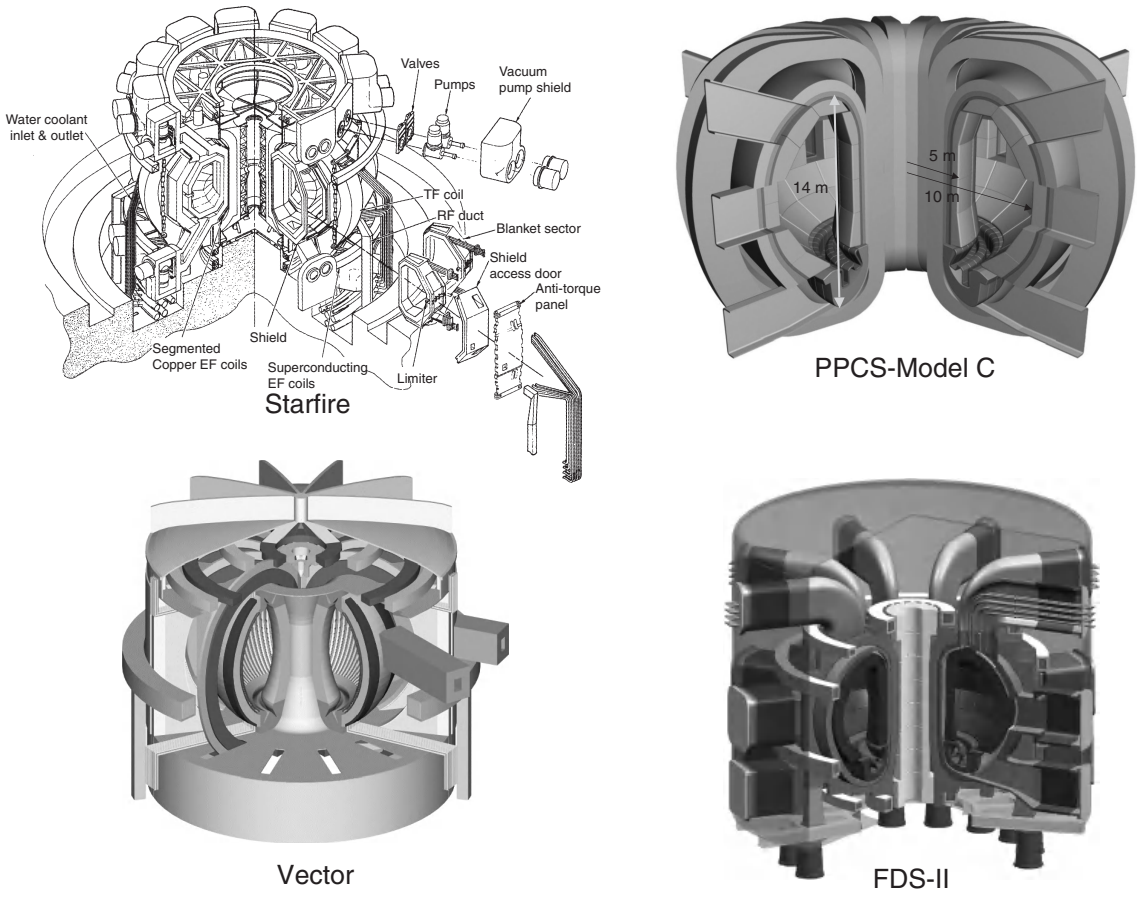

Figure 35.3 Isometric views of STARFIRE and selected EU, Japanese, and Chinese power plants (not to scale).

composites as the main structure. Even though the high-field TF coils and high thermal conversion efficiency improved the attractiveness of this first-stability regime of operation, ARIES-I did not adequately satisfy the economic requirement. The second-stability regime of ARIES-II/IV [25] had better performance, but the experimental database for this physics regime is very limited. Two blanket options were examined in ARIES-II/IV: liquid lithium with vanadium structure and lithium oxide ceramic breeder with SiC/SiC composite structure. Next, the ARIES-RS study [26] with reversed-shear (RS) plasma and a Li/V blanket offered similar economic performance. Nevertheless, the physics database for this RS regime, while small at the time of the study, is continuing to evolve and improve. The advanced tokamak (AT) plasma confinement regime was incorporated in the last ARIES-AT design [4], displayed in Figures 35.1 and 35.2, to assess the physics and technology areas with the highest leverage for achieving attractive and competitive fusion power. Indeed, the ARIES-AT design demonstrated superior performance and benefited greatly from several developments: high toroidal beta (9%), new SiC/SiC composite structure and LiPb blanket operating at high temperature ($\sim$1000°C) with high thermal conversion efficiency (59%), and high system availability (85%) with an efficient horizontal maintenance scheme.

35.3 INTERNATIONAL TOKAMAKS

Europe, Japan, and China have produced a number of tokamak fusion power plant studies. There are technical similarities and differences related to strategic objectives, technology readiness, and general approaches. For instance, the emphasis given to the economic competitiveness of power plants varies significantly between countries. The United States is highly motivated to obtain a fusion power plant that is at least as economically competitive as other available electric power sources. On the other hand, Europe and Japan take the view that the first generation of fusion power plants will enter the energy market because of the significant safety and environmental advantages and large fuel reserve, even if they produce electricity at a somewhat higher cost.

A series of European studies delivered two reports [27, 28] in the 1990s on the safety and environmental assessment of fusion power (SEAFP). The lessons learned from SEAFP were applied to the successor EU study of commercial power plants: European Power Plant Conceptual Study (PPCS) [29]. This four-year study focused on five power core models that spanned a wide range of near-term and advanced physics/technology tokamaks operating in steady-state mode. Models A, AB, and B are considered near-term concepts while Models C and D are more advanced concepts. The models deliver ~1500 MW_e output power, but differ substantially in plasma parameters, physical size, fusion power, materials, blanket and divertor technologies, breeding capacity, economic performance, and safety and environmental impacts. Figure 35.3 displays an isometric view of the Model C power plant. The cost of electricity for fully matured tenth-of-a-kind model plants is thought to be competitive with other sources of energy. In addition to this valuable comparison, the PPCS study highlighted the need for specific R&D activities as well as the need to establish the basic features of the Demo [30]—a device that bridges the gap between ITER and the first-of-a-kind fusion power plant.

In Japan, several studies have been made of tokamak power plants. SSTR [31] is a pioneer Japanese study developed in the early 1990s and aimed at achieving high power density through high field of 16.5 Tesla at the TF magnets. More advanced SSTR studies followed and recommended higher magnetic fields (20–23 T) with 20°K magnets. A major design challenge for such a high magnetic field approach is the sizable magnet structure needed to support the much larger electromagnetic forces on the TF coils. The DREAM study [32] promoted the approach of easier and faster power core segment maintenance in order to achieve high overall availability and thus reduce the cost of electricity. With 12 toroidal sectors and a high plasma aspect ratio (A) of 6, an entire sector can be pulled out radially between the outer legs of TF composites as the main structure coils—a similar approach to the STARFIRE, ARIES-RS, and ARIES-AT maintenance designs. The successor, more compact CREST study [33] adopted DREAM's maintenance philosophy, but with an increased number of 14 TF magnets and 14 sectors. The most recent very compact tokamak reactor (VECTOR) [34], shown in Figure 35.3, is even more compact with a major radius of 3.75 m and >16 T superconducting TF magnets operating at 20°K. VECTOR's design features were incorporated in the design of a compact Demo (SlimCS) with low aspect ratio and slim central solenoid [35]. Demo-CREST [36] has also been proposed as an alternate Demo based on the CREST approach.

In China, a series of fusion design studies (FDS) [37] has been developed over the past 10 years covering a broad range of tokamak concepts, including a hybrid tokamak to transmute fission products and breed fissile fuels (FDS-I), electricity generator (FDS-II), hydrogen producer (FDS-III), and spherical tokamak (FDS-ST) to examine innovative approaches. The FDS-II single-null tokamak design [38], shown in Figure 35.3, is based on advanced plasma physics and employs a LiPb breeder and reduced-activation ferritic steel structure. The dual-cooled LiPb/He reference blanket produces a 700°C LiPb outlet temperature while the backup He-cooled quasi-static LiPb blanket has a 450°C He outlet temperature. The FDS-II configuration is designed with modularized blankets to alleviate the thermal stress and impact of electromagnetic force caused by plasma disruption. There are 240 blanket modules and divertor cassettes that are maintained, removed, and replaced individually through equatorial and lower ports, respectively. Preliminary assessments indicated the conceptual design satisfies the FDS-II requirements in terms of tritium breeding, mechanical performance, fabricability, maintainability, safety, and economics.

35.4 D-He3 TOKAMAKS

Most fusion studies and almost all operational experiments have employed the D-T fuel cycle—the least demanding to reach ignition. Since the 1970s, researchers around the globe examined other fuel cycles based on "advanced" fusion reactions with much less neutron production, such as D-He3. These advanced concepts [39] offer several advantages: no need for a tritium breeding blanket, much longer-lived or permanent components, and possibly direct energy conversion of charged particles into electricity with conversion efficiencies approaching 60%. However, the D-He3 plasma has its own set of issues and concerns, such as the limited availability of He3 and the attainment of the higher plasma parameters that are required for D-He3 fusion conditions. Moreover, the D-He3 cycle is not completely without neutrons, requiring shielding components to protect the magnets and externals. It has a very low presence of energetic neutrons, due to side D-D reactions generating 2.45 MeV neutrons and T and the side D-T reactions generating 14.1 MeV neutrons. Several studies have addressed the physics and engineering issues of D-He3 fueled power plants while a few publications [40, 41] addressed the pertinent issues of utilizing today's technology and a strategy for D-He3 fusion development. Most of the D-He3 efforts of the 1970s and 1980s focused on alternate confinement concepts with high beta and high magnetic field, such as the field-reversed configuration, tandem mirrors, and Ring Trap concept. In the early 1990s, the University of Wisconsin developed a series of tokamak-based D-He3 Apollo designs [42] while the D-He3 ARIES-III tokamak [43] was developed by the ARIES project. The Apollo and ARIES-III designs acknowledged

the challenging physics, but postulated the reduction in radioactivity and the advantageous effect of the D-He3 safety characteristics that include low radioactivity and decay heat levels, very low-level waste, and low releasable radioactive inventory from credible accidents.

35.5 ROADMAP FOR DEVELOPING FUSION ENERGY

All power-plant studies developed thus far identified the characteristics of fusion power plants in a fully mature, commercial fusion market (tenth-of-a-kind plant), believing strongly that fusion should be an option in the 21st century energy mix. Recently, optimism about fusion has increased with the initiation of construction of the large ITER tokamak experiment in France. However, it is recognized that developing fusion energy will cost billions of dollars and would span decades. The key strategic questions are What physics and engineering technologies remain to be developed, matured, and validated for a viable fusion power plant? What other facilities will be needed between ITER and the first power plant to reduce programmatic risk? What will it cost? How long will it take to construct the first plant? and How efficiently will the plant operate and be maintained? A Demo plant is viewed as the last step before the first commercial power plant and will provide validated subsystems for the first plant. Assuming ITER operates successfully, several countries have recommended constructing a few facilities to qualify materials, components, and physics for the Demo. Other countries feel confident that ITER and existing experiments will provide adequate technology development to directly embark on their Demo. The proposed facilities include the International Fusion Materials Irradiation Facility (IFMIF), Fusion Nuclear Science Facility (FNSF), and Advanced Physics Testing Facility. The tentative names of these preliminary facilities are indicative of the facility function.

In each country, the pathway to fusion energy is influenced by the timeline anticipated for the development of the essential physics and technologies for Demo and power plants as well as the demand for safe, environmentally attractive, economical, and sustainable energy sources. As expected, the international roadmaps are taking different approaches due to their power plant concept and degree of technical optimism and extrapolation beyond ITER. Several Demos with differing approaches could be built in the United States, European Union, Japan, China, Russia, Korea, India, and other countries to cover a wide range of near-term and advanced fusion systems. Recognizing the capabilities of national and international fusion facilities, it appears that the construction of the first fusion power plant could start as early as 2030, with completion and supply of electricity to the grid by 2035, providing sufficient funding and governmental support is available.

Acknowledgments

The author is very appreciative to the following colleagues for their inputs and reviews: L. Waganer (Boeing consultant), J. Santarius (University of Wisconsin - Madison), D. Maisonnier (EC, Brussels), K. Tobita (Japan Atomic Energy Agency, Japan), and Y. Wu (Chinese Academy of Sciences, China).

REFERENCES

1. L. A. El-Guebaly, History and evolution of fusion power plant studies: past, present, and future prospects. Chapter 6 in book: *Nuclear Reactors, Nuclear Fusion and Fusion Engineering*, A. Aasen and P. Olsson, ed., NOVA Science Publishers, Hauppauge, NY, 2009, pp. 217–271.
2. Worldwide Tokamak Experiments: http://www.toodlepip.com/tokamak/conventional-large-tokamaks.htm, accessed March 2011.
3. The ITER Project: http://www.iter.org/, accessed March 2011
4. F. Najmabadi, A. Abdou, L. Bromberg, T. Brown, V. C. Chan, M. C. Chu, et al., The ARIES-AT advanced tokamak, advanced technology fusion power plant. *Fus. Eng. Des.*, 2006, **80**, 3–23.
5. F. Najmabadi, R. W. Conn and the ARIES Team, *The Pulsed-Tokamak Fusion Power Plant—The Pulsar Study—Final Report*. University of California San Diego Report UCSD-ENG-003, 1999.
6. D. Ward, Newly developing conceptions of DEMOs: pulsing and hydrogen. *Fus. Sci. Tech.*, 2009, **56**, 2, 581–588.
7. L. A. El-Guebaly and L. M. Waganer, Radiation shielding schemes and advanced fabrication techniques for superconducting magnets. Chapter 8 in book: *Superconducting Magnets and Superconductivity: Research, Technology and Applications*, A. Aasen and P. Olsson, ed., NOVA Science Publishers, Hauppauge, NY, 2010.
8. The ARIES project: *http://aries.ucsd.edu/ARIES/*, accessed March 2011.
9. T. Ihli, L. V. Boccaccini, G. Janeschitz, C. Koehly, D. Maisonnier, D. Nagy, C. Polixa, J. Rey, and P. Sardain, Recent progress in DEMO fusion core engineering: improved segmentation, maintenance and blanket concepts. *Fus. Eng. Des.*, 2007, **82**, I15–24, 2705–2712.
10. S. J. Zinkle, Advanced materials for fusion technology. *Fus. Eng. Des.*, 2005, **74**, 1-4, 31–40.
11. S. J. Zinkle and J. T. Busby, Structural materials for fission and fusion energy. *Materials Today*, 2009, **12**, 11, 12–19.
12. L. El-Guebaly, V. Massaut, K. Tobita, and L. Cadwallader, Goals, challenges, and successes of managing fusion active materials. *Fus. Eng. Des.*, 2008, **83**, 7-9, 928–935.
13. R. Raffray, L. El-Guebaly, S. Malang, I. Sviatoslavsky, et al., Advanced power core system for the ARIES-AT power plant. *Fus. Eng. Des.*, 2006, **80**, 79–98.
14. A. R. Raffray, L. El-Guebaly, T. Ihli, S. Malang, X. Wang, and B. Merrill, Engineering design and analysis of the ARIES-CS power plant. *Fus. Sci. Tech.*, 2008, **54**, 3, 725–746.

15. L. A. El-Guebaly and L. Cadwallader, Recent developments in safety and environmental aspects of fusion power plants. Chapter 9 in book: *Nuclear Reactors, Nuclear Fusion and Fusion Engineering*, A. Aasen and P. Olsson, ed., NOVA Science Publishers, Hauppauge, NY, 2009, 321–365.
16. C. G. Bathke, Systems analysis in support of the selection of the ARIES-RS design point. *Fus. Eng. Des.*, 1997, **38**, 59–86.
17. R. L. Miller, Systems context of the ARIES-AT conceptual fusion power plant. *Fusion Technology*, 2001, **39**, 2, 439.
18. T. Hamacher, H. Cabal, B. Hallberg, R. Korhonen, Y. Lechon, R. M. Saez, and L. Schleisner, External costs for future fusion plants. *Fus. Eng. Des.*, 2001, **54**, 405–411.
19. D. Ward, N. Taylor, and I. Cook, Economically acceptable fusion power stations with safety and environmental advantages. *Fus. Eng. Des.*, 2001, **58-59**, 1033–1036.
20. J. Sheffield, W. Brown, G. Garret, J. Hilley, D. McCloud, J. Ogden, et al., A study of options for the deployment of large fusion power plants. *Fus. Sci. Tech.*, 2001, **40**, 1, 1–36.
21. B. Badger, M. A. Abdou, R. W. Boom, R. G. Brown, E. T. Cheng, R. W. Conn, et al., *UWMAK-I—A Wisconsin Toroidal Fusion Reactor Design*. University of Wisconsin Fusion Technology Institute Report, UWFDM-68, 1973. Available at: http://fti.neep.wisc.edu/pdf/fdm68.pdf.
22. B. Badger, K. Audenaerde, H. Avci, J. Beyer, D. Blackfield, R. W. Boom, et al., *NUWMAK—A Tokamak Reactor Design Study*. University of Wisconsin Fusion Technology Institute Report, UWFDM-330, 1979. Available at: http://fti.neep.wisc.edu/pdf/fdm330.pdf.
23. C. C. Baker, M. A. Abdou, R. M. Arons, A. E. Bolon, et al., *STARFIRE—A Commercial Tokamak Fusion Power Plant Study*. Argonne National Laboratory report ANT/FPP-80-1, 1980.
24. F. Najmabadi, R. W. Conn, P.I. Cooke, E. Ibrahim, et al., *The ARIES-I Tokamak Fusion Reactor Study—The Final Report*. University of California Los Angeles Report UCLA-PPG-1323, 1991.
25. F. Najmabadi, R. W. Conn, C. G. Bathke, C. B. Baxi, L. Bromberg, J. Brooks, et al., ARIES-II and ARIES-IV second-stability tokamak reactors. *Fusion Technology*, 1992, **21**, 3, Part 2A, 1721–1728.
26. F. Najmabadi, C. G. Bathke, M. C. Billone, J. P. Blanchard, L. Bromberg, E. Chin, et al., Overview of ARIES-RS reversed shear power plant study. *Fus. Eng. Des.*, 1997, **38**, 3–25.
27. J. Raeder, I. Cook, F. H. Morgenstern, E. Salpietro, R. Bunde, and E. Ebert, Safety and environmental assessment of fusion power (SEAFP): report of the SEAFP project. European Commission DGXII, *Fusion Programme*, EUR-FUBRU XII-217/95, Brussels, Belgium, 1995.
28. I. Cook, G. Marbach, L. Di Pace, C. Girard, P. Rocco, and N. P. Taylor, Results, conclusions and implications of the SEAFP-2 programme. *Fus. Eng. Des.*, 2000, **51–52**, 409–417.
29. D. Maisonnier, I. Cook, P. Sardain, R. Andreani, L. Di Pace, R. Forrest, et al., *A Conceptual Study of Fusion Power Plants*. European Fusion Development Agreement Final Report EFDA-RP-RE-5.0, 2005. Available at: http://www.efda.org/eu_fusion_programme/scientific_and_technical_publications.htm.
30. D. Maisonnier, D. Campbell, I. Cook, L. Di Pace, L. Giancarli, J. Hayward, et al., Power plant conceptual studies in Europe. *Nuclear Fusion*, 2007, **47**, 11, 1524–1532.
31. M. Kikuchi, M. Azumi, S. Tsuji, K. Tani, and H. Kubo, Steady state tokamak reactor based on the bootstrap current. *Nuclear Fusion*, 1990, **30**, 343.
32. S. Nishio, Y. Murakami, J. Adachi, H. Miura, I. Aoki, and Y. Seki, The concept of drastically easy maintenance (DREAM) tokamak reactor. *Fus. Eng. Des.*, 1994, **25**, 289–298.
33. K. Okano, Y. Asaoka, R. Hiwatari, N. Inoue, Y. Murakami, Y. Ogawa, et al., Study of a compact reversed shear tokamak reactor. *Fus. Eng. Des.*, 1998, **41**, 511–517.
34. S. Nishio, K. Tobita, S. Konishi, T. Ando, S. Hiroki, et al., Tight aspect ratio tokamak power reactor with superconducting TF coils. *Proceedings of* 19th *IAEA Fusion Energy Conference*, Lyon, FT/P/1-21, 2002. Available at: http://www-pub.iaea.org/MTCD/publications/PDF/csp_019c/html/node362.htm#74213.
35. K. Tobita, S. Nishio, M. Sato, S. Sakurai, T. Hayashi, et al., SlimCS—compact low aspect ratio DEMO reactor with reduced-size central solenoid. *Nuclear Fusion*, 2007, **47**, 892–899.
36. R. Hiwatari, K. Okano, Y. Asaoka, and Y. Ogawa, Analysis of critical development issues towards advanced tokamak power plant CREST. *Nuclear Fusion*, 2007, **47**, 378–394.
37. Y. Wu, Conceptual design activities of FDS series fusion power plants in China. *Fus. Eng. Des.*, 2006, **81**, 23-24, 2713–2718.
38. Y. Wu, Conceptual design of the China fusion power plant FDS-II. *Fus. Eng. Des.*, 2008, **83**, 1683–1689.
39. UW website for D-He3 Fuel Cycle: http://fti.neep.wisc.edu/proj?rm=dhe3 and http://fti.neep.wisc.edu/ncoe/dhe3, accessed March 2011.
40. J. Santarius, G. Kulcinski, L. El-Guebaly, and H. Khater, Can advanced fusion fuels be used with today's technology? *Journal of Fusion Energy*, 1998, **17**, 1, 33–40.
41. G. L. Kulcinski and J. F. Santarius, New opportunities for fusion in the 21st century—advanced fuels. *Fusion Technology*, 2001, **39**, 480–485.
42. G. L. Kulcinski, J. P. Blanchard, L. A. El-Guebaly, G. A. Emmert, et al., Summary of Apollo, a D-He3 tokamak reactor design *Fusion Technology*, 1992, **21**, 4, 2292.
43. F. Najmabadi, R. W. Conn and the ARIES Team, *The ARIES-III Tokamak Fusion Reactor Study—The Final Report*,.UCLA report UCLA-PPG-1384, 1994. Available at: http://aries.ucsd.edu/LIB/REPORT/ARIES-3/final.shtml.

36

SAFETY AND ENVIRONMENTAL FEATURES

LEE CADWALLADER[1] AND LAILA A. EL-GUEBALY[2]
[1]*Fusion Safety Program, Idaho National Laboratory, Idaho Falls, ID, USA*
[2]*Fusion Technology Institute, University of Wisconsin-Madison, Madison, WI, USA*

Controlled fusion has long been sought for its safety and environmental advantages over other energy sources. Some of the safety advantages are an inherently safe process to operate the fusion plasma, low radioactive inventories stored in the plant, and low radioactivity fuel. Fusion power plants have the potential to be low risk to the public, with no need for evacuation in case of an accident event. Worker safety is also incorporated into fusion designs, so that workers are protected. We will look at both the safety advantages for the public and station personnel and the environmental benefits of fusion as an energy source.

Since the inception of the fusion power plant design activities in the late 1960s, designers realized the environmental advantages of fusion. Some of the advantages are that deuterium exists in natural water and is relatively easy to retrieve in the needed kilogram quantities. Very low levels of tritium exist in nature, but plans call for breeding tritium fuel in as-needed kilogram quantities. These characteristics make fusion's fuel production more environmentally benign than the types of mining used to retrieve the required tens or hundreds of tons of coal or uranium power-plant fuels. Also, the fusion product of these hydrogen nuclei is helium, which does not pose an environmental issue like uranium fission products or coal combustion products. Another particular advantage is the low level of waste produced. While a fusion power plant has radio-activation of the interior walls, the fusion reactions do not depend on the wall materials—leaving the designers free to select low activation materials for the walls and other power core components.

36.1 SAFETY ASPECTS OF FUSION

The safety discussions use the ITER project as the fusion point of reference. ITER is an experimental magnetic fusion design that is scheduled for construction at the Cadarache nuclear complex in France (www.iter.org). ITER follows the safety and environmental rules of France.

French regulations for research facilities are very similar to U.S. regulations for nuclear facilities. The U.S. fusion safety policy has five main requirements [1]:

1. The public shall be protected such that no individual bears significant additional risk to health and safety from the operation of those facilities above the risks to which members of the general population are normally exposed.
2. Fusion facility workers shall be protected such that the risks to which they are exposed at a fusion facility are no greater than those to which they would be exposed at a comparable industrial facility.
3. Risks both to the public and to workers shall be maintained as low as reasonably achievable (ALARA).
4. The need for an off-site evacuation plan shall be avoided.

Nuclear Energy Encyclopedia: Science, Technology, and Applications, First Edition (Wiley Series On Energy).
Edited by Steven B. Krivit, Jay H. Lehr, and Thomas B. Kingery.

5. Wastes, especially high-level radioactive wastes, shall be minimized.

36.1.1 Public Safety Discussion

Public safety for fusion entails the confinement of radioactive and hazardous materials. Fusion facilities will attain this by using defense-in-depth design principles:

1. **Preventing** releases that could harm the public by minimizing radiological and hazardous inventories, using highly reliable components, employing conservative design margins, and integrating a rigorous quality assurance program into processes.
2. **Protecting** by using a succession of physical barriers and multiple means (inherently safe, passively safe, actively safe) before a release could occur.
3. **Mitigating** occurrences with confinement buildings, cleaning systems, ventilation stacks, emergency procedures, and passive heat sinks.

The fundamental characteristics of fusion are used as the foundation for the ITER safety approach and for fusion in general [2]:

- The fuel inventory in the plasma is small. A fusion machine injects puffs of gas or tiny frozen pellets into the plasma. Fusion fuel is consumed in milligram quantities at a time, similar to coal-fired power plants that feed pulverized coal into the combustion chamber, so very little fuel is at risk of release at any given time. Fusion power plant routine releases of gases and liquids are expected to be less than fission power plant annual releases. No public evacuation plan for nearby populations would be necessary in case of accidents.
- Fusion superconducting magnets use large amounts of cryogenic coolants, liquid helium, and nitrogen. Any releases from the cryogenic plant are non-radioactive and present no hazard to people outside the site boundary, like other cryogenic production facilities in commercial operation today.
- Fusion uses high magnetic and radio frequency fields for deuterium and tritium ion confinement and heating. These energies are contained within the facility. The natural attenuation of these energy forms with distance means that there is no public exposure at the plant boundary.
- Fusion plasma cannot sustain itself after fueling is stopped; the plasma terminates. The fusion process lasts only a few seconds with each fuel addition.
- Plasma burn is self-limiting with regard to power excursions, excessive fueling, and excessive additional heating. In the event that the plasma produces extra heat, the additional heat would melt or vaporize the armor tiles or wall coatings, sending relatively cool particles into the plasma and terminating the plasma.
- In the event of impurity ingress under abnormal conditions (e.g., by evaporation or gas release or by coolant leakage into the vacuum chamber), the plasma burn is passively and quickly terminated (in a few milliseconds).
- The fusion thermal energy per unit volume and thermal power per unit volume (the energy and power densities) in a fusion machine are low. Fusion plants have only low levels of releasable radioactive fuel and materials.
- Extensive heat-transfer surfaces and large masses exist and are available as passive heat sinks.
- Confinement barriers must be leak-tight for operational reasons, and the fusion fuel inventory is stored in specially designed multiple confined areas that have been functioning well for fusion research for many years.

Table 36.1 gives the ITER project numerical safety goals for the public [2]. The ITER goals are well below the allowable regulatory limits of participant countries, which include most of the industrialized nations that use fission power. The U.S. Environmental Protection Agency set a 1 rem limiting value for protection of the public in emergency situations as a value that would not have acute effects on public health and would have very low risk of any delayed effects to public health [3].

In the United States, fission requirements have a once-in-a-lifetime reference value of 250 mSv (25 rem) public dose that is used to help set public exclusion areas and low population areas around fission power plants for protection against potential accidents at those plants [5]. The U.S. routine release limits for normal power plant effluent exposures by the public are less than 1 mSv (100 mrem) [4]. The ITER goals are 10% and 4% of those values, respectively. A typical person in the United States receives 3.6 mSv/year (360 mrem/year) naturally from radiation in the air (i.e., radon gas), natural decay of elements in the earth, direct radiation emissions from building materials, naturally radioactive foodstuffs, and cosmic rays [6]. Figure 36.1 shows a comparison of radiation exposures.

When a facility's safety objectives are established, safety researchers assess the design to determine the highest consequence but credible events that could occur and compare the release consequences of those events to the goal values. These analyses are performed with computational modeling to assess the maximum possible releases from the plant with the use of conservative

TABLE 36.1 The ITER Design Safety Objectives and U.S. Fission Limits for the Public

	ITER [2]	Fission [4]
Normal operations situations	≤0.1 mSv/year (10 mrem/year)	≤1 mSv/year (100 mrem/year) or ≤0.02 mSv/hour (2 mrem/hour)
Incidents	0.1 mSv (10 mrem) per incident	250 mSv (25 rem) evaluation guideline, any public dose from any accident event must be well below this value
Accidents	No sheltering or evacuation <10 mSv (1000 mrem) No restriction on consumption of animal or vegetable products	
Hypothetical accidents beyond design basis	No disproportionate increase in risk from beyond design basis accidents (no cliff edge effect); possible counter-measures limited in time and space	

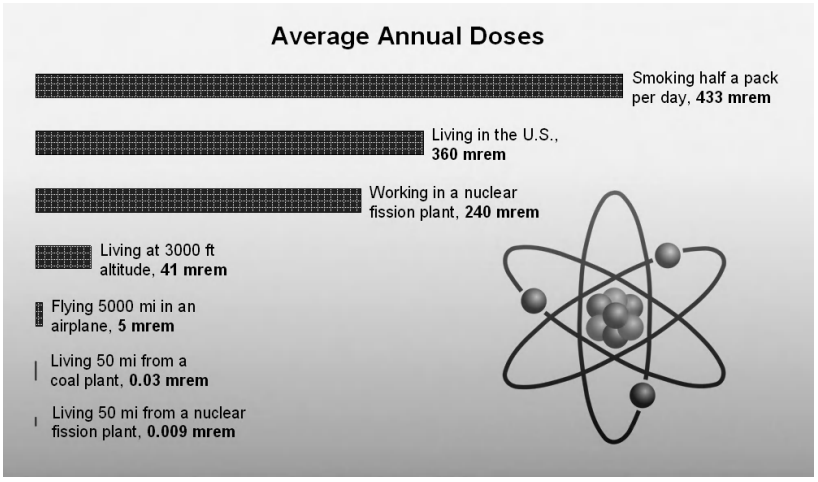

Figure 36.1 A comparison of typical annual radiological doses [7].

overestimates. Regulatory agencies then review the safety analysis in great detail and sometimes give direction for additional analysis. In the case of ITER, 25 of the worst conceivable incidents and accidents were studied, including loss of power, cooling water system failure, air or water ingress into the vacuum vessel and cryostat, events during maintenance, tritium release, fires, magnet system failures, and confinement failures [8]. All have consequences well within the Table 36.1 goal values; in many cases, the accident consequences are zero public exposure or trivial exposure [9]. The French regulatory agency, Autorité de Sûreté Nucléaire (ASN), has found the ITER safety analysis report to be complete and valid in its preliminary reviews; the ASN accepted the report in December 2010 to begin detailed technical review. The public hearings on the ITER safety analysis report are scheduled to begin in 2011. Approval is expected because of ITER's low radiological inventories and prudent design that will protect the public.

In the United States, fusion researchers have also extrapolated the technology to fusion power plants of the future and have assessed the public safety of two leading designs [10, 11]. The two designs are the Advanced Reactor Innovations and Evaluation Study (ARIES) advanced tokamak and the ARIES compact stellarator power plants. The advanced tokamak design uses lithium-lead (LiPb) as the coolant and tritium breeder and silicon carbide/silicon carbide (SiC/SiC) composites for the blanket and divertor structural materials. Being able to refurbish and reuse the LiPb in several cycles could considerably reduce the amount of activated material produced and thereby reduce costs. The compact stellarator confines the plasma with magnetic fields generated by external coils and uses a dual-cooled LiPb blanket with ferritic steel structural material to remove heat. Both designs are tenth of-a-kind fusion power plants believed to be operating several decades in the future. (Because these are conceptual extrapolations, the safety assessment does not have the detail or rigor of the ITER assessment.)

The ARIES advanced tokamak safety analysis [10] considered two worst consequence events: a large loss of vacuum accident, or LOVA, where the fusion vacuum vessel is breached to building air, and an in-vessel loss-of-coolant accident (LOCA) where water coolant leaks into the vacuum vessel. In both cases, the intrusion fluid (either

air or water) causes a plasma disruption that mobilizes tritium fuel and erodes dust from the protective coating on the divertor. For the LOVA, the effluents from the vessel enter the tokamak building and are drawn into the ventilation system where they are filtered, cleaned, and released through the facility vent stack. The estimated releases were 0.09 grams of tritium and 0.04 grams of tungsten dust from the tiles. The in-vessel LOCA was postulated to cause a bypass of the confinement and a ground level release of 7.6 grams of tritium (0.5 mSv), 207 grams of tungsten dust (0.345 mSv), and activated products of the LiPb material used to breed tritium fuel. The activated product releases were 4.7 μg of polonium (Po-210, 0.0085 mSv) and 6.3 mg of mercury (Hg 203, 0.035 mSv). In both cases, the releases are small and are less than 9% of the no-evacuation limit of 10 mSv (1 rem) dose to any member of the public.

The ARIES compact stellarator accidents analyzed were in-vessel LOCAs, loss of flow accidents (LOFAs), and an ex-vessel LOCA of LiPb [11]. Several of the events gave no public exposure because there were no off-site releases due to the design provisions of passive decay heat removal and defense-in-depth confinement. The worst consequence event was the ex-vessel LOCA because LiPb coolant contains several radioactive products. In this event, the hot but low-pressure LiPb coolant is leaked as the result of a pipe failure. The LiPb pool releases Hg 203 and Po 210 to the building air. After filtration and release from the facility vent stack, the 29 μg of Po 210 and the 40 μg of Hg 203 result in a dose of 0.51 mSv (51 mrem) to the maximum exposed individual member of the public. This dose is ≈5% of the 10 mSv (1 rem) threshold value for public evacuation.

Fusion power plant designs have little or no on-site inventories of high-level radioactive materials, which is a much smaller amount than that of fission power plants, and fusion inventories are also generally less radioactive than the ash piles of coal-fired power plants. As a comparison, coal-fired power plants emit radioactive and toxic species in flue gases and fly ash as they operate. Early studies of this fact in the 1970s and 1980s showed that the public in the immediate vicinity, a few miles, of large coal-fired power plants were receiving 0.01 to 0.05 mSv/year (1 to 5 mrem/year) from routine plant operation [12]. The newest coal-fired plants with additional pollution controls have reduced their airborne releases by several orders of magnitude, giving exposure of 0.05 μSv/year (0.005 mrem/year) in the immediate vicinity of the power plant [13].

36.1.2 Personnel Safety Discussion

The safety of power plant personnel falls into two basic areas, radiological safety and traditional industrial safety. Radiological safety is concerned with keeping personnel exposure to direct radiation and to radioactive materials as low as possible. Fusion designers have taken efforts to plan for isolation of plant operating areas to protect personnel from high magnetic and radio-frequency fields, ionizing radiation, and tritium fuel. Robotic maintenance is used to replace the fusion chamber components when needed so personnel do not receive any radiological exposure. Table 36.2 shows the ITER project safety goals and U.S. fission power plant exposure limits for facility personnel.

36.1.3 Radiological Safety

Fusion power plants will use the same fundamental principles as other radiological facilities to reduce personnel exposures: reduce exposure time, increase the distance between personnel and the hazardous materials, and use shielding to attenuate the ionizing radiation. Specifically, fusion designs have incorporated features to keep personnel radiation exposure low, including minimizing radiological inventories, confining these inventories in as small a volume as possible, identifying zones in the building to denote no-access and limited access radiation areas, controlling the time personnel work within these areas,

TABLE 36.2 The ITER Safety Objectives and U.S. Limits for Fission Facility Workers

	ITER [2]	U.S. Fission Facility Personnel [14]
Normal operations situations	Maximum individual dose ≤10 mSv/yr (1000 mrem/yr) Average individual dose ≤2.5 mSv/yr (250 mrem/yr)	≤50 mSv/year (5000 mrem/year) ≤150 mSv/year (15 rem) for lens of eye ≤500 mSv/year (50 rem) for skin
Incidents	<10 mSv/yr (1000 mrem/yr) per incident	
Accidents	Take into account the constraints related to the management of the accident and the post-accident situation	Occupational dose may exceed annual limits in accidents and emergencies
Hypothetical accidents beyond design basis	No disproportionate increase in risk from beyond design basis accidents (no cliff edge effect); possible counter-measures limited in time and space	

using radiation shielding placed as close to the inventory as possible, and using remote handling tools to perform tasks within radiation zones. All of these features reduce worker exposure. An example of this safety approach is seen with the ITER international project [15]. In addition to the low allowable values for individual worker radiation exposure per year, the ITER project also has a collective worker annual dose goal of 500 person-mSv (50 person-rem) for maintenance and inspection activities. This is the same goal planned for the Next Generation Nuclear Plant, a new high-temperature gas-cooled fission reactor [16]. This goal is possible because of the inherent safety in the ITER design, which incorporates good shielding, use of remote handling equipment, and good work planning. The United States also has a nuclear worker occupational exposure limit of 50 mSv/year (5 rem/year) [14]. As seen in Table 36.2, the ITER project goal is 20% of that value.

36.1.4 Industrial Safety

According to the U.S. fusion standard, fusion workers will be protected so the risks they are exposed to are no greater than those at a comparable industrial facility [1]. The two most comparable industrial facilities to fusion have been judged to be particle accelerators and fission power plants. Comparisons of industrial injury rates have been made between these types of facilities, and a goal for ITER of 0.3 lost workday cases per 100 workers per year has been suggested [17]. The JET Joint Undertaking (see www.jet.uk), the largest operating tokamak, and U.S. nuclear power plants have reached this low value. From 2003 to 2008, the U.S. national average lost workday case rate was 1.3 [18]. Following many of the same principles used for ionizing radiation safety (e.g., building zones, shielding, reducing exposure time), ITER also has made worker safety provisions for protection against cryogenic gases and liquids, vacuum in vacuum chambers, high temperature/high pressure coolant systems, pressurized gas systems, non-ionizing radiation, hazardous chemicals, magnetic fields, and other industrial hazards to fusion personnel [19]. Future power plants will also use these proven approaches for personnel safety [20]. The ITER international project will follow the occupational safety rules of France, the host country where the experiment will be built.

36.2 ENVIRONMENTAL ASPECTS OF FUSION

As mentioned earlier, fusion designers have the freedom to select materials with low neutron activation to build the fusion power plant. Carefully selecting the alloying elements of materials and controlling their impurities can reduce the long-lived by-products. Thus, low-activation materials have been developed worldwide with the main goal of generating only low-level waste, avoiding the need for deep geological disposal and its detrimental burden on future generations. Three main structural materials were developed over the past five decades: ferritic steel, vanadium alloy, and SiC/SiC composites [21]. These materials exhibit a potential for high performance under the challenging fusion radiation environment and satisfy the requirements of short-term activation and low decay heat. Therefore, fusion power plant radioactive waste is low-level waste similar to that of hospitals and industry. The fusion plant waste decays within 100 years rather than remaining radiotoxic for millennia.

The impact of the structural material choice on the activation and decay heat of the first wall (the most radioactive components in any fusion device) is displayed in Figure 36.2. A realistic level of impurities was included in the compositions of ferritic steel [11], vanadium alloy [22], and SiC/SiC composites [10]. For comparison, the activity of the fission spent fuel decreases by three to four orders of magnitude over a millennium. Within one day (the time scale of importance for the loss of flow/coolant events), the SiC/SiC decay heat reduces significantly, a salient safety feature of the SiC/SiC composites. In fact, the main safety advantages of fusion can be obtained with the use of the low-activation ferritic steel [11, 23, 24]. Advanced

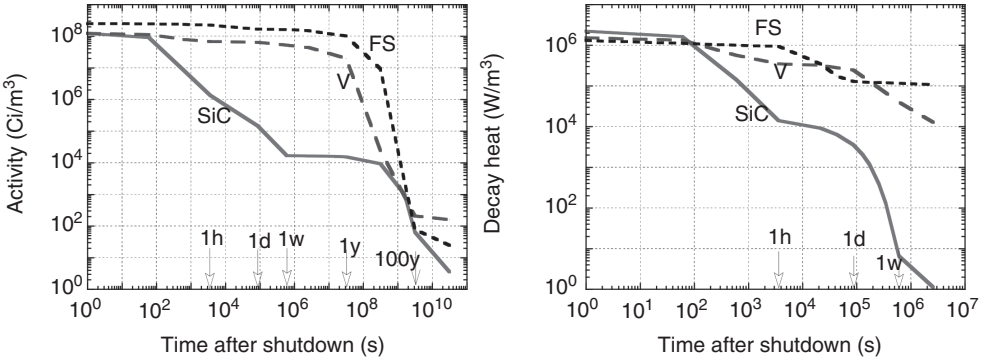

Figure 36.2 Specific activity and decay heat of first wall structure (100% dense materials).

materials (such as vanadium and SiC) demonstrate the full safety potential of fusion. Additionally, they offer economic advantages, permitting the first wall/blanket to operate at higher neutron wall loading (allowing more compact machines) and higher temperature (meaning higher thermal conversion efficiency and higher electrical power generation for a given plant size).

Over the past decades, the criteria that define an acceptable nuclear system evolved for two main reasons: (1) Existing commercial U.S. repositories will reach their maximum capacity by 2050 to 2060 [25] (even before building the first fusion power plant), and (2) the political difficulty of opening new repositories in the United States has lately proven to be extremely difficult with strong negative public perception. In reality, the actual environmental impact of nuclear facilities is not only determined by the level of waste (high or low), but also by the volume of radioactive materials a device generates. Because fusion power plants (tokamaks, spherical torii, stellarators) are sizable, the amount of mildly activated materials involved in the fusion power core is relatively large when compared to an advanced fission power plant core [27]. As such, fusion designers in many countries around the world developed a new framework for managing the large volume of activated materials that will be generated during fusion plant operation and after decommissioning [26]. The proposed integrated management strategy calls for recycling and clearing the fusion activated materials as much as practically possible to minimize the amount of radioactive waste assigned for geological disposal.

A promising approach to reducing the volume of low-level waste for disposal is recycling the material for further use, particularly steel and other metals with finite resources. Another approach is the clearance of very mildly activated materials. Clearance is unconditional release of material with only slight traces of radioactivity to the commercial market, or disposal in a non-nuclear landfill. The maturation of the recycling/clearance approach requires developing an integrated, life-cycle management scheme and understanding the levels of activation throughout the fusion power core, considering the remote handling issues, properties of recycled materials, and economic implications [25]. These essential needs are certainly influenced by the fusion design configurations, materials selection, and operational performance. Over the past 10 years, numerous fusion studies indicated that fusion would be greatly helped by recycling and clearance, and, from a science perspective, these approaches are technically feasible for any fusion device employing low-activation materials, advanced radiation-resistant remote handling equipment, and clearance guidelines for slightly radioactive materials. In reality, the actual environmental impact of fusion is not only determined by the level of waste (high or low), but also by the volume of radioactive materials a fusion device generates. Because fusion power plants (tokamaks, spherical torii, and stellarators) are sizable, the amount of mildly activated materials involved in the fusion power core is relatively large when compared to an advanced fission power core [29]. Thus, fusion would be greatly helped by recycling and clearance.

36.2.1 Recycling

The primary goal for recycling is to reuse the activated materials within the nuclear industry only, not in the commercial market. This process includes storage in continuously monitored facilities (to allow the radioactivity to decay), segregation of materials, crushing, melting, and re-fabrication [28]. At present, limited scale recycling within the nuclear industry has been proven feasible and economical in Europe and at several U.S. national laboratories. In the United States, mildly radioactive materials have been recycled. For example, the Idaho National Laboratory recycled over 100 tons of lead from shielding casks to be used as a shielding wall at the Idaho Accelerator Center [29]. It is expected that recycling within the fission industry will continue to develop at a fast pace to support the fission spent-fuel reprocessing systems. The fusion industry will certainly benefit from fission recycling experience and its related governmental regulations.

Past fusion studies have indicated that all components can potentially be recycled after a specific storage period using conventional and advanced remote handling (RH) equipment that can handle high dose rates of 10,000 Sv/hour or more [25–27]. Figure 36.3 illustrates the variation of the recycling dose rate with time for typical fusion components, indicating strong component dependence. These curves essentially determine the remote handling needs (hands-on, conventional, or advanced tools) and the interim storage period necessary to meet the dose limit. Besides the dose to equipment, other important recycling criteria include the decay heat level during reprocessing, economics of remote fabrication, physical properties of recycled materials, efficiency of the detritiation system that removes tritium before recycling, and the acceptability of the nuclear industry to recycled materials.

36.2.2 Clearance

Under clearance, slightly radioactive components (such as the bioshield) can be declassified into non-radioactive waste and handled as if they are no longer radioactive. Such materials with traces of radioactivity can be reused (after a specific cooling period) without restrictions in the commercial market and recycled into consumer products.

As Figure 36.3 indicates, all recyclable fusion in-vessel components (first wall, blanket, shield, divertor, and

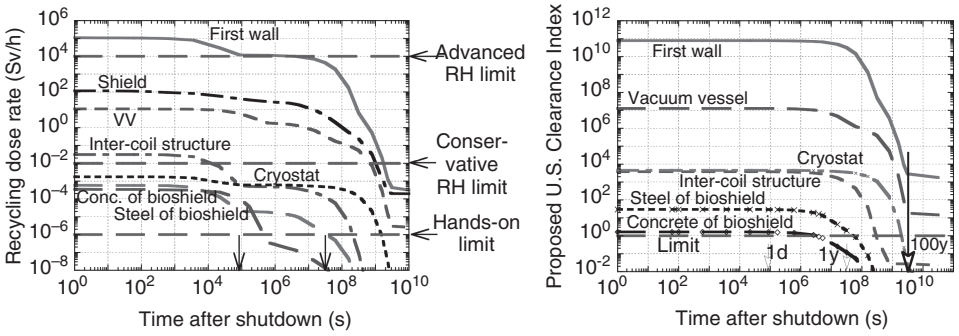

Figure 36.3 Recycling dose rate and clearance index for typical fusion components.

vacuum vessel) cannot be cleared even after an extended storage period of 100 years [30]. Fortunately, the bioshield along with the cryostat and some magnet constituents qualify for clearance, representing ≈70% of the total fusion material volume [11].

During the 2000s, clearance guidelines for mildly radioactive materials were issued by the U.S. Nuclear Regulatory Commission [31], International Atomic Energy Agency [32], and other organizations. In the United States, the free release of clearable fission materials has been performed only on a case-by-case basis during decommissioning projects. A clearance market currently exists in Germany, Spain, Sweden, Belgium, and other European countries [30], but not in the United States.

36.3 REMARKS AND CONCLUSIONS

Fusion energy holds promise as a safe and environmentally benign energy source for electrical power generation. Magnetic confinement fusion has several inherent safety aspects, including the nature of fusion plasma and its controllability, low fuel inventories, and the energies used to control the plant (e.g., magnetic fields and radiofrequency energy) do not propagate from the plant site to nearby communities. Fusion has the advantages of breeding tritium fuel as needed. Fusion also allows designers to select low-activation materials that will reduce on-site inventories and reduce waste generation. Fusion designers can conceive plant layouts that will protect workers and the public, as evidenced by the ITER international project.

Effective progress in the environmental field hinges on how any source of energy handles the waste: radioactive, chemical, or hazardous. For over a half-century, the nuclear fission industry struggled with the disposal of high- and low-level radioactive wastes as the prediction of deep geological storage conditions is less accurate for long times into the future. Fusion power plants would have less environmental impact than other types of power plants, such as coal or nuclear fission. Fusion radioactive wastes are low-level waste, less radiotoxic than fission product high-level waste. Fusion wastes are similar to hospital and industrial wastes that decay reasonably quickly to stable nuclides. The mandate of fusion to promote nuclear fusion as a clean source of energy will be significantly strengthened if the fusion problem of large radioactive waste volume is solved by adopting the recycling and clearance approaches, thus avoiding deep geological disposal. This strategy calls for major rethinking and research to make these approaches a reality. Admittedly, a substantial challenge lies in influencing the policy, regulatory, and public acceptance aspects, particularly in the United States. The ongoing related developments in the areas of fission spent fuel processing and fission reactor dismantling during decommissioning will be of great importance to fusion before committing to commercialization in the 21st century.

REFERENCES

1. U.S. Department of Energy, *Safety of Magnetic Fusion Facilities: Requirements*, DOE-STD-6002-96, 1996.
2. N. P. Taylor, D. Baker, S. Ciattaglia, P. Cortes, J. Elbez-Uzan, M. Iseli, S. Reyes, S. Rosavallon, and L. Topilski, Key Issues in the safety and licensing of ITER, *9th IAEA Technical Meeting on Fusion Power Plant Safety*, Vienna, Austria, July 15–17, 2009, ITER document D_2M5X89 v1.1.
3. U.S. Environmental Protection Agency, *Manual of Protective Action Guides and Protective Actions for Nuclear Incidents*, EPA 400/R/92-001, revised 1991.
4. U.S. Code of Federal Regulations, *Dose Limits for Individual Members of the Public*, 10CFR20.1301, November 25, 2008.
5. U.S. Code of Federal Regulations, *Determination of Exclusion Area, Low Population Zone, and Population Center Distance*, 10CFR100.11, November 25, 2009.
6. Agency for Toxic Substances and Disease Registry, *Toxicological Profile for Ionizing Radiation*, profile #149, U.S. Department of Health and Human Services, September 1999.
7. Idaho Department of Environmental Quality, *INL Oversight Program: Guide to Radiation Doses and Limits*, available at http://www.deq.idaho.gov/inl_oversight/radiation/radiation_guide.cfm, visited November 29, 2009.

8. S. Reyes, L. Topilski, N. Taylor, B. J. Merrill, and L. Sponton, Updated modeling of postulated accident scenarios in ITER. *Fus. Sci. Tech.*, 2009, **56**, 789–793.
9. N. Taylor, D. Baker, V. Barabash, S. Ciattaglia, J. Elbez-Uzan, J.-P. Girard, C. Gordon, M. Iseli, H. Maubert, S. Reyes, and L. Topilski, Preliminary safety Analysis of ITER. *Fus. Sci. Tech.*, 2009, **56**, 573–580.
10. D. A. Petti, B. J. Merrill, R. L. Moore, G. R. Longhurst, L. El-Guebaly, E. Mogahed, D. Henderson, P. Wilson, and A. Abdou, ARIES-AT Safety design and analysis. *Fus. Eng. Des.*, 2006, **80**, 111–137.
11. B. J. Merrill, L. A. El-Guebaly, C. Martin, R. L. Moore, A. R. Raffray, D. A. Petti, and the ARIES-CS Team, Safety assessment of the ARIES compact stellarator design. *Fus. Sci. Tech.*, 2008, **54**, 838–863.
12. J. Tadmor, Radioactivity from coal-fired power plants: a review. *J. Environ. Radioact.*, 1986, **4**, 177–204.
13. T. Zeevaert, L. Sweeck, and H. Vanmarcke, The radiological impact from airborne routine discharges of a modern coal-fired power plant. *J. Environ. Radioact.*, 2006, **85**, 1–22.
14. U.S. Code of Federal Regulations, *Occupational Dose Limits for Adults*, 10CFR20.1201, December 1, 2009.
15. P. Cortes, N. Taylor, and J. Elbez-Uzan, Workers and members of the public radiation protection concerns for ITER and fusion power plants. *9th IAEA Technical Meeting on Fusion Power Plant Safety*, Vienna, Austria, July 15-17, 2009, ITER document D_2MNTBH v1.0.
16. J. W. Collins, *Next Generation Nuclear Plant System Requirements Manual*, INL/EXT-07-12999, revision 3, Idaho National Laboratory, September 2009.
17. L. C. Cadwallader, Occupational injury rate estimates in magnetic Ffusion experiments. *Fus. Sci. Tech.*, 2007, **52**, 1017–1021.
18. U.S. Department of Labor, *Bureau of Labor Statistics*, http://www.bls.gov/, visited November 28, 2009.
19. International Atomic Energy Agency, *ITER Technical Basis*, ITER EDA Documentation Series No. 24, January 2002, Chapter 5.
20. L. C. Cadwallader, Personnel safety for future magnetic fusion power plants. *9th IAEA Technical Meeting on Fusion Power Plant Safety*, Vienna, Austria, July 15–17, 2009, INL/CON-09-15949.
21. S. Zinkle, Advanced materials for fusion technology. *Fus. Eng. Des.*, 2005, **74**, 31–40.
22. D. Steiner, L. El-Guebaly, S. Herring, H. Khater, E. Mogahed, R. Thayer, and M. S. Tillack, ARIES-RS safety design and analysis. *Fus. Eng. Des.*, 1997, **38**, 189–218.
23. H. Y. Khater, E. A. Mogahed, D. K. Sze, M. S. Tillack, X. R. Wang, and the ARIES Team, ARIES-ST safety design and analysis. *Fus. Eng. Des.*, 2003, **65**, 285–301.
24. I. Cook, Analyses performed within the European Safety and Environmental Assessment of Fusion Power (SEAFP). *Fus. Eng. Des.*, 1995, **30**, 171–190.
25. L. A. El-Guebaly and L. Cadwallader, Integrated management strategy for fusion activated materials: U.S. position and regulations. *9th IAEA Technical Meeting on Fusion Power Plant Safety*, Vienna, Austria, July 15–17, 2009.
26. M. Zucchetti, L. Di Pace, L. El-Guebaly, B. N. Kolbasov, V. Massaut, R. Pampin, and P. Wilson, The back end of the fusion materials cycle. *Fus. Sci. Tech.*, 2009, **52**, 109–139.
27. L. El-Guebaly, V. Massaut, K. Tobita, and L. Cadwallader, Goals, challenges, and successes of managing fusion active materials. *Fus. Eng. Des.*, 2008, **83**, 928–935.
28. V. Massaut, R. Bestwick, K. Brodén, L. Di Pace, L. Ooms, and R. Pampin, State of the art of fusion material recycling and remaining issues. *Fus. Eng. Des.*, 2007, **82**, 2844–2849.
29. L. El-Guebaly, V. Massaut, K. Tobita, and L. Cadwallader, *Evaluation of Recent Scenarios for Managing Fusion Activated Materials: Recycling and Clearance, Avoiding Disposal*, UWFDM-1333. University of Wisconsin Fusion Technology Institute, 2007, available at http://fti.neep.wisc.edu/pdf/fdm1333.pdf.
30. L. El-Guebaly, P. Wilson, and D. Paige, Evolution of clearance standards and implications for radwaste management of fusion power plants. *Fus. Sci. Tech.*, 2006, **49**, 62–73.
31. U.S. Nuclear Regulatory Commission, *Radiological Assessments for Clearance of Materials from Nuclear Facilities*, NUREG-1640, 2003, available at: http://www.nrc.gov/reading-rm/doc-collections/nuregs/staff/sr1640/.
32. International Atomic Energy Agency, *Application of the Concepts of Exclusion, Exemption and Clearance*, IAEA Safety Standards Series, No. RS-G-1.7, 2004, available at: http://www-pub.iaea.org/MTCD/publications/PDF/Pub1202_web.pdf.

37

INERTIAL FUSION ENERGY TECHNOLOGY

ROKAYA A. AL-AYAT, EDWARD I. MOSES AND ROSE A. HANSEN
Lawrence Livermore National Laboratory, Livermore, CA, USA

37.1 ENERGY REQUIREMENTS

Providing for the world's growing energy needs is one of the most urgent, and difficult, challenges facing us. With the United Nations predicting world population growth from 6.6 billion in 2007 to 8.2 billion by 2030, demand for energy will increase substantially over that period, and beyond. The Reference Scenario outlined by the International Energy Agency projects that worldwide energy demand will grow 40% between 2009 and 2030. Over 70% of the increased energy demand is from developing countries, led by China and India. During that same time period, electricity demand will require at least 4800 GW of additional capacity (equivalent to five times the existing capacity of the United States). This scenario also projects that over 1.3 billion people will still lack access to electricity. Both population growth and increasing standards of living in developing countries will cause vigorous growth in energy demand.

Currently proposed solutions to match demand with supply predict strong regional dependencies and a portfolio composed of fossil fuels, renewables, and nuclear power. These studies invariably raise a potentially intractable problem—requiring very large fractions of renewable energy at a level that is often inconsistent with other societal pressures (e.g., land use for housing or farming). Or they require nuclear power at a level that demands breeding and reprocessing cycles, high volumes of radioactive waste storage, and complex governance procedures to mitigate the danger of nuclear proliferation.

Auspices Statement: This work performed under the auspices of the U.S. Department of Energy by Lawrence Livermore National Laboratory under Contract DE-AC52-07NA27344.

37.2 WHAT IS FUSION ENERGY?

Fusion, the energy source that drives the Sun and the stars, has long been pursued as a solution to this energy supply conundrum. It is a nuclear process that forces nuclei of light atoms, like hydrogen, together to form the nuclei of heavier elements. In contrast, nuclear fission splits the nuclei of heavy elements like uranium and plutonium into lighter elements. Fusion, like fission, needs only a small amount of fuel to release vast amounts of energy. Harnessing fusion energy requires construction of a system able to heat matter to temperatures comparable to those found at the center of the Sun and to sustain power output from the system at a level that significantly exceeds the power required to initiate the fusion process.

Nuclear Energy Encyclopedia: Science, Technology, and Applications, First Edition (Wiley Series On Energy).
Edited by Steven B. Krivit, Jay H. Lehr, and Thomas B. Kingery.

The simplest fusion fuel is a mixture, in equal amounts, of the two heavy isotopes of hydrogen (deuterium and tritium), because this fuel requires the lowest amount of energy to initiate the process. Deuterium is extracted from water, and tritium is derived from the metal lithium, a relatively abundant resource. Because the energy released in burning fusion fuels is a few million times greater than burning fossil fuels, only a small amount of material is needed. As such, the fuel is virtually inexhaustible. The lithium in one laptop battery plus the deuterium from half a bathtub of water would meet an individual's electricity production needs for 30 years.

37.3 FUSION AS PART OF GLOBAL ENERGY STRATEGY

Fission, fusion, and renewable energy (including biofuels) are the only energy sources capable of satisfying the Earth's need for power for the next century and beyond without the negative environmental impacts of fossil fuels. Substantially increasing the use of nuclear fission and renewable energy now could help reduce dependency on fossil fuels. However, fusion has the potential of becoming the ultimate baseload energy source. It offers profound benefits in the context of a sustainable, low-carbon economy:

- An abundant, effectively limitless fuel supply.
- Very high generating capacity, at an optimum level per plant for central electricity generation ($\sim$0.5–2 GWe).
- No greenhouse gas emissions.
- Low environmental impact. The principal external by-product is waste heat, which could be used as part of an integrated energy network. The "ash" from burning the fuel is non-radioactive helium. The residual by-products within the power plant itself are short-lived radioisotopes that can be disposed of as low-level waste.
- Inherent safety, with no danger of runaway reactions or meltdown. The principal hazardous material is tritium (a radioactive isotope of hydrogen), but the amount that is present in the reacting plasma at any time is small.
- Compatibility with the existing electricity grid infrastructure (plant location and transmission lines).
- Produces power on demand, consistent with baseload grid requirements.
- Provides options for utility-specific adaptation to different configurations (including fission waste disposal).

These environmental, commercial, and security benefits have motivated a multibillion-dollar research effort spanning over five decades. This worldwide effort has yielded major progress. The roadmap for transforming fusion energy into a source of electricity can be thought of as a five-step process: (1) Demonstrate that the underlying principle of achieving fusion is sound; (2) achieve net energy gain from a fusion system; (3) retire technical challenges in a directed research, development, and engineering effort; (4) build and demonstrate a prototype power plant; and (5) build commercial power plants.

Substantial amounts of fusion energy were produced during brief pulses in laboratory experiments during the 1990s, and the principles of how to produce fusion energy in a controlled and repeatable manner are understood. For example, 5 to 10 megajoules of fusion energy per pulse were repeatedly and predictably produced in the TFTR (Princeton, NJ, USA) and JET (Culham, UK) facilities using a deuterium–tritium fuel mixture. While step 1 can therefore be considered complete, improved scientific understanding and technical advances are still needed to achieve the subsequent steps.

By the time this text is published, step 2 may well have been achieved (see National Ignition Facility section below). Net energy gain means getting more energy out of the fusion reaction than was injected into the fuel to make it burn. Demonstrating substantial energy gain will be a major achievement along the path to develop commercially viable fusion power.

37.4 APPROACHES TO FUSION ENERGY

Scientists have developed a variety of devices and systems in an effort to contain and heat the deuterium and tritium fuel to the densities and temperatures needed to sustain thermonuclear fusion reactions. Two main paths are being pursued: magnetic confinement fusion (MCF) and inertial confinement fusion (ICF).

The MCF approach (see separate chapter) uses magnetic fields to confine the plasma—a hot, electrically charged gas—at the required density until it is heated to the required temperature (about 100 million degrees) for fusion reactions to occur. The magnetic field must also insulate the hot plasma so that the energy is confined long enough to achieve net energy gain. Practical limits on the strength of magnetic fields place upper limits on the pressure of the extremely hot fuel. As a result, the density of the hot fuel must be much less than the air we breathe, and the energy must be confined for up to a few seconds. For power plants based on MCF, the burning of fusion fuel is envisioned to take place on a continuous basis, or at least in a series of long pulses, with each one lasting for hours.

The ICF approach is the focus of this chapter. It uses the inertia associated with the mass of the fuel to replace the need for a magnetic field. For this approach to work, a small capsule of fuel must to be compressed to more than 100 times solid density before the fuel is ignited. The inertia of the fuel delays the expansion just long enough (roughly a nanosecond) to allow sufficient fuel to fuse and yield energy gain. No magnetic field is needed to hold or insulate this plasma. However, these pulses must be repeated often enough to provide a continuous source of heat.

Small research efforts are exploring a third approach, called magneto-inertia fusion (MIF), which is a hybrid of the two main approaches. Like ICF, it relies on inertia to confine the plasma, but it adds a magnetic field in the fuel to help insulate the fuel from losing heat too quickly. This reduces the requirements on the speed and intensity of the compression of the fuel capsule. Power plants based on this approach would require a lower repetition rate, but must deal with more energy per event than in an ICF-based plant.

37.5 PATH TO FUSION ENERGY THROUGH INERTIAL CONFINEMENT

An ICF-based power plant would operate conceptually like a car engine: Fuel is injected (in the form of a ball-bearing-sized capsule of hydrogen isotopes); a piston is then used to compress and heat the fuel to the point of ignition (with the piston being a large laser or other driver); and finally, the spent fuel is exhausted, and the cycle repeats. Repetition rates of up to 10 times a second (similar to an idling car engine) are sufficient to produce a gigawatt (GW) of electrical power from an inertial fusion energy (IFE) plant.

To heat and compress the fuel, energy is delivered for a few nanoseconds to the outer layer of the fuel capsule using some type of "driver." Three types of drivers—lasers, heavy-ion accelerators, and Z-pinches—are described later. The heated outer layer explodes outward, producing a reaction force against the remainder of the target, accelerating the target material inward, and sending shock waves into the center. A sufficiently powerful set of shock waves can compress and heat the fuel at the center so much that fusion reactions occur. The energy released by these reactions will then heat the surrounding fuel, which may also begin to undergo fusion. The goal is to produce a condition known as ignition, where this heating process causes a chain reaction that burns a significant portion of the fuel (see Fig. 37.1).

"Burning" the fuel means fusing deuterium and tritium nuclei together to form a helium nucleus and a neutron. The energy produced is carried by the helium nucleus (3.5 MeV) and the neutron (14.1 MeV). The energetic helium nuclei heat the fuel to sustain the fusion reactions. The neutrons are used to breed tritium from lithium in a "blanket" that covers the outside of the fusion chamber. IFE plants would deliver a successive stream of fuel-bearing targets (up to 10 per second) to the fusion chamber and convert the released energy into heat. That heat would be carried from the chamber by a fluid to drive the turbine and generator to produce electricity.

The small amount of helium generated would be collected and become a useful by-product. A fusion power plant would produce no climate-changing gases.

37.5.1 Components of an IFE Power Plant

An IFE plant will have separate areas for the driver, a factory for making the targets, a chamber where the fusion reactions occur, and a turbine to generate electricity (see Fig. 37.2).

This separability of plant components is a major benefit of the IFE approach. It provides design flexibility and

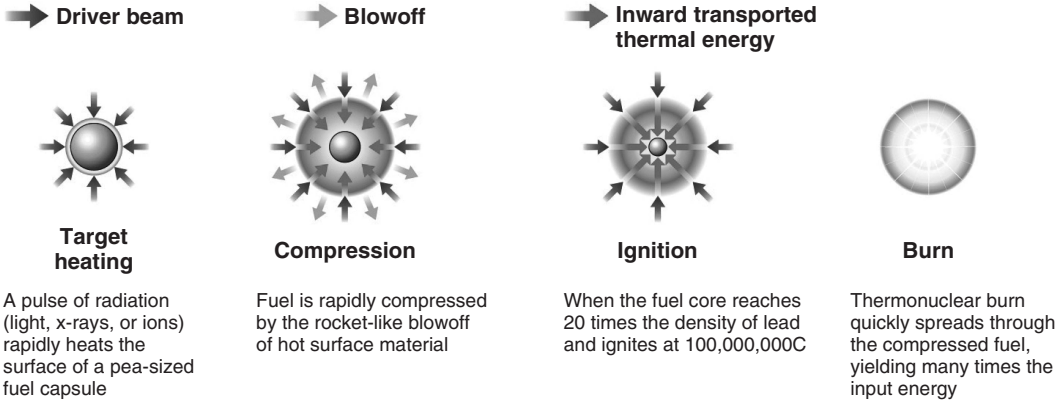

Figure 37.1 The figure illustrates target heating, compression, ignition, and then burn (*courtesy Lawrence Livermore National Laboratory*).

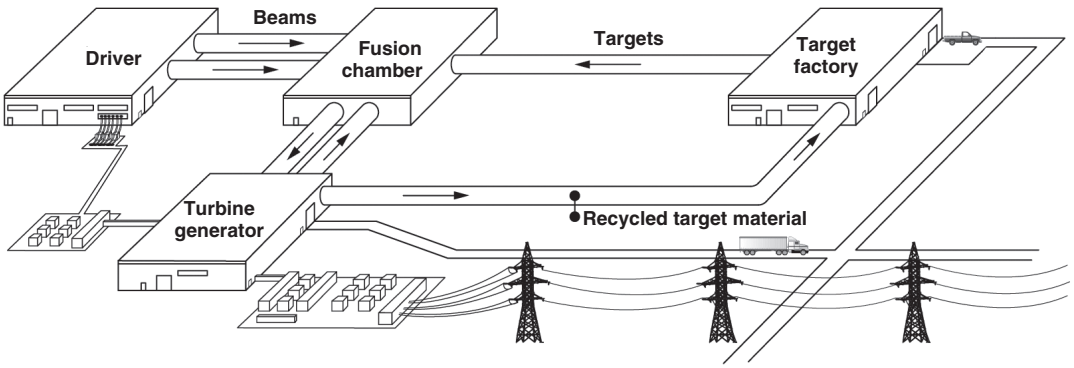

Figure 37.2 Basic layout of an IFE power plant, showing the driver, target factory, fusion chamber, and turbine generator to produce electricity. The beam component would only be present for certain types of drivers. In reality, these components could be assembled in a single building (*courtesy of Lawrence Livermore National Laboratory).*

allows the driver and target factory to be protected from the fusion radiation environment. It also allows each aspect of the system to be developed and optimized separately, such that the timescale from one generation to the next can be much shorter than for an integrated system. The separability also enables the integration of improvements into the system as they become available through concurrent development activities. For commercial power plants, the modularity of subcomponents (e.g., the driver) will reduce maintenance and construction costs, while maximizing system availability and reliability.

37.5.2 Next Steps in Developing IFE

As described above, the second step in the five-step process of developing fusion energy is demonstrating net energy gain. The next section of this chapter describes two experimental facilities that are focused on this demonstration. It is possible that the first facility may have demonstrated ignition and net energy gain by the time this book is printed.

Such an achievement should launch a major effort to demonstrate the integration of this ignition process into a prototype power plant, which is step 4 in the five-step process. The design and construction of such a prototype will require the development of materials, technologies, and systems not required in existing research facilities (step 3), as well as improving the performance of those presently used. This includes increasing the repetition rate of implosions by a factor of 100,000. Subsequent sections of this discussion outline these requirements, and describe the drivers, ignition techniques, and associated technologies that are being studied to meet these requirements.

Building and testing of a prototype plant will be necessary to provide the confidence that an IFE power plant can achieve commercial plant requirements, including those of safety, economics, and environmental features.

37.6 DEMONSTRATING IGNITION AND HIGH-ENERGY GAIN

The two world-class engineering research facilities described in this section—the National Ignition Facility (NIF) at Lawrence Livermore National Laboratory in Livermore, California, and the Laser Mégajoule (LMJ) being built near Bordeaux, France—are the culmination of over five decades of advances in scientific understanding, computing power, and a host of advanced technologies. Among their missions is the demonstration of step 2—achieving ignition and demonstrating high energy gain on the path to commercial fusion power.

37.6.1 National Ignition Facility

The National Ignition Facility (NIF), a laser-based ICF facility designed to achieve thermonuclear fusion ignition and burn and net energy gain in the laboratory, was completed at the Lawrence Livermore National Laboratory (LLNL) in the United States in 2009 (see Fig. 37.3). NIF consists of 192 laser beams, housed in a 10-story building the size of three football fields. In March 2009, NIF achieved over a 1 MJ of energy—60 times more than any previous laser system. NIF experiments using all its beams have set new records for power delivery by a laser.

Experiments designed to pursue the ignition goal were begun in 2010, using laser energies of 1 to 1.3 MJ. Fusion yields of the order of 10 to 35 MJ (or net energy gains of 10 to 25) are expected before the end of 2012. By optimizing target and laser performance, net energy gains of up to 70 could ultimately be demonstrated on NIF.

If successful, NIF will be the first laboratory facility of any type to demonstrate ignition and net energy gain.

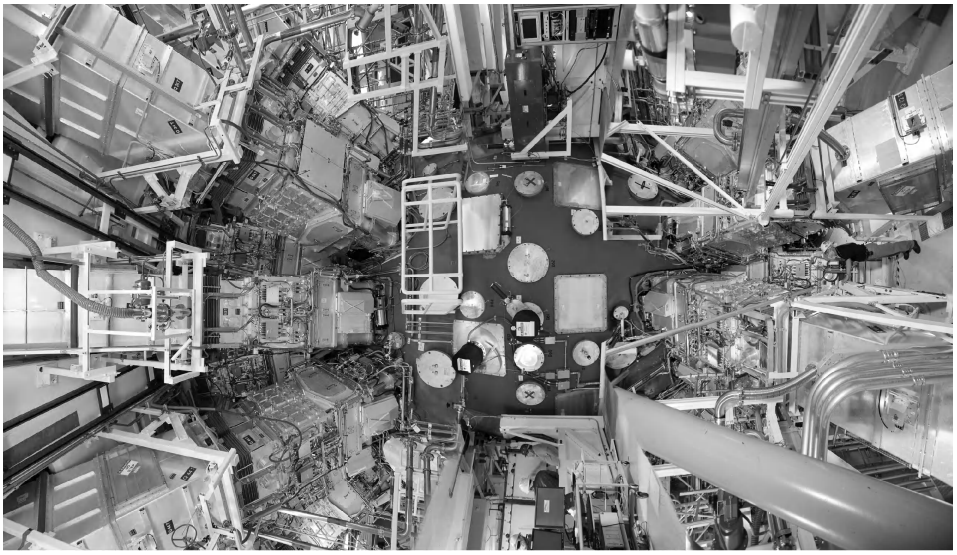

Figure 37.3 The National Ignition Facility's massive 10-meter-diameter target chamber (central sphere). The men wearing hard hats at the left center of the picture provide a scale of the size of the chamber. The square openings and the ducts attached to the target chamber are the paths for NIF's 192 laser beams (four beams per duct). The round openings accommodate nearly 100 pieces of diagnostic equipment (*courtesy of Lawrence Livermore National Laboratory).*

37.6.2 Laser Mégajoule

Laser Mégajoule (LMJ) is an experimental ICF facility being built near Bordeaux, France, by the French atomic energy commission, CEA (see Fig. 37.4). The LMJ baseline design contains 240 laser beamlines arranged in eight groups of 30, making it similar to its U.S. counterpart, NIF. The initial ignition experiments will use 160 beams, delivering up to 1.4 MJ of laser energy to its targets. Currently, the LMJ system is expected to commence operations in 2014. It is the largest ICF experiment to be built outside the United States.

37.6.3 How NIF and LMJ Work

NIF and LMJ use solid-state, neodymium glass amplifiers pumped by the energy from large flashlamps. The lasers deliver about 5 MJ of infrared laser energy in a few-nanosecond pulse. The laser pulse is sent through the amplifiers several times by an optical switch to maximize the energy extracted and thus enhance the system efficiency. A deformable mirror is used to remove imperfections in the beams.

Before reaching the target chamber, the energetic beams are reflected off mirrors to arrange their entry into the spherical chamber from all sides. The beam energy coming out of the amplifiers is so high that the cross-section of each beam must be kept larger than a square foot to avoid damaging the optics. Just before entering the chamber, the beams pass through optical frequency multipliers to convert the infrared laser light into ultraviolet light. This conversion to a shorter wavelength enhances the efficiency of the interaction with the fuel-bearing target. As the large beams enter the chamber, they are each focused to a very small spot size at the chamber center. The beams hit the target with a precision of better than 50 microns (about the thickness of a piece of paper).

Although both facilities are designed to achieve ignition and net energy gain, neither is designed to harness the enormous potential of fusion for energy generation. A fusion power plant would require extensions and additions to the technologies used in these facilities.

37.7 KEY REQUIREMENTS FOR AN IFE POWER PLANT

Following industry best practice, a fusion power plant must meet a number of top-level requirements consistent with commercial operation. These include standardized, proven technology, maintainability and constructability, a high level of quality assurance, competitive economics, and environmental sustainability. For IFE, this translates into the need to improve performance in the following four areas:

1. *High Energy Gain and Efficiency*: The efficiency of the driver in converting energy from the electrical power grid to the energy needed to compress the capsule, coupled with the energy gain of the fuel

Figure 37.4 General view of the Laser Mégajoule laser hall, where the beam amplification structures are being assembled *(Courtesy CEA)*.

capsule, must be sufficient to yield substantial net energy. Generally, the product of capsule energy gain and driver efficiency must be about 10 or greater for acceptable power plant economics. As a result, the fusion energy output must be roughly 50–150 times greater than the driver energy input to the capsule, depending on the 7% to 20% efficiencies projected for the various drivers. The flashlamp-pumped lasers used in NIF and LMJ will not be able to reach these efficiencies or the required repetition rates.

2. *Repetition Rate*: The driver and the fabrication and insertion of the target (which includes the fuel capsule) must operate at a repetition rate that is sufficient to produce economically useful power. The chamber must be reset to a sufficiently inactive state after each shot to allow insertion of the next target and for the transmission and focusing of the next pulse of energy from the driver to that target. Repetition rates of 0.1 to 10 per second are needed, depending on the driver. By comparison, the repetition rates for NIF and LMJ at full power are only a few shots per day.
3. *Energy Conversion and Tritium Breeding*: The energy released from the ignited target is mainly in the form of energetic ions, neutrons, and x-rays. This energy must be absorbed by a "blanket" in the chamber and converted into heat that can be efficiently used to drive electric generators. The blanket must also use the emitted neutrons to breed sufficient new tritium from lithium and allow for the extraction of the tritium to sustain the fuel supply. LMJ and NIF do not have blankets.
4. *Durability, Availability, and Reliability*: The components in an IFE system must carry out the above functions with sufficient durability for the high-capacity factors required in an attractive energy system. Reliable automated systems must be engineered to replace any components that have a short working lifetime. All the major plant components and systems must operate consistently and reliably, for a better than 90% overall availability.

This complex set of interrelated performance requirements presents major challenges to the scientists and engineers dedicated to demonstrating IFE as an attractive energy source. Each of the three drivers being studied leads to conceptual IFE plants with different potential advantages and challenges.

Fortunately, great advantage can be taken from the separability of the plant components. As previously pointed out, the components can be developed and tested separately and often at lower cost than fully integrated facilities. However, the IFE power plant ultimately requires successful integration of all the components. Fusion system studies help guide the research by pointing out opportunities and problem areas. As understanding and demonstrated performance progress, the potential of the various approaches can be assessed with more certainty, and the details of a prototype power plant design will become clearer.

37.8 DRIVERS

This section describes the IFE drivers that are being studied, including some of the facilities used in those studies. When the above performance measures are applied to drivers, they place constraints not only on the repetition rate, reliability, and efficiency of energy delivered to a high-gain target, but also on the capital cost of the driver. System studies indicate that this capital cost should be less than about $400 per joule of energy delivered to the target, depending on the specific driver characteristics and associated target gain.

37.8.1 Lasers

Lasers are attractive because of their demonstrated ability to compress energy into the very short timescales and spatial scales required to implode fusion fuel capsules. The type of lasers used in NIF and LMJ are the drivers that have been most intensely studied and developed; however, efficiency and rep-rate limitations prevent serious consideration of flashlamp-pumped lasers for use in IFE power plants. To overcome these limitations, research is being carried out on both krypton-fluoride (KrF) gas lasers and diode-pumped solid-state lasers (DPSSL).

37.8.1.1 KrF Lasers The laser medium in a KrF laser is a gas that can be circulated for heat removal in high pulse-repetition-rate applications such as IFE. Faster cooling makes it easier to achieve the required repetition rates of 5 to 10 Hz. High rep-rate operations have been tested using the Electra facility at the U.S. Naval Research Laboratory in Washington, DC.

Target physics experiments are being conducted using the Nike KrF laser, also at that laboratory. KrF lasers operate at a shorter wavelength (248 nm) than the typical frequency-tripled wavelength (351 nm) of the DPSSLs. This shorter wavelength allows higher intensities to be applied before triggering instabilities in the target. As a result, the required gains of 140 are predicted for less energy (1.1 MJ) delivered. This advantage is partially offset by lower predicted driver efficiency of about 7% for KrF versus 10% for DPSSLs. In addition, the KrF lasers team is exploring high beam uniformity for optimum laser–target physics, the brightness to achieve the required intensity on target, a modular architecture for low development costs, and a pulsed power-based industrial technology that scales to a power-plant-sized system.

37.8.1.2 Diode-Pumped Solid State Lasers DPSSLs, which build on NIF laser technology, use diodes instead of flashlamps to pump a solid-state laser, dramatically reducing the cool-down time needed between laser firings. Further improvement in repetition rate has been achieved using new laser architecture. LLNL's Mercury laser, for example, is a prototype DPSSL capable of the required 10 Hz rep rate. However, it has a smaller aperture than a NIF beamline, and therefore lower power. Another repetition rate challenge for the DPSSL approach is the development of a high-average-power frequency converter to 351 nm light. DPSSLs may ultimately improve the power and cost of solid-state lasers enough to enable their use as fusion power plant drivers.

Progress continues on durability issues for different components needed for KrF laser and DPSSL drivers. For KrF lasers, the goal is two years of continuous operation at 5 Hz. The diode arrays for a DPSSL are projected to last 30 years at 10 Hz.

Final optics presents another durability issue for both the KrF and DPSSL. In both systems, these optics must survive the high-intensity ultraviolet light of the laser beam and the debris, neutrons, and x-ray radiation from the exploding target. One approach uses grazing incidence metal mirrors. Aluminum-coated silicon carbide is one of the types being considered. Multilayer dielectric mirrors offer another potential option, and transmissive fused silica lenses may provide an option for DPSSLS.

37.8.2 Heavy-Ion Accelerators

Heavy-ion (HI) drivers for fusion share the same basic technology as existing accelerators used for a range of scientific and engineering pursuits. This experience indicates that an HI driver could meet the efficiency, repetition rate, and durability performance measures.

Magnetic lenses outside the target chamber would focus the HI beams on the target. The penetration of heavy ions into dense matter is greater than ultraviolet or x-ray photons. This feature yields more efficient energy coupling to the target. It also allows more efficient penetration through the higher vapor pressures in the target chamber that would occur if liquid thick-walled blankets were to be used (see target chamber discussion below). These features could result in comparatively low capital costs.

A major challenge for the HI approach is to demonstrate the ability to focus an energetic (10 KJ) beam onto a target with the required short-pulse length (few ns) and small spot size (few mm radius). U.S. researchers are developing designs that use induction accelerators, while European and Japanese groups prefer radio-frequency accelerators, similar to those used in high-energy physics. To manage the significant excess electric charge of the ions, U.S. conceptual designs (for example, Fig. 37.5) accelerate many beams in parallel, and Europeans plan to accumulate charge gradually in a series of storage rings. Both approaches also require the beam duration to be severely reduced from its initial value, by about three orders of magnitude for induction machines and six for radio-frequency accelerators. The present research is

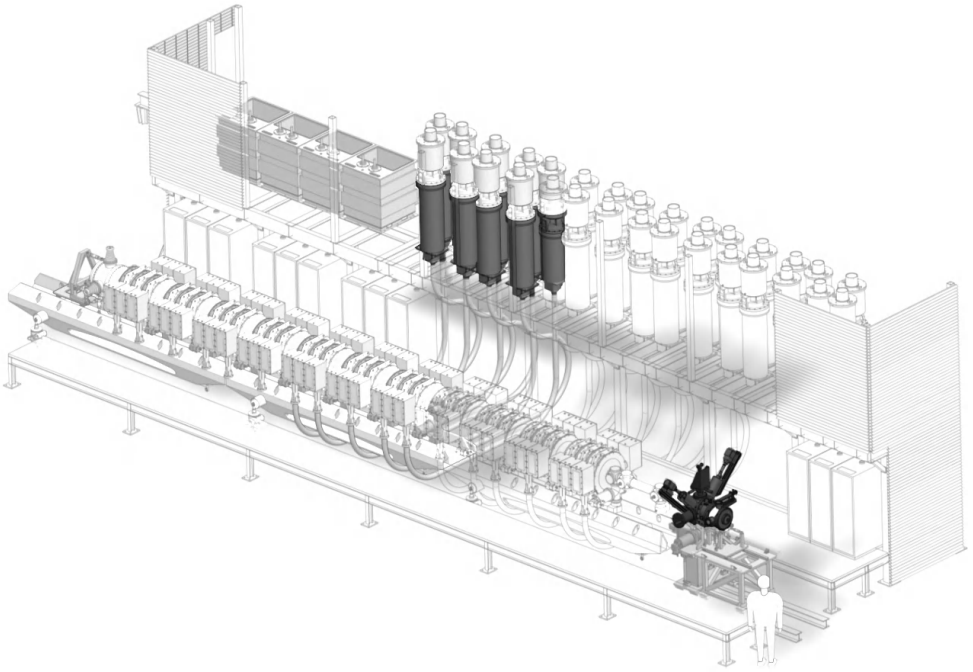

Figure 37.5 Sketch of the Neutralized Drift Compression Experiment-II, an energy-efficient induction accelerator under development at the Lawrence Berkeley National Laboratory. Transmission lines for creating high-voltage pulses to power the accelerator cells are in the top center of the image. Beam-neutralizing plasma injectors and the chamber that focuses the beam on the target are shown in the lower right *(Courtesy of Lawrence Berkeley National Laboratory)*.

primarily directed toward meeting these stringent requirements.

37.8.3 Z-Pinch

A Z-pinch driver for IFE is being studied at Sandia National Laboratories in the United States (see Fig. 37.6). The Z-pinch approach offers the potential for the highest driver efficiency of those being studied. Experiments on Sandia's Z machine demonstrated 15% efficiency in converting electrical energy to x-rays. The intense x-rays are used to implode the fuel capsule.

One type of target contains a cylindrical array of very fine tungsten wires surrounded by a cylindrical metal enclosure, or hohlraum. The large pulsed-power system in the Z machine sends a current of millions amperes through the fine wires, converting them into super-hot plasma. The plasma fills the hohlraum with intense x-rays, and the hohlraum helps contain the x-rays during the implosion of the capsule. The energy that the present Z machine can deliver to the target is not sufficient to ignite a fuel capsule.

Designs for a next-generation Z-pinch driver are based on linear transformer driver technology that offers high repetition rates, greater reliability, and twice the efficiency of the Marx generator technology on Z. A recyclable transmission line (RTL) connects the driver to the target, eliminating the need for final optics, beam focusing, and target tracking. This approach also allows the use of thick liquid blankets to protect the chamber wall. However, the replacement of the RTL (10–100 kg) every 10 seconds presents substantial technical and cost challenges.

The lower repetition rate (0.1 Hz) in the Z-pinch approach is compensated by increasing the yield per pulse by tenfold, and by having 8 to 10 fusion chambers operating together in a 1 GWe power plant.

37.9 FAST IGNITION: AN ALTERNATIVE APPROACH TO IFE

In the conventional approach to inertial confinement, the drivers that compress the fuel capsule also heat it to ignition. Fast ignition decouples the compression and heating phases of the implosion (see Fig. 37.7). Fast ignition, if successful, could require less driver energy than the conventional approach, which could make fusion energy production even more economically attractive.

The fast ignition concept uses one of the drivers (HI accelerator, laser, or Z-pinch) to compress the target, and then uses an extremely intense laser beam to ignite a propagating thermonuclear burn wave in the compressed, but relatively cold, fuel capsule. The technique relies on the

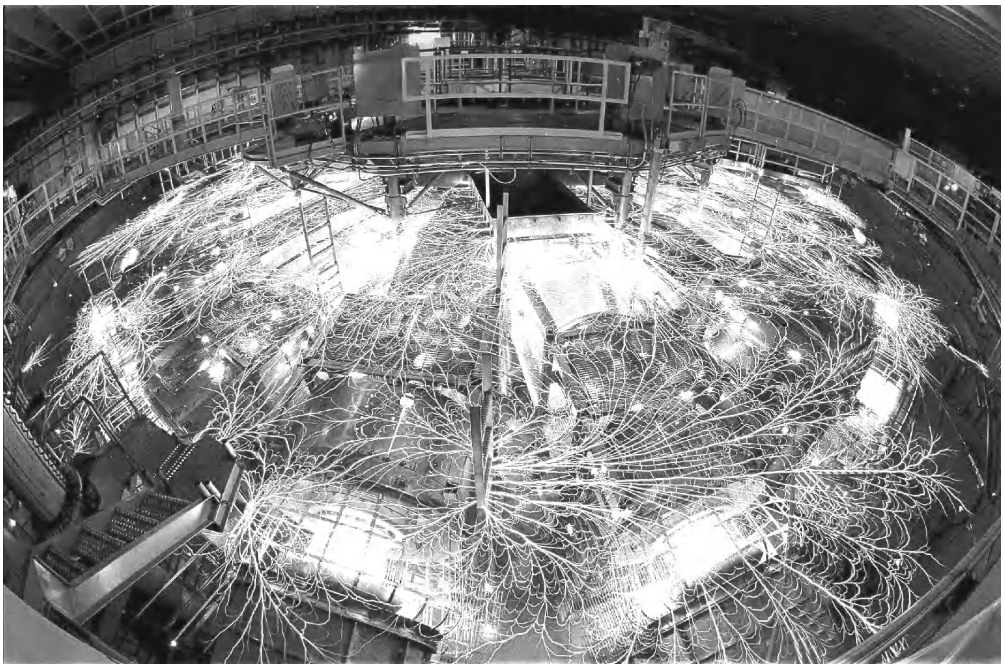

Figure 37.6 Sandia National Laboratory's Z-pinch device, the Z machine, in action *(Courtesy of Sandia National Laboratory)*.

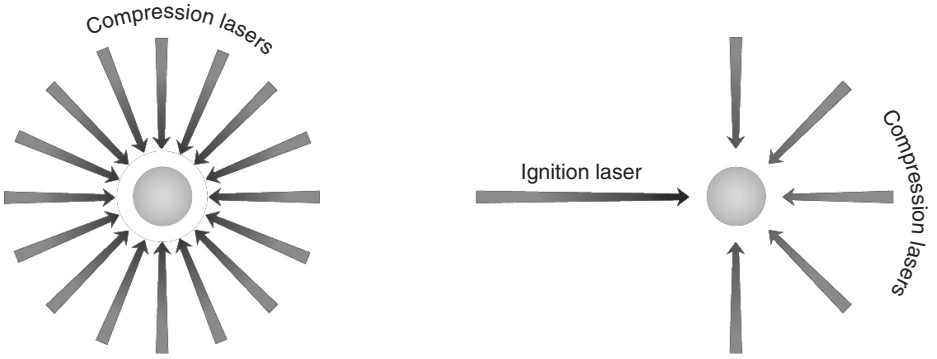

Figure 37.7 The left figure shows the symmetrical arrangement of lasers for compressing and heating a fuel capsule for convention inertial confinement fusion. The right figure illustrates how, in fast ignition, the compression and heating functions are performed by separate drivers, with different timing and geometry *(Courtesy of Lawrence Livermore National Laboratory)*.

extremely short pulse (~10 ps) of a petawatt (10^{15} W) laser to heat and ignite a small portion of the fuel near the edge of the compressed capsule. This concept has the potential of increasing target gain and/or relaxing the constraints on chamber and driver specifications because no central hot spot is required. The concept is at an early stage of investigation, with complex physics and engineering issues still to solve.

Experiments for the fast ignition approach were conducted at the GEKKO XII laser at Osaka University in Japan in 2001, working with a team of UK scientists. Several projects are currently underway to explore the fast ignition approach, including upgrades to the OMEGA laser at the University of Rochester, the GEKKO XII device in Japan (where the FIREX1 construction project is adding a powerful laser to GEKKO for fast ignition), and an entirely new facility, known as HiPER, to be constructed in the European Union starting around 2015. If successful, fast ignition could dramatically lower the total amount of energy needed to drive the target; the HiPER design, for example, will use much smaller lasers than conventional designs, yet produce fusion power outputs of similar magnitude.

37.10 OTHER IFE POWER PLANT COMPONENTS

As indicated in Figure 37.2, the major plant components in addition to the driver are the fusion chamber, target factory, and turbine generator. This section focuses on how the key requirements for an IFE plant will dictate the design of these components and some of their subsystems.

37.10.1 Fusion Chamber

IFE systems studies have resulted in a variety of designs for fusion chambers, but the basic functions are similar. The structure must maintain a vacuum in the central cavity where the target is placed and ignited. The material on the inner surface of that cavity, called the first wall, is exposed to the products of the ignited targets. A "blanket," at or just behind the first wall, allows for the breeding of tritium and extracts high-grade heat to be sent to the turbine generator. Shielding on the outside of the chamber protects equipment and workers from the radiation environment produced by the ignited targets. Penetrations through these layers of the chamber are required to allow for target injection, and for the delivery of the driver beams or electrical power used to implode the target. The chamber and all of its subsystems need to be designed using materials that avoid the necessity of high-level waste disposal.

37.10.1.1 First Wall Each fusion target releases a burst of fusion energy in the form of high-energy neutrons (about 70% of the energy), x-rays, and energetic ions, along with the debris from the structural material of the target. The first wall must survive these repeated bursts. Various first-wall designs have been proposed and fall into three major classes:

- Dry wall, where the innermost surface is a solid material designed to handle the full target energy impact.
- Wetted wall, where a thin liquid layer coats the first wall and absorbs the short-range x-rays and ions before they can damage the wall.
- Thick liquid wall, where more than 50 centimeters of liquid (lithium-bearing metal or molten salt) flows between the target and first wall and provides protection from x-rays, ions, and neutrons.

Not only must the first wall survive the repeated energetic bombardments from the ignited targets, it must also effectively manage the intra-shot recovery—the conditions inside the chamber (such as vapor and droplet density) that must be recovered between each shot so that the next target can be injected and the laser or HI beams can propagate through the chamber to the target. In the case of the Z-pinch, the transmission line and new target need to be installed and readied for the next electrical pulse during this period.

37.10.1.2 Blanket The blanket converts the sequence of energy pulses into a steady flow of high-grade heat, and it breeds sufficient tritium to continue to fuel the IFE plant. To accomplish these two functions, the blanket has to be thick enough to slow and absorb the energetic neutrons to extract their energy, and it must contain lithium to react with those slowed neutrons to create the tritium. The x-rays, ions, and other products from the exploding target would also heat the blanket.

A variety of blanket designs are being considered. When liquids such as lithium, lithium-bearing liquid metals, or lithium-bearing molten salt are used for tritium breeding, the liquid is generally circulated as the primary coolant for the fusion chamber. When solid breeders such as lithium oxide are used, high-pressure helium serves as the chamber coolant. The blanket must operate at temperatures of more than 500°C in order to achieve high efficiency in the power-conversion system. The tritium must be extracted from the blanket to sustain the supply of fuel.

The blanket and some other internal components of the chamber may need to be replaced periodically, depending on the design. The structural part of the fusion chamber would be spared the damage from radiation and debris.

37.10.1.3 Target Injection and Tracking In LMJ and NIF, targets are held in place at the center of the chamber, and the beams are aligned to the ideal fixed position for each laser shot. For the high rep-rate (5 to 10 Hz) laser- and HI-driven power plant designs, the targets would need to be injected at speeds greater than 100 meters a second and tracked in flight to provide data to a real-time beam-pointing system needed to ensure the precise illumination required to achieve ignition and high-energy gain.

Target injection, steering, tracking, and engagement can be demonstrated with surrogate targets and low-power lasers or HI beams in separate facilities. Target injection experiments using gas guns have been conducted at General Atomics in San Diego, California, with room-temperature surrogates. Conceptual designs for other types of injectors, such as electromagnetic accelerators, and for target tracking and beam pointing systems have also been completed.

Lower repetition rates (0.1 Hz) are needed for Z-pinch driven systems to allow for the replacement between each shot of the transmission line that provides electrical power to the target. Since the transmission lines are attached to the target, no target tracking or beam steering systems are needed, but the chamber would need to withstand the higher energy release per shot and the longer times between pulses of heat.

While laser- and HI-driven systems do not have to replace transmission lines each shot, they do have the

challenge of protecting or replacing the "final optics" that are exposed, to some extent, to the debris and radiation from each ignited target. The final optics are the magnets or optical components on the fusion chamber that provide the precision focusing and aiming of the HI beams or laser beams onto the target.

37.10.2 Turbine Generator

By flowing a coolant through the blanket in the fusion chamber at a steady rate, the pulsed fusion energy can be extracted at a constant rate and delivered to the power conversion system, which converts the thermal power to electrical power. The primary coolant from the blanket circulates through heat exchangers. The secondary coolant from the heat exchangers then drives the turbine generator to produce electricity. The efficiency of the power conversion system depends on the outlet temperature of the primary coolant, which is limited by the materials used in the construction of the blanket and chamber. With advanced material being developed for fusion and other applications, conversion efficiencies of 40 to 50% should be possible. Some work has also been done on ideas for converting a portion of the target energy output directly to electricity.

37.10.3 Target Factory

The target factory must produce a continuous supply of high-quality targets at an acceptable cost—typically 25¢ for a target that produces 300 megajoules of energy. Many types of targets are being considered for IFE, including indirect drive (like those being shot on NIF), direct drive (currently being tested on the OMEGA laser at the University of Rochester), and advanced designs such as fast ignition. In all cases, the fusion fuel is contained in a spherical fuel capsule. Near-term experiments planned for NIF will use capsules made of plastic, beryllium, carbon, or carbon-hydrogen polymers, but for IFE plants, it is likely that polymer capsules will be the preferred material. The fuel capsule must be cold enough for deuterium–tritium fuel to freeze and form a layer of ice on the inner wall of the capsule.

For direct-drive targets, the capsule is directly and symmetrically irradiated by the laser or HI beams. For indirect-drive targets, the capsule is placed inside a hohlraum, a tiny, can-shaped container made with high-atomic-mass materials like gold and lead with holes at each end for laser beam entry. For HI drivers, the holes are not needed because of the longer penetration depth of HI beams. If the power plant operates at five shots a second, the target factory will have to produce more than 400,000 targets a day.

LLNL materials science experts, working with General Atomics in San Diego, California, have shown that fully automated, low-cost, large-volume target manufacturing can be adapted from other mass-production industries. Researchers have begun using existing computer codes for NIF fusion targets to design precise, low-cost fusion targets for IFE plant concepts that would be scalable to mass production.

Sandia Laboratory is studying the best indirect drive target designs to ensure efficient and repeatable coupling of electrical energy to x-rays and then to capsule implosion. It is also studying how to mass-produce these targets and the attached recyclable transmission lines in a way that minimizes material inventory and cost for Z-pinch devices.

For IFE, a target gain greater than about 100 is needed in order to minimize the portion of generated electric power that has to be recirculated within the plant to operate the laser. Fast ignition targets are expected to give gains of several hundred. A lower recirculating power fraction would result in more power being available for sale, so the cost of electricity would be lower.

37.11 HOW MUCH WOULD IFE POWER COST?

Economic models based on experience with NIF, coupled with industry-standard models, show that inertial fusion energy could be highly cost-competitive with alternate sources of low-carbon baseload electricity. These models provide price requirements for the consumable elements (fuel pellets, optics, etc.) and guide the path to implementation. An important aspect of fusion energy, in contrast with many other energy sources, is that the cost of production is not expected to grow as more plants are deployed. In the case of wind energy, for example, the first wind farms are built in ideal locations for maximum efficiency. Later wind farms must build in less suitable locations—possibly competing with other land use needs or in locations far from energy demand—and thus for higher costs. With fusion energy, the production cost of plants will not increase significantly as more plants are built. Since the fusion fuel itself is derived from abundant, readily available materials, the fuel prices will remain stable and affordable, as fossil and fission fuel prices rise precipitously.

37.12 FUSION–FISSION HYBRIDS

Approaches for the use of fusion–fission hybrids for power generation have been discussed since the 1970s. These approaches were originally considered as a means to breed fuel for fission reactors. More recently, scientists have begun to explore the possibility of combining fusion and fission to generate electricity while at the same time disposing of nuclear waste.

One such concept now under study at LLNL is the Laser Inertial Fusion Energy, or LIFE, concept, which would use a solid-state laser driver. The proposed LIFE power plant could be configured as a pure fusion IFE plant or be surrounded by a subcritical fission blanket to function as a hybrid plant. In a LIFE hybrid power plant, a laser focused on very small fuel capsules would produce about 300–700 megawatts of fusion power. The fusion process also generates high-energy neutrons that, in the hybrid plant design, bombard a blanket of fertile or fission fuel. The blanket's fissile reactions multiply the energy from the fusion process and produce the heat that is used to drive turbines similar to those in current electrical power plants, generating safe, environmentally friendly power. The fuel could be thorium, light-water reactor spent nuclear fuel, weapons-grade plutonium, highly enriched uranium, or natural and depleted uranium. Using leftover fuels such as these, LIFE could supply U.S. electricity needs for more than 1,000 years.

The fusion source of neutrons allows the LIFE engine to burn its fuel to more than 99 percent FIMA (fission of initial metal atoms) without refueling or reprocessing. The nuclear waste produced in this process has very low concentrations of long-lived actinides compared to the spent fuel from conventional reactors. And because the fuel is burned so completely, LIFE engines could reduce the quantity of spent fission fuel destined for long-term underground storage by a factor of 15 to 20 per unit of energy generated.

Such a hybrid reactor would operate at a substantially subcritical state, so that the fissile fuel in a LIFE engine could not spontaneously generate enough neutrons to start or maintain a nuclear chain reaction. This could ease regulatory requirements, reduce development and implementation costs and delays, and make the technology more attractive to private industry.

Depending on how it is configured, a LIFE engine would require a ramp-up time of days to about one year before reaching full electrical power. If configured as a fusion–fission hybrid, the continuous power phase lasts for five to more than 40 years, followed by an incineration or burn-down phase in which nearly all actinides are converted to fission by-products.

37.13 THE FUTURE OF IFE

Following decades of effort, IFE research is at a key juncture. The demonstration of fusion ignition and energy gain in an experimental setting will spark the transition from scientific research to the delivery of a pilot fusion plant based on the integration of the required IFE components. The pilot plant will test and validate the system integration and scaling of various systems, options, and technologies and determine what is needed to roll out a series of commercial power plants. A commercial demonstration plant would follow, illustrating the plant's reliability, availability, and maintainability, and establishing the detailed economics and licensing regime. Timescale estimates suggest that a prototype plant could be operational in the mid-2020s, with commercial rollout commencing a few years thereafter.

Renewable energy sources will be an increasing and important part of the energy portfolio over the next 50–100 years, as will continued emphasis on increasing the energy efficiency of our power-consuming devices. But providing for 22nd century energy demand will require that revolutionary responses be pursued in parallel with evolutionary ones. Researchers are hoping that ICF technology can take up that challenge and scale to meet future commercial energy needs.

SUGGESTED READING

Fusion as Part of a Global Energy Strategy

R. J. Hawrykuk, S. Batha, W. Blanchard, et al., Fusion plasma experiments on TFTR: A 20 year retrospective. *Phys. Plasmas*, 1998, **5**, 1577–1589.

A. Gibson and the JET Team, Deuterium-tritium plasmas in the Joint European Torus (JET): Behavior and implications. *Phys. Plasmas*, 1998, **5**, 1839–1847.

Path to Fusion Energy through Inertial Confinement

E. Moses, Ignition on the National Ignition Facility: a path towards inertial fusion energy. *Nucl. Fusion*, 2009, **49**, 104022.

Demonstrating Ignition and High Energy Gain

S. Glenzer, B. MacGowan, P. Michel, N. Meezan, L. Suter, S. Dixit, J. Kline, G. Kyrala, D. Bradley, D. Callahan, E. Dewald, L. Divol, E. Dzenitis, M. Edwards, A. Hamza, C. Haynam, D. Hinkel, D. Kalantar, J. Kilkenny, O. Landen, J. Lindl, S. LePape, J. Moody, A. Nikroo, T. Parham, M. Schneider, R. Town, P. Wegner, K. Widmann, P. Whitman, B. Young, B. Van Wonterghem, L. Atherton, and E. Moses, Symmetric inertial confinement fusion implosions at ultra-high laser energies. *Science*, 2010, **327**, 1228–1231.

P. Chang, R. Betti, B. Spears, K. Anderson, J. Edwards, M. Fatenejad, J. Lindl, R. McCrory, R. Nora, and D. Shvarts, Generalized measurable ignition criterion for inertial confinement fusion. *Phys. Rev. Lett*. 2010, **104**, 135002.

N. Meezan, L. Atherton, D. Callahan, E. Dewald, S. Dixit, E. Dzenitis, M. Edwards, C. Haynam, D. Hinkel, O. Jones, O. Landen, R. London, P. Michel, J. D. Moody, J. Milovich, M. Schneider, C. Thomas, R. Town, A. Warrick, S. Weber, K. Widmann, S. Glenzer, L. Suter, B. MacGowan, J. Kline, G. Kyrala, and A. Nikroo, National ignition campaign hohlraum energetics. *Phys. Plasmas*, 2010, **17**, 056304.

Key Requirements for an IFE Power Plant

R. Linford, R. Betti, J. Dahlburg, J. Asay, M. Campbell, P. Colella, J. Freidberg, J. Goodman, D. Hammer, J. Hoagland, S. Jardin, J. Lindl, G. Logan, K. Matzen, G. Navratil, A. Nobile, J. Sethian, J. Sheffield, M. Tillack, and J. Weisheit, A review of the US Department of Energy's inertial fusion energy program. *J. Fusion Energ*., 2003, **22**, 93–126.

Drivers

R. Betti, D. Hammer, G. Logan, D. Meyerhofer, J. Sethian, and R. Siemon, *Advancing the Science of High Energy Density Laboratory Plasmas*, Fusion Energy Science Advisory Committee report from its Panel on High Energy Density Laboratory Plasmas. U.S. Department of Energy, January 2009.

KrF

J. Sethian, M. Friedman, and R. Lehmberg, Fusion energy with lasers, direct drive targets, and dry wall chambers. *Nucl. Fusion*, 2003, 43, 1693–1709.

S. Obenschain, D. Colombant, A. Schmitt, J. Sethian, and M. McGeoch, Pathway to a lower cost high repetition rate ignition facility. *Phys. Plasmas*, 2006, **13**, 056320.

DPSSL

Y. Kozaki, Way to ICF reactor. *Fusion Eng. Des*., 2000, **51–52**, 1087–1093.

C. Orth, S. Payne, and W. Krupke, A diode pumped solid state laser driver for inertial fusion energy. *Nucl. Fusion*, 1996, **36**, 75–116.

HI Accelerators

S. Yu, W. Meier, R. Abbott, J. Barnard, T. Brown, D. Callahan, C. Debonnel, P. Heitzenroeder, J. Latkowski, B. Logan, S. Pemberton, P. Peterson, D. Rose, G. Sabbi, W. Sharp, and D. Welch, An updated point design for heavy ion fusion. *Fusion Sci. Technol*., 2003, **44**, 266–273.

B. Logan, L. Perkins, and J. Barnard, Direct drive heavy-ion-beam inertial fusion at high coupling efficiency. *Phys. Plasmas*, 2008, **15**, 072701.

P. Roy, S. Yu, E. Henestroza, A. Anders, F. Bieniosek, J. Coleman, S. Eylon, W. Greenway, M. Leitner, B. Logan, W. Waldron, D. Welch, C. Thoma, A. Sefkow, E. Gilson, P. Efthimion, and R. Davidson, Drift compression of an intense neutralized ion beam. *Phys. Rev. Lett*., 2005, **95**, 234801.

Z-Pinch

M. Matzen, M. Sweeney, R. Adams, J. Asay, J. Bailey, G, Bennett, D. Bliss, D. Bloomquist, T. Brunner, R. Campbell, G. Chandler, C. Coverdale, M. Cuneo, J. Davis, C. Deeney, M. Desjarlais, G. Donovan, C. Garasi, T. Haill, C. Hall, D. Hanson, M. Hurst, B. Jones, M. Knudson, R. Leeper, R. Lemke, M. Mazarakis, D. McDaniel, T. Mehlhorn, T. Nash, C. Olson, J. Porter, P. Rambo, S. Rosenthal, G. Rochau, L. Ruggles, C. Ruiz, T. Sanford, J. Seamen, D. Sinars, S. Slutz, I. Smith, K. Struve, W. Stygar, R. Vesey, E. Weinbrecht, D. Wegner, and E. Yu, Pulsed-power-driven high energy density physics and inertial confinement fusion research. *Phys. Plasmas*, 2005, **12**, 055503.

D. Ryutov, M. Derzon, and M. Matzen, The physics of fast *Z* pinches. *Rev. Mod. Phys*., 2000, **72**, 167–223.

S. Slutz, C. Olson, and P. Peterson, Low mass recyclable transmission lines for Z-pinch driven inertial fusion. *Phys. Plasmas*, 2003, **10**, 429–437.

Fast Ignition

M. Tabak, J. Hammer, M. Glinsky, W. Kruer, S. Wilks, J. Woodworth, E. Campbell, M. Perry, and R. Mason, Ignition and high gain with ultrapowerful lasers. *Phys. Plasmas*, 1994, **1**, 1626–1634.

N. Basov, S. Yu, and L. Feokistov, Thermonuclear gain of ICF targets with direct heating of ignitor. *J. Sov. Laser Res*., 1992, **13**, 396–399.

S. Atzeni, A. Schiavi, and C. Bellei, Targets for direct-drive fast ignition at total laser energy of 200–400 kJ. *Phys. Plasmas*, 2007, **14**, 052702.

IFE Power Plant Components

S. Reyes, R. Schmitt, J. Latkowski, and J. Sanz, "Liquid wall options for tritium-lean fast ignition inertial fusion energy power plants. *Fusion Eng. Des*., 2002, **63–64**, 635–640.

W. Meier, A. Raffray, S. Abdel-Khalik, G. Kulcinski, J. Latkowski, F. Najmabadi, C. Olson, P. Peterson, A. Ying, and M. Yoda, IFE chamber technology—status and future challenges. *Fusion Sci. Technol*., 2003, **44**, 27–33.

Fusion–Fission Hybrids

E. Moses, T. de la Rubia, E. Storm, J. Latkowski, J. Farmer, R. Abbott, K. Kramer, P. Peterson, H. Shaw, and R. Lehman, A sustainable nuclear fuel cycle based on laser inertial fusion energy. *Fusion Sci. Technol*., 2009, **56**, 547–565.

W. Meier, R. Abbott, R. Beach, J. Blink, J. Caird, A. Erlandson, J. Farmer, W. Halsey, T. Ladran, J. Latkowski, A. MacIntyre, R. Miles, and E. Storm, Systems modeling for the laser fusion-fission energy (LIFE) power plant. *Fusion Sci. Technol*., 2009, **56**, 647–651.

38

HYBRID NUCLEAR REACTORS

Jose M. Martinez-Val[1], Mireia Piera[2], Alberto Abánades[1] and Antonio Lafuente[1]
[1]*Institute of Nuclear Fusion-UPM, Madrid, Spain*
[2]*ETSII-Dp Ingenieria Energetica, UNED, Madrid, Spain*

38.1 INTRODUCTION AND BACKGROUND: THE CONCEPT OF HYBRID NUCLEAR REACTORS

In standard nuclear reactors, neutron multiplication is produced by the fission reaction, which is induced by a free neutron created in a previous fission reaction. This fact leads to the concept of chain reaction, which is self-maintained in a so-called critical reactor. On the contrary, in a subcritical reactor, the nuclear properties of the nuclear fuel and other components are unable to keep the chain reaction going on, and both the neutron population and the fission reaction rate vanish in a very short time (in less than one second, although the thermal power of the system does not go to zero so fast, because of the existence of an afterheat produced by radioactive decay). On the other hand, a supercritical reactor is an unwanted system where both the neutron population and the fission reaction rate grow at an exponential speed, and so does the thermal power, which means that a true catastrophic accident can take place, as it was in April 1986 in the Chernobyl-4 reactor [1, 2].

Criticality is therefore a very important feature of the nuclear reactors. Fortunately, the physics of fission reactors helps us a lot for exploiting them, because of the existence of the so-called delayed neutrons and because the reactors are naturally stable (within some working windows of their relevant parameters), and they strongly stick to the critical state, making it very easy to control them by means of neutron-absorbing control rods.

In Chernobyl-4 accident, reactors conditions were (stupidly) modified in order to make a thermal experiment, and the reactor became unstable (namely, over-moderated, in the terminology of reactor physics). The pumping power loss [2] conveyed by the experiment they wanted to carry out was the final trigger for the reactor to initiate an exponential power rise, reaching 500 times its nominal value, which destroyed the reactor elements and most of the structural components.

With such a precedent, it is obvious that *criticality* is a condition that has to go side by side with *stability*. This is something that always happens in under-moderated thermal reactors, but the physics is not so clear in fast reactors (the word "fast" meaning that neutrons are not moderated before they are absorbed by a nucleus). For instance, molten-metal cooled fast reactors can have a positive feedback due to coolant boiling or loss, and any positive feedback is a source of instabilities [3, 4]. The need for fast reactors is rooted in the so-called nuclear breeding, a feature that will be introduced later on, and it is of paramount importance for exploiting nuclear raw materials.

It is out of the scope of this chapter to analyze in depth the physics of critical fast reactors, and the same can be said about over-moderated thermal reactors. Nevertheless, it is worth pointing out again the problems potentially associated with a supercritical state, which is something very close to the critical state.

And what about reactors in a subcritical state? It was already said that both the neutron population and the fission reaction rate vanish in a very short time in this case.

Nuclear Energy Encyclopedia: Science, Technology, and Applications, First Edition (Wiley Series On Energy).
Edited by Steven B. Krivit, Jay H. Lehr, and Thomas B. Kingery.

Hence, they are useless for generating energy. However, they have a very interesting property: If a subcritial reactor is fed with neutrons coming from an independent neutron source (a source not depending on the neutron flux of the reactor), both the neutron population and the neutron-induced reaction rates stabilize at a constant level that depends on the degree of subcriticality and the strength of the independent neutron source [5].

The degree of subcriticality is measured by the value of the *neutron multiplication factor* of the reactor, k. For $k = 1$, the reactor is critical. For $k > 1$, it is supercritical; and for $k < 1$, it is subcritical. The value of k depends on the material composition of the reactor components (fuel, moderator, coolant, structural material, control rods) and its size. So, the degree of subcriticality is $1 - k$, which has an important role in the physics of the hybrid.

And what about an independent neutron source? There are some artificial heavy nuclei, as Cf-252, with a sizable strength of neutron emission (neutron per second per gram of material) and some mixtures of heavy radioactive nuclei with Be (beryllium) also have a non-negligible rate of neutron emission. However, more powerful sources are needed to feed a subcritical reactor if we want to have a power density similar to that of a critical reactor. And this is the basis of the hybrid reactor concept, where neutron generation is not produced just in neutron-induced fissions, but also in a second type of nuclear reaction, not induced by neutrons. This additional reaction is the core of the independent neutron source, and there mainly are two reactions for doing that:

- Deuterium-tritium fusion reactions, and the system is called a fusion-fission hybrid (FFH). In this reaction, a 14 MeV (mega-electron-volt) neutron appears, as well as a He4 nucleus, which is the result of the fused reactants, H2 (deuterium) and H3 (tritium). The 14 MeV neutron is somehow injected in the subcritical fission reactor (which is surrounding some parts of the fusion chamber).
- Spallation reactions induced by an accelerated proton impinging in a target of a heavy element, as lead [6]. This is an Accelerator Driven System (ADS), because it includes a particle accelerator, where electric fields accelerate beams of charged particles, as ionized hydrogen (protons). For instance, a proton accelerated until 600 MeV can create about 25 neutrons when impinging on a lead target. These neutrons are naturally injected into the subcritical fission reactor, because the spallation target is placed close to the center of the reactor.

A sketch of the hybrid phenomenology is depicted in Figure 38.1, which is applicable either for spallation neutron sources or for fusion devices. The core of those phenomena

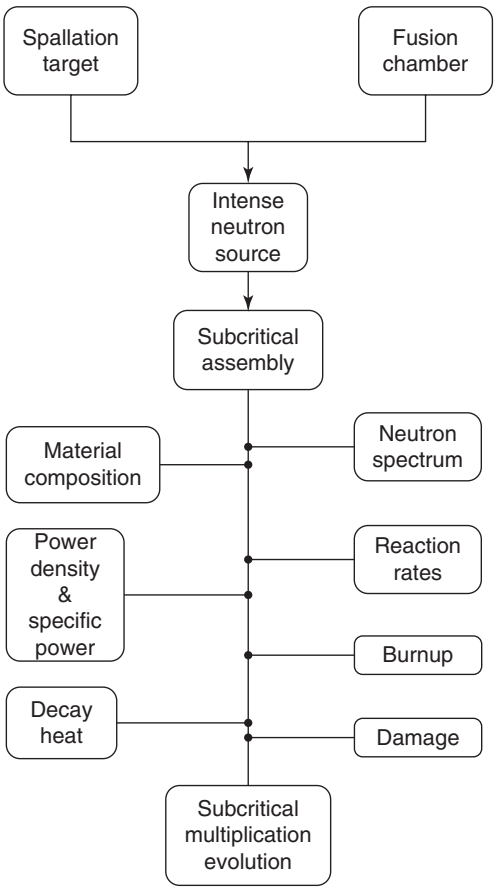

Figure 38.1 A schematic view of the main topics for the analysis of a hybrid blanket.

is the subcritical multiplication of the neutron population, which drives the reaction rates and the power production. In Figure 38.2 a sketch is presented on the neutron-induced reactions in a hybrid. Of course, the essential companion of the neutrons is the composition and configuration of the material of the subcritical assembly.

Although most of the physics of the subcritical assembly is the same for FFH and ADS, there is a difference in the use of the neutrons. In both cases, neutrons can be used for

- Generating energy (mainly through fissions reactions).
- Transforming non-fissile nuclei, namely U238 or Th232, into highly valuable fissile nuclei, Pu239 or U233, respectively.
- Incinerating long-term radioactive nuclei into stable or short-term nuclei, which is usually called "rad-waste transmutation," although transmutation means a change in the nuclear entity, in general.

In FFH there is an additional use: to produce H3 (tritium), because it does not exist in nature. It has to be produced by neutron capture in Li6 (the lightest and rarest

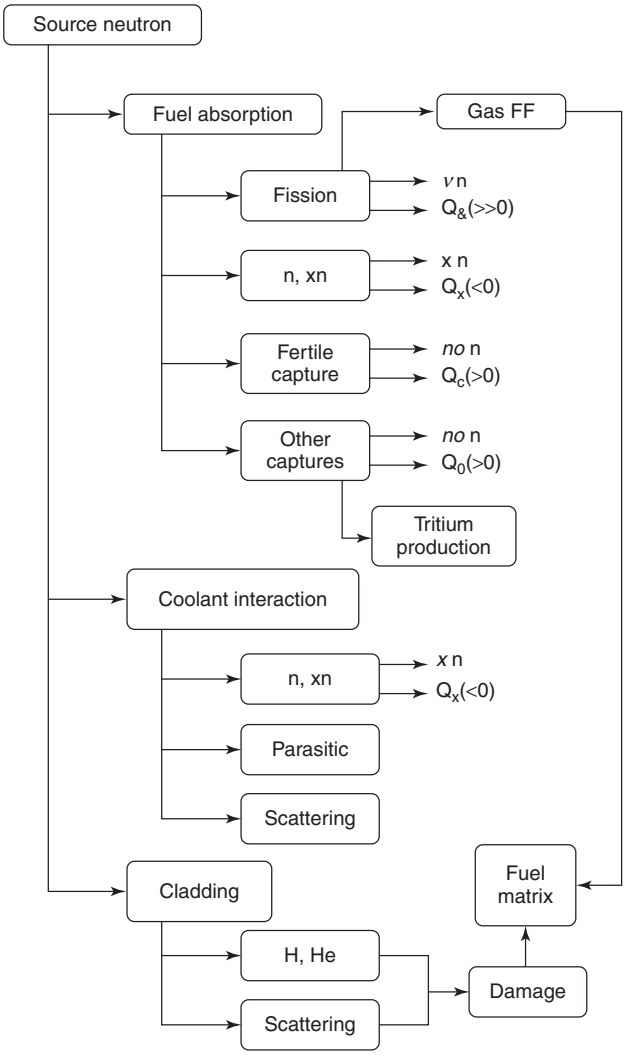

Figure 38.2 Neutron-induced reaction tree to guide specific calculations of hybrid blankets.

isotope of lithium). The subcritical assembly has to embody some part, or some material, to produce the tritium needed for feeding the fusion chamber.

In summary, hybrids can be described as subcritical assemblies of fissionable material, which are activated by a powerful external neutron source. For some decades, hybrids were studied in the most prominent laboratories and a large bibliography was produced [7–37]. In spite of the appealing inherent characteristics of the hybrids, they have not been developed for a series of reasons related to the deployment of nuclear energy, strongly dominated by critical reactors from the very beginning, in a framework where sustainable development and nuclear sustainability were not household concepts. The scenario can change dramatically in favor of the hybrids if those concepts become an important part of future nuclear policies.

38.2 NEUTRONICS OF HYBRID NUCLEAR REACTORS

A sketch of the neutron cycle in an FFH is shown in Figure 38.3, which explains how a fraction of the fusion-born neutrons enter into the subcritical assembly of fissionable material, also called a blanket, where they will trigger secondary neutron reactions, notably fissions. Because the neutrons have different behavior-inducing reactions when they have different energies (different speeds), a parameter has to be included for characterizing the fusion-born neutrons, and it is called "importance" and is represented by "I" in the figure. The importance is related to the adjoin flux of the system, which is a mathematical function very useful for a better understanding of the physics of a system [38]. A suitable explanation of the importance function can be seen in most textbooks on nuclear reactors, and an application to hybrids is shown in reference [5]. The value of "I" is slightly above 1 (and this is why it is omitted in some approximate analyses).

The most relevant term included in this picture is the factor $1/(1 - k)$, which is called "subcritical multiplication." It is obvious that it goes to infinity as the neutron multiplication k tends to 1. This is so because a critical system ($k = 1$) is able to self-sustain the neutron flux by itself through the chain reaction. So, a continuous addition of neutrons by an independent source would linearly increase the neutron flux, theoretically going to infinity. Figure 38.4 shows the behavior of neutron multiplication in a subcritical assembly. In the real world, the thermal power associated with a continuously increasing flux would

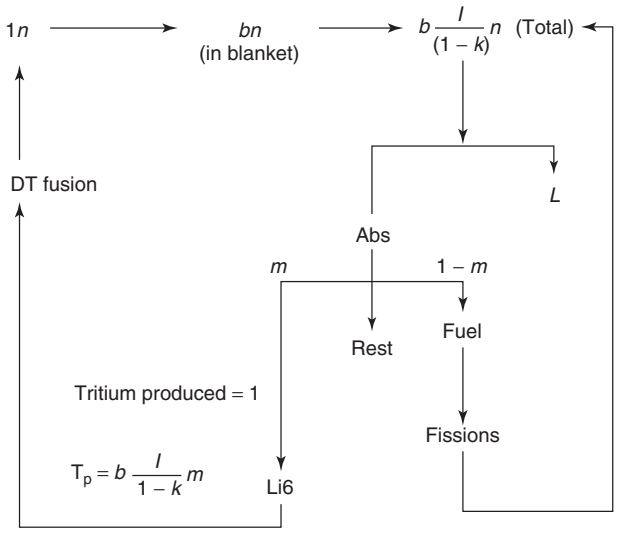

Figure 38.3 An outline of the neutron cycle in a fusion hybrid. "b" is the fraction of fusion-born neutrons which enter into the blanket; "I" is the importance of the fusion neutrons for the subcritical blanket (see ref. [26]) and it is slightly above 1. "m" is the fraction of neutrons absorbed in Li6.

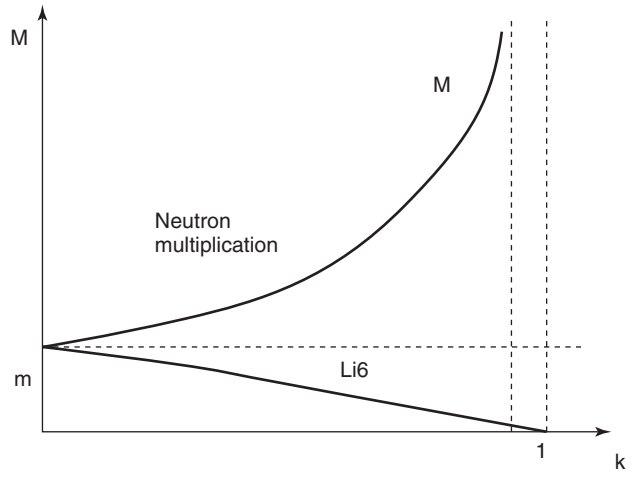

Figure 38.4 Dependence of the total neutron multiplication, M, in a fusion hybrid, versus k-effective of the blanket. The value required in "m" to meet the tritium breeding condition is also depicted, "m" being the fraction of neutrons absorbed in Li6. It is worth remembering that k cannot reach the value 1 in a hybrid, as explained in Figure 38.3. This limit is signaled by a vertical line close to k = 1, representing the maximum multiplication factor k allowed in the hybrid. This value can change from a design to other.

also increase linearly and would reach such levels that the reactor operation would be stopped by the control system, eliminating the neutron population in several seconds. Otherwise, some solid materials would melt down, and the reactor would lose its functionality for keeping the chain reaction, because a destruction of its geometry, which could be the initiating event of an accident, because of losing confinement of radioactive material. It goes without saying that a hybrid must never reach the critical state, and this can be achieved by design in such a way that criticality cannot be reached by any conceivable change in the system, either coming from changes in its material composition, or from changes in geometry, or any other action (as a wrong extraction of all control rods). In summary, the hybrid has a "degree of freedom" that a critical reactor does not have, because the independent neutron source enables the reactor to operate at the required level of subcriticality. On the contrary, a critical reactor has to have its multiplication factor k = 1 always. However, it does not need any additional expensive component, such as a fusion chamber or a proton accelerator. In fact, there are over 400 commercial critical reactors operating all over the globe, and there is not a single operating hybrid. Of course, this situation stems from a particular history with well-known roots, going back to the Chicago Pile 1 constructed by Enrico Fermi and collaborators in December 1942, which was the first critical (and slightly supercritical) reactor. Once critical reactors were available, there were no reasons for developing more complex and expensive systems. The hybrids, even if they seem to be safer, remain subcritical and cannot suffer from power surges that can destroy a reactor and provoke an accident (as it was the ill-fated experiment leading to the Chernobyl-4 accidents).

However, it was already said that under-moderated light water reactors, LWRs, are inherently safe and cannot undergo accidents as Chernobyl-4. The most severe accident in LWR was Three Mile Island 2 (Harrisburg, 1979), but it was not an accident involving a power surge. It was a loss-of-cooling accident caused by several wrong decisions by the operators, who were misled in some occasions by wrong information about the actual state of some valves. Although the reactor was severely damaged, the leakage of radioactive products was almost negligible, and the aftermath was totally different than the Chernobyl situation, because the power surge in Chernobyl had destroyed all confinement barriers, and a fraction of the reactor core, including a sizable amount of plutonium isotopes, had been spread across a wide radius.

From the point of view of safety, LWRs are excellent machines. Very likely, the so-called Generation-3 LWRs will still be better, because they will embody the right answers to the lessons learned from Harrisburg (and also from Chernobyl, although Chernobyl was an RBMK reactor, totally different from Western and far-East LWRs). But all kinds of LWRs have an inherent limitation for exploiting the natural material that can become nuclear fuel. In nature, there are only two chemical elements fitting this label: uranium, which is mainly made of two isotopes: U235 (0.71%) and U238 (99.29%); and thorium, with only one isotope, Th232. And here comes an important feature of nuclear physics: The properties of a nucleus depend a lot on the parity of the numbers of their constituents, protons and neutrons. Note that U235 has 92 protons and 143 neutrons, while U238 has also 92 protons (this is the U label) but 146 neutrons. Th232 has 90 protons and 142 neutrons. And it happens that even-even nuclei (as U238 and Th232) are very stable (so to speak) and do not fission with neutrons of minimum energy, called thermal neutrons, which are the dominating particles in a LWR, because they are moderated and thermalized by the hydrogen nucleus of the water molecules. On the contrary, even-odd nuclei, as U235, undergo fission very easily when they interact with a thermal neutron. This is why U235 is the very fuel of LWR, and this is why thorium has not been yet commercialized as nuclear fuel. This is why LWRs need enriched fuel, i.e., uranium with a U235 content higher than the natural value (about 4% in current LWR). However, not all the fuel loaded in an LWR is fissioned. In fact, only about 4% is

fissioned, the rest of the fuel being downloaded as spent fuel (but not a waste, properly speaking). If a balance of energy is done, taking as a reference the potential energy contained in the mineral extracted from the mine to feed the fuel cycle to fabricate the fuel for the reactor, the energy released (as heat) in the reactor is a bare 0.5% of the reference natural value. Incredibly low, and even so, LWRs are economically competitive in producing electricity.

We need to complete the neutronic mechanisms inside a reactor (either critical or subcritical) by explaining the concept of "nuclear conversion" and its extension, "nuclear breeding." When a neutron is captured into a U238 nucleus, it becomes U239, which is short-lived and decays into Np239, which is also short-lived and decays into Pu239, which has a decay period of 24,000 years. Pu329 is a very good fission fuel for reactors (even better than U235), which is a very positive effect of exploiting the very abundant U238 by transmuting it into Pu239. Similarly, a neutron capture in Th232 leads to U233, also a very good fission fuel. This change in the fuel composition is called nuclear conversion, and U238 and Th232 are called "fertile" nuclei. When the conversion effect is so strong that the rate of even-odd nuclei (U235, Pu239 and the like, which are denominated "fissile" nuclei) generation is higher than the destruction rate of these nuclei, we call it "nuclear breeding."

In Figure 38.5, the percentage of energy utilization is depicted as a function of the reactor conversion ratio, which is the fundamental parameter in this context (see definition below, Eq. (38.1)). Because fissile nuclei are the fundamental ones for the chain reaction, the aforementioned conversion ratio, CR, is a key parameter to characterize a nuclear reactor. It is defined as

$$\mathrm{CR} = \frac{\textit{Rate of production of fissile nuclei}}{\textit{Rate of destruction of fissile nuclei}} \tag{38.1}$$

Because fissile nuclei are produced by fertile captures (in U-238 or Th-232), the conversion ratio can be expressed as

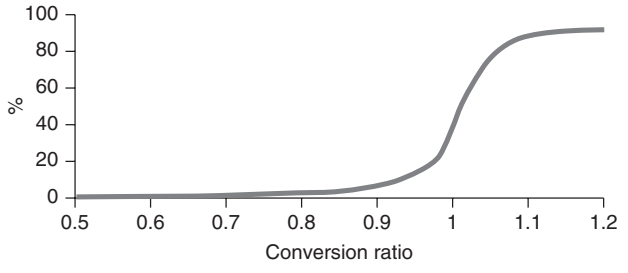

Figure 38.5 Percentage of natural resources utilization as a function of the conversion ratio (CR).

follows

$$\mathrm{CR} = \frac{\sigma_{\mathrm{cu}}\mathrm{U}}{\sigma_{\mathrm{ap}}\mathrm{P}} \tag{38.2}$$

where U stands for the concentration (or for the inventory) of fertile nuclei, P stands for the concentration (or for the inventory) of fissile nuclei, and σ_{cu} and σ_{ap} are the average cross-sections for fertile capture and fissile absorption (fission plus capture).

As can be seen in Figure 38.5, reactors with a conversion ratio larger than 1 can achieve a very high percentage of energy utilization. Fast breeder reactors (FBR) have this high a value of CR. Fast reactors are characterized because a suitable neutron spectrum is tailored (by means of an adequate composition in the fuel and the coolant, and adequate volume fractions for each material) so that the neutrons are very poorly moderated.

In fact, the fissile material inventory in a FBR becomes larger at the end of an operation cycle than at the beginning of it. Thus, it can feed a new reactor with the excess of fissile material, once reprocessed. Of course, spent fuel reprocessing is needed to recover the fissile nuclei and the fertile ones. Fission fragments must be separated for being properly confined until they decay down to naturally occurring radioactive levels (what happens after 500 years, in round numbers). Minor actinides (MA) are also present in the spent fuel, and are particularly important for the long-term radiotoxicity of the nuclear waste [39].

There is a potential alternative, not yet supported by an experimental program, which is not based on external reprocessing, but on extending burn-up of the nuclear fuel as much as possible. This alternative cannot be done with critical reactors, because they need to unload spent fuel and upload fresh fuel in order to keep criticality. It could be possible with a hybrid, but this is still a challenge to be answered.

All these features have been discussed and reviewed several times in national and international programs, particularly in the INFCE initiative (International Nuclear Fuel Cycle Evaluation, 1978–1980). INFCE [40] was mainly oriented to hamper the deployment of the so-called plutonium economy.

In the last years, new initiatives on nuclear waste transmutation were proposed [41] in order to reduce the long-term radiotoxicity of the wastes by eliminating a high fraction of the transuranics (TRU) from the spent fuel before its final disposal.

It has already been said that hybrid reactors have a particular degree of freedom because of the independent source that helps maintain the neutron flux. This means that the neutron spectrum (the statistical distribution of the

neutrons taking into account their kinetic energy) can be tailored into a hybrid for a given purpose, without affecting too much the hybrid neutronic multiplication. So to speak, it is easier to design a hybrid for acting as a nuclear breeder than to design a critical reactor with that feature.

Because of that, hybrids [7–37] have been considered for decades as potential tools for exploiting the natural nuclear resources in an optimized way. It has already been explained that their use can be aimed at

- Generating energy in the subcritical reactor.
- Breeding fissile nuclei from fertile ones (particularly Pu239 from U238 and U233 from Th232) to be burned up in other reactors.
- Transmuting radioactive waste, notably transuranium isotopes.

Theoretically, all three objectives can be pursued in a given installation, but there are some obvious restrictions that must be taken into account in the design of a hybrid. Some of those restrictions stem from the inherent features of neutron-induced reactions, and some others would depend on the type of nuclear energy scenario where the hybrid would have to operate. The final decisions would have to be taken on the basis of nuclear energy sustainability, which will include considerations on the actual risk of proliferation of the hybrids and their fuel cycles.

Besides that, tritium breeding will be specifically considered for fusion–fission hybrids. In a pure fusion reactor, it will be difficult to meet this requirement. In a hybrid, it will be seen that the requirement will become particularly easy for high k-effective (k-eff) blankets.

A third goal that could be reached with hybrids is the incineration of nuclear waste [42]. This is very important because the existence of nuclear waste throughout very many centuries is a fact that has hampered the development of nuclear energy (see Fig. 38.6).

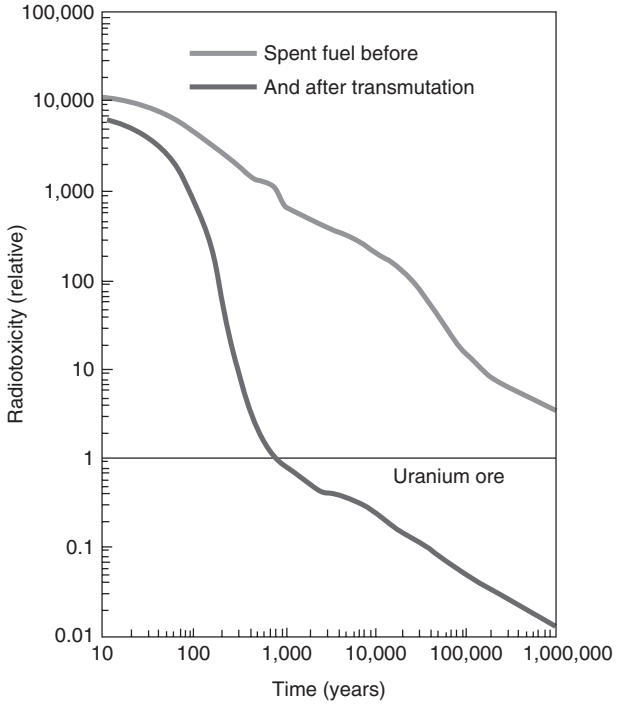

Figure 38.6 Relative radiotoxicity of the spent fuel extracted from a given amount of natural ore in current LWR fuel cycle. The upper line shows the natural decay of the spent fuel, and it is seen that it takes more than one million years to decay to the natural level of the natural uranium ore. However, if 99.9% of actinides (transuranics) are removed from the fuel and transmuted by fission into fission products, the natural level is reached after 700 years. This is tremendous change of scale and can induce a waste management policy not simply based on burying the spent fuel in deep geological repositories. Of course, actinide transmutation conveys some risks and technical challenges that must be solved before implementing it. It is obvious that those risks must be lower than the long-term risk of burying the spent fuel in a repository. In this context, hybrids can be efficient and safe tools for transmuting most of the actinides.

38.3 WHAT DO HYBRIDS LOOK LIKE?

Hybrids were mainly proposed in the 1970s for several reasons, including the fact that nuclear fusion started to be considered as a lengthy process of R&D needing a long time span and very huge budgets. Hybrids [7–37] seemed to be a potential way to shorten the road for getting energy from fusion. However, hybrids needed a parallel strong development of nuclear fission blankets, including new fuels and new reprocessing techniques, and such programs were not developed, because of the strong cut in fission R&D after 1980. However, the hybrid concept remained as a potential tool for getting the best of both domains—the neutron richness of fusion with the energy richness of fission—without needing a full development of fusion reactors, and without using critical reactors, which present more problems on safety than subcritical reactors. In fact, in last years, the concept has been revisited from different viewpoints, particularly in the shadow of the U.S. National Ignition Facility commissioned in Lawrence Livermore National Laboratory in 2009. LLNL has proposed the LIFE conceptual design [43–51] as a long-term quest for exploiting the natural fission materials in an inherently safe hybrid fed with the neutrons coming from a NIF-type fusion chamber. Although hybrids are much older than LIFE, we can use LIFE artwork for explaining how a fusion–fission hybrid is structured.

38.3.1 Fusion–Fission Hybrid Description

There is not a unique structure for a fusion–fission hybrid, because there are two different modes to harness fusion reactions inside a reaction chamber: magnetic confinement and inertial confinement. Even a brief description of each approach is out of the scope of this chapter, and this information can be found in other chapters of this Encyclopedia. In magnetic confinement, the most relevant project is ITER, to be built in Cadarache (France) as an international facility (www.iter.org). In magnetic confinement, the fusion plasma is at extremely low densities, and it is heated and confined by means of electric currents and electromagnetic fields.

In inertial confinement, a very tiny target made of deuterium plus tritium and other materials is imploded up to very high temperatures and densities by the action of a set of laser beams depositing a tremendous power in a very short time (of some nanoseconds) on the outer part of the target. This is the case of the National Ignition Facility, which is the base of the reactor system depicted in Figure 38.7 (https://lasers.llnl.gov/about/nif/about.php).

Most of the space in those buildings is occupied by the laser bays, where the laser light is amplified and powered up to very high power. The laser beams are perfectly synchronized and are finally divided into 192 beamlets in order to have a uniform illumination on the spherical target, although other asymmetric illumination patterns are possible. All the beamlets coincide, crashing against the outermost shell of the target, which is blown off instantaneously and produces a sort of rocket effect pushing the inner part of the target toward its center. There, the collapse of shock waves forms a central hot spark that ignites the fusion burn inside the deuterium-tritium overdense plasma. A microexplosion takes place, and a burst of x-rays, ions, and, mainly, neutrons flies away, impinging on the chamber wall and going through it,

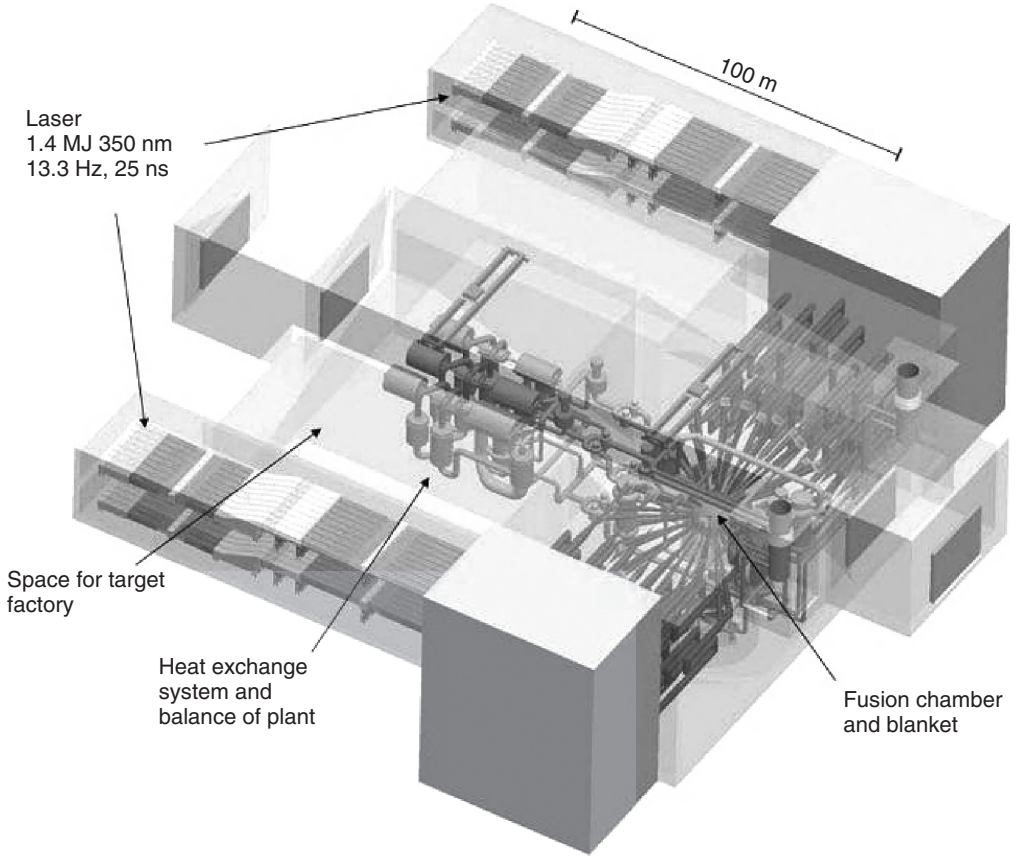

Figure 38.7 Conceptual design of a LIFE engine based on the inertial fusion yields of 35 MJ expected from indirectly driven hot-spot ignition targets on NIF from 1.4 MJ laser pulses. The diode-pumped solid-state laser operates with at 13.3 Hz and a wavelength of 350 nm. The 2.5 m radius chamber is shown, and the final optics are 25 meters from the target (*Courtesy of Ed Moses, LLNL*).

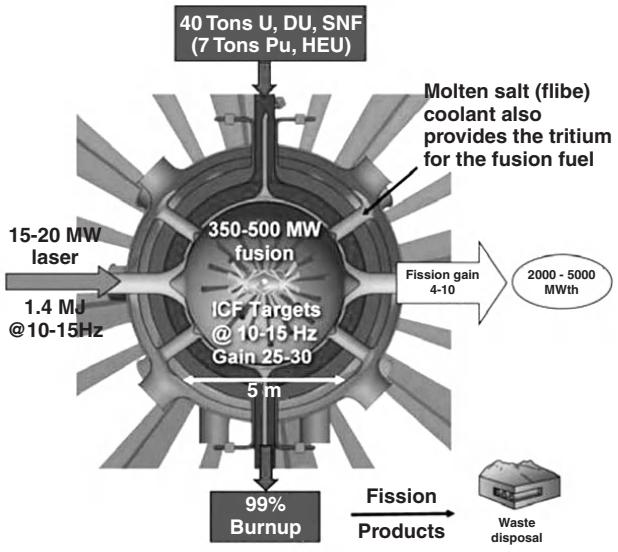

Figure 38.8 The energy and materials flow for the NIF/NIC-based Laser Inertial Fusion Energy (LIFE) engine. LIFE provides an option for a once-through, closed nuclear fuel cycle that starts with a 15–20 MW laser system to produce 375–500 MW of fusion power and uses a subcritical fission blanket to multiply this to 2000–5000 MWth (*Courtesy of Ed Moses, LLNL*).

particularly the neutrons, which are retained in the blanket. This blanket is the place where a subcritical reactor can be placed, resulting in a fusion–fission hybrid.

Figure 38.8 shows a schematic view of the hybrid reactor vessel of LIFE [45] that uses a molten salt, FLiBe, as coolant. Lithium (Li) is used for tritium generation, as already said. Beryllium is used because it is a good neutron multiplier, and F is right chemical companion of both Li and Be to have a salt. Other potential candidates for coolants are FliNaK, F_2Be, and the eutectic LiPb.

The stream of fission fuel is also depicted in Figure 38.8, although it is not, properly speaking, a fluid stream despite the fact that there is also a proposal [49] for using a molten salt also for the fuel. In the first approach, the stream is made of TRISO balls, made of graphite, SiC, and other products, including the fission fuel. An example of those balls is shown in Figure 38.9. It must be noted that most of the ball volume is occupied by ceramic shells and matrices acting as confinement barriers to retain fission products and actinides. The fuel is at the very center of small particles (about 1 mm diameter) surrounded by porous and pyrolitic graphite and silicon carbide (SiC). Those balls were the fuel of the pebble-bed reactor tested in Germany in the 1970s and 1980s. They are currently considered for modular commercial reactors in South Africa, and indeed present very appealing features. In particular, they are very resistant to high levels of neutron radiation. The LIFE project estimates that those balls could withstand nuclear fuel burn-ups close to 100%, without reprocessing. This fact would be extremely positive against proliferation, because the fuel would always be kept inside the TRISO balls (originally devised for high temperature reactors [52–59]), and it would be possible because the reactor is subcritical (a hybrid). Such a fact would be absolutely impossible in a critical reactor. We will come back to this point later on.

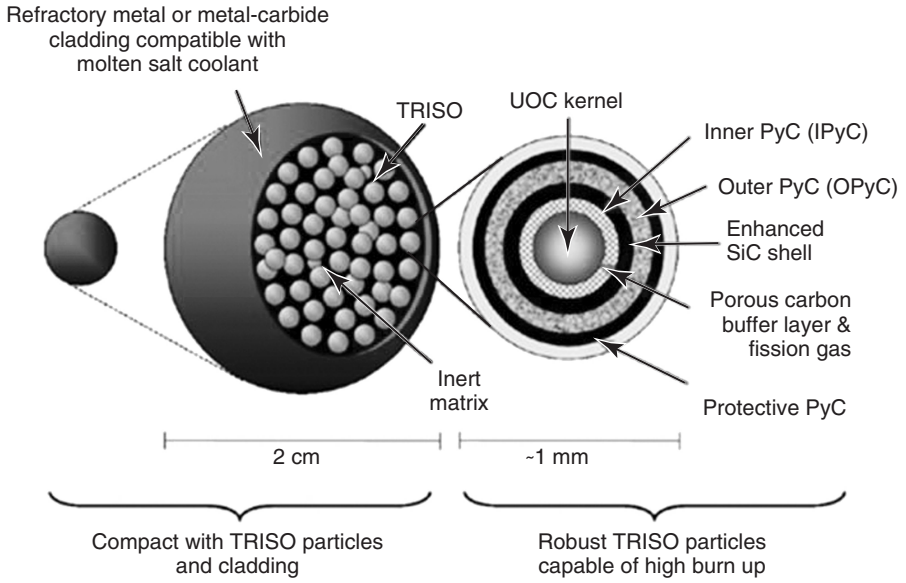

Figure 38.9 An enhanced TRISO fuel, with a more robust SiC capsule to enable fission-gas containment, is being considered as one possible fuel option for LIFE (*Courtesy of Ed Moses, LLNL*).

In summary, fusion–fission hybrids will be characterized by having two parts:

- Systems and components for activating the fusion reactions, particularly D-T fusions, where very fast neutrons would be produced and injected into:
- A subcritical fission reactor, where energy generation will overrun the energy needed by the fusion system, and nuclear breeding and/or waste incineration could also take place.

In turn, the fusion system will depend on the type of plasma confinement used in the machine, either magnetic or inertial. The inertial case has been shown, because those machines have been considered to be more fitted to act as powerful neutron sources.

38.3.2 Accelerator Driven Systems (ADS)

Spallation big targets can also act as strong neutron sources, and they are the base of the second type of drivers, usually called Accelerator Driven Systems (ADS) [60, 61]. As in the previous case, the system is composed of two parts:

- The spallation source, which in turn can be studied as made of two subsystems
  - The proton accelerator, which can deliver proton beams with very different features in total intensity, proton energy, and other magnitudes.
  - The spallation target, made of a high Z material, as lead (Pb), although lead-bismuth (PbBi) eutectic and other materials have been considered as target material.
- The subcritical fission reactor, which can adopt different structures and compositions depending on the aims of the ADS, already explained. In fact, the subcritical fission reactor, or subcritical assembly, can be very similar to the systems devised for fusion–fission hybrids, with a main difference: ADS do not have to produce tritium (on the contrary, tritium would be an offending by-product of the ADS operation and would have to be treated accordingly).

Spallation targets offer an advantage in comparison to fusion–fission systems: They are smaller than fusion chambers, and the subcritical assembly can be closer to the source neutrons. However, they present the problem of very high power densities in the target, with strong cooling requirements and with important effects in radiation damage. Moreover, spallation is a complex reaction similar to a nuclear cascade where the initial proton produces a shower of primary neutrons that in turn produce secondary neutrons and so on. This cascade produces a collection of radioactive products that are grouped into two main sets: nuclei that are close to the original ones, with a few nucleons less, which have been extracted from the original ones by direct interactions; and a set of fission-fragments, because some of the original nuclei can be split into two pieces plus some neutrons by high energy protons or very fast spallation-born neutrons.

A key feature of spallation targets is the number of neutrons produced per incoming proton. This value depends a lot on the target material composition and on the proton energy. In general, the higher the A number of the nucleus and the higher the proton energy, the higher the number of neutrons produced. Of course, this fact also conveys a larger inventory of radioactive products. The limit in the type of material for a spallation target is natural uranium, and this was the case of the FEAT experiment [62] carried out at CERN in 1994, under the leadership of Nobel laureate in physics Carlo Rubbia.

Of course, the target, and the subcritical assembly around it, was irradiated for a very short time, so as not to accumulate a radioactive burden in an experiment, but it was enough to assess the physics of the system at a very low power level, because there was not an external cooling loop for removing heat from the water that filled the assembly vessel. A top and a side view of the system can be seen in Figures 38.10(a) and (b). The fuel bars (natural uranium) were inside aluminum tubes, and the multiplication factor k was well below 1 (under any conceivable condition, even if all bars were packed together). With all these conditions, it was possible to perform very accurate experiments from the point of view of neutronics and thermal measurements, which led to the determination of the energy gain, shown in Figure 38.11.

Several designs have been proposed on accelerator driven systems, since the pioneering work by Van Atta and colleagues in 1970 [7], but they always correspond to a fission reactor very similar to the conventional ones, although subcritical, with an empty space somewhere in the central part of the reactor core, where the spallation source is located. The most modern project of this type of devices is MYRRHA, depicted in Figure 38.12.

An accelerator-driven system can be devised for different objectives, as already explained, but the most complete case is to aim at all the goals at the same time. That was the spirit of the energy amplifier [60, 62–64] proposed by Carlo Rubbia, summarized in Figure 38.13. The accelerator is a two-step cyclotron fed by the proton injectors. The second step is a booster to accelerate the beam up to 600 MeV per proton or so, in order to have a good source performance.

The source is located in the middle of the reactor core axis, which is in the bottom of a reactor vessel filled with molten lead (Pb) or Pb-Bi eutectic. The reactor vessel is very tall for enhancing natural convection of the molten metal, but that option conveys an important structural

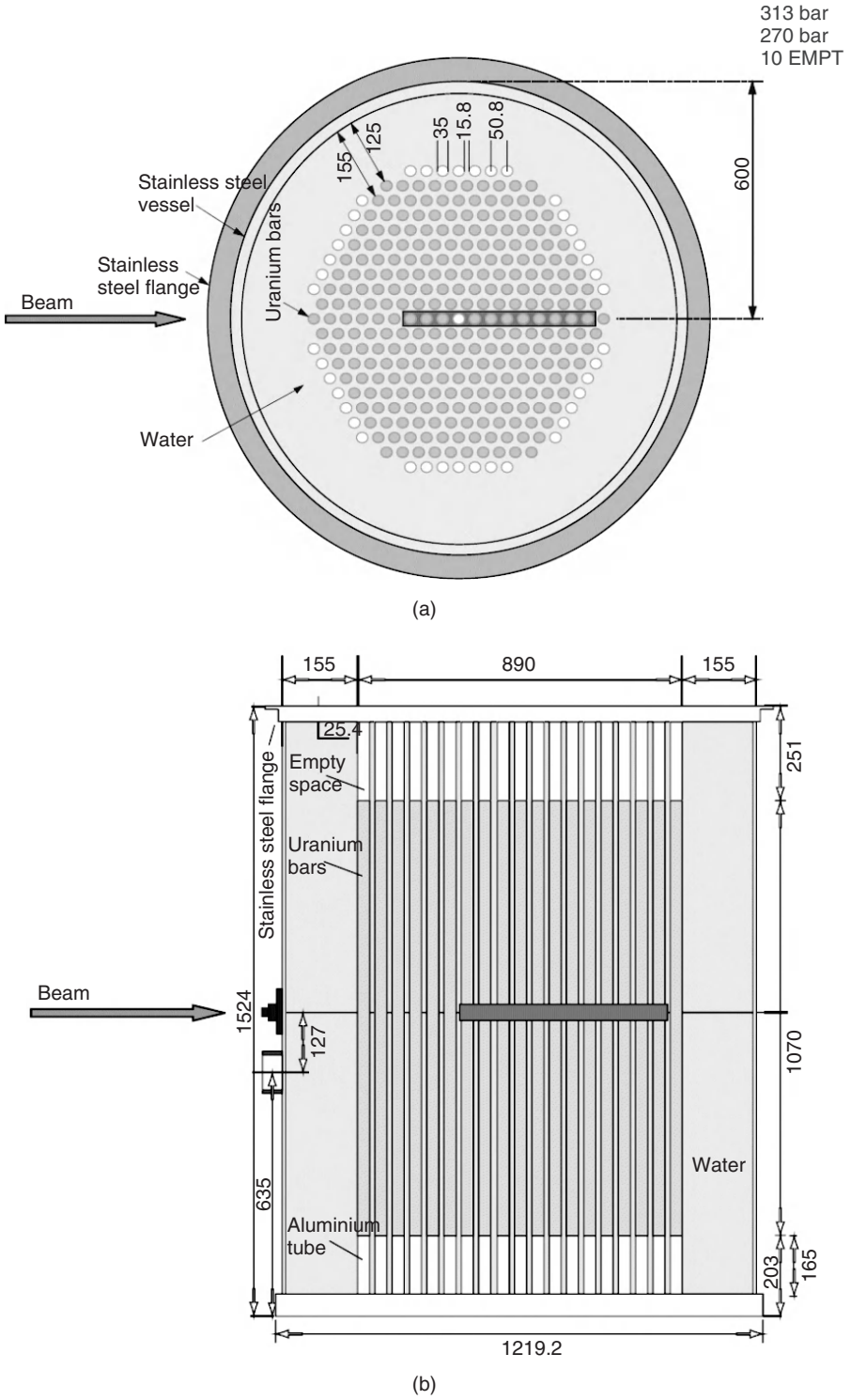

Figure 38.10 (**a**) Top view of the critical assembly of the FEAT experiment. **(b)** Side view of the critical assembly of the FEAT experiment.

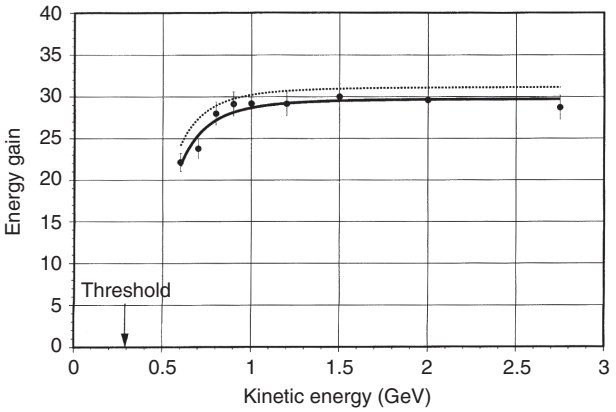

Figure 38.11 Energy gain of the FEAT [62] experiment as a function of the proton energy. The concept of energy gain, or energy multiplication, is explained later on. *(Source: S. Andriamonje et al., Physics Letters B 348 (1995) 697–709.)*

burden because of the very high density of the coolant. Other alternatives are based on shorter vessels where the coolant is propelled by electromagnetic pumps.

It is worth pointing out in the fuel cycle of the energy amplifier (Fig. 38.13) that it is aimed at working in a perfect equilibrium, because it takes 2.9 tons of Th and gives back 2.9 tons of fission fragments, after producing 2 GW (thermal) for five years (1,500 effective days at full power). In fact, the weight of the fission fragment will be slightly less than that, because 0.1% of that mass had disappeared in the fission process, being converted into heat. Of course, the system can also work with uranium, but this option could disturb the standard market of nuclear fuels for LWRs. This proposal of exploiting Th [65] has two reasons: Th is not used in LWRs, and Th reserves are bigger than U reserves. Anyway, the hybrid option presents this possibility, which is another signal of its high energy potential.

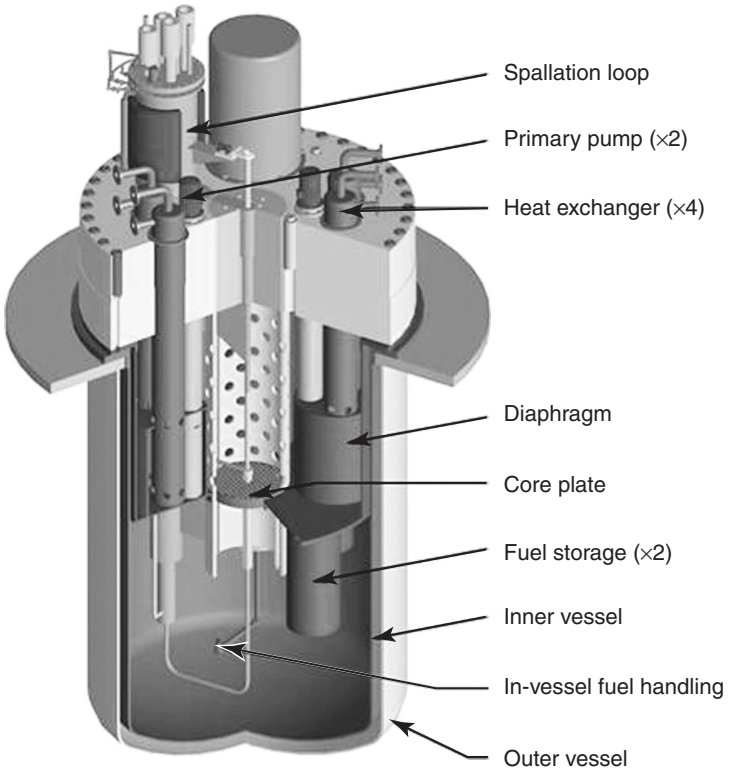

Figure 38.12 The MYRRHA project being developed at Mol Nuclear Research Center (Belgium) is a hybrid experimental reactor aimed at testing all components of this type of reactor. It is a subcritical reactor with a spallation source in its central axis, where the protons of an accelerated beam impinge. The spallation source has a special refrigeration loop, separated from the main cooling loop of the nuclear fuel, because the spallation molten metal will have to be cleaned continuously in order to avoid the build-up of an offending radioactive inventory inside it, because the spallation reaction happens in the molten metal stream that is at the end of the beam tube coming from the proton accelerator. The MYRRHA reactor will be particularly intended for transmutation of minor actinides and material irradiation.

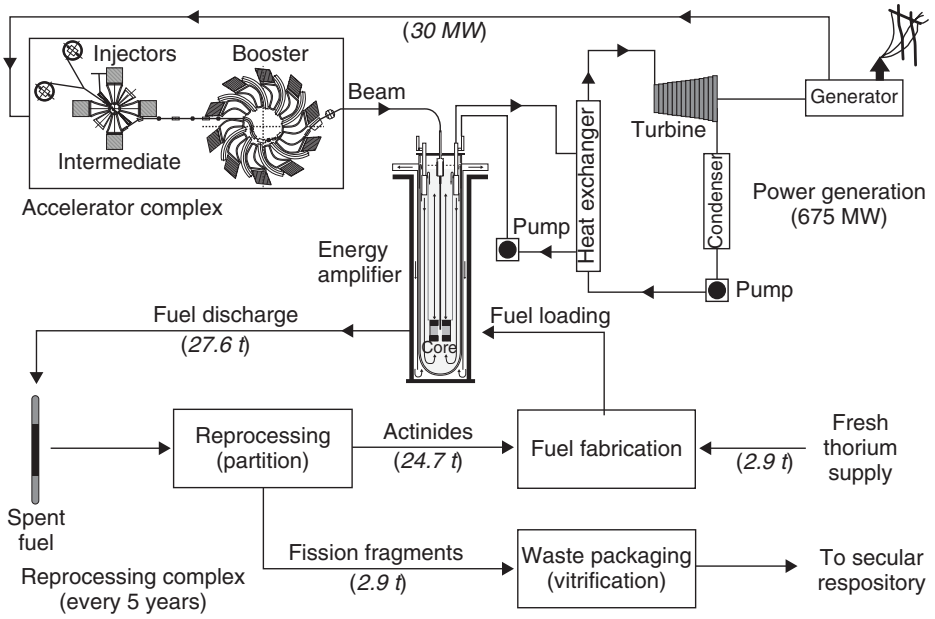

Figure 38.13 An outline of Carlo Rubbia's energy amplifier [60], including all components for making electricity. The corresponding fuel cycle is also shown, including reprocessing and recycling, and the supply of natural fuel, which is Th in this case. The concept also includes the incineration of most of actinides inside the subcritical assembly, and the waste is only made of fission fragments. This means that those wastes would reach the natural level of radiotoxicity after 700 years, approximately.

38.4 NEUTRONIC CHARACTERIZATION OF A HYBRID REACTOR

Although a hybrid has a degree of freedom that can be used to some extent for optimizing a given goal, it is obvious that hybrid performance is limited by a number of factors, which can be either thermal restrictions or properties of the nuclear components.

In the thermal field, a subcritical reactor has to comply with the same requirements of critical reactors, particularly those restrictions oriented to guarantee the integrity of the confinement barriers, both at nominal operation and accidental conditions. Those limitations apply to the maximum power density allowed in the reactor, which can be expressed in some cases in terms of maximum linear power density, or maximum heat flux. The main criterion is to make sure that solid materials, notably claddings of the fuel, remain in solid form and are able to withstand the mechanical requirements from weight, pressure differences, and temperature gradient (which can produce significant mechanical stresses).

In the nuclear field, a hybrid also has some limits in its performance to exploit the nuclear fuel, because a neutron cannot do two reactions at the same time, so to speak. This is why it is important to analyze the basics of their neutronic performance [5].

A hybrid can be considered a subcritical blanket surrounding a source where Q neutrons per second are born. A fraction ζ of the fusion-born neutrons reach the blanket, which is made of a fissile material (P), a fertile material (U), and other nuclei such as structural materials and the coolant. The fuel composition will be characterized by E, which stands for the fissile-to-fertile concentration ratio.

$$\mathrm{E} = \frac{\mathrm{P}}{\mathrm{U}} \tag{38.3}$$

A simple subcritical accounting leads to the following calculation of the total number T of neutrons disappearing in the blanket, through absorption or leakage, per source neutron

$$\mathrm{T} = \zeta \frac{\psi^*}{1 - \mathrm{k}} \tag{38.4}$$

where ψ^* is an importance factor [38], formerly represented by I; but ψ^* is a more common representation, because of being closely related to the adjoint function. The physical interpretation of ψ^* can be derived from the reciprocity principle between direct and adjoint fluxes and sources [38]

$$(\psi^+ \mathrm{S}) = (\mathrm{S}^+ \psi) \tag{38.5}$$

The adjoint source S^+ can represent either a definite cross-section or the function 1/v, which enables one to relate the importance function ψ^+ either to a reaction rate or to the number of neutrons produced in the reactor.

The basic parameters chosen to characterize the blanket neutronics are

- v' mean number of secondary neutrons per multiplicative reaction (in most of the hybrids, this will be very close to v, the number of neutrons per fission).
- η' mean number of secondary neutrons per absorption in the fuel (accounting for all types of fuel nuclei, not only for fissile ones).
- x probability of a neutron in the blanket to be absorbed in the fuel.
- z the probability of an absorption in the fuel to be a fertile capture.

Any relevant integral magnitude of the hybrid can be expressed in terms of the former parameters. For instance, the effective multiplication factor k

$$k = \eta' x \tag{38.6}$$

and the breeding ratio B (i.e., the conversion ratio (Eq. (38.1)) of this reactor, that would be larger than 1)

$$B \geq \frac{z}{1-z} \tag{38.7}$$

where the equality holds for $\sigma_{cU} = \sigma_{aU}$, that is, when the rate or multiplicative (fission) reactions in the fertile material U is negligible. In general, it will be so, because most of the neutron multiplication reactions will take place in the fissile nuclei.

On the other hand, these parameters are interrelated through

$$z + \frac{\eta'}{v'} \leq 1 \tag{38.8}$$

the equality being fulfilled for $\sigma_{cp} = 0$, i.e., when all the fissile absorptions are multiplicative reactions. In suitable hybrid reactors working as converters, more than 80% of the absorptions will convey neutron multiplication.

The value of those parameters will depend on the fuel composition and the spectrum. As a very rough estimate, for a thermal blanket with uranium it can be fitted to

$$\eta' = \frac{2.1E}{E + 0.01} \tag{38.9}$$

and for a fast blanket (with plutonium)

$$\eta' = \frac{3E + 0.006}{E + 0.03} \tag{38.10}$$

It is obvious that the fuel composition is the fundamental factor defining the values of the former parameters, and the fuel composition has to be tailored to get the required values for a given goal. In this context, it must be noted that the fuel composition and the breeding ratio are related through a spectral index w, defined as follows

$$w = \frac{\sigma_{cU}}{\sigma_{aP}} = EB \tag{38.11}$$

where E and B have been defined in Eqs. (38.3) and (38.7). It is worth quoting that for thermal spectra, $w \sim 0.01$ (or even smaller); for epithermal spectra, $w \sim 0.05$, and for fast ones, $w \sim 0.1$ or even larger. It is possible to obtain higher w figures with intermediate spectra generated by incomplete moderation.

One of the main consequences of last equation is the definition of the maximum fissile to fertile ratio E^* achievable in a breeding regime ($B \geq 1$), which is equal to the spectral index:

$$E^* = w \tag{38.12}$$

The previous findings will be used now to qualify the performance of the hybrid in relation to the main objectives: to generate energy and produce fissile fuel.

38.4.1 Fissile Production (Breeding)

If ε stands for the number of fertile captures produced per source neutron, we have

$$\varepsilon = \frac{\zeta \psi^*}{1 - \eta' x} zx \tag{38.13}$$

and taking into account Eq. (38.8),

$$\varepsilon \approx \frac{\zeta \psi^*}{1 - v'(1-z)x} zx \tag{38.14}$$

$$\left(\frac{d\varepsilon}{dz}\right)_{v'x} = \frac{\zeta \psi^* (1 - v'x)x}{(1 - v'(1-z)x)^2} \tag{38.15}$$

It is clearly observed that the sign of the derivative depends on $(v'\ x - 1)$. For $v'\ x > 1$, the derivative is negative, i.e., ε increases as z decreases, but the minimum value of z is bounded because criticality is attained at

$$z_{min} = \frac{v'x - 1}{v'x} \tag{38.16}$$

As $z \to z_{min}$, ε tends to infinity, but this is an asymptotic behavior related to the mathematical fact that the neutron flux in a critical reactor tends to infinity if it is neutronically fed by an external source.

Of course, this situation is utterly impossible, because the power would also be infinite.

38.4.2 Neutron Subcritical Multiplication

The most important reaction in this subject is fission, which yields $Q_f \sim 200$ MeV per reaction. We must also include the capture contribution with $Q_c \sim 6.5$ MeV and the (n, 2n) and (n, 3n) energy-consuming reactions with $Q_{n,2n} = -6$ MeV and $Q_{n,3n} = -12$ MeV.

If γ stands for the energy multiplication in the blanket per unit of source energy, then

$$\gamma = \frac{Q_f}{Q_s}\zeta\frac{\psi^*}{v}\frac{k}{1-k}\frac{1+\frac{Q_{n,2n}}{Q_f}\frac{\Sigma_{n,2n}}{\Sigma_f}+\frac{Q_{n,3n}}{Q_f}\frac{\Sigma_{n,3n}}{\Sigma_f}+\frac{Q_c}{Q_f}\frac{\Sigma_c}{\Sigma_f}}{1+\frac{2}{v}\frac{\Sigma_{n,2n}}{\Sigma_f}+\frac{3}{v}\frac{\Sigma_{n,3n}}{\Sigma_f}}+1 \quad (38.17)$$

In the usual cases where fission dominates both energy and neutron multiplication, it can be written

$$\gamma = \zeta\frac{\psi^*}{v}\frac{\eta' x}{1-\eta' x}\frac{Q_f}{Q_s}+1 \quad (38.18)$$

which tends to infinity as the blanket approaches criticality ($\eta' x = 1$). Safety requirements, particularly subcriticality margins, set the maximum k allowable, and therefore the maximum energy multiplication factor.

38.4.3 Effective Fissile Production

Taking into account that a light water reactor yields a discharge burn-up (in percent) very close to the feed enrichment (in percent as well) in a once-through cycle, the potential energy can be defined by Q_f (200 MeV) times the number of fissile nuclei produced, ε. Hence, the support ratio would be

$$S = \frac{Q_f}{Q_s}\frac{\varepsilon}{\gamma} = \frac{\xi\psi^* z x \nu' Q_f}{\xi\psi^* k Q_f + \nu'(1-k)Q_s} \quad (38.19)$$

which is expressed in terms of the basic parameters of the blanket and the source.

When the energy balance in the hybrid is dominated by the blanket (because k is not very far from 1) an upper limit of S can be found, which corresponds to

$$S = \frac{z\nu'}{\eta'}$$

In fact, this is only true for $k = 1$, but it gives a general indication of the importance of the blanket parameters.

If Eq. (38.8) is taken into account for the simplest case of $\sigma_{cp} = 0$, it holds

$$z = 1 - \frac{\eta'}{\nu'} \quad (38.20)$$

and the support ratio becomes

$$S = \frac{\nu' - \eta'}{\eta'} \quad (38.21)$$

For a fast spectrum subcritical blanket, one can have $\nu' = 3$ and $\eta' = 1$. This means that S will be close to 2. If neutron parasitic captures are taken into account, this value can decrease by 10% or so. It is important to note that this value of η' includes all types of neutron absorptions in the fuel isotopes, both fissile and fertile ones.

The former value indicates that a breeder can produce fissile fuels for LWR reactors with a total power twice as large as the breeder power. From this general calculation, it could be said that natural resources utilization could reach 65% with this scheme, instead of 0.5 or 1%. Such a potential makes a strong difference in the quest for safely exploiting the natural nuclear ores.

38.5 NUCLEAR ENERGY SUSTAINABILITY

Current commercial reactors are not good at exploiting the nuclear natural resources, burning barely 0.6%. Reaching a percentage approaching 100% will need breeders, and this is a formidable challenge, because critical fast reactors could suffer from some reactivity effects [2–4], leading to positive feedback between thermal hydraulics and nuclear power, which can produce exceedingly large power surges. When the coolant density decreases, eventually reaching zero in an accident, two effects increase the reactivity of the reactor: The neutron spectrum hardens, because of a lower moderation effect, and the neutron capture rate decreases, because of the absence of an absorbing material (the coolant).

Those well-known facts were discussed at depth in the INFCE [40] international study (1978–1980), carried out under the umbrella of United Nations Organization and the IAEA agency, and representing a severe blow against the fast reactor research and development program. However, 30 years later it seems mandatory to start a new phase of nuclear energy development policy, aimed at finding the most suitable ways for nuclear fission to be a significant contributor to the generation of electricity in the mid and long term, in the context of sustainable development and the fight against global warming by excessive greenhouse effect gases.

After reviewing the risks and the benefits of nuclear fission, a proposal for sustainability technical criteria in nuclear energy can be established on the following technical guidelines:

- Enhanced safety in nuclear reactors and nuclear fuel facilities (an example of this idea is given in Figure 38.14).

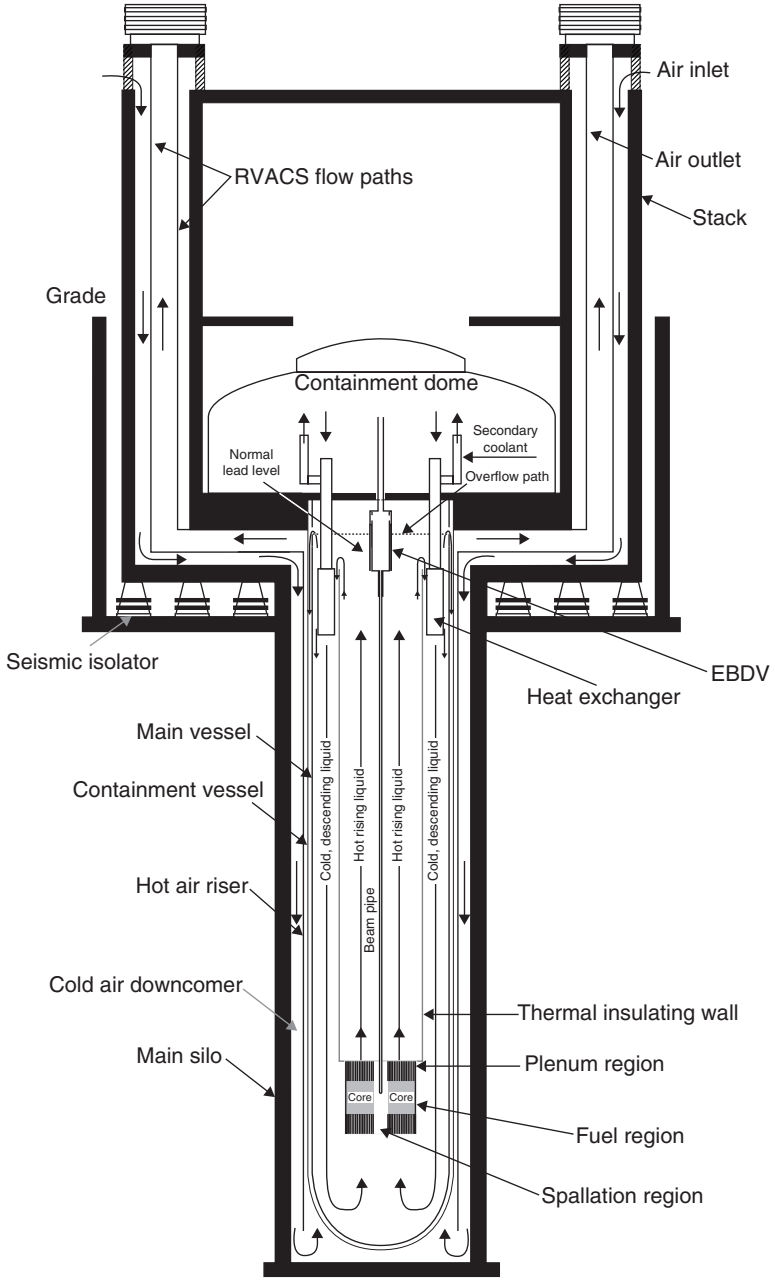

Figure 38.14 An outline of the reactor vessel of Carlo Rubbia's energy amplifier [60], where molten lead is the reactor coolant and moves by natural convection, transferring heat to the secondary circuit through the heat exchangers placed in the upper place of the molten lead pool. Cooling by natural convection of air was also considered to remove the residual heat after stopping the beam, if the full system could not operate. Passive safety is an important complementary feature in hybrids.

- High-level exploitation of natural nuclear materials (which is in connection with Figure 38.5, where the concept of nuclear breeding was introduced; which in turn is connected with the spectral index given in Figure 38.15).
- Minimization of the radioactive inventory in the waste.
- Development of proliferation-resistant technologies.

The last point seems to be very critical for the future of nuclear energy in a large scale [66–69], and it could

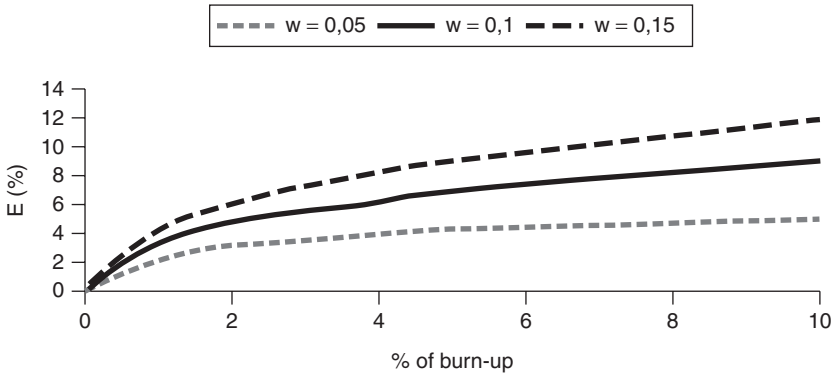

Figure 38.15 Fissile-to-fertile ratio (E) evolution along burn-up as a function of the spectral index w.

dominate the definition of R&D activities in the future, both in terms of reactors and fuel cycles. However, this is mainly a political and diplomatic problem, and it can be said that in all countries having nuclear weaponry, the military program was not taking any benefit from the civilian program (in some countries, there was not any civilian program). Nevertheless, developing proliferation-free facilities would ease a lot a larger deployment of civilian nuclear energy. This also affects reprocessing, because it is a potential way of diverting nuclear fissile material from the reprocessing stream. In summary, more attention should be paid to proliferation-resistant features, because some reprocessing methods [69] produce a stream of Pu/Np that could be considered not totally safe for non-proliferation purposes [70].

On the other hand, limitations in mineral reserves led to the concept of sustainability of energy in a finite world [66], although the very concept of sustainable development needed some more time to be formulated [71]. Anyway, the key for addressing this challenge is how to propose and develop new technologies for properly exploiting the available resources. In the case of nuclear energy, this quest has produced several proposals on critical reactors [72–74].

Breeder reactors are needed for a complete exploitation of natural resources, but critical fast breeders have a supercriticality problem associated to variations of coolant density. These concerns are not unfounded and have dogged the history of fast reactors from its very beginning when, back in the 1970s, the engineering and safety problems encountered in the Enrico Fermi Nuclear Generating Station [75], the first American breeder reactor, led to a failed license renewal. The closure, in 1983, of the high-profile Clinch River Breeder Reactor [76] was another signal of the importance of the problem. It is worth noting that it was the Reagan Administration that finally decided the halt the U.S. Fast Breeder Program in 1983, although INFCE had been launched by President Carter.

Hybrids are very appealing machines in this context because they can be designed to remain subcritical even in severe accidental conditions, such as the full void of the molten metal acting as core coolant. Although sodium was the standard choice for fast reactors [3], lead has become an interesting alternative, although it also conveys the problem of a positive reactivity coefficient or coolant voids and reduction in density. Of course, this problem is much less severe in a hybrid, as the energy amplifier [60], but the problem of positive feedback still exits, although at a much lower scale. In fact, the subcritical margin of a hybrid can be chosen to make it sure that criticality is not reached even if the worst positive feedback happens. Nevertheless, as can be seen in Eq. (38.17), an increase in k conveys an increase in thermal power, and that could entail a severe cooling problem.

38.5.1 Systematic Approach for Hybrid Performance Analysis

There are three main ways to use hybrids, in relation to the fission natural fuel, which are exposed in the following paragraphs. Another point is the contribution of fusion–fission systems for producing the tritium contents needed to feed the fusion chamber, which was already introduced in Figure 38.3.

Regarding the potential of hybrids to exploit the fission natural fuel, three ways could be followed:

- The energy amplifier scheme [60], in which the spent fuel is reprocessed to separate fission fragments (waste) from transuranium elements. The latter fraction is recycled (after fuel refabrication) to continue energy extraction from the original fuel. In general terms, the system can work as a breeder, and a part of the fuel recovered by reprocessing would be sent for feeding other reactors.

- The LIFE approach [42], which does not include reprocessing, because the fuel remains always inside the balls of fuel, which embody a series of shell and matrices to keep the radioactive products inside them forever. The subcritical reactor composition is tailored to have a conversion ratio above 1, to keep the multiplication factor almost constant. The spent fuel balls would be downloaded once exhausted, i.e., without any remaining fissile inventory. The spent fuel balls would be sent to an isolation plant or repository. Of course, this is a quest with many challenges, because of the very high contents of fission fragments (some of them, in gaseous form) accumulated in a hot graphite fuel.
- The third option is what can be called the "fissile factory," based on the proposal by Van Atta and colleagues [7] followed by Takahashi [35] and others, and reformulated by Martinez-Val and Piera [33]. It is based on keeping the hybrid at low temperature, with moderate power density, in order to minimize the effects of loss of coolant accidents and to improve the integrity of confinement barriers. Of course, the only goal in this case would be fissile breeding, to be burned up in other reactors, notably Gen-3 ones, which seem to have very high safety standards.

As depicted in Figure 38.16, two types of reactors would be needed to close this nuclear fuel cycle. On the one hand, burner reactors would be responsible for producing the required energy. In our approach, these reactors would be LWR type. The second type of reactors, "converters," would produce the nuclear conversion and could be fed from reprocessed fuel, from depleted uranium, or from natural thorium. Those breeders would be hybrid reactors.

In the interest of hybrids being combined with Generation-3 reactors, as depicted in Figure 38.17, takes into account the very high safety level of these reactors and the enormous capability of hybrids to breed fissile material. This could be a way to satisfy the requirements formerly cited on nuclear energy sustainability.

It is obvious that the other ways to run hybrids, in the line of the energy amplifier or LIFE, are more ambitious, and they would produce energy in the subcritical assembly with very high temperature for having a high energy efficiency and to breed fissile fuel both for replacing the spent fuel in the reactor and to discharge part of it for reprocessing and preparation of new fuel elements for other reactors, either critical or subcritical. In this case, the risk of thermal accidents would be higher than in the previous case, because the specific power and the power density would be much higher than in Gen-3 reactor, which can be considered as the reference about safety.

The three alternatives presented cannot be evaluated as general proposals, because they will depend a lot on the composition used in each case. They would also depend on the general economic and international scenario, because having or not having commercial reprocessing will represent a big change in the evaluation criteria, and that point will mainly be related with the proliferation problem.

It should be added that a breeder hybrid can produce [33] fissile fuels for LWR reactors with a total power twice as large as the breeder power. This value can be considered very modest, but it would imply that natural resources utilization could reach 65% with this scheme,

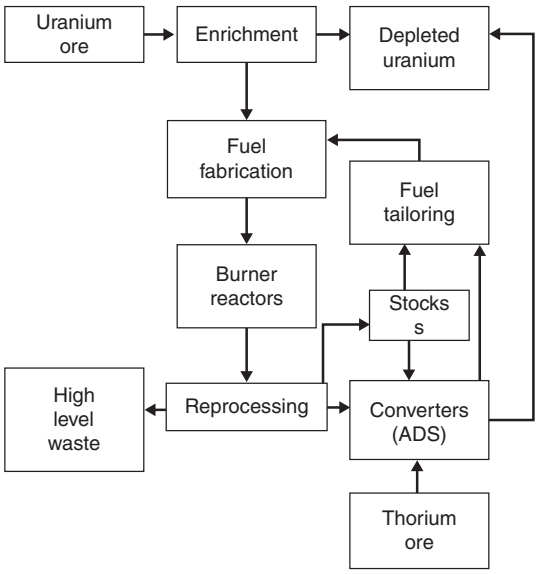

Figure 38.16 The hybrid "fissile factory," performing as a breeder to fabricate fuel for critical "burner reactors" with very high safety standards, as LWRs of the second and third generations.

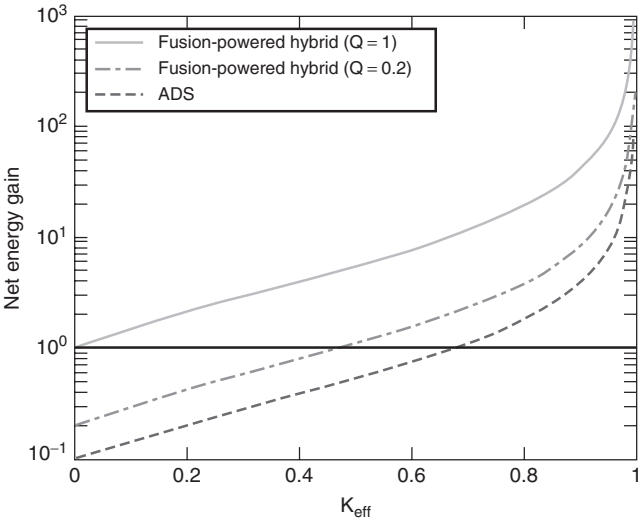

Figure 38.17 Net energy gain as a function of the K_{eff} for different system's drivers.

instead of 0.5 or 0.6% as in current LWRs. Those breeder-hybrids would not be intended for energy production, so that safety standards could rely on very low values of the thermal magnitudes, allowing for very large safety margins for emergency cooling. Similarly, subcriticality would offer a very large margin for not reaching prompt-criticality in any event.

It is worth remembering that current and anticipated LWR present very robust safety standards, but they are not suited for an effective exploitation of the natural resources, which need fertile-to-fissile breeding. This goal can be achieved in a fast breeder reactor (and less probably, in a thorium thermal (critical) breeder), but safety analysis on those reactors, particularly FBR, identified some major problems in connection with reactivity trips and nuclear-thermal-hydraulic feedback. Those risks were analyzed in the INFCE initiative, which was a serious blow against the FBR development [40].

38.5.2 Is a Comparison Possible between ADS and Fusion–Fission Hybrids?

Yes and no. Some papers have been published on this topic, particularly the recent one by Salvatores [37], but many assumptions are needed for establishing such a comparison, and one can discuss endlessly the value of those assumptions. Anyway, a main difference lies in the fact that accelerators are always energy-consuming machines, and fusion devices could eventually produce net energy. This point is relevant for the comparison because of the importance of the energy invested in generating one neutron injected into the fission assembly, which is in turn connected with the subcritical neutron multiplication in said assembly.

In this comparison, a fundamental result is depicted in Figure 38.17 (where data from the paper by Slessarev [34]) have been used. In this figure, net energy gain means the ratio between the output electrical power of the reactor and the electric power needed to operate it, and it is depicted as a function of the K_{eff}. This relationship is of paramount importance, because it sets a threshold in the multiplication factor of the subcritical assembly, for each type of hybrid.

The lowest curve represents the results for an accelerator-driven system whose source produces an average of 20 neutrons per spallation reaction, each one with an importance of 1.3, and assuming both an electrical and accelerator efficiency of 45%.

On the other hand, the upper lines show the same evolution for a D-T fusion-powered system when Q equals 1 or 0.2, with Q being the total electric energy outcome in a period of time, divided by the total energy invested in the fusion reactor for triggering or keeping the fusion power along that period. Note that $Q = 1$ corresponds to the 'breakeven point' and $Q<1$ corresponds to the 'negative energy balance of a fusion installation. Obviously, for $Q = 1$, the threshold in K is zero, because the fusion reactor per se is already in the fusion threshold to be an energy producer. For an ADS, high K values are needed, because of the energy balance in the accelerator. For instance, Rubbia's energy amplifier was devised to work over $K = 0.95$, and some of the designs were aimed at $K = 0.98$.

However, one can question the interest of having a hybrid (with a large radioactive inventory of fission fragments and actinides) if fusion has reached breakeven. The answer is twofold: It can make fusion cheaper, and it can exploit natural materials (as thorium), which represent a high total energy content and seem not to have other ways of exploitation.

38.6 SUMMARY AND FUTURE WORK

Hybrids present a wide range of performance possibilities and can therefore be a powerful tool for the deployment of nclear energy in a much larger scale than today. Moving toward that goal, some nuclear sustainability criteria must be met to dramatically reduce the drawbacks of nuclear energy. From the technical point of view, it is very important to achieve a very high percentage of exploitation of the raw nuclear materials (U and Th), which is currently a mere 0.6% for the former and 0% for the latter, but this must be done in a system of very high safety standards. For both purposes, hybrids present a very good potential, although they would require a tremendous effort of technological R&D. Challenges for this development depend quite a lot on the type of hybrid. For inertial-fusion-driven hybrids, a very complete specialist's account can be found in last section of the paper by E. Moses [45]. In the field of accelerator-driven systems, some roadmaps have been elaborated by different institutions, and a good recollection at specialist level is given in Chapter 7 of the document *Accelerator-Driven Systems (ADS) and Fast Reactors (FR) in Advanced Nuclear Fuel Cycles* [77] prepared by the Nuclear Energy Agency of OECD, available at http://www.nea.fr/ndd/reports/2002/nea3109.html.

A complete exploitation of the natural resources would likely need reprocessing and recycling, and this point has to be properly counterbalanced against the risk of proliferation posed by a given fuel cycle. A difficult point in this context is that the no-proliferation criterion has a lot of political weight, and the goal of exploiting the resources is mainly economical.

Waste is also important in the same balance, because the amount of waste per unit of generated energy will be lower in closed cycles with high burn-ups and actinide recycling. This is in connection to reprocessing, but is also in connection to safety, because of the nuclear properties of higher actinides. In particular, they have much lower values

of the fraction of delayed neutrons, as compared to U235, which is very negative for reactivity control.

This fact is another important reason for the evaluation of the hybrids to be very dependent on the blanket composition. Similarly, coolant composition is also of fundamental concern for the power stability in the blanket. Moreover, the blanket must not reach criticality under any condition, including loss of coolant accidents.

On the other hand, the blanket multiplication factor k also dominates the problem of tritium breeding in a fusion–fission hybrid. It was seen in Figures 38.3 and 38.4 that the higher the k-eff value, the smaller the fraction "m" of neutrons absorbed in the Li6 of the blanket to produce tritium. This is an advantage because a higher fraction of neutrons is absorbed in the fuel, either producing energy (through fission) or breeding new fissile nuclei (by fertile capture).

Although many papers on hybrids were published years ago, much more work must be done on many lines, including the selection of fuel (including the Th cycle) and the final selection of coolant for a given purpose.

In spite of the pending work, it should be said that very important properties of neutron interaction with some relevant nuclei are particularly suited for being exploited in a hybrid scenario.

Hybrids are still out of mainstream research, and an effort must be made by hybrid proponents in order to convince the scientific community and policymakers that hybrids deserve more study and support.

Acknowledgments

Courtesy of Carlo Rubbia about using pictures of his energy amplifier is highly recognized. Some of the authors were Carlo's collaborators at CERN, in the Emerging Energy Technologies initiative.

Information provided by Ed Moses and the LIFE team from Lawrence Livermore National Laboratory was very important for guiding the elaboration of this paper, and it was also useful for properly illustrating the fusion–fission hybrid.

Special thanks are given to Belgium's SCK-CEN at Mol, for information provided on the MYRRHA project and European activities in this field.

REFERENCES

1. INSAG 2006, *The Chernobyl Accident: Updating INSAG-1*, Safety Series 75. www.iaea.org, IAEA, Vienna, 2006.
2. J. M. Martínez-Val, J. M. Aragonés, E. Mínguez, J. M. Perlado, and G. Velarde, An analysis of the physical causes of the Chernobyl accident. *Nuclear Technology*, 1990, **90**, 3, 371–388.
3. F. Storrer, *Introduction to the Physics of Fast Power Reactors*, IAEA series 143, Vienna, 1973.
4. W. M. Stacey Jr., Improved reactivity table models for LMFBR dynamics. *Nuclear Science and Engineering*, 1972, **49**, 213–231.
5. M. Piera and J. M. Martínez-Val, Neutronic characterization and analysis of performance of fusion-fission hybrids. *Kerntechnik*, 1987, **50**, 197.
6. D. Ridikas and W. Mittig, Neutron production and energy generation by energetic projectiles: protons or deuterons? *Nuclear Instruments and Methods in Physics Research Section A: Accelerators, Spectrometers, Detectors and Associated Equipment*, 1998, **418**, 2–3, 449–457.
7. C. M. Van Atta, J. D. Lee, and W. Heckrotte, *The Electronuclear Conversion of Fertile to Fissile Material*. Lawrence Livermore Laboratory Report UCRL-52144, 1970.
8. H. A. Bethe, The fusion hybrid. *Physics Today*, 1979, **5**, 44.
9. D. J. Bender, Performance parameters for fusion-fission power systems. *Nuclear Technology*, 1979, **44**, 381.
10. M. Z. Youssef et al. Tritium and fissile fuel exchange between hybrids, fission power reactors and tritium produce reactors. *Nuclear Technology*, 1980, **47**, 397.
11. J. K. Presley et al., Nuclear fuel trajectories of fusion-fission symbionts. *Nuc. Science and Engineering*, 1980, **74**, 193.
12. S. I. Abdel-Khalik et al., Impact of fusion-fission hybrids on world nuclear future. *Atomkernenergie*, 1981, **38**, 1.
13. D. H. Berwald and J. Maniscalco, An economics method for symbiotic fusion-fission electricity generator systems. *Nuclear Technology/Fusion*, 1981, **1**, 128.
14. R. P. Rose, The case for the fusion hybrid. *J. of Fusion Energy*, 1981, **1**, 185.
15. J. D. Lee and R. W. Moir, Fission-suppressed blankets for fissile fuel breeding fusion reactors. *J. of Fusion Energy*, 1981, **1**, 299.
16. E. Greenspan and G. H. Miley, Fissile and synthetic fuel production ability of hybrid reactors. *Atomkernenergie*, 1981, **38**, 12.
17. A. A. Harms and C. W. Gordon, Fissile fuel breeding potential with paired fusion-fission reactors. *Annals of Nuclear Energy*, 1976, **3**, 411.
18. S. Taczanowski, Neutron multiplier alternatives for fusion reactor blankets. *Annals of Nuclear Energy*, 1981, **8**, 29.
19. A. A. Harms and M. Heindler, *Nuclear Energy Synergetics*. Plenum, New York, 1982.
20. R. W. Moir, The fusion breeder. *J. Fusion Energy*, 1982, **2**, 351.
21. R. W. Moir, Design of a He-cooled, molten salt fusion breeder. *J. Fusion Technology*, 1985, **8**, 465.
22. R. W. Moir et al., Fusion breeder reactor design studies. *Nuclear Technology/Fusion*, 1983, **4**, 589.
23. J. D. Lee, US-DOE fusion breeder program-blanket design and system performance. *Atomkernenergie*, 1984, **44**, 35.
24. S. J. Piet, Safety evaluation of the blanket comparison and selection study. *Fusion Technology*, 1985, **8**, 77.
25. J. Garber, and I. Maya, Safety assessment of the fusion breeder. *Fusion Technology*, 1985, **8**, 474.

26. B. R. Leonard Jr., A review of fusion-fission (hybrid) concepts. *Nuclear Technology*, 1973, **20**, 161.
27. C. Powell and D. J. Hahm, Energy balance of a hybrid fusion-fission reactor. *Atomkernergie*, 1973, **21**, 172.
28. L. M. Lidsky, Fusion-fission systems: hybrid symbiotic and augean. *Nuclear Fusion*, 1975, **15**, 939.
29. A. A. Harms, Hierarchical systematics of fusion-fission energy systems. *Nuclear Fusion*, 1975, **15**, 989.
30. N. G. Cook and J. A. Maniscalco, J.A., Uranium-233 breeding and neutron multiplying blankets for fusion reactors. *Nuclear Technology*, 1976, **30**, 5.
31. J. Maniscalco, Fusion-fission hybrid concepts for laser induced fusion. *Nuclear Technology*, 1976, **28**, 98.
32. V. L. Blinkin and V. M. Novikov, Symbiotic system of a fusion and a fission reactor with very simple fuel reprocessing. *Nuclear Fusion*, 1978, **18**, 7.
33. J. M. Martínez-Val and M. Piera, Nuclear fission sustainability with hybrid nuclear cycles. *Energy Conversion and Management*, 2007, **48**, 1480–1490.
34. I. Slessarev and P. Bokov, On potential of thermo-nuclear fusion as a candidate for external neutron source in hybrid systems (applied to the WISE concept). *Annals of Nuclear Energy*, 2003, **30**, 16, 1691–1698.
35. H. Takahashi et al., Fissile fuel production by linear accelerator. *Trans. Am. Nucl. Soc*., 1982, **43**, 138.
36. S. Sahin, Neutronic analysis of fast hybrid thermoionic reactors. *Atomkernenergie*, 1981, **39**, 41.
37. M. Salvatores, Physics features comparison of TRU burners: fusion/fission hybrids, ccelerator-driven systems and low conversion ratio critical fast reactors. *Annals of Nuclear Energy*, 2009, **36**, 11–12, 1653–1662.
38. J. Lewins, *Importance: The Adjoint Function: The Physical Basis of Variational and Perturbation Theory in Transport and Diffusion Problems*. Pergamon Press, Cambridge, UK, 1965.
39. *Advanced Nuclear Fuel Cycles and Radioactive Waste Management*. Nuclear Energy Agency, OECD, 2006
40. N. Oi and L. Wedekind, *INFCE, Changing Global Perspectives* Available: http://www.iaea.org/Publications/Magazines/Bulletin/Bull401/article2.html.
41. NEA/OECD 2002, *Accelerator-driven System (ADS) and Fast Reactors (FR) in Advanced Nuclear Fuel Cycles: A Comparative Study*, NEA/OECD Report, 2002.
42. C. Rubbia, S. Buono, Y. Kadi, and J. A. Rubio, *Fast Neutron Incineration in the Energy Amplifier as Alternative to Geological Storage: The Case of Spain*. CERN/LHC/97-01, 1997.
43. LIFE project; http://lasers.llnl.gov/missions/energy-for-the-future/life.
44. K. Kramer, *Laser Inertial Fusion-Based Energy: Neutronic Design Aspects of a Hybrid Fusion-Fission Nuclear Energy system*. Unpublished PhD thesis, University of California, Berkeley, Berkeley, CA, 2010.
45. E. I. Moses, T. Diaz de la Rubia, J. F. Latkowski, J. C. Farmer, R. P. Abbott, K. J. Kramer, P. F. Peterson, H. F. Shaw, and R. F. Lehman II, A sustainable nuclear fuel cycle based on laser inertial fusion energy (LIFE). *Fusion Science and Technology*, August 2009, **56**, 2, 566–572.
46. K. J. Kramer, J. F. Latkowski, R. P. Abbott, J. K. Boyd, J. J. Powers, and J. E. Seifried, Neutron transport and nuclear burnup analysis for the laser inertial confinement Fusion-Fission energy (LIFE) engine. *Fusion Science and Technology*, August 2009, **56**, 2, 625–631.
47. R. P. Abbott, M. A. Gerhard, K. J. Kramer, J. F. Latkowski, K. L. Morris, P. F. Peterson, and J. E. Seifried, Thermal and mechanical design aspects of the LIFE engine. *Fusion Science and Technology*, August 2009, **56**, 2, 618–624.
48. S. C. Wilks, B. I. Cohen, J. F. Latkowski, and E. A. Williams, Evaluation of several issues concerning laser beam propagation through the LIFE target chamber. *Fusion Science and Technology*, August 2009, **56**, 2, 652–657.
49. R. W. Moir, H. F. Shaw, A. Caro, L. Kaufman, J. F. Latkowski, J. Powers, and P. E. A. Turchi, Molten salt fuel version of laser inertial fusion-fission energy. *Fusion Science and Technology*, August 2009, **56**, 2, 632–640.
50. K. J. Kramer, W. R. Meier, J. F. Latkowski, and R. P. Abbott, Parameter study of the LIFE engine nuclear design. *Energy Convers. Manage*., 2010, **51**, 9, 1744–1750.
51. W. R. Meier, R. Abbott, R. Beach, J. Blink, J. Caird, A. Erlandson, J. Farmer, W. Halsey, T. Ladran, J. Latkowski, A. MacIntyre, R. Miles, and E. Storm, Systems modelling for the laser fusion-fission energy (LIFE) power plant. *Fusion Science and Technology*, August 2009, **56**, 2, 647–651.
52. The High Temperature Reactor and Nuclear Process Heat Applications (special issue). *Nuclear Engineering and Design*, 1984, **78**.
53. K. Kugeler and R. Schulten, *Hochtemperaturreaktortechnik*. Springer Verlag, Heidelberg, Germany, 1989.
54. K. Kugeler and P. W. Philippen, The potential of self-acting safety features of high temperature reactors. *Kerntechnik*, 1996, **61**, 5.
55. G. Lohnert, Technical design features and essential safety-related properties of the HTR Module. *Nucl. Eng. Des*., 1990, **121**, 259.
56. K. Krueger, A. Bergerfurth, S. Burger, P. Pohl, M. Wimmers, and J. C. Cleveland, Preparation conduct and experimental results of the AVR Loss of coolant accident simulation test. *Nucl. Sci. Eng*., 1991, **107**, 99.
57. W. Heit and H. Huschka, Status of qualification of HTGR fuel element spheres. *Nucl. Technol*., 1985, **69**, 44.
58. K. Sawa et al., Safety criteria and quality control of HTR fuel. *Nucl. Eng. Design*, 2001, **208**, 305.
59. J. T. Maki, D. A. Petti, D. L. Knudson, and G. K. Miller, The challenges associated with high burnup, high temperature and accelerated irradiation for TRISO-coated particle fuel., *Journal of Nuclear Materials*, 2007, **371**, 1–3, 270–280.
60. C. Rubbia et al., *Conceptual Design of a Fast Neutron Operated High Power Energy Amplifier*. CERN/AT/95-44, 1995.
61. H. Aït Abderrahim and P. D'hondt, MYRRHA: a European experimental ADS for R&D applications. *Journal of Nuclear Science and Technology*, 2007, **44**, 3, 491–498.

62. S. Andriamonje, A. Angelopoulos, A. Apostolakis, F. Attale, et al., Experimental determination of the energy generated in nuclear cascades by a high energy beam. *Phys. Lett. B*., 1995, **348**, 697.

63. H. Arnould, C. A. Bompas, R. Del Moral, V. Lacoste, et al., Experimental verification of neutron phenomenology in lead and transmutation by adiabatic resonance crossing in accelerator driven systems. *Phys. Lett. B*, 1999, **458**, 167.

64. A. Abánades, J. Aleixandre, S. Andriamonje, A. Angelopoulos, et al., Results from the TARC experiment: spallation neutron phenomenology in lead and neutron-driven nuclear transmutation by adiabatic resonance crossing. *Nuclear Instr. & Methods* A, 2002, **478**, 577.

65. Thorium fuel utilization: options and trends. Proceedings of three IAEA meetings held in Vienna in 1997, 1998, and 1999. IAEA-TECDOC-1319.

66. W. Hafele, *Energy in a Finite World. Paths to a Sustainable Future. Energy in a Finite World. A Global System Analysis*. Ballinger, Cambridge, MA, 1981.

67. CEA, Systems nucleaires du future. Generation IV. *Clefs*, 2007, **55**.

68. NEA-OECD, *Innovation in Nuclear Energy Technology*. OECD, 2007.

69. IAEA, *Guidance for the Evaluation of Innovative Nuclear Reactors and Fuel Cycles: Report of Phase IA of the International Project on Innovative Nuclear Reactors and Fuel Cycles (INPRO)*. IAEA-TECDOC-1362, 2003.

70. Arms Control Center, *The Limited Proliferation-Resistance Benefits of the Nuclear Fuel Cycles of AFCI*, 2006. www.armscontrolcenter.org/archives/001711.php.

71. G. Brundtland, Chairman, World Commission on Environment and Development, *Our Common Future (The Brundtland Report)*. Oxford University Press, Oxford, United Kingdom, 1987.

72. NEA-OCDE, *Nuclear Energy in a Sustainable Development Perspective*, 2000, www.nea.fr/html/pub/webpubs/welcome.html.

73. Sustainable Nuclear Energy Technology Plantform, 2008,. www.snetp.eu.

74. U.S. Department of Energy, *The Path to Sustainable Nuclear Power*, www.er.doe.gov/bes/reports/files/PSNE_rpt.pdf, 2003.

75. R. L. Scott Jr., R.L., Fuel-melting incident at the Fermi Reactor on Oct. 5, 1966. *Nuclear Safety*, 1971, **12**, 2–10.

76. R. J. Slember, Safety-related design considerations for the Clinch River Breeder Reactor Plant. *Proceedings of the International Meeting on Fast Reactor Safety and Related Physics*. Chicago, IL, 1977, p. 112.

77. *Accelerator-Driven Systems (ADS) and Fast Reactors (FR) in Advanced Nuclear Fuel Cycles*. Nuclear Energy Agency, OECD, 2002. http://www.nea.fr/ndd/reports/2002/nea3109.html.

39

FUSION MAINTENANCE SYSTEMS

LESTER M. WAGANER
Fusion Consultant, O'Fallon, MO, USA

Future fusion power plants, both magnetically and inertially confined, will be ideally suited for production of electricity, hydrogen, and process heat. Since they will likely be capital intensive, they would be best utilized as base-loaded plants. Furthermore, they should be highly reliable and easily maintainable to achieve the highest level of plant capacity or availability so the plants can be commercially viable. To accomplish these goals, fusion power plants must have very efficient maintenance systems to achieve this high level of plant availability, on the order of 90% similar to fission or hydrocarbon-fueled power plants. This means the plant must be capable of operating 90% of the time at full capacity.

39.1 RATIONALE FOR REMOTE MAINTENANCE

The first generation of fusion power plants, possibly available in two to four decades, will likely burn or fuse two hydrogen isotopes, deutritium (D) and tritium (T). Fusing these hydrogen isotopes in a high-temperature plasma with sufficient temperature and pressure will create a helium alpha particle (3.5 MeV) and a high energy (14.1 MeV) neutron. This fuel combination is favored for the first-generation fusion power plants because it has the lowest temperature and pressure requirements for the fusion process.

The choice of these D and T fuel elements (and resultant particles) presents challenges in design and maintenance of the power core. Tritium is a radioactive hydrogen isotope with a half life of 12.33 years, decaying to helium-3 by beta decay with the release of 18.6 keV of energy. Beta radiation cannot penetrate the skin, so tritium is dangerous only if inhaled or absorbed as tritiated water through the skin. Since tritium is a hydrogen isotope with a small nuclear cross-section, it is highly mobile and can easily penetrate many materials and pass through small cracks or gaps. Because of those characteristics, efficient tritium containment is an important design and maintenance consideration in the power core.

Within the fusion plasma, the created 3.5 MeV alpha particle is charged and can be magnetically directed to specific parts of the power core inner surfaces. The most likely contact surface will be the divertor that is designed to absorb the alpha particle kinetic energy; however, the divertor will accrue some surface erosion damage over time that will require periodic replacement.

The high energy 14.1 MeV neutron is the primary energy and damage source because this neutron can penetrate deeply through the power-core elements before releasing its kinetic energy. The main power and fuel-producing component inside the power core is the blanket. This blanket typically contains lithium or a lithium compound to generate the tritium fuel. Interaction of the high-energy neutrons will transmute lithium (Li7 or Li6) into tritium and helium. Tritium and helium are removed from the blanket, and the tritium gas is separated for use in the fuel cycle. The high-energy neutrons interact with the blanket and other power-core components to thermalize their kinetic energy. This energy is recovered using a high-temperature coolant that is used in a thermal conversion system. Damage to the

Nuclear Energy Encyclopedia: Science, Technology, and Applications, First Edition (Wiley Series On Energy).
Edited by Steven B. Krivit, Jay H. Lehr, and Thomas B. Kingery.

materials in the power core is manifested as displacements per atom (dpa) to the detriment of the materials' physical properties. For fusion power plants of reasonable size, having a fusion power of 2000–3000 MW, this neutron damage can limit the interior power core subsystems' lifetimes to four to five years given today's technology. The economic lifetime of these fusion power plants is envisioned to be on the order of approximately 50 years, so this means about nine or more full change-outs of the damaged interior power core elements. These highly energetic neutrons can transmute elements they encounter and, in some cases, create radioactive elements or isotopes. One of the principal tenets of the fusion plant is to create a safe and environmentally friendly power source. This means not only creating any high-level radioactive waste, but also minimizing the low-level waste produced. Low-activation materials, alloying elements, and impurities are carefully selected to avoid the generation of high-level waste (i.e., the majority of radioisotopes produced are slightly radioactive and will decay in a reasonably short period of time).

The second-generation fusion power plants may use advanced fusion fuels (such as D-D and D-He3, P-B11, and He3-He3) that produce much fewer high-energy neutrons. Thus, much of the material damage and transmutation can be avoided. However, this advantage is offset by much more difficult physics and confinement requirement for the plasma.

39.2 DESIGN PROCESS

Most of the previous discussion applies equally to both magnetically and inertially confined fusion power plants. Maintenance approaches are highly design specific, so for the remainder of this article, only magnetically contained fusion facilities will be discussed. Since the tokamak approach is the currently favored magnetic approach and it has been most thoroughly investigated, it will be used as the illustrative example.

The U.S.–sponsored Advanced Research Innovation and Evaluation Study (ARIES) team has produced and analyzed many conceptual fusion power plant designs. The most current and widely accepted tokamak designs are the ARIES-RS [1] and ARIES-AT [2]. See Figure 39.1 for an illustration of the ARIES-AT power-core design. Both of these power plant conceptual designs are intended to be very compact and highly maintainable with many advanced physics and engineering features.

Early fusion experimental facilities that used DT plasmas (i.e., TFTR [3] and JET [4]) had very low duty cycles, and they did not require extensive maintenance. TFTR had initially planned to use an articulated boom for internal maintenance, but funding limitations reduced the number of DT experiments to ~1,000 over a three-year period. The dose levels were sufficiently low that the minor in-vessel maintenance that was required could be accomplished with hands-on maintenance and long-handled tools. JET carried out ~100 DT experiments over a one-month period and used extendible, articulated booms that entered the interior plasma chamber via two large maintenance ports to replace divertor modules and execute minor repairs. The weight of the modules to be handled was somewhat limited, and the module size was restricted to the port size. These maintenance operations were very slow and methodical and usually quite unique to the configuration and weight of the module being replaced.

ITER [5] is a much larger fusion experiment that is currently under construction. It uses the module removal approach, a toroidal running rail that is deployed and

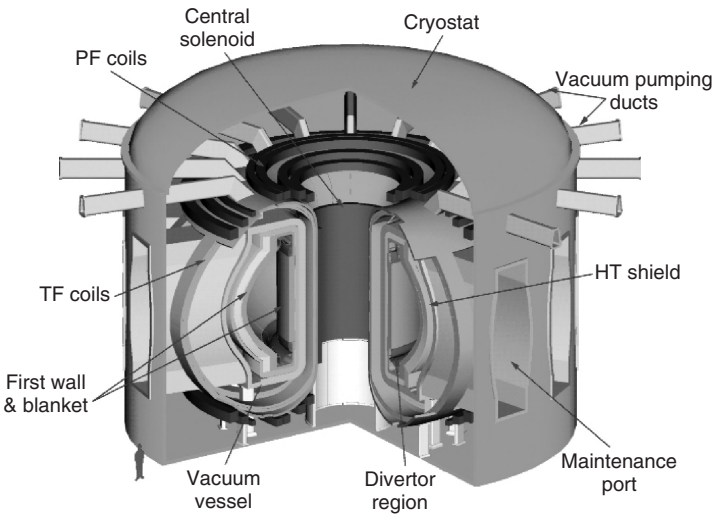

Figure 39.1 ARIES-AT fusion power core cutaway.

supported in the vacuum vessel, allowing an articulated manipulator to be positioned to the right hand of the shielding blanket modules, which do not produce useful energy or tritium for fuel. ITER has a single-null divertor comprised of much larger assemblies that are removed on tracks through larger maintenance ports. Once outside the power core, these modules are transported in a sealed mobile cask to the hot cell for refurbishment or processing and disposal. The time for these maintenance operations is anticipated to be very lengthy, on the order of months, but this is quite acceptable for an experimental facility.

Remote maintenance in existing fusion experiments has provided information about maintenance in a high vacuum, but much more efficient and expedient maintenance is a critical requirement for a commercial power plant to achieve the necessary plant availability. ARIES-AT [6] defined and analyzed its maintenance approach to estimate the necessary power-core maintenance times for an overall plant availability of 88%. It should be noted that this ARIES-AT study and most conceptual fusion power plant studies assumed a tenth–of-a-kind plant, thus all developmental problems will have been solved and all processes are highly optimized. This level of plant availability should be reasonably consistent with other competitive base-loaded electrical generating power plants at the time of the fusion plant operation.

The articulated boom maintenance approach is acceptable for experiments but is not amenable to rapid and precise remote maintenance needed for the power plant fusion power core. Instead, a sector removal approach has generally been adopted for conceptual design studies of tokamak fusion power plants. In tokamak reactors there are typically 16 distinct toroidal field (TF) superconducting coils placed around the outside of the D-shaped power core. It was found that if the TF coils were enlarged slightly, both in height and width, a sector of the power core could be taken out between the stationary TF coils. It is advantageous to keep the de-energized coils secured while remaining at cryogenic temperature. Figure 39.2 illustrates the shape of the coils and the other power-core subsystems. The intent is to remove all the life-limited power-core components from within a sector by taking them out between the TF coil outer legs and through a large maintenance port in the vacuum vessel.

The power core is typically designed to have all internal subsystems that require periodic replacement engineered to be on the same replacement cycle, nominally four to five years. This would include the first wall and

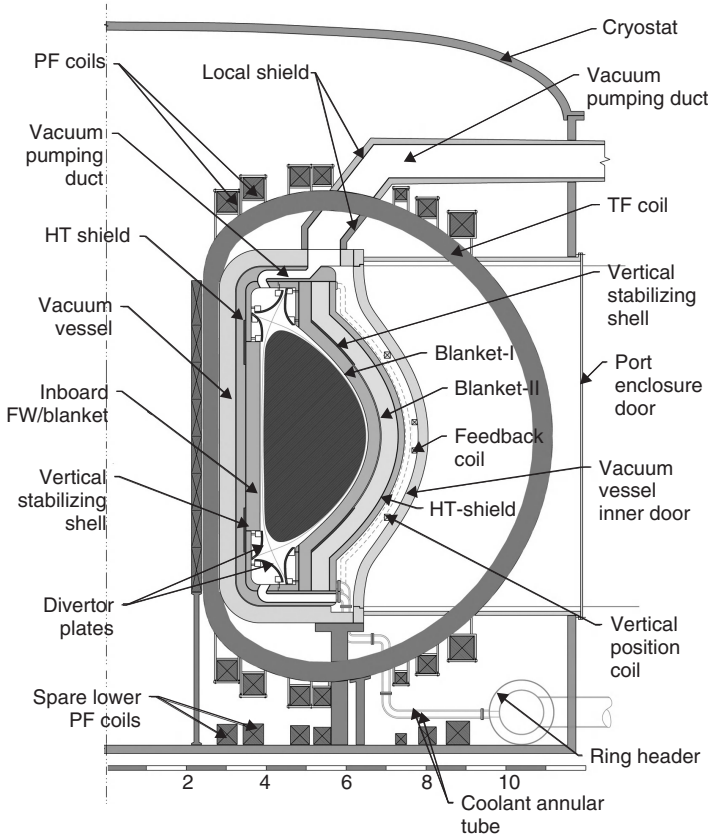

Figure 39.2 ARIES-AT power core configuration.

blanket, divertor, and the other plasma-facing components. Figure 39.2 illustrates the inboard and outboard first wall and blanket and the upper and lower divertor subsystems (double-null divertor configuration). The back part of the outboard blanket receives much lower neutron flux and consequently has a longer lifetime than the front part (closest to the plasma). The ARIES-AT blanket designers took advantage of this difference and separated the blanket into two distinct zones, Blanket I and II. This enables the Blanket II to be designed as a life-of-plant component.

In order to have a structurally sound assembly to withdraw, the replacement sector, shown in Figure 39.3, will include the first wall and blanket (I and II, inboard and outboard), upper and lower divertor, lifetime high-temperature shielding, and high-temperature structure with heat-transfer fluid manifolds. The intent is to move the entire sector to the hot cell where the life-limited subsystems are replaced, and the refurbished sector can be returned to service. This entire structural assembly of the sector is supported on the base of the vacuum vessel with aligning supports at the upper vacuum vessel flange.

If the horizontal sector removal maintenance approach is selected, the basic vacuum vessel shape might be a cylinder with an upper flange and lower flange (as shown in Figure 39.4) that completely encases the power-core

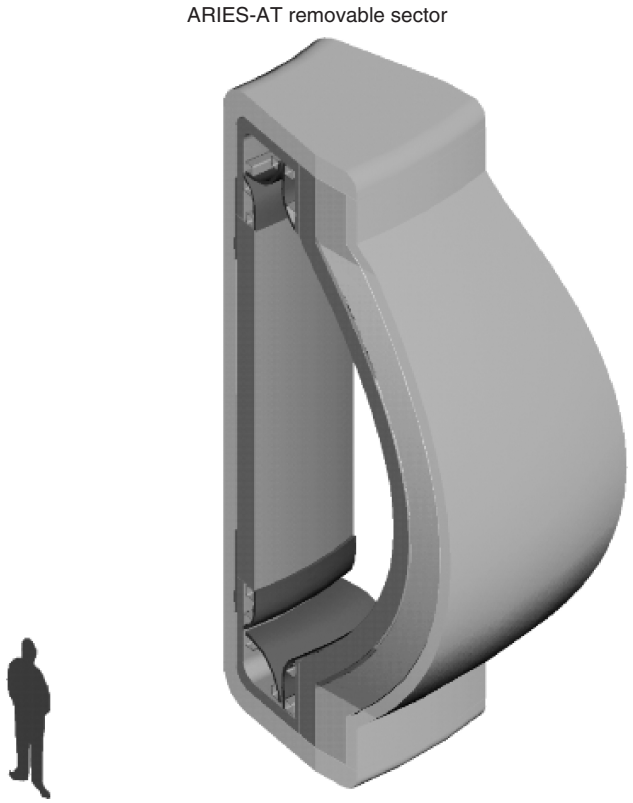

Figure 39.3 Removable sector.

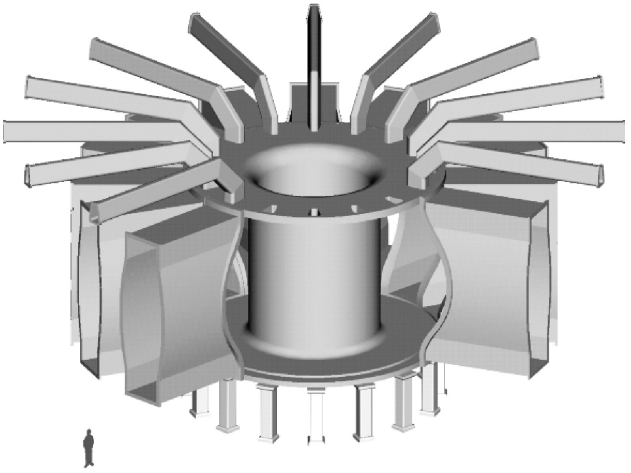

Figure 39.4 ARIES-AT vacuum vessel with port extensions and pumping ducts.

sectors. This vacuum vessel inner component is assembled in place because the inner TF coil legs (not shown in Figure 39.4) will pass down through the inner diameter of the vacuum vessel, and the outer legs will go between the maintenance ports. Sixteen large maintenance ports are attached to the outer periphery of the vacuum vessel spool assembly. Vacuum doors are provided at both the inner and outer portions of the maintenance ports (as seen in Figure 39.2). Gravity supports are provided below the assembly to support the entire power core.

While discussing the initial assembly, it should be noted that it is necessary to initially assemble the entire power core with the remote maintenance equipment. It is not mandatory from the safety standpoint, but instead, after the power core is operated, it becomes neutron activated, so it must be disassembled with robotic equipment. Therefore, the initial assembly is a verification process. This equipment is specially made to perform the task, thus there is no need to have workers, lifts, cranes, scaffolds, etc, when this system is available.

The design approach described above relates to horizontal removal of a large power-core sector. There is another design approach that employs vertical movement of large power-core sectors, either upward or downward. This approach requires a different vacuum vessel designed to accommodate this vertical movement. The ARIES-ST (spherical torus) power plant study [7] features a very low aspect ratio power core that would favor vertical core replacement. It has a shielded copper toroidal field coil center-post (inboard leg) that could be removed from the bottom separately from the remainder of the power core, if necessary. Figure 39.5 shows the ARIES-ST power-core configuration with removal of the center-post and the entire power core. This approach is likely much quicker than the

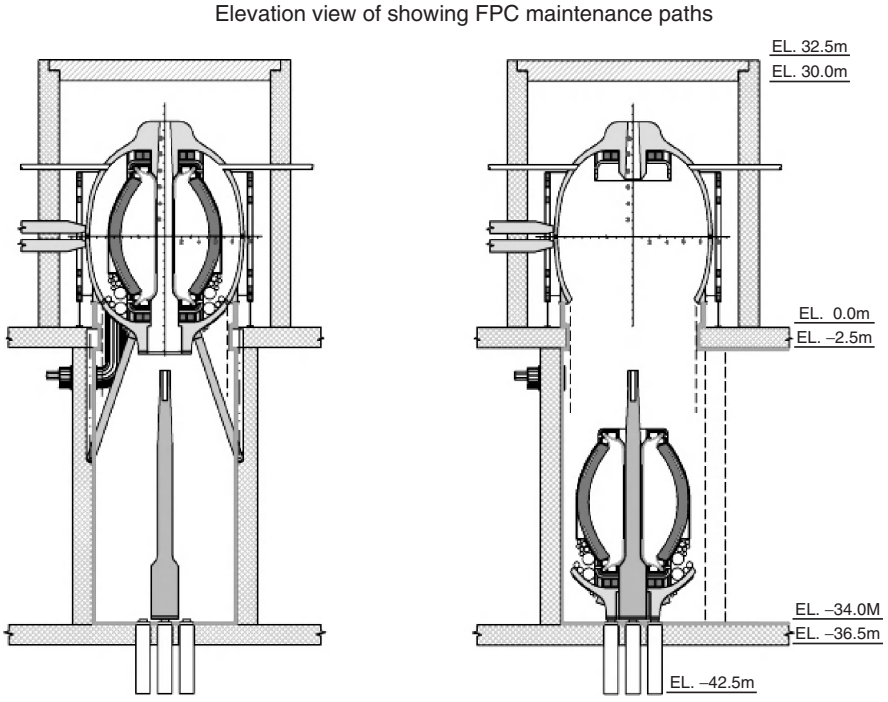

Figure 39.5 ARIES-ST vertical removal of center-post and entire power core.

tokamak sector removal approach, but it requires duplication of the entire power core plus a second replacement for a spare.

The EU is pursuing a vertical maintenance approach for its tokamak DEMO, per T. Ihli [8, 9]. In these papers on maintenance and the MMS (Multi-Module Segment) attachment concept for the DEMO, it is evident that the ITER-like segmentation and maintenance schemes for the blanket would not be relevant to a demonstration plant and future power plants. The EU is pursuing the MMS approach of attaching multiple blanket modules to a strong back structure, similar in approach to the ARIES-RS [1] and ARIES-A [2] design and maintenance designs. Presently, they are investigating both a low-temperature shield and a hot (high)-temperature shield (HTS) option. The HTS can also serve as a strong back structure with coolant manifolds as in the ARIES design. The EU DEMO approach reduces the number of elements to replace during blanket maintenance down to 52 (20 inboard and 32 outboard), plus the divertor assemblies. As a point of departure from the U.S. approach, the EU DEMO vertically removes and replaces the MMS assemblies through a limited number of maintenance ports on the top of the power core. Presently, two vertical ports seem to be most desirable. To enable removal of all the multiple MMS assemblies, all the divertor cassettes at the bottom of the core must be removed and replaced with remote transfer machines with gripper/manipulation devices to radially and poloidally move the MMS assemblies under the vertical maintenance ports. With only two MMS maintenance ports, each port services half the core, one-quarter on each side of the port. If a random blanket failure occurs, requiring a blanket module replacement, the worst case scenario is that one-quarter of the inboard or outboard core MMS assemblies plus the related divertor assemblies would have to be removed and replaced, which would entail a long replacement period. The planned replacement of the DEMO divertor is very similar to the ITER maintenance approach. The times for this MMS tokamak vertical maintenance scheme are probably midway between the single blanket module replacement with articulated booms and the large sector replacement of ARIES.

39.3 MAINTENANCE PROCESS

There are two guiding principles for the design and operation of the fusion power plant—it must be safe and economical to operate. As stated above, the fusion reactions create hazardous conditions for humans inside the thick radiation shield walls that surround the reactor (called the biological shield, not shown yet) during operations and during periods of non-operation due to induced radioactivity in the power-core materials. Because of this, all operations inside the bioshield must be conducted remotely, including

maintenance. And to be commercially competitive, the plant must operate at full rated power at a high level of availability, on the order of 90%. Fission plants were considered to be economical at 75% in the 1950s and 1960s where the capital, operations and maintenance (O&M), and fuel costs were significantly lower. As these costs gradually escalated, the most affordable option to remain competitive was to raise the plant reliability, maintainability, and availability. This implies that all subsystems must be highly reliable, have a long operational lifetime, and be capable of being quickly replaced to get the plant operational as soon as possible. The maintenance of the power core is critical because many of the internal subsystems are connected in a serial fashion and cannot be coupled in parallel to provide subsystem redundancy with a higher reliability value. The power core is of the most interest because it is both the most difficult to maintain and crucial for operation. Thus, it will be the main topic of discussion.

During the development period before the design of the first power plant, aggressive maintenance research and development programs will enhance robotic maintenance systems that can quickly and efficiently inspect, diagnose, repair, remove, replace, and inspect all components of the power core. The equipment and procedures will be verified in both non-nuclear and nuclear facilities prior to committing to a final integrated plant design for both the life-limited and the life-of-plant components. It is anticipated that fully automated, radiation-resistant, autonomous maintenance machines will efficiently accomplish the remote maintenance operations for the commercial fusion power plant. Vision, position, and feedback control will be enhanced to provide precise position and motion control. The use of expert systems will be expanded to help develop experience databases for maintenance systems. Fuzzy logic will be applied to help analyze new variations on unique maintenance situations. Optimization programs will refine the maintenance procedures to speed the overall process. The ability to predict wear-out and incipient component failures will continue to be improved.

As discussed earlier, the present data on the preferred materials suggest a limited lifetime of the first wall, inner portions of the blanket, divertor and other plasma-facing components such that these components would need to be replaced on approximately a four-year schedule. The power core could be replaced (a) once a year (one-quarter of the power core), (b) every two years (one-half of the power core), or (c) every four years (entire power core). The scheduled maintenance period of the power core must be carefully coordinated with the other power plant scheduled plant maintenance actions to accomplish as much maintenance as possible at the same time to minimize the overall maintenance periods. This is very crucial because every time the plasma is shut down, there will be an approximate 24-hour period of time allotted for a thermal cool-down of the power core, decay of the radiation by about two orders of magnitude to a safe level for radiation-resistant maintenance equipment, and increasing the pressure in the core to ambient conditions. An additional six hours is provided in the shutdown period to drain the heat-transfer fluids, open all vacuum port doors, and stage the maintenance equipment. The startup time would be slightly longer (perhaps 34 hours) to account for the reverse of the shutdown procedures plus a full checkout of power-core systems. These operations timelines were estimated in reference [6]. These shutdown and startup times are very aggressive in light of current and past experimental facility experience; however, these time durations are representative of those needed to achieve the desired plant availability.

If the power-core maintenance schedule is frequent, fewer sets of maintenance equipment and spare power core sectors are needed. However, the 2.6 days (64 h) for shutdown and startup add to each and every maintenance period, greatly reducing the plant availability with the more frequent maintenance periods. When the entire core is replaced at one time, this represents the minimum time allowed for scheduled shutdown and startup, but the entire power core must be duplicated and ready for replacement, plus many sets of maintenance equipment are required for efficient change-out of the core. The ARIES team [6] decided to adopt the scheduled replacement of half the replaceable power-core elements roughly every other year, pending a more detailed optimization plan. This is probably a reasonable compromise because a loss in plant availability represents millions in lost revenue per day, but the complexity of removing the entire power core will be challenging.

39.3.1 Power Core Layout and Maintenance Equipment

As discussed earlier, the power core must be designed specifically to accommodate the sector replacement maintenance approach. The TF coils must be large enough to allow dimensional clearance of the vacuum vessel maintenance ports and the passage of the sector. The outer PF coils near the midplane must be permanently located above and below the maintenance ports (see Fig. 39.2 for typical PF coil placement). The plan view of the ARIES-AT power-core operational state is shown in Figure 39.6. When the power core is operational, the primary vacuum vessel door is in place, speculatively held with mechanical screw jacks to provide positive clamping force on metal vacuum O-ring seals. For additional vacuum integrity, a second door provides additional sealing protection at the outer end of the maintenance port. In Figure 39.7, the same plan view is shown in the maintenance state. In this figure, the outer door has been removed, the screw jacks disengaged and

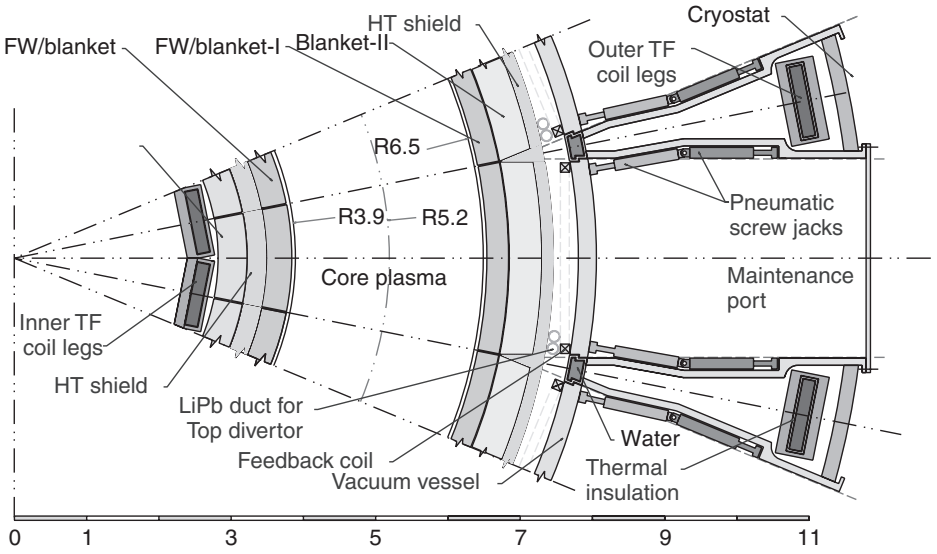

Figure 39.6 Power core plan view of the ARIES-AT operational state.

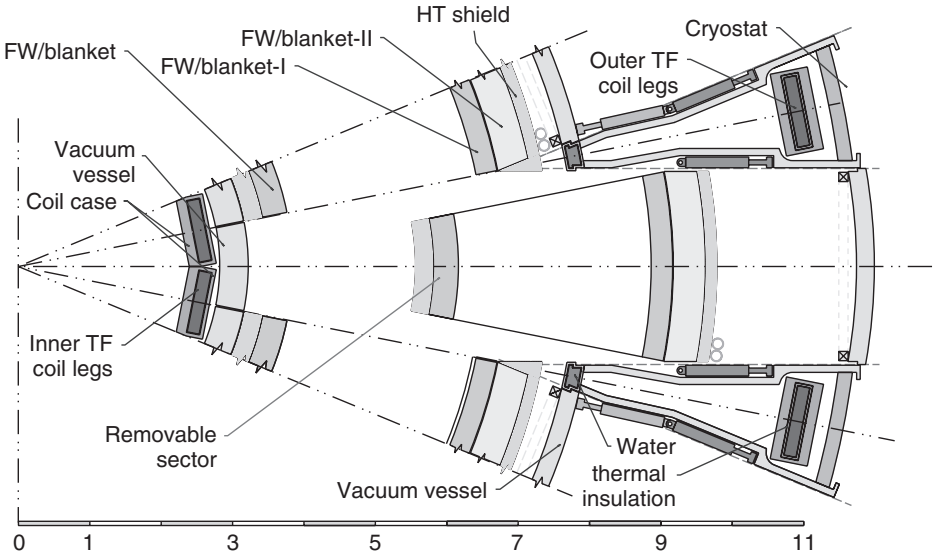

Figure 39.7 Power core plan view of the ARIES-AT maintenance state.

swung out of the way, the inner vacuum door has been removed, and the sector transporter (not shown) has begun operations to remove the sector.

Figure 39.8 shows how the sector maintenance transporter might look when it engages the sector before removal. The shape of the transporter is not important except that it needs to be as close to the sector as possible. It will connect an auxiliary cooling system to remove waste heat in the sector. It also disconnects any structural supports and plumbing and electrical connections from the stationary portion of the power core. It will activate the sector-lifting mechanisms and commence to pull the sector out of the power core and into the mobile transport cask. This cask will then take the doors and sector to the hot cell and return with either a new or refurbished sector.

Figure 39.9 is a plan view of half the tokamak power core, illustrating the sequence of maintenance actions. As seen, several operations can be performed simultaneously with multiple transporters operational on different sectors. The transporters resemble bulldozers or wheeled vehicles that move heavy loads. These transporters will enter the maintenance corridor just outside the power core through an airlock and proceed to remove and set aside a concrete bioshield door, which weighs approximately 140 tonnes. Next, the transporter will disengage the outer vacuum door to the maintenance port and set it at the outer perimeter

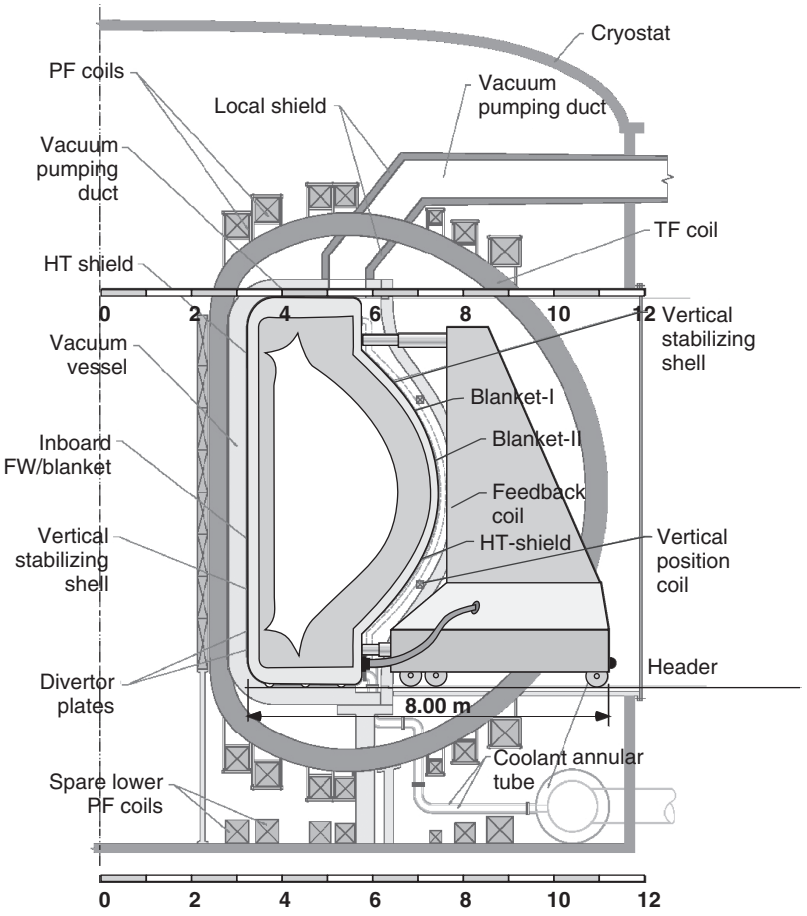

Figure 39.8 Maintenance transporter engaging power-core sector.

of the maintenance corridor near the bioshield door. The next component to be removed is the inner curved vacuum vessel door. During operation, this door is filled with cooling water, but it would be drained of coolant during maintenance operations and would weigh on the order of 14 tonnes. Before removal, the cooling lines will have to be disconnected. This door can be removed and placed near the wall of the outer bioshield. The next operation will be to engage the removable power core sector, disconnect all plumbing and electrical connections, disconnect the structural attachments, activate the lifting mechanisms, and remove the sector from the power core. In the ARIES-AT design [10], the structural material for the first walls, blankets, and divertor was silicon carbide (SiC/SiC) composite material, cooled with high-temperature liquid lithium lead (LiPb). The weight of an empty sector would be approximately 120 tonnes. Other choices of structural materials and solid breeder blanket modules might weigh considerably more. The power core is designed such that any of the sectors can be removed and replaced in any order, allowing great freedom in replacing the core. In theory, 16 transporters could be working simultaneously; however, it might be more practical to use four transporters to lower the capital cost of the maintenance equipment and reduce the complexity of the maintenance procedure. The core sector and transporter will then proceed to the hot cell, where a new or refurbished sector from a prior maintenance action will be returned to the core for installation. The approach shown in Figure 39.9 is intended to show feasibility and is not intended to be an optimized design. Certainly the operations would be staggered to provide flexibility without crowding.

The time to accomplish this removal and replacement of a single sector is a debatable issue at this point without a firm design and minimal relevant experience with remotely and autonomously handling large structures. However, this is a crucial operation and should be accomplished accurately, reliably, and rapidly to achieve the necessary plant availability. ARIES-AT [6] defined each operational step with an estimated time to accomplish the maintenance, arriving at a time of 35 hours to remove and replace each sector (not counting cool-down and startup times). This time is quite optimistic, but necessary for the overall availability goal. Using the cool-down, startup, and

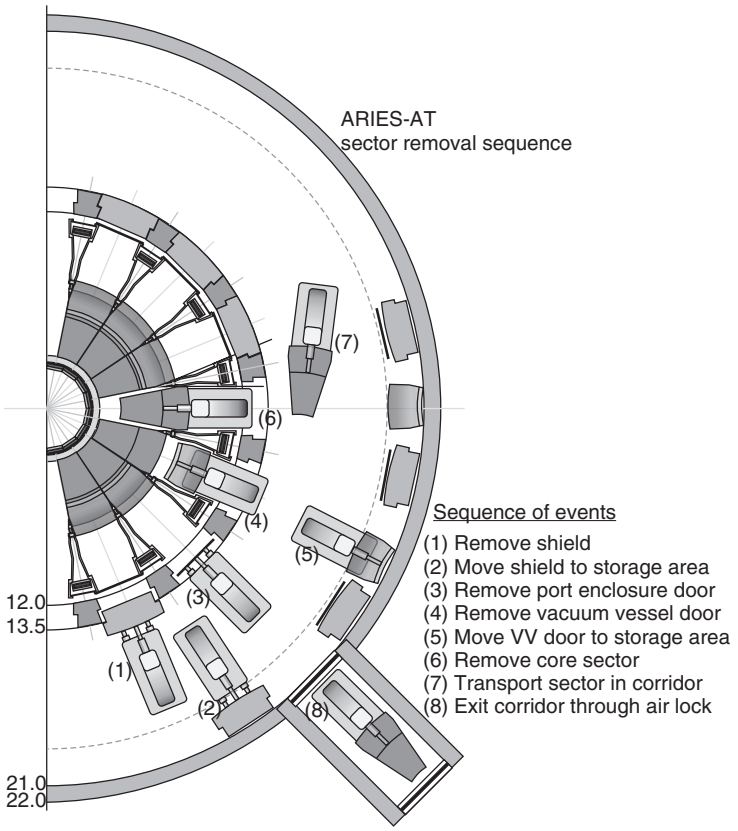

Figure 39.9 Sequence of power core maintenance actions to remove sectors.

single sector replacement times along with the number of transporters and the fraction of the core to be replaced, a scheduled maintenance period duration can be estimated.

Figure 39.9 also shows an interesting, but as yet undecided, shielding approach. It shows a two-part bioshield. The inner bioshield is 1.5 m thick reinforced concrete, just outside the cryostat, with fixed portions just outside the TF coils and movable door portions outside the power-core sectors. The outer bioshield is about one meter thick for a total bioshield thickness of approximately 2.5 meters, which would be necessary to protect the workers and public [11]. It is placed at a radius that is established to provide a maintenance corridor for storage of the bioshield doors and the two vacuum doors plus transit of the transporters and sectors. The outer bioshield is permanent (fixed). To allow egress and ingress of transporters and sectors, there is an airlock that is adjacent or near to the hot cell. This approach has the advantage of the containment of the activated materials in slightly smaller volume; however, the disadvantage is the time required to remove the heavy bioshield doors. The alternate bioshield approach is to have a single bioshield of approximately 2.5 meters at the outer perimeter of the maintenance corridor. The advantage of the latter approach is that there are no bioshield doors, but the activated volume is larger.

Another option and deferred decision is to have a mobile cask located directly outside the power core (not shown) to enclose the transporter and sector. This approach is used by ITER [5] for module maintenance, but it could be applied for sector maintenance. The mobile cask would be undocked and moved around the maintenance corridor to the airlock and the hot cell. The advantage of the mobile cask approach is to contain the migration of activated dust into the maintenance corridor, airlock, passageway, and hot cell. The disadvantages of the cask approach are that the casks represent additional maintenance equipment, larger corridors and passageways are needed, and added complexity and time are needed to accomplish the maintenance task. The alternate approach would be to not have a mobile cask and move the bare sector and transporter to the hot cell, as shown in Figure 39.9. The severity of the contamination issue will probably be the deciding factor between the ARIES and ITER approaches.

All of these designs and maintenance approaches are very preliminary and certainly will be revised many times before being validated on the demonstration power plant. However, these design concepts are thought to be compatible with the basic tokamak configuration and may achieve the necessary plant availability. Certainly, these

designs will evolve and improve. At this time, it is likely that the robotic maintenance operations will be completely autonomous for all routine activities. As the anomalous activities are encountered and solved, they will be added to a maintenance actions database.

The prior discussions concentrated on the design approaches and the procedures to accomplish major scheduled power-core maintenance actions to replace the life-limited components. An equally important maintenance issue is how the unscheduled maintenance will be accomplished on internal power-core components and subsystems. These maintenance actions are related to random failures before the expected end-of-life. If the failure is a major one related to the replaceable first wall, blanket, divertor, hot shield, and hot structure/manifold, a single sector can be removed in roughly 100 hours (30 h + 35 h + 34 h), per the ARIES-AT [6] analysis. This would result in a reduction of the plant availability of just over one percentage point per year for each occurrence. This cannot happen too often or the overall plant availability would be severely impacted. The reliability of these components must be extremely high, which means excellent quality control and rigorous testing. If the failure of any of these components is minor, but results in a plasma shutdown, the plant must be shut down and started up again for a minimum duration of approximately 64 hours (30 hours for shutdown and 34 hours for startup and checkout). If the failure is a leak, it might be possible to enter the interior of the plasma chamber or the heat transfer or coolant pipes and manifolds and repair a leak in a few additional hours. There are presently some internal plumbing robots that can repair pipes and other components. In the future, these might be adapted for this use and radiation hardened to provide some plumbing repairs without component removal. The shutdown also might be a large disruption that requires a plasma-facing surface inspection. These and many other minor failures would each result in 64+ hours of maintenance downtime, which equates to a reduction in availability of 0.75% or more for per occurrence. Again, it mandates that all operations-critical components be extremely reliable.

Scheduled maintenance on other plant equipment external to the power core, such as RF amplifiers and vacuum pumps and those associated with the balance of plant, may be done at the same time as the power-core maintenance period or online while the plant is operating. These maintenance actions would not impact the plant availability.

39.4 HOT CELL OPERATIONS

The hot cell area is a shielded and environmentally controlled region of the power-core building that will control, contain, and process activated materials. This area will be responsible for inspecting, refurbishing, or disposing of all activated powercore components and subsystems while the power plant is conducting normal operations. The hot cell must be configured to accommodate full-size, upright sectors. In the time period when fusion plants are operational, it is anticipated that all operations in the hot cell would be remote with much of the repair, replacement, and inspection operations being autonomous and highly automated. Decay heat of all activated materials will be accommodated and/or removed. All solid and liquid waste products are processed in the hot cell and will be either shipped off-site or stored to allow further radioactive decay. This building, as well as the power core building, has atmospheric tritium recovery units to clean up tritium in the event of a tritium leak. At plant decommissioning, the hot cell will probably process the entire power-core for recycling or disposal.

39.5 MAINTENANCE TIMES AND PLANT AVAILABILITY

The principal metric to judge the maintenance approach, equipment, and procedures is the time to reliably replace the power-core subsystems for both scheduled and unscheduled maintenance. These times can be analytically estimated using simulators and physical sub- and full-scale mockups or models. Most fusion conceptual design studies typically assumed a plant availability with no analysis or substantiating data. ARIES-AT [6] estimated the main maintenance actions to provide a "reasonable, but aggressive" estimate of the times required for the necessary plant availability. The ARIES-CS [12] compact stellarator power-plant study defined a more detailed set of maintenance actions and times to develop a higher fidelity maintenance timeline and plant availability calculation. These timelines set very aggressive development goals for the maintenance simulations, models, and demonstration plants to achieve.

39.6 SUMMARY

The tokamak magnetic confinement approach is probably the leading and most well-developed fusion confinement concept at this time. Numerous preconceptual and conceptual fusion plant design studies have been completed to illustrate and examine potential physics and engineering solutions. A few of these studies have integrated their designs with maintenance approaches to allow replacement of life-limited and failed components. Only a few designs offered and analyzed maintenance approaches that might achieve the necessary plant availability for competitive plant economics. These are only visions of designs, approaches and procedures for concepts yet to be conceived, developed, and matured as viable fusion power

plants. At present, visions have to be accepted at face value, recognizing that they are our studied engineering approach to the future.

REFERENCES

1. F. Najmabadi, and the ARIES Team, Overview of the ARIES-RS reversed-shear tokamak power plant study. *Fus. Eng. Des.*, 1997, **38**, 3–25.
2. F. Najmabadi, and the ARIES Team, The ARIES-AT advanced tokamak, advanced technology fusion power plant. *Fus. Eng. Des.*, 2006, **80**, 3–23.
3. G. Loesser, P. Heitzenroeder, D. Kungl, H. Dylla, G. Böhme, M. Selig, and G. Cerdan, Remote maintenance of in-vessel components in tokamak fusion test reactor. *Vacuum*, **41**, 1990, 1523–1527.
4. A. Rolfe, P. Brown, P. Carter, R. Cusack, A. Gaberscik, L. Galbiati, B. Haist, R. Horn, M. Irving, D. Locke, A. Loving, P. Martin, S. Mills, R. Minchin, J. Palmer, S. Sanders, S. G. Sanders, and R. Stokes, A report on the first remote handling operations at JET. *Fus. Eng. Des.*, 1999, **46**, 299–306.
5. A. Tesini and J. Palmer, ITER remote maintenance system. *Fus. Eng. Des.*, 2008, **83**, 810–816.
6. L. Waganer, ARIES—AT maintenance system definition and analysis. *Fus. Eng. Des.*, 2006, **80**, 161–180.
7. F. Najmabadi and the ARIES Team, Spherical torus concept as power plants—the ARIES-ST study. *Fus. Eng. Des.*, 2003, **65**, 143–164.
8. T. Ihli, D. Nagy, C. Koehly, and J. Rey, High availability remote maintenance approach for the European DEMO breeder blanket options. *Proceedings of the 21st IAEA Fusion Energy Conference*, Chengdu, China, October 16–22, 2006, International Atomic Energy Agency, http://www-naweb.iaea.org/napc/physics/fec/fec2006/html/node295.htm#58758, 2006, FT/P5-11, (8 pages) [proceedings not published in paper form, only in HTML on web].
9. T. Ihli, L. Boccaccini, G. Janeschitz, C. Koehly, D. Maisonnier, D. Nagy, C. Polixa, J. Rey, and P. Sardain, Recent progress in DEMO fusion core engineering: improved segmentation, maintenance and blanket concepts. *Fus. Eng. Des.*, 2007, **82**, 2705–2712.
10. A. Raffray, L. El-Guebaly, S. Malang, I. Sviatoslavsky, J. M. Tillack, X. Wang, and the ARIES Team, Advanced power core system for the ARIES-AT power plant. *Fus. Eng. Des.*, 2006, **80**, 79–98.
11. L. El-Guebaly and the ARIES Team, Nuclear performance assessment of ARIES-AT. *Fus. Eng. Des.*, 2006, **80**, 99–110.
12. L. Waganer, R. Peipert, Jr., X. R. Wang, S. Malang, and the ARIES Team, ARIES-CS maintenance system definition and analysis. *Fus. Sci. Tech.*, 2008, **54**, 3, 787–817.

40

FUSION ECONOMICS

LESTER M. WAGANER

Fusion Consultant, O'Fallon, MO, USA

Economics plays an important role in the development and the viability of fusion power plants. Energy is a market-driven product that is influenced by many factors, including the ability to produce excess energy, provide adequate safety to plant workers and the general public, be environmentally friendly, cause no significant depletion or adverse use of natural resources, and have a high plant availability (i.e., reliable and maintainable components). Even if all of these criteria are met, it must produce economical power with reasonable capital and operating and maintenance costs. This chapter will discuss how the economics of the future fusion power plants are estimated.

40.1 PLANT DEFINITION

It is vitally important to the validity of the cost estimate to have a sufficient level of plant subsystem on which to base the cost estimate. A work breakdown structure (WBS) and the corollary cost breakdown structure (CBS) must be defined early to make sure all systems and subsystems are considered and estimated. There will be certain plant systems and subsystems that will be of the most interest, and these will be defined in more detail. Other areas will be lacking both in interest and detail, but these must be also defined and estimated or the complete cost estimate will be flawed.

Early in the history of studies of fusion power plant designs, standard cost accounts were defined in 1978 in the Schulte report, *Fusion Reactor Design Studies—Standard Accounts for Cost Estimates* [1], to provide a common cost standard. At this period in the development of fusion, it cannot be expected to have detailed design drawings and specifications, but the design should be sufficiently well developed to specify the overall size, power, capacity, and materials required for the cost estimators.

40.2 BASIC DEVELOPMENTAL AND PHYSICAL PLANT SITE

In the Schulte report [1], it was recommended that if a mature power industry is assumed (which is normally the case), it should be a tenth-of-a-kind (10^{th} OAK) plant with appropriate learning curve factors applied. The tenth-of-a-kind nomenclature denotes that a common, standardized design has been used for the prior first nine plants as opposed to the U.S. fission plant experience of rather unique designs with very little detailed design commonality. With the 10^{th} OAK plant, all developmental effort would have been completed, and no R&D costs would be charged against the plant capital costs. Only minimal plant engineering would be required for site-specific and plant design modifications. The commonality of the design also allows for more standardized procurement, which maximizes the applicable learning associated with the costs of the plant elements.

The physics and engineering technologies employed in the power-core design and operation are typically founded in current technology with some advance technology enhancements incorporated, provided there is a sound technical basis, and this technology is likely to be available in the time frame of the future fusion plant.

Multiple power plants per site are allowed, but the usual practice is to only consider one plant per site. Obviously, more plants sharing a common site would result in a lower

Nuclear Energy Encyclopedia: Science, Technology, and Applications, First Edition (Wiley Series On Energy).
Edited by Steven B. Krivit, Jay H. Lehr, and Thomas B. Kingery.

cost of electricity (COE). However, this option has not been commonly proposed as it might imply that fusion must have multiple plants at a site to be economically sound.

The power level or physical size of the power plants is usually determined to nominally produce 1000 MWe net. The related fusion power is established by the plant's neutron multiplication factor, thermal conversion efficiency, and necessary auxiliary power. The use of a common 1000 MWe net plant size allows comparison with other fusion power plants without scaling from a different power basis. There were a few exceptions to the 1000 MWe rule, such as the early UWMAK-1 [2] 1973 fusion plant design that developed 5000 MW fusion power with 1200 MWe net output. Later, UWMAK-II [3] and UWMAK-III [4] designs had fusion powers of 5000 MW and electric powers of 1716 and 1985 MWe net, respectively, due to improved thermal efficiency and lower recirculating power. These power plant designs were viewed as being too big at 5000 MW fusion, and the trend was to create smaller power designs with improved performance and economics. STARFIRE [5], at 4000 MW fusion and 1200 MWe net, was a more compact design compared to its predecessors, but it was physically large compared to the current tokamak designs. With the advent of the ARIES [6] (Advanced Research Innovation and Evaluation Study) series of design reactors, the net electrical output was decreased to a nominal 1000 MWe with the related fusion. It is recognized that the economy of scale for larger plants would decrease the cost of electricity (COE); however, the capital cost is significantly increased for the larger plants. Even though the lower COE would be much more favorable, the higher capital cost would be a considerable hindrance to financing the plant. Fusion plants smaller than 1000 MWe net have poor COE values and generally have not been pursued.

There is a common basis for the physical site. The *Fusion Reactor Design Studies—Standard Accounts for Cost Estimates* [1], Appendix A, provided a set of reference site characteristics and parameters for all design studies and cost estimates to use as common basis. This is a 1000-acre site, located in the Midwest and close to a river for cooling and barge facilities for transportation of large components. This site description also contains topographical, meteorological, and climatological data to provide a common basis. The cost of the land has been updated periodically to reflect current Midwest land values. Assuming there would be a sizable premium to obtain a contiguous site of 1000 acres with water access, it is not unreasonable to assume that the current land price would be $20,000 per acre in 2009 dollars. There is also a description of the nearby population centers to help determine environmental impact, possible evacuation plans, and public utility services.

40.3 ECONOMIC ASSUMPTIONS

In the Standard Accounts for Cost Estimates report [1], it was recommended that the financing assumptions to be used would be for commercial electric power plant designs based on the premise that the facility is financed, constructed, and owned by an investor-owned (private) electric utility organization. The cost of all labor, materials, and equipment would be estimated using present (current) year price levels, adjusted for the time period of the design study. There are a multitude of different historical cost indices for a wide variety of special interests, such as Consumer Price Index, Handy-Whitman Index of Public Utility Construction Costs, Gross Domestic Product, and many other useful indices. As a practical matter, it was useful to use a single inflation index, thus the Gross Domestic Product Price Level Deflator has become the de facto index to correlate all prior fusion plant cost estimates. This index is maintained by the U.S. Department of Commerce, Bureau of Economic Analysis [7]. This is also the index used by the Economic Modeling Working Group of the Generation IV International Forum as documented in its Economic Guidelines report [8].

40.4 METHOD OF CAPITAL COST ESTIMATION

The intent of fusion economics is to estimate the capital and operating costs of a future fusion electrical generating power plant. The difficulty is that this subject plant is envisioned to be built roughly 50 years in the future. This was true in the time period of the UWMAK and STARFIRE power plant designs some 30 to 35 years ago and, unfortunately, it is still true today due to budgetary constraints. Plasma experiments have been quite successful and have grown in size and fidelity, but they are not yet at the threshold of achieving a power-plant relevant plasma and technology. The ITER facility [9], currently under construction, will be the first fusion plasma that has limited power plant relevancy. This latter statement is a subject of debate between the United States and other fusion-literate nations.

The current quandary is that the design of the 10^{th} OAK commercial fusion power plant remains at least 40 to 50 years in the future, given the past and current funding scenarios. If the need for fusion power becomes urgent, it is technically possible to advance that commercial time threshold and compress the plant design, development, and validation by a decade or two with sufficient funding. Thus, the designers of the future power plant must extrapolate today's technology some years in the future. This entails some technical and programmatic risk, but 40 to 50 years is a long time, and many new technologies can be developed, providing there is sufficient need and funding. The currently

proposed designs express optimism that difficult issues can be solved, pointing the way to more desirable solutions.

Cost estimation of this mix of current technology in facility and balance of plant (BOP) design along with the advanced materials and hardware is quite challenging. A detailed, bottom-up cost estimate is too time consuming and expensive, and the engineering details are simply not available to do a credible estimate. Also, the design is certain to change in the years before actual construction. Therefore, any fusion power plant estimate has to be accomplished using costing algorithms and rules to provide a less precise, but adequate cost estimate to be able to determine the viability of the fusion energy option and assess the attractiveness of alternative design and system options. All reasonably comprehensive fusion power plant studies from the UWMAK series to the current ARIES series of fusion power plant studies have employed this methodology. STARFIRE [5] probably had the most detailed plant design and economic analysis. All the conceptual design economic analyses documented their assumptions to varying degrees.

Algorithm cost estimation entails researching relevant cost bases, either actual facility or hardware costs, or valid cost estimates. There are usually one or more size or performance parameters that determine the cost of the item. The intent is to provide the installed cost (materials, fabrication labor, and installed labor) of each subsystem. These relevant metrics can be an area in the case of land or divertors, volume for some components and structures, transmitted force in the case of support structures, power handled for heating and current drive, and so on.

The cost of the magnetic-fusion power core is of great interest as it contains the first wall, divertor, power- and fuel-producing blankets, neutron shields, hot structure, vacuum vessel and ducts, heating and current drive subsystems, magnetic coils, and cryostat. Many of these power-core subsystems can be modeled using their volume multiplied by an installed material cost per mass. A database is developed that includes the type of material for each subsystem. Additional cost data can be provided for different confinement concepts to account for different system complexities. This material cost database method usually applies to the first wall, blanket, divertor, shielding, magnet coils, vacuum vessel, cryostat, bioshield, and main structure. The current drive and heating, vacuum pumping, cryogenics, fueling and fuel handling, radioactive materials treatment and management, and heat transport systems are usually estimated with their relevant parameters. The maintenance equipment is usually estimated as number of pieces of equipment times the unit price. The instrumentation and control system is usually estimated with near-constant cost parameters.

Other plant equipment, such as the turbine plant, electrical plant, heat rejection, and miscellaneous plant equipment are usually estimated as a constant times the normalized thermal power$^{0.5}$, electrical power$^{0.5}$, rejected power$^{1.0}$, or electrical power$^{0.6}$, respectively.

The Special Materials account covers materials added to the fusion power plant just before testing and validation commences. The common categories for these materials are some tritium breeding materials, heat-transfer fluids, cover gases for material handling systems and buildings, breathing air, and specialty gases or liquids not preloaded into the plant systems. These materials are considered to be capital equipment, but they are not to be procured with the various plant systems. Replenishment of these materials is considered to be an operational expense. The current trend in fusion power plant design studies is to use a liquid tritium breeding fluid, typically lithium metal compounds that also serve as the power-core coolant or heat-transfer media. The most popular lithium lead breeder is inexpensive, but the lithium component must be enriched with more costly ^{6}Li to provide adequate tritium breeding.

STARFIRE [5] had the most complete and highest fidelity building estimates because the design team had an A&E contractor determine the building size and then developed a detailed cost estimate of all the buildings. Many of the succeeding plant estimates used the Starfire basis, scaling the buildings according to volume (power core building), turbine building (normalized thermal power$^{0.5}$), heat rejection structures (normalized rejected power$^{0.5}$), and other buildings as related the appropriate scaling parameter. Some buildings, such as the control room, are estimated as a constant value as their size and complexity do not scale with any parameter.

40.5 ESTIMATION METHOD FOR INDIRECT COSTS

Many fusion power plant conceptual design studies [5, 10–12] developed improved cost account modeling that were implemented into the ARIES design studies. Table 40.1 reflects the current categories and bases for the indirect capital costs as a function of the direct and indirect costs. Again, these values are only meant to be representative, and any future plant will have more definitive values defined for that project.

40.6 CONTINGENCY

The contingency allowance is for unforeseen or unpredictable expenses that might be incurred during facility construction and startup resulting from potential acts of nature and non-design related construction problems. Uncertainties from technical design (Process Contingency) should be accounted for in design allowances, thus design allowances

TABLE 40.1 Recommended ARIES-AT Indirect Cost Factors (% of Direct Costs)

Account	Factors[a]
90 Direct Costs	1.00000
91 Con Serv & Eq	0.11300
92 Home Office Engr	0.05200
93 Field Office Engr	0.05200
Subtotal (ID costs)	**0.21700**
94 Owner's Cost (%Direct + Indirect)	0.1500
Total Indirect Costs	**0.39960**
Total Dir + Indir costs	**1.39960**
95 Process Contingency	0
96 Project Contingency (%Direct + Indirect)	0.1465
Total Overnight Costs	**1.6046**

[a]Factors are a ratio of indirect cost item to direct cost (90) unless noted (94 and 96).

should be minimal for a 10th OAK plant. In 1989, a report [13] by Schulte et al. on standard unit costs for fusion reactor studies recommended 15% of accounts 21 through 25 be provided to account for unforeseen expenses. At that time, Starfire [5] adopted these guidelines at 15% of the direct costs for each of the specified accounts (21–25), omitting the cost of spares.

On the other hand, the Delene 1990 Generomak cost model update [14] altered the contingency allowance to relate to both direct and indirect costs. The ARIES project [6] adopted contingency allowances with a lower factor of 14.65% applied to both the direct and indirect costs.

40.7 FINANCIAL ASSUMPTIONS AND COST METHODOLOGIES ASSOCIATED WITH PLANT CONSTRUCTION

The prior sections addressed the methodologies and algorithms for developing the direct and indirect capital costs for a fusion power plant. Those total costs are considered to be the total overnight costs (OC), in that no time-related interest or escalation (inflation) effects are considered.

This section addresses the assumptions, methodologies, and algorithms associated with the financing of the procurement and construction of the plant and its facilities. These factors consider the cash flow necessary to procure and construct the facility, any inflationary effects on the cash flow, and the accrual of interest and other factors charged to the incremental cash flow.

40.7.1 Cash Flow

First, the expected distribution of the cash flow during the construction period must be established. In actual practice, this expenditure curve would not be a continuous function; rather, it would be composed of many unequal step functions depending on the timing of the long-lead items and the integrated procurement, construction schedule, and the contractual arrangements with suppliers and subcontractors. For simplicity, conceptual and preliminary design studies usually assume a continuous and smooth skewed "S"-shaped expenditure curve [5, 15, 16] with 50% of the cash flow occurring at 60% of the construction time.

40.7.2 Time Value of Money

At the start of construction, the total overnight costs have been identified that are necessary to procure and construct the plant. However, the plant cannot physically be procured or constructed overnight and requires some elapsed time for this process to be financed and completed. The prior section identifies a prescriptive cumulative cash flow curve necessary to complete the project. There are two primary time-related analysis approaches that determine the total cost necessary at the end of construction: escalation due to inflationary effects from the start of construction and interest compounded from the date of cash accrual to the start of plant operation.

There are two methodologies used to evaluate the time-related effects that occur during the construction period. One is called "constant dollars" defined by Harrnett and Phung [17], which assumes that the purchasing power of the dollar remains constant throughout the construction period—the cost for an item measured in money with the general purchasing power as of some reference date. Hence, there is no inflation. However, there are costs associated with the true (or real) interest value. This will not be a realistic situation in the actual world because there are always inflationary (or deflationary) effects, but this "constant dollar" analysis provides a more easily understood economic metric that avoids making the assumptions about future inflationary/deflationary effects. The rate of interest is usually in the range of 3% to 6% without inflation. Cumulative interest is accrued from the beginning of the construction period and is called "interest during construction" (IDC), and it is dependent on the cash flow curve.

The second evaluation methodology described by Harrnett and Phung [17] is called "then-current dollars." Other authors may refer to this methodology as "nominal dollars." Nominal dollar cost is the cost for an item measured in as-spent dollars and includes inflation effects. Nominal dollars are sometimes referred to as "current" dollars, "year of expenditure" dollars, or "as spent" dollars. Most fusion plant economic analyses express their estimates in both constant and then-current (nominal) dollars; however, the former is more commonly used for comparison.

Since this analysis technique includes both escalation (related to inflation) and interest, the total cost due to escalation at the end of construction is highly dependent on the cash flow schedule. The interest rate, when stated in current or nominal dollars, inherently includes an escalation factor. The total capital investment required at the end of construction = initial capital investment x (1 + IDC + EDC) with appropriate interest and escalation rates applied over the cash flow schedule. Figure 40.1 illustrates the differences between constant and then-current dollar analysis. In the Starfire analysis, the constant dollar interest was 5% (IDC = 0.1303), and in the then-current dollar analysis, the escalation (inflation) was 5% (EDC = 0.1896) and inflated interest was 10% (IDC = 0.3164). These values were determined from a numerical integration with steps that approximated a true integral function.

40.7.3 Evaluating the Interest and Escalation Rates

The 1978 PNL report [1], *Fusion Reactor Design Studies—Standard Accounts for Cost Estimates*, established a methodology for handling time-related costs using the constant and then-current dollar analyses, then using an interest rate of 5% for the constant dollar case, an interest rate of 10%, and an escalation rate of 5% for the then-current dollar case. Generomak [10, 11] originally assumed a real interest rate of 3% in the constant dollar analysis, an escalation rate of 6%, and an interest rate of 9% in the current year analysis for an eight-year construction period. In 1989, J. Delene updated the draft Generomak model [18], which reduced the escalation rate from 6% to 5% and changed the average cost of money from 5.1% and 11.4% to 6.05% (without inflation) and 11.35% (with inflation), respectively. These rates were used for the allowance for funds used during construction (AFUDC). Delene noted the U.S. Tax Reform Act of 1986 decreased the federal tax rate from 45% to 34%. With this tax rate change, the AFUDC should use the average cost of money rather than the tax-adjusted cost of money, which is 9.7% nominal and 4.35% constant or real. The ARIES systems code used for the evaluation of ARIES-AT [19], as well as other prior ARIES studies, the Delene cost of money as 6.05% (without inflation) and 11.35% (with inflation) average cost of money for its IDC and EDC computations.

The Gen-IV economic guidance [8] is that only the constant dollar analysis approach be employed.

> The EMWG (Economic Modeling Working Group) decided to use 5% and 10% real (i.e., excluding inflation) discount rates because these rates bracket the cost of capital for most nuclear energy plant owners. The 5% real discount rate is appropriate for plants operating under the more traditional "regulated utility" model, where revenues are guaranteed by captive markets. The 10% real discount rate would be more appropriate for a riskier "deregulated" or "merchant plant" environment, where the plant must compete with other generation sources for revenues.
>
> In the context of the GIF guidelines, the discount rate is equal to the real cost of money.

Further, the EMWG decided to keep the economic groundrules as simple as possible. The EMWG defined the escalation rate as the rate of cost or currency change. This rate can be greater or less than the general inflation rate, as measured by the Gross Domestic Product Implicit

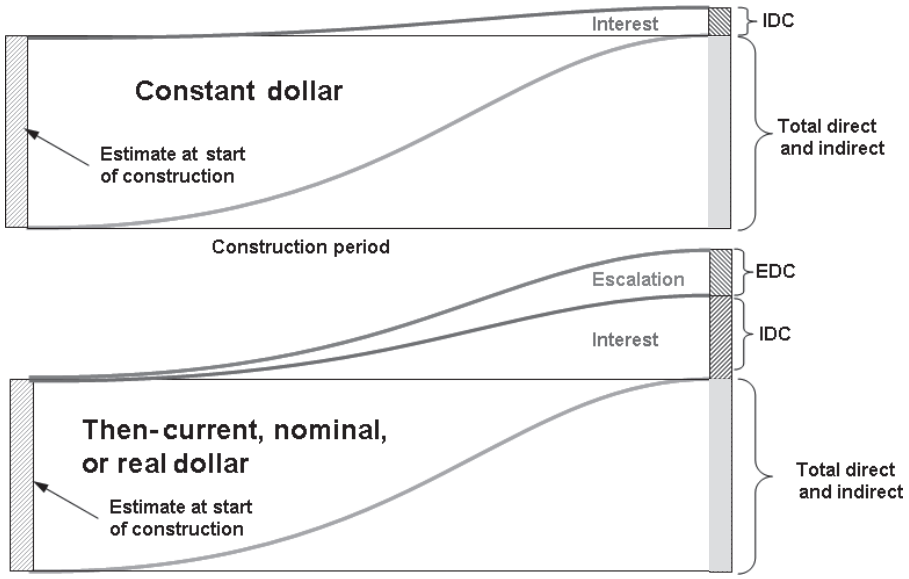

Figure 40.1 Comparison of constant and then-current dollar accumulation.

Price Deflator [7]. The EMWG chose to consider these two metrics to be equal for its estimate.

The ARIES project recently re-evaluated the assumed interest and escalation rates and adopted the Gen-IV simplified approach. This approach eliminates the need to estimate future tax rates, tax incentives, and other cost of money effects. Table 40.2 provides the IDC values for several interest rates and construction durations. The recommended interest rate of 5% from Gen-IV and a six-year construction duration yields an IDC value of 0.1303. The deregulated value of 10% interest rate would yield an IDC value of 0.2744.

40.7.4 Financial Assumptions and Methodologies for Annual Costs

The busbar cost of electricity is the most important consideration for utilities or independent power producers in choosing an electrical generating power plant. The plant must be an affordable, reliable, and maintainable energy source and all of these factors are contained in the cost of electricity. The busbar cost of electricity is given by:

$$\mathrm{COE} = [\mathrm{C_{AC}} + (\mathrm{C_{O\&M}} + \mathrm{C_{SCR}} + \mathrm{C_F}) * (1 + \mathrm{y})^{\mathrm{Y}}]/(8760 * \mathrm{P_E} * \mathrm{p_f}) + \mathrm{C_{D\&D}},$$

where

- C_{AC} is the annual capital cost charge (total capital x FCR)
- $C_{O\&M}$ is the annual operations and maintenance cost
- C_{SCR} is the annual scheduled component replacement cost
- C_F is the annual fuel costs
- y is the annual escalation rate (0.0 for constant dollar and y for current dollar)
- Y is the construction and startup period in years
- P_E is the net electrical power (MWe)
- p_f is the plant capacity factor (~plant availability)
- $C_{D\&D}$ is the annual decontamination and decommissioning converted to mills/kWh

40.7.5 Annual Capital Cost Charge

The annual capital cost charge is determined by applying a fixed charge rate (FCR) to the total capital cost of the power plant.

40.7.6 Fixed Charge Rate

The fixed charge rate (FCR), a charge to total investment costs that is annualized over the operating life of the plant, typically considers the cost of capital, depreciation, interim replacement, property insurance, and federal and state taxes for both constant and current (nominal) economic analysis approaches. Early analyses and studies assumed the annual FCR was 10% for the constant dollar and 15% for the current dollar analysis approach.

The Sheffield and Delene Generomak report [11] adopted the economic and financial parameters from the Nuclear Energy Cost Data Base (NECDB) [20] to determine a more realistic FCR involving tax rates, depreciation, salvage value, cost of money, and construction period. In 1992, ARIES [12] began using a FCR of 0.0966 (constant dollars) based on this guidance.

The Gen-IV guidance [8] takes a much more simplified approach in that tax and depreciation considerations are not considered. Their formulation for the FCR is much easier to compare to other power generation systems in other countries:

$$\mathrm{FCR} = \mathrm{X}/[1 - (1 + \mathrm{X})^{-\mathrm{Lecon}}],$$

where X is assumed as the real discount rate of 5% and 10% in constant dollars.

And L_{econ} is the economic or regulatory life of plant (40 years) equal to commercial operation.

The Gen-IV economic guidance report [8] determines the FCR values as 0.05828 for the 0.05 discount rate and a FCR of 0.10226 for the 0.10 discount rate. ARIES has recently adopted the Gen-IV FCR recommendation because of the simplified approach of not considering the changing aspects of the tax laws and depreciated assets. A 40-year economic life will also be adopted to be consistent with the current technology baseline, which is identical to Gen-IV plant lifetime.

TABLE 40.2 Recommended ARIES-AT Interest during Construction Cost Factors

		ID C with no Escalation								
	Interest	**0.02**	**0.03**	**0.04**	**0.05**	**0.06**	**0.07**	**0.08**	**0.09**	**0.10**
Years	**2**	0.0165	0.0248	0.0330	0.0413	0.0495	0.0578	0.0661	0.0743	0.0826
	3	0.0249	0.0374	0.0500	0.0627	0.0754	0.0882	0.1011	0.1140	0.1270
	4	0.0334	0.0503	0.0674	0.0847	0.1021	0.1198	0.1376	0.1556	0.1737
	5	0.0419	0.0633	0.0851	0.1072	0.1296	0.1524	0.1755	0.1990	0.2228
	6	0.0505	0.0766	0.1032	**0.1303**	0.1580	0.1862	0.2150	0.2444	**0.2744**
	7	0.0593	0.0900	0.1216	0.1540	0.1872	0.2213	0.2562	0.2920	0.3287
	8	0.0681	0.1037	0.1404	0.1783	0.2173	0.2576	0.2990	0.3417	0.3858

40.7.7 Annual Operations and Maintenance Cost

The annual operations and maintenance (O&M) accounts include salaries, supplies and equipment, outside support services, general and administrative costs, coolant makeup, fuel handling costs, and miscellaneous costs. Fusion plants would likely be more highly automated than traditional fission plants with a much reduced staffing need from those of current fission plants. The O&M costs for generally all fusion power plant studies were estimated to be in the \$70M to \$90M/yr range (2009 dollars). Gen-IV [8] O&M algorithm had a fixed and variable portion with a total annual cost \$68.6M in 2009 dollars, based on IAEA data.

Until more detailed assessments of the O&M costs are conducted, ARIES decided to use the general costing algorithm:

$$C_{O\&M} = \$80M \text{ x}(P_{e\ net}/1200)^{0.5}$$

in 2009 dollars.

40.7.8 Scheduled Component Replacement

There is a need to separately identify and monitor the cost of the high-cost power-core components that have a limited life less than the economic life of the plant. Especially identified were the first wall and blanket modules, divertor modules, and heating and current drive components. In the constant dollar mode, no escalation is considered, so the annual cost is represented by the initial cost of the components divided by their lifetime with plant availability factored into their specific lifetime. In the constant or nominal dollar mode, the annual costs are multiplied by the escalation factor, $(1 + y)^B$, where y is the escalation rate and B is the construction and startup period in years.

A second category, identified by Starfire [5], included other lower-cost replaceable components, such as crossed field (RF) amplifiers, vacuum isolation valves, ECRH gyrotrons, atmospheric tritium recovery system components, power supplies, LHe refrigerators, and shield door seals. These are replaced on different schedules then the power core components.

$Cost_{SCR}$ = Total cost of replaceable blankets, divertors, RF launcher plasma−facing components, and other regularly replaced items divided by their scheduled lifetime.

40.7.9 Fuel Cost

Purchase of deutritium would be a stable cost for a tenth−of-a-kind power plant. The annual cost of D is ∼\$0.7M (2009\$). A nominal cost of \$1 M/y in 2009 dollars would reasonable for the cost of deuterium pending a new updated cost.

Tritium is a no-cost fuel element, as it would be continuously bred within the blanket in sufficient quantities [5] for the power plant usage. The cost of the initial supply of tritium for the first fusion power plant might be a sizable one-time cost, but within a very short period of time, the plant should be tritium-self-sufficient and will produce an excess of tritium to start a new power plant. In the long run, the net cost of tritium should be zero, and any initial costs will be balanced by the sale of tritium to another power plant starting operation after ∼5 years.

The cost of liquid tritium breeding materials, such as lithium or lithium compounds, either natural or enriched, could be included along with annual offsite fuel processing and disposal costs. All other solid tritium breeding materials, cladding, neutron multipliers, etc., would be accounted for in the SCR cost account.

40.7.10 Decontamination and Decommissioning

Sheffield [11] added this decontamination and decommissioning (D&D) cost item as a separate annual cost of 0.5 mill/kWh based on fission experience in decommissioning power plants. Delene [14] thought that the fission disposal costs were highly speculative and increased the D&D allowance to 1.0 mill/kWh for plants with fission-similar safety and environmental conditions, whereas very safe and environmentally attractive plants would have no D&D charge. The ARIES study [12] adopted the Delene approach, but chose to charge 0.25 mill/kWh for the safer and environmentally friendly case. ARIES's current recommendation is to link the decommissioning cost is linked to the waste volume with considerations for the Class A and Class C low-level waste classification and the recycling/clearance [21, 22]. ARIES is recommending an assessment of 1.0 to 1.5 mill/kWh in 2009\$ for D&D of future fusion power plants.

40.8 SUMMARY

This chapter identifies how fusion plant economics are determined, based on their physical design and operational scenario. The economic assumptions are shown. The method of capital and indirect cost estimation are discussed in detail related to the work breakdown structure. Financial assumptions and cost methodologies associated with plant construction and financing are provided. Annual costs are defined to allow determination of the cost of electricity (COE).

The economics of fusion power are vitally important to determine the economic viability of a proposed conceptual design approach. Methods appropriate to this level of design definition were discussed. Interaction of the economics and the engineering has produced more cost-effective

approaches for proposed power plants. More work is needed in physics, engineering, and economics to be able to better quantify the competitiveness the proposed fusion power plant in relation to its peers at the proposed time of introduction into a power grid.

REFERENCES

1. S. Schulte, T. Wilke, and J. Young, *Fusion Reactor Design Studies—Standard Accounts for Cost Estimates*. Pacific Northwest Laboratory, PNL-2648, May 1978.
2. B. Badger, M. Abdou, R. Boom, R. Brown, E. Cheng, R. Conn, J. Donhowe, L. El-Guebaly, G. Emmert, G. Hopkins, W. Houlberg, A. Johnson, J. Kamperschroer, D. Klein, G. Kulcinski, R. Lott, D. McAlees, C. Maynard, A. Mense, G. Neil, E. Norman, P. Sanger, W. Stewart, T. Sung, I. Sviatoslavsky, D. Sze, W. Vogelsang, W. Wittenberg, T. Yang, and W. Young, *UWMAK-I - A Wisconsin Toroidal Fusion Reactor Design*, UWFDM-68, November 20, 1973 (revised March 15, 1974).
3. B. Badger, R. Conn, G. Kulcinski, M. Abdou, R. Aronstein, H. Avci, R. Boom, R. Brown, E. Cheng, J. Davis, J. Donhowe, G. Emmert, Y. Eyssa, N. Ghoniem, S. Ghose, W. Houlberg, J. Kesner, W. Lue, C. Maynard, A. Mense, N. Mohan, H. Peterson, T. Sung, I. Sviatoslavsky, D. Sze, W. Vogelsang, R. Westerman, L. Wittenberg, T. Yang, J. Young, and W. Young, *UWMAK-II, A Conceptual D-T Fueled, Helium Cooled, Tokamak Fusion Power Reactor Design*, UWFDM-112, October 1975.
4. B. Badger, R. Conn, G. Kulcinski, C. Maynard, R. Aronstein, H. Avci, D. Blackfield, R. Boom, A. Bowles, E. Cameron, E. Cheng, R. Clemmer, S. Dalhed, J. Davis, G. Emmert, N. Ghoniem, S. Ghose, Y. Gohar, J. Kesner, S. Kuo, E. Larsen, E. Ramer, J. Scharer, D. Schluderberg, R. Schmunk, T. Sung, I. Sviatoslavsky, D. Sze, W. Vogelsang, T. Yang, and W. Young, W., *UWMAK-III, A High Performance, Noncircular Tokamak Power Reactor Design*, UWFDM-150, December 1975.
5. C. Baker, M. Abdou, R. Arons, A. Bolon, C. Boley, J. Brooks, R. Clemmer, C. Dennis, D. Ehst, K. Evans Jr, P. Finn, R. Fuja, Y. Gohar, V. Jankus, J. Jung, S. Kim, S. Piet, R. Mattas, B. Misra, J. Rest, H. Schreyer, D. Smith, H. Stevens, L. Turner, S. Wang [Argonne National Laboratory], D. DeFreece, C. Trachsel, N. Bond, D. Bowers, L. Carosella, J. Davis, M. Delaney, C. Dillow, D. Driemeyer, M. Gordinier, J. Haines, P. Heaton, G. Morgan, D. Ruester, P. Stones, L. Waganer, R. Watson, H. Zahn, [McDonnell Douglas Astronautics Company], D. Graumann, J. Alcorn, W. Chen, R. Creeden, P. Drobnis, R. Field, T. Hino, E. Johnson, G. Lutz, R. Pratner, H. Varga [General Atomics Company], J. Kokoszenski, K. Barry, G. Arvay, R. Cavazo, M. Cherry, J. de La Mora, J. Geere, L. Gise, D. Hegberg, S. Huang, R. Jarvis, B. Kenessey, H. Klumpe, P. MacCalden, M. Mercade, R. Hixdorf, L. Pardee, W. Polk, A. Soderbolm. [The Ralph M. Parsons Company], *STARFIRE—A Commercial Tokamak Fusion Power Plant Study*, Argonne National Laboratory report ANL/FPP-80-1, September 1980.
6. The ARIES Project Bibliography: http://aries.ucsd.edu/ARIES/DOCS/bib.shtml.
7. U.S. Department of Commerce, Bureau of Economic Analysis, *Gross Domestic Product Web Page*, http://www.bea.gov/index.htm.
8. The Economic Modeling Working Group of the Generation IV International Forum, *Cost Estimating Guidelines for Generation IV Nuclear Energy Systems*, GIF/EMWG/2007/004, Revision 4.2, September 26, 2007.
9. The ITER Project: http//www.iter.org/ or ITER Technical Basis, Report G A0 FDR 1 01-07-21R0.4, July 2001.
10. J. Delene, R. Krakowski, J. Sheffield, and R. Dory, *GENEROMAK Fusion Physics, Engineering, and Costing Model*. Oak Ridge National Laboratory report, ORNL/TM-10728, June 1988.
11. J. Sheffield, R. Dory, S. Cohn, J. Delene, L. Parsly, D. Ashby, and W. Reiersen, Cost assessment of a generic magnetic fusion reactor. *Fusion Technology*, March 1986, **9**, 199–249.
12. C. Bathke, R. Krakowski, R. Miller, and K. Werley, Chapter 2. *Systems Studies of the ARIES-II and ARIES-IV Tokamak Fusion Reactor Study—The Final Report*, UCLA report UCLA-PPG-1461, 1992.
13. S. Schulte, W. Bickford, C. Willingham, S. Ghose, and M. Walker, *Fusion Reactor Design Studies—Standard Unit Costs and Cost Scaling Rules*. Pacific Northwest Laboratory report, PNL-2987 (UC-20), September 1979.
14. J. Delene, *Generomak Cost Model Update*, Informal note, June 4, 1990.
15. *Guide for Economic Evaluation of Nuclear Power Plant Design*, NUS Corporation, NUS-531, January 1969.
16. D. Phung, *A Method for Estimating Escalation and Interest During Construction (EDC and IDC)*. Institute for Energy Analysis, Oak Ridge Associated Universities, ORAU/EA-78-7, 1978 (OSTI ID:6765917).
17. R. Harrnett and D. Phung, *The Three Modes of Energy Cost Analysis—Then Current, Base-Year, and Perpetual- Constant Dollar*, Technical Report. Institute for Energy Analysis, Oak Ridge Associated Universities, ORAU/IEA-78-10(M), January 1979 (OSTI ID:6268636).
18. J. Delene, *Generomak Model Update*, Informal note, February 21, 1989.
19. F. Najmabadi and the ARIES Team, The ARIES-AT advanced tokamak, advanced technology fusion power plant. *Fusion Engineering and Design*, 2006, **80**, 3–23.

20. *Nuclear Energy Cost Data Base—A Reference Data Base for Nuclear and Coal-Fired Power Plant Generation Cost Analysis*, DOE/NE-0044/3, US Department of Energy, Office of Nuclear Energy, August 1985.

21. L. El-Guebaly, V. Massaut, K. Tobita, and L. Cadwallader, Goals, challenges, and successes of managing fusion active materials. *Fusion Engineering and Design*, 2008, **83**, 7–9, 928–935.

22. L. El-Guebaly and L. Cadwallader, *Lifecycle Waste Disposal and Decommissioning Costs for ARIES Systems Code*, presented at ARIES Project Meeting May 2008. Available at: http://aries.ucsd.edu/ARIES/MEETINGS/0805/ or http://fti.neep.wisc.edu/aries/TALKS/lae_lifecycle0508.pdf.

PART VI

LOW-ENERGY NUCLEAR REACTIONS

41

DEVELOPMENT OF LOW-ENERGY NUCLEAR REACTION RESEARCH

STEVEN B. KRIVIT

New Energy Times, San Rafael, CA, USA

41.1 INTRODUCTION

"Cold fusion" is a term that prompts disgust and scorn in some people and inspiration and hope in others. Rarely has the modern world witnessed a scientific (and sometimes unscientific) topic so polarizing. It's also a term and a concept that is long overdue for retirement from scientific venues—but not without the recognition of the legitimate science that has evolved from it.

When the cold fusion concept first made headlines in 1989, the idea was promoted as the panacea for the world's energy problems and, soon after, denounced and discredited in its entirety by the science establishment of the day. Nuclear experts had never known of any kind of nuclear energy that did not produce commensurate levels of dangerous radioactive emissions. The controversy has been chronicled in a number of nonfiction accounts [1].

The evidence has grown year after year and now shows that the hypothesis of cold fusion lacks strong experimental support as well as a viable theoretical explanation. Partially hidden among the unscientific claims in this two-decade controversy, a legitimate set of scientific phenomena has emerged. This set of phenomena is known as low-energy nuclear reactions (LENRs), and it does not presume or assert a fusion mechanism. The potential benefit for society ranges from trivial to revolutionary; it is the energy wild card.

One of the most revealing aspects of the cold fusion controversy is the extent and the intensity of the associated human drama. This drama reveals that scientists—humans, just like the rest of us—have strong opinions and passions. It reveals that scientific inquiry is not nearly as dispassionate as many of us have come to believe. This chapter, and the following chapters, will provide an overview of a subject that could have extremely broad and significant impact in a multitude of applications for society.

41.2 A NUCLEAR CHEMISTRY REVOLUTION

Not since the mysterious days of ancient alchemy has anyone believed that chemistry could cause elemental changes. For more than a century, the realm of chemistry was limited to the electrons surrounding an atom; the nuclear realm was limited to the subatomic particles inside the atom. And the twain never met—until now.

On March 23, 1989, electrochemists B. Stanley Pons (University of Utah) and Martin Fleischmann (University of Southampton), along with administrators from both universities, boldly announced in a press conference that they had achieved a nuclear fusion reaction by means of a chemical process [2].

Neither discoverer has retracted his fundamental claim, although Fleischmann has expressed regret about claiming it as fusion rather than as an anomalous nuclear reaction. Pons has been silent and has chosen to remain out of the public spotlight for more than a decade.

However, unlike Fleischmann, Pons was not attached to the cold fusion hypothesis. On April 12, 1989, at the American Chemical Society meeting in Dallas, TX, Pons revealed to reporters at a press conference that his group's normal-water cells were also showing a slight but

Nuclear Energy Encyclopedia: Science, Technology, and Applications, First Edition (Wiley Series On Energy).
Edited by Steven B. Krivit, Jay H. Lehr, and Thomas B. Kingery.

significant signal of excess heat. Normal-water excess heat disproves the cold fusion hypothesis. A news report from a later press conference quoted Fleischmann dismissing the possibility of excess heat from normal water. Fleischmann also told Mahadeva Srinivasan of the Bhabha Atomic Research Centre of his disbelief in normal-water excess heat. Research by Francesco Piantelli, George Miley, Francesco Celani, Tadahiko Mizuno, James Patterson, and Randell Mills also adds support for the possibility that normal hydrogen may produce excess heat in benchtop experiments.

After the 1989 announcement, the pair pursued their idea for several years in a laboratory in southern France, but that association dissolved around 1995. Little is publicly known of the causes of their dissolution, but the ideological disparity of Fleischmann's cold fusion hypothesis versus Pons' more open-minded philosophy is a likely component of the breakup. Although several cold fusion startups have attempted to involve Fleischmann as a figurehead, Fleischmann and Pons have effectively abandoned their personal efforts in the research.

Fleischmann, the idea man of the pair, had been curious about the behavior of hydrogen/deuterium in palladium at least as early as 1947. In 1922, during the decades when great discoveries were made in nuclear physics, two American chemists, Clarence E. Irion and Gerald L. Wendt, performed experiments in which they claimed the decomposition of tungsten atoms into helium, effectively LENRs [3].

In 1926, Fritz Paneth and Kurt Peters of the University of Berlin preceded Pons and Fleischmann with a similar experiment [4]. However, after significant peer pressure, Paneth and Peters retracted their claim, stating that their observations had been the result of experimental error and contamination from the atmosphere. Only a thorough historical investigation will reveal whether Paneth and Peters believed they had made an error or, like Galileo, recanted under coercion from science authorities.

41.3 COLD FUSION: SCIENTIFIC CONTROVERSY OF THE CENTURY

In 1993, nuclear chemist John Huizenga published a book titled *Cold Fusion: The Scientific Fiasco of the Century* after he organized the first U.S. Department of Energy cold fusion review in 1989 [5, 6].

His account was one-sided and considered only the flaws of the cold fusion concept. Huizenga's complete dismissal of the phenomena was premature. The topic is more accurately identified as "the scientific controversy of the century."

Many people with a variety of scientific backgrounds have been believers in the cold fusion concept, accepting aspects of the cold fusion claim on faith and, to some extent, ignorance [7].

Huizenga was helpful, however, in making clear why cold fusion seemed so unlikely, considering what is known of thermonuclear fusion. He mockingly called these contradictions the "three miracles" of cold fusion:

- The mystery of how the Coulomb barrier is penetrated
- The lack of strong neutron emissions
- The lack of strong emission of gamma or x-rays

Misinformation, disinformation, and scientific research misconduct have played a significant part in the controversy. These LENR chapters have been selected carefully to represent the best experimental and theoretical work in the field.

41.4 LENR: THE END OF COLD FUSION

In 2000, the Web magazine *New Energy Times* began to investigate and publish news and information on cold fusion. Ten years later, in the July 30, 2010, *New Energy Times* Special Report "Cold Fusion Is Neither," *New Energy Times* concluded that the claims for cold fusion as a fusion process were unsupported, although the subject and potential for energy were not at all cold [8].

New Energy Times concluded that evidence for nuclear processes, likely the result of weak interactions and neutron capture processes, were clearly supported by the best available experimental data. The report indicated that the unsubstantiated hypothesis of cold fusion put forth by many of the researchers who pursued LENRs is the most significant cause of the sweeping dismissal of the subject. In spite of this, many of the researchers who have advocated the cold fusion concept for two decades remain wedded to their ideological belief that LENRs are the result of a fusion process. Other LENR researchers simply continue to use the term "cold fusion" out of habit. In recent years, some of the researchers have recognized that the "cold fusion" concept is obsolete, and they have attempted to redefine "fusion" to be synonymous with non-fusion processes.

41.5 THEIR D-D FUSION HYPOTHESIS

The Pons-Fleischmann experiment used an electrolytic cell in a palladium-deuterium system (Fig. 41.1) [9].

The configuration and process were intricate and subtle, and numerous critics, downplaying the significance of these factors, used these constraints as excuses to dismiss their own failures to replicate the excess-heat effect. Invariably, such critics turned out to be poorly informed of the crucial details of the Pons-Fleischmann experiment.

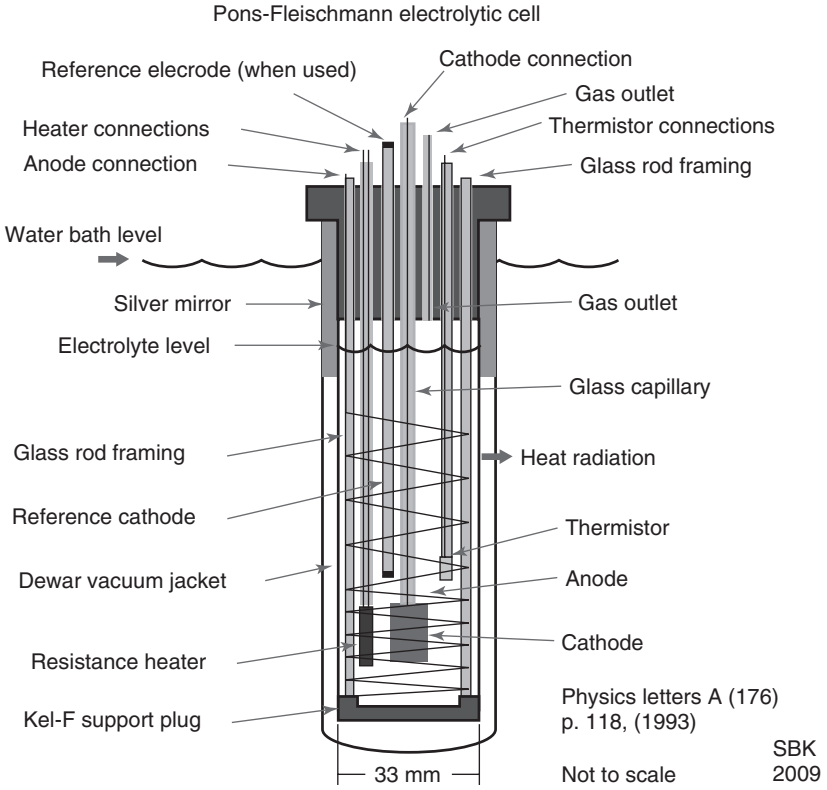

Figure 41.1 Schematic of Pons-Fleischmann electrolytic cell.

To their detriment, Pons and Fleischmann did not have conclusive data on neutrons, tritium, transmutations, or isotopic anomalies when they went public in 1989. These data would come in later years from other researchers. What Pons and Fleischmann had at the time was excess heat. They did not have the benefit of a background in nuclear physics or nuclear chemistry, however; electrochemistry and measuring heat via calorimetry were their domains of expertise.

When they performed their experiments, they observed that more heat was coming out of the cell than could be accounted for by the electrical energy going into the cell. The amount of heat energy coming out of the cell was up to 1,000 times greater than it should have been, based on their knowledge of possible chemical reactions. They assumed, correctly, that they were triggering a nuclear reaction. They did not speculate that their results were caused by fission, because their results were missing key characteristics of fission reactions, and they were not using materials required to create fission reactions.

Initially, Pons and Fleischmann hypothesized that they had discovered a new kind of fusion process. Weeks later, they added a more circumspect alternative speculation: a "hitherto unknown nuclear process or processes." They knew that it didn't look like fusion as they and the rest of the world knew fusion. They were troubled by the fact that there was no associated deadly gamma radiation and no high flux of deadly neutron emissions. Because they were looking for neutrons (and frustrated that they found none commensurate with the heat), Pons and Fleischmann were specifically not looking for a new "clean" version of fusion. That objective seems to have developed only in hindsight for them and the University of Utah. Fleischmann has cited the 1930s "cold explosions" research by Percy Bridgman, a professor of physics at Harvard and a Nobel Prize winner, as one of the influences for his ideas [10].

Once Pons and Fleischmann knew they had discovered a novel effect, fusion was their best guess for an explanation because they, as well as most other scientists at that time, were not aware of a third nuclear possibility: weak interaction processes. Key aspects of electroweak theory had been experimentally confirmed only a few years earlier—and in high-energy physics, not chemistry. Even people who knew about weak interactions had no idea that weak interactions could, in fact, be very energetic, enough to explain the nuclear-scale heat that Pons and Fleischmann observed.

A Pons-Fleischmann experiment performed in 1992 (Fig. 41.2) shows the typical amount of time required for their cells to load the minimum amount of deuterium into palladium, a requirement for the anomalous heating effect. After day 16, after no changes to the input energy for the previous 13 days, the temperature suddenly rises.

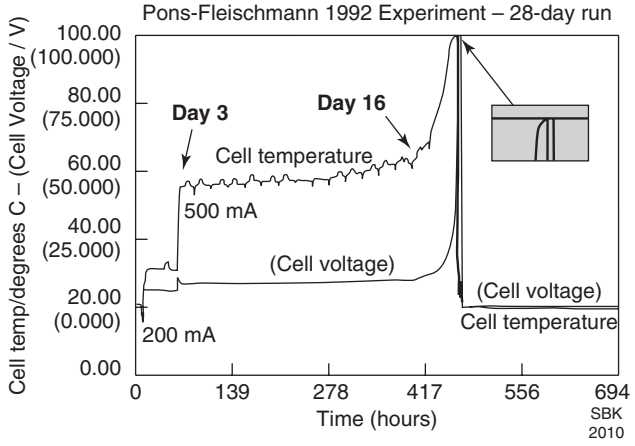

Figure 41.2 Pons-Fleischmann 1992 heat measurements.

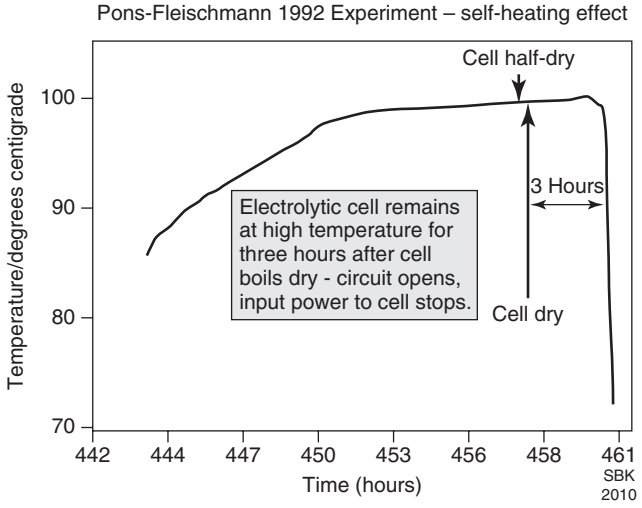

Figure 41.3 Pons-Fleischmann 1992 self-heating effect.

Figure 41.3 shows the final 19 hours of the heating effect. The cell remained close to 100°C after the electrolyte boiled and the circuit opened. Some kind of LENR process had begun and kept the palladium cathode hot for three hours.

41.6 DEVELOPMENT OF EXPERIMENTAL EVIDENCE

The Pons and Fleischmann research inspired hundreds (initially thousands) of researchers to attempt to replicate and develop the concept. Few succeeded, and those who did observed remarkable anomalies: excess heat beyond that possible by ordinary chemistry, rare but clear cases of tritium production (Fig. 41.4), neutron emissions (Fig. 41.5), temporal correlations of helium-4 and

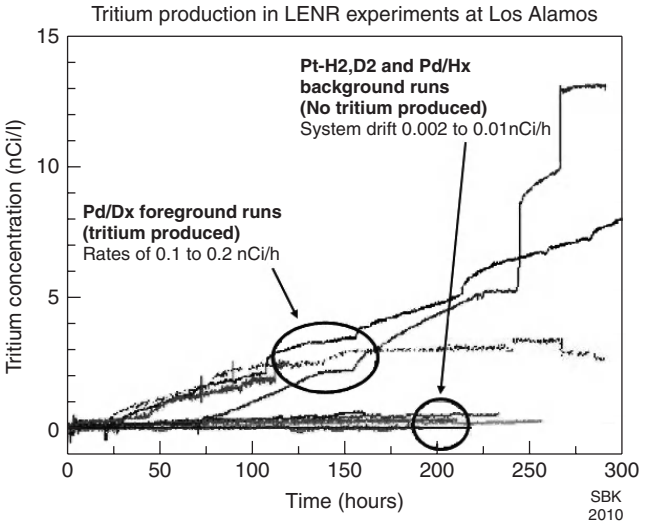

Figure 41.4 Tritium generation rates up to 25 times larger than control experiments.

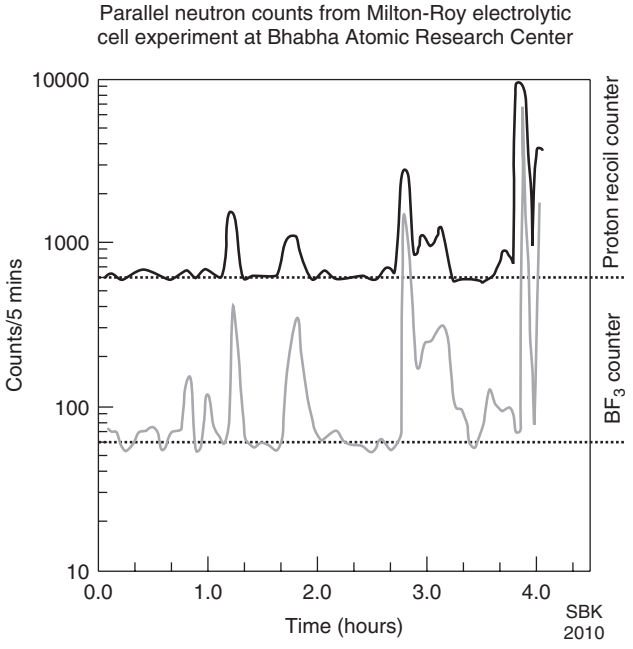

Figure 41.5 Neutron counts measured at BARC in LENR experiment.

excess heat evolution (Fig. 41.6), melting (Fig. 41.7) and vaporization (Fig. 41.8) of metals from just a few watts of input energy.

On April 24, 1989, a group led by John O'Mara. Bockris at Texas A&M University observed extremely high concentrations of tritium in its experiments. The researchers later reported that 11 of a set of 24 cells produced tritium at levels "100 to 10^{15} times above that expected from the normal isotopic enrichment of electrolysis" [11].

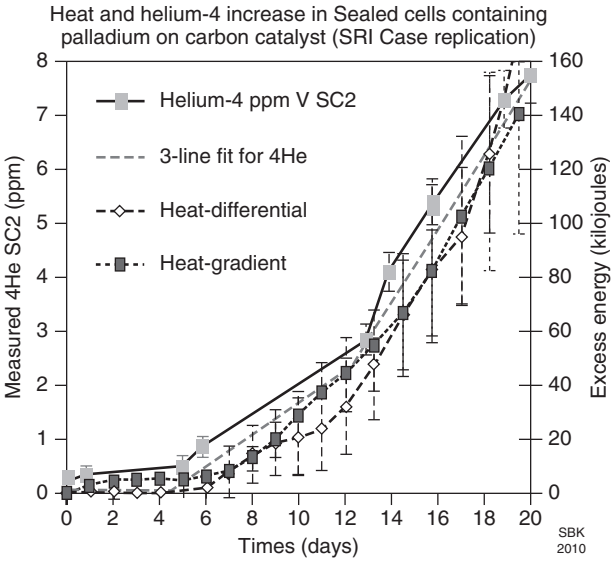

Figure 41.6 Temporal correlation of excess heat and helium production in deuterium gas cell designed by Lester Case.

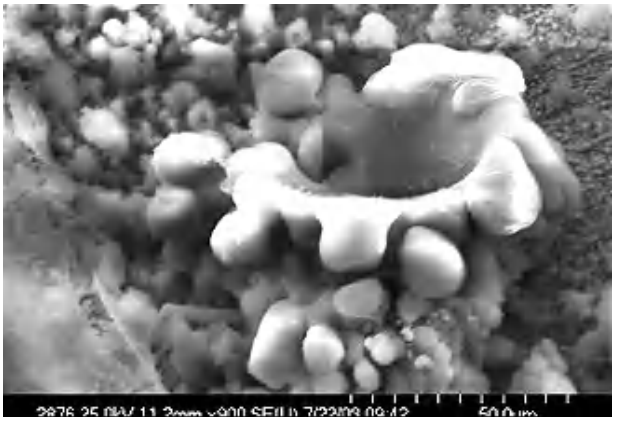

Figure 41.7 Apparent molten metal on cathode after LENR experiment (*image courtesy SPAWAR Pacific*).

Other groups who reported tritium (Figs. 41.4 and 41.9) in LENR experiments include Padmanabha Krishnagopala Iyengar and Mahadeva Srinivasan at the Bhabha Atomic Research Centre in Trombay, India, who witnessed a tritium burst on April 21, 1989 [12]. Later, a group led by Thomas Claytor at Los Alamos National Laboratory found tritium as well, as did other groups [13].

On April 21, 1989, researchers at Bhabha Atomic Research Center performed LENR experiments using a Milton-Roy electrolytic cell (Fig. 41.5). They registered similar tracks of neutron signals during the experiment using two kinds of detectors: a BF3 counter embedded in paraffin blocks for thermal neutrons and a proton recoil plastic scintillator counter for fast neutrons. They monitored

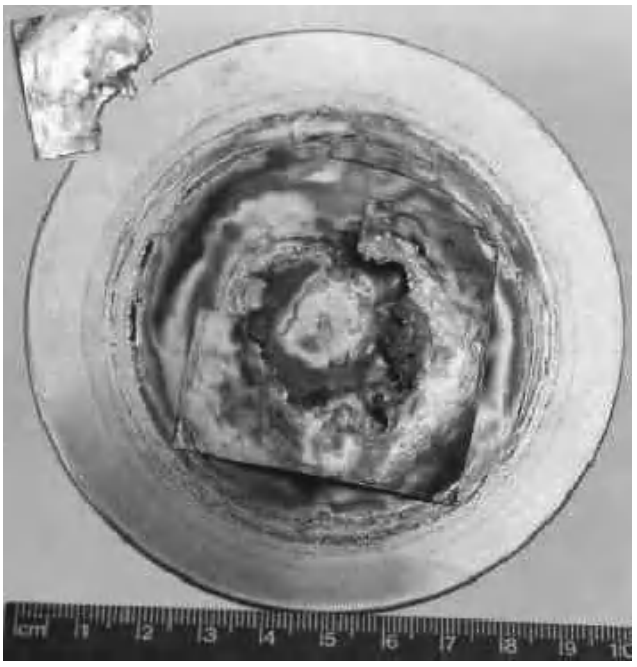

Figure 41.8 Vaporized section (in center) of palladium foil used in LENR acoustic cavitation experiment; acoustic energy inputs varied from 5 to 16 W with exposures of 5 minutes to several weeks in duration (*image courtesy Roger Stringham*).

background signals using He3 counters. Several other groups at BARC also registered neutrons (Fig. 41.9) [14].

41.7 THE DEVELOPMENT OF THE COLD FUSION BELIEF

Some researchers attempted to follow closely in the footsteps of Pons and Fleischmann, striving to replicate precisely their electrochemical cell. Many others ventured out on their own, trying experiments with deuterium gas as well as more common materials such as nickel and ordinary hydrogen or light water. A dozen other experimental approaches and configurations evolved, many having little to do with the original Pons and Fleischmann experiment.

In time, a subgroup among these researchers focused on the hypothesis that the Pons and Fleischmann experimental results were the result of a fusion process. This ideological pursuit, and the failure to distinguish rigorously between observations and speculations, caused many observers of the field to reject the entire field; they perceived its proponents as adherents to a religion, guided by faith rather than by science.

The cold fusion subgroup held a simple belief: If deuterium was present in the experiment as an input and helium-4 was present as an output, then nuclear fusion was occurring, even if the idea of room-temperature cold

Summary of results from groups reporting tritium and neutrons in BARC electrolysis experiments (1989–1990)

Division	Cathode material	Geometry	Area Cm^2	Anode	Neutron yield	Tritium yield	n / T ratio
Desalin*	Ti	Rod	104	SS pipe	$3\times10^{+7}$	$1.4\times10^{+14}$	2×10^{-7}
Neut. Phy*	Pd-Ag	Tubes	300	Ni pipe	$4\times10^{+7}$	$8\times10^{+15}$	5×10^{-7}
HWD*	Pd-Ag	Tubes	300	Ni pipe	$9\times10^{+7}$	$1.9\times10^{+15}$	5×10^{-7}
HWD*	Pd-Ag	5 Disks	78	Porous Ni	$5\times10^{+4}$	$4\times10^{+15}$	1.2×10^{-9}
Anal.Ch.@	Pd	Hol. Cyl.	5.9	Pt Mesh	$3\times10^{+6}$	$7.2\times10^{+13}$	4×10^{-8}
ROMg@	Pd	Cube	6.0	Pt Mesh	$1.4\times10^{+6}$	$6.7\times10^{+11}$	1.7×10^{-4}
ROMg@	Pd	Pellet	5.7	Pt Mesh	$3\times10^{+6}$	$4\times10^{+12}$	1×10^{-4}
App. Ch.@	Pd	Ring	18	Pt Mesh	$1.8\times10^{+8}$	$1.8\times10^{+11}$	1×10^{-3}

* = 5M NaOD electrolyte @ = 0.1M LiOd electrolyte SBK 2009

Figure 41.9 Tritium and neutron results at BARC.

fusion contradicted 70 years of experimental and theoretical groundwork. It seemed as simple as $2 + 2 = 4$. That is, two deuterons make one helium-4 atom. But it was far from simple.

Among other problems with the theory of room-temperature fusion is that, normally, temperatures in the millions of degrees are required to cause nuclear fusion. More significant than the contradiction to prevailing theory was the fact that the cold fusion subgroup overlooked a crucial empirical consideration.

In the early days of the cold fusion controversy, the researchers were challenged by skeptics to find commensurate nuclear products associated with the claimed excess heat. Fairly early on, they did find quantities of helium-4 that, in some cases, were sufficient to explain the heat as a nuclear process.

But some of them quickly closed their minds to alternative explanations. They also ignored and, in some cases, denied experimental evidence suggesting that more-complex reactions and diverse phenomena were taking place. These researchers came to believe that deuterium was the sole reactant and that heat and helium-4 were the sole products. They failed to consider and thus quantify other significant nuclear products and effects in the experiments. Without considering the broader range of possible reactants and products, they assumed a direct and exclusive proportionality between helium and excess heat. Additionally, many of them worked only in the D/Pd system and ignored and dismissed research with nickel and hydrogen.

Through the 1990s, researchers discussed the cold fusion idea in papers and conference presentations, primarily as a hypothesis, and this generally followed scientific protocol. Beginning around 2000, however, the character of the discussion shifted. Some LENR researchers—for example, "cold fusion" theorist Scott Chubb—began discussing the cold fusion idea as an "official fact," not an hypothesis.

This ideological shift didn't take place because the researchers made new discoveries, however. Instead, in order to support their hypothesis, the "cold fusion" subgroup invented theories that relied on new physics, invented new untested concepts of metallurgy, and were very selective about the data they chose to consider and report as accurate. In one case of research misconduct at SRI International that took place in 1994 and was reported in 2000, a researcher made up data points and made changes to results without scientific justification [15]. Once the misconduct became public knowledge in 2010, the claims from that experiment quietly disappeared [16].

In 2006, a theoretical breakthrough occurred that offered insight into the two-decade mystery. Theorists Lewis Larsen and Allan Widom proposed that LENR phenomena could be explained accurately by weak interactions and neutron capture processes, not by fusion [17]. Their proposed theory requires no new physics or miracles and has been verified by independent third parties to be mathematically sound. Perhaps not surprisingly, their theory

drew bitter opposition and hostility from researchers who were wedded to the idea and name of "cold fusion."

41.8 LENR: WHAT GOES IN

For comparison, in D-D thermonuclear fusion, the input materials are very simple: deuterium gas or deuterium pellets. LENR systems, on the other hand, consist of a complex and highly variable mixture of elements and materials. The inputs—that is, potential reactants—may include (but are not limited to) deuterium in heavy water, deuterium gas, hydrogen in normal water, hydrogen gas, lithium, carbon, platinum, palladium, titanium, nickel, aluminum, and tungsten. Given the complex mixture of elements and input materials, it is naive to assume that the primary, let alone only, reactant is deuterium and the primary, or only, nuclear product is helium-4.

41.9 LENR: WHAT COMES OUT

In D-D thermonuclear fusion, the nuclear products are well-known: strong fluxes of neutrons, gamma radiation, helium-3, and tritium. Helium-4 is a rare output in D-D thermonuclear fusion reactions.

In LENR, the complex array of nuclear products barely overlaps with D-D thermonuclear fusion. Strong fluxes of neutrons are extremely rare, and gamma radiation is almost entirely absent. Helium-3 and tritium do appear, but infrequently. Low fluxes of neutrons and energetic alpha particles have been measured by a variety of groups [18, 19].

Helium-4 has been measured in the parts-per-million range, and some researchers have made bold claims that its remote association to the third branch of D-D thermonuclear fusion proves the observed products are the result of a fusion process [20]. Some researchers have gone to great lengths to build the case for the cold fusion hypothesis. From 1998 to 2007, Michael McKubre, a researcher at SRI International, retroactively made a dozen unsubstantiated changes, additions, and deletions in his reporting of an experiment he performed in 1994 in an attempt to show data that supported the hypothesis of cold fusion [21]. The attempt to equate LENRs to the third branch of D-D thermonuclear fusion was, in fact, moot for several reasons.

First, there are other nuclear products in LENR systems besides helium-4; hence, other nuclear processes must be occurring. Tritium is one example; high-energy alpha particles are another. Most important, numerous reports of heavy-element transmutations and anomalous isotopic abundances have been presented at conferences throughout the last two decades.

The subgroup of cold fusion advocates has tended to avoid looking for heavy-element transmutation products and isotopic anomalies because this would cast significant doubt on the cold fusion hypothesis. Instead, they tended to look only for heat and helium-4. LENR transmutation products are inexplicable by any cold fusion theory. Additionally, the production of transmutation products throws a monkey wrench into the simplistic accounting that the cold fusion subgroup believes takes place in its $D + D \Rightarrow 4He + 24$ MeV (heat) cold fusion hypothesis. This hypothesis dictates that all the evolved heat results only from the fusion of two deuterons into an atom of helium-4, that helium-4 is the sole product of LENRs, and that the helium-4 is born with an energy of 20.2 KeV or less. The cold fusion hypothesis fails simply because of the presence of numerous other products as well as MeV-scale alpha particles.

In some cases, LENR researchers have claimed to measure neutron emissions using solid-state nuclear track detectors. Based only on optical comparisons of track dimensions, rather than electronic detectors, they say they have observed particle track diameters from LENR experiments similar to particle track diameters from 2.45 MeV neutrons in calibration tests. On this basis, some researchers have also staked a claim of cold fusion. They propose that, if low fluxes of neutrons are emitted from a LENR experiment at or near 2.45 MeV, similar to the neutrons seen from the high fluxes resulting from DD thermonuclear fusion, then such LENR data provide evidence for cold fusion [22]. However, there has never been any evidence to support the suggestion that the low flux of neutrons in LENRs can in any way explain the observed level of heat output in LENRs.

Some researchers have also suggested that secondary D-T reactions may be responsible for the low fluxes of neutrons seen in LENR. A significant problem with this hypothesis is that no tritium is used as a starting material. Another problem with this suggestion is that tritium is rarely seen as a product in LENR experiments, although when it is observed, it appears in significant amounts [23].

Many researchers in the field think that their peers have confirmed that, in excess-heat-producing LENR experiments, a proportionate quantity of helium gas is released relative to the excess heat. They have suggested that LENR experiments produce 24 MeV of heat per helium-4 atom produced, thus giving the appearance of an emulation of the third branch of D-D thermonuclear fusion. But the logic is flawed, for reasons stated above and because the reported heat results span a wide range, from 12 to 89 MeV per helium-4, assuming no other nuclear processes (such as transmutations) take place in the experiment, a key assumption of the cold fusion hypothesis that is arguably false.

41.10 ANOMALOUS LENR TRANSMUTATIONS

The quality of LENR transmutation experimental observations is varied, but some work, such as the Mitsubishi Heavy Industries gas permeation experiments developed by Yasuhiro Iwamura, have been performed with meticulous care [24].

The researchers at Mitsubishi, using a process with little resemblance to the Pons-Fleischmann experiment, developed a method of passing deuterium gas through a multilayer substrate (Fig. 41.10). Through gas pressure and a low-grade heater alone, they cause the simultaneous increase of a target element and the decrease of a starting (given) element. While it may sound like alchemy, the multimillion-dollar apparatus is a long way from providing a cost-effective method to create rare elements from common elements.

The Mitsubishi researchers have repeated this type of observation many times, with several pairs of elements:

- 133Cs ⇒ 141Pr
- 88Sr ⇒ 96Mo
- 137Ba ⇒ 149Sm
- 44Ca ⇒ 48Ti

The gradual increase of one element and the temporally correlated gradual decrease of another element are consistent features of their experiment. In Figure 41.11 their XPS data show similar patterns among three sets of experimental runs.

The Mitsubishi group has confirmed its LENR transmutations by a variety of methods, including TOF-SIMS, XANES, x-ray fluorescence spectrometry, and ICP-MS. Some of the analyses have been performed *in situ*, and some have been performed at the Japanese Spring-8 Synchrotron.

41.11 ANOMALOUS ISOTOPIC ABUNDANCES

Reports of anomalous isotopic abundances in LENR experiments have been available for two decades. Figure 41.12 represents the changes to the palladium isotopic ratios that took place as the result of a heavy-water LENR electrolysis experiment performed by researcher Tadahiko Mizuno in 1991. A variety of significant changes is evident. Figure 41.13, from the same experiment, also shows a significant anomalous shift in the isotopes of chromium.

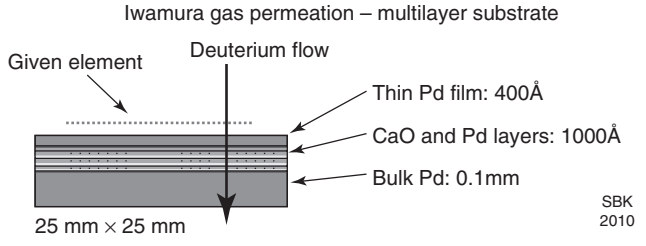

Figure 41.10 Mitsubishi Heavy Industries/Iwamura multilayer substrate.

41.12 ENERGY RELEASE FROM LENR TRANSMUTATIONS

In November 1999, Thomas Passell, a former program manager with the Electric Power Research Institute and Albert Machiels, another EPRI program manager, reported LENR transmutations from a cathode (palladium rod) that had been used by Pons in a heavy-water electrolysis experiment that generated lots of excess heat. Passell arranged for nuclear activation analysis at the well-respected University of Texas, Austin, research facility.

The samples—sections of the cathode—that were tested in the University of Texas reactor came from an experiment conducted by Pons, possibly in the laboratories of the Toyota-sponsored Institut Minoru de Recherche Avancée in Nice, France. Exactly when Pons conducted this experiment is unknown. The experiment may have taken place in the mid-1990s, because Passell cites similar work by Pons, T. Roulette, and J. Roulette published in October 1996 [25].

The University of Texas analysis (Table 41.1) shows a wide variety of transmutations in the cathode. The researchers reported four times the amount of cobalt (Co), 5.4 times the amount of chromium (Cr), 2 times the amount of cesium (Cs), 1.3 times the amount of europium (Eu), 56 times the amount of iron (Fe), and 11 times the amount of zinc (Zn) that is found in the virgin material.

Electrolytic experiments, as opposed to gas experiments, are often but not necessarily easily critiqued for the possibility that rogue elements from the electrolytic solution may deposit on the cathode. However, some of the elements reported in Table 41.1 represent large concentrations, and thus the value of such critiques is limited.

The anomalous isotopic ratio of palladium-108 to palladium-110 merits attention. Authors of the EPRI report wrote, "Pd108 was depleted in the active sample over the virgin material by an apparent 28% with the one sigma error limits extending from 7% to 49%."

41.13 LENR TRANSMUTATIONS: CATHODE FROM AN EXPERIMENT WITH LOTS OF HEAT

According to Passell and Machiels, the authors of the EPRI report, that Pons experiment produced lots of heat [23]. The authors of the EPRI report did not know

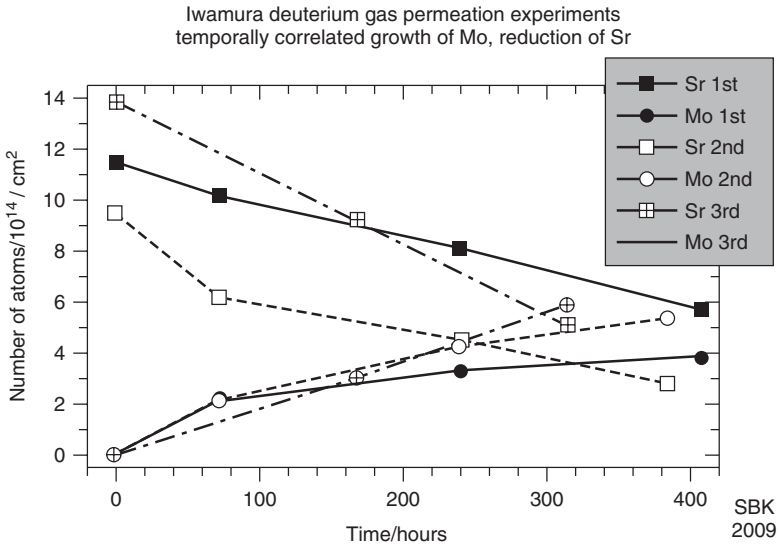

Figure 41.11 Temporally correlated gradual decrease and increase of elements.

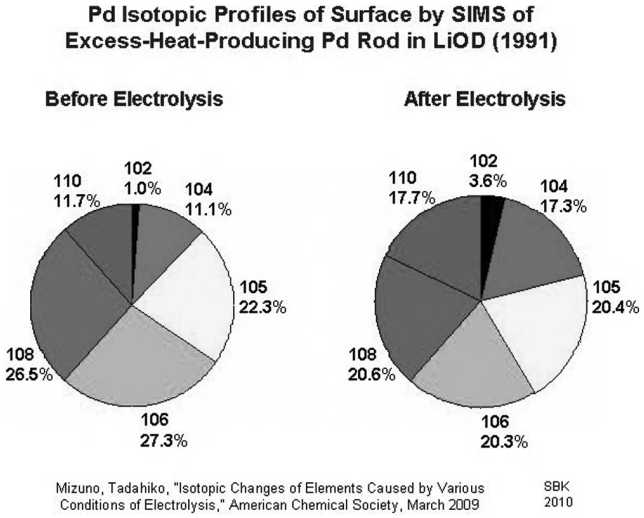

Figure 41.12 Changes to palladium isotopic ratios. *(Mizuno, Tadahiko, "Isotopic changes of elements caused by various conditions of electrolysis," American Chemical Society, March 2009.)*

what type of nuclear process to attribute the reactions to. They speculated, based on their understanding of nuclear chemistry, "that the excess power episodes observed with the cathode integrated over the time of the episodes must have totaled 160 kilojoules."They also had information from Pons about similar experiments for comparison.

"Pons of IMRA volunteered a cathode that had experienced such episodes of excess heat well above the required levels of several hundred kilojoules," the researchers wrote. "It was this cathode and its virgin counterpart that were analyzed in this study."

The researchers were not given the excess-heat data from Pons, but they back-calculated the minimum amount of energy release based on the facts they obtained from the NAA along with their knowledge of nuclear binding energy. They based their interpolation on the most conservative estimate of depleted Pd110 atoms (7%), and from this, they extrapolated an amount of energy in the same ballpark as that which Pons had reported by his calorimetry.

Passell and Machiels explained their calculations [23]:

> If we take the 7% number as the value, this implies a loss of 2.3E18 atoms of Pd108," Passell and Machiels wrote. "At 10 MeV per atom lost, this amounts to 3.6 megajoules for the sample, and extrapolating to the total cathode assuming homogeneity gives 163 megajoules of excess heat. Of course, total homogeneity is not likely in the electrochemical cell. The total excess heat generated by this cathode has not been made available to us as yet.

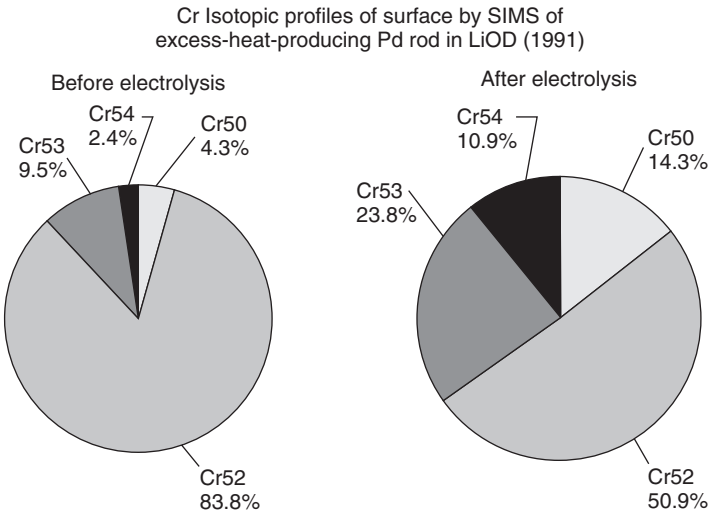

Figure 41.13 Changes to chromium isotopic ratios. *(Mizuno, Tadahiko, "Isotopic changes of elements caused by various Conditions of electrolysis," American Chemical Society, March 2009.)*

TABLE 41.1 Trace Elements in Electrolyzed and Virgin Palladium (Neutron Activation Analysis of Pons Cathode Performed at University of Texas, Austin)

Element	Symbol	Electrolyzed Pd	Virgin Pd	Ratio
Cerium	(Ce)	<5 ppm	<5 ppm	NA
Cobalt	(Co)	2 ppm	<0.5 ppm	>4
Chromium	(Cr)	27 ppm	<5 ppm	>5.4
Cesium	(Cs)	14 ppm	<7 ppm	>2
Europium	(Eu)	0.04 ppm	0.03 ppm	1.3
Iron	(Fe)	13,870 ppm	247 ppm	56
Hafnium	(Hf)	<0.5 ppm	<0.4 ppm	NA
Rubidium	(Rb)	<20 ppm	<20 ppm	NA
Selenium	(Se)	<3 ppm	<3 ppm	NA
Zinc	(Zn)	60 ppm	5 ppm	12

To get 163 megajoules of excess heat would require an episode with an excess power of 10 watts for 4,527 hours, or about 0.5 years. The conclusion we must draw is that homogeneity is unlikely for excess-heat episodes or that our measurement of Pd108 depletion is in error. However, it should be noted that Roulette, Roulette, and Pons report one cell giving a total net excess heat of 294 megajoules and another yielding 102 megajoules.

41.14 LENR TRANSMUTATIONS WITHIN DRY, SEALED, HOLLOW-CORE ELECTROLYTIC CATHODE

Passell pursued the search for rigorous LENR evidence further. He knew that some skeptics might dismiss the LENR transmutations (but not the isotopic shifts) as impurities from electrolytic solutions.

He found a unique experiment developed by Yoshiaki Arata and Yue-Chang Zhang at Osaka University that was designed with a double-structure electrolytic cathode (See Fig. 41.14). This cathode contained a hollow core in which finely divided palladium, also called palladium-black, was inserted before the experiment began. After insertion of the palladium-black, the core was welded shut. The palladium-black material was protected from the electrolyte inside the gas-pressure-tight core of the cathode.

Passell was given three samples from post-electrolysis experiments and one virgin sample. He sent them to The University of Texas, Austin, for neutron activation analysis (Table 41.2). The most striking finding was 6.6 to 14.4 times the zinc-64 isotope relative to the virgin palladium [26].

In addition to the increase of zinc-64 relative to virgin palladium, Table 41.2 shows the following anomalies:

- 7–15 times the zinc-64 by weight

TABLE 41.2 Analysis of Palladium within Dry, Sealed, Hollow-Core Electrolytic Cathode (Neutron Activation Analysis of Arata-Zhang Pd-Black by University of Texas, Austin)

Sample	Zn64 Content PPM by Weight	Zn64 Ratio Relative To Virgin Pd (One Sigma)	Iridium Content PPM by Weight	Gold Content PPM by Weight	Pd110/Pd102 Relative to the Ratio Observed in Virgin Pd (One Sigma)
A	50	6.6 (1.6)	4.1	55	1.24 (0.11)
B	121	14.4 (3.2)	0.2	11	1.06 (0.06)
C	58	8.3 (2.1)	3.1	17	1.21 (0.11)
D (Virgin Pd)	8	1.0 (DNA)	0.5	10	1.00 (DNA)

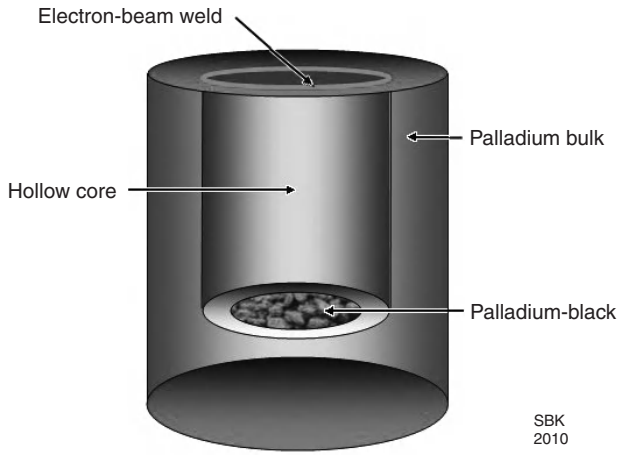

Figure 41.14 Arata-Zhang double-structure palladium cathode.

- 8 times the iridium content by weight from sample A
- 0.4 times (decrease) the iridium content by weight from sample B
- 6 times the iridium content by weight from sample C
- 5.5 times the gold content by weight from sample A
- 0.1 times the gold content by weight from sample B
- 0.7 times the gold content by weight from sample C
- 24% increase in Pd110/Pd102 ratio over virgin palladium from sample A
- 6% increase in Pd110/Pd102 ratio over virgin palladium from sample B
- 21% increase in Pd110/Pd102 ratio over virgin palladium from sample C

Several years later, Passell arranged for further NAA studies on these same samples, analyzing the isotopic ratio anomalies more extensively. He speculated on the nuclear binding energy that would be released as a result of the nuclear products from the LENR transmutations.

> The precise amount of excess heat produced by the cathodes in which the powdered palladium was contained has not yet been made available," Passell wrote. "Arata and Zhang's

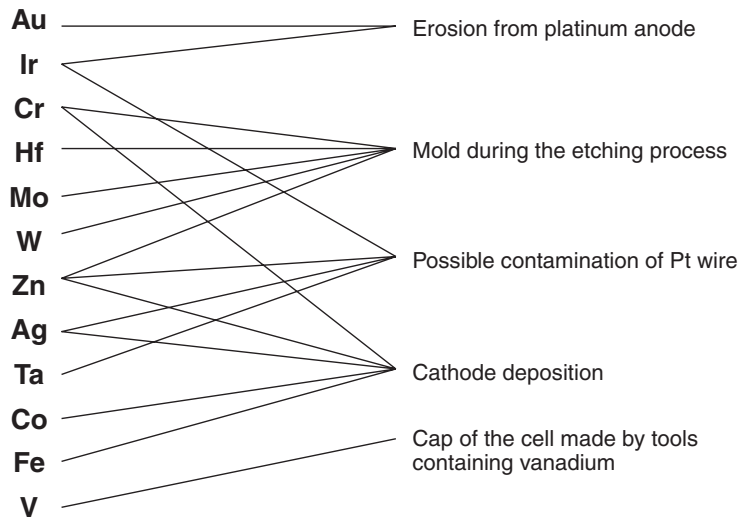

Figure 41.15 Vittorio Violante group's (ENEA-Frascati) explanation of LENR elemental anomalies. *(Source: A. Rosada, E. Santoro, F. Sarto, V. Violante, P. Avino–Impurity measurements by Instrumental Neutron Activation Analysis on Palladium, Nickel and copper thin films, ICCF-15, Rome, Italy, 2009.)*

published work shows data from similar cathodes which produced about 30 to 40 megajoules of excess heat over the most active two-month period of their electrolysis [27]. If one assumes that some nuclear process produced each excess zinc-64 atom at about 10 MeV per atom, that some 12 grams of powdered palladium was contained in each cathode hollow core, and that our sample of 5 to 15 milligrams was a representative sample of the full 12 grams present, then one obtains expected excess heat of 20 megajoules.

41.15 RESISTANCE FROM ADVOCATES OF COLD FUSION HYPOTHESIS

In the first decade of the research, the greatest resistance to the idea of cold fusion came from researchers affiliated with the thermonuclear fusion community. In the second decade, factionalism within the LENR field was far more volatile than any disputes outside the largely isolated field. Certain LENR researchers have attempted to explain away and deny even their own LENR transmutations. Although none of those researchers has admitted it, the reason is obvious: LENR transmutations contradict and disprove the hypothesis of cold fusion, an idea that they fought long and hard to have recognized.

In an experiment reported in 2009, Vittorio Violante of ENEA Frascati attempted to explain that LENR transmutations observed in a "clean room" experiment came from a complex mixture of ad-hoc, contrived sources of error (Fig. 41.15). Violante did not detail how the various contamination scenarios might have occurred [28].

In an experiment presented in 2002 and 2003 with a nickel-hydrogen thin-film system, Violante reported a set of LENR transmutations supported by nuclear activation analysis measurements of isotopic shifts in silver (47.37%) and SIMS measurements of isotopic shifts in copper (1,360%). He reported a threefold increase in Cu65 and a sixfold decrease in Cu63. [29–31] He chose to search for copper because of its chemically unique mass/charge peaks at 63 and 65.

By 2004, Violante had performed a second round of experiments. He replicated the results and observed apparent isotopic shifts with four of the five electrolyzed

Figure 41.16 1990 SPAWAR first-generation cold fusion co-deposition cell (*Courtesy of S.B. Krivit*).

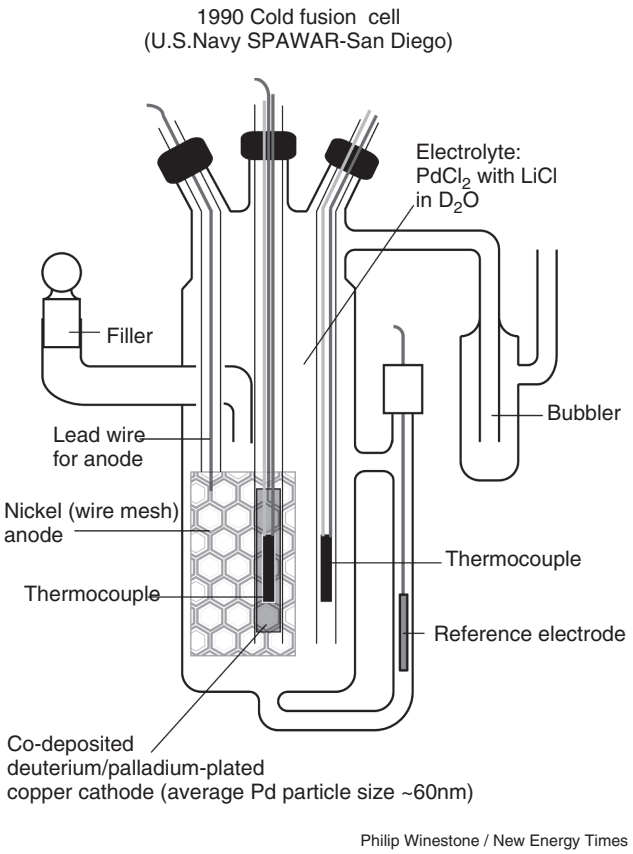

Figure 41.17 Schematic for 1990 SPAWAR first-generation cold fusion co-deposition cell (*image courtesy New Energy Times*).

runs. Five reference films showed no isotopic shifts.[32] In 2006, he began a search for alternative explanations and initially speculated that a Ni58/Li7 compound could have contributed to the 65 m/e peak. [33] In 2009, he denied seeing any evidence of transmutations because, he wrote, the first SIMS instrument he used created an organic compound (C5H5) that gave an erroneous 65 m/e peak. [34]

However, he did not provide any evidence to indicate the quantity of C5H5 versus the quantity of Cu65 that composed the peak. Also, he did not explain why the creation of C5H3 (which he also claimed was created by the SIMS instrument) would lead to a sixfold decrease in the 63 m/e peak. Violante also did not explain why the SIMS instrument did not create C5H5 on the five reference films.

41.16 STATE OF THE ART

The state of the art in LENRs is far from the potential that many participants and observers consider to be possible from this field of research. There are no substantiated practical applications, and the research is generally limited to pure science. The field has been beleaguered by a variety of obstacles: financial, ideological, political, and technical. Nevertheless, all indicators suggest that the field of LENRs could be vitally important to the development of clean, carbon-free sources of energy.

The majority of LENR researchers do not know what causes the nuclear energetic reactions when, partly by chance, they get them to occur. In general, they know what conditions will *not* lead to excess heat and nuclear products. They know the minimum requirements for a successful experiment and, from this, they have been able to identify why the early replication attempts in 1989 failed. The parameter space is extremely large, and they struggle to identify its bounds. The most reliable experiments have not been replications of the Pons-Fleischmann excess-heat experiment but rather other ideas, such as electrolytic co-deposition or gas permeation experiments.

As early as 1989, researchers at SPAWAR Pacific, in San Diego, California, began developing a method of depositing palladium, atom by atom, in an electrolytic solution rather than using a solid palladium cathode, as Pons and Fleischmann had done. Their 1990, first-generation co-deposition cell (Fig. 41.16) reveals intricate custom glassblowing. Figure 41.17 provides a schematic diagram of this cell.

The co-deposition method provided the SPAWAR researchers with an experiment that appears to repeatedly demonstrate production of high-energy alpha particles and perhaps low fluxes of neutrons (See Fig. 41.18). The SPAWAR researchers' understanding of the experiment is limited to the phenomenology; they do not appear to have a clear theoretical direction [35].

The SPAWAR researchers have made great strides in simplifying the cell configuration. Simple modifications to off-the-shelf acrylic boxes (See Figs. 41.19 and 41.20) became their standard base cell in 2007.

The production of heat has been the most frustrating line of research in the field. Hundreds of experiments have demonstrated milliwatts of excess heat. Many of these have been performed with accurate calorimetry, and measures have been taken to eliminate conventional explanations. On rare occasions, experiments have produced tens of watts of heat, at levels many times the input energy. But

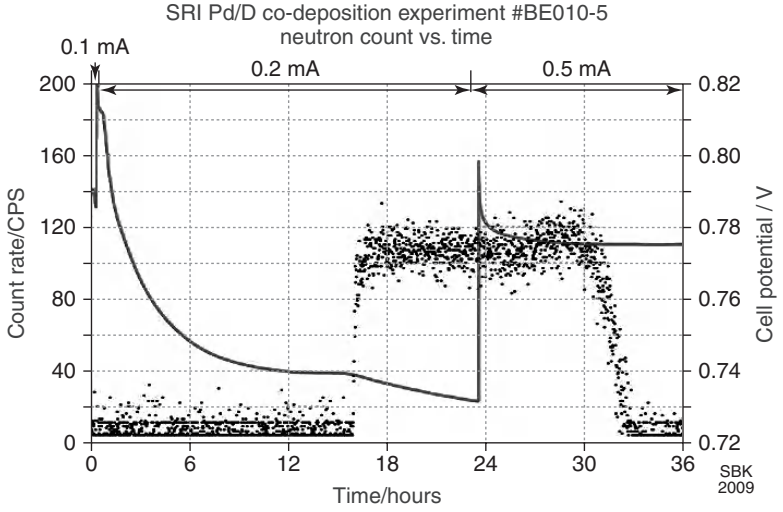

Figure 41.18 SRI International Replication of SPAWAR co-deposition experiment. Neutron 14x greater than background during 14-Hour burst. Measurement by BF_3 ionizing neutron detector placed about 10 cm from operating cell. Drop in cell potential temporally correlated with onset of neutron signal suggests cell heating [36].

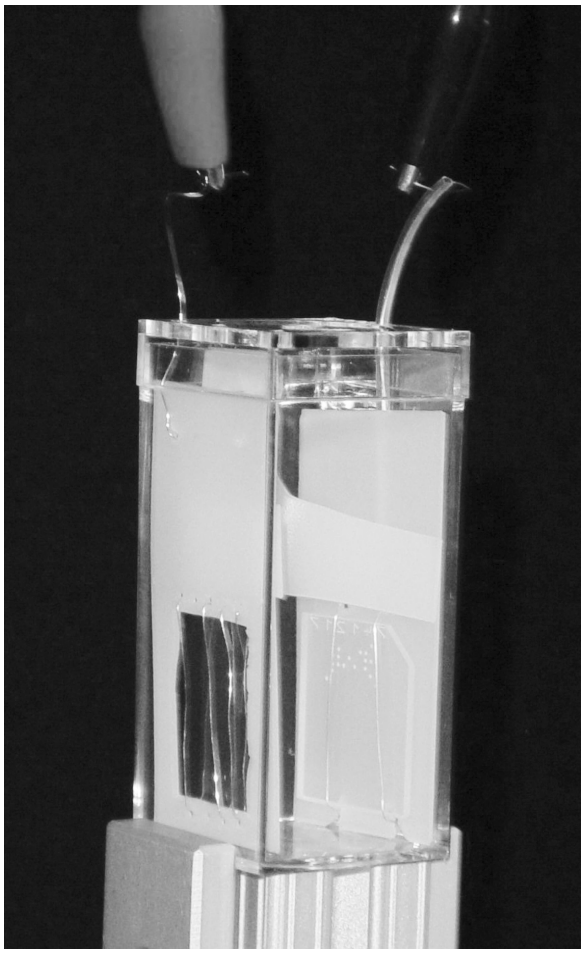

Figure 41.19 2.5-inch-high acrylic LENR co-deposition cell. Anode windings mounted on left polyethylene support, cathode windings on right support, CR-39 (solid-state nuclear track detector) sits under cathode wires (*Courtesy of S.B. Krivit*).

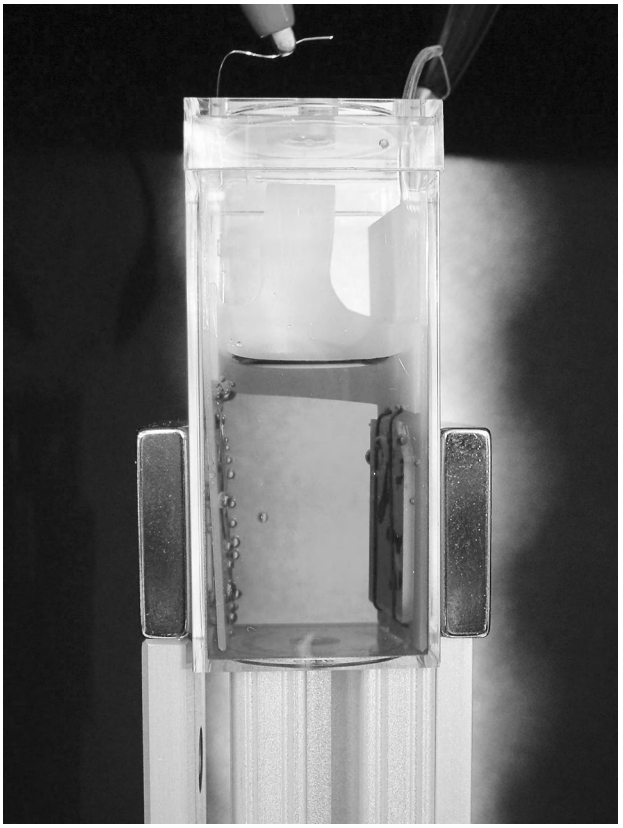

Figure 41.20 LENR co-deposition cell built by Winthrop Williams at University of California, Berkeley (*Courtesy of W. Williams*).

the researchers do not know what specific conditions in these experiments were responsible for such significant results. Some of them think that nanotechnology will bring the required tools and methods to more effectively investigate LENRs. Once the experimentalists understand the mechanisms and develop full control over them, they can begin to consider practical applications.

41.17 NICKEL-HYDROGEN LENR

If made practical, LENRs using hydrogen gas and nickel are far more practical than any kind of electrolytic device using deuterium and palladium, from the perspective of engineering and cost-efficiency.

Many nickel-hydrogen LENR research studies were performed in the 1990s. An excellent review of this work is provided in a 1998 paper by Giuliano Mengoli et al. [37].

One of the most significant sets of Ni–H research was performed by a group led by Francesco Piantelli, of the Department of Physics at the University of Siena, and Sergio Focardi, of the Department of Physics at the University of Bologna. Their group has presented and published a dozen papers on the topic. Whereas electrolytic D/Pd experiments have typically produced scientifically meaningful levels of excess heat, such effects were generally observed only in the milliwatt range. The Piantelli group's Ni–H gas experiments produced excess heat in the tens of watts.

The researchers explain that an anomalous heating effect in the Ni–H cell takes place "when a cell containing a nickel rod is maintained at temperatures above a critical value and is filled with gaseous hydrogen at subatmospheric pressures." The critical value is obtained by a heater in the cell that provides constant input power to initially raise and keep the cell temperature at its working value, about 700 K. When the heat production rises above the equilibrium condition, the authors identify this as the excited state. Because the experiment can run in the excited state for months at a time, the researchers were also able to observe sporadic evidence of both neutrons and gamma rays, which

are generally hard to detect in D/Pd electrolytic LENR systems because those experiment run for much shorter periods.

Whereas excess-heat-producing electrolytic D/Pd experiments typically ran for days before the electrode corroded or the researcher stopped replenishing electrolyte, the Piantelli group hydrogen gas experiments ran continuously in a stable state for months at a time. In November 1998, the group reported two experiments in *Il Nuovo Cimento* [38].

Cell "A" produced 38.9 +/−1.5 watts of heat, and cell "B" produced 23.0 +/−1.3 watts of heat. The cells produced excess power continuously at a slowly increasing rate during that period: cell "A" for 278 days; cell "B" for 319 days. The integrated excess energy was 900 MJ for cell "A" and 600 MJ for cell "B."

41.18 THE PROMISE

Although LENRs do not look like fusion, they hold great promise as a clean nuclear energy source. Theoretical work by Widom and Larsen, which uses collective effects, quantum electrodynamics, the Standard Model, particle physics, condensed matter physics and nuclear physics, suggests that, despite the likelihood that LENRs are explained by weak interactions and neutron capture processes, highly energetic reactions are possible. Their theory claims to explain both deuterium-palladium and nickel-hydrogen systems.

If net-positive, cost-effective energy production can be demonstrated on a small scale, the chances that the effect can be scaled up by additional research and development are great. Other applications, such as the production of neutrons and heavy-element transmutations—if cost-effective—may lead to other, unimagined opportunities.

Two decades of experiments on lab benchtops have proved that, at least at experimental levels, biosafety risks of LENRs are negligible. The prospect of fueling LENRs with common materials, for example ordinary water and certain base metals, is alluring.

All of these characteristics, combined with the ability of researchers to investigate LENRs without large-scale physical installations, could lead the field to potentially explosive growth if the research community develops a better understanding of how to control the phenomena experimentally.

Acknowledgments

The author would like to thank the sponsors of New Energy Institute for their support, the technical reviewers for their time and care, and editors Cynthia Goldstein and Sally Robertson for their assistance.

REFERENCES

1. Cold fusion history, LENR, CMNS Book Index. *New Energy Times*, http://www.newenergytimes.com/v2/books/books.shtml.
2. M. Fleischmann and S. Pons, Electrochemically induced nuclear fusion of deuterium. *Journal of Electroanalytical Chemistry*, April 10, 1989, **261**, 2, Part 1, 301–308. Errata: M. Fleischmann, S.Pons, and M. Hawkins, 1989, **263**, 187–188.
3. G. L. Wendt and C. E. Irion, Experimental attempts to decompose tungsten at high temperatures. *J. Am. Chem. Soc*., 1922, **44**, 9, 1887–1894.
4. F. Paneth and K. Peters, "Über die verwandlung von wasserstoff in helium" *Berichte der Deutschen Chemischen Gesellschaft*, 1926, **59**, 2039–2048.
5. J. R. Huizenga, *Cold Fusion: The Scientific Fiasco of the Century*. University of Rochester Press, Rochester, NY and Boydell & Brewer Inc., 1992.
6. *Cold Fusion Research*, Report of the Energy Research Advisory Board to the United States Department of Energy, DOE/S-0073 DE90 005611, November 1989. http://www.newenergytimes.com/v2/government/DOE1989/contents.htm.
7. S. B. Krivit and N. Winocur, *The Rebirth of Cold Fusion: Real Science, Real Hope, Real Energy*. Pacific Oaks Press, Los Angeles, CA, October 2004.
8. S. B. Krivit, Cold fusion is neither, New Energy Times Special Report, July 30, 2010. http://www.newenergytimes.com/v2/news/2010/35/SR35900outline.shtml.
9. M. Fleischmann, S. Pons, M. W. Anderson, L. J. Li, and M. Hawkins, Calorimetry of the palladium-deuterium-heavy water system,. *Journal of Electroanalytical Chemistry*, July 1990, **287**, 293–351.
10. M. Fleischmann, Background to cold fusion: the genesis of a concept in *Low-Energy Nuclear Reactions Sourcebook*, J. Marwan and S. B. Krivit, eds. American Chemical Society/Oxford University Press, Washington, DC, August 2008.
11. N. J. C. Packham, K. L. Wolf, J. C. Wass, R. C. Kainthla, and J. O'M. Bockris, Production of tritium from D2O electrolysis at a palladium cathode *Journal of Electroanalytical Chemistry*, 1989, **289**, 451.
12. P. K. Iyengar, Cold fusion results in the Bhabha Atomic Research Center (BARC) experiments, in *Proceedings of the Fifth International Conference on Emerging Nuclear Energy Systems*, Karlsruhe, Germany, World Scientific, July 3–6, 1989, 29–33.
13. T. N. Claytor, D. D. Jackson, and D. G. Tuggle, *Tritium Production from a Low Voltage Deuterium Discharge on Palladium and Other Metals*. Los Alamos National Laboratory, LAUR#95-2687, August 9, 2002.
14. M. Srinivasan, M., *Observation of Neutrons and Tritium in a Wide Variety of LENR Configurations: BARC Results Revisited*. 237th American Chemical Society National Meeting March, 2009, Salt Lake City, UT.

15. S. B. Krivit, When nuclear is not enough: A tangled tale of two experiments, *New Energy Times*, July 30, 2010, http://newenergytimes.com/v2/news/2010/35/SR35903tangledtale.shtml.
16. S. B. Krivit, Editorial: Progress is this way, *New Energy Times*, Jan. 31, 2011, http://newenergytimes.com/v2/news/2011/36/3601editorial.shtml.
17. A. Widom and L. Larsen, Ultra low momentum neutron catalyzed nuclear reactions on metallic hydride surfaces. *European Physical Journal C–Particles and Fields*, 2006, **46**, 1, 107.
18. P. K. Iyengar and M. Srinivasan, eds, *BARC Studies in Cold Fusion Government of India Atomic Energy Commission*, April -September 1989, December 1989.
19. A. G. Lipson, A. S. Roussetski, G. H. Miley, and E. I. Saunin,, *Phenomenon of an Energetic Charged Particle Emission from Hydrogen/Deuterium Loaded Metals*. Tenth International Conference on Cold Fusion, Cambridge, MA, 2003.
20. B. F. Bush, J. J. Lagowski, M. M. Miles, and G. S. Ostrom, Helium production during the electrolysis of D2O in cold fusion experiments. *J. Electroanal. Chem*., 1991, **304**, 271–278.
21. S. B. Krivit, When nuclear is not enough: a tangled tale of two experiments. *New Energy Times*, July 30, 2010, 35.
22. A. Lipson, F. Lyakhov, A. Roussetski, T. Akimoto, N. Asami, R. Shimada, S. Miyashita, and A. Takahashi, Evidence for low-intensity D-D reaction as a result of exothermic deuterium desorption from Au/Pd/PdO:D heterostructure. *Fusion Science and Technology*, 2000, **38**, 238–252.
23. P. A. Mosier-Boss, J. Y. Dea, L. P. G. Forsley, M. S. Morey, J. R. Tinsley, J. P. Hurley, and F. E. Gordon, Comparison of Pd/D co-deposition and DT neutron-generated triple tracks observed in CR-39 detectors. *European Physical Journal, Applied Physics*, July 7, 2010, **51**, 2, (Online).
24. Y. Iwamura, M. Sakano, and T. Itoh, Elemental analysis of Pd complexes: effects of D2 gas permeation. *Japanese Journal of Applied Physics A*, 2002, **41**, 4642–4648.
25. B. F. Bush and J. J. Lagowski, *Trace Elements Added to Palladium by Electrolysis in Heavy Water*, Machiels, A., and Passell, T.O., project managers, EPRI TP-108743, November 1999.
26. T. O. Passell and R. George, Trace elements added to palladium by exposure to gaseous deuterium. *Proceedings of the Eighth International Conference on Cold Fusion*, *Italian Physical Society*, Lerici (La Spezia), Italy, 2000.
27. Y. Arata and Y. Zhang, Achievement of solid-state plasma fusion ("cold fusion"), *Proceedings of the Sixth International Conference on Cold Fusion*, Toya, Japan, Vol. 1, 129–135, October 13–18, 1996.
28. A. Rosada, E. Santoro, F. Sarto, V. Violante, and P. Avino, Impurity measurements by instrumental neutron activation analysis on palladium, *Nickel and Copper Thin Films*, ICCF-15, Rome, Italy, 2009.
29. V. Violante, P. Tripodi, D. Di Gioacchino, R. Borelli, L. Bettinali, E. Santoro, A. Rosada, F. Sarto, A. Pizzuto, M. McKubre, and F. Tanzella, X-ray emission during electrolysis of light water on palladium and nickel thin films, *Procedings of the Ninth International Conference On Cold Fusion*, Beijing, 2003.
30. V. Violante, E. Castagna, C. Sibilia S., and Paoloni, F. Sarto, Analysis of ni-hydride thin film after surface plasmons generation by laser technique, *Proceedings of the Tenth International Conference on Cold Fusion*, Cambridge, MA, 2003.
31. V. Violante, M. L. Apicella, L. Capobianco, F. Sarto, A. Rosada, E. Santoro, M. Mckubre, F. Tanzella, and C. Sibilia, Search for nuclear ashes in electrochemical experiments, *Proceedings of the Tenth International Conference on Cold Fusion*. Cambridge, MA, 2003.
32. M. Apicella, E. Castagna, G. Hubler, M. McKubre, F. Sarto Sarto, C. Sibilia, A. Rosada, E. Santoro, F. Tanzella, and V. Violante, Progress on the study of isotopic composition in metallic thin films undergone to electrochemical loading of hydrogen, *Eleventh International Conference on Cold Fusion*, Marseilles, France, 2004.
33. M. Apicella, E. Castagna, G. Hubler, M. McKubre, F. Sarto Sarto, C. Sibilia, A. Rosada, E. Santoro, F. Tanzella, and V. Violante, Progress on the study of isotopic composition in metallic thin films undergone to electrochemical loading of hydrogen, *Proceedings of the Twelfth International Conference on Cold Fusion*, 2006.
34. M. L. Apicella, E. Castagna, S. Lecci, M. Sansovini, F. Sarto, and V. Violante, Mass spectrometry: critical aspects related to the particles detection in the condensed matter nuclear science, Fifteenth International Conference on Cold Fusion, Rome, Italy, 2009.
35. P. A. Mosier-Boss, S. Szpak, F. E. Gordon, and L. P. G. Forsley, Characterization of tracks in CR-39 detectors obtained as a result of Pd/D co-deposition. *Eur. Phys. J. Appl. Phys*. April 17, 2009, **46**, 30901, DOI: 10.1051/epjap/2009067, April 17, 2009.
36. F. Tanzella, B. P. Earle, and M. C. H. McKubre, The search for nuclear particles in the Pd-D co-deposition experiment. *Eighth International Workshop on Anomalies in Hydrogen/Deuterium Loaded Metals*, Catania, Italy, October 13–18, 2007.
37. G. Mengoli, M. Bernardini, C. Manducchi, and G. Zannoni, Anomalous heat effects correlated with electrochemical hydriding of nickel, *Il Nuovo Cimento*, **20D**, 1998, 331–352.
38. S. Focardi, V. Gabbani, V. Montalbano, F. Piantelli, and S. Veronesi, Large excess heat production in Ni–H systems, *Nuovo Cimento*, **111A**, 1998, 1233–1242.

42

LOW-ENERGY NUCLEAR REACTIONS: A THREE-STAGE HISTORICAL PERSPECTIVE

LEONID I. URUTSKOEV

Moscow State University of Printing Arts and State Atomic Energy Corporation "Rosatom", Moscow, Russia

First, it is crucial to note that the term "cold nuclear fusion" seems highly inappropriate. A more correct premise, and inquiry, is this: *Are controlled low-energy nuclear reactions possible at all*? This, indeed, calls for an analysis of the history of this scientific problem.

There are three stages to review. The first is during the mid 1920s when a number of publications [1–5] appeared in the leading scientific journals in which authors asserted that some chemical elements transformed into others when strong electrical current was passed through condensed matter (including metallic wire [1], molten salts [2], and vapor of quicksilver [3, 4]).

Most notable of the work from this period is that by two American chemists, Clarence E. Irion and Gerald L. Wendt [1]. The authors were prompted then by several obvious facts. Accordingly, they established through (optical) spectral analysis of light that their spectra did not contain any typical optical lines in the heavy element range. The surface temperature of the Sun, found to be about 6000 K (Kelvin), had been already measured by that time through the same type of optical measurements. However, on the other hand, as shown by J. Anderson's experiments [6], discharging a condenser battery into a small wire results in the formation of a 20,000 K temperature plasma.

Based on those facts, the American scientists surmised: "What if absence of the heavy element spectral lines in the starlight emanation can be explained by the fact that heavy elements become unstable when subjected to 6000 K temperature?" They wondered if they could take a thin heavy element wire, that is, tungsten, transmit heavy electrical current through it, having heated it up to 20,000 K, and watch "decomposition of tungsten atoms," as they called it at the time.

The idea itself was indeed great, and it's not at all important that it was really wrong. In those times, there was no quantum mechanics, no electrodynamics, no neutrons, no neutrinos, no strong or weak nuclear interactions . . . not even nuclear physics as a science. There was not even a simple oscilloscope. But Irion and Wendt were enthusiastic enough, and they took up the case. They dared to carry out a fantastic experiment, in a quite peculiar but thorough way, using such seemingly simple means that even now, 90 years later, their article on the subject invokes sincere pleasure and deep respect for their professional competence.

Leaving out unnecessary description of superfluous details, let us get right down to the matter of their experiment itself. Approximately one cubic cm of gas (under normal conditions, of course) was formed from the electro-explosion of a thin tungsten wire. Through optical spectroscopy, the experimenters identified this as helium. One more relevant factor is worth mentioning here: No typical spectral hydrogen lines were registered when analyzing the optical spectrum of the gas obtained. This is particularly significant because it shows that the experiment was "clean." If not, optical lines of atmospheric hydrogen, absorbed on the surface of the explosion chamber, would have inevitably appeared.

Thus, it can be quite certainly asserted that in 1922, when experimenting with thin tungsten wire, Irion and Wendt registered a phenomenon that, using language of our time, could be called *induced cluster radioactivity*. It's also worth reminding readers that one cubic cm of gas (under normal

Nuclear Energy Encyclopedia: Science, Technology, and Applications, First Edition (Wiley Series On Energy).
Edited by Steven B. Krivit, Jay H. Lehr, and Thomas B. Kingery.

conditions) contains about 10^{19} particles, meaning that the resulting effect is indeed of macroscopic nature.

Feeling confident of the experiment's invalidity, Sir Ernest Rutherford, a pioneer of modern physics, responded quite negatively to the article by Irion and Wendt in *Nature*. The scholarly public naturally followed and believed Professor Rutherford rather than the two unknown chemists.

Later, in the mid-1920s, well-known scholars (F. Goldschnidt, A. Smits, A. Karssen, H. Nagaoka [2–5])—quite independently of each other—spoke about transforming heavy elements into lighter ones (lead into mercury and mercury into gold) under powerful electrical discharge through melting the elements, solutions, or through a vapor of the elements. However, as shown by quantum mechanics, which was already well developed by that time, there is great difference between atomic and nuclear energy scales and as a consequence, all these experimental results were dismissed as mere artifacts without verification. This terminated the research in this direction as it appeared to have been discredited.

The second stage of growing interest in the "cold nuclear fusion" problem was initiated provisionally in 1989 through the work reported by Martin Fleishmann and Stanley Pons [7]. Their idea was based on the fact that palladium easily adsorbs hydrogen, though this is nothing new for either physicists or chemists. Accordingly, a palladium sample can be rather easily loaded with hydrogen by 60-80%. This means 6 to 8 atoms of hydrogen per 10 atoms of the palladium matrix. Incidentally, this characteristic is typical (much less obvious, though) of a number of other metals in the transitional group, such as titanium, for example. As noted by Fleishmann and Pons, electrolyzing in heavy water, where palladium is the electrode (cathode), the deuterium atoms are adsorbed by palladium. Their prediction was that, under a sufficiently high degree of saturation of the palladium matrix with deuterium atoms, the deuterium nuclei, being so close to each other, would interact in a nuclear way to form helium. Such a phenomenon in physics is called fusion, a process that takes place in stars under high temperatures accompanied with significant energy release. Fleishmann and Pons tried to carry out the process under "room temperature" conditions, which was later reflected in the name of this quite hypothetical occurrence. Qualitatively, quantum mechanics does not forbid such low temperature fusion, but its probability is negligibly small. Nevertheless, it was exactly on the basis of this idea that they embarked on their experiment.

By no means was the initial intuitive idea of Fleischmann and Pons' experiment decisively wrong. It will suffice to remind readers, for example, of the discovery of the phenomenon of natural radioactivity. This resulted from Antoine Henri Becquerel's testing of Henri Poicare's wrong hypothesis, not to mention the great discoveries in physics made through the adventurous spirit of creative experimentalists of the early 1900s.

Somewhat haphazardly, Fleischmann and Pons guessed at the explanation as nuclear fusion reactions. Complaints from skeptics in 1989 centered around the concern that Fleischmann and Pons were not measuring neutrons correctly. Their critics gave little credibility to Fleischmann and Pons' measurements of excess heat. Most problematic of all was that Fleischmann and Pons could not consistently repeat their experiment at the time of announcement. Thus, having poor (at best) measurements of nuclear phenomena, the authors—at the behest of the University of Utah—went forward with the infamous press conference. As to the "fusion" term, we tend to think it erroneous. Rather, what Fleishmann and Pons observed is just a new class of nuclear reactions that is yet to be studied and learned.

Thus, as to its cogency and professionalism, the scientific level of work of Fleishmann and Pons, however paradoxically it may seem, is much lower than that from the early 20th century as mentioned above. Therefore, there is nothing surprising in the practically immediate refutations of the Fleishmann-Pons work that, accordingly, caused great disappointment in the respective academic environment. Nevertheless, due to simplicity of the conclusions made by Fleishmann and Pons, hundreds of inquisitive people (students, retirees, and even university professors) believed in this idea and started experimenting with heavy-water electrolyses. The fact that so many people began to explore this work is particularly meritorious. The very important results of Fleischmann and Pons reopened the doors to this work.

As shown during the last two decades, the main typical features of the phenomenon include low-energy transformation of chemical elements' nuclei and excess (in relation to the electrical energy contributed by electrolysis) heat release. It was also discovered, through significant contributions by Russian researchers, that low energy nuclei transformation can be observed not only under electrolysis but also under glow discharge in the presence of deuterium [8], titanium wire explosion in liquid [9], and other electromagnetic processes in condensed matter [10]. The common component in all these experiments is the electrical current passed through the non-equilibrium weakly ionized plasma, although certain specific conditions must be present when performing any low-energy nuclear reaction research.

The range of experiments leading to the above-referenced nuclear reactions is much broader than just electrolysis in heavy water and the production of new light elements such as tritium and helium. This realization resulted in the changing of the very name of this scientific (or *pseudo-scientific*, as some people have often called it) pursuit: from "cold fusion" to "low energy nuclear reactions (LENR)." With LENRs, no significant fluxes of free neutrons or residual radioactivity have yet been registered as expected from thermonuclear fusion reactions. This means

that there are no predominant strong interactions in the LENR mechanism. Another obvious feature of LENRs is that they are collective. However, collective interactions are typical for plasma physics [11] but not yet well known in nuclear physics.

Some of the more observant LENR researchers noticed that when experimenting with heavy-water electrolysis, even after the electrical voltage was cut, something was still going on in the working cell, and significant levels of heat continued to be released from it. As a result of this self-heating phenomenon, some researchers looked for tracks of nuclear radiation.

Initially, searches for neutrons and gamma-rays were unsuccessful, but later, particularly through the nuclear emulsion methods [12], and the use of CR-39 solid-state nuclear track detectors [13], it became possible to register and repeatedly reproduce certain strange traces. Initially, the researchers tried to ascribe them to alpha particles and later also to hypothetical heavy particles and hypothetical bi-neutrons as other possibilities.

We paid particular attention in our work [9] to strange irradiation interacting with the magnetic field. This research supported the assumption that unusual tracks on the nuclear emulsions were somehow connected with hypothetic particles called *magnetic monopoles*, whose existence had been predicted by theorists long ago. The distinctive feature of the phenomenon is intermittence of these tracks and their abundant nature; they are most often formed on the detector surface. As of today, there is no consensus on this subject yet, but the probability of its reality remains. The knowledge so far is based on limited and rather obscure information, and this limits our ability to understand the physical mechanism of low energy nuclear reactions.

Due to the growing number of recent experimental publications on LENR, intuitive analysts, including J. Loshak [18] (pupil of Louis de Broglie), H. Stumpf [19] (pupil of V. Heisenberg), and many other talented scholars, attempted to theoretically explain the phenomena observed. These publications are the beginning of the third stage of LENR.

The experimentalists observe macroscopic (from the physics viewpoint) transformations of nuclei under low energy. They see that a great number of nuclei interact at or near room temperature, apparently overcoming the Coulomb barrier. This is inexplicable, so far, by classical electrodynamics, also, the macroscopic nature of the effect is inexplicable by quantum mechanics. Classical electrodynamics cannot explain the effects relative to the Coulomb barrier. Quantum mechanics can explain the tunneling through the Coulomb barrier, but such theoretical effect is very microscopic and cannot explain LENR. Quantum electrodynamics cannot explain the macroscopic nature of the effect either because it deals only with small allowances. The value of the *Lamb shift* or that of the anomalous electron magnetic moment can be quite elegantly computed (with great precision, by the way) through quantum electrodynamics methods, within quantum field theory. However, quantum electrodynamics is absolutely hopeless in trying to explain these very macroscopic collective phenomena. In the case of LENR, we have a situation with the macroscopic phenomena that is taking place in condensed matter, under conditions of non-equilibrium plasma.

Thus, we now seem to face a rather paradoxical situation in present-day physics: On the one hand, the said LENR effect is experimentally observed but, on the other hand, the existing hypothetical approaches do not help us much to understand its physical mechanism. So there remains (as often happens in the history of physics) the well-known phenomenological approach. The main questions to be answered first can be formulated as follows: *If LENRs are possible, then nuclei of what particular elements can take part in the process? What new elements can such reactions produce and what will the isotopic distribution of the newly formed elements be*?

The first step in this direction was made in works of Roussetski et al. [14] and Kuznetsov et al. [15]. However, the phenomenological models and principles of low-energy elemental transformation, based on experimental observations, were described with greater consistency and detail by D. Filipov in [15]. As already mentioned above, no high-flux free neutrons or residual radioactivity are observed in LENR. Accordingly, this fact seems to be worth trusting since it is emphasized practically by all respective experimental groups. To paraphrase the great Russian writer Leo Tolstoy, "*everybody is mistaken in his own way but the true answer is always one*." In other words, in our view, when explaining the LENR physical mechanisms, we can rely only on weak nuclear interactions. Or, to be more exact, a still unknown but exceptionally wide-range branch of such interactions. Another possibility is to complement existing nuclear physics with some other, principally new class of nuclear interactions. In [15], the first option was chosen for taking the phenomenological model under consideration.

Underlying the Filipov model of LENR are four conservation laws: energy, baryon, lepton, and electrical charges. This model surmises all nuclear processes to run only due to weak interactions (β^--decay and k-electron capture). Furthermore, this model sets up parameters for certain atomic isotopes of the chemical elements under consideration enabling interaction through a computerized LENR program to extrapolate the nuclear reaction products. Such a model became possible thanks to personal computers and the quantity of the Mendeleyev Table stable isotopes being final and not overly large. Due to this, availability of modern PCs allows for screening all the respective options within reasonable spans of time.

Subsequently, the results of computer-modeling computations are quite comparable with experimental results. Accordingly, with computer -modeling, in the plasma mixture of titanium and vanadium atoms that occurs in our experiments from electrical explosion of titanium foil in a solution of vanadium salt, Fe57 isotope is expected to be formed. Fe57 isotope is rather rare, and its content in the natural iron atomic mixture comprises just about 2%. Therefore, it is easy to diagnose it by contemporary experimental methods. Such an experiment has been carried out and the excess Fe57 isotope (about 6%) was confidently registered. The statistical probability of the experimental result as a random coincidence, which can be easily determined, turns out to be negligibly small. While helping us to better understand the physical mechanism of LENR, this fact nevertheless does confirm that while not violating the laws of conservation, such reactions somehow only contradict the probability laws.

This naturally calls for a question: Are LENRs some "exotic" phenomenon or widespread but yet, so far, hidden phenomena? Or are LENRs phenomena that have been hidden in plain sight for many years? Although no definite answer has yet been found, more and more scientific publications keep asserting that LENRs play a significant part in the life activity of biological objects [16, 17]. We normally consider the biological cell growth process (that is, greater quantity of atoms in the cell) to be the result of cellular intake of different chemical elements from the outside necessary for cell construction and their redistribution *in situ*.

However, it is quite possible to assume that this growth can be connected with outside intake of only certain chemical elements (e.g., oxygen, carbon, nitrogen, hydrogen + perhaps something else) while the formation of all other necessary chemical elements rather, is caused by the LENR processes in the very cell. These suggest, in other words, that LENR may be a basic underlying aspect of living matter and the role of the respective chemical processes may come down to the control of nuclear processes. The above assumption may seem something like fantasy but should it turn out to be true then the LENR physical mechanism can be assumed to be of very delicate and fine nature, since biological objects are exceptionally sensitive to temperature ranges. In any case, we are certainly quite far from a true understanding of the role of LENR in biological life systems.

In view of the macroscopic nature of LENR effects, some gross and simple explanation is to be sought even if older concepts in the cornerstone principles of physics must be changed. Because the body of research is not at all irrefutable, evidence is needed to guide researchers as to which of the stones is to be, very carefully, turned over. It is worthwhile to consider how to pursue such an endeavor that, if successful, might expand the body of scientific knowledge while at the same time, retain the existing foundation of science and build on it.

At the moment, no one knows how fundamental this expansion may be. Thus, the logical question: Is there any need or value to disrupt the foundation? Just one single instance of macroscopic nuclear transformation may or may not provide the chance to understand nature in a radically novel way. Let us not forget a well-known episode from the history of physics: Were it not for the experimental banding of optical spectra, no one would have paid attention to the "nonsense" by Max Planck and Albert Einstein as regards light quantum. One reliable experimental fact turned out to be enough to give a start to a new science—quantum mechanics.

REFERENCES

1. G. L. Wendt and C. E. Irion, Experimental attempts to decompose tungsten at high temperatures, //*Amer. Chem. Soc*., 1922, **44**, 1887.
2. A. Smits and A. Karssen, Vorläufige Mitteilung über einen Zerfall des Bleiatoms, *Naturwiss*, 1925, **13**, 699.
3. H. Nagaoka, Preliminary note on the transmutation of mercury into gold, *Nature*, 1925, **116**, 95; Zuschriften und vorläufige Mitteilungen, *Naturwiss*, 1925, **13**, 682.
4. E. Tiede, A. Stammreich, and F. Goldschnidt, Zur Frage der Bildung von Gold aus Quecksilber, *Naturwiss*, 1925, **13**, 745.
5. A. Miethe and H. Stammreich, Der Zerfall des Quecksilberatoms, *Naturwiss*, 1924, **12**, 597.
6. J. Anderson, *Astrophis. J*., 1920, **51**, 37.
7. M. Fleishmann and S. Pons, Electrochemically induced nuclear fusion of deuterium, *J. Electroanal. Chem*., 1989, **261**, 301.
8. A. B. Karabut, Y. R. Kucherov, and I. B. Savvatimova, Nuclear product ratio for glow discharge in deuterium, *Phys. Letters, A*, 1992, **170**, 265.
9. L. I. Urutskoev, V. I. Liksanov, and V. G. Cinoev, Experimental detection of "strange" radiation and transformation of chemical elements, *Applied Physics*, 2000, **4**, 83 [in Russian].
10. V. F. Balakirev and V. V. Krymskii, *Transformation of Chemical Elements*. Ekatirenburg publishing, 2003. [in Russian].
11. B. B. Kadomcev, *Collective Phenomena in Plasma*. Nauka, 1988 [in Russian].
12. L. I. Urutskoev, Review of experimental results on low-energy transformation of nucleus, *Ann. Fond. L. de Broglie*, 2004, **29**, 1149; D. Priem, G. Racineux, G. Lochak, G. Daviau, D. Fargue, M. Karatchentcheff, and H. Lehn, Explosion électrique d'un fil de titane dans de l'eau en milieu confiné, *Ann. Fond. L. de Broglie*, 2008, **33**, 129.
13. A. S. Roussetski, *CR-39 Track Detectors in Cold Fusion Experiments*, Pub. in 11-IC CMNC, Marseille, France, 2004.
14. V. D. Kuznetsov, G. V. Mishinsky, F. M. Penkov, V. I. Arbuzov, and V. I. Zhemenik, Low energy transmutation of atomic nuclei of chemical elements, *Ann. Fond. L. de Broglie*, 2003, **28**, 173.

15. L. I. Urutskoev and D. V. Filipov, On the possibility of nuclear transformation in low-temperature plasma from the viewpoint of conservation laws, *Applied Physics*, 2004, **2**, 30. [in Russian].
16. C. L. Kevran, *Biological Transmutations*. Happiness Press, USU (Magalia, California), 1998.
17. V. I. Vysotskii and A. A. Kornilova, *Nuclear Fusion and Transsmutation of Isotops in Biological Systems*. Moscow, Mir, 2003 [in two languages, Russian and English]
18. G. Loshak, The equation of a light leptonic magnetic monopole and its experimental aspects, *Z. Naturforschung*, 2007, **62a**, 231.
19. H. Stumpf, Change of electroweak nuclear reaction rates by CP- and isospin symmetry breaking—A model calculation, *Z. Naturforschung*, 2006, **61a**, 439.

43

LOW-ENERGY NUCLEAR REACTIONS: TRANSMUTATIONS

MAHADEVA SRINIVASAN[1], GEORGE MILEY[2] AND EDMUND STORMS[3]

[1]*Bhabha Atomic Research Centre (Retired), Chennai, TN, India*
[2]*University of Illinois at Urbana-Champaign, Fusion Studies Laboratory, Urbana, IL, USA*
[3]*Kiva Labs, Santa Fe, NM, USA*

43.1 INTRODUCTION

This chapter describes different aspects of low-energy nuclear reactions (LENR), which investigate the occurrence of various types of nuclear reactions in certain "host" metals such as palladium, titanium, nickel, etc when they are "loaded" or "charged" with deuterium (or hydrogen) to form the corresponding metallic deuterides (or hydrides).

Deuterium, a heavier isotope of hydrogen, is present in natural waters in minute quantities in the proportion of one deuterium atom to 6000 atoms of hydrogen. The nucleus of the deuterium atom is termed deuteron and is composed of a proton and a neutron. The chemical molecule composed of two atoms of deuterium and one of oxygen is called "heavy water," similar to light water, which is primarily made of hydrogen and oxygen. Heavy water (and hence deuterium) is available plentifully in natural water bodies such as oceans, rivers, and lakes, and indeed there are industrial-level production plants in many countries that produce heavy water commercially in quantities of several tens of tons per annum, by separating it out from ordinary water. (Heavy water is used as a "neutron moderator" in the type of nuclear fission reactor developed originally in Canada known as the CANDU reactor.)

Ever since the announcement on March 23, 1989, by Martin Fleischmann and Stanley Pons of the discovery of the phenomenon that initially was called "cold fusion" but later more appropriately described as low-energy nuclear reactions (LENR), physicists have been speculating on the nature of the anomalous nuclear reactions that appear to be taking place in the near surface regions of deuterated metals and that often generate significant amounts of excess heat. Sometimes such devices, which produce more energy than what they consume, are referred to as "over unity systems."

It has by now been confirmed that in excess-heat-producing LENR experiments a proportionate quantity of helium gas is released. Evidence accumulated over the last two decades has revealed that at times when the right experimental conditions are met, helium or at times low fluxes of sporadic emission of neutrons and also a radioactive isotope of hydrogen known as tritium (in whose nucleus there are two neutrons attached to a proton) are generated. As well, in other carefully conducted experiments, energetic charged particles such as alpha particles (which are basically the nuclei of helium atoms stripped of their two orbiting electrons) and protons have also been detected.

Thus, the extensive experimental evidence accumulated over the last two decades has led to the conclusion that when metals such as palladium, titanium, nickel, or others are loaded with deuterium to a sufficient degree (meaning high deuterium to metal atom ratios) and these deuterated metals are triggered appropriately, nuclear reactions take place involving the deuterons, catalyzed by the special lattice structure of the host metal. In all these inter-deuteron nuclear reactions, the host metal appears to serve primarily as a facilitating agent, witnessing the nuclear reactions between the deuterons but not directly taking part in it.

Nuclear Energy Encyclopedia: Science, Technology, and Applications, First Edition (Wiley Series On Energy).
Edited by Steven B. Krivit, Jay H. Lehr, and Thomas B. Kingery.

Viewed from the perspective of the generally accepted understanding of nuclear physics, the occurrence of nuclear fusion reactions between a pair of deuterons at room temperatures as described above would be considered "impossible." The basic issue is the strong repulsion between two positively charged deuterons referred to as the "Coulomb barrier," which has to be overcome before a nuclear reaction can take place. Theoreticians are racking their brains to explain in what manner the electronic properties and the geometrical arrangement of the ordered atomic lattice of the host metal and the possible presence of impurity atoms and/or lattice defect/vacancy sites could be playing an unexpectedly favorable role in enabling nuclear reactions to take place between deuterons embedded in the matrix of the atomic lattice.

Under these circumstances any suggestion or speculation of the possible occurrence of nuclear reactions between the deuterons and the nuclei of the host metal such as palladium, titanium, or nickel (or others), resulting in the transformation of the host metal nucleus would be considered as totally unthinkable! This is because the magnitude of the repulsive Coulomb barrier between deuterons and the nucleus of the host metal atom is enormously larger than that between a pair of deuterons.

Yet there were indeed some researchers who, right from day one of the "cold fusion" saga, wondered whether such "magical" nuclear reactions might be occurring in deuterated metallic solids and devised experiments in quest of evidence for them. For if the deuteron could invade the nucleus of the host metal atom in simple laboratory experiments (of the type described later on in this chapter) and succeed in altering the nucleonic composition of the host metal nucleus, resulting in its isotopic composition changing or transmuting its elemental nature, then it would imply that the age-old claims of alchemy have been effectively validated, and it would have to be admitted that nuclear science is witnessing a silent revolution, with deep scientific implications.

However, since the stakes are so high, before reaching such an extraordinary conclusion, *the phenomenon would have to be unequivocally confirmed to be true, meeting the highest standards of scientific rigor and scrutiny*. In this chapter we review the ongoing and fascinating quest for evidence of occurrence of nuclear transmutation reactions in simple experimental configurations.

Throughout the last 21 years, researchers have used an immensely broad variety of experimental and diagnostic approaches to seek and measure elemental and isotopic anomalies in LENR experiments. As a result of this variety, it is not yet practical to perform a full synthesis of the collective results. This chapter will instead provide the reader with an overview of some of the highlights of the work.

43.2 FIRST REPORTS OF OBSERVATION OF Pd ISOTOPIC ANOMALIES

The first reports of the possible occurrence of nuclear reactions involving a host metal nucleus was discussed as early as October 1989 at the NSF/EPRI Workshop on Anomalous Effects on Deuterated Materials held at Washington, DC. Rolison and O'Grady of the U.S. Naval Research Laboratory presented results of their mass spectrometric measurements, which hinted at the possibility of changes having taken place in the isotopic composition of the Pd in samples taken from near surface layers of Pd cathodes electrolyzed in D_2O [1].

The atomic number of Pd is 46 and its natural isotopic abundance is Pd^{102} (1.02%), Pd^{104} (11.14%), Pd^{105} (22.33%), Pd^{106} (27.33%), Pd^{108} (26.46%), Pd^{110} (11.72%). Rolison and O'Grady reported that time-of-flight secondary ion mass spectrometry (TOF-SIMS) measurements had indicated that samples from two D_2O electrolyzed Pd cathodes had exhibited an increase of about 20% in the intensity of the $(m/z) = 106$ peak with a corresponding decrement in $(m/z) = 105$ peak intensity. Note that Pd^{105} is the only natural isotope of Pd which has an odd number of neutrons, namely 59, in its nucleus. The pre-electrolysis control Pd sample and H_2O electrolyzed "control" sample showed only natural Pd isotopic composition. This result elicited considerable excitement at the meeting as it implied a direct neutron transfer reaction between a deuteron and a Pd^{105} nucleus.

However experts in mass spectrometric measurements were skeptic and cautioned that there could be experimental artifacts caused by molecular ions having an (m/z) close to 106 giving rise to false peaks. At the March 1990 ICCF 1 meeting held at Salt Lake City five months later, the authors did concede there might have been trace levels of ZrO on the Pd electrode as a surface contaminant in the LiOD experiments but emphasized that the Li_2SO_4 electrolyzed samples that did not have this impurity interference still indicated isotopic shifts near the expected (m/z) region. This result, the authors asserted [2, 3], could not be dismissed away as an artifact, but doubts still persisted in the minds of peers. The original authors too did not persist with their claims since they too could not replicate the results in subsequent measurements.

The Rolison–O'Grady exploratory work however played an important role in highlighting the challenges involved in carrying out such transmutation measurements. It is obvious that the quantity of new isotopes or new elements produced in LENR experiments would be in such low concentrations that skeptics would always dismiss the results as impurities possibly deposited on the electrode from the electrolytic solution or migrated to the surface of the cathode from the interior layers of the bulk cathode material, accumulating at selected hot spots on the surface.

Interestingly, it has also been reported that nuclear reactions seem to be taking place even when no host metal is present at all, as in the so-called carbon arc experiments or in the case of the phenomenon referred to as biological transmutations, which are both discussed later in this chapter. While reading this chapter, it is therefore advisable to be mindful of the fact that we are treading a very new and unexplored area of nuclear science.

As the story of the possible occurrence of nuclear transmutations in the LENR field unfolded over the years, periodic status reviews were carried out by Miley [4, 5, 6]. Also, Storms had painstakingly collected and compiled in tabular form (reproduced as Appendix A), for inclusion in his 2007 book titled *The Science of Low Energy Nuclear Reaction* [7] a large number of experimental reports on the occurrence of transmutation reactions. The present authors have taken advantage of these prior review papers and compilations while preparing this updated overview.

43.3 MILEY-PATTERSON THIN FILM LIGHT WATER ELECTROLYSIS EXPERIMENTS

The pioneering work of George Miley of the University of Illinois and James Patterson of CETI company and their collaborators, which was first presented in September 1996 [8] and later again in October 1996 [9], has played a seminal role in establishing recognition for the possible occurrence of LENR transmutations. This work is therefore discussed first at the start of this review, although historically [10] during the interim period between 1989 and 1996, there were also many reports of observation of new elements on post-run cathodes both in electrolysis experiments and in the impressive glow discharge experiments carried out by Russian groups, which are discussed in later sections.

To place the Miley-Patterson work in perspective, one has to first discuss the so called Patterson Power Cell [8]. Figure 43.1 is a schematic representation of Patterson's flowing packed bed electrolytic cell. The unique feature of this cell was that it used for a cathode a packed bed of 1 mm dia plastic or glass microspheres (or beads), which were coated with thin films of Ni and/or Pd. Typically, there were about 1000 microspheres in the cell forming a four- or five-layer bed that constituted the cathode. Both single and multilayer coated bead configurations were investigated, with coating thicknesses varying in the range of 500 A to 3000 A. Some beads had Ni only coatings, others Pd only, and the rest multilayer coatings made up of alternating layers of Ni and Pd.

Miley's group developed a novel technique of producing robust thin-film-coated beads using a special sputtering process after appreciating the advantages of spherical substrates invented by Patterson, rather than the conventional flat plate support structures that he had been deploying in his earlier thin film electrolysis studies. The distinct advantage of using thin-film cathodes is that whatever new reaction products are formed it would constitute a significant percentage of the host metal atoms, rendering the results more trustworthy. The freshly generated products would no more constitute such minute levels that skeptics could readily dismiss the results as probable impurities deposited from the electrolyte. Besides, high deuterium or hydrogen loadings could be obtained with thin films in time durations as short as an hour or two compared to days or weeks required when thicker electrodes (Pd and Pt rods) are used.

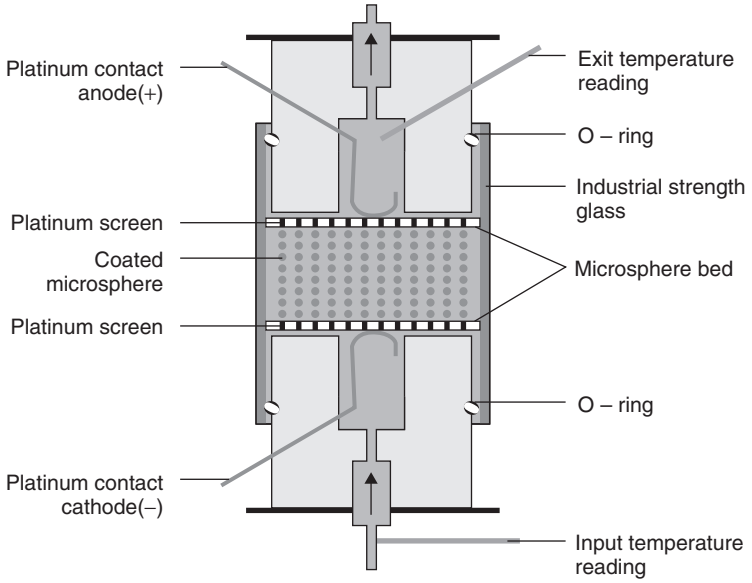

Figure 43.1 Schematic of Patterson power cell.

The electrolyte deployed in the Miley-Patterson studies was a light water solution of 1M Li_2SO_4 (lithium sulphate), which was circulated in a closed loop through a heat sink, for purposes of excess heat measurements. Knowing the mass flow rate and the temperature differential between outlet and inlet, the power output could easily be computed; the input power is the product of voltage applied and cell current. In several runs excess heat production was observed with multilayer coatings giving excess power values as much as 4 watts. Details of their calorimetry and excess heat results are discussed in references [8, 9].

Unlike their early excess-heat-oriented studies, for purposes of transmutation measurements, Miley and Patterson constructed a new system that eliminated metallic components to the extent possible, thereby minimizing possible sources of impurities. During the electrolysis runs the thin metallic films quickly get loaded to a high ratio of H-to-film metal atoms, which is then believed to undergo nuclear transmutation reactions involving the hydrogen and host metal nuclei. After several weeks of electrolysis, beads from the top layers of the packed bed cathode were carefully removed and analyzed for the presence of new elements not present in the control beads prior to electrolysis. In all, more than a dozen experiments were carried out with cathode beads of various types of coatings as described earlier.

A variety of measurement techniques such as Secondary Ion Mass Spectrometry (SIMS), Energy Dispersive X-ray (EDX) analysis, Auger Electron Spectroscopy (AES), and Neutron Activation Analysis (NAA) were employed. While EDX gave confirmatory data for the higher concentration elements, AES was used for depth profiling of these elements. SIMS was used to obtain an overall picture of the various nuclides present and their relative isotopic ratios while NAA gave a quantitative measure of eight key elements, namely Al, Ag, Cr, Fe, Cu, V, Co, and Zn, present in a gross sample containing 10 microspheres. In the case of Cu and Ag, NAA helped establish deviations of isotopic composition from their natural abundance values. NAA has the advantage that it circumvents the molecular ion interference problem that often plague mass spectrometric measurements. The University of Illinois Triga research reactor was used for these studies with calibration carried out using NIST standards. Since NAA typically gives an average value integrated over 10 beads, it averages out the significant bead-to-bead variations in the reaction product yields, which are known to be sensitive to the location of the microspheres in the packed bed. Other techniques helped probe a local area of coating on a single microsphere.

The results of elemental analysis showed the presence of a wide range of new elements in the post-run thin films. Surprisingly, the reaction products had mass numbers ranging both below and above the atomic mass number of the host metal, spanning across the entire periodic table. Figure 43.2 shows a consolidated plot of the reaction rate (yield) vs. product mass number for the case of several Ni-Pd composite multilayer thin film cathode runs, reproduced

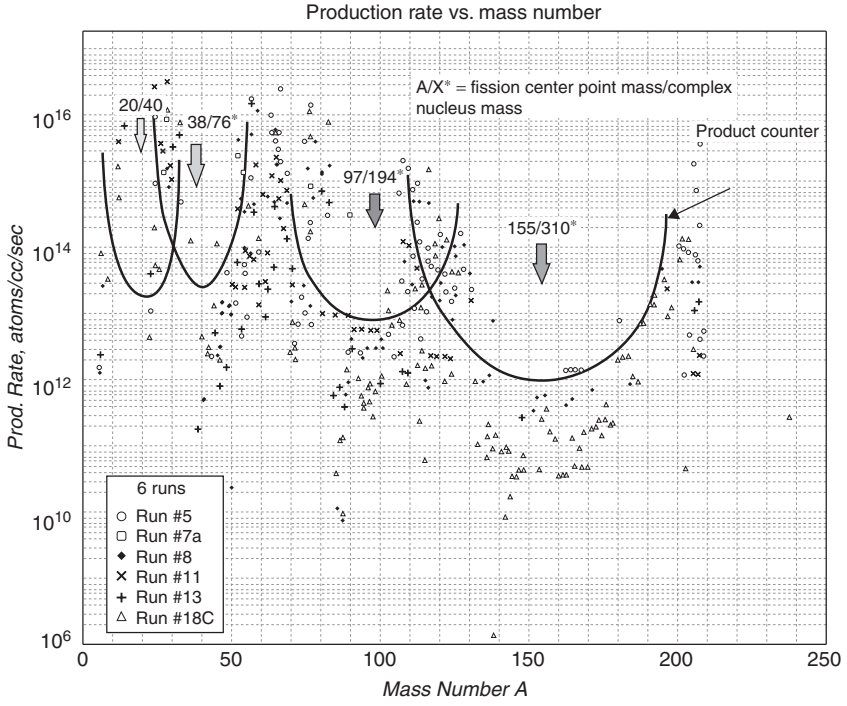

Figure 43.2 Miley's Pd-Ni thin film light water electrolysis experiments: Log rate of reaction product yield as a function of its mass number.

from Ref. [9]. The raw experimental data from different analytical measurements were appropriately normalized prior to plotting. Data from several different runs are plotted in this figure. The outer envelope enclosing all the data points brings out the distinctive grouping of the high yield elements into four broad zones of mass numbers (A ~22 to 23, 50 to 80, 103 to 120, and 200 to 210).

Figure 43.3 shows the same data plotted as production rates against the atomic number (Z value) of the reaction product elements. The characteristic four-humped yield spectrum is once again evident with humps occurring at Z = 6–18 (peak at Mg-Si), Z = 22–30 (peak at Fe-Zn), Z = 44–50 (peak at Ag-Cd), and Z = 75–85 (peak at Au). In some of the runs, as much as 40% of the initial metal atoms of the thin film coating was transmuted. It is speculated that each of these groups of elements is derived from one of the main elemental components used in the construction of the cell such as sulphur, nickel, palladium, and platinum (anode material). Interestingly, this type of grouped reaction product yield curve is found to be consistent with the results reported by other investigators too such as Mizuno, as will be seen in the next section.

From the SIMS data which indicates the isotopic composition of the elements, it is observed that most of the elements showed substantial isotopic deviation from natural abundance, whereas analysis of the control beads corresponded to natural isotopic ratios only. The NAA data for Ag and Cu also confirmed statistically significant deviations from natural abundance. However, it was not possible to discern any systematics in the isotopic shift results, since there was considerable scatter in the isotopic ratios depending on the location of the bead in the cathode bed as well as depth of the sample within the coated film layer. The original papers on these studies [8, 9, 11, 12] have dealt with the expected criticism, namely, the possibility that the observed post-run reaction products could have arisen from impurity deposition from the electrolyte. The NAA quantitative comparisons of the levels of the key transmutation elements in pre- vs post-run beads provide very strong support for the reliability of the transmutation results, since impurity deposition cannot explain the isotopic shifts. The original papers have also discussed the differences in yield spectrum between different base metal coatings, differences in product yield between plastic beads and glass microspheres and differences between H_2O runs and D_2O runs.

There is considerable speculation on the nature of the mechanism that could be responsible for production of such a wide variety of elements. The similarity of these four humped yield curve with the well-known double-humped yield curve observed in the neutron-induced fission process has led to speculation that there could be a similar proton- or deuteron-induced fission of the compound nucleus formed between a host metal nucleus and one or more protons or deuterons in LENR configurations [13, 14].

43.4 MIZUNO AND OHMORI: TRANSMUTATION PRODUCTS ON Pd CATHODES IN D_2O ELECTROLYSIS EXPERIMENTS

At about the same time in 1996 when Miley and his team were performing the above experiments, Mizuno and his collaborators at Hokkaido University in Sapporo, Japan, started carrying out a systematic analysis of their post-run Pd cathodes that had earlier been electrolyzed in heavy water solutions at high-current density, high temperature and high pressure, in search of evidence for the presence of new elements not present in the virgin cathode material. They were inspired by the deliberations at the First International Conference on Low Energy Nuclear Reactions held at College Station, Texas, in June 1995 under the

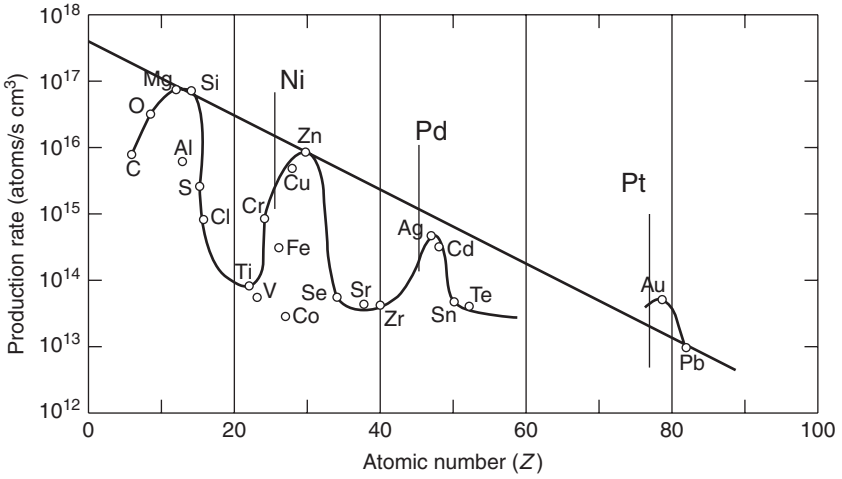

Figure 43.3 Miley's Ni-H_2O experiments: Reaction product yield vs. atomic number.

leadership of Prof. Bockris, who is considered a pioneer [15] in the field of LENR research. Using several different analytic methods, Mizuno, Ohmori, and Enyo [16] found reaction products with mass numbers varying from 6 to 220, comprising a wide range of elements from hydrogen to lead.

Figure 43.4, reproduced from Ref. [16], shows a semilog plot of the EDX spectrum of a Pd cathode rod before and after electrolysis as recorded by them. This rod had shown an integrated excess energy output of ~10 MJ. Peaks corresponding to Pt, Cr, and Fe are seen to be comparable in magnitude to the bulk Pd peak, while signals corresponding to Sn, Ti, Cu, and Pb are relatively smaller in magnitude. EDX analysis performed at different locations on the cathode surface indicated that the counts corresponding to newly formed elements varied by as much as a factor of 10 between different locations, bringing out the highly localized nature of the transmutations (indeed the entire LENR) phenomenon, a feature that has been highlighted by Miley and most other workers also.

Figure 43.5, reproduced from the same reference [16], shows the yield spectrum of the reaction products deduced from the SIMS count rates generated using O_2^+ ions to bombard the Pd sample. The data are plotted as a function of the atomic number of the detected isotope. (The explanation for labeling the X-axis as "counting correction RSF/cm^{-3}" is discussed in detail in ref. [16].) It is surprising that in the spectrum, the maxima correspond to inert gases. The authors have speculated that perhaps during SIMS analysis, the inert gas atoms may have been more efficiently ejected when bombarded by oxygen ions, giving false peaks corresponding to their atomic positions.

Figure 43.6 shows the reaction product yield spectrum plotted as a function of the mass number of the isotope. Note that this too shows a four-humped spectrum remarkably similar to that of Miley et al, presented in Figure 43.2.

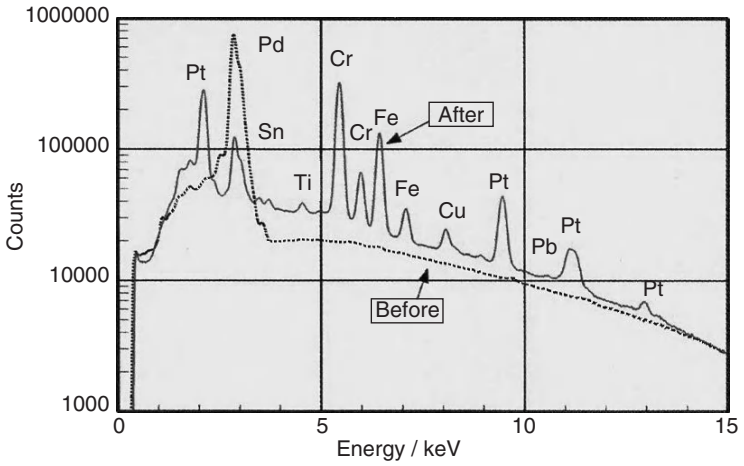

Figure 43.4 EDX Spectra from a Pd cathode rod before and after electrolysis.

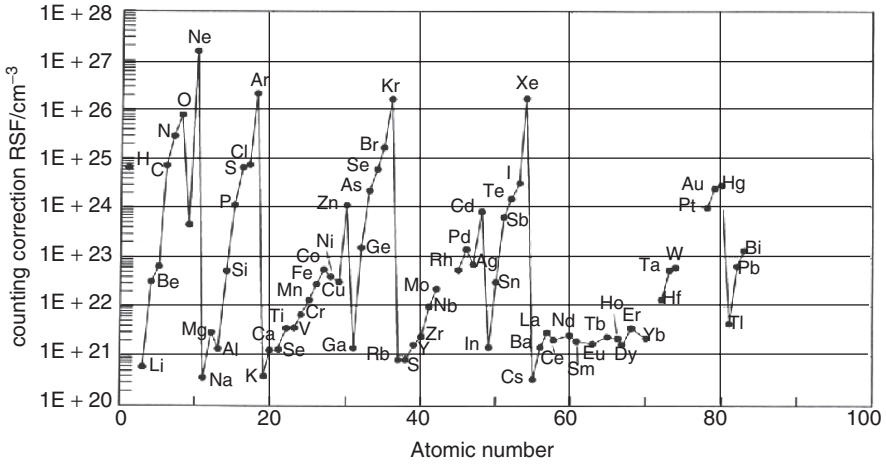

Figure 43.5 Mizuno's Pd-D_2O experiments: Yield of elements formed on surface vs. atomic number.

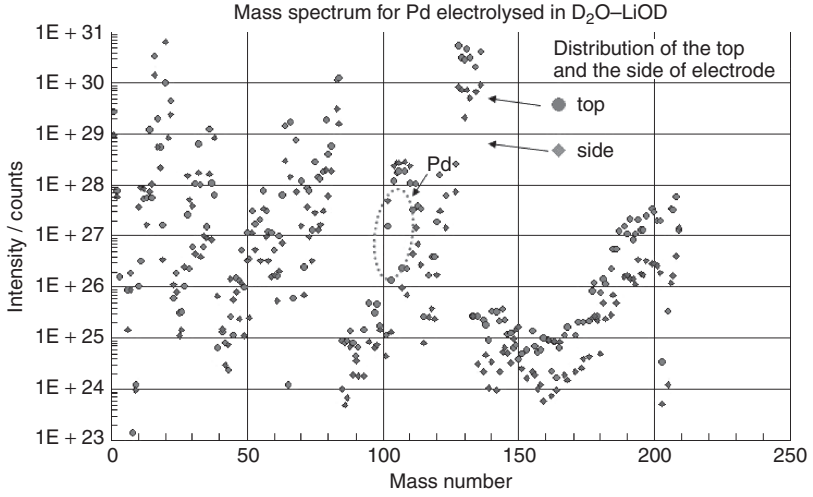

Figure 43.6 Mizuno's isotopic analysis of Pd cathode electrolyzed in heavy water solution: SIMS count rates vs. mass number.

Mizuno also reports that the isotopic distributions of almost all of the newly produced elements are drastically different from their natural abundances [17]. Figure 43.7 shows one such example for the case of Cr isotopes detected on a Pd cathode that had shown excess heat. The left figure shows variation of atomic concentration of the Cr isotopes with depth, while the right part shows the depth profile of the isotopic ratios. Significant variations are seen in the top 10 micron region.

As emphasized already, while isotopic shift measurements are notoriously subject to interference effects caused by molecular ions having m/z values in the region of the signal of the isotope under study, it is equally difficult to conceive of the presence of a plethora of interfering molecular ion species readily available in the cell components to give false peaks at every one of the mass spectrum locations observed by Mizuno and Ohmori.

43.5 NEUTRON ACTIVATION ANALYSIS OF DEUTERATED Pd SAMPLES THAT HAD PRODUCED SIGNIFICANT AMOUNTS OF EXCESS HEAT

Tom Passell of the Electric Power Research Institute (EPRI) had arranged for samples of Pd cathodes, which were

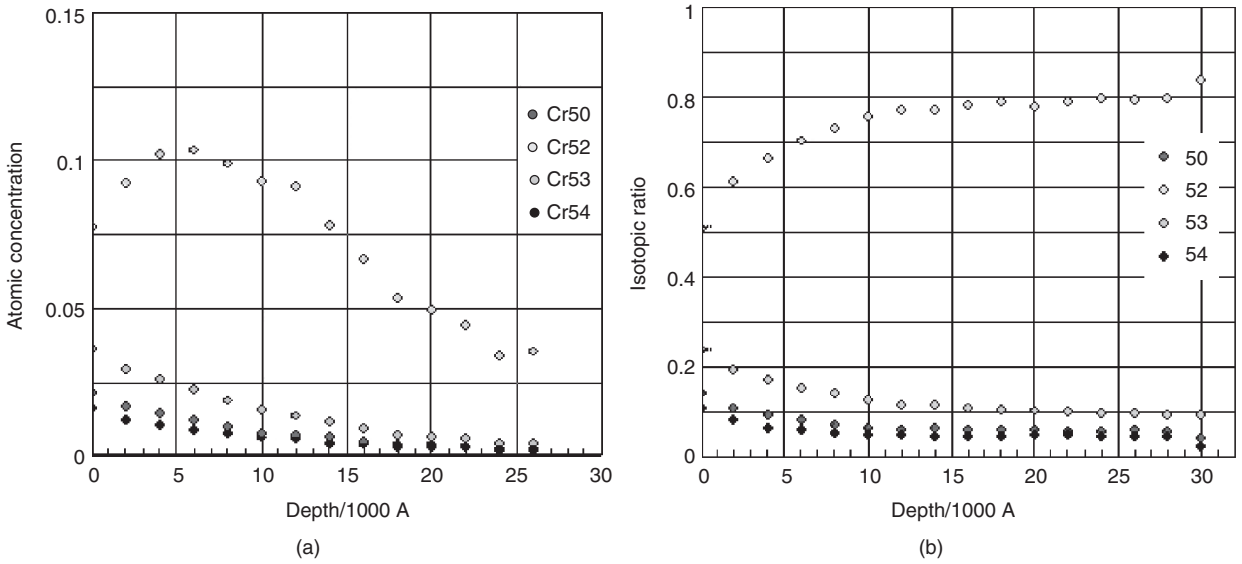

Figure 43.7 (a) (b) Depth profile of Cr isotopic ratios on surface of Pd cathode that had shown excess heat.

known to have "exhibited episodes of excess heat beyond all inputs" during electrolysis in LiOD, to be analyzed for possible changes in trace element nuclide composition using Neutron Activation Analysis (NAA). He was clearly motivated to do this following reports of isotopic anomalies observed by other workers using the NAA technique, which is more appealing to nuclear physicists than mass spectrometry, which is subject to molecular ion interference issues. Also, NAA gives an integrated overall global result and is not sensitive to local variations within a sample. Mo et al. from China too had reported [18] at ICCF 7 in 1998 a 20 to 34% increase in (Zn^{64}/Zn^{68}) activity ratio in samples of thin Pd wires exposed to gaseous hydrogen isotopes using NAA techniques.

Passell obtained his first samples for analysis by NAA from Stanley Pons; these were thin slices from the 2 mm dia Pd cathode rods used in the Icarus 9 experiments conducted at IMRA, Europe. One was taken from an active Pd cathode (22.1 mg in weight) that had generated significant amounts of excess power during electrolysis, while the second (29.3 mg) was a control taken from a similar but virgin rod. The NAA measurements were carried out by Benjamin Bush and J. J. Lagowski of the department of Chemistry, The University of Texas, Austin campus. These measurements [19] indicated that the Pd^{108} to Pd^{110} isotopic ratio of the active Pd sample was depleted by about 28% relative to the virgin cathode sample. In addition, the concentration of several trace elements were found to be higher relative to the control sample, the most noticeable being Fe (56 times) and Zn (12 times). The concentrations of Co, Cr, Cs, and Eu also indicated an increase by a few times.

In a follow-up series of measurements reported first at ICCF 8 [20] and again at ICCF 10 in Cambridge, Massachusetts [21], samples of Pd black powder, taken from the inner plenum of a double-structured cathode provided by Arata of Osaka University, were analyzed at The University of Texas (UT), Austin, in a project managed by Tom Passell. In his report, Passell wrote that "the precise amount of excess heat produced by the cathodes in which the powdered palladium was contained has not yet been made available. Arata and Zhang's published work shows data from similar cathodes which produced about 30 to 40 megajoules of excess heat over the most active two-month period of their electrolysis." A fourth sample was virgin Pd black powder from the same batch. Since the active powder samples were from the central hollow portion of the double-structure cathodes, they would not have had any possibility of getting contaminated from impurity elements during electrolysis.

The samples (5 to 15 mg each) were loaded in standard small polythene vials and irradiated simultaneously in The University of Texas nuclear reactor facility for 80 mins. The 13.4 hr Pd^{109} activity gave a measure of the Pd^{108} content, while the 7.45 day Ag^{111} activity was taken as representative of the Pd^{110} content. All data were normalized to the corresponding gamma counts obtained for the virgin powder sample. The areas under the respective gamma photo peaks were integrated using procedures routinely used at this NAA laboratory. The results clearly showed a statistically significant 8% decrease of the Pd^{108} to Pd^{110} ratio for active cathode sample B. Interestingly, this cathode sample also showed a corresponding increase in Zn^{64} ($\sim$15 times) and Co^{59} activity ($\sim$60% higher) implying anomalous production of Zn and Co as well during the electrolysis runs.

Passel suggests that Fe, Zn, Co, and other elements that are found in the active Pd samples could have been fragmented products arising from deuteron-induced fission of Pd nuclides, the depletion of Pd^{108} being indicative of a relatively higher fissioning rate of the Pd^{108} nuclide relative to the Pd^{110} nuclide. It may be pointed out that NAA gives information only about nuclides that get activated during exposure to a neutron flux, and all isotopes of Pd do not respond in the same manner during NAA analysis.

43.6 ANOMALIES IN TRACE ELEMENT COMPOSITION OF NEWLY FORMED STRUCTURES ON CATHODE SURFACE IN CO-DEPOSITION EXPERIMENTS (SPAWAR GROUP)

The co-deposition protocol has been successfully developed into a very powerful technique for the investigation of LENR phenomena by Stanislaw Szpak, Pamela Boss, and others at the U.S. Navy SPAWAR Systems Center in San Diego from the very beginning of this field of research [22]. In the work [23] reviewed here, the main innovation introduced was placing the co-deposition cell in an electrostatic field applied perpendicularly to the direction of flow of the electrolytic current, as illustrated in Figure 43.8.

The Pd and deuterium atoms are simultaneously deposited onto the surface of the Au strip substrate, forming a thin cohesive layer of PdD. The experimental protocol, refined after years of research, calls for the cell current to be initially maintained at 1 mA for the first 24 hrs, after which it is stepped up to 3 mA; this is continued until the solution becomes colorless (implying Pd^{2+} is fully reduced). The current is then raised to $\sim$40 mA for a few hours until vigorous D_2 gas evolution is observable; this indicates that the D/Pd atomic ratio has stabilized and become uniform. Figure 43.9 shows the typical structure of the co-deposited PdD film at this time, as imaged by a Scanning Electron Microscope (SEM). The PdD is seen to have a "characteristic cauliflower" like structure made up of globules 3 to 7 μm in dia. (see insert in figure). The corresponding EDX

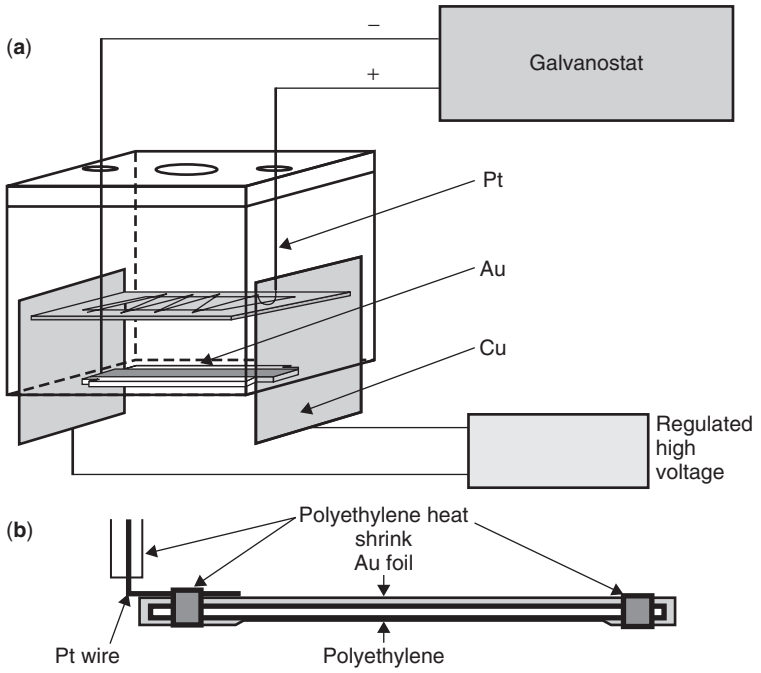

Figure 43.8 SPAWAR co-deposition electrochemical cell setup and assembly of Au cathode.

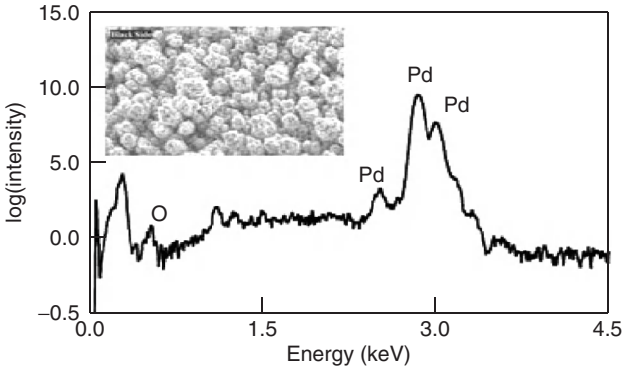

Figure 43.9 Scanning electron microscope (SEM) image in absence of electric field and EDX scan of the co-deposited PdD film.

scan of the PdD layer shows only the expected Pd and D, having composition of Pd (95.17 wt%) and O (4.83 wt %).

At this point, an external 6 KV cross electric field is switched on while simultaneously jacking up the current to 100 mA. This is maintained for about 48 h. At the end of this procedure, the SEM scan of the electrode shows the appearance of several new structural forms having morphologies suggestive of localized melting. The researchers have characterized the newly produced morphologies as having "boulder like," "crater like," "blister like," and so on features. What is interesting, however, is that the EDX scan of these new structures indicates the presence of a variety of trace elements such as Al, Ca, Mg, Si, and others that were not present either in the electrolyte or in the cauliflower-like structure of the initial PdD deposit. The quantum of the newly formed elements is at times as high as several tens of percent. Equally intriguing is the fact that the composition and magnitude of the additional elements is different in the central and peripheral regions of some of these morphological structures.

The experimenters had confirmed that the concentration of all these newly appeared trace elements were below detection limit in the initial electrolytic solution. The total quantity of all impurities in the electrolytic solution was less than 0.5 mg and could not account for the total magnitude of the newly appeared elements. The authors have concluded that the only logical explanation is that these elements must have been generated by some type of nuclear transmutation reactions occurring in the PdD cathode structure. A comprehensive discussion of the various arguments that have lead the authors to such a conclusion is presented in their original paper [23].

43.7 OBSERVATIONS OF TRACE ELEMENT DISTRIBUTION ON CATHODE SURFACES FOLLOWING ELECTROLYSIS AT PORTLAND STATE UNIVERSITY (JOHN DASH)

John Dash of Portland State University, Oregon, has been researching LENR phenomena since 1989, with the help of

graduate students. A notable feature of his experiments is their simplicity since they are designed as student projects [24]. His main tools are open electrolytic cells and an SEM equipped with an Energy Dispersive Spectrometer (EDS) with which he can measure surface morphology as well as elemental composition of cathode samples on a microscopic scale before and after electrolysis. He also has available a Secondary Ion Mass Spectrometer (SIMS) with which the mass spectrum of ionic species ejected from the surface during sputtering by Cs ions can be recorded. By peeling off layers one after the other, he has the capability to depth profile the mass spectrum of ejected ions.

In a recent review [25] of his two-decade-long pursuit of isotopic anomalies, Dash has highlighted the fact that after a mere 6 minutes of electrolysis (at a current density of 0.25 A/cm^2), he was able to detect changes in trace element composition on the surface of his cathodes, as well as isotopic anomalies using the quadrupole mass spectrometer of the SIMS instrument. He is, of course, fully aware of the pitfalls of mass spectrometry, namely possibility of interference caused by molecular ion species having m/e values very close to that of the nuclide being measured. These issues are addressed in detail in his papers.

Dash was among the earliest to report [25] presence of Au and Ag on the Pd cathodes after electrolysis in an electrolyte comprised of H_2SO_4 and D_2O or H_2SO_4 and H_2O, at ICCF 6 in Lake Toya, Hokkaido, in 1996. (Note that Ag is the upper neighbor of Pd in the periodic table of elements and Au the higher mass neighbor of Pt, which was the anode material in his cells.) Dash operated two identical cells in series—one containing acidified D_2O electrolyte and the other a control cell loaded with acidified H_2O electrolyte. The 40 μm thick Pd foils used for fabricating his 2 cm long, 0.8 cm wide cathodes were cold-rolled from 500 μm thick Pd metal sheets. A Pt lead wire was spot-welded to the vertically suspended cathode foil at the upper edge. A SIMS scan of the post-electrolysis cathodes revealed isotopic inversion of Pd isotopes on the near surface layers of the foil that had been electrolyzed in acidified D_2O, as compared to the virgin foil. The (Pd^{108}/Pd^{106}) ratio was somewhat higher than the natural abundance value (which is close to unity). Sputtering exposed deeper layers, and the isotopic ratio anomaly steadily decreased reaching natural abundance levels at a depth of 0.3 microns.

Figure 43.10, which brings out this observation clearly, indicates that whatever processes are responsible for nuclear transmutation phenomena are confined to the outermost layers of the cathodes. This type of behavior was noticed at 10 different spots on the same cathode. For comparison, the corresponding variation of the concentration of the Pd isotopes for the case of a foil electrolyzed in light water solutions is presented in Figure 43.11. Isotopic ratio inversion is not seen here.

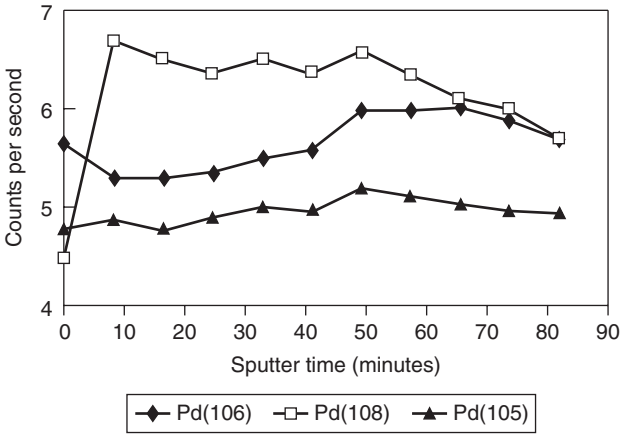

Figure 43.10 Pd isotopic distribution: SIMS counts after 6 minutes of electrolysis in heavy water electrolyte.

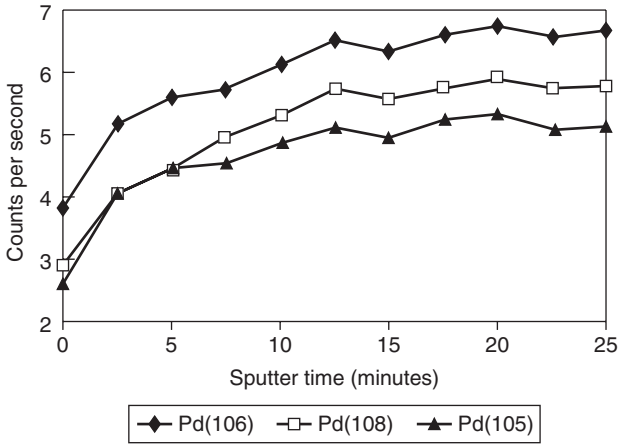

Figure 43.11 Pd isotopic distribution: SIMS counts after 6 minutes of electrolysis in light water electrolyte.

One very interesting observation reported by Dash was that several days after the above mentioned SEM/EDS study was completed and the Pd foil that had been put away in storage at room temperature and ordinary atmosphere was reexamined, they discovered that a new oval-shaped structure had developed at a spot wherein significant amounts of Ag had been freshly generated. When this spot was again examined a month later, the additional presence of cadmium (upper-side neighbor of Ag in the periodic table) was observed, suggesting that the silver had been further transmuted to Cd during the intervening one-month period when it was in the storage cabinet!

In a later paper Dash had reported that vanadium concentration was found to have increased on the surface of Ti cathodes after electrolysis. Note again that the atomic number of V is 47, which is one unit higher than that of Ti which is 46.

43.8 RUSSIAN GLOW DISCHARGE EXPERIMENTS (KARABUT, SAVVATIMOVA, AND OTHERS)

Karabut and Savvatimova from Russia were among the earliest researchers in the LENR field to present experimental findings indicative of the occurrence of nuclear transmutation reactions and anomalous isotopic shifts in deuterided metals [26]. This group has been carrying out exhaustive studies for almost two decades using high-current, high-voltage glow discharge devices in a deuterium (or hydrogen) plasma to investigate LENR phenomena. Figure 43.12 is a schematic diagram of their glow discharge apparatus, which is basically a double-walled quartz vacuum chamber with a Mo anode and a cathode.

The design of the setup permits use of different cathode materials for study. The chamber is evacuated to about 10^{-3} Torr and filled with D_2 gas to a pressure in the region of 3 to 10 Torr. The region of the cathode bombarded by the plasma ions is typically $\sim$1 cm^2 in area. The cathode, anode, and the quartz chamber housing are each separately cooled by circulating water. Temperature sensors located at appropriate locations in the cooling circuits permit calorimetric measurements. The voltage applied is varied from 50 V to 1.2 KV while the discharge current is $\sim$100 mA. The power dissipated, inclusive of excess heat if any is generated, is removed by the three cooling water circuits.

While they have reported observing excess heat consistently with near 100% reproducibility, they did not detect the expected normal (D-D) fusion reaction products such as neutrons, tritium, or even helium in quantities commensurate with the magnitude of the heat generated.

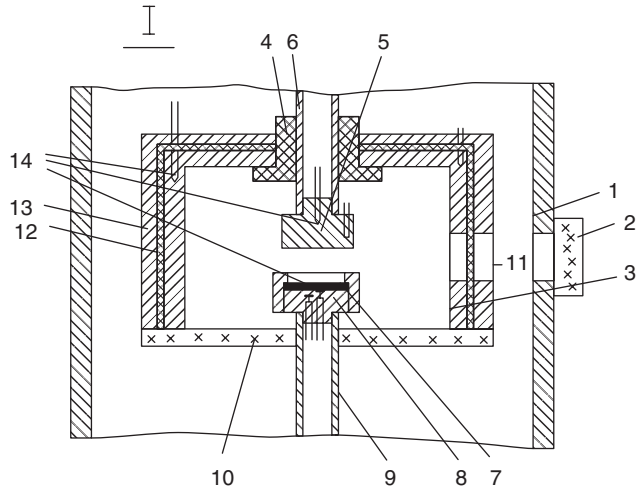

Figure 43.12 Schematic diagram of glow discharge apparatus used by Karabut et al.

The studies reported in this review were mainly conducted with a Pd planchet (cathode) and deuterium plasma. In quest of the mystery of the missing reaction products, they carefully analyzed the surface of the Pd cathode after it had been subjected to several tens of hours of glow discharge in deuterium gas. The bulk impurity content of the virgin Pd cathode material (supposedly 99.99% purity) was first analyzed [27, 28] using spark mass spectrometry at the GIREDMED mass spectrometry laboratory. The detection limit of the set up was 10^{-6}% (atom percent). The scan showed presence of the following impurity elements with concentrations above 10^{-4}%: Mg, Ca, Fe, Rh, Ag, Ta, Pt, and Au. A few other elements were also present but with lower concentration. It was confirmed that the total impurity content of the virgin material was indeed under 0.01%.

The post-discharge Pd cathode buttons were subjected to detailed investigations using the following techniques:

- Surface topography by scanning electron microscopy.
- Element and isotopic composition using spark mass spectrometry, SIMS, and XRF.
- Autoradiography for evidence of any remnant radioactivity.
- Thermal Ionization Mass Spectrometry (TIMS).

Several different laboratories in the Moscow-Podolsk region were involved in carrying out these investigations.

As emphasized already, the presence of new elements after discharge alone cannot be taken as evidence of formation of new elements by transmutation processes. However, in the case of gaseous plasma experiments, there is no electrolytic solution involved and the possibility of impurity deposition from the electrolyte is absent. Alternate routes of impurity migration from the discharge environment need to be thoroughly examined and ruled out.

The Russian investigators carried out detailed isotopic composition measurements on the cathode samples at the Tomsk Polytechnik Institute using SIMS. This study clearly indicated significant deviations from natural abundance values for most elements. Karabut et al. [28] bring out this feature elegantly. But this data can only be taken as representative, since the reaction product yield is known to notoriously vary from spot to spot on the surface of the cathode, a feature that has been independently observed by several workers in the LENR field. At the Nagoya ICCF 3 meeting in 1992, Karabut et al. reported [28] finding as much as 0.1% of Na, Mg, Br, Zn, S, Mo, and Si in the upper crust of the Pd and had speculated that these elements could in principle be explained through occurrence of multiple deuteron captures in one of the isotopes of the Pd cathode, followed by fission of the complex intermediate compound nucleus.

An obvious question that bothered the investigators right from the beginning was the possibility of mass transport of impurity ions onto the cathode surface from various metallic components used in the discharge environment, such as the silica and alumina insulators and the molybdenum anode. The top 1 μm layer of the Pd sample was examined at several spots in the front portion, the back portion, and shielded area with a spatial resolution of 1 μm using an x-ray microprobe analyzer. It was found that the content of some elements increased by tens to hundreds of times relative to initial content in virgin Pd. A paper by Savvatimova et al. [29], for example, gives the concentration of many elements for discharge run times of 4 hours and 40 hours respectively.

The Russian groups have continued to report similar but fresh observations in almost every ICCF conference since 1992, refining and improving their experimental procedures. At ICCF 5 held in Monaco in 1995 [30], they again reported that the quantity of the newly appearing "impurity" products varied significantly from spot to spot as detected by an x-ray microprobe analyzer. In some spots, the Ag content was as high as 12 to 15% and Mo about 5 to 7%. The concentration of elements such as As, Br, Rb, Sr, Y, and Cd, which are not present in any of the construction materials used in the experimental apparatus, was in the range of 0.1 to 0.2%. A new result reported at the Monaco meeting was that even with hydrogenous plasma, they observed elements not present in the virgin cathode, but in general the products' yield with deuterium gas was orders of magnitude higher.

At ICCF 9 held in Beijing in 2002, Karabut reported [31] new results obtained by subjecting the discharge device to an "impulsive periodical power source" (pulsed voltage), which led to generation of intense x-ray laser beams. Discussion of this discovery, though very interesting, is beyond the scope of this review. The difference in "impurity" elements content before and after the experiment is taken as the yield of nuclides produced in the experiment. The main impurity nuclides (with more than 1% content) registered in the top 100 nm thick surface layer are Li^{7}, C^{12}, N^{15}, Ne^{20}, Si^{29}, Ca^{44}, Ca^{48}, Fe^{56}, Fe^{57}, Co^{59}, Zn^{64}, Zn^{66}, As^{75}, Ag^{107}, Ag^{109}, Cd^{110}, Cd^{111}, Cd^{112}, and Cd^{113}.

It is apparent that one can identify two broad categories of impurity elements: those with masses roughly half of that of Pd (probably caused by deuteron induced fission) and those with masses close to but above that of Pd (possibly caused by multiple deuteron captures).

Karabut speculates that the excess heat measured in the glow discharge experiments must have been caused by these two categories of transmutation reactions, leading to the production of the plethora of observed product nuclides. Details of his arguments are presented in his original paper [31]. Table 43.1 presents the impurity nuclide yields for the discharge experiments with Pd cathode and D_2 plasma as a function of depth in the cathode sample.

At ICCF 12, held in Yokohama in December 2005, Karabut presented [32] further results from discharges carried out with V, Nb, and Ta cathodes and in the inert gases of Xe and Kr besides D_2. In general, with cathodes other than Pd, "impurity" element yield was significantly lower. In these experiments, Karabut measured the impurity content yield after peeling off some atomic layers using plasma etching and then again analyzed the elemental content using SIMS. Table 43.1 presents the impurity nuclide yields for the discharge experiments with Pd cathode and D_2 plasma as a function of depth in the cathode sample.

At the same conference in Yokohama, Savvatimova presented [33] a very detailed and exhaustive account of her independently conducted glow discharge results with hydrogen, deuterium, argon, and argon-xenon mixture plasmas. The influence of various experimental parameters such as nature of plasma gas, total dose of bombarding ions, discharge current density (mA/cm^2), and type of applied voltage (direct or pulsed) on the yield of "additional" elements was studied systematically. This time she also used multilayer cathodes comprising several foils of 100 μm thickness stacked one on top of the other to study differences in product yield characteristics with depth. In particular, special attention was paid to the structural changes associated with the hot spot sites (especially grain boundaries) where the additional elements are generally found to be concentrated. The greatest changes in "additional" element content and isotope shifts were found in certain "hot spots," where a micro-explosion or plasma micro-discharges had appeared to have taken place. The author makes special mention of elements with mass numbers 59(C0), 55(Mn), and 45(Sc), which were always found in plenty in the post-discharge samples but never in initial samples.

On the whole, Savvatimova finds that the more deeply she investigates the LENR glow discharge phenomenon, the more complex it is found to be, as brought out by her in the 13 tables of results included in the Yokohama paper [33]. For example, while investigating the effect of time duration of discharge, Savvatimova found that while a 30 minute run resulted in the content of Zr increasing by a factor of 570 to 340, that of V by a factor of 100, and Cr by 160, continued irradiation did not yield significantly more products, a behavior observed by them several years earlier also. On the other hand, Mo, which is an element used in the construction of some components of the discharge chamber, showed an increase commensurate with total dosage of ions (current x time). The author speculates that with a fresh a cathode sample there may have been many defect sites that promote transmutation reactions, but these might have all been consumed or destroyed on continued experimentation.

If the additional elements appear as a result of cathode sputtering or redistribution, one would expect a higher yield

TABLE 43.1 Impurity Nuclide Yields for the Discharge Experiments with Pd Cathode and D_2 Plasma as a Function of Depth in the Cathode Sample. [32]

V - H				V - D			
A Impurity nuclide	1 scan 10 nm, content, %	2 scan nm, content, % 50 nm, content, %	3 scan nm, content, % 700 nm, content, %	A Impurity nuclide	1 scan 10 nm, content, %	2 scan 50 nm, content, %	3 scan 700 nm, content, %
99Ru	**ND**	**ND**	**ND**	**99Ru**	0.42	0.11	0.02
102Ru	0.66	0.73	0.4	**102Ru**	0.74	0.51	0.4
103Rh	0.25	0.14	0.02	**103Rh**	0.19	0.23	0.34
104Pd	0.16	0.04	0.3	**104Pd**	0.22	0.2	0.37
106Pd	0.15	0.02	0.02	**106Pd**	0.29	0.16	0.12
108Pd	0.45	0.04	0.06	**108Pd**	0.21	0.24	0.12
111Cd	0.05	0.16	0.01	**111Cd**	0.15	0.2	0.07

of "impurity" elements with bombardment by heavier ions such as argon or xenon as compared to deuterium runs. But the results always show maximum quantity and maximum variety of additional elements with deuterium discharges, much less with hydrogen, and least with argon.

One intriguing new result reported at Yokohama was that the isotopic changes continued to occur for at least three to five months after glow discharge exposure, reminiscent of the self-heating phenomenon reported by many LENR researchers. (Readers may recall that a similar observation made by Dash has been noted by us earlier in this chapter.) Several isotopes with masses less than those of W and Ta increased by factors ranging from 5 to 1,000 times.

The exhaustive two decade-long series of experiments [26 to 37] conducted by two separate Russian groups using the glow discharge technique clearly indicates that the plethora of observations pertaining to additional element production and their deviation from natural isotopic composition are indeed very complex in nature and strongly support the postulate that both fusion- and fission-type nuclear transmutation reactions seem to be occurring in Pd cathodes subjected to deuterium plasma bombardment. The accumulated evidence also points to the occurrence of such reactions preferentially in certain selected sites or "hot spots," which appear to be associated with grain boundaries.

It is noteworthy that precisely the same conclusion was arrived at from the transmutation measurements in electrolysis experiments discussed in earlier sections.

43.9 REPLICATION OF GLOW DISCHARGE TRANSMUTATIONS BY YAMADA'S GROUP AT IWATE UNIVERSITY, JAPAN

The glow discharge apparatus employed by this group [38, 39], which was made of Pyrex glass to avoid contamination from metallic impurities, is shown in Figure 43.13. Yamada used a Pd plate (10 mm square and 1 mm thick) as a cathode and a gold foil as anode. Great care was taken to

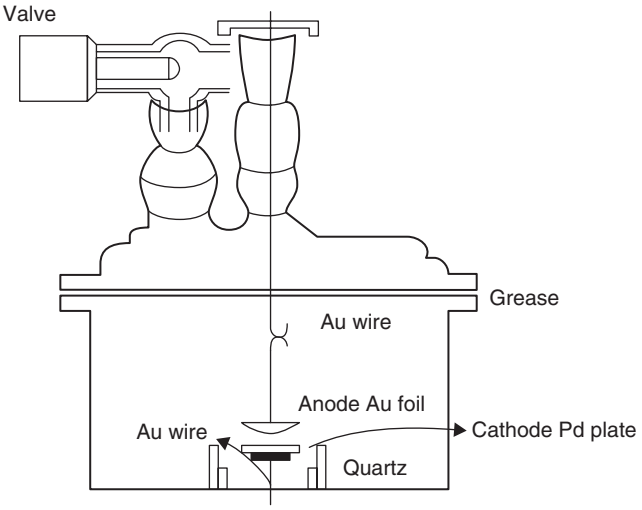

Figure 43.13 Glow discharge apparatus used by Yamada's group.

avoid contamination of the Pd sample (99.95% purity) prior to experimentation. The Pd samples were first preloaded *in situ* by a gas-loading procedure by evacuating the discharge chamber and filling it with D_2 or H_2 gas at 5 to 10 atmospheres for two days. Discharge runs (600 to 800 V and 2 mA) were then conducted for about an hour either with deuterium or hydrogen gas at 10^{-3} torr.

The impurity composition of every sample was analyzed by high resolution TOF-SIMS both before and after discharge runs. Prior to discharge, the following elements were found to be present in the Pd samples: B, Na, Al, Mg, Si, Ca, K and Mn, and to a lesser extent Li, Fe, Cr, and Cu. The post-run samples were analyzed for those elements that were not present prior to discharge. Be and Ni, whose masses are less than that of Pd, were invariably found in the post-run samples, both in case of D_2 and H_2, but never in pre-run samples. The quantity of Li, an element whose mass is substantially smaller than that of Pd, increased in 3 out of 10 runs, while the presence of Ba, whose mass is heavier than that of Pd, was surprising.

Ni and Ba were also found in Pd samples discharged in hydrogen plasma. The authors have pointed out that the TOF-SIMS measurement system used by them for isotopic analysis could easily distinguish between Ba^{138} and Pd-Si molecular ion species (both ^{108}Pd-^{30}Si and ^{110}Pd-^{28}Si). The details of their results are presented in the tables given in ref 10.2. The authors speculate that the appearance of elements such as Li and Ni, lighter than Pd, could indicate the occurrence of some type of fission of Pd, while presence of Ba, which is heavier than Pd, could indicate a fusion-type reaction.

43.10 IWAMURA (MHI): TRANSMUTATION REACTIONS OBSERVED DURING D_2 GAS PERMEATION THROUGH Pd COMPLEXES

Yasuhiro Iwamura and his colleagues at the Mitsubishi Heavy Industries (MHI) laboratories of Japan have been systematically investigating the occurrence of nuclear reactions during the loading and diffusion of deuterium in Pd foils since 1993. In the beginning, they used a simple gas loading/deloading method and reported detecting neutrons and tritium [40]. The problem with gas loading, however, is that in general it is very difficult to obtain D/Pd loadings >0.8. Subsequently, they employed electrolytic loading from one side of the foil and looked for charged particles on the other side [41]. In the next phase, they loaded the Pd foil electrolytically, then deposited a thin copper layer on the surface to seal the loaded foil to prevent deuterium degassing. This loaded and sealed foil was then transferred to a vacuum chamber where, on heating, the loaded deuterium gas was released. During this process, they observed nuclear reaction products such as neutrons and tritium [42], like so many other workers in the field throughout the world.

Iwamura's group had thus independently arrived at the conclusion that to cause nuclear reactions one needs both a decent loading as well as some method to cause the deuterons to rapidly diffuse within the Pd. At this point, they intuitively speculated that perhaps impurities play an important role in enhancing the nuclear reaction processes and decided to incorporate a third entity such as CaO, which has a very low "work function" (1.60 to 1.86 ev) into the PdD, inspired by their Electron Induced Nuclear Reaction (EINR) model [43, 43a]. Accordingly, they prepared a new multilayer cathode comprised of a 1 mm thick Pd sheet, followed by 10 alternating layers of CaO (20A) and Pd (180A) and topped off with a 400A Pd overlayer. This experiment was carried out at room temperature using an Ar ion beam sputtering apparatus. Details of preparation of this multilayer complex as well as the calorimetry measurements performed by them to measure excess heat production are described in ref. [43].

Figure 43.14 shows a sectional view of their "electrolytic continuous diffusion apparatus." The electrochemical cell made of Teflon is separated from a vacuum chamber by an O-ring gasket. 1M LiOD was used as the electrolyte. Deuterium was loaded by electrochemical potential on one side of the Pd complex and released from the vacuum side, the rate of diffusion of deuterons through the complex being controlled by the cell current as well as gas pressure on the vacuum side.

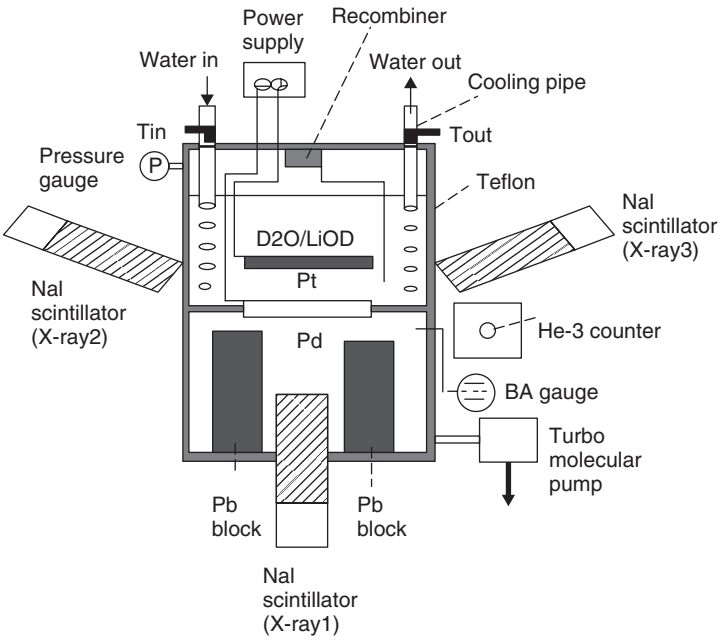

Figure 43.14 Iwamura's electrolytic continuous diffusion setup.

Using an Electron Micro Probe Analyzer (EPMA), they detected an anomalously large (20 μg) amount of Ti as well as extra amounts of Fe and Cu on the inner electrolyzed surface of the post-run Pd complex. These results were perhaps Iwamura's first hints of observation of transmutation reactions in LENR devices. SIMS measurement of the isotopic composition of iron isotopes showed that (Fe^{57}/Fe^{56}) ratio varied in the region of 0.24 to 0.66, which is more than an order of magnitude higher than its natural abundance ratio value of 0.023. Later, at ICCF 8 held in Lerice, Italy, in May 2000, Iwamura's group reported [44] measuring (Fe^{57}/Fe^{56}) values even as high as 1.8 at some spots on the post-electrolyzed cathode. Such high ratios, in comparison to the natural abundances, are indeed a clear indication of the occurrence of nuclear transmutation processes.

At Lerici, Iwamura also presented details of their improved gas diffusion apparatus [44], which had facilities for *in situ* measurements of the surface concentration of selected elements and isotopes using X-ray Photoelectron Spectroscopy (XPS). These new elements are thought to be generated through transmutation reactions during the simple process of diffusion of deuterium through Pd complexes. In this experiment "permeation" of D_2 gas is solely due to the gas pressure differential of 1 atmosphere between the two faces of the Pd complex. Maintaining the foil temperature at 70°C is found to facilitate permeation. Since no electrochemistry is involved, it is a clean experiment with less scope for impurities to enter. Figure 43.15 depicts their gas diffusion apparatus comprising two SS vacuum chambers separated by the Pd foil complex; on one side is D_2 gas, while the other side is evacuated by means of a turbo molecular vacuum pump.

The system incorporates an x-ray gun and electrostatic analyzer for XPS, a mass spectrometer, and a Ge semiconductor detector for charged particle measurements. The great advantage of this setup is that the surface of the Pd sample can be analyzed without taking the sample out of the experimental chamber, thereby avoiding the possibility of contamination. Prior to introduction of D_2 gas into the system, the Pd surface was first analyzed. After filling the gas, diffusion was permitted to take place for a period of about a week or two. At the end of the permeation period, XPS measurement was carried out, after evacuating the deuterium gas for a short while. As is well known to surface scientists, carbon is always present as an impurity on the Pd foil complex even under high vacuum conditions. In the initial experiments when a pure Pd foil was used for permeation studies, there was no change in C content before and after permeation. But when the permeation was carried out with the Pd-CaO-Pd multilayer complex, after 40 hours the carbon content had decreased to almost zero, but the levels of Mg, Si, and S increased. Mg, Si, and S have never been detected in their samples before permeation commenced. Figure 43.16 depicts these results. Further permeation (after 116 hrs in all) resulted in the amount of Mg decreasing marginally while Si and S went up correspondingly.

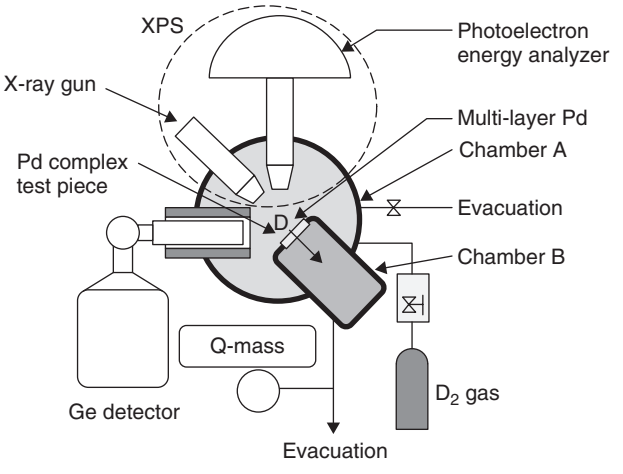

Figure 43.15 Iwamura's gas diffusion apparatus with *in situ* XPS analyzer and quadrupole mass spectrometer.

Iwamura explains these results using his EINR theoretical model [47], which suggests that ${}_6C^{12}$ somehow captures (may not be a direct reaction) 6 deuterons to become ${}_{12}Mg^{24}$ as follows:

$$ {}_6C^{12} + 6({}_1d^2) \rightarrow {}_{12}Mg^{24} $$

Likewise, the right part of Figure 43.16 is explained by postulating the following reactions:

$$ {}_{12}Mg^{24} + 2({}_1d^2) \rightarrow {}_{14}Si^{28} $$

and

$$ {}_{12}Mg^{24} + 4({}_1d^2) \rightarrow {}_{16}S^{32} $$

In all these reactions, deuterons seem to be getting captured in multiples of 2, 4, 6, and so on.

In a repeat experiment (his experiment. No. 4) wherein the initial C content was somewhat higher, the time variation of the C, Mg, Si and S content, shown plotted on the right part of Figure 43.16, further corroborates the possible occurrence of the above sequential nucleosynthesis reactions scheme, through his multiple "even number of deuteron captures" hypothesis.

SIMS analysis of the isotopic composition of sulphur isotopes on the multilayer complex after D_2 gas permeation showed that the ratio (S^{33}/S^{32}) was anomalously large (0.25) as compared to the corresponding natural isotopic abundance ratio of 0.0079, once again confirming the occurrence of nuclear phenomena.

In further studies, Iwamura and his colleagues electrolytically deposited Li as a dopant on the surface of the multilayer complex and then carried out the D_2 gas permeation

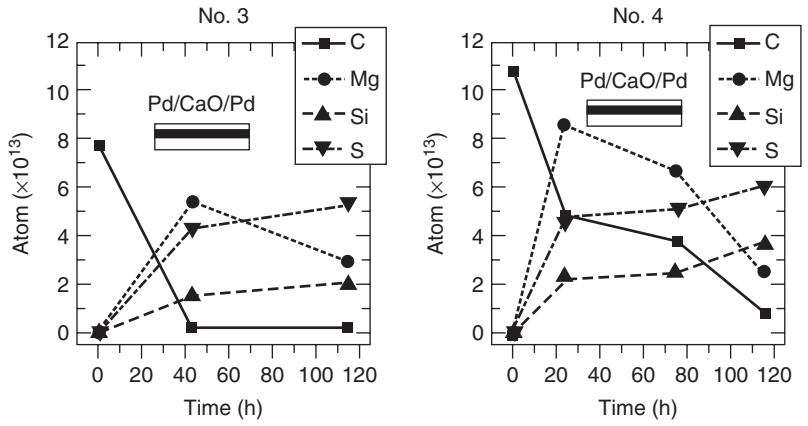

Figure 43.16 XPS measurement of time dependence of C, Mg, Si, and S on the surface of multilayer Pd samples after D_2 gas permeation.

experiment. *In situ* XPS analysis showed (see Fig. 43.17) the production of fluorine first, which then appears to have transmuted to Al during the second half of the permeation process as follows:

$$_3Li^7 \rightarrow _9F^{19} \rightarrow _{13}Al^{27}$$

In each step, either six deuterons or four deuterons seem to have been effectively added to the nucleus.

For Iwamura's group, these results were possibly the first taste of reliable and trustworthy transmutations effected during the simple process of D_2 gas permeation. The reactions investigated so far involved mainly light elements, up to mass number 27. As a next step, they decided to attempt transmutations with higher mass nuclides. During the last decade, Iwamura's group has laboriously carried out [45 to 50] a series of systematic experiments, using essentially the same experimental procedure described above, and investigated the occurrence of nuclear transmutation reactions with nuclides having Z values up to 56 and mass values up to 138 during D_2 gas permeation. The D_2 molecule appears to undergo "dissociative chemisorption" and diffuses through the solid complex in the form of deuterons. They have experimentally confirmed that permeation-induced transmutation reactions do not occur either on pure Pd foils or with complexes wherein MgO is used as a dopant instead of CaO. Thus, the presence of CaO in the environment seems to be absolutely essential. In all these experiments, deuterons are effectively captured always in multiples of 2, namely either 4, 6, or 8. It has also been established that the phenomenon occurs only at certain "hot spots" and that too within the top 100 μm layer of the surface. Iwamura's group has presented regular updates on their spectacular results at every one of the consecutive ICCF conferences held during the last decade. Since the experimental methodology and analytical techniques were essentially the same, we summarize below only the highlights of their more recent experiments and observations.

It was at Beijing in 2002 that Iwamura first presented [49, 50] the group's Cs to Pr and Sr to Mo transmutation results, which have been hailed as one of the turning points in the history of transmutation research in the LENR field. In these studies, a very thin layer of Cs or Sr was first

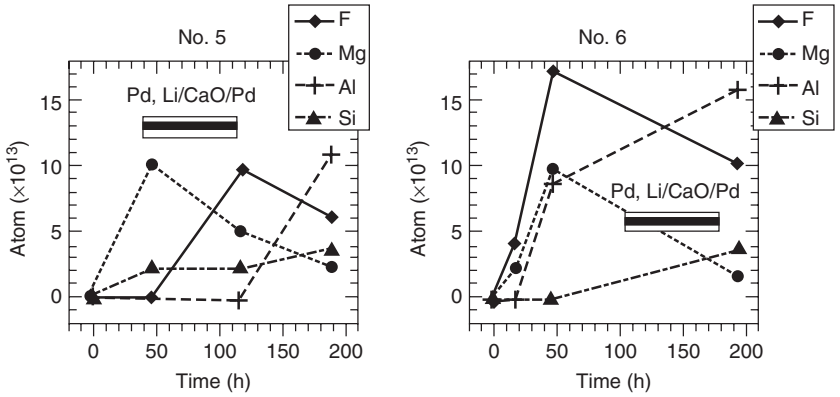

Figure 43.17 Time dependence of F, Mg, Al, Si, detected on the Pd, Li/CaO/Pd samples.

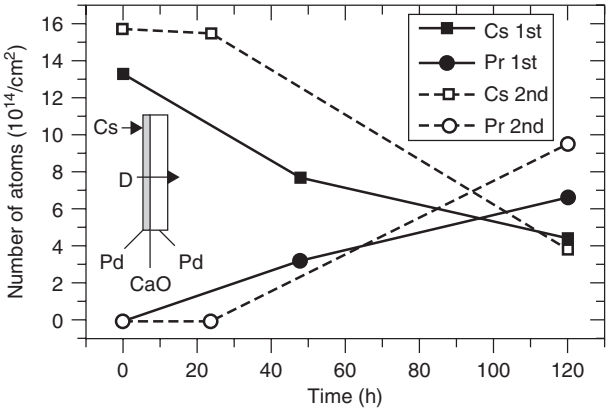

Figure 43.18 Time variation of Cs and Pr atomic density during D_2 gas permeation.

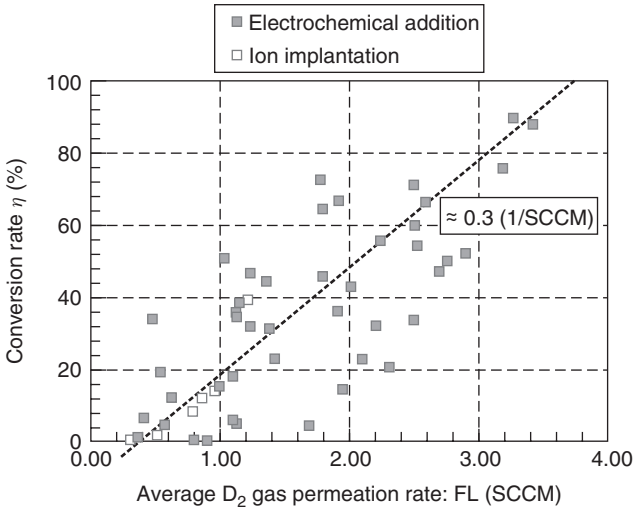

Figure 43.19 Correlation between D_2 permeation rate and conversion rate.

deposited on the Pd complex by an electrolytic method. (It took only 10 seconds for the Cs or Sr layer to be formed when electrolyzed in a very dilute solution of either $CsNO_3$ or $Sr(OD)_2$.) Figure 43.18 presents the time variation of the concentration of Cs and Pr during D_2 gas permeation. The gradual decrease of Cs concentration and gradual increase of Pr atom density is plainly visible. Note that there was no Pr present prior to permeation. The results of two runs are shown plotted in Figure 43.18, suggesting that the reproducibility of such experiments is reasonably good.

Ref. [45] gives the time variation of the XPS spectra for Cs, Pr, and Pd and shows that while the Cs peaks decrease and Pr peaks increase, Pd remains steady with time. These researchers have also experimentally established that in these permeation experiments the reaction rate correlates linearly with the flux of flowing deuterium atoms (see Fig. 43.19).

Similar results for Sr to Mo transmutation are presented in Figure 43.20. The only difference is that the permeation time for this study was 14 days because the transmutation rate was lesser for this reaction.

The following transmutation reactions corresponding to the above measurements are thought to occur:

$$_{55}Cs^{133} \rightarrow {}_{59}Pr^{141} \text{ and } {}_{38}Sr^{88} \rightarrow {}_{42}Mo^{96}$$

In each of these reactions, four deuterons are "effectively captured" by the initial test (or given) nuclide. Interestingly, the authors themselves do not specifically claim, anywhere in their papers, that the four deuterons are directly captured. As per their EINR theory, this reaction happens through an intermediate step of dineutron formation following electron capture by deuterons. But a detailed description of the theoretical conjectures of how such a complex reaction may be taking place is beyond the scope of this chapter.

The energy released in the above reactions, based on mass deficit calculations, works out to 50.3 MeV and 53.5 MeV respectively per reaction. This translates into an excess power of a few milliwatts for the amounts of new elements generated in their measurements and was well below the detection sensitivity of their calorimetry method. So they could not state whether any excess energy could have been generated. Iwamura has also categorically stated that they did not detect any x-rays or gamma rays during the permeation experiments, since they did in fact have an appropriate detector kept switched on and monitoring the setup during permeation.

As controls, they repeated the experiments with H_2 gas permeation and also with D_2 gas but with a pure Pd foil with no CaO-Pd multilayer complex present. In both cases, the Cs level did not change, nor was any Pr observed on the post-permeation samples.

For isotopic composition studies, the samples were taken out and analyzed using a SIMS and O_2^+ ions for bombardment of the sample. The mass resolution of the

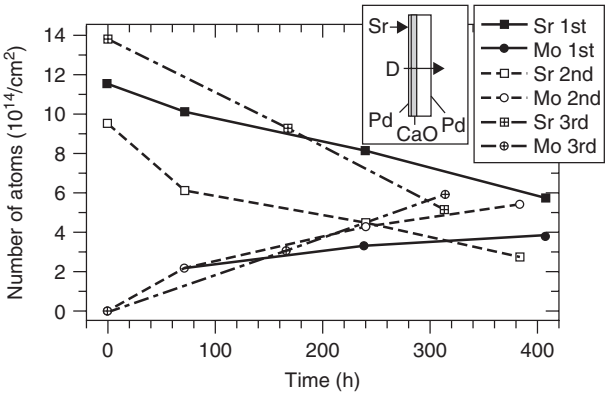

Figure 43.20 Time variation of Sr and Mo atomic density during D_2 gas permeation.

measurements was about 300. SIMS typically scans an area of 150 μm dia as compared to XPS, which analyzes a spot 5 mm in size. The authors have emphasized [45] that their SIMS analyses was performed by the "offset voltage technique" to suppress the effects of molecular ions on mass spectra. Thus, while the isotopic composition of the initial Cs as well as the bulk Pd corresponded to that of their natural abundances, the isotopic spectrum of the newly produced Mo was significantly different from natural abundance. In fact, it had a huge peak at mass number 96, exactly where one would expect it if it was generated from Sr^{88} capturing four deuterons.

At the ICCF 10 conference held in Cambridge, Massachusetts, in 2003, Iwamura presented [47] a yield vs. deuterium gas flow rate (or flux) correlation curve for the Cs to Pr transmutation reaction. The maximum gas flow rate achieved was close to 4 cm^3 per min. To obtain adequate permeation rates, the sample is maintained at an elevated temperature of 70°C. Although there was considerable scatter in the data, one could fit an approximate linear correlation, from which an estimate for the reaction cross-section was derived as 1 barn. Also, in the newer work, the Cs and Pr levels in the samples were measured by ICP-MS as well, making it the fifth technique of quantification of concentration levels, besides XPS, TOF-SIMS, XANES, and XRF.

However, the main innovation introduced this time was depth profiling of the Cs and Pr on the samples using TOF-SIMS. To facilitate this, the Cs layer deposition on the Pd foil complex was carried out by an ion implantation technique in order to obtain a controlled depth profile of Cs atoms in the target sample prior to permeation. Figure 43.21 presents the results of one such depth profile measurement before and after permeation. (In this figure the X-axis scale is indicated as sputtering time, but it was translated into depth through auxiliary calibration measurements. Thus, as shown at the top of the figure, 1000 secs corresponds to a depth of about 500A.)

It is seen that before permeation, the depth profile of Pr is flat at zero level, while Cs concentration steadily decreases with depth. The maximum penetration of the Cs ions into the sample was 500 A. After permeation, the level of Pr increases with the depth reaching a maximum at about 50 or 60 A, then falling back to zero beyond 100 A. Correspondingly, the Cs level has decreased, but only in the top 50 A or so. Beyond this depth there is no change in Cs concentration levels. This confirms that the transmutation of Cs into Pr takes place only on the top near-surface layers within a depth of 100 A.

At ICCF 11 held at Marseilles, France, in 2004, Iwamura presented results of the transmutation of $_{56}Ba$ into $_{62}Sm$, during which reaction six deuterons are effectively captured by Ba, resulting in the Z number increasing by six units and mass number increasing by 12 units. Barium has seven

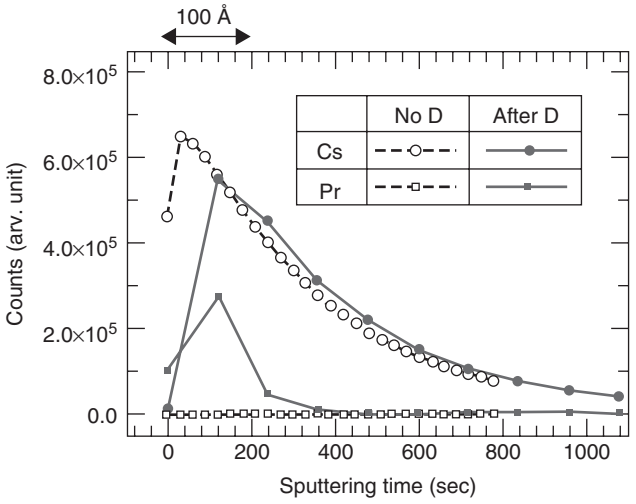

Figure 43.21 Depth profiles of Cs and Pr before and after permeation.

natural isotopes with masses varying from 130 to 138. But the most abundant Ba isotopes are Ba^{137}(11.3%) and Ba^{138}(71.7%). Sm too has seven natural isotopes ranging in mass from 144 to 154. This makes the interpretation of the results quite complicated. In spite of this, Iwamura's group carried out permeation studies with natural barium as well as with enriched Ba^{137} and Ba^{138} respectively. While the interpretation of SIMS data from natural Ba was somewhat complicated, as expected, they did find strong evidence to indicate that Ba^{137} yielded Sm^{149} while Ba^{138} produced Sm^{150}. Figure 43.22, reproduced from Ref. [48], shows the mass correlation between the starting and final elements on the surface of the foil complex. When Ba^{137} was used to start with, Sm^{150} was obtained, and when Ba^{138} was used, Sm^{149} was obtained; in each case the atomic number increased by six units while the mass increased by 12 units.

At ICCF 12 held in December 2005 at Yokohama, Iwamura presented results obtained using a significant improvement in the measurement technique [49]. He and his team used the powerful Spring 8 Synchrotron light source facility at Hyogo for carrying out *in situ* two-dimensional XRF spectrometry of the permeated samples for studying the surface distribution of the transmuted elements. Figure 43.23, shows the experimental setup. The test micro x-ray beam from the synchrotron is seen to enter the set up from the left side. Fresh Pd complex samples with either a Cs or Ba layer on top were prepared, and permeation was carried out *in situ* at the Spring 8 facility. The x-ray beam was filtered by a pair of rectangular slits to produce a square cross-section beam of 1 mm square. The Pd sample was mounted on an X -Y motion table operated by stepping motors. A microscope with camera permitted taking surface topography photographs of the portion being scanned by the XRF spectrometer. With this arrangement it

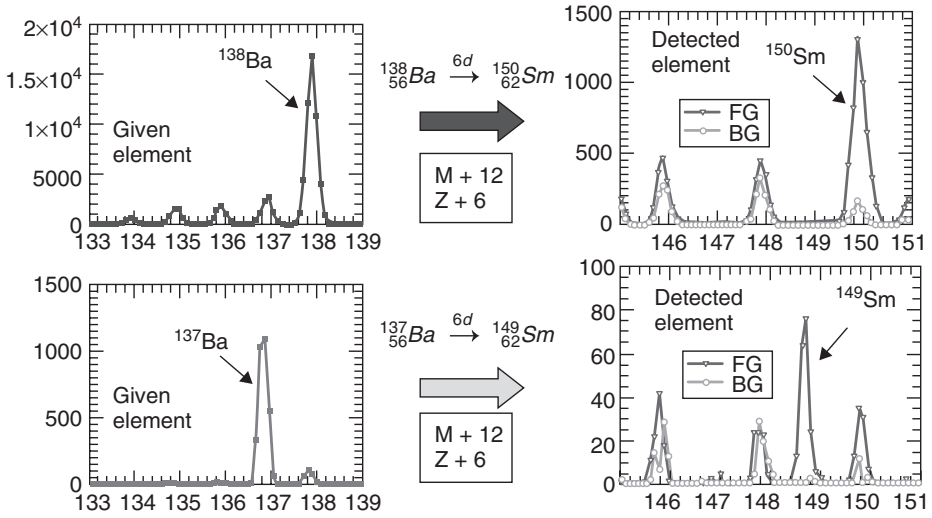

Figure 43.22 Mass correlation between the elements in the before and after permeation samples.

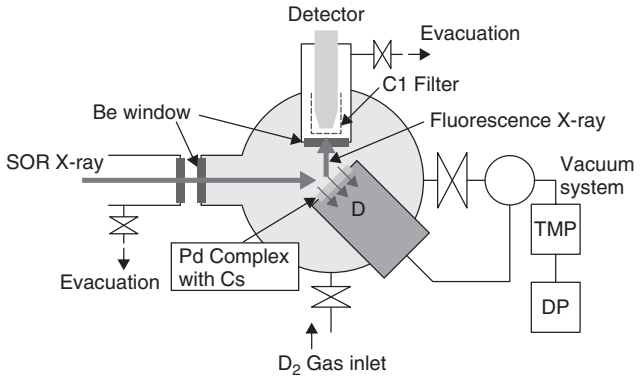

Figure 43.23 Experimental setup used by Iwamura at Spring 8 Synchrotron facility for *in situ* measurement of spatial variation of new element production during D_2 gas permeation.

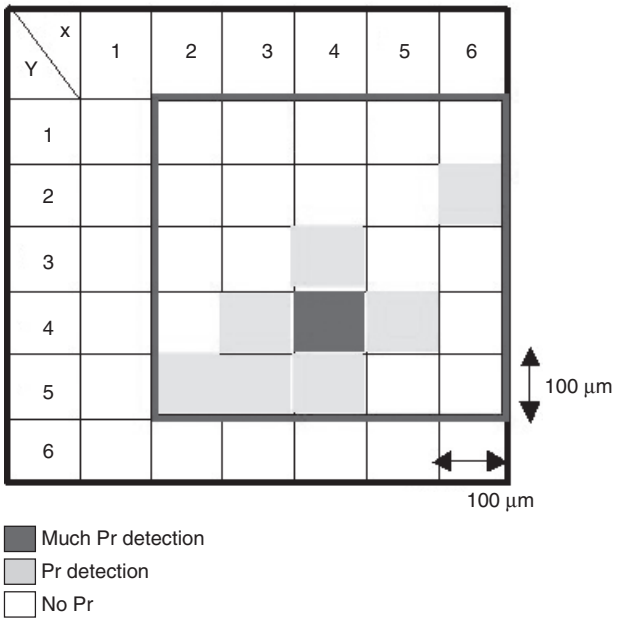

Figure 43.24 Mapping of surface distribution of Pr using 100-micron X-ray beam within a 500 micron square zone.

was possible to correlate the distribution of elements with the corresponding surface images. Figure 43.24 illustrates three neighboring 100 micron square regions where Pr content was high, medium and nil. Figure 43.25 presents the corresponding XRF spectra of Cs and Pr at these three selected spots.

The main observation to emerge from these studies was that Cs to Pr conversion does not take place all over the entire surface but only at highly localized "hot spots," something that has been observed by other LENR researchers also using diverse experimental procedures as described already in the present chapter.

The exhaustive decade-long experimental studies conducted by Iwamura's team under "clean conditions" employing sophisticated analytical methods has confirmed that complex multibody elemental transmutations do seem to be taking place when deuterons interact with certain metallic lattices. The observation that these reactions take place during the simple act of permeation of D_2 gas through specially prepared Pd multilayer complexes is a remarkable discovery. The fact that these reactions seem to occur only in selected spots on the near surface region corroborates similar observations of other researchers. Their finding that for these reactions to occur certain special additives such as CaO (and not MgO) besides the bulk metal Pd are required is a very significant hint regarding the nature of the Nuclear Active Environment (NAE).

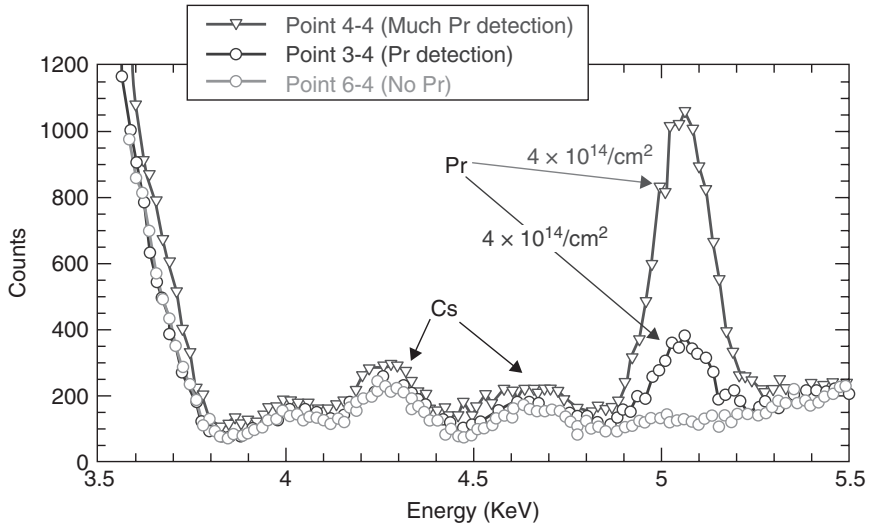

Figure 43.25 XRF spectrum of Cs and Pr at three selected points on surface using 100 micron x-ray probe of Spring 8 facility.

43.11 REPLICATION OF MHI PERMEATION EXPERIMENT BY OTHER GROUPS

Higashiyama and others of Osaka University were among the first groups to replicate the MHI D_2 gas permeation transmutation experiment [50]. The Osaka group started with multilayer Pd complexes (comprising substratum bulk Pd plate over which 1000 A thick alternate layers of CaO and Pd had been formed, topped off with a 400 A thick Pd film) supplied by the MHI group. They then deposited a thin Cs layer on the top surface by performing rapid electrolysis in 1 mM $CsNO_3$ solution by applying 1V electric field for 10 seconds. Prior to this, the top surface of the foil complex was pre-cleaned to get rid of any likely surface hydrocarbon contamination.

The Osaka group then carried out the D_2 gas permeation studies following the protocol provided by the MHI group. The Cs side of the foil complex was subjected to a D_2 gas pressure of 1 atm and the bulk Pd side was evacuated by a turbo molecular pump. The foil complex was maintained at a temperature of 70°C as recommended in the protocol. The MHI group had indicated that for obtaining successful results the gas flow rate has to be maintained at a level of at least 1 sccm (cm cube per min under standard conditions). To attain this, the temperature of the Pd foil complex had to be adjusted appropriately. To avoid moisture in the setup, they had to bake the chamber and flush it with N_2 gas. As they had not taken this precaution earlier, the gas flow rate in the first two runs was less than optimal.

It was only in the third attempt, which lasted over 120 hours, that they succeeded in obtaining the requisite gas flow rate of over 2 sccm. But unfortunately, by then they started running out of D_2, gas whose pressure steadily decreased, resulting in the flow rate falling to below 0.5 sccm. In spite of the experimental conditions not being ideal, production of Pr on the surface was confirmed in all three runs.

Elemental analysis was performed by two independent techniques, namely ICP-MS and Neutron Activation Analysis (NAA). The results of the ICP-MS analysis carried out at the MHI Labs is summarized in Table 43.2 below: The amounts of Cs and Pr measured after the permeation runs are given in the table. When there was more Cs present initially, more Pr was produced, and there was also more left over Cs.

The NAA analysis, which was performed at the Japan Atomic Energy Research Institute's 14 MeV Fusion Neutron Source facility, also confirmed presence of Pr in all three runs. For details, the original paper of Higashiyama et al. [50] may be referred to.

The replication experiment confirms that Cs^{133} is transmuted to Pr^{141} with mass number increasing by 8 and atomic number by 4. Takahashi, who is a co-author of this replication paper, has proposed a multibody resonance fusion model via formation of energetic Be^8 nuclei as an intermediate step for explaining this transmutation reaction [51].

43.12 CARBON ARC EXPERIMENTS

In this very simple experiment, the claim is that when an arc is struck between a pair of carbon rods dipped in water, by applying a voltage of some tens of volts, the powder debris that falls from the arcing region to the bottom of the vessel would contain significant amounts of iron as well as other metals in the Fe, Co, Ni region [52]. It was speculated

TABLE 43.2 Transmutation of Cs into Pr: Replication by Higashiyama et al. ICP-MS Results [54]

	Pr(ng)	Cs(nq)	Max Flow(sccm)	Average(sccm)	Minimum (sccm)
1st run	**18**	**180**	**173**	**0.93**	**0.43**
2nd run	**5.1**	**141**	**.61**	**.35**	**0.29**
3rd run	**36**	**330**	**2.17**	**0.76**	**0.27**

by these early researchers that the basic reaction involved could be a multibody heavy ion fusion reaction involving two carbon nuclei and two oxygen nuclei as follows:

$$2\{{}_6C^{12} + {}_8O^{16}\} \rightarrow \text{(intermediate compound nucleus)} \rightarrow {}_{26}Fe^{56}$$

$$\text{or alternately } 2\{{}_6C^{12} + {}_8O^{18}\} \rightarrow {}_{26}Fe^{56} + {}_2He^4 + 56.55 \text{ Mev}$$

As an intermediate step, an atom of oxygen and an atom of carbon may combine to generate ${}_{14}Si^{28}$, since in some experiments, presence of silicon in the debris has also been reported.

Historically, the credit for the "invention" of this process is attributed to George Oshawa [52] of Japan, who was a close friend of Michio Kushi; both were admirers of Louis Kervran during the early 1960s. The word "invention" is used here because it was not an accidental discovery, but rather a carefully crafted experiment with the objective of producing iron. It is reported that the first successful synthesis was carried out in 1964, and the mixture of elements that was so generated was found to contain some Ni and Co also, so the product was called "George Oshawa Steel." Arcing between the carbon rods is reported to have been successfully performed both in air and under water with comparable end results. Thus, the origin of this very simple transmutation experiment goes back almost a quarter of a century prior to the Fleischmann-Pons announcement and was inspired by the "Biological Transmutation" (discussed in the next section) works of Louis Kervran.

Roberto Monti has reported that he has independently verified the production of iron and other elements during the arcing of carbon several times [53]. It was after listening to a talk given by Monti at the Bhabha Atomic Research Centre (BARC) in Mumbai in 1992 that a group at BARC set up the experiment disbelieving and challenging Monti to demonstrate production of iron. But in the end, they confirmed finding iron in the debris [54]. Simultaneously, Sundaresan of BARC, who was a postdoctoral fellow at the Texas A & M University (TAMU) at that time, and Prof. Bockris also independently set up the carbon arc experiments and confirmed production of Fe at College Station [55]. (Both the BARC paper and TAMU paper were peer reviewed simultaneously and published in same issue of *Fusion Technology* in 1994.) At ICCF 7 held at Vancouver in 1998, Jiang et al of the Beijing University of Aeronautics and Astronautics reported finding Fe^{58} content increasing from its natural value of 0.3% to 0.5% and other elements such as Cr, Co, and Zn in the debris [56]. The enrichment of Fe^{58} isotope was deduced through Neutron Activation Analysis.

As an illustration of this simple experiment, we describe below the carbon arc studies conducted by Sundaresan and Bockris [55]. Figure 43.26 gives a schematic diagram of the experimental setup. The 6.14 mm dia, 300 mm long spectroscopically pure carbon rods were procured from Johnson Mathey and were certified to have an initial iron impurity content of ~2.0 ppm. (This was independently also verified by the experimenters.) The rods were mounted in a Pyrex glass trough as shown in the figure, with the tips being about 5 cm below the surface of the water. The voltage applied was typically ~10 V. The current drawn to strike the arc was initially higher but quickly settled to a steady value of between 5 and 15 A depending on various experimental factors. A simple manually operated screw-driven arrangement, as depicted in the figure, permitted re-adjustment of the gap between the tips in order to keep the arc sustained as the rods were consumed.

The ultra-pure distilled water was additionally passed through an ion exchange column to attain a resistivity of 13 MΩ. It was then further purified by percolating it through finely crushed carbon powder (made from same stock of carbon rods), so as to minimize the iron content

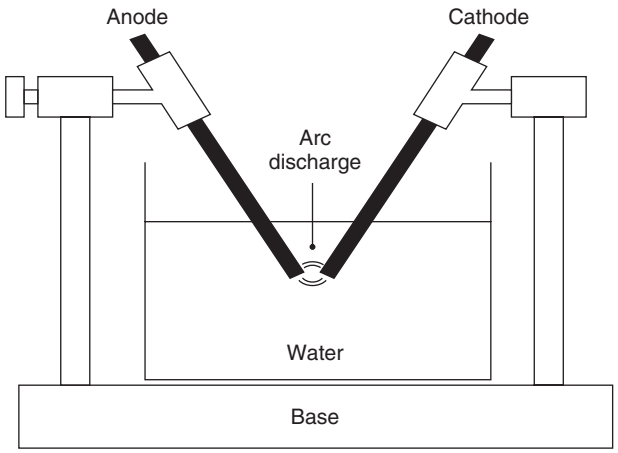

Figure 43.26 Schematic of carbon arc experimental setup.

of the water prior to commencement of the transmutation experiments.

Arcing under water was performed for a few hours until an adequate quantity of detritus accumulated at the bottom of the vessel. For each new run, a fresh set of carbon rods was deployed. In a second series of experiments with a given pair of rods, the collected powder was taken out every few hours for analysis; at this time the vessel water too was replaced. This way it was possible to study the variation of the quantum of iron formed with time duration of arcing.

The Fe content in the detritus powder was measured by a standard spectrophotometer method using a Perkins Elmer Lambda instrument. This technique measures the optical density of a solution of a colored complex of iron thiocyannate at 470 nm wavelength. Calibration was done using standard solutions having known iron content. The results of the first series of 14 runs are summarized in Table 43.3.

It is seen that the iron concentration in the detritus powder varies in the range of 30 to 167 ppm, which translated to several tens of μg of total Fe production in each run, or an average the rate of about 4 to 5 μg of Fe per hour of arcing. The second series of runs indicated a nominally linear correlation between duration of arcing and total quantity of iron generated. Electrode pair No. 3, which was subjected to arcing for a total of 10 hours, yielded altogether about 40 μg of Fe.

Before concluding that nuclear transmutation reactions were indeed responsible for the generation of iron, the authors did consider other possible modes of "adventitious" entry of iron into the system. First, ingress of iron from the water was ruled out since the total content of iron in the entire inventory of water in the trough was calculated to be well below the amounts detected in the debris. Alternately, it may be suggested that the entire initial content of iron in the carbon rods could have diffused to the tips of the rods and accumulated in the powder debris collected at the bottom of the vessel. Since the rods are immersed in water, their temperature is well under 100°C, except for the very small portion near the tips, which could have been close to say a 1000°C. ("The rods were cool to touch at distances beyond 2 cm from the tip.") Even at 100°C, the diffusion coefficient of iron in carbon is so low (10^{-26} cm^2 sec^{-1}) that the diffusion-concentration mechanism cannot be attributed to be the source of the iron measured in the debris.

Interestingly, the authors found that when the arcing was carried out with nitrogen gas dissolved in the water in place of oxygen, no additional Fe was detected in the debris. This experiment thus not only ruled out the diffusion-concentration theory but also supported that oxygen is indeed necessary for the generation of iron as suggested by the multibody transmutation reaction proposed by the original proponents of this experiment.

Sundaresan et al. have also pointed out in their paper that the average rate of iron production, namely 5 μg/hr, implies a nuclear heat production of 135 watts, assuming 55.65 Mev per atom of Fe generated. This is to be compared with an electrical power input of between 50 to 150 W, depending on the steady current level. Following simple external heating calibration, they did have indication of detectable "excess heat." The authors have recorded that, in general, overheating of the water was indeed a problem, requiring them to periodically stop the arcing in order to allow the water to cool down and thereby avoid reaching near boiling temperatures.

TABLE 43.3 Table III of Sundaresan's Paper [55]

Experiment Number	Weight of Carbon Detritus (mg)	Iron Content (μg)	Iron in Carbon (ppm)
1	269	45	167
2	116	—	—
3	167	—	—
4[a]	361	45	125
5[a]	103	15	146
6	231	—	—
7	192	11	57
8	183	5.5	30
9	163	13.5	80
10	143	—	—
11	138	—	—
12	130	5.5	42
13[a]	471	53	112
14[b]	477	196	410

[a] Same rod.

[b] This value and the last value in Table 1 are abnormally high, and the analyses were performed on the same day; it is possible that an instrument malfunction might have caused the error.

43.13 VYSOTSKII'S MICROBIAL TRANSMUTATION STUDIES

This section discusses the remarkable "Microbial Transmutation" experiments conducted during the last decade by Vladimir Vysotskii and his collaborators at Kiev, Ukraine, which confirm that certain biological entities such as microbes are able to catalyze nuclear transmutation reactions [57, 58] under certain special conditions. Vysotskii's experiments have a great bearing on the prospects of converting radioactive nuclear waste into stable products and so deserve careful scrutiny.

The origin of the concept of "Biological Transmutations" in fact goes back to the 1960s, decades before the Fleischmann-Pons effect became known, when Louis Kervran of France published three books pertaining to this topic. An English version of Kervran's books became available in 1972 [59]. In his works, Kervran had

exhaustively compiled previous experimental publications and scientific reports that indicated that non-radiative elemental transmutations might be occurring in plants, animals, and indeed even human beings. Over a century ago, keen observers had been puzzled by the fact that hens lay dozens of eggs that contain a lot of calcium, but the food eaten by the hens (mostly mica) did not appear to contain the requisite amount of calcium content. During 1799 to 1815 Vauquelin analyzed the excreta of hens and found that there is more Ca in it than in the oats fed to them. In 1822 an English physiologist by the name of Prout reported incinerating and analyzing freshly hatched chicks to find that the ash contains more Ca than present in the eggs from which the chicks hatch. These reports suggested that the following nuclear reaction possibly takes place in these biological systems:

$$_{14}Si^{28} + _{6}C^{12} \rightarrow _{20}Ca^{40}$$

During the second half of the 19th century, several workers, notably Herzeele, reported through carefully conducted experiments that while seeds germinate, there is a change in their trace element composition through elemental transmutations. Prof. Baranger of the Ecole Polytechnic in Paris has claimed [60] that he has independently repeated and confirmed Herzeele's experiments. Baranger states that seeds of "cerdagne vetch" growing in distilled water showed no change in phosphorus or potassium content, but when germinated in a calcium chloride solution, they showed an increase of phosphorus or potassium content by over 10%.

Kervran himself repeated the germinating seeds experiments and has reported [59], from analysis of 840 seeds and 403 sprouts, finding strong evidence for $_{19}K^{39}$ (potassium) absorbing a proton to yield $_{20}Ca^{40}$ during germination.

It is seen from Figure 43.27 that the decrease in the amount of potassium (33 mg) is approximately equivalent to the increase in quantity of calcium (32 mg).

In a another experiment Kervran placed "tench" fish in a tank of water containing 1.4% sodium chloride (NaCl) solution for four hours and found that the concentration of KCl in the blood of the fish increased by 66% and that in the tank from 3.95 g/l to 5.40 g/l, suggesting the occurrence of the following transmutation reaction:

$$_{11}Na^{23} + _{8}O^{16} \rightarrow _{19}K^{39}$$

Kervran's book is full of such very interesting examples. Unfortunately, many of the quoted experimental studies were not published in mainstream peer-reviewed physics journals, and the scientific community, especially the nuclear physicists, never took these "claims" seriously since occurrence of such transmutation reactions is not possible as per contemporary knowledge of nuclear physics.

During the period 1967 to 1992, Komaki of Japan had conducted several experiments, some of them jointly with Kervran [61 and cross-references therein] that indicated the occurrence of nuclear transmutation reactions in nutrient cultures in which certain micro-organisms thrive. These investigators determined the amounts of potassium, magnesium, iron, and calcium in the dried cells of selected micro-organisms such as *Aspergillus niger, Penicillium chrysogenum*, etc., cultured in normal media as well as media deficient in one of the test elements such as potassium, magnesium, iron or calcium. Komaki has specifically mentioned [60] that these experiments, which were carried out under more controlled conditions than previously, were quite reproducible.

Vysotskii was inspired by the experiments of Kervran and Komaki but was unhappy that they had not analyzed the isotopic composition of the newly formed elements because this would have partly answered the criticisms of the skeptical nuclear physicists. By the time Vysotskii entered the field, in the early 1990s, high-resolution mass spectrometers capable of identification of individual nuclides became more commonly available. He therefore set about conducting a fresh set of meticulously planned experiments, aimed at measuring the isotopic composition of the newly formed chemical elements.

To begin with, Vysotskii identified the following nuclear reaction for investigation [62]:

$$_{25}Mn^{55} + _{1}d^{2} \rightarrow _{26}Fe^{57}$$

He categorizes this reaction as an example of transmutation of "light and intermediate" isotopes. He selected the Fe^{57} isotope not only because iron is an integral part of most living organisms, but because it is a rare isotope whose abundance in natural iron is only 2.2%. More importantly, the detection of the Fe^{57} isotope can be carried out

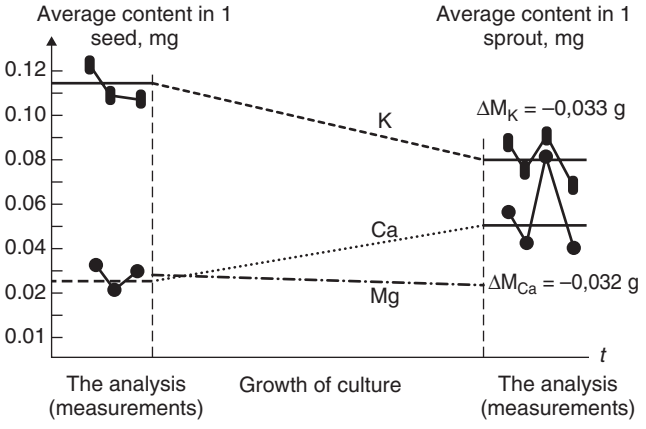

Figure 43.27 Changes in K and Ca content following sprouting of seeds.

very simply and elegantly using the Mossbauer technique. Vysotskii proceeded to attempt synthesis of Fe^{57} through the above reaction in biological systems. He selected several different bacterial cultures as well as a culture of yeast for initial tests. One culture in which he was particularly interested was *Deinococcus radiodurans* M-1 because this culture is known to withstand high radiation doses. (The motivation for choosing this will become apparent later in this chapter.) Other micro-organisms were selected because of their known ability to multiply in cultures containing heavy water.

After preliminary treatment, the cultures were placed in a dish containing standard salt-sugar nutrient medium, incorporating various salts such as Mg, S, Ca, K, etc., and heavy water. Control studies were initially done in a medium containing only light water. For transmutation, $MnSO_4$ salt was added. Natural manganese comprises of only one stable isotope, namely Mn^{55}, thus rendering the interpretation of the results unambiguous. Before commencement, the Fe^{57} content of all the dry ingredients used in the cultures were analyzed using Mossbauer spectroscopy, and it was confirmed that the initial Fe^{57} content in all cases was below detection limit. There were in all four experimental flasks, three of which served as controls. The culture growth periods were 24, 48, or 72 hours. The temperature of the flasks was maintained at 32°C by a thermostat, and the flasks were kept continuously stirred.

At the end of the growth period, the biological substances were separated in a centrifuge, rinsed in distilled water, dried, and then ground to powder. A small portion (~0.3 g) of this was tested in the Mossbauer spectrometer using standard Mossbauer spectrometry procedures. It was found that only the fourth flask, which contained both Mn and D_2O, indicated presence of Fe^{57}.

Vysotskii then selected the following transmutation reaction representing "middle range atomic numbers" for study, deploying the microbiological culture known as *Bacillus subtilis*.:

$$_{11}Na^{23} + {}_{15}P^{31} \rightarrow {}_{26}Fe^{54} + 22.4\text{Mev}$$

Both the reacting nuclides occur in nature as single isotopes while the reaction product is a low natural abundance (5.8%) isotope of iron. He placed the microbial culture in a nutrient medium that was deficient in iron and then added controlled quantities of sodium in the form of $NaNO_3$ and phosphorus in the form of K_2HPO_4. There were two identical flasks in which all ingredients were same except that in one there was no phosphorus additive. The quantity of Fe^{54} generated was measured using mass spectrometry. The isotopic ratio of (Fe^{54}/Fe^{56}) increased from its natural value of 0.06 to about 0.20 to 0.25 in various repeat experiments. The details of the experiment and results are described in ref. [63].

Vysotskii has performed a large number of auxiliary experiments to determine how the yield of these biological transmutation reactions can be improved. His new 2009 book [58] discusses the biotechnology approaches adopted by him for this purpose in great detail. The main lesson learnt by him was that instead of using "one-line" cultures, if a mixture of a large variety of cultures are deployed, the transmutation yield improves substantially. To achieve this, he has invented what he calls a "Microbial Catalyst Transmutator" (MCT). The MCT is composed of special granules of concentrated biomass of metabolically active micro-organisms, sources of energy and nutrients such as N, C, P, and others bound together by a gluing substance that keeps all compounds in the granules stable in water solutions for long times under any external conditions. The basis of the MCT is microbes' syntrophin associations, which contain thousands of varieties of micro-organisms that are in a state of complete symbiosis. These organisms represent different physiological groups displaying a very wide variety of microbe metabolism and accumulation mechanisms. According to Vysotskii, the state of complete symbiosis of the syntrophin associations is the key feature that is responsible for maximum adaptation to external environment.

Vysotskii has repeated the Fe^{57} generation experiment using MCTs in place of the single species microbes use by him earlier. Figure 43.28 shows the Mossbauer spectrum of the Fe^{57} so generated.

The quantum of Fe^{57} present was also independently confirmed using Thermal Ion Mass Spectrometry (TIMS). The results of the TIMS measurement are summarized in Table 43.4. The decrease in the amount of Mn^{55} approximately matches the increase in amount of Fe^{57} in the

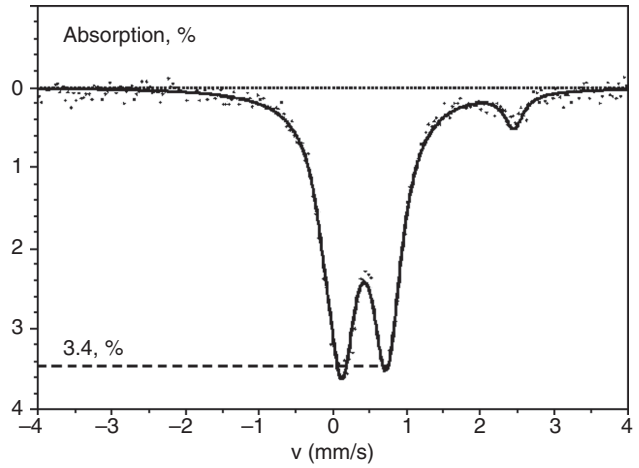

Figure 43.28 Mossbauer spectrum of the Fe^{57} generated in presence of D_2O and Mn^{55} using MCT granules.

TABLE 43.4 Mass Spectrometric Measurements of Fe^{56}/Fe^{57} Isotopic Ratios in Control and Transmuted Cultures [64]

Isotope (natural concentration)	Natural Isotopic Ratio (in relation to Fe^{56})	Concentration in Dried Biological Substance in Control Experiment: $H_2O + MnSO_4$ +*nutrient medium*	Isotopic Ratio in Control Biological substance	Concentration in Dried Biological Substance in Experiment on Transmutation $D_2O + MnSO_4$ +*nutrient medium*, (normalized)	Isotopic Ratio in the Experiment on Transmutation
Mn^{55}, 100%	_	0.15 ± 0.012	$Mn^{55}/Fe^{57} = 6.6$	0.13 ± 0.012	$Mn^{55}/Fe^{57} = 7.7$
Fe^{56}, 91.7%	1	1	1	1	1
Fe^{57}, 2.2%	$Fe^{56}/Fe^{57} = 41.7$	0.024 ± 0.002	$Fe^{56}/Fe^{57} = 42.5$	0.051 ± 0.003	$Fe^{56}/Fe^{57} = 19.5$

powder of the transmutation flask. Also it may be seen that the (Fe^{56}/Fe^{57}) isotopic ratio has decreased from the natural iron value of 41.7 to 19.5. These results clearly confirm the occurrence of nuclear processes in these microbiological cultures.

Vysotskii then turned his attention to the possibility of transmutation or "accelerated deactivation" of a "heavy mass" radioactive nuclide such as Cs^{137} using the MCT approach. But prior to tackling radioactive Cs^{137}, he first developed the procedures using Cs^{133} and verified that the following reaction does take place in microbial cultures [58]:

$$Cs^{133} + p^1 \rightarrow Ba^{134} + 8.3 \text{ Mev}$$

However, details of this study are not discussed in this review. Instead, the Cs^{137} study [64] is discussed in more detail because it has great relevance to the problem of deactivation of radioactive waste for the nuclear industry.

Cs^{137} decays with a half life of ~30 years, emitting a 661 Kev gamma ray in the process. Vysotskii started with 20 Kbq of Cs^{137} dissolved in distilled water. 10 ml each of this active water was transferred into each of 8 thin-walled closed glass vials. The eighth vial served as a control, and no other ingredient was added into it. In each of the other seven vials he added the same quantity of MCT granules. The seventh vial also served as control because no nutrient salt was added in it. In the remaining six vials, one of the following six salts was added into the active water: K, Ca, Na, Fe, Mg, and P. These additive elements are vitally necessary for the cultures to grow. According to Vysotskii's hypothesis "each of these specific additives completely blocks all transmutation channels in which any of the biochemical analogs of the specific chemical element can be used [58]; this blockage is a consequence of the need to attain an optimal balance of micronutrients."

The cultures were grown at a temperature of 20°C for 45 days. Every seven days, the activity of the closed flasks was counted in a low background Ge gamma counting system sitting on the 661 kev peak. Figure 43.29 displays the results of this experiment.

It is seen that the activity of the seventh vial, which contains only active water and MCT (no salts), follows the natural 30-year half-life decay rate, whereas the fastest decay corresponding to a half-life of 310 days occurs for the vial containing $CaCO_3$ as additive. This means the decay rate has been speeded up by a factor of 35 times. However,

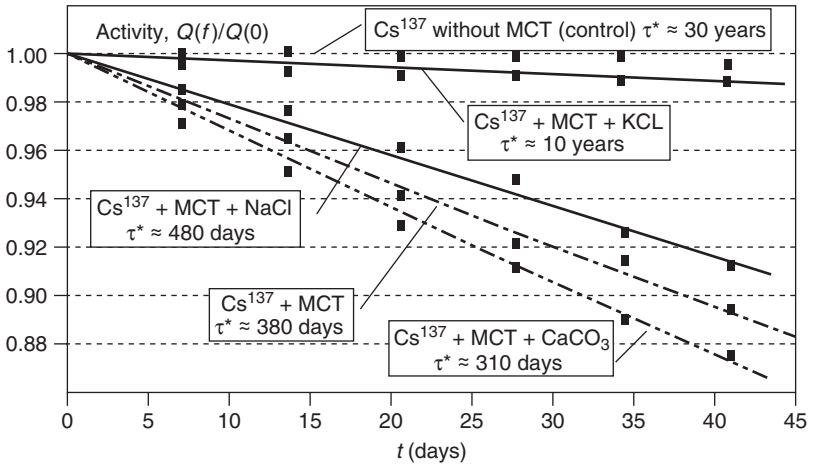

Figure 43.29 Accelerated decay of Cs137 isotope in "biological cells" in presence of different chemical elements.

it is to be noted that all the six salts did result in speeding up the decay to a greater or lesser extent.

Vysotskii hypothesizes that the following exhothermic proton capture reaction occurs in all six vials where there was some "nutrient salt" besides the MCT granules, resulting in stable Ba^{138}:

$$Cs^{137} + {}_1p^1 \rightarrow Ba^{138} + \Delta E(5.58\ \text{Mev})$$

In references [58 and 64], the author has offered his explanation as to why the speed-up rate for transmutation is better when the concentration of Ca is increased.

In general, Vysotskii theorizes that for optimal growth of microbial cultures, a balanced mix of trace elements is essential. A deficiency of even one of the required elements hinders the growth of the entire biological object. According to Vysotskii, the phenomenon of occurrence of transmutation of chemical elements and isotopes in biological systems is based upon the heuristic proposition that if some of the essential elements are not present in the environment (in this case, the nutrient medium), then, *provided certain prerequisites are met*, these elements will be synthesized through appropriate nuclear transmutation reactions. Vysotskii has arrived at such a proposition following more than a decade of experimental investigation of the topic of biological transmutations. His new book [58], presents a detailed exposition of his experimental findings and theoretical conjectures.

Needless to emphasize, Vysotskii's works are of great relevance to the urgent task of dealing with the problem of radioactive waste generated by nuclear power stations. His microbial transmutation technique appears to have great promise and deserves study and replication.

43.14 SUMMARY AND CONCLUSIONS

A brief summary of the major experimental investigations and results in the LENR field pertaining to the occurrence of a gamut of nuclear transmutation reactions in simple experimental configurations has been presented. There are, in fact, many more such studies that could not be covered in this chapter due to space constraints. For purposes of completeness, we reproduce as Appendix A an exhaustive updated tabulation of 101 transmutation experiments compiled by Storms and given initially in his book [7], which includes most of the major studies that we have discussed so far.

The sheer variety of experimental approaches in which transmutations have been reported rules out the probability that experimental artifacts could be responsible for erroneous interpretation of the observations and compels us to take serious note of the results, notwithstanding the fact that the presently accepted understanding of nuclear phenomena does not provide any scope at all for such reactions to take place. However, in view of the deep implications of the claim that nuclear transmutation reactions can and do occur in simple experimental configurations (almost validating the age old claims of alchemy!), it is absolutely imperative that some of these very simple experiments be replicated by groups outside of the limited LENR community, enabling critical evaluation by a wider section of the scientific community and leading to eventual publication and endorsement by mainstream journals. The purpose of the present chapter is precisely to encourage such an effort.

A careful scrutiny of the reported results brings out some insightful features [65]. During transmutation, the atomic weight and atomic number of some of the nuclides present in the reaction environment appear to have increased in "multiples of several deuterons." In addition, isotopes having a fraction of the atomic weight (and atomic number) of the initial nuclei present in the experimental zone are detected in post-experimental samples, suggesting that perhaps some large-sized nuclei may have "fissioned" into smaller nuclear fragments. These features are evident in Figure 43.30, which illustrates the number of occasions wherein various elements have been observed on the surface of the Pd cathode following electrolysis in a D_2O-based solution. Also, the presence of Au ($Z = 79$) and Pb ($Z = 82$) at the higher atomic number end appears to be attributable to multiple deuteron captures in Pt ($Z = 78$), which is obviously sourced from the anode material.

Figure 43.31 gives the Z vs. A representation of the stable isotopes of elements (shown as dots) in the $Z = 46$(Pd) to $Z = 55$(Cs) region, extracted from a standard periodic table of elements. The X-axis represents the atomic weight while the Y-axis gives the atomic number. All combinations of Z and A, other than that shown as dots, are unstable and would imply radioactive nuclides. Since in LENR experiments, radioactive products have seldom been observed, only the stable isotopes represented by the dots are relevant to our discussions. The three straight lines emanating from the dot corresponding to Pd^{110} nuclide indicate how the Z vs. A plot will vary if a series (or clusters) of protons, deuterons or neutrons are captured by Pd^{110} nucleus.

Addition of a single neutron to Pd^{110} would hypothetically lead to formation of radioactive Pd^{111}, which is a beta emitter with a 23.4 min half-life. Further addition of neutrons would result in beta emitters with even shorter half-lives. Decay of these isotopes would lead to other radioactive species, until the decay chain terminates in a stable end product nuclide. Given that the vast majority of the well-instrumented LENR experiments have been performed in aqueous electrolytic cells, beta emissions from cathodes in LENR experiments would be very difficult to detect as they would not travel out beyond the electrolyte; hence, they would not be detectable.

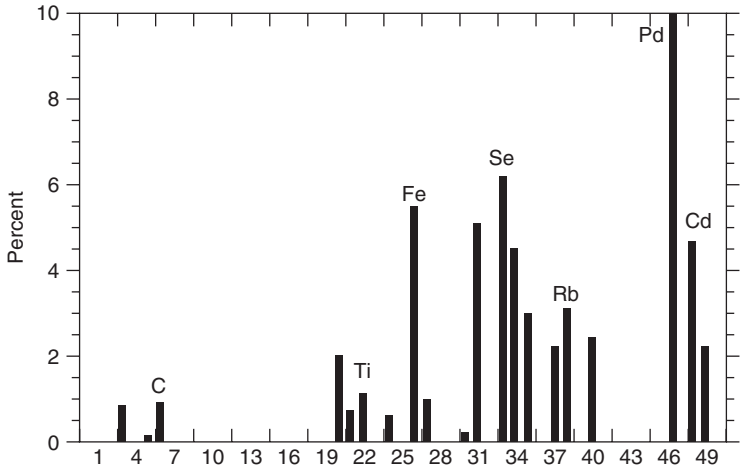

Figure 43.30 Frequency of observation of elements on surface of Pd cathodes after electrolysis in D_2O-based electrolytes.

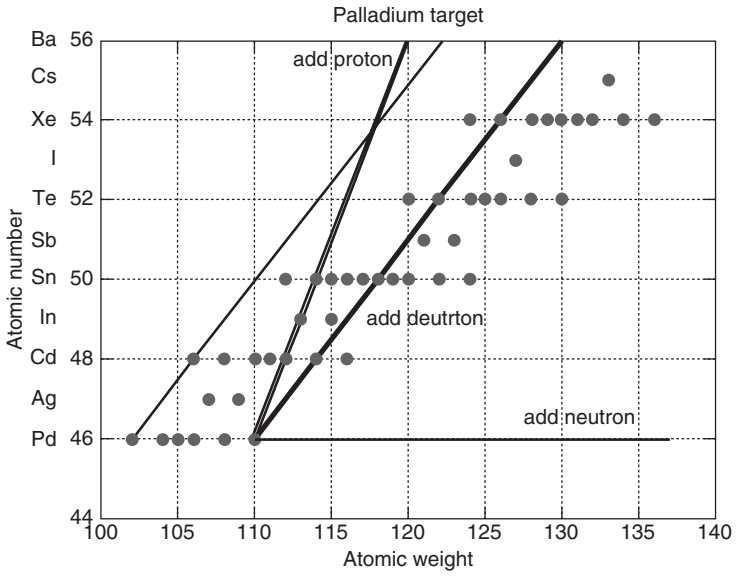

Figure 43.31 Isotopic compositions of stable elements with $Z \geq 46$ (Pd) shown as dots and the effect of adding one or more protons, deuterons, or neutrons to the Pd^{110} nucleus.

If we next follow the line marked "add proton" in Figure 43.31, we note that sequential addition of several protons to Pd^{110} can lead only to a few stable elements with tin (Sn) being the heaviest. Beyond that, one again ends up in radioactive isotopes that are not observed.

Therefore, hypothetically, only the addition of one or more deuterons seems to enable the full range of observed *stable elements* to be synthesized, at least in Pd-D_2 experiments. Note also that, in general, stable isotopes are produced only when even numbers of deuterons are added. In this context, the remarkable observations of Iwamura et al. during D_2 gas permeation studies discussed earlier are relevant. It may be recalled that these authors had found, during transmutation studies involving single nuclides, always only even numbers of deuterons, namely 4, 6, or 8 deuterons, were added and that too in such a manner that radioactive isotopes were not formed. However, we do recognize in electrolysis experiments that palladium is not the only target nucleus available; platinum, lithium, silicon, oxygen, and possibly a few impurity atoms also are present on the surface of the cathode where transmutation products are formed. This complicates the task of theoretical interpretation of these processes.

The newly emergent science of Low Energy Nuclear Reactions (LENRs) is thus wide open and indeed offers exciting challenges and opportunities to the future generation of nuclear scientists!

APPENDIX: SUMMARY OF EXPERIMENTAL STUDIES IN WHICH NUCLEAR TRANSMUTATION REACTIONS HAD BEEN REPORTED AS OF 2007

(Reproduced from Edmund Storms' book [7])

Source	Substrate	Environment	Method	Detected
Wang et al. [66]	Pd	$H_2SO_4 + D_2O$	electrolytic	Ag,Ni,Fe,Ti,S,Pt
Wang et al. [66]	Ti	$H_2SO_4 + D_2O$	electrolytic	Ag,Ni,Fe,Ti,S,Pt
Szpak et al.[67, 68]	Pd	$LiOD + D_2O$	electrolytic	Si,Mg,Zn,Ca,Al
Savvatimova et al. [69]	Ti	D_2 gas	plasma	Al,Mg,Br,Sr,Rb,S,F,O,Ni,Cr, Fe,Sn (isotope ratio change)
Mizuno et al. [70]	W	$K_2CO_3 + H_2O$	plasma	Ca,Fe,Zn
Lochak and Urutskoev [71]	Ti	H_2O	fuse	Na,Mg,Al,Si,K,Ca,V,Cr,Fe,Ni, Cu,Zn
Karabut [72, 73]	Pd	D_2 gas	plasma	Li,C,N,Ne,Si,Ca,Fe,Co,Zn, As, Ag,Cd,In (isotope ratio change)
Focardi [74]	Ni	H_2 gas	ambient	Cr,Mn
Cirillo and Iorio [75]	W	$K_2CO_3 + H_2O$	plasma	Re,Os,Au,Hf,Tm,Er,Y
Celani et al. [76]	Pd	C_2H_5OD+ Th,Hg	electrolytic	Cu,Zn,Rb,Cs,Pb.Bi
Campari [77]	Ni	heated H_2 gas	ambient	Na,A,Si,S,Cl,K,Ca,Fe,Zn
Yamada et al. [78]	Pd	H_2 gas	diffusion	Ti,Cr,Mn,Fe,Ni,Cu,Ag
Violante et al. [79]	Ni	D_2O	electrolytic	Cu (isotope ratio change)
Passell [80]	Pd	D_2 gas	plasma	Pd isotope change, Co,Zn,Au,Ir
Ohmori et al. [81]	Re	$K_2CO_3 + D_2O, H_2O$	plasma	K (isotope ratio change)
Celani et al. [82]	Pd	C_2H_5OD + Th,Hg,Sr	electrolytic	Sr → Mo (isotope ratio change)
Violante et al. [83]	Ti	$D_2O + Li_2SO_4$	electrolytic	Zn,Cu,Ag (isotope ratio change)
Yamada et al. [84]	Pd	$H_2O + Na_2CO_3$	electrolytic	Li,B,Mg,Al,K,Ca,Ti,Cr,Mn, Fe, Co,Ni,Cu,Zn,Ba,Pb (isotope ratio change)
Warner et al. [85]	Ti	$D_2O + H_2SO_4$	electrolytic	Au
Vysotskii et al. [86]		Cs	biological	Ba
Matsunaka et al. [87]	Pd	D_2O	electrolytic	Fe,Zn
Karabut [88]	Pd	D_2 gas	plasma	C,Ca,Ti,Fe,Co,Zn,As,Ag,Cd (isotope ratio change)
Iwamura et al. [89, 90]	Pd	D_2 gas	diffusion	Cs → Pr, Sr → Mo
Goryachev [91]	Ni	27 MeV electron	bombard	Ni → Rh
Di Giulio et al. [92]	Pd	PdD	laser	Ca,Fe,S,Zn,Ti,Cu,Cr
Arapi et al. [93]	Pd	D_2 gas	plasma	Li,Be,Fe,Ni,Cu,Ba
Yamada et al. [94]	Pd	D_2 gas	plasma	Fe,Cu
Warner and Dash [95]	Ti	$D_2O + H_2SO_4$	electrolytic	Cr
Wang et al. [96]	TiH	H^+	bombard	He^4
Vysotskii et al. [97]		Na, P	biological	Na + P → Fe
Passell and George [98]	Pd	D_2 or D_2O	electrolytic	Zn
Nassisi and Longo [99]	Pd	PdD	laser	Zn
Mizuno et al. [100]	W	$K_2CO_3 + H_2O$	plasma	Al,Si,Ca,Ti,Cr,Fe,Ni,Zn,Ge, Pd,Ag,In
Li et al. [101]	Pd	$Pd + D_2O$		Ni
Iwamura et al. [102]	Pd	D_2gas + C	diffusion	Mg,Si,S
Iwamura et al. [102]	Pd	$LiOD + D_2O$	electrolytic	F, Al, Si

Source	Substrate	Environment	Method	Detected
Hanawa [103]	C	H_2O	plasma	Si,S,Cl,K,Ca,Ti,Cr,Mn,Fe,Co, Ni,Cu,Zn
Dufour et al. [104]	Pd	H_2 gas	plasma	Mg,Zn,Fe
Castellano et al. [105]	Pd	PdD	laser	Na,Mg,Al,P,S.Cl.Ca,Ga,Fe, Ni,Zn,Cu,Sn
Campari et al. [106]	Ni	heated H_2 gas	ambient	F,Na,Mg,Al,Si,P,S,Cl,K,Ca,Cr, Mn,Fe,Cu,Zn
Bernardini et al. [107]	Ti	$K_2CO_3 + D_2O$	electrolytic	Sc (radioactive)
Ransford [108]	C	H_2O	plasma	Fe,Cr
Ohmori and Mizuno [109]	W	$Na_2SO_4 + H_2O$	plasma	Cr,Fe,Ni,Re,Pb
Focardi et al. [110]	Ni	heated H_2 gas	ambient	C,O,Mg,Si,K,S,Cl,Al, Na,Fe,Cu
Klopfenstein and Dash [111]	Ti	$D_2SO_4 + D_2O$	electrolytic	Al.S,Ca,Fe (Ti isotope change)
Qiao et al. [112, 113]	Pd	D_2	ambient	Zn
Ohmoi et al. [114]	Au	Na_2CO_3 or $Na_2SO_4 + H_2O$	electrolyte	Hg,Kr,Ni,Fe,Si,Mg (isotope change)
Ohmori and Mizuno [115]	W	$K_2CO_3 + H_2O$	plasma	Ni,C,Fe,Cr,Pb (isotope change)
Notoya et al. [116]	Ni	$K_2CO_3 + H_2O$	electrolytic	Os,Ir,Pt,Au,K
Nassisi [117, 118]	Pd	H_2, D_2 gas	XeCl laser	**Al**,Au,C,Ca,Cl,Cr,**Fe**,K,Mg,Na, Nd,Ni,V,Zn,O,S,**Si**, delayed n
Jiang et al. [119]	Pd	$NaOD + D_2O$	electrolytic	Mg,Al,Si,Fe,Cu,Zn,Pt
Jiang et al. [120]	C	H_2O	plasma	Fe
Iwamura et al. [116, 120]	Pd	$LiOD + D_2O$	electrolytic	Ti,Cu,Fe (isotope change)
Nakamura et al. [113]	Ni, (C anode)	$(NH_4)_2MoO_4 + H_2O$	plasma	radioactivity
Ohmori et al. [124]	Au	Na_2SO_4, K_2SO_4, K_2CO_3, KOH $+ H_2O$	electrolytic	Fe (isotope change)
Qiao et al. [125]	Pd	H_2	ambient	Zn,Tb
Kopecek and Dash [126, 127]	Ti	$H_2SO_4 + D_2O$	electrolytic	S,K,Ca,V,Cr,Fe,Ni,Zn
Ohmori and Enyo [128]	Au, Pd	$Na_2SO_4 + H_2O$	electrolytic	Fe (isotope change)
Yamada et al. [129]	Pd	D_2 gas	plasma	C
Karabut et al. [130]	Pd	D_2	plasma	Na,Mg,Br,Zn,S, Mo.Si
Miley et al. [131–133]	Ni	$Li_2SO_4 + H_2O$	electrolytic	Major elements: Cr,Fe,Mn,Cu,Zn,Se,As,Cd, Ag (isotope change)
Savvatimova and Karabut [134]	Pd	H_2, D_2 gas	plasma	As,Br,Rb,Sr,Y,Cd (isotope change)
Notoya [127–137]	Ni	$H_2O + Cs_2SO_4$	electrolytic	Ba
Mizuno et al. [138, 139]	Pt	solid electrolyte SrCeNbY oxide	electrolytic	Pt (radioactive), Al,Ca,Mg,Bi, Sm,Gd,Dy
Sundaresan and Bockris [140]	C	H_2O	plasma	Fe
Singh et al. [141]	C	H_2O	plasma	Fe
Mizuno et al. [142, 143]	Pd	$LiOH + D_2O$	electrolytic	Ti and Cr (isotope change), Ca,Mn,Fe,Co,Cu,Zn,Cd,Sn, Pt,Pb
Dash et al. [144, 145]	Pd	$H_2SO_4 + D_2O$	electrolytic	Ag
Matsunoto [146]	Pd	$K_2CO_3 + H_2O$	plasma	Ni,Ca,Ti,Na,Al,Cl,Cd,I
Bush and Eagleton [147, 148]	Ni	$Rb_2CO_3 + H_2O$	electrolytic	Sr (radioactive)
Savvatimova et al. [149]	Pd	D_2 gas	plasma	Li,B,V,Cr,Fe,Ni,Cu,Sr,Zr,Na,Al, Si,Ti,Nb,Mo,Ag,In (isotope ratio change)

Source	Substrate	Environment	Method	Detected
Notoya [150]	Ni	$K_2CO_3 + H_2O$	electrolytic	$K \rightarrow Ca$
Komaki [151]		H_2O	biological	$Na \rightarrow K$, $Na \rightarrow Mg$, $K \rightarrow Ca$, $Mg \rightarrow Ca$
Dillon and Kennedy [152]	Pd	$LiOD + D_2O$	electrolytic	Zn,Cu,Cr,Fe
Bush and Eagleton [153, 154]	Ni	$Rb_2CO_3 + H_2O$	electrolyte	$Rd \rightarrow Sr$
Ohmori and Enyo [155]	Ni	$K_2CO_3 + H_2O$	electrolytic	$K \rightarrow Ca$
Rolison and O'Grady [156]	Pd	$Li_2SO_4 + D_2O$, H_2O	electrolytic	Rh,Ag
Williams et al. [157]	Pd	$LiOD + D_2O$	electrolytic	Li,Cu,Zn,Fe,Pb,Si,Pt
Divisek et al. [158]	Pd	$LiOD + D_2O$	electrolytic	Pb, Cu
Greber [159]	Pd	$LiOD + D_2O$	electrolytic	Pb,Hg,Bi,Zn

The following are examples of observation of isotopic enrichment:

Source	Method	Isotope Change	Remarks
Donohue and Petek [160]	Electrolysis, D_2O	Pd	no change
Savvatimova et al. [134, 149]	Plasma, Pd in D_2 gas	$+Fe_{54}$, $+Fe_{57}$, $+B_{11}$, $+V_{51}$, $+Cr_{53}$, $+Ni_{61}$, $+Cu_{63}$, $+Sr_{87}$, $+Zr_{90}$	Many elements produced
Mizuno et al. [142, 143]	Plasma, Pd in D_2O	$100\%Cu_{63}$, $+Fe_{57}$, $-Fe_{56}$, $+Cr_{53}$, $-Cr_{52}$, $-K_{39}$, $-Zn_{64}$, $+Ir_{91}$, $-Ir_{93}$, $+Re_{185}$, $-Re_{187}$	Many elements produced
Ohmori and Enyo [124, 128]	Electrolysis, Pd and Au in H_2O	$+Fe_{54}$, $+Fe_{57}$	Fe increased as excess energy increased
Savvatimova et al. [161]	Plasma in Ar + Xe gas	$+Pd_{104}$	Many elements produced
Miley [162]	Electrolysis, Ni in H_2O	$+Ag_{107}$, $-Ag_{109}$, $+Cu_{63}$, $-Cu_{65}$	Many elements produced
Iwamura et al. [163]	Electrolysis, Pd in D_2O	$+Fe_{57}$,	Pd-CaO-Pd cathode
Ohmori et al. [164]	Plasma, W in H_2O	$+Fe_{56}$, $+Cr_{52}$, $+Pb_{206}$, $-Pb_{208}$	Cr and Fe found together on the W
Karabut [88]	Plasma, Pd in D_2 gas	$+Fe_{57}$, $+Cd_{110}$	Many elements produced
Celani et al. [82]	Electrolysis, Pd in $D_2O + C_2H_5OD$	$+Cu_{63}$, $+K_{39}$,	Many elements produced
Ohmori et al. [81]	Plasma, Re in $H_2O/D_2O + K^+$	$+K_{41}$	
Violante et al. [79] [165]	Electrolysis, Ni in H_2O	$+Cu_{65}$	Laser light used
Kim and Passell [166]	Various methods	$+Li_7/Li_6$	
Savvatimova and Gavritenkov [69]	Plasma, Ti in D_2 gas	$+Ti_{40}$	Many elements produced

Electrolyte = solution through which current is passed to initiate a Faraday-type reaction.

Plasma = Sufficient voltage is applied to either a gas or liquid to form gaseous ions as an arc or spark.

Laser = Laser light is applied in order to stimulate nuclear reactions.

Diffusion = Deuterium or hydrogen is diffused through palladium from the gas phase.

Fuse = Metal is rapidly melted by high current while under water.

Ambient = Metal substrate is placed in the indicated gas.

Bombard = Substrate is bombarded with the indicated charged particle.

Biological = Transmutation products are made in the presence of living organisms.

+ = indicates increase in concentration

− = indicates decrease in concentration

REFERENCES

1. D. R. Rolison and W. E. O'Grady, Proc. NSF/EPRI Workshop, Washington, DC, October 1989.
2. D. R. Rolison and W. E. O'Grady, Observation of elemental anomalies at the surface of palladium after electrochemical loading of deuterium or hydrogen. *Anal. Chem*. 1991, **63**, 1697–1702.
3. D. Rolison, W. O'Grady, R. Doyle, Jr, and P. Trzaskoma, Anomalies in the surface analysis of deuterated palladium. *Proc. 1st International Conference on Cold Fusion*, March 28-31, 1990, Salt Lake City, Utah. National Cold Fusion Institute: University of Utah Research Park, Salt Lake City, Utah, 1990, p. 272.
4. G. H. Miley and P. J. Shrestha, On transmutation reactions and associated LENR effects in solids," in Condensed matter nuclear science: *Proc.10th International Conference on Cold Fusion*, August 24-29, 2003, Cambridge, MA; P. L. Hagelstein and S. R. Chubb, eds. World Scientific Publishing Co.: Singapore, 2006, pp. 361–378.
5. G. H. Miley and P. J. Shrestha, Overview of light water/hydrogen-base low energy nuclear reactions. *Proc. 12th Int. Conf. on Cold Fusion*, A. Takahashi, K. Ota, and Y. Evamura, Y., eds. Yokohama, Japan, November 27-December 2, 2005. World Scientific, 2006, pp. 34–43.
6. G. H. Miley and P. J. Shrestha, Transmutation reactions and associated LENR effects in solids, in *Low Energy Nuclear Reactions Sourcebook*, J. Marwan and S. B. Krivit, eds. American Chemical Society, Washington, DC, Oxford University Press, 2008.
7. E. Storms, *The Science of Low Energy Nuclear Reaction*. World Scientific, Singapore, 2007.
8. G. H. Miley and J. Patterson, Nuclear transmutations in thin-film nickel coatings undergoing electrolysis. *J. New Energy*, 1996, **1**, 3, 5.
9. G. H. Miley, G. Narne, M. J. Williams, J. Patterson, D. Cravens, and H. Hora, Quantitative observations of transmutation products occurring in thin-film coated microspheres during electrolysis. *Proc. 6th Int. Conf. on Cold Fusion*, Hokkaido, Japan, Oct. 13-18, 1996, M. Okamoto, ed. New Energy and Industrial Technology Development Organization, Tokyo, 1996, pp. 629–644.
10. J. O. M. Bockris and E. F. Mallove, The occurrence of cold nuclear reactions widespread throughout nature? *Infinite Energy*, 1999, **27**, 29–38.
11. G. H. Miley, Product characteristics and energetics in thin-film electrolysis experiments. *Proc. 7th Int. Conf. on Condensed Matter Nuclear Science*. Vancouver, British Columbia, Canada, ENECO, ed., Salt Lake City, Utah, 1998,, pp. 241–246.
12. G. H. Miley, H. Heinrich, A. Lipson, S. O. Kim, N. Luo, C. H. Castano, and T. Woo, Progress in thin-film LENR research at the University of Illinois. *Proc. 9th Int. Conf. on Cold Fusion*, Beijing, China, May 19–24, 2002, X. Z. Li, ed. Tsinghua Univ. Press, Beijing, China, 2002, pp. 255–260.
13. E. Storms and B. Scanlan, Role of cluster formation in the LENR process. *Proc. 15th Int. Conf. on Condensed Matter Nuclear Science*, Roma, Italy, October 5-9, 2009, V. Violante and F. Sarto, F., eds. ENEA Publications, Frascati, Rome, Italy, 2010.
14. E. Storms and B. Scanlan, What is real about cold fusion and what explanations are possible? *AIP*, 2011, *J. Cond. Matter Nucl. Sci.*, 2011, **4**, 17–31.
15. J. O. M. Bockris, History of the discovery of transmutations at Texas A & M University. *Proc. 11th Int. Conf. on Condensed Matter Nuclear Science*, J. P. Biberian, ed., October 31-November 5, 2004, Marseilles, France, World Scientific, 2006, Singapore, pp. 562–586.
16. T. Mizuno, T. Ohmori, and M. Enyo, Isotopic changes of the reaction products induced by cathodic electrolysis in Pd. *J. New Energy*, 1996, **1**, 3, 31.
17. T. Mizuno, Transmutation reactions in condensed matter, in *Low Energy Nuclear Reactions Sourcebook*, J. Marwan and S. B. Krivit, eds. American Chemical Society, Washington DC Oxford University Press, 2008.
18. D. W. Mo et. al., The evidence of nuclear transmutation phenomena in PdH system using NAA (Neutron Activation Analysis). *Proc. 7th Int. Conf. on Condensed Matter Nuclear Science*, April 19-24, 1998, Vancouver, Canada, 1998, pp. 259–293.
19. B. F. Bush and J. J. Lagowski, "*Trace Elements Added to Palladium by Electrolysis in Heavy Water*, EPRI Report TP-108743 (1999). Electric Power Research Institute, Palo Alto, CA (Unpublished).
20. T. O. Passel and R. George, Trace elements added to palladium by exposure to gaseous deuterium. *Proc. 8th Int. Conf. on Cold Fusion*, F. Scaramuzzi, ed., Lerice, (La Spazia), Italy, May 21–26, 2000, Society Italiana Fisica, Bologna, Italy, 2000, pp. 129–134.
21. T. O. Passel, Pd^{110}/Pd^{108} ratios and trace element changes in particulate palladium exposed to deuterium gas. *Proc. 10th Int. Conf. on Condensed Matter Nuclear Science*, P. L. Hagelstein and S. R. Chubb, eds., August 24–29, 2003, Cambridge, MA. World Scientific Publishing Co., Singapore, 2006, pp. 399–404.
22. S. Szpak et al., LENR research using co-deposition. *Proc. 14th Int. Conf. on Condensed Matter Nuclear Science*, August 10-15, 2008, Washington, DC.
23. S. Szpak, P. A. M. Boss, C. Young, and F. E. Gordon, Evidence of nuclear reactions in the Pd lattice. *Naturwiss*., 2005, **92**, 8, 394–397.
24. J. J. Dash, J. J. Noble, and J. Diman, Surface morphology and microcomposition of palladium cathodes after electrolysis in acidified light and heavy water: correlation with excess heat. *Transactions in Fusion Technology*, 1994, **26**, 299.
25. J. Dash, Q. Wang, and D. S. Silver, Excess heat and anomalous isotopes and isotopic ratios from the interaction of palladium with hydrogen isotopes, in *ACS Low Energy Nuclear Reactions Sourcebook*, Vol. 2, Oxford University Press, Oxford, USA, 2010.
26. A. B. Karabut, Y. R. Kucherov, I. B. Savvatimova, The investigation of deuterium nuclei fusion at glow discharge cathode. *Fusion Technology*, 1991, 20, 4, Part 2, 924.

27. A. B. Karabut, Y. R. Kucherov, I. B. Savvatimova, Nuclear product ratio for glow discharge in deuterium. *Physics Letters A*, 1992, *170*, 265.
28. A. B. Karabut, Y. R. Kucherov, I. B. Savvatimova, Possible nuclear reactions mechanism at glow discharge in deuterium. *Proc. 3rd Int. Conf. on Condensed Matter Science*, H. Ikagami, ed., October 21–25, 1992, Nagoya, Japan. University Academy Press Inc., Tokyo, Japan, 1992, pp. 165–168.
29. I. B. Savvatimova, Y. R. Kucherov, and A. Karabut, Cathode material change after deuterium glow discharge experiments. *Proc. 4th Int. Conf. on Condensed Matter Nuclear Science*, Maui, Hawaii, December 6–9, 1993; *Transactions of Fusion Technology*, 1994, **26**, 389–394.
30. I. B. Savvatimova and A. Karabut, Nuclear reaction products registration on the cathode after glow discharge. *5th International Conference on Cold Fusion*, Monte-Carlo, Monaco, April 9–13, 1995, S. Pons, ed., IMRA Europe, Sophia Antipolis Cedex, France, pp 213–222.
31. A. B. Karabut, Excess heat power, nuclear products and X-ray emission in relation to the high current glow discharge experimental parameters., *Proc. 9th Int. Conf. on Cold Fusion*, X. Z. Li, ed., May 19-24 2002, Beijing, China. Tsinghua University Press, Beijing, China, 2002, pp. 151–154.
32. A. B. Karabut, *Research into Low Energy Nuclear Reactions in Cathode Sample Solid with Production of Excess Heat, Stable and Radioactive Impurity Nuclides*. The 12th International Conference on Condensed Matter Nuclear Science, Yokohama, Japan, 2005.
33. I. B. Savvatimova, Reproducibility of experimental and glow discharge and process accompanying deuterium ions bombardment. *Proc. 8th Int. Conf. on Condensed Matter Nuclear Science*, F. Scaramuzzi, ed., May 21–26, 2000, Lerici (La Spezia), Italy. Societa Italiana Di Fisica, Bologna, Italy, 2000, p. 277.
34. A. B. Karabut, Analysis of experimental results on excess heat power production, impurity nuclides yield in the cathode material and penetrating radiation in experiments with high current glow discharge. *8th International Conference on Cold Fusion*, Scaramuzzi, F. ed., May 21–26, 2000, Lerici (La Spezia), Italy. Italian Physical Society, Bologna, Italy. 2000, pp. 329–334.
35. I. B. Savvatimova, and D. V. Gavritenkov, Influence of the parameters of the glow discharge on change of structure and the isotope composition of the cathode materials. *Proc. 12th Int. Conf. on Condensed Matter Nuclear Science*, November 27-to December 2, 2005, Yokohama, Japan. World Scientific, Singapore, 2006 p. 231.
36. I. Savvatimova, G. Savvatimov, and A. Kornilova, Decay in tungsten irradiated by low energy deuterium ions. *Proc. 13th Int. Conf. on Condensed Matter Nuclear Science*, Sochi, Russia, 2007.
37. I. Savvatimova, Creation of more light elements in tungsten irradiated by low-energy deuterium ions, *Proc.13th Int. Conf. on Condensed Matter Nuclear Science*, June 25–July 1, 2007, Sochi, Russia, 2008, p. 505.
38. H. Yamada et al., Producing a radioactive source in a deuterated palladium electrode under direct-current glow discharge, *C. Fusion Technology*, 2001, **39**, 253.
39. A. Arapi et al., Experimental observation of the new elements production in the deuterated and/or hydride palladium electrodes, exposed to low energy DC glow discharge, *Proc. 9th Int. Conf. on Condensed Matter Nuclear Science*, May 24-29, 2002, Tsinghua University, Beijing, China. Tsinghua University Press, Beijing China, 2002, p. 1.
40. Y. Iwamura, K. Itoh, and I. Toyoda, Observation of anomalous nuclear effects in D_2-Pd system, *Fourth International Conference on Cold Fusion*, Lahaina, Maui, Dec. 6–9, 1993, Passell, T. O., ed., Electric Power Research Institute 3412 Hillview Ave., Palo Alto, CA, 160–164.
41. T. Itoh, Y. Iwamura, N. Gotoh, and I. Toyoda, Observation of nuclear products under vacuum condition from deuterated palladium and high l Loading ratio. 1ccf 5, pp 189–196.
42. Y. Iwamura, Y. et al., Correlation between behavior of deuterium in palladium and occurance of nuclear reactions observed by simultaneous measurement of excess heat and nuclear products, *Sixth International Conference on Cold Fusion*, Progress in New Hydrogen Energy, Lake Toya, Hokkaido, Japan, ct. 13–18, 1996, Okamoto, M., ed., New Energy and Industrial Technology Development Organization, p. 274.
43. Y. Iwamura et al., Detection of anomalous elements, x-ray, and excess heat in a D_2-Pd system and its interpretation by the electron-induced nuclear reaction model. *Fusion Technology*, 1998, **33**, 476.

43a. Y. Iwamura et al, Detection of anomalous elements, x-ray and excess heat induced by continuous diffusion of deuterium through multilayer cathode (Pd/Cao/Pd). *Proc. 7th Int. Conf. on Cold Fusion*, F. Jaeger, ed., April 19–24, 1998, Eneco, Inc., Salt Lake City, UT, 1998, pp. 167–172.

44. Y. Iwamura, T. Itoh, and M. Sakano, Nuclear products and their time dependence induced by continuous diffusion of deuterium through multi-layer palladium containing low work function. *Proc. of ICCF8*, May 21–26, 2000, Lerici, Italy. *SIF Conf. Proc*., 2000, **70**, 141–146.
45. Y. Iwamura, M. Sakano, and S. Sakai, S., Elemental analysis of Pd complexes: effects of D_2 gas permeation. *Jpn. J. Appl. Phys*., 2002, **41**, 4642–4648.
46. Y. Iwamura, et al., Observation of low energy nuclear reactions induced by D2 gas permeation through Pd complexes. iccf9, 2002, pp 141–146.
47. T. Iwamura, T. Itoh, M. Sakano, S. Sakai, and S. Kuribayashi, Low energy nuclear transmutation in condensed matter induced by D2 gas permeation through Pd complexes: correlation between deuterium flux and nuclear products, *Proc. ICCF10*, August 24–29, 2003, Cambridge, USA. World Scientific, Singapore, 2003, pp. 435–446.
48. Y. Iwamura, T. Itoh, M. Sakano, S. Kuribayashi, Y. Terada, T. Ishikawa, and J. Kasagi, Observation of nuclear transmutation reactions induced by D2 gas permeation through Pd complexes, Proc. ICCF11, October 31–November 5, 2004, Marseilles, France. World Scientific, Singapore, 2004, pp. 339–350.

49. Y. Iwamura, et al., Observation of surface distribution of products by x-ray fluorescence spectrometry during D_2 gas permeation through Pd complexes. ICCF 12, November 27–December 2, 2005, Yokohama, Japan. pp. 178–187.
50. T. Higashiyama, M. Sakano, H. Miyamaru, and A. Takahashi, Replication of MHI transmutation experiment by D_2 gas permeation through Pd complex. Tenth International Conference on Cold Fusion, Cambridge, MA, August 24–29, 2003, Hagelstein, P. L., Chubb, S. R., ed., World Scientific Publishing Co., Singapore, pp. 447–454.
51. A. Takahashi, The basics of deuteron-cluster dynamics as shown by a Langevin equation, in *ACS Low-Energy Nuclear Reactions and New Energy Technologies Sourcebook*, Marwan, J., Krivit, S. B., ed., American Chemical Society, *Vol. 2* 2010, pp. 193–217.
52. C. Hugus, ed., *Kushi Institute Study Guide*, Issue No. 10 Kushi Institute, Brookline Village, MA, 1980.
53. R. A. Monti, Low energy nuclear reactions: the revival of alchemy. *Proceedings of the International Conference Space and Time*, St. Petersburg, Russia, 2001, p. 178.
54. M. Singh, M. D. Saksena, V. D. Dixit, and V. B. Kartha V.B., "Verification of the George Oshawa experiment for anomalous production of iron from carbon arc in water. *FusionTechnol*., 1994, **26**, 266–270.
55. R. Sundaresan and J. O. M. Bockris, Anomalous reactions during arcing between carbon rods in water. *Fusion Technol*., 1994, **26**, 261–265.
56. X. L. Jiang, L. J. Han, and W. Kang, Anomalous element production induced by carbon arcing under water. *Proc. 7th Int. Conf. on Cold Fusion*, F. Jaeger, ed., April 19–24, 1998, Salt Lake City, UT,. Eneco Inc., Salt Lake City, UT, 1998, pp. 172–179.
57. V. I. Vysotskii and A. A. Kornilova, *Nuclear Fusion and Transmutation of Isotopes in Biological Cultures*. Mir Publishers, Moscow, 2003.
58. V. I. Vysotskii, A. A. Kornilova, *Nuclear Transmutation of Stable and Radioactive Isotopes in Biological Systems*. Pentagon Press, New Delhi, India, 2009.
59. L. C. Kervran, *Biological Transmutations*. Swan House Publishing Co., New York, 1972.
60. P. Bahrangar, *J. Biol. Sciences*, 1960, **3**, 2, 57–85.
61. H. Komaki, Observations on the biological cold fusion or the biological transmutation of elements. *Proc. 3rd Int. Conf. on Condensed Matter Science*, H. Ikagami, ed., October 21–25, 1992, Nagoya, Japan. University Academy Press Inc., Tokyo, Japan, 1992, pp. 555–558.
62. V. I. Vysotskii, A. A. Kornilova, and I. I. Samoylenko, Experimental discovery of the phenomenon of low-energy nuclear transmutation of isotopes (Mn55 → Fe57) in growing biological cultures., *Proc. 6th Int. Conf. on Cold Fusion*, Toya, Japan, 1996, pp. 687–693.
63. V. I. Vysotskii, A. A. Kornilova, and I. I. Samoylenko, Experimental observation and study of controlled transmutation of intermediate mass isotopes in growing biological cultures. *Proc. 8th Int. Conf. on Cold Fusion*, May 21–26, 2000, Lerici, Italy. *SIF Conf. Proc*., 2000, **70**, 135–140.
64. V. I. Vysotskii, A. B. Tashyrev, and A>A. Kornilava, Experimental observation and modelling of Cs137 isotope deactivation and stable isotopes transmutation in biological cells, in *American Chemical Society Sourcebook*, Vol. 1. Oxford University Press, 2008, pp. 295–303.
65. E. K. Storms and B. Scanlan, Role of cluster formation in the LENR process, *15th International Conference on Condensed Matter Nuclear Science*. ENEA, Rome, Italy, 2009.
66. Q. Wang and J. Dash. Effect of an additive on thermal output during electrolysis of heavy water with a palladium cathode, in *12th International Conference on Condensed Matter Nuclear Science*, Yokohama, Japan, 2005, p. 140.
67. S. Szpak, P.A. Mosier-Boss, and F. Gordon. Precursors and the fusion reactions in polarized Pd/D-D_2O systems: Effect of an external electric field,. in *11th International Conference on Cold Fusion*, 2004. World Scientific, Marseilles, France, 2004, p. 359.
68. S. Szpak et al., Evidence of nuclear reactions in the Pd lattice. *Naturwiss*., 2005, **92**, 394.
69. I. Savvatimova and D.V. Gavritenkov. Results of analysis of Ti foil after glow discharge with deuterium, in *11th International Conference on Cold Fusion*, 2004. World Scientific, Marseilles, France, 2004, p. 438.
70. T. Mizuno et al. Generation of heat and products during plasma electrolysis, in *11th International Conference on Cold Fusion*, 2004. World Scientific, Marseilles, France, 2004, p. 161.
71. G. Lochak, and L. Urutskoev. Low-energy nuclear reactions and the leptonic monopole, in *11th International Conference on Cold Fusion*, 2004. World Scientific, Marseilles, France, 2004, p. 421.
72. A. Karabut, Excess heat production in Pd/D during periodic pulse discharge current in various conditions, in *11th International Conference on Cold Fusion*, 2004. World Scientific, Marseilles, France, 2004, p. 178.
73. A. B. Karabut, Analysis of experimental results on excess heat power production, impurity nuclides yield in the cathode material and penetrating radiation in experiments with high-current glow discharge, in *8th International Conference on Cold Fusion*, 2000, Lerici (La Spezia), Italy. Italian Physical Society, Bologna, Italy, 2000, p. 329.
74. S. Focardi et al., Evidence of electromagnetic radiation from Ni-H systems, in *11th International Conference on Cold Fusion*, 2004. World Scientific, Marseilles, France, 2004, p. 70.
75. D. Cirillo and V. Iorio, Transmutation of metal at low energy in a confined plasma in water, in *11th International Conference on Cold Fusion*., 2004. World Scientific, Marseilles, France, 2004, p. 492.
76. F. Celani et al., Innovative procedure for the, *in situ*, measurement of the resistive thermal coefficient of H(D)/Pd during electrolysis; cross-comparison of new elements detected in the Th-Hg-Pd-D(H) electroytic cells, in *11th International Conference on Cold Fusion*, 2004. World Scientific, Marseilles, France, 2004, p. 108.
77. E. G. Campari et al., Photon and particle emission, heat production and surface transformation in Ni-H system,

in *11th International Conference on Cold Fusion*, 2004. Marseilles, France: World Scientific, Marseilles, France, 2004, p. 405.

78. H. Yamada et al., Analysis by time-of-flight secondary ion mass spectroscopy for nuclear products in hydrogen penetration through palladium, in *Tenth International Conference on Cold Fusion*, 2003, Cambridge, MA. World Scientific, 2003, p. 455.
79. V. Violante et al., Analysis of Ni-hydride thin film after surface plasmons generation by laser technique, in *Tenth International Conference on Cold Fusion*. 2003. Cambridge, MA. World Scientific, 2003, p. 421.
80. T. O. Passell, Pd110/Pd108 ratios and trace element changes in particulate palladium exposed to deuterium gas, in *Tenth International Conference on Cold Fusion*, 2003. Cambridge, MA. World Scientific, 2003, p. 399.
81. T. Ohmori et al., Enrichment of ^{41}K isotope in potassium formed on and in a rhenium electrode during plasma electrolysis in K_2CO_3/H_2O and K_2CO_3/D_2O solutions. *J. Appl. Electrochem*., 2003, **33**, 643.
82. F. Celani et al., Thermal and isotopic anomalies when Pd cathodes are electrolyzed in electrolytes containing Th-Hg salts dissolved at micromolar concentration in C_2H_5OD/D_2O mixtures, in *Tenth International Conference on Cold Fusion*, 200, Cambridge, MA. World Scientific, 2003, p. 379.
83. V. Violante et al., X-ray emission during electrolysis of light water on palladium and nickel thin films. in *The 9th International Conference on Cold Fusion, Condensed Matter Nuclear Science*, 2002, Tsinghua University, Beijing, China. Tsinghua University Press, 2002, p. 376.
84. H. Yamada et al., Production of Ba and several anomalous elements in Pd under light water electrolysis, in *The 9th International Conference on Cold Fusion, Condensed Matter Nuclear Science*, 2002, Tsinghua University, Beijing, China. Tsinghua University Press, 2002, p. 420.
85. J. Warner, J. Dash, and S. Frantz, Electrolysis of D_2O with titanium cathodes: enhancement of excess heat and further evidence of possible transmutation, in *The Ninth International Conference on Cold Fusion*, 2002, Tsinghua University, Beijing, China. Tsinghua University Press, 2002, p. 404.
86. V. I. Vysotskii et al., Catalytic influence of caesium on the effectiveness of nuclear transmutation on intermediate and heavy mass isotopes in growing biological cultures, in *The 9th International Conference on Cold Fusion, Condensed Matter Nuclear Science*, 2002, Tsinghua Univ., Beijing, China. Tsinghua University Press, 2002, p. 391.
87. M. Matsunaka et al. Studies of coherent deuteron fusion and related nuclear reactions in solid, in *The 9th International Conference on Cold Fusion, Condensed Matter Nuclear Science*, 2002, Tsinghua University, Beijing, China. Tsinghua University Press, 2002, p. 237.
88. A. B. Karabut, Excess heat power, nuclear products and X-ray emission in relation to the high current glow discharge experimental parameters. in *The 9th International Conference on Cold Fusion, Condensed Matter Nuclear Science*, 2002, Tsinghua University, Beijing, China. Tsinghua University Press, 2002, p. 151.
89. Y. Iwamura et al., Observation of low energy nuclear reactions induced by D_2 gas permeation through Pd complexes, in *The Ninth International Conference on Cold Fusion (ICCF9)*, 2002, Beijing, China. Tsinghua University Press, 2002, p. 141.
90. Y. Iwamura, M. Sakano, and T. Itoh, Elemental analysis of Pd complexes: effects of D_2 gas permeation. *Jpn. J. Appl. Phys. A*, 2002. **41**, 7, 4642.
91. I. V. Goryachev, Registration of synthesis of $_{45}Rh^{102}$ in media of excited nuclei of $_{28}Ni^{58}$, in *The 9th International Conference on Cold Fusion, Condensed Matter Nuclear Science*, 2002, Tsinghua University Beijing, China. Tsinghua University Press, 2002, p. 109.
92. M. Di Giulio et al., Analysis of nuclear transmutations observed in D- and H-loaded films. *J. Hydrogen Eng*., 2002, **27**, 527.
93. A. Arapi et al., Experimental observation of the new elements production in the deuterated and/or hydride palladium electrodes, exposed to low energy DC glow discharge, in *The 9th International Conference on Cold Fusion, Condensed Matter Nuclear Science*, 2002, Tsinghua University, Beijing, China. Tsinghua University Press, 2002, p. 1.
94. H. Yamada et al., Producing a radioactive source in a deuterated palladium electrode under direct-current glow discharge. *Fusion Technol*., 2001, **39**, 253.
95. J. Warner and J. Dash, Heat produced during the electrolysis of D_2O with titanium cathodes, in *8th International Conference on Cold Fusion*, 2000, Lerici (La Spezia), Italy. Italian Physical Society, Bologna, Italy, 2000, p. 161.
96. T. Wang et al. Nuclear phemonena in $P + Ti_2H_x$ experiments, in *8th International Conference on Cold Fusion*, 2000, Lerici (La Spezia), Italy. Italian Physical Society, Bologna, Italy, 2000, p. 317.
97. V. Vysotskii et al., Experimental observation and study of controlled transmutation of intermediate mass isotopes in growing biological cultures, in *8th International Conference on Cold Fusion*, 2000, Lerici (La Spezia), Italy. Italian Physical Society, Bologna, Italy, 2000, p. 135.
98. T. O. Passell and R. George, Trace elements added to palladium by exposure to gaseous deuterium, in *8th International Conference on Cold Fusion*, 2000, Lerici (La Spezia), Italy. Italian Physical Society, Bologna, Italy, 2000, p. 129.
99. V. Nassisi and M. L. Longo, Experimental results of transmutation of elements observed in etched palladium samples by an excimer laser. *Fusion Technol*., May 2000, **37**, 247.
100. T. Mizuno et al., Confirmation of heat generation and anomalous element caused by plasma electrolysis in the liquid, in *8th International Conference on Cold Fusion*, 2000, Lerici (La Spezia), Italy. Italian Physical Society, Bologna, Italy, 2000, p. 75.
101. X. Z. Li et al., Nuclear transmutation in Pd deuteride, in *8th International Conference on Cold Fusion*, 2000, Lerici (La

Spezia), Italy. Italian Physical Society, Bologna, Italy, 2000, p. 123.

102. Y. Iwamura, T. Itoh, and M. Sakano, Nuclear products and their time dependence induced by continuous diffusion of deuterium through multi-layer palladium containing low work function material, in *8th International Conference on Cold Fusion*, 2000, Lerici (La Spezia), Italy. Italian Physical Society, Bologna, Italy, 2000, p. 141.
103. T. Hanawa, X-ray spectroscropic analysis of carbon arc products in water, in *8th International Conference on Cold Fusion*, 2000, Lerici (La Spezia), Italy. Italian Physical Society, Bologna, Italy, 2000, p. 147.
104. J. Dufour et al., Hydrex catallyzed transmutation of uranium and palladium: experimental part, in *8th International Conference on Cold Fusion*, 2000, Lerici (La Spezia), Italy. Italian Physical Society, Bologna, Italy, 2000, p. 153.
105. Castellano et al., Nuclear transmutation in deutered Pd films irradiated by an UV laser, in *8th International Conference on Cold Fusion*, 2000, Lerici (La Spezia), Italy. Italian Physical Society, Bologna, Italy, 2000, p. 287.
106. E. G. Campari et al. Ni-H systems, in *8th International Conference on Cold Fusion*, 2000, Lerici (La Spezia), Italy. Italian Physical Society, Bologna, Italy, 2000, p. 69.
107. M. Bernardini et al., Anomalous effects induced by D_2O electrolysis at titanium, in *8th International Conference on Cold Fusion*, 2000, Lerici (La Spezia), Italy. Italian Physical Society, Bologna, Italy, 2000, p. 39.
108. H. E. Ransford, Non-stellar nucleosynthesis: transition metal production by DC plasma-discharge electrolysis using carbon electrodes in a non-metallic cell. *Infinite Energy*, 1999, **4**, 23, 16.
109. T. Ohmori and T. Mizuno, Nuclear transmutation reaction caused by light water electrolysis on tungsten cathode under incandescent conditions. *Infinite Energy*, 1999, **5**, 27, 34.
110. S. Focardi et al., On the Ni-H system, in *Asti Workshop on Anomalies in Hydrogen/Deuterium Loaded Metals*, 1997, Villa Riccardi, Italy. Societa Italiana Di Fisica, 1997, p. 35.
111. M. F. Klopfenstein and J. Dash, Thermal imaging during electrolysis of heavy water with a Ti cathode, in *The Seventh International Conference on Cold Fusion*, 1998. Vancouver, Canada, 1998, Eneco Inc, Salt Lake City, UT, USA, p. 98.
112. G. S. Qiao et al., Nuclear products in a gas-loading D/Pd and H/Pd system, in *The Seventh International Conference on Cold Fusion*, 1998, Vancouver, Canada. Eneco Inc, Salt Lake City, UT, USA p. 314.
113. L. C. Kong et al., Nuclear products and transmutation in a gas-loading D/Pd and H/Pd system. *J. New Energy*, 1998, **3**, 1, 20.
114. T. Ohmori et al., Transmutation in a gold-light water electrolysis system. *Fusion Technol*., 1998, **33**, 367.
115. T. Ohmori and T. Mizuno, Excess energy evolution and transmutation. *Infinite Energy*, 1998, **39**, 20, 14.
116. R. Notoya, T. Ohnishi, and Y. Noya, Products of nuclear processes caused by electrolysis on nickel and platinum electrodes in solutions of alkali-metallic ions, in *The Seventh International Conference on Cold Fusion*, 1998, Vancouver, Canada. ENECO, Salt Lake City, UT, 1998, p. 269.
117. V. Nassisi, Transmutation of elements in saturated palladium hydrides by an XeCl excimer laser. *Fusion Technol*., 1998, **2**, 468.
118. V. Nassisi, Incandescent Pd and anomalous distribution of elements in deuterated samples processed by an excimer laser. *J. New Energy*, 1997, **2**, 3/4, 14.
119. X.-L. Jiang et al., Tip effect and nuclear-active sites, in *The Seventh International Conference on Cold Fusion*, 1998, Vancouver, Canada. ENECO, Salt Lake City, UT, 1998, p. 175.
120. X.-L. Jiang, L.J. Han, and W. Kang, Anomalous element production induced by carbon arcing under water, in *The Seventh International Conference on Cold Fusion*, 1998, Vancouver, Canada. ENECO, Salt Lake City, UT, 1998, p. 172.
121. Y. Iwamura et al., Detection of anomalous elements, X-ray and excess heat induced by continuous diffusion of deuterium through multi-layer cathode (Pd/CaO/Pd). *Infinite Energy*, 1998, **4**, 20, 56.
122. Y. Iwamura et al., Detection of anomalous elements, X-ray, and excess heat in a D_2-Pd system and its interpretation by the electron-induced nuclear reaction model. *Fusion Technol*., 1998, **33**, 476.
123. K. Nakamura, Y. Kishimoto, and I. Ogura, Element conversion by arcing in aqueous solution. *J. New Energy*, 1997, **2**, 2, 53.
124. T. Ohmori et al., Transmutation in the electrolysis of light water - excess energy and iron production in a gold electrode. *Fusion Technol*., 1997, **31**, 210.
125. G. S. Qiao et al., Nuclear transmutation in a gas-loading system. *J. New Energy*, 1997, **2**, 2, 48.
126. R. Kopecek and J. Dash, Excess heat and unexpected elements from electrolysis of heavy water with titanium cathodes. *J. New Energy*, 1996, **1**, 3, 46.
127. J. Dash, R. Kopecek, and S. Miguet, Excess heat and unexpected elements from aqueous electrolysis with titanium and palladium cathodes, in *32nd Intersociety Energy Conversion Engineering Conference*, 1997. p. 1350–1355.
128. T. Ohmori and M. Enyo, Iron formation in gold and palladium cathodes. *J. New Energy*, 1996, 1, 15.
129. H. Yamada et al., Carbon production on palladium point electrode with neutron burst under DC glow discharge in pressurized deuterium gas. *J. New Energy*, 1996, **1**, 4), 55.
130. A. Karabut, Y. Kucherov, and I. Savvatimova, Possible nuclear reactions mechanisms at glow discharge in deuterium. *J. New Energy*, 1996, **1**, 1, 20.
131. G. H. Miley et al., Quantitative observations of transmutation products occuring in thin-film coated microspheres during electrolysis, in *Sixth International Conference on Cold Fusion, Progress in New Hydrogen Energy*, 1996, Lake Toya, Hokkaido, Japan. New Energy and Industrial Technology Development Organization, Tokyo Institute of Technology, Tokyo, Japan, 1996, p. 629.

132. G. H. Miley and J.A. Patterson, Nuclear transmutations in thin-film nickel coatings undergoing electrolysis. *J. New Energy*, 1996, **1**, 3, 5.

133. G. H. Miley, Possible evidence of anomalous energy effects in H/D-loaded solids-low energy nuclear reactions (LENRS). *J. New Energy*, 1997, **2**, 3/4, 6.

134. I. Savvatimova and A. Karabut, Nuclear reaction products registration on the cathode after glow discharge, in *5th International Conference on Cold Fusion*, 1995, Monte-Carlo, Monaco. IMRA Europe, Sophia Antipolis Cedex, France, 1995, p. 213.

135. R. Notoya, Nuclear products of cold Fusion caused by electrolysis in alkali metallic ions solutions, in *5th International Conference on Cold Fusion*, 1995, Monte-Carlo, Monaco. IMRA Europe, Sophia Antipolis Cedex, France, 1995, p. 531.

136. R. Notoya, Low temperature nuclear change of alkali metallic ions caused by electrolysis. *J. New Energy*, 1996, **1**, 39.

137. R. Notoya, Low temperature nuclear change of alkali metallic ions caused by electrolysis. *J. New Energy*, 1996, **1**, 1, 39.

138. T. Mizuno et al., Formation of ^{197}Pt radioisotopes in solid state electrolyte treated by high temperature electrolysis in D_2 gas. *Infinite Energy*, 1995, **1**, 4, 9.

139. T. Mizuno et al., Excess heat evolution and analysis of elements for solid state electrolyte in deuterium atmosphere during applied electric field. *J. New Energy*, 1996, **1**, 1, 79.

140. R. Sundaresan and J.O.M. Bockris, Anomalous reactions during arcing between carbon rods in water. *Fusion Technol*., 1994, **26**, 261.

141. M. Singh et al., Verification of the George Oshawa experiment for anomalous production of iron from carbon arc in water. *Fusion Technol*., 1994, **26**, 266.

142. T. Mizuno, T. Ohmori, and M. Enyo, Anomalous isotopic distribution in palladium cathode after electrolysis. *J. New Energy*, 1996, **1**, 2, 37.

143. T. Mizuno, T. Ohmori, and M. Enyo, Isotopic changes of the reaction products induced by cathodic electrolysis in Pd. *J. New Energy*, 1996, **1**, 3, 31.

144. J. Dash and S. Miguet, Microanalysis of Pd cathodes after electrolysis in aqueous acids. *J. New Energy*, 1996, **1**, 1, 23.

145. S. Miguet and J. Dash, Microanalysis of palladium after electrolysis in heavy water. *J. New Energy*, 1996, **1**, 1, 23.

146. T. Matsumoto, Experiments of underwater spark discharge with pinched electrodes. *J. New Energy*, 1996, **1**, 4, 79.

147. R. T. Bush and R.D. Eagleton, Evidence for electrolytically induced transmutation and radioactivity correlated with excess heat in electrolytic cells with light water rubidium salt electrolytes. *Trans. Fusion Technol*., 1994, **26**, 4T, 344.

148. R. T. Bush, Electrolytic stimulated cold nuclear synthesis of strontium from rubidium. *J. New Energy*, 1996, **1**, 28.

149. I. Savvatimova, Y. Kucherov, and A. Karabut, Cathode material change after deuterium glow discharge experiments. *Trans. Fusion Technol*., 1994, **26**, 4T, 389.

150. R. Notoya, Cold fusion by electrolysis in a light water-potassium carbonate solution with a nickel electrode. *Fusion Technol*., 1993. **24**, 202.

151. H. Komaki, An approach to the probable mechanism of the non-radioactive biological cold fusion or so-called Kervran effect (part 2). in *Fourth International Conference on Cold Fusion*, 1993, Lahaina, Maui, HI. Electric Power Research Institute, Palo Alto, CA, 1993, p. 44.

152. C. T. Dillon and B.J. Kennedy, The electrochemically formed palladium-deuterium system. I. Surface composition and morphology. *Aust. J. Chem*., 1993, **46**, 663.

153. R. T. Bush and R.D. Eagleton, Experimental studies supporting the transmission resonance model for cold fusion in light water: I. Correlation of isotopic and elemental evidence with excess energy, in *Third International Conference on Cold Fusion, & Frontiers of Cold Fusion,"* 1992, Nagoya. Japan. Universal Academy Press, Tokyo, Japan, 1992, p. 405.

154. R. T. Bush, Electrolytically simulated cold nuclear synthesis of strontium from rubidium. *J. New Energy*, 1996, **1**, 1, 28.

155. T. Ohmori and M. Enyo, Excess heat production during electrolysis of H_2O on Ni, Au, Ag and Sn electrodes in alkaline media, in *Third International Conference on Cold Fusion, &Frontiers of Cold Fusion,"* 1992, Nagoya, Japan. Universal Academy Press, Tokyo, Japan, 1992, p. 427.

156. D. R. Rolison and W.E. O'Grady, Observation of elemental anomalies at the surface of palladium after electrochemical loading of deuterium or hydrogen. *Anal. Chem*., 1991, **63**, 1697.

157. D. E. G. Williams et al., Upper bounds on 'cold fusion' in electrolytic cells. *Nature (London)*, 1989, **342**, 375.

158. J. Divisek, L. Fuerst, and J. Balej, Energy balance of D_2O electrolysis with a palladium cathode. Part II. Experimental results. *J. Electroanal. Chem*., 1989, **278**, 99.

159. T. Greber et al,. Cold fusion experiments in Fribourg, in *Understanding Cold Fusion Phenomena*, Conference Proceedings **24**, R.A. Ricci, E. Sindoni, F. De Marco, ed., SIF, Bologna, 1989, 219.

160. D. L. Donohue and M. Petek, Isotopic measurements of palladium metal containing protium and deuterium by glow discharge mass spectrometry. *Anal. Chem*., 1991, **63**, 740.

161. I. B. Savvatimova, A.D. Senchukova, and I.P. Chernov, Transmutation phenomena in a palladium cathode after ions irradiation at glow discharge, in *The Sixth International Conference on Cold Fusion*, 1996, Lake Toya, Japan. The Institute of Applied Energy, 1996, p. 575.

162. G. Miley, Characteristics of reaction product patterns in thin metallic films experiments, in *Asti Workshop on Anomalies in Hydrogen/Deuterium Loaded Metals*, 1997, Villa Riccardi, Rocca d'Arazzo, Italy. Italian Phys. Soc., 1997, p. 77.

163. Y. Iwamura et al., Detection of anomalous elements, X-ray and excess heat induced by continous diffusion of deuterium through multi-layer cathode (Pd/CaO/Pd), in *The Seventh International Conference on Cold Fusion*, 1998, Vancouver, Canada. ENECO, I Salt Lake City, UT, 1998, p. 167.

164. T. Ohmori and T. Mizuno, Strong excess energy evolution, new element production, and electromagnetic wave and/or

neutron emission in the light water electrolysis with a tungsten cathode, in *The Seventh International Conference on Cold Fusion*, 1998, Vancouver, Canada. ENECO, Salt Lake City, UT, 1998, p. 279.

165. V. Violante et al., Search for nuclear ashes in electrochemical experiments, in *Tenth International Conference on Cold Fusion*, 2003, Cambridge, MA. World Scientific, 2003, p. 405.

166. Y. E. Kim and T.O. Passell, Alternative interpretations of low-energy nuclear reaction processes with deuterated metals based on the Bose-Einstein condensation mechanism, in *11th International Conference on Cold Fusion*, 2004, Marseilles, France. World Scientific, 2004, p. 718.

44

WIDOM–LARSEN THEORY: POSSIBLE EXPLANATION OF LENRs

JOSEPH M. ZAWODNY[1] AND STEVEN B. KRIVIT[2]
[1]*NASA Langley Research Center, Hampton, VA, USA*
[2]*New Energy Times, San Rafael, CA, USA*

Alternative theories explaining LENR that do not rely on D-D "cold fusion" have been proposed since the 1989 Pons and Fleischman announcement, although few have been published in the peer-reviewed literature. One such alternate explanation came to light in 2006 when Allan Widom and Lewis Larsen published their paper, "Ultra Low Momentum Neutron Catalyzed Nuclear Reactions on Metallic Hydride Surfaces," in the reputable, peer-reviewed *European Physical Journal C* [1]. Widom–Larsen Theory (WLT), as it has become known, does not rely on or even require traditional fusion processes based on the strong nuclear force. Instead, WLT proposes that the mechanism for energy production is initiated by electron capture by a proton (the inverse of the weak force's beta decay) to produce a neutron. That neutron is absorbed by a nearby nucleus, which subsequently emits an energetic photon or particle.

After Widom and Larsen's initial paper, a series of non-peer-reviewed papers followed to further refine the proposed mechanism and to explore some of the other physical applications of the theory. WLT is a complex theory in that it requires that a multitude of physical conditions and processes be present and active. Fortunately, each of these processes is based on well-established physics. Acceptance of WLT becomes an issue of whether the conditions are reasonable and consistent with the existing body of experimental evidence and whether the physical processes are in fact occurring in these experiments.

44.1 FOUR-STEP WIDOM–LARSEN PROCESS

The Widom–Larsen ultra-low-momentum neutron-catalyzed theory of LENRs involves four fundamental steps, as shown graphically in Larsen's image (Fig. 44.1) and legend (Fig. 44.2).

Summaries of the four steps follow:

1. *Creation of Heavy Electrons*
   Electromagnetic radiation in LENR cells, along with collective effects, creates localized regions of very high E-M fields. Electrons within these fields become heavy electrons.
2. *Creation of ULM Neutrons*
   An electron and a proton combine, through electron capture (inverse beta decay), into an ultra-low-momentum (ULM) neutron and a neutrino.
3. *Capture of ULM Neutrons*
   That ULM neutron is captured by a nearby nucleus, producing either a new, stable isotope or an isotope unstable to beta decay.
   A free neutron outside of an atomic nucleus is unstable to beta decay; it has a half-life of approximately 13 minutes and decays into a proton, an electron, and a neutrino.
4. *Creation of New Elements and Isotopes*
   When an unstable nucleus decays, one or more particles are emitted along with a release of energy. In beta decay, a neutron inside the nucleus decays into a proton, an energetic electron, and a neu-

Nuclear Energy Encyclopedia: Science, Technology, and Applications, First Edition (Wiley Series On Energy).
Edited by Steven B. Krivit, Jay H. Lehr, and Thomas B. Kingery.

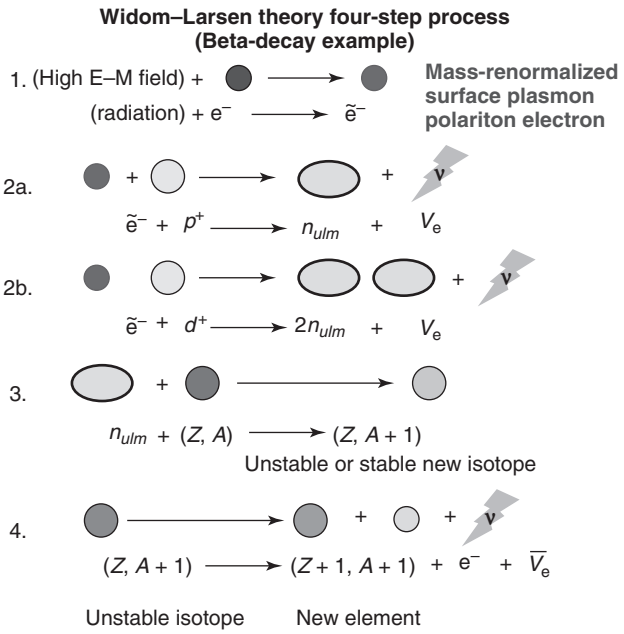

Figure 44.1 Visual representation of Widom-Larsen four-step process in the beta-decay example. (*Image courtesy of Lewis Larsen*). *(Source: Adapted by New Energy Times with minor modification from, copyright, Lewis Larson, Lattice Energy LLc, Slide presentation. Nov. 25, 2009.)*

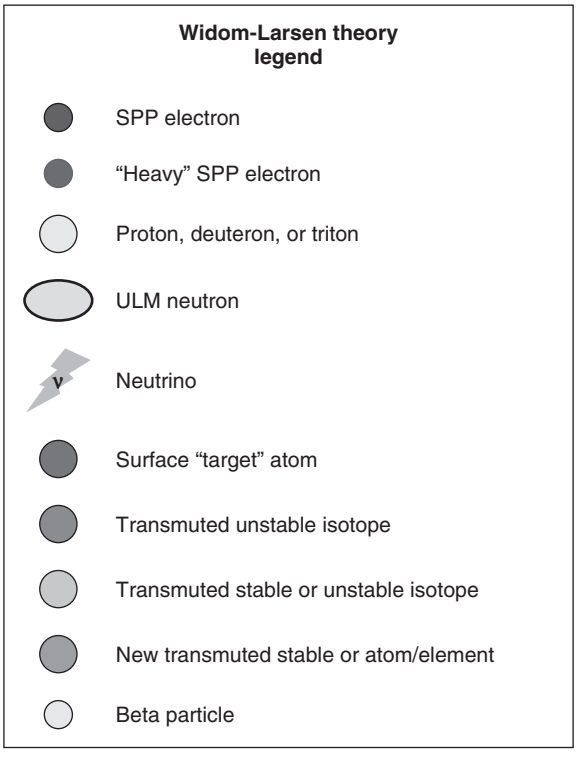

Figure 44.2 Legend for Widom-Larsen four-step process (*Image courtesy of Lewis Larsen*).

trino. The energetic electron released in a beta decay exits the nucleus and is detected as a beta particle. Because the number of protons in that nucleus has gone up by one, the atomic number has increased, creating a different element and transmutation product. Similarly, alpha particles may be emitted decreasing the number of proton and neutrons in the nucleus by two each. In either case, the newly transmuted nucleus may be left in an excited state which eventually decays to the ground state by emitting a gamma ray. Other types of decays are also possible with neutron-rich isotopes.

In the graphic above, step 2 is listed twice: 2a depicts a normal hydrogen reaction; 2b depicts the same reaction with heavy hydrogen. All steps except the third are weak-interaction processes. Step 3, neutron capture, is a strong interaction but not a nuclear fusion process. Given that the fundamental basis for the Widom–Larsen theory is weak-interaction neutron creation and subsequent neutron-catalyzed nuclear reactions, rather than the fusing of deuterons, the Coulomb barrier problem that exists with fusion is irrelevant in this four-step process.

The most unusual and by far the most significant part of the Widom–Larsen process is step 1, the creation of the heavy electrons. Whereas many researchers in the past two decades have speculated on a generalized concept of an inverse beta decay that would produce either a real or virtual neutron, Widom and Larsen propose a specific mechanism that leads to the production of real ultra-low-momentum neutrons.

44.2 THE ROLE OF SURFACE PLASMON POLARITONS

It is reasonably safe to say that one of the most accepted conditions required for the initiation of LENRs is the presence of a metal that forms an interstitial hydride and is loaded with an isotope of hydrogen to near stoichiometry (equal numbers of metal and hydrogen nuclei). Upon entry into the metal, the hydrogen nucleus loses its electron to the sea of conduction electrons that make a metal conductive and becomes a bare nucleus (a proton for hydrogen, a proton and neutron for deuterium, . . .). These hydrogen nuclei take up residence in between the metal nuclei in the regular crystal lattice. Each allowed location in the lattice can hold a single hydrogen nucleus. These locations represent stable energetic minima where hydrogen settle.

Furthermore, these nuclei can oscillate in these locations with the oscillations occurring at specific frequencies that depend on the lattice geometry and the mass of hydrogen. As a metal is loaded with increasing amounts of hydrogen, the hydrogen nuclei at first act like a gas and diffuse

through the metal in random fashion independent of one another. The hydrogen nuclei are rather unique in that they can and do migrate rather freely within the metal crystal. This property of interstitial metal hydrides allows metal films and sheets to be used as an effective filter for purifying hydrogen gas. As increasing amounts of hydrogen are forced into the lattice, the system undergoes a series of phase changes. The lattice can no longer accommodate the strain the additional hydrogen places on the crystal, and the lattice expands to a new size/spacing. This expansion does require energy input and is a primary reason why reaching stoichiometry is difficult. As the lattice becomes full of hydrogen, the individual hydrogen nuclei are no longer free to randomly diffuse through the lattice. The hydrogen motions become synchronized. One hydrogen nucleus cannot move without affecting the others nearby. This effect can be very long range at stoichiometry. This collective motion of the hydrogen nuclei is an essential aspect of WLT.

The surfaces of good electrical conductors, such as metals, allow for an interesting mode of propagation of electromagnetic radiation (photon of light). At the interface between a conductor (metal) and an insulator/dielectric (vacuum, water, air, ...) a photon can become attached to the surface of the conductor. The mode of propagation is called a Surface Plasmon Polariton (SPP). As an SPP travels along the surface of the conductor, the usual oscillating electric and magnetic fields exist in the dielectric; however, the electric field cannot exist in the conductor. Instead, the SPP in the metal is comprised of an oscillating surface charge wave. The conduction electrons from the metal form a localized traveling packet of excess charge that follow and match the electric fields dielectric above the conductive surface. SPPs can be created by a wide range of disturbances to the steady state charge distribution on the surface of the metal. In addition to the thermal statistical (blackbody) fluctuations in charge density, incident light, ions, electrical currents, and fields all generate SPPs. SPPs on the surface of a metal are ubiquitous.

According to WLT, the first step in the process of initiating LENRs is to resonantly couple the hydrogen oscillations in the lattice to the SPPs. Since the conduction electrons in the metal are much more mobile, they effectively shield the electric fields from penetrating into the bulk of the metal. Although charged and mobile, the hydrogen nuclei (proton plasma) generally do not respond directly to the SPP fields. However, if the fields associated with the SPPs are large enough and at the correct frequency, the initial oscillation of the conduction electrons can resonantly couple to the protons in the lattice. This process of the electrons acting as an intermediary is known as a breakdown of the Born-Oppenheimer Approximation. Resonant exchanges of energy can be very rapid and energetic. As the resonant proton motion increases in amplitude, the proton motions are synchronized on the scale of the SPP wavelength (several microns) and the fluid-like constraints of the motions within the lattice cannot be maintained. WLT holds that at this point transient micron-scale surface patches or pools of bare hydrogen nuclei emerge onto the surface of the metal. For a fully loaded metal hydride driven at resonance, the surface of the hydride is "shimmering" in transient pools of correlated protons.

Associated with these surface patches are regions of very strong and localized electric field gradients. These fields arise as a result of surface topology, surface contamination, lattice defects (such as cracks or grain boundaries), or differences in the band structure between the metal lattice and the surface protons. Although the voltage of these fields is rather small, perhaps only a few tens of eV, they occur on such a small physical scale that the voltage gradient can be very large, in excess of 10^{11} eV/m. It is well known from quantum electrodynamics that an electron in such a field has its mass renormalized and effectively becomes a heavy electron [2]. In a sufficiently strong field, the electron mass can be increased several-fold. These heavy electrons are essential to several processes in WLT.

Normally, the mass of an electron is 0.51 MeV. The combined mass of an electron and a proton is less than the mass of a neutron by 0.78 MeV. As such, the process of an electron, at rest, being captured by a proton, also at rest, to form a neutron is energetically inhibited. Extra energy or mass is required for electron capture to proceed. WLT states that this extra mass becomes available in the form of the heavy electrons that exist in the strong electric fields near the surface patches. Once a heavy electron becomes slight more than 2.5 times its rest mass, it can be readily absorbed by a proton. The probability of electron capture increases rapidly with heavy electron mass.

The neutrons produced by this electron capture process have one other unusual property initially. WLT relies on the concept of "collective effects" to produce neutrons with very low momentum—Ultra-Low-Momentum Neutrons (ULMNs). Because of the collective motions of the protons driven at resonance, the wave functions of the protons have a spatial extent comparable to the scale of the motion or several microns. Since the extent of the wave function (de Broglie wavelength) is inversely related to the momentum, the momentum of these neutrons is exceptionally sub-thermal. Such neutrons are highly reactive and undergo rapid neutron absorption by nearby nuclei. These neutrons are so reactive that essentially none of them escape from the vicinity where they are produced.

The absorption of one or more neutrons into a target nucleus is usually followed by the emission of a soft gamma ray (photon), a beta particle (electron), or for some neutron rich isotopes, an alpha particle (helium nucleus). Except for those instances where only a gamma ray is emitted, the neutron absorption results in transmutation of the original

nucleus. Although moderate energy beta and alpha particles are readily absorbed and their energy thermalized in the vicinity of their creation, the heavy electrons are required to absorb and convert the gamma rays to thermal photons [3]. Recall that one of the primary advantages and a hallmark of LENRs is that the nuclear-like energy release is not accompanied by any statistically significant observations of long-range energetic particles (expected neutrons) or photons (prompt gammas).

Through a combination of condensed matter physics, plasmonics, quantum electro-dynamics, electro-weak theory, and nuclear physics, WLT achieves a plausible explanation for LENR, which addresses the following issues:

- Overcoming the Coulomb barrier—there is none in either the electron capture or neutron absorption processes.
- Lack of energetic particles—neutrons and gamma rays both readily absorbed; Transmutation of elements within the sample, which may also result in unnatural isotopic enrichments.

44.3 NUCLEAR PROCESSES

While the exact reactions and amounts of energy release depend on the composition of the metal hydride and trace impurities, the following example illustrates the basic steps and mechanisms. The first step in the process according to WLT is for a proton to capture an electron to form a neutron. The reaction process of electron capture can be written as follows:

$$\mathrm{p} + \mathrm{e}* \Rightarrow \mathrm{n} + \overline{\upsilon}_e$$

where p is a proton, e is an electron, n is a neutron, and $\overline{\upsilon}_e$ is an antineutrino (electron type). The asterisk on the e indicates that this is a heavy or energetic electron.

Alternatively, in the case of deuterium, the reaction process can be written as follows:

$$\mathrm{d} + \mathrm{e}* \Rightarrow 2\mathrm{n} + \overline{\upsilon}_e$$

Additional energy or mass is required since the process of electron capture by a proton to form a neutron is inhibited by 0.78 MeV. This first step actually costs energy and must be input into the system before any net energy can be released. This process and energy cost occurs once for every new neutron produced.

A key concept of the WLT is that many reactions become possible in the LENR environment once the ULMN is created. A variety of pathways to create He4 are possible, as Larsen shows in the image below (Fig. 44.3).

A common trace element, lithium (Li), is present in many experiments. The original WLT uses the following series of reaction starting with a common isotope of lithium.

$$\mathrm{Li6} + \mathrm{n} \Rightarrow \mathrm{Li7}$$

$$\mathrm{Li7} + \mathrm{n} \Rightarrow \mathrm{Li8}$$

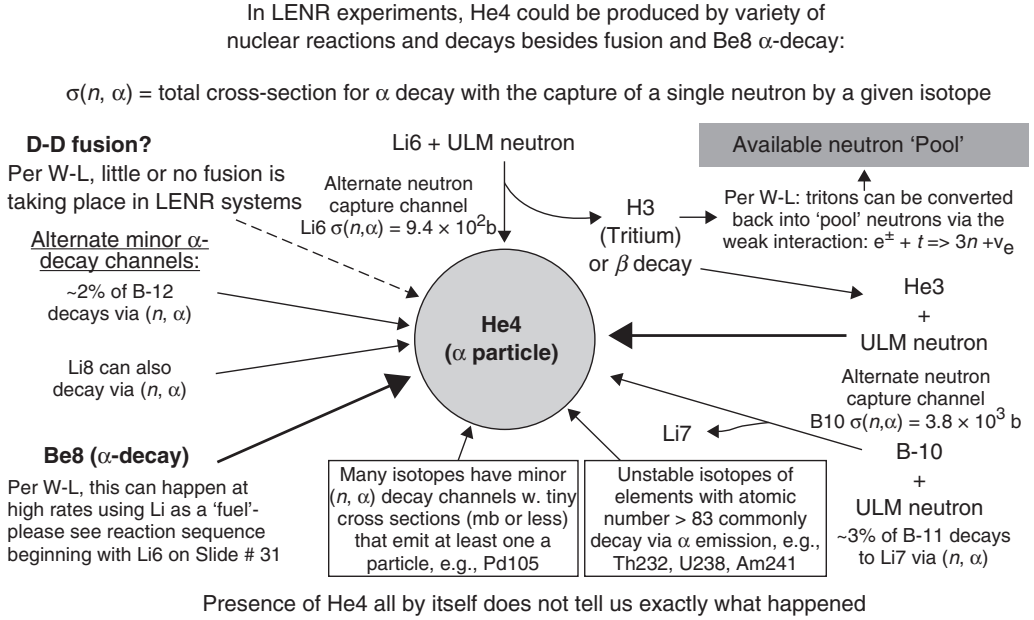

Figure 44.3 Lewis Larsen's graphical display of the variety of pathways to create helium-4 in LENR (*Image courtesy of Lewis Larsen*). *Source:* Adapted by New Energy Times with minor modifications from, and copyright Lewis Larsen, Lattice Energy LLC, slide presentation June 25, 2009.

$$\text{Li8} \Rightarrow \text{Be8} + \beta + \upsilon_e$$

$$\text{Be8} \Rightarrow \text{He4} + \text{He4}$$

The most abundant naturally occurring isotope of lithium is Li6, which has 3 protons and 3 neutrons. The first two process steps are the absorption of neutrons by Li6 to form Li8. Li8 is unstable and quickly decays to beryllium through emission of a beta particle (energetic electron) and a neutrino. The Be8 isotope is also unstable and splits to produce two helium atoms. Both of these last two steps release a significant amount of energy (~27 MeV) and only required ~1.6 MeV input (2×0.78 MeV) to produce the two neutrons partaking in the first two steps of the process. Through this process, WLT predicts that helium will be produced when lithium is present.

Helium can undergo neutron absorption.

$$\text{He4} + n \Rightarrow \text{He5}$$

$$\text{He5} + n \Rightarrow \text{He6}$$

$$\text{He6} \Rightarrow \text{Li6} + \beta + \upsilon_{\text{e}}$$

If the helium just produced absorbs two additional neutrons to form He6, it will decay to lithium and release additional energy. Note that this returns the lithium atom consumed in the first set of neutron capture steps and is therefore a catalytic cycle. If both helium atoms are converted back to lithium, the cycle is super-catalytic and releases the most energy from this simple system of reaction. In this cycle, 6 protons and 3 electrons are converted to a new Li6 and 9 (anti)neutrinos with a net release of ~28 MeV. In this case, energy is released without the net production of any helium.

Depending upon the fraction of the helium atoms produced and subsequently converted back into lithium, any value for the energy per helium atom in the range from ~9 MeV (allowing for energy lost via neutrinos) to infinity can be obtained. Therefore, the observed values of net energy per helium only provide information on the fraction of lithium atoms catalytically restored and are not a clear indication of the specific processes (e.g., D-D fusion's 23.8 MeV/He4) occurring. Real-world experiments are more complicated with several nuclear cycles occurring within the apparatus as evidenced by the wide variety of nuclear transmutation products.

Note: The "Four-Step Widom–Larsen Process" section is reprinted courtesy of New Energy Times.

REFERENCES

1. A. Widom and L. Larsen, Ultra low momentum neutron catalyzed nuclear reactions on metallic hydride surfaces. *Eur. Phys. J. C*, 2006, (DOI) 10.1140/epjc/s2006-02479-8.
2. V. B. Berestetskii, E. M. Lifshitz, and L. P. Pitaevskii, *Quantum Electrodynamics* (Sec. 41). Butterworth Heinemann, Oxford, UK, 1997.
3. V. B. Berestetskii, E. M. Lifshitz, and L. P. Pitaevskii, *Quantum Electrodynamics* (Sec. 101). Butterworth Heinemann, Oxford, UK, 1997.

45

POTENTIAL APPLICATIONS OF LENRs

WINTHROP WILLIAMS[1] AND JOSEPH ZAWODNY[2]
[1]*University of California, Berkeley, Berkeley, CA, USA*
[2]*NASA Langley Research Center, Hampton, VA, USA*

45.1 INTRODUCTION

Low energy nuclear reactions (LENRs) are the subject of research intended to lead to applications in energy generation and transmutation of nuclear fission waste into nonradioactive materials. The research may also provide tools to probe the structure of matter and expand our understanding of physics.

As an energy source, LENR offers the possibility to meet basic human needs anywhere on the globe, without requiring access to special locations or limited resources, thus encouraging peaceful coexistence. Some of the human need for purpose and meaning could be met through new philanthropic, scientific, and environmental initiatives fueled by abundant energy.

LENR research and applications may engage new interest in science, change the role of energy in our economy and our decision making, and engage social shifts supported by abundant energy and the possibility of new discovery. LENR and its secondary technological and social shifts may eventually become enablers of space exploration.

The LENR research throughout the last two decades, while problematic in certain regards, has nevertheless consistently shown signs of advantageous characteristics of these phenomena without showing any major disadvantages, such as dependency on rare materials or operating characteristics that would interfere with day-to-day applications.

45.2 POSSIBLE LENR FUEL COMBINATIONS AND ENERGY DENSITY

LENR has been observed primarily (although not exclusively) in solid-state materials consisting of nickel or palladium into which normal or heavy hydrogen had been introduced with some non-equilibrium driving force. Observed energy outputs exceed what is possible chemically, and nuclear transmutations, from light to heavy elements, have been observed repeatedly [1, 2]. Energy output varies orders of magnitude between experiments, and small changes in materials preparation can make a difference between a positive or null result. Nevertheless, these outcomes indicate that nuclear reactions are taking place in these systems. It is therefore likely that nuclear-scale energy density can be achieved using LENR, and that at least two fuel combinations (Ni-H and Pd-D) appear to be viable although the role of other potential active materials is still unclear.

LENR is observed under non-equilibrium conditions; an action or flow or oscillation of some kind is intentionally introduced into the system in order to trigger the reaction. The energy output of such a system may be expressed as the sum of the heating that results from the triggering input (e.g., frictional or ohmic heating loss equal to the input power) plus whatever additional energy is released by the reaction. This additional energy is termed the excess heat. In many experiments the application of the triggering stimulus must be continued for the reaction

Nuclear Energy Encyclopedia: Science, Technology, and Applications, First Edition (Wiley Series On Energy).
Edited by Steven B. Krivit, Jay H. Lehr, and Thomas B. Kingery.

to continue producing excess heat. However, there is a growing body of examples where LENR systems have produced atypically large amounts of heat and sustained heat output well after all external stimuli had ceased. Some research shows evidence of localized melting of metal indicative of microscopic concentrations of very high levels of heat.

45.3 LENR RADIATION AND PORTABILITY FACTORS

Intriguingly, LENR experiments have never produced much in the way of radiation or long-lived radioactivity. Thus, neither shielding nor remote isolation of the LENR system is expected to be required. The radiation that has been observed is relatively benign, being either non-penetrating (alpha or beta particles for example), small in quantity, or short lived. Tritium (a short-lived radioactive isotope of hydrogen) has been seen intermittently in some experiments. Tritium decays via beta radiation (emission of an electron from the nucleus of the tritium atom). The emitted electrons are of too low an energy to penetrate the skin, thus tritium is only harmful to humans if large quantities (hundreds of millicuries) are ingested, inhaled, or absorbed through the skin [3–5]. In addition, the "biological half-life" of tritium in the body is only 10 days; in other words, it flushes out rather quickly. The amounts produced in LENR experiments (up to a few microcuries) are detectable using readily available detectors having high sensitivity to beta radiation, such as x-ray film.

45.4 EARLY APPLICATIONS OF LENR NOT REQUIRING SIGNIFICANT HEAT OR ENERGY OUTPUT

As researchers continue to develop a better understanding of LENR, they will hopefully be led to deeper understandings of fundamental physics, and the new insights may lead to applications that enable researchers to use these phenomena to probe the atomic and crystalline structure of these materials and nuclear structure. This will be a natural spin-off of research already under way to characterize and quantify the phenomena using surface-imaging techniques [6–8]. Therefore, such applications may provide utility even if they don't provide any significant net energy output.

LENR research may spawn other new areas of research and breathe new life into old ones, both directly and indirectly. New lines of inquiry will be stimulated directly as spin-offs and also as a result of ideas stimulated by the growing understanding of LENR. In addition, LENR may open new areas of research that will awaken interest in further exploration of other lines of research that have been dormant, including ones completely unrelated to LENR.

An example of an industrial application that doesn't require energy as a product is the use of LENR to remediate radioactive wastes, forming non-radioactive materials (or shorter lived isotopes that quickly decay), thus eliminating the radioactivity [9, 10].

Should LENR remediation be proven and scaled up, the need for sequestration and storage of "hot" waste will be reduced or eliminated. If LENR can be successfully combined with biological remediation, then the need for sequestration of low-level radioactive wastes (which by mass and volume make up the vast majority of all radioactive wastes) may be eliminated as well.

45.5 APPLICATIONS OF RESEARCH-STAGE ENERGY DEVICES

It is conceivable the first LENR devices that produce useful energy will be fabricated in small batches by specialists, possibly using expensive or specialized nanotechnology tools. Such products might initially have small form factors and low-power output. They are likely to be used in specialized applications that are not cost-sensitive and that benefit from longer running times for a given weight. Similarly, it may be that early large-scale power generation will require expert monitoring and maintenance. If so, such systems (if greater than a few megawatts) could still be competitive and not sensitive to the cost of custom construction and operation.

45.6 APPLICATIONS OF LOW-GRADE LENR HEAT

Energy applications that require only low-grade heat include the augmentation of heating systems formerly reliant on electricity alone, such as heating the passenger compartments of trains and electric automobiles. In such cases, whatever additional energy the reaction yields, even if small, reduces electricity consumption.

45.7 LARGE-SCALE LENR APPLICATIONS

As soon as the heat output from a LENR system is high enough to where it can cost-effectively compete with combustion fuel systems, it can be applied to heating water and buildings in place of natural gas and/or heat pump systems.

This level of efficiency (about three times as much heat output as electrical input) is approximately the same point at which Carnot efficiency becomes sufficient for LENR

to power a generator that sustains the energy required for the reaction input. Even with no net electrical output, such systems open up large-scale applications such as greenhouse heating and evaporative desalination to make pure enough water for farming and reforestation.

45.8 MATURING TECHNOLOGIES: ELECTRICAL GENERATION AND COMBINED HEAT AND POWER

As LENR applications mature and scientists understand which fundamental parameters are needed to control LENR, it is likely that efficient LENR systems will be developed.

When the level of efficiency becomes "good enough," it will tip the balance for decision makers—who might otherwise have waited longer for even greater scientific advancements—to begin deployment and rapid scale-up.

Rather than building additional central power plants, however, and the extra grid infrastructure they would demand, decentralized generation can pick up the load for new buildings and industry. Local systems can offer combined heat and power, as existing chemically fueled local generation systems do today, and this shift to shared reliance on grid power and local power can mitigate (or eventually avoid entirely) central points of potential failure. In addition, local generation better distributes any waste heat that goes unused, avoiding the kind of environmental harm that has sometimes resulted from waste heat disposal concentrated near electrical generating stations. Even if such systems are bulky at first, they may also find use in some mobile applications such as cruise lines and cargo ships.

While it could turn out that one LENR technology can be scaled to applications of all sizes, it is also possible that different LENR technologies will find application in devices of different power scales, from a few kilowatts to heat and/or power a home, to 10 or more gigawatts to launch something into low earth orbit.

45.9 ENVIRONMENTAL REMEDIATION OPTIONS

Potential low-cost LENR energy sources may also find applications in a variety of remediation endeavors. Such proposals as pulling CO_2 out of the atmosphere, indirectly by removing it from the surface layers of the ocean, may become feasible. One approach proposed for this is the electrolysis of sea water resulting in formation of a deposit rich in carbonate. The deposit has even been proposed as a building material and dubbed "sea concrete." This concept has also been suggested as an approach for restoring coral reefs [11, 12].

45.10 PORTABLE AND FIXED TERRESTRIAL APPLICATIONS

If LENR can be made compact, sufficiently lightweight, and able to routinely withstand acceleration, then vehicles of all sizes may be powered with it, including personal aircraft. Some LENR phenomena are observed in the gas phase, and in the interaction of gas with a solid catalyst. Descendants of these systems could be naturally insensitive to acceleration and lead directly to use in vehicles. However, many other LENR experiments involve electrolysis of a low-viscosity liquid (which only partially fills its container) and solid electrodes from which gas bubbles rise (to join gas produced at the other electrode) and then recombine (in closed systems) before returning to the liquid. Clearly these experimental systems (which rely on gravity to separate gas from liquid) are not suitable for application in moving vehicles. It will be necessary to immobilize the electrolyte (as in modern batteries) and separate gas and liquid phases (perhaps as presently done in fuel cells), in order to prevent unwanted mixing during a vehicle's maneuvers.

As a result of LENR technology, our use of land and oceans may change significantly as well. Habitation will be possible nearly anywhere on the globe, and quality of life can be improved for billions of people living off the grid. Rather than being limited to energy production that brings pollution, LENR could provide power for cost-effective desalination of water, pumping deep wells, running long supply lines, condensing water from the air, as well as heating or cooling farming and living spaces.

In a futuristic scenario not unlike the TV program *The Jetsons*, buildings and entire cities could expand both horizontally and vertically if new transportation modalities—personal aircraft, for example—become so ubiquitous as to replace elevators and allow direct flight from building to building, like bees among hives [13].

45.11 SPACE EXPLORATION

Assuming LENR can be optimized for sufficient power-to-weight and energy density, and with engine designs capable of achieving high exit velocity, single-stage launches to orbit and beyond become feasible. Furthermore, it is possible that fuel to power the LENR system, as well as reaction mass to eject through the rocket motor creating thrust, will be available at way-points throughout the solar system. This would make extended multi-stop missions feasible and significantly reduce the launch weight of these and more traditional round-trip missions. Even if power-to-weight were to remain too low for earth launch, high-energy density would suffice to propel missions from earth orbit to asteroids and planets with sufficient speed to avoid the

crew's being exposed to excessive radiation from space, and provide essentially indefinite power for habitat heating and life support [14, 15].

REFERENCES

1. G. H. Miley, and P. Shrestha, Review of Transmutation Reactions in Solids, *Proceedings of the Tenth International Conference on Cold Fusion*, Cambridge, Mass., 2003.
2. V. Vysotskii, et al., Experimental discovery of phenomenon of low-energy nuclear transformation of isotopes (Mn55 = Fe57) in growing biological cultures, *Infinite Energy*, **2** (10), p. 63. http://www.lenr-canr.org/acrobat/StormsEanewmethod.pdf.
3. United States Nuclear Regulatory Commission Office of Public Affairs, Backgrounder on Tritium, Radiation Protection Limits, and Drinking Water Standards. http://www.nrc.gov/reading-rm/doc-collections/fact-sheets/tritium-radiation-fs.html.
4. T. J. Dolan, Fusion Research, Pergamon Press, 1982. http://npre421.ne.uiuc.edu/2007%20files/Dolan%20book%20chapters/Fusion%20Research%201%20file%20original%20with%20hidden%20text.pdf.
5. P. D. Ritter, T. J. Dolan, G. R. Longhurst, Environmental tritium transport monitoring at TFTR, Journal of Fusion Energy, 1993, **12**, 145–148.
6. V. Violante, et al., Material science on Pd-D system to study the occurrence of excess power. *Proceedings of the Fourteenth International Conference on Condensed Matter Nuclear Science*. Washington, DC, 2008.
7. A. Ramachandrana, W. M. Tuchoa, A. L. Mejdellb, M. Stangec, H. J. Venvikb, J. C. Walmsleyd, R. Holmestada, R. Bredesenc, and A. Borga, Surface characterization of Pd/Ag23wt% membranes after different thermal treatments, *Applied Surface Science*, 2010, **256**, (20), 6121–6132.
8. M. L. Bosko, D. Yepes, S. Irusta, P. Eloy, P. Ruiz, E. A. Lombardo, L. M. Cornaglia, Characterization of Pd–Ag membranes after exposure to hydrogen flux at high temperatures, *Journal of Membrane Science*, 2007, **306**(1-2), 56–65.
9. Larsen, Lewis, LENRs for nuclear waste disposa: How weak interactions can transform radioactive isotopes into more benign elements, *Institute of Science in Society*. http://www.i-sis.org.uk/LENR_Nuclear_Waste_Disposal.php.
10. O. Reifenschweiler, Some experiments on the decrease of tritium radioactivity, *Fusion technology*, 1996, **30**, (2), 261–272. http://cat.inist.fr/?aModele=afficheN&cpsidt=2504851.
11. P. van Treeck, H. Schuhmacher, Initial survival of coral nubbins transplanted by a new coral transplantation technology-options for reef rehabilitation, *Marine Ecology Progress Series*, 1997, **150**, 287–292. http://www.int-res.com/articles/meps/150/m150p287.pdf.
12. T. Goreau, W. Hilbertz, Reef restoration using seawater electrolysis in Jamaica, *Proceedings of 8th International Coral Reef Symposium*, Panama, 1996. http://www.globalcoral.org/reef_restoration_using_seawater.htm.
13. Arthur St. Antoine, At Last: A Jetpack of Your Very Own, 2010. http://iactionfigure.com/jetpack/.
14. J. P. Biberian, Low energy nuclear reactions in gas phase: A comprehensive review, *Low-Energy Nuclear Reactions and New Energy Technologies Sourcebook*, 2009, ***2***, 9–34. http://pubs.acs.org/doi/abs/10.1021/bk-2009-1029.ch002.
15. R. Adams, R. Alexander, J. Chapman, S. Fincher, R. Hopkins, A. Philips, T. Polsgrove, R. Litchford, B. Patton, G. Statham, P. White, Y. Thio, *Conceptual Design of In-Space Vehicles for Human Exploration of the Outer Planets*, NASA/TP—2003–212691, 2003. http://ntrs.nasa.gov/archive/nasa/casi.ntrs.nasa.gov/20040010797_2004001506.pdf.

PART VII

OTHER CONCEPTS

46

ACOUSTIC INERTIAL CONFINEMENT NUCLEAR FUSION

Rusi P. Taleyarkhan[1], Richard T. Lahey Jr.[2] and Robert I. Nigmatulin[3]

[1]*Purdue University, College of Engineering, West Lafayette, IN, USA*
[2]*Rensselaer Polytechnic Institute, Troy, NY, USA*
[3]*Russian Academy of Sciences, Moscow, Russia*

46.1 OVERVIEW OF ACOUSTIC INERTIAL CONFINEMENT NUCLEAR FUSION (AICF/BNF)

Acoustic Inertial Confinement (aka Bubble) nuclear fusion (hereafter referred to as AICF) is an approach using highly focused acoustic waves for attaining super-compression-induced based high temperature ($>10^7\,^\circ$K) plasma states within imploding deuterium (i.e., H2, a heavy isotope of hydrogen) or deuterium and tritium (H3, an even heavier form of hydrogen) bearing vapor bubbles. AICF is somewhat similar to laser-energy-induced super-compression inertial confinement fusion. However, instead of using pulsed energetic laser beams focused on tiny fuel pellets, AICF utilizes focused acoustic energy to attain thermonuclear fusion within imploding cavitation bubbles. Also, unlike laser-based fusion, which aims to produce relatively large quantities of fusion energy with every laser pulse (at a targeted repetition rate of about 1 per minute), the AICF process produces sub-nano-scale thermonuclear reactions at the rate of over 20,000 per second. The goal of AICF is to eliminate the conventional uncontrolled nature of thermonuclear devices, which release their energy within microseconds, instead having many much smaller fusion reactions in a controlled manner and stretched out in time to the desired extent to attain the net power level that is required.

For thermonuclear fusion to occur [Gross, 1984] due to super-compression, the density and temperature of the compressed vapor/plasma must be high enough to overcome the Coulomb barrier, preventing positively charged ions (i.e., deuterium with deuterium or tritium) from fusing. In the AICF method (Fig. 46.1), tiny vapor bubbles, on the scale of nanometers, are nucleated in a highly tensioned metastable liquid hydrocarbon, such as deuterated acetone. This liquid is composed of molecules that contain either deuterium or a combination of deuterium and an even heavier form of hydrogen called tritium. Tension-inducing (i.e., sub-vacuum) pressures in the liquid overpowers the intermolecular forces so that tiny (nano-scale) cavitation bubbles can be nucleated using ionizing radiation such as from energetic (multi-MeV) neutrons, heavy ions, photons, or even the recoiling nuclei of heavy elements such as dissolved uranium undergoing radioactive decay. Once the nucleated bubbles are greater than a critical dimension, these bubbles will grow rapidly (within microseconds), by factors of over 10^6 to visible dimensions in the muli-mm scale [Lahey et al., 2006]. During the evaporation-induced growth phase, molecules of the host liquid enter the vapor bubble. Thereafter, when the impressed external pressure field becomes positive (i.e., is compressive) these bubbles implode within time spans of nano-to-pico seconds. As the liquid/vapor interface collapses, the pressure in the bubble starts to rise, and some of the vapor inside the bubble condenses back into the liquid. As the interface and surrounding fluid accelerates beyond the speed of sound, a converging shock wave is formed in the vapor, which leads to dissociation and ionization of the vapor molecules. Close to the point of maximum compression near the center of the bubble, a flash of light (typically in the UV range) is emitted by a process [Gaitan, 1992] referred to as sonoluminescence

Nuclear Energy Encyclopedia: Science, Technology, and Applications, First Edition (Wiley Series On Energy).
Edited by Steven B. Krivit, Jay H. Lehr, and Thomas B. Kingery.

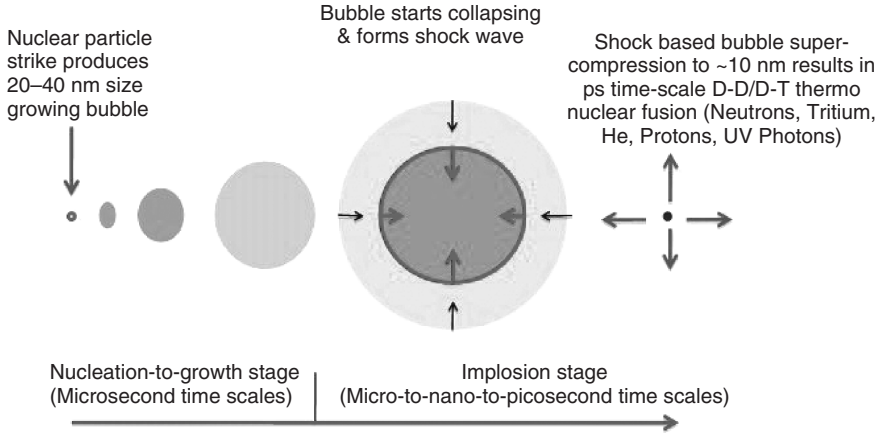

Figure 46.1 Illustration of acoustic inertial confinement (bubble) fusion process.

(SL), together with the telltale signatures of thermonuclear fusion (viz., neutron and tritium production), and this is followed by an audible shock wave [Taleyarkhan et al., 2002]. Young [2004] and Walton [1984] provide good summaries of sonoluminescence phenomena.

46.2 THERMONUCLEAR D/D AND D/T FUSION AND AICF

A significant amount of fusion of D (H2) with D atoms (i.e., D/D fusion) or with T (H3) atoms (i.e., D/T fusion) requires plasma temperatures in the range of 10^7 K and above.

Fusion of D and D atoms at high temperatures results in two reaction pathways of roughly equal probability [Gross, 1984]:

$$^2\mathrm{H} + ^2\mathrm{H} \rightarrow n + ^3\mathrm{He}$$

or,

$$^2\mathrm{H} + ^2\mathrm{H} \rightarrow ^3\mathrm{H} + ^1\mathrm{H}$$

Also, fusion of H2 and H3 atoms at high temperatures results in a single reaction pathway:

$$^2\mathrm{H} + ^3\mathrm{H} \rightarrow ^4\mathrm{He} + \mathrm{n}.$$

For a plasma temperature in the $10^7\,^\circ$K range, the deuterium/tritium reaction rate is over 100 times greater than that for deuterium/deuterium reactions. In addition, the energy of neutrons resulting from a deuterium/deuterium fusion reaction is ~2.45 MeV, whereas the neutron energy from deuterium/tritium reactions is over five times greater at ~14 MeV.

Despite the fact that the deuterium/tritium reaction produces more energy and is also 100 times more probable compared with deuterium/deuterium reactions, such a reaction is not easy to use for two key reasons. First, tritium is radioactive. Thus, cost and special handling requirements make it unsuitable for laboratory-scale studies at universities. Second, tritium (i.e., a tritiated liquid) is not readily available in significant quantities at reasonable cost. For this reason, all reported AICF studies and experiments to date have relied on deuterium/deuterium fusion reactions.

46.3 CONTRASTING AICF BUBBLE NUCLEAR FUSION AND SINGLE BUBBLE SONOLUMINESCENCE (SBSL) EXPERIMENTAL APPROACHES

Controlled sonoluminescence was first announced in the early 1990s [Gaitan, 1992] wherein a stationary, levitated bubble, having a diameter of ~10 μm, was expanded and compressed by oscillating acoustic pressures in the ±1 bar range for baseline atmospheric pressure conditions. Each time, the levitated air bubble grew by a factor of about 10, to ~100 μm, and imploded to produce a flash of blue light (in the ultra-violet range) lasting for tens of picoseconds. This process was referred to as Single Bubble Sonoluminescence (SBSL). Shock-physics-based simulations [Moss, 1996] of SBSL predicted the possibility of attaining plasmas and $\sim 10^6\,^\circ$K temperatures, and even higher, if the implosion stage could be made more intense by using larger acoustic pressures. Since the early 1990s, SBSL experimental studies have demonstrated the attainment of plasma states [Flannigan, 2005] and the contents of the interior of the bubbles have been estimated to reach temperatures close to $10^6\,^\circ$K [Camara, 2004]. Unfortunately, due to inherent hydrodynamic instabilities, impressed pressure amplitudes above ~1 bar lead to bubble ejection and breakup of the gas-filled bubble [Lahey et al., 2006]. Thus, conditions suitable for fusion cannot be achieved using the standard SBSL experimental approach.

TABLE 46.1 Bubble Nuclear Fusion (AICF) vs Conventional Single Bubble Sonoluminescence

Parameter	AICF/BNF	SBSL
Bubble shape and quantity	Over 100 (in cluster form) spherical bubbles during growth and implosion; bubbles re-dissolve in liquid but can be formed on demand	1 (single) spherically shaped during growth and implosion phases; single bubble resides continuously in acoustic antinode
Max. radius to initial radius	~100,000	~10
Bubble nucleation	On demand via neutron, ion, alpha recoil, or photon-based interactions	Pre-existing bubble via a hot-wires or gas entrainment
Non-condensible gas in bubble(s)	~0%	~100%
External drive pressure amplitude/stability limitations	±15 bar and above with no known inherent stability limitations	~ ±1 bar (higher drive pressures ejects bubble from acoustic antinode)
Working liquid's accommodation coefficient	~1.0 (Organic, large molecular weight)	~0.05 (Inorganic; e.g., water)
Sonoluminescence?	Yes	Yes
Maximum temperature during implosion	$\sim 10^{8\,\circ}$K	$10^{6\,\circ}$K
D/D fusion demonstrated and replicated?	Yes ($\sim 10^6$ neutrons and tritons per second)	No
Fusion patent protection?	No (pending)	Yes
Natural solution to first-wall problem of tokamaks or laser fusion?	Yes	Yes

The AICF (i.e., bubble nuclear fusion) process was developed to overcome the inherent limitations in the SBSL experimental approach. Key differences are summarized in Table 46.1. As seen, AICF starts out with a cluster of vapor bubbles rather than one non-condensable bubble as in SBSL. The intent here is to utilize the power of acoustic streaming and the focusing of reflected wave energy to amplify the externally generated pressure field by factors of over 100. The second major difference involves on-demand nucleation of vapour bubble clusters in AICF versus using a single pre-existing gas-filled bubble in SBSL. Such an approach relies on first placing the working liquid under intense tension (i.e., −15 bar or more versus only ~0 bar for SBSL). This creates a much larger amount of liquid super heat for growing larger bubbles. AICF expansion ratios are about 100,000 versus only 10 for SBSL, which permits a relatively huge amount of potential energy buildup in the liquid prior to implosion. The third major difference concerns the type of working liquid used. SBSL uses low molecular weight (MW) inorganic liquids such as water, which possesses a very low accommodation coefficient of about 0.05 (a measure of how fast vapor will either form or condense), versus very high accommodation coefficients (i.e., about 1.0, the maximum possible) for AICF, which typically employs high molecular weight organic liquids such as acetone and benzene. In addition, the use of high MW organic liquids permits attaining large tensile pressures prior to externally induced nucleation (without spurious cavitation), and also permits the generation of stronger shocks during the implosion phase since sound velocity is well-known to be inversely proportional to the square root of the MW. The non-condensable gas (e.g., air) content in the working liquid is close to 0% (i.e., the liquid is degassed as much as possible), versus about 100% in SBSL. This was intentional since AICF aims to concentrate shock-based heating onto deuterium-atom-bearing molecules and not dissipate the same in the form of shock cushioning by non-condensable gas molecules. Finally, a key issue related to the first-wall damage that plagues conventional (i.e., tokamak- and laser-based inertial confinement) thermonuclear fusion methods is naturally overcome by the AICF approach. In conventional systems, the fixed (first) wall immediately facing a $10^{7\,\circ}$K type plasma can get readily eroded if the plasma or fusion reaction products come in contact with the first wall, even for brief periods of time. In the AICF approach, the liquid surface surrounding the imploding bubbles is continuously replenished and becomes a natural sacrificial first wall. All of these factors, when taken together, allowed AICF to continuously (up to $\sim 10^2$ to 10^4 times a second for several hours of operation) attain high enough plasma temperatures to result in neutron and tritium emission rates of about 10^6 sec^{-1}. [Taleyarkhan et al., 2002, 2004, 2006]. Although proponents [Putterman, 1997] of the SBSL approach for attaining thermonuclear fusion have been awarded patent rights (by the U.S. Patent and Trademark Office), the SBSL approach has not been demonstrated to be capable of producing fusion. AICF is in the patent-pending mode since the initial filing in 2003, despite demonstration of operability and multiple replications by others skilled in the art.

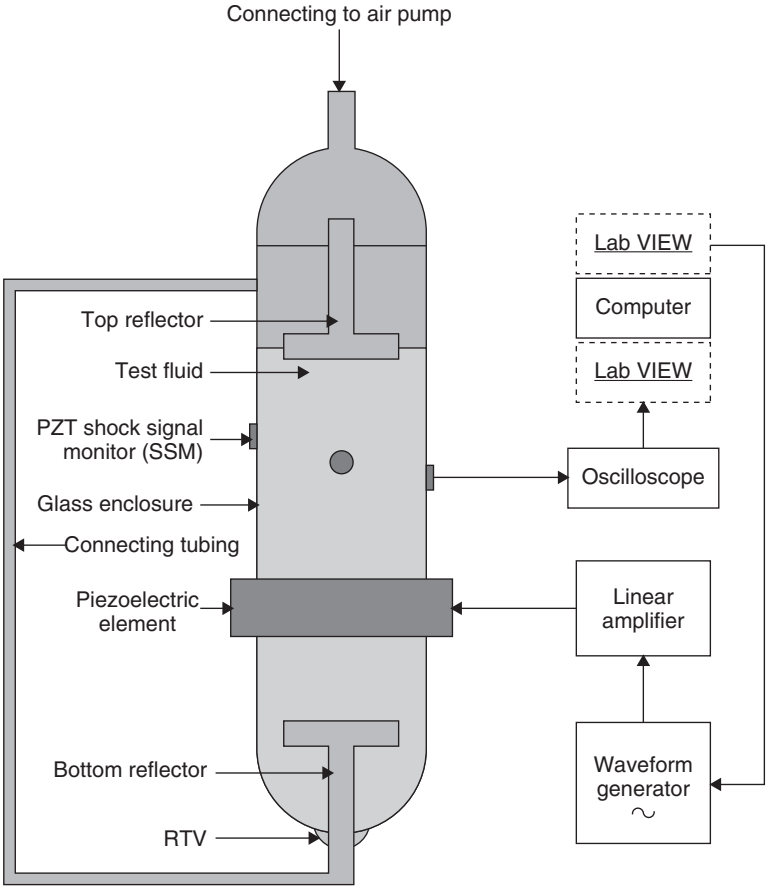

Figure 46.2 AICF reactor test cell and drive train schematic.

46.4 AICF SETUP AND EXPERIMENTATION

A typical AICF test cell and drive components are shown schematically in Figure 46.2. As can be seen, the apparatus consists of a glass chamber (about 6 cm in diameter and about 15 cm tall) within which the deuterated working liquid is placed. A lead-zirconate-titanate (PZT) ring transducer is epoxied to the outer wall of the test cell and driven harmonically at the resonance frequency of the test cell using a combination of a wave-form generator and an amplifier. To establish the proper acoustic boundary conditions, hollow glass reflectors are positioned just below the free surface of the liquid and also within the liquid pool close to the bottom. The liquid within the test cell is first degassed using a combination of acoustic agitation in combination with ionizing radiation (using either an external source of neutrons or through the use of dissolved radioactive material such as uranium). The entire test cell is maintained close to vacuum conditions at as low a liquid temperature as feasible. In the reported successful experiments, the liquid in the test cell was maintained at a temperature of about 273°K. Figure 46.3 depicts the overall experimental approach used in the first published study [Taleyarkhan et al., 2002]. As noted therein, a burst of external neutrons nucleated nano-scale bubbles when the liquid was in highest state of tension. These bubbles grew and then imploded to produce flashes of light and neutrons from D/D fusion. Later, a shock wave was picked up by the pill-microphones mounted on the outside of the glass walls of the test cell.

Separate sensors were used for detecting the SL light flashes and the 2.45 MeV D/D neutrons leaving the test cell, after some of them collide with intervening atoms of the working liquid as well as the glass walls and other obstructions such as ice-containing thermal-shields (when used). A fast response photomultiplier tube was used for SL light detection. In earlier reported studies [Taleyarkhan et al., 2002] a fast-response liquid scintillation (LS) neutron/gamma detector was used. Later, when demonstrating AICF without the use of an external beam of pulsed neutrons for the nucleation of vapor bubble clusters [Taleyarkhan et al., 2006], three independent neutron detectors were used together with a separate NaI gamma photon detector, using the setup shown schematically in Figure 46.4.

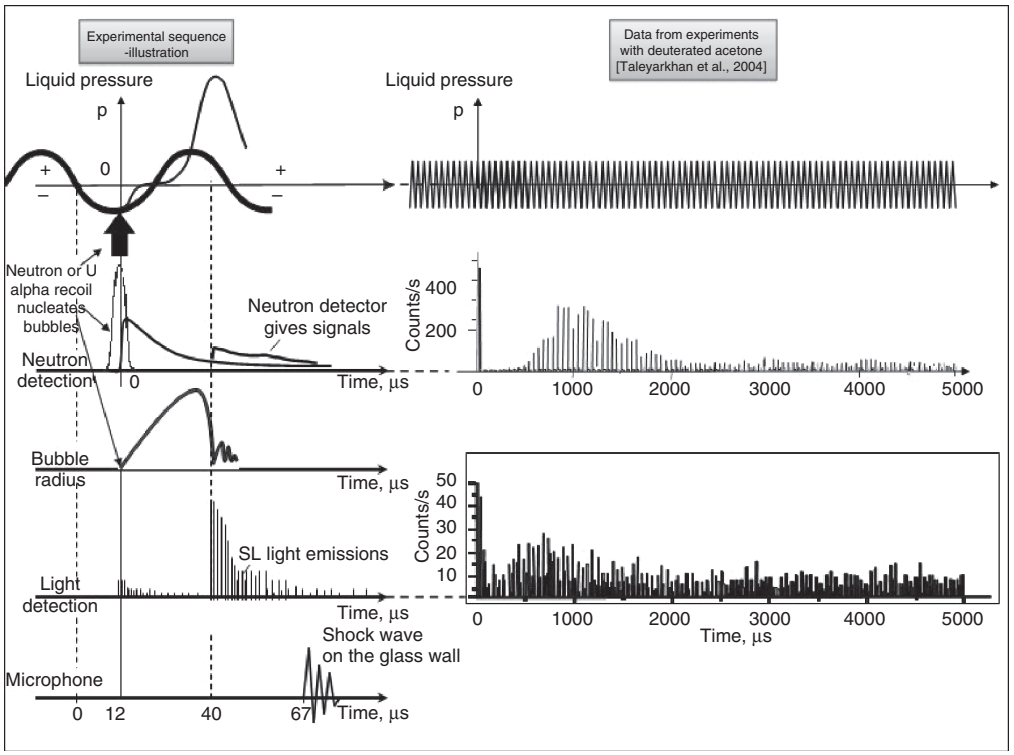

Figure 46.3 Illustration of experimental sequence of events and actual measured data (*Source: Nigmatulin et al., 2005*).

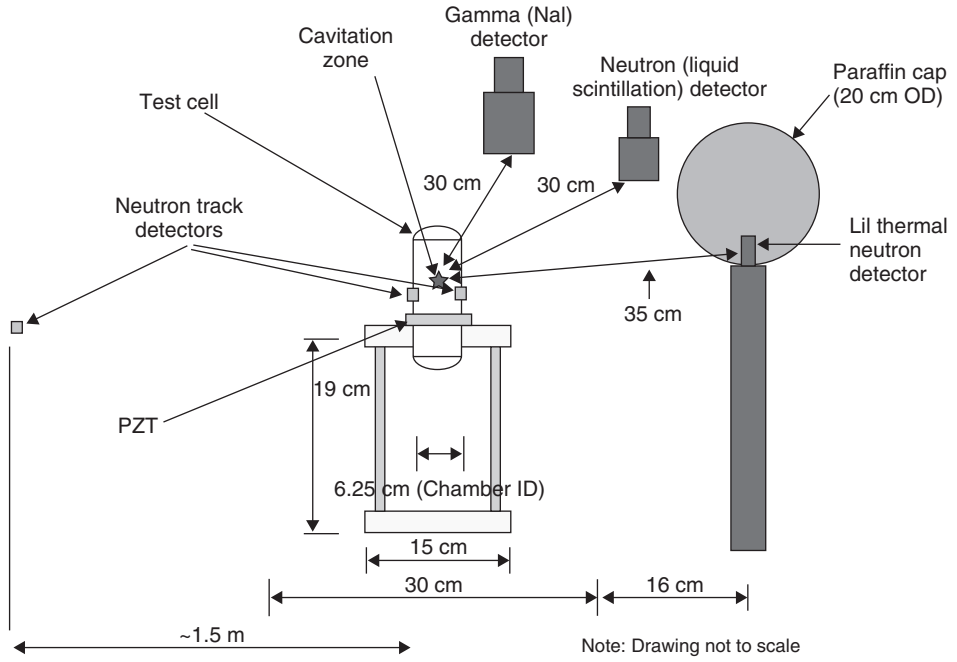

Figure 46.4 Experimental test cell and neutron-gamma detector schematic (Note: Not shown is the enclosure around test cell with ~3 cm ice-packs on enclosure walls).

Another nuclear particle, tritium, was also detected. Tritium, a radioactive beta radiation emitter, remained within the working liquid. To test for the buildup of tritium, a sample of test liquid was removed before and after the experiments and mixed with a scintillation cocktail [Taleyarkhan et al., 2002, 2004]. The beta rays emitted by the tritium produced flashes of light proportional to the amount of tritium present in the liquid within the cocktail. Such light flashes were a direct measure of tritium buildup and were counted using a state-of-art spectrometer.

46.5 WHEN NOT TO EXPECT AICF

All successful reports of AICF have relied on the generation and implosion of spherical bubble clusters. Typical high-speed movie images are shown in Figure 46.5a. They show the bubble cluster generation and evolution toward eventual dissipation. During the time when the bubble cluster is imploding in a spherical fashion, neutron and gamma emissions may be detected. However, non-optimized test cells can drive the nucleated bubbles toward non-spherical shapes, as shown in Figure 46.5b. Under these conditions,

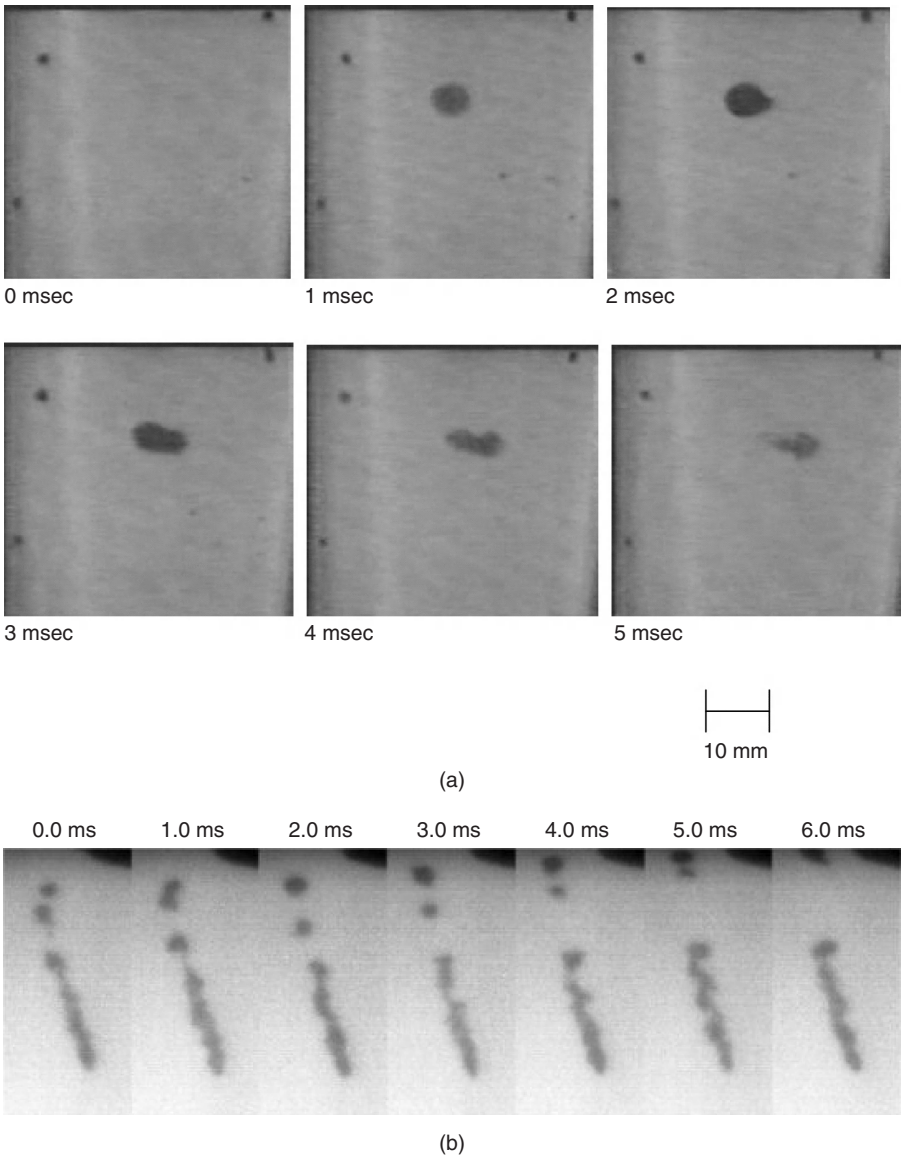

Figure 46.5 (a) Evolution of AICF bubble clusters from nucleation to dissolution [Taleyarkhan et al., 2004] (Note: D/D fusion and SL output depends on cluster shape remaining spherical; output drops after ~2msec.). (b) Non-AICF/BNF bubble clusters [Xu et al., 2005] (Note: D/D fusion reactions terminate if bubble clusters tend towards and/or turn towards such comet-like shapes).

the implosion intensity is significantly reduced, and AICF does not occur. Other factors resulting in the non-attainment of AICF conditions involve the presence of dissolved non-condensable gas in the working liquid and the improper buildup and resonance focusing of acoustic energy. Also, a large vapor content in the imploding bubbles reduces the intensity of collapse, a condition that can occur if the liquid pool temperature is too high.

46.6 DUE DILIGENCE Y THE AICF DISCOVERY TEAM

The following due diligence steps were taken by the discovery team to provide credible evidence for the attainment of AICF and to further bubble fusion technology:

a. Monitor for neutrons using multiple, independent detectors.
b. Ensure neutron energy is $\leq$2.5 MeV while accounting for pulse-pileup and gamma photon leakage.
c. Monitor neutrons to assess if they are time-correlated to occur during emission time of light flashes.
d. Monitor gamma photons with two independent detectors.
e. Ensure gamma photon energy is commensurate with D/D neutron interactions (e.g., photon emission from capture in hydrogen and other atoms in environment of the experiment).
f. Monitor gamma photons to ensure they are not time-correlated with light flashes nor neutron emissions; this accounts for the time required for the down-scattering of neutrons from the MeV energy levels to eV energy levels where radiative capture processes can occur.
g. Monitor the relative emission of neutrons and gamma photons and ensure neutron-to-gamma ratios are $\sim$10:1 (i.e., in line with expectations).
h. Monitor for tritium buildup in the liquid pool.
i. Ensure the neutron to tritium production rate ratios are $\sim$1:1.
j. Verify that the nuclear emissions are inversely related to liquid temperature; this ensures harmony with the physics of vapor condensation-related implosion intensification, as predicted by theory [Nigmatulin et al., 2005].
k. Verify the absence of neutron-tritium-gamma signals for control experiments.
l. Ensure experimental observations are in line with theory.
m. Use theoretical framework to make predictions.
n. Conduct blind experiments to validate theoretical predictions.
o. Follow time-honored anonymous peer review process and publish results in pre-eminent scientific/engineering journals.
p. Demonstrate evidence of successful AICF to public.
q. Enable and facilitate other scientific groups and researchers to replicate findings.
r. Facilitate spinoff-applications, further direct and indirect confirmations.

46.7 SUMMARY OF EXPERIMENTAL EVIDENCE FOR AICF

The AICF discovery team has produced experimental evidence of 2.45 MeV D/D neutrons (with over 30 standard deviation (SD) statistical significance), which are time-correlated with emission of SL light flashes, indicative of neutron emission during highly compressed conditions [Taleyarkhan et al., 2002; 2004; 2006]. Gamma photon emission at the expected energy was also measured with over 10 SD significance, and it was shown to be non-time correlated with the observed SL light flashes. The intensity of the gamma photons was roughly 10 times smaller than that for the neutron emissions, which is in line with expectations from nuclear particle transport theory assessments for the experimental configurations. The tritium emission rates were found to be consistent with the neutron emission rates, to within bounds of experimental uncertainty. The neutron emission rates were monitored using three independent detectors, all of which produced similar results. Notably, control experiments were conducted with a non-deuterated working liquid, giving null results. Sample results are shown in Figures 46.6, 46.7, and 46.8 for neutron/gamma emissions and in Figure 46.9 for tritium. Significantly, the rate of tritium production agreed with the D/D neutron production rate.

46.8 THEORETICAL MODELING AND SIMULATION OF AICF

A comprehensive theoretical model was developed by members of the discovery team [Nigmatulin et al., 2005] resulting in their *HYDRO* code simulations. The modeling framework included all major aspects of the AICF process and included shock-wave-induced phenomena such as the transient dissociation and ionization of the organic vapor molecules in the imploding bubbles to produce a plasma mixture of ions and electrons. Actual shock-induced experimental data were used to formulate the necessary equations-of-state. Effects of cluster pressure amplification

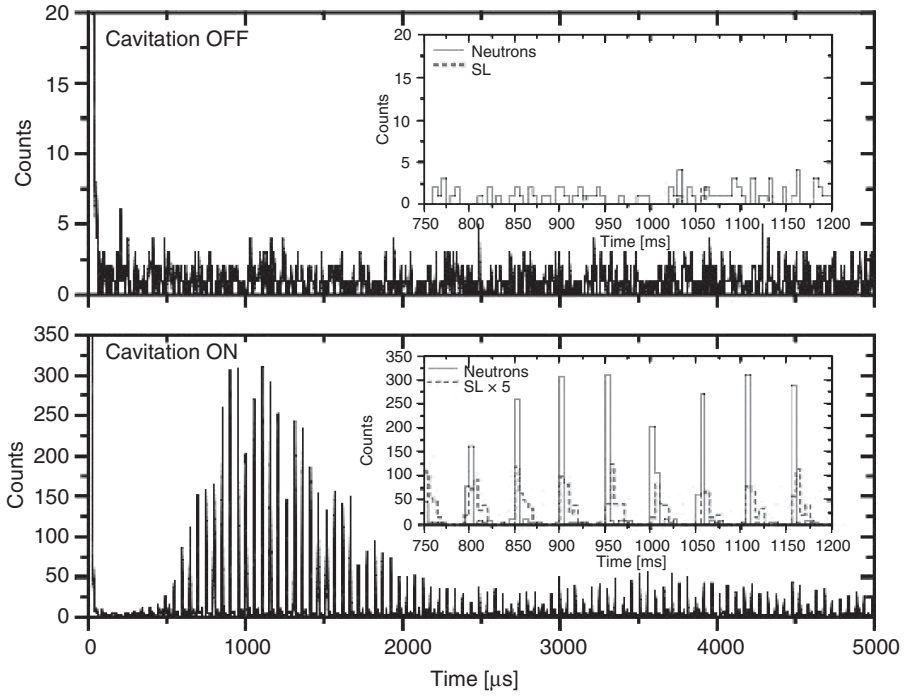

Figure 46.6 Time-correlated neutrons and SL emissions in AICF Experiments [Taleyarkhan et al., 2004] (deuterated acetone test liquid at ~0°C; SL emissions are shown as dashed lines in red.)

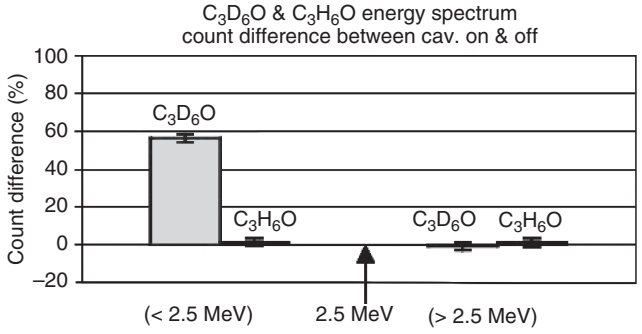

Figure 46.7 Aggregate energy spectra for deuterated and control liquid AICF tests [Taleyarkhan et al., 2004] (over 30 SD statistically significant data; neutron counts largely ≤2.45 MeV).

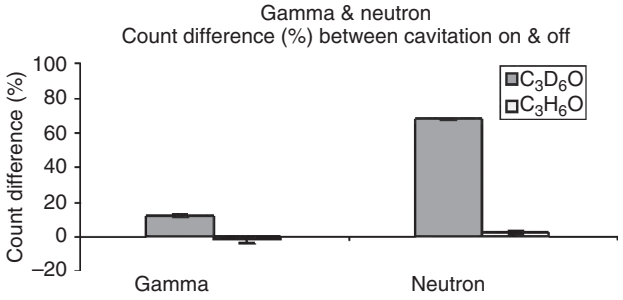

Figure 46.8 Relative neutron to gamma emissions in AICF tests [Taleyarkhan et al., 2004] (gamma photon levels are ~10% of neutron levels and arise from neutron radiative capture).

were included as was the evaporation and condensation at liquid/vapor interface. Significantly, this theoretical framework predicted that experiments using deuterated water (i.e., heavy water), rather than a deuterated hydrocarbon, would not produce AICF-type nuclear emissions. Later experiments showed this to be true. Sample results from the *HYDRO* code are shown in Figure 46.10. As can be noted, in the various stages of shock wave propagation inwards (i.e., from right to left) and shock reflection from the center of the bubble (i.e., from left to right), the predicted plasma temperatures reached are over 10^8 °K, the pressures are over 100,000 Mbar, and the vapor densities are an order of magnitude higher than the liquid density.

46.9 SUCCESSFUL REPLICATIONS AND CONFIRMATIONS

The first successful reports on the confirmation of independent observations of AICF were reported in 2005 [Xu et al., 2005], by the group led by Dr. Xu (presently with Westinghouse Electric Company). Figure 46.11a shows the published neutron energy pulse-height spectra for the cases of a deuterated liquid and control experiments with a

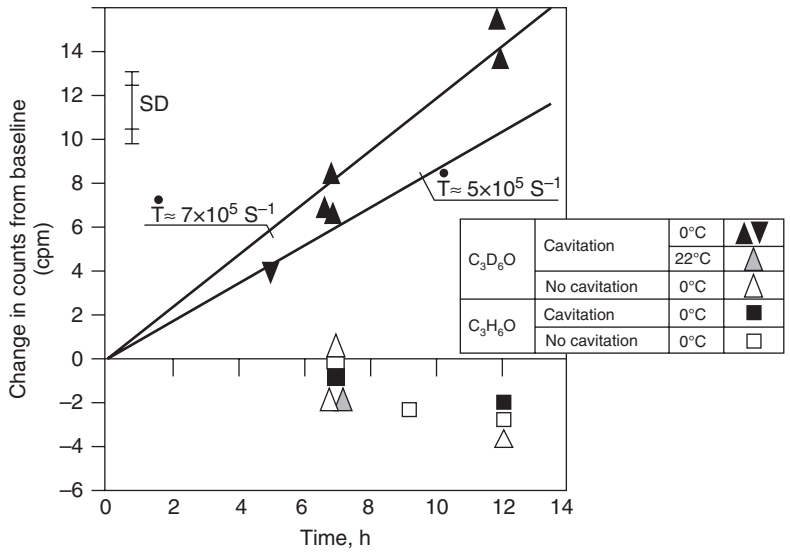

Figure 46.9 Tritium evolution with time (Nigmatulin et al., 2005) (tritium emission rate is similar to that for neutron rates).

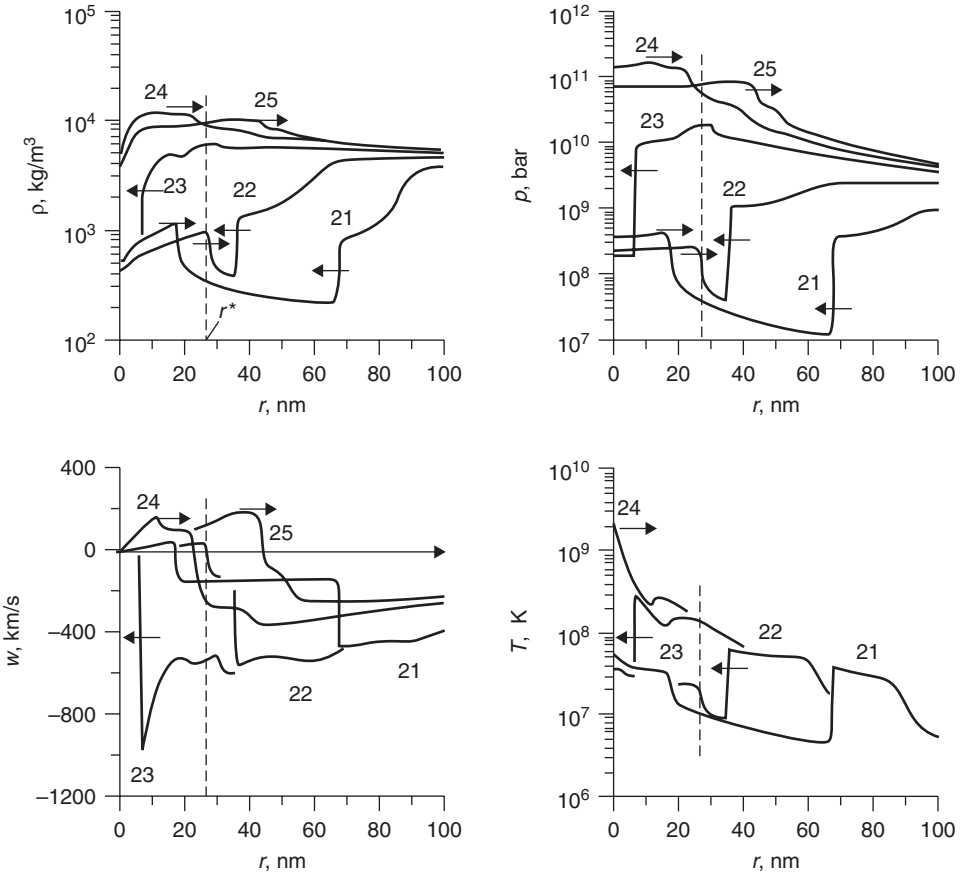

Figure 46.10 Theoretical HYDRO code predictions for AICF experiments [Nigmatulin et al., 2005] (over 10^5 Mbar and 10^{9°K attained during final stages of implosion; dissociation/ionization effects included).

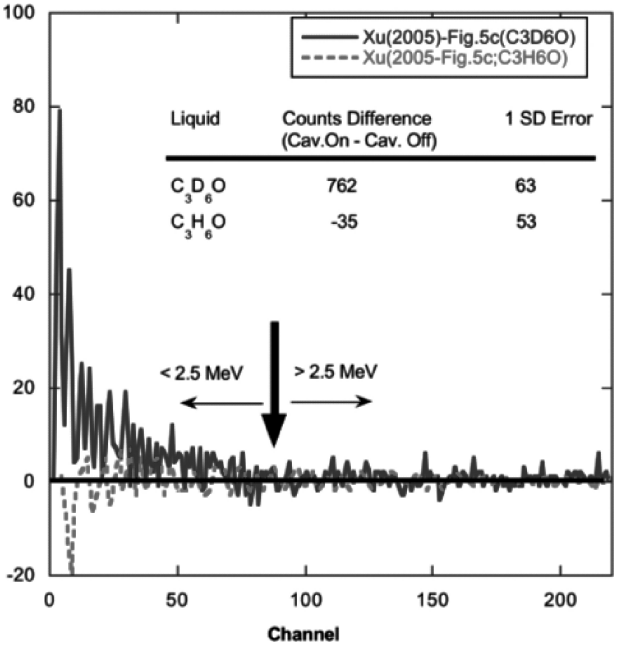

(a)

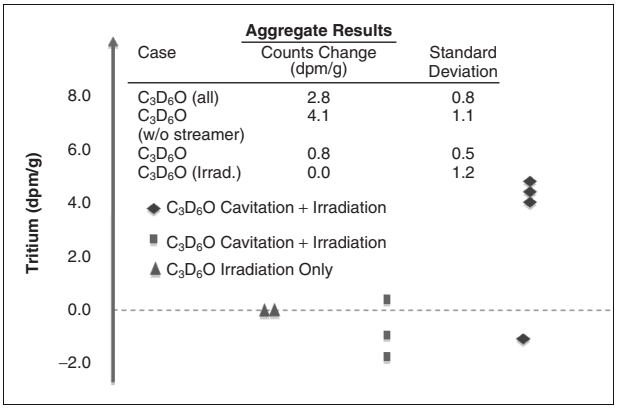

(b)

Figure 46.11 Confirmation results from replication experiments by Xu et al. [Xu, 2005]. (a) Neutron pulse-height spectra. (b) Tritium production (including for control experiments) [Note: Figures redrawn with best possible estimates from original published values].

non-deuterated liquid. Over 10 SD statistically significant neutron emission data for 2.45 MeV D/D neutrons were reported, and as can be seen in Figure 46.11b, compatible tritium production rates were also measured.

The second successful report on AICF confirmation [Forringer et al., 2006] was by the group led by Dr. Forringer (from LeTourneau University, Texas, USA). This group also reported neutron pulse-height spectra, with over 10 SD significance, which was indicative of D/D fusion, and, unlike previous measurements, their measurements were also made using passive neutron track detectors. Published results are shown in Figures 46.12a and b. Also, Forringer et al. conducted control experiments and confirmed null results.

A third successful report of AICF confirmation was documented [Bugg, 2006] in an electronic report of findings by W. Bugg (of Stanford University, Stanford, CA and University of Tennessee, Knoxville, TN). Like Drs. Forringer and Xu, Dr. Bugg also reported statistically significant neutron emission data for testing with deuterated liquids but null results for all control experiments using an undeuterated liquid.

A separate announcement of the successful attainment of statistically significant neutron emissions for cavitated deuterated acetone and null results for control experiments using regular acetone was also made by R. Tessein [2006] of Impulse Devices, Inc. at the 2006 Innovative Confinements Concepts Workshop.

46.10 PUBLIC DEMONSTRATIONS OF SUCCESSFUL AICF

In addition to these replications and confirmations by groups unaffiliated with the original discovery team, AICF was successfully demonstrated to the public on two separate occasions in 2006 at Purdue University by Taleyarkhan et al.

46.11 OTHER ATTEMPTS AT REPLICATION

During mid-2001, on a single afternoon, a group of two scientists (Shapira and Saltmarsh) at Oak Ridge National Laboratory (ORNL) used their own LS detector system and monitored for the evolution of neutrons and SL light flash data during two 1 h trial runs in the ORNL laboratory of the discovery team. The results of monitoring, despite issues related to instrument saturation from gamma photon flashes, resulted in statistically significant (with over 10 SD accuracy) nuclear emissions that were time-correlated with the SL flash emissions. These results have been documented (e.g., see Ref. 31 of Taleyarkhan et al., 2002) and are archived (www.rpi.edu/̃laheyr/SciencePaper.pdf). Sample results are shown in Figure 46.13. Shapira and Saltmarsh (S/S) did not monitor for tritium and prematurely concluded that their neutron emission levels did not match the expected emission rate as published in 2002 by the original discovery team. The S/S team published their views first as a Ref. 31 in the 2002 *Science* paper by the discovery team [Taleyarkhan et al., 2002], and later presented their data in a separate publication elsewhere. This second publication caused significant confusion since it implied that valid AIFC data were not observed and that

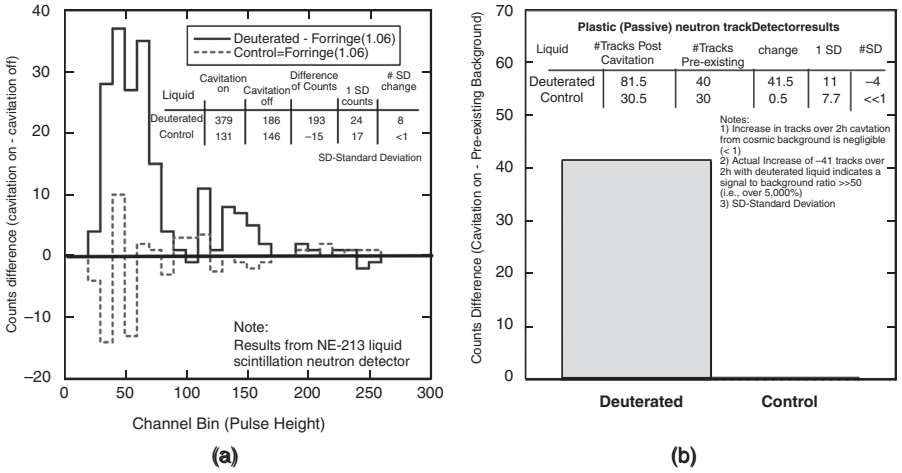

Figure 46.12 Confirmation results from replication experiments by Forringer et al. [Forringer, 2006]. (a) Liquid scintillation neutron detector data. (b) Plastic (passive) neutron track detector data [Note: Figure 11a redrawn with best possible estimates from original published values].

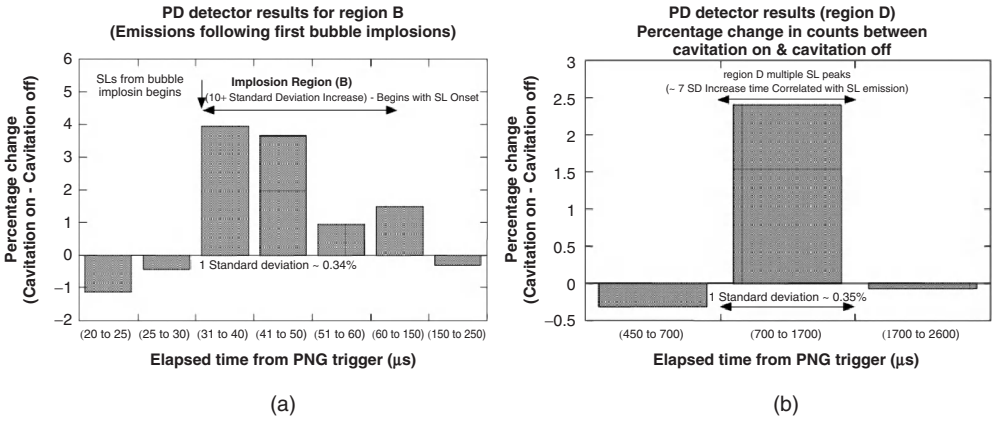

Figure 46.13 Confirmation of excess nuclear emissions from measurements of Shapira and Saltmarsh [Shapira, 2002]. (a) Emissions during first bubble implosion (SL) period. (b) Emissions during second time region of SL emitting bubbles [figures from raw data provided by Shapira to Taleyarkhan in 2001; archived: www.rpi.edu/~laheyr/SciencePaper.pdf].

S/S had conducted their own separate and comprehensive AICF experiments. In fact, as noted above, statistically significant nuclear emissions were indeed observed by S/S with cavitating deuterated liquid experiments and none for the control non-cavitating liquid. Since the S/S group failed to conduct tritium monitoring on that day, their argument of mismatch with the neutron-gamma signals they measured with the tritium data of the discovery team from a different experiment on a different day is irrelevant. A good archival review of this situation has been given by Nigmatulin et al. [2005] in *J. Power and Energy*.

Another attempt to replicate the published 2002 experimental AICF data in *Science* was undertaken by a group led by Putterman et al. of the University of California at Los Angeles (UCLA). This group published their results in 2007 [Camara et al., 2007] claiming an inability to reproduce the AICF data of the original discovery team. Some fundamental flaws in the UCLA attempt are highlighted in Figure 46.14. The UCLA team inexplicably failed to properly utilize the top reflector for intensifying the reflected acoustic energy within the bulk of the liquid pool; they added air to the working liquid; they failed to attain and control spherical bubble clusters as required; and finally, the UCLA team failed to build a test cell using the recommended design for the top and bottom reflectors. With such deviations, non-attainment of successful replication was to be expected, in sharp contrast to the replication attempts by other groups [Xu et al., 2005; Forringer et al., 2006, 1,2; Bugg, 2006; Tessein, 2006] that successfully measured AICF.

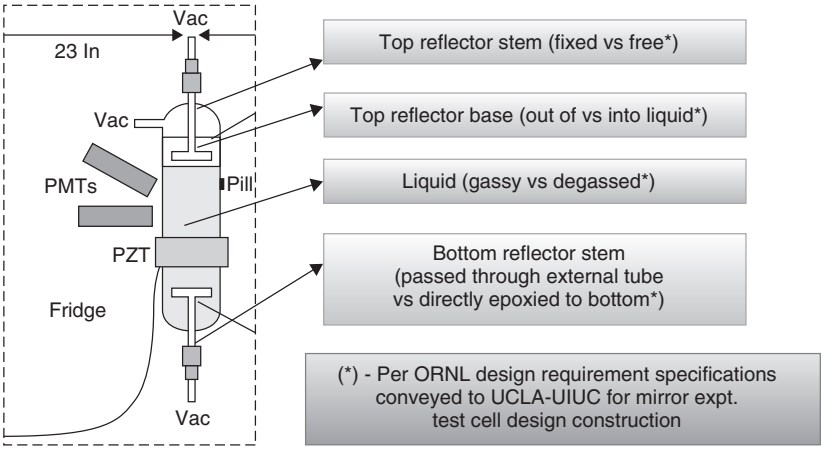

Figure 46.14 Variances in UCLA-UIUC replication attempt vs ORNL* design. (C.G. Camara, S.D. Hopkins, K.S. Saslick, and S.J. Petterman Physics and Astronomy Department, University of California, Los Angeles, California 90095, USA; Chemistry Department, University of Illinois, Urbania, Illinois 61801, USA.)

46.12 FLAWED THEORETICAL SPECULATIONS BY THE UCLA TEAM

A UCLA researcher also conducted flawed Monte Carlo-based nuclear particle transport simulations [Naranjo, 2006; Reich, 2006] for the self-nucleated AICF experiments published in 2006 by the discovery team [Taleyarkhan et al., 2006]. The fundamental problem with their results is that the UCLA team modeled the AICF test cell as having a direct line of sight with the LS neutron detector. The all-important fact that about 3 cm of thermal ice-pack shielding was used in the specific AICF experimental enclosure was left out. As such, the energy spectrum of the fusion neutrons reaching the neutron detector was calculated improperly and was reported [Reich, 2006] in *Nature* with the hyped message that there was only a one in 100 million chance that the January 2006 published neutron spectra [Taleyarkhan et al., 2006] of the discovery team could be from D/D fusion, but instead was a consequence of the inappropriate use of a Cf252 isotope neutron-gamma source. Although this misinformation was successfully clarified via the publication of peer reviewed facts in *PRL* [Taleyarkhan et al., 2006], the erroneous news reports in *Nature* in 2006 initiated a political-motivated congressionally mandated investigation. After more than two years of thorough investigation by various committees, all serious allegations were dismissed as groundless.

Nevertheless, to settle any lingering doubts, the discovery team proactively embarked on performing their own comprehensive Monte Carlo nuclear particle transport and detector response simulations, not just for the seminal 2006 *PRL* journal publication by the discovery team, but for all published AICF experiments—some of which used thermal-shielding and others did not or else utilized other envelopes over the test cell. After detailed calibration, and developing two independent approaches for predicting with all major 3D effects accounted for, the neutron energy spectra were obtained for all published AICF experiments. Furthermore, the team also accounted for AICF-specific issues such as pulse-pileup from simultaneous emanation of neutrons within picoseconds. The entire framework and results were documented as a comprehensive archival manuscript, which was peer reviewed and published in *Nuclear Engineering & Design* [Taleyarkhan et al., 2008]. These results convincingly demonstrated the invalidity of the insinuations implicit in the 2006 *Nature* article [Reich, 2006] that resulted from the flawed UCLA computer predictions. Indeed, the results of these simulations matched not one but "all" of the published experimental data—which, at their times of publication were reported in a "blind" fashion by the various experimental teams. Figure 46.15 shows sample results of the predictions using two independent modeling approaches, both of which demonstrate excellent agreement (as noted from the goodness of fit statistics) with the reported experimental data of AICF experiments conducted from 2002 through 2006 in stark contrast to the erroneous information published in *Nature* [Reich, 2006]. These findings should conclusively confirm the principal conclusion that the results from all published experiment efforts (2002–2008) are compatible with the occurrence of thermonuclear D/D fusion in AICF experiments.

46.13 BREAKEVEN ENERGY PRODUCTION: STATUS AND PATHWAY

The pathway for attaining breakeven and the scale-up of power production appears promising and has been discussed

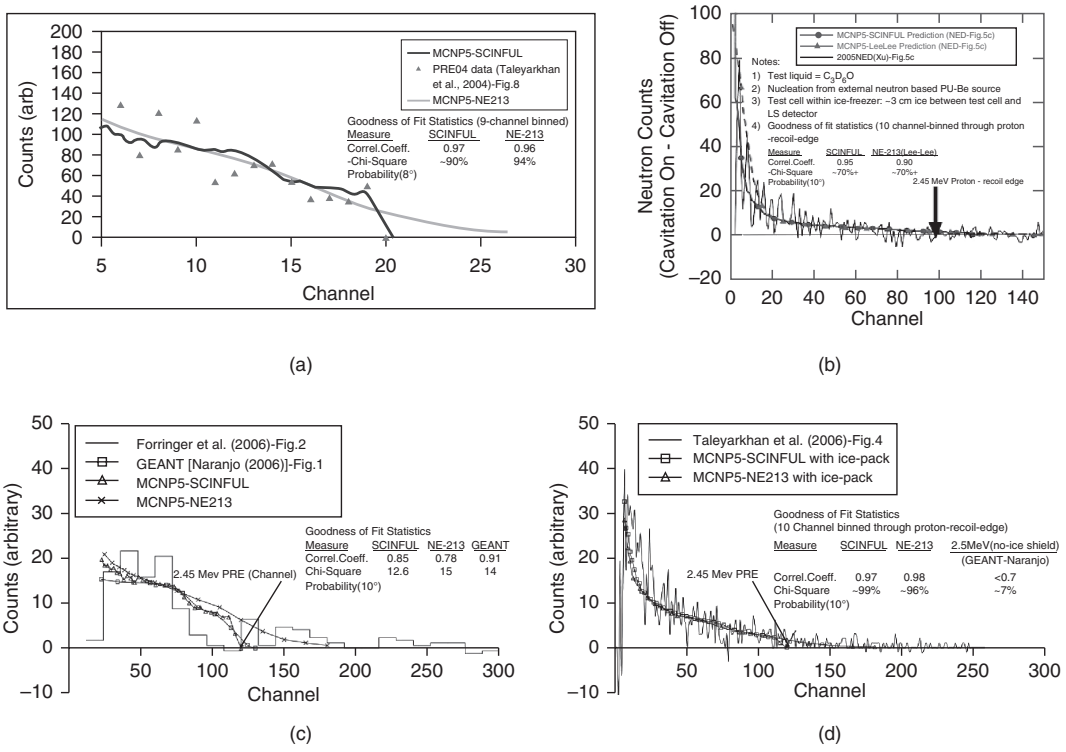

Figure 46.15 Monte Carlo 3D simulation predictions vs 2002–2006 AICF experiment data (Source: Taleyarkhan et al., 2008). (a) Predictions [Taleyarkhan, 2008] vs data of Taleyarkhan et al. [Taleyarkhan, 2004, 2002]. (b) Predictions [Taleyarkhan, 2008] vs confirmatory data of Xu et al. [Xu, 2005]. (c) Predictions [Taleyarkhan, 2008] vs confirmatory data of Forringer et al. [Forringer, 2006] and GEANT predictions [Naranjo, 2006]. (d) Predictions [Taleyarkhan, 2008] vs self-nucleation data of Taleyarkhan et al. [Taleyarkhan, 2006].

elsewhere [Lahey et al., 2007, 2006]. However, a summary is presented herein. For super-compression AICF conditions leading to temperatures in the 10^8 °K range, the fusion energy output for D/D fusion in the ORNL experiments [Taleyarkhan et al., 2002] (based on the well-known Lawson criterion) was about four orders of magnitude lower than breakeven. The ORNL experiments provide a fusion "spark" vs a "burn" in a typical breakeven system. However, scale-up appears to be feasible. For example, with D/T vs D/D reactions, the energy output would already provide three orders of magnitude enhancement and come very close to breakeven, since the energy of D/T neutrons is 14.1 MeV compared to 2.45 MeV for D/D neutrons. Experience with fusion experimentation has also revealed an exponential dependence on parameters like the forcing pressure; with the implosion-induced pressure rising by over three orders of magnitude for a twofold increase of forcing pressure. Also, improving implosion and fusion reaction dynamics using other optimal liquids could readily provide improved performance. For example, there is about four orders of magnitude difference in the fusion output between heavy water and deuterated acetone-benzene mixtures. Once breakeven conditions are reached, aspects such as controlled output, economic, regulatory, and other such aspects will need to be addressed [Taleyarkhan et al., 2005]. At present, despite the many challenges successfully addressed by the discovery team, AICF is in a situation that is somewhat analogous to being between the discovery of nuclear fission by Otto Hahn and Lisa Meitner and the demonstration of a controlled chain fission reaction by Enrico Fermi's team. Nevertheless, this exciting new technology appears to be inherently safe (no significant decay heat after shutdown) and also addresses one of the fundamental problems (i.e., the first-wall problem) facing conventional thermonuclear fusion approaches (e.g., tokamak and laser-based fusion) [Lahey et al., 2006].

46.14 SPINOFF AND OTHER POTENTIAL APPLICATIONS OF AICF TECHNOLOGY

The AICF experience in attaining super-compression in imploding cavitation bubbles has motivated some interesting spinoff applications: (1) transforming ordinary hexagonal graphite to nano-scale diamond states by a British-Asian

scientific group [Khachatryan et al., 2008], providing a powerful albeit, indirect, confirmation for the technique's ability to attain super-compressed pressure states and on the soundness of its underlying physics, and, (2) producing transformational nuclear particle sensors for combating nuclear terrorism [Taleyarkhan, 2008; Archambault, 2008]. Others have also strived to utilize the shock-based super-compression to attain actinide nuclear transmutations [Cardone, 2009], an area that is still in its infancy. Other areas for using sonofusion technology may be to offer new ways to parametrically study plasma physics and neutron cross-sections in nuclear fusion; the development of novel pico-second duration pulsed neutron-photon sources for scientific/engineering studies; the production of tritium; and various medical applications for therapy and diagnostics.

REFERENCES

B. Archambault, J. A. Webster, J. Wang, J. Lapinskas, S. Zielinski, and R. P. Taleyarkhan, Towards Leap-Ahead Advances in Radiation Detection. Professional 16th International Conference on Nuclear Enginering. (ICONE-16), May 11–15, 2008, Orlando, Florida, USA.

W. Bugg, *Report on Activities on June Visit*, Report to Purdue University, June 9, 2006 (transmitted from W. Bugg to R. P. Taleyarkhan, Purdue University).

C. Camara, S. Putterman and E. Kirilov, "Sonoluminescence from a single bubble driven at 1megahert." *Phys. Rev. Lett*, 2004, **92**, 124301-1–124301-4.

C. G. Camara, S. Hopkins, K. Suslick, and S. Putterman, Upper bound for neutron emission from sonoluminescing bubbles in deuterated acetone. *Phys. Rev. Lett*., 2007, **98**, 064301.

F. Cardone, R. Mignani, and A. Petrucci, "Piezonuclear decay of thorium," *Phys. Letters* A, 2009, **373**, 1956–1958.

R. A. Gross, *Fusion Energy*. John Wiley and Sons, New York, USA, 1984.

D. Flannigan and K. Suslick, Plasma formation and temperature measurement during single-bubble cavitation. *Nature*, March 5, 2005, **434**, 52–53.

E. R. Forringer, D. Robbins, and J. Martin, Confirmation of neutron production during self-nucleated acoustic cavitation. *Trans. Am. Nucl. Soc*., November 2006, **95**, 736.

E. R. Forringer, D. Robbins, and J. Martin, Confirmation of neutron production during self-nucleated acoustic cavitation of deuterated benzine and acetone mixture. *Proc. Intl. Conf. Fusion Energy*, Albuquerque, NM, USA, November 2006.

D. F. Gaitan, L. A. Crum, R. A. Roy, and C. C. Church, 1992–06. Sonoluminescence and bubble dyanamics of a single, stable, cavitation bubble, *The Journal of the Acoustical Society of America*, **91**(6), 3166–3183.

A. K. Khachatryan, S. G. Aloyan, P. W. May, R. Sargsyan, V. A. Khachtrayan, and V. S. Baghdasaryan, Graphite to diamond transformation induced by ultrasound cavitation. *J. Diamond and Related Materials*, 2008, **17**, 931–936.

Le Tourneau University Press Release, Nov. 17, 2006, *Bubble Fusion Confirmed by LeTourneau University Research*.

R. T. Lahey Jr., R. P. Taleyarkhan, R. I. Nigmitalun, and I. S. Akhatov, Sonoluminescence and the search for sonofusion *Advances in Heat Transfer*, 2006, **39**, 1–168.

R. T. Lahey Jr., R. P. Taleyarkhan, and R. I. Nigmatulin, Sonofusion technology revisited. *Nuclear Engineering & Design*, 2007, **237**, 1571–1585.

W. C. Moss, D. B. Clarke, and D. A. Young, D.A., Sonoluminescence and the prospects for table-top micro-thermonuclear fusion. *Phys. Lett. A*, 1996, **211**, 69.

B. Naranjo, Comment 149403 on Taleyarkhan et al., PRL 96, 034301, 2006. *Phys. Rev. Lett*., October 2006, **97**, 149403.

New Energy Times, Inc. bubble fusion web-portal site, http://newenergytimes.com/v2/news/2009/NET33Cdfkj5.shtml, Special Edition, Issue #33, November 20, 2009.

R. I. Nigmatulin, I. Akhatov, R. K. Bolotnova, A. S. Topolnikov, N. K. Vakhitova, R. T. Lahey, and R. P. Taleyarkhan, The theory of supercompression of vapor bubbles and nano-scale thermonuclear fusion. *Physics of Fluids*, 2005, **17**, 107106–1.

R. I. Nigmatulin, R. P. Taleyarkhan, and R. T. Lahey, Evidence for nuclear emissions during acoustic cavitation revisited. *J. Power and Energy*, 2005, **218**, Part A, Special Issue Paper.

S. P. Putterman, B. Barber, R. Hiller, R. Maire, and J. Lofstedt, *Converting Acoustic Energy into Other Useful Energy Forms*. United States Patent #5,659,173, August 1997.

E. Reich, Evidence for bubble fusion called into question, Nuclear fusion in collapsing bubbles—Is it there? An attempt to repeat the observation of nuclear emissions from sonoluminescence, *Nature*, March 9, 2006, **440**, 142.

D. Shapira and M. Saltmarsh, Comments on the possible observation of d-d fusion in sonoluminescence, *Phys. Rev. Lett.*, 2002, **89**, 104302; also on Refs. 31–32 of Taleyarkhan et al. (2002); www.rpi.edu/~lahey r/Sonofusion.pdf; and on www.bubblegate.com.

R. P. Taleyarkhan, C. West, J. S. Cho, R. T. Lahey, R. I. Nigmatulin, and R. C. Block, Evidence for nuclear emissions during acoustic cavitation. *Science*, 2002, **295**, 1868.

R. P. Taleyarkhan, R. C. Block, C. D. West, and R. T. Lahey, Comments on the Shapira and Saltmarsh Report. *Science*, 2002, **295**, Ref. 32; also on www.bubblegate.com.

R. P. Taleyarkhan, J. S. Cho, C. West, R. T. Lahey, R. I. Nigmatulin, and R. C. Block, Additional evidence for nuclear emissions during acoustic cavitation. *Phys. Rev. E*., 2004, **69**, 036109-1–036109-11.

R. P. Taleyarkhan, R. T. Lahey, Jr., and R. I. Nigmatulin, Bubble nuclear fusion technology—status & challenges. *Multiphase Science & Technology*, 2005, **17**, 3, 191–224.

R. P. Taleyarkhan, C. West, R. T. Lahey, R. I. Nigmatulin, R. C. Block, and Y. Xu, Nuclear emissions during self-nucleated acoustic cavitation. *Phys. Rev. Lett*, 2006-1, **96**, 034301–1.

R. P. Taleyarkhan et al., Response to B. Naranjo comment 149403, *Phys. Rev. Lett*., October 2006-2, 149404.

R. P. Taleyarkhan, J. Lapinskas, Y. Xu, J. S. Cho, R. C. Block, R. T. Lahey, Jr., and R. I. Nigmatulin, Modeling, analysis and prediction of neutron emission spectra from acoustic cavitation bubble fusion experiments. *Nuclear Engineering and Design*, 2008-1, **238**, 2779–2791.

R. P. Taleyarkhan, J. Lapinskas, and Y. Xu, Tensioned metastable fluids and nanoscale interactions with external stimuli—theoretical-cum-experimental assessments and nuclear engineering applications. *Nuclear Engineering and Design*, 2008-2, **238**, 1820–1827.

R. Tessein, *Testimonial for Successful AICF,* March 2006, www.bubblegate.com.

A. J. Walton and G. T. Reynolds, Sonoluminescence. *Adv. Phys*. 1984, **33**, 595.

Y. Xu, and A. Butt, Confirmatory experiments for nuclear emissions during acoustic cavitation. *Nuclear Engineering and Design*, 2005-1, **235**, 1317.

Y. Xu, A. Butt, and S. Revankar, Bubble dynamics and tritium emission during Bubble Fusion Experiments, Paper #548, *Proceedings of the 11th International Conference on Nuclear Reactor Thermal Hydraulics*" Avignon, France, October 2–5, 2005-2.

F. R. Young, *Sonoluminescence*, CRC Press, Boca Raton, FL., 2004.

47

DIRECT ENERGY CONVERSION CONCEPTS

PAVEL V. TSVETKOV

Department of Nuclear Engineering, Texas A&M University, College Station, TX, USA

47.1 DIRECT ENERGY CONVERSION

The world of the 21st century is an energy-consuming society. Due to increasing population and living standards, each year the world requires more energy and new efficient systems for delivering it. Furthermore, the new systems must be inherently safe and environmentally clean. These realities of today's world are among the reasons leading to serious interest in considering direct energy conversion (DEC) as one of the promising methods of producing electricity. The absence of any intermediate conversion stages in an ideal DEC system provides the potential for significant design simplifications, improved conversion efficiency, and broadened application areas. Inherent safety and environmental purity are realistically achievable design characteristics of innovative DEC systems. However, all current DEC systems exhibit much lower energy conversion efficiencies than those expected in theoretical studies. This discrepancy comes from challenges of engineering implementation. The most simple and direct way to convert some type of energy to a usable form may not be practical due to tremendous engineering challenges that may be required to realize what appears to be a simple and straightforward conversion principle [1, 2].

All DEC systems depend on a primary energy source. Thermionic energy conversion takes advantage of electron emission from heated surfaces (cathode) followed by their collection on cooled surfaces (anode). A nuclear reactor could serve as a source of needed heating to realize thermionic energy conversion. Thermionic converters operate best at temperatures above 1000°C. The optimum cathode temperatures are close to 2200°C. Such high temperatures can be found in modern Generation-IV nuclear reactors, especially in Very High Temperature Reactors. Some authors recognized this as an opportunity for thermionic conversion as an additional energy conversion method [2].

Thermoelectric energy conversion is another method to directly convert thermal energy to electricity. Thermoelectrics is founded on Seebeck effect, in which difference in joined materials forming a circuit between cold and hot junctions will produce a voltage. The addition of an electrical load provides the ability to generate a current. Modern designs of thermoelectric converters are expensive and inefficient. However, their simplicity and absence of moving parts lead to applications in systems requiring autonomity and reliability with minimized or no maintenance [2]. Radioisotope thermoelectric generators (RTG) are widely used in space applications to produce electricity or thrust. The radioisotope thruster concept is derived from the RTG technology. The thermoelectric converters from the RTG are removed, and energy from the RTG nuclear fuel capsules is used to heat a propellant "working fluid," such as hydrogen, water, helium, etc., to temperatures of 1500 to 2000°C and then expand the hot gas through a nozzle. In an isotope power supply, the heat is produced by the natural decay of a radioisotope, which in all U.S.-launched systems is Pu238.

Both thermionic and thermoelectric devices are heat engines and therefore subject to Carnot efficiency limitations. Direct fission fragment energy conversion (DFFEC) is based on the direct collection of fission fragments as the primary charged particles (positively charged ions) that are released in nuclear fission. Since charge is converted

Nuclear Energy Encyclopedia: Science, Technology, and Applications, First Edition (Wiley Series On Energy).
Edited by Steven B. Krivit, Jay H. Lehr, and Thomas B. Kingery.

to electricity directly, this method avoids thermal energy conversion. The following subsections discuss direct fission fragment energy conversion and its realization potential.

47.2 DIRECT FISSION FRAGMENT ENERGY CONVERSION

The energy resulting from nuclear fission is mainly released in the form of kinetic energy of fission fragments (~80%). Emitted neutrons and other particles and radiations, resulting from the nuclear fission reaction, carry away the remaining amount of the released energy. The approximate distribution of the energy released by nuclear fission (neglecting the energy of the delayed neutrons) is given in Table 47.1 [1].

The energies of fission fragments, prompt and delayed neutrons, prompt γ-rays, as well as, the energies of the β-particles and γ-rays due to fission product decay constitute the recoverable components of the nuclear fission energy. The energy of neutrinos accompanying FP decay cannot be recovered in practical systems.

The conversion of nuclear fission energy to utilizable energy forms can be accomplished in several ways [2, 3]. Energy transformations and relevant nuclear energy conversion (NEC) methods are shown in Figure 47.1. As illustrated, energy conversion can involve single or multiple steps. Single-step conversion is represented by the DFFEC system based on the direct collection of fission fragments.

TABLE 47.1 Distribution of the Released Nuclear Fission Energy for Fission of U235

Component of Energy Release in Fission	Energy (MeV)	Fraction (%)
• Kinetic Energy of FFs	168	81.16
• Kinetic Energy of Fission Neutrons	5	2.42
• Energy of Prompt γ-Rays	7	3.38
• Total Energy of β-Particles	8	3.86
• Energy of Delayed γ-Rays	7	3.38
• Energy of Neutrinos	12	5.80
• Total Energy Release per Nuclear Fission Event	207	100.00

Conventional methods of nuclear fission energy conversion do not utilize the kinetic energy of fission fragments directly. As fission fragments slow down, they dissipate their kinetic energy in a fuel element. The energy dissipation process results in conversion of the FF kinetic energy into heat, the natural final energy form shown in Figure 47.1. The generated heat is removed by a coolant and can be utilized to produce power.

The traditional, and most widely applied, approaches for the utilization of heat, are heat engines, which are limited by the Carnot efficiency [2, 3]. The Carnot theorem (principle) states that no heat engine operating between two given reservoirs (in a closed cycle) can be more efficient than a Carnot engine operating between the same two reservoirs (in a closed cycle) [4]. Current technological

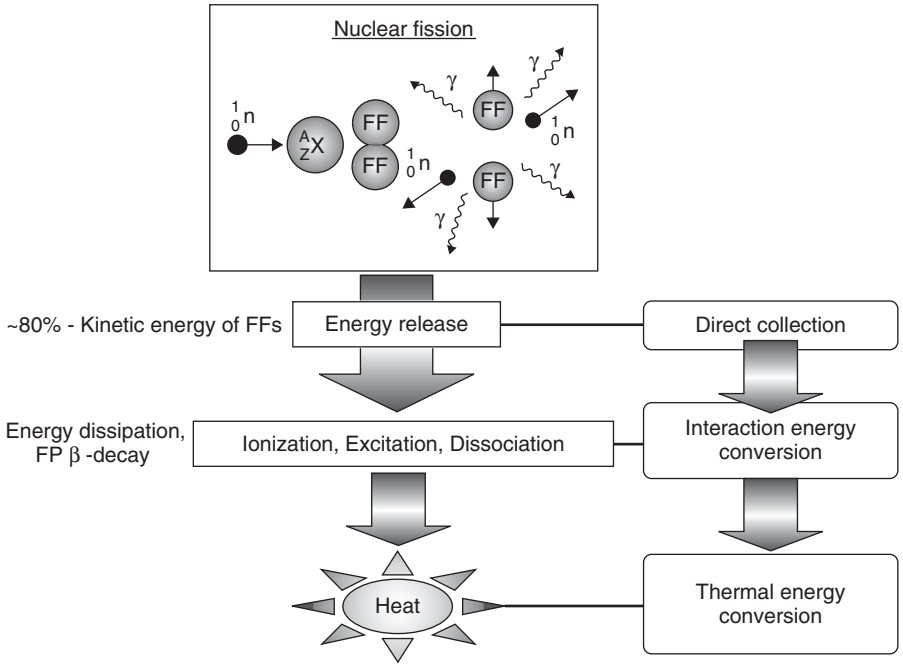

Figure 47.1 Nuclear fission energy transformations and NEC methods.

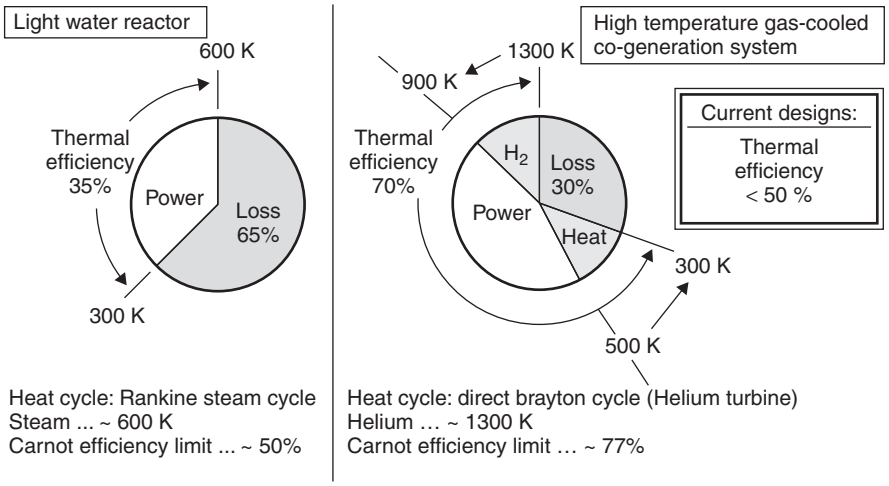

Figure 47.2 Achievable thermal efficiencies of NEC systems with LWRs and HTGRs.

advances provide possibilities for the achievement of high conversion efficiencies that come close to the corresponding Carnot efficiency limit. Achievable thermal efficiencies for advanced LWRs and HTGRs are shown in Figure 47.2 [5, 6].

The DEC approach is an alternative to conventional heat engines [7]. This is illustrated in Figure 47.1. Direct conversion of nuclear fission energy to electrical power may be accomplished if the kinetic energy of fission fragments can be collected before it is turned into heat. Because there is no intermediate conversion to thermal energy, the efficiencies of DEC systems are not subject to the classical Carnot efficiency limit. Existence of the fundamental Carnot efficiency limitation for heat engines makes the DFFEC systems uniquely advantageous.

Because heat cycles utilize conventional mechanical rotary machinery, thermal energy converters are complex multi-stage systems. A typical Nuclear Energy Conversion (NEC) system with intermediate thermal energy conversion stages is shown in Figure 47.3 [8]. Intrinsic design simplicity is offered by the DFFEC concept because of the absence of any intermediate thermal energy conversion stages.

The possibility of using DEC methods to produce electricity from the kinetic energy of charged particles emitted as a result of nuclear reactions was first suggested in 1913 [9]. At that time, using a radium source, H. G. C. Moseley and J. Harling demonstrated that charged particle emission could be used to build up a high voltage. Use of various other radionuclides was suggested. Several scientists considered artificially produced radioactive nuclides as possible replacements for a radium source to build up a voltage by charged-particle emission. It was proposed to use a β-emitter to overcome the high self-absorption inherent with α-radiation sources [10].

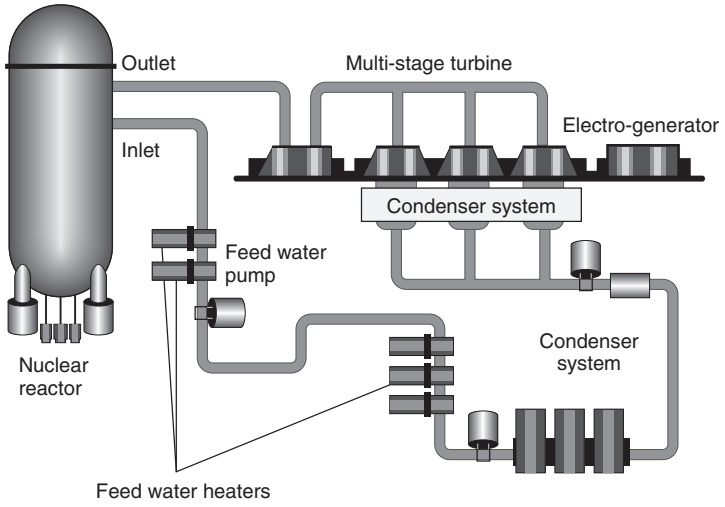

Figure 47.3 NEC system with ABWR and intermediate thermal energy conversion stages.

The DEC concept utilizing the kinetic energy of fission fragments was originally proposed by E. P. Wigner in 1944 [2]. In 1957, G. M. Safonov performed the first theoretical study of the DFFEC concept [11]. Investigations of various aspects of the DFFEC concept were conducted during the 10 years that followed Safonov's study [12–22]. Research was very intense, especially for space applications [17, 22]. The most important of the earlier studies were those in which DFFEC components (cells) were constructed and irradiated in research reactors [14–17, 21].

All DFFEC systems utilize, as their basic power source, the kinetic energy of fission fragments that escape from a very thin fuel layer, called the fission fragment emitter or fuel-coated cathode. In the approach that has historically received the most emphasis, fission fragments are collected on the fission fragment collector (or anode) located only a few centimeters away from the emitter. The fuel layer thickness and electrical potential of the fission fragment collector are the most important factors determining the attainable energy conversion efficiency. If an attractive electrical efficiency is to be achieved, a significant fraction of the fission fragments must escape from the fuel layer. Since typical ranges for fission fragments in fuel materials are less than 10 microns, the fuel layer thickness needs to be less than a few microns, i.e., significantly smaller than the fission fragment range. For high electrical efficiencies, the fission fragment collector must maintain a high positive electrical potential relative to the fission fragment emitter.

The early DFFEC systems employed a lattice of fission electric cells, with each cell consisting of the fission fragment emitter, fission fragment collector, and additional components for secondary electron suppression, i.e., a grid or electro-magnetic coils [14, 16]. Several types of fission electric cells have been proposed [13, 16, 21]. They differ mainly according to the technique used to suppress electrons originating at the fission fragment emitter from reaching the fission fragment collector. One of the fission electric cell (FEC) concepts, the "Triode" FEC design, is shown in Figure 47.4 [16].

Nuclear reactor cores based on fission electric cells pose significant problems for reactor designers. All of the fission electric cell components inside the nuclear reactor core are subjected to significant fluxes of neutrons, γ-rays, and β-particles (electrons). Since the fission electric cells contain thin metallic components and electrical insulators, prolonged exposure to such radiation fields may have deleterious effects on the fission electric cell performance. Several specific problem areas were identified in the early research efforts:

- The fabrication and performance of fuel elements with ultra-thin fuel layers.
- The suppression of secondary electrons emitted along with fission fragments.
- Criticality and long-term operation without suffering damage to the fuel layer and other components.
- The stability of high voltage differentials in a radiation environment.
- The development of insulators for a high radiation environment.

Experiments validated the basic physics of the fission electric cell concept, but a variety of technical challenges limited the efficiencies that were achieved [16, 17, 21].

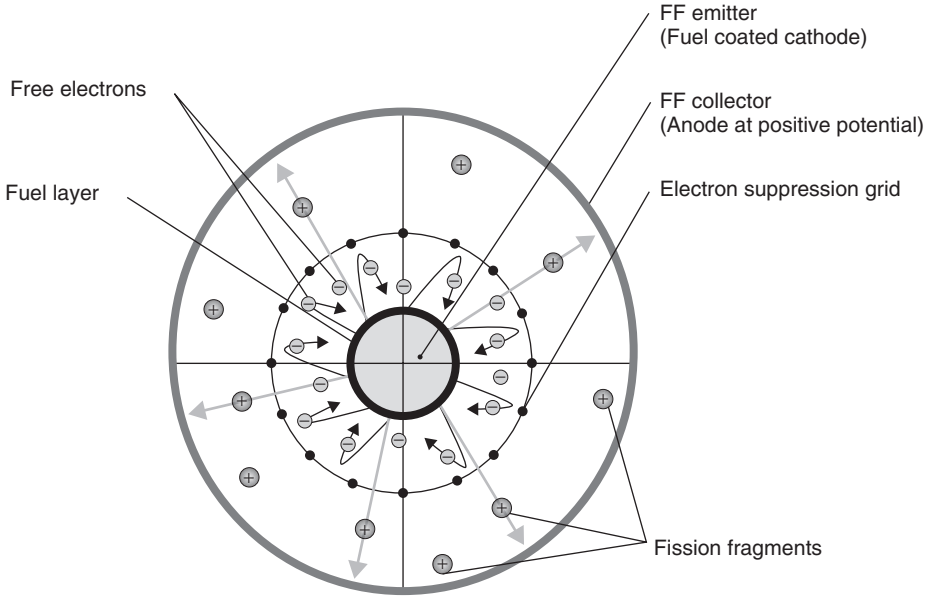

Figure 47.4 "Triode" FEC design.

None of the irradiated devices was able to achieve the high voltage indicative of a high electrical efficiency. Because of the poor performance of the early DFFEC systems, most of the DFFEC research ceased by the late 1960s.

The most recent research work on the DFFEC concept has been performed under the US DOE NERI DEC Project [23]. The original goal of this new research program was to re-examine the technological feasibility of DFFEC concepts, taking into consideration scientific and technological advances since the 1960s. Although there has been limited research activity in recent years in the DFFEC field [24–26], other research programs concerning pulsed power, magnetic insulation, and nuclear fusion have made significant developments that could find application in advancing and improving the DFFEC technology. Results of the systematic analysis performed under the NERI DEC project indicate that one of the considered concepts, known as the fission fragment magnetic collimator reactor (FFMCR), could offer promising performance. The first three years of the DOE-NERI Direct Energy Conversion (DEC) Power Production Program (1999–2002) produced a feasible design for terrestrial applications [23, 55]. That effort was followed by the three-year Proof-of-Principle Project (2002–2005) to verify the design performance principles experimentally [56].

The FFMCR concept is an advanced DFFEC system that combines design solutions that have been developed for fission reactors and fusion systems [27–29]. Because the FFMCR is a nuclear reactor utilizing DFFEC, the FFMCR core consists of a lattice of non-neutron absorbing structural elements on which a thin layer of fissile fuel has been deposited. The FFMCR core is similar to the core proposed earlier for a fission fragment rocket [30]. These fuel elements (FEs) are the analog of the FF emitters of the traditional fission electric cell design approach. However, in the FFMCR concept, fission fragments exit the fuel element, and then they are directed out of the nuclear reactor core and through magnetic collimators by an external magnetic field to direct collectors located outside of the nuclear reactor core. This approach has the advantage of separating (in space) the generation and collection of fission fragments. In addition, achieving and maintaining criticality of the neutron chain reaction is easier for the FFMCR concept, because the metallic collection components can be located outside the nuclear reactor core. The governing principles of the FFMCR concept are illustrated in Figure 47.5.

A conical design is envisioned for the magnetic coils used to create the magnetic field for the FFMCR collimators [27]. At the end of the collimator a venetian-blind (VB)-type charged particle collector might be employed to recover the FF kinetic energy [28]. Experimental studies already performed with multi-stage VB-type collectors have demonstrated the achievement of high conversion efficiencies [29].

The FFMCR concept is a new DFFEC concept that has not been extensively studied. Preliminary simplified analysis had demonstrated that an acceptable efficiency may be achievable. The computational study of DFFEC utilizing magnetic collimation (DFFEC-MC) is the next stage in FFMCR concept development.

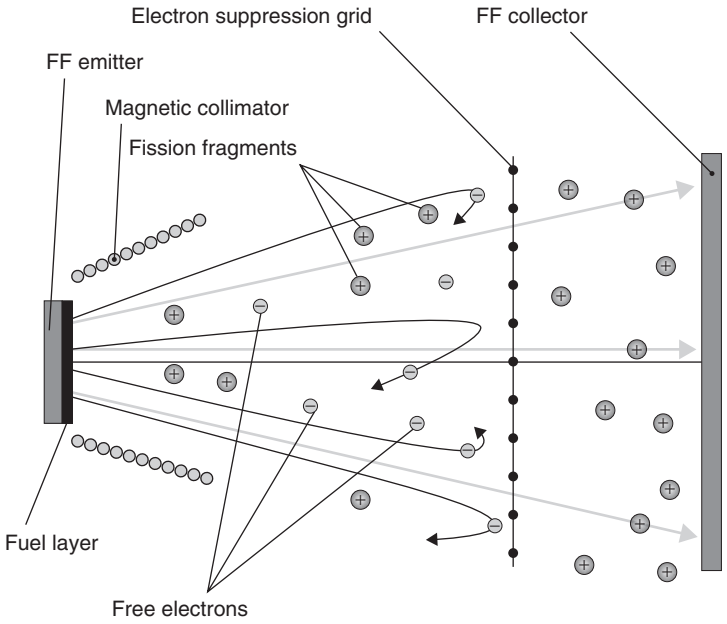

Figure 47.5 Principles of the FFMCR concept.

47.3 OUT-OF-CORE DIRECT FISSION FRAGMENT ENERGY CONVERSION

As originally conceived, nuclear reactor systems, which incorporate DFFEC, exploit in-core direct conversion of the FF kinetic energy. They use a thin fuel layer as an emitter of the positively charged fission fragments. The kinetic energy is harvested using a metallic collector held at an appropriate positive electrical potential relative to the fission fragment emitter. The emitter-collector pair forms a fission electric cell.

Efficient performance of the emitter-collector pairs within the nuclear reactor core is the principal requirement for successful operation of conventional fission electric cell systems. The fission electric cell design is complicated by the fact that several hundreds of low-energy (secondary) electrons are emitted from the fuel layer along with fission fragments [14]. If electrons are able to reach the fission fragment collector, they can be quickly collected negating the collected positive charge of the fission fragments. For high efficiency, the electric potential difference from emitter to collector needs to be on the order of millions of volts.

Alternatively, the DFFEC-MC concept applies out-of-core direct conversion of the fission fragment kinetic energy. The nuclear reactor core of the DFFEC-MC system consists of a lattice of non-neutron-absorbing elements coated with ultra-thin layers of fissile fuel. These fuel elements are the analog of the fission fragment emitters of the traditional DFFEC design approach that utilizes fission electric cells. After fission fragments exit the fuel element, they are captured on magnetic field lines and are directed out of the nuclear reactor core and through magnetic collimators to direct collectors located well outside of the nuclear reactor core. The concept of guiding fission fragments out of a nuclear reactor core using a magnetic field was originally proposed for a fission fragment rocket [30].

The high electric fields (millions of volts per centimeter) needed for the DFFEC systems with traditional fission electric cells are mitigated in the DFFEC-MC system by transporting fission fragments outside the nuclear reactor core for direct collection. Also, since the DFFEC-MC system does not use traditional fission electric cells, it has the advantage of allowing the electromagnetic components fission fragment collectors and superconducting coils needed for the fission fragment transport and collimation) to be located outside the strong radiation environment of the nuclear reactor core. Furthermore, absence of the metallic electromagnetic components within the nuclear reactor core greatly simplifies the task of achieving and maintaining criticality.

Generalized schemes of the in-core and out-of-core DEC approaches are illustrated in Figure 47.6. Depending on the specific implementation in the DFFEC-MC system design, the out-of-core DEC approach adds an energy transport step between the energy emission and conversion points within a system. Because of the energy transport step, the DFFEC-MC system does not have the critical issues of the DFFEC system with fission electric cells.

Independent of the specific design, technological feasibility for the DFFEC-MC system needs to be demonstrated in the following areas:

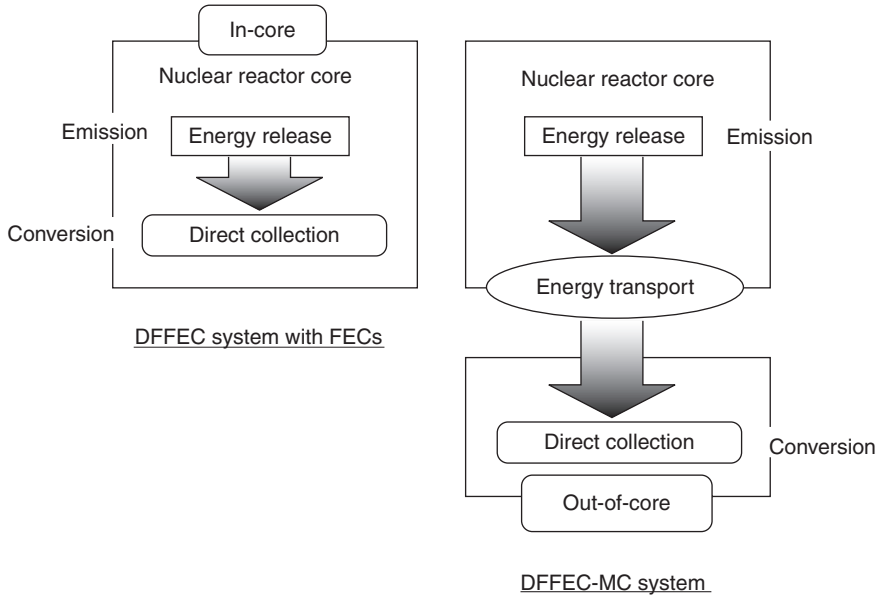

Figure 47.6 Alternative approaches of direct conversion of the fission fragment kinetic energy.

- Long-term energy emission and sustainable component integrity.
- Reliable and efficient energy transport.
- Efficient out-of-core direct conversion of the fission fragment kinetic energy.

47.4 COMPONENTS OF THE DFFEC-MC SYSTEM

The principal components of a DFFEC-MC system and their arrangement are shown in Figure 47.7. The DFFEC-MC system considered here employs features originally formulated to apply DEC methods to mirror-based fusion systems [31]. An out-of-core DEC system that utilizes magnetic collimation involves four main components:

- Nuclear reactor core consisting of fuel elements with ultra-thin fuel layers.
- Central solenoid (CS).
- Conical magnetic collimators (CMCs).
- Multi-stage direct energy collectors.

The DFFEC-MC concept requires the fissile fuel to be contained in thin layers, no more than a few microns thick, so that the fission fragments can escape the fuel element with a significant fraction of their initial kinetic energy. The nuclear reactor core has to be designed in such a way that the fission fragments, which escape the fuel element, can be magnetically guided to the out-of-core collectors, ideally without colliding with other fuel elements and structures. The concept requirements lead to an extremely low average density for the fissile fuel in the nuclear reactor core, i.e., the core consists of very thin fuel layers on widely spaced fuel elements. This fact complicates reactor core design, both in achieving criticality and in maintaining the required excess reactivity over a practical refueling interval.

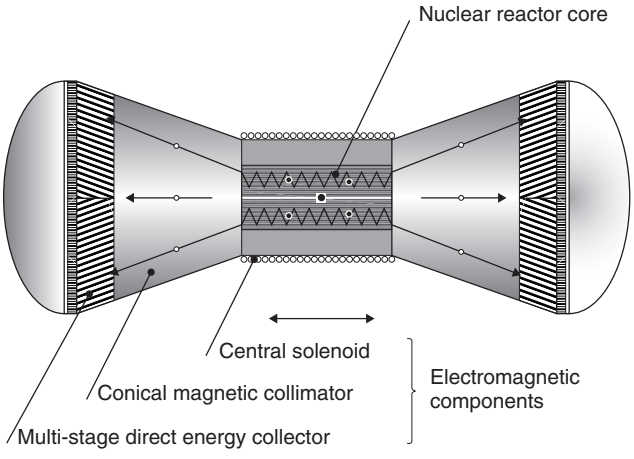

Figure 47.7 Principal component arrangement of the DFFEC-MC system.

The criticality of the DFFEC-MC nuclear reactor core is only achievable for a technologically feasible core size if highly fissile nuclides are utilized as fuel and if an efficient neutron reflector surrounds the core. Utilization of plutonium and higher actinides (for example, Am242m or Cm245) with large fission cross-sections, low capture cross-sections, and high neutron releases per fission can help in achieving criticality. Considering possible fuels for the DFFEC-MC system, fuel compositions based on HEU (~100% of U235), reactor-grade and weapon-grade Pu, and compositions with Am242m are taken into account in the present study.

The source of the magnetic field within the fuel element lattice is a solenoid surrounding the nuclear reactor core. The DFFEC-MC central solenoid serves to trap the escaping fission fragments on magnetic field lines and isolate them from collisions with other fuel elements and structures. The applied magnetic field must be chosen so that the trajectories (each trajectory is characterized by the corresponding gyroradius and axial motion per revolution) of the trapped fission fragments allow most of them to avoid collisions with neighboring fuel elements and other internal components and structures. Arrangement of the fuel elements should also minimize interactions of the escaping fission fragments with fuel elements (other than the one in which the fission fragment is born) and structures within the nuclear reactor core.

Once fission fragments are trapped and exit the nuclear reactor core, the next step is a magnetic expansion that is used to convert the rotational kinetic energy of fission fragments around the magnetic field lines to translational kinetic energy parallel to the magnetic field lines. Thus, a "beam" of fission fragments is formed that is more favorable for direct collection. This magnetic expansion is performed by the conical magnetic collimators [27]. In addition, the CMC volumes provide an intrinsic reduction of the fission fragment density, decreasing potential space-charge and heating effects at the direct collector entrance.

The integrated design of the nuclear reactor core, central solenoid, and conical magnetic collimator coils has to provide efficient extraction of the escaping fission fragments from the core with minimal collision losses and essential neutron confinement within the core or neutron trapping prior to the collector entrances. If neutrons are allowed to reach the direct collectors, they can damage collection stages. Neutron confinement is preferable to trapping, since confinement reduces neutron leakage and preserves neutron population in the nuclear reactor core.

At the end of the collimator a direct energy collector is employed to recover the fission fragment kinetic energy and convert it to power. The method envisioned for direct

energy conversion is the deceleration of fission fragments in a stationary electrostatic field [31]. There are two design requirements for the DFFEC-MC system collectors:

- High efficiency for positively charged particle collection.
- Capability for operation at high power densities.

Satisfaction of the first requirement is needed to achieve a high overall efficiency of the system. The second requirement provides technologically realistic dimensions for the DFFEC-MC system components.

Due to the distribution of the fission fragment kinetic energies at the CMC exit, it is necessary to design multi-stage direct energy collectors. Use of the external charge collection (out-of-core multi-stage collection) eliminates the necessity to have the extremely large electric fields needed for fission electric cells. A multi-stage venetian blind (VB)-type charged particle collector located at the CMC end is considered to be one of the most efficient direct collectors for such a system [28]. In the VB-design, multi-stage collection is achieved using the angular dependence of the fission fragment transmission through collection stages (plates), arranged such that they resemble a venetian blind. A VB-collector can be operated at a relatively high density of the entering fission fragments because particles are transmitted through the multiple collection blinds. As a result, this feature reduces the CMC dimensions. Experimental studies previously performed with VB-collectors have demonstrated high efficiencies and very promising agreement between theoretically estimated and experimentally observed values of the collection efficiencies [29, 31].

The escaping fission fragments and free electrons must be separated before collection to avoid charge neutralization at the collection stages. The required charge separation can be accomplished using electrostatic or magnetic fields. Three basic methods have been suggested as solutions of the analogous problem for fusion systems [31]:

- Grid wires with a negative bias placed in front of the collectors.
- Weak transverse magnetic fields superimposed at the exits of the collimators.
- Sharp curved magnetic field lines at the exits of the collimators.

All three methods appear to be theoretically possible. However, each of them has some negative impact on the overall efficiency of the DFFEC-MC system. Furthermore, the technological feasibility of each of these methods is still under consideration. Selection of the best method of charge separation for implementation in the DFFEC-MC system is beyond the scope of the present analysis.

TABLE 47.2 Components of the DFFEC-MC System and Existing Technologies

DFFEC-MC System Component	Existing Technologies
Long-term energy emission and sustainable component integrity	
Advanced Actinide Fuel	• Actinide Inventory [32, 33] • Separation Pyroprocesses for Actinides and Lanthanides [34]
Element with Ultra-Thin Fuel Layer	• Fuel-Coated Elements [16, 21] • Ultra-Thin Film Fuels with Long Lifetimes [14, 35] • Graphite Fibers [36–38] • Nano-Tube Technology [39–41]
Reliable and efficient energy transport	
Central Solenoid	• ITER Central Solenoid Model Coil [42–46] • KLOE Solenoid [47] • A Dual 6T Persistent-Mode SC Solenoid Ion-Optical System [48]
Conical Magnetic Collimator	• SWIFT Ion Implantation System [49] • VASIMIR Engine [50–52]
Vacuum Vessel	• ITER Vacuum Vessel [53, 54]
Efficient out-of-core direct conversion of the FF kinetic energy	
Multi-Stage VB-type Collector	• 2-Stage VB-type Collector [29]

As discussed above, because of the high energies of the escaping fission fragments, the DFFEC-MC concept requires large external magnetic fields that can only be maintained in the system utilizing superconducting coils. Similar to fusion systems, the superconducting coils of the DFFEC-MC system are expected to be among the most critical and expensive components. Depending on the specific system layout and characteristics, the CS superconducting coil may need to be designed for an axial magnetic field of 7.5 T with the CMC coils designed for an axial magnetic field of 0.9 T. These coils have a significant influence on the overall dimensions of the DFFEC-MC system.

The working volume of the DFFEC-MC system consists of the CS, CMC, and VB-collector internal volumes. A high vacuum must be maintained in the working volume to minimize parasitic interactions of the escaping fission fragments. The vacuum vessel (VV) of the DFFEC-MC system is the outer boundary of the entire working volume. This is also the main radioactivity confinement barrier for the system. The VV structure must be designed to withstand normal operation, design basis accidents, and off-normal operation events.

47.5 EXISTING TECHNOLOGIES AND POTENTIAL FEASIBILITY OF THE DFFEC-MC CONCEPT

The DFFEC-MC concept is an innovative approach to utilize the enormous amount of energy released in a nuclear fission event. While founded on the original ideas suggested at the beginning of the nuclear era, this concept incorporates current technological advances that afford the possibility of practical applications. To be deemed feasible for further development and to be considered viable for eventual deployment, the DFFEC-MC concept must achieve satisfactory performance in the following principal areas:

Operation:

- The nuclear reactor core of the DFFEC-MC system, which is composed of the elements coated with the extremely thin layers of fissile fuel, must be able to reach criticality.
- The nuclear reactor core of the DFFEC-MC system must be able to attain useful fuel burn-up levels over a long period of sustainable operation without severe degradation of the fissile fuel layer, supporting elements, and other core components.
- The DFFEC-MC system must be able to reliably transport and utilize fission fragments with minimal losses within transport components.
- Fission energy that is not available for direct recovery, for example, the fission fragment kinetic energy that does not escape the fuel elements must be reliably removed from the nuclear reactor core.
- The DFFEC-MC system must have favorable size, controllability, non-proliferation and safety characteristics.

Efficiency of direct energy conversion (efficient out-of-core direct conversion of the fission fragment kinetic energy):

- The secondary electrons emitted along with fission fragments from the fuel layer must be suppressed so that they do not reach the collectors.
- The energy conversion efficiency of the DFFEC-MC system should be competitive with or exceed that of alternative technologies.

Applicability of the DFFEC-MC system output:

- The high voltage, direct current output of the DFFEC-MC system must be adaptable for interconnection to an external power grid of the particular application.
- Potential needs for the DFFEC-MC systems must be clearly identified.

Although the DFFEC-MC system is an innovative direct nuclear energy conversion concept, most of its components can be based on existing technologies that have been either implemented or experimentally proven. Existing technologies applicable to individual DFFEC-MC components are listed in Table 47.2. This information indicates that a prototype of the DFFEC-MC system might be built within a relatively short development period. Systematic experimental research with the prototype could verify results of the computational modeling and prove the feasibility of the DFFEC-MC concept. Commercial applications could then follow.

REFERENCES

1. J. R. Lamarsh, *Introduction to Nuclear Engineering*, 2nd ed. Addison-Wesley, Reading, Massachusetts, 1983.
2. M. M. El-Wakil, *Nuclear Energy Conversion*, 4th ed. American Nuclear Society, Inc., La Grange Park, Illinois, 1992.
3. G. H. Miley, *Direct Conversion of Nuclear Radiation Energy*. American Nuclear Society, Inc., La Grange Park, Illinois, 1970.
4. J. Weisman, *Elements of Nuclear Reactor Design*, 2nd ed. Robert E. Kreiger Pub. Comp., Inc., Malabar, Florida, 1983.
5. *Hydrogen as an Energy Carrier and Its Production by Nuclear Power*, IAEA-TECDOC-1085, International Atomic Energy Agency, Vienna, Austria, 1999.
6. *Safety Related Design and Economic Aspects of HTGRs*, IAEA-TECDOC-1210, International Atomic Energy Agency, Vienna, Austria, 2001.
7. S. W. Angrist, *Direct Energy Conversion*, 3rd ed. Allyn and Bacon, Inc., Boston, Massachusetts, 1976.
8. A. Tsuji, A. Endoh, and Y. Asada, Completion of ABWR Plant—Kashiwazaki-Kariwa Nuclear Power Station Unit Nos. 6 and 7. *Hitachi Review*, 1998, **47**, 157.
9. H. G. C. Moseley, J. Harling, The attainment of high potentials by the use of radium. *Proc. Royal Soc*., 1913, **88**, 471.
10. C. B. Amphlett, The production of electrical power from separated fission products. *J. Nuclear Energy*, 1955, **1**, 173.
11. G. M. Safonov, *Direct Conversion of Fission to Electric Energy in Low Temperature Reactors*, RM-1870, Science and Technology Program, RAND Corporation, Santa Monica, California, 1957.
12. C. J. Heindl, *Efficiency of Fission Electric Cells*, JPL-32-105, Jet Propulsion Laboratory, Pasadena, California, 1961.
13. C. J. Heindl, *Comparison of Fission Electric Cell Geometries*, JPL-32-101, Jet Propulsion Laboratory, Pasadena, California, 1961.
14. J. N. Anno, Secondary electron production from fission fragments emerging from thin layers of uranium dioxide. *J. App. Phys*., 1962, **33**, 1678.
15. J. N. Anno, A direct energy conversion device using alpha particle. *Nucl. News*, 1962, **3**, 12.

16. J. N. Anno Jr. and S. L. Fawcett, The triode concept of direct conversion. *Battelle Techn. Review*, 1962, **10**, 3.
17. C. J. Heidl, W. F. Krieve, and R. V. Meghreblian, Fission fragment conversion reactors for space. *Nucleonics*, 1963, **21**, 80.
18. J. L. Shapiro, *The Two-Region Fission-Electric Cell Reactor*, JPL-32-685, Jet Propulsion Laboratory, Pasadena, California, 1965.
19. J. L. Shapiro, *Design Study of a Fission-Electric Cell Reactor*, JPL-32-741, Jet Propulsion Laboratory, Pasadena, California, 1965.
20. G. H. Miley, Fission-fragment transport effects as related to fission-electric-cell efficiencies. *Nucl. Sci. Eng*., 1966, **24**, 322.
21. W. F. Krieve, *JPL Fission-Electric Cell Experiment*, JPL-32-981, Jet Propulsion Laboratory, Pasadena, California, 1966.
22. D. J. Mokski, *Fluid Systems Design Concept for a Large Gas-Cooled Fission-Electric Cell Reactor Space Power Plant*, JPL-33-283, Jet Propulsion Laboratory, Pasadena, California, 1967.
23. G. E. Rochau, An overview of the direct energy conversion power production program. *Proc. 10th International Conference on Nuclear Engineering (ICONE10)*, Arlington, Virginia, April 14–18, 2002, Track 8, ICONE10-22478, p. 347, American Society of Mechanical Engineers, Fairfield, New Jersey, 2002.
24. I. Ursu and I. I. Purica, Synergetics of the fission electric cells., *J. Energy Research*, 1980, **4**, 19.
25. I. Ursu, A. I. Badescu-Singureanu, and L. Schachter, Some developments in direct nuclear energy conversion: neutron flux dependence of the fission electric cell output parameters. *J. Energy Research*, 1985, **9**, 165.
26. I. Ursu, A. I. Badescu-Singureanu, and L. Schachter, Estimated output parameters at high neutron flux values for an experimental fission electric cell. *J. Energy Research*, 1990, **14**, 63.
27. R. R. Smith, *Plasma Expander for Venetian Blind Direct Converters*, UCRL-51373, Lawrence Livermore National Laboratory, Livermore, California, 1973.
28. R. W. Moir and W. L. Barr, Venetian-blind direct energy converter for fusion reactors. *Nucl. Fusion*, 1973, **13**, 35.
29. R. W. Moir and W. L. Barr, *Experimental Results on the Two-Stage, Venetian Blind, Direct Energy Converter*, UCID-16429, Lawrence Livermore National Laboratory, Livermore, California, 1974.
30. G. F. Chapline, P. W. Dickson, and B. G. Schitzler, "*Fission Fragment Rockets—a Potential Breakthrough*, EGG-M-88285, Lawrence Livermore National Laboratory, Livermore, California, 1988.
31. G. H. Miley, *Fusion Energy Conversion*. American Nuclear Society, Inc., La Grange Park, Illinois, 1976.
32. A. Shelley, H. Akie, H. Takano, and H. Sekimoto, Plutonium and minor actinide once-through burning in LWRs. *Proc. 8th International Conference on Nuclear Engineering (ICONE8)*, Baltimore, Maryland, April 2—6, 2000, Track 6, ICONE8-8740, p. 154, American Society of Mechanical Engineers, Fairfield, New Jersey, 2000.
33. C. H. M. Broeders, E. Kiefhaber, and H. W. Wiese, Burning of transuranium isotopes in thermal and fast reactors. *Nucl. Eng. Design*, 2000, **202**, 157.
34. Actinide and fission product partitioning and transmutation. *Proc. 6 th Information Exchange Meeting on Nuclear Development*, Madrid, Spain, December 11–13, 2000, NEA-OECD-EC, EUR 19783EN, Nuclear Energy Agency, Issy-les-Moulineaux, France, 2000.
35. R. A. Meyers, ed., *Encyclopedia of Lasers and Optical Technology*. Academic Press Inc., San Diego, California, 1991.
36. M. E. Beauharnois, D. D. Edie, and M. C. Thies, Carbon fibers from mixtures of AR and supercritically extracted mesophases. *Carbon*, 2001, **39**, 2101.
37. F. R. Jones, *Handbook of Polymer-Fiber Composites*. Longman, Inc., London, United Kingdom, 1994.
38. D. D. L. Chung, *Carbon Fiber Composites*. Butterworth-Heinemann, Inc., Boston, Massachusetts, 1994.
39. G. Fasol, "anowires: small is beautiful". *Science*, 1998, **280**, 545.
40. B. S. Files, Carbon nanotubes. *Advanced Materials and Processes*, 1999, **10**, 47.
41. Y. Zhang, T. Ichihashi, E. Landree, F. Nihey, and S. Iijima, Heterostructures of single-walled carbon nanotubes and carbide nanorods. *Science*, 1999, **285**, 1719.
42. T. Kato, First test results for the ITER central solenoid model coil. *Fusion Eng. Design*, 2001, **56–57**, 59.
43. R. Toschi, How far is a fusion power reactor from an experimental reactor. *Fusion Eng. Design*, 2001, **56–57**, 163.
44. R. Aymar, ITER R&D: executive summary: design overview., *Fusion Eng. Design*, 2001, **55**, 107.
45. H. Tsuji, ITER R&D: magnets: conductor and joint development. *Fusion Eng. Design*, 2001, **55**, 141.
46. H. Tsuji, ITER R&D: magnets: central solenoid model coil. *Fusion Eng. Design*, 2001, **55**, 153.
47. D. E. Andrews, A. J. Broadbent, M. Greenslade, S. M. Harrison, and D. M. Jenkins, Progress in the design, manufacture and testing of the KLOE solenoid for the DAPhiNE ring at Frascati. *Proc. 1997 Particle Accelerator Conference (PAC97)*, Vancouver, British Columbia, Canada, May 12–16, 1997, p. 3413, Institute of Electrical and Electronic Engineers, Inc., Piscataway, New Jersey, 1998.
48. F. D. Becchetti, A dual 6T persistent-mode SC solenoid ion-optical system for radioactive nuclear beam research. *IEEE Trans. Applied Superconductivity*, 2001, **11**, 1601.
49. C. K. C. Jen and J. Gordon, SWIFT—a new ion implantation system for parametric applications. *Semiconductor Fabtech*, 2001, **13**, 279.
50. F. R. C. Diaz, The development of the VASIMIR engine. *Proc. International Conference on Electromagnetics in Advanced Applications (ICEAA99)*, Torino, Italy, September 13–17, 1999, p. 798, Institute of Electrical and Electronic Engineers, Inc., Piscataway, New Jersey, 1999.

51. F. R. C. Diaz, Research status of the variable specific impulse magnetoplasma rocket. *Trans. Fusion Techn*., 1999, **35**, 87.
52. J. P. Squire, Experimental status of the development of a variable specific impulse magnetoplasma rocket. *Trans. Fusion Techn*., 1999, **35**, 243.
53. G. Kalinin, ITER R&D: vacuum vessel and in-vessel components: materials development and test. *Fusion Eng. Design*, 2001, **55**, 231.
54. K. Koizumi, ITER R&D: vacuum vessel and in-vessel components: vacuum vessel. *Fusion Eng. Design*, 2001, **55**, 193.
55. P. Tsvetkov, R. R. Hart, and T. A. Parish, Highly efficient power system based on direct fission fragment energy conversion utilizing magnetic collimation. *Proc. 11th Intern. Conf. on Nucl. Eng*. (ICONE 11), Tokyo, Japan, April 20–23, 2003, ICONE11-36275, American Society of Mechanical Engineers, Fairfield, New Jersey, 2003.
56. P. Tsvetkov, R. R. Hart, and D. B. King, Fission fragment magnetic collimator reactor: current status of the experimental program., *Trans. Amer. Nucl. Soc*., 2004, **91**, 927, Amer. Nucl. Soc., Inc., La Grange Park, Illinois.

INDEX

Nuclear Energy Encyclopedia: Science, Technology, and Applications, First Edition (Wiley Series On Energy).
Edited by Steven B. Krivit, Jay H. Lehr, and Thomas B. Kingery.